PB82-227901

Proceedings of Third Conference on Waste Heat Management and Utilization, Held at Miami Beach, Florida on May 11-13, 1981

Miami Univ.
Coral Gables, FL

Prepared for

Industrial Environmental Research Lab.
Research Triangle Park, NC

May 82

U.S. Department of Commerce
National Technical Information Service
NTIS

PB82-227901

EPA-600/9-82-008
May 1982

PROCEEDINGS: THIRD CONFERENCE ON WASTE HEAT MANAGEMENT AND UTILIZATION (May 1981, Miami Beach, FL)

S.S. Lee and Subrata Sengupta, Compilers
Mechanical Engineering Department
University of Miami
Coral Gables, Florida 33124

EPA Purchase Order D5835NAET

EPA Project Officer: Theodore G. Brna
Industrial Environmental Research Laboratory
Office of Environmental Engineering and Technology
Research Triangle Park, NC 27711

Cosponsors: Department of Energy, Electric Power Research Institute, Environmental Protection Agency, Florida Power and Light Company, Nuclear Regulatory Commission, and University of Miami's School of Continuing Studies (In cooperation with American Society of Mechanical Engineers' Miami Section)

Prepared for
U.S. Environmental Protection Agency
Office of Research and Development
Washington, DC 20460

REPRODUCED BY
NATIONAL TECHNICAL
INFORMATION SERVICE
U.S. DEPARTMENT OF COMMERCE
SPRINGFIELD, VA 22161

FOREWORD

The first conference on Waste Heat Management and Utilization held in Miami during May 9-12, 1977 was well attended. A three volume proceedings was published. In response to continued interest, the second comprehensive conference on the subject was held during December 4-6, 1978. This established a biannual frequency and allowed significant progress during meetings. The third conference, which was held during May 11-13, 1981, further helped in meeting the needs of the Waste Heat Community.

The third conference had working sessions covering important topics in the subject area. Each working session featured an invited lecturer to set the tone for the session. The session reports are included in these proceedings.

Continued support from private and public sponsoring agencies and their representatives have made this effort worthwhile.

Subrata Sengupta

Samuel S. Lee

TECHNICAL REPORT DATA
(Please read Instructions on the reverse before completing)

1. REPORT NO.	2.	3. RECIPIENT'S ACCESSION NO.
EPA-600/9-82-008	ORD Report	PB82 227901

4. TITLE AND SUBTITLE	5. REPORT DATE
Proceedings: Third Conference on Waste Heat Management and Utilization (May 1981, Miami Beach, FL)	May 1982
	6. PERFORMING ORGANIZATION CODE
7. AUTHOR(S)	8. PERFORMING ORGANIZATION REPORT NO.
S.S. Lee and Subrata Sengupta, Compilers	
9. PERFORMING ORGANIZATION NAME AND ADDRESS	10. PROGRAM ELEMENT NO.
University of Miami Department of Mechanical Engineering P.O. Box 248294 Coral Gables, Florida 33124	11. CONTRACT/GRANT NO. EPA Purchase Order D5835NAET
12. SPONSORING AGENCY NAME AND ADDRESS	13. TYPE OF REPORT AND PERIOD COVERED
EPA, Office of Research and Development* Industrial Environmental Research Laboratory Research Triangle Park, NC 27711	Proceedings; 1-6/81
	14. SPONSORING AGENCY CODE EPA/600/13

15. SUPPLEMENTARY NOTES IERL-RTP project officer is Theodore G. Brna, Mail Drop 61, 919/541-2683. EPA-600/9-79-031a and -031b were proceedings of the 2nd conference. Cosponsors: DOE, EPRI, Florida Pwr and Light Co., NRC, and Univ. of Miami.

16. ABSTRACT The proceedings document presentations at the Third Conference on Waste Heat Management and Utilization in Miami Beach, FL, 5/11-13/81. The conference addressed programs in waste heat management and utilization, utilization of waste heat from industrial processes, thermal discharges and related phenomena, cooling towers and their effects, greenhouse applications of waste heat, environmental effects of waste heat discharges to water bodies, and management and regulatory aspects of waste heat. The conference (jointly sponsored by DOE, EPA, NRC, EPRI, Florida Power and Light Co., and the University of Miami) involved the participation of researchers, state and federal officials, process developers and users, and consultants.

17. KEY WORDS AND DOCUMENT ANALYSIS

a. DESCRIPTORS	b. IDENTIFIERS/OPEN ENDED TERMS	c. COSATI Field/Group
Pollution	Pollution Control	13B
Heat Recovery	Stationary Sources	20M,13A
Industrial Processes	Waste Heat	13H
Cooling Towers	Thermal Discharge	07A,13I
Greenhouses		02C
Management		05A
Regulations		05D

18. DISTRIBUTION STATEMENT	19. SECURITY CLASS (This Report)	21. NO. OF PAGES
Release to Public	Unclassified	
	20. SECURITY CLASS (This page) Unclassified	22. PRICE

EPA Form 2220-1 (9-73)

ORGANIZING COMMITTEE

John Neal
Department of Energy

Theodore G. Brna
Environmental Protection Agency

Frank Swanberg
Nuclear Regulatory Commission

John Maulbetsch
Electric Power Research Institute

C.C. Lee
Environmental Protection Agency

Charles D. Henderson
Florida Power & Light Company

Samuel S. Lee
Conference Chairman
University of Miami

Subrata Sengupta
Conference Co-Chairman
University of Miami

ADVISORY COMMITTEE

Charles H. Kaplan
U.S. Environmental Protection Agency

Richard Dirks
National Science Foundation

Donald R.F. Harleman
Massachusetts Institute of Technology

Charles C. Coutant
Oak Ridge National Laboratory

G.S. Rodenhuis
Danish Hydraulic Institute, Denmark

H. Fuchs
Consulting Engineers, Inc., Switzerland

P.F. Chester
Central Electricity Research Laboratory, England

A.J. Policastro
Argonne National Laboratory

P.R. Kamath
Bhabha Atomic Research Centre, India

W. Aung
National Science Foundation

J.R. Hendricks
Duke Power Company

CONFERENCE SUPPORT

Arrangements:

Ruben Fuentes
The School of Continuing Studies

Coordinator:

Dipankar Dasgupta

Secretaries:

Berta Souto
Sook Rhee

ACKNOWLEDGMENT

The conference committee is grateful to the keynote speaker, Mr. Floyd Culler. The participation of Mr. Leonard Weiss, the banquet speaker, is greatly appreciated.

The advisory committee played a significant role in shaping the contents of this conference. The efforts of the session chairmen and co-chairmen are gratefully acknowledged.

The sponsoring organizations and the scientists and managers, who have provided leadership in sustaining continued growth in the important field of waste heat research, have our sincerest gratitude.

The authors and other participants have played the most important role in defining the present status and future directions.

Conference Committee

Miami, May 1981

CONTENTS

WASTE HEAT MANAGEMENT AND UTILIZATION CONFERENCE

PAGE No.

OPENING SESSION (Session I)

GENERAL SESSION (Session II).....II-1

OVERVIEW OF DOE WASTE HEAT RECOVERY PROGRAMS.....II-3
J. Neal, Department of Energy, Washington D.C.

ENVIRONMENTAL APPROACHES TO WASTE HEAT UTILIZATION.....II-9
T.G. Brna, EPA, Research Triangle Park, North Carolina
C.C. Lee, EPA, Cincinnati, Ohio

EPRI ACTIVITIES IN WASTE HEAT MANAGEMENT AND UTILIZATION.....II-18
J. Maulbetsch and J. Bartz, Electric Power Research Institute
Palo Alto, California

ALTERNATIVES FOR WASTE HEAT UTILIZATION IN THE.....II-28
PETROLEUM REFINING AND PETROCHEMICAL INDUSTRIES
E.H. Mergens, Shell Oil Company, Houston, Texas

UTILIZATION I (Session III-A).....III-A-43

USING INDUSTRIAL REJECT HEAT FOR DISTRICT HEATING,.....III-A-45
A CASE STUDY, BELLINGHAM, WASHINGTON
M. Olszewski, Oak Ridge National Laboratory, Oak Ridge, TN
L.B. Katter, Rocket Research Company, Redmond, Washington

WASTE HEAT AND CHILL STORAGE IN AQUIFER SYSTEMS.....III-A-56
J.R. Ellison, Battelle Northwest Laboratory Systems
Richland, Washington

CO-GENERATION ELECTRICAL INTERCONNECTION EQUIPMENT.....III-A-66
COSTS AND ISSUES
J.B. Patton, Systems Control, Inc., Palo Alto, California

PERFORMANCE ANALYSIS OF DEDICATED HEAT PUMP WATER.....III-A-80
HEATING IN AN OFFICE BUILDING APPLICATION
L.S. Morrison, Solar Energy Research Institute, Golden, Colorado

HEAT TRANSPORT SYSTEM FROM A SWISS WASTE INCINERATION.....III-A-92
PLANT TO INDUSTRIAL CONSUMERS AND TO DISTRICT HOSPITALS
E. Gautschi, Motor-Columbus Consulting Engineers, Baden, Switzerland

THERMAL DISCHARGE I (Session III B).....III-B-103

DISCHARGE INDUCED SHEAR STRESSES.....III-B-105
F.J. Mogolesko, Boston Edison Company, Boston, Massachusetts

INSTALLATION OF CLOSED CYCLE COOLING SYSTEM TO REDUCE.....III-B-114
IMPACT OF EXISTING ONCE THROUGH COOLING SYSTEM
H.A. Frediani, Jr., Envirosphere Company, Atlanta, Georgia

A SIMPLIFIED MATHEMATICAL THERMAL MODEL FOR SPRAY CANALS....III-B-121
K.E. Trout, Black, and Veatch, Kansas City, Missouri
W.E. Stewart, Jr., University of Missouri, Kansas City, Missouri
A.T. Leard, Kansas University, Manhattan, Kansas

COOLING WATER DISPERSION UNDER THE INFLUENCE OF GROYNS.....III-B-127
V. Kaleris & M. Schatzmann, University of Karlsruhe, West Germany

THERMAL DISCHARGE II (Session IV A).....IV-A-137

EVAPORATION FROM HEAT LOADED LAKES: A SUMMARY.....IV-A-139
B.L. Sill, Clemson University, Clemson, South Carolina

INVESTIGATION OF LAKE BELEWS.....IV-A-152
S.K. Mathaven, Florida Power & Light Company, Miami, Florida
W.J. McCabe, Duke Power Company, North Carolina
S.S. Lee & S. Sengupta, University of Miami, Coral Gables, Florida

THERMAL PLUME EVALUATION OF THE ST. LUCIE UNIT 1 DIFFUSER....IV-A-158
N.S. Shasidhara & H.A. Nagel, Envirosphere Company, New York,
New York

2-D CONVECTION DOMINATED THERMAL DISPERSION IN COASTAL.....IV-A-177
WATERS
H.P. Miller & K.C.S. Tong, United Engineers & Constructors, Inc.
Philadelphia, Pennsylvania

A THERMAL IMPACT ASSESSMENT MODEL WITH MEASURED.....IV-A-185
FIELD DATA APPLIED TO THE TIDAL RIVER WESSER
J. Hauser, D. Eppel, A. Muller & A. Nehisen, Institute
of Physics, West Germany
F. Tanzer, Universitat Giessen, West Germany

MATHEMATICAL MODELLING OF HYDROTHERMAL RECIRCULATION.....IV-A-200
FOR PASIR GUDANG POWER STATION MALAYSIA
V.S. Thaker, B.M. Patil, & K.G.K. Murty, Central Water
and Power Research Station, Pune, India

COOLING TOWERS (Session IV-B).....IV-B-211

AERODYNAMIC LOSSES OF NATURAL DRAFT COOLING TOWERS,.....IV-B-213
ESPECIALLY WITH HIGH FLARE
F.K. Moore & M. Garde, Cornell University, Ithaca, New York

MODEL STUDIES ON THE DESIGN AND ARRANGEMENT OF FORCED.....IV-B-227
DRAFT COOLING TOWERS TO MINIMIZE RECIRCULATION & INTERFERENCE
P.R. Slawson & H.F. Sullivan, University of Waterloo, Ontario
Canada

COOLING TOWER FAN MOTOR POWER MEASUREMENTS.....IV-B-237
A.E. Johnson & K.H. Belfer, Pacific Gas & Electric
Company, San Ramon, California

HEAT TRANSFER CHARACTERISTICS OF A PLATE-FIN CONDENSER.....IV-B-248
WITH DELUGED WATER AUGMENTATION FOR COOLING TOWERS
H.D. Fricke & K. McIlory, Union Carbide, Tonawanda, New York
J.A. Batz, Electric Power Research Institute, Palo Alto, California

STATUS REPORT ON ADVANCED COOLING TOWER (ACT) PROJECT.....IV-B-263
R.T. Allemann & B.M. Johnson, Battelle Northwest, Richland,
Washington

UTILIZATION II (Session IV C).....IV-C-275

WASTE HEAT RECOVERY TECHNOLOGIES FOR GASEOUS DIFFUSION.....IV-C-277
PLANTS AND OTHER LOW TEMPERATURE SOURCES
E. Schneider, W.P. Teagan, P.C. Manata & J. Burke, Arthur
D. Little, Inc., Cambridge, Massachusetts

INDUSTRIAL REFRIGERATION FROM 140F° WASTE HEAT.....IV-C-292
S.J. Hynek, Foster-Miller Associates, Inc., Waltham,
Massachusetts

SOME PROBLEMS IN DESIGNING THE WASTE HEAT POWER.....IV-C-304
STATION OF YUN XI
Liu-De Chang & Z. Ming-ru, Huazhong Institute of
Technology, Wuhan, China

DESIGN OF THE PROPOSED WATTS BAR WASTE HEAT PARK.....IV-C-310
C.F. Bowman & R.E. Taylor, TVA, Knoxville, Tennessee

COOLING TOWER PLUMES (Session V A).....V-A-321

AN IMPROVED METHOD FOR PREDICTING SEASONAL AND.....V-A-323
AND ANNUAL SHADOWING FROM COOLING TOWER PLUMES
R.S. Carhart & W.E. Dunn, University of Illinois,
Chicago, Illinois
A.J. Policastro, Argonne National Laboratory, Argonne, Illinois

COOLING TOWER DRIFT STUDY AT THE OAK RIDGE.....V-A-337
GASEOUS DIFFUSION PLANT
S.H. Park, Union Carbide, Oak Ridge, Tennessee

GREENHOUSE I (Session V B).....V-B-353

INDUSTRIAL WASTE HEAT FOR GREENHOUSES.....V-B-355
I.J. Crumbly, Fort Valley State College, Fort Valley, Georgia
T.G. Brna, U.S. Environmental Protection Agency,
Research Triangle Park, North Carolina

AN UPDATE ON HEATING GREENHOUSE IN NORTHERN.....V-B-369
CLIMATES WITH POWER PLANT REJECTION HEAT
G.C. Ashley, J.S. Hietala, Ashley Engineering, Inc.,
St. Paul, Minnesota

FISHERIES/AQUACULTURE (Session VI A).....VI-A-375

STRIPED BASS AND MANAGEMENT OF COOLING LAKES.....VI-A-377
C.C. Coutant, Oak Ridge National Laboratory, Oak Ridge,
Tennessee

TILAPIA CULTURE IN HEATED EFFLUENTS: ECONOMIC ASPECTS.....VI-A-385
R.G. Nelson, L.L. Behrends, E.L. Waddell, & D.W. Burch,
TVA, Muscle Shoals, Alabama

FISHERIES AND THE DESIGN OF ELECTRIC POWER PLANTS:.....VI-A-393
THE LAKE ERIE EXPERIENCE
J. Reuter & C.E. Herdendrof, The Ohio State University,
Columbus, Ohio

ABALONE CULTURE AT A COASTAL ELECTRIC GENERATING.....VI-A-407
J.C. Kelley & A. Weir, Jr., Southern California Edison
Company, Rosemead, California

TILAPIA CULTURE IN HEATED EFFLUENTS: POTENTIAL.....VI-A-417
FOR COMMERCIALIZATION IN TEMPERATE CLIMATES
L.L. Behrends, D.W. Burch, J.J. Maddox, R.G. Nelson
& E.L. Wanddel, TVA, Muscle Shoals, Alabama

THERMAL DISCHARGE III (Session VI B).....VI-B-425

MATHEMATICAL MODELLING OF THERMAL PLUME INTERACTION.....VI-B-427
AT WATERFORD NUCLEAR POWER STATION
S.Y.H. Tsai, Argonne National Laboratory, Argonne, Illinois

HYDRAULIC MODELLING OF THERMAL DISCHARGES INTO.....VI-B-441
SHALLOW TIDAL AFFECTED STREAMS
H.W. Copp, Washington State University, Pullman, Washington
N.S. Shasidhara, Ebasco Services, New York, New York

MATHEMATICAL MODELLING OF WASTE HEAT DISCHARGE.....VI-B-456
IN LARGE WATER BODIES
A.K. Runchal, Analytical and Computational Research, Inc.
Los Angeles, California
D. Ian Austin, Dames and Moore, Los Angeles, California

EFFECT OF MODEL DISTORTION ON THE NEAR FIELD.....VI-B-468
BEHAVIOR OF THERMAL SURFACE DISCHARGES
D. Hoogendoorn & A. Quist, Delft Hydraulics Laboratory
Delft, Netherlands

MATHEMATICAL MODELS FOR POWER PLANT WASTE HEAT DISCHARGE.....VI-B-479
P.G. Kharche & P.C.K. Variyar, Tata Consulting Engineer,
Bangalore, India

GREENHOUSE II (Session VII A).....VII-A-491

GREENHOUSE HEATING SYSTEM DESIGN AND ECONOMICS.....VII-A-493
FOR WASTE HEAT UTILIZATION
D.M. Stipanuk & R.E. Friday, Cornell University, Ithaca,
New York
B. Chezar, Power Authority of the State of New York,
New York, New York

GREENHOUSE HEATING OPTIONS: CAN WASTE HEAT COMPETE?.....VII-A-508
R.E. Friday, D.M. Stipanuk & G.B. White, Cornell University
Ithaca, New York

MONTOUR WASTE HEAT GREENHOUSE.....VII-A-525
R.P. Johnson, Pennsylvania Power and Light Company,
Washingtonville, Pennsylvania

THERMAL DISCHARGE IV (Session VII B).....VII-B-539

ASSESSMENT OF MODELS USED TO PREDICT EVAPORATIVE LOSS AT.....VII-B-541
COOLING IMPOUNDMENTS
E. Eric Adams, K.R. Helfrich, A.L. Godbey & D.R.F. Harleman,
Massachusetts Institute of Technology, Cambridge, Massachusetts

USE OF NON SITE SPECIFIED WIND SPEED DATA IN PREDICTING.....VII-B-556
LAKE TEMPERATURE AND EVAPORATION
A.M. Mitry, Duke Power Company, Charlotte, North Carolina
B.L. Sill, Clemson University, South Carolina

COOLING POND PERFORMANCE AND RIVER IMPACT DUE TO CYCLIC.....VII-B-566
DAILY POWER GENERATION
Y.J. Tsai & W. Yow, Stone and Webster, Engineering Corporation,
Boston, Massachusetts

HEAT REJECTION FROM COOLING WATER OF A THERMAL POWER.....VII-B-577
PLANT BY RECIRCULATION IN WATER BODY
A.K. Agarwal & M. Prasad, Indian Institute of Technology,
Kanpur, India

NUMERICAL SIMULATION OF THERMAL DISCHARGE FROM OCONEE.....VII-B-585
POWER PLANT INTO LAKE KEOWEE
S.K. Sinha, E.V. Nwadike, S. Sengupta, S.S. Lee, University
of Miami, Coral Gables, Florida

ENVIRONMENTAL EFFECT (Session VII C).....VII-C-591

LIFE HISTORY, POPULATION STRUCTURE AND PHYSIOLOGY OF.....VII-C-593
TEREDO BARTSCHI, A SHIPWORM INTRODUCED INTO TWO NUCLEAR
POWER PLANT EFFLUENTS
K.E. Hoagland, Lehigh University, Bethleham, Pennsylvania

IMPACT OF SALINE AEROSOL DRIFT FROM BRACKISH WATER COOLING....VII-C-607
TOWERS ON CROPS
C.L. Mulchi, J.A. Armbuster, & D.C. Wolf, University of
Maryland, College Park, Maryland

SECTION 316(b) AND MODELLING OF ICHTHYOPLANKTON.....VII-C-624
ENTRAINMENT
D.S. Vaughan, Oak Ridge National Laboratory, Oak Ridge, Tennessee

RNA/DNA RATIO IN TROPICAL FISH EXPOSED TO THERMAL.....VII-C-636
DISCHARGES IN RANA REATAP SAGAR LAKE
P.R. Kamath, K.G. Varughese, & R.P. Gurg, Bhabba
Atomic Research Center, Trombay, Bombay, Inda

WORKSHOPS

ECOLOGICAL EFFECTS (Session W1).....W-1-641

ECOLOGICAL EFFECTS ASSESSMENT REQUIREMENT Vs STATE.....W-1-643
OF ART
D.H. McKenzie, Battelle Pacific Northwest Laboratory,
Richland, Washington

MATHEMATICAL MODELLING (Session W2).....W-2-655

COMMON PROBLEMS IN MODELLING OF THERMAL PLUME IN AIR.....W-2-657
AND WATER
A.J. Policastro, Argonne National Laboratory, Argonne, Illinois

UTILIZATION (Session W3).....W-3-671

CO-GENERATION.....W-3-673
A. Streb, Department of Energy, Washington, D.C.

THERMAL DISCHARGE V (Session VIII A).....VIII-A-695

A CASE STUDY OF AL-KHOBAR COOLING WATER INVESTIGATION.....VIII-A-697
P. Mortensen, A. McCowan & G.S. Rodenhuis, Danish Hydraulic
Institute, Horsholm, Denmark

REMOTE- SENSING STUDY ON MESO-SCALE, MIXING PROCESSES.....VIII-A-710
OFF SAN ONOFRE NUCLEAR GENERATING STATION
C.J. Sonu, Tekmarine Incorporated, Arcadia, California
R.S. Grove, Southern California Edison Company, Rosemead, California

COMBINED EFFECTS OF CITY AND COOLING TOWER HEAT RELEASE.....VIII-A-718
ON THE THERMAL STRUCTURE AND VELOCITY FIELD OF THE LOWEST
AIR LAYERS OF THE ATMOSPHERE
C.A. Jacobs & J.P. Pandolfo, The Centre for Environment and
Man Incorporated, Hartford, Connecticut
D. Haschke, Swiss Federal Institute of Reactor Research,
Wurenlingen, Switzerland

UTILIZATION III (Session VIII B).....VIII-B-729

ENERGY APPLIED SYSTEMS TEST FACILITY.....VIII-B-731
F.J. McCrosson, P.W. Yngve, & F.H. Zander, South Carolina
Energy Research Institute, Columbia, South Carolina

UTILIZATION IV (Session IX A).....IX-A-745

THE POTENTIAL FOR WASTE HEAT UTILIZATION RESULTING FROM.....IX-A-747
THE USE OF POTABLE WATER SUPPLIES PRIOR TO TREATMENT
FOR COOLING WATER
R.H. Ramsey III, R.D. Bowersock, L.V. Urban, J.H. Strickland
& R.M. Sweazy, Civil Engineering, Texas Tech University, Texas

RENOVATION AND REUSE OF COOLING TOWER BLOWDOWN USING.....IX-A-762
WASTE HEAT DISTILLATION
D. Burkhart, Southern California Edison, Rosemead, California
W. Chow, Electric Power Research Institute, Palo Alto, California
Hugo H. Sephton, University of California, Berkeley, California

WASTE-HEAT DESALINATION OF SEA WATER FOR BOILER FEED.....IX-A-769
H.H. Sephton, Envirotech-Sephton Development Center,
Emeryville, California
S.J. Senatore, EBASCO, New York, New York

IMMISCIBLE LIQUID CYCLE IN LARGE SCALE MEDIUM TEMPERATURE.....IX-A-779
WASTE HEAT RECOVERY
B.M. Burnside, University of Carleton, Ottawa, Canada

THE FUNCTION OF CHAINS IN THE TRANSFER OF LOW GRADE.....IX-A-795
HEAT IN ROTARY KILNS
M.C. Patterson & F.D. Moles, University of Surrey, Guildford,
Surrey, England

PROCESS STEAM LINE FROM THE NUCLEAR POWER STATION TO.....IX-A-811
CARDBOARD INDUSTRY AT NIEDERGOESGEN
I. Daglio, Motor-Columbus, Consulting Engineers
Baden, Switzerland

THERMAL DISCHARGE VI (Session IX B).....IX-B-819

FINITE ELEMENT MODELLING OF A COMPLEX EMBAYMENT SYSTEM.....IX-B-821
D.P. Galya & P.M. Colangelo, Stone and Webster Eng'g Corp.,
Boston, Massachusetts

MANAGEMENT AND REGULATION (Session IX C).....IX-C-831

REGULATORY REQUIREMENTS FOR THERMAL DISCHARGES AND.....IX-C-833
DEMONSTRATION OF COMPLIANCE
N.S. Shashidhara, Envirosphere Company, New York, New York

MANAGEMENT OF WASTE HEAT FROM THERMAL POWER PLANTS.....IX-C-847
AS RELATED TO RISING COST OF FUEL
M. Mesarovic, Energoprojekt, Belgrade, Yugoslavia

REGULATORY ASPECTS OF WASTE HEAT MANAGEMENT.....IX-C-861
William A. Anderson, Hunton & Williams, Richmond, Virginia

UTILIZATION V (Session X A).....X-A-873

WASTED LATENT HEAT RECOVERY FROM LOW TEMPERATURE GASES.....X-A-875
Y.H. Kiang, Trane Thermal Company, Conshohocken, Pennsylvania

ECONOMIC EVALUATION OF COMPETING INDUSTRIAL WASTE-HEAT.....X-A-885
RECOVERY TECHNOLOGIES
P. Grogan, Argonne National Laboratory, Argonne, Illinois
B.B. Hamel & H.L. Brown, General Energy Associates,
Cherry Hill, New Jersey

HEAT RECOVERY FROM TURBINE EXHAUST GAS.....X-A-901
G. Hesse, GEA-Power Cooling Systems, Inc., San Diego
California

PREDICTING THE PERFORMANCE AND COST OF ORC WASTE.....X-A-911
HEAT RECOVERY SYSTEMS
J.L. Krazinski, Argonne National Laboratory, Argonne, Illinois

ENERGY UTILIZATION IN THE PRODUCTION OF ANHYDROUS.....X-A-921
ETHYL ALCOHOL FOR GASOHOL
N.B. Smith, Stanley Consultants, Muscatine, Iowa

THERMAL DISCHARGE VII (Session X B).....X-B-931

DYNAMIC BEHAVIOR OF THERMAL PLUME.....X-B-933
J. Cataldo & S. Quense, The Cooper Union, Cooper Square,
New York

A THREE DIMENSIONAL FINITE DIFFERENCE MODEL FOR THE.....X-B-947
PREDICTION OF THERMAL DISCHARGES
G.D. Raithby & R.V. Elliott, University of Waterloo,
Ontario, Canada

PREDICTION OF LOW-FLOW PLUME CONFIGURATION FOR 316 (a).....X-B-961
STUDIES OF OPERATING POWER PLANTS
P.P. Paily, Georgia Institute of Technology, Atlanta, Georgia

SESSION II

GENERAL SESSION

PB82-227919

AN OVERVIEW OF THE DEPARTMENT OF ENERGY WASTE HEAT RECOVERY PROGRAM

John W. Neal
Deputy Director
Office of Coal Utilization
Department of Energy
Washington, D.C., U.S.A.

ABSTRACT

Proper utilization of scarce energy resources is one of the goals of the Department of Energy (DOE). At present about 85 Quadrillion BTU's (Quad) of energy is consumed in the United States every year. Out of this, 15-20 Quads/year constitute "avoidable loss" in conversion process and another 15-20 Quads/year may be termed "avoidable waste," which could be saved. Therefore, potential energy savings could amount to 30-40 Quads/year. Converting this to equivalent barrels of oil per day, a savings of about half this amount (15 Quads) would more than offset our current daily oil import levels of 6.5 to 7.0 million barrels.

The waste heat recovery programs of DOE were triggered by the energy crisis. To date, feasibility studies, market studies, and development and demonstration programs have been funded by DOE to identify, investigate and utilize energy recovery potentials. Some of the major sources of waste heat are powerplants, gaseous diffusion plants, industrial processes, chemical plants, petroleum refineries, boiler exhausts, diesel engine and gas turbine exhausts, furnace exhausts, etc. The temperature range of these waste heat sources can vary from 100-1500°F, and the source medium may be in the form of gas, liquid, or condensing vapor. The quantity of available heat also varies from source to source.

Based on the above factors, several options of heat recovery can be considered. First, is the direct heat utilization by using heat exchangers, recuperators and distribution system. This is feasible when applications are appropriate for the temperature level of the source. The second option is the utilization of a heat pump to boost the temperature of the waste heat to a useful level in order for it to be used in applications that can generate steam or high-temperature liquids. With this approach a greater number of industrial applications can be satisfied. The third option is to generate shaft/electric power using organic (or steam) Rankine cycle engines. This has the advantage of feeding power to the utility and grid if application is not found in the immediate vicinity of the waste heat. Other options include thermal cooling, desiccant dehumidification and so on.

Present Government programs include development and demonstration of the above mentioned system options and to identify market potential of each system. Some notable programs include Residual Energy Applications Program (REAP), which involves gaseous diffusion plants and similar low- and high-temperature sources and the Conservation and Solar Applications Industrial

Preceding page blank

Program whose activities include implementing specific industrial applications. Development of heat pumps (open and closed cycle), efficient turbines, and effective heat exchangers are underway to encompass all aspects of heat recovery from industry, utility, and other sources. If waste heat recovery and the energy savings momentum are continued through final development and commercialization by industry, oil imports which amount to over 13 Quads/year or about 6.5 million barrels per day can be drastically reduced.

1. THE DOE HEAT RECOVERY PROGRAM

With the pressures of growing world population and increasing industrialization, world demand for energy is rapidly outpacing the growth of conventional fuel sources. In the United States, this phenomenon has led to an increased dependence on foreign sources of oil, which now account for 17.5 percent of all energy consumed annually. The serious consequences of such dependence first became apparent during the 1973-1974 Arab oil embargo. Not only do we lack a secure source of energy supply, but increasing outflows of payments to foreign governments due to the increase in the quantity and price of fuel imports has also contributed to a serious strain on the national balance of payments. This has resulted in the emergence of a national goal to reduce our dependence on foreign sources of oil through the exploration of possibilities for the domestic production of alternative fuels and the substitution of more plentiful national resources such as coal.

One of the greatest potential domestic "sources" of fuel which can be of particularly great short term value to offset our energy needs while we fully develop these alternative supplies is an effective program of waste heat utilization. At present, approximately 85 Quads of energy are consumed in the United States every year. Of this total, 15 to 20 Quads per year represent heat loss during conversion processes that could be recovered with waste heat utilization techniques. In addition, 15 to 20 quads could be saved through the use of more efficient conversion processes. Therefore, the potential energy savings from waste heat utilization and the improvement of conversion processes alone could amount to 30 to 40 Quads a year.

The principal sources of waste heat are shown in Exhibit I and include:

Source	Energy Equivalent (10^{15} Btu/year) (estimates)
Condenser Cooling Water (1)	1.1
Industrial Process Water and Process Streams (1)	5.7
Boiler Exhaust Gases (1)	1.0
Furnace Exhaust Gases (1)	2.8
Diesel and Gas Turbine Exhaust (1)	0.4
Powerplant Condenser Cooling Water (2)	12.4

The temperature range of these sources can vary from 100° to 1500°F and source medium may be in the form of gas, liquid, or condensing vapor.

The enormous potential of waste heat utilization as an energy source has made it an important aspect of DOE program activity. Within the Heat Engines and Heat Recovery activity of Fossil Energy's Office of Coal Utilization, the Residual Energy Applications Program (REAP) was estabished to examine three techniques for the recovery of waste heat. The first two techniques are focused on waste heat utilization at low temperatures, up to 200°F. The first technique, direct heat utilization, makes use of two main elements: a heat exchanger and a distribution system. The second technique is the use of a heat pump to boost the temperature of waste heat in order to generate steam or high-temperature of waste heat in order to generate steam or high-temperature liquid, which have a greater number of industrial applications. The third technique is the use of organic or steam Rankine cycle engines for waste heat recovery at high temperatures, between 200° and 1000°F. Waste heat recovered using this method can be used to generate shaft/electrical power and has the advantage of being able to feed power to a utility grid if there are no uses for the power in the immediate vicinity. In addition, DOE's Conservation and Renewable Resources Industrial Program Office is exploring several techniques for achieving energy savings through waste heat recovery including programs in high-temperature recuperator systems, industrial heat pump systems, air/fuel ratio control systems, and oxygen-enriched combustion. In the next few minutes, I would like to briefly highlight for you the overall major activities underway within DOE.

The principal barriers to waste heat utilization have been the lack of awareness of potential users and the lack of sufficient operating experience to establish credibility with potential users. To remove these barriers, REAP activities have been aimed at information dissemination, and demonstration and development of waste heat utilization technology to increase the confidence of potential users and provide the basis for commercialization in the future. The REAP program is organized into three paths designed to achieve these goals: demonstrate the economically feasible recovery of low grade residual (less than 200°F) heat from DOE production facilities; construction of an Energy Applied Systems Test (EAST) facility for the testing of heat recovery system components; and the implementation of waste heat recovery projects with utilities and industry.

The first of these paths, the projects to evaluate the feasibility, on a site specific basis, the recovery of residual heat from DOE coal-fired nuclear production facilities, examines the possibilities of applying direct and heat pump recovery technologies on a commercial scale at three DOE facilities: the gaseous diffusion plants at Oak Ridge, Tennessee; Paducah, Kentucky; and Portsmouth, Ohio. Based on engineering prudence and to obtain crucial experience quickly, it was decided that prior to undertaking a commercial scale project, a smaller scale precursor experiment should be conducted. The Portsmouth, Ohio, facility was selected as the site for this initial system application evaluation. The use of waste heat from the facility is being evaluated for a potential application to heat a nearby school and to operate a greenhouse. Initial engineering studies for this project have been completed under DOE sponsorship; the next step will involve final design and construction. In addition, the Department of Energy is considering the award of two contracts for feasibility studies of full scale heat recovery activities at these facilities. One would investigate the feasibility of a central energy management system at the Portsmouth gaseous diffusion plant and the other would examine the feasibility of an ethanol plant at the Paducah gaseous diffusion plant. DOE is also considering the issuance of a Program Opportunity Notice to identify potential applications at the Oak Ridge plant.

The second path is the construction of the Energy Applied Systems Test facility at the Savannah River plant. The EAST facility is designed to reduce uncertainties associated with waste heat utilization technology in the areas of cost, performance and maintenance. Through this project, hardware developed in REAP for system application evaluation or project use will undergo performance rating, availability, maintainability, and cost determination and reliability, and cost determination and reliability testing. Dupont, the operating contractor at DOE's Savannah River plant, has been charged with designing the EAST facility, and this effort is presently underway. The facility will be designed to test both high- and low-temperature equipment such as:

- o low-temperature power cycles
- o industrial heat pumps, closed and open cycles
- o advanced cooling systems
- o high-temperature power systems
  - organic Rankine Cycle engines
  - innovative steam systems

The facility will be constructed in two stages. The first will consist of a core facility designed to handle one low-temperature heat engine, one heat pump and one high-temperature organic Rankine cycle engine. The second-stage expansion will permit testing of three of each of these pieces of equipment.

The third area of the REAP project activity involves joint sponsorship of development activities with utilities and industry. These activities have demonstrated concepts for advanced bottoming cycles and they are continuing to pursue other promising industrial applications. To date, for example, joint DOE-funded demonstrations have been successfully conducted at four utility plants; tests recently began at an industrial powerplant; and two additional facility tests are planned. In addition, as a result of DOE-supported Rankine cycle engine development, the Navy is in the process of installing such a system at its installation in Bermuda. If operation at that site is successful, it is expected that the Navy will install other Rankine systems at a variety of remote locations.

These activities will be discussed in greater detail by subsequent speakers later today.

2. INDUSTRIAL ENERGY CONSERVATION

Within DOE's Office of Conservation, several programs are underway directed toward developing and encouraging waste heat utilization. Principal among these are the Office of Industrial Program's effort aimed at reducing energy loss in industrial and agricultural processes by improving equipment and processes commonly used. To this end, there are two principal groups of activities currently underway: waste heat recovery and utilization, and industrial cogeneration.

Waste heat recovery and utilization activities focus on the development and use of advanced combustion and heat exchange techniques. Current activities are designed to supplement rather than duplicate private industry's efforts in this area, and include developmental work on the following projects:

- Five high-temperature recuperator systems that will extend to thermal ranges and applications not covered by currently available systems.

- Four industrial heat pump systems that operate at higher temperatures with improved performance than present systems.

Future work planned will build on developments resulting from current activities and investigate additional applications for the technologies being developed.

A second area of industrial conservation program activities is industrial cogeneration. It is estimated that cogeneration systems could produce energy savings of 200,000 BPDE by 1985 and 1,000,000 BPDE by the year 2000 at low levels of market penetration. Program activities are designed to assist market penetration by developing optimized inter-industrial/utility cogeneration activities, minimizing requirements for gas and petroleum fuels and developing and commercializing improved conversion system technologies. They are focused on industry-specific projects: steel, aluminum, glass and cement in the high-temperature area; and textile, paper and pulp, and product manufacturing in the low-temperature and end-product process areas. In addition, projects have focused on agricultural and food processes. Specific projects are designed to:

- Conduct a feasibility study for industrial cogeneration fuel cell applications.

- Develop a turbomachinery device, to be powered by waste energy from a glass furnace, that will generate electricity to boost the molten material tank.

- Conduct cogeneration cost studies to determine financial, regulatory, institutional and environmental factors that influence investors' decisions and to summarize industrial experience with systems to date.

- Determine optimum conditions for cogeneration systems on a site-specific basis.

- Demonstrate new systems more optionally suited for use as cogeneration hardware.

Let me conclude by being very frank in my comments on the Government's ability to carry all of these projects to fruition. As you all know, there is a significant change in the DOE energy R&D policy under the new Administration as well as fundamental changes in the role of the Federal Government with respect to funding of energy related activities. These changes are, simply stated, that the Federal role will be relagated to longer-range higher-risk but high payoff R&D. The private sector will be expected to assume almost total responsibility for demonstration and commercialization efforts. This philosophy is evident in the FY 1981 and FY 1982 Federal budgets where, in particular, competition for the Federal dollar in energy related areas is even more keen due to a greater overall emphasis on defense combined with the National need to affect an overall curtailment in the growth of Federal spending.

These factors translate to a reduction in DOE's ability to support the complete spectrum of previously planned heat recovery activities. Consequently, development of a National program in heat recovery will now place a much greater reliance on the private sector to develop and promote the recovery of waste heat, specifically in the areas of demonstration projects. However, the Federal Government remains firmly committed to its belief that waste heat utilization is a National resource of great potential, and plans to continue to support base technology development activities in this area in cooperation with an increased private sector commitment to demonstrate and commercialize this energy resource as an alternative to critical imported energy such as oil and gas.

Natural and human factors affect the magnitude and quality of waste heat from power plants and industries. Seasonal changes in ambient temperature of cooling water affect steam-electric plant thermal efficiency and the demand for electrical energy is affected by season. Seasonal temperatures also impact process heating requirements and the energy mix in cogeneration facilities. For power plants, a lower ambient water temperature can reduce waste heat through more efficient electrical energy generation, while increased electrical energy demands without offsetting efficiency gain entails greater heat rejection. In these plants closed cycle (off-stream) cooling in lieu of open cycle (on-stream) cooling leads to higher heat rates (lower thermal efficiencies) with correspondingly higher heat rejection rates. Consequently, closed cycle cooling is accompanied by higher heat rejection rates (more waste heat) at slightly higher rejection temperatures relative to open cycle cooling. Both of these factors favor waste heat utilization from closed cycle cooling over that from open cycle cooling.

In 1974 EPA issued guidelines for steam-electric generating stations which were based on use of the best available technology. Consideration of the impacts of thermal discharges from these stations led to increased use of closed cycle cooling systems, particularly evaporative cooling towers. Despite a court remand of these guidelines in 1976 and no subsequently issued replacement Federal guidelines, off-stream cooling appears to be the trend for new plants. This cooling approach, which results in less thermally efficient plants as noted earlier, is consistent with protecting aquatic life through limiting water withdrawals from natural bodies and the lack of available water for on-stream cooling at otherwise favorable sites.

2. BENEFITS OF WASTE HEAT UTILIZATION

From an environmental viewpoint, waste heat utilization/reduction reduces adverse environmental impacts. Environmental benefits attributed to waste heat utilization/reduction include:

1. Reduction of pollutant generation and release for a given useful energy requirement.
2. Energy and cost savings through decreased need for pollution abatement equipment.
3. Conservation of energy through improved utilization.
4. Elimination of adverse environmental effects associated with obtaining, processing, and supplying the energy equivalent to the beneficially used waste heat.
5. Potential generation of revenue to offset costs of pollution abatement equipment.

3. EPA PROGRAM IN WASTE HEAT UTILIZATION/REDUCTION

EPA's Office of Research and Development has funded waste heat utilization/reduction research, development, and demonstration projects since the receipt of its first separate budget in 1977. Since various program offices and ORD laboratories have supported waste heat utilization projects, the total level of support and complete listing of projects sponsored is not provided here. However, funding for waste heat utilization/reduction has progressively declined in recent years and is essentially nil today. Higher priority for other program areas for limited funds has been the recent trend and is expected to continue. However, other Federal agencies have missions more attuned to energy conservation and waste heat utilization and currently fund programs in these areas.

Within EPA the Industrial Environmental Research Laboratories in Research Triangle Park (IERL-RTP) and Cincinnati (IERL-Cinn) have responsibilities for energy conservation and waste heat utilization programs. IERL-RTP manages work on the beneficial use of condenser cooling water from industrial and utility plants, while IERL-Cinn has responsibility for industrial energy conservation and the beneficial use of thermal discharges at temperatures above those associated with condenser cooling water. Both have specifically assigned responsibilities for thermal pollution control technology from non-steam power plant discharges from industrial heat sources.

Because of their high potential application for supporting the Agency's environmental mandates, EPA programs for waste heat utilization have stressed the following three options:

1. Utilization of waste heat discharged from industrial and utility plants for agriculture, aquaculture, and non-cogeneration purposes.
2. Cogeneration.
3. Development of integrated energy production/use facilities which are more energy-efficient.

The first option concerns heat after its discharge from a process or facility, while the others involve reduction of waste heat through optimized design and managment. Table 1 lists projects under Option 1, all of these being managed by IERL-RTP.

TABLE 1. BENEFICIAL USE OF WASTE HEAT FOR AGRICULTURAL, AQUACULTURAL AND OTHER NON-COGENERATION USES

Project	Contractor/Grantee	Status
Demonstration of Beneficial Uses of Warm Water from Condensers of Electric Generating Plants	Northern States Power Company	Completed, May 1980 (For final report, see Reference 1)
Greenhouse Production of Bedding and Foliage Plants with Industrial Waste Heat	Fort Valley State College	Completed, September 1980 (For final report, see Reference 2)
Biological Recycling of Nutrients from Livestock Wastes through Use of Waste Heat	Tennessee Valley Authority	Final Report being drafted
Soil Heating to Extend Growing Season for Field Crops	Tennessee Valley Authority	Completed, January 1981
Waste Heat Vertical Tube Foam-Enhanced Evaporation for Water Purification & Recycle	University of California	Final Report being drafted; field testing to continue in 1981
Fish Farming with Warm Water from Condensers of Power Plants	Northern States Power Company	Two-year project began in Fall 1980

4 Table 2 gives projects under Option 2; these are managed by IERL-Cinn. Option 3 has received limited attention from the perspective of waste heat utilization.

TABLE 2. BENEFICIAL USE OF WASTE HEAT FOR COGENERATION

Project	Contractor/Grantee	Status
Environmental, Economic, and Conservation Aspects of Cogeneration	Georgia Institute of Technology	Final Report being drafted
Twin Cities District Heating/Cogeneration: An Environmental Assessment and Regulatory Procedures	Oak Ridge National Laboratory	Final Report due in 1982
Cogeneration: Status and Environmental Issues	TRW, Inc.	Final Report being drafted

Since previously completed studies for EPA concerning waste heat utilization have been reported to previous meetings of this conference [3,4], the projects discussed here will be limited to those now underway or recently completed. In addition, the discussion will be restricted to projects listed in Tables 1 and 2.

3.1 Agricultural, Aquacultural, and Non-Cogeneration Uses of Waste Heat

Because of its favorable potential for near-term (through 1985) energy savings and reducing thermal discharges to water bodies or air, agricultural applications of waste heat dominate the listing in Table 1. They primarily utilize waste heat from electric utility cooling systems, involve low temperatures (38°C (100°F) or less), represent a very small fraction of the waste heat available from modern steam-electric generating stations, and have seasonal limitations. The projects listed result in reduced thermal discharges to water bodies, even for the aquacultural applications. This contrasts with normal aquacultural uses of waste heat which do not reduce thermal pollution but make beneficial use of natural waters heated by thermal discharges.

EPA partially supported the waste heat utilization study at the Sherburne County (Sherco), Minnesota, Plant of the Northern States Power Company (NSP). The details of this demonstration which involved the beneficial use of warm condenser cooling water for greenhouse heating are presented elsewhere [1]. The program with horticultural objectives was concluded in 1980 and resulted in obtaining 3 years of crop growth, economic, and space conditioning data in the 0.2-hectare (0.5-acre) greenhouse. The program was an unqualified success and led to the commercial growth of roses and vegetables (hydroponic farming) at the plant site. Expansion of the waste heat commercial greenhouse area from its currently used 0.6 hectare (1.7 acres) is now underway, and about 6 hectares (14 acres) are available for future warm water heated greenhouses. Although most of the demonstration greenhouse is now used by a commercial rose grower, one 5.2 m x 29.3 m (17 ft x 96 ft) bay serves a fish raising study. In this study by the University of Minnesota with the bulk of the funding from NSP, catfish and tilapia are being grown in six 1.5-m^3 (400-gal.) tanks, two each containing water from the closed cycle cooling system of the plant, a mixture of cooling system water and river water (makeup), and water from a well serving the greenhouse area [5]. Preliminary data covering the initial 12 weeks of the study show no

fish mortality, weight gains near projections, highest weight gains by catfish, and highest weight gains for both species in the mixture and lowest gains in the cooling system water. Based on NSP's present rates for warm water, the estimated annual cost for greenhouse heating at the Sherco site is about $50,000/hectare ($20,000/acre), less than half the projected cost with fuel oil.

While the Sherco demonstration addressed growth of roses and other seted flowers, vegetables, and conifer seedlings, the Fort Valley State (Georgia) study focused on the growth of bedding and foliage plants using simulated industrial waste heat in a location requiring about 35 percent of the heating needed annually at the northern site. These crops were grown under high humidity conditions in adjacent research and control greenhouses, the research greenhouse being heated with waste heat while the other was conventionally heated. Data from 9 months of testing show comparable plant survival and growth in both greenhouses, satisfactory heating with waste heat, and promising economics for waste heat relative to natural gas and fuel oil heating. Additional information on this study will be presented later in this conference [6].

Since 1975, the Office of Environmental Engineering and Technology (formerly the Office of Energy, Minerals and Industry) in EPA's Office of Research and Development has coordinated the Federal Energy/Environment Research and Development Program involving 17 governmental agencies. Through this program, EPA and TVA have jointly supported studies by TVA in Muscle Shoals, Alabama, on using waste heat for soil heating to extend the growing season for field crops and for the biological recycling of nutrients in livestock wastes. The former study has been completed, while the final report for the latter study is now being prepared.

The purpose of the field crop study was to determine if soil heating enhanced maturation and yields of selected crops (bush beans, cantaloupe, corn, okra, peanuts, squash, and watermelon). Using buried plastic pipes at optimized row spacings and soil depths, soil heating increased maturation and yields of the crops noted above during the spring months. No change or slightly decreased yields were evident for squash and watermelon during the summer. While the spring-grown crops with soil heating were available for market about a week earlier than conventionally grown crops, the results show that soil heating in the Muscle Shoals, Alabama, area is not now economically viable.

The biological recycling of swine wastes involved several facets. Initially, TVA used these wastes to grow algae which were harvested and fed to fish. Later the wastes were applied in several concentrations to tanks containing fish (tilapia and silver and bighead carp) at different water temperatures. Waste slurries from these tanks corresponding to three retention times were then supplied to sand beds containing water chestnuts. Tilapia weight increases from 50 to over 500 g in 6 months were obtained, while the harvested water chestnuts were of excellent quality and the chestnut hay was well-suited for ruminant forage. Water from the sand beds was low in nutrients (nitrogen and potassium) and was greatly improved in biological quality relative to the entering effluent from the fish tanks. Fish growth and survivability in holding ponds receiving swine wastes were also evaluated under two conditions. Initially, wastes were supplied directly to these ponds; later biogas production, and fish production in these ponds with digester effluent were evaluated. Biogas production does not remove major plant nutrients (nitrogen, phosphorous, and potassium) but can significantly reduce the biological oxygen demand of manure and the risk of oxygen depletion in aquatic systems fertilized with digester effluent. The system using warm condenser cooling water for producing fish and water chestnuts through recycling swine

wastes was nearly twice as productive when flowing water systems replaced static water (pond) systems. An economic analysis based on a 2000-head swine facility and an investment of about $400,000 was projected to produce a 20 percent rate of return, save the equivalent of 57,235 m^3 (360,000 barrels) of oil through the use of waste heat, and produce the equivalent of 477 m^3 (3,000 barrels) of oil via biogas generation. Information on tilapia culture in heated effluents, based in part from the study just described, is scheduled for presentation later in this conference [7,8].

The recycling of effluents from power plants is of major interest in water-short and low-water-quality regions. The use of waste heat for the production of potable water or the improvement of water quality of effluents or salt-laden waters was investigated in a vertical tube foam-enhanced evaporator (VTFE) process developed under an EPA grant to the University of California-Berkley. Following design, construction, and pilot testing of this 189-m^3/day (50,000-gpd) facility at the Sea Water Conversion Laboratory, the unit was field tested using cooling-tower blowdown at a power plant. Support for the field testing was provided by the Electric Power Research Institute (EPRI) and the Envirotech Corporation as these sponsors believe this system has potential application for treatment of certain power plant wastewaters. Testing is expected to continue in 1981 at Etiwanda Station under the guidance of a steering committee composed of representatives from Envirotech, EPA, EPRI, and Southern California Edison. Field testing results obtained last year indicate that this unit, which uses turbine exhaust steam for heating, has improved both heat transfer and the economics relative to commercially available systems for recycling power plant wastewaters. Later presentations in this conference will address the performance [9] and projected economics [10] of this VTFE in its recycling of cooling tower blowdown.

3.2 Cogeneration

Cogeneration is the simultaneous generation of electricity or mechanical energy and useful thermal energy. EPA studies have focused primarily on the cogeneration of electrical power and thermal energy, since recent legislation has improved the economics of this process by ensuring sale of excess electricity to the utility grid at an attractive price. Cogeneration systems may be divided into three classes, depending upon the quality of the thermal energy delivered and the distance of delivery. Distinguishing systems by these two factors is important because it dictates the air quality impacts of using cogeneration systems. These impacts may be positive or negative, unlike the thermal energy impacts of cogeneration which are in almost all cases beneficial to the environment. The three classes of systems are: (1) district heating, (2) in-plant cogeneration, and (3) energy parks.

District heating utilizes waste heat from electric utilities in the form of hot water (although steam is sometimes used) for the space heating of a community. While the economics of a distribution system dictate that district he heating is most suited for densely populated urban areas, suburbs can also be heated by this method. Generally, hot water can be transported 30 to 40 km with less than a 10 percent loss of thermal energy. As a result, new cogenerating central station power plants need not be built in downtown areas to supply a district heating system. This can reduce pollution control costs for the plant, particularly if the urban area is in non-attainment with respect to national ambient air quality standards (NAAQS).

By building a district heating system, a municipality can also gain several fuel benefits. Scarce oil and gas burned by numerous small boilers and furnaces

are replaced by coal-fired central generating facilities. Municipal solid waste may be burned to produce thermal energy, thus reducing land-fill requirements.

Air quality benefits can also result from district heating by shifting from numerous (often uncontrolled) emission sources which have small stack heights to large cost-effectively controlled facilities having taller stacks. The ground-level air quality will usually improve, principally because of the shift to taller stacks which promote higher dispersion of emissions. This improvement can be quite dramatic, as appears to be the case in Sweden where oil is the principal fuel for both small and large sources. Those cities with district heating have SO_2 concentrations that are lower by factors of 3 to 5, compared with those cities without such centralized systems. EPA is currently undertaking an environmental assessment of the impacts of developing a 2600 MW(t) district heating system which has been proposed for Minneapolis-St. Paul (the "Twin Cities"). This study complements one by DOE which projected reductions in annual average SO_2 concentrations if the system was completed in 1987 (the most distant year for which fuel use projections are available) [11]. The EPA study is looking at not only the annual average decrease in ground-level total suspended particulate (TSP) concentrations, but also the impact on short-term (24-hour) SO_2 and TSP concentrations. Preliminary results indicate that improvements are seen in both time frames, even though more than half of the fuel which will be displaced by coal is natural gas.

It is important to note that district heating (and cogeneration in general) must be considered on a case-by-case basis when investigating air quality impacts. The fuel switching which frequently accompanies system development and increased load factors at the cogeneration facility often results in increased emissions. Thus, there is the potential for very local (within 2 km) increases in pollutant concentrations, particularly during short-term adverse meteorological conditions. In addition, while employing tall stacks may improve local air quality, it may, depending on control equipment used, contribute to long-range increases in pollutant concentrations.

In-plant cogeneration is the production of electricity at an industrial facility which is primarily concerned with producing process steam. (This term can also be applied to commercial establishments which generate electricity with diesel engines and use the heat in the hot exhaust gas for space heating.) One example of such a system is cogeneration at an alcohol plant using a gas turbine, as will be described elsewhere in this conference [12]. TRW, Inc. is just completing a study for EPA which identifies the environmental impacts of switching from separate sources of process steam and electricity to such cogenerating systems. This study shows that while there may be local increases in emissions, the overall emissions in the region can often be expected to decrease. However, the net change in emissions is dependent upon the fuels involved and the size of the cogeneration system; some cogeneration systems are so small that they are not, and probably will not be, regulated. Unregulated facilities potentially would contribute more pollutants per unit of useful energy output than well-controlled electric power plants. The TRW, Inc. study shows that thermal pollutants can be expected to decrease, while solid wastes may increase, depending on the fuel switching which occurs.

A third study, for which IERL-Cincinnati will publish a report this year, explores the energy, economic, environmental, and social impacts of developing an energy park. Here an energy park is a set of industries which lie within 2 or 3 km (1 or 2 mi) of a central cogenerating facility. The study, which was performed by the Georgia Institute of Technology, considers a hypothetical

energy park consisting of six chlorine plants supplied steam by a coal-fired electric utility. Environmentally, the study finds that, while area emissions are likely to be lower compared to what would occur if energy was produced at separate facilities, local emissions may increase significantly. In fact, an energy park is likely to have more intense local air quality problems than district heating or in-plant cogeneration. Similarly, water consumption and water pollution problems (with the exception of thermal pollution) may increase because of the dense population of industry. On the other hand, the close proximity of facilities and the availability of process steam can contribute to more cost-effective pollution control technologies and to the reduction of pollutants through recycling or reuse by other industries.

3.3 Integrated Energy Production/Use Facilities

This option offers promise for waste heat utilization/reduction over the long-term (beyond the year 2000) and is especially applicable to new facilities. The application would have facilities designed for operational compatibility according to energy form, load characteristics, and equipment lifetime. Through joint utility/industry cooperation, this option could increase energy utilization by 10 percent or more over current values.

Integrated energy facilities in the United States have been precluded by institutional problems, the incompatibility of production and user systems, financial risk, lack of capital, inappropriate planning, and relatively inexpensive energy. Appropriate candidates for integrated energy facilities include district heating, power parks with process heating and electrical energy from the same source, surplus electrical energy from industries to electrical utilities, off-peak storage and on-peak use of energy, and combinations of these candidates.

While integrated energy facilities would improve environmental quality and energy conservation, these factors have not yet led to development of such facilities. Energy prices have not risen to the level to spur such development, nor do regulatory guidelines or legislative mandates require use of such facilities. Still higher fuel prices and more limited energy resources seem to be prerequisites for the development of integrated energy facilities.

4. CONCLUSIONS

Effective utilization/reduction of waste heat promotes improved environmental quality and energy conservation. In the past EPA has provided significant support for studies on the beneficial use of waste heat, but higher priorities in other program areas for available resources have forced declining support for this area. Although the Agency's program recognizes three waste heat utilization/reduction options, primary emphasis has been given to near-term applications, such as agricultural uses. The results of these programs have been significant and include a successful greenhouse demonstration which led to commercializaton of waste heat at a power plant site. Potential environmental benefits and recent legislation which makes cogeneration more attractive to industry have also encouraged EPA studies in this area. The studies focusing on district heating, in-plant cogeneration, and energy parks have addressed both potential positive and negative impacts. While long-term waste heat utilization has the potential for major energy savings and environmental benefits, additional incentives are needed to spur development of integrated energy production/use facilities.

ACKNOWLEDGEMENT

The authors extend their appreciation to Ben Blaney, EPA/IERL-Cincinnati, for his contributions to the Cogeneration section and his timely review of this paper.

REFERENCES

1. L. L. Boyd et al., A Demonstration of Beneficial Uses of Warm Water from Condensers of Electric Generating Plants, EPA-600/7-80-099 (NTIS No. PB 80-196793), May 1980.

2. I. J. Crumbly, Greenhouse Production of Bedding and Foliage Plants with Industrial Waste Heat, EPA-600/7-81-034 (NTIS No. PB 81-178279), April 1981.

3. D. J. Graham, EPA Views on Waste Heat Management and Utilization, Proc. Conf. Waste Heat Management and Utilization, Vol. I, pp. I-3-I-12, 1977.

4. T. G. Brna, EPA Programs in Waste Heat Utilization, Proceedings: 2nd Conference on Waste Heat Management and Utilization, Vol. 1, EPA-600/9-79-031a (NTIS No. PB 80-112311), pp 26-37. August 1979.

5. R. V. Stansfield, Northern States Power Co., Minneapolis, MN. Private Communication to T. G. Brna.

6. I. J. Crumbly and T. G. Brna, Industrial Waste Heat for Greenhouses, Proc. 3rd Conf. Waste Heat Management and Utilization (to be published).

7. R. G. Nelson et al., Tilapia Culture in Heated Effluents: Economic Aspects, Proc. 3rd Conf. Waste Heat Management and Utilization (to be published).

8. L. L. Behrends et al., Tilapia Culture in Heated Effluents: Potential for Commercialization in Temperate Climates, Proc. 3rd Conf. Waste Heat Management and Utilization (to be published).

9. D. Burkhart et al., Renovation and Reuse of Cooling Tower Blowdown Using Waste Heat Distillation, Proc. 3rd Conf. Waste Heat Management and Utilization (to be published).

10. H. H. Sephton and S. J. Senatore, Waste Heat Desalination of Sea Water for Boiler Feed, Proc. 3rd Conf. Waste Heat Management and Utilization (to be published).

11. M. A. Kornitz et al., District Heating/Cogeneration Application Studies for the Minneapolis-St. Paul Area: Impact of a District Heating/Cogeneration System on Annual Average SO_2 On Quality in the Twin Cities, Oak Ridge National Laboratories No. ORNL/TM-6830/P11, 1981.

12. W. Kury et al., Energy and Environmental Policy Implications of Alcohol Fuel Production by Cogeneration, Proc. 3rd Conf. Waste Heat Management and Utilization (to be published).

related to some aspect of waste heat management and utilization. Table 1 lists the cognizant divisions and programs, specifies the primary focus of the research for each, and identifies a few lead projects in each area.

The total research budget allocated to waste heat research in the three areas is approximately $2.8 million in 1981. A summary description of the content and plans of these, as well as all the other EPRI programs is available in the EPRI R&D Program Plan Documents (References 1,2, and 3). A complete list of available reports is provided in the EPRI Guide. (Reference 4). The paper will deal primarily with the work in the Water Quality Control and Heat Rejection Program.

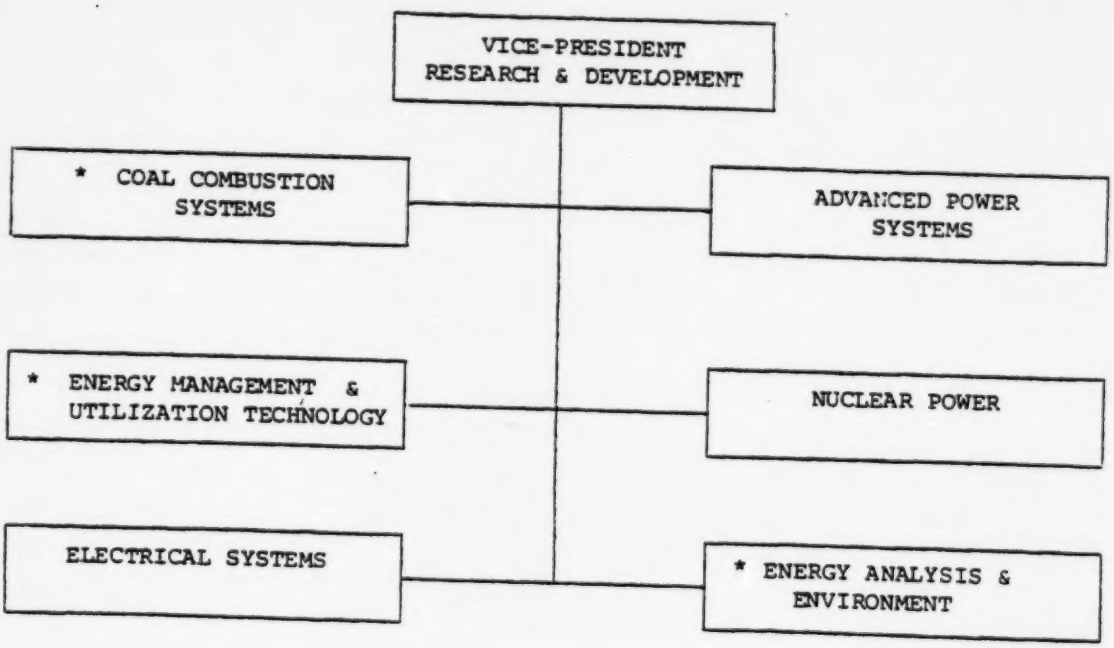

* Waste Heat Management and Utilization activities

FIGURE 1

EPRI DIVISION/PROGRAM	EMPHASIS	MAJOR PROJECT
Coal Combustion Systems/Water Quality Control & Heat Rejection	• Water conservation	• Advanced Dry Cooling
	• Environmental controls	• Cooling tower plumes/Intakes
	• Plant efficiency	• Cooling tower performance
Energy Management & Utilization/ Industrial Applications	• Reject heat utilization	• District heating
		• Industrial cogeneration
Energy Analysis & Environment/ Ecological Effects	• Environmental effects	• Cooling system effects

WASTE HEAT MANAGEMENT AND UTILIZATION RESEARCH AT EPRI

Table 1

3. RESEARCH IN THE WATER QUALITY CONTROL AND HEAT REJECTION PROGRAM

The relevant work in the Water Quality Control and Heat Rejection Program focuses on the management rather than the utilization of reject heat. The program has responsibility for the hardware and the processes, from the turbine flange to the discharge plume, required to accomplish the economical and efficient cooling of a steam-electric power plant.

3.1 Premises

The research plan is based on the following premises:

- power plant cooling sets a major siting constraint on power plants

  -Virtually all reject heat is transferred from the plant condenser to the environment by the evaporation or warming of the water.

  -The availability of large quantities of water for withdrawal, and sometimes for consumption, is an essential requirement of a plant site.

  -In many regions of the country, this is becoming the primary constraint on the location of a new plant.

- power plant cooling systems are an obvious subject of environmental concerns and objections:

  -While thermal discharge regulations are no longer a pacing environmental issue, the question of environmental damage as a result of intake losses has become so, leading to major delays and expense in siting.

  -Closed-cycle cooling systems, sometimes used for environmental reasons, can produce visible plumes, ground-level fogging and icing, and saline drift dispersion, which are difficult to predict or control.

- cooling system performance has a first-order effect on plant efficiency.

  -Towers with insufficient cooling capability can result both in reduced plant capacity on hot, humid summer days when utilities normally experience peak loads and in increased heat rate over the rest of the year.

3.2 Objectives

The objectives of the heat rejection research are:

- to reduce the cost and improve the efficiency of water-conserving cooling systems,

- to predict and mitigate the physical, environmental effects of power plant cooling,

- to improve the technical basis for the specification, selection, and testing of cooling equipment to ensure adequate performance at

acceptable cost.

3.3 Dry & Dry/Wet Cooling (References 5,6, & 7)

For cooling systems that conserve water, the most serious concern centers on the cost of such systems. Although technology is commercially available for dry cooling, a dry-cooling system is about four times as expensive in total cost as a corresponding conventional evaporative system. Emphasis in the EPRI program has been placed on reducing the cost of water-conserving cooling systems substantially, by about a factor of two. Such systems will provide the industry with the most economical alternative to evaporative cooling when water scarcity rules out or severely constrains the consumptive use of water for power plant cooling.

EPRI's main endeavor in this area is development of a demonstration facility for advanced wet-dry cooling technologies. Recently constructed at Pacific Gas and Electric Co.'s Kern Power Plant in Bakersfield, California, the EPRI facility uses air-cooled heat exchangers, with water for supplemental cooling. The facility also features a steam condenser with heat transfer enhancements to improve efficiency. The system, which uses ammonia as the transport fluid, offers potential annual savings to the industry of about $1 billion over commercially available wet-dry technology.

A three-year test program is planned. Operation and testing will be funded by DOE, EPRI and a consortium of U.S. and overseas utilities. Close cooperation is being maintained through an information exchange agreement with Electricite de France which is building a similar demonstration facility near Paris.

Progress on the analysis, design, and construction of this facility has been reported on at this Conference in the past, both in detailed technical papers and in this General Forum. Construction is now complete; shakedown is underway; and formal testing is scheduled to begin by mid-summer. We will summarize briefly what we expect to learn and to prove at Bakersfield.

The overall test objectives are:

- to demonstrate performance and operational feasibility
- to demonstrate operability under "normal" steady-state and transient conditions.
- to demonstrate the ability to handle non-standard operation, such as recovery from an accident or power loss.

Specifically, the demonstration will prove that ammonia, phase-change dry cooling is state-of-the-art. To this end, the design and construction was performed using an architect-engineering firm and component suppliers who build and sell commercial equipment. The materials and components were obtained from competitive sources. We expect to demonstrate that we were able to predict the system's performance over the range of expected operating conditions.

The economic results will not constitute a direct proof of our cost projections, since the facility will not benefit from economies of scale and will have only indirect tie-in to plant performance. However, the results should

(1) show that the performance curves used in the economic analyses are

correct, and

(2) be extrapolable to full-size systems since the modular sizes of the major components were chosen to permit this.

Operational feasibility will be demonstrated by showing that the system assumes a stable and predictable state during normal operations and that transitions from one state to another during normal transients (shut-up, shut-down, loss of load, and load following) are smooth and predictable. Non-standard conditions, such as fouling of air-cooled surfaces or loss of pump or fan power, will be imposed to demonstrate these events can be handled satisfactorily. Finally, the tests will provide familiarity with the idea and promote confidence in the technology.

Supportive Projects

In a companion project, a capacitive cooling system is being designed for possible inclusion in the test facility. The system, which consists of a water tank that functions as a thermal capacitor plus associated hardware, eliminates water consumption for cooling and operates in a zero discharge mode. Economics of the capacitive system are comparable to a wet/dry cooling system.

The comparative economics of various water-conserving cooling systems are being evaluated. In this study, the ammonia-based technology is being compared to both the direct and indirect (closed water loop) systems. Economic comparisons are being made among optimized cooling systems over a range of power plant sizes, fuel costs, and quantities of water consumption Results of the study should aid utilities in selecting the best type of water-conserving cooling system for their application.

In a related project, performance testing of a commercial wet-dry cooling tower has been completed at Southern California Edison Co.'s San Bernardino Station. A water saving of 20% was achieved during the testing, and a further saving should be possible under optimal operating conditions. This effort included the validation of a predictive model for wet-dry cooling -tower performance. The final report is available. (Reference 8).

Evaluating the costs of using dry or wet-dry cooling must include consideration of the costs of reduced capacity and efficiency at the plants on which they are installed. These costs are closely tied to utility expansion plans, load projections, and system economics. A technique was developed that accounts for these factors in the design methods and operating strategies for wet-dry cooling systems. This technique was demonstrated in a case study of a 1000 MW(e) coal-fired baseload station. The results indicated that using available cooling water in an optimal manner would save $650/MW annually. (Reference 9). An analysis was subsequently performed on cycling plants which represent about one-third of the plants now being designed (Reference 10). It was found that the effective value of cooling water may be more than 50% greater to a cycling plant than for a baseloaded plant. A user's manual for the computer simulation program is available (Reference 11).

3.4 Physical Effects of Plant Cooling

The responsiblity of the Water Quality Control and Heat Rejection Program is to identify the physical effects of power plant cooling systems

on the environment. It is the role of the Environmental Assessment Department to analyze and interpret these effects in light of their environmental or ecological consequences and determine to what extent mitigation is required. The two active areas are cooling tower plumes and intake screening.

Tower Plumes

The focus of the work to date has been the development of improved mathematical models for visible plumes and drift deposition for natural- and mechanical-draft cooling towers. The approach has been to use the most extensive data base available in order to ensure proper understanding and modeling of all major physical trends and to isolate specific elements of the models where improvements in the physics could substantially improve the overall predictions. (Reference 12)

In the prediction of visible plumes, a need for improvement was identified in three areas: proper representation of mixing coefficients; tower wake effects; and moisture thermodynamics.

Estimates of the mixing on dilution rates can be made both on the basis of plume trajectory (rate or bending) or visible plume length (rate of mixing with dry ambient air). Bending rates suggest higher mixing rates than plume lengths, and some alternative mechanisms were required to match both sets of observations. This is related to proper treatment of wake effects. Field data shows frequent downwash at high (>1.5) wind-speed to tower-exit-velocity ratios. Laboratory data suggest that this region is important in increasing dilution.

In the treatment of condensation, the assumption of instantaneous equilibrium gives excessive plume rise rates while suppression of condensation precludes proper modeling of long, high voluminous plumes.

Improvements in these areas have led to a model which appears to represent an improvement on previously available models. It was compared with five other models which were designed to handle both single and multiple tower plumes and were calibrated to all or part of the same data base.

The model performed best in the prediction of plume rise for single plumes (77% of the cases within a factor of x2) with its poorest performance being on short plumes. Plume lengths were predicted within a factor of x2 in 60% of the cases. While this performance is comparable with other good quality models, there was a significant reduction in the number of grossly incorrect predictions (in error by a factor of x5 or more). In the prediction of laboratory data, where ambient conditions are controllable and describable, the improved model was clearly superior.

An important factor for utility application is the ability to handle multiple merging plumes. The model was designed to satisfy two important observed characteristics of the data set: that plume rise is higher when the wind is parallel to a line of sources than when it is perpendicular; and that plumes begin round in cross section and merge into an elliptical stage, and then become round again. The model demonstrates the best predictive capability for multiple plumes.

A similar approach was taken to drift modeling. The elements of the model which required improved physical representation were droplet evaporation; dry particle formation; and droplet deposition. The data base in the

drift area is far less extensive and reliable than that in the visible plume area, and hence less effective in guiding or validating model improvement. The bulk of the comparisons were with data from the Chalk Point Cooling Tower Project and from a drift deposition study at Pacific Gas and Electric's Pittsburg Plant. When a successful prediction is defined as one in which the predicted deposition rate is within a factor of x3 of the measured data, the Chalk Point measurements (single natural draft cooling tower) were predicted successfully in 24 out of 26 sample comparison, while the Pittsburg data (two 13-cell mechanical draft towers) were successfully predicted for 50% of the samplers on four out of five days.

Follow-on efforts involve the development of methods to generate statistically reliable predictions of weather and tower operating conditions on the basis of data typically available to siting engineers. The objective of this effort is a flexible, reliable tool for use in environmental impact and plant siting studies. Workshops in the fall of 1981 and 1982 are being planned to disseminate this code to the industry.

This analytical work is complemented by related laboratory studies. At the Massachusetts Institute of Technology, a wind tunnel has been constructed to evaluate various methods of plume droplet drift measurement against a calibrated reference method that is being developed; the evaluation program is scheduled for 1981. In work recently completed at the University of Iowa's Institute of Hydraulic Research, laboratory tests were performed on hydraulic scale models of mechanical-draft cooling towers to determine plume recirculation and interference effects between towers. The results of these water flume experiments are reported in Reference 13 and Reference 14. This testing technique represents a useful and relatively inexpensive tool for tower siting studies by utilities. Such a physical modeling effort was recently performed for the Tennessee Valley Authority by the Institute of Hydraulic Research.

Intake Screening

Several projects are under way that focus on the entrainment and entrapment of aquatic species in once-through cooling systems and on changes in intake design to alleviate these problems. A porous dike intake structure at the Brayton Point Station of the New England Electric System is being tested by New England Power Service Co. and Marine Research, Inc. Results to date indicate that no serious clogging or fouling problems have occurred. The second year of laboratory work and field tests is in progress. In a related effort at Oak Ridge National Laboratory, a series of entrainment mortality studies is being conducted using a condenser simulator; this work will continue in 1981.

As part of a project on screening systems for power plant intakes, a clearing-house is being organized for the collection, analysis, and dissemination of biological data, information on operating experience and problems, and engineering and cost data.

3.5 Cooling System Performance

Work on the performance of conventional power plant cooling systems has emphasized the ability to specify, site, predict the performance of, and test cooling towers. The projects range from the development of computer programs for physical modeling of interference and recirculation, to

the demonstration of field testing procedures.

Performance models of cross-flow and counterflow natural-draft towers have been developed and validated (Reference 15). The computer code is currently being used by utilities in cooling-tower performance studies. Work to extend the code to mechanical-draft cooling towers is in progress. Model validation, through comparison to existing tower test performance data, is being performed as part of this effort. A workshop in the fall of 1981 is being planned to disseminate this code to the industry.

Plans are presently being developed for a cooling tower test facility. The test facility will be used as a tool for developing improved methods of predicting the thermal performance characteristics of cooling towers, especially in terms of bid evaluation and retrofit studies. The present work will identify interested utilities, possible test sites, and instrumentation and structural requirements. Through application of the performance prediction code, this project will enable many analytical studies to be performed (off-design performance, effect of air and water maldistributions, etc.).

The Ralph Parsons Laboratory at MIT is continuing an effort to improve the ability to predict cooling-pond performance and evaporative loss. After a review of available test data and evaporative loss formulations, a workshop was held in September 1980 to identify promising field measurement techniques. This project includes a scoping study for a field test program. In preparation for that test program, a limited series of field tests is scheduled for the spring of 1981, to screen and evaluate various advanced techniques of evaporation measurement.

REFERENCES

1. 1981-1985 Research and Development Plan: Overview and Strategy, EPRI Planning Staff, P-1710-SR, October, 1980.

2. 1981-1985 Research and Development Plan: Program Descriptions, P-1726-SR, January, 1981.

3. 1981 Research and Development Plan: P-1727-SR, January, 1981.

4. EPRI GUIDE: A Directory of Technical Reports, Spring, 1981.

5. "Advanced Concept of Dry/Wet Cooling for Power Plants", EPRI Report No. CS-1668, February 1981.

6 "Power Plant Waste Heat Rejection Using Dry Cooling Towers", CS-1324-SY, February 1980.

7. "ACT Facility Measurement and Test Plan", CS-1530, September 1980.

8. "Test Report: Wet/Dry Cooling Tower Test Module", CS-1565, October 1980.

9. "Optimization-Simulation Methodology for Wet/Dry Cooling", FP-1096, May 1979.

10. "Wet/Dry Cooling for Cycling Steam-Electric Plants", CS-1474, August 1980.

11. "User's Manual for WDSCSIM II Wet/Dry Cooling Computer Program", CS-1594, October 1980.

12. "Studies on Mathematical Models for Characterizing Plume and Drift Behavior From Cooling Towers", CS-1683 Volumes 1-5 plus Executive Summary, January 1981.

13. "Development and Verification of Laboratory Model Techniques for Prediction of Near-Field Behavior of Cooling Tower Plumes", CS-1370, March 1980.

14. "An Analytical and Experimental Study of Multiple Plumes", CS-1547, September 1980.

15. "Validation of Cooling Tower Analyzer (VERA) Volume 1", FP-1279, December 1979.

PB82-227927

ALTERNATIVES FOR WASTE HEAT UTILIZATION IN THE PETROLEUM INDUSTRY

Edward H. Mergens
Shell Oil Company
Houston, Texas

ABSTRACT

The challenge of the energy management job in petroleum refining and petrochemical companies is to make the term "waste heat" obsolete in the jargon of the industry. The thesis is: heat which is no longer any potential use to anyone, can no longer be called a waste.

The potential use of low level heat is often limited by the extent to which equipment and costs allow a practical solution. Process innovation is continually expanding the horizons of practicality in a physical sense, and fossil fuel scarcity is broadened practicality in an economic sense.

Only a few percent of the energy used during the processing of petroleum remains in the products of that operation. Almost all of the energy, in the form of heat, is rejected to the environment at varying temperature levels.

For the petroleum refiner or petrochemical operator there is a limited capability to absorb low level heat within the confines of the plant operation. The potential for additional low level heat recovery exists outside the plant, but the petrochemical and refinery operator must convert the heat into a usable energy source for these other needs.

Today's petroleum processors can do a better job of minimizing the temperature level at which heat is rejected by better utilizing the heat sinks created by their operating needs. The potential of waste heat utilization is even greater if the energy needs outside the process area are met through low level heat conversion.

The opportunities for eliminating waste heat from the petrochemical and refining process are discussed. Practical examples and limitations experienced in the petroleum industry are presented. The extension of technical applications in order to provide energy needs beyond the petroleum process requirements are discussed and some estimates of the impact of government programs and economic policy are made.

1. INTRODUCTION

The petroleum industry has long practiced the art of reusing the BTU of energy within the process. The heat which was finally rejected by the refiner or petrochemical operator wasn't really considered a waste since there wasn't any further practical use for it. Producing "waste heat" wasn't part of the

processor's perception. It was only the inevitable decay of energy resulting from an increase in entropy, which at some point, must be accepted.

Over the past few years, the perception of that point has been changed. Recovery of energy at lower and lower temperature levels is now practical, economically and technically. Our perceived view of the future, shown in Figure 1, indicates that the value energy, relative to the cost of equipment to recover it, will continue to rise. Thus, the incentive to apply more sophisticated methods of energy recovery will be there. And, the perception of what is and what is not a waste will continue to change with time.

2. PETROLEUM INDUSTRY ENERGY CONSUMPTION

For today's discussion, I'd like to profile the energy consumption pattern in petroleum refining to illustrate where low level heat rejection occurs, and outline the options the petroleum processor has to utilize that low level heat. The refiner requires the energy from one out of every ten barrels processed in order to operate. The process temperatures required usually are 1,000°F to 400°F with rejected heat predominately available below 400°F.

In a study sponsored by the Department of Energy, Gulf Oil Company provided a profile of energy consumption and its rejection for their Alliance, Louisiana refinery [1]. The 200 MB/D refinery is fairly typical of industry which in 1979 reported a consumption of 550,000 BTU's for each barrel processed [2]. The end use of that energy is illustrated in Figure 2. Approximately two-thirds of the fuel is used in heating petroleum, and one-third for boilers producing steam. Less than ten percent of the total energy used is in the form of electricity.

In the process there are several low level heat sinks which can be used before heat is rejected to the atmosphere. A small amount of heat can be taken up in petroleum products. The water used to make steam, and the air used for combustion of fuel can be preheated. Of course, each of these heat sinks are used to some extent today, but more heat is still rejected to air coolers, cooling water towers and through furnace flue ducts. Figure 3 shows the amount of heat rejection found in the study made by Gulf Oil (op sit). Heat, equivalent to 110,000 BTU/Barrel, is rejected at levels of 200°F and higher in water and air coolers. Flue gas heat rejected above 200°F is equivalent to about 50,000 BTU/Barrel.

3. LOW LEVEL HEAT RECOVERY

Using the readily available heat sinks has been the energy managers' first priority. The following are some examples of techniques now being used. Of course each application has technical or economic limits of practicality which will be discussed.

Heat Pumps for use in supplying for low level distilling column energy are used in configurations such as illustrated in Figure 4. Practical limitations to the use of the technology include the size of equipment, and molecular weight range of the distilled components. In order to be economical, the heat load needs to be fairly large (i.e. 50 to 100 million BTU/HR) to justify the equipment. Secondly, the column temperature differential must be small (i.e. 2 to 10°F) to use the thermodynamic principle. Considering the typical refinery operating configurations, we estimate the potential to replace low pressure steam demand by this means, equivalent to 5,000 BTU/Barrel.

Combustion Air Preheaters have been the norm for most boiler applications for a long time. Preheaters are now being applied to process fluid heaters (See Figure 5 for a typical case). The economics have been helped marginally by the ten percent additional investment tax credit allowed now [3]. Heater size has to be large enough to justify the equipment (cu. 40 to 50 million BTU/HR or larger) and in some cases furnace configuration or space may prove a barrier to installation. Environmental constraints may also limit application. Because of higher flame temperatures, slightly more nitrogen oxide is emitted and in some areas of the country this can be a constraint. In addition, recovery of heat below ca. 300°F is impractical since corrosive combustion products are condensed in the flue gas. Despite limitations, considerable recovery potential exists and we estimate 40,000 BTU/Barrel may be possible.

Boiler Feed Water Preheating can be another use of low level heat. A typical refinery may generate 220 lbs. of steam per barrel of petroleum processed. About one-third is generated from waste process heat and the remainder in direct fired boilers. In Figure 6 an example of low level process heat for BFW heating is shown. The exchanger investment is helped marginally by a 10% additional investment tax credit now allowed [op sit]. Practical limitations may be the proximity of equipment to the boiler house and the process complications of linking various units together in this manner. Although a good heat sink, the potential is not too large. If we assume a fifty percent condensate return to the boiler house (i.e. fifty percent makeup water required), about 10 to 12,000 BTU/Barrel could be used for makeup water heating. Typical feed water deaerators using waste steam then produce feed water at 250°F. An additional 4 to 5,000 BTU/Barrel might further be added to boiler feed water from low level heat sources to raise the temperature to 275°F.

Product heat retention normally represents only a few percent of the total heat consumption in petroleum processing. Low level heat utilization in this area provides limited opportunity. Even assuming the average product temperature could be increased 25°F, the heat sink represents only 3 to 4,000 BTU/Barrel processed for the refinery.

4. ALTERNATIVE LOW LEVEL HEAT RECOVERY

We have discussed energy recovery within the confines of the petroleum process area and these are summarized in Figure 7.

A potential of about 60,000 BTU/Barrel out of 160,000 BTU/Barrel of heat over 200°F could be used onsite. Potentials for use offsite are possible using heat for district heating/cooling or through electrical generation using low temperature level organic Rankine cycle units.

District Heating is conceptually practical and Shell Oil has reported such an operation at its Gothenburg refinery in Sweden [4]. The project had potential energy recovery equivalent to 70,000 BTU/Barrel--a significant savings. The application in this instance was aided by several favorable circumstances. The housing complex already had an operating central heating water system. The refinery supplied only a portion of the heat load, and both systems had installed alternative heat/cooling equipment. The housing was relatively close to the refinery. In spite of the favorable circumstances, a government subsidy was necessary in order to make the project economically viable for all parties.

Organic Rankine Cycle heat recovery has a potentially good application to use low level heat from petroleum processing. ORC units converting heat to electricity are currently available in small sizes (ca. 1 megawatt) at an

installed cost around $2,000 per kilowatt. Electricity generation obviates some of the drawbacks associated with district heating (i.e. specialized application and proximity). In addition, special recognition of this cogeneration technique have been afforded in the Energy Tax Act [op sit], as amended, and the Public Utilities Regulatory Policy Act [5]. In some sections of the country these units already show a reasonable economic return. For example: 1000 KW x 8000 hrs/yr x 5.0¢/KWH = $400,000/yr or a five year simple pay back on $2 million.

The prototype units appear to be relatively simple to operate, yet they have some drawbacks.

Most heat recovery opportunities appear to be in services where air cooling is currently used by the refinery. ORC units currently available require cooling water, and the cost of supplying cooling water can often negate most of the potential savings.

Development work is proceeding however, on new turbine technology, air-cooled units, and newer Rankine cycle working fluids and these are being tested by several manufacturers. Application of these ORC machines across the processing industry can be expected in the future.

5. PUBLIC POLICY

From the foregoing discussions it is apparent that low level heat recovery has certain limitations--either practical technology or economics. I have complete faith in the ability of our engineering technology to make the laws of nature work for us. A reaffirmation of that belief was witnessed a few hundred miles north of this spot by the space shuttle project. I wish I had similar conviction in the social lawmaking arena. We have an excellent system of market forces which inevitably leads to a rational use of resources. However, we have overlaid it with some conflicting and confusing social forces. We cannot undo thirty years of tinkering overnight, but we must react to the realism of today's energy situation.

Fuel costs must be restored to reflect true replacement values. The user must see the real cost in order to adjust consumption patterns. An accelerated decontrol of natural gas prices is required. While recognizing the short term pricing inequities we should seek to stimulate recapitalization of our manufacturing facilities through accelerated depreciation and investment incentives. Finally, we need to revisit some of the environmental decisions made in a climate of trying to make a poor situation perfect, we need to determine whether reasonable cost/benefit results are being obtained.

6. CONCLUSIONS (Figure 8).

a. There are reasonable uses for heat currently rejected from petroleum processing operations. Approximately two-thirds of the identified sources will probably be used in applications outside of the process plant fuel use area.

b. Technology limits will not present a major obstacle to waste heat utilization. Many technologies are already being applied or are ready to be applied.

c. Clear economic signals and incentives are needed to prompt accelerated utilization of low level heat sources and more efficient equipment installa-

tion.

d. Government should review past policies in light of present day world energy position.

REFERENCES

[1] R. W. Maier et al, Refinery Energy Profile - Final Report ORO 5262-S, NTIS, January 1979.

[2] American Petroleum Institute - Report to Department of Energy - Office of Industrial Programs - Form CS-189S, June 1980.

[3] The Energy Tax Act of 1978, PL 95-618 Title III, Section 301. As amended by Title II, Section 221, Windfall Profits Tax Act 1979.

[4] Shell World, September/October 1979, No. 7, vol. 4, Shell International Petroleum Company, Shell Centre, London SE1 7NA.

[5] The Public Utilities Regulatory Policy Act of 1978, PL 95-617 Title II, Section 210.

[6] M. Sittig, Practical Techniques for Saving Energy in the Chemical, Petroleum and Industries - 1st edition. Noyes Data Corporation, New Jersey, 1977.

Figure 1
Mergens

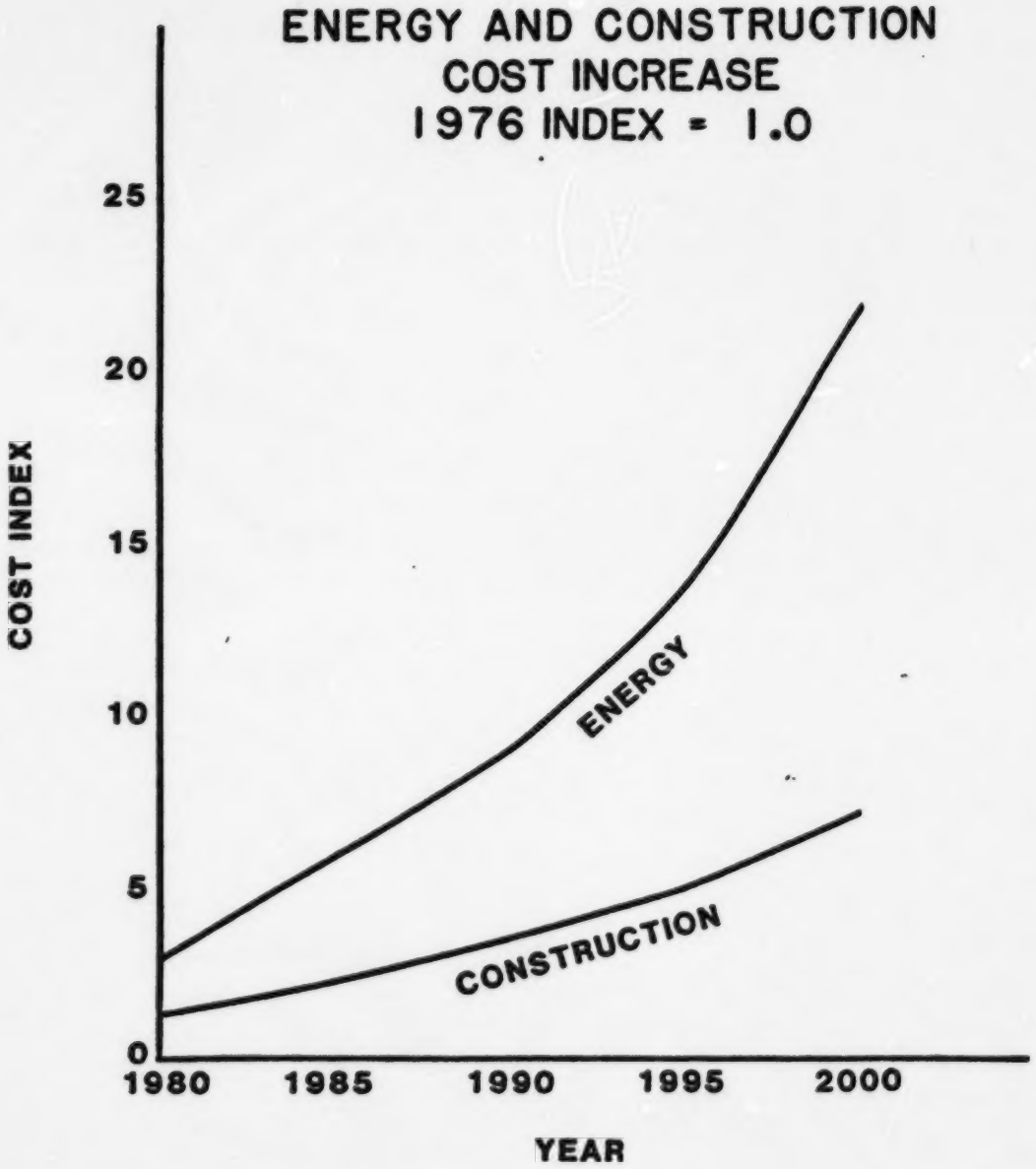

Figure 2
Mergens

PETROLEUM INDUSTRY ENERGY CONSUMPTION

	MBTU/BBL INTAKE
AVERAGE 1972	650
AVERAGE 1979	550
USE BY TYPE 1979	
PROCESS FLUID HEATERS	360
STEAM BOILERS	150
ELECTRICITY	40

Figure 4
Mergens

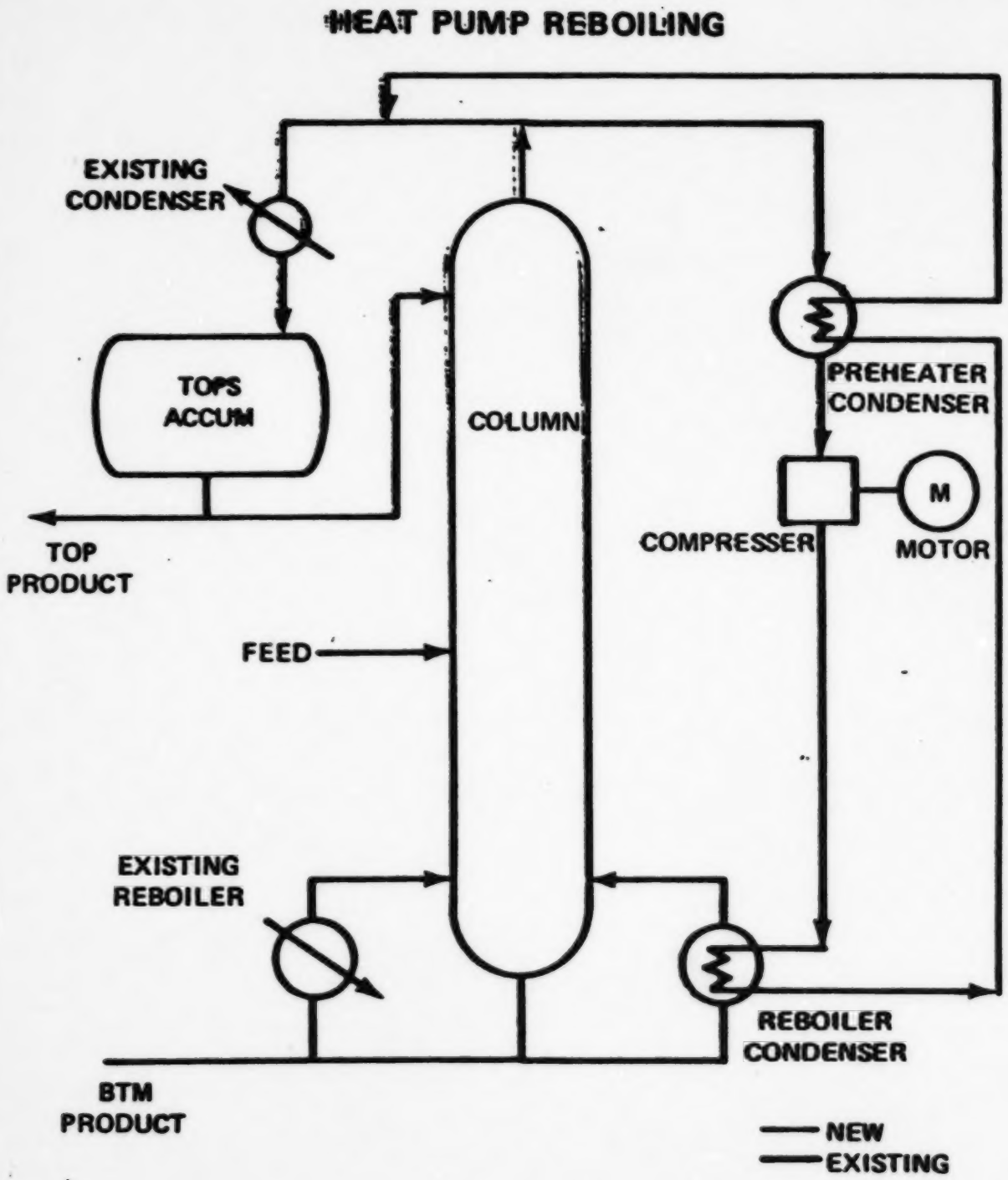

COMBUSTION AIR PRE-HEAT

Figure 5
Mergens

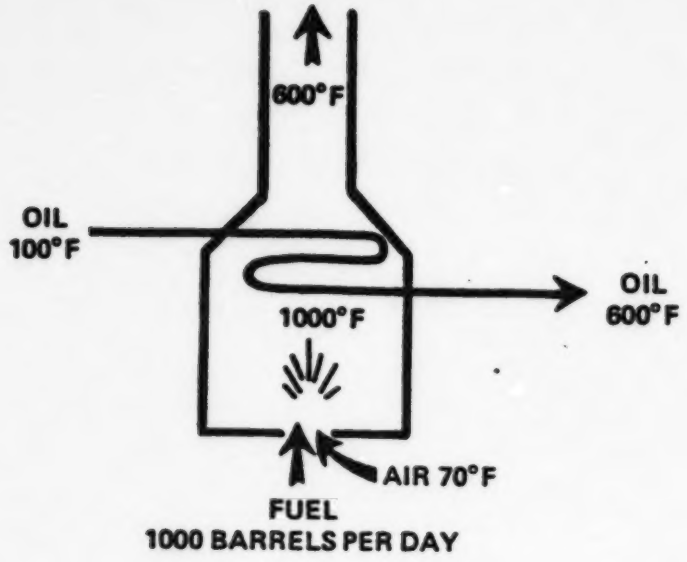

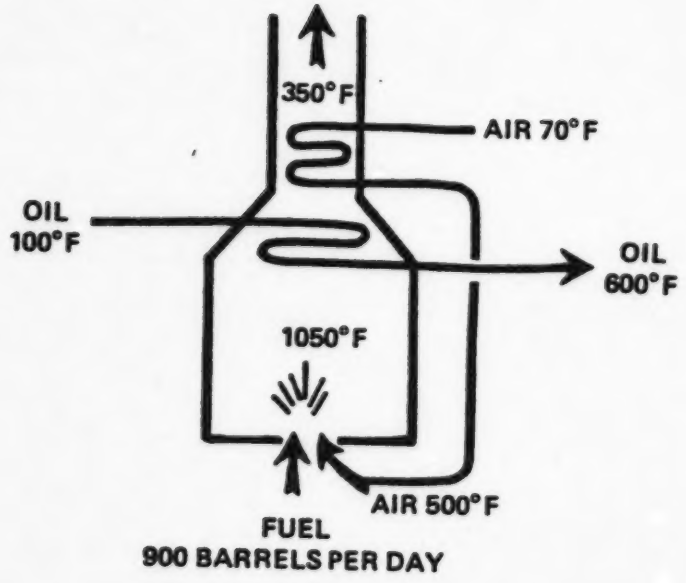

Figure 6
Mergens

HEAT TRANSFER LOOP
EXAMPLE OF MULTIPLE UNIT HEAT INTEGRATION

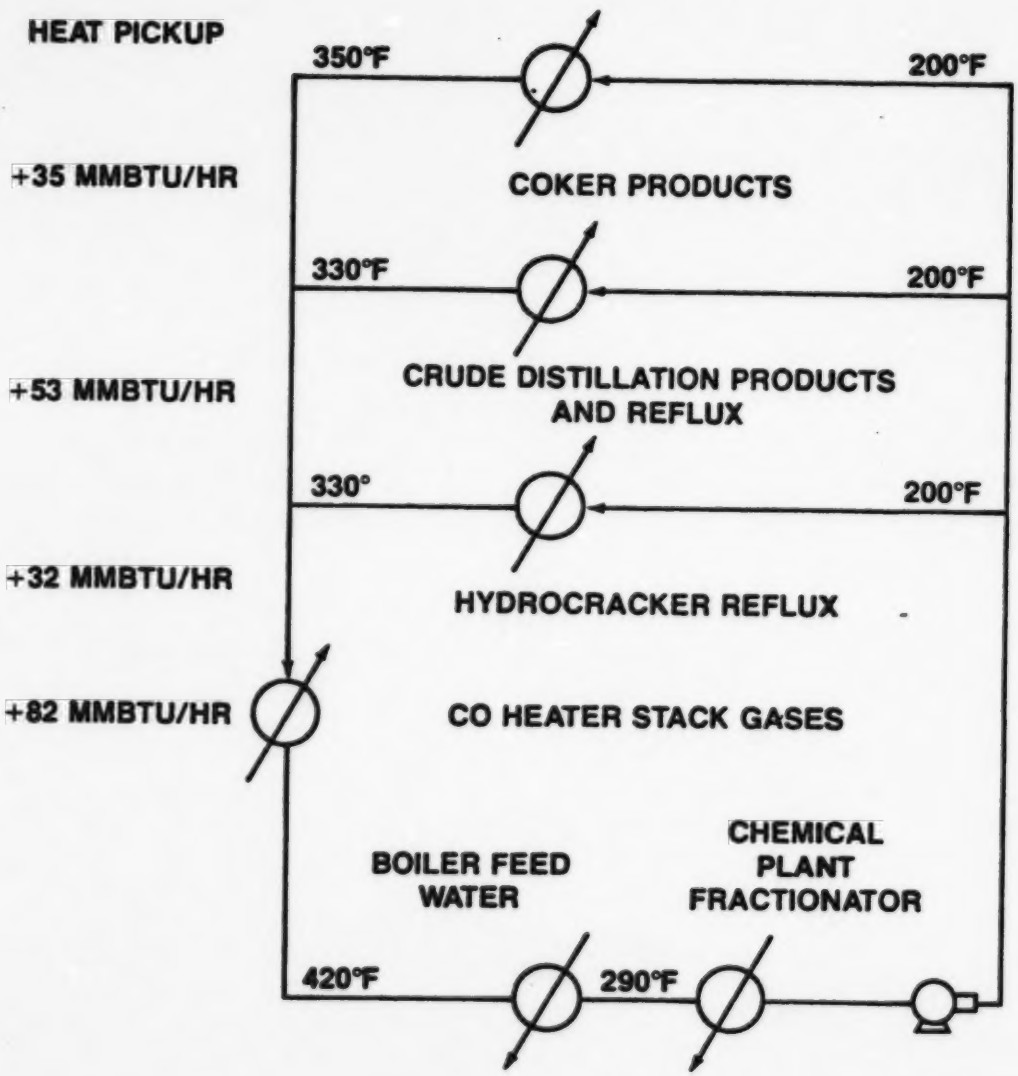

Figure 3
Mergens

PETROLEUM REFINING
LOW LEVEL HEAT REJECTION PROFILE

AIR & WATER COOLERS

TEMP RANGE °F	MBTU/BBL
200-250	57
250-300	29
300-320	6
320-400	9
400-430	9
TOTAL	110

FLUE GAS - COMBUSTION PROCESSES

TEMP RANGE °F	MBTU/BBL
200-350	18
350-450	13
450-550	9
550-750	3
750+	8
TOTAL	51

Figure 7
Mergens

HEAT SINKS FOR LOW LEVEL HEAT

WITHIN THE PROCESS AREA	BTU/BBL
- LOW TEMPETURE DISTILLATION	5,000
- PRODUCTS	3,000
- COMBUSTION AIR	40,000
- BOILER FEEDWATER	13,000
TOTAL	61,000

OUTSIDE THE REFINERY

- DISTRICT HEATING
- ORGANIC RANKINE CYCLE

Figure 8
Mergens

CONCLUSIONS

1. LOW LEVEL HEAT CAN BE USED.

2. TECHNOLOGY IS NOT LIMITING.

3. REPLACEMENT COST ENERGY PRICING.

4. GOVERNMENT POLICIES NEED REVAMPING.

SESSION III-A

UTILIZATION I

Preceding page blank

PB82-227935

USING INDUSTRIAL REJECT HEAT FOR DISTRICT HEATING, A CASE STUDY, BELLINGHAM, WASHINGTON (UTILIZATION I)

Dr. Mitchell Olszewski
Oak Ridge National Laboratory
Post Office Box X, Bldg. 4500N
Oak Ridge, Tennessee 37830

Mr. Lincoln B. Katter
Rocket Research Company
York Center
Redmond, Washington 98052

ABSTRACT

A project in northwestern Washington state is investigating using low-grade waste heat as a source for a district heating system. Current efforts are focused upon testing at the two ends of the system: the source and the user. The following paragraphs present a review of the project approach, the plan and early results of the current phase of effort with emphasis on the energy recovery equipment.

1. PROJECT APPROACH

Since 1977, a project has been underway to develop a district heating system for the City of Bellingham, Washington. Research sponsored by the Division of Thermal & Mechanical Energy Storage Systems, U.S. Department of Energy, Union Carbide Corporation-Nuclear Division administers the project. Lead investigation work for the project to date has been conducted by Rocket Research Company (RRC), a division of ROCKCOR, Inc. Support is being provided at no cost to the government by Intalco Aluminum Corporation of Ferndale, Washington, and by the City of Bellingham. Costs of Intalco and city activities are provided as cost sharing to the project by each organization.

Figure 1 displays the relationship of the four phases of the project.

1.1 Phase I

The project began with a survey of the primary aluminum industry within the United States, directed at identifying applications for energy storage technology.

During this effort the waste energy borne by the gaseous pollution control system was identified as the most likely recoverable energy source, but of relatively low grade (100 to 180°C). Space heating and domestic hot water production were identified as the most cost effective uses to which the energy could be applied. The Bellingham-Intalco site was chosen as an example. A preliminary design was made to estimate the effects of energy storage coupling the constant source to the variable demand. The result of this effort was a prediction of 31,800m^3 (200,000 barrels) of oil saved annually from the example site alone and over 800,000m^3 (5 million barrels) if the concept were applied to the entire aluminum industry. The technology could be applied to low-grade

Preceding page blank

Project Phasing Diagram

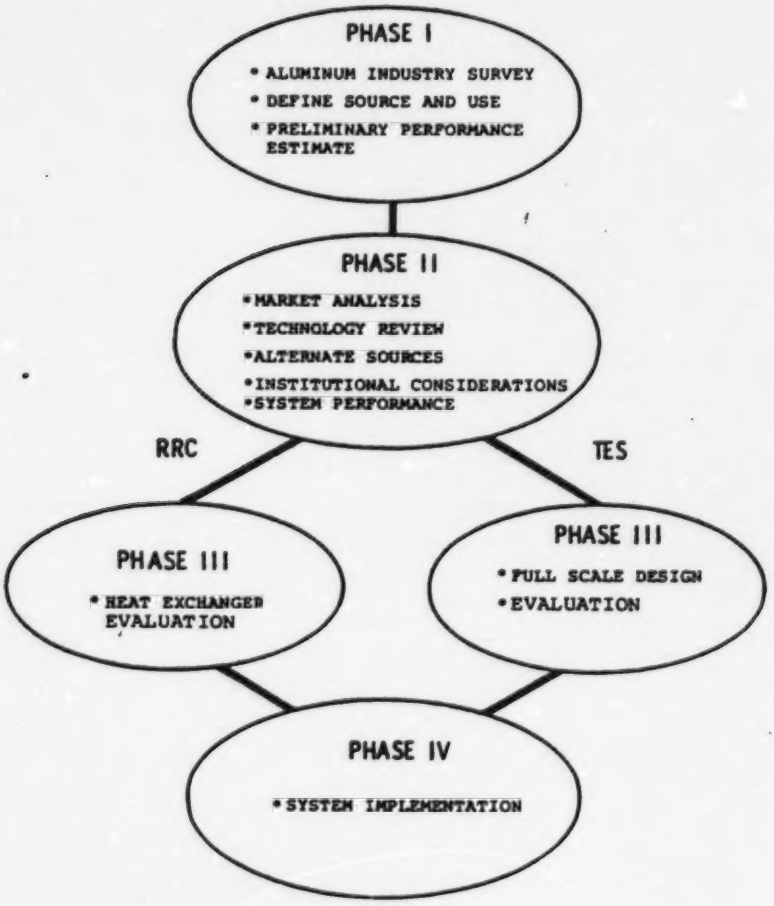

Figure 1

waste energy from any industry. It is estimated that 160 million m^3 (one billion barrels) of oil per year could be saved from application of this technology to all low-grade industrial waste heat.

1.2 Phase II

Based upon the favorable results of Phase I, Phase II was initiated to improve the accuracy of system performance predictions. Limitations of scope in Phase I did not allow in-depth analytical treatment in four key areas 1) demographics of the market area, 2) equipment technology and supply, 3) energy sources and 4) institutional, legal and environmental considerations Phase II of the project accommodated greater levels of complexity and volumes of data to improve accuracy of system performance forecasts and institutional characterization to establish greater levels of confidence in project feasibility and cost effectiveness prior to major commitments of funds. Each of the areas of investigation above became a separate task in Phase II; a fifth task provided an overall system cost analysis.

Resulting from the market area analysis, a near optimum service area has been identified in the City of Bellingham as shown in Figure 2. Market penetration analysis predicts a subscription rate of 85 percent for small residential (less than five units) and 92 percent for larger structures, for an overall average of 90 percent penetration. At that rate there will be 2727 small residential subscribers, 555 commercial/industrial subscribers, 107 large residential (multiple) subscribers and 86 institutional consumers. The design peak energy demand is 93.4 MW, calculated at an ambient temperature of -18°C (0°F).

Under task two, the analysis of the overall system was divided into five subsystems; 1) energy recovery, 2) transmission, 3) control/storage/peaking center, 4) distribution and 5) user conversion subsystems. Schematics were prepared for each subsystem from which materials and parts lists were created. A search was made of the domestic industrial equipment market for each required item. Cost estimates and delivery times were solicited from at least two suppliers of each major item, as well as evidence of reliable performance under similar use to that proposed for this project. Table 1 displays the overall compilation of hardware costs (in $ 1980).

TOTAL SYSTEM COST BY SUBSYSTEM

	$ 1980	%
1 Heat Recovery	5,596,000	9.23
2 Heat Transmission	9,348,000	15.42
3 Peaking Boiler, Storage and Control Center	4,006,000	6.60
4 Distribution Network	26,282,000	43.36
5 Consumer Equipment	15,381,000	25.38
Total	60,613,000	

All major items were found available in the domestic market, although in some cases foreign suppliers were significantly less expensive. No unusually long delivery times were found. Many instances of long service with minimum

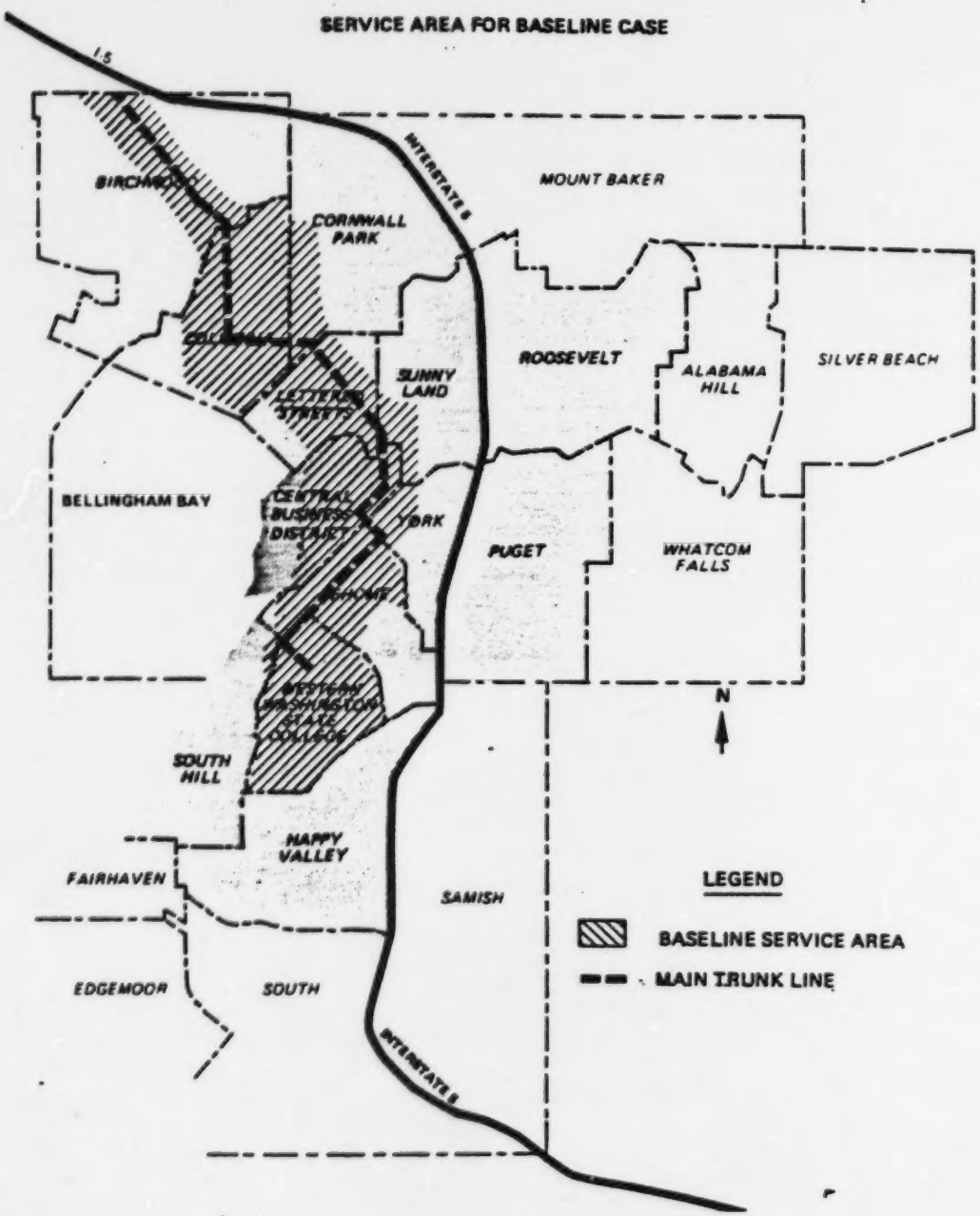
SERVICE AREA FOR BASELINE CASE
I-5
INTERSTATE 5
MOUNT BAKER
CORNWALL PARK
ROOSEVELT
ALABAMA HILL
SILVER BEACH
SUNNY LAND
LETTERMAN STREET
BELLINGHAM BAY
CENTRAL BUSINESS DISTRICT
YORK
PUGET
WHATCOM FALLS
WESTERN WASHINGTON STATE COLLEGE
SOUTH HILL
HAPPY VALLEY
FAIRHAVEN
SAMISH
EDGEMOOR
SOUTH
N
LEGEND
BASELINE SERVICE AREA
MAIN TRUNK LINE

Figure 2

maintenance under similar service conditions were cited by the various suppliers, hence no particular element could be isolated as a "weak link" in the reliability chain.

Alternate energy storage technologies were evaluated as another subtask. Above ground insulated steel tanks were the most cost effective near term storage means. A two tank system, one for hot supply water and one for warm return water, is preferred as a first module. Total energy storage is 200 megawatt hours (thermal). The storage volume for each tank is 3407 cubic meters (900,000 gallons) as optimized for the defined service area. A viable storage technology for future system expansion is found from consideration of an abandoned coal mine lying beneath the northern city limits. Whereas the mine itself is too large to be coupled efficiently to any conceivable district heating system, a portion of the mine could be isolated and provide a storage volume some 100 times the proposed tankage. This option can be exercised in the future, if the district heating system experiences strong growth. The possibility of energy storage using the heat well concept was investigated but appears unlikely. An extensive search of the available geological data in the region failed to locate a suitable aquifer. Neither unconsolidated nor consolidated deposits bear strong promise of a suitably thick, suitably porous stratum. Two exploratory borings through unconsolidated deposits accomplished on a separate companion project, did not identify a suitable aquifer. Consolidated deposits show numerous sandstone layers, however these are generally of very low porosity. The conclusions drawn from the storage technology review is that the project can benefit from surface tank-type storage during the construction and early operating years. An expansion to approximately 150 percent of proposed system size is possible in future years, through the transition to seasonal energy storage, should city growth patterns result in increased thermal demand density in the areas near-by the defined service area. Cavern type storage technology using the coal mine will be preferred over aquifer storage technology in that event.

Another area of technological investigation concerns the effect upon aluminum plant operations from the installation and operation of the heat exchangers with which energy will be transferred from the pollution control fume stream to the heat transport medium (water). Several possible locations for these heat exchangers were evaluated. The best site for these heat exchangers from most consideration (operating safety, installation safety, operating simplicity, installation simplicity) is just upstream of the pollution control dry scrubbers. In this location the potential interference with the primary plant processes is minimal. This location, however, does appear to produce the most stubborn deposits on cooled surfaces (heat exchanger fouling). Investigation into the potential for fouling and corrosion of heat transfer surfaces accordingly forms a large portion of the current effort described later in this report.

A search of chemical literature was made to predict the effect of lowering the temperature of the dry scrubbing process upon the scavenging efficiency. The result of this investigation is that it is unlikely that the dry scrubbing process will be impaired. A project groundrule is that NO impairment in this efficiency can be tolerated. Hence, the ongoing experimental phase will measure this effect.

Under task three, nine industries in the local area were investigated concerning their suitability for incorporation as additional energy sources for the district heating system. Each industry was assessed regarding the magnitude and temperature of waste energy, the time phase of this energy availability and the potential for future growth which would significantly change the

temperature, magnitude or time available. These data were then compared to the needs of the district heating system for topping power (peak mode operation), backup power (failure mode operation) and baseload power (future growth). One of these sources (the city municipal solid waste plant incinerator) shows promise as a peaking plant. A detailed analysis of this source is not possible at this time, as the city plans to move the operation, with a site and new design as yet undefined. The municipal solid waste, however, remains a viable additional energy source for all applications and the city is being urged to consider energy recovery as they plan for future solid waste incineration. None of the plants studied was sufficient to serve as a backup heat source for the system. The expense of incorporating enough plants to serve as a backup function is unjustified compared to the small expenditure for natural gas backup boilers and the low quantity of natural gas required. As an additional baseload source for future growth, the pulp and paper mill operated by Georgia Pacific Co. in downtown Bellingham shows promise. Their current operation, however, only allows them to commit to supply energy on an interruptable basis.

Resulting from the institutional issue investigation of task four, a municipal utility is identified as the most likely owning/operating entity. The City has existing water and sewer utilities with billing structures, meter reading and maintenance functions established. Tax exempt financing is possible for such a utility. Both the political leadership and their constituents have demonstrated an active interest disposed towards the district heating system. The City of Bellingham and Intalco have executed a Memorandum of Understanding with the Department of Energy detailing their support, participation, willingness to cost share and payback provisions. The City has retained bond counsel and executed an agreement with national and regional investment banking firms to assist with developing a financing plan beginning with this early stage of the project. Bellingham has established and staffed a district heating office. A community Advisory Group with diverse members of the community has been meeting for the last 18 months and continues to provide direction and linkage with major sectors of the public.

A combination of general obligation, revenue and local improvement district bonds is the most promising mechanism for financing the system. Because of the limits on allowable indebtedness and impact on other capital projects of general obligation bonds, revenue bonds are necessary for a major share of funding. Long-term contracts between the system and energy suppliers and the system and energy consumers are essential to secure the lowest possible interest rate on this debt. Local improvement districts can assist in financing transmission lines and hookups.

The net impact on environments involved in the district heating system as a whole is significantly positive, in large part because the district heating system would displace a variety of small heating systems which contribute incrementally to air pollution. Negative impacts are limited to disruptions during system construction. Some concern has been expressed about transmission line water crossing; these concerns can be met with appropriate emergency hardware. Longer range concerns the future concentration of development along the district heating system transmission line, as it sometimes does along highways and sewer lines, can be addressed by city and county planners through zoning ordinances.

During the fifth task the results of the previous tasks were incorporated into the technical and economic system performance predictions. The sensitivity of system economic performance was predicted over ranges of key economic variables.

The system annual energy sales are predicted at 225 GW hr_t/yr. Fuel use in the area is 46 percent natural gas, 29 percent electricity and 25 percent fuel oil. It is therefore predicted that 143,000m^3 (5.05 million therms), 65.26 million Kw hr_e electric energy and 7900m^3 (2.06 million gallons) of fuel oil will be displaced in the market area. The system will consume 10,000m^3 (0.36 million therms) of natural gas in its boilers for peaking energy supply, hence the net natural gas displacement is predicted at 133,000m^3 (4.7 million therms). Electric power is consumed by the system mainly to operate fans at the energy source and pumps for water transmission. The aggregate of all predicted parasitic power requirements is 22.25 million Kw hr/yr. Thus, the system will displace a net of 43 million Kw hr_e per year from the grid. The system does not require fuel oil in the normal operating mode, hence the requirement to supply 7900m^3 (2.06 million gallons) will be removed from the supply system. Assuming that electric energy is displaced from oil-fired thermal plants of 34 percent overall efficiency and natural gas displaced will be used directly in place of oil, system implementation displaces 31,800m^3 (200,000 barrels) of oil annually.

The system was analyzed in an economic environment derived from extrapolation of current inflationary trends (since the oil embargo of 1973) through the next decade, with subsequent decreases in inflation, to the end of the system life in the year 2015. Escalation in the real value of energy was found to be the most influential variable. A span for analysis was chosen constant with the world oil price prediction results of Ref. 1.

Baseline system economic performance is that for the first year of full system operation (1990), the system is just competitive with other energy forms. Thereafter, throughout the system lifetime, the cost of supplying heat from the district heating system remains nearly constant, while inflation and escalation in the real cost of energy both increase the cost of competitive energy forms. Economic performance comparisons via traditional parameters (NPV, IRR) suffer two difficulties. The first is that these are designed from the private capital point of view rather than the non-profit stance of the public utility. The second is that they are defined upon data from the full 25 year system life and, therefore, are as strongly dependent upon inflation and escalation assumptions late in system life as in early system life. Emphasis has been placed upon noting the time in the system life when income rises to meet expenses, NPV and IRR are calculated for comparison purposes only. Figure 3 presents the effect of energy charge on system revenue during the construction phase and over the first decade of full system operation. It can be seen that the non-profit utility must charge the full value of its service (no cost edge over competing forms) during the first year of system operation. Thereafter, a price edge of 10 percent per year favors the district heating subscriber.

1.3 Phase III

At the present time, the project is entering Phase III (Ref. Figure 1), which is the last phase in which DOE funding is planned. Phase IV is the full system implementation which will be financed locally and which includes planned partial payback to DOE for R&D equipment installed during Phase III activities. During Phase III of this project, three major efforts will be undertaken. The first of these involves heat exchanger development at the aluminum plant, primarily oriented towards testing system reliability at the source end. The second major effort entails the validation of models concerning the design and dynamic behavior of a district heating system using dispersed storage (i.e. stratified storage units at each substation). This effort will also be concerned with the development of control strategies and systems to

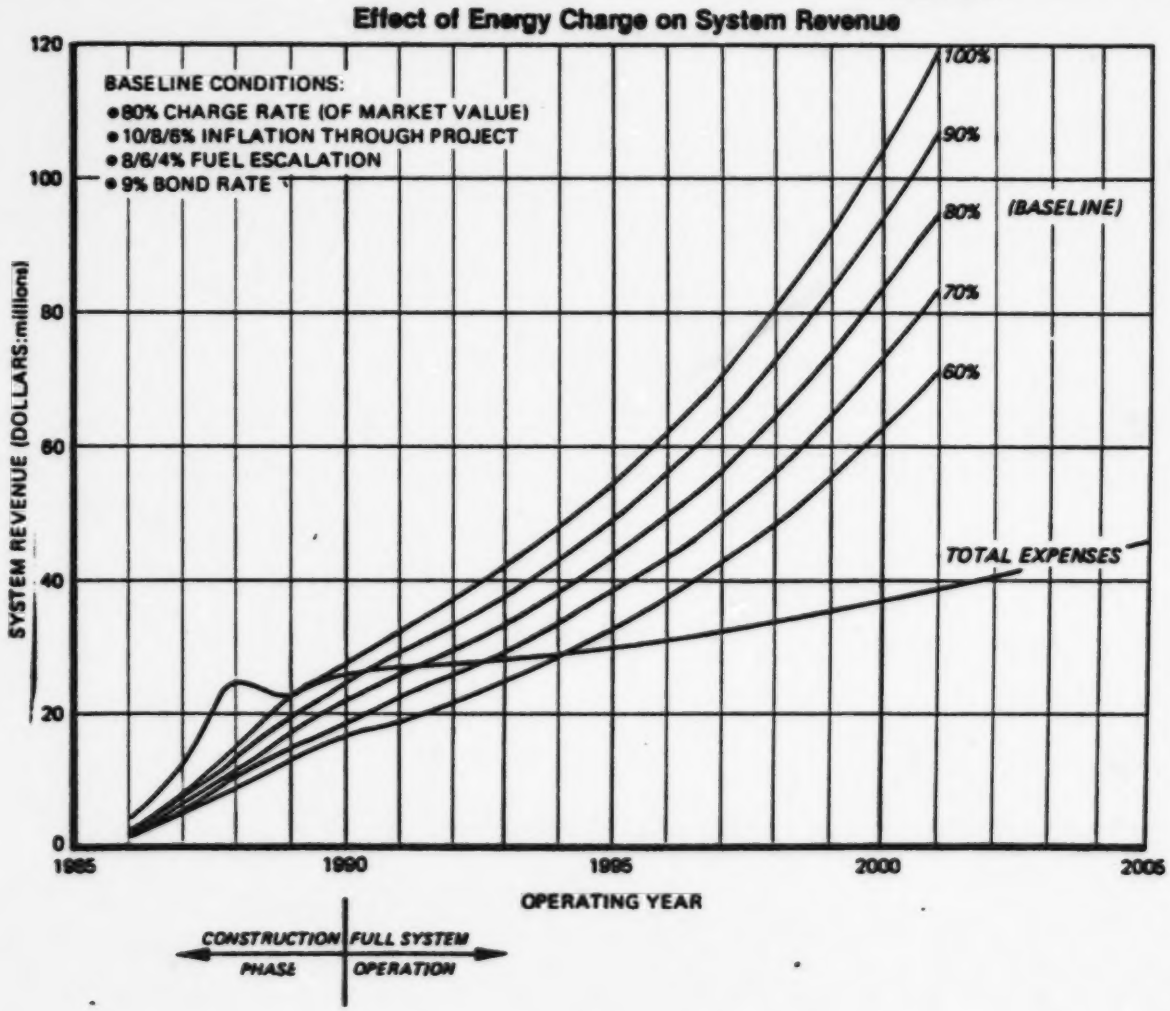
Effect of Energy Charge on System Revenue
BASELINE CONDITIONS:
• 80% CHARGE RATE (OF MARKET VALUE)
• 10/8/6% INFLATION THROUGH PROJECT
• 8/6/4% FUEL ESCALATION
• 9% BOND RATE
100%
90%
80% (BASELINE)
70%
60%
TOTAL EXPENSES
SYSTEM REVENUE (DOLLARS: millions)
120
100
80
60
40
20
0
1985
1990
1995
2000
2005
OPERATING YEAR
CONSTRUCTION PHASE
FULL SYSTEM OPERATION

Figure 3

make optional use the constant heat source. A small-scale district heating system (equivalent to one substation in the overall system) will be constructed and operated to test the storage and control system, validate the models, and verify the merits of the storage control strategy.

1.4 Phase IV

The fourth project phase will continue with city-arranged financing. A municipal utility will secure financing through the issuance of a mix of revenue and general obligation bonds to fund the full system construction. It is the stated intent of parties concerned that Phase III funds which are applied to hardware later incorporated in the full-scale system will be repaid from Phase IV revenues.

2. PHASE III HEAT EXCHANGER EVALUATION

The heat exchanger evaluation proceeds in five tasks: chemical analysis, corrosion investigation, probe testing, subscale testing and full-scale testing.

The first three tasks support the design for the subscale heat exchanger and are currently in process. Task four testing is scheduled to begin in the fall of 1981 with full-scale testing one year later.

The final system will incorporate 12 heat exchangers, each designed to remove 3.7 megawatts (12.5×10^6 Btu/hr) from the fume stream. These will be located just upstream of the dry scrubbers at ground level. Ductwork between the reduction cells and the heat exchangers will be insulated with 5 cm (2") of fiberglass insulation.

Fume will enter the heat exchangers at an average temperature of 121°C (250°F) and exit at 74°C (165°F). Water will enter the heat exchangers at 57°C (135°F) and exit at 99°C (210°F). Heat exchangers will be shell and tube type, multipass crossflow configurations.

The major choices left in the heat exchanger design concern are 1) the tube material and 2) the spacing or absence of fins.

Mild steel is the favored material at this stage, with aluminum and monel as backup/alternate possibilities. The duct environment is known to be mildly corrosive due to the presence of fluorine bearing compounds and sulfur oxides. The fume stream is remarkably low in water vapor, which if present would aggregate the corrosiveness.

A thirty year lifetime is desired for the heat exchanger. To date the mild steel ductwork has survived eight to nine years. However, the temperature is high and the stress levels are lower in the ductwork than are anticipated for the heat exchangers. Both effects will tend to increase corrosion attack in the heat exchanger application.

Access ports have been made for experiment installation at five locations in the ductwork. The material removed from the duct has been submitted for metallographic-microscopic analysis for surface corrosion and corrosion induced cracking. New samples of material candidates have been prepared for exposure to the fume environment in stressed and non-stressed states. The choice of material for the subscale heat exchanger will be made based upon analysis of the duct coupons. Should a change of material for the full-scale heat exchanger be warranted, comparative data in the accelerated (stressed) state

will be available to support the choice.

Two preliminary designs for the full-scale heat exchanger have been performed, one with bare tubes and one incorporating 3 fins/inch at 3/4" fin length. The two designs differ primarily in cost, weight and air-side pressure drop. The cost and weight of the bare tube designs are roughly double those of the finned tube. An additional penalty for the bare tube design is an increase of 60 percent in gas side pressure drop over the finned tube designs.

Probe testing is incorporated to support the decisions regarding the heat exchanger tube geometry. Two types of surface fouling are seen on cooled surfaces in the fume stream. A soft friable material, likely to be removable with air jets (soot blowers) and a hard slate-like material. The latter may have a more wax-like texture at medium temperature. It is this material which strongly influences the choice of tube geometry. On small bare tube probes this material has been seen to build up to a thickness of roughly 5 milimeters within 24 hours exposure and show little or no increase in thickness for the next 720 hours. It is believed that the mechanism limiting buildup may be surface temperature. In that case, it is possible that the presence of fins on the tube surface could result in much thicker hard deposit.

Probes consisting of short segments of finned and bare heat exchanger tubing have been equipped with cooling water flow and appropriate thermocouples. These are installed in the fume stream near the baghouse where the subscale heat exchanger will be installed. These probes will be cooled continuously and monitored for fouling twice weekly over the next several months. Heat transfer coefficient measurements are made by emptying the probe of cooling water and observing the transient thermal response without cooling. The probe is removed, dusted free of loose foulant and the test repeated with only the hard material present.

After the first week of exposure the results are summarized as follows:

1) The buildup of hard foulant is significantly less than predicted at 0.5 mm (.020").

2) Heat transfer coefficients are measured
$$1.94 \times 10^{-3} \pm 1.36 \times 10^{-4} \ \frac{\text{Cal}}{\text{Cm}^2 \ \text{Sec}^\circ\text{C}} \ (14.3 \pm 1) \ \text{Btu/hr ft}^2 \ ^\circ\text{F}$$
on the finned probe.

3) Heat transfer coefficient is measured as
$$2.17 \times 10^{-3} \pm 1.8 \times 10^{-4} \ \frac{\text{Cal}}{\text{Cm}^2 \ \text{Sec}^\circ\text{C}} \ 16 \pm 1.3 \ \text{Btu/hr ft}^2 \ ^\circ\text{F}$$
on the bare probe.

4) After one week both units exhibit a 20 percent decrease in heat transfer coefficient.

5) After one week when only the hard foulant remains on the probe, heat transfer is not significantly different from the performance in the clean state.

These preliminary results indicate that the best geometry choice will be the finned tube arrangement. Probe monitoring will continue for the next few weeks. Thereafter a final design cycle will be made using the probe measured heat transfer coefficients and fabrication of the subscale heat exchanger will be initiated.

The subscale heat exchanger will be arranged at 1/12 scale, to recover heat from the fume from five reduction cells. This exchanger will have the same water and gas flow lengths, same number of passes and the same tube configuration proposed for the full-scale.

A short section of ductwork will be fabricated containing two stub sections and three butterfly valves. This section can be rapidly installed in the existing ductwork without interference in ongoing operations. The five ducts from the reaction cells, the collective header and all downstream ductwork will be insulated with 2" of fiberglass insulation and a weatherproof coating.

New ductwork, also insulated, will be fabricated to lead the fume flow to the heat exchanger pad at the side of the building.

The energy recovered from the subscale heat exchanger will be furnished to the shower room approximately 250 meters (820 feet) distant. Both space heating and hot potable water demands will be served. It is estimated that over 95 percent of the present natural gas consumption for this building can be displaced with the energy recovered during the test.

After the initial startup and checkout transients, industrial water inlet to the test heat exchanger will be controlled in temperature by mixing makeup process water (ambient temperature) with water returning from the shower room. Excess return water will be blended with process water and directed to the outfall. The proposed district heating system return temperature of 57°C (135°F) will be simulated by this means. Water flow through the heat exchanger will be controlled to yield the desired output temperature of 99°C (210°F). Fume temperatures will be monitored before and after the heat exchanger.

The subscale heat exchanger and its associated control and dissipation systems will be monitored throughout the 1981-1982 heating season. Periodic inspection for hard foulant buildup will be made and hard foulant cleaning techniques tried if the buildup is significant. A continuous analysis of the baghouse performance will be made during this test and compared to data collected from the system in its unmodified state. While it is unlikely that a modification involving only 8 percent of the fume will result in measurable performance change, the comparison will place an upper bound on the possible performance change for the full-scale experiment to follow.

3. CONCLUSION

The application of low-grade industrial waste heat to space and domestic water heating through district heating systems has the potential to effect very large decreases in national oil imports.

The City of Bellingham, Washington, coupled to the Intalco Aluminum plant, forms an excellent site to test and develop the required technology and test the concepts under U.S. economic conditions.

Reference

1. Energy Information Administration, "Annual Report to Congress, 1979, Volume 3: Projections" DOE/EIA-0173 (79)/3, U.S. Department of Energy.

PB82-227943

WASTE HEAT AND CHILL STORAGE IN AQUIFER SYSTEMS

Jay R. Eliason
Seasonal Thermal Energy Storage Program
Battelle Northwest Laboratory
Richland, Washington, U.S.A.

ABSTRACT

Seasonal storage of thermal energy in aquifers has the potential to make a significant near-term contribution towards relief of the national energy shortage. Winter chill, summer heat, and various forms of industrial waste heat and chill can be stored for future demand, thus reducing the need for generating primary energy. This seasonal storage of heat and chill in aquifer systems is being assessed as part of the Seasonal Thermal Energy Storage (STES) Program. The STES Program is managed by the Pacific Northwest Laboratory (PNL) for the U.S. Department of Energy (DOE). The program is designed to conduct research and development studies required to provide the technical base for implementation of the Aquifer Thermal Energy Storage (ATES) concept.

1. INTRODUCTION

Winter chill, summer heat, and various forms of industrial waste heat and chill stored in aquifer systems for future demand can reduce the need for generating primary energy and lessening the nation's dependence on imported petroleum fuels. It appears that it is technically feasible to supply about 7.5% of the nation's total energy demand through aquifer thermal energy storage, with about a third of this energy initially supplied by industrial waste heat. The feasibility of this technology is now being investigated by the U.S. Department of Energy through the Seasonal Thermal Energy Storage Program, which is conducting research studies to develop this concept (Reilly 1980).

ATES appears to be the most promising of the several technologies proposed for long-term (or seasonal) storage of large amounts of thermal energy. A major key to ATES's attractiveness is its simplicity of design and construction. The storage device in its simplest form consists of two ordinary water wells drilled into an aquifer, connected at the surface by piping and a heat exchanger. During the storage cycle water is pumped out of the aquifer, through the heat exchanger to absorb thermal energy, and then back down into the aquifer through the second well. The thermal energy remains in the aquifer "storage bubble" until required for use, when it is recovered by reversing the storage operation. For many applications the installation can probably be designed and constructed using existing site-specific geohydrologic information and modern well-drilling techniques.

Another key to the attractiveness of ATES is its potential for cost-effective operation. The storage medium, water, is inexpensive. The wells,

pumps and other equipment costs constitute the only capital storage expense, as the cost of acquisition and use of the storage container (aquifer) is essentially free and independent of the amount of energy to be stored. Therein lies the major advantage of ATES over other storage technologies, where cost of the container is typically proportional to volume stored. It is likely that initial storage efficiencies of 70% will be encountered for commercially-sized units. Efficiencies are expected to increase over time, possibly to the 90%+ range, as the aquifer heats or cools.

There are concomitant benefits. Large-scale ATES development has the potential for improvement of the environment, primarily due to reduced pollution from extraction, refining, and combustion of fossil fuels. Therefore, normal pollution is reduced, as is the cost of equipment presently required to treat that pollution. Storage as part of a district heating system should increase the overall system reliability.

The potential for market penetration of ATES is immense. Aquifers are estimated to underlie roughly two-thirds of the nation. Both winter chill and summer heat are technically feasible energy sources for many parts of the country, and the potential for electrical cogeneration and for capture of industrial waste heat is vast.

Widespread implementation of ATES is not without difficulties, however. The more exotic energy sources present technical problems, and work needs to be done to evaluate the implications of widespread heat storage at depth. Perhaps the most significant barriers to commercialization, however, are institutional. As this is a new technology, numerous legal questions need to be addressed, including liability for thermal pollution of the aquifer and protection of the stored resource from capture by others. Because district heating of residential housing requires extensive pipelines, development is needed for the means of financing these highly capital-intensive ventures and to create incentives and/or leadership.

The existing body of information on ATES indicates that it is a cost-effective, fuel-conserving technique for providing thermal energy to residential, commercial, and industrial users. The negative aspects are minor and highly site-specific, and do not seem to pose a threat to widespread commercialization. With a suitable institutional framework, ATES promises to supply a substantial portion of the nation's future energy needs.

2. PROGRAM ORGANIZATION

The STES Program is designed to conduct research and development studies required to provide a sound technical base for the demonstration of seasonal thermal energy concepts. The ATES concept has been identified as one of the most promising which could provide a significant near-term contribution to alleviation of the national energy shortage. In order to provide the necessary technical base for commercialization of this concept, the following program goals have been established:

- Develop field research facilities to obtain data
- Perform analytical, laboratory, and field research activities
- Provide a center of knowledge and information for STES
- Transfer STES technologies to the commercial sector

The research and development tasks established to achieve these goals include: Legal/Institutional Assessment, Economic Assessment, Environmental Assessment, Field Test Facilities, Compendia, Physicochemical Analysis, and Numerical Simulation.

2.1 Legal/Institutional Assessment

The principal objective of this task is to catalog and analyze the legal, regulatory, and institutional issues that are likely to affect implementation of STES concepts. Issues are to be addressed at the federal, state, and, to a lesser extent, the local level of government. Initial effort has been focused on assessment of issues related to the development of the ATES concept.

2.2 Economic Assessment

The objectives of the economic assessment task are to determine the economic performance of seasonal thermal energy storage concepts, to estimate their market penetration potential, and to develop economic assessment methodologies for STES concepts.

2.3 Environmental Assessment

The objectives of the environmental assessment task are to provide assistance in identifying, acquiring, and assessing environmental-related information and preparing environmental documentation as required to support the STES Program.

2.4 Field Test Facilities

The objectives of the Field Test Facilities task are to develop field research facilities that can provide accurate data on aquifer characterization, design, operation, and economics of proposed ATES concepts.

2.5 Compendia

The objective of the Compendia Task is to collect, summarize, and transmit STES-related information. The task will provide a central source of information which will assist with the development of STES technologies and will also aid in the transfer of these technologies to the commercial sector.

2.6 Physicochemical Analysis

The objectives of this task are to conduct laboratory tests on the physical and chemical properties of aquifer materials subjected to ATES conditions, develop laboratory and field analysis facilities dedicated to the support of ATES projects, and develop geochemical modeling capabilities tailored to ATES operational and environmental concerns.

2.7 Numerical Simulation

The objectives of this task are to document the state-of-the-art of

numerical simulation applicable to ATES systems and to develop and/or utilize simulation technologies capable of predicting the transport and retrieval of a thermal energy resource within the ground-water environment.

3. STATUS

The STES Program was established at PNL in FY 1979 and activities have focused primarily on ATES concepts. In addition to the research and development tasks now being conducted, the program includes an ATES demonstration program which is designed to provide site-specific conceptual designs for ATES systems. Three contracts were selected through a competitive request for proposal to develop ATES demonstrations. They are TRW, Dames and Moore, and the University of Minnesota. The demonstrations have focused on aquifer characterization during FY 1981. The following table shows the location, energy source and projected use at each site:

Site	Prime Contractor	Energy Source	Storage Temperature	Application
Bethel, Alaska	TRW, Inc.	Diesel-Electric Utility	<105°C	District Heating
Stony Brook, New York	Dames & Moore	Winter Chill	4°C	District Cooling
St. Paul, Minnesota	University of Minnesota	University Heating Plant	>150°C	District Heating

Initial aquifer characterization studies have been conducted at each of the demonstration test sites. These data will be available in report form at the end of FY 1981.

Program plans are now being developed which include continued research studies at the University of Minnesota to obtain data on high temperature ATES. These studies will complement studies conducted at the low temperature FTF site at Mobile, Alabama.

3.1 Legal/Institutional Assessment

Legal and institutional issues that may effect ATES are being assessed under this task. These issues are discussed in the following paragraphs.

Initiation of an ATES project will necessarily involve compliance with certain permits and regulatory requirements. In most western and some eastern states, a permit to withdraw ground water will be required from the appropriate state water resources agency. Most states have requirements related to well drilling, construction, and abandonment. In many states, a separate permit to reinject the thermally altered ground water will be required from the appropriate pollution control agency. A few states prohibit such reinjection, and a variance will be necessary if an ATES project is to be implemented. Eventually, a permit from a state agency or the U.S. Environmental Protection Agency under the underground injection control (UIC) program established by the Safe Drinking Water Act of 1974 will be required. This requirement will likely supersede existing underground

injection requirements. Final UIC requirements for the well classification likely to include ATES wells will probably not be issued for several years.

An ATES operator should be aware of several possible sources of liability. Liability is most likely for interference with the property rights of others in the storage aquifer. Interference with existing users of an aquifer as a potable water source is of greatest concern. Alleged interference would most likely be for increased water temperature, although it is also possible that an ATES operation could lead to some chemical or biological contamination of ground water.

Surface drilling and injection activities can also potentially lead to liability through such things as noise, vibrations and fluid spills. Proper care in surface operations can minimize these possibilities.

A central concern of the ATES operator will be assurance of the ability to store, protect, and recapture the thermal energy when desired. At a minimum, the ATES operator will need to purchase or, when necessary, condemn (assuming statutory authority) sufficient surface property rights to provide site access, drill needed wells, and provide adequate spacing from nearby land use activities.

Many legal, institutional, and regulatory issues will occur at the stage of heat or chill delivery. A principal issue is locating an entity with sufficient incentive to construct and operate an ATES and delivery system. It may be difficult to find an investor-owned entity with sufficient economic incentive; consequently, the responsibility may fall to a public body. A variety of other issues related to financing, rate setting, service areas, taxation, and other areas will require resolution. These issues are likely to be most complex for a residential district heating system.

A technical document containing the results of investigations to date under this study entitled, "Legal and Regulatory Issues Affecting the Aquifer Thermal Energy Storage Concept" was published in October 1980 (Hendrickson 1980).

3.2 Economic Assessment

Economic assessment methodology development has been focused on developing a computer code, AQUASTOR, to evaluate the economic performance of ATES configurations. This code combines demand, aquifer, and supply characterisitcs with climate, cost functions, and economic parameters in one systematic model. It provides the flexiblity to individually or collectively evaluate the impact of different economic and technical parameters, assumptions, and uncertainties on the cost of providing heat (chill) from an aquifer storage system.

The model consists of two major parts: the aquifer resource submodel, and the distribution submodel. The resource submodel calculates the life cycle cost of energy production by simulating the exploration, development, and operation of an ATES system and the transmission of this energy to a distribution center. The distribution submodel calculates the life-cycle cost of delivered energy by simulating the construction and operation of a distribution system.

The code is extremely flexible and can simulate heating (with stored hot water), chilling (with stored cold water or with hot water and absorption

chillers), or both (using hot water with absorption chillers). The distribution submodel simulates large-scale district heating (cooling) networks, point demands, or various combinations. Each of the submodels is considered to be its own operating entity with a tailored financial configuration, including different tax rates and incentives, capital structure, and depreciation schedules.

The AQUASTOR model has been used to conduct preliminary economic assessments of both the heat and chill storage concepts. These results have been published in the proceedings from The Mechanical, Magnetic, and Underground Energy Storage 1980 Annual Contractor's Review and the 15th Intersociety Energy Conversion Engineering Conference (Reilly et al. 1980(a); Reilly et al. 1980(b)). These studies included analysis of several of the key parameters which will determine the economics of ATES. The studies have shown that under appropriate demand, supply, and geologic conditions, operation of both ATES heating and cooling systems can be competitive with conventional systems.

A document providing an overall analysis of ATES was published in June 1980. It is entitled, "A Descriptive Analysis of Aquifer Thermal Energy Storage Systems" (Reilly 1980). In October 1980, a document entitled, "Guidelines for Conceptual Design and Evaluation of Aquifer Thermal Energy Storage" was authored by Meyer and Hauz of G.E. Tempo. These descriptions of ATES concepts and guidelines were prepared as tools for those considering the use of ATES systems. The guidelines will assist in the preliminary design effort and in evaluation of the technical and economic feasibility of using the ATES technology.

3.3 Environmental Assessment

A programmatic Environmental Assessment (EA) for the ATES Program was finalized and submitted to DOE Headquarters for final approval and publication. The assessment documents the finding of no significant environmental impact associated with the planned ATES activities.

The programmatic EA basically concludes that the environmental consequences of the ATES Program will be site-specific in nature. Potential adverse local environmental impacts could occur which may reduce aquifer permeability, alter ground-water quality, and ground- water microbology. These potential impacts can be eliminated, however, if sites are carefully selected, systems are properly designed, and monitoring programs are included. Site-specific institutional issues related to water use are expected to be important for ATES type developments. Adverse impacts to surface water hydrology, aquatic ecology, terrestrial ecology, air quality and the host communities are not anticipated. Site-specific monitoring programs, which are comprehensive in scope, must be developed to ensure that mitigatory measures are adequate and to detect any unforeseen impacts. Potential environmental benefits are anticipated from reducing the amount of waste heat discharged to the environment and from reducing dependence on conventional energy sources for space heating and cooling. The ATES technology was assessed to be closer to implementation than its alternatives.

3.4 Field Test Facilities

Field Test Facilities (FTF) are being operated to obtain engineering design and geohydrologic data for support of ATES concept development. Test

sites are being developed at Mobile, Alabama, and the University of Minnesota. The site at Mobile, Alabama will provide test data on heat storage in an unconsolidated confined aquifer at temperatures ranging from 55°C to 125°C. The site at the University of Minnesota will provide data on storage in a consolidated, confined aquifer at temperatures ranging from 100°C to 150°C. Field test data have also been collected at each of the ATES demonstration sites and at Texas A&M University.

The Mobile, Alabama and University of Minnesota test sites are now being operated to obtain data on ATES heat storage. The Mobile, Alabama test site has been operated since 1976 and a report describing testing through December 1979 entitled, "Experimental Study of the Storage of Thermal Energy in Confined Aquifers" authored by Molz, Parr and Andersen of Auburn University, has been issued. Since December 1979 the well field design has been modified and additional test wells have been drilled. A series of experiments are now being conducted. Injection, storage, and recovery cycles are planned at injection temperatures of 59°C, 90°C and 125°C. The initial test is now in the recovery stage and the injection and recovery system has performed well. Injection of water at 90°C is now scheduled for July 1981. The University of Minnesota test site is designed to operate at temperatures up to 150°C. This site is now being characterized and physical facilities are being installed. Injection cycles are scheduled for July 1981, provided well structures are completed without complications.

Field tests at Texas A&M and the Dames & Moore demonstration project at the State University of New York (SUNY) have conducted injection and storage cycles with chilled ground water. The Texas A&M study utilized a spray pond in the winter as a chill source. A cooling tower has been used as the chill source at the SUNY test site. These data sets are now being analyzed and will be made available in formal reports by the end of FY 1981.

3.5 Compendia

Under the compendia task, a library containing STES related information has been established. It now contains over 1700 documents with a wide range of key references on topics related to thermal energy storage. The bibliographic information from the STES Library has been entered into a computerized information system, called the STES Technology Information System (STES-TIS). Each library article is represented by a citation, which consists of a number of fields including author, title, publisher, publication date, keywords, abstract, etc. Each citation also contains fields that can be used by the STES librarian to keep a record of the status of the document represented by the citation. The STES-TIS also provides the capability to conduct customized, on-line literature searches. A bibliography is scheduled to be published by the end of FY 1981.

The STES-TIS has been designed to fill the informational needs of the STES Program by providing the capability to store and manipulate various types of data files and numerical models. In general, the STES-TIS contains four types of resources: (1) administrative, (2) bibliographic, (3) computational, and (4) communications. The administrative resources include files containing task descriptions, weekly highlights, a quarterly newsletter, and conference information. The bibliographic resources consist of various data files related to the STES Libary. The computatonal resources provide automated access to various computers on which the economic and hydrologic models developed for the STES Program can be run. The communications resources

include electronic mail, conferencing, and the capability to link with or write to the terminal of another user.

A quarterly STES Newsletter is published and distributed internationally. It contains brief reports on STES activities being conducted throughout the world.

Summary reports on regional aquifer assessments and reinjection experience in groundwater cooling operations have been published. The regional aquifer assessment qualitatively describes the ATES potential of major aquifers throughout the United States (Century West 1981). The reinjection experience report was prepared to document ATES-related activities (Snyder and Lee 1980).

3.6 Physicochemical Analysis

This task has been directed toward evaluation of physical and chemical changes induced by ATES operations which could effect ground water flow and/or quality.

A laboratory flow loop and a field injectivity test stand for analysis of aquifer materials and ground water are being developed. The laboratory system is designed to permit testing of aquifer materials under simulated ATES conditions of temperature, pressure, flow direction, flow rates, and ground-water chemistries. The injectivity test stand is designed for on-site sampling of fluids being injected into the aquifer. Primary emphasis is on the suspended solids and how these particulates might impact injection well performance.

A geochemical computer model is being modified specifically for STES applications. This model will include mass transfer (mineral precipitation/dissolution), kinetic control for major aquifer minerals, and ground-water speciation compilations at temperatures from 25°C to 150°C. Another goal is the development of a package of acceptable field data collection and analyses techniques suitable for field site managers.

Documentation on the analysis systems being developed and the geochemical model will be published in proceedings of the Annual Contractors' Review Meeting scheduled for August 1981.

3.7 Numerical Simulation

Numerical simulation models for design and assessment studies of proposed ATES concepts are being developed and verified utilizing data from the field test facilities. A state-of-the-art review of modeling has been conducted to identify available codes and to identify modeling needs. This document entitled, "Review of Simulation Techniques for Aquifer Thermal Energy Storage (ATES)" was authored by Mercer, Faust, Miller, and Pearson of Geo Trans, is now being published.

At this time three saturated ground-water flow models are being evaluated for ATES simulation studies. They are the Conduction Convection and Compaction (CCC) code of Lawrence Berkeley Laboratories, the Deep Well Disposal Model (DWDM) of the USGS and the Coupled Fluid, Energy, and Solute Transport (CFEST) code of PNL.

The physics of energy transport in unsaturated media is currently being studied by members of the soils science faculty of Oregon State University. A

literature review has been completed, and both a preliminary interpretive report and an annotated bibliography have been written. Using our current knowledge of the physics of nonisothermal flow in unsaturated media, Lawrence Berkeley Laboratory has initiated the development of a simulation code for the coupled unsaturated-saturated nonisothermal ground water environment. An isothermal code for the analysis of transient flow in unsaturated and saturated porous media (TRUST) is being expanded to include nonisothermal effects.

Generic simulations and parameter studies are being conducted to produce a graphical solution process which, when given the aquifer and utilization parameters of the ATES facility, can predict the response of the aquifer. Dimensionless parameter groups appropriate to the planning and design of practical projects have been defined and are being studied. Since many simulations must be made in a study of functional dependence, a simplified model has been employed.

4. CONCLUSIONS

The studies of ATES concepts which are now being conducted indicate that the overall energy saving potential for ATES is significant and the technology should be a near-term energy storage option. Field studies now being conducted and planned for the near future will provide needed data for accurate assessment of ATES concepts. Economic assessment of ATES has shown that with reasonable geohydrologic and design assumptions, both heat and chill storage systems should be economical for intermediate to large scale systems. The environmental and legal studies indicate that although there may be local restrictions, ATES systems in general are expected to be able to meet requirements. Research and development activities now being conducted under the STES Program should provide a sound technical base for the development of ATES systems.

1. Century West Engineering, Regional Assessment of Aquifers for Thermal Energy Storage, Pacific Northwest Laboratory, Richland, WA., Draft Report.

2. P. L. Hendrickson, Legal and Regulatory Issues Affecting the Aquifer Thermal Energy Storage Concepts, Pacific Northwest Laboratory Rept. PNL-3437, Oct. 1980.

3. J. W. Mercer, C. R. Faust, W. J. Miller, and F. J. Pearson, Jr., Review of Simulation Techniques for Aquifer Thermal Energy Storage (ATES), Pacific Northwest Laboratory, March 1981.

4. C. F. Meyer and W. Hausz, Guidelines for Conceptual Design and Evaluation of Aquifer Thermal Energy Storage Systems, Pacific Northwest Laboratory Rept. PNL-3581, Richland, WA., Oct. 1980.

5. F. J. Molz, A. D. Parr, and P. F. Andersen, Experimental Study of the Storage of Thermal Energy in Confined Aquifers, Oak Ridge National Laboratory Rept. ORNL/Sub-7338/1, Oak Ridge, TN, May 1980.

6. R. W. Reilly, A Descriptive Analysis of Aquifer Thermal Energy Storage Systems, Pacific Northwest Laboratory Rept. PNL-3298, Richland, WA., June 1980.

7. R. W. Reilly, D. R. Brown, and H. D. Huber, Economic Assessment of Aquifer Thermal Energy Storage, Mechanical, Magnetic, and Underground Energy Storage

1980 Annual Contractors' Review, vol. 1, pp. 39-41, 1980(a).

8. R. W. Reilly, D. R. Brown, and H. D. Huber, The Economics of Aquifer Storage of Chilled Water for Air Conditioning, 15th Intersociety Energy Conversion Engineering Conference, vol. 2, pp. 1265-1276, 1980(b).

9. M. Snyder and C. H. Lee, Survey of Reinjection Experience from Groundwater Cooling Applications, Pacific Northwest Laboratory Rept. PNL-3740, Richland, WA., In press.

PB82-227950

COGENERATION ELECTRICAL INTERCONNECTION EQUIPMENT -- COSTS AND ISSUES

J. B. Patton
Systems Control, Inc.
1801 Page Mill Road
Palo Alto, California 94304, U.S.A.

ABSTRACT

This paper summarizes a study undertaken to relate common utility policy requirements for utility-cogeneration interconnections to potential cogenerators and utilities with little or no cogeneration experience [1]. Several utilities were contacted to determine their policy specifications. The interconnection issues and cost ramifications of alternative interconnection policies are discussed here.

1. INTRODUCTION

Interconnecting on-site cogeneration with utilities can potentially offer many attractive benefits. Utility interconnection helps improve the energy conversion efficiency by balancing the electrical and thermal energy output. By providing excess power to the utility at times of peak system load, cogeneration can help reduce oil consumed in less efficient generating units. Furthermore, interconnection improves the reliability of the customer's power system with the utility as a back-up supply.

Utilities require that the addition of new cogeneration facilities should not result in a degradation of the quality or reliability of power delivered to other customers. This basic requirement is implemented by establishing a formal specification identifying the equipment necessary to prevent disruption of the utility system as the result of incidents at the cogeneration facility.

The utility's cogeneration policy includes its own protection practices and any special conditions due to the lack of utility control over customer-owned equipment. These relaying practices, applied even to utility-owned generation, are not standardized. Historically, protective relaying has been considered an engineering art -- dictated by the designer's judgment in weighing reliability versus cost.

2. UTILITY INFORMATION

Information related to interconnection policies and specifications was gathered from the following utilities:

* PACIFIC GAS AND ELECTRIC

* SOUTHERN CALIFORNIA EDISON
* SAN DIEGO GAS AND ELECTRIC
AMERICAN ELECTRIC POWER
BALTIMORE GAS AND ELECTRIC
CONSUMERS POWER
DUQUESNE LIGHT COMPANY
PORTLAND GENERAL ELECTRIC
CLEVELAND ELECTRIC ILLUMINATING COMPANY
DETROIT EDISON
* GEORGIA POWER
* NEW ENGLAND ELECTRIC SERVICE
ROCHESTER GAS AND ELECTRIC

The marked (*) utilities have specific technical guidelines. The others have only a general policy, study each application on a case-by-case basis, or have no experience with cogeneration. From this data, a consensus of utility opinion concerning interconnection policy was obtained.

The following sections discuss factors influential in determining the costs of interconnection. The first section details the protective relaying called for by those utilities having guidelines. The second section discusses operations requirements the customer must meet in order to parallel his generator with the utility grid for the purpose of selling power. The third section examines other economic aspects of interconnection that utilities and potential cogenerators must examine before reaching an agreement to buy and sell power.

2.1 Protection Practices

From the survey of electric utility interconnection practices, it was found that, of those utilities having guidelines, a consensus of opinion had formed in the specification of certain protective relay functions. Disagreement was noted in other aspects of the protective scheme. This section presents for comparative analysis, the interconnection device specifications.

The relaying functions listed in Table 2.1 are those that are most commonly called for in relaying the interconnection. Generator protection functions such as generator differential, loss of excitation, field ground, over/under voltage are not included. The utilities generally specify interconnection protection assuming no knowledge of the relaying functions that are included in the generator protection package. Similarly, the protection associated with the particular substation transformer (e.g., transformer differential, sudden pressure relay) are not included here. The functions listed are the minimum requirements specified by the particular utilities for the interconnection.

First, in nearly all cases, some kind of protection from paralleling the two voltage sources out of synchronism is called for. Although most of the utilities stated that energization of a dead utility bus by a cogenerator would not be allowed, only two (San Diego Gas and Electric and New England Electric Service) require an interlock to prevent such an operation.

All the utilities require some form of overcurrent protection. This protection may consist of time and/or instantaneous overcurrent, directional overcurrent, overcurrent with voltage restraint, or impedance relaying. The particular function used depends on the load and utility system characteristics. This subject is further discussed in [1].

Table 2.1 Minimum Protective Relay Requirements

SITUATION IDENTIFIER	PROTECTION CONFIGURATIONS																							
	GEORGIA POWER						PACIFIC G. AND E.			SOUTHERN CAL. ED.	SAN DIEGO G.&E.		NEW ENGLAND ELEC. S.	CLEVELAND ILL. CO.	IEEE	GOFF, ROOK, POWELL							
Size range for which Protection Configurations apply from 200 KW to 80 MW	5 MW ∧I	5 MW ∧I	5 MW ∧V	5 MW ∨	5 MW ∧I	5 MW ∨	400 KW ∧I	400 KW ∧I	400 KW ∨	200 KW ∧I	200 KW ∧	5 MW ∨	5 MW ∧I	4.	200 KW ∧	200 KW ∧								
network or radial line feed	✓		✓	✓	✓	✓	✓	✓		✓	✓	✓	✓	✓	✓	✓								
network bus feed		✓					✓	✓		✓														
fused transformer primary				✓		✓					-													
customer load much greater than generation					✓	✓								✓										
delta-delta distribution transformer connection			✓	✓				✓																
wye-grounded wye (dist. primary to generator v.)						✓																		
grounded wye-delta							✓		✓															
delta-grounded wye (with or without resistance)	✓	✓			✓										✓	✓								
grounding bank may be required								✓		✓														
SYNCHRONISM PROTECTION																								
relay to prevent energization of utility dead bus											✓	✓	✓	✓										
synchro check relay										✓				✓		✓								
hot line reclose inhibit	✓	✓	✓	✓	✓	✓	✓	✓	✓	✓				✓										
auto-synchronizer required							✓																	
OVERCURRENT PROTECTION																								
time and/or instantaneous overcurrent	✓	✓	✓	✓	✓						✓	✓		✓	✓	✓								
directional overcurrent (looking into utility)										2.			✓											
overcurrent with voltage restraint							✓	✓	✓	✓			or											
impedance	✓						or ✓	or ✓	or ✓	or ✓			✓		✓	✓								
SYSTEM BALANCE PROTECTION																								
phase current balance							✓	✓	✓		✓													
negative sequence				✓		✓																		
GROUND FAULT PROTECTION											3.													
ground overcurrent (in transformer or ground bank neutral)	✓	✓	1.		✓	✓	✓	✓	✓			✓		✓	✓	✓								
zero sequence voltage (broken delta connection)	✓		✓							✓			✓		✓									
single phase over/under voltage				✓								✓		✓		✓								
SYSTEM VOLTAGE PROTECTION																								
over voltage	✓		✓	✓			✓	✓	✓	✓		✓	✓											
under voltage	✓		✓	✓			✓	✓	✓	✓	✓	✓	✓		✓									
SYSTEM FREQUENCY PROTECTION																								
over frequency							✓	✓	✓	✓		✓	✓											
under frequency	✓		✓	✓			✓	✓	✓	✓		✓	✓	✓	✓	✓								
REVERSE POWER RELAY					✓	✓				✓				✓										

1. The neutral current in the CT residual connection is sensed.
2. Directional overcurrent and undervoltage relay supervision is specified.
3. Neutral overvoltage at the generator neutral is used.
4. Data is based on one 5 MW installation - not policy based.

The problem of system unbalance protection is approached in several ways. Although most of the utilities recommended negative sequence protection for the generator, few found it necessary at the interconnection.

In every system, some form of ground fault protection was found necessary. The particular scheme depends to a large extent on how the customer transformer is connected and how the primary circuit is grounded.

Usually, under and over voltage and frequency relays were required at the interconnection. Some disagreement was noted as to the need for an over-frequency relay. It is assumed by those not specifying over-frequency protection that the turbine governor response is sufficient to control overspeed.

The detection of reverse power under conditions where no power is expected to flow back to the utility is used by some utilities to indicate abnormal system conditions or a condition where the reverse power exceeds the expected level. Georgia Power Company recognizes this condition and removes its requirements for voltage and frequency relays at the interconnection. Southern California Edison requires no special interconnection protection if the customer's generation is less than 20% of his load.

2.2 Interconnection Equipment - Influencing Factors Due to Operations Requirements

In addition to the technical characteristics of the utility-cogenerator system, utility operations and maintenance practices and requirements can affect the cost of interconnection. Utility policy regarding operations requirements is less defined than that concerning protection requirements. The data available is presented here by relating specific utility comments on:

- metering
- load reporting requirements
- safety
- voltage regulation
- communications
- maintenance

Metering. The metering required at the interconnection is dependent upon the contract terms of the agreement to buy and sell power. Differing rates for power purchases and sales necessitate the installation of two watt hour meters ratcheted to record incoming and outgoing power. Almost every utility contacted requires this arrangement and supplies the appropriate meters at the utility's expense. New England Electric Service requires only one meter, allowing it to run backwards to credit the customer for power generated into the system. Pacific Gas and Electric requires the customer to supply two kilowatt-hour meters, two kilovar-hour meters, a magnetic tape load recorder, and a voltage recorder for installations greater than 100 kW. San Diego Gas and Electric supplies nearly the same equipment at its own expense. Southern California Edison monitors the two way demand, two way energy flow, and reactive power into the plant with company-owned meters and reserves the right to install mag tape recorders at its expense.

Load Reporting. For most utilities, the individual contract negotiated determines the load reporting requirements. The sale of customer capacity requires the installation to be demand-monitored. Pacific Gas and Electric requires daily load reports for machines greater than 100 kW, hourly load reports for machines greater than 5 MW, and telemetering for units over 10 MW. San Diego Gas and Electric requires telemetering of any unit over 1 MW.

American Electric Power does not require special load reporting until the units reach the 50 MW to 100 MW range. No relation of utility size to load reporting requirements is apparent from this data. A common policy or a consensus of utility opinion concerning cogenerator size versus need and application of load reporting equipment does not exist. The administrative and technical costs of load reporting are highly dependent on the utility's requirements for accurate load data. In nearly every case involving special equipment or personnel responsible for load reports, the associated costs are expected to be borne by the customer. An exception, San Diego Gas and Electric Company, stated that the costs of telemetry and supervisory control would "probably" be split evenly between the customer and utility.

Communications. Utility policy on communications requirements for supervisory control and pilot-type relaying follow closely the requirements for telemetering. A generator size is determined, based on the impact of its sudden loss on the rest of the system, and any unit larger than this size requires special communications facilities. Usually, a blanket policy is not written; load flow and transient stability studies are performed for each case to determine the need for special communications. Table 2.2 shows the available utility policy information.

Maintenance. The policy of utilities toward maintenance is reflected in their protection policies. Those utilities who have protection guidelines also specify that the customer must maintain or contract with the utility to maintain protective equipment. Maintenance records must be made available for utility review. Those utilities without protection guidelines lack maintenance policies as well.

Interconnection equipment that is placed on utility property is maintained by the utility. Though the customer may pay for the equipment, it is controlled by the utility. Most of the utilities surveyed prefer this arrangement. Those utilities allowing interconnection equipment on customer property demand access to customer maintenance records and the right to open the interconnection breaker if they are not satisfied. Maintenance scheduling is not usually required unless the generator capacity is sold. All the utilities reserve the right to separate the cogenerator from the system for their own maintenance purposes. Table 2.3 summarizes the available information on maintenance policy.

Safety and Voltage Regulation. Finally, utility operations requirements concerning safety and voltage regulation may be imposed. A means of establishing a visible disconnect between the utility and the customer must be provided and made accessible to the utility at all times. In addition, the customer is expected to maintain acceptable voltage at all times. He must purchase equipment to satisfy his reactive demand or negotiate the purchase of reactive power from the utility.

2.3 Other Requirements and Costs

The costs considered thus far are the minimum costs that a cogenerator can expect to pay. However, there may be interconnection costs not related to system protection and operation. These additional costs may involve:

- replacing utility equipment
- purchasing higher quality equipment than expected
- hiring consultants to do design evaluation
- hiring contractors to do equipment installation

Table 2.2 Communications Requirements

Georgia Power

- GPC "may require leased telephone, power line carrier, pilot wire circuits, microwave, or other means determined by GPC" for protective relaying.

San Diego Gas and Electric

- Units greater than 1 MW will be telemetered.
- Units greater than 5 MW will have supervisory control or 24 hour manned operation.

Southern Cal Edison, Pacific Gas and Electric

- Units greater than 10 MW require full telemetry.
- Supervisory control requirements will depend on terms of contract for energy and capacity sales.

American Electric Power

- No special requirements for telemetering or supervisory control for units under approximately 50 MW.

Table 2.3 Maintenance Requirements

Georgia Power Co.

- Protective equipment "will be owned and maintained by GPC. Where not possible, the customer is encouraged to contract with GPC for routine maintenance. Complete maintenance records must be available for GPC review."

San Diego Gas and Electric

- The utility will maintain all meters.
- The "customer is responsible for damage caused to other customers or to the serving utility as a result of misoperation or malfunction of his generator or its controls."
- Note - Interconnection protection equipment is on customer property.
- Sold capacity necessitates coordination in maintenance scheduling.

Southern Cal Edison

- SCE will maintain all interconnection protective equipment.
- The customer must keep and make available all maintenance records.
- Note - Interconnection equipment is on utility property.
- Sold capacity necessitates coordination in maintenance scheduling.

Pacific Gas and Electric

- PG and E will test and maintain all meters at customer expense.
- Maintenance records are required and are subject to utility review.
- Sold capacity necessitates coordination in maintenance scheduling.

Rochester Gas and Electric

- The customer must keep maintenance records open for inspection.

- hiring manufactuers to do checkout and servicing

Utility Equipment Replacement. When a large cogenerator is connected to the system, the possibility exists that some utility breakers will have to be replaced with breakers of a higher interrupting rating. This is because the cogenerator will add to the short-circuit capacity of the bus, and faults at certain locations on the utility system will draw additional fault current from the generator through a utility breaker. If the breaker is not sized to interrupt the total fault current, severe damage can result. Most of the utilities contacted require the customer to pay the additional expense incurred in changing out equipment as a result of connecting cogeneration. The final cost to the customer is a matter of negotiation. The cost of interconnecting could be affected dramatically.

Utility Grade Equipment. The cost of protective relays may be prohibitive for small cogenerators who believe this equipment is the only addition they need to make to their system in order to interconnect. The requirement by utilities is that utility grade relays be used. As opposed to industrial grade relays, utility grade relays are generally more reliable, respond better, are more easily adjusted, are more accurate, and cost more. The utility equipment requirements should be understood by the potential cogenerator.

Installation and Maintenance. A cost consideration is involved in financing and performing the installation and maintenance. For example, Southern California Edison will purchase and install all interconnection equipment and charge the customer 1.5% of the capital cost per month. In general, where the interconnection equipment is on utility property, the utility will assume responsibility for obtaining the capital. These costs may be passed on to the customer. Where the interconnection equipment is located on customer property, the customer is directly responsible for financing. In addition, the construction and maintenance costs are higher for a customer involving a general contractor and manufacturer in the installation and servicing. The utility can usually provide labor at a price cheaper than the contractor or manufacturer. For instance, the cost of a manufacturer's representative to do maintenance of relays will cost between $40 and $50 per man-hour. The customer will probably prefer to pay the utility to maintain the relays if necessary.

Special Customer Requirements. Customer requirements for high reliability will affect the cost of interconnection. A customer needing an unusually high level of reliability may consider additional protection equipment. In general, the amount of protection will reflect the capital investment in the plant or process. The addition of cogeneration and multiple utility feeds will enhance the system reliability but will complicate the protection scheme. The added complexity will increase the amount of protection equipment, switchgear, transformers, engineering time, and installation time.

Preliminary Studies. Finally, the costs in making preliminary power system studies should be considered. The design of a large cogeneration system must specify adequate ratings of protection equipment. In general, short-circuit studies, relay coordination studies, transient stability studies, normal and contingency load-flow studies, and possibly motor starting studies are necessary to insure a well-engineered design. Rarely will the cogenerator have the capability to make these studies himself. A consultant is usually hired to analyze the design using these tools. The utility may perform some of these studies. Upon judging the design sound, the customer can proceed with the installation.

3. COST OF INTERCONNECTION EQUIPMENT

In order to investigate the costs of interconnection equipment, five example schemes were chosen to represent typical interconnections. The objectives in choosing these interconnections were to obtain cost figures for the protective functions of Table 2.1, illustrate the effect of key variables on the interconnection costs, and provide a means for approximating the costs of other interconnections.

From discussions in the utility survey, five key variables were indentified as primary interconnection cost determinants:

- generator size
- interconnection voltage level
- installation man-hours required
- engineering man-hours required
- ownership responsibility (maintenance and liability) as reflected in interconnection policy

It is obvious that the interconnection cost will increase with generator size. However, it is not obvious how the costs of switchgear, protective relaying, installation labor, engineering labor, and maintenance man-hours are affected. Furthermore, the generator size need not be related to the interconnection transformer size if the customer load is large.

The effect of interconnection voltage is reflected in the relative costs of different voltage class equipment. It is desired to observe the cost difference in specifying 15 kV class equipment instead of 7.5 kV class equipment where the interconnection can be made at either voltage level. Also of interest are the cost implications of interconnecting at transmission voltage.

Most of the major equipment installation charges are included in the price of the equipment and are minor compared to the total cost. The installation cost of protective relaying and metering is not insignificant compared to the equipment cost. It is desired to see how the installation and equipment costs are related.

The amount of engineering man-hours required to design an installation will obviously increase as the complexity and amount of equipment increase. It is desired to know how these costs are estimated and the overall effect.

Finally, it is of interest to know the cost differences reflected by utility policy concerning ownership. Some of the equipment the utility requires to be purchased may already be supplied by the customer at the generator. The cost of this duplication of equipment is of interest. Since the maintenance responsibility generally belongs to the owner of the interconnection equipment, it is desired to know the man-hours involved.

3.1 Five Interconnection Schemes

After reviewing the available utility policy data, five interconnection schemes were chosen to represent the effects of the key variables discussed above. Detailed one-line diagrams and equipment descriptions are presented in [1]. A major equipment summary of the five interconnection schemes is given in Table 3.1.

Table 3.1 Major Equipment for Interconnection Schemes

Scheme A	20 MVA generator at 13.8 kV - 15 kV, 2000 Amp, indoor metalclad switchgear - 115 kV/13.8 kV, 20/26/35 MVA transformer - 115 kV, 1200 A, oil circuit breaker (interconnection with utility at 115 kV)
Scheme B	5 MVA generator at 4160 V - 7.5 kV, 2000 Amp, indoor metalclad switchgear - 13.8 kV/4160 V 10/13 MVA transformer - 15 kV, 1200 A, oil circuit breaker (interconnection with utility at 13.8 kV)
Scheme C	4.2 MVA generator - 13.8 kV vacuum circuit breaker - self-standing protective relaying package (interconnection with utility at 13.8 kV)
Scheme D	1000 kVA generator at 480 V - 13.8 kV/480 V, 2500 kVA transformer - 13.8 kV unit sub with air circuit breaker (interconnection with utility at 480 V)
Scheme E	200 kVA generator at 480 V - 13.8 kV unit substation with 13.8 kV/480 V 750 kVA transformer - 480 V distribution switchgear (interconnection with utility at 480 V)

Having specified the characteristics of the interconnections to be studied, the equipment, installation, engineering, and annual maintenance costs were estimated for the different configurations. The assumption was made that all equipment was new. No attempt was made to estimate site preparation costs.

A summary of the interconnection costs are given in Table 3.2. A detailed breakdown of these costs is given in [1]. A "sub-total" is shown in Table 3.2 - indicating that not all costs are included. Specifically, cabling and some substation auxiliary equipment are not included. However, this table indicates where the major cost items occur and the relative effect of the generator and transformer size, interconnection voltage level, protection scheme, installation and engineering labor, and maintenance costs.

Generator Size. The cost effect of connecting different size generators with identical interconnection arrangements to a utility system can be observed by comparing the cost summaries of Scheme A and Scheme B in Table 3.2. The direct effects of a generator size increase is an increased switchgear cost. The protective relaying, relay installation, engineering labor, and maintenance man-hours are identical for these installations. To estimate the cost of interconnecting another size generator in Schemes A or B, a fault study must be made to determine if the high and low voltage switchgear can withstand the added fault current contributed by the larger generator. If no change in switchgear is needed, the cost of connecting the larger generator is unchanged. The need to replace switchgear will depend on the level of short-circuit capacity at the substation bus compared to the breaker withstand ratings. The utility can supply the data and can tell a potential cogenerator the maximum size unit he can install without needing new switchgear.

Interconnection Voltage. The effect of interconnecting at a higher voltage can also be seen by comparing Schemes A and B. The cost of transmission voltage switchgear ($173,000) is much higher than the 15 kV class switchgear ($50,000). Unless the customer plant load is great enough to require transmission voltage switchgear, it is cheaper to interconnect at a lower voltage. For example, the minimum available continuous current rating of the 115 kV circuit breaker is 1200A. This corresponds to a rated load of 240 MVA. This breaker is overrated for a plant load much less than 240 MVA. The cost effects of interconnecting at a higher voltage are reflected in the switchgear costs. The relay, installation, design, and maintenance costs are not affected significantly.

The effect of using primary fuses instead of interrupting with a circuit breaker is shown in the high voltage switchgear figure of Table 3.2, Scheme E. The cost is substantially reduced from a typical $30,000 figure to $10,000.

Transformer. The interconnection of a cogenerator to the utility system will not usually result in the need to replace the transformer. The size of the transformer is determined by the customer's peak load, and the cogenerator size will nearly always be a fraction of the peak load. Nevertheless, the cost of the transformer is a large part of the interconnection cost. To estimate the cost of transformers, forty percent of the indicated values should be subtracted if the transformer is fitted with a load tap changer. The dollars per kilovoltampere can be calculated and the cost extrapolated to higher ratings to obtain the basic transformer cost. Forty percent of this cost is then added for the load tap changer to achieve a final rough estimate.

Installation Costs. The installation costs listed in Table 3.2 are those associated with the relay installation. The major substation elements are ordinarily estimated and purchased on an installed equipment basis. Table 3.2

Table 3.2 Interconnection Cost Summary

	generation size	transformer size	interconnection voltage	installed HV swgr and instrument transformers	installed transformer	protective relaying and metering	relay installation	installed LV swgr	engng labor	SUBTOTAL	maintenance man-hrs per year
Scheme A	20 MVA	20 MVA	115 kV	173	314	27	24	123	30	691	96 man-hrs
Scheme B	5	10	13.8 kV	50	160	21	22	100	30	339	96
Scheme C	4.2	10	13.8 kV	29	160	10	8	100	26	319	82
Scheme D	1	2.5	480 V	39	31	6	5	17	12	104	38
Scheme E	200 kVA	750 kVA	480 V	10	16	3	4	17	10	60	30

(in thousands of dollars)

reveals that the relay installation costs can be approximated by the cost of the relays themselves. The complexity of the protective scheme determines the number and types of relays. The effect of differing utility protection policies is reflected by the number and type of relaying functions required. Nearly all the relaying functions found in the survey were included in the cost data to allow this application.

Engineering Design Costs. The engineering labor required for designing an installation is roughly proportional to the number of equipment elements. A good measure of engineering man-hours required is reflected by the number of design drawings needed to specify and install the equipment. The cost involved is the time taken in preparing specifications, evaluating bids, reviewing vendor equipment, and making detailed construction cost estimates. An estimate of the engineering drawings needed can be made by visualizing the field equipment, the drawings needed per device, and the drawings needed to interconnect the power and control cabling. The ability to estimate the number of design drawings is gained through experience. The accuracy of such an estimate is always questionable; no attempt is made here to outline a method.

Ownership. The effects on interconnection costs of ownership responsibilities and liabilities are reflected in the utility's protection and maintenance requirements. The installed relay cost data can give a potential cogenerator an indication of the cost he will incur in paying a utility for interconnection equipment it has purchased. The avoided costs of not having to maintain the interconnection equipment can be calculated from the maintenance data given in Table 3.2. No costs were associated with the maintenance man-hours since these services may come from a variety of sources with widely varying charge rates.

RESULTS AND CONCLUSIONS

In performing the utility survey, it was found that very few utilities have adopted written policies concerning cogeneration interconnections. Of those having policies, most have agreed on the abnormal system conditions that must be addressed. These conditions are:

- the utility and cogenerator voltage sources being synchronized out of phase
- overcurrent conditions
- system unbalance
- ground fault conditions
- low or high system voltage
- low or high system frequency

Differences in utility policies were observed in the specifiec protection practices. There are many ways to achieve a single protection goal. The relaying practices of one utility, suitable for its system, may not be applicable to another system. Furthermore, the protection practices were found to be highly_situation-dependent for a utility with a large variety of possible interconnection conditions. Every utility stated that its policy constituted guidelines; the individual situation should be reviewed to determine if an exception to the policy should be made.

The interconnection costs estimated for the five typical cogeneration schemes revealed that:

- The need to replace existing switchgear is the most cost-intensive interconnection requirement. It is determined by comparing the

ratings of existing switchgear to the new system short-circuit capacity. The added short-circuit capacity is proportional to generator size.

- Normally, the customer transformer need not be replaced for a typical cogeneration facility to be interconnected.
- The cost of relaying is generally independent of generator size but depends on the quality of protection. The installation cost is approximately equal to the total device material cost.
- The installation and engineering man-hours required are directly related to the number of devices and do not vary greatly for different size cogenerators employing the same interconnection schemes.
- Ownership responsibility affects the interconnection cost. Maintenance and liability responsibilities are usually assigned to the party upon whose property the interconnection equipment is located. It is cheaper for the utility to maintain equipment, and most utilities prefer to have interconnection equipment located on utility property.

The above costs do not include operating, maintenance, and several miscellaneous cost components which include:

- the replacement of existing equipment
- the equipment quality for certain customer-purchased devices
- hiring consultants, contractors, and manufacturers to do design evaluation studies, equipment installation, and equipment servicing.

These costs would, of course, add to the estimated costs of the typical cogeneration arrangements.

REFERENCES

1. J. Patton, "Survey of Utility-Congeneration Interconnection Practices and Costs", Final Report prepared by Systems Control, Inc., for the U.S. Department of Energy, Office of Electric Energy Systems, June 20, 1980.

PB82-227968

PERFORMANCE ANALYSIS OF DEDICATED HEAT PUMP WATER HEATERS IN AN OFFICE BUILDING

Louise S. Morrison
Building Systems Development Branch
Solar Energy Research Institute
1617 Cole Boulevard
Golden, Colorado 80401 U.S.A

ABSTRACT

Implementing energy conservation measures in office and light commercial buildings has great potential. This paper evaluates the performance of two generic dedicated heat pump water heaters (HPWHs) in supplying the domestic hot water (DHW) needs of a medium-sized office building in Colorado. The HPWHs are sized for residential use, since no industrial-grade HPWHs were manufactured at the start of the experiment. Results are based on preliminary data measurements, and assumptions are made to compensate for a faulty flow meter. A stand-alone heat pump plumbed to a conventional tank obtains a coefficient of performance (COP) of 2.4 but only delivers load water temperatures of about 41°C (105°F) because of the 15,142 L/day (4000 gal/day) recirculating loop flow. An industrial-grade stand-alone HPWH will replace this unit, and results will be forthcoming. An integral heat pump/tank unit is being tested, but results are not available because of compressor starting problems. Recirculating loop losses account for 75% of the energy delivered by the HPWHs. These losses could be reduced by 75% if the recirculating loop were insulated, thus reducing the DHW fuel costs by 50%. The insulation expense could be paid in less than 3 years by savings in DHW fuel costs.

1. BUILDING AND HVAC EQUIPMENT DESCRIPTION

Two generic dedicated HPWHs are operated singly, for individual performance evaluation, in supplying water to the recirculating DHW system of a 4-story office building. The building houses about 200 office workers of the Solar Energy Research Institute (SERI) in Golden, Colo. The HPWHs use waste heat from a gas boiler and a compressor in an unconditioned top-floor room [58 m x 52 m (19 ft x 17 ft)], which is vented through the roof (see Fig. 1). The boiler* heats water for a closed 4-pipe space heating and cooling system that supplies the building's fan coil distribution units. The compressor operates the pneumatic thermostats. During the cooling season, the HPWHs use warm air that infiltrates from the conditioned space and the outdoors.

One HPWH is an integral unit with a heat pump housed on top a 310-L (82-gal) tank (see Fig. 2). The heat exchanger/condenser is installed in the tank bottom and is connected to the heat pump through the tank top. The other HPWH is a stand-alone heat pump hard-plumbed with flexible copper tubing to a well-insulated 159-L (42-gal) tank (see Fig. 3). Water is pumped from the tank bottom to the heat exchanger/condenser in the heat pump and back to the tank top. In each system, a heat pump extracts heat from the room air and rejects it to the tank water. R-12 is the working fluid in the refrigerant

*Rated at 2.1 million kJ/hr (2 million Btu/hr) input and 1.7 million kJ/hr (1.6 million Btu/hr) output (adjusted for altitude).

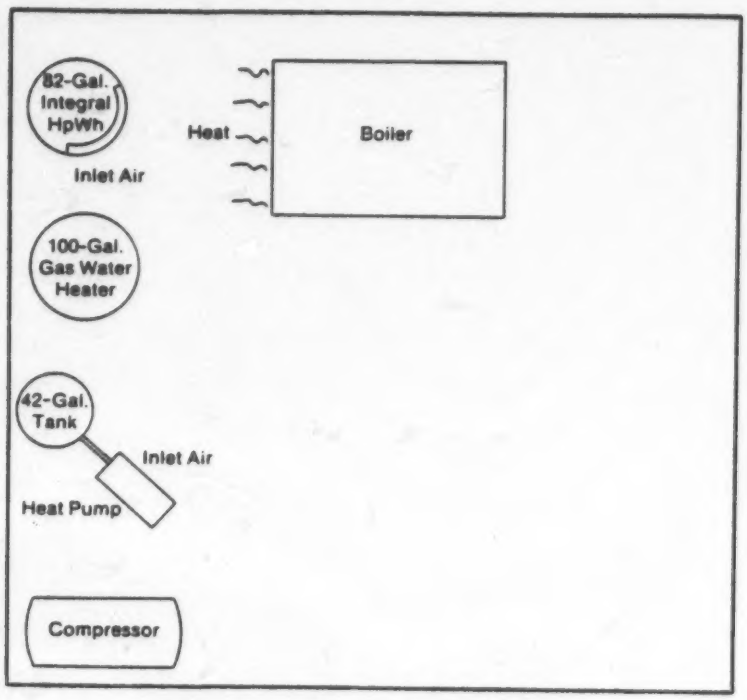

Figure 1. Boiler Room Equipment

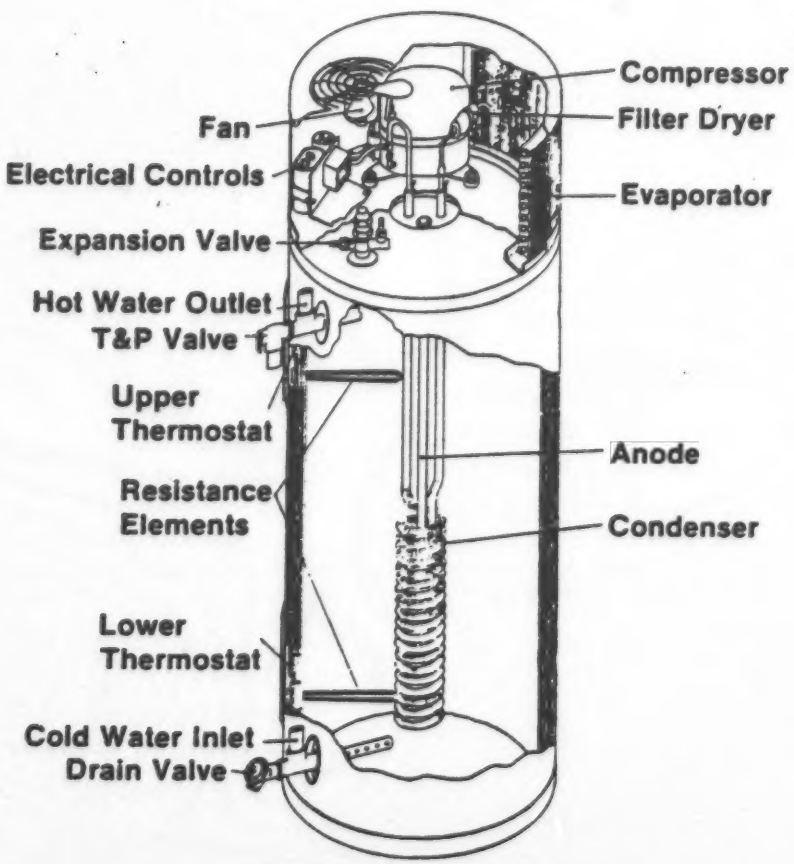

Source: [1]

Figure 2. Integral HPWH

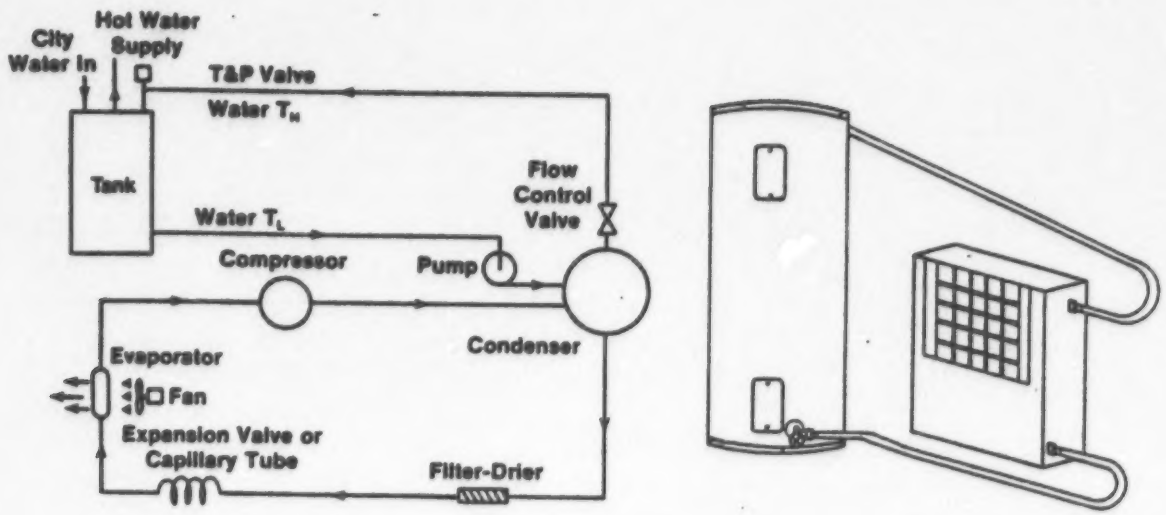

Source: [2]

Figure 3. Stand-Alone HPWH

loop of the integral unit, and R-22 is used in the stand-alone unit. A 208-volt power supply is used with 220-230-volt equipment. The HPWHs are sized for residential applications because no industrial-grade HPWHs were being manufactured at the start of the experiment. The equipment replaces the 379-L (100-gal) gas water heater (see Fig. 4) in supplying the building's hot water needs, which consist primarily of warm water for washing hands. Hot water is also used in small employee convenience kitchens on each floor and after working hours to clean the building. The delivery temperature of the water has been about 71°C (160°F) with gas water heating, but a temperature of 49°C (120°F) would be adequate for most of the building's hot water uses and would reduce the losses of the recirculating loop, tanks, and pipes. Instantaneous electric water heating units provide hot water in some kitchen areas.

This application is of special interest because the building has a large space heating load that creates substantial waste heat and a minimal water heating load. The COP of the HPWH increases as inlet air temperature increases and decreases as inlet and outlet water temperatures increase. In this application the COP is enhanced by the high room air temperature and the low outlet water temperature (relative to residential applications).

An experiment is being conducted to measure the thermal performance of each HPWH in the office building application and to analyze the thermal performance of the recirculating loop. Each can be operated in either heat pump or resistance mode. In resistance mode, the water of the integral HPWH unit is heated by two 2500-W (8532 Btu/hr) resistance elements not interlocked. In heat pump mode, heat pump operation is controlled by a thermostat near the bottom resistance element, and the top resistance element is used to assist fast recovery. The electrical usage of the heat pump alone is about 975 W (3328 Btu/hr). The thermostats are set at 49°C (120°F). In resistance mode, the water of the stand-alone HPWH system is heated by two 4500-W (15,358 Btu/hr) interlocked resistance elements. In heat pump mode, heat pump operation is controlled by a special thermostat near its bottom resistance element. No auxiliary backup is used. About 1260 W (4300 Btu/hr) of electricity are used by the heat pump. When the water drops below 49°C (120°F), water is pumped from the tank bottom, through the heat pump unit, and back to the tank top. This continues until the thermostat registers about 56°C (133°F). A variable flow control valve reduces the water flow, as necessary, to

Figure 4. HPWHs, Gas Water Heater, and Boiler

return water to the tank at a minimum of 41° C (115° F). A 62-W (1/12-hp) pump circulates water through the building to supply the DHW load. The pump is installed immediately before the tank and draws water from the loop by suction. A thermostat activates the pump when the water temperature drops below 46° C (115° F).

2. INSTRUMENTATION

Thermocouples are used to measure the cold water supply temperature, the outlet water temperature of each tank, the return water temperature of the recirculating loop, the inlet and outlet water temperatures of the stand-alone heat pump unit, and the inlet air temperature of each heat pump. The cold water supply sensor is installed on the line before it enters the boiler room to prevent radiative and convective heat gain from the boiler room equipment. Check valves and nonconductive plastic pipe are installed in the cold water supply line to the tanks and boiler to minimize nocturnal and weekend conductive heat loss back up the line. Nightly and weekend increases in cold water supply temperature readings occur, nevertheless, because the lack of water draw allows heat conduction in the stagnant pipe water. The air temperature thermocouples are installed with radiation shields to protect them from thermal radiation of the water tanks and boiler and from air currents of the HPWH evaporator fans.

Heat flux transducers are used to measure the heat flow through the tank walls. A transducer is attached on the front of each tank between the insulation and tank skin.

Another, protected by a radiation shield, is attached to the rear tank surface. Front heat loss measurements vary widely in response to boiler cycling and flue drafts. A watt-hour meter measures the quantity of electrical energy used by each system in each mode. In heat pump mode, the integral unit requires electricity for its fan and compressor; the stand-alone unit requires electricity for its fan, compressor, and water pump. Turbine flow meters, with pulse rate/voltage converters, are used to measure the flow rates of the cold water supply line and the recirculating DHW loop. An elapsed time indicator records recirculating loop pump operation. A thermocouple-activated strip chart recorder profiles boiler operation. A 16-channel data logger scans data measurements at an 8 channels/sec rate. Instantaneous and average data measurements are recorded every 5 min.

3. ANALYSIS METHODS

I calculated 24-hour COPs for weekdays (Mon-Fri), as well as separate COPs for the workday period (6:30 a.m.-8:00 p.m.) and for the nighttime period (midnight-6:30 a.m. and 8:00 p.m.-midnight). I also calculated 24-hour COPs for weekend days, but weekly COPs are estimated. HPWH performance differs for these periods primarily because of the minimal hot water usage at night and on weekends. (The circulating loss load is substantial at all times.) The COP of each HPWH is calculated as follows. The quantity of energy delivered to the recirculating loop is

$$Q_{DEL} = M_{SUPPLY} \cdot C_p(T_{OUT} - T_{SUPPLY}) + M_{CIRC} \cdot C_p(T_{OUT} - T_{RETURN}) \quad (1)$$

where M_{SUPPLY} is the mass of water delivered to the load; M_{CIRC} is the mass of water returning to the tank from the recirculating loop; T_{OUT}, T_{SUPPLY}, and T_{RETURN} are the average tank outlet, cold water supply, and recirculating return water temperatures, respectively; and C_p is the specific heat of water. The quantity of energy lost through the tank surface during a period of time t is

$$Q_{LOSS} = h \cdot t \cdot A_s \quad (2)$$

where h is the average of the heat loss rates measured at the front and rear of the tank and A_s is the tank surface area. E_{AUX}, the quantity of electrical energy supplied to the HPWHs' fan, compressor, and pump or resistance element, is calculated from the watt-hour measurements. The COP is

$$COP = \frac{Q_{DEL} + Q_{LOSS}}{E_{AUX}} . \quad (3)$$

Since the average tank water temperature is nearly the same at the beginning and end of each period of data analysis, there is no calculation of the change in internal tank energy.

An estimate of the average temperature of the water supplied to the building taps is

$$T_{LOAD} = \frac{T_{OUT} + T_{RETURN}}{2} . \quad (4)$$

T_{OUT} and T_{RETURN} are averaged during the period 6:30 a.m.-8:00 p.m. (Mon-Fri only), since virtually all of the DHW load occurs during this time. T_{LOAD} is estimated rather than measured because of the many taps in the building. (The water temperature at a tap decreases as its distance from the tank's outlet increases). An estimate of the daily quantity of energy delivered to the load is

$$Q_{LOAD} = M_{SUPPLY} \cdot C_p(T_{LOAD} - T_{SUPPLY}) \quad (5)$$

An estimate of the losses of the recirculating loop is

$$Q_{CIRC} = M_{SUPPLY} \cdot C_p(T_{OUT} - T_{LOAD}) + M_{CIRC} \cdot C_p(T_{OUT} - T_{RETURN}) \quad (6)$$

where the first term is an estimate of the energy lost between the tank outlet and the tap by the water delivered to the load. The second term is an estimate of the energy lost by the water returning to the tank as it passes through the entire recirculating loop.

4. PERFORMANCE RESULTS

Preliminary results are presented for measurements taken in April 1981 immediately following completion of instrumentation. Performance analysis is only given for the stand-alone HPWH because the integral HPWH is experiencing compressor starting problems. Typical weekday and weekend results for the stand-alone HPWH, operating in heat pump mode, are presented in Tables 1-3. Because there is a transition in HPWH performance at the beginning and end of the weekend, weekday results are given for a Tuesday and weekend results are given for Saturday noon to Sunday noon.

Daytime ambient high temperatures are about 23°C (73°F) and nighttime lows are about 7°C (44°F) during the period of data collection. The frequency and duration of boiler operation, and thus waste heat availability, are inverse functions of ambient temperature. The boiler is sized to maintain 20°C (68°F) indoor building temperature at -23°C (-10°F) outdoor temperature with continuous operation. During the period of data collection, the boiler cycling varied from 2.5-min duration every 5 min on colder nights to 1-min duration every 30-45 min on warmer afternoons.

The stand-alone HPWH obtains a COP of about 2.3 at night and on the weekend during periods of time when there is little or no draw. This validates the performance predicted by the manufacturer's literature (see Fig. 5) for the average heat pump inlet air and water temperature of 23°C (73°F) and inlet water temperature of 40°C (104°F). Because of a faulty supply water flow meter, the quantity of water drawn at the taps is unknown. Based on the validation of the manufacturer's performance curves (see Fig. 6) at night and on the weekends, it is assumed that an average of 11,600 kJ (11,000 Btu/hr) of energy are transferred by the heat pump to the water during the Tuesday workday when heat pump inlet air and water temperatures average 23°C (74°F) and 35°C (95°F), respectively. From an energy balance on the tank, it is estimated that approximately 871 L (230 gal) of water were drawn at the taps that day. The resultant calculated workday COP of 2.6 is subject to considerable uncertainty.

On weekdays the stand-alone heat pump operates continuously because the HPWH is sized for residential installation and cannot maintain sufficiently high tank outlet water temperatures. A larger capacity industrial-grade heat pump would facilitate heating the 7570-15,140 L/day (2000-4000 gal/day) recirculating return flow. The 19-mm (3/4-in.) copper tubing of the HPWH restricts the flow of the 25-mm (1-in.) pipe of the recirculating loop. In addition, a valve restricts flow through the stand-alone heat pump unit to 5.7-7.6 L/min (1.5-2.0 gal/min). Since the recirculating flow is about 10.6 L/min (2.8 gal/min), a large amount of water bypasses the heat pump and goes directly to the tank outlet. This water is warmed only by mixing with hot water at the tank top. The average tank outlet water temperature of 39°C (102°F) weekdays is lower than optimum and is lower than the heat pump outlet water temperature of 46°C (114°F) because of the water which bypasses the heat pump. The average tap water temperature near the end of the recirculating loop of 37°C (99°F) on weekdays is even lower. The average outlet water temperature of the heat pump, 46°C (114°F), is approximately the expected design value from its average inlet water temperature of 35°C (95°F). The tank heat loss rate for the stand-alone HPWH is about 23 kJ/hr-°C (12 Btu/hr-°F). Air temperature readings near the tank are 21°-24°C (70°-75°F), and average tank outlet temperatures are 39°-48°C (102°-118°F).

Table 1. STAND-ALONE HPWH OPERATION

Tuesday, April 15

	6:30 am-8:00 pm	Midnight-6:30 am 8:00 pm-Midnight	Daily
Quantity of Water to Load	871 L (230 gal)	0	871 L (230 gal)
Quantity of Water Returning from Recirculating Loop	8483 L (2241 gal)	6677 L (1764 gal)	15,161 L (4005 gal)
Cold Water Supply Temperature	13°C (56°F)	—	13°C (56°F)
Tank Outlet Water Temperature	39°C (102°F)	44°C (111°F)	41°C (106°F)
Recirculating Return Water Temperature	37°C (99°F)	40°C (104°F)	38°C (101°F)
Heat Pump Inlet Air Temperature	23°C (74°F)	21°C (70°F)	22°C (72°F)
Heat Pump Inlet Water Temperature	35°C (95°F)	38°C (101°F)	37°C (98°F)
Heat Pump Outlet Water Temperature	46°C (114°F)	46°C (115°F)	46°C (114°F)
Energy Delivered to Taps	9.0×10^4 kJ (8.5×10^4 Btu)	0	9.0×10^4 kJ (8.5×10^4 Btu)
Energy Delivered to Recirculating Loop	1.5×10^5 kJ (1.4×10^5 Btu)	1.1×10^5 kJ (1.0×10^5 Btu)	2.6×10^5 kJ (2.4×10^5 Btu)
Energy Lost in Recirculating Loop	6.0×10^4 kJ (5.9×10^4 Btu)	1.1×10^5 kJ (1.0×10^5 Btu)	1.7×10^5 kJ (1.6×10^5 Btu)
% of Energy Delivered to Loop that is Lost	42%	100%	65%
Tank Heat Loss Rate	21 kJ/hr-°C (11 Btu/hr-°F)	25 kJ/hr-°C (13 Btu/hr-°F)	23 kJ/hr-°C (12 Btu/hr-°F)
Energy Lost Through Tank Surface	3987 kJ (3784 Btu)	5443 kJ (5163 Btu)	9430 kJ (8947 Btu)
HPWH Electrical Usage Rate	1257 W (4290 Btu/hr)	1260 W (4300 Btu/hr)	1258 W (4293 Btu/hr)
Electrical Energy Supplied to HPWH	6.1×10^4 kJ (5.8×10^4 Btu)	4.7×10^4 kJ (4.5×10^4 Btu)	1.1×10^4 kJ (1.0×10^4 Btu)
HPWH COP	2.6	2.4	2.5

Table 2. STAND-ALONE HPWH PERFORMANCE

Saturday-Sunday, April 11, 12
12:00 Noon - 12:00 Noon

Quantity of Water to Load	0
Quantity of Water Returning from Recirculating Loop	7192 L (1900 gal)
Tank Outlet Water Temperature	48°C (118°F)
Recirculating Return Water Temperature	40°C (104°F)
Heat Pump Inlet Air Temperature	24°C (75°F)
Heat Pump Inlet Water Temperature	44°C (111°F)
Heat Pump Outlet Water Temperature	48°C (118°F)
Energy Delivered to Taps	0
Energy Delivered to Recirculating Loop	2.3×10^5 kJ (2.2×10^5 Btu)
Energy Lost in Recirculating Loop	2.3×10^5 kJ (2.2×10^5 Btu)
% of Energy Delivered to Loop that is Lost	100%
Tank Heat Loss Rate	27 kJ/hr-°C (14 Btu/hr-°F)
Energy Lost Through Tank Surface	13,000 kJ (12,000 Btu)
HPWH Electrical Usage Rate	1252 W (4273 Btu/hr)
Electrical Energy Supplied to HPWH	1.1×10^5 kJ (1.0×10^5 Btu)
HPWH COP	2.3

Table 3. STAND-ALONE HPWH PERFORMANCE

Weekly Performance Results (Estimated)

COP	2.4
% of Energy Supplied to Recirculating Loop that is Lost	76%
% of Energy Supplied to Water by Heat Pump and Lost Through Tank Surface	5%

The recirculating loop pump operates almost continuously on weekdays during HPWH operation because the recirculating return water temperatures are below its thermostat set point temperature of 46°C (115°F). The reduction in recirculating flow on the weekend is because of decreased pump operation. Parasitic power consumption would be included in system efficiency calculations if performance comparisons were being made between HPWH and conventional DHW systems.

To comply with building codes, the stand-alone heat pump was hard plumbed to its tank instead of being attached with the supplied nylon hoses. Because of the quantity of dust in the boiler room, it is necessary to periodically clean the heat pump evaporator grills. Both HPWHs are equipped to handle condensate resulting from the dehumidification effects of operation. Because the office building is located in the dry climate of Colorado, condensate is not noticeable.

5. ECONOMIC ANALYSIS

The present nonsubsidized cost of each of the HPWH systems used in the experiment is about $1100-$1200 including tank and installation. HPWH purchases can cost less in demonstration programs and are eligible for tax credits and utility subsidies in some states. An industrial-grade stand-alone HPWH unit with 4 times the capacity of the experimental equipment is now being marketed at a wholesale cost of $2000 without tank or installation.

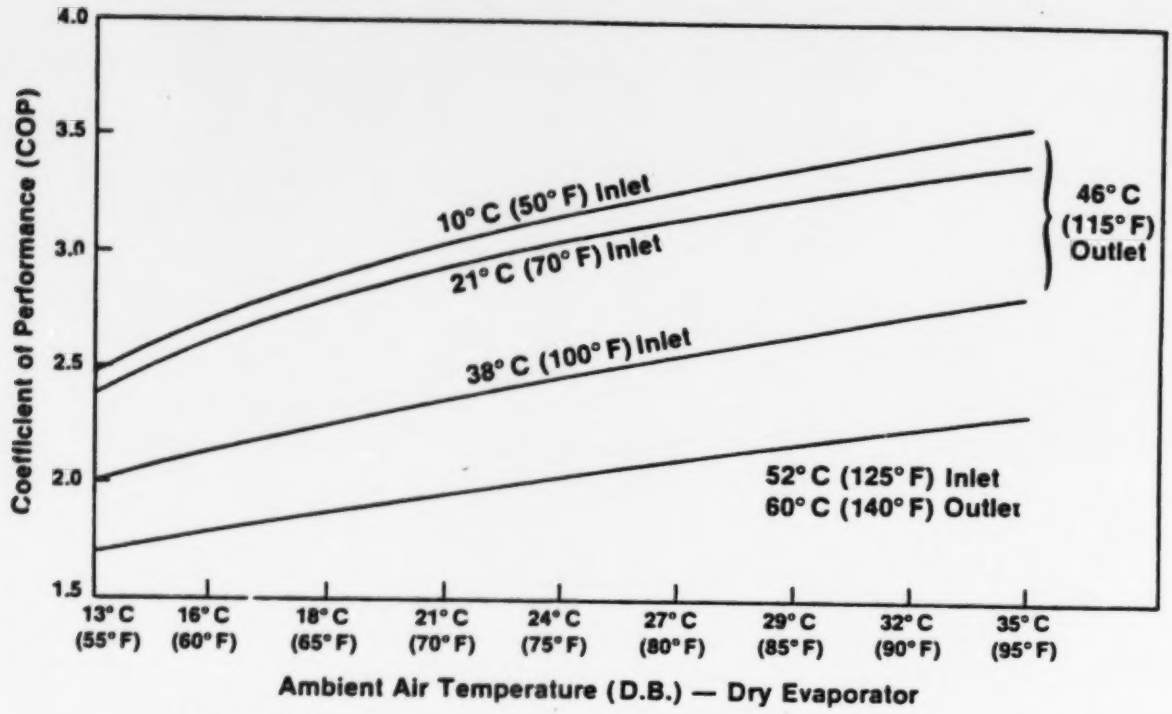

Source: [2]

Figure 5. COP vs. Ambient Temperature for Stand-Alone HPWH

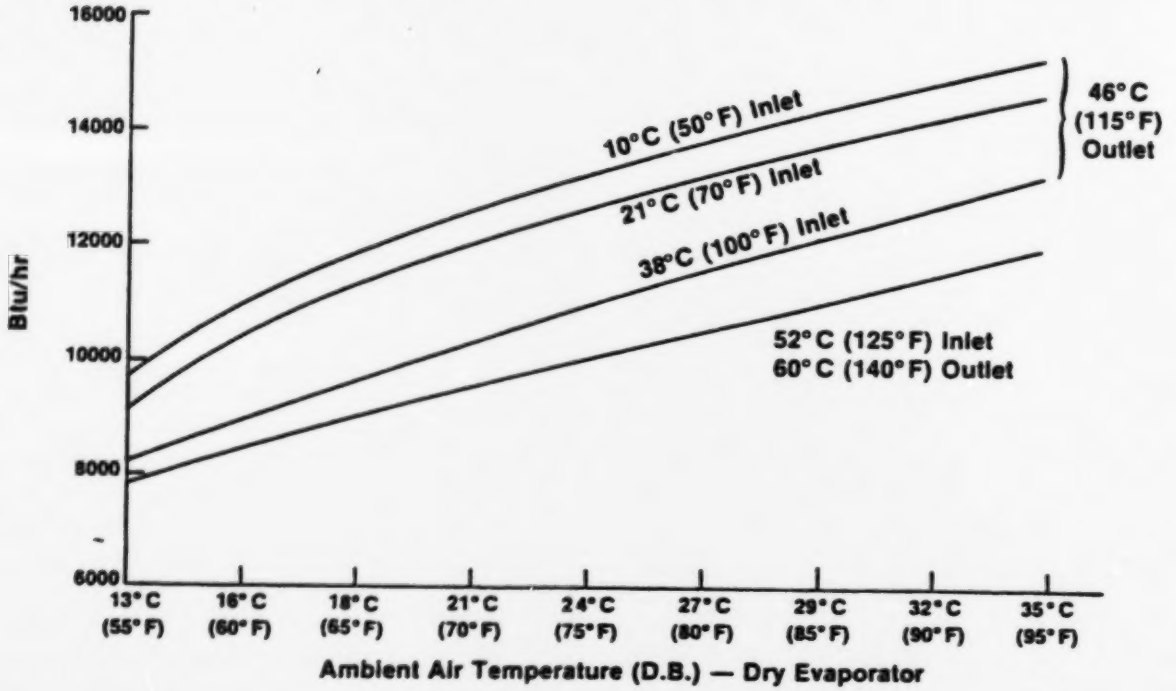

Source: [2]

Figure 6. Heating Rate vs. Ambient Temperature for Stand-Alone HPWH

The gas water heater had been operated with a set point temperature of 71°C (160°F). Recirculating loop losses are greatly decreased by the lowered tank outlet temperatures to the loop. Even so, about 75% of the energy delivered to the loop by the HPWHs is lost; 25% is delivered to the taps. The energy delivered by the HPWHs to the water also includes tank losses, which are about 5% of the total.

When the stand-alone HPWH is operating, the average daily and weekend recirculating water temperatures are 40°C (104°F) and 44°C (111°F), respectively. If an average building air temperature of 32°C (72°F) is assumed, the rates of heat loss of an insulated recirculating loop would be 1839 kJ/hr (1743 Btu/hr) and 2240 kJ/hr (2124 Btu/hr), respectively [3] instead of the measured values of 7032 kJ/hr (6667 Btu/hr) and 9668 kJ/hr (9166 Btu/hr). This represents an approximate by 75% reduction in recirculating loop losses and more than a 50% reduction in the energy required for domestic water heating. The recirculating loop losses benefit the space heating load but penalize the space cooling load. To maintain a constant building temperature, space heating and cooling occur simultaneously in various parts of the building during most months of the year. Thus, it is difficult to determine the space conditioning impacts of the losses.

The installed cost of fiberglass pipe insulation for commercial buildings is about $7.38-$8.20/m ($2.25-$2.50/ft). The recirculating loop is 244-m (800-ft) long, it could be insulated in new construction for a total of $1,800-$2,000. At present electricity costs in Golden, Colo., the monthly DHW electricity bill for the stand-alone HPWH is $122. If this cost were reduced to $60 with recirculating loop insulation, the pay-back of the insulation would be less than 3 years. The reduced heat loss of insulated pipe with water at temperatures of 49°C (120°F) or higher would represent even larger monthly dollar savings.

6. CONCLUSIONS

The stand-alone HPWH obtains a weekly COP of 2.4 in heating the 871 L/day (230 gal/day) draw and the 7570-15,140 L/day (2000-4000 gal/day) recirculating loop flow. However, because it is sized for residential applications, the HPWH is only able to maintain workday tank outlet water temperatures of about 41°C (106°F). This is less than the desirable temperature level of 49°C (120°F). SERI will replace the present HPWH with a newly marketed, high-capacity industrial-grade stand-alone HPWH and will test its performance in supplying the office building's DHW needs. Industrial-grade stand-alone HPWHs should prove to be high performing and more cost-effective than resistance water heaters. Performance analysis of the integral HPWH will be forthcoming after equipment repairs are made.

Approximately 75% of the energy delivered to the recirculating loop is lost from the uninsulated pipes. If the loop were insulated, the losses would be reduced by 75% thus reducing the monthly fuel bills for DHW by 50%. The cost of insulation could be paid in less than 3 years with savings in DHW fuel costs.

ACKNOWLEDGMENTS

I wish to express appreciation to the members of the SERI Building Systems Development Branch Performance Testing Group and to Michael Holtz, Henry Kelly, Dave Claridge, Joel Swisher, and Dick Murphy.

REFERENCES

1. Energy Utilization Systems, Inc., Demonstration of a Heat-Pump Water Heater vol. 1, Design Report, Oak Ridge National Laboratory, ORNL/SUB-7321/3, Oak Ridge, TN, 1979.

2. E-Tech, Inc., "Efficiency II Water Heating Heat Pump" (Manufacturer's Literature), E-Tech, Inc., Atlanta, GA, 1981.

3. Owens/Corning Fiberglas, "Mechanical Insulation Systems" (Manufacturer's Literature), Owens/Corning, Fiberglas Tower, Toledo, OH, 1981.

BIBLIOGRAPHY

1. Energy Utilization Systems, Inc., Research and Development of a Heat-Pump Water Heater, vols. 1 and 2, Final Summary Report, Oak Ridge National Laboratory, ORNL/SUB-7321/1, Oak Ridge, TN, Aug. 1980.

2. Energy Utilization Systems, Inc., "Status of Field Demonstration of TEMCOR Heat Pump Water Heater," (Manufacturer's Literature), Energy Utilization Systems, Inc., Pittsburg, PA, Apr. 1980.

3. Energy Utilization Systems, Inc., "TEMCOR, Heat Pump Water Heater," (Manufacturer's Literature), Pittsburg, PA, 1981.

4. E-Tech, Inc., "Efficiency II Water Heating Heat Pump, Field Test Data" (Manufacturer's Literature), E-Tech, Inc., Atlanta, GA, 1981.

5. E. Hirst, "Is Solar Really the Best Way?" ASHRAE Journal, p. 60-62. Jan. 1980.

6. Louise Morrison and Joel Swisher, "Analysis of the Performance and Space Conditioning Impacts of Dedicated Heat Pump Water Heaters," Proceedings of the ASME Systems Simulation and Economic Analysis Conference, Reno, NV, 1981.

7. D. O'Neal, J. Carney, and E. Hirst, Regional Analysis of Residential Water Heating Options: Energy Use and Economics, Oak Ridge National Laboratory, ORNL/CON-31, Oak Ridge, TN, Oct. 1978.

8. E. Powell, "New Energy-Saving Heat Pump Water Heater," Popular Science, vol. 216, no. 4, pp. 49-52, 57, April 1980.

9. Purdue University, Proceedings of the Conference on Waste Heat Recovery for Energy Conservation-Residential and Light Commercial Heat Pumps, Air Conditioning, and Refrigeration Systems, DOE Report CONF-800966, West Lafayette, IN, 1980.

10. State Industries, Inc., "Censible 5 Energy Efficient, Residential Round Electric Water Heater with Foamite Insulation" (Manufacturer's Literature), State Industries, Inc., Ashland City, TN, 1980.

11. Tennessee Valley Authority, Heat Pump Water Heater Field Test, Interim Report, Load Management Branch, Chattanooga, TN, 1980a (Summer).

12. Tennessee Valley Authority, Summary of the DOE/TVA Heat Pump Water Heater Workshop, Chattanooga, TN, April 1980b.

13. C. A. Wan, Energy Test Method Development for Electric Heat Pump Water Heaters, National Bureau of Standards, NBSIR 79-1951, Washington, D.C., Jan. 1980.

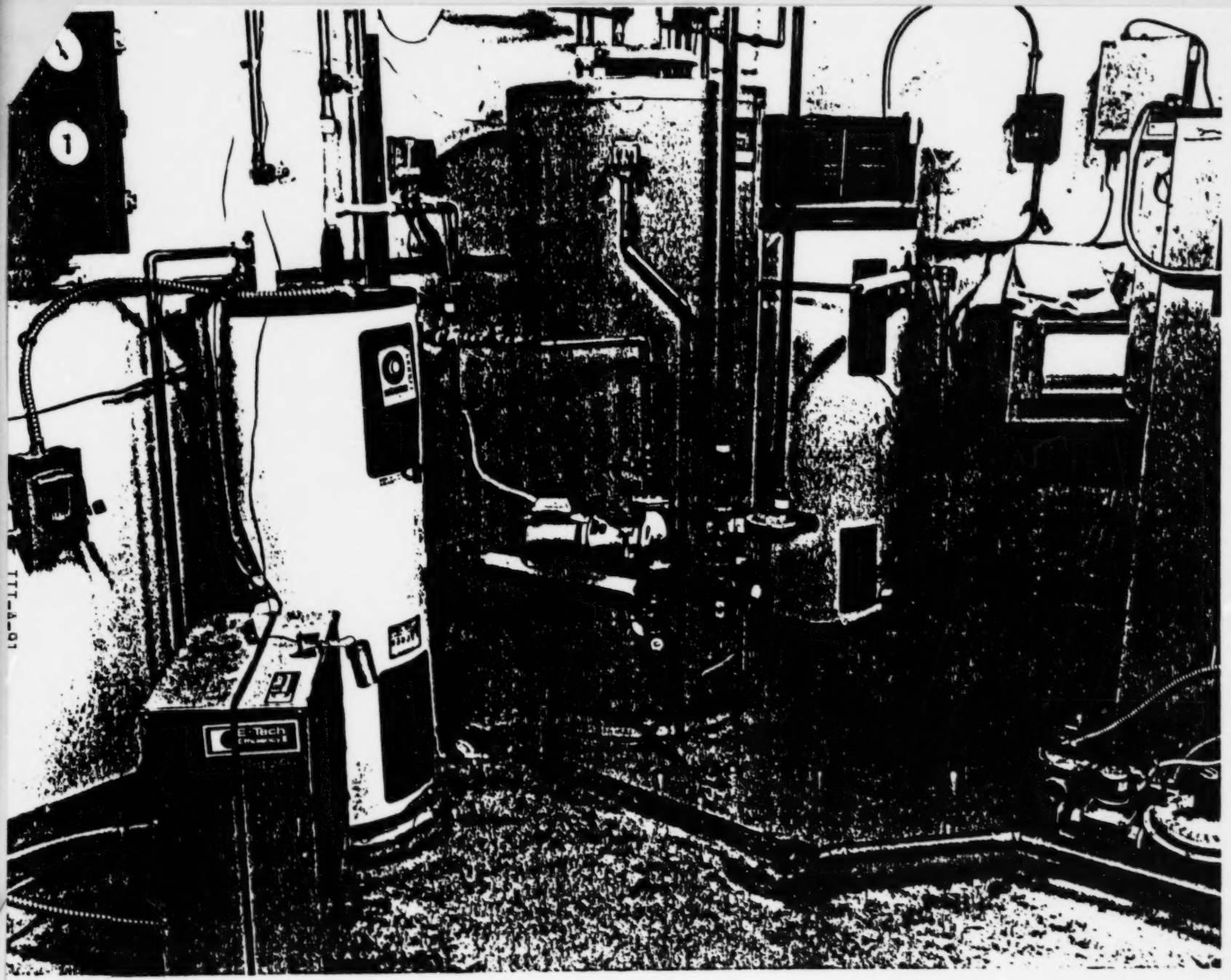

TTT-A-01

PB82-227976

HEAT TRANSPORT SYSTEM FROM A SWISS WASTE INCINERATION PLANT TO INDUSTRIAL CONSUMERS AND TO A DISTRICT HOSPITAL

Edgar Gautschi
Motor-Columbus Consulting Engineers, Inc.
CH-5401 Baden, Switzerland

ABSTRACT

Due to the increased prices of primary energy, heat utilization from civil vaste incineration plants is becoming increasingly competitive despite the heavy investments involved. Three kinds of heat utilization are discussed: heat production, electricity production and combined heat and electricity production. For the extension of the Buchs incineration plant in Switzerland, the evaluation of the marginal conditions led to the selection of a heat production scheme which will supply process steam to industrial consumers, and hot water to a district hospital which will be provided with heat accumulators. The supply commitments and the load variations, as well as the yearly overhaul shutdown of the incinerator pointed to a project with a variable load incineration furnace, a small additional boiler to cover the peaking demands, and an oil/gas fired boiler capable of taking over the heat generation during the overhaul periods in summer. The costs of generated thermal energy are shown.

A. POSSIBILITIES OF WASTE HEAT UTILIZATION FROM INCINERATION PLANTS

Considering the increasing prices of primary energy, heat utilization from incineration plants is becoming increasingly economical and, therefore, interesting despite the necessary investments.

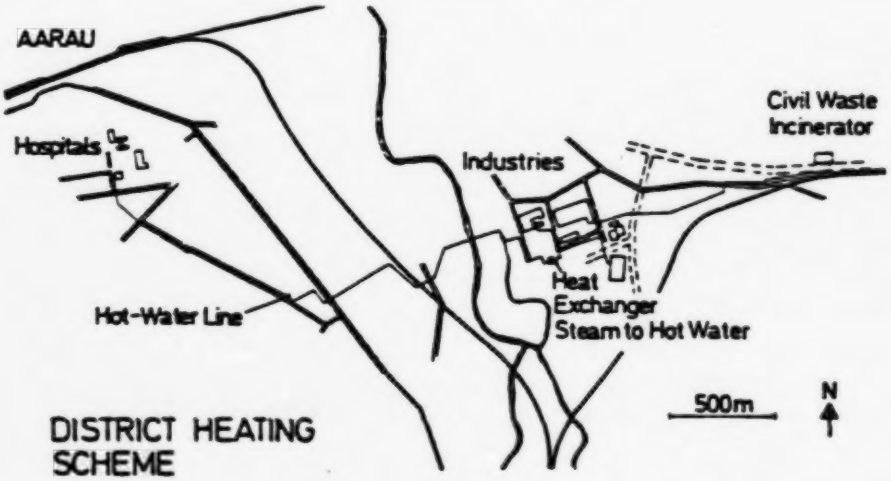

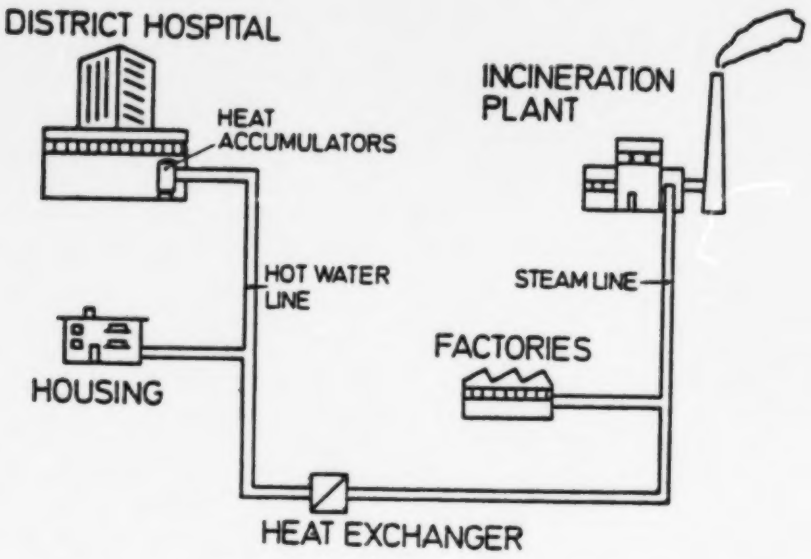

At the present state-of-the art the following three heat utilization possibilities are technically feasible and meaningful:

(1) Heat production and supply (by means of heat distribution lines to nearby consumers)

(2) Electricity production and supply

(3) Heat as well as electricity production and supply (combined heat and electric power generation)

(1) Heat Supply

A meaningful utilization of waste heat is generally the supply of steam or hot water to industry, commercial business or for comfort heating purposes. For the supply of heat, a continuous operation of the incineration plant is absolutely necessary. In addition a replacement unit operated with conventional fuels (oil, gas, coal etc.) should be available to take over the heat supply commitments during overhaul periods of the waste incineration plant.

A pre-requisite for an economic heat supply is the presence of sufficiently large consumers taking as much as possible of the available heat. This spectrum of consumers should be so arranged that a base load of large consumers is able to establish an equilibrium between heat generation and heat demand. Therefore, having continuous industrial process heat consumers is extremely advantageous, since they represent an economically desired base load.

(2) Electricity Generation

If there is no heat demand at all, or if the supply conditions are unfavourable (small amounts, large distances), a quite different type of heat utilization must be considered. In this case, and if the amount of waste has a certain volume, the production and supply of electricity seems to be the only reasonable way. Electricity generation and supply is relatively simple and can be

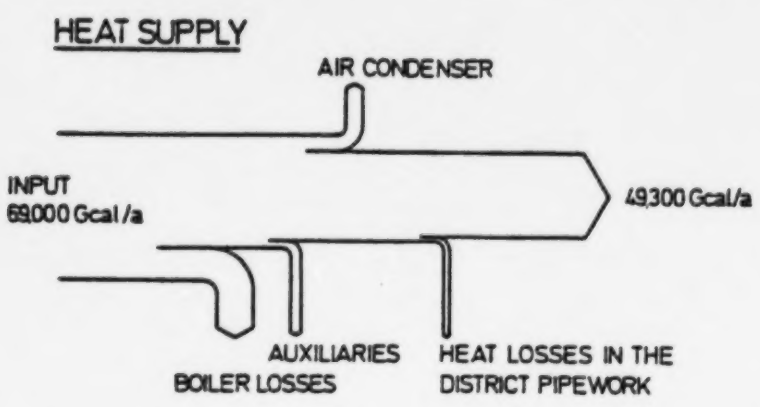

INVESTMENTS 22.0 Mio SFr.
ANNUAL RUNNING COSTS AND
ADDITIONAL FUEL 1.98 Mio SFr.

done at any time even if the prices are not always interesting.

Waste incineration itself must not consider outside conditions (heat demand) and is, therefore, usually simpler. The necessity of an additional boiler is generally limited to startup operations (since no electricity supply commitments must be met).

(3) Combined Heat and Electric Power Generation

If the heat supply possibility is relatively small or subjected to large variations in the amount of heat (e.g. large difference between summer and winter heat demand), it is usually reasonable to realize a combined heat and electric power generation system.

Since, due to expensive district heat lines, a combined heat and electric power generation is only considered if good possibilities for heat supply exist, the heat supply is the main objective. Therefore, the operation of the waste incineration plant must consider heat supply in accordance with demand, i.e. continuous operation with additional boiler.

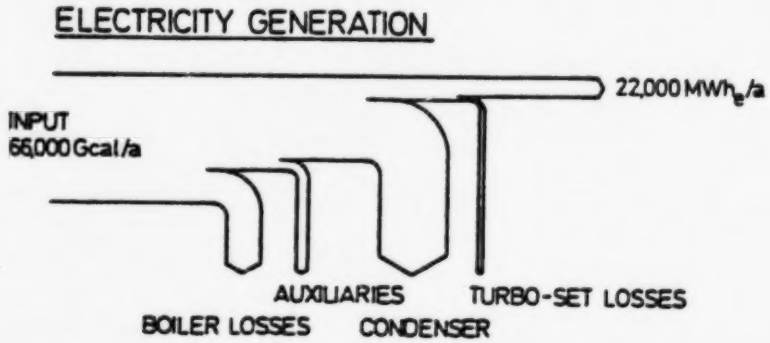

INVESTMENTS 23.0 Mio SFr.
ANNUAL RUNNING COSTS 1.8 Mio SFr.

B. THE MOST FAVOURABLE POSSIBILITY OF HEAT UTILIZATION

The recommendation of the Swiss Overall Energy Concept (GEK) calls for substitution of oil products and clearly leads to the concept of heat utilization by heat supply to consumers presently burning fuel oil.

The heat demand of industrial consumers in the area and of the cantonal hospital at Aarau is high enough to give preference to heat supply from the nearby incineration plant, rather than to electricity production.

Generally, the waste heat utilization in this case is as follows:
The existing Buchs waste incineration plant will be extended by a third incineration unit equiped with a steam vessel. Some of the steam will be delivered via a 1,5 km long district heating line to the industrial facilities. The remaining steam is used for the generation of hot water in a heat exchanger at the end of the steam line which is then supplied to the cantonal hospital via a 3 km long hot water line. Due to the availability of heat storage at the hospital, heat can be supplied even at times with little demand, thereby improving the heat supply conditions.

This concept of heat utilization in the Buchs incineration plant allows 80 % of the heat produced from the waste to be supplied as useful heat.

In addition to the heat produced from the waste and because of supply commitments, approx. 7 % per year must be produced by the oil/gas fired boilers. These boilers take over the peak load in winter and the full heat supply to the industry during one summer month, while the Buchs incineration plant is being overhauled.

C. THE CONCEPT

Supply Commitments

Based on the concept (and the heat supply contracts), the continuous supply of heat from the incineration plant is an obligation. This puts even

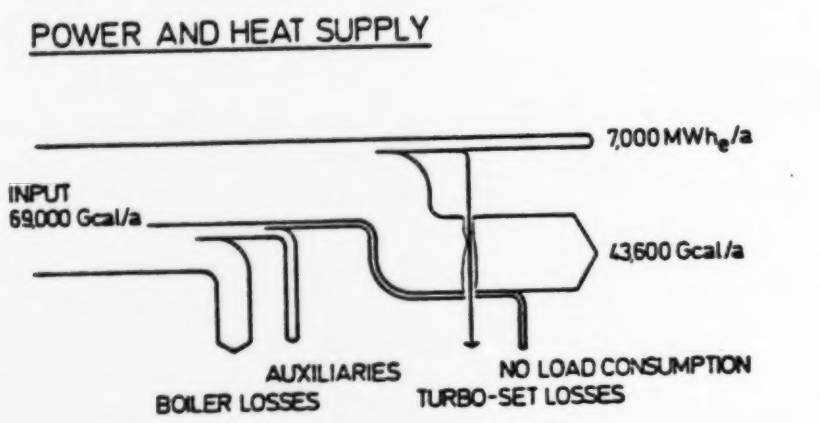

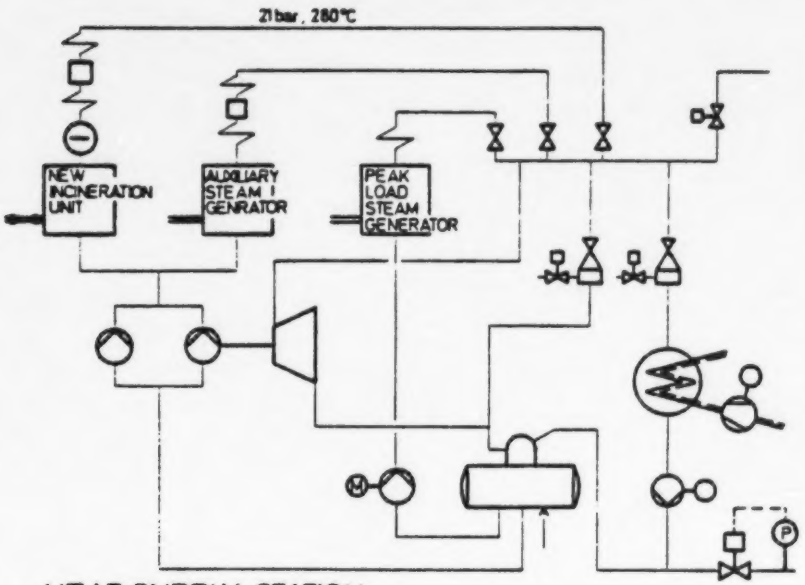

HEAT SUPPLY STATION

more emphasis on the important criterion of operational reliability of the waste incineration plant. No unusual shut-downs due to incidents should occur, since the oil/gas boilers would have to take over. The scheduled plant overhaul should only take place in a month with small waste quantity and little heat demand (July or August). Through special construction characteristics a guaranteed operation time of 8,000 hours/year must be achieved.

- Heat Transportation System

The required high operational security of the system, and full reliability of heat supply to the industry, as well as consideration of minimum investment and operational costs, led to the selection of a steam line for the heat supply to industry, and a hot water line for heat supply to the hospital.

- Additional Fuels

The chosen heat utilization concept and the heat demand of the consumers limit the use of additional fuels to relatively small amounts for peak loads during the winter months and for the overall heat production during overhaul periods of the waste incineration system.

According to the present market situation and consideration of possible additional fuels, heavy oil is suggested as main energy source. However, dual-purpose boilers with the possibility of switching to natural gas will be installed.

- Technical Design for Firing the New Furnace/Boiler Unit

To reduce the firing of additional fuel, the incineration furnace is being designed to allow load variations between 60 and 100 %, thus improving waste economy by operating at reduced output during the night.

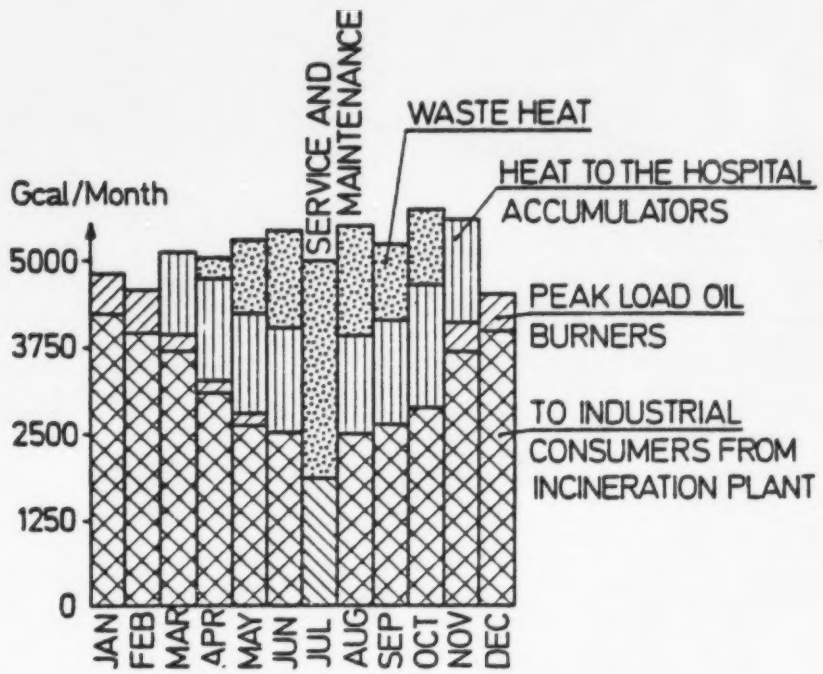

The Plant

1. The Waste Incineration Plant

The heart of the new waste incineration scheme as a heat production plant is the new waste-fired steam vessel. The vessel is equiped with a steam superheater and a hot steam temperature control, in order to have the necessary superheat for covering the heat loss in the relatively long steam line. The steam produced in the vessel is supplied to the main steam distributor of the plant. This steam distributor is also supplied by the two additional oil fired boilers. During winter time the small additional boiler is in parallel operation with the waste boiler and its output is controlled by the pressure in the live steam line. The large additional boiler is in operation only in summer to generate the heat required by the industrial consumers. The main feed water pumps are driven by steam turbines in order to reduce the purchase

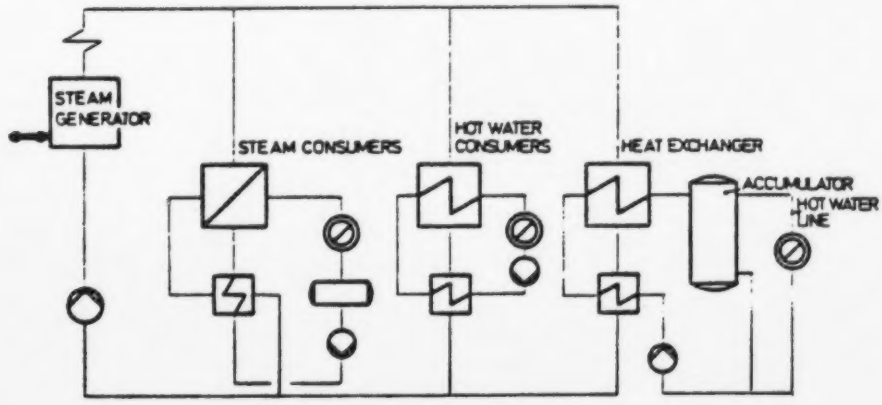

HEAT TRANSPORTATION SYSTEM

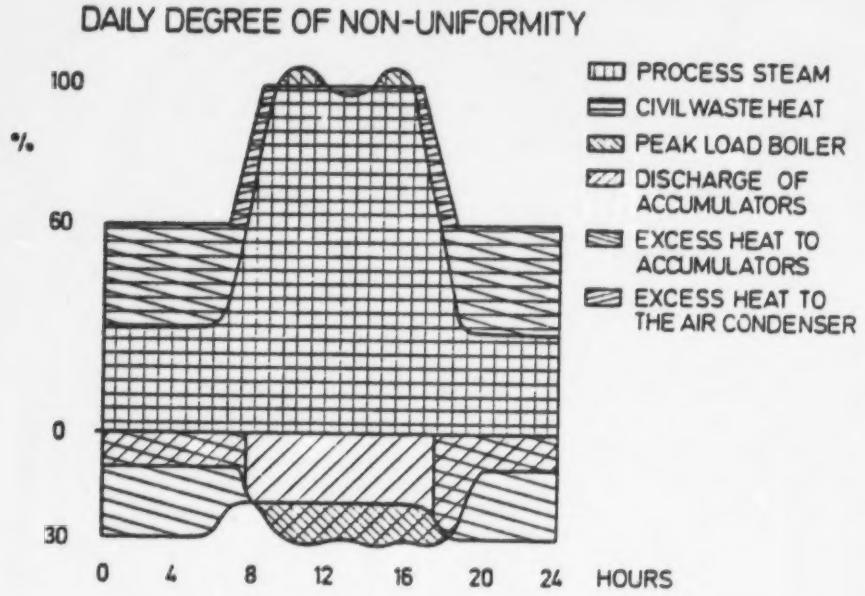

of electricity from the public network. The small additional boiler (5 t of steam per hour) is equipped with two motor-driven feedwater pumps.

During periods with little steam demand, the excess steam is precipitated in the existing air-cooled condenser.

2. The Steam District Heating System

- The superheated steam with an operating overpressure of 21 bar and a temperature of 280 °C is transported via the steam line to the transforming stations of the various consumers.

- Every 200 m the steam line is equipped with a condensate collection tank. This is necessary for start-up operations, in order to keep the steam line

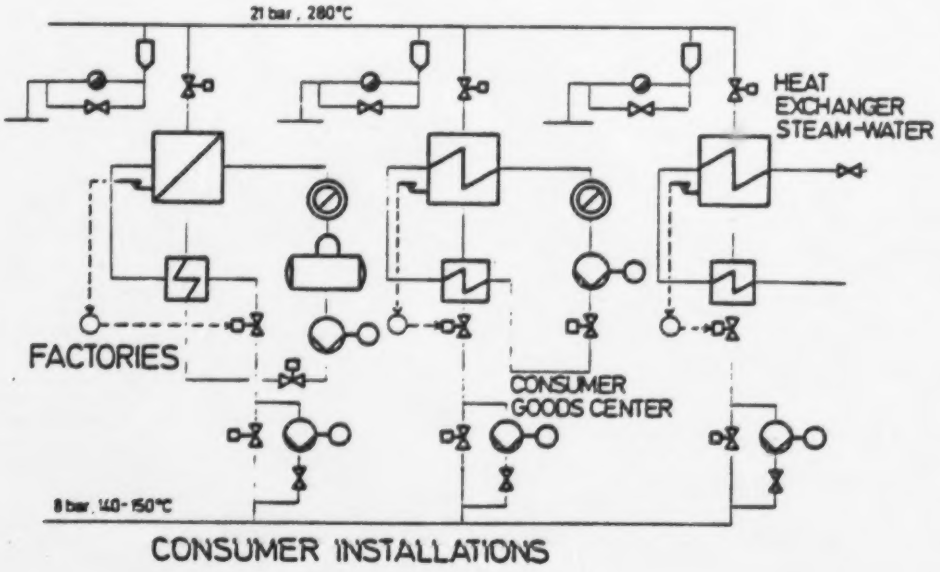

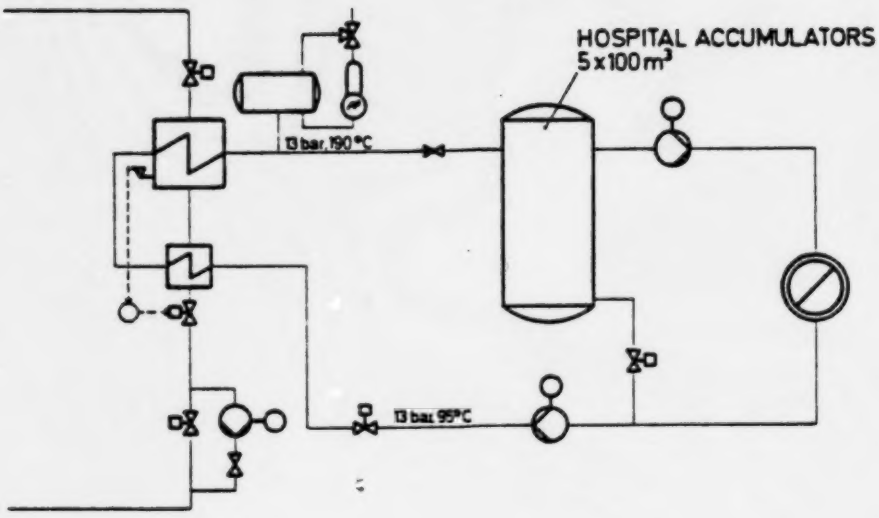

dry. During operation the steam line will remain dry, since superheated steam is transported.

- The steam condensed in the consumer's sub-stations is transported back by the live steam pressure into the feedwater tank of the incineration plant via the condensate line. For start-up operations, electrically driven pumps are used on a temporary basis.

The Hot Water District Heating System

- The hot water, with a temperature of 190 °C and an operating overpressure of 13 bar, is produced from steam in the transforming station in the industrial area.

- Pumps in the substation supply hot water from the transforming station to the hospital from where heat is transported via heat accumulators to the internal hot water grid.

- The expansion vessel installed in the substation of the industrial area has the following functions:

  -- absorption of hot water expansion
  -- pressure control
  -- level control with water supply

To improve operational reliability of the hot water district heating system the installation of an additional heat source is necessary, in order to avoid evaporation in the hot water system in case of rapid heat loss on the primary side (steam). This auxiliary boiler is fed by the public electricity network.

4. Heat Production Accounting

The heat units produced in the incineration plant and supplied to the consumers via the district steam line, as well as the heat units of the returning

condensate are registered in the plant, added, totalised and displayed on a counter. Simultaneously, heat output and steam temperature and overpressure are registered.

5. Heat Consumption Accounting

Each heat consumer has a heat metering device as described above. To achieve correct results, in particular mass flow accounting must be individually considered for every consumer.

E. THE AVERAGE HEAT PRODUCTION AND TRANSPORTATION COSTS

The average annual amounts of heat supplied by the waste incineration plant are, in 1985, 49,300 Gcal/ year (industry: 25,900 Gcal; hospital: 23,400 Gcal).

The running costs with 15 years depreciation and 4,5 % interest,	1.98 million Sfr.
= average production costs per Gcal at the entry of steam line	Sfr. 40.30

For the industrial connections, i.e. the fully supplied heat consumers of the steam net, the costs will increase by those factors necessary for construction and operation of the steam line.

The running costs with 15 years depreciation and 4.5 % interest,	0.51 million Sfr.
per Gcal:	Sfr. 10.40
= average steam production costs at consumers entry	total = Sfr. 50.70

For the hot water net, the costs will increase by the depreciation and operation of the hot water district line.

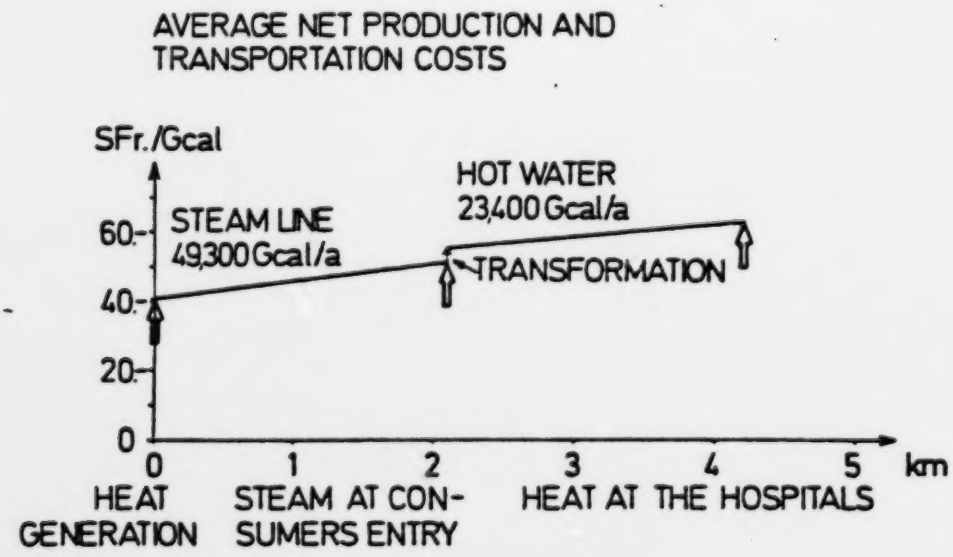

BREAKDOWN OF HEAT UNIT COSTS

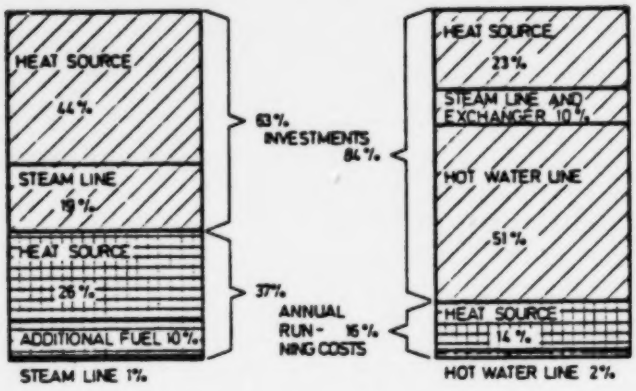

The running costs with 25 years depreciation and 4.5 % interest per Gcal	0.58 million Sfr.
	Sfr. 11.80
= average hot water costs at the hospital	total = Sfr. 62.50

For heavy-oil fuelled boilers, the average heat production costs per Gcal of steam are between Sfr. 50.00 and 60.00. These costs will have the tendency to increase rapidly in the near future, mainly for the following reasons:

1) The generally expected price increase for mineral oil

2) Ever more light components such as gasoline, light oils, etc. are being extracted from crude oil, causing the remaining heavy oils to get scarce and, therefore, more expensive, while at the same time decreasing their calorific value and increasing their sulphur contents.

3) The increasing environmental impact due to heavy oil sulfur emission through stacks will have to be restricted. This will lead to expensive flue gas cleaning processes.

Whilst today the competitiveness of heat from waste incineration is still only modest, the situation will undoubtedly change in the near future.

F. THE PORTIONS OF THE VARIOUS COST COMPONENTS OF THE AVERAGE HEAT PRODUCTION COSTS OF THE CONCEPT

The costs arising from the incineration itself are not considered in these calculations, since they are borne by the waste disposal corporate entity. Only heat utilization is charged to the heat supply calculations.

For the steam network the costs per Gcal supplied are as shown in the left figure. It can be seen from the figure that the depreciation costs take a considerable portion of the heat extraction and transportation costs (total 63 %).

Considering the average heat production costs for the hot water network, the following division of various components will result (right side of fig-

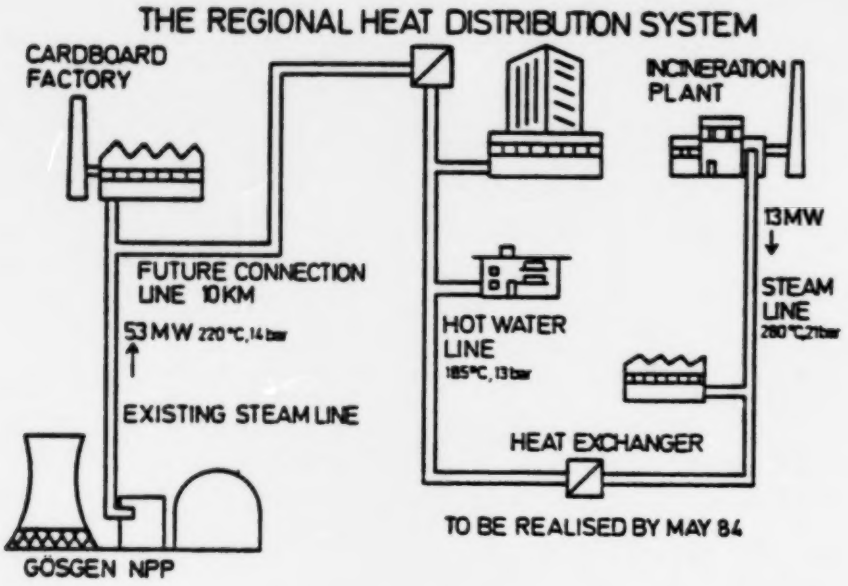

ure). The high depreciation costs are due to the necessary investments for energy transformation (steam/hot water) and the long transportation distance.

G. GOVERNMENTAL SUPPORT

Since the usual energy sources, for well-known reasons, have become very expensive, and their prices will further increase, it is essential to utilize new energy sources. The responsible cantonal authorities have requested government and communities to give the necessary support to the project.

With pre-investments and acting as a coordinator, the Canton of Argovia has shown its readiness to support and realize the project. The financial engagement of the Canton is subject to negotiations. However, in May 1984 the first industrial facility will be fully supplied with district heat.

H. THE REGIONAL HEAT SYSTEM

In the future, the hot water district line could also be supplied with heat from the Gösgen nuclear power plant, located some 12 km away, and which is already supplying heat to a cardboard factory. A region with a population of approx. 25,000 can be supplied with comfort and process heat through a 10 km long pipeline.

The expected heat load density of 25 MW/km^2 should enable the overall project to be realized financially. By connecting the waste incineration plant to a nuclear power plant a full civil waste heat utilization and a nearly 100 % supply reliability will result.

SESSION III-B

THERMAL DISCHARGE I

PB82-227984

DISCHARGE INDUCED SHEAR STRESSES

Fred J. Mogolesko
Nuclear Engineering Department
Boston Edison Company
Boston, MA 02199

Joseph Laznow
M & L Environmental Consultants
Holliston, MA.

ABSTRACT

Within a fluid flow-field, organisms can be expected to experience their greatest potential damage in the immediate vicinity of solid surfaces. In addition, it can be anticipated that a source of mechanical damage exists in a flow-field possessing high levels of turbulence. The most critical region in a highly turbulent flow-field is at the interface of eddies. The quantification of the magnitude of shear stress experienced by a passively entrained organism will be the main theme of the paper.

1. INTRODUCTION

The Federal Water Pollution Control Act Amendments of 1972 require steam electric generating power stations such as Pilgrim Station to have the best available control technology by 1983 for minimizing the discharge of pollutants. This has been interpreted for thermal discharges as some form of closed-cycle cooling. Under the 316(a) exemption, alternate effluent limitations may be granted if the Applicant can demonstrate that the effluent limitations are more stringent than are: "...necessary to assure the protection and propagation of a balanced indigenous population of shellfish, fish and wildlife in and on the body of water into which the discharge is to be made...". With respect to the effects associated with the intake, Section 316(b) of the Federal Water Pollution Control Act Amendments of 1972 specifies that the location, design, construction, and capacity of the cooling water intake structure shall reflect the best technology available for minimizing adverse environmental impact.

The data for the analysis of ecological, engineering, and hydrologic information on which the 316 demonstration is based are reported in the Applicant's Environmental Report and Nuclear Regulatory Commission Environmental Impact Statements for Pilgrim Station. Various reports and results of environmental and engineering studies associated with Pilgrim Station have been used. Pertinent scientific literature has also been used and referenced in preparation of the demonstration. The demonstration contains assessments of Pilgrim Station's impact on the representative species. The analysis considers the effects of entrainment into the circulating water system, entrapment at the intake structures, and effects relating to the thermal discharge of the station. The impact assessment approach in this document

Preceding page blank

is to identify potential impacts which could occur, and, based on available data and expected station characteristics, to quantify the effects of the station on representative species.

This type of analysis requires that a number of conservative assumptions be made which overstate the magnitude of the station-induced effects. This results, however, in quantitative impact determinations which otherwise would not be possible.

In addition to thermal effects, certain other stresses are considered. The most important of these stresses (author's opinion) is passive entrainment. Passive entrainment of early life stages refers to the situation in which small planktonic forms incapable of significant movement are carried through the thermal plume. It is believed that passive entrainment at Pilgrim Station will not induce detectable mortality among aquatic organisms because (1) the residence time (and thus the exposure to elevated temperatures within the plume) is very short, (2) the currents and tides in the area preclude organisms from remaining near the discharge for an extended period, (3) the maximum temperature elevation with both Units 1 and 2 in operation is 23°F, and (4) the volume of water at the highest temperatures is, as the result of rapid dilution, very small.

To date, most of the open literature has attempted to quantify the magnitude of potential damage to planktonic organisms due to mechanical sources. To this extent, estimates of damage to these organisms have been associated with the damage that could occur within pumps and circulating water lines of cooling water systems for electricity generating power plants. Marcy [2] has sampled fish eggs and larvae in the discharge canal of the Connecticut Yankee Nuclear Power Plant to obtain an estimate of mechanical damage. The analysis of this data indicates that about 80 percent of the entrained juveniles failed to survive their journey through the plant. It must be noted that the data examined was obtained from the discharge canal of an operating circulating water system, but artificial heat attributed to power production was not present.

Within a fluid flow-field, organisms can be expected to be subject to their greatest potential damage in the immediate vicinity of solid surfaces. In addition, it can be anticipated that a source of mechanical damage exists in a flow-field possessing high levels of turbulence. The most critical region in a highly turbulent flow-field is at the interface of eddies. The quantification of the magnitude of shear stress experienced by a passively entrained organism will be the main theme of this paper. The magnitude of these stresses will be compared to values found in the open literature.

2. MECHANISM OF DAMAGE

Ulanowicz [8] has outlined the three major forces that an entrained organism can experience if exposed to significant flow-field velocity variations. These forces are (1) shear stresses, (2) pressure changes, and (3) accelerations. The attempt in this discussion will be to concentrate on the shear stresses that a passively entrained organism can encounter due to the interaction of the flow from a surface discharging power plant with the ambient coastal receiving waters.

3. SURFACE DISCHARGE MODELING

The mathematical models that serve as the basis for the analytic determination of shear stress levels are the Shirazi-Davis Model [4] (S-D) and the Stolzenbach-Harleman Model [5] (S-H). The S-H model is formulated from the three-dimensional, time averaged equations of mass, momentum and energy conservation for a turbulent-incompressible fluid. Heat conduction and viscous transfer, representative of molecular processes are assumed to be negligible. The model takes into account buoyancy, but is based upon non-buoyant jet theory and buoyant spreading is accounted for via a lateral spreading velocity. In addition, crossflow velocities are assumed to be small.

The specific limitations of the S-H model are typical of other three-dimensional integral models. Specifically, this model does not account for bottom contact of discharged effluent and the resultant limitation of vertical entrainment.

To this extent, the S-H model is typically applied with confidence to the situations that mirror the model assumptions. A second limitation of the S-H model lies in the fact that the model is based upon the presence of ambient currents that are less than 10% of the outfall velocity.

The S-D model makes use of available data (field and laboratory) to calibrate and modify the existing three-dimensional integral model attributed to Prych [6]. As a result of the Shirazi-Davis examination of pertinent data, modifications were made to the original Prych model. The Prych model is an extension of the S-H model that additionally allows for the inclusion of entrainment due to ambient turbulence in the mass flux equation. The momentum flux equation includes buoyancy forces, shear forces between jet and ambient fluids, drag force due to crossflow, and entrainment of ambient momentum. The heat flux equation allows for surface heat loss.

The most noted modification to the original Prych model by Shirazi-Davis, involved the treatment of buoyant spreading. The specific limitations of the S-D model includes the original limitations of the Prych model as a subset. The lateral spreading assumptions are questionable since spreading attributed to entrainment and spreading attributed to buoyancy are not typically additive when the magnitude of each is essentially identical [7]. The S-D modification in this area is not purely defensible, but appears to improve the predicative capabilities of the original Prych model.

A further drawback to the S-D model lies in the range of distances from the outfall over which it is truly applicable. This drawback will not interfere in the use as proposed in this paper because the area of major interest is close to the discharge location.

To summarize, there exists a set of limitations that all integral type models exhibit. Typically, a rectangular outfall channel is assumed. The violation of this assumption is not judged to be serious. The second major limitation is the lack of conformance to the deep water assumption. The deep water assumption allows the jet to act as a free jet, totally unconfined by bottom interference. In reality, the discharge does not have to satisfy the

condition of being in an infinitely deep receiving body. Futhermore, the receiving body should be wide enough such that it does not inhibit the idealized free jet. Further limitations are the existence of non-stratified receiving waters, uniform ambient currents, constant outfall conditions and no wind momentum transferred to the plume [7]. These remaining limitations are not judged as severe as the former set, since the resolution of the integral models as a class are not typically good enough to make a significant difference by their inclusion.

The application of the two selected integral models is believed to produce conservative results. The application of these models to the non-ideal prototype situation and specifically to the regions to be identified, are judged to be quite reasonable.

4. STATION DESCRIPTION [3]

Pilgrim Station Units 1 and 2 are considered base-loaded, nuclear-powered electrical generating units designed to produce 655 mW and 1,180 mW of electrical energy, respectively, under full load conditions. The units are planned for an anticipated capacity factor of 80 percent. This represents operation of the units over a wide range of load conditions, such that the overall capacity averages 80 percent. For the purpose of this study, it is assumed that the station operates at 100 percent load all of the time (a very conservative assumption).

The station withdraws cooling water from Cape Cod Bay via intake structures located south of Rocky Point in Plymouth, Massachusettts. The cooling water is returned to Cape Cod Bay via a discharge channel which is designed to promote rapid dilution of the heated effluent. The cooling water is used primarily to remove heat from the station condensers. Additionally, a small quantity of heat is removed from the station service water systems.

The total heat rejection during full load operation of Pilgrim Station will be approximately 1.34×10^{10} Btu/hour. This reflects operation of both Units 1 and 2. Unit 1 has a circulating water flow of 690 cfs at a maximum temperature rise of 32°F, and a service water flow of 23 cfs at a maximum temperature rise of 15°F. Unit 2 will have a circulating water flow of 1,770 cfs at a maximum temperature rise of 20°F, and a service water flow of 78 cfs at a maximum temperature rise of 10°F. The combined flow will be 2,561 cfs at a temperature rise of 22°F. Table 1 summarizes the contribution of each system. Under reduced load conditions the circulating water flow rates will not normally be reduced, except for substantially reduced power levels over extended time periods. Table 2 presents anticipated, typical operating characteristics over a range of possible load conditions.

Units 1 and 2 will utilize a common discharge channel to return cooling water to Cape Cod Bay. The circulating water will leave the discharge channel as a high velocity surface jet, and will rapidly mix with the surrounding sea water. Figures 1 and 2 illustrate the discharge channel geometry. The channel is trapezoidal in cross-section with a bottom width of 20 feet and side slopes of 2:1 (H:V). The invert elevation runs level at elevation -4.8 MSL from the seal wells to the point where the channel intersects the beach slope, which it then follows. Minor variations in flow and temperature rise will

occur under various tidal conditions due to the hydraulic characteristics of the circulating water system. Table 3 presents approximate flow characteristics for a range of tidal conditions.

The greatest velocity variations occur in the zone of flow establishment. Having defined the critical region with respect to shear stress, two state-of-the-art mathematical models for surface discharges will be used in the determination of shear stresses. The mathematic models that serve as the basis for the analytic determination of shear stress are the Shirazi-Davis Model (4) and the Stolzenbach-Harleman Model [5] (9).

5.1 CASE STUDY NUMBER 1

This case will be based upon the S-D Model and the shear stress will be determined from the product of the dynamic eddy viscosity and the velocity gradient. The eddy viscosity is obtained from a review of the open literature and the velocity profile from the S-D Model.

The turbulent shear stress can be defined mathematically as follows:

$$\tau = \rho \varepsilon \, \partial u / \partial z \qquad (1)$$

where ε = Eddy viscosity,

ρ = Density of fluid

and $\partial u / \partial z$ = Velocity gradient

In order to proceed with the determination of the shear stress, an estimate of the eddy viscosity term, ε, is needed. For this purpose, it is useful to note that the Prandtl Number, which defines the ratio of eddy viscosity (ε) to eddy diffusivity (k), is defined as:

$$P = \varepsilon / k \qquad (2)$$

P = (1.0 - for wall turbulence [1]
(0.7 - for free turbulence [1]

Furthermore, for free turbulence, Prandtl's second hypothesis has been found to be quite useful (1). That is, the eddy viscosity can be expressed as

$$\varepsilon = \varepsilon_o \tilde{u}_c b \qquad (3)$$

where

ε_o = a constant dependent on the problem under consideration,

$\tilde{u}_c$ = jet centerline velocity,

and b = jet half width where the velocity is one-half of Uc.

The value of ε_o has been found from experimental data to be 0.037 if the above definition for b is accepted [1]. This value is valid for the area of flow where the discharge is essentially a two dimensional jet.

Since the S-D Model does not specify the magnitude of the eddy viscosity, it is necessary to estimate its magnitude. To that extent, it is noted that the entrainment coefficient, E_o=0.05 is specified by S-D. From Equation 2, ξ= PK, and since the case under consideration is likened to the freely turbulent situation, a value of eddy viscosity quite consistent with the experimetnally determined one, is obtained. For this calculation, ξ = 0.035, will be used.

The velocity profile is obtained from Reference 4.

$$u_r = u \cdot \exp\left(-\frac{n^2}{B^2}\right) \cdot \exp\left(\frac{z^2}{H^2}\right) + V\cos\theta \qquad (4)$$

where n and z are distances perpendicular to the plume centerline in the lateral and vertical directions, respectively,

U = centerline velocity,
B = local characteristic width of jet,
H = local characteristic thickness of jet,
V = uniform ambient current,
θ = angle that surface discharge makes with ambient current.

The velocity gradient is expressed as

$$\frac{\partial u_r}{\partial z} = u \cdot \exp\left(-\frac{n^2}{B^2}\right) \cdot \left(-\frac{2z}{H^2}\right) \cdot \exp\left(-\frac{z^2}{H^2}\right) \qquad (5)$$

To determine $(\partial u_r/\partial z)_{max.}$, the second derivative of the velocity profile is calculated and set equal to zero. The second derivative is

$$\frac{\partial^2 u_r}{\partial z^2} = u \cdot \exp\left(-\frac{n^2}{B^2}\right)\left[-\frac{2}{H^2} - \left(\frac{2z}{H^2}\right)^2\right]\left[\exp\left(-\frac{z^2}{H^2}\right)\right] \qquad (6)$$

and if $\left(\partial^2 u_r/\partial z^2\right) = 0$, an expression for z is obtained.

That is $z = \frac{H}{\sqrt{2}}$ and furthermore

$$\left(\frac{\partial u_r}{\partial z}\right)_{MAX} = \left.\frac{\partial u_r}{\partial z}\right|_{\substack{z=\frac{H}{\sqrt{2}} \\ n=0}} = -0.8578\left(\frac{U}{H}\right) \qquad (7)$$

To determine the magnitude of the shear stress, the characteristics for the Pilgrim Discharge Channel (see Figure 2) must be considered. The seaward end of the discharge channel, characterized by Station (STA) 8 + 78 is at Elevation (mean sea level reference) = -7.8'. From a knowledge of the discharge flow-rate and discharge velocity, an estimated critical depth of water within the trapezoidal channel can be obtained from the classical continuity equation. Based upon the trapezoidal cross section of the Pilgrim discharge

channel a quadratic equation evolves for the determination of the critical depth (ho). Selecting the positive root of the above-mentioned expression produces a critical depth, ho = 6.4 feet.

The maximum shear stress now calculated by noting that U = 12.2 fps (Table 3).

$$\tau_{max.} = \rho \varepsilon \left[0.8578 \left(\frac{U}{h_o}\right)\right] \tag{8}$$

$$\tau_{max.} = 54.5 \text{ dynes/cm}^2$$

$$\tau_{max.} = 0.114 \text{ lb/ft}^2$$

5.2 CASE STUDY NUMBER 2

This case will be based upon the S-H Model and the procedure will be identical to that used in Case 1 except that the velocity profile will be obtained from the core region. For this region, the velocity profile is expressed as

$$U = (U_c) \cdot (F_y(y)) \cdot (F_z(z)) \tag{9}$$

where U_c = centerline velocity

$$F_y = \begin{cases} 1 \\ f(\xi_y) \\ 0 \end{cases} \quad \begin{cases} 0 < y < s \\ s < y < b+s \\ b+s < y \end{cases} \tag{10}$$

and

$$F_z = \begin{cases} 1 \\ f(\xi_z) \\ 0 \end{cases} \quad \begin{cases} -r < z < n \\ -r-h < z < -r \\ z < -r-h \end{cases} \tag{11}$$

and

$$\xi_z = \frac{-z-r}{h}$$

$$\xi_y = \frac{y-s}{b} \tag{12}$$

$$f = (1 - \xi^{3/2})^2$$

The terms associated with Equations 9 through 12 are defined on Figure 3. From Equations 9 through 12, u/uc can be expressed as

$$\frac{U}{U_c} = (1 - \xi^{3/2})^2 \tag{13}$$

From Equation 13 the velocity gradient is expressed as

$$\left.\frac{\partial u}{\partial \xi}\right|_{y=0(0<\xi<1)} = U_c \frac{\partial}{\partial \xi}\left[\left(1-\xi^{3/2}\right)^2\right] \qquad (14)$$

or

$$\frac{\partial u}{\partial \xi} = -3U_c\left[\left(\xi^{1/2}-\xi^2\right)\right]$$

The maximum velocity gradient criterion is established from

$$\left.\frac{\partial^2 u}{\partial \xi^2}\right|_{y=0(0<\xi<1)} = 0 \qquad (15)$$

From Equation 15 it is observed that $\xi = 0.3968$. The maximum velocity gradient can be expressed in terms that are identified in the equation for shear stress. From the chain rule for partial differentiation, the following is noted

$$\frac{\partial u}{\partial z} = \left(\frac{\partial u}{\partial \xi}\right)\cdot\left(\frac{\partial \xi}{\partial z}\right) \qquad (16)$$

$$\frac{\partial u}{\partial z} = 3\left(\frac{U_c}{h}\right)\left[\xi^{1/2}-\xi^2\right]$$

To calculate the maximum shear stress, $\frac{\partial u}{\partial z}$ must be maximized:

$$\left(\frac{\partial u}{\partial z}\right)_{MAX.} = \left.\frac{\partial u}{\partial z}\right|_{\xi=0.3968} \qquad (17)$$

$$\left(\frac{\partial u}{\partial z}\right)_{MAX.} = 1.4172\left(\frac{U_c}{h}\right)$$

The critical value of h can be determined from an examination of the S-H Model in the core region. Based upon this determination, Uc=Uo (initial discharge velocity, 12.2 ft/sec). The maximum shear stress is expressed as follows:

$$\tau_{MAX.} = \rho\varepsilon\left[(1.4172)\cdot\left(\frac{U_c}{h}\right)\right] \qquad (18)$$

From Equation 18, it is observed that τ_{max} would occur for the situation where $h \rightarrow o$. Selecting a realistic and critical location where planktonic organisms would exist, such as between 10 and 20 feet off the discharge, the shear stress would range between 262 and 131 dynes/cm^2, respectively. Based upon the complexities of the hydrodynamic flow field induced by the interaction of the jet-like discharged effluent and highly variable alongshore currents, it is difficult to support the critical location selected

above. This location and the resulting shear stress should be considered as the worst case.

6. CONCLUSIONS

Even at the worst case shear stress level, the exposure time is critical. Using this concept and the information for duration vs. mortality presented to Ulanowicz (8), it is noted that the shear stresses that a passively entrained organism would experience at the coastal location of Pilgrim Nuclear Power Station are typically low.

TABLE 1

PILGRIM STATION COOLING WATER CHARACTERISTICS (3)
(FULL LOAD)

	Flow (cfs)	Temp Rise (°F)	Heat Rejection (Btu/Hr)
Unit 1			
Circulating Water	690	30	4.7×10^9
Service Water	23	15	7.8×10^7
Total	713	30	4.8×10^9
Unit 2			
Circulating Water	1,770	20	8.0×10^9
Service Water	78	10	1.8×10^8
Total	1,848	20	8.2×10^9
Units 1 and 2 Total	2,561	22	1.3×10^{10}

TABLE 2

TYPICAL LOAD-DEPENDENT OPERATING CONDITIONS [3]
(UNITS 1 AND 2 COMBINED)

Load %	Flow (cfs)	Temp Rise (°F)	Heat Rejection (Btu/Hr)
100	2,561	22.0	1.30×10^{10}
80	2,118	21.3	1.04×10^{10}
60	2,118	16.0	0.78×10^{10}
40	1,723	13.1	0.52×10^{10}
20	1,723	6.6	0.26×10^{10}
0	0	0	0

PB82-227992

INSTALLATION OF CLOSED CYCLE COOLING SYSTEM TO REDUCE IMPACT OF EXISTING ONCE-THROUGH COOLING SYSTEM

H. A. Frediani, Jr.
Envirosphere Company
Norcross, Georgia, U.S.A.

ABSTRACT

A description of a proposed installation of a new steam electric generating station, adjacent to an existing station which utilizes once-through cooling, is presented. The new station has been designed to utilize the existing station's intake and discharge structures. This design eliminates the need for new construction in the Receiving Body of Water (RBW). The combined effect of the makeup intake and blowdown discharge locations of the proposed new station would have several effects on both stations. It will provide dilution for the concentrated chemical discharge from the new station's cooling tower blowdown. In summer, when extreme ambient conditions can cause the absolute discharge temperature of the once-through station to rise to unacceptable levels, the cooling tower blowdown is expected to be at a lower temperature, thus reducing the combined discharge temperature. In winter, when cooling tower blowdown is expected to be at its maximum temperature rise over ambient RBW temperatures, the discharge temperature from the once-through station is estimated to reduce the overall combined discharge temperature rise over ambient.

1. INTRODUCTION

A common situation for an electric utility today is to desire to install existing generating capacity at a site that already contains one or more operating units. In many cases, such a site was originally intended for expansion, and has been provided with transmission and/or fuel handling capability to support additional units. In addition, many of these existing units utilize once-through cooling systems and have been criticized because of the impact of their thermal discharge on the RBW. In this situation, the addition of even the relatively small discharge from a recirculating cooling system can be environmentally unacceptable to an already stressed RBW. An alternative concept is to integrate a new unit's makeup and blowdown system with the once-through system of the old unit(s) in order to reduce the total quantity of heat discharged to the RBW.

2. DISCUSSION

The following discussion is based on a concept developed for an actual proposed new installation adjacent to an existing once-through station in the Southeastern United States. The existing station utilizes salt water for cooling and consists of approximately 1200 Mwe of capacity at a design flow

rate of 560,000 gpm and a temperature rise of 19 degrees F. The proposed station consists of approximately 1200 Mwe of capacity and is designed to utilize cooling towers for heat dissipation. Its design makeup and blowdown rates are 36750 and 24500 gpm, respectively, for a design solids concentration of 1.5 cycles.

The existing station utilizes open channels to convey circulating water both to and from the condenser. This feature makes it a relatively simple operation to install the makeup and/or discharge structure for the new station within the circulating water system of the existing station. It was proposed to locate the makeup intake structure so that it withdraws water from the discharge channel of the existing station. This location has the following advantages:

1. No new construction or dredging is required in the source water body. Thus no construction impact would occur there.

2. There would be no impingement or entrainment of organisms except those which have already passed through the existing station. Thus, the fish protection system of the existing station would also serve the new station.

3. Withdrawal of a portion of the heated discharge from the existing station would transfer some of the heat load from the RBW to the heat dissipation system of the new station. This transfer should compensate for the added heat load of the blowdown from the new station.

Two possible locations were conceived for the blowdown discharge. The first location would inject the blowdown into the intake canal of the existing station. A block diagram of this system is shown in Figure 1. This blowdown location would have the following advantages:

1. No construction or dredging would be required in the RBW.

2. Full mixing of the blowdown with the once-through flow would provide rapid dilution of the blowdown.

3. Operation of the new station, when the existing station is shut down, would not lead to recirculation of the blowdown back into the makeup.

4. A portion of the flow rate through the old station would be replaced by blowdown, thus reducing the net inflow from the river. This would presumably reduce the entrainment impact of the existing station.

This blowdown location also has the following disadvantages:

1. It would increase the temperature and salinity at the intake to the condensers of the existing station.

2. It would increase the salinity of the makeup water to the new station.

3. The thermal impact on organisms in the intake water might be significantly adverse.

The second location of the blowdown discharge would inject the blowdown into the discharge canal of the existing station, downstream of the proposed makeup withdrawal. A block diagram of this system is shown in Figure 2.

This blowdown location would have the following advantages:

1. No new construction or dredging is required in the RBW.

2. A properly designed discharge structure would provide full mixing of the blowdown with the once-through flow for dilution.

3. Operation of the new station would have no effect on the condensers of the existing station.

4. The thermal impact on organisms within the discharge canal would not be expected to be significant.

This blowdown location would have one serious disadvantage in that operation of the new units while the existing units are shut down would cause recirculation of blowdown into the makeup.

Quantification of the impacts associated with the advantages and disadvantages of each of the configurations discussed above was required in order to select the preferred arrangement. This required estimates of flow rates and water temperatures associated with both the new station and the existing station.

Cooling tower evaporation rates and cold water temperatures were estimated from vendor-supplied performance curves and meteorological data from the nearest longterm weather monitoring station. Blowdown rates were calculated from the evaporation rates and the design makeup flow rate. Flow rates and intake and discharge temperatures for the existing station were obtained from plant records. Simulation of how both stations would have performed, for both blowdown discharges, were carried out.

The temperature rise above ambient, for both the once-through discharge and the blowdown from the cooling tower system, is presented in Figure 3. These temperatures are presented for average monthly conditions. During the months from May through November, the average blowdown temperature is less than the average discharge temperature from the once-through system. Thus, mixing the two flows would actually result in a lowering of the discharge temperature below that of the existing once-through system during the summer months. This is the time when absolute temperature limits can be a problem for the once-through system.

During the months from December through April, the blowdown temperature rise is greater than that of the once-through discharge. At this time, mixing the two flows would result in dilution of the excess temperature in the blowdown. These winter months are the period in which temperature rise criteria can be a problem for the blowdown discharge.

The first blowdown location (see Figure 1) results in an increased intake temperature into the once-through units. This increase, at the design flow rates, varies between 0.8 degrees F in January, and 0.2 degrees F in July. This increase is offset by a decrease in discharge flow rate of about 6% due to the withdrawal of makeup. The change in heat rejection rate, which is proportional to the product of flow rate and temperature rise, is shown as the solid line in Figure 4. It can be seen from this Figure that the overall effect of this blowdown discharge location is to decrease the heat rejection rate. Thus the reduction in flow rate has more effect than the increase in temperature rise. However, there is a slight increase in January and March.

FIGURE 1

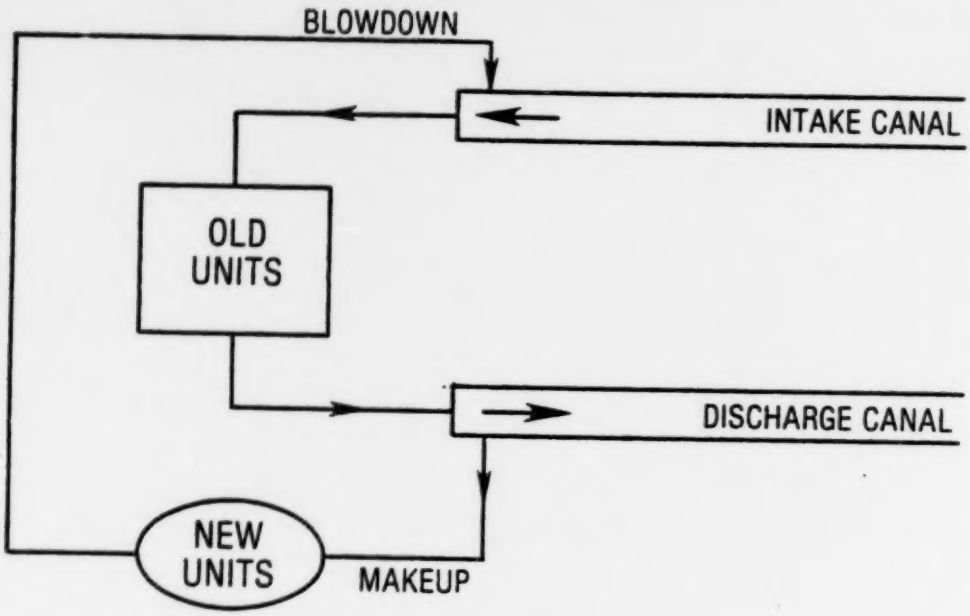

FIGURE 2

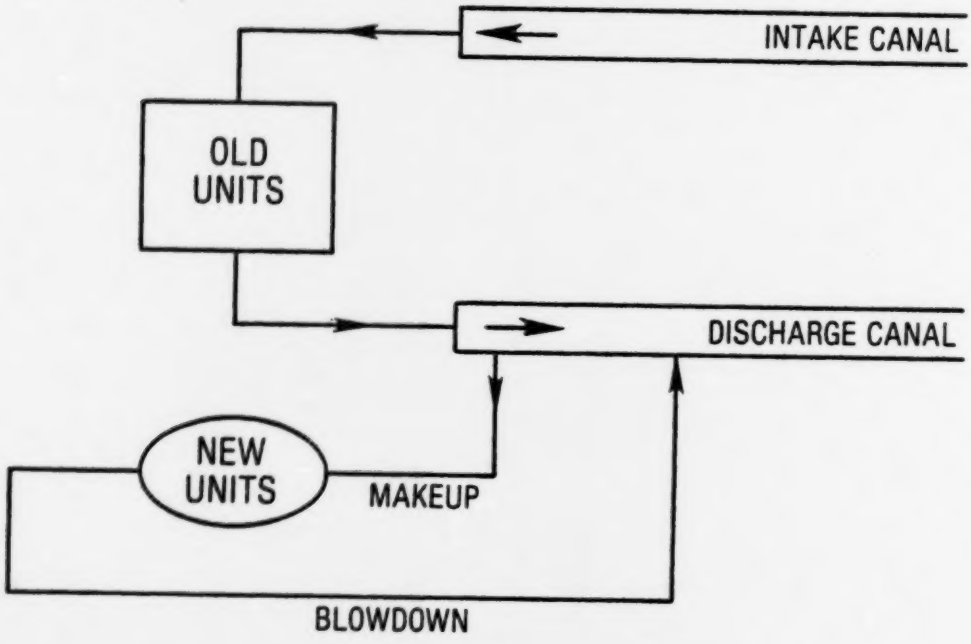

The second blowdown location (see Figure 2) has no effect on the operation of the once-through units. Essentially, it reduces the discharge flow rate by about 2%, and replaces about 4% of the once-through flow with cooling tower blowdown. This results in a change in discharge temperature rise ranging between an increase of 0.4 degrees F in March, and a decrease of 0.5 degrees F in September. The change in heat rejection rate for this blowdown discharge location is shown in Figure 4 as the broken line.

It can be seen from this Figure that the changes in heat load are very similar to the changes resulting from the first discharge location. Each change is slightly more positive than in the first case. The change is a slight increase in January, February, and March. The overall effect, however, is a decrease in the heat rejection rate.

Another important factor in selecting the blowdown discharge location is the concentration of dissolved solids in the discharge. The first blowdown discharge location recirculates a portion of the solids from the blowdown to the makeup. Thus the cooling towers operate slightly above the design concentration of 1.5 cycles above ambient. The actual operating level at design conditions is approximately 1.54 cycles of concentration over ambient, in the towers. The corresponding discharge concentration is then about 1.023 cycles of concentration above ambient.

Using the second blowdown discharge location establishes 1.5 cycles of concentration in the cooling towers. The corresponding discharge concentration is about 1.022 cycles above ambient. Thus, the second blowdown discharge location has a slight advantage over the first, with respect to discharge concentrations.

Because of the slight differences in effects of the two blowdown discharge locations, further quantification of those effects must be provided under conditions of reduced flow rate through the existing once-through station. The results at a flow rate of 140,000 gpm (25% of rated capacity) are summarized below:

Blowdown Discharge Case	1	2
Maximum Temperature Rise Increase (degrees F)	3.1	1.6
Minimum Temperature Rise Increase (degrees F)	0.8	-1.8
Maximum Heat Rejection Rate Increase (%)	-0.5	+8.6
Minimum Heat Rejection Rate Increase (%)	-22.2	-20.8
Number of Months of Heat Rate Decrease	12	9
Discharge Number of Cycles of Concentration	1.119	1.096

3. RESULTS

Both configurations of makeup intake and blowdown discharge locations within the circulating water system of the existing once-through station have advantages over the construction of new structures within the RBW. The first configuration (blowdown discharge into the existing intake canal) provides the greater reduction in total discharge flow rate, and total discharge heat rate, from the combined operation of the existing and the proposed station. However, it also provides the greater increase in discharge temperature rise and discharge solids concentration.

The second configuration (blowdown discharge to the existing discharge canal) provides less reduction in total discharge flow rate and total

FIGURE 3

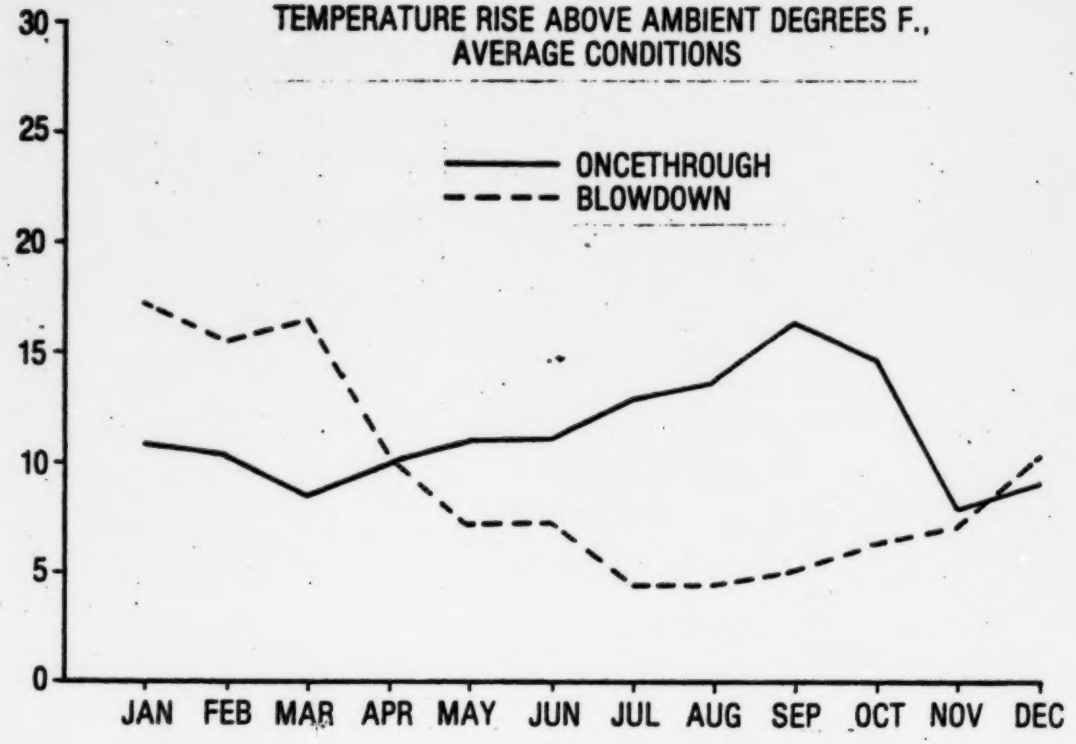

FIGURE 4

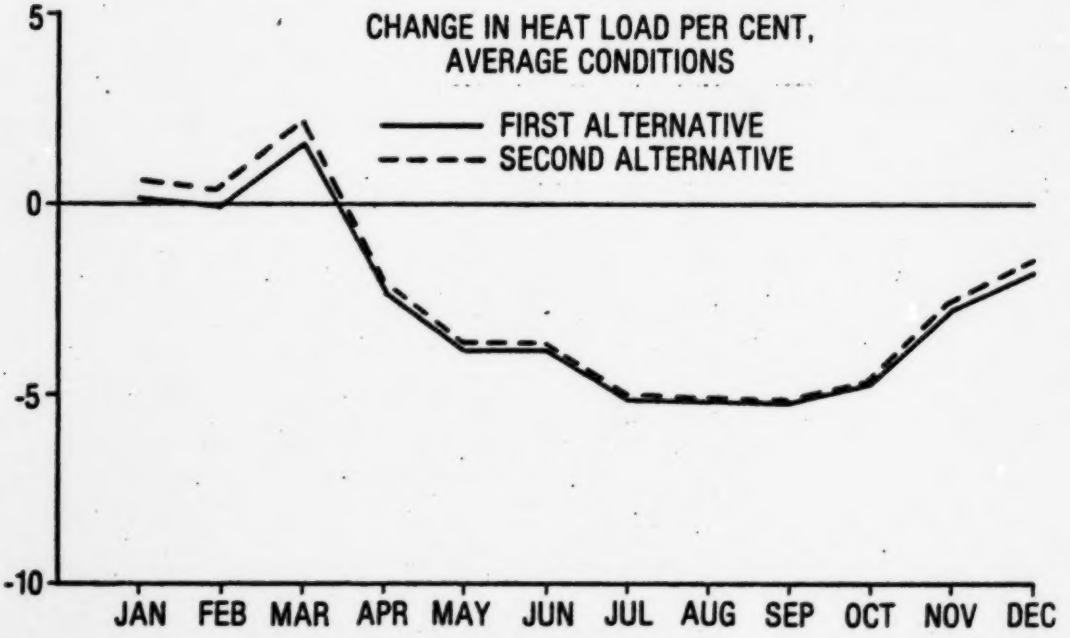

discharge heat rate. It does provide a reduction in discharge temperature during summer months, and a lower level of solids concentration.

With respect to impact on organisms in the cooling water, the first configuration has the advantage of reducing net inflow from the river, and the disadvantage of providing a thermal impact in the intake canal, upstream of the fish protection system. The net result of these two factors is not readily quantifiable, but could easily be an adverse impact.

Mathematical modeling of the discharge from the existing once-through station, and the discharge expected from the combined operation of both stations, for both blowdown discharge locations, has also been performed. The following results have been derived from that effort.

The major effect of reducing the flow rate leaving the discharge system of the existing station is a slight reduction in the discharge velocity and, consequently, a slight reduction in the discharge densimetric Froude number. This reduction causes a reduction in initial mixing, and a correspondingly larger surface area of the thermal plume. The major effect of a change in discharge temperature is that an increase in discharge temperature results in a larger surface area of the thermal plume. The combination of these two effects produces a thermal plume larger than that for the once-through station alone when the first configuration of blowdown discharge is assumed. The thermal plume produced when the second configuration of blowdown discharge is assumed is larger than that for the once-through station during the cooler months, but smaller during the summer months. It is always smaller than the plume produced by the first blowdown discharge configuration.

4. CONCLUSIONS

The makeup and blowdown system, including the second blowdown discharge location (see Figure 2) was selected as the preferred system. It provides the following advantages:

1. During months of high ambient receiving water temperatures, this configuration will provide a reduced discharge temperature, and reduced thermal plume surface area, with respect to the existing once-through discharge.

2. This configuration has no effect on the water quality of cooling water entering the once-through station, and no effect on the existing fish protection system.

3. This configuration provides maximum dilution of the chemical discharge from the new closed cycle station.

4. This configuration should not increase entrapment or impingement of organisms because it only withdraws water which has already been screened.

This configuration has the one main disadvantage of recirculating solids to the cooling towers when the existing station is not operating. Based on the past history of the existing station, such an event is expected to occur approximately 0.3% of the time. This event can be provided against by installing the necessary piping for both potential blowdown discharge configurations and only utilizing the first location when the existing station is shut down.

PB82-228008

A SIMPLIFIED MATHEMATICAL THERMAL MODEL FOR SPRAY CANALS

K.E. Trout
Black & Veatch
Consulting Engineers
Kansas City, MO

W.E. Stewart, Jr.
University of Missouri-KC
Kansas City, MO

A.T. Leard
Kansas State University
Manhattan, KS

ABSTRACT

A simplified mathematical model has been developed for predicting the thermal performance of spray cooling canal systems. The model is useful as a preliminary design tool for conceptual power plant heat rejection studies. The model calculates spray canal size requirements based on design conditions and calculates off-design performance which can be used to estimate operating costs. With the model, the feasibility of spray cooling canals can be compared to other recirculating heat dissipation alternatives such as cooling towers or cooling ponds/lakes.

INTRODUCTION

A simplified mathematical model has been developed for predicting the thermal performance of a spray canal system. The heat and mass transfer from a single water droplet is determined in a step-wise transient manner, based upon the mass mean instantaneous spray droplet diameter and droplet velocity, ambient conditions, condenser flowrate, and the heat load on the spray canal.

Essentially two different situations were analyzed. The first consisted of knowing all the design parameters, including the design condenser inlet and outlet water temperatures, and the program predicts the number of sprays required to dissipate the heat load. This situation applies also to the off-design case of operating fewer than the installed number of sprayers.

Secondly, the off-design case of specifying the number of sprays and having the program calculate the condenser inlet and outlet water temperatures to dissipate the heat load was modeled.

ANALYSIS

Several basic premises and assumptions were made in the mathematical development of the computer program. Based upon previous work in the area, the approaches can be separated into two general areas. One method essentially follows that developed for wet cooling towers, utilizing the NTU (number of transfer units) method. The NTU method must be based on and correlated to field experimental data. This technique has the obvious limitation of poor correlation to the real case if field data is not readily available and if all the dominant parameters are not considered in the correlation.

The other approach is to consider the heat and mass transfer from individual

droplets, basing the calculations on a variety of assumptions and parameters, as each investigator deemed appropriate. Several papers considered the situation where a cell of air surrounds the droplet throughout the entire flight time. The increase in humidity in the air cell due to evaporation of water from the drop is used to calculate the decrease in mass transfer and to predict the increase in the overall humidity of the air passing by the spray canal from the wind. These calculations are then used to calculate interference between sprays.

As in most investigations, the results are compared to data poorly defined, usually not noting all of the design parameters used to obtain the results.

Because of this inconsistency in method and data to which results cannot be correlated, it was proposed to develop a computer code which addresses the fundamental processes of heat and mass transfer which occur simultaneously at the drop surface.

It was proposed that the end result be a prediction of the number of sprays required to dissipate the heat load. Several investigators have reported varying effects of wind influence on individual spray performance and interference with downwind sprays. In some instances, the wind increased the canal thermal performance and has likewise been reported to significantly decrease performance due to interference. The wind effects have been ignored in this analysis and buoyancy has been considered of a sufficient effect that the droplet always exists in a constant wet and dry bulb environment.

Water loss due to evaporation is normally less than 3 per cent. Drift, usually limited to less than 1 per cent of the total flow, has been ignored. Evaporation is obviously considered since it plays the dominant role in decreasing droplet temperature.

Heat gains or losses and evaporation losses from the canal water surface have likewise been ignored.

Based upon these assumptions and limitations and others to be noted below, the following analysis was performed.

The droplet is assumed to exist in spherical form the moment the droplet exits the spray until the canal surface is reached. It should be noted here that as the droplet proceeds through its flight it decreases in temperature due to convective heat and mass transfer, decreases in mass due to mass transfer, and decreases in velocity from that of frictionless flight due to drag.

The heat transfer from constant surface temperature spheres has been well documented and was approximately correlated by

$$Nu_d = \frac{h_f d}{k_f} = 2.0 + 0.6 + Re_f^{1/2} Pr_f^{1/3} \qquad (1)$$

where all properties of the fluid are evaluated at the fluid temperature, $T_f = \frac{T_s + T_\infty}{2}$, where T_s is the instantaneous drop temperature and T_∞ is the constant dry bulb temperature, and are all variable with time.

The heat transfer from the spherical drop over some small time interval is then

$$Q_{conv} = \frac{k_f}{d} (Nu_d) A(Ts - T_\infty) (\Delta t) \quad (2)$$

where

A = surface area of droplet, d^2, ft^2

Δt = a small step-wise increment of time, seconds

The mass transfer is likewise well documented and assumes in equation form an identical correlation to that of the heat transfer equation, except the Prandtl number is replaced by the Schmidt number, as

$$Nu_D = \frac{k_{xm} d}{C_f D_{AB_f}} = 2.0 + 0.6 \, Re_f^{1/2} \, Sc_f^{1/3} \quad (3)$$

where

k_{xm} = mean mass transfer coefficient, $\frac{\text{lb-moles}}{ft^2 - sec}$

C_f = concentration of the fluid, $\frac{P_{ATM}}{\bar{R}T_f}$, $\frac{\text{lb-moles}}{ft^3}$

The mean mass transfer of water at any instant of time is given by, assuming ideal gas behavior,

$$W_{W_m} = k_{xm} A \frac{X_{wo} - X_{w_\infty}}{1 - X_{wo}} \quad (4)$$

where

X_{wo} = mole fraction of water at droplet surface, (Pwsat @ Ts)/P_{ATM}

X_{w_∞} = mole fraction of water in the surrounding free stream,

$(P_w @ T_\infty)/P_{ATM}$

Based upon the initial drop temperature, which is assumed uniform, the drop temperature at the next time step is decreased uniformly based upon the heat loss experienced in the previous time step as

$$T_D(t + \Delta t) = T_D(t) - \frac{Q_{total}}{m(t) Cp_w(t)} \quad (5)$$

where

m(t) = mass of drop at time t,

$Cp_x(t)$ = specific heat of water at T_D at time t, Btu/lbm F

$T_D(t)$ = uniform drop temperature at time t, F

Q_{total} = combined heat transfer due to convective heat and mass transfer

The initial velocity is prescribed and the final velocity over the time step Δt is determined as

$$a_y = -g \pm C_D A_p \rho_f u_\infty^2(t) \sin \alpha / 2m(t), \quad \begin{matrix} + \text{ for } v_y > 0 \\ - \text{ for } v_y < 0 \end{matrix} \quad (6)$$

$$a_x = -C_D A_p \rho_f u_\infty^2(t) \cos \alpha / 2m(t) \quad (7)$$

$$V(t + \Delta t) = V(t) - \sqrt{a_x^2 + a_y^2} \, \Delta t \quad (8)$$

A mean velocity was then determined as

$$u_{\infty}(t) = \frac{V(t + \Delta t) + V(t)}{2} \qquad (9)$$

This value of mean velocity was used at each time step in the determination of Reynolds number through the flight of the drop.

The calculation of drop velocity and direction allows the determination of flight time based upon the initial drop velocity, initial discharge angle α, and height above the canal surface.

The calculations noted above are repeated throughout the flight of the drop. The heat and mass transfer experienced by an individual drop is then applied to the whole discharge from the spray, the resulting canal temperature being

$$T_{canal} = \frac{(mT)_{sprays} + (M_{canal} - M_{spray})T_{canal}}{M_{canal}}. \qquad (10)$$

The procedure is repeated throughout the canal, adding sprays until the desired canal outlet temperature is attained.

RESULTS

There is very limited amounts of experimental data to correlate the results of the program to and as such the results have been compared to only a few cases. The comparisons agree very well though.

Overall spray performance shows a general increase with increasing wind velocity. Hence, the analysis being based upon the case of zero wind should in most cases be conservative.

Typical results are shown in Figure 1. These data are from actual operating spray canal systems. Using the mass median drop diameter as the initial condition, the program predicted a greater number of spray nozzles than required for the two typical cases shown. The number of sprays predicted exceeds those actually required by about 13 per cent. This is reasonable accuracy for preliminary design considerations.

CONCLUSIONS

The results obtained from the model show the following:

- o The initial drop diameter has the greatest effect on the overall thermal performance.
- o Large diameter drops dissipate relatively small amounts of energy and are ineffective.
- o The results compare favorably with published manufacturer's data.
- o The assumptions are reasonably valid, e.g., neglect of drift and wind effects are within the scatter of available data.

REFERENCES

1. Baird, R.D., Myers, D.M., and Shah, A., "The Thermal Performance Characteristics of Large Spray Cooling Ponds," Proc. Waste Heat Management and Utilization, Miami Beach, Florida, 9-11 May, 1976.
2. Porter, R.W., and Chaturvedi, S.K., "Atmospheric Spray-Canal Cooling Systems for Large Electric Power Plants," Proc. Waste Heat Management and Utilization, Miami Beach, Florida, 9-11 May, 1976.
3. Weinstein, H., et.al., "Dispersion of Heat and Humidity from Atmospheric

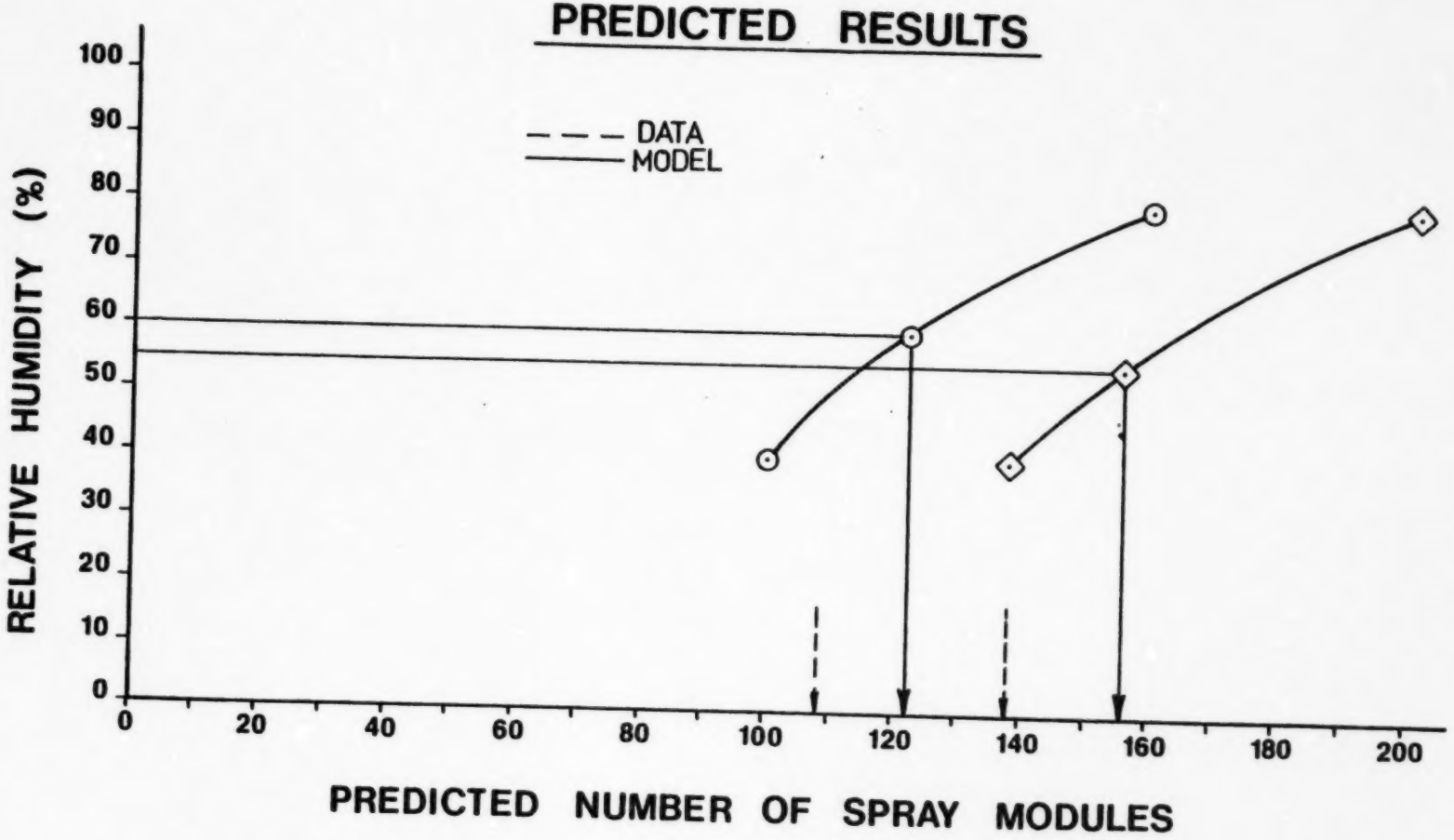
PREDICTED RESULTS
DATA
MODEL
RELATIVE HUMIDITY (%)
100
90
80
70
60
50
40
30
20
10
0
0
20
40
60
80
100
120
140
160
180
200
PREDICTED NUMBER OF SPRAY MODULES

FIGURE 1

Spray-Cooling Systems," Proc. Waste Heat Management and Utilization, Miami Beach, Florida, 9-11 May, 1976.
4. Frediani, H.A., Jr., and Smith, N., "Mathematical Model for Spray Cooling Systems," Trans. ASME, Journal of Engineering Power, April, 1977, pp. 279-283.
5. Bird, R.B., Stewart, W.E., and Lightfoot, E.N., Transport Phenomena, J. Wiley and Sons, 1960.
6. Chen, K.H., and Trezek, G.J., "Thermal Performance Models and Drift Loss Predictions for a Spray Cooling System," Trans. ASME, Journal of Heat Transfer, 99: 274-280 (May, 1977).
7. Arndt, C.R., and Barry, R.E., "Simulation of Spray Canal Cooling for Power Plants—Performance and Environmental Effects," ASME Paper 76-WA/HT-28, 1976.
8. Schrock, V.E., Trezek, G.J., and Kleiman, L.R., "Performance of a Spray Pond for Nuclear Power Plant Ultimate Heat Sink," Trans. ASME, Journal of Engineering Power, October, 1977, pp. 650-655.
9. Porter, R.W., and Chen, K.H., "Heat and Mass Transfer of Spray Canals," Trans. ASME, Journal of Heat Transfer, August, 1974, pp. 286-291.
10. Elgawhary, A.M., and Rowe, A.M., "Spray Pond Mathematical Model for Cooling Fresh Water and Brine," Environmental and Geophysical Heat Transfer, ASME HT 4 (1971).
11. Hoffman, D.P., "Spray Cooling for Power Plants," Proc. American Power Conference, 35: 702-712 (1975).

PB82-228016

COOLING-WATER DISPERSION UNDER THE INFLUENCE OF GROYNES

Vassilios Kaleris and Michael Schatzmann

Sonderforschungsbereich 80
University of Karlsruhe
Kaiserstrasse 12, 7500 Karlsruhe, W. Germany

ABSTRACT

Laboratory studies have been carried out to investigate the effects of different outfall exit conditions on the lateral mixing of cooling-water side-discharges into rivers with groyne-protected banks. Buoyant and non buoyant discharges were used to study plume dynamics. Through use of the steady-state diffusion equation, a simple equation was developed for quantifying the geometrical and dynamical impact of outfall and river conditions on lateral spreading. The results obtained show that, contrary to expectation, the outfall discharging a given cooling-water flux with large transverse momentum does not necessarily provide the largest initial dilution rate. In the presence of groynes, a very buoyant plume is protected from interaction with the ambient current for a short distance into the river giving it the opportunity to stratify and spread into the river. Later interaction with the ambient current beyond the groynes leads to a vertically fully-mixed plume with good dilution characteristics. For the design of an outlet structure which maximizes the rate of initial mixing it is important to carefully adjust the entire set of initial parameters based on the properties of the particular river section.

1. INTRODUCTION

Compared to the large American rivers, the widths and depths of even the largest European rivers are rather small. As a result, the discharge of cooling water into rivers through submerged diffusers located at the river bottom can be found only in very special cases. For the sake of ship- traffic safety, regulatory agencies in Europe usually require bank discharges.

Whether the cooling water is released through submerged diffusers or as side discharges employing free-surface channels, the intensity of near-field mixing is highly sensitive to the particular choice of geometrical and dynamical outfall conditions. Since mathematical models [3] are still limited in generality and accuracy, hydrothermal model studies can best provide an optimal set of initial conditions which could guarantee a maximum of temperature reduction within a certain distance from the outfall.

A set of design criteria for bank-discharge outlet-structures which permits large initial dilution rates was presented in an earlier article [5]; these criteria had been inferred from the results of laboratory experiments. In those experiments, the dependence of initial mixing on the geometrical and dynamical characteristics of several outlet struc-

CASE A (WITHOUT GROYNES)

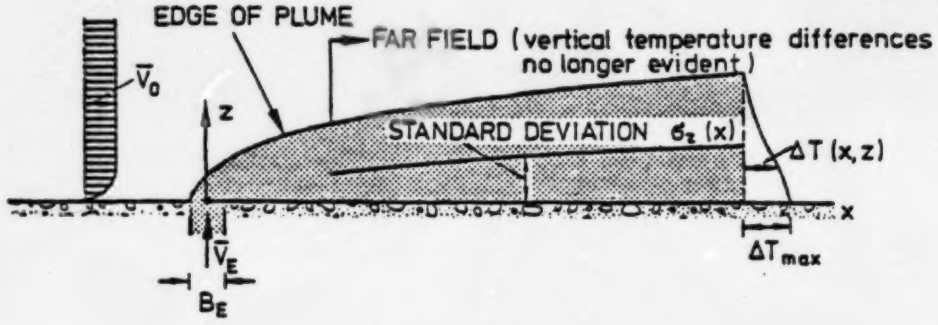

CASE B (WITH GROYNES)

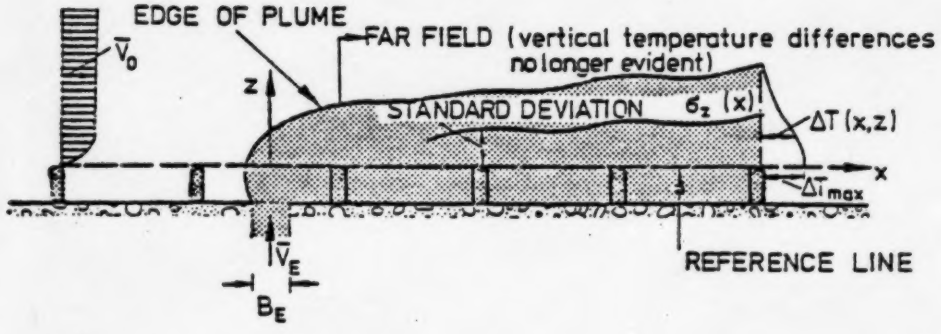

Fig. 1: Definition sketch

tures was investigated. In the laboratory model, warm water was discharged into a river of idealized shape. At the same time, other experiments were carried out in which the river was modified by insertion of a number of groynes positioned in a regular pattern at the discharge bank (Fig. 1). Groynes are sometimes employed in German rivers for shoreline erosion purposes. Their effects on plume dispersion is the subject of study in this paper. A comparison between the results of the plume studies with and without groynes will be presented below.

2. EXPERIMENTAL INVESTIGATION

Experiments were conducted in a straight laboratory flume with a test section of length 20 m and width 1,82 m. Table 1 presents information of the range of flume flow and outfall parameters investigated in case A (without groynes) and B (with groynes) in addition to data on the groyne geometry used in case B. To generate turbulence characteristics similar to that found in nature, an undistorted Froude model (F_o = 0.13) was used with carefully adjusted channel roughness [4, 6]. The groynes were not submerged and the distance between them was kept constant throughout the experiments. Both the distance between the groynes and the groyne geometry were chosen according to situ-

ations typical for the Rhine river. The outlet structures utilized were always positioned exactly in the middle between two groynes (see Table 1). For each outfall structure, a systematic sequence of steps was carried out encompassing the measurement program. First, water of the same density as the water in the flume was colored in preparation for discharge. Then the temperature was increased up to a maximum excess temperature (above river ambient) of 20°C in order to evaluate the effect of buoyancy on initial mixing. The exit densimetric Froude number range covered in the experiments was $0.21 \leq F_D \leq \infty$ ($F_D = \bar{V}_E / \sqrt{(\Delta\rho_E/\rho) \cdot g \cdot B_E}$). In all experiments, the width of the plume was considerably smaller than the width of the flume, so that the spreading of the plume remained always unaffected by the opposite bank. A few flow visualization studies were carried out as well to support the physical interpretation of the results obtained.

			CASE A	CASE B
Flume parameters (Index o)	Depth of flume flow	y_o	6 cm = const	6 cm = const
	Width of flow section	B_o	1.82 m = const	1.43 m = const
	Velocity (cross sectional average)	$\bar{V}_o$	10 cm/s = const	10 cm/s = const
	Shear velocity on bottom of flume	$V_*/\bar{V}_o$	0.147 = const	0.150 = const
	Distance between the groynes	x_G	—	1.5 m = const
Outfall parameters (Index E)	Geometry of outlet structure (top view)			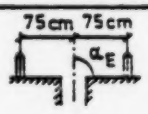
	Angle of discharge	α_E	90°	90°
	Width of outlet channel	B_E	4.5 cm; 30 cm; 60 cm	4.5 cm; 30 cm; 60 cm
	Depth of outlet channel	y_E	6 cm	6 cm
	Discharge velocity	$\bar{V}_E$	$0.3\bar{V}_o$; $2\bar{V}_o$; $4\bar{V}_o$	$0.3\bar{V}_o$; $2V_o$; $4V_o$
	Initial excess temperature	$\Delta T_E = T_E - T_o$	0; 5; 10; 15; 20°C	0; 5; 10; 15; 20°C
Groyne geometry	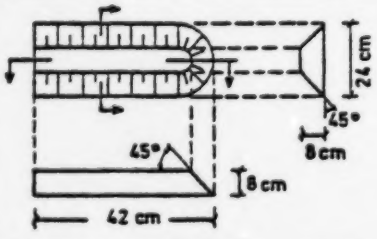		Non-submerged groynes throughout the experiments	

Table 1: Summary of flume flow and outfall parameters

3. QUANTIFICATION OF THE EFFECT OF CHANGES IN THE OUTFALL PARAMETERS

Rivers like the Rhine are characterized by comparatively large flow velocities and high turbulence levels. Therefore, vertical temperature gradients diminish rapidly; moreover, the so-called far-field of the plume, defined as the region of the plume in which vertical temperature stratification is no longer evident, starts at only a few hundred

meters downstream from the outfall. In this far-field buoyancy effects are negligible and heat spreads horizontally as if it were a passive tracer.

The fact that the plume becomes approximately two-dimensional (fully-mixed vertically) within a short distance (a few meters in our small-scale laboratory model) is used later as part of our analysis to quantify the mixing characteristics resulting from different discharge parameters. Under steady-state conditions, lateral spreading in the far-field can be computed by means of the depth-averaged conservation equation for a passive tracer, e.g. temperature T,

$$\bar{V}_0 \, y_0 \frac{\partial T}{\partial x} = \frac{\partial}{\partial z} \left(e_z \, y_0 \frac{\partial T}{\partial z} \right) \qquad (1)$$

Here, e_z is the transverse mixing coefficient and all other variables are defined in Table 1. The mixing coefficient e_z is essentially a "catch-all" parameter describing the combined effects on lateral mixing of (1) turbulent diffusion, (2) dispersion due to non-uniformities in the velocity profile of the flume flow, and finally (3) secondary flows.

Equation (1) can be solved easily [1] if one assumes that the water depth y_o is approximately constant and that a space-averaged e_z is representative of the whole flow field under consideration. In such case, an expression results for the dependence on flume-flow properties of the squared standard deviation σ_z^2 (x) of far-field lateral temperature profiles :

$$\sigma_z^2 (x) = \frac{2 e_z}{\bar{V}_0} x + \sigma_{z0}^2 \qquad (2)$$

The initial value σ_{zo}^2 can be obtained by extrapolating the σ_z^2(x) - curve into the upstream direction (Fig. 2). The σ_{zo} represents physically the nominal width of a virtual reference area source which discharges an effluent without excess momentum or buoyancy into a co-flowing stream, leading to an identical temperature or concentration pattern in far-field cross sections as is generated by the side discharge being modeled [2].

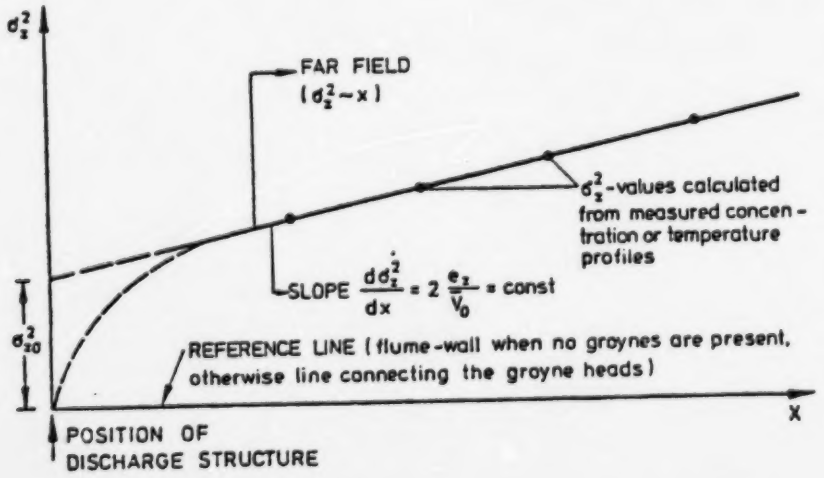
σ_z^2
FAR FIELD
($\sigma_z^2 \sim x$)
σ_z^2-values calculated from measured concentration or temperature profiles
SLOPE $\frac{d\sigma_z^2}{dx} = 2\frac{e_z}{\bar{V}_0}$ = const
σ_{zo}^2
REFERENCE LINE (flume-wall when no groynes are present, otherwise line connecting the groyne heads)
x
POSITION OF DISCHARGE STRUCTURE

Fig. 2: Sketch of method for quantifying effect of outfall parameters on near-field mixing

Clearly, the far-field rate of increase of the squared standard deviation $\sigma_z^2(x)$ with distance is constant (equ. 2) for a river section with approximately constant depth-averaged velocity $\overline{V}_o$ and mixing coefficient e_z. As a result, for the same ambient flow the $\sigma_z^2(x)$ - curves resulting from outfalls with different mixing characteristics must all be parallel in the far-field. The more the near-field mixing is intensified by the combined effects of initial parameters like transverse exit momentum or buoyancy and their interaction with ambient properties like river turbulence, the larger is the σ_{zo}^2 - value that results. Consequently, σ_{zo}^2 provides a clearly defined measure characterizing the mixing capability of a particular set of discharge conditions for a fixed set of river flow conditions.

4. RESULTS AND THEIR INTERPRETATION

The above method to quantify the effect of the exit conditions on transverse mixing proved successful. In both cases - without groynes (case A) and with groynes (case B) - Gaussian temperature (or concentration) profiles were found and a linear increase of $\sigma_z^2(x)$ with distance was observed. The standard diviation, $\sigma_z^2(x)$, was calculated according to the equation :

$$\sigma_z^2(x) = \frac{\int_0^\infty \overline{V}(x,z)\cdot\Delta T(x,z)\cdot z^2\,dz}{\int_0^\infty \overline{V}(x,z)\cdot\Delta T(x,z)\,dz} \simeq \frac{\sum_{i=1}^{n} \overline{V}_i\cdot\Delta T_i\cdot z_i^2\cdot\Delta z_i}{\sum_{i=1}^{n} \overline{V}_i\cdot\Delta T_i\cdot\Delta z} \qquad (3)$$

In the case with groynes, the lateral temperature (or concentration) distributions were measured in cross sections in line with the longitudinal axis of the groynes. It should be noted that the standard deviation $\sigma_z^2(x)$ has been calculated with respect to the discharge bank as the reference line (Fig. 2) for situations without groynes (A) and the line connecting the groyne heads for situations with groyne fields (B).

4.1 Results of Mixing Experiments without Groynes

The experimental results for cases without groynes are presented in detail in [2 , 5]. According to equation (2), the lateral mixing coefficient was determined from the slope of the $\sigma_z^2(x)$ - curves and was found to be $e_z = 1.18\ cm^2/s$. Presented in nondimensionalized form $e_z/(V_* y_o) = 0.134$. It was found that the outfall parameters dominating the rate of initial mixing are the excess temperature ΔT_E (characterising the buoyancy effect), the velocity ratio $\overline{V}_E/\overline{V}_o$ (characterising the initial momentum), and the dimensionless width B_E/y_o which is proportional to the exit volume flux $Q_E/(\overline{V}_o\, y_o^2)$. Geometrical details of the outlet structure such as rounded corners (or even the depth of the outlet channel) played a comparatively minor role.

The experiments showed that when the outfall temperature was set equal to the ambient temperature, the initial mixing parameter σ_{zo}^2 increased with increasing velocity ratio as well as with increasing volume flux (see Fig. 3). The exit excess momentum flux causes an increase in plume turbulence and consequently intensifies the initial mixing of the (buoyancy-free) effluent. The diagram in Fig. 3 implies that outlet structures having equal σ_{zo}^2 - values, i.e., outfalls with the same mixing capability, may be designed with different combinations between velocity ratio and volume flux.

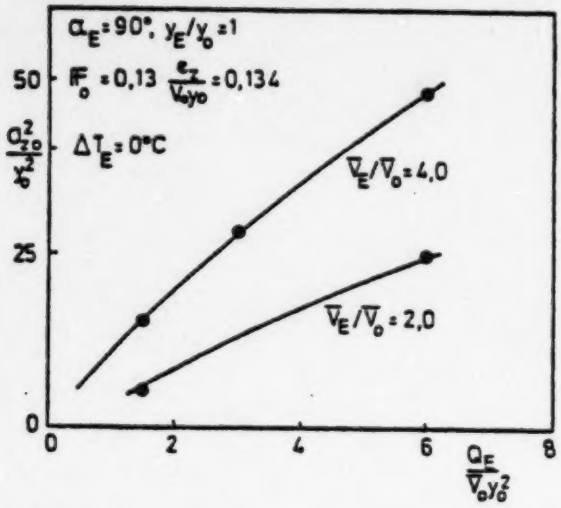

Fig. 3 Dependence of the initial mixing parameter σ^2_{zo} on velocity ratio and volume flux for plumes with zero degree excess temperature

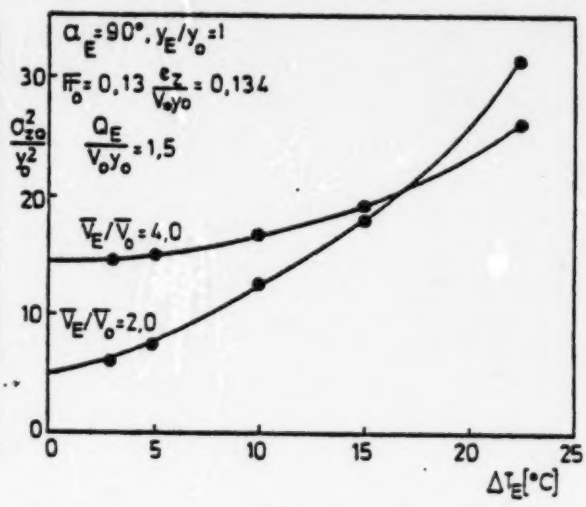

Fig. 4 Dependence of the initial mixing parameter σ^2_{zo} on exit temperature excess for different velocity ratios

When excess temperatures are increased, and all other parameters kept constant, σ^2_{zo} shows a general increase (see Fig. 4). However, the contribution of buoyancy to the total value of the initial mixing parameter σ^2_{zo} is not independent of other initial and ambient parameters such as exit momentum or river turbulence. If the level of ambient- and plume-generated turbulence is sufficiently low, and, at the same time, the local buoyancy sufficiently large, then the heated effluent can stratify and from a warm water wedge at the surface before turbulence finally destroys the stratification. This, of course, would lead to a substantial increase in σ^2_{zo} due to enlarged lateral spreading caused by the large buoyancy.

If, on the other hand, the outfall is designed such that the effluent is emitted with large momentum transverse to the flume flow, ($\bar{V}_E/\bar{V}_o = 4.0$ in Fig. 4), then initial stratification is being prevented with the result that, for our example with excess temperatures of up to 10° C, the contribution of buoyancy to σ^2_{zo} is negligible. For a given cooling water flux Q_E, a specific set of discharge conditions, and a river flow characterized by y_o, $\bar{V}_o$ and e_z, Fig. 4 shows that the rate of near field mixing is highly sensitive to the particular combination of ΔT_E and $\bar{V}_E$. To maximize initial dilution (i.e., maximize σ^2_{zo} in Fig. 4), an increase or reduction of the exit velocity may be necessary, depending on the actual excess temperature of the cooling water.

4.2 Results of Mixing Experiments with Groynes

If the experiments are repeated in a river model containing a non-submerged groyne field located at the discharge bank, local inhomogeneities in turbuelnce intensity along with secondary currents generated at the groyne heads result in an increased space-averaged lateral mixing coefficient e_z [1]. Since in our experiments the widths of the plumes in far-field always exceeded the lateral extend of the zone with flow disturbances due to the groynes, also in situation B a unique e_z - value could be determined from the slope of the $\sigma_z^2(x)$ - curves (Fig. 5). For cases with groynes we found that e_z was equal to 1.5 cm^2/s and $e_z/(V_* \, y_o)$ was equal to 0.167.

However, not only the river flow parameters (e_z, V_*, etc.) are affected when a groyne field is inserted at the river bank. Since the particular combination of river flow and exit parameters determines initial mixing, a discharge structure with given dynamical characteristics performs differently when the river flow properties change. As is demonstrated in Fig. 6, for the same outfall exit conditions, generally different initial mixing parameters σ_{zo}^2 were obtained in situations A and B.

Fig. 6 indicates that after implementation of a groyne field into a river the initial mixing parameter in low buoyancy cases is slightly ($\bar{V}_E / \bar{V}_o$ small) or significantly ($\bar{V}_E / \bar{V}_o$ large) reduced compared with situation A. For large exit excess temperatures, on the other hand, the same alteration at the river bank results in σ_{zo}^2 - values larger ($\bar{V}_E / \bar{V}_o$ small) or only marginally smaller ($\bar{V}_E / \bar{V}_o$ large) than in case of a river without groynes.

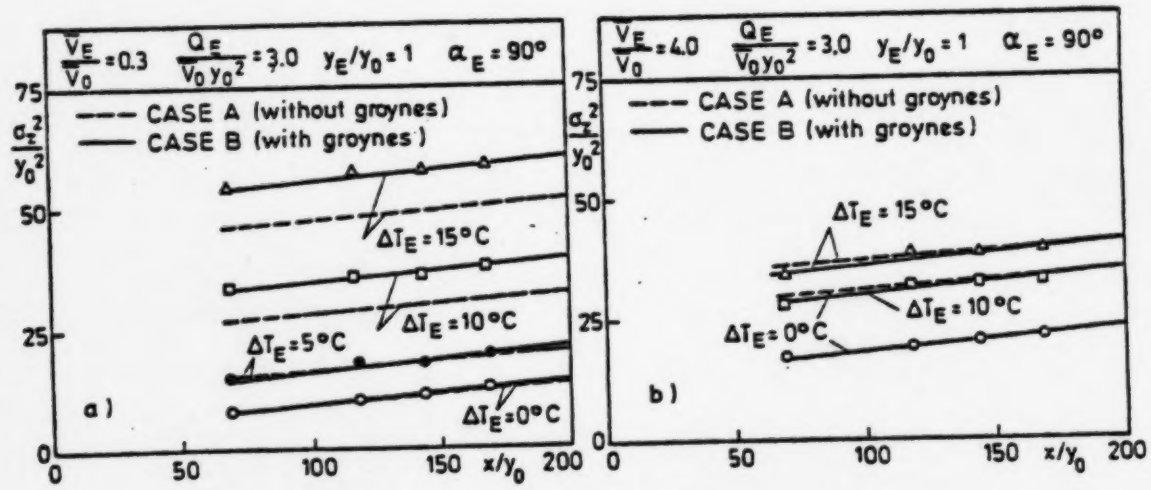

Fig. 5: Nondimensional standard deviation as a function of nondimensional distance for two distinct exit velocity ratios, a sequence of exit excess temperatures, and all other parameters kept constant throughout the measurements

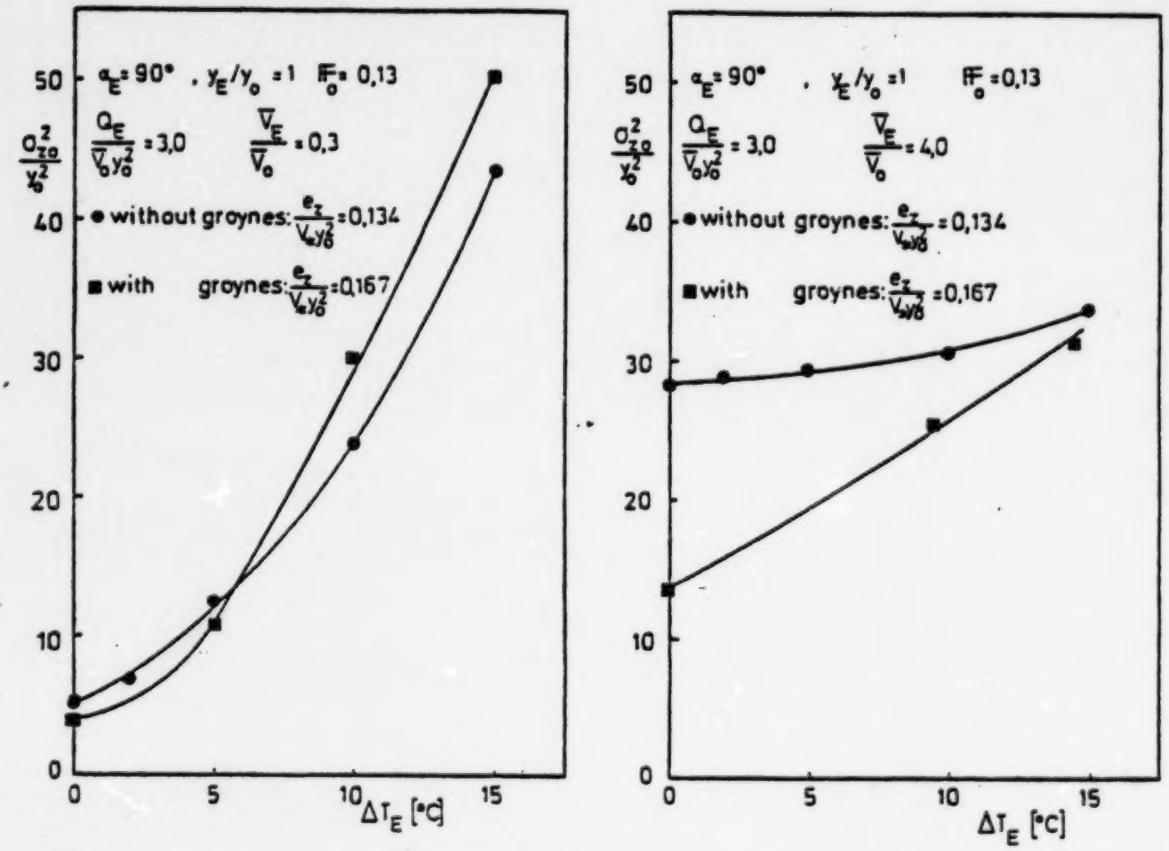
$\alpha_E = 90°$. $y_E/y_o = 1$ $Fr_o = 0,13$
$\frac{Q_E}{\bar{v}_o y_o^2} = 3,0$ $\frac{\bar{v}_E}{\bar{v}_o} = 0,3$
● without groynes: $\frac{e_z}{\bar{v}_o y_o^2} = 0,134$
■ with groynes: $\frac{e_z}{\bar{v}_o y_o^2} = 0,167$
$\frac{\sigma_{zo}^2}{y_o^2}$
ΔT_E [°C]
$\alpha_E = 90°$. $y_E/y_o = 1$ $Fr_o = 0,13$
$\frac{Q_E}{\bar{v}_o y_o^2} = 3,0$ $\frac{\bar{v}_E}{\bar{v}_o} = 4,0$
● without groynes: $\frac{e_z}{\bar{v}_o y_o^2} = 0,134$
■ with groynes: $\frac{e_z}{\bar{v}_o y_o^2} = 0,167$
$\frac{\sigma_{zo}^2}{y_o^2}$
ΔT_E [°C]

Fig. 6: Dependence of the initial mixing parameter σ_{zo}^2 on exit conditions for discharges into a river with and without groyne-protected banks

These at first glance contradictory results can be easily understood when the fact is taken into consideration, that in case B the cooling water is discharged into a dead-water zone between two groynes whereas in case A the effluent is discharged directly into the freely-flowing river. Before in situation B the cooling water jet approaches the reference line (connecting the groyne heads), all jet properties have already been changed to an extend which depends on the actual set of exit parameters.

In case of a discharge with small exit velocity the jet can be so weak that parts of it are engulfed by the recirculating eddy behind the groyne upstream from the outfall (Fig. 7a). In this case we observed, that the colored effluent initially spread over the whole dead-water zone from where it then was re-entrained into the jet. The discharge of colored water into the free river flow occured mainly in the direct vicinity of the groyne downstream from the outlet structure over a very limited section of the reference line. Since in this particular example transverse momentum was small in any way, and the entrainment rate of river water into the jet seemed to be very small within the dead-water zone, it is not surprising that nearly identical σ_{zo}^2 - values were obtained in situations A and B.

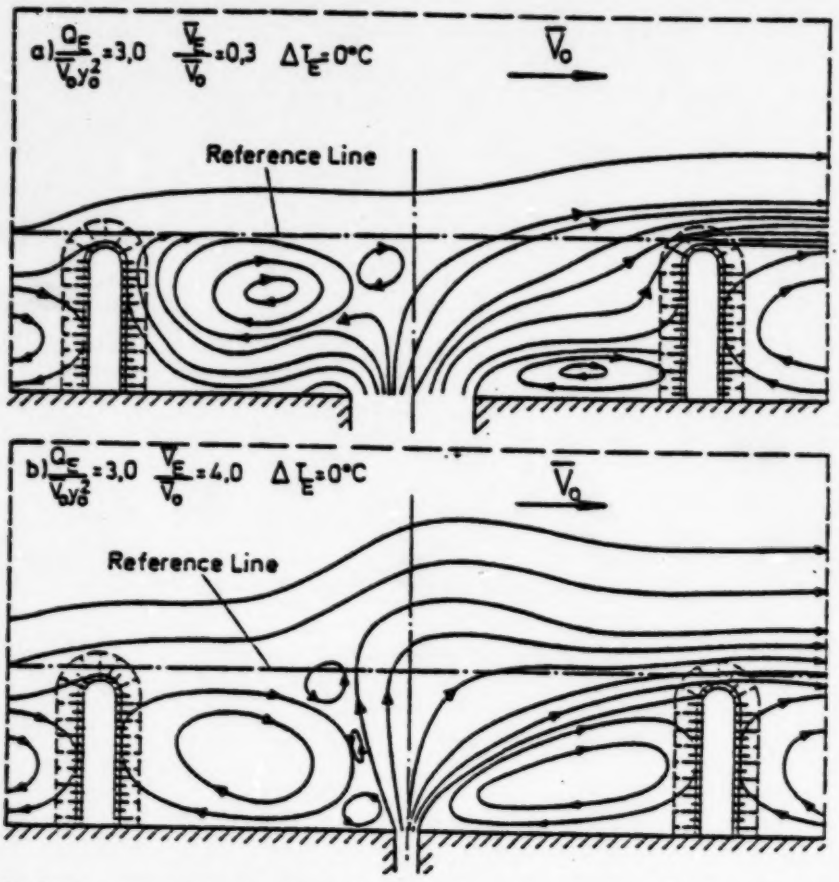
a) $\frac{Q_E}{V_o y_o^2}$ = 3,0 $\frac{V_E}{V_o}$ = 0,3 ΔT_E = 0°C
$\bar{V}_o$
Reference Line
b) $\frac{Q_E}{V_o y_o^2}$ = 3,0 $\frac{V_E}{V_o}$ = 4,0 ΔT_E = 0°C
$\bar{V}_o$
Reference Line

Fig. 7: Surface streamline pattern for non-buoyant jets with identical exit volume flux but different discharge velocity ratio

In case of a non-buoyant jet with large exit velocity (Fig. 7b) the part of the dead-water zone on the left from the outfall remained nearly free of contamination, which indicates that now the steady vortex upstream from the outlet structure was obviously not able to engulf parts of the jet fluid. On the way through the dead-water zone the jet entrained ambient water, thereby distributing its momentum over a larger amount of fluid and loosing excess velocity. Compared with situation A (without groynes), a much "weaker" jet passed the reference line and penetrated into the free river flow. In addition, pressure differences on both sides of the jet supported initial bending. Consequently, a significantly reduced σ^2_{zo} - value was obtained.

As is indicated in Fig. 6, the effect of buoyancy on σ^2_{zo} is generally larger in case B than in case A. For a given excess temperature ΔT_E, sufficiently high that buoyancy effects become important at all, the cooling water might not be able to form a warm water wedge in case A whereas it may be able to do so in situation B as a result of the reduced turbulence level in the dead-water zone between the groynes. In case B as in case A, the initial temperature stratification will be sooner or later destroyed by the river turbuelnce. Nevertheless, in cross sections remote enough from the outfall that the far-field is reached in both cases, we observe mostly a larger σ^2_z in situation B due to the fact that buoyancy was able to contribute significantly to initial lateral spreading.

That in our experiments for the velocity ratio $\overline{v}_E / \overline{v}_o = 4.0$ larger σ^2_{zo} - values were found in case A than in case B is not contradictory to the theory presented above. This particular result reflects only that (1) in case of extremly large exit velocity ratios and moderate excess temperatures, initial mixing mainly depends on transverse momentum, and (2) that momentum dominated jets mix better in rivers without groyne-protected banks. In our example, exit excess temperatures of more than 15°C would have been needed to obtain larger σ^2_{zo} - values in case B than in situation A.

5. CONCLUSIONS

Although the range of parameters covered in our laboratoy experiments is narrow, sufficient data were obtained to show that the implementation of groynes into a river can result into a drastic change of initial mixing characteristics of a given outlet structure. For the design of an discharge structure which maximizes the rate of initial mixing it is therefore important to carefully adjust the entire set of initial parameters based on the properties of the particular river section.

ACKNOWLEDGEMENTS

The authors should like to thank Prof. E. Naudascher for many helpful discussions, and Dr. A.J. Policastro for his suggestions regarding the grammatical formulations of the paper.

REFERENCES

1. Holley, E.R. and Abraham, G. 1973. Laboratory Studies on Transverse Mixing in Rivers. Journal of Hydraulic Research, Vol. 11, pp. 219 - 253.

2. Naudascher, E., Fink, L. and Schatzmann, M. 1979. Das Ausbreitungsverhalten von Abwärme- und Abwassereinleitungen in Gewässern. E. Schmitt Verlag, Bielefeld, Germany.

3. Rodi, W. and Srivatsa, S.K. 1980. A Mathematical Model for the Flow in Channels Containing Groynes. University of Karlsruhe, Report SFB 80/T/160.

4. Sayre, W.W. and Albertson, M.L. 1963. Roughness Spacing in Rigid Open Channels. Transactions, ASCE, Vol. 128.

5. Schatzmann, M. and Naudascher, E. 1980. Design Criteria for Cooling-Water Outlet Structures. Journal of the Hydraulic Division, ASCE, Vol. 106, pp. 397 - 408.

6. Webel, G. and Schatzmann, M. 1980. The Role of Bed Roughness in Turbulent Diffusion and Dispersion. Proc. Symp. on River Engineering and its Interaction with Hydrological and Hydraulic Research, Paper D17, Belgrade.

SESSION IV-A

THERMAL DISCHARGE II

PB82-228024

EVAPORATION FROM HEAT LOADED LAKES: A SUMMARY

Ben L. Sill
Department of Civil Engineering
Clemson University
Clemson, S. C.

1. INTRODUCTION

Accurate calculation or measurement of evaporation from lakes is difficult. Water loss rates are typically small, lakes are often irregular in shape in widely varying terrain, and effects such as atmospheric stability, dynamic weather conditions and wind generated waves all hinder the determination of evaporation. If these problems are compounded by superimposing a thermal discharge on the natural lake conditions, then the resulting analysis is quite complicated. The most important factor to consider is that usually the surface of a heat loaded lake is not isothermal, but often exhibits substantial temperature variations. One of the primary interests in determining the evaporation from heated lakes is to assess the amount of the heat load which goes toward increasing the natural lake evaporation.

The purpose of this paper is to present a brief summary of present approaches for determination of evaporation from thermally loaded lakes. The discussion will include the most widely used techniques for both measuring and predicting lake evaporation with emphasis on their applicability to heated lakes. One of the most widely used approaches for prediction of evaporation is through use of mathematical models. Application of some simple models to heated lakes and the accuracy of such approaches will also be presented. The paper concludes with a discussion of the relative merits of various methods.

2. EVAPORATION MEASUREMENT

Techniques for measurement of evaporation may be divided into two broad categories: point measurement, and budget techniques. Since the surface temperature of a thermally loaded lake typically varies with location, the measurement of evaporation at a point will only yield the actual rate at that point. It cannot be directly extrapolated to the entire water body. In general, warmer surface waters will evaporate more rapidly, cooler more slowly.

Budget measurement techniques are better suited for heat loaded lakes. One of the most widely used is the water budget (or mass conservation). With this approach, an accounting of all the water inflows and outflows yields

Preceding page blank

Change in Water Stored = Inflow Rate − Outflow Rate + Precipitation (Surface runoff)

− Evaporation ± Groundwater Seepage

Of these terms, precipitation, storage and outflow (through a spillway) are usually the simplest to measure. For lakes with numerous tributaries, it is often not economically feasible to gage all inflow contributions on a continuous basis. Also, leakage through an earthen dam or into the lake bottom can often be on the same order as the evaporation rate. Since evaporation is calculated from the difference in these terms, it depends heavily on the accuracy of each. In some situations, this technique can provide satisfactory results (Ref. 1) and it has the advantage of eliminating the need to know the surface temperature distribution. A summary of the required measurements is given in Table I.

TABLE I

DETERMINATION OF LAKE EVAPORATION BASED ON FIELD MEASUREMENTS

	NON HEATED			HEATED		
MEASUREMENTS	WATER BUDGET	ENERGY BUDGET	DALTON	WATER BUDGET	ENERGY BUDGET	DALTON (DUHAMEL)
POINT						
Inflow, outflow (Seepage and temperature)	X	X		X	X	
Precipitation (and its temperature)	X	X		X	X	
Lake Level(storage)	X			X		
Meteorological (wind, temperature, radiation, etc.)		X	X		X	X
Surface Temperature at a point		X	X			
LAKEWIDE						
Surface Temperature Distribution					X	X
Vertical Temperature Profiles		X			X	
Surface Runoff Seepage	X	X		X	X	

A second commonly used method is the thermal energy budget. It is based on energy conservation and may be stated

Change in energy stored	=	Advected Energy Inflow	−	Advected Energy Outflow	+	Precipitation Energy Inflow	−	Evaporative Energy Flux

+	Long wave Atmospheric Radiation	+	Short Wave Radiation	−	Reflected Short Wave Radiation	−	Long Wave Radiation from Water	−	Energy Conducted from Water surface

While the energy budget approach has been widely used for unheated lakes, it is more difficult to apply to heated lakes. The long wave radiation emitted by the water and the energy conducted from the surface as sensible heat are both functions of the surface temperature. As a result, these terms vary from place to place in the lake. Additionally, it is not possible to accurately measure the energy stored in a heated lake without taking temperature profiles at numerous representative locations. A direct consequence of these drawbacks is that it is difficult to employ energy budget methods on heated lakes. Even so, successful energy budget studies have been conducted on both non-heated (Ref. 1) and heated (Ref. 2) lakes.

3. EVAPORATION CALCULATION FROM NON-HEATED LAKES

From an engineering viewpoint, two basic approaches for calculation of unheated lake evaporation rates have found wide usage. These are: (1) Dalton (or bulk aerodynamic) type equations, and (2) the energy budget technique.

Dalton type expressions assume the evaporation rate is driven by the difference in the saturated water vapor pressure at the surface temperature and the vapor pressure of the ambient air (e_s and e_a respectively) and is proportional to this difference. The proportionality constant depends (at least) on the wind speed u and is often termed the "wind speed function", f. This form of the evaporation rate is written as (Ref. 3)

$$E = f(u) \quad (e_s - e_a) \tag{1}$$

There are several problems with the use of this equation but the most important is with the definition of f. Examination of existing literature indicates that there are on the order of one hundred proposed expressions for the wind speed function. Figure 1 gives some of these (see Ref. 3, 4, 5 and 14 for tabulations) and vividly demonstrates the scatter. As a result, there is not a universally accepted wind speed function. The primary reasons for this are that f depends on atmospheric stability (Ref.6) and lake shape and terrain (Refs. 7, 8) in addition to wind speed, although the exact dependencies have not been determined. Since the value of evaporation calculated by equation (1) is directly proportional to f, a 10% uncertainty in f yields a 10% uncertainty in predicted evaporation. In other words, the computed value of evaporation is directly linked to the adequacy of the wind speed function.

A second way to calculate evaporation from non-heated lakes is with the energy budget approach. Results from a computer model which predicts lake temperature distributions allow calculation of the long wave radiation

from the water surface and advected energy changes. Solar and atmospheric radiation inputs can also be computed based on atmospheric conditions. Assuming that the conducted energy transfer is proportional to the evaporative flux (through the Bowen ratio B, where $B = 0.26\ (e_s - e_a)$ mmHg/$(T_s - T_a)$ ^{o}F) the evaporative energy flux Q_E is obtained from Eq. 1 as

$$Q_E = \frac{1}{1+B}\left(\left((\rho q C_v T)_{in} - (\rho q C_v T)_{out}\right)/A_T + (Q_s + Q_A - Q_B - Q_n)\right) \quad (2)$$

where qC_vT represents the advected energy terms with flow rate q, and specific heat C_v, Q_s and Q_a the net solar and long wave atmospheric radiation, respectively, Q_B long wave radiation emitted at the surface, and Q_n the stored energy which corresponds to the net flux at the surface (units on heat flux terms, Q's, are BTU/day/ft^2).

For long time periods (e.g. a year) it may be appropriate to assume that energy stored in the lake can be neglected. If the advected energy difference is small compared to the radiation flux, equation (2) can be simplified to

$$Q_E = \frac{Q_r}{1+B} \quad (3)$$

with Q_r the net radiative energy transfer over the time period.

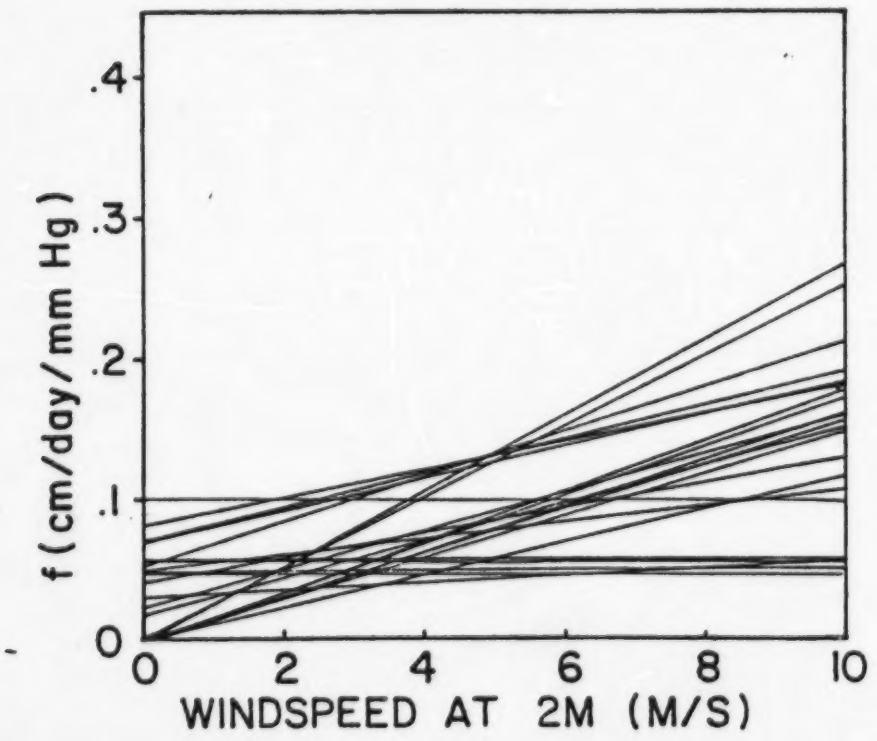

Figure 1. Examples of several of the many proposed wind speed functions.

4. EVAPORATION CALCULATION FOR HEAT LOADED LAKES

There are two basic ways to obtain the evaporation from a heated lake. First, extensive field measurements from an existing lake can be used to find the evaporation. Secondly, mathematical models can be used to predict temperatures (from either existing or proposed lakes) which in turn are used to calculate evaporation. Table I summarizes the field measurements which are required to allow calculation of evaporation from thermally loaded lakes.

4.1 Lake Measurements

The water budget approach using field surveys is applied in the same manner for heated and non-heated lakes, requiring accurate measurements of flow rates. Only point measurements are needed except for estimation of seepage and surface runoff. Measurement of all tributary inflows is often quite difficult.

Requirements for the energy budget technique have been discussed previously so that only the differences in measurements need be mentioned. The primary change is that a complete surface temperature distribution is needed to compute the long wave radiation from the surface. For short time periods, the energy storage term must be accurately determined requiring many vertical temperature profiles. For longer periods (say 1 year) the net energy stored may be relatively small, but the surface temperatures needed for the long wave radiation term (Q_B) must be monitored for the entire period to provide a satisfactory average. For either short or long time periods the presence of a surface temperature gradient substantially complicates the application of an energy budget approach.

Dalton type equations can be used directly to calculate evaporation from heated lakes based on field measurements. This is done by assuming that the velocity field over the lake is not coupled to the mass flux or temperature distribution of the surface. Such an approach (a modification of Duhamel's theorem, Ref. 9) has been successfully used to compute heat flux from flat plates with arbitrary surface temperature distributions. At the present time, work is in progress at Clemson University to apply Equation (1) to the prediction of evaporation from thermally loaded lakes with specified surface temperatures. The advantage of such an approach is in its ability to analyze complex surface temperature distributions. A disadvantage is that the resulting computed value of evaporation is limited by the accuracy of the value of the wind speed function.

4.2 Predicted Lake Evaporation

Since the water budget technique requires measured flow rates, it can be used only for existing water bodies, and will not be discussed in this section. Discussion here will be limited to the application of Dalton type expressions and the energy budget approach. The presentation will focus on errors resulting from the predictive approach. First, the error in calculated evaporation due to errors in improper prediction of surface temperature will be examined. Next, the error in evaporation prediction relative to a specified error in the wind speed function will be examined.

To analyze the effect of errors in predicted surface temperature, it will be assumed that the true expression for f is known for a particular lake. A schematic showing typical surface temperatures for a one dimensional situation is given in Figure 2. Based on these assumptions, the

actual total lake evaporation is

$$E_a = \int f\,(e_s - e_a)\,dA \tag{4}$$

where e_s is a function of the measured surface temperature, T_s. The evaporation computed from the modelled surface temperature is

$$E_c = \int f\,(e_{sc} - e_a)\,dA \tag{5}$$

in which the water vapor pressure at the surface e_{sc} is based on computed temperatures, T_{sc}. If the vapor pressure error ε_e is defined as $e_{sc} - e_s$, and the Dalton difference $e_s - e_a = b(T_s - T_d)$ with $b = \partial e_s/\partial T_s$ given as (Ref. 3)

$$b = 0.255 - .0085\,T^* + .000204\,(T^*)^2 \quad \frac{\text{mmHg}}{^\circ\text{F}} \tag{6}$$

with T^* the average of the surface and dew point temperatures (in $^\circ$F). We can then write

$$\frac{E_c}{E_a} = 1 + \frac{\int b\varepsilon_s\,dA}{\int b(T_s - T_d)\,dA} \tag{7}$$

where ε_s is the error in the surface temperature (Fig. 2). Assuming that the variation of b over the lake surface is relatively small, then the simple expression

$$\frac{E_c}{E_a} = 1 + \frac{\bar{\varepsilon}_s}{\bar{T}_s - T_d} \tag{8}$$

is obtained, where overbars denote area averages. Since ε_s can be positive or negative, the minimum error in calculated evaporation occurs when surface temperatures are overpredicted for a portion of the lake and unpredicted for the remainder. If a lake model predicts to within 2° C and the difference in average surface temperature and the dew point is 10° C then evaporation calculated by Equation (5) using the modelled surface temperatures would be 20% different than that calculated using actual surface temperatures. This error is in addition to any errors involved in the use of an inaccurate wind speed function.

Error analysis of this type can be carried one step further without an undue amount of complication. This is done by examining the effect of an error in the wind speed function on surface temperature prediction and subsequent evaporation calculation using the same incorrect wind speed function. Since evaporative rates are directly proportional to f, if too large an f is used, too much heat (latent) is removed from the lake and surface temperatures are under-predicted. However, the use of the same f with low surface temperatures (and thus vapor pressures) provide some compensation in evaporation calculation. Several simple examples of this effect are discussed below.

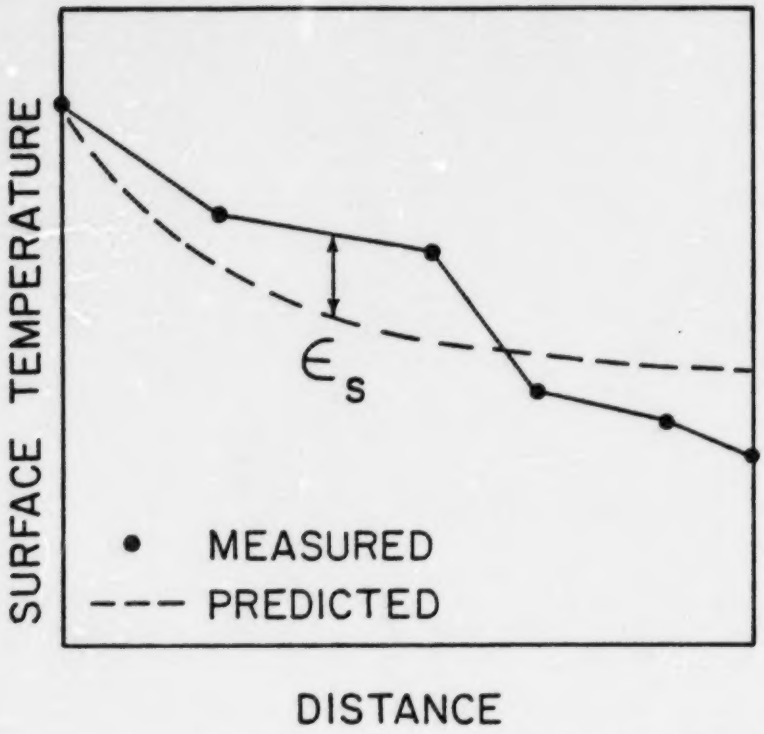

Figure 2. Schematic showing examples of measured and predicted lake surface temperatures with resulting errors.

4.2.1 Dalton Equations

The commonly used expression for decay of the surface temperature T_s is

$$\frac{T_s - T_E}{T_{so} - T_E} = \exp\left(-\frac{KA}{\rho C_v q}\right) \tag{9}$$

where T_E is the equilibrium temperature, K the surface heat exchange coefficient, A surface area, ρ water density, C_v constant volume specific heat, q the flow rate, and T_{so} the initial surface temperature. The net surface energy flux is written as

$$Q_n = -K\,(T_s - T_E) \tag{10}$$

The exchange coefficient K depends on f as (Refs. 3, 10),

$$K = C_1 + C_2\, f \tag{11}$$

so long as f is not a function of surface temperature. Assuming that C_2 is constant over some range of temperature, $\partial E/\partial f$ is calculated for Equation (1) using Equations (9), (10), and (11), and noting that $b = \partial e_s/\partial T_s$ yields

$$\frac{\partial E}{\partial f} = \frac{E}{f}\left[1 - \left(\frac{\Theta}{1+\Theta}\right)\left(1 - \frac{C_1}{K}\right)\ln\left(\Theta_o/\Theta\right)\right] \tag{12}$$

where

$$\Theta = (T_s - T_E)/(T_E - T_d) \tag{13}$$

To evaluate the percentage error in evaporation $\Delta E/E$ resulting from a specified percentage error in wind speed function, equation (12) is written as

$$H_D = \frac{(\Delta E/E)}{(\Delta f/f)} = 1 - (1 - \frac{C_1}{K})(\frac{\Theta}{1+\Theta}) \ln (\Theta_o/\Theta) \tag{14}$$

with subscript D denoting use of a Dalton formulation. Based on this expression, H is unity when $\Theta = \Theta_o$ and $\Theta = 0$. These conditions occur at the discharge point (where the temperature is specified) and very far downstream (where $T_s = T_E$). Since the surface temperature is known for both these locations, errors in evaporation are directly proportional to errors in f, hence H = 1. For intermediate stations, the surface temperature is predicted by equation (9) and H benefits from the compensating effects discussed earlier. Figure 3 shows this variation for a typical value of Θ_o. The error in calculated evaporation from modelled surface temperatures is always equal to or less than the error in the wind speed function as shown by the ratio H.

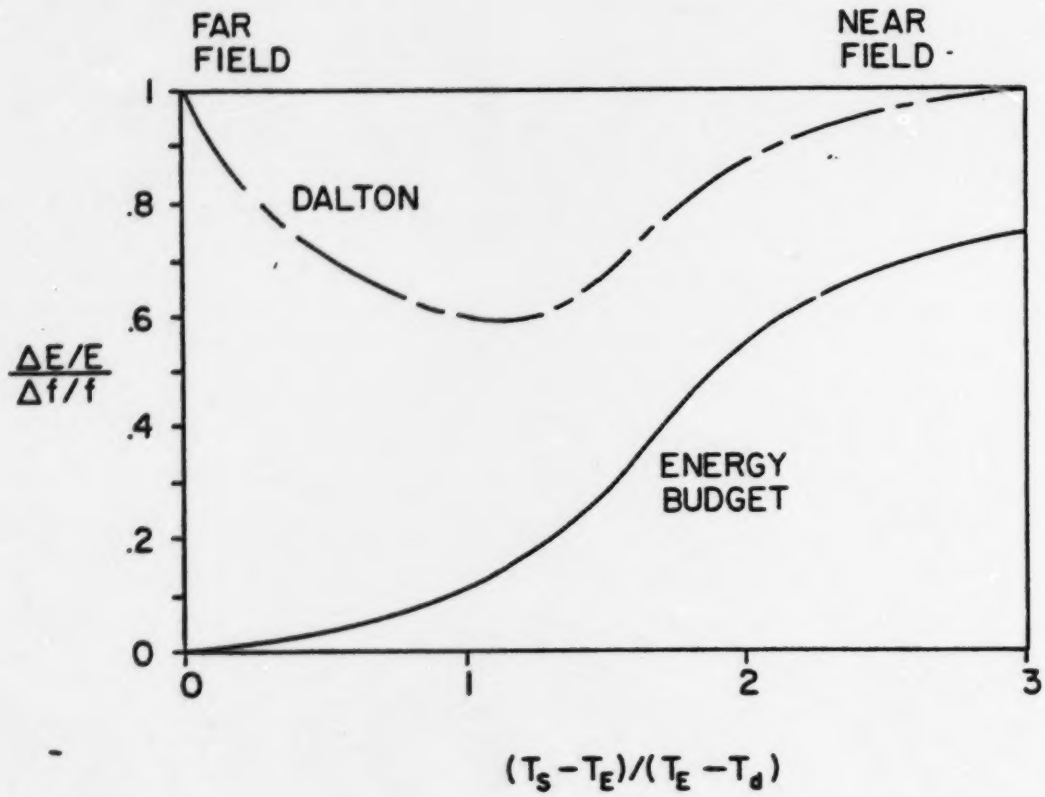

Figure 3. Percentage error in evaporation prediction relative to a specified error in the wind speed function for two modelling approaches, $\theta_o = 3$, $C_1/K = .2$.

4.2.2 Energy Budget

The same type of analysis can be performed if evaporation rates are calculated by an energy budget approach. Assuming B is independent of f, differentiating Equation (2) and using Equations (9), (10) and (11) gives

$$H_B = H_D - \frac{1}{(1+\Theta)} \tag{15}$$

where it is assumed that $(1 + C_2/b)/(1+B) = 1$. Equation (15) is also plotted in Figure 3 and demonstrates that the energy budget method is less sensitive to errors in wind speed function that is the Dalton type formulation. In fact the energy budget analysis becomes increasingly less sensitive as the effluent moves away from the discharge point. The error goes to zero (i.e. the evaporation prediction becomes independent of f) at large distances since $T_s = T_E$ and the heat exchange coefficient (which depends on f) drops from the equation. Then the analysis is essentially that for an unheated lake.

Accuracy of predicted evaporative rates with the energy budget approach also can suffer from errors in terms other than Q_s and Q_n. These errors resulting from cloud cover measurement, reflectivity of the water surface, advected energy transfer, or errors in the Bowen ratio, are usually considered fairly small but are not always negligible.

5. EVAPORATION ATTRIBUTABLE TO A THERMAL LOADING

It is possible to estimate the percentage of heat rejected from a thermal discharge through increased evaporative rates. This has been done by Harbeck (Ref. 11) for a completely stirred pond and using basically a Dalton equation approach. Results from his analysis depend heavily on the wind speed function in the form

$$\frac{\Delta E}{Q_p} = \frac{f}{a_1 + a_2 f} \tag{16}$$

where a_1, and a_2 are computed constants, and ΔE is the increase in lake evaporation resulting from the heat input Q_p. Both a_1 and a_2 vary with lake temperature. For a wind speed range of 5 to 20 mph and lake temperatures of from 45° F to 90° F, Equation 16 gives values of 37 to 73 per cent (as given in Ref. 11). An error analysis of this approach is given in Ref. 15.

A second way to estimate $\Delta E/Q_p$ is with the energy budget technique. First, natural lake evaporation is obtained and then the increase due to a thermal loading is calculated by the same procedure. This technique has been presented in Ref. 12 and will be briefly outlined here.

The terms comprising the energy flux are (see Ref. 3)

1. surface inflow - $\rho C_v q_{si}(T_{si} - T_b) = Q_{si}$

2. groundwater inflow - $\rho C_v q_{gi}(T_{gi} - T_b) = Q_{gi}$

3. surface outflow - $\rho C_v q_{so}(T_{so} - T_b) = Q_{so}$

4. groundwater outflow - $\rho C_v q_{go}(T_{go} - T_b) = Q_{go}$

5. precipitation - $\rho C_v q_r(T_r - T_b) = Q_r$

6. net incoming solar radiation - Q_s given (or calculated)

7. long wave atmospheric radiation - $K_1 T_a^6(1+.17C_c^2) = Q_A$

8. back radiation from water surface - $K_2 T_s^4 = Q_B$

9. evaporative (latent heat) flux - Q_E

10. sensible heat (conduction) $BQ_E = Q_C$

11. energy lost with evaporated water - $Q_w = \frac{C_v}{h_v}(T_s - T_b)\, Q_E$

In these expressions, T_b is a base temperature, q's are water flow rates, K's constants, h_v the latent heat of vaporization and C_c the fractional cloud cover. The net change in lake energy content Q_n is then

$$Q_n = (Q_s + Q_A - Q_B - Q_E - Q_C - Q_W)A_T + Q_{si} - Q_{so} + Q_{gi} - Q_{go} + Q_r \qquad (17)$$

with A_T the total lake area. Definitions 1 - 11 are substituted into equation (17) and integrated for a period of one year. The water surface and air temperatures are assumed to vary sinusoidally through the year and all higher order terms resulting from the integration for Q_A and Q_B are neglibible and are dropped. It is further assumed that the sum of the advective terms (last five terms in equation (17)) is small and is neglected. A final simplification is obtained by writing

$$\int Q_E\left(1+B+\frac{C_v}{h_v}(T_s - T_b)\right) A_p\, dt = A_p S \int Q_E\, dt \qquad (18)$$

with S a constant, so that the expression for annual natural evaporation is (for dimensions see Refs. 3, 10 or 12) for time t = 365 days

$$E_N(m) = \frac{1}{S}\left[Q_{sT} + \left((1.17 \times 10^{-13})\,(1 + .17C_c^2)\,\bar{T}_a^{\,6} - 4 \times 10^{-8}\,\bar{T}_s^{\,4}\right)(365)\right] 4.75 \times 10^{-6} \qquad (19)$$

Here Q_{sT} is the yearly total <u>net</u> solar radiation (in BTU/ft^2), S = 1.31 for the Piedmont Carolinas (by comparison with data, Ref. 13), and $\bar{T}_a$ and $\bar{T}_s$ are the annual average air and lake surface temperatures respectively (in $^\circ$R). Predictions of equation (19) for eight lakes on the

Catawba River, N.C., using a minimum of thirteen years of surface temperature data yielded evaporations within 3% of those in Ref. 13. Values varied from .88 m/yr. to 1.09 m/yr. No attempt was made to determine the variation of S with location.

The same procedure can be used for estimating the forced evaporation due to a thermal load. An additional term is added to the right side of equation 17 to represent the external heat source as $-dQ_{ex}/dA$. Subtracting equation 17 from the thermally loaded expression and noting that many of the terms are independent of water surface temperature gives upon integration over time

$$E_F - E_N = \frac{1}{S}\left[\int (Q_{BN} - Q_B)\, dt - \int \frac{dQ_{ex}}{dA}\, dt\right] \tag{20}$$

with F and N subscripts denoting forced and natural conditions respectively. Utilizing equation 9, dQ_{ex}/dA becomes (for a one dimensional flow)

$$\frac{dQ_{ex}}{dA} = -(T_{so} - T_E)\, K \exp\left(-\frac{KA}{\rho C_v q}\right) \tag{21}$$

and linearizing the expression for Q_B and Q_{BN} gives (assuming $T_{SN} = T_E$)

$$Q_B = Q_{BN}\,(1 + 4\,(T_S - T_E)/(T_{SN} + 460)\,) \tag{22}$$

These equations are substituted into equation 20 and integrated over the entire lake area. The order of integration is reversed (integrate over area first) and the result is divided by the heat input by the plant $\rho C_v q(T_{so} - T_{si})N$ to obtain the fraction of the thermal load used to increase evaporation. Here T is the time period (number of days; 365 typically) of interest and $T_{so} - T_{si}$ the difference in power plant discharge and intake temperatures respectively. Assuming S = 1.31 as before

$$\frac{\Delta E}{Q_p} = \frac{1}{1.31}\left(\frac{T_{so} - T_E}{T_{so} - T_{si}}\right)\left[1 - \left(\frac{\overline{T_{ST} - T_E}}{T_{so} - T_E}\right) - \frac{4K_2}{T}\int_0^T \frac{(T_{SN}+460)^3}{K}\, dt\right] \tag{23}$$

If the plant intake temperature equals the temperature at the extreme end of the lake ($T_{si} = T_{ST}$) and the lake is sufficiently large so that $T_{ST} = T_E$ then (with T = 365 days)

$$\frac{\Delta E}{Q_p} = 0.76\left[1 - 4K_2\,\frac{\overline{T_{SN} + 460^3}}{K}\right] \times 100\% \tag{24}$$

with $K_2 = 4 \times 10^{-8}$ BTU/ft^2/day/^{o}f^4. For lakes in the Piedmont Carolinas, this equation yields values of 55% to 65% for $\Delta E/Q_p$ and equation (23) gives slightly lower values. It is important to note that even in the energy budget approach which produces Equations (23) and (24), f appears implicitly in the heat transfer coefficient K.

6. DISCUSSION

The present paper presents several techniques which can be used for the determination of evaporation from heat loaded lakes and enumerates problem areas which leads to inaccurate predictions. Results are given for both the measurement and calculation of evaporation from heated lakes.

Water bodies subject to a thermal loading often exhibit substantial surface temperature gradients. For these conditions, budget measurement techniques are most readily utilized. At the present time, the energy budget and water budget approaches are most widely used. The primary problem with either of these is that calculation of evaporation is accomplished by summing a number of large magnitude terms to obtain a relatively small number. Consequently even small percentage errors in any of these quantities can substantially effect the predicted value of evaporation.

An additional way to calculate evaporation directly from field data is to apply a Dalton type equation over the lake surface by using surface temperature measurements to compute surface water vapor pressures. While this approach is direct and requires a minimum of lakewide field information, it depends directly upon the accuracy of the wind speed function.

Both the Dalton and energy budget approaches can be coupled with a predictive lake temperature model to calculate evaporation. Predicted lake temperatures depend on the wind speed function. Consequently an error in f will yield an error in surface temperature and finally an error in calculated evaporation. These errors are often partially compensating. It is demonstrated that the energy budget approach is less sensitive to errors in f than is the use of a Dalton equation. The analyses presented assume that a proper expression for f is known and the predicted evaporation errors are measured from the accurate value. In reality this is not the case, and we can only draw the conclusion that the accuracy of the energy budget technique will suffer less than will the Dalton method when applied to an entire lake.

Present measurement techniques have three basic disadvantages: they are costly, restricted to existing lakes, and tedious to employ for extended periods. Present mathematical modelling efforts suffer primarily from a lack of knowledge of an accurate wind speed function for a particular site, and to a lesser degree in approximations in the lake model itself. While f may be "tuned" for an existing lake, the best present method to do this has not been satisfactorily determined. Further, predictive use of the poorly known wind speed function may produce errors of substantial magnitude.

REFERENCES

1. Water Loss Investigations: Lake Hefner Studies, Technical Report, U.S. Geological Survey Professional Paper 269, U.S. Printing Office, Washington, D.C., 1954.

2. Harbeck, G.E., Hoberg, G.E., and Hughes, G.H., "The Effect of the addition of heat from a power plant on the thermal structure and evaporation of Lake Colorado City, Texas," USGS Professional Paper No. 272-B, 1959.

3. Ryan, P.J., and D.R.F. Harleman, An Analytical and Experimental Study of Transient Cooling Pond Behavior, Ralph M. Parsons Laboratory, Department of Civil Engineering, Report No. 161, Massachusetts Institute of Technology, Cambridge, Mass., January, 1973.

4. Paily, P.P., E.O. Macagno and J.F. Kennedy, Winter Regime Surface Heat Loss from Heater Streams, Report No. 155, Iowa Institute of Hydraulic Research, 1974.

5. Wunderlich, W.O., Heat and Mass Transfer Between a Water Surface and the Atmosphere, Engineering Laboratory, Tennessee Valley Authority, Lab. Report No. 14, 1972.

6. Pruitt, W.O., et al, "Momentum and Mass Transfers in the Surface Boundary Layer", Quarterly Journal of the Royal Meteorological Society, Vol. 99, 1973, pp. 370-386.

7. Harbeck, G.E., "A Practical Field Technique for Measuring Reservoir Evaporation Utilizing Mass-Transfer Theory", U.S.G.S. Professional Paper 272-E, 1962.

8. Brutsaert, W. and Shaw-Lei Yu, "Mass Transfer Aspects of Pan Evaporation," Journal of Applied Meteorology, Vol. 7, No. 4, 1968.

9. Eckert, E.R.G. and R.M. Drake, Jr., Heat and Mass Transfer, McGraw-Hill Book Co., New York, NY 1959.

10. Edinger, J.E.,and J.C. Geyer, "Heat Exchange in the Environment," Publication No. 65-902, Edison Electric Institute, New York, June, 1965.

11. Harbeck, G.E., Jr., "Estimating Forced Evaporation from Cooling Ponds," Journal of the Power Division, ASCE, Vol. 90, No. PO3, October, 1964.

12. Sill, B.L., Heat Transfer and Evaporation from Open Water Bodies, Duke Power Company Technical Report, DUKEPWR/76-02, August, 1976.

13. Geraghty, J.J., D.W. Miller, F. Van der Leeden, and F.L. Troise, Water Atlas of the United States, Water Information Center Publication, Port Washington, NY, 1973.

14. Edinger, J.E., D.K. Brady, and J.C. Geyer, "Heat Exchange and Transport in the Environment," Report No. 14, Electric Power Research Institute Research Project RP-49, The Johns Hopkins University, Baltimore, Maryland, Nov. 1974.

15. Ward, G.H., Jr., "Accuracy of Harbeck Diagram for Forced Evaporation," Journal of the Energy Division, ASCE, Vol. 106, No. EY1, April, 1980.

PB82-228032

INVESTIGATION OF LAKE BELEWS

S. K. Mathavan
Florida Power & Light Company
P. O. Box 529100, Miami Florida 33152

W. J. McCabe
Duke Power Company
500 South Church Street, Charlotte, NC 28242

S. S. Lee and S. Sengupta
University of Miami
Coral Gables, Florida 33124

ABSTRACT

In 1976-1977, an investigation of Lake Belews was conducted to investigate its capability as a cooling pond. The investigation included infrared scanning of surface temperatures, in situ measurements of temperatures and currents and three-dimensional computer simulation. Field investigations of summer 1976 and winter 1977 are presented in this paper. The investigation shows that the lake is stratified most of the year and exhibits complete mixing once a year during winter. The thermal discharge is cooled completely and there is no recirculation of the hot effluent.

1. HISTORY OF LAKE BELEWS

Lake Belews was created by Duke Power Company by building a dam on Belews Creek in 1970, to serve as a cooling pond for two Belews Creek coal fired units of 1143 MW_e each. The lake has a surface area of 3863 acres. It lies northeast of Winston-Salem, North Carolina. The lake has two separate parts connected together by a canal. (See Figure 1.) The smaller portion of the lake is rather shallow with a maximum depth of 13.72 meters. This part of the lake is referred to as The Mixing Pond in this paper. The larger part of the lake is quite deep with a maximum depth of 38.2 meters. This portion of the lake is referred to as The Main Lake in this paper. The surface area of the Main Lake is approximately eleven times the surface area of the Mixing Pond and the volume of the Main Lake is approximately twenty-two times the volume of the Mixing Pond. The plant intakes condenser cooling water from the Main Lake and the heated effluent is discharged into the Mixing Pond. (See Figure 1.) The design rise in temperature is 10°C during summer and 15°C during winter. Initial mixing of the effluent occurs in the Mixing Pond and from there it flows through the canal into the Main Lake where most of the cooling occurs.

2. STUDY METHODOLOGY

The study of Lake Belews included three procedures. Firstly, the surface temperatures were scanned with an infrared scanner flown at an altitude of 609.6 meters above the water surface. A Daedalus multispectral scanner carried aboard a Beachcraft airplane was used for this purpose. Several passes were made over the lake using an 8-14 micron window and a mosaic of all the passes provided a mapping of the surface temperatures. Secondly, measurements of surface and subsurface temperatures and current velocities were made from boats. Thirdly, a three-dimensional numerical simulation of the thermo-hydraulics of the lake was carried out to simulate the thermal discharge, wind driven circulation and atmospheric heating and cooling of the lake.

The investigations were conducted for four seasons over a two-year period from 1976 to 1977. Field investigations for the summer of 1976 and the winter of 1977 are presented in this paper. The complete study is documented in the doctoral dissertation of Mathavan [1]. A discussion on the Mixing Pond was presented at the First Waste Heat Management and Utilization Conference [2].

3. INVESTIGATION OF SUMMER 1976

The summer investigation was conducted on August 26, 1976. Surface isotherms for the morning are given in Figure 1 and for the afternoon in Figure 2. Vertical temperature profiles at various depths below the water surface are given in Figure 5. A comparison of the morning and afternoon surface isotherms shows that the lake surface was approximately 1°C warmer in the afternoon. The surface temperatures varied from 39°C to 29°C. Vertical temperature profiles show that the Mixing Pond was fairly well mixed while the Main Lake exhibited stratified thermal behavior. In the Main Lake thermocline existed at approximately 11.5 meters. Ambient surface temperature was 29°C while the ambient bottom temperature was 11°C. The thermal discharge was accumulated in the top six meters of the lake and the accumulation of the thermal energy was maximum near the discharge and gradually reduced to zero near the plant intake.

Wind on this day was from S-SW and varied from 5.0 m/sec to 3.7 m/sec. Such a wind direction helped spread the discharge over the lake surface, thus increasing the discharge heat transfer area and helping the discharge cooling. The discharge flow rate was 228.9 x 10^6 kg/hr which represented a waste heat equivalent to 2658 MW at 10°C of temperature rise.

4. INVESTIGATION OF WINTER 1977

The winter investigation was conducted on January 25, 1977. Surface isotherms for the morning are given in Figure 3, for the afternoon in Figure 4 and the vertical temperature profiles below the water surface are given in Figure 6. A comparison of the morning and the afternoon surface isotherms shows that the surface was slightly warmer in the afternoon. The surface temperatures varied from 23°C to 7°C. The vertical temperature profiles show that the Main Lake ambient conditions were well mixed. The

thermal discharge was accumulated in the top six meters of the lake. The thermal accumulation was at a maximum near the discharge and gradually reduced to zero near the intake. The ambient temperature of the Main Lake was 7°C. The average temperature in the Mixing Pond was about 20°C.

Winds on this day varied from 3.7 m/sec, W to 6.6 m/sec, NW. Air temperature on this day was around 4.3°C. The thermal discharge temperature was 23°C and the flow rate was 143.9 x 10^6 kg/hour, which represented a waste heat equivalent to 2674.4 MW at 16°C of temperature rise.

CONCLUSIONS

Investigation shows that the Main Lake behaves as a monomictic lake exhibiting one overturning during the winter season. The thermal discharge is contained in the top six meters of the Main Lake and the ambient conditions exist below this depth. The lake provides sufficient surface area for cooling the thermal discharge which is cooled down to the ambient temperature before entering the intake. The velocities in the Main Lake were too small to be measured accurately with the velocity meter (Endeco-Type 146, Environmental Monitoring System).

ACKNOWLEDGEMENT

The investigation of Lake Belews was conducted jointly by the University of Miami, Duke Power Company and the National Aeronautics and Space Administration, Kennedy Space Center. The authors express their sincere appreciation to those involved in the project.

REFERENCES

1. Mathavan, S. K. 1977. Experimental and numerical study of current and temperature fields in Lake Belews, an artificial cooling pond. University of Miami, doctoral dissertation.

2. Mathavan, S. K; Lee, S.S. and Sengupta, S. 1977. Numerical and remote sensing studies of Lake Belews, an artificial cooling lake. Waste Heat Management and Utilization Conference, Miami Beach, Florida.

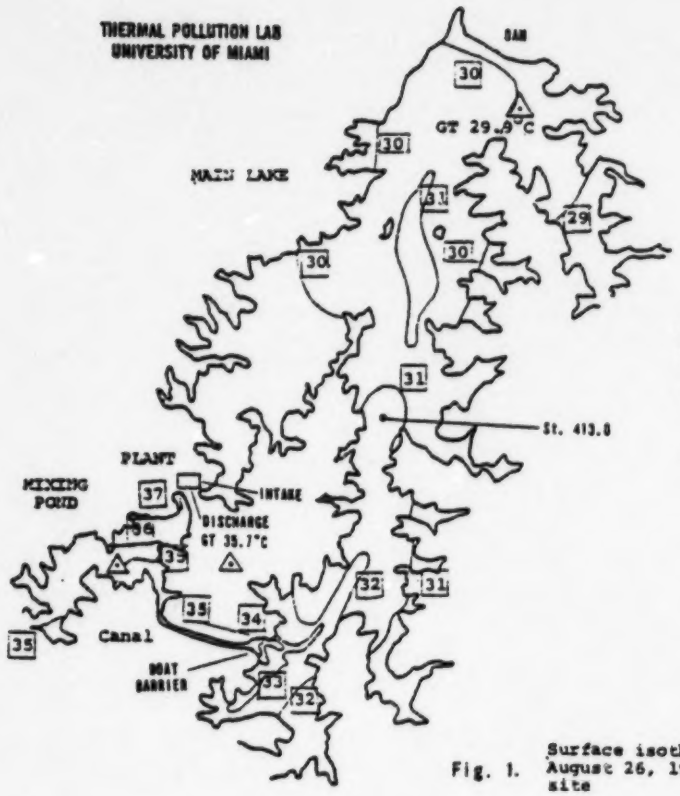

Discharge Temp. : 38.9°C (102.1°F)
Air Temp. : 23.9°C (75°F)
Wind : 3.7 m/sec (8.2 MPH) S-SW
Flight Altitude : 609.6 m (2000 ft.)

I.R. Correction: 1.8°C

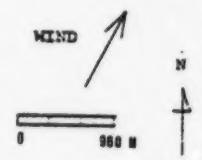

Fig. 1. Surface isotherms obtained by infrared scanning on August 26, 1976 at 9.03 - 10.03 EDT at Lake Belews site

Discharge Temp. : 39.1°C (102.4°F)
Air Temp. : 28.9°C (84°F)
Wind : 5.01 m/sec (11.2 MPH) S-SW
Flight Altitude : 609.6 m (2000 ft.)

I.R. Correction: 1.44°C

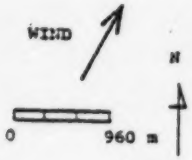

Fig. 2. Surface isotherms obtained by infrared scanning on August 26, 1976 at 15.08 - 16.05 EDT at Lake Belews Site

Fig. 3. Surface isotherms obtained by infrared scanning on January 25, 1977 at 10.52 - 11.28 EST at Lake Belews site.

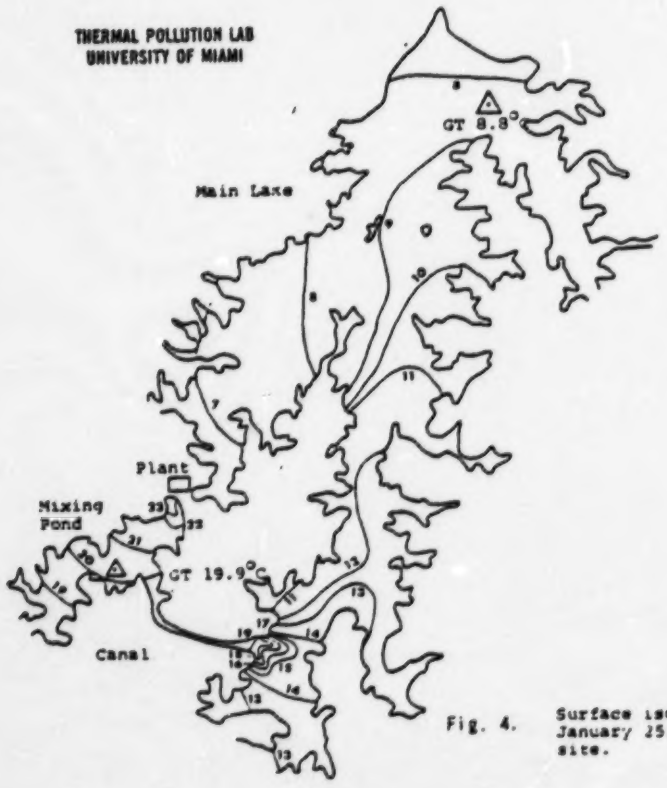

Fig. 4. Surface isotherms obtained by infrared scanning on January 25, 1977 at 16.33 - 17.14 EST at Lake Belews site.

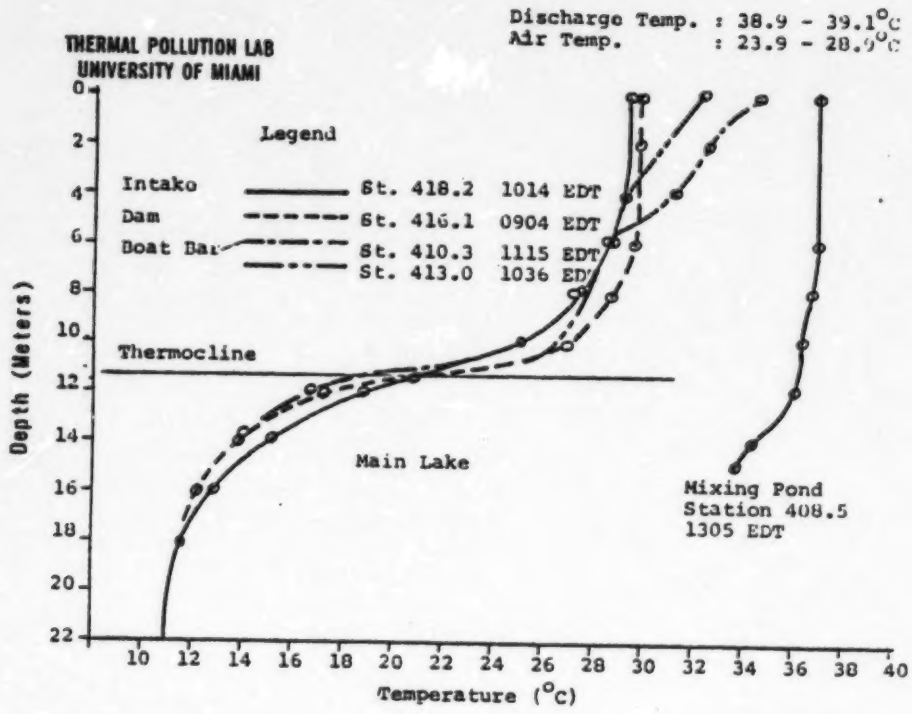

Fig. 5. Vertical Temperature profiles at different stations on August 26, 1976 at Lake Belews site.

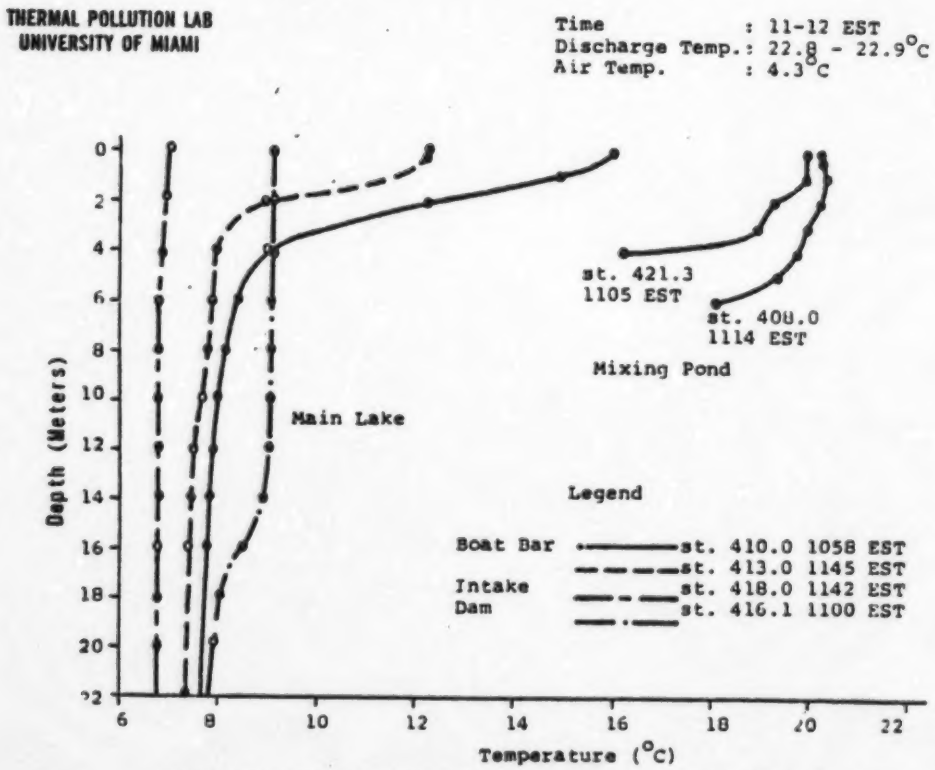

Fig. 6. Morning vertical temperature profiles at different stations on January 25, 1977 at Lake Belews site.

PB82-228040

THERMAL PLUME EVALUATION OF THE ST. LUCIE UNIT 1 DIFFUSER

N.S. Shashidhara and H.A. Nagel
Envirosphere Company
A Division of Ebasco Services Incorporated
Two World Trade Center
New York, New York, 10048, U.S.A.

ABSTRACT

Florida Power and Light Company's St Lucie Nuclear Power Plant (Unit 1) has been in operation since 1976. In 1977 Envirosphere Company, a Division of Ebasco Services, Inc performed a study to evaluate the performance of the discharge diffuser in terms of (i) Maximum Surface Temperature Rise and (ii) Area of the Surface Isotherms. The study included a field monitoring program, performed under known plant operating conditions, and verification of the mathematical models previously used for the design of the diffuser system. The field surveys included definition of ambient conditions, mapping of temperature distribution at three depths and airborne infrared thermal imagery. Verification of the mathematical models involved predictions of near and far-field temperature distribution and comparison with corresponding field measurements. As a result of these investigations it was concluded that the diffuser performs satisfactorily as previously predicted with mathematical and physical model studies.

1. INTRODUCTION

Condenser cooling water from St Lucie Unit 1 is discharged into the Atlantic Ocean through a Y-port diffuser with a nozzle diameter of 7.5 feet[1]. At the point of discharge there is a short sloping trench lined with tremie concrete and excavated to a depth of -34 feet (MLW). The design discharge is 1150 cfs. The Y-nozzle has been designed as a high velocity jet (13 fps) to enhance entrainment and mixing with the ocean water. This results in a relatively low temperature rise at the surface. The ocean depth outside the trench is -23 feet (MLW).

A field survey was conducted during the period of March 25 to April 4, 1977 to characterize the thermal discharge plume and ambient water conditions. This field monitoring program included measurements of temperature distrubution with a boat mounted fast scanning mobile mapping system, continuous recording of water temperature and current at four stations with moored in situ instruments, vertical temperature profiling and airborne infrared mapping. Subsequently, an analytical study was undertaken to compare and verify mathematical model results and evaluate the performance of the as-built diffuser.

2. METHODOLOGY

2.1. Description of Field Program

The field monitoring program included mapping of the thermal plume and ambient conditions using a mobile mapping system supplemented by vertical temperature profiles and airborne infrared photography. In addition, in situ temperature and current instruments were moored at a depth of about 10 feet below the surface at four points, two on each side of the diffuser, to obtain continuous records of water temperature and current (Exhibit 1).

Tri-level mapping was performed using a string of three thermistors with a towed V-fin depressor, a digital data display printer and a recorder. Boat position was established using a Mini-Ranger III navigation system with two ranges to shore-based transponders. Concurrent temperature at three depths, position, and time were automatically recorded on cassette tapes for data acquisition can be selected manually between 2 to 10 second intervals, depending on the resolution required. Airborne infrared mapping was performed with a Texas Instrument RS-310 D infrared line-scanning system.

2.2. Thermal Surveys

To reflect differences between near and far-field areas, field surveys were conducted in two phases. For the near-field, boat speed was lowered to about 4 knots and the interval of data logging was set at 2 seconds. At this combination of boat speed and rate of data collection, temperatures would be measured at 15 foot intervals. Track spacing was 30 to 45 feet apart and track lengths were usually 1200 feet. Ten to fifteen tracks were run for each near-field map. One boat transect intersected the boil spot to measure peak surface temperature.

In the far-field, a zig-zag pattern of transects was used. Before each mapping, current measurements were taken to determine the direction of the current to select appropriate transect orientation. Towing speed was increased to 8 or 10 knots and the data recording interval was gradually increased from 4 to 10 seconds with distance from the diffuser. Distances covered, both offshore and longshore, ranged up to 1.5 miles. The mobile mapping unit was calibrated against an ASTM traceable mercury thermometer graduated to 0.1° F, before and after each survey. Accuracy of the scanner for the airborne infrared mapping was within 0.5° F. Reference temperatures for calibration for infrared mapping were taken near the intake canal headwall and from a floating dock in the discharge canal using an ASTM traceable thermometer.

To supplement the temperature measurements with the mobile mapping system, vertical temperature measurements were conducted at 4 to 7 stations in the plume area. Temperatures were measured at 1, 3, 5, 10, 15 and 25 foot depths with a thermistor probe and deck read-out unit.

In-situ temperature and current data were recorded at half hour intervals from 1230 - March 25 to 0930 - April 4, 1977 to define ambient conditions for each survey. A record of plant operating conditions from 1000 - March 25 to 0700 - April 3, 1977 was also provided by plant operating personnel. This included hourly readings of discharge and intake canal temperatures, wind direction and speed, air temperature, relative humidity and discharge canal

level. In addition, percent power output and on/off status of the four circulating water pumps and the intake cooling water pumps were also provided to determine total flow rate in the circulating water system. A summary of plant operating and ambient conditions is presented in Table 1.

2.3. Field Data Analysis

In situ temperature data were analyzed for variability among stations, diurnal ranges and day-to-day changes of 24-hour mean temperature. The *in situ* current data were analyzed for direction and speed at times coinciding with mobile mapping surveys.

Data from the mobile mapping surveys were processed and reduced into a listing of time, range A, range B, and temperature at three levels. In addition to this listing, track charts (Scale 1 inch equals 100 feet, near-field, and 1 inch equals 300 feet; far-field) were plotted to show.

Infrared images for three overflights coinciding with mobile mapping surveys were prepared by Texas Instruments and presented as computer processed digital thermal maps. These maps showed relative temperature increases at 0.5° F intervals using the intake canal temperature as a reference. This relative temperature distribution was analyzed at 1° F intervals.

2.4. Mathematical Models

For modeling thermal discharges, the Koh and Fan[2] mathematical model was utilized to describe the near-field submerged jet region and the Pritchard[3] mathematical model was utilized to describe the far-field region to the point where plume temperature differential reached 1.5° F.

3. RESULTS

3.1. Results of Field Surveys

In Situ Temperature and Current Measurements.

In situ temperature data (Table 2) indicate significant variability of ambient temperature. Highest daily temperatures occurred at Station IN from March 26 to 31, coinciding with a period of strong southeasterly winds and a continuous northward current. From April 1 to 4, a period of calm conditions, highest daily temperatures were monitored at Station ON. In view of wind and current conditions, the high temperatures at Stations IN and ON indicate advective transport of the plume northward.

In situ current data show a persistent longshore current northward for all stations when moderate winds are from the southeast quadrant, except for a 16-18 hour interval of southward longshore flow associated with the passage of a cold front on March 25. During a prolonged period of 15 to 20 knot winds, March 26 to 30, current speeds varied between 0.3 and 1.0 fps. When the coastal winds subsided from March 31 to April 2, the current became more variable with speeds generally less than 0.3 fps. Current reversals due to astronomical tides became more noticeable during this period of light winds.

Vertical Temperature Profile Measurements.

Vertical temperature profile data were collected from March 31 to April 2, 1977, at locations shown in Exhibit 1. The temperature profile nearest to the diffuser was measured on the seaward side of the surface boil area. The profiles at Station 1 show a vertically mixed thermal layer to a depth of 25 feet. Temperature was stratified at most other stations in the far-field, with colder water usually below the 15 foot level. The profiles for Stations 10 and 11 appear to reflect the edge of the thermal plume. The temperature gradient from the surface to the 15 foot level at these stations indicates mixing of the discharge as well as strong diurnal heating. The profiles at Stations 5, 6, 8, 9 and 12 show a sharply stratified layer in the top 3 feet at the surface. In contrast, this feature was missing in some other cases due to wind mixing and diurnal cooling in the late afternoon on March 31 and April 1.

Ambient Temperature.

Analysis of in situ records and background measurements taken before and during each survey revealed significant temporal and spatial variations in the temperature field. These variations may reflect intrusions of Gulf Stream surface water, upwelling and downwelling phenomena, or transport of warm or cold water masses from the Indian and St Lucie Rivers tidal exchange. On relatively calm days, diurnal warming and stratification of the nearshore surface water can exceed 2° F and completely mask the 1.5° F Δ T isotherm, relative to isothermal conditions in the ambient field. For example, the temperature measured at Stations IS and OS showed a variability of up to 4° F from 0700 to 1800 March 31 when the plume transport was oriented away from these two stations. Vertical temperature gradients up to 3.3°F over an 8 foot layer were also observed.

Temperature measurements at Station IS agreed closely with background measurements taken at the 10 foot depth near the velocity cap (See Table 1). Exhibit 2 correlates temperature measured at these locations and in the intake canal. Since the prevailing currrent was generally longshore toward the north and Station IS is at mid-depth, the temperature measured at Station IS, at the time of the near-field measurement closely represents the ambient temperature of water entrained in the discharge plume.

In evaluating the surface temperature rise as well as the areal extent of the 1.5° F Δ T-isotherm, a temperature more representative of the ocean surface layer was used. The temperature measured at the 2 foot depth near the intake velocity cap appeared to represent ambient temperature and was used to assess the effective maximum temperature rise and the area of the 1.5° F Δ T isotherm.

Near-field Temperature Distribution.

Exhibits 3 and 4 show examples of the near-field measurements and isotherms for the 2 foot depth, ie, surface, and the 10 foot depth respectively. Most isotherm analyses show a tongue of colder water separating the boil areas identifying the two diffuser ports (See Exhibit 3). The maximum surface temperature for all surveys varied from 72.1° F on March 31 to 74.7° F on April 1. Surface temperature differential (ΔT) relative to ambient temperature measured at the 2 foot depth, varied from 2.3 to 4.8° F. The highest maximum surface temperature differential (relative to the

ocean temperature at the 2 foot depth) coinciding with normal plant load and total flow rate of 1150 cfs was 4.8° F. When the plant load was decreased and conditions changed to three pump operation with total flow of 950 cfs, the maximum surface temperature difference was 4.3° F.

Far-field Temperature Distribution.

The plume axis initially coincided with the orientation of the Y-nozzle, and, depending on ambient current direction and speed, its orientation approached the ambient flow direction in the far-field region. The far-field isotherm patterns for March 25, 1977 is shown in Exhibit 5 for the 2 foot depth and in Exhibit 6 for the 7-foot. In general, the area enclosed by a given isotherm at the 2 foot depth is larger than that at the 7 or 10 foot depth which shows the broader fanning pattern of the plume at the surface.

On March 31 and April 1, ambient temperature was significantly temperature boundary as shown in Exhibit 7 for March 31, 1977. This boundary as found on March 31 separated the plume from warm ambient water near the shoreline and to the north of the plume. Offshore toward the east-southeast, temperatures indicated the presence of cool ambient water, whereas southward there was a pocket of relatively warmer water that suggested a residual plume. The 69° F nearshore isotherm closely followed the 15 foot contour. Temperature changes measured between the plume and cool ambient water decreased steadily on the seaward edge of the plume then increased several tenths of a degree before further decreasing into the cool ambient water area. The thermal trough between the steady decline and slight rise identified the approximate minimum temperature boundary of the plume on the seaward side.

Infrared Imagery.

Areas contained within isotherms as analyzed from the infrared thermal (IRT) maps depended upon temperature calibrations from the intake and discharge canals at the time of overflight. For the 1052 March 31 IRT map, the area within the 70.2° F isotherm was 61 acres. This compared favorably with the 67 acre area within the 70° F isotherm as determined from the surface mobile map and listed in Table 3. At 1821 April 1, the areas within the 71.2° F and 72.2° F isotherms were 79 and 11 acres respectively. These areas are less than the mobile mapping areas as listed. Similarly, the 70.1° F area of 49 acres, 71.1° F area of 11 acres and 72.1° F area of 2 acres at 1128 April 2 were also smaller than the corresponding areas found by mobile mapping. Differences between results of the two survey techniques may be attributed to the ambient reference temperature and the natural stratification conditions that existed. Maximum surface temperatures defined by IRT imagery are also listed in Table 3. Generally, the infrared maximum temperatures agree with those measured by mobile mapping.

3.2. Results of Mathematical Modeling

Maximum Surface Temperature Rise.

Maximum surface temperature rises (ΔT max), predicted with the Koh-Fan Model, are presented in Table 4. In this analysis, the temperature rise at the lower edge of the impingement zone (along the plume centerline and at an

assumed subsurface distance of one-sixth the ocean depth from the water surface) is taken as the ΔT max. Other investigations (4) and (5) of jets have shown that at distances above this point temperature decay is significantly smaller than that decay in the remainder of the water column.

In Table 4, Column 6 presents the temperature rise expected at the surface. The maximum predicted surface temperature rise is 4.7° F for four pump operating conditions and 4.5° F for three pump operations. The differences between columns 4 and 6 are due to the temperature variability between the surface (2 foot depth) and the 10 foot level.

Surface Areal Extent of the 1.5°F Isotherm.

The surface areal extent of the isotherms was predicted utilizing Pritchard's model. The maximum surface (hot spot) temperature rise and width with the Koh-Fan near-field model and from both plant heat rejection rate and depth of the thermal layer determined from field measurements.

During the survey, it was found in some cases when significant natural temperature variability existed, the isotherm value, T_{IS} + 1.5°F, was not observed in the plume area (Exhibit 7). This required a definition of ambient water temperature which represents actual field conditions. As discussed in Section 3.1, ambient water temperature was taken to be the temperature at the 2-foot level near the intake velocity cap and the computations of areal extent for the 1.5°F isotherm were modified. On this basis, the predicted areas of the 1.5°F isotherm were compared to field measurements. The results of the computations are presented in Table 4. The area varies from 88 to 300 acres for four pump operations and from 51 to 121 acres for three pump operation. The degree of stratification during three pump operation was greater than that during four pump operation. This resulted in a reduced area of the 1.5°F isotherm for the three pump operation case. Under isothermal conditions, however, a three pump operation with reduced flow and higher ΔT should yield a larger areal extent than a four pump case.

3.3. Discussion of Results and Conclusions

Maximum Surface Temperature Rise.

In all but one case (i.e., Test 4), the predicted results (Table 4 and Exhibit 8) are higher than measured maximum temperature rises. The observations of temperature rises range from 2.3 to 4.8°F for four pump operation (condenser ΔT of 19.5 and 23.7°F) and from 3.4 to 4.3°F for three pump operation (condenser ΔT of 25.2 and 26.3°F). The corresponding predicted results range from 3.2 to 4.7°F for four pump operation and from 3.6 to 4.5°F for three pump operation. The difference between observed and predicted values of maximum surface temperature rise range from 0.2 to 1.0°F. In Test 4 the predicted result was lower than the observed value by 0.8°F. These differences are within the range of precision available from models.

The as-built Y-nozzle diffuser was designed to provide dilution of about 4.4 for a flow of 1150 cfs and a condenser ΔT of 24°F. In Test 2, which closely corresponds with design conditions with regard to flow rate and condenser rise, the predicted dilution was about 4.7. The dilution factor

based on field measurements was calculated to be 4.9. Dilution factors for all other cases are presented in Table 4. Based on the near-field analysis, it is concluded that (1) diffuser performance is in close agreement with the expected performance and (2) near-field modeling gives satisfactory comparison between predicted and measured values.

Areal Extent of the 1.5°F Isotherm.

Table 4 shows that the predicted areas are larger than measured areas for the 1.5°F isotherm. Differences between measured and predicted areas can be explained by temperature variations in the ambient field. In Test 1, the survey showed that the ambient temperature was almost isothermal. Pritchard's model showed satisfactory comparison between predicted and measured results for this case. Differences between the observed and predicted areas of the 1.5°FΔT isotherm is less than 10 percent. In Tests 3, 5 and 6 variability survey areas and the predicted areas are considerable. Pritchard's model is insensitive to variability in ambient surface temperature and considers the ocean surface to be isothermal. In situations where the assumption of isothermal ambient temperature is violated the Pritchard model over-predicts the area of the isotherms.

At assumed design conditions, St Lucie Unit 1 rejects approximately 6.4 x 10^9 Btu/hr. This was predicted previously to result in a surface area of 400 acres for 1.5°FΔT isotherm for assumed design plant and oceanographic conditions.(1) The present field studies showed a 1.5°FΔT isotherm area of 2 to 278 acres for heat rejection rates ranging from 5.1 x 10^9 to 6.64 x 10^9 Btu/hr. The predicted areas for measured field conditions range from 51 to 300 acres. These results are also presented in Table 4. This indicates that the oceanographic conditions at the St Lucie site during the field monitoring period were more favorable for dispersion and dilution of the thermal plume than the assumed design conditions.

REFERENCES

1. St. Lucie Plant Unit No. 1, U.S.A.E.C. Final Environmental Statement Docket No: 50-335, June 1973.

2. R.C.Y. Koh and L.N. Fan, Mathematical Models for the Prediction of Temperature Distribution Resulting from the Discharge of Heated Water. U.S.E.P.A. Report, Program No. 16130, DWO October 1970.

3. D.W. Pritchard, Design and Siting Criteria for Once-Through Cooling Systems. Proc. AICHE 68th National Meeting, March 1970.

4. G.H. Jirka, G. Abraham and D.R.F. Harleman, An Assessment of Techniques for Hydrothermal Prediction. R.M. Parsons Laboratory Report No. 203. Mass. Inst. Tech. July 1975.

5. J.J. Shin, Momentum, Heat and Mass Transfer Around the Stagnation Region of a Surfacing Plume, Ph.D. Thesis, The Univ. of Delaware June 1974.

TABLE 1

SUMMARY OF PLANT OPERATING AND AMBIENT CONDITIONS

	March 25 1356-1515	March 31 0953-1034	March 31 1347-1428	April 01 0851-0922	April 01 1444-1536	April 02 0928-1050
Test Number	1	2	3	4	5	6
Discharge Rate (cfs)	1,150	1,150	1,150	1,150	900	950
Tide Adjustment (ft#)	+1.3	+0.3	+2.6	+1.2	+2.9	+0.7
Percent Power Output	99	94.5	98	99.3	90.4	88.9
Number of Pumps Online	4	4	4	4	3	3
Discharge Canal Temp. (°F)	93.4	91.9	89.8	90.7	94.3	95.0
Intake Canal Temp. (°F)	70.5	68.2	70.3	67.3	69.1	68.7
Ambient Temperature (°F)						
a. In situ Station IS	70.5	67.0	70.5	66.8	68.6	67.7
b. 100 to 200 ft seaward of velocity cap**						
2 ft depth	70.5	68.6	71.0	67.8	71.2	69.9
6 ft depth	70.5	67.6	70.6	67.5	70.3	69.6
10 ft depth	70.5	67.0	70.3	66.4	68.7	67.6
Ambient Current Direction and Speed (fps)*						
Sta IN	0.10 (N)	0.08 (ON)	0.29 (S)	0.08 (S)	0.07 (S)	0.32 (S)
Sta IS	0.08 (N)	0.11 (NW)	0.13 (OFF)	0.03 (ON)	0.14 (OFF)	0.25 (S)
Sta ON	0.30 (N)	0.15 (SE)	0.14 (SE)	0.31 (N)	0.23 (N)	0.28 (S)
Sta OS	0.23 (N)	0.13 (N)	0.17 (N)	0.10 (N)	0.14 (OFF)	0.50 (S)

* N: Northerly, S: Southerly, ON: Onshore, OFF: Offshore, NW: Northwest, SE: Southeast.
**Temperature data were collected at 2.5 and 7 foot depths on March 25.
Tide Adjustment plus 18 feet would provide the total ambient ocean water depth.

TABLE 2

SUMMARY OF IN SITU TEMPERATURE MEASUREMENTS

Daily Mean Temperatures (^{o}F)

Date, 1977		STATION IN	IS	ON	OS	Range
March	25+	71.0*	70.9	70.4	70.4	0.6
March	26	71.5*	71.3	70.5	70.7	1.0
March	27	71.5*	70.8	70.1	70.4	1.4
March	28	71.8*	71.2	70.9	71.0	0.9
March	29	74.0*	72.8	73.6	73.2	1.2
March	30	71.8*	70.5	70.6	69.9	1.9
March	31	70.5*	69.1	68.8	68.6	1.9
April	1	69.1	68.6	69.6*	69.0	1.0
April	2	69.5	69.3	70.1*	69.6	0.8
April	3	68.5	67.7	69.1*	68.2	1.4
April	4+	66.5	66.5	67.2*	67.1	0.7
11-Day Mean		70.5	69.9	70.1	69.8	
Range		7.5	6.3	6.4	6.1	

Notes: +Partial day only

*Highest daily average among stations

TABLE 3

MAXIMUM SURFACE TEMPERATURE AND ISOTHERM AREAS

Date & Time	Isotherm (°F)	ΔT* (°F)	Area (Acres)
March 25	72	1.5	278
1356-1508	72.5	2.0	98
	73	2.5	8.4
	74	3.5	1.5
Maximum Temperature	74.2	3.7	<0.02
March 31	70	1.4	67
1032-1137	70.2 (IRT)**	1.6	61 (IRT)**
	70.5	1.9	22
	71	2.4	3.0
Maximum Temperature	72.1	3.5	<0.2
IR Maximum	71.9	3.3	0.25
March 31	72	1.0	3.0
1428-1500	73	2.0	1.1
Maximum Temperature	73.3	2.3	<0.02
April 1	70	2.2	54
0956-1041	70.5	2.7	11
	71	3.2	1.9
	72	4.2	0.3
Maximum Temperature	72.6	4.8	<0.02
April 1	71.5	0.3	12
1536-1624	72	0.8	8
	73	1.8	1.5
Maximum Temperature	74.6	3.4	<0.02
April 1	71.2 (IRT)**	0.0	79 (IRT)**
1812-1835	71.8	0.6	96
	72	0.8	40
	72.2 (IRT)**	1.0	11 (IRT)**
	73	1.8	4.1
	74	2.8	1.8
Maximum Temperature	74.6	-	<0.02
IR Maximum	74.7	-	-
April 2	70.1 (IRT)**	0.2	49 (IRT)**
	70.8	0.9	87
1052-1136	71	1.1	37
	71.1 (IRT)**	1.2	11 (IRT)**
	72	2.1	6.1
	72.1 (IRT)**	2.2	2.0 (IRT)**
	73	3.1	1.8
Maximum Temperature	74.2	4.3	<0.02

* Temperature difference ΔT is relative to 2-foot temperature in vicinity of intake structure.

** Infrared surface temperature and area.

TABLE 4

COMPARISON OF MEASURED AND PREDICTED PLUME CHARACTERISTICS**

Test No.	Disch. Temp. Rise*	Disch. Heat Rate	Pred. Temp. Rise#	Pred. Max. Surface Temp.	Pred. Max. Temp. Rise/Dilution Factor	Meas. Max. Temp. Rise/Dilution Factor	Isotherm Area 1.5°F Pred.	1.5°F Meas.	3°F Pred.	3°F Meas.
1	22.9	6.0	4.7	75.2	4.7 / 4.87	3.7 / 6.19	300	278	18	4
2	24.9	6.64	5.3	72.3	3.7 / 4.70	3.5 / 4.88	98	52	6	-
3	19.3	5.1	3.7	74.2	3.2 / 5.22	2.3 / 6.89	88	12	5	-
4	23.9	6.3	5.0	71.8	4.0 / 4.78	4.8 / 4.12	154	-	10	4
5	25.7	5.3	6.2	74.8	3.6 / 4.15	3.4 / 4.28	51	8	3	-
6	27.3	6.0	6.7	74.4	4.5 / 4.07	4.3 / 4.20	121	20	8	2

** Units for Temperature in: °F, Area: in Acres, Heat Rate in: (BTU/HR) x 10^9

* With reference to T_{IS}

At the edge of the impingement zone

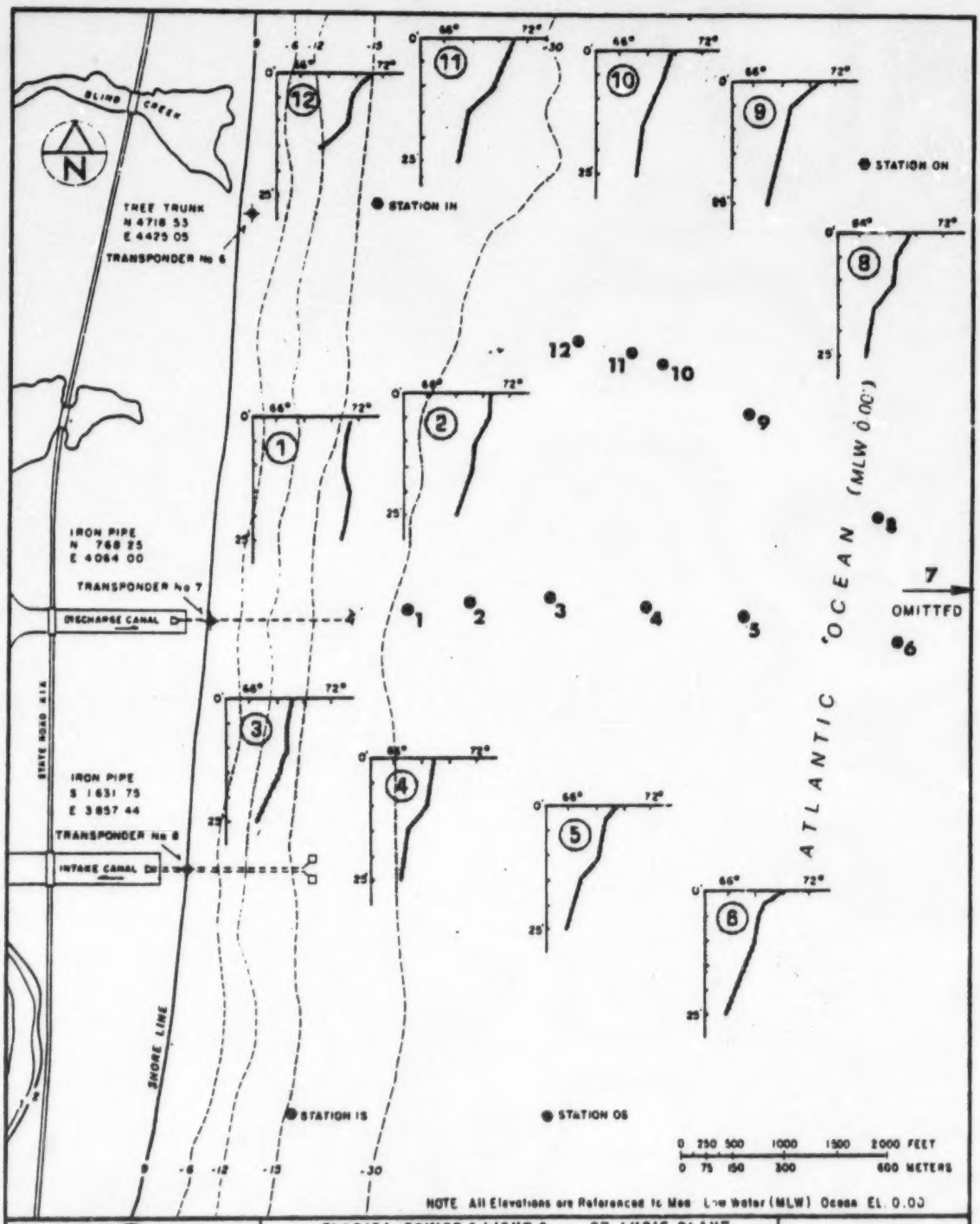

envirosphere company

FLORIDA POWER & LIGHT Co. – ST. LUCIE PLANT

OCEAN DISCHARGE STUDY

VERTICAL TEMPERATURE PROFILES AND STATION LOCATIONS, 1050 - 1135 APRIL 1, 1977

DATE:

EXHIBIT 1

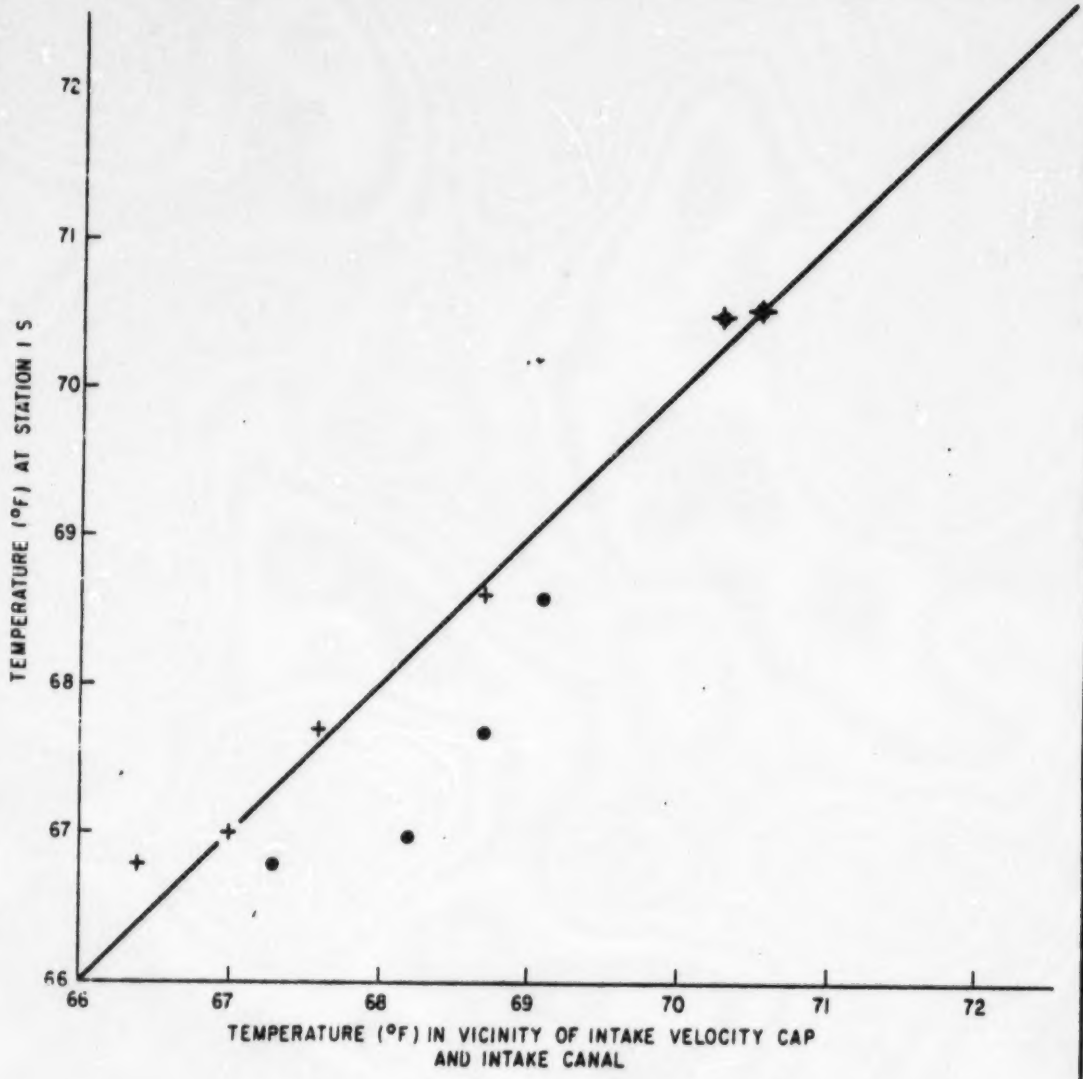

envirosphere company

FLORIDA POWER & LIGHT Co. – ST. LUCIE PLANT

OCEAN DISCHARGE STUDY

CORRELATION OF TEMPERATURES AT STATION 1S, 10 FT LEVEL NEAR THE VELOCITY CAP & INTAKE CANAL

EXHIBIT 2

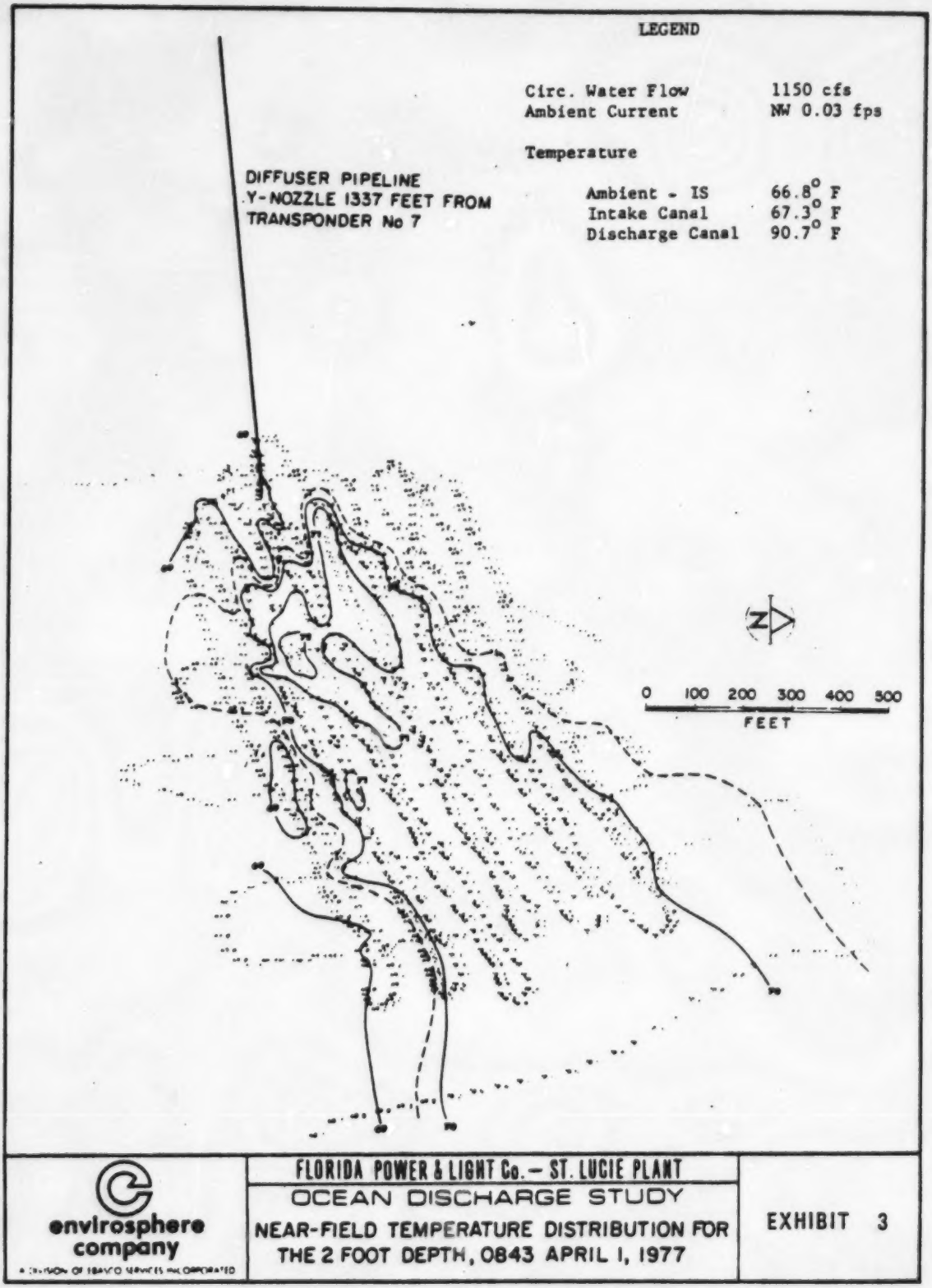
LEGEND
Circ. Water Flow 1150 cfs
Ambient Current NW 0.03 fps
Temperature
Ambient - IS 66.8° F
Intake Canal 67.3° F
Discharge Canal 90.7° F
DIFFUSER PIPELINE
Y-NOZZLE 1337 FEET FROM
TRANSPONDER No 7
N
0 100 200 300 400 500
FEET
envirosphere company
FLORIDA POWER & LIGHT Co. – ST. LUCIE PLANT
OCEAN DISCHARGE STUDY
NEAR-FIELD TEMPERATURE DISTRIBUTION FOR THE 2 FOOT DEPTH, 0843 APRIL 1, 1977
EXHIBIT 3

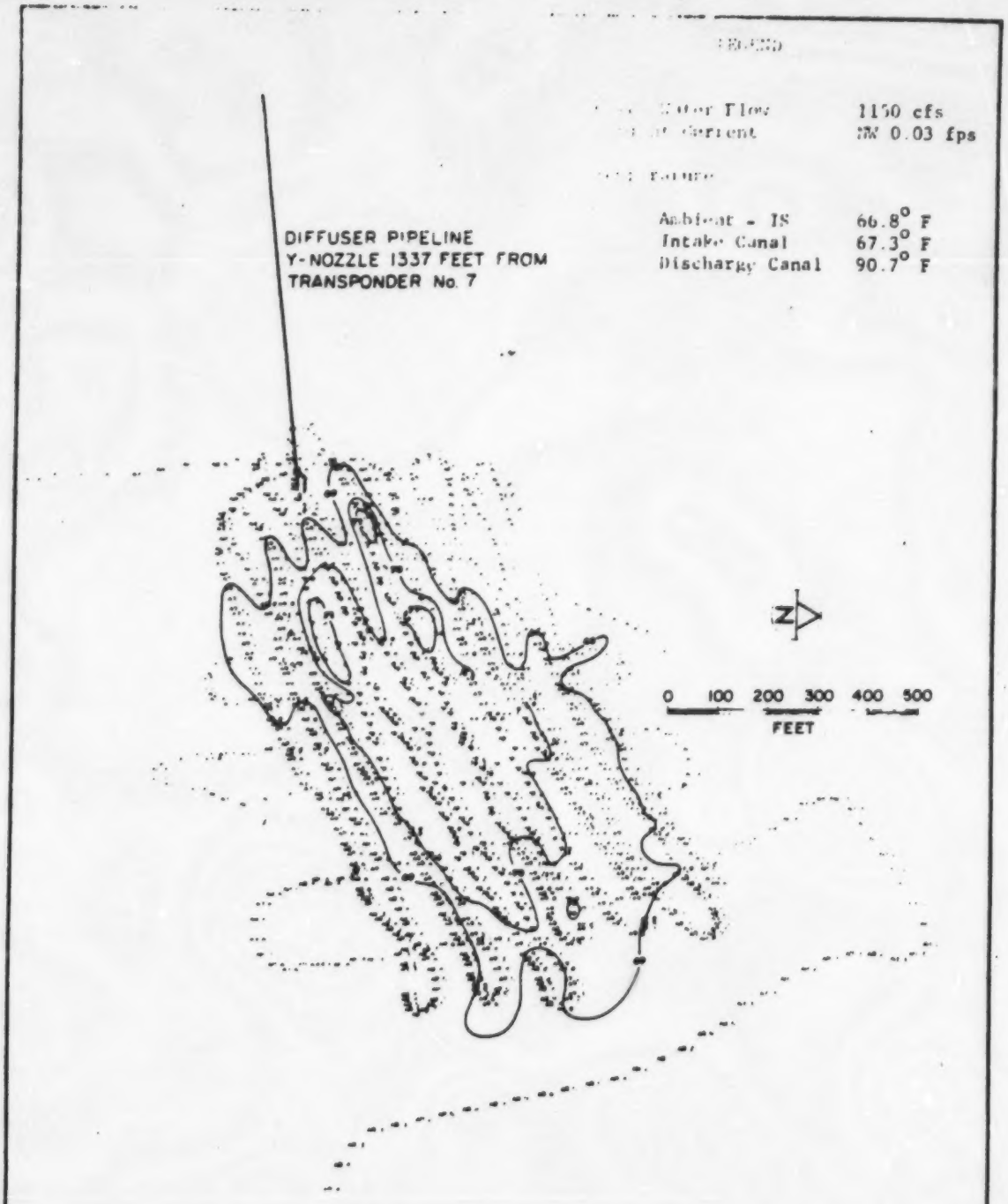

envirosphere company

FLORIDA POWER & LIGHT Co. – ST. LUCIE PLANT

OCEAN DISCHARGE STUDY

NEAR-FIELD TEMPERATURE DISTRIBUTION FOR THE 10 FOOT DEPTH, 0843 APRIL 1, 1977

EXHIBIT 4

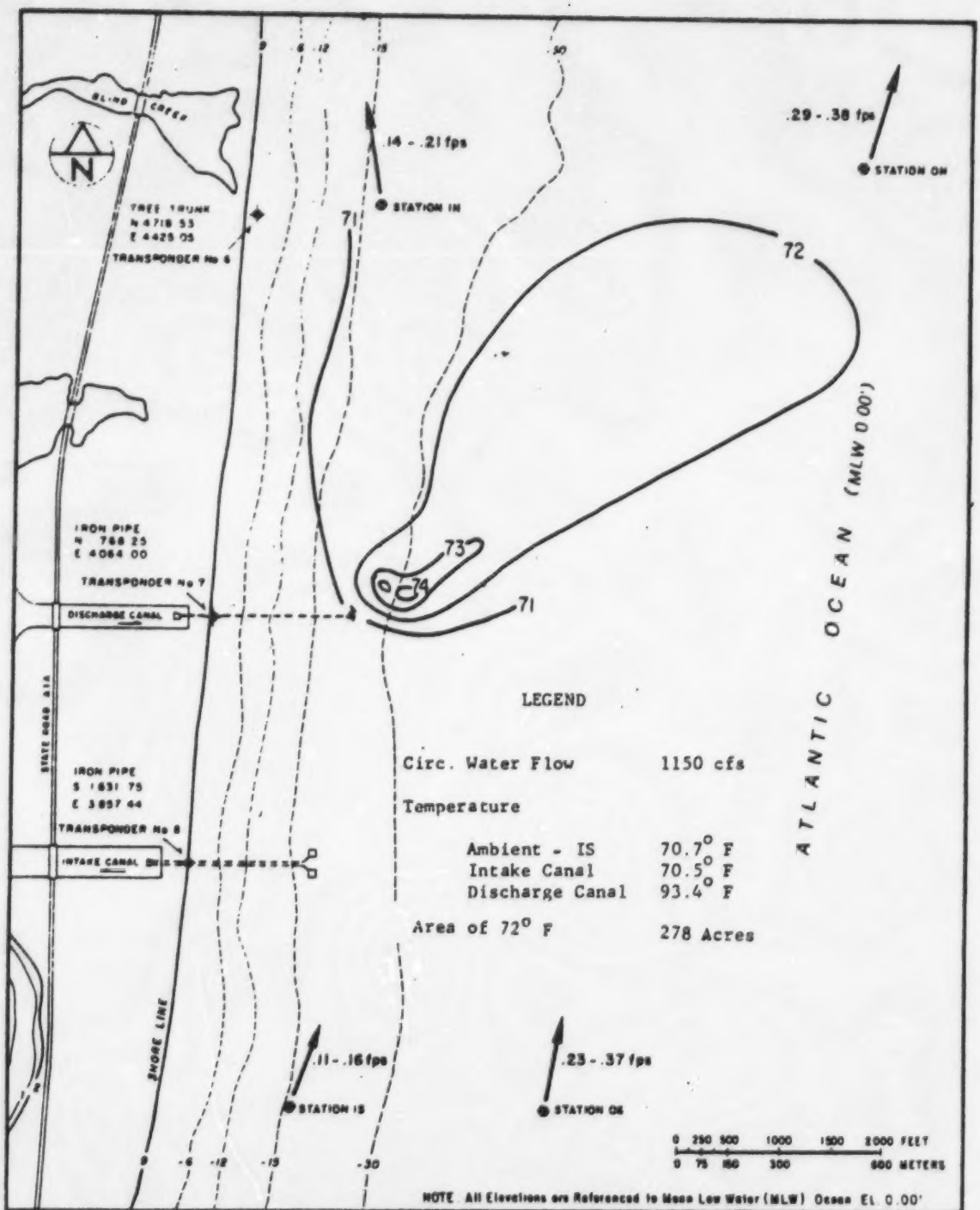

envirosphere company

FLORIDA POWER & LIGHT Co.– ST. LUCIE PLANT

OCEAN DISCHARGE STUDY
FAR-FIELD ISOTHERMS AT THE 2 FOOT DEPTH, 1356 - 1508 MARCH 25, 1977

DATE:

EXHIBIT 5

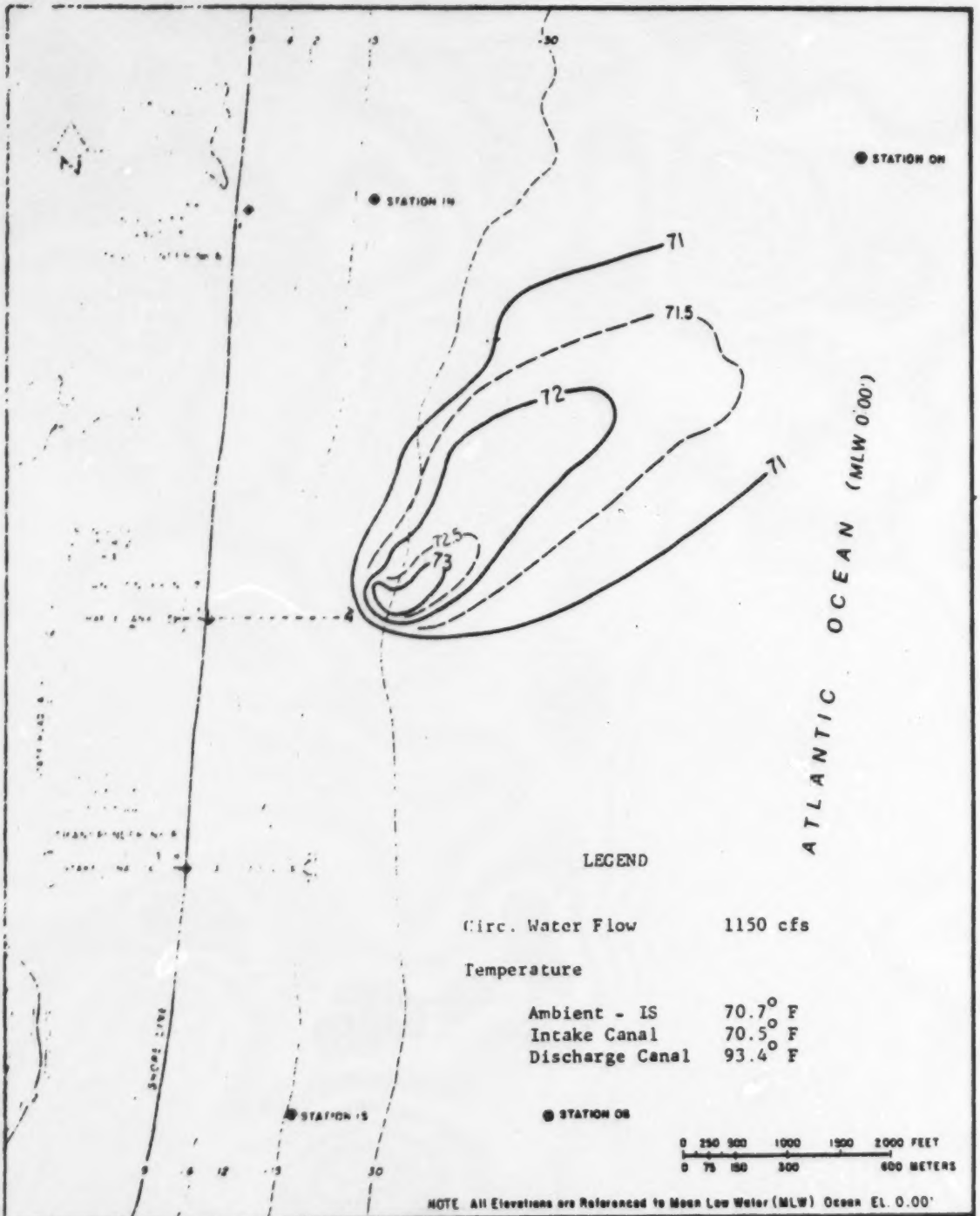

envirosphere company

FLORIDA POWER & LIGHT Co.— ST. LUCIE PLANT

OCEAN DISCHARGE STUDY

FAR-FIELD ISOTHERMS AT THE 7 FOOT DEPTH, 1356 - 1508 MARCH 25, 1977

DATE:

EXHIBIT 6

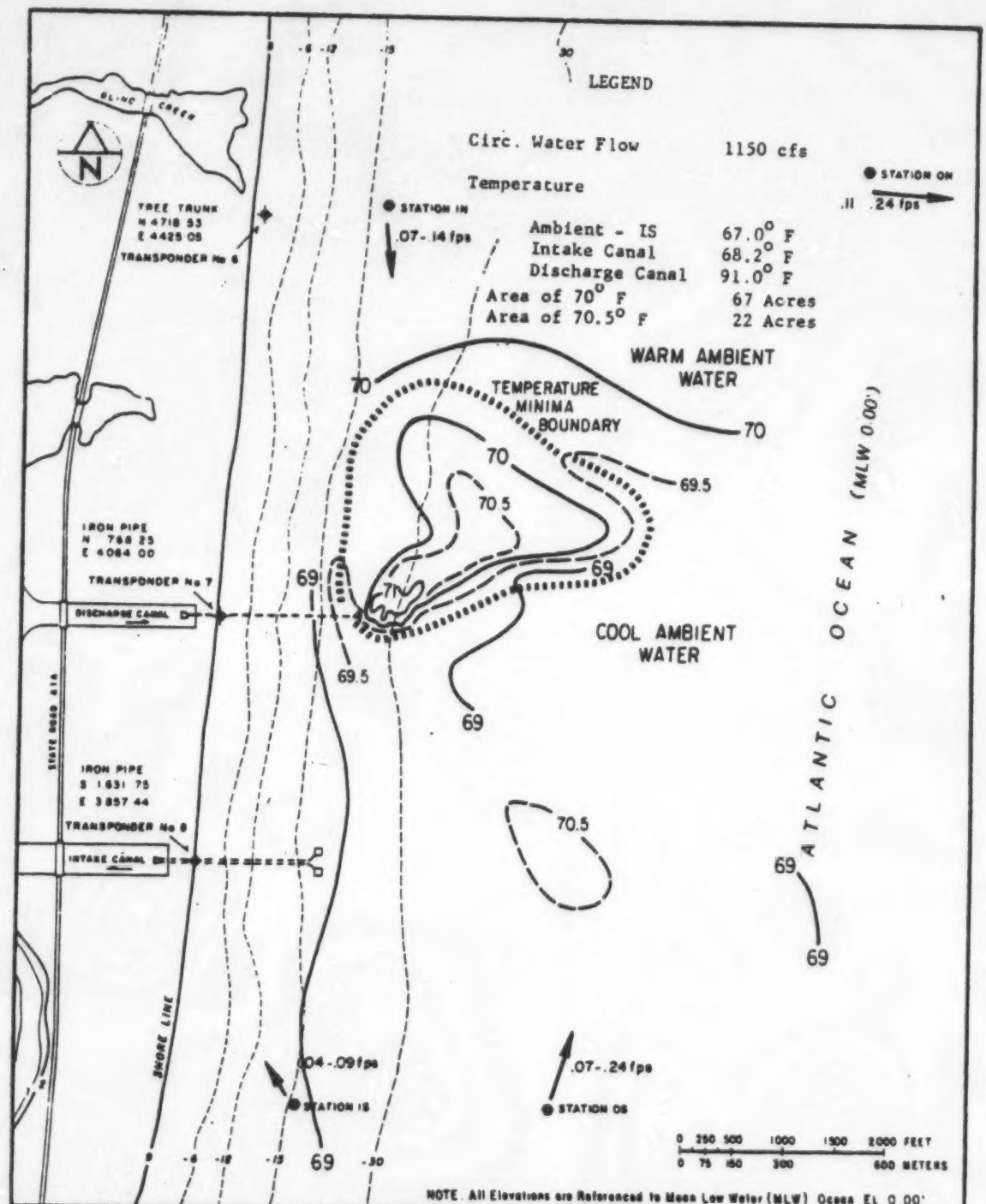
LEGEND
Circ. Water Flow 1150 cfs
Temperature
Ambient - IS 67.0° F
Intake Canal 68.2° F
Discharge Canal 91.0° F
Area of 70° F 67 Acres
Area of 70.5° F 22 Acres
STATION IN
.07-.14 fps
STATION ON
.11 .24 fps
WARM AMBIENT WATER
TEMPERATURE MINIMA BOUNDARY
COOL AMBIENT WATER
ATLANTIC OCEAN (MLW 0.00')
TREE TRUNK
N 4718 53
E 4425 08
TRANSPONDER No 6
IRON PIPE
N 768 25
E 4084 00
TRANSPONDER No 7
DISCHARGE CANAL
IRON PIPE
S 1831 75
E 3857 44
TRANSPONDER No 8
INTAKE CANAL
STATE ROAD A1A
SHORE LINE
.04-.09 fps
STATION 18
.07-.24 fps
STATION 08
0 250 500 1000 1500 2000 FEET
0 75 150 300 600 METERS
NOTE. All Elevations are Referenced to Mean Low Water (MLW) Ocean El 0.00'
envirosphere company
FLORIDA POWER & LIGHT Co.— ST. LUCIE PLANT
OCEAN DISCHARGE STUDY
FAR-FIELD ISOTHERMS AT THE 2 FOOT DEPTH, 1032 - 1137 MARCH 31, 1977
DATE:
EXHIBIT 7

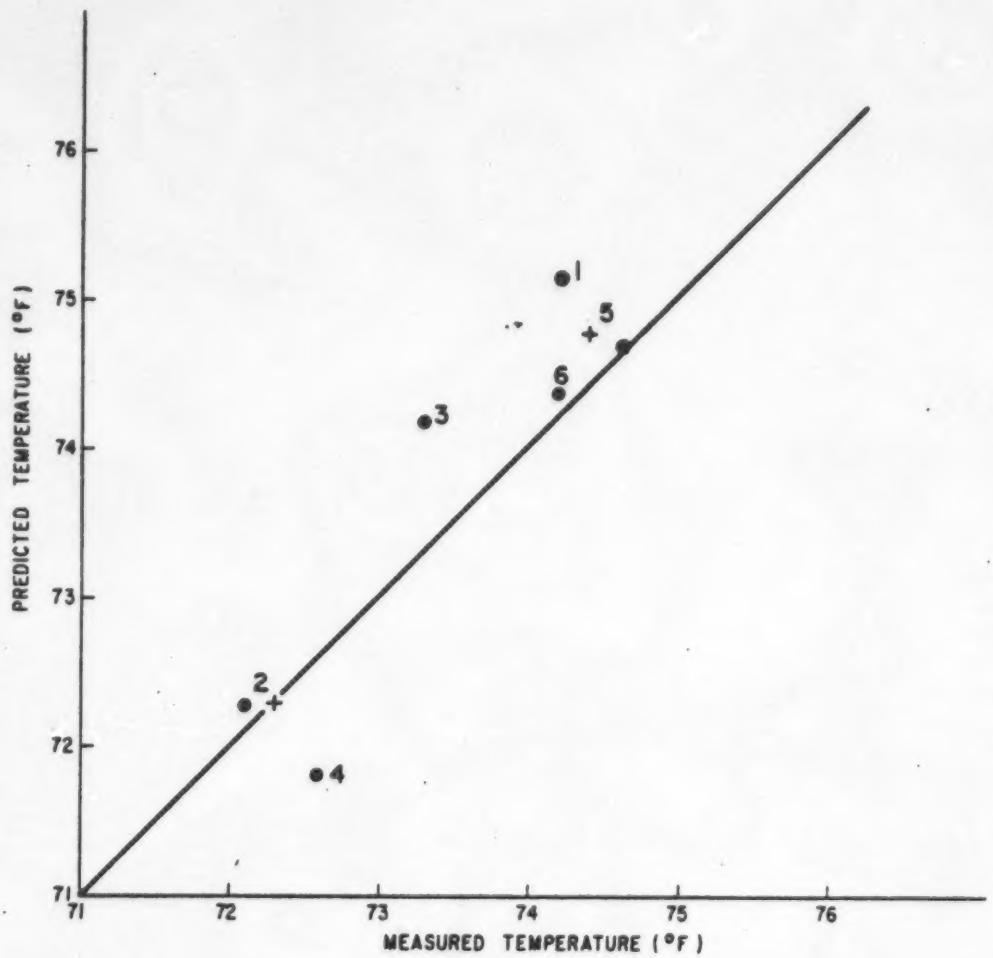

LEGEND

● MEASURED BY ENVIROSPHERE CO.

+ MEASURED BY T. I.

NOTES: NUMERALS REFER TO TEST CASES - 1 - 6

(AMBIENT TEMPERATURE BASED ON 15-STATION AND ASSUMED UNIFORM OVER THE DEPTH)

envirosphere company	FLORIDA POWER & LIGHT Co. – ST. LUCIE PLANT OCEAN DISCHARGE STUDY COMPARISION OF PREDICTED VS. MEASURED "HOT SPOT" TEMPERATURE	EXHIBIT 8

PB82-228057

2-D CONVECTION DOMINATED THERMAL DISPERSION IN COASTAL WATERS

H. P. Miller and K. C. S. Tong
United Engineers & Constructors Inc.
Philadelphia, Pennsylvania

ABSTRACT:

An ad-hoc numerical method, using the flux-corrected transport (FCT) method developed for compressible, nonlinear flows, has been applied to one and two-dimensional incompressible convection dominated flows for predicting thermal dispersion at a hypothetical coastal site. The FCT method was further simplified for the case of a slowly varying current velocity, which is justifiable for relatively small integration time steps. The results predicted by the simplified FCT method compare rather well with the exact solution, and demonstrably yield a more realistic simulation than conventional differencing schemes. A one-dimensional comparison with a first upwind differencing scheme clearly illustrates the benefits of using the simplified FCT method by numerical modellers. The method is ad-hoc in the sense that a minimum of ten grid points of the initial distribution is required to approximate the continuum solution.

1: INTRODUCTION

An ad-hoc numerical method for significantly reducing numerical dispersion in convection dominated compressible flows has been developed by Book, Boris and Hain [1, 2]. This paper presents a simplication and applications of this method to one and two-dimensional incompressible flows for the case of slowly varying currents. The FCT method is applied to a hypothetical coastal site with current variations in two-dimensions.

Explicit finite difference schemes have their shortcomings in attempting to reproduce the continuum solution for convection. So-called numerical diffusion results in some differencing schemes, and numerical dispersion invariably results in all differencing schemes [3]. Although some schemes do yield conservative as well as transportive approximate solutions, interpretation of the results is quite difficult. Basically, numerical diffusion/dispersion is caused by the inherent numerical truncation/grid interpolation error propagation with time associated with differencing the convection terms in explicit schemes [4].

Comparison of a conventional differencing scheme (upwind) for the convection terms with the FCT method is given to clearly demonstrate the effectiveness of the latter corrective procedure. It should be noted that when physical diffusion strongly dominates convective transport this pathological behavior is comparatively small and becomes less significant in numerical models [5], and the FCT method need not be employed.

2: CONVECTION-DIFFUSION EQUATION

The two-dimensional dispersion of heat or mass in a turbulent flow can be expressed in cartesian coordinates as:

$$\frac{\partial A}{\partial t} + u\frac{\partial A}{\partial x} + v\frac{\partial A}{\partial y} = B_x\frac{\partial^2 A}{\partial x^2} + B_y\frac{\partial^2 A}{\partial y^2} + S \qquad (1)$$

in which A = C(x, y, t) or T (x, y, t), that is, the specie mass concentration or temperature, respectively; B_x and B_y = x and y components of turbulent eddy transport coefficient; and, S = source term. The left side of Eq. (1) represents the convective change upon A; where u and v = x and y component of current velocity and the right side represents diffusive transport and a source term. With appropriate initial and boundary conditions, Eq. (1) can be used to describe either mass or thermal dispersion in a domain of interest. For slowly varying currents, Eq. (1) need not be cast into the conservative form, although Book et al developed their method for a system of nonlinear, compressible conservation equations.

Note, for the case of thermal dispersion the source term is usually represented by the Edinger and Geyer [6] surface heating/cooling mechanism, whereas, for particle dispersion this term is generally set equal to zero [7, 8]. Since, the inclusion of the Edinger and Geyer term does not affect numerical stability and convergence in thermal dispersion models, it will not be considered here. Although, other terms would appear in the momentum equation, viz. coriolis and pressure gradients, the convection/diffusion terms most commonly dictate numerical stability criteria. Lastly, the mass continuity equation can also be solved by implementing the FCT method.

3: NUMERICAL STABILITY CRITERIA

Eq. (1) can be approximated by a finite difference equation in explicit schemes by discretizing the infinitesimal variations in x, y and t such that: Δx = grid size in x-direction; Δy = grid size in y-direction; and, Δt = appropriately selected time step. For an explicit scheme, Δt is based upon the dominant transport process, that is, whichever process yields the smaller time step. Proceeding as follows; where the subscript c and d = convection and diffusion, respectively;

$$\Delta t_c < \frac{\Delta x}{u_{max}} \text{ and } \frac{\Delta y}{v_{max}} \qquad (2)$$

and

$$\Delta t_d < \frac{(\Delta x)^2}{2B_x} \text{ and } \frac{(\Delta y)^2}{2By} \qquad (3)$$

Therefore,

$$\Delta t = \min(\Delta t_c, \Delta t_d) \qquad (4)$$

In order to ensure numerical stability, even with the FCT method, Eq. (2) must be satisfied for convection dominated flows. Note, that for strongly convection dominated flows, reducing the time step by even a factor of 100 does not obviate the need for the FCT method, since significant numerical dispersion still results in conventional differencing methods.

4: FCT METHOD IN TWO-DIMENSIONS

The flux corrected transport method (FCT) for convection can be simplified to incompressible flow in two-dimensions, for a slowly varying current field (u, v), as follows for the case of thermal dispersion, in which for the "x-cycle":

$$f^n_{I+\frac{1}{2}} = 1/8\ (T^n_{I+1} - T^n_I) \tag{5}$$

$$F^d_I = T^n_I + (f^n_{I+\frac{1}{2}} - f^n_{I-\frac{1}{2}}) \tag{6}$$

$$\epsilon^{\pm}_I = \tfrac{1}{2} \pm u^n_I\ (\Delta t/\Delta x) \tag{7}$$

$$Q^+_I = \epsilon^-_I/(\epsilon^+_{I+1} + \epsilon^-_I) \tag{8}$$

$$Q^-_{I+1} = 1 - Q^+_I \tag{9}$$

$$F^{td}_I = 4(Q^+_I)^2\ f^n_{I+\frac{1}{2}} - 4(Q^-_I)^2\ f^n_{I-\frac{1}{2}} + Q^+_I\ (T^n_I) + Q^-_I(T^n_I) \tag{10}$$

$$\delta F^t_I = F^{td}_I - F^d_I \tag{11}$$

$$\delta F^{td}_{I+\frac{1}{2}} = F^{td}_{I+1} - F^{td}_I \tag{12}$$

$$f^t_{I+\frac{1}{2}} = f^n_{I+\frac{1}{2}} + 1/8(\delta F^t_{I+1} - \delta F^t_I) \tag{13}$$

$$f^c_{I+\frac{1}{2}} = \mathrm{SGN}\ (f^t_{I+\frac{1}{2}})\ \mathrm{MAX}\ (0,\ \mathrm{MIN}(\mathrm{SGN}(f^t_{I+\frac{1}{2}})\ \delta F^{td}_{I-\frac{1}{2}}),\ \mathrm{ABS}\ (f^t_{I+\frac{1}{2}}),\ \mathrm{SGN}\ (f^t_{I+\frac{1}{2}}) \cdot \delta F^{td}_{I+3/2})) \tag{14}$$

$$T^{n+1}_I = F^{td}_I - (f^c_{I+\frac{1}{2}} - f^c_{I-\frac{1}{2}}) \tag{15}$$

Introducing shorthand notation, let the operator L $\{T^n_I,\ u^n_I,\ \Delta x,\ \Delta t\}$ define Eqs. (5) through (15), then for the x-cycle:

$$T^{n+1}_I = L\ \{T^n_I,\ u^n_I,\ \Delta x,\ \Delta t\} \tag{16}$$

Eqs. (A2) and (A3) in Book et al [1] have been simplified by considering that $v^o_x = v^{hx}_x = u$ over a time step Δt for slowly varying currents. Similarly, Eqs. (A4) and (A5) in Ref. [1] can be simplified by considering $v^x_y = v_y{}^{hy} = v$ and therefore, the y whole step becomes:

$$T^{n+1}_{I,J} = L\ \{T^{n+1}_I,\ v^n_j,\ \Delta y,\ \Delta t\} \tag{17}$$

in which T^{n+1}_I = temperature at grid location (I, J) advanced one full time step Δt from T^n_I as computed for the x-cycle; $T^{n+1}_{I,J}$ = temperature at grid location (I,J) advanced one full time step Δt from $T^n_{I,J}$ for both the x-cycle and the y whole step; I and J = the grid indices in the x and y - direction, respectively; n = time level; Δx and Δy = grid size in x and y - directions,

respectively; Δt = time step; d = diffused; td = transported and diffused; and c = flux-corrected. The remaining symbols are directly defined by Eqs. (5) through (15).

Now, if the effect of physical diffusion must be considered, and the FCT method is used to reduce numerical error propagation, the combined effects of convection and diffusion may be superimposed, due to the linearity [9] of Eq. (1). Thus,

$$T_{I,J}^{n+1} = L\,(T_I^{n+1},\ v_J^n,\ \Delta y,\ \Delta t) + (B_x\Delta_x^2\,T^n + B_y\Delta_y^2 T^n)\Delta t \tag{18}$$

where,

$$\Delta_x^2 T^n = \frac{T_{I+1,J}^n + T_{I-1,J}^n - 2T_{I,J}^n}{(\Delta x)^2} \tag{19}$$

$$\Delta_y^2 T^n = \frac{T_{I,J+1}^n + T_{I,J-1}^n - T_{I,J}^n}{(\Delta y)^2} \tag{20}$$

where central differencing in space has been used for the horizontal diffusion terms.

5: NUMERICAL EXAMPLE #1

A sample problem, for the case of thermal dispersion was constructed to demonstrate the extent to which numerical diffusion/dispersion is reduced in comparison with a conventional upwind differencing scheme for the convection term. Assuming a thermal parcel in a uniform flow region with periodic motion, the values of grid size, time step, turbulent eddy diffusivities, and other physical parameters used in this computer run are as follows:

$\Delta x = \Delta y = 2025$ ft (617.2m)
$\Delta t = 360$ sec
$B_x = B_y = 6$ ft^2/sec (0.56m^2/sec)
$u = \sin\omega t$ (ft/sec), in which $\omega = 2\pi f$ ($=2\pi/12$)
$v = 0$
$T(x, y, t = 0) = 77.5^oF$ (25.3°C) for $17 \leq I \leq 26$
$T(x, y, t = 0) = 77^oF$ (25°C) elsewhere

The surface heating term was ignored, since the intent of this simulation is to compare the FCT method to the upwind differencing method for the case of dominant convective transport. The addition of this term would not affect the stability or convergence of the predicted solution.

For this example convection strongly dominates in the x-direction, whereas, only physical diffusion is present in the y-direction. For the sake of illustration, the results of thermal dispersion in the x-direction are given to clearly indicate the significant benefits available to the modeller using the FCT method in lieu of upwind differencing for a convection dominated flow.

Figure 1 presents the initial temperature distribution along a J-transect, and the evolving temperature distribution after 3 hrs., 6 hrs., 9 hrs., and 12 hrs. for the case of employing the FCT method. Figure 2 gives the corresponding results of using conventional upwind differencing for the full tidal cycle. As

can be readily seen, the FCT method yields much the same results as the exact solution, except for numerical distortion in the neighborhood of the end points. However, the extent of this error does not significantly grow with the passage of time, and a substantial portion of the initial temperature distribution properly convects (in a Lagrangian sense) during the course of the tidal cycle. Thus, the FCT methods yields both conservative and transportive solutions.

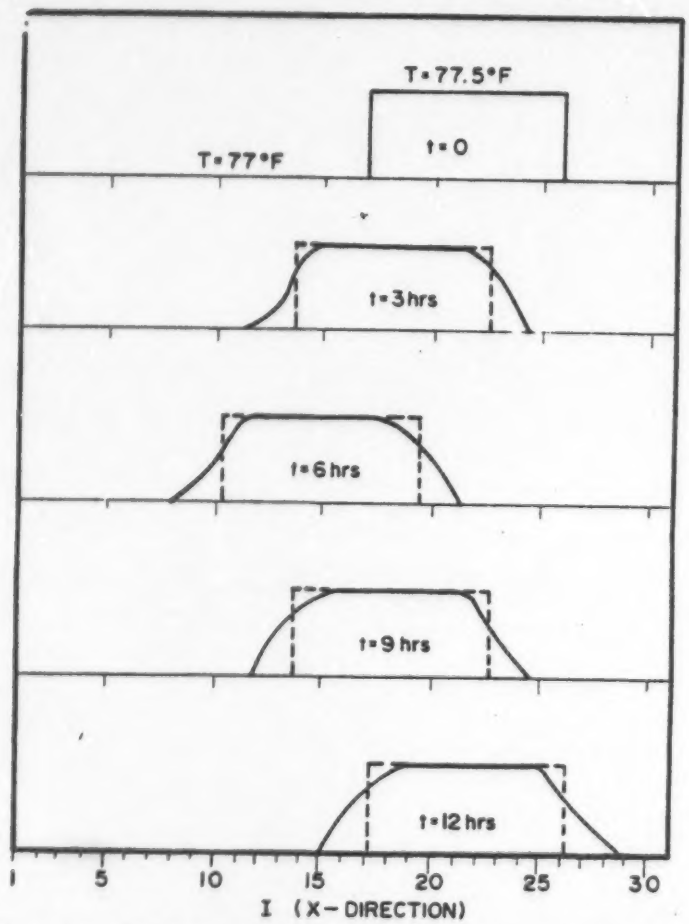

Fig.1 Evolution of initial temperature distribution over one tidal cycle using flux-corrected transport method.

Figure 2 for the case of upwind differencing, indicates increasing numerical diffusion/dispersion behavior during the course of the tidal cycle. The spreading of the initial temperature distribution increases significantly with time. This was not evidenced by implementing the FCT method. Furthermore, although the resulting temperature distributions shown in Figure 2 do possess conservative and transportive properties, interpretation of these results can be misleading and is difficult in the sense of general application.

Therefore, this simple numerical example demonstrates the distinct advantage of using the FCT method as opposed to conventional differencing schemes for one-dimensional convection dominated flows. The large extent to which numerical diffusion/dispersion produce excessive smearing effects in conventional schemes, makes application of the FCT method, or some comparable correc-

tive method, imperative to the modeller.

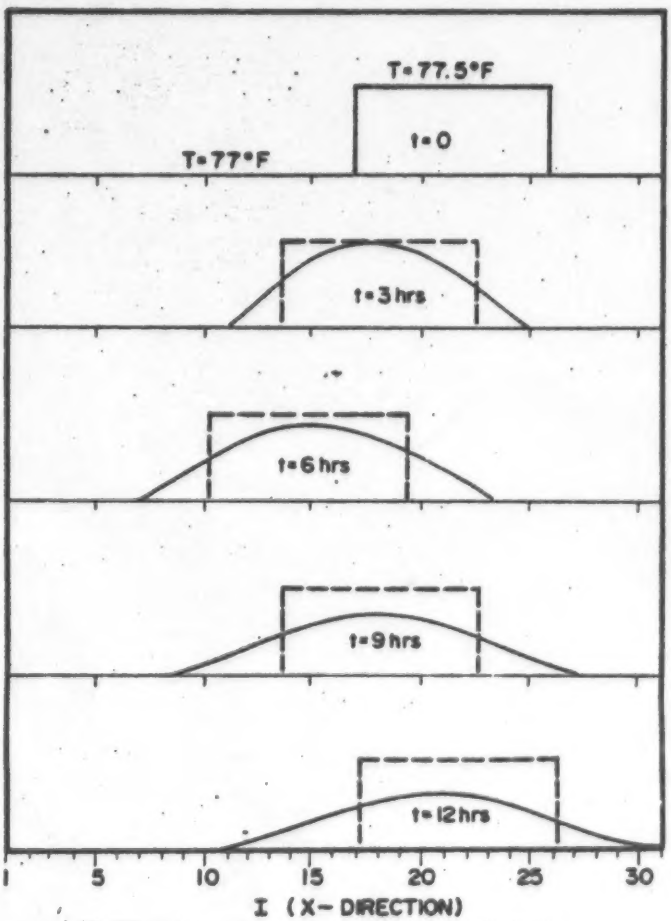

Fig.2 Evolution of initial temperature distribution using upwind differencing method.

6: NUMERICAL EXAMPLE #2

A two-dimensional case of implementing the FCT method is shown in this example. Assuming a thermal parcel in a uniform flow region with periodic motion, the parameters are the same as in Example 1; Δx, Δy, Δt, B_x, By are given; however,

$u = \sin\omega t$ (ft/sec), in which $\omega = 2\pi f$ $(=2\pi/12.)$
(.305 $\sin\omega t$ m/sec)
$v = 0.1$ ft/sec (.0305 m/sec)
$T(x, y, t = 0) = 77.5^{o}F(25.3^{o}C)$ for $15 \leq I \leq 26$
$T(x, y, t = 0) = 77.^{o}F(25^{o}C)$ $8 \leq J \leq 18$

elsewhere.

Note, for most oscillating flow regions, for a sinusoidal component of current parallel to the shoreline, a cosinusoidal component of current would exist normal to the shoreline. However, the case in Figure 3 was run for the normal component of current constant, to indicate the maximum distance

convected in the y-direction by the thermal parcel.

Figure 3 shows the grid system for this example, the initial temperature distribution, and the temperature distribution at t = 3, 6, 9 and 12 hours. As can be seen in Figure 3, the initial temperature distribution does not distort at t = 3, 6, 9 and 12 hours, due to the inherent accuracy of using the adhoc FCT method. Figure 3 does not indicate the distortion illustrated in Figure 1, since Figure 3 is based upon interpolating values such that only values of 77.5°F are shown. Thus, Figure 1 would similarly illustrate the exact solution. Physical diffusion is not observed since its magnitude is so small.

Therefore, the FCT method can be applied readily to 1-D as well as 2-D incompressible flows for u and v relatively constant over Δt, by utilizing Eqs. (5) - (17).

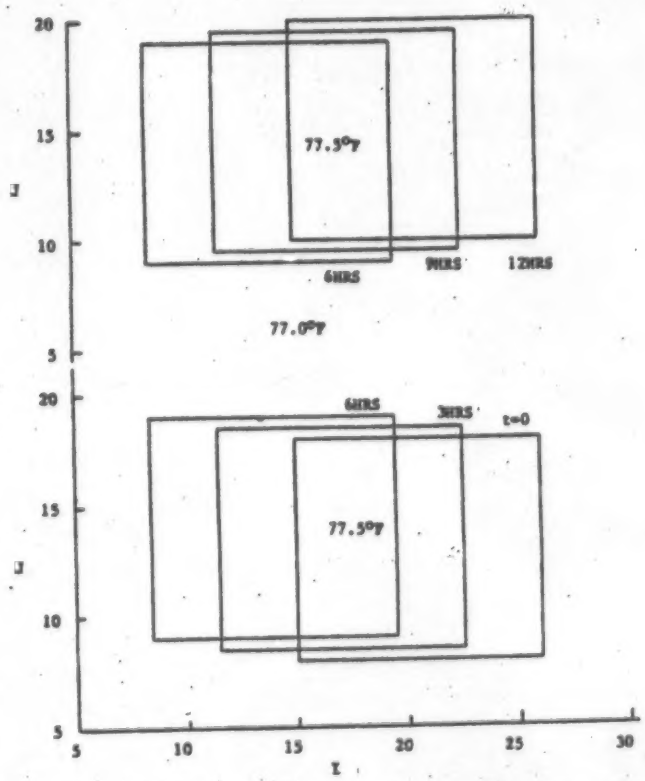

Fig.3 Evolution of initial 2-D temperature distribution over one tidal cycle using flux-corrected transport method.

7: SUMMARY AND CONCLUSIONS

The flux-corrected transport (FCT) method has been simplified to significantly reduce numerical diffusion/dispersion associated with an explicit finite difference solution to the convection-diffusion equation for the case of one and two-dimensional, incompressible, convection dominated flows. The exact (continuum) solutions are reproduced rather well over the course of one

tidal cycle for the numerical examples given, which are representative of coastal sites. Significant distortion of the numerical solution is shown for the case of conventional upwind differencing in one-dimension to demonstrate the value of the FCT method to the numerical modeller.

The FCT method, which was developed for nonlinear, compressible flows, was vastly simplified to an incompressible, slowly varying 2-D current field. The method is ad-hoc in the sense that many points must be used to achieve accurate convection (numerical examples #1 and #2 used a minimum of 10 points, and Book et al used about 20 points) and, therefore, must be carefully implemented. For the coastal site conditions selected, the integration time step is small compared to the time scale of the current velocity variation, thus the simplification of the nonlinear FCT method was justified. The site conditions are common, however, and, therefore, this simplified FCT method should provide an additional modeling technique for various environmental studies.

REFERENCES

1. Book, D. L., Boris, J. P., and Hain, K., Flux-Corrected Transport II: Generalizations of the Method, Journal of Computational Physics, 18, 248-283 (1975).
2. Boris, J. P. and Book, D. L., Flux Corrected Transport I. SHASTA, A Fluid Transport Algorithm That Works, Journal of Computational Physics, 11 , 38-69 (1973).
3. Fromm, J. E., A Method for Reducing Dispersion in Convective Differencing Schemes, Journal of Computational Physics, 3 , 176-189 (1968).
4. Roache, P. J., Computational Fluid Dynamics, Hermosa Publishers (1972).
5. Lee, S. S. and Sengupta, S., Three-Dimensional Thermal Pollution Models, NASA CR-144858 (1977).
6. Edinger, J. E., and Geyer, J. C., Heat Exchange in the Environment, E.E.I. Publication No. 65-902, Edison Electric Institute (1971).
7. Sengupta, S., Lee, S. S. and Miller, H. P., Three-Dimensional Numerical Investigations of Tide and Wind-Induced Transport Processes in Biscayne Bay, Sea Grant Technical Bulletin No. 39 (1978).
8. Sheng, Y. P., The Wind-Driven Currents and Contaminants Dispersion in the Near-Shore of Large Lakes, Report H-75-1, Department of Earth Sciences, Case Western Reserve University (1975).
9. Garabedian, P. R., Partial Differential Equations, John Wiley & Sons (1964).

PB82-228065

A THERMAL IMPACT ASSESSMENT MODEL WITH MEASURED FIELD DATA APPLIED TO THE TIDAL RIVER WESER

J. Häuser, D. Eppel, A. Müller, A. Nehlsen
Institut für Physik, GKSS-Research Center
2054 Geesthacht, Germany

F. Tanzer
1. Phys. Institut, Universität Giessen
6300 Giessen, Germany

ABSTRACT

This paper presents the fundamental principles, the general outline, and a specific application of the model UTRANS (unified transport system) with emphasis on the results of application. The model simulates the temperature distribution, generated by the nuclear power plant KKU (1300 MWe), in the lower Weser river (within tidal cycle) for october 3, 1979. The model was run for a period of 24 hours. The solution area of some 15 kilometers (km 44 to km 59) consists of about 1100 discrete elements (DE) of variable size and irregular shape.

For that day numerous temperature profiles were recorded by in situ measurements at different depths along with temperature surveys of the solution area by remote sensing infra-red measuring techniques from 7 am to 9 pm. Furthermore the necessary meteorological parameters were measured as half-hourly values.

The meteorological data and the data of the power plant in conjunction with an accurate depth survey along with the calculated flow field were input into the model but no calibration was performed to fit the calculations. The necessary bottom friction coefficient was determined by the measurements of Palmer. Computer simulation results for the two-dimensional temperature distribution in the vicinity of the power plant and for selected cross sections and their comparisons with the field-measured data are presented.

1. INTRODUCTION

Since water cooling is the easiest way, most of the power plants in Europe use once-through cooling from a nearby river, lake, or estuary. In view of the magnitude of the power output of the operational installations, condenser waste heat can be a critical aspect of power plant licensing and siting. Hence, in Germany certain temperature standards must be observed when once-through cooling is used [1]. The present paper describes the calculations of the thermal distribution resulting from the heated discharge water of the nuclear power plant KKU (1300 MWe) into the Weser. Extensive field-measurements were carried out to provide the necessary data for verification of the model.

Since the Weser is a tidal river the assumption of an infinite receiving body of water as a sink for the dilution of the discharge water is not valid. Hence, a sufficient quantity of new dilution water (that is, water not influenced by previous discharges) is not always supplied to the inshore region, where the plant is sited. However, the determination of a background tempera-

ture (i.e. estimation) of the ambient water is not necessary because the model equations are derived from the conservational principles of mass, momentum, and energy for a turbulent, incompressible fluid.

The equations are mean-time averaged and depth-averaged and upon being integrated are solved numerically. For the simulation of the thermal plume the modul HETRAN (heat transfer program) of UTRANS (unified transport system) [2,3] is used. The model accurately describes the complex shoreline geometry which is an important factor for plume dispersion, in particular for plumes of large longitudinal extension (up to 30 km) and small plume width. Since the application of the model is for environmental impact analysis in tidal rivers and estuaries a nearly complete vertical mixing is assumed. If the vertical temperature profile is known the resulting horizontal transport can be considered in the model. For the present study of the Weser simulation it was found from measurements that these additional transport terms need not be accounted for.

Due to the low discharge velocity of the effluents no jet formation is observed because the outfall structure, located at a distance of about 400 m from the shore, is designed to diffuse the cooling water at the river bottom. Hence, typical near field phenomena need not be regarded (of course a temperature stratification in the vicinity of the discharge condenser was found).

2. COMPUTER MODELS FOR TIDAL RIVERS, BAYS AND ESTUARIES

This section outlines the different requirements for tidal river models and oceanographic models and shows that this results in the building of different models. Furthermore it describes the necessary general features of mathematical models applied to the simulation of transport processes in tidal rivers, bays and estuaries. For these solution areas the vertical extension is normally orders of magnitude smaller in comparison with lateral and longitudinal extensions. Thus, the mathematical models employed for these purposes are two-dimensional, depth-averaged models. Since tidal effects with severe reversing flow conditions must be incorporated the time-dependent equations must be solved and steady-state equations are definitely not acceptable. Although two- and three-dimensional oceanographic models are available [4-10] the subsequent discussion shows that different models must be used. Hence some care must be taken if one wishes to use these models for tidal rivers. Since in rivers, bays or estuaries the solid boundaries, due to their length, have a strong influence on the flow-field and the calculated concentration distribution, it is important that the model provides a proper handling of these boundaries; i.e., the curvature and irregular shape of the boundary should be accounted for. Thus, models with equidistant meshes in the x- or y-direction and a rectangular representation of curved boundaries may cause artificial geometrical effects and can lead to possible gross errors in local mass balance.

Furthermore, calculations of thermal plumes in tidal rivers demand a fine spatial resolution, e.g., resolutions of 50 m in lateral and 150 m in longitudinal directions are needed near outfalls. In general, oceanographic models employ rather large grid specings and thus need not have improved numerical procedures to reduce computer time; so, for example, the simple FTCS (forward time, centered space) algorithm leads to a stability criterion of $\Delta t \sim (\Delta x)^2$ for the diffusion equation. Hence a reduction of Δx causes a considerable increase in computer time. The use of implicit schemes eliminates this problem only to a certain extent since the time step is still bounded in order to meet the desired accuracy conditions. As transport processes normally contain advection terms, the two principle errors, namely amplitude and phase errors (due to advection) are encountered in the solution and while the amplitude error can be substantially reduced by implicit schemes, the corresponding phase error (e.g., Crank-Nicolson) can be larger than that of some explicit schemes [11].

From the above discussion it is obvious that the two types of models must have different numerical solution procedures where a river model demands a more sophisticated algorithm. In addition, thermal plumes in tidal rivers have a width of 200 m to 500 m and are parallel to the shore and banks. Hence a coarse mesh, in particular an equidistant mesh, is insufficient to represent the accurate shape and location of the plume. As is known from infra-red remote sensing techniques, the thermal plume of a power plant is strongly influenced by islands situated in the solution area; i.e., the island frequently separates the plume from the rest of the river water. Hence a simulation model must provide a reasonable resolution of geometrical structures to account for the impact of the geometry on transport processes. In general a reasonable resolution by rectangles is not acceptable since the necessary number of DE is prohibitive from computer time and storage considerations. So the model uses cubic splines for the description of curved boundaries which reduces the number of base points and substantially simplifies the algorithm which determines all interior mesh points since the boundary curve is differentiable (exception: end points of a segment, see sec. 4, which require special treatment).

Since during a field campaign a lot of measured data are taken the model should provide the facility, at least to a certain extent, to directly input the measured data; e.g., temperature values are not normally measured at the coordinates of the computational mesh but along various transects. It should be possible to avoid the tedious and error-prone interpolation process of measured values on the computational mesh. All input data should be checked for consistency and error messages and warnings should be issued. Although checking and interpolating of input data takes a few seconds of computer time it may save hours or days of the time of the user.

As is known from observations thermal plumes in rivers from a single power plant can have extensions of up to 35 km. Hence simulation models for rivers must be capable to cover regions of that length with a fine enough resolution. Since sharp bends can occur the commonly used technique, which is employed in most models, of storing two-dimensional quantities in two-dimensional arrays, is extremely uneconomical since large parts of the arrays will contain no information. Thus, the length of the river section which can be modeled is substantially reduced by storage limitations. To avoid this problem the more expensive linked list technique must be used to store all quantities in one-dimensional arrays so that no empty list elements occur.

For the numerical solution of the parabolic partial differential equation (PDE) the PDE is reduced to a nonautonomous system of weakly coupled, ordinary differential equations which is integrated from specified initial conditions by a fourth order Runge-Kutta method. One ordinary differential equation is established for each discrete element so that an actual problem consists of 500 to 2500 equations. The spatial discretization employs the donor-cell method for the calculation of half-point values. This method is conservative and transportive. The numerical scheme used can be accelerated in two ways. First, and most important, the spatial approximation can be replaced by splines. Investigations for one-dimensional and regular two-dimensional problems have been carried out and the application to irregular multiconnected areas is being investigated. Since in fluid problems only first and second derivatives occur, the construction of spline functions being twice continuously differentiable is sufficient. The better accuracy of the spline method, in particular for the approximation of the advection term, allows much larger grid spacings and subsequently leads to enhanced time steps. Although splines are computationally more costly than upwind differencing computer time is reduced substantially. Second, attention is given to the superstep-method [12] to accelerate time integration. Although this method was primarily developed to calculate stationary

solutions, the third order method of W. Gentzsch should be sufficient to accurately represent the time-dependent solution.

Although river models and oceanographic models are derived from the same fundamental physical equations, the model building process for these two types of application is different, because a tidal river model demands :

(i) description of irregularly shaped boundaries with a reasonable degree of accuracy including multiconnected solution areas,

(ii) more effective numerical solution algorithms because of fine spatial resolution,

(iii) more sophisticated storage techniques to avoid the problem of empty arrays in order to allow consideration of large solution areas of desired resolution [2, 27].

3. FUNDAMENTAL EQUATIONS USED IN UTRANS

We now give a brief description of the mathematical formulation of the governing equations and the numerical solution technique. A more detailed description is found in [3, 13, 14]. The mathematical model is based on the conservation principles of mass, momentum and energy. Since the modul HETRAN relies on known velocity data, the Navier-Stokes equations need not be solved.

The conservation for mass and energy are therefore necessary and sufficient for the mathematical formulation of the governing equations. The continuity equation is used in the form

$$\frac{\partial}{\partial t}\int_V \rho\, dV + \oint_{A(V)} \rho\, v_i\, dA_i = \oint_{A(V)} \rho\, dQ \qquad (1)$$

The contribution on the right hand side,

$$\oint_{A(V)} \rho\, dQ \qquad (Q\ [m^3/s] \text{ is the volumetric flow rate}) \qquad (2)$$

represents mass flow across the surface due to external sources or sinks, such as intake or discharge buildings of power plants.

The heat transport is described by the equation

$$\rho c \frac{\partial}{\partial t}\int_V T\, dV + \rho c \oint_{A(V)} T\, v_i\, dA_i = \rho c \oint_{A(V)} T\, dQ + \oint_{A(V)} \lambda \frac{\partial T}{\partial x_i}\, dA_i + \int_R \phi\,(T, x_1, x_2, t)\, dx_1, dx_2 \qquad (3)$$

where $c = c_v = c_p$ $(J\,kg^{-1}\,K^{-1})$ denotes the specific heat of water and λ $(J\,s\,m^{-1}\,K^{-1})$ is the thermal conductivity. The term

$$\rho c \oint_{A(V)} T\, dQ$$

accounts for the influence of intake- or discharge structures but may also contain volumetric flow rates resulting from thermally stratified water bodies.

The last term of Eq. (3) considers the transient heat flux $\phi(J/m^2s)$ across the free water surface $R(m^2)$. The formulas for radiation, convection and evaporation along with the measured meteorological parameters are given in sec. 4. Eqs. (1,3) are integrated over each discrete element, where a DE is formed by its free surface (determined by the mesh and the boundaries) and its associated depth (time dependent). Thus, the integration process results in the following system,

$$\frac{\partial T_{i,j}(t)}{\partial t} = F_{i,j}(t, T_{i\pm1,j}; T_{i,j\pm1}; T_{i,j}; \phi_{i,j}(t)) \qquad (4)$$

$$T_{i,j}(t_o) = (T_o)_{i,j} \qquad \text{(initial conditions)}$$

which is solved numerically. The model is, of course, not restricted to the calculation of temperature distributions. Any other water quality parameter is handled in the same way.

For the calculation of the transient flow-field the one-dimensional model FLUSS [15] was used, which calculates the cross-section averaged velocity from measured water-levels. This program employs the continuity equation in conjunction with accurately measured time-dependent cross-sections. Future calculations will use slightly modified version of the Hansen model [4,5] to obtain additional information for flow fields. The original version of that program used classical central differencing which is undesirable because unrealistic diffusion coefficients (for tidal rivers) must be chosen to ensure stability. It is now accepted that donor-cell differencing, where the values are evaluated in the direction of the flow, should be preferred [28]. So the model was modified to reflect this improvement. However, it is planned to resort to a numerical method with higher truncation error for the approximation of the convection term in order to allow larger grid spacings without loss of accuracy. For that purpose a flux corrected transport technique [16], convective difference schemes with Hermite interpolation [17] or quadratic upstream interpolation [18] can be used. Spline approaches also give excellent results in most cases [19,20] (see sec. 2).

Interpolation from the coarse staggered mesh, used for the flow calculations, to the nonuniform mesh utilized by UTRANS is not feasible because this procedure is too time-consuming as it must be performed at least every second or third time step. The present version of UTRANS treats the flow-field as input data in form of spline functions which are determined from one-dimensional calculations to simulate the transient flow-field.

4. RESULTS FOR THE LOWER WESER RIVER

4.1 Model Simulation and Field Measurements for the Weser

The area of interest has a length of approximately 15 km (Weser km 644 to km 659). A nonuniform mesh is spanned over the solution area [Fig. 1] with fine spatial resolution near the discharge condenser and larger grid spacings far from the outfall structure. The lateral resolution of the grid is fine near the shore where the plume is observed and gradually increases to avoid combination of very large and very small discrete elements.

The model simulates the temperature distribution for 3 october, 1979 from 0 am to 12 pm. For this day seventeen cross-section temperature profiles were measured where three temperature sensors were kept at different depths to de-

tect continuously the water temperature [21]. The profiles were recorded near the discharge condenser of KKU nuclear power plant between km 49.9 and 53.5. The plant has a cooling water intake flow rate of 61 m^3/s. The temperature increase of the cooling water in the condenser is 10 K. The KKU is the main discharger in the region modelled. Additional temperature values and water quality parameters are taken from a set of ten continuously measuring stations located at fixed positions between km 43.3 and 60.5. Six of these stations are situated near the outlet structure of the power plant. In conjunction with the in situ measurements infra-red remote sensing surveys were carried out (7.38 am to 20.42 pm) providing a nearly synoptic (half-hour time lag) thermal mapping of the heated effluents of the lower Weser river. The infra-red photo images were quantified assigning a color code to the zones of the picture for fourteen-different temperature intervals ranging from 8.75 °C to 19.25 °C, producing an interval size of 0.75 K. The necessary meteorological data, that is, wind speed and direction, air temperature, air humidity, and surface radiation heat transfer are supplied by the KKU meteorological station. Surface evaporation heat transfer and surface convection heat transfer are calculated from the meteorological data, which are considered representative for the whole solution area. The input for the river topography was produced from the latest lower Weser survey. The daytime variations of the water levels were taken from the lower Weser water gauges.

For the calculation of the turbulent diffusion a linear relation between turbulent heat conduction and the mean temperature gradient was assumed, that is, the influence of the turbulent transport is described by eddy-viscosity. The magnitude of the eddy-viscosity coefficient is given as a function of depth and horizontal velocity. The remaining free parameter ε, describing the bottom roughness, was determined from the work of Palmer [21] who has measured de Chèzy's coefficient for various bottom types. A different approach using Prandl's turbulence ansatz is given in [22]. The mixing length is determined analytically as a function of the bottom and free surface elevations. Both models, however, do not describe the transport of turbulence. Although more sophisticated turbulence models [30] are available their application in combination with transport models for large flow regions is prohibitive from computer time considerations.

4.2 Meteorological Data, Water Levels and Flow Field Formulation for the Weser Sample

The heat flux across the free surface consists of the following three terms, namely, radiation, evaporation, and convection. Since the absorbed day-time solar irradiation was measured (Table 1) only the formula for the black-body back radiation is necessary (the program accepts half-hourly measured values of solar irradiation, air temperature, relative air humidity and wind speed or approximates the temporal course of these quantities by builtin formulas).

$$\phi_{R_2} = -\sigma \gamma_E (T - \Delta T + 273.16)^4 \tag{5}$$

where $\sigma = 5.6703 \times 10^{-8}$ W/m^{4}K^4 is the Stefan-Boltzmann constant, $\gamma_E = 0.97$ the emissivity of the water surface, T temperature of DE and $\Delta T = 1$ K is the difference between the temperature of the DE and its water surface. The equation for the evaporation term is given by

$$\phi_E = \begin{cases} (\alpha_1 + \alpha_2 (|\vec{v}_w|)^r) \; (p(T - \Delta T) - p(T_D) R_D) & ; \quad T_D \leq T \\ 0 & \text{otherwise} \end{cases} \tag{6}$$

where $\alpha_1 = 0.0612$ m/s, $\alpha_2 = 0.0230$ (s/m)$^{r-1}$ (note that α_2 is a dimensionless factor for $r = 1$), $|\vec{v}_w|$ is the wind speed (Table 1), $r = 1$, $p(T-\Delta T)$ partial

pressure (air humidity) of water in air [N/m^2] (a fourth order polynominal in T), T_D (time-dependent) is air temperature and R_D is relative air humidity [Table 1].

The convection is described by

$$\phi_c = \begin{cases} -\beta(\gamma_1 + \gamma_2(|\vec{v}_w|^r))\ (T - \Delta T - T_D) & ;\quad T > T_D \\ 0 & \text{otherwise} \end{cases} \tag{7}$$

where $\beta = 0.62$ J/m^3 K Bowen's ratio, $\gamma_1 = 5.0$ m/s and $\gamma_2 = 2.85(s/m)^{r-1}$. The transient water level was determined by cubic spline interpolation of measured water levels (Fig. 2) where hourly values were used (this method proved to be much more accurate than Fourier analysis). Two additional nodes at the left and right boundary of the interval were employed to avoid inaccuracies associated with the natural spline condition; that is, the free end conditions $f''(t_o) = f''(t_n) = 0$ were utilized [29]. Hence the formula for the transient water level reads

$$H(x,y,t) = H_L(x,y) + 2.5 + H_{spl}(x,y,t) \tag{8}$$

The phase shift ist calculated by

$$t_o = \frac{s}{v_{td}}$$

where $H_L(x,y)$ low water [m], H_{spl} spline interpolated values v_{td} tidal wave speed, 39 000 m/h, s distance on x-axis with respect to river km 50.375 (negative or positive).

For the turbulent heat conduction (molecular heat conduction is negligible) the formulation derived in [24] is used

$$\lambda = k_o\, \varepsilon\, H(u^2(x,y,t) + v^2(x,y,t))^{1/2}\, \frac{m^3}{(2m-1)\ (3m-1)} \tag{9}$$

where $k_o = 0.41$ Karman's constant, $\varepsilon = 0.0763$ bottom friction coefficient (mud) for the Weser determined from the measurements of Palmer [22], $m = 10$ as suggested by measurements [25, p. 535]. For a maximum velocity (Fig. 2) of 1 m/s, one obtains

$$\lambda = 0.41 \times 0.0763 \times 10\,m \times 1\,m/s \times 1.815 = 0.568\ m^2/s. \tag{10}$$

The magnitude v^H of the temporal course of the flow, as determined by FLUSS (Fig. 2), was interpolated by cubic splines,too. Again hourly measured values were used.

The expressions for the four different modes of surface heat transfer Eqs. (7-9), Table 1 were employed to compute heat transfer rates per unit area. The effects of the four terms nearly cancelled during 9 am to 4 pm. Hence, the model computed no changes in temperature for areas not influenced by the thermal plume (e.g., opposite shore of KKU). This is, however, in agreement with recorded temperature measurements. Thus any temperature changes were mainly caused by power plant discharges.

Fig. 3 shows the location and shape of the thermal plume obtained by infra-red survey taken at 8.15 am (flood). Fig. 4 depicts the locations where the seventeen temperature profile were recorded. Fig. 5 represents the computer simulation results for the two-dimensional temperature distribution along

with the comparison of the corresponding distribution obtained by remote sensing. Fig. 6 gives a comparison between simulated and measured temperature profiles for various transects (see Fig. 4) at different times.

Although the program gives a lot of diagnostics and detects input errors the following error messages appeared quite frequently when the lower Weser sample was computed (this signalled the attempt of improper use of the program):

***** warning: sr solve: DE xxxx depth = xxx.xx is likely to be errorneous

***** warning: sr solve: DE xxxx temperature not okay T = xxx.xx

The first warning indicates that an incorrect depth value was detected; that is, $H(x,y,t) < 0$ for the whole calculation period. The program allows for negative depths which are utilized as one possibility (the second one uses time dependent scale factors; the two methods may be combined) to simulate areas which run dry. This warning occurs, when the program has insufficient information to interpolate or extrapolate the depths values of the computational mesh from the user specified transects. Thus additional depth values must be supplied.

The second warning signals that unrealistic temperatures are calculated; e.g., temperature values of $-2.5^{\circ}C$ or $+500^{\circ}C$ may occur. In general, the two warnings are issued together and unrealistic temperatures are frequently the outcome caused by unrealistic depths. In addition, one of the following reasons can produce errorneous temperature values:

(i) unrealistic large time step (the program estimates a maximum time step (rather restrictive) and outputs a warning if the user exceeds this value),

(ii) unphysical velocity field which may lead to gross errors in mass balance,

(iii) volume ratio of neighbored discrete elements too large,

(iv) volumes of discrete elements representing discharges too small,

(v) unrealistic meteorological data,

(vi) approximation at open boundaries caused unrealistic energy inflow or outflow (can occur if the thermal plume leaves the solution area with too a large gradient).

5. CONCLUSIONS AND OUTLOOK

A short-time transient, two-dimensional, depth-averaged model for simulation of water-quality parameters in tidal rivers, bays and estuaries is presented. The UTRANS mathematical model was applied to the lower Weser river for the assessment of the thermal impact KKU (1300 MW_e) power plant for 3 october 1979. The model was run for a period of 24 hours, starting at midnight.

The flow field was obtained by the one-dimensional model FLUSS. Measured water levels and calculated velocity data were interpolated over a period of 24 hours. The spline routines [29] were used to simulate the transient behavior of the current field and the water levels. Meteorological data were measured for 24 hours. In addition seventeen temperature profiles were measured at

various cross-sections (at three different depths) in the vicinity of the power plant from 7 am to 9 pm. Furthermore, five temperature surveys were recorded employing remote sensing infra-red measuring techniques.

The wide experimental campaign provided the data to convalidate the mathematical model to be used for planning purposes in the presence of relatively complex environmental conditions such as those to be prevailing in tidal rivers.

No parameters were adjusted during the computational process. Hence the results clearly indicate the validation of the model and its predictive capability (within certain limits) for the assessment of thermal impact of discharged effluents in tidal rivers, bays and estuaries.

It should be stated that the results of UTRANS mathematical model depend on the available input information. It is therefore advantageous that the model incorporates the hydrodynamic calculations. Although the conservation of energy (or any other concentration) principle is exactly statisfied the modul HETRAN possesses limitations associated with the required input data.

In the near future the model will be extended to simulate additional water quality parameters (relevant parameters and areas of further application are found in [26].

To reduce computer time and storage more effective numerical methods both for time and space integration are being investigated. Although the second upwind differencing form of the convective terms has desirable stability conditions, methods with higher truncation error (see 4.1) should be preferred to obtain improved accuracy and to lessen numerical diffusion.

REFERENCES

1. Lawa, 1977. Grundlagen für die Beurteilung der Wärmebelastung von Gewässern. Dr. Hanns Krach, Postfach 2730, 6500 Mainz.

2. Häuser, J. and Tanzer, F., 1978. Algorithms for a Mathematical Model to Predict Environmental Effects from Thermal Discharges in Rivers and in Coastal and Offshore Regions. Second Conference on Waste Heat Management and Utilization, Miami.

3. Häuser, J., Eppel, D., Tanzer, F., 1980. Analysis of Thermal Impact in Tidal Rivers and Estuaries, Water Research, Vol 14, pp. 1409-1419, Pergamon Press.

4. Hansen, W., 1956. Theorie zur Errechnung des Wasserstandes und der Strömungen in Randmeeren nebst Anwendungen, Tellus, Vol 8, Nr. 3.

5. Backhaus, J., 1976. Zur Hydrodynamik im Flachwassergebiet. Ein hydrodynamisches Modell, Deutsche Hydrographische Zeitschrift, Bd. 29, Heft 6.

6. Leendertse, Jan J., Liu, S.K., May 1977. A three-dimensional model for estuaries and coastal seas. Volume IV, The Rand Corporation, R-2187-OWRT.

7. Liu, S.K., Nelson, A.B., May 1977. A three-dimensional model for estuaries and coastal seas. Volume V, The Rand Corporation, R-2188-OWRT.

8. Liu, S.K., Leendertse, J.J., 1978. Three-dimensional subscridscale energy model of eastern Bering sea, The Rand Corporation, P-6237.

9. Rodenhuis, G.S., Kjaer, O.B., Bertelsen, J.A., May 2-5, 1977. A north sea model that can provide detailed hydrographic information, 9th Annual OTC, Houston, Texas.

10. Abbott, M.B., 1979. Computational Hydraulics, Pitman.

11. Verboom, G.K., 1975. The advection-dispersion equation for an an-isotropic medium solved by fractional-step methods, delft hydraulics laboratory, publication no. 157.

12. Gentzsch, W., 1980. Über ein verbessertes explizites Einschrittverfahren zur Lösung parabolischer Differenzialgleichungen, DFVLR-TS, Göttingen.

13. Eraslan, A.H., 1975. A transient, two-dimensional, discrete-element, far-field model for thermal impact analysis of power plant discharges in coastal and offshore regions, ORNL-4940.

14. Eraslan, A.H., Kim, K.H., Dec. 4-6, 1978. Cost effective mathematical modeling for the assessment of hydrodynamic and thermal impact of power plant operations on controlled-flow reservoirs, Second Conference on Waste Heat Management and Utilization, Miami Beach.

15. Fiedler, H., Müller, A., Nolte, D., 1981. FLUSS - ein eindimensionales Modell des Wärme- und Stofftransportes in Flüssen, GKSS 81/E/12, Geesthacht.

16. Boris, J.P., Book, D.L., 1973. I. SHASTA, A Fluid Transport Algorithm that Works, J. of Comp. Phys. 11, 38-69.

17. Fischer, K., 1978. Convective Difference Schemes and Hermite Interpolation, Intl. J. For Numerical Methods in Eng., Vol 12, 931-940.

18. Leonhard, B.P., 1979. A Stable and Accurate Convective Modelling Procecure Based on Quadratic Upstream Interpolation, Computer Math. in Applied Mech. and Eng., 19, 59-98.

19. Rubin, G., Khosla, P.K., 1976. Higher Order Numerical Solutions Using Cubic Splines, NASA CR-2653.

20. Häuser, J., Eppel, D., Tanzer, F., 1981. Solution of Fluid Flow Problems by a Direct Spline Interpolation Method, paper to be presented at the Conference of Numerical Methods in Laminar and Turbulent Flow, Venice.

21. Institut für Physik der GKSS, 1980. Gewässeranalytische Untersuchungen auf der Unterweser im Herbst 1979, GKSS/E/27.

22. Palmer, S.L., 1978. A Calibrated and Verified Thermal Plume Model for Shallow Coastal Seas and Embayments, Second Conference on Waste Heat Management and Utilization, Miami.

23. Dinelli, G., 1976. Evaluation of Thermal Impact of Cooling Water Discharges into Mediterranean Coastal Waters. Future Energy Production Systems (J.C. Denton, N.H. Afgan, Eds.), Washington, Hemishere Publishing Corp..

24. Müller, A., et al., 1981. Simulation and Interpretation eines Tagesganges der Temperatur im Einflußbereich des Kraftwerkes Unterweser, in preparation, GKSS/81/E/.

25. Schlichting, H., 1958. Grenzschicht-Theorie, G. Braun.

26. Onislu, Y. et al., 1981. Critical review, radionuclide transport, sediment transport, and water quality mathematical modeling, and radionuclide adsorption/desorption mechanisms, NUREG/CR-1322, PNL-2901.

27. Duwe, 1980. Institut für Meereskunde, Universität Hamburg.

28. Dunn, W.E. et al., 1975. Water resources research program, surface thermal plumes. Evaluation of mathematical models for the near and complete field, ANLIWR-75-3, Part I, II.

29. Boor, C.de., 1978. A practical Guide to Splines, Springer.

30. Rodi, W., 1980. Mathematical Modelling of Turbulent Diffusion in Open Channel Flow, EUROMECH 130.

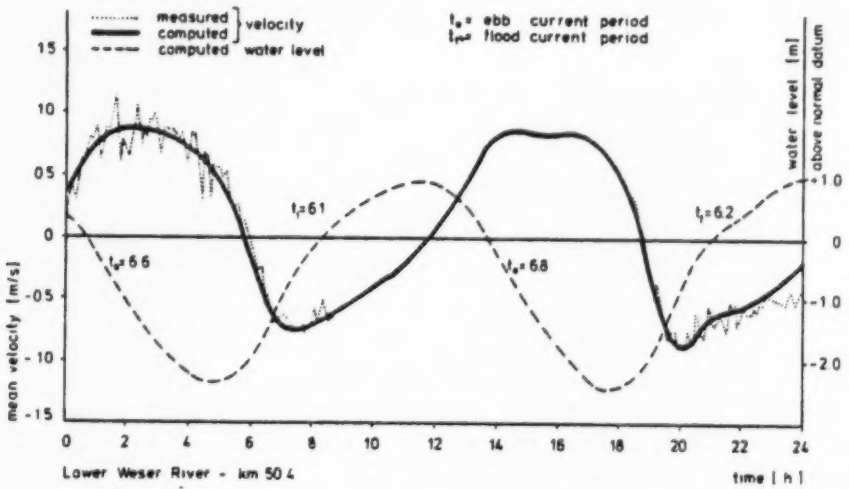

Fig. 2: The dotted line represents the measured velocity, the solid one shows the velocity computed by model FLUSS.

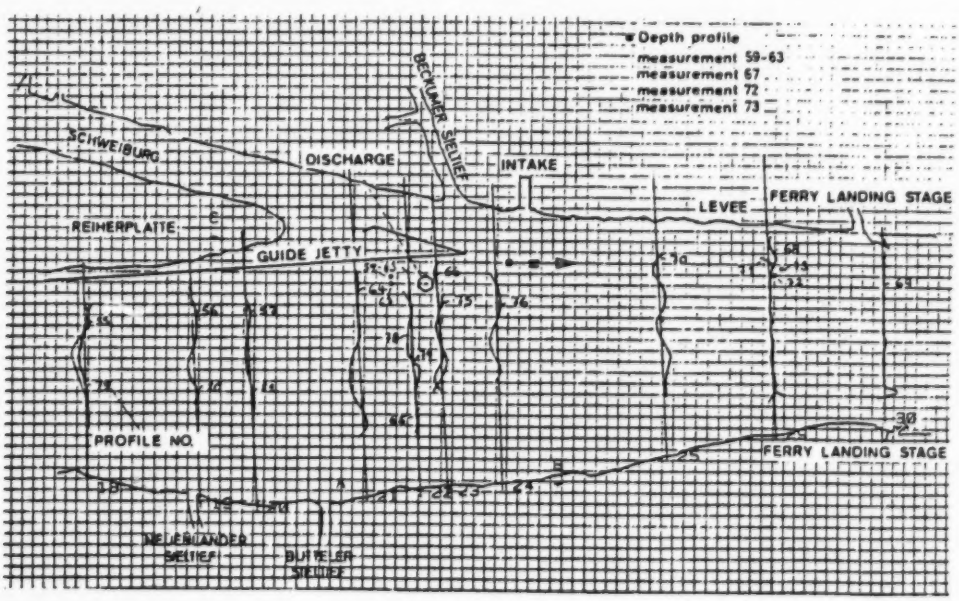

Fig. 4: Recorded temperature profiles at various cross sections at 3 october 1979.

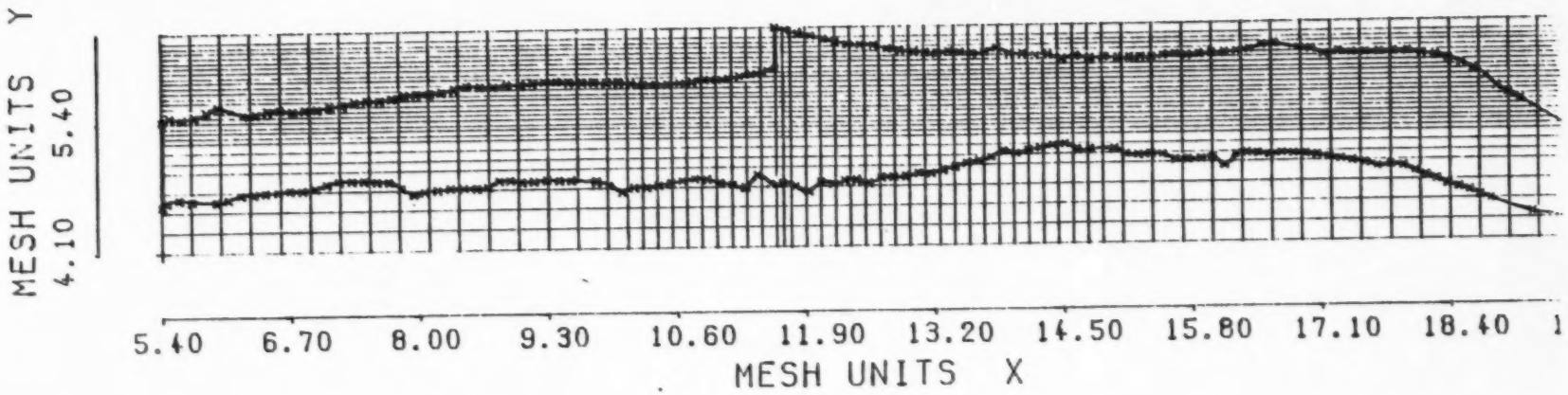

Fig. 1: Solution area used for temperature calculations of the lower Weser river reaching from km 44 to km 5
nonequidistant mesh is spanned over the region of interest with a fine resolution near the discharge
denser and along the upper shore. To account for the irregular geometry model employs discrete elemen
with curved boundaries. A time-step of 60 seconds was utilized (1 km = 1.0 MU).

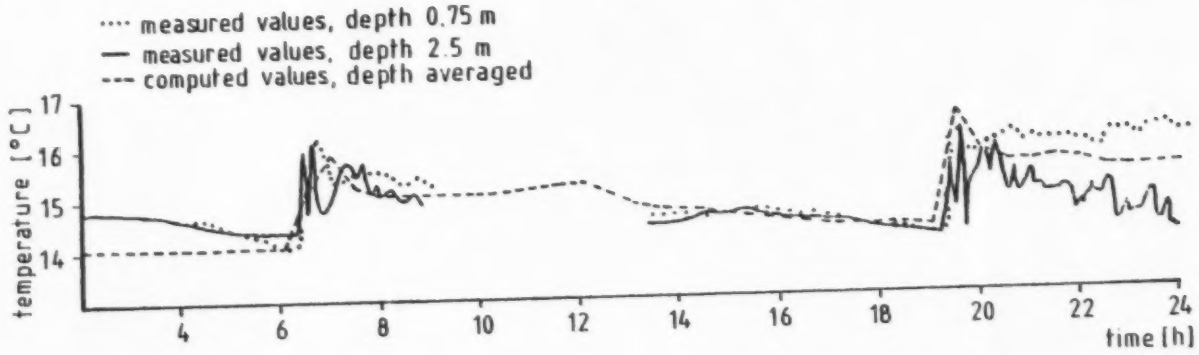

Fig. 7: Measured and calculated daily variations of temperature at lower Weser km 50.4. Temperatures were re
ed by a fixed measuring station. The first few hours should be discarded since the model was started
night using an estimated temperature distribution.

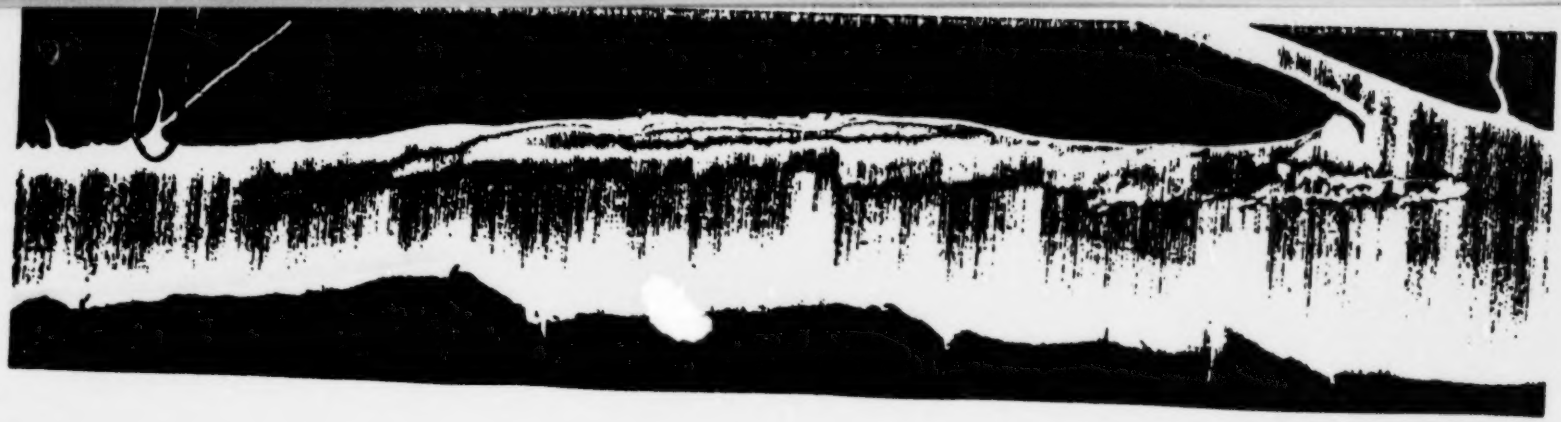

Fig. 3: Temperature distribution for 3 october 1979 at 8.15 am as obtained by remote sensing survey. The plume stretches along the shore and has an extension of some 5.3 km with an average width of about 260 m. This demands an extremely high spatial resolution for the numerical calculations.

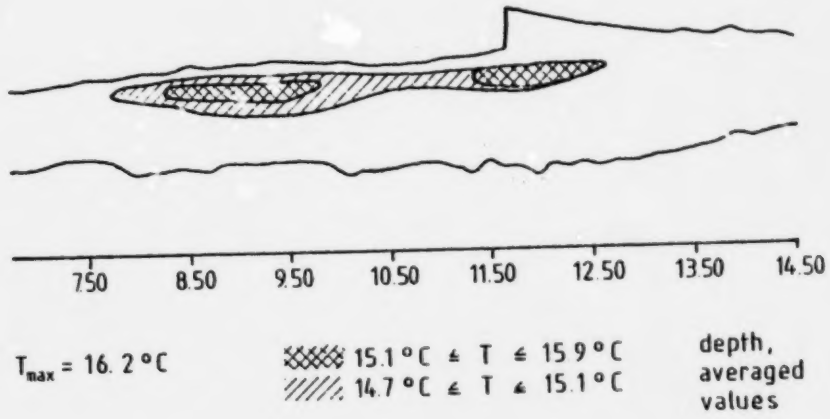

Fig. 5: Shape and extension of computed thermal plume for 3 october 1979 at 8 am. The plume has a calculated length of 5.4 km where the plume boundary was determined by an excess temperature of 0.5 K.

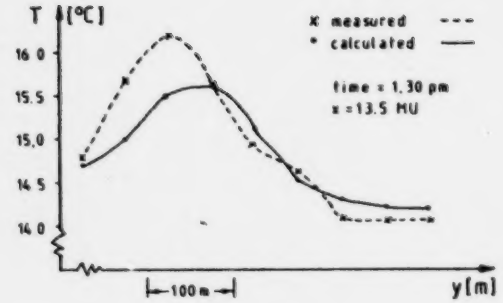

Fig. 6c

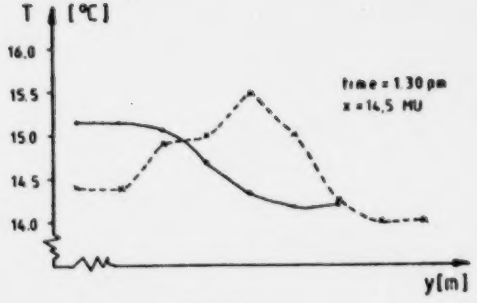

Fig. 6d

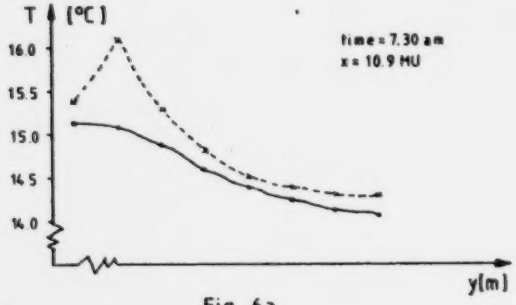

Fig. 6a

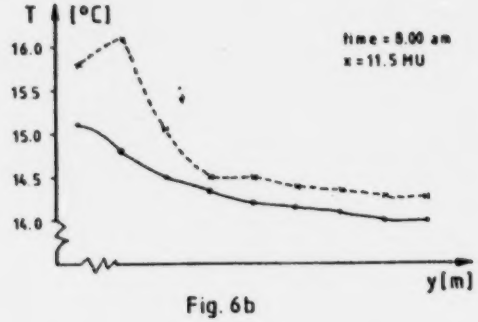

Fig. 6b

Fig. 6: Comparison of measured and calculated temperature profiles at various cross sections at different tim
It should be noted that the calculated temperature values are averaged over the volume of a DE, hence
sharp peaks do not normally occur because they are averaged out, while measured values are recorded a
a (nearly) fixed x-position. This value need not be a good representative of the mean value. Although
very fine spatial resolution is employed it is known from Fourier analysis that wavelengths less than
2 Δx (grid spacing) cannot be resolved, thus high frequencies of the temperature distribution are not
visible. While Fig. 6a - 6c show a reasonable agreement, Fig. 6d depicts large deviations. Here it is
obvious that the simple flow field calculation is insufficient for that instant at this cross-section
It is likely to obtain improved results if a two-dimensional hydrodynamic model is utilized.

Meteorological data of 3 october 1979 at river km 52

time	solar irradiation [kW/m^2]	air temperature [°C]	air humidity [%]	wind speed [m/s]	wind direction [° ≙ N]
0.00	0.27	7.0	77	6.3	90
0.30	0.28	7.0	78	6.6	90
1.00	0.28	6.5	79	6.3	88
1.50	0.28	6.5	81	6.6	94
2.00	0.28	6.3	81	6.6	94
2.30	0.27	6.0	81	6.6	94
3.00	0.28	6.0	81	6.0	97
3.30	0.29	5.8	82	5.4	97
4.00	0.29	5.8	84	6.3	97
4.30	0.29	5.5	85	6.2	94
5.00	0.30	5.5	86	6.6	90
5.30	0.29	5.5	86	7.2	94
6.00	0.28	5.3	85	5.7	99
6.30	0.31	5.2	85	6.0	99
7.00	0.29	5.2	84	6.7	99
7.30	0.37	5.2	85	6.2	106
8.00	0.41	5.5	84	6.9	103
8.30	0.43	6.0	83	7.0	103
9.00	0.40	6.5	82	7.5	101
9.30	0.47	7.0	80	6.0	106
10.00	0.44	7.5	78	7.5	103
10.30	0.56	8.0	75	7.8	108
11.00	0.70	8.5	72	7.8	103
11.30	0.58	9.5	68	8.1	99
12.00	0.49	10.0	65	8.1	104
12.30	0.52	11.0	62	9.0	112
13.00	0.58	11.5	59	8.7	104
13.30	0.58	11.5	57	8.8	101
14.00	0.60	11.5	58	8.4	99
14.30	0.58	11.5	57	9.3	101
15.00	0.66	11.8	58	8.7	101
15.30	0.37	11.8	59	8.7	90
16.00	0.42	11.5	59	6.9	103
16.30	0.35	11.0	61	5.7	94
17.00	0.32	11.0	62	4.8	97
17.30	0.36	10.5	63	5.1	86
18.00	0.33	10.5	64	4.5	83
18.30	0.34	9.5	68	3.6	79
19.00	0.30	9.5	68	3.9	90
19.30	0.29	8.7	71	3.9	79
20.00	0.29	8.8	71	4.5	86
20.30	0.29	8.0	75	4.2	79
21.00	0.29	7.5	78	4.8	79
21.30	0.29	7.5	79	4.2	84
22.00	0.29	7.0	81	4.5	77
22.30	0.30	7.0	83	4.5	85
23.00	0.30	6.8	83	4.5	85
23.30	0.30	6.3	86	3.9	79
24.00	0.30	6.5	85	4.2	86

Table 1.

PB82-228073

MATHEMATICAL MODELLING OF HYDROTHERMAL RECIRCULATION FOR PASIR GUDANG POWER STATION, MALAYSIA
(Thermal Discharge II)

V.S. Thakar, B.M. Patil and K.G.K.Murthy
Central Water & Power Research Station,
Pune, India

ABSTRACT

A thermal power station, with an initial installed capacity of 240 MW, has been proposed to be set up at Pasir Gudang in Malaysia. Cooling water would be drawn from the Johore Strait, into which it would be let back after undergoing a temperature rise of about 10°C. The Strait is a navigable tidal estuary, with a fairly irregular geometry.

A study of the hydrothermal recirculation in the estuary is important in relation not only to the proposed power station at Pasir Gudang, but also to two other thermal power stations which already exist along the Strait. The present study employs mathematical models based on the vertically averaged two-dimensional equations of hydrodynamics and heat dissipation. The principal objectives are the study of the hydrodynamic circulation patterns, and estimation of the far-field temperature distributions and recirculation of heat.

1. INTRODUCTION

A thermal power station has been proposed to be set up at Pasir Gudang, on the northern shore of Johore Strait dividing Malaysia and the Singapore island (Fig.1). In the first stage of construction the installed capacity would be 240 MW, proposed to be raised in the next two stages to 540 MW and 840 MW respectively. Cooling water needed for the power station would be drawn from the Johore Strait. After undergoing a temperature rise of about 10°C in cooling the condensers, the water would be let back into the Strait. The cooling water requirements would rise from 40,800 m^3/hr, in the first stage, to 91,800 and 1,42,800 m^3/hr respectively in the second and third stages of construction.

The present mathematical model study aims at obtaining information on the hydrodynamic circulation in the Strait, and deriving estimates of the likely recirculation of heated water discharges from the power house.

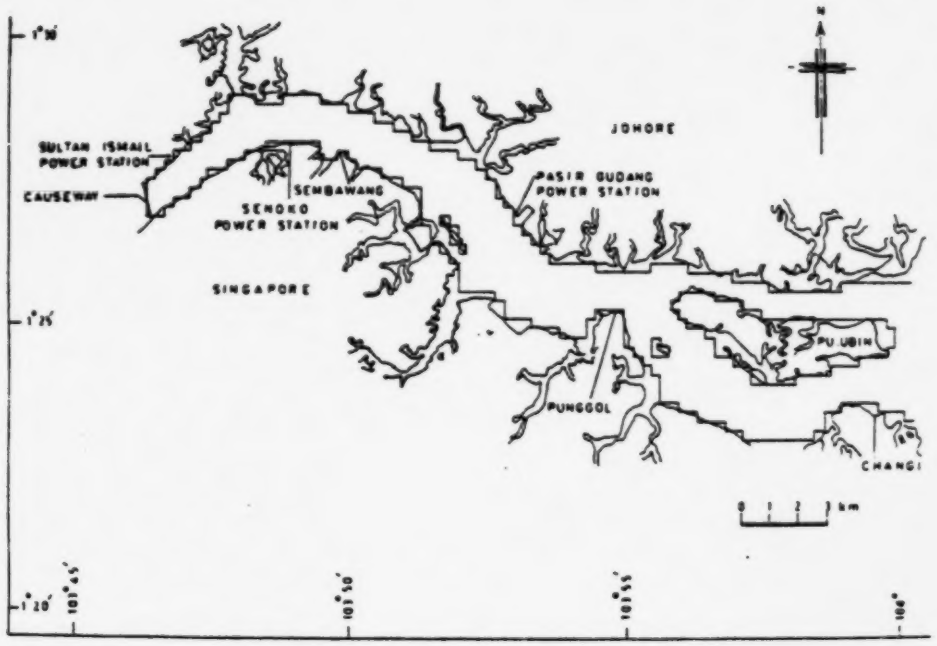

FIG. 1. JOHORE STRAIT, WITH MODEL BOUNDARIES

2. PROBLEM REGION

The Johore Strait is a navigable tidal estuary, with its width varying from 1 to 2.75 km. The depths along the deepest channel vary from 10 to 20 m. A causeway across the estuary forms a solid barrier to the flow. The Pasir Gudang power station is to be situated about 14 km east of the causeway. There are two other power stations along the Strait, the Sultan Ismail and Senoko. Both utilise the waterway for the intake and discharge of cooling water.

There are three tidal gauge stations in the region of interest, at Sembawang, Punggol and Changi respectively. The tides are semidiurnal, the range varying from 0.2 m to 3.4 m. The magnitude of the currents varies from 0.1 to 0.3 m/s. The maximum wave heights in the region are of the order of 1.5 m.

The intake system of the Pasir Gudang power station is proposed to consist of an open channel connecting the forebay and pumphouse to the Strait, fitted with a skimmer wall. The outfall system would consist of a seal well protected by a rubble mound, the structure being so designed as to provide a free fall into the Strait at all stages of the tide.

3. MODELLING TECHNIQUES

The hydrothermal problem in regions very close to the intake and outfall structures would be essentially three-dimensional in nature. As one moves away from these structures, the problem may be considered to be two-dimensional in the horizontal plane, on the assumption of vertically well-mixed conditions.

Close to the outfall, in the 'near field' region, entrainment of the hot water jet with the ambient fluid is the most important phenomenon. In the 'far field', convection, dispersion and surface cooling are the significant characteristics to be considered. Physical and mathematical modelling both have their respective limitations in the study of these phenomena. In the far field, mathematical modelling techniques have been fairly developed, and enable information to be obtained on the hydrothermal circulation. Wind stress, Coriolis force and surface heat loss can be simulated on the mathematical model; representation of these phenomena on the physical model may prove to be difficult.

The hydrodynamic mathematical model, based on the dynamic and continuity equations, yields time histories of water levels and currents in the flow region. The thermal mathematical model, describing convection and dispersion of heat, utilises as input the time histories of flow derived from the hydrodynamic model.

4. PRESENT MODEL

The present study is based on a finite difference solution of a system of two-dimensional, vertically integrated equations.

The governing hydrodynamic and heat transport equations are stated below. In these equations, the x-y plane is taken in the horizontal undisturbed water surface, the x- and y- axes are directed towards the local East and North respectively, the z-axis is directed vertically upwards, and the bottom stress is introduced through Chezy's formula.

Dynamic equations:

$$\frac{\partial u}{\partial t} + u\frac{\partial u}{\partial x} + v\frac{\partial u}{\partial y} - fv + g\frac{\partial \zeta}{\partial x} + \frac{g u (u^2+v^2)^{\frac{1}{2}}}{C^2(h+\zeta)} = 0$$

$$\frac{\partial v}{\partial t} + u\frac{\partial v}{\partial x} + v\frac{\partial v}{\partial y} + fu + g\frac{\partial \zeta}{\partial y} + \frac{g v (u^2+v^2)^{\frac{1}{2}}}{C^2(h+\zeta)} = 0$$

Continuity equation:

$$\frac{\partial \zeta}{\partial t} + \frac{\partial}{\partial x}[(h+\zeta)u] + \frac{\partial}{\partial y}[(h+\zeta)v] = 0$$

Heat transport equation:

$$\frac{\partial}{\partial t}[(h+\zeta)\Delta T] + \frac{\partial}{\partial x}[u(h+\zeta)\Delta T] + \frac{\partial}{\partial y}[v(h+\zeta)\Delta T]$$

$$-\frac{\partial}{\partial x}[(h+\zeta)k_x\frac{\partial \Delta T}{\partial x}] - \frac{\partial}{\partial y}[(h+\zeta)k_y\frac{\partial \Delta T}{\partial y}] + \frac{K\Delta T}{\rho C_p} - \frac{W}{\rho C_p} = 0$$

Here u,v: vertically averaged velocity components in x- and y-directions respectively
f: Coriolis parameter
h: water depth below reference plane
ζ: elevation of water surface above reference plane
g: acceleration due to gravity
C: Chezy's coefficient
t: time
ΔT: temperature rise above ambient
k_x, k_y: diffusivities along x- and y-directions respectively
K: heat transfer coefficient
ρ: density of water
Cp: specific heat of water
W: heat source or sink, per unit area per unit time.

Several finite difference schemes have been proposed and used for the solution of these equations. The hydrodynamic model in the present study follows the 'multi-operation' technique developed by Leendertse (ref.1). The method employs a space-staggered scheme. The solution proceeds through two steps at each time level. In the first step, the ζ, u and v fields at time $(n+\frac{1}{2})$ are dervied from the fields at time (n) by an operation which is 'implicit' in ζ and u, and explicit in v. The fields at time (n+1) are then obtained from those at time $(n+\frac{1}{2})$ by an operation which is 'implicit' in ζ and v, and 'explicit' in u. The scheme has been found to be unconditionally stable in most situations, which is its main advantage over other fully explicit schemes which place stringent restrictions on the time step for purposes of stability.

The basic computer code of ref.1 has been modified for the present study. The basic code needs computations to be performed in a rectangular space, in which the area of interest may be situated. In the case of very irregularly shaped water bodies, such as the estuary under consideration, it may be seen from fig.1 that the area of the land portion included in the rectangular area may be much larger than that covered by water. This may lead to a wastage of computer memory, time and cost. A technique has been added to the basic method and code so that the main computations could be performed only over the water area. This requires some book-keeping on the computer. The boundary of the water area is shown by the zig-zag line in fig.1. The water area contains about 710 grids, whereas the full rectangular area contains about 3,300 grids; which gives an indication of the savings effected by the program modification.

The heat transport model in the present study has been based on a method described by Tsai and Chang (ref.2), which employs an alternating direction implicit technique.

The intake and outfall structures of the Pasir Gudang power station are proposed to be located at 400 m from each other. The width of the estuary in this region is of the order of 3 km. In order to obtain a fine enough representation of the hydrodynamics in the region of the power station, it may be necessary to construct a model with a mesh size of, say, 100m. It would be prohibitively expensive of computer memory and cost to construct a model from the causeway to Changi with such a mesh size. An alternative, though not a very desirable, procedure could be to construct a model with a coarser grid, and derive boundary conditions for an inner model with a finer grid. However, the best procedure would be to operate the coarse model and the inner fine model(s) simultaneously.

The present model has been constructed with a grid size of 304.8 m. The estuary bed has been schematised by averaging over each grid. The intake and outfall are taken to be situated three grids apart. This would obviously affect the representation of hydrothermal circulation in the region very close to the intake and outfall. However, it may be expected that this 'schematisation' of the intake-outfall region will not appreciably affect the hydrothermal behaviour of the model in regions located away from the intake and outfall. It may also be expected that the representation of long-term distributions of heat in the estuary may not be affected much too adversely by this schematisation. The veracity of these statements can perhaps be judged only after the present results are compared with those dervied from a fine enough representation of the intake-outfall region, which is proposed to be done during the next phase of the study.

In the hydrodynamic model, with a grid size of 304.8 m and maximum depth of 21.3 m, the half time step has been chosen to be 120 sec. It may be noted that the maximum value 21.3 m of the water depth obtains only in a small area near Changi, typical depths in the model being much smaller, of the order of 10 to 12 m. The heat transport model employs a half time step of 360 sec. and utilises the information derived at the corresponding time levels during the operation of the hydrodynamic model.

5. HYDRODYNAMIC MODEL

It is possible to operate the hydrodynamic mathematical model under any desired variation of the water level at the open boundary, over any desired length of real time. This enables calibration of the mathematical model against the actual observed data. Averaged data corresponding to a representative tidal cycle, may also be used.

For the calibration, data available for the tidal level variation at Changi, corresponding to the period 24-26 Dec.1972, has been used to derive the condition for the open boundary near Changi (Fig.2(A)). Several tidal cycles, with varying ranges and other irregularities, have been covered.

An important aspect of the computer techniques, in studies such as the present one, is the necessity to store intermediate results, analyse them and restart the model with any modifications that may be called for. In the present calibration study, a set of C values ranging from 22 to 33 $m^{\frac{1}{2}}/s$ over the estuary yielded tidal elevation curves at Sembawang and Punggol showing good agreement with observed data. These are the only two places in the model region, where tidal elevation data is available.

Fig.2(B) shows the results of the calibration study, relating to the tidal level at Punggol. The mathematical model generates values of the tidal level every 4 minutes of real time. However, the output has been restricted to a printout of values after each one hour of real time. The observed data is also available at one hour intervals. The correspondence between the mathematical model results and observational data appears to be fairly close.

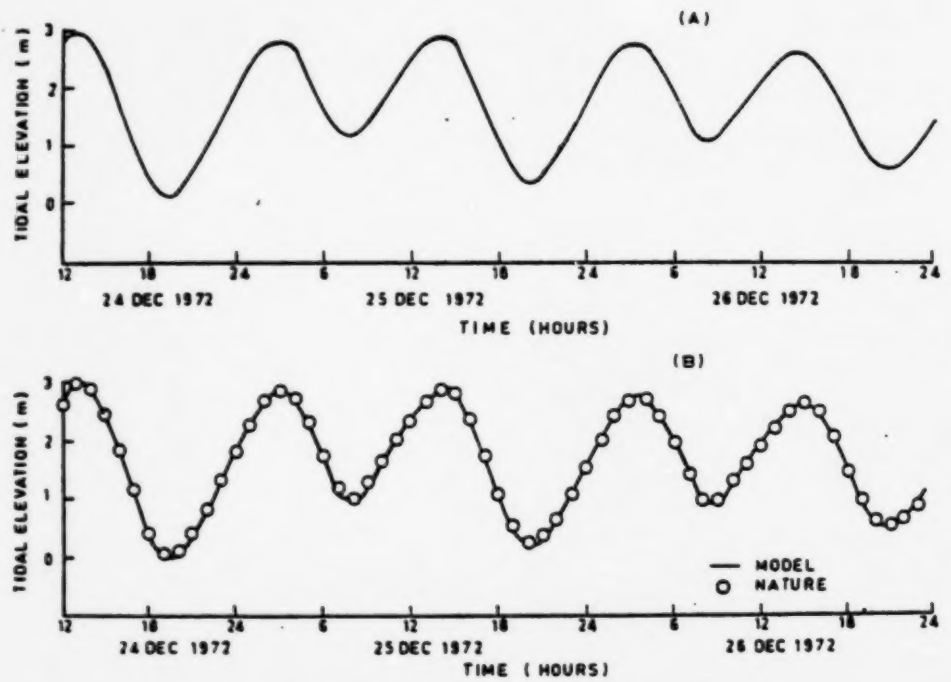

FIG. 2. BOUNDARY CONDITION AND CALIBRATION

Current data corresponding to the tides under consideration have not been available. However, field observations at a few places corresponding to tides with similar ranges compare well, qualitatively, with the model velocities.

Fig.3 shows the velocity field in the model, as a representative output, at about the time when the maximum flood velocity occurs.

6. HEAT TRANSPORT MODEL

The thermal model needs values, at each grid point, of depth, water level and velocity components in the x- and y-directions, at the desired time steps over a tidal cycle. These are derived from the hydrodynamic model and stored on tape. In addition to these data, the thermal model employs values of diffusion and heat transfer coefficients, and needs data on heat input and withdrawl. With this information the model yields, under appropriate boundary conditions, the temperature rise over ambient at each grid over a tidal cycle. It is assumed that there is little change in the temperature at the open boundary at Changi. This assumption has been partly verified by the fact that extending the model by 4 km beyond Changi has practically no effect on the behaviour of temperatures near Changi.

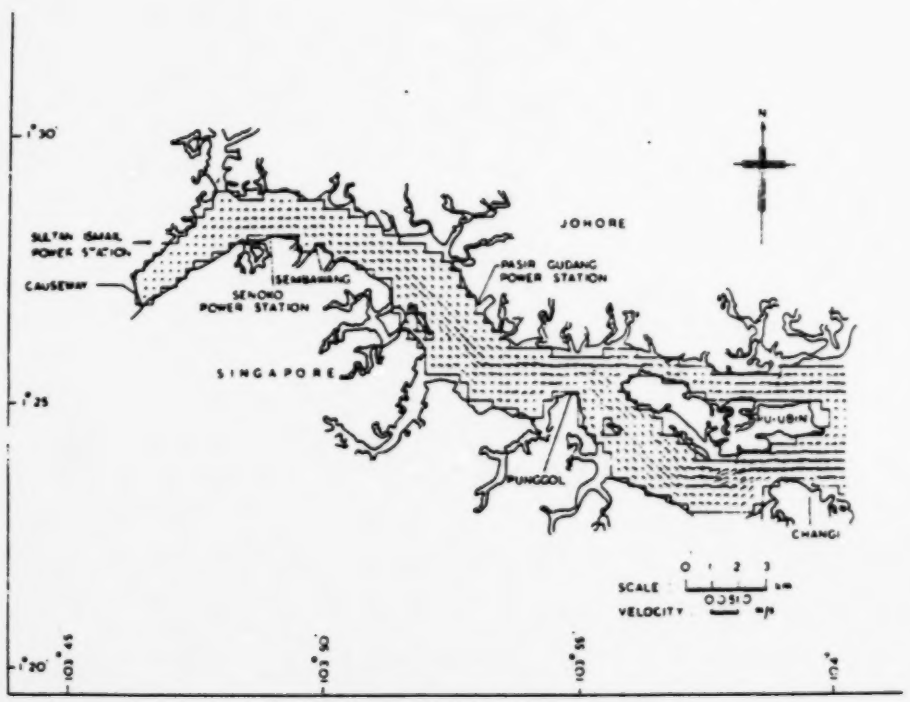

FIG. 3. VELOCITY FIELD

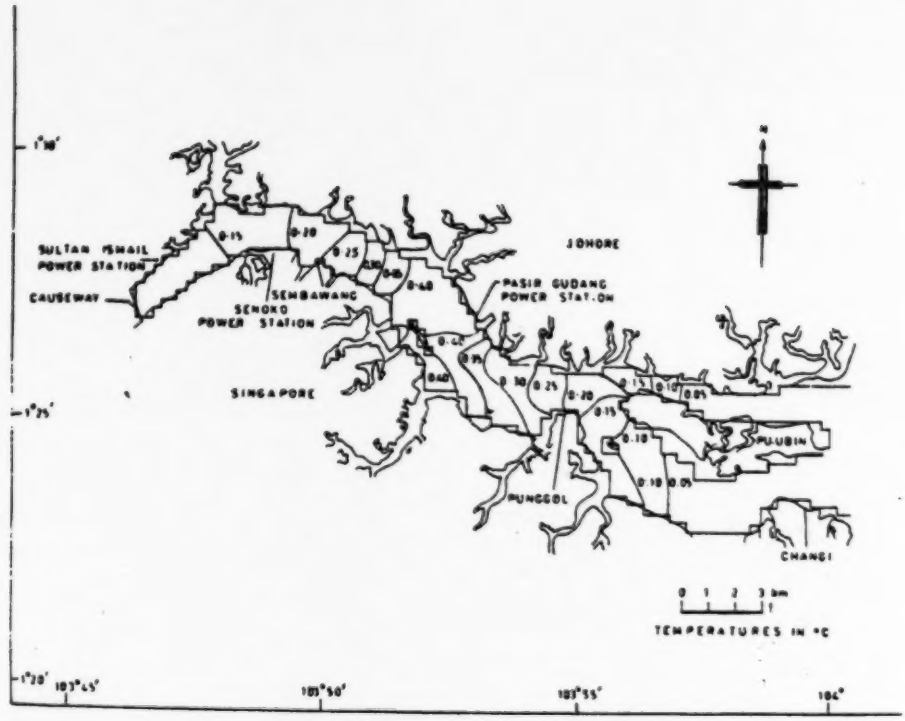

FIG. 4. ISOTHERMS AT HIGH TIDE

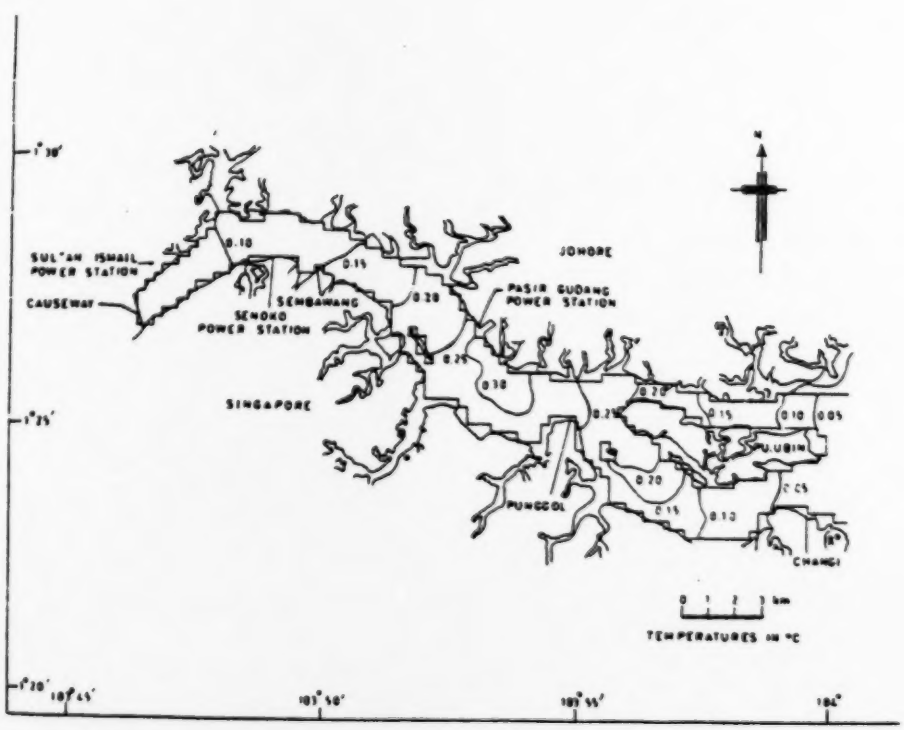

FIG. 5. ISOTHERMS AT LOW TIDE

In order to reach a quasi-steady state temperature distribution over a tidal cycle, it is necessary to run the model for several successive tidal cycles. This has been done by deriving hydrodynamic boundary conditions from tidal averaged data.

Experiments have been carried out with different sets of values of the diffusion and heat transfer coefficients, under the proposed first stage conditions. Typical results, corresponding to $k_x = k_y = 37.16\ m^2/sec$, and $K = 8.48\ Cal/°C.m^2.sec$, are shown in figs. 4 and 5. The figures show the isotherms in the estuary waters at around the time of high tide and low tide respectively. The results indicate the extent to which heated waters are pushed by tide towards the causeway, and the extent towards the other end to which the heat may travel. Figs. 4 and 5 also give an indication of the maximum range over which the temperatures at any place in the estuary may be expected to vary. However, the variation over a tidal cycle of the temperature, tidal level and velocity in the region near the intake in the model is shown in further detail in fig.6.

It appears from these figures that, for the first stage of construction of the Pasir Gudang power house as studied, the temperature near the intake in the model may rise by a maximum of 0.42°C. Near the Senoko and Sultan Ismail power stations, however, the rise of temperature may be expected to be less than 0.20°C.

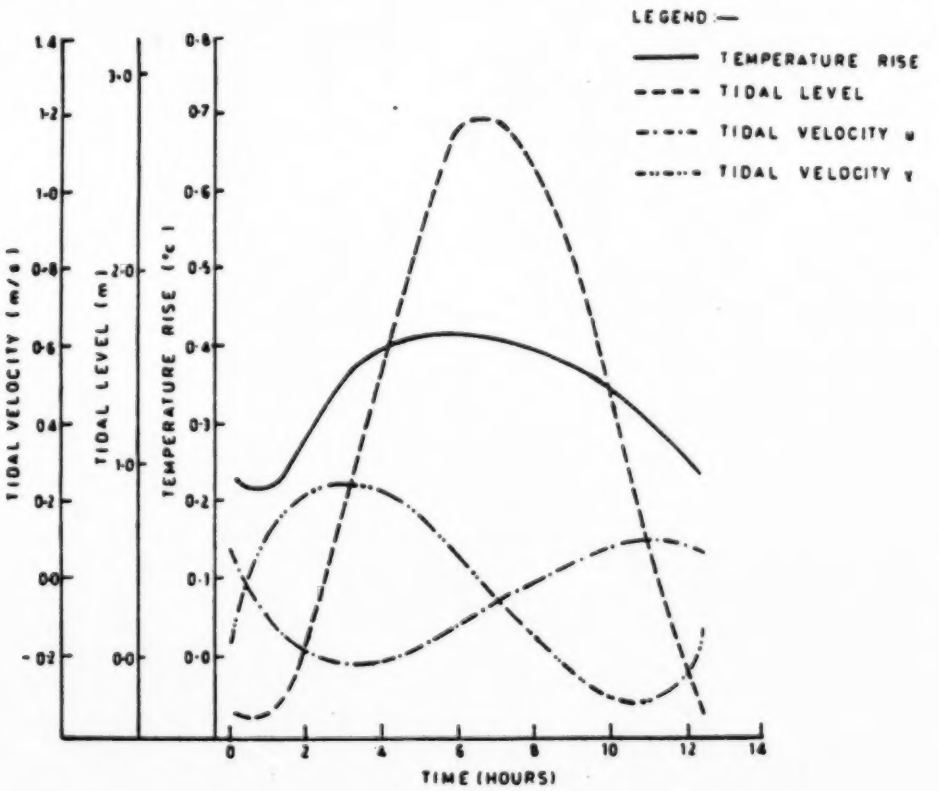

FIG. 6. VARIATION OF TEMPERATURE, TIDAL LEVEL AND VELOCITY NEAR INTAKE

7. CONCLUSIONS

A two-dimensional mathematical model has been constructed for the study of hydrothermal recirculation in Johore Strait. The model has been used to derive the likely extent to which temperatures in the estuary may rise due to the operation of the proposed power station at Pasir Gudang, in the first stage of its construction. The model consists of two parts: hydrodynamic, and thermal. The hydrodynamic model has been calibrated against data from nature, covering successive tidal cycles of varying ranges. Tidal averaged data has also been used. The results have been used as inputs to the thermal model.

The study has yielded information on the pattern of hydrothermal recirculation in the estuary, and the extent to which temperatures are likely to rise at various locations owing to the operation of the first stage of construction of the Pasir Gudang power station. Although the representation of the intake and outfall in the model is rather schematic, the results are expected to indicate heat distributions over extended periods of time. Further studies are proposed with a refinement of the model grid in the intake-outfall region. Temperatures in the estuary would further rise with the larger discharges of heated waters in the second and third stages of construction of the Pasir Gudang power station; studies for which have also been proposed.

REFERENCES

1. Leendertse,J.J., Aspects of a computational model for long period water wave propagation, RM-5294-PR, Rand Corporation, Santa Monica, California, May 1967.

2. Tsai, Y.J. and Chang, Y.C., Two-dimensional transient hydrothermal mathematical model, Proc. of the First World Congress on Water Resources, vol.IV, pp. 76-88, Chicago, Illinois, U.S.A., 1973.

SESSION IV-B

COOLING TOWERS

Preceding page blank

PB82-228081

AERODYNAMIC LOSSES OF HIGHLY FLARED NATURAL DRAFT COOLING TOWERS

F. K. Moore and M. A. Garde
School of Mechanical and
Aerospace Engineering
Cornell University
Ithaca, N.Y. U.S.A.

ABSTRACT

A study is made of the potential improvements of natural-draft tower performance to be gained by use of shell shapes which are highly flared at entrance. Draft height requirement is strongly reduced by flare. Heat-exchange surface requirement may be made independent of flare for dry towers by suitable choice of surface. Conventional wet fill requirement would increase with flare. Entrance loss has been studied experimentally, giving new estimates applicable to large flare. Results indicate that entrance heights may be reduced with flare, further reducing overall tower height. Flared tower design should provide a densimetric Froude number of about 0.6, to prevent cold inflow.

1. INTRODUCTION

Natural-draft cooling towers are, conventionally, concrete shells of a rather standard configuration dictated largely by structural considerations. A typical ratio of shell height to exit diameter is 2, and a typical degree of flare would show a ratio of base to exit diameters of 1.6. The average slope of the tower profile, expressed as the ratio of diameter difference to shell height,

$$f \equiv \frac{D - D_e}{H} \tag{1}$$

would have the rather small value of 0.3. Hereafter, we shall use the quantity f to describe degree of "flare" of a cooling tower shell. That and other symbols are defined in the Appendix.

It would seem possible, and even likely, that a higher than conventional degree of flare would provide improved performance in some circumstances, because the bulk velocity at the tower base could be reduced thereby, and the flow resistance offered by the heat-exchange elements located near the tower base would be reduced. Thus, the tower could potentially be lower in height. Cost and siting advantages might then follow. This paper describes results of a study of the performance benfits of high flare, supported chiefly by Owens-Corning Fiberglas and also by NSF (Heat Transfer Program).

In order to exploit any potential advantage of high flare, one must first have in mind a mode of construction that, unlike concrete, would permit extreme flare. Owens-Corning became interested in this topic because of the

IV-B-213

design flexibility offered by a fabric-structure approach. They have pioneered in the field of large fabric structures, such as the Haj Terminal at the Jeddah International Airport in Saudi Arabia, and the Pontiac Silverdome, DakotaDome, and UNI-Dome in the U.S. Owens-Corning is interested in applying large fabric structure principles to the design of natural-draft cooling towers of optimized aerodynamic performance, having in mind the potential for siting flexibility, and the increasing cost and construction time for the usual concrete shells. The ability to deal with highly flared shapes is just one of the potential advantages of fabric tower construction, of course.

To form a basis for evaluating high flare, three key performance issues are considered in this paper. namely

Heat-exchanger performance. Heat exchanger resistance and heat transfer rate are both affected by widening the tower base. In principle, both are reduced, and the relative degrees of reduction, in the context of a cooling-tower design, would indicate the basic merit of flare. It is shown that the Stanton vs Reynolds number relationship is crucial in this regard, and that a favorable result would be easily achievable for dry towers, and could possibly be achieved for wet.

Entrance loss. A highly-flared shape, with a very large base diameter, might be thought to require a high entrance opening, in order to control entrance loss. If so, any advantages of flare might be negated by high construction or pumping costs. Lowe and Christie [1] and Rish [2] have provided the methods now in general use for estimating entrance loss. Rish's method is more conservative, and is used for comparison in the present paper. Those methods, which are empirical, do not deal with unconventional degrees of flare.

This paper describes experiments conducted by Garde [3] to measure entrance loss of three tower shapes of increasing flare and various degrees of heat-exchanger resistance, but no wind. Entrance guide rings and annular fill distribution were also studied. Results show an entrance-height requirement which is substantially less than Rish's method would give, and calculations show that the overall tower height required is in fact a decreasing function of flare, for a given heat-exchanger resistance coefficient.

Exit loss. It is necessary to specify an exit condition in order to fix the geometry of a natural-draft cooling tower, because a low, wide tower may be thought to have the same performance as a tall, narrow tower (see Moore [4]). If the tower is highly flared, it is perhaps not obvious what exit proportion is appropriate. It is argued that "cold inflow' is the determining concern, and recent studies of this phenomenon by Mr. A. Dayal and Mr. V. Modi, graduate students at Cornell, give confidence that the proper exit condition is a specification of exit densimetric Froude number.

Finally, the simple design rules which result from the forgoing studies are summarized, and conclusions are drawn as to the future potential for highly-flared natural-draft cooling towers for charge power plants.

2. HEAT EXCHANGER PERFORMANCE

The heat exchangers of a natural-draft tower may be evaporative (wet) or dry, and these two basic types must be considered separately. Throughout this paper, we will assume counterflow heat exchangers, generally covering the disc formed by the base of the tower shell. (Tower notation is shown on Fig. 1).

2.1 Wet heat exchange

Following Rish [2], the heat-transfer coefficient for wet packing in the form of vertical plates which provide film-type heat transfer may be expressed as

$$K_e = G\left[\frac{2}{f_1} + 71.6\left(\frac{L}{G}\right)^{-1/4}\right]^{-1} \qquad (2)$$

where L and G are water and air mass flows per unit plan area of the fill. f_1 is a loss factor depending on L/G. For a given duty, the ratio L/G is fixed because the air-water proportion for the tower as a whole is fixed. K_e is an evaporation coefficient, equivalent to a heat-transfer coefficient $(\bar{h})$ when multiplied by heat of vaporization.

G, of course, is proportional to a free-flow velocity (V_c) of air upward through the heat exchanger. Thus, equation (2) in effect states that

$$\bar{h} \sim V_c \qquad (3)$$

for plate fill, with film heat transfer. Clearly, if a tower is widely flared, so that plan area of the shell, which is also the frontal area (A_f) of the heat-exchange array, is increased, V_c must decrease in proportion. Equation (3) says that $\bar{h}$ also decreases in the same proportion. Now, for a given duty, if the heat-transfer coefficient $\bar{h}$ decreases, the total wetted fill area (A_a) of all the plates must correspondingly increase. Thus,

$$A_a \sim (\bar{h})^{-1} \sim A_f \qquad (4)$$

and one sees that the cost of fill will simply increase in proportion to flare, even though flare would decrease the required shell height because flow resistance of the fill would drop.

In a conventional plate-fill wet tower, flare would certainly increase fill cost, but might decrease shell cost, to the degree that height is more important than base diameter. The optimum degree of flare would depend, obviously, on relative costs; expensive fill would work against flare.

2.2 Dry heat exchange

Next we consider the situation for dry towers (sensible heat transfer with finned tubes or plate-fin surfaces). Kays and London [5] present St_a and f_a vs Re relationships for a variety of such heat exchangers: over a given Re range of interest, one may infer a power law for the air side in the form

$$St_a \sim (Re)^{n-1} \quad ; \quad f_a \sim St \qquad (5)$$

where n depends on the surface and Re range. Usually one may take friction factor and Stanton numbers to be proportional. In place of equation (5) one may use the usual definitions of St and Re to write

$$\bar{h} \sim V_c^n / r_{h_a}^{1-n} \qquad (6)$$

where r_{h_a} is "air-side hydraulic radius", a measure of the transverse scale of the air passages.

Equation (3) corresponds to the special case n = 1. Actually, n ranges between 0 and 1. For finned tubes (Fig. 10-75 of [5]), about 0.8 would be an appropriate value. For many plate-fin surfaces, on the other hand, n is virtually 0 (Fig. 10-56 of [5]).

If n = 0, then

$$\bar{h} \sim (r_{h_a})^{-1} \tag{7}$$

and $\bar{h}$ is independent of V_c, and hence of flare. In that case, A_a would also be independent of flare, and heat exchanger cost would be unaffected, leaving only the draft-height advantage to consider.

For purposes of illustration, dry tower shell and heat exchanger sizes were calculated for a given duty, as follows:

Heat: $3.85 \cdot 10^9$ Btu/hr: water: 291,000 gpm
Water temperature °F: 138 (in), 125 (out)
Air temperatures °F: 89 (in), 112 (out)

Heat exchangers of the two extreme types (n = 0 and 1) were assumed, and the analysis of [4] was used. In that notation, St_a Re = 12 was chosen for n = 0 and St_a = 0.021 for n = 1. For both cases, f_a/St_a = 2.7, E = 1, and F = 1 were assumed. The frontal area A_f was taken to be 1.75 times free-flow area A_c. The tower exit Froude number

$$F_d = \frac{V_e}{\sqrt{\frac{\Delta\rho}{\rho} g D_e}} \tag{8}$$

was chosen to be 0.55 in order to control cold inflow (see Section 4 to follow). The head loss, exclusive of heat-exchanger loss, was taken as 3 times exit loss (see Section 3 to follow). The following simple formulas result from the analysis:

Draft (shell) height: $H = (1.23\ 10^6/A_f)^2 + 174$ (ft) (9)

Heat exchange area

n=0: $A_a = 6.62 \cdot 10^{10}\ r_{h_a}$ (ft^2)

n=1: $A_a = 58.2\ A_f$ (10)

Heat exchanger depth

n=0: $11.6 \cdot 10^{10}\ r_{h_a}^2/A_f$ (ft)

n=1: $425\ r_{h_a}$ (11)

In these formulas, one may choose A_f and r_{h_a}, which will yield relations between flare and heat exchange area. Results are shown in Fig. 2. If equation (3) applies (n=1, corresponding to plate-fill wet towers), A_a increases as flare increases, independent of heat-exchanger fineness (r_{h_a}). If, on the other hand, equation (7) applies (n =0, a plate-fin surface), then A_a depends only on fineness (r_{h_a}), and not on flare. In the latter case, flare seems purely beneficial, and also opens the possibility of an additional benefit from "fineness".

Heretofore, the slope of the St_a vs Re line has not been considered important, but it seems clear that n=0 is reasonably available as a design

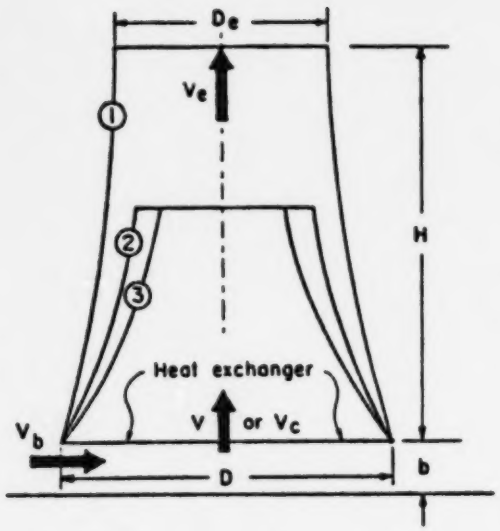

TOWER	1	2	3
D (in)	8.0	8.0	8.0
D_e (in)	5.2	4.48	8.12
H (in)	10.0	6.0	6.0
$f = \frac{D - D_e}{H}$	0.28	0.59	0.81

Fig. 1 Model Tower dimensions and notation.

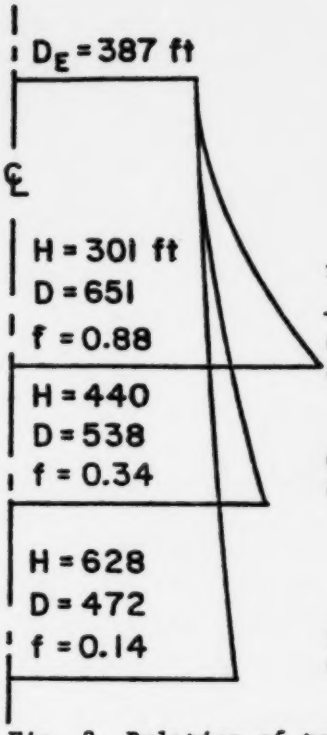

r_{h_a} (ft)	A_a (10^6 ft^2) n=1	n=0
0.001	19.4	6.6
0.002	19.4	13.3
0.001	13.3	6.6
0.002	13.3	13.3
0.001	10.2	6.6
0.002	10.2	13.3

Fig. 2 Relation of tower flare to heat-exchange area, for dry towers of two different types of heat-transfer laws; n=1 ($\overline{h} \sim V_c$) and n=0 ($\overline{h} \sim 1/r_{h_a}$).

option for dry towers. For wet towers, the case is more doubtful. Probably, a fill which produces fine droplets in a controlled way, and avoids the consequences of the re-agglomeration which usually occurs after a foot or so of fall, would tend to show small values of n, and therefore be interesting in combination with flare.

Even if flare is advantageous in terms of shell height as shown in Fig. 2 the overall height includes entrance height; the relation of entrance height requirement to base diameter is the subject of the next section.

3. ENTRANCE LOSS

The total resistance to airflow through a natural-draft tower depends on the heat exchanger, and on the entrance and the exit velocity, but entrance loss is more complex; degree of flare, entrance height and heat-exchanger resistance all presumably affect entrance loss. In the experimental study to be described (conducted by Mr. M. S. Garde as his MS Thesis [3]), three tower shapes (Fig. 1) were studied ranging in flare from f = 0.28 (Tower 1) to 0.81 (Tower 3).

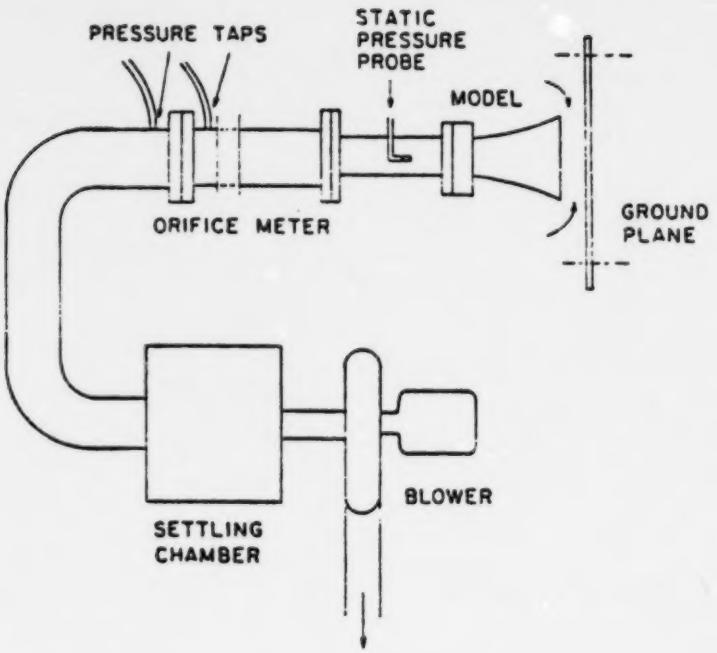

Fig. 3 Sketch of experimental setup

3.1 Description of experiment

The scheme of the experiment is shown in Fig. 3. The models, constructed of fiberglass by Owens-Corning, were connected to an ASME standard orifice meter. The ground plane was moved in and out to change entrance height (b). Static pressure at the tower "exit" compared with room pressure, when related to measured mass flow, yielded the entrance loss. In dimensionless form referred to entrance head $^1/_2\rho V^2$, the entrance-loss coefficient is

$$R_{ent} = R_{tot} - K - (D_e/D)^4 \qquad (12)$$

where R_{tot} is the measured pressure-drop coefficient, K is the (known) heat exchanger resistance, and the last term represents the loss of exit dynamic head. This experiment dealt only with entrance loss. Actual exit phenomena were not modeled, nor were wind effects considered. However, it was verified by total-head probe traverse that the "exit" velocity profile was uniform to within 0.05 in. of the wall.

The heat exchanger resistance was provided by sheets of stainless steel screening, of 60 mss epoxied across the mouth of the tower. One such screen had 0.011 in. dia. wire, and provided a resistance of K = 14.5 entrance heads (typical of dry towers) and one with 0.0075 in. dia wire gave K = 5.5. By overlaying these screens various values of K could be achieved.

The models were hyperboloidal in shape, with zero exit flare, and each had 8 in. dia. entrances to simplify comparisons between cases. The flow

velocity V at entrance was about 23 ft/sec. providing a Re per inch of 12000. The ground plane consisted of a 4 ft X 4 ft plywood sheet mounted on a movable stand. Pressures were measured with differential water manometers. Errors in the various measurements were estimated to be about 5%.

3.2 Results

Fig. 4 shows typical results for a range of entrance heights and a screen resistance K = 14.5. Usually, D/b ranges from 11 to 15 in large natural-draft wet tower designs. D/b may be as small as 5 for dry designs. Fig. 5 shows that changing K to 29 had only a slight effect on dimensionless entrance loss.

Also shown on Figs. 4 and 5 are the predictions of Lowe and Christie [1] and Rish [2]. Rish suggested that the formula, taken from [1],

$$R_{ent} = 0.167\ (D/b)^2 \tag{13}$$

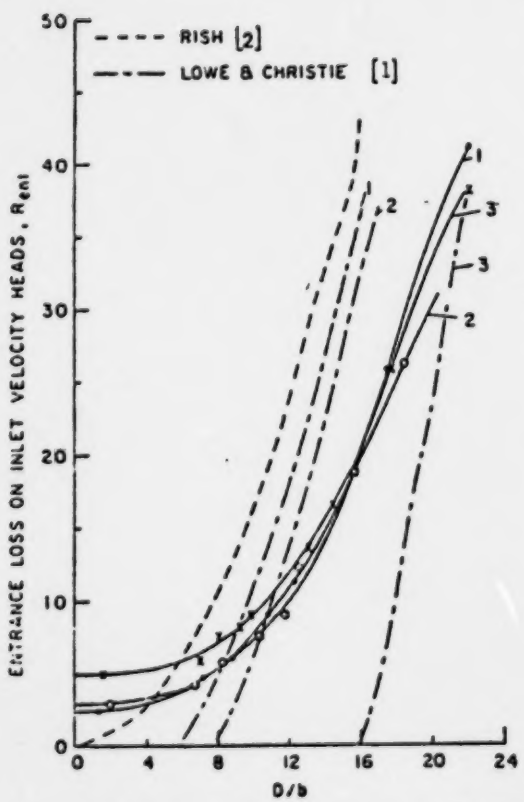

Fig. 4 Effect of tower shape on entrance loss for screen resistance = 14.5; numerals refer to models described in Fig. 1.

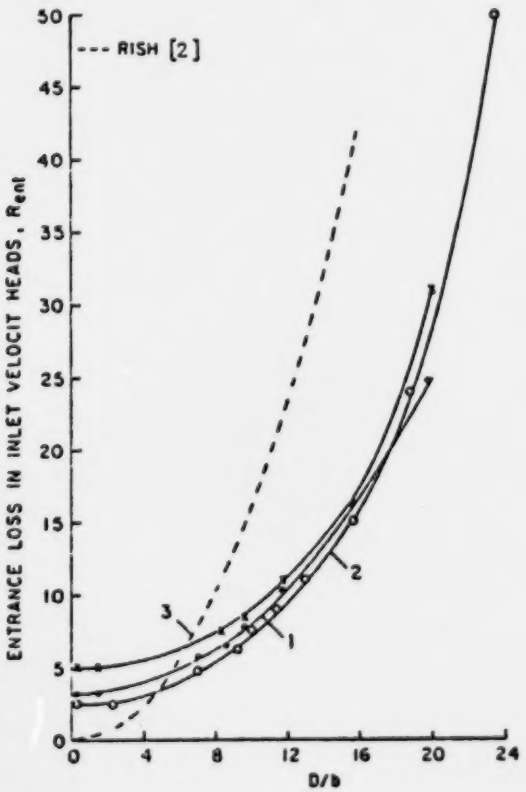

Fig. 5 Effect of tower shape on entrance loss for screen resistance = 29

be used for the entrance loss, although in [1] that equation logically represents $R_{ent} + (D/D_e)^4$. Thus, in Figs. 4 and 5, the lines ascribed to Rish are from equation (13), while those ascribed to Lowe and Christie are from equation (13) less $(D/D_e)^4$. Clearly, the Lowe and Christie theory is quite inappropriate to the present experiments, and so, in fact, is the Rish formula. However, both formulas fortuitously (empirically) cross the data in the range of D/b which is typical of practice. Neither formula predicts the observed effect of flare.

The effect of flare is apparently almost entirely accounted for by expressing R_{ent} in terms of entrance head. In fact, the present results can be well represented by the following formula, for all flares and screen resistances:

$$R_{ent} = 3 + 0.055\ (D/b)^2 \tag{14}$$

While there is no direct theoretical support for equation (14), it is worth noting that the total pressure loss Δp_L through a slot of width equal to the entrance height could be expressed in the form

$$\frac{\Delta p_L}{1/2\rho V_b^2} = C \tag{15}$$

where the loss coefficient C would be of order 1, and V_b would be the radial (bulk) velocity entering under the sill. Now, $V_b = (1/4)(D/b)V$, and therefore

$$\frac{\Delta p_L}{1/2\rho V^2} = (0.067)\ (D/b)^2\ C$$

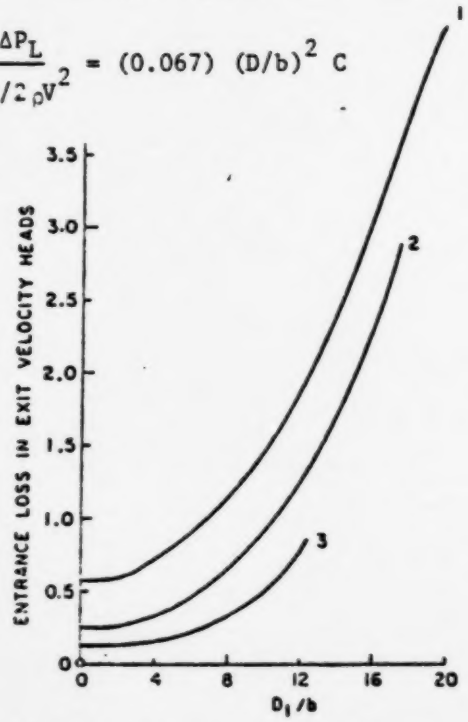

Fig. 6 Effect of tower shape on entrance loss for screen resistance = 29, expressed in exit dynamic heads. In abscissa, D_1 is the diameter of Tower 1.

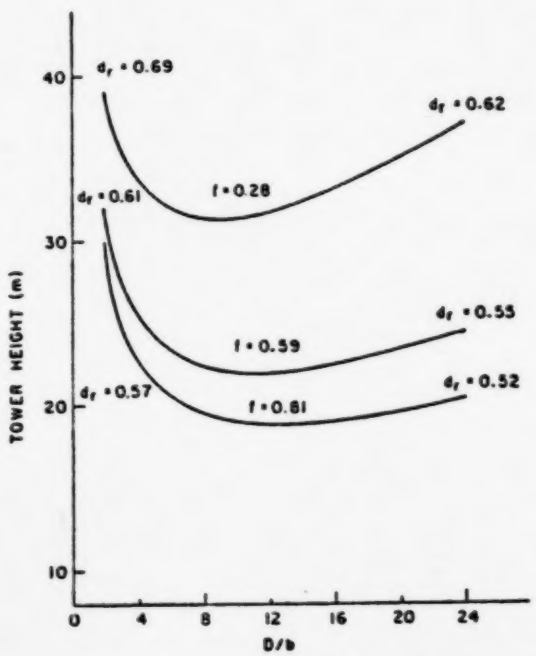

Fig 7 Effect of tower shape on calculated total tower height for constant flare. Three values of flare are assumed.

Thus, in the limit of low height, the measured entrance loss (equation 14) could be considered as that of a slot having a loss coefficient C = 0.8.

If the entrance loss in terms of entrance head is nearly independent of flare, then entrance loss in terms of exit head would decrease strongly with flare. Fig. 6 illustrates this effect. In that figure, the D_1 in the abscissa is that of Tower 1; in effect, the abscissa is 1/b with no effect of flare. Inasmuch as exit head would generally be fixed in design (to limit cold inflow), Fig. 6 shows that for a given allowable entrance loss, increased flare actually permits a substantially lower entrance height.

3.3 Illustrative example

In order to illustrate the effect of flare on tower height more specifically, draft calculations were made in [3] for a cooling tower rejecting 20 MW of heat to ambient air at 86°F, with $\Delta\rho/\rho = 0.1$ and a specific constant choice of heat-exchanger resistance coefficient as K = 28, corresponding to typical wet cooling towers. Exit Froude number F_d was chosen to be 0.71. Entrance loss was evaluated using equation (14), and the three values of flare given in Fig. 1 were used. Results appear in Fig. 7.

For each value of flare*, there is a minimum total (shell plus entrance) height. To the right of the minimum, the entrance itself is wastefully high; to the left of the minimum, the shell is high to compensate for excessive entrance loss. Apparently, high flare permits a lower optimum shell height, and the best D/b shifts to higher values for higher flare. For construction or pumping-power reasons, it may be important to notice that the curve is quite flat for high flare; there is only a slight height penalty for halving the optimum entrance height. These calculations suggest a substantial construction and aesthetic advantage of the flared shapes that might be feasible with novel methods of construction based, perhaps, on fabric technology.

3.4 Entrance-flow modifications

It remains to discuss certain possibilities for entrance loss reduction which were studied as part of this research.

Turbulence generators. Attempts were made to make the entrance velocity profile more uniform by adding vortex generators to the ground plane. 3/8 in. x 1/2 in. strips, 1 in. were erected on the ground plane, in a circle 9 in. in diameter (1/2 in. in front of the tower entrance). The airfoils were set at an incidence of 20°. Tests showed no beneficial influence of these devices.

---

*With flare defined as in the Appendix, the exit to inlet diameter ratio (d_r) is not quite constant when f is constant.

Inlet guide ring. With the thought in mind that the entrance loss might be reduced by providing a smooth nozzle-like entrance, a large toroidal ring was added to Tower 3 as shown in Fig. 8. The ring minor diameter was 2 in., and it was fixed so that its tangent was horizontal at the entrance. Fig 8 also shows that the guide ring indeed had a beneficial effect, but only for low entrance heights. Recalling Fig. 7, one finds that the ring would only slightly shift the optimum value of D/b from about 12 to about 14, but, more significantly, it would flatten the curve, permitting quite low entrance heights with reasonable entrance loss. The merits of entrance rings need further study, to optimize their dimensions aerodynamically.

Central blockage. It seems possible that flare of the shell might be used directly to reduce entrance loss by permitting a given heat-exchanger plan area to be brought nearer the entrance lip, in an annular pattern. Fig 9 shows how this change was accomplished in the present experiment, by blocking off the central part of the screen with a solid disc. In order to isolate the effect of "central blockage", the more flared models 2 and 3 were fitted with discs which left the annular screen area in the same proportion to exit area as was true for the least-flared Model 1 with no blockage. Disc diameters were, therefore, 0, 0.9, and 2.05 in. for models 1, 2, and 3, respectively.

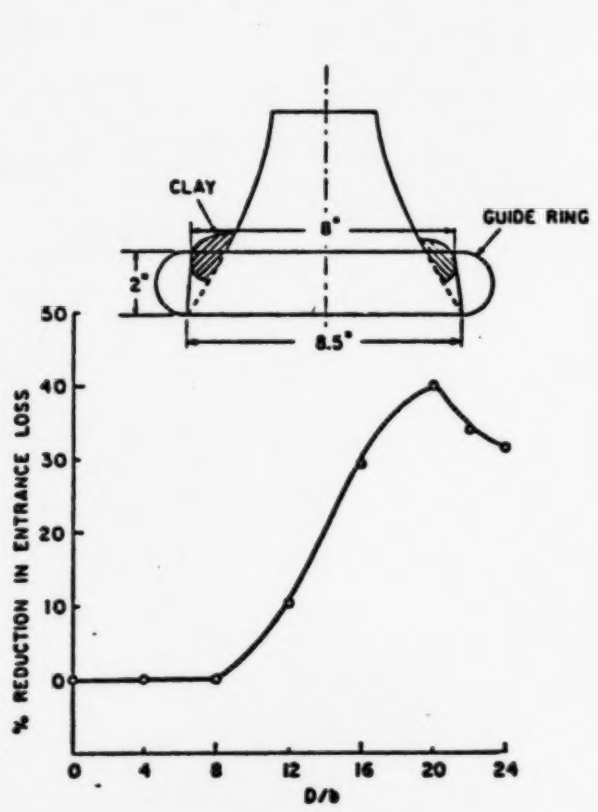

Fig. 8 Percent reduction in entrance loss using an inlet guide ring on Tower No. 3, for screen resistance = 29.

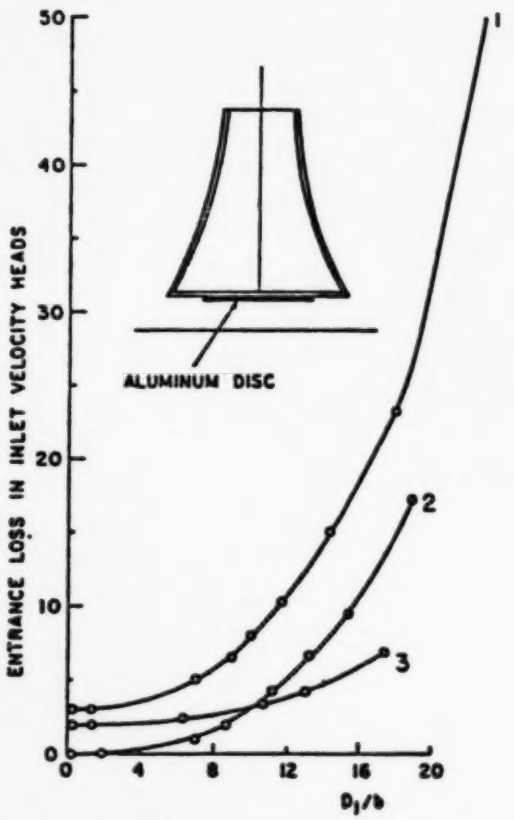

Fig. 9 Effect of central blockage for screen resistance = 29. In abscissa, D_1 is diameter of Tower 1.

By using this scheme, all three models were made exactly equivalent on a one-dimensional flow basis.

Results are shown in Fig. 9, plotted versus reciprocal entrance height (D_1 being the entrance diameter of unblocked Tower 1.) In Fig 9, then, nothing is changed from model to model, except the way the screen opening is shaped. Evidently, flare with corresponding central blockage does reduce entrance loss. The improvement is marked for slight flare and a rather high entrance. High flare is helpful only at very low entrance heights. Of course, any advantage of lowered draft height gained by introducing central blockage would have to be balanced against the implied increase of shell size. Before attempting to optimize this approach, wind effects should be evaluated.

EXIT LOSS

Finally, we consider exit loss. Exit loss is a strong function of wind; however, we do not consider wind in this paper. Rather, we have considered it best to specify an exit Froude number in the range 0.5 - 0.7, in order to secure the draft against "cold inflow". This subject was discussed in the second of these conferences [6], and, here, recent progress will be discussed, tending to support the choice of Froude number mentioned above.

A cooling tower contains a mass of slowly-moving air which is only slightly buoyant compared with ambient air. If it were not for the motion (expressed by densimetric Froude number F_d), cold air would obviously spill into the tower at its upper edge. Such "cold inflow" is apparently always present to some degree, but would seriously diminish draft only if F_d is too low.

In [6] and in subsequent work to appear in a Cornell MS Thesis by A. Dayal, the basic plume theory of Morton, Taylor and Turner [7] was matched to a simple draft equation to see how the plume initially separates from the tower, whether at the lip or down inside; if the latter, a loss of draft is implied. With entrainment considered, it turns out that the governing parameter is εF_d^2, which we shall call Φ:

$$\Phi \equiv \frac{\varepsilon \, V_e^2}{\frac{\Delta\rho}{\rho} g \, D_e} \tag{17}$$

where ε is the turbulent entrainment coefficient, typically about 0.1 in value.

If Φ is greater than 1/8 ($F_d \approx 1.12$), the exit jet is very vigorous, and spreads as it leaves the tower. If Φ is less than 1/8, the plume will initially converge, and therefore might "fall in" the tower. Calculations show that as the tower shape is made lower and wider, the plume may fall in until the gap between its boundary and the tower lip is so narrowed that the assumed entrainment rate at the plume margin cannot be maintained. In dimensionless form, the maximum draft loss is indicated in Fig. 10. The theory suggests that the draft is "secure" if Φ exceeds 0.043, or, if $\varepsilon = 0.1$, F_d exceeds 0.66.

The foregoing rule is given a degree of support by recent hot-wire studies of the physical nature of cold inflow, conducted with NSF support at Cornell by V. Modi, with supervisory assistance of Prof. K. E. Torrance. In those tests,

Reproduced from best available copy.

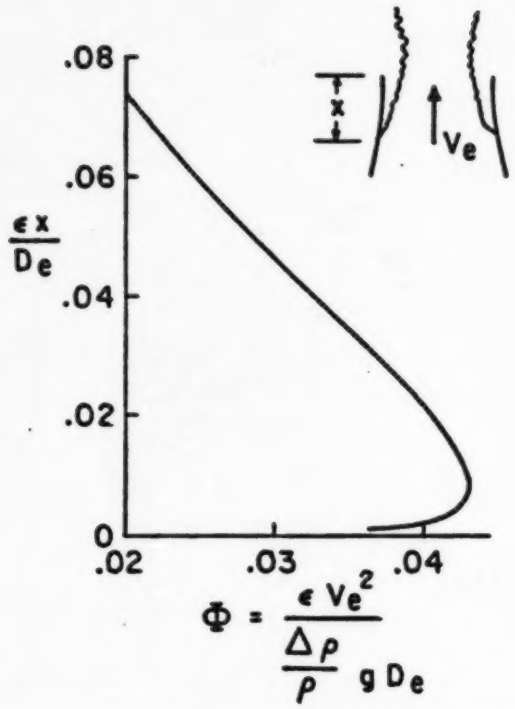

Fig. 10 Maximum depth of plume origin below tower lip. $\Phi = \epsilon F_d^2$.

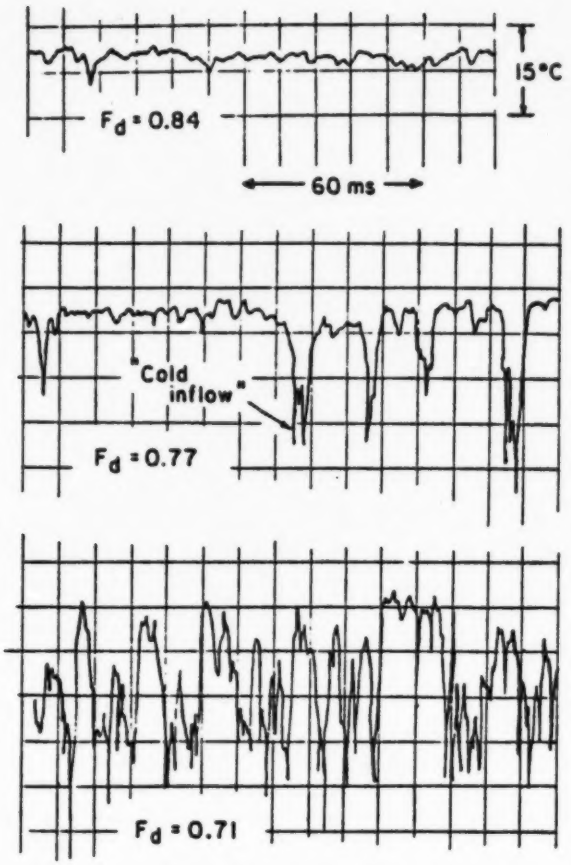

Fig. 11 Hot-wire traces in hot-air flow near exit of simulated tower.

electrically heated air is supplied to a "tower" of 25 cm dia., and temperature and velocity measurements are made simultaneously with a two-wire probe, the data being processed by computer in real time.

Records obtained with the probe tip 1.6 cm inward from the wall and 0.5 cm below the tower lip have the character shown on Fig. 11. When F_d is 0.84, the temperature fluctuations are at the level of the main-flow turbulence. When F_d is reduced to 0.77, spikes of low temperature (cold inflow) occur, but probably are not extensive enough to affect draft. When F_d is 0.71, an extremely turbulent temperature field exists near the wall. Other measurements show that when F_d is 0.58, the disturbed region has penetrated down the wall to about 1/3 the exit diameter, and inward from the lip about 1/4 of the radius. Presumably a serious disruption of draft could occur in these circumstances.

Various means may be considered (see the recent EPRI Symposium proceedings [8]) to reduce cold inflow. These matters are beyond the scope of this paper. We may, however, conclude that an exit F_d of 0.6 will make the draft secure, whatever the shape of the tower below.

5. CONCLUSIONS

There is potential for improving the design of large natural-draft cooling towers by aerodynamic refinement, especially if a large degree of flare is permitted, through use of novel construction techniques. One may look for lower draft height, lower construction costs and pumping power, and greater aesthetic acceptability and siting flexibility through such developments. In this paper, a number of research results bearing on the advantages of tower flare have been presented, and are recapitulated below.

A highly flared tower shape will have a dramatically lower draft requirement (height above the heat exchangers) than a conventional shape. The heat-exchange surface requirement would be nearly unaffected by flare for dry towers with typical plate-fin surfaces, or possibly wet towers with suitable spray packing. Wet towers with conventional plate-type fill would have increased surface requirement if flare is increased. Further research is needed to explore the crucial slope of the Stanton-Reynolds number curve for a variety of dry and wet surfaces.

Extreme flare does not require a high entrance. Tests over a wide range of flares and resistances have shown that entrance loss, in entrance dynamic heads, can be well represented by a simple formula (equation (14)) which is independent explicitly of flare and of heat-exchanger resistance. The entrance loss is found to depend chiefly on inward velocity under the sill, and that decreases with increased flare. Present results give substantially lower entrance loss for the low relative entrance heights desired if flare is large, than do presently used methods of estimation. In fact, required total tower height (draft plus entrance height) is shown to be substantially reduced when flare is large, for certain typical examples.

The addition of a large toroidal ring to a flared-tower entrance will reduce entrance loss, but only for very low entrance heights. Using flare to redistribute heat-exchanger surface out toward the tower periphery will reduce required entrance height, but at the cost of a larger structure.

Tower design, whether flared or not, should provide an densimetric Froude number at exit of about 0.6 to insure that draft is not disrupted by cold inflow.

Finally, it should be emphasized that wind effect of highly flared towers is certain to be important, because both entrance and exit wind effects depend on the air flow around the tower shell. Further reasearch on the prospects for flared towers should emphasize performance under wind.

ACKNOWLEDGMENTS

We thank Mr. Robert D. Mitchell for many helpful discussions about this research and Messrs. T. R. Ketcham and M. R. Canty of Owens-Corning for their help and support.

REFERENCES

1. H. J. Lowe and D. G. Christie: "Heat transfer and pressure drop data on cooling tower packings and model studies of the resistance of natural draught towers to air flow". Int. Dev. in Heat Transfer, Part V. ASME, N.Y. pp 933-950. 1962.

2. R. F. Rish: "Design of a natural draught cooling tower" Int. Dev. in Heat Transfer, Part V, ASME N.Y. pp. 951-950, 1962.

3. M. A. Garde: "Experimental evaluation of entrance losses of flared natural draft cooling towers", M. S. Thesis, Cornell University, January 1981.

4. F. K. Moore, Dry Cooling Towers, Advances in Heat Transfer, Vol. 12, pp 1-75, Academic Press, New York, 1976.

5. W. M. Kays and A. C. London, Compact Heat Exchangers, 2nd Ed. McGraw-Hill New York, 1964.

6. F. K. Moore "Cold Inflow and its Implications for Dry Tower Design", Second Waste Heat Management and Utilization Conference, "Miami Beach, U. Fla., 4 Dec., 1978.

7. B. R. Morton, "Forced Plumes," Jour. Fluid Mech., Vol. 5, p. 151, 1959.

8. Proc. EPRI Cooling-Tower Workshop (Ed: J.A. Bartz), San Francisco, Sept. 1980.

APPENDIX-SYMBOLS

A_a	total heat exchange surface (air side)
A_c	free-flow area of heat exchanger
A_f	frontal area of heat exchanger, $\pi D^2/4$
b	entrance height
C	loss coefficient
D	diameter of tower shell at entrance
D_e	diameter of tower shell at exit
d_r	ratio, De/D
E,F,K	notation in [4]
F_d	densimetric Froude number, $V_e^2/(\frac{\Delta\rho}{\rho} g D_e)$
f	flare, (D-De)/H
f_a	friction factor of heat exchanger (air side)
f_1	loss coefficient (equation (2))
G	air mass flow per unit frontal area
g	acceleration of gravity
H	tower draft height from heat exchanger to exit
h	heat-transfer coefficient
K	heat-exchanger (screen) resistance coefficient in transverse dynamic heads
K_e	heat transfer coefficient for wet packing (equation (2)).
L	water mass flow per unit frontal area
n	exponent in St_a, Re relation (equation (5))
Re	Reynolds number
R_{ent}	entrance loss in entrance heads $1/2\ \rho V^2$
r_{ha}	air side hydraulic radius [5]
St_a	Stanton number of heat exchanger (air side)
V	bulk velocity of tower at heat-exchanger level
V_b	inward velocity at entrance (Fig. 1)
V_c	free-flow velocity at heat exchanger
V_e	exit velocity
x	distance below tower exit where plume originates
ε	turbulent entrainment coefficient of plume (about 0.1)
ϕ	cold-inflow parameter, εF_d^2
ρ	air density
$\Delta\rho/\rho$	fractional density change across heat-exchanger

PB82-228099

MODEL STUDIES ON THE DESIGN AND ARRANGEMENT OF FORCED DRAFT COOLING TOWERS TO MINIMIZE RECIRCULATION AND INTERFERENCE

P.R. Slawson and H.F. Sullivan
University of Waterloo
Waterloo, Ontario
Canada

EXTENDED ABSTRACT

Physical model studies were conducted in a water flume to measure recirculation and interference for two conceptual configurations of forced draft dry cooling towers, a rectangular array and a multiple round tower arrangement. The objective of this study was to investigate and make recommendations on the design and arrangement of cooling towers in order to provide optimum ambient air distribution to the heat transfer surfaces. Optimum air distribution is maintained by minimizing recirculation (re-ingestion of a tower's own effluent) and interference (ingestion of an adjacent tower's effluent plume).

The proposed dry cooling tower "array concept" under study consisted of individual rectangular cells with suggested dimensions of 10ft by 40ft x 10ft high. These dimensions were proposed based on the economics of manufacturing. These cells were to be arranged in rows of 20 cells to each row. Each cell was to have 8 fans.

The proposed multiple round tower configuration studied consisted of two rows of approximately 5 towers each, with each tower having nominal dimensions of approximately 200 ft diameter by 80 ft high.

Physical experiments were thus conducted on a "two-dimensional" four row section of the rectangular array as well as on a section of the two row proposed round tower arrangement.

As one might expect, very high recirculation and interference measurements of 40 to 70% existed for the rectangular array concept, while values of 20 to 30% were measured for the round tower arrangement.

The degree of recirculation and interference depended on such things as: tower spacing, tower exit air velocity to ambient wind speed ratio and clustering and shrouding of fans.

Details of the experiments and explanations of the measured results are given.

1. INTRODUCTION

As large electric generating stations increase in number, the need for

multiple cooling tower installations (both wet, dry or a combination thereof) will also increase. When more than one cooling tower is required at a given site, there exists the possibility that the heated effluent from one tower may adversely affect its own performance as well as that of an adjacent tower through "recirculation" and "interference". Recirculation occurs when the effluent air from a single cooling tower is presented to the heat exchange surfaces of that tower as a consequence of aerodynamic downwash. "Interference" occurs when the heated effluent of one tower is ingested across the heat exchange surfaces of an adjacent tower. It is clear that recirculation and interference have the potential of reducing tower performance by decreasing the operating temperature difference approaching the tower.

There is little quantitative experimental data on recirculation and or interference. The majority of the data that does exist is the result of physical modelling studies performed in water flumes or wind tunnels. Reisman (1972) performed a series of single tower scale model studies on recirculation in a wind tunnel. Chan et al (1974) conducted water flume studies on recirculation and interference on scale models of both rectangular and round mechanical draft cooling towers. The results of these studies indicate that, (a) downwash and recirculation vary considerably with rectangular tower orientation to the wind (b) circular towers suffer less recirculation than rectangular towers (c) recirculation varies with the tower exit velocity to wind speed ratio (d) the three dimensional end vortices of rectangular towers dominate tower wake mixing near the ends of the tower and can thus influence greatly tower recirculation (e) for adjacent rectangular towers recirculation is increased for both upwind and downwind towers over that found for a single tower under identical ambient flow conditions. Crawford and Slawson (1978) attempted to numerically model the three dimensional recirculation zone adjacent to two rectangular mechanical draft cooling towers separated by one tower length. They compared their predicted plume with field observations with limited success.

The objective of the work reported here was to investigate recirculation and interference for two conceptual configurations of forced draft dry cooling towers, a rectangular array and a multiple round tower arrangement. The array concept consisted of individual rectangular cells with suggested dimensions (based on economics of manufacture) of 10 ft. by 40 ft by 10 ft. Each rectangular cell was to have two heat exchangers of approximate dimensions 8 ft by 40 ft and have 8 fans. The cells were to be arranged in 30 rows of 20 units per row. The spacing between each row was to be some 23 ft. Two air distribution lanes 150 feet wide were to run through the array. The main attributes of the array concept were low installation cost, ease of manufacture of the heat exchange units, and low maintenance. The proposed round tower configuration for study consisted of two rows of approximately five towers each, with each tower having nominal dimensions of approximately 200 feet in diameter by 80 ft high. Further details on the experiments may be found in Sullivan and Slawson (1978).

2. EXPERIMENTAL DESIGN AND TECHNIQUE

The array concept for cooling towers had been proposed purely because of the ease with which the individual cells could be manufactured, assembled and put in place. It was recognized from the outset that this array configuration would lead to severe recirculation problems. Thus, one of the objectives of this work was to quantify the expected recirculation of the array and to investigate other possible tower configurations with equivalent heat transfer area but with minimal recirculation. This led to consideration of multiple

round tower arrangements as one possible alternative to the array.

2.1 Array Configuration of Cooling Tower Cells

A model scale of 1:240 was chosen for the array. A section of the array of some three cells long by four rows deep was chosen for the model studies to be conducted in a water flume of cross-sectional dimensions 1.5 ft by 2 ft. The separation distances between rows was one of the parameters to be adjusted to determine its effect on recirculation and interference. Thus row separations of one, two and four model heights were used. The array section to be modelled corresponded to a portion from near the centre of the array and thus two-dimensional modelling of the flow normal to the rows was necessary in order to avoid "end effects" that occur at the edges of the array (end of rows). The two dimensional flow simulation was approximated by placing plexiglas walls at the ends of the model rows of cells and parallel to the water flume sides. Simulation of the flow near the ends of rows of the array was achieved by removing one of the plexiglas walls.

Figures 1 and 2 illustrate schematically the experimental equipment and set-up for the two dimensional array section experiments. Heated water flowed from an overhead tank to the individual models through a series of flexible hoses. Hand valves in the individual lines were used to balance the flow rates to the models to ensure uniformity of flow from the separate rows. Ambient fluid was withdrawn from the models at exactly the same rates at which the heated water was supplied in order to simulate the inlet-outlet flow conditions of the cooling tower units.

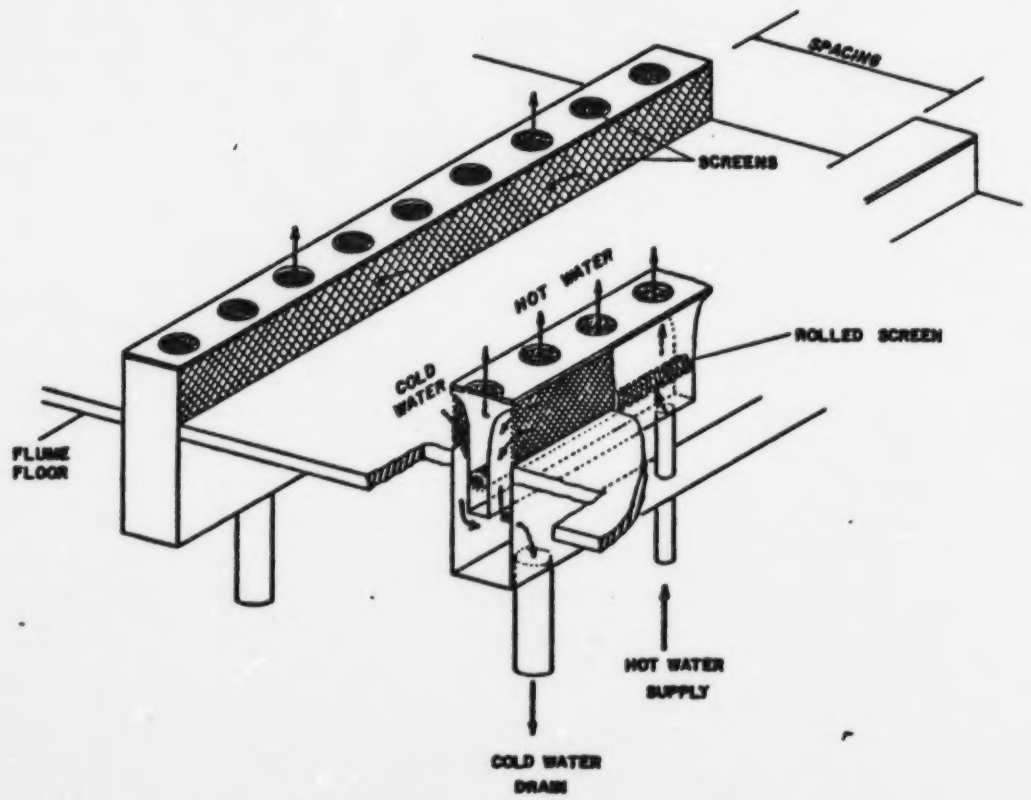

Fig.1. Schematic diagram of model construction

2.2 Round Cooling Towers

A model scale of 1:480 was selected for the round tower models which thus correspond to prototype towers of 200 ft in diameter by 80 ft high. Figures 3 and 4 illustrate schematically the nature of the individual round tower model construction and the geometric arrangement of a two tower and multiple tower configuration respectively. For purposes of measuring tower performance, the drain sections of the towers were divided into four quadrants and separate temperature measurements of each drain quadrant were made. The top plate of the tower consisted of a plexiglas plate with twenty-seven (11/16 inch) holes which simulated individual fans exit ports of 28 ft in diameter. The half-tower models shown in Figure 4 were constructed similar to the full towers. Both the two tower in-line and the multiple tower configurations were adjustable to separation distances of one-half and one full tower diameter. Froude number similarity was maintained between the proposed prototype tower units and the models. The densimetric Froude number is given by

$$F_r \equiv \frac{u_j}{(gD\,\frac{\Delta\rho}{\rho_a})^{1/2}}$$

where u_j is the exit velocity of the fans, D is fan (exit port) diameter, $\Delta\rho$ is the density difference between the exit fluid and ambient, ρ_a is the density of ambient fluid and g is the acceleration due to gravity. Constant Froude numbers of 10.5 for the array concept of tower unit and 6.5 for the round tower unit were maintained during the experiments. In addition, a particularly important scale parameter for near exit simulation of jets and plumes, the velocity ratio $K \equiv u_j/u_a$, where u_a is ambient near field velocity at the height of the exit ports, was varied over a range of 0.5 to 3.5. Recirculation

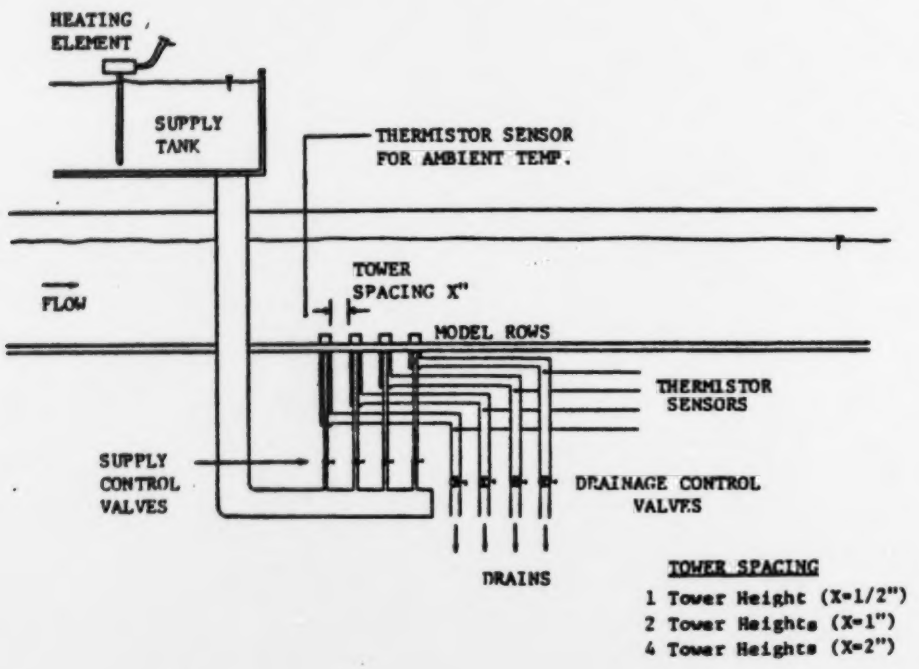

Fig. 2. Schematic Diagram of Flow System

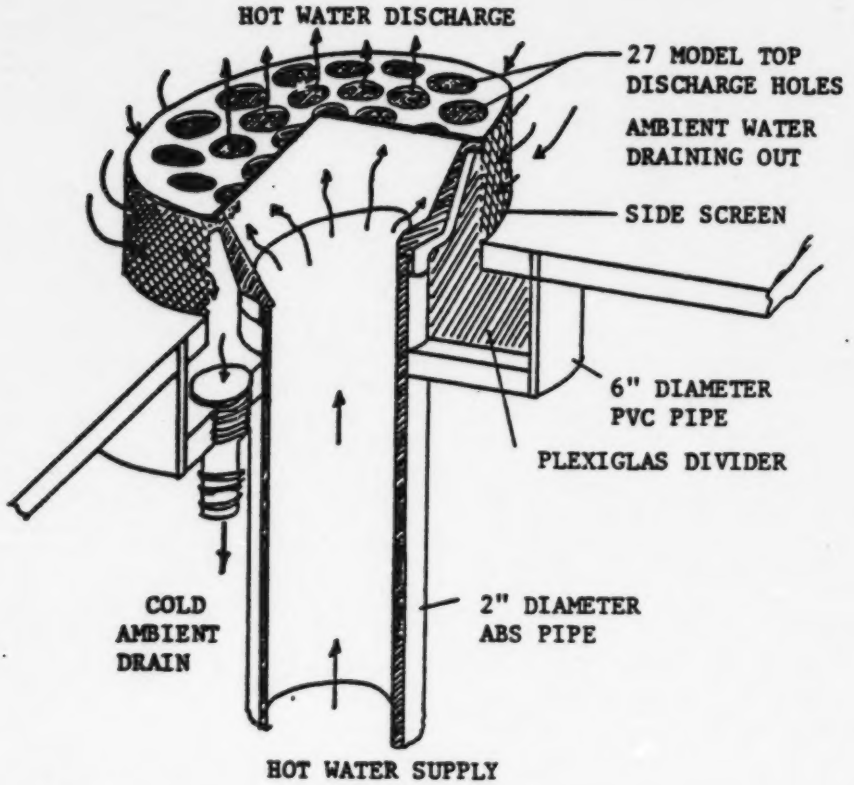

Fig.3. Schematic diagram of model construction

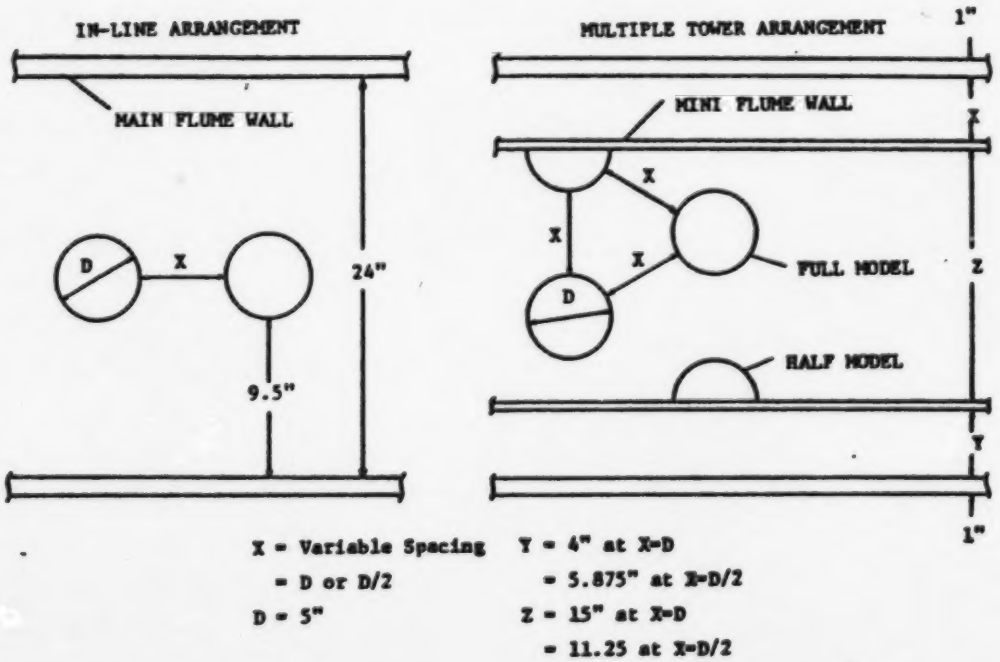

Fig.4. Schematic arrangement (plan view) for round tower modeling

R (and interference) for a given model was calculated using the following equation:

$$R_i = \frac{T_{wi} - T_a}{T_j - T_a}$$

where T_{wi} is the temperature of water drained from position i, T_a is the ambient flume water temperature and T_j is the model jet discharge temperature.

In addition to recirculation and interference measurements as functions of the velocity ratio K and separation distance of rows or towers, documentation of the flow was achieved through dye injection flow visualization observations and in-plane (wake) temperature measurements. The temperature measurements were made in a plane normal to the flow at several distances downstream from the tower units as well as between towers and rows.

3. RESULTS

3.1 Array Configuration

Figure 5 illustrates some of the results of the recirculation and interference measurements for the two-dimensional 4 row section of the array. The observations indicate that:

(a) recirculation decreases as the separation distance between rows of towers increases except for row one.

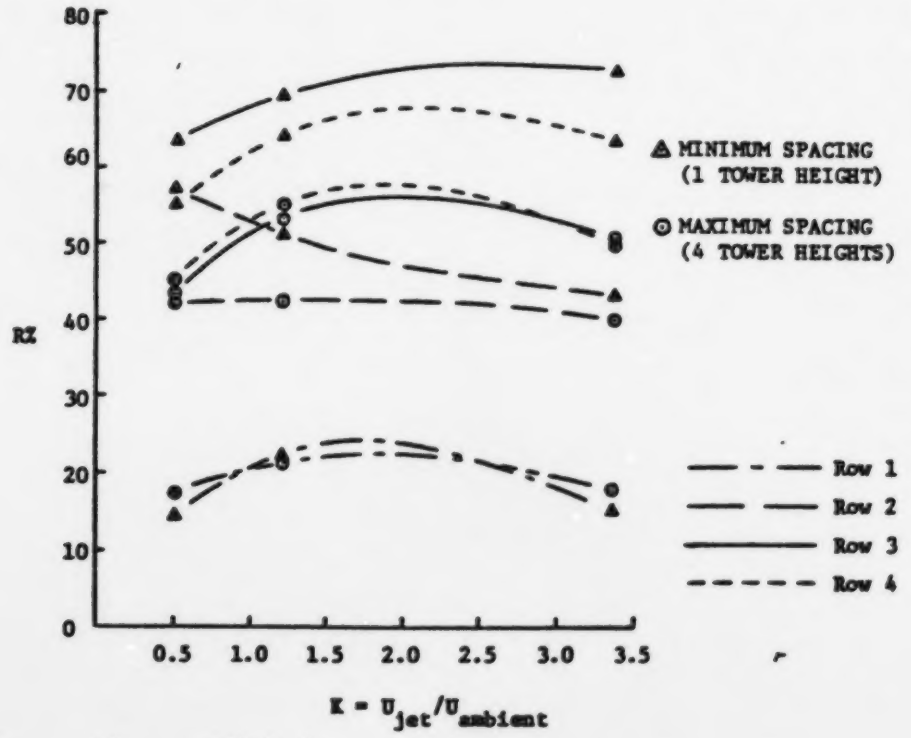

Fig. 5. Recirculation RZ as a function of velocity ratio K

(b) recirculation increases dramatically from rows one through three but remains much the same for rows three and four

(c) recirculation values on rows two through four are in the range 40 to 70% (unacceptably high)

Removing one end wall from the array models and repeating the recirculation measurements resulted in approximately a 15% reduction in average recirculation and interference for the four rows.

The dye injection and flow visualization observations indicated that there is significant upstream diffusion of the adjacent downstream tower's effluent into the low pressure zone in the immediate wake of the upstream tower at all tower spacings tested.

The measurements of the plume and wake temperature fields indicated near uniform temperatures in the immediate wake zones between adjacent towers indicating a well mixed zone as might be implied from the dye visualization results. Also, very similar recirculation values were obtained using these near tower wake temperature measurements in place of the tower drain measurements.

3.2 Round Tower Configurations

Figure 6 illustrates the effect of tower separation on recirculation and interference for two round towers at one and one-half tower diameter separations respectively. There was no measurable difference in the recirculation values for the first tower at both tower separation distances. There was a sharp decrease in recirculation for the downstream tower as K increased (decrease in ambient wind speed as was expected).

Figure 7 illustrates recirculation results for the multiple round tower configuration. At the one-half tower diameter spacing, recirculation increases with K (lower wind speeds) for the downstream (second) row of towers while the variation is much less when the towers are at one tower diameter separation.

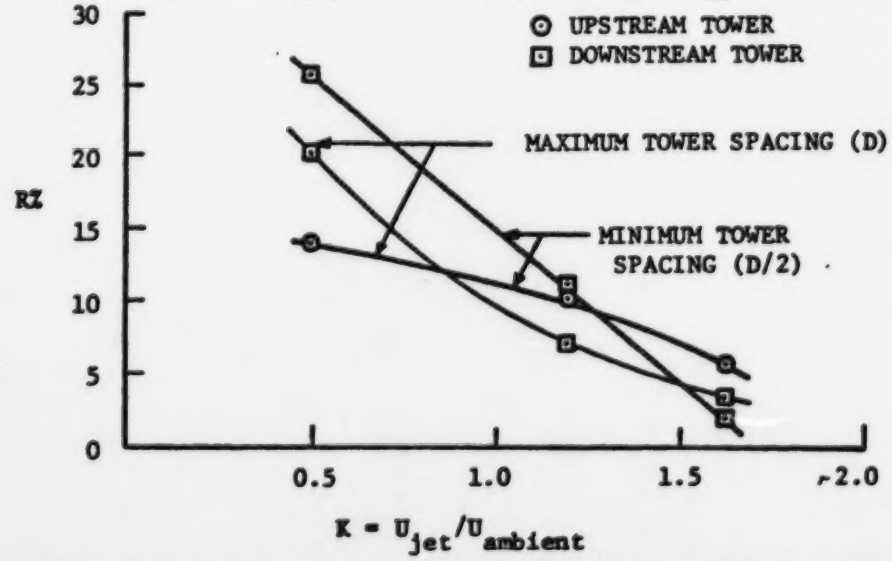

Fig.6. Recirculation RZ as a function of velocity ratio K for upstream and downstream towers of a dual tower in-line arrangement

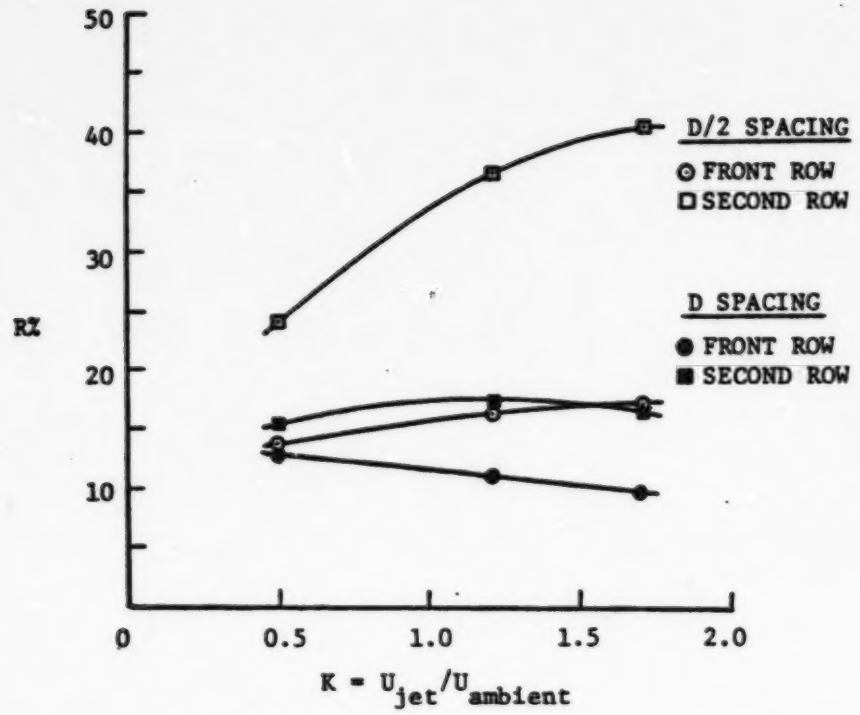

Fig.7. Recirculation RZ as a function of velocity ratio K for front row and second row full towers in a multiple tower arrangement

At all K values, the plumes were under downwash conditions. Subsequently they were fully mixed to the flume floor in the immediate wake of the towers. However, the lateral growth of the tower wakes increased with increasing K (lower ambient velocities). As a result, the extent of the interaction zone of the upstream tower's effluent with the downstream tower increased with increasing K value. This was adequately illustrated from dye visualization. Figure 7 shows this resulting increase in R with increasing K, in particular at the 1/2 D spacing, for the second row towers where the recirculation appears to be reaching a maximum at an R value just beyond 1.5. The tower effluent plumes and wakes form complex interactions at various K values and required well documented dye visualization experiments to sort out.

Figure 8 illustrates the effects of fan shrouding on recirculation for a single round tower. There is a clear reduction in recirculation at all measured K values when a fan shroud is used.

The flow visualization of the round tower plumes clearly illustrated the effects of shielding by the upstream plume on the downstream plume. The downstream plume in a two tower in-line arrangement rose much more sharply than the upstream plume leading to less downwash in the wake of the downstream tower. However, the downstream tower still had higher recirculation values than the upstream tower because it had its own recirculation as well as interference from the upstream tower.

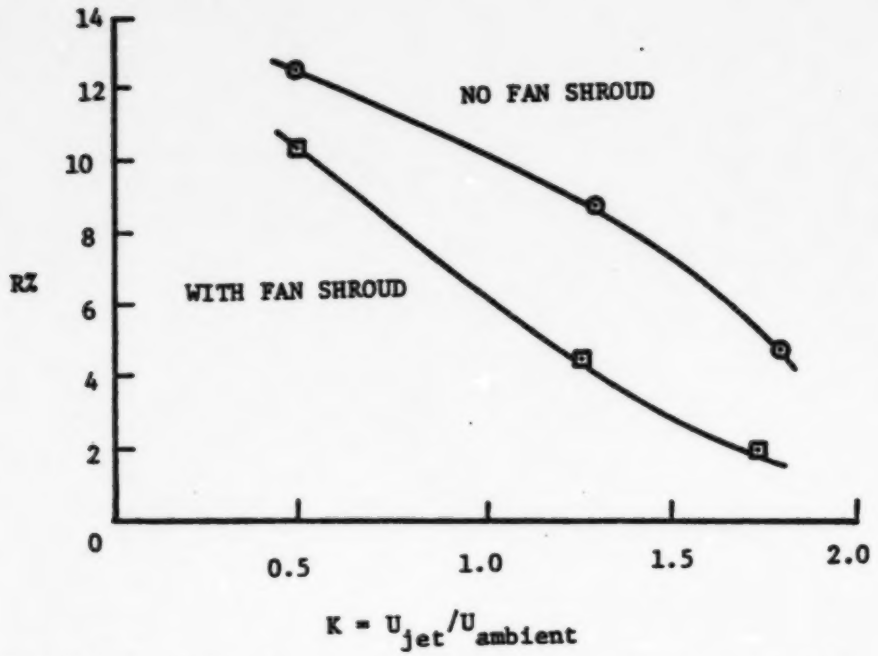

Fig.8. Recirculation R% as a function of velocity ratio K for a single round tower.

4. CONCLUSIONS

As one might anticipate, very high recirculation and interference occurs with the array concept. Even with the reduction in recirculation for the array due to end effects, the overall values for the array are expected to be in the range 38 to 67%. This translates into an expected 20 to 35% reduction in heat rejection capability for the array.

The multiple round tower experiments (two row arrangement) produced improved recirculation values over the array configuration of 50 to 75%. At one-half a tower diameter spacing the recirculation values ranged from 20 to 30% (depending on velocity ratio) while at one tower diameter spacing they were measured at 14 to 15%.

Further reductions in recirculation of 20 to 60% (depending on velocity ratio) for a single round tower were achieved with the clustering of fans about the tower exit axis and with the provision of fan shrouding. Thus, further detailed model studies on the effects of fan configuration and shrouding appear to be warranted for the round tower design.

REFERENCES

1. Chan, T.L., Hsu, S.T., Lin, J.T., Hsu, K.H., Huang, N.S., Jain, S.C., Tsai, C.E., Croley, T.E. II, Homer Fordyce and John F. Kennedy, "Plume Recirculation and Interference in Mechanical Draft Cooling Towers", Iowa Institute of Hydraulic Research The University of Iowa, Iowa City, Iowa, IIHR Report No. 160, 1974.

2. Crawford, T.L. and Slawson, P.R., "Modeling Near-Field Behaviour of Plumes from Mechanical Draft Cooling Towers" Proc. 2nd Conf. on Waste Heat Management and Utilization, Dec. 4-6, 1978, Miami Beach, Florida (11p.), 1978.

3. Onishi, Y., and Trent, D.S. "Mechanical and Experimental Investigations on Dispersion and Recirculation of Plumes from Dry Cooling Towers at Wyodak Power Plant in Wyoming", Battelle Pacific Northwest Laboratories, 1976.

4. Reisman, J.I., "A Study of Cooling Tower Recirculation", presented at the ASME 93rd Winter Annual Meeting, 22p, Nov. 1972.

5. Sullivan, H.F., and Slawson, P.R., "Dry Cooling Tower Design and Arrangement for Optimum Air Distribution" Envirodyne Ltd. Report 120p, July, 1978.

PB82-228107

COOLING TOWER FAN MOTOR POWER MEASUREMENTS

A. E. Johnson
K. H. Belfer
Pacific Gas and Electric Company
San Ramon, California

ABSTRACT

During the past few years, much effort has been expended to improve cooling tower thermal performance test accuracy. Both the Cooling Tower Institute Test Code ATC 105 and American Society of Mechanical Engineers Test Code PTC23 have outlined procedures and test equipment to measure circulating water flow rate, hot and cold water temperatures, and inlet wet bulb temperatures. These codes, however, become vague and general regarding fan motor power measurements. Fan horsepower is directly related to airflow through each cooling tower cell by the equation $CFM_2 = CFM_1(BHP_2/BHP_1)^{1/3}$ where CFM = air flow rate in feet^3/min and BHP = measured brake horsepower of the fan motor at conditions 1 and 2. Our experience is that cooling tower fan power measurements made with commonly used wattmeters or ammeters and voltmeters are typically in error by 5 to 7%, but errors as high as 20% have been seen. A fan motor power measurement with a ±10% accuracy means airflow is known to only 3.2% and, therefore, calculated tower performance is only accurate to ±3.2%. A fan power measurement 20% in error will yield a calculated tower performance that could be 6.3% in error. An outline of a procedure to accurately measure power to a typical cooling tower fan motor is presented herein.

1: INTRODUCTION

During the past few years much effort has been put forth to improve the test methods and, therefore, test accuracy for cooling tower thermal performance tests. The Cooling Tower Institute Test Code ATC105 and American Society of Mechanical Engineers Test Code PTC-23 have detailed descriptions of allowable test equipment and procedures to measure circulating water flow rate, hot and cold water temperatures, and inlet wet bulb temperatures. These test procedures insure the most accurate measurement of these parameters possible. However, these codes become somewhat vague and general regarding fan motor power measurements. In particular the existing CTI Code states that "power input shall be determined by measurement of the voltage, current, and power factor, or by direct measurement of the kilowatt input." The same CTI code has a seven page addendum dealing solely with measurement of inlet wet bulb temperatures. More emphasis should be placed on obtaining accurate fan horsepower measurements than is given. The usual reason for a lack of concern regarding the accuracy of the fan power measurements is the fact that the measured power is taken to the third root. However, a power measurement with a ±10% accuracy means the airflow is known to only 3.2% and,

therefore, the calculated tower performance is only accurate to ±3.2%. A power measurement 20% in error will yield a calculated performance that is 6.3% in error. Therefore, it is possible to have the results of an acceptance test indicate the tower is meeting its design specifications when in actuality it is 6% short. Our experience is that cooling tower fan power measurements made with commonly used wattmeters or ammeters and voltmeters are typically in error by 5 to 7% but errors as high as 20% have been seen.

The purpose of this paper is to outline the theory of power measurements and discuss the usual methods of cooling tower fan power measurement and their shortcomings. A proposed method of measurement along with its advantages over the other systems will also be discussed. None of these are either the ASME or IEEE power test codes. These codes are not convenient to use because of the typical wiring of tower fan motors. In conclusion, an outline of the steps necessary to measure power to a typical cooling tower fan motor using the proposed method as well as examples of the measurements and calculations necessary to determine fan motor brake horsepower will be presented.

2: THEORY

By using the "Fan Laws," it can be shown that the airflow through each cooling tower cell is directly related to fan motor horsepower:

$$CFM_2 = CFM_1 \left(\frac{BHP_2}{BHP_1} \right)^{1/3}$$

where:

$CFM_{1,2}$ = airflow in cubic feet/minute at Conditions 1 and 2.
$BHP_{1,2}$ = brake horsepower of fan motor at Conditions 1 and 2.

Further, a review of the relationships that exist among voltage, current and power in electrical circuits is also necessary. In d-c measurements the power in a circuit equals the product of the current in the circuit and the voltage across the terminals. In a d-c system, if current and voltage are constant, consumed power is determined by the product of the measured voltage and the measured current.

Alternating current (a-c) power measurements present considerably greater problems than d-c power measurements especially in polyphase circuits. The current in an a-c circuit changes direction constantly, and the voltage constantly changes polarity, therefore power becomes more difficult to measure. In a purely resistive circuit, the voltage and current are in phase. Power is calculated by:

$$P = EI$$

where:

P = power
E = voltage (measured)
I = current (measured)

Unfortunately, a-c circuits almost always exhibit some inductance and/or capacitance, so the voltage and current are out of phase. Power can no longer be found by multiplying the voltage by the current.

Phase-angle, , is defined as the difference in degrees by which the current leads the voltage in a capacitance circuit or lags the voltage in an inductive circuit. The power factor of a three phase a-c circuit is equal to the true power in watts divided by the apparent power in volt-amperes. The apparent power is the product of volts and amps. True power for a three phase a-c circuit is defined as:

3-phase true power = $\sqrt{3}EI \cos\theta$.

where:

E = measured voltage
I = measured current
Cosθ = power factor

2.1 Wattmeter Method of Measuring Power

The wattmeter method for measuring power utilizes a clamp-on analog wattmeter. The clamp-on method is used because the power must be measured without disrupting the load. A clamp-on wattmeter has both current and voltage inputs. The current jaws are clamped around the leads going from the switchgear to the fan motor. The voltage clip leads are attached to the 480 volt bus directly. A 3-phase, 3-wire system, which is a common power system for cooling tower fan motors, requires two power measurements. The total power is the algebraic sum of the two measurements. If the load is balanced and at unity power factor, each measurement will be half the load. At 50% power factor, one measurement will be the total load and the other will be zero. A typical power factor for a 200 horsepower fan motor is 88%. One measurement will be approximately two-thirds of the total load and the other will be approximately one-third.

Stray magnetic fields which are very common in power plants and electrical switchgear affect the accuracy of a clamp-on wattmeter. The plane or angle at which the wattmeter is held also has an effect on accuracy. To achieve highest accuracy the clamp-on wattmeter should be used in the same plane as it was calibrated. This is difficult if not impossible to do when working near electrical switchgear.

The jaws of a typical clamp-on wattmeter are about 3 inches in diameter. Errors of 3 to 5% have been found by the movement of the cable within this area. This error is called a proximity error. A clamp-on wattmeter used under optimum conditions is accurate to about ±3%. Overall errors as high as 15% have been found using this method of power measurement.

Example 1 will show the necessary measurements and calculations.

2.2 Voltmeter and Clamp-on Ammeter Method

This method uses a clamp-on ammeter, a voltmeter, and the motor manufacturer's claimed power factor to determine motor input horsepower. The clamp-on ammeter is used to measure the current flowing in the motor cables without disrupting the load. It is clamped around the leads between the switchgear and the fan motor. The voltmeter is used to measure the bus voltage, which supplies power to the total bank of motors. It can be attached either to the 480 volt bus directly, or to the 120 volt side of the metering

potential transformers used for the 480 volt protection scheme. Example 2 will show the measurements and calculations necessary to determine fan motor power using this method.

The clamp-on ammeter is similar to the clamp-on wattmeter in operation and presents the same type of problems. Stray fields, proximity errors, and the instrument not being used in the same plane in which it was calibrated all effect accuracy. Again under optimum conditions current measurements have an accuracy of ±3%.

The power factor cannot be measured when using this method of power measurement. Therefore, the motor manufacturer's supplied power factor must be used. A difference of 3% between manufacturers power factor and measured power factor has been found when checking a bank of 10 fan motors. Total errors as high as 20% caused by the compounding effect of all of the above have been found using this method of power measurement.

2.3 Proposed Method - Power Meter and Split Core Current Transformer

This system consists of a digital power meter and two or more split core current transformers. Whether a digital or an analog power meter is selected, it should be capable of measuring 3-phase, 3-wire; and 3-phase, 4-wire as well as single phase power.

One type of digital power meter measures volts, amps, and watts single phase or polyphase with an accuracy of 0.25% of reading. Self-contained range coverage is up to 600 volts and 20 amps. Front panel pushbuttons are used to select volts, amps, or watts for any phase plus total system power. This instrument also has simultaneous 0 to 5 volt analog outputs for all functions which can be fed to a computer, data logger, analog recorder, or digital panel meters scaled for direct readout in engineering units.

When input values for either volts or amps exceed the self-contained rating of the instrument, external metering transformers suitable for power measurements must be used. Inexpensive transformers meant for use with only ammeters or voltmeters should not be used with a power meter. They may have large phase angle errors which have no effect on current or voltage readings but can cause large errors in power measurements. Transformers with low ratio errors and phase angle errors should be used.

A split core metering current transformer is made to clamp around the power cables, measuring the current by induction, drawn by the load, without disrupting it. A transformer is a device which is minimally affected by stray fields, or the plane in which it is used.

Current transformers, which are parallel wound, will have a proximity error that is minimal. The power meter with split core current transformers is the proposed way to measure power. This system will give three phases of voltage, three phases of current, three phases of power along with total power. From these measurements phase angle and power factor can be calculated. As a result, total measurement errors can be less than 1%.

3: PROPOSED POWER MEASUREMENT PROCEDURE

The proposed procedure for measuring fan motor horsepower with a power meter and two split core current transformers will now be given. It should

be stressed that untrained personnel should not attempt to make the measurements as there are many potentially lethal accidents that can occur. The outline presented below is not meant to be a "cookbook" procedure for measuring power to all cooling tower fan motors, but a guideline of the general principles involved.

Step 1. Prior to the test, procure schematic diagrams, both single line and three line, of the motor control circuits and 480 volt bus, which are associated with the fan motors in question. Become familiar with the protection circuits and motor wiring before the test. From the plan drawing of the cooling tower determine the wire lengths from the switchgear to the fan motors.

Step 2. Connect the current and potential leads to the back of the power meter. Connect the split core current transformers to the other end of the current leads. Plant personnel should be alerted before performing Steps 3 and 4.

Step 3. Put split core current transformers around A and C phases of the first fan motor to be tested.

Step 4. Clip potential leads from the power meter to the 120 volt side of the 480 to 120 volt metering potential transformers on the 480 volt bus which supplies power to the motors. Insure that the split core current transformers are in phase with the metering potential transformers.

Step 5. Record measurements. If a measurement is fluctuating take the average. Remember that if the power source is a 3-phase, 3-wire system with a typical 88% power factor, one power reading will be about half the other, and that the total of the two will be the power delivered to the motor at the point of measurement.

Step 6. For an accurate determination of fan motor horsepower, lead losses are an important parameter and must be taken into consideration. Lead losses (I^2R) are the product of square of the average phase current and the resistance of the wire going from the switchgear to the motor in question. The type of copper wire used is important, since soft, medium, or hard drawn copper cable have different resistances.

Step 7. After subtracting the lead losses from the measured power calculate the motor brake horsepower. The brake horsepower is found by multiplying the motor efficiency by the measured horsepower corrected for lead losses. The motor efficiency is obtained from the motor manufacturer.

4: EXAMPLES OF MEASUREMENTS AND CALCULATIONS

4.1. Example 1. Clamp-on Wattmeter Method (Figure 1).

Known information:

1. Manufacturer's motor efficiency = 93% at full load

Measurements:

1. B-A phase voltage with A phase current, 110 KW
2. B-C phase voltage with C phase current, 55 KW

Calculations:

Total power = 110 + 55 = 165 KW
Horsepower = (165 KW)/(.7457 HP/KW) = 221 HP
Fan motor brake horsepower = (221)(0.93) = 206

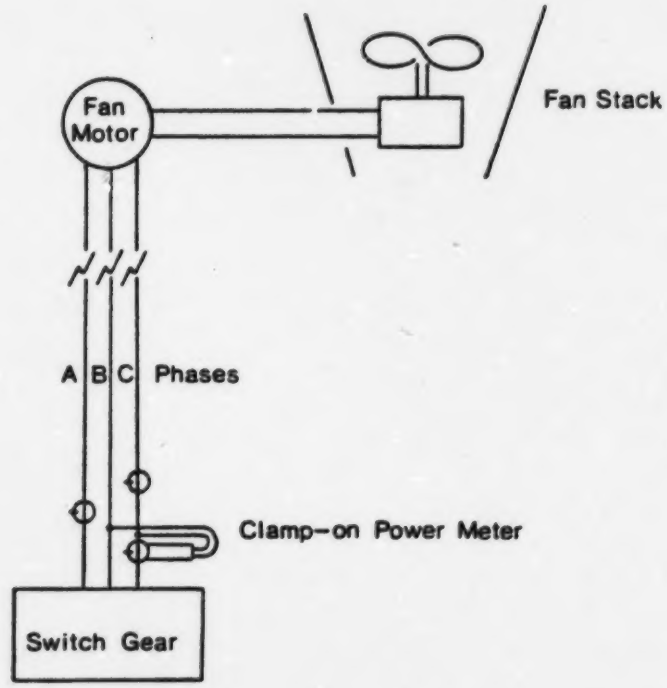

FIGURE 1. Typical power measurement diagram using clamp-on wattmeter.

4.2. Example 2. Clamp-on Ammeter and Voltmeter Method (Figure 2).

Known information:

1. Potential transformer ratio, 4 to 1
2. Wire data: 155 ft of 500 MCM medium drawn copper wire from switchgear to Fan Motor No. 1
3. Wire resistance: 0.00002116 ohm/ft (from electrical handbook)
4. Manufacturer's motor efficiency = 93% at full load
5. Motor manufacturer's power factor = 88%

Measurements:

1. A phase current, 210 amps
2. C phase current, 210 amps
3. B-C phase voltage, 122.8 volts
4. B-A phase voltage, 122.9 volts

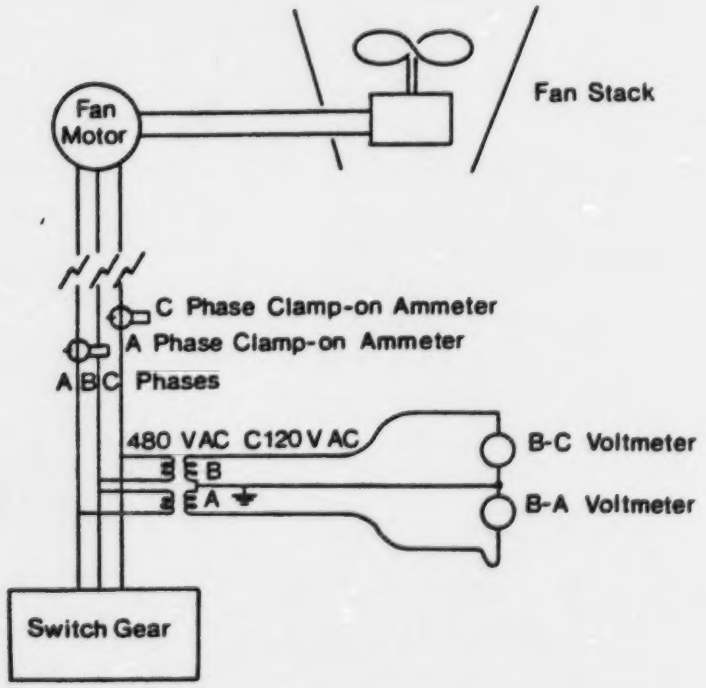

FIGURE 2. Typical power measurement diagram using clamp-on ammeters and voltmeters.

Calculations:

1. Current:

   A phase current = 210 amps
   C phase current = 210 amps
   Average current = 210 amps

2. Voltage = (measured volts)(potential transformer ratio)

   B-C phase voltage = (122.8)(4) = 491.2 volts
   B-A phase voltage = (122.9)(4) = 491.6 volts
   Average voltage = 491.4 volts

3. Input motor power = true power = $\sqrt{3}$(average current)(average voltage)(manufacturer's power factor)

   Input motor power = (1.732)(210)(491.4)(0.88) = 157,000 watts

   $$\text{Input motor horsepower} = \frac{157 \text{ KW}}{0.7457 \text{ KW/HP}} = 211 \text{ HP}$$

   Fan motor brake horsepower = (Input motor horsepower) (manufacturer's motor efficiency)

   Fan motor brake horsepower = (211)(0.93) = 196

4. Since the accuracy of the current measurements is ±3% at best, correction for lead losses is not made as the lead losses would be less than 3%.

4.3. Example 3. Proposed Method - Power Meter and Split Core Current Transformer (Figure 3).

Known information:

1. Current transformer ratio, 100 to 1
2. Potential transformer ratio, 4 to 1
3. Wire data: 155 ft of 500 MCM medium drawn copper wire from switchgear to Motor No. 1 terminals.
4. Wire resistance: 0.00002116 ohm/ft (from electrical handbook)
5. Motor efficiency = 93% at full load
6. Motor manufacturer's power factor = 88%

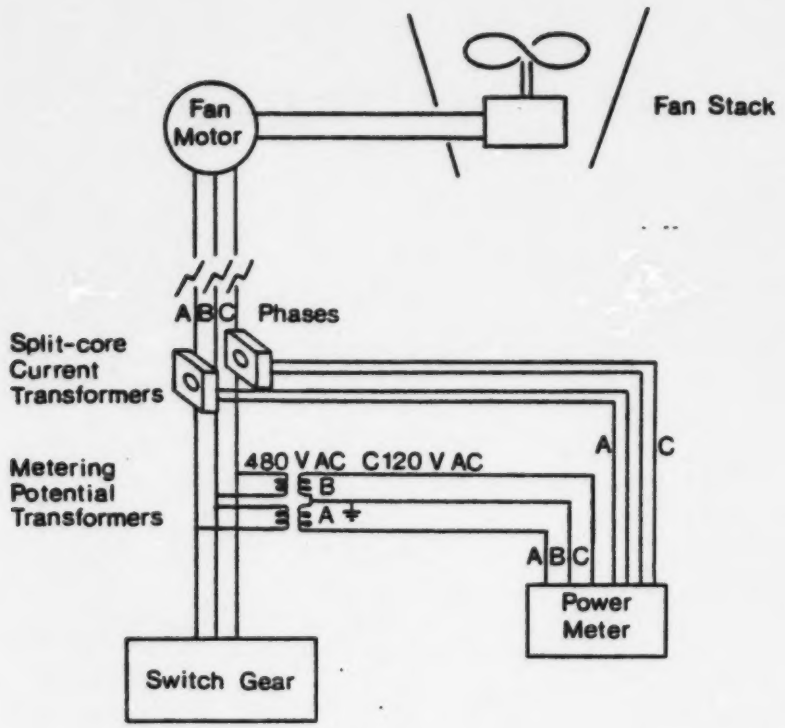

FIGURE 3. Typical power measurement diagram using power meter and split-core current transformers.

Measurements:

1. A phase current, 2.067 amps
2. C phase current, 2.083 amps
3. B-C phase voltage, 122.8 volts
4. B-A phase voltage, 122.9 volts
5. B-C phase power, 0.2541 KW
6. B-A phase power, 0.1263 KW

Calculations:

1. Current = (measured current)(current transformer ratio)

   A phase current = (2.067)(100) = 206.7 amps
   C phase current = (2.083)(100) = 208.3 amps
   Average current = 207.5 amps

2. Voltage = (measured volts)(potential transformer ratio)

   B-C phase voltage = (122.8)(4) = 491.2 volts
   B-A phase voltage = (122.9)(4) = 491.6 volts
   Average voltage = 491.4 volts

3. Input motor power = true power = (B-C phase measured power + B-A phase measured power)(current transformer ratio)(potential transformer ratio) - lead losses

   Input motor power = true horsepower = (0.2541 + 0.1263)(100)(4) = 152.2 KW - lead losses

   Input motor horsepower = true horsepower = $\frac{152.2 \text{ KW}}{0.7457 \text{ KW/HP}}$ = 204.1 HP - lead losses

4. Lead resistance from switchgear to fan motor

   Resistance = (No. of wires)(length per wire)(resistance per foot of wire)

   Resistance = (3)(155)(0.00002116) = .009839 ohm

5. Lead losses = (average current)^2(lead resistance)

   Lead losses = $(207.5)^2(0.009839)$ = 423.7 watt

   Lead losses = $\frac{423.7 \text{ watt}}{745.7 \text{ watts/HP}}$ = 0.57 HP

6. Input motor horsepower = true power - lead losses

   Input motor horsepower = 204.1 - 0.57 = 203.5 HP

7. Fan motor brake horsepower = (input horsepower)(motor efficiency)

   Fan motor brake horsepower = (203.5)(0.93) = 189.3 BHP

8. Apparent power = $\sqrt{3}$(average measured voltage)(average measured current)

   Apparent power = $3(491.4)(207.5)$ = 176,600 volt-amps

9. Power factor = $\frac{\text{true power}}{\text{apparent power}}$

   Power factor = $\frac{152.2\text{-}0.42 \text{ watt}}{176{,}600 \text{ volt-amp}}$ = 0.8596 (Note difference between actual and claimed power factor)

5: SUMMARY AND CONCLUSIONS

Both the ASME and CTI test codes have written procedures if followed, that will accurately determine the capability of a cooling tower. Methods for measuring water temperatures and flow rates as well as inlet wet bulb temperature have been scrutinized resulting in the current procedures. It is now time to examine that remaining test parameter, fan power measurements. Equipment is now available which can provide accurate power measurements. Why strive to obtain temperatures and flow rates with 1% or better accuracy when the accuracy of most presently used cooling tower fan power measurement methods is often

in the five to 7% range? The chart below illustrates the differences in measured capability found using each of the three fan power measurement methods on an actual ten-cell mechanical draft tower.

Method	Measured Input Horsepower	Calculated Capability %
Clamp-on Wattmeter	221	96.8
Clamp-on Ammeter + Voltmeter	211	98.3
Power Meter and Split Core Current Transformer	203.5	99.5

In this case the clamp-on wattmeter results were 2.7% in error when compared to the more accurate power meter - current transformer method. Had the clamp-on wattmeter results been used in an acceptance test, the tower purchaser may have been inclined to ask for 2.7% of the cost of the tower in refund. In this case the tower cost $3 million and the refund would have been $81,000. The purchase and use of the more accurate power system would have been easily justified for the tower vendor.

REFERENCES

1. Power Measurements for Energy Cogeneration, Plant Electrical Systems, pp. 36-42, January 1980.

2. Electrical Power Measurement Handbook, Yokogawa Corporation of America, pp. 3-16, 1979.

PB82-228115

HEAT TRANSFER CHARACTERISTICS OF A PLATE-FIN CONDENSER WITH DELUGED WATER AUGMENTATION FOR COOLING TOWERS

Hans D. Fricke and Ken McIlroy
Union Carbide Corporation, Linde Division
Tonawanda, New York 14150

John A. Bartz
Electric Power Research Institute
Palo Alto, California 94304

ABSTRACT

This paper describes an EPRI-funded, experimental evaluation of an advanced, air-cooled ammonia condenser for a phase-change dry/wet-dry cooling system for electric power plants. A condenser of similar design, but much bigger, is about to be tested in a 10 MWe demonstration plant at the Pacific Gas & Electric Kern Station in Bakersfield, California.

In this cooling concept, the reject heat from the power plant is transferred to liquid ammonia in a steam condenser/ammonia reboiler, rather than by conventional condensation of steam by coolant water. The ammonia vapor generated is subsequently condensed in a cooling tower by heat rejection to the atmosphere.

This condenser, comprised of an aluminum plate-fin/tube assembly (8 ft. x 7 ft. frontal area), was tested under representative operating conditions in Union Carbide's ammonia phase-change pilot plant (0.3 MWe) in both the dry and wet (water deluge on air-side) mode.

Heat transfer and air-side pressure loss characteristics were measured under varying air face velocities from 300 to 800 FPM and initial temperature differences (ITD) from 10 to 50°F. Deluge rates varied from 0 to 3.0 gpm/ft. of core width. In the dry mode, overall heat transfer coefficients ranged from 7 to 12 BTU/hr-ft^2°F (based on air-side surface) depending on face velocity. During wet operation increasing water deluge greatly enhanced the heat rejection capacity over dry operation - as high as 4 times, depending on operating conditions. This deluge augmentation was greater for lower air relative humidities and lower ITD's.

For reference, the paper includes pertinent results* from prior experiments with a bench-scale size condenser (2-1/2 ft. x 2 ft. frontal area) and with an integral shaved fin/extruded aluminum tubing. A brief description of the recently completed ammonia phase-change dry/wet-dry cooling demonstration plant at the Kern Station is also presented.

---

* Previously published.

1. INTRODUCTION

For over a decade, considerable interest has existed in dry (non-evaporative) cooling to dissipate heat from steam-electric power stations. Dry cooling offers the elimination of thermal pollution of lakes and streams caused by once-through cooling, as well as a method to avoid water makeup, blowdown, and fogging problems associated with wet (evaporative) cooling. In addition, dry cooling increases siting flexibility, particularly for locations in arid Western coal fields.

However, dry cooling requires considerable capital investment for the cooling towers. Hence, the development of efficient (low cost) heat transfer surfaces in conjunction with new cooling processes is very important for this approach to be economically feasible. Extensive studies have indicated that although heat exchangers contribute about 35% of the cost, the entire heat transport system, not merely the heat exchangers, need to be evaluated to achieve an attractive alternative [1]. This must include acceptable transport fluids to transfer the heat from the steam condenser to the ambient air, effective methods to transfer heat and methods of achieving augmented cooling during hot dry weather.

Beginning in 1975 the Electric Power Research Institute (EPRI) sponsored a program of dry cooling research proposed by Union Carbide Corporation, Linde Division and Westinghouse Electric Corporation. The primary object of this effort was to study, select and demonstrate a heat-rejection cycle of substantially increased thermal performance to reduce the large penalties commonly associated with conventional dry cooling where circulating water (the coolant in an indirect dry system) is heated in the steam condenser and, subsequently cooled in the cooling tower. The recommended concept consisted of an isothermal ammonia phase-change heat rejection cycle with heat transfer enhancements on the heat exchanger surfaces. The reject heat from the power plant is transferred to liquid ammonia in a steam condenser/ammonia reboiler* and the ammonia vapor thus generated is condensed in a cooling tower by heat rejection to the atmosphere.

In order to demonstrate the feasibility of this concept, a test pilot plant (0.6 MW_{th}) was designed, built and operated by Union Carbide under EPRI contract. Primary objectives were to demonstrate the integrated performance of this cooling scheme using Union Carbide's heat transfer enhancements in the steam condenser/ammonia reboiler and to test the performance of advanced air-cooled ammonia condensers in the cooling tower. Aside from having successfully demonstrated the feasibility of ammonia phase change for dry cooling at the pilot plant scale, three ammonia condensers were tested: the Curtiss-Wright integral shaved fin - extruded aluminum tubed heat exchanger (designed for dry operation) and two different-size condensers of the same basic Hoterv aluminum plate-fin tube configuration. The latter entailed a bench scale size (2.5 ft. wide x 2.0 ft. high) core and a pilot model (8.0 ft. wide x 7.2 ft. high), which were tested in the dry and water deluged mode. Water deluge entails wetting the air-side surface of the condenser to improve the heat

* Featuring Union Carbide's doubly-enhanced heat transfer tubing.

transfer performance of dry cooling towers during periods of high ambient air temperature. Augmentation of the convective tube-to-air heat transfer is achieved by the evaporative cooling of the water as it flows over the external surface. This technique will result in an economical peak shaving approach with minimal water consumption.

The experimental studies by Union Carbide of the Curtiss-Wright and the Hoterv bench scale condenser were previously reported [2]. More recently, however, a test program with the larger Hoterv heat exchanger was completed and is the subject of this paper. Other efforts related to this ammonia phase change dry cooling work are fully described in [3] and [4]. The specific objectives of the subject experiments, were to:

(1) measure the heat transfer and air-side pressure loss characteristics of this plate-fin air-cooled condenser with and without water deluge.
(2) assess scale-up effects - evaluate the performance under less controllable air flow and temperature conditions than exist under laboratory type environments.

The bench scale condenser had been tested inside an air duct with baffles for supplying a uniform air flow at constant temperature. The pilot model, however, was installed in a larger cooling tower, located outside where it was subjected to random variations of the ambient weather conditions (wind velocity etc).

Where appropriate, test data were compared to results from the prior bench scale condenser experiments [2] and [3] and from Battelle's WATA test program [5].

2. TEST FACILITY

An ammonia phase change dry/wet cooling pilot plant was built and tested for demonstrating the concept and for measuring the heat transfer performance of augmented heat exchangers [3]. A simplified schematic of the concept is shown in Fig. 1.

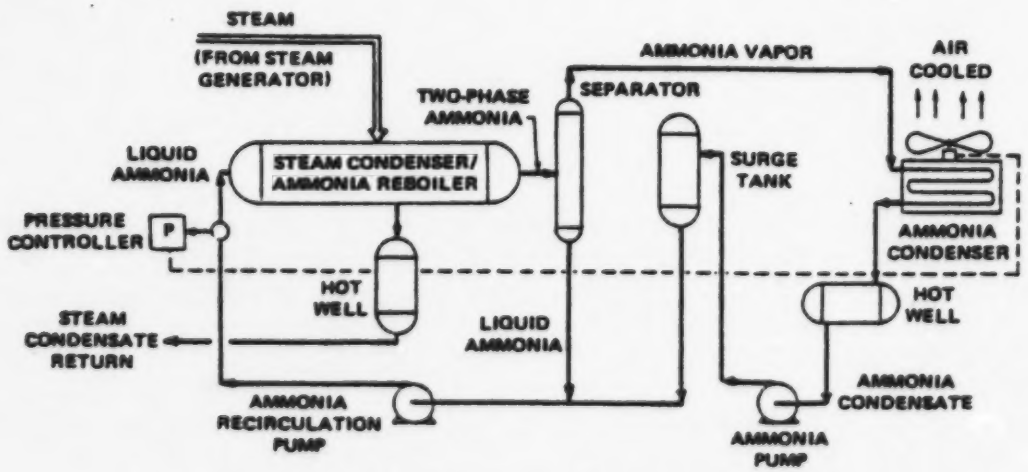

FIG. 1. ADVANCED DRY COOLING PILOT PLANT FLOW SCHEMATIC

There are two primary flow loops: the anhydrous ammonia isothermal phase change circuit which transports the heat from the steam condenser/ammonia reboiler to the ammonia air-cooled condenser in the cooling tower and the steam/condensate loop which provides the source of low pressure steam to the condenser/reboiler from a commercial steam generator.

Basically, the liquid ammonia is pumped from the surge and phase separator tanks into the steam condenser/ammonia reboiler where it boils inside High Flux* tubes, extracting heat of condensation from the shell-side condensing steam. Two-phase ammonia exits the condenser/reboiler and enters the phase separator from which the vapor is subsequently condensed in the air-cooled condenser installed in the cooling tower. The liquid is collected in the hotwell to be pumped back to the surge tank. Steam is condensed in the condenser/reboiler on the outside of the tubes which also incorporate a Union Carbide condensing enhancement. The steam condensate is collected in the hotwell and returned to the generator to be recycled.

The system was designed for a nominal heat load of 0.6 MWth when condensing steam at 5 inches Hg absolute pressure (T_{sat} = 134°F). At design condition, this would translate to condensing steam at 2000 lb/hr, boiling and condensing 4500 lb/hr of ammonia at 315 psig (T_{sat} = 129°F) with an air flow rate of 75,000 CFM across the ammonia condenser at 93°F ambient air temperature.

A more detailed schematic of the pilot plant's test cooling tower is presented in Fig. 2.

Saturated ammonia vapor flows from the phase separator to the test condenser in the tower. The condensate is returned from the hotwell to the surge tank. The system ammonia pressure can be varied from 150 to 350 psig to control the condensing temperature and thereby the ITD**.

A dual-compartment water distribution system was installed above the condenser for testing in the wet mode. It was designed to water deluge the heat exchanger at rates up to 3 gpm/ft. of core width.

The deluge injection system (of same basic design as used in the Battelle tests [5]) consists of two perforated aluminum pipe (2 in. diameter) manifolds delivering water to a bed of plastic distribution rings nested directly on top of the test core. Guide vanes, at the distributor pipe, direct the discharging water spray over the rings. Prior to the actual tests both injection systems were operated at varying water flow rates (either separately or in combination) until a uniform water coverage over the entire air-side (top to bottom) was achieved, depending on the desired air face velocity. Excess water was collected in a basin below the condenser.

A heater in the loop, raises the temperature of the supply augmentation water to that of the ambient air.

---

* Union Carbide patented porous boiling surface which greatly enhances boiling heat transfer by typically 5-10 times that of a plain surface.

** Initial Temperature Difference = Ammonia Saturation Temp.-Inlet Air Temp.

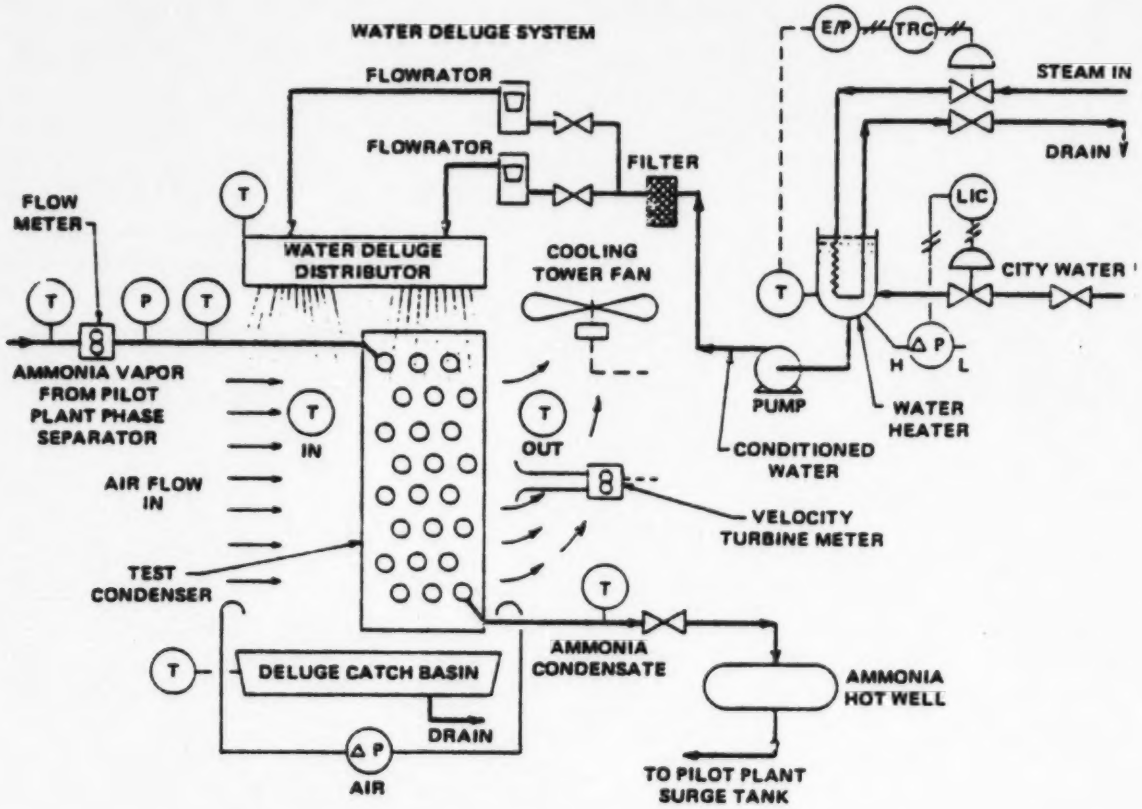

FIG. 2 HOTERV PILOT MODEL CONDENSER TEST SYSTEM SCHEMATIC

A variable-pitch fan, on top of the cooling tower, induces the ambient air flow across the condenser core.

As noted in the figure, thermocouples (in the ammonia, water and air streams), pressure transducers (absolute and differential), and turbine flow meters were provided to measure the heat transfer and air-side pressure loss characteristics of the test condenser.

This unit is of identical design as the previously tested bench scale heat exchanger except it is much larger. It has 11 times more frontal area and has a heat rejection capability of up to 2×10^6 BTU/hr at an air velocity of 800 FPM and a 50°F ITD. The condenser's total air-side area is 4543 ft^2. It is basically an aluminum plate-fin/tube configuration, developed and manufactured by the Hoterv Institute, a Hungarian organization and supplied by Babcock & Wilcox, the licensee and U.S. distributor. It is typically used for water-cooled heat exchanger applications.

As noted in Fig. 3, the assembly basically consists of two rectangular headers, manifolding the staggered horizontal tubing which pass through a closely spaced stack of aluminum plate-fins (8.9 fins/inch). Because of the relatively high operating pressures (up to 400 psig) used in the tests, carbon-steel liners (0.57 in. I.D. x 0.67 in. O.D.) were employed inside the

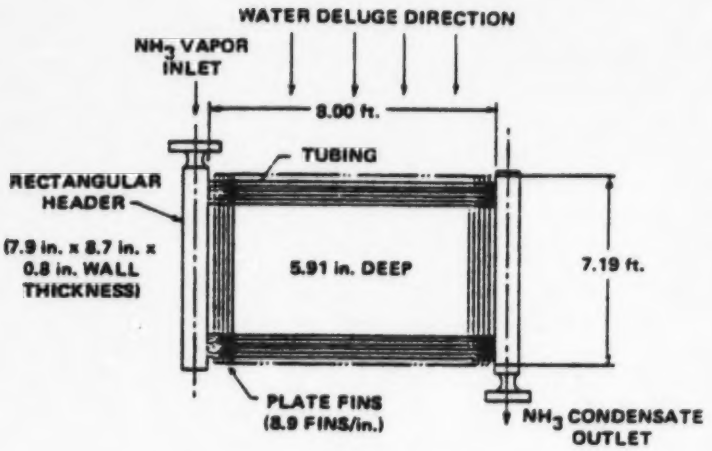

FIG. 3. HOTERV AMMONIA CONDENSER

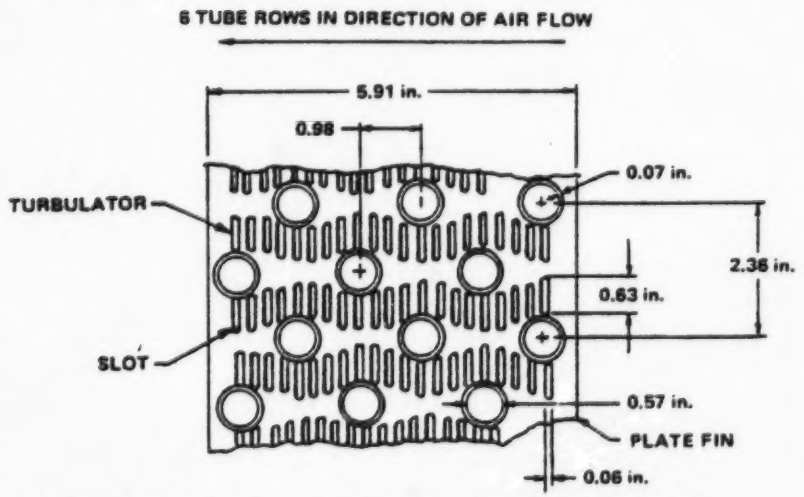

FIG. 4. HOTERV CONDENSER PLATE–FIN CONFIGURATION

aluminum tubes (0.71 in. O.D.). The air-to-condensing side area ratio was 17.3.

As illustrated in Fig. 4 the plate-fins of the condenser feature patterns of slots and raised turbulators to enhance the air-side heat transfer, which is the controlling resistance. Typically, 63% of the total thermal resistance is on the air-side, 30% on the condensing ammonia side and 7% is due to the tube wall resistance.

2.1 Test Variables and Procedure

In the dry mode the condenser was tested at air inlet velocities of 400, 600, and 800 FPM (probable velocity range for a full size system) and at ITD's ranging from 10 to 50° F. The desired air velocity (measured with a turbine flow

meter) was achieved by adjusting the variable pitch of the fan blades. The air-side pressure (static) loss across the core was measured via a differential pressure cell. ITD was controlled by varying the system ammonia pressure to a level such that the corresponding vapor saturation temperature differed from that of the ambient air by the desired amount. This was accomplished by controlling the amount of ammonia to be vaporized in the condenser/reboiler, which entailed adjusting the steam flow (heat duty) to the condenser/reboiler. Once the system reached steady-state, the pertinent parameters were recorded with the data acquisition system and the performance was automatically evaluated and printed with the on-line desk computer.

For the wet-mode testing the condenser was operated at three selected air-side pressure drops* (ΔP); namely 0.28, 0.55 and 0.84 in. of water. These ΔP's are equal to those of the dry mode cases when the corresponding air face velocity was 400, 600 and 800 FPM. The probable method of utilizing a deluge system in practice, is to have certain sections of heat exchanger cores within a cooling tower operating under deluge conditions with other sections operating dry. Thus, the air flow through each core will be self-regulating such that the ΔP through each is equal. Hence, it was decided that the performance comparison between the dry and deluged operation would be more meaningful if the ΔP across the condenser would remain constant.

Water deluge ranged from 0.5 to 3.0 gpm/ft. of core width with ITD's at 10 and 20°F. An effort was made to evaluate the deluged unit over a range of ambient air relative humidities for each test conditions; however, the available humidity ranged between 30 to 65%.

3. DISCUSSION OF RESULTS

The results from the dry mode experiments are first summarized, followed by a discussion of the water deluge tests.

A parameter of key interest to the designer is the power consumed by the tower fans to draw the air through the condenser. Hence, in Fig. 5, the overall heat transfer coefficient, U, of the Hoterv surface, is plotted as a function of fan power.

The coefficient and fan power are expressed per square foot of core frontal area and the heat rejected is based on the measured rate of ammonia condensation. This figure illustrates the trends and is specific for an ITD of 20°F. The fan power here is defined as the product of the measured air velocity and pressure loss. It is cautioned that actual fan power will of necessity be greater and include windage losses, frictional drag of mechanical parts and motor inefficiencies.

As expected, U increases with fan power. Higher power entails more air flow resulting in greater turbulence and improved air-side heat transfer. The data from the two Hoterv condensers agree within approximately 7%. Scale-up effects and non-uniform air flow into and within the cooling tower could have

* By changing the induced air flow via the fan-blade pitch.

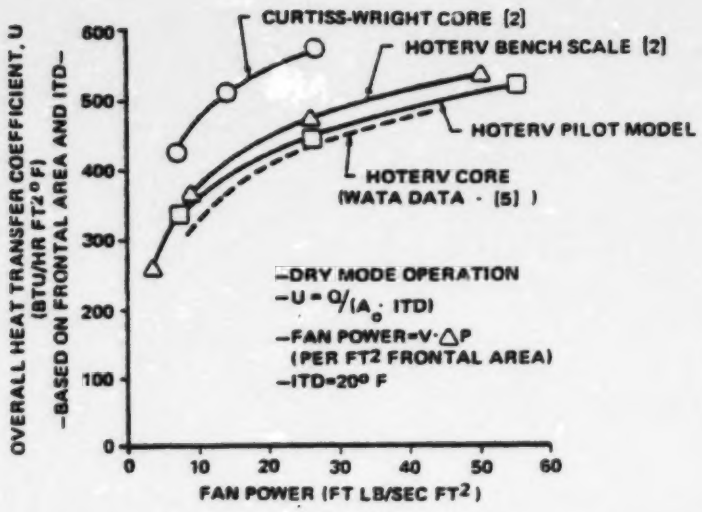

FIG. 5. OVERALL HEAT TRANSFER COEFFICIENT VS. FAN POWER

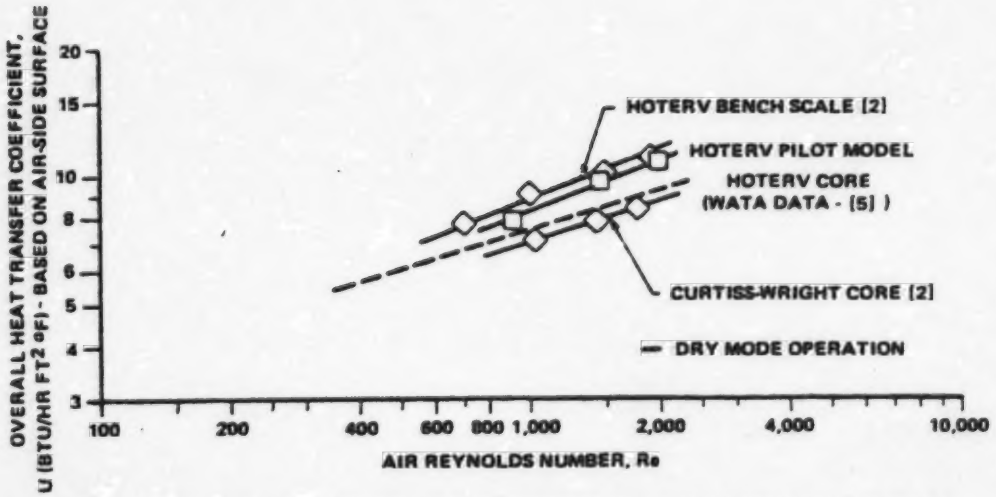

FIG. 6. OVERALL HEAT TRANSFER COEFFICIENT vs AIR REYNOLDS NUMBER

caused this slight disagreement. Included in the figure are Battelle's data [5] which agree with those of the pilot model condenser. For reference, results on the Curtiss-Wright heat exchanger [2] have been superimposed. Although this unit shows a larger heat transfer coefficient than the Hoterv core at any specific fan power, it must be cautioned that the ultimate criterion of cost-effectiveness must be determined by comparing not only the capital cost of each surface (including supporting structures) but also assessing the power consumption, operating and maintenance cost over the life of the plant.

Fig. 6 presents U as a function of air Reynolds number (based on minimum air-side cross-sectional flow area) for the pilot model condenser. Included

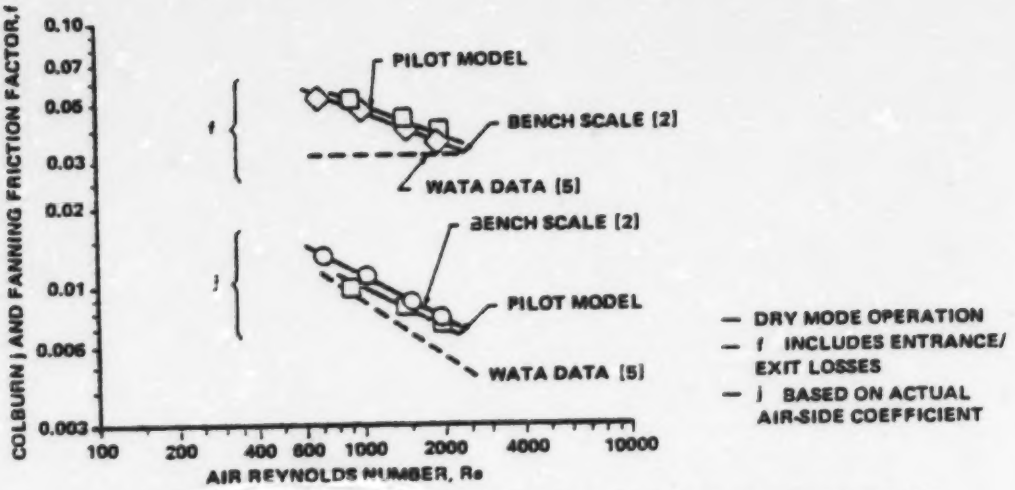

FIG. 7. COLBURN j AND FANNING FRICTION FACTOR AS A FUNCTION OF AIR REYNOLDS NUMBER FOR THE HOTERV SURFACE

are results on the Curtiss-Wright core, from the bench-scale tests and Battelle's measurements on a similar core. The coefficient was determined from the measured heat rejection rate, log mean temperature difference (LMTD), and air-side surface area. It includes the thermal resistance due to the condensing ammonia, tube wall, and air-side. The ammonia condensing coefficient was computed by an iterative type integration procedure employing the Rosson and Meyers correlation [6].

The familiar, dimensionless heat transfer and air-side pressure loss parameters, Colburn j and Fanning friction factor, f, are presented in Fig. 7 as a function of air Reynolds number. Even though the conventional friction factor representation is without the heat exchangers entrance/exit pressure losses, the f-factor shown includes these. As expected both parameters decrease with increasing air Reynolds number. Reasonable agreement between the different frontal area condenser surfaces can be observed.

In studying the wet performance of the Hoterv condenser, one of the important comparison parameters for a given size and cost of heat exchanger is the ability to efficiently reject heat based on an equal air-side pressure loss. It was, therefore, decided that the air-side ΔP across the deluged condenser should be adjusted to correspond to that obtained for the dry cases, as explained in Section 2.1.

The effect of water deluging the air-side surface on the degree of cooling enhancement is shown in Fig. 8 to 10 for the three selected air-side ΔP's and for 10 and 20°F ITD. The indicated air relative humidity (R.H.) is the average value ($\pm$ one standard deviation) measured over the particular test series. The enhancement is defined as the ratio of the quantity of heat rejected with the surface deluged to the amount rejected dry (Q_{wet}/Q_{dry}) at equal air-side ΔP

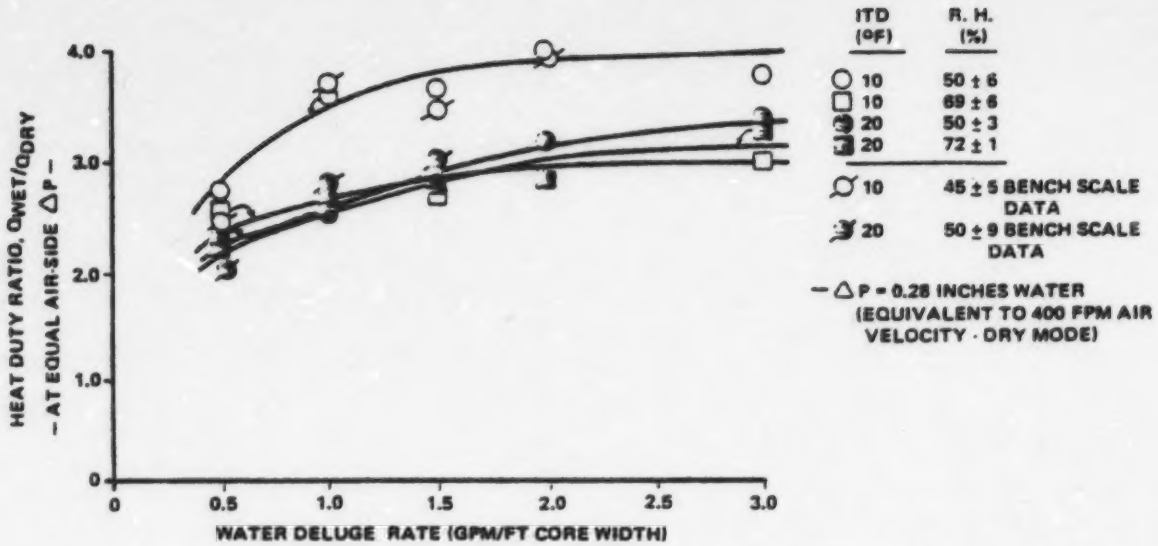
HEAT DUTY RATIO, Q_{WET}/Q_{DRY} – AT EQUAL AIR-SIDE ΔP –
WATER DELUGE RATE (GPM/FT CORE WIDTH)
ITD (°F)
R. H. (%)
10 50 ± 6
10 69 ± 6
20 50 ± 3
20 72 ± 1
10 45 ± 5 BENCH SCALE DATA
20 50 ± 9 BENCH SCALE DATA
— ΔP = 0.28 INCHES WATER (EQUIVALENT TO 400 FPM AIR VELOCITY - DRY MODE)

FIG. 8. HEAT TRANSFER ENHANCEMENT AS A FUNCTION OF WATER DELUGE RATE

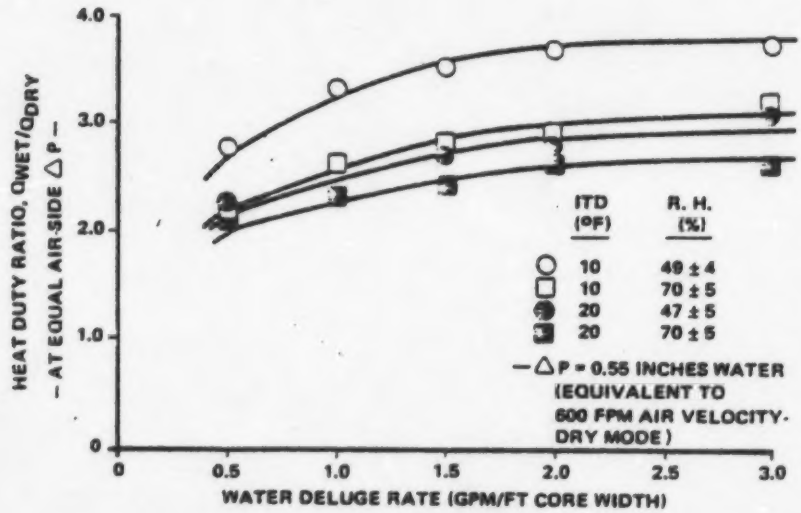
HEAT DUTY RATIO, Q_{WET}/Q_{DRY} – AT EQUAL AIR-SIDE ΔP –
WATER DELUGE RATE (GPM/FT CORE WIDTH)
ITD (°F)
R. H. (%)
10 49 ± 4
10 70 ± 5
20 47 ± 5
20 70 ± 5
— ΔP = 0.55 INCHES WATER (EQUIVALENT TO 600 FPM AIR VELOCITY - DRY MODE)

FIG. 9. HEAT TRANSFER ENHANCEMENT AS A FUNCTION OF WATER DELUGE RATE

and ITD. Q_{wet}/Q_{dry} ratios as high as 4 were measured depending on operating conditions. Higher ratios can be expected at much lower air relative humidities as indicated later. As noted especially from Fig. 10 the enhancement ratio is higher at lower ITD's because Q_{dry} will decrease as the ITD becomes smaller, whereas Q_{wet} will remain relatively high, providing the relative humidity is less than 100%. Also note that the rate of enhancement improvement (over dry operation) with increasing deluge rates essentially diminishes as deluge rates exceed 1.5 to 2 gpm/ft. core width - regardless of the tested ITD and air-side ΔP. This is explained by the fact that, (1) there is a limit to the total quantity of deluge water that is effective (can be evaporated under

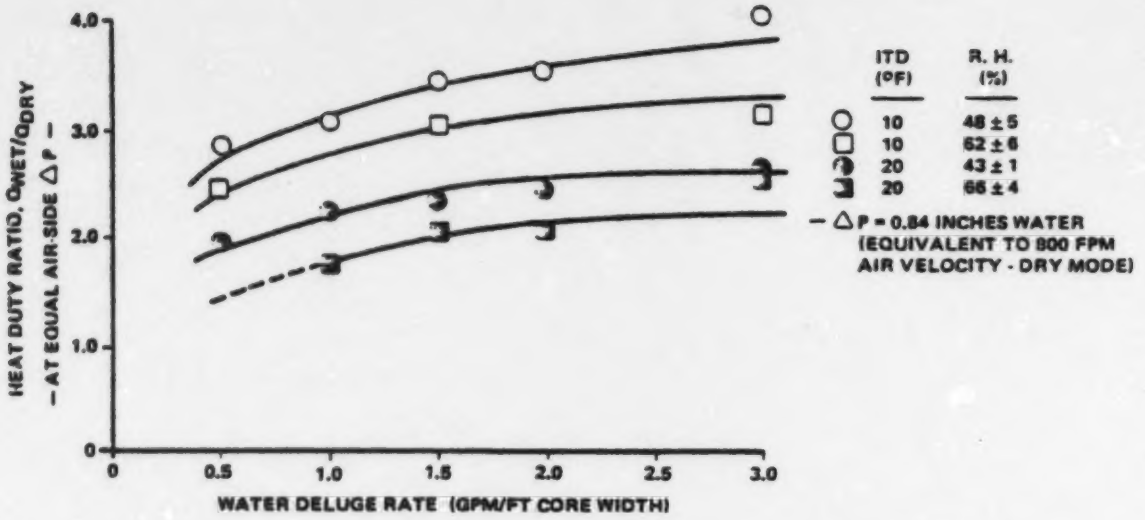

FIG. 10. HEAT TRANSFER ENHANCEMENT AS A FUNCTION OF WATER DELUGE RATE

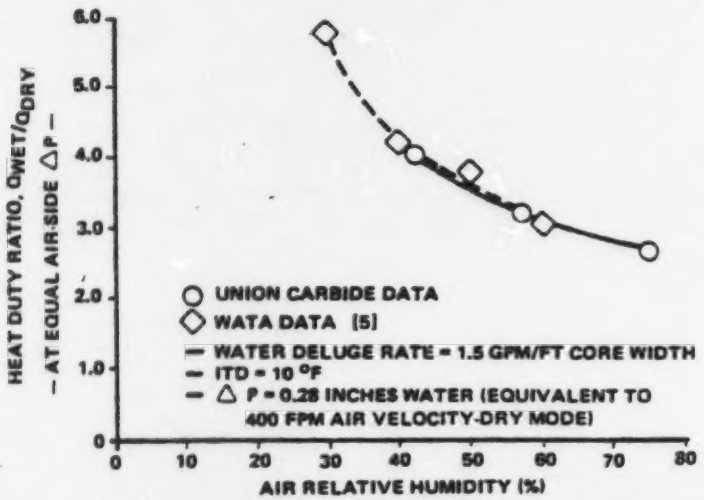

FIG. 11. DELUGE ENHANCEMENT AS A FUNCTION OF AIR RELATIVE HUMIDITY

particular ambient conditions) and the resulting rate at which heat can be rejected; and (2) as deluge rate is increased, air flow through the core necessarily decreases due to increasing restriction to air flow. The figures also demonstrate that the enhancement due to the evaporative cooling of the water is higher at lower inlet air humidity levels. The reason is that the evaporation rate of the deluge water increases as the air relative humidity decreases, thereby increasing the heat dissipation capability. To better illustrate this effect, Q_{wet}/Q_{dry} was plotted as a function of air relative humidity in Fig. 11 for a typical operating condition of 10° F ITD and 1.5 gpm water deluge/ft. core width. The strong influence of ambient air humidity can be observed in this

figure. Good agreement is noted with results from Battelle's tests [5] on a similar deluged heat exchanger.

4. CONCLUSIONS

For dry operation, the overall heat transfer coefficients of the Hoterv ammonia air-cooled condenser ranged from 7 to 12 BTU/hr ft^2°F (based on air-side surface) depending on air Reynolds number. Water deluging the condenser improves heat transfer performance manyfold. The greatest enhancement is achieved at low air relative humidities and lower ITD's. The improvement increases with higher deluge rates up to a point where any further increase in deluge offers little improvement. Fortunately the augmentation is greatest at low ITD's when it is needed most--during high ambient air temperatures.

However, it must be emphasized that even though considerably higher heat rejection rates can be obtained with increasing deluge, the economics of the entire cooling system must ultimately be evaluated. For an optimum system, fan power, capital costs, water resources and cost, maintenance, etc. must be considered and compared against alternative peak shaving concepts. Also, one important consideration is corrosion and scaling tendencies of the air-side surface due to water deluge which could cause performance degradation. To minimize these effects "treated" water should be used or following water-deluge a "softened" and de-ionized rinse water be applied to clean the surface. This, obviously, increases cost and tends to somewhat offset the economic advantages of higher performing water-augmented cooling tower condensers.

It can also be concluded from these experiments that, within the experimental error, the heat transfer and air-side pressure loss characteristics between the pilot model and bench scale Hoterv condenser are essentially identical and agree well with Battelle's results on a similar, small size Hoterv heat exchanger. This implies that condensers of the plate-fin configuration could be designed for a full size (e.g. 1000 MWe) cooling tower system using performance parameters measured on much smaller (bench scale size) test cores.

5. DEMONSTRATION PLANT

A consequence of experimental work described and other related studies [3], [5], [7] has resulted in the design and construction of an ammonia phase-change dry/wet cooling tower demonstration plant at Pacific Gas and Electric's existing Kern Power Station in Bakersfield, California [8],[9]. It is called the Advanced Concept Test (ACT) Facility. It was designed and constructed under EPRI sponsorship, and will be operated with funding from DOE, EPRI, PG & E and a utility consortium. Battelle (Pacific Northwest Laboratories) is the project manager, C. F. Braun and Company is the Architect and Engineering firm and Union Carbide the project advisor, a major component supplier and a test participant.

The chief objective of the ACT Project is to develop and demonstrate safe and reliable dry/wet cooling tower systems that can be applied to conserve water resources, increase power plant siting flexibility, and give

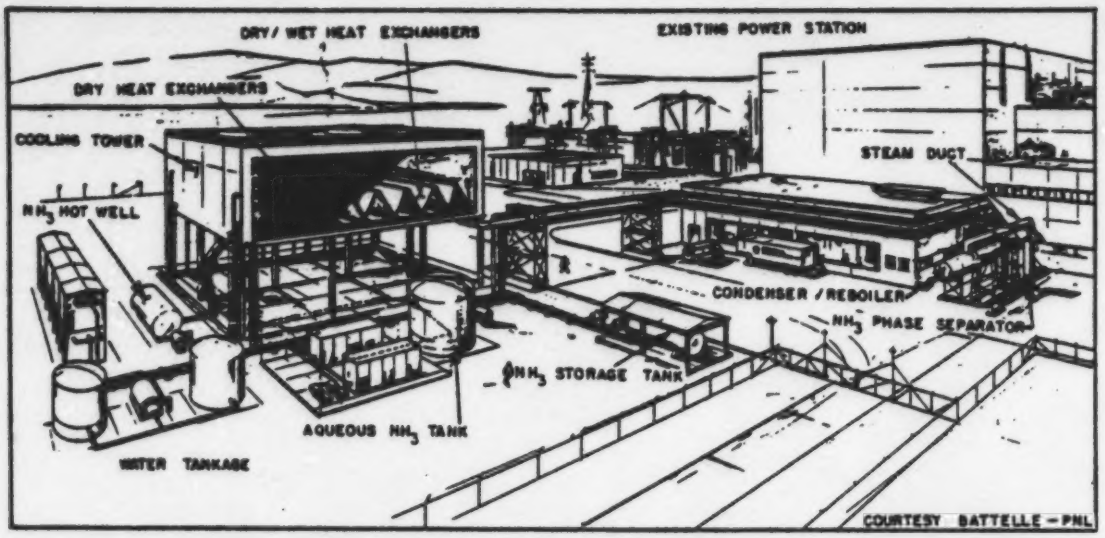

FIG. 12. ADVANCED CONCEPT TEST FACILITY AT THE P.G. & E. KERN POWER STATION

efficient power plant performance over a year's cycle, at costs (capital plus operating) substantially below systems presently available from manufacturers.

The project is focused on large scale testing of advanced concepts of dry and dry/wet cooling of electric power stations.

The significant advantages of an ammonia heat transport system include: 1) less cooling tower surface due to a larger heat transfer temperature driving force with the isothermal condensation of ammonia; 2) smaller transfer lines due to the low volumetric flow rates and high latent heat of vaporization of ammonia; 3) no low-temperature safety freeze protection systems in the cooling tower; and 4) no power requirements to move vapor to the tower and little power is needed to return the liquid ammonia to the steam condenser/ammonia reboiler.

The ACT system is basically identical to Union Carbide's pilot plant except its heat rejection capability will be 30 times greater. The facility shown in Fig. 12 as an artist's sketch will operate by redirecting the exhaust steam from the existing 6 MWe house turbine to the enhanced steam condenser/ ammonia reboiler, where steam is condensed against boiling ammonia. The resultant two-phase ammonia mixture passes through a separator from which the vapor is sent to air-cooled condensers in the cooling tower and the liquid is recycled back to the steam condenser/ammonia reboiler. The latter is Union Carbide's shell and tube heat exchanger of a removable bundle design featuring 1369 aluminum tubes (20 ft. long x 1 in. O.D.). The tubes incorporate Union Carbide's heat transfer enhancements: High Flux Porous Boiling Surface on the inside and on the outside a Thin Film Condensing Promoter. This heat exchanger will nominally condense 60,000 lb/hr of steam flow corresponding to

about 10 MWe, at a 5°F temperature difference. This is based on an overall service (includes fouling resistance) U of 1700 BTU/hr ft^2°F which was measured in the pilot plant.

The induced draft cooling tower contains four (15 ft. diameter) 50 HP variable pitch fans and houses Curtiss-Wright aluminum shaved-fin condenser modules (for dry mode testing) and Trane's aluminum plate-fin type condenser for dry or wet operation. Testing of either surface will be done independently. The dry cores (60 ft. long x 18 ft. high) are installed on two opposite sides of the rectangular tower whereas the dry/wet units are mounted in delta configuration across the elevated bottom platform within the tower structure.

Plywood panels are employed to prevent air flow through the surfaces not being tested.

The total face area of the Curtiss-Wright condensers is 2160 ft^2. These units were designed to remove 61.2×10^6 BTU/hr at an ITD of 70°F and an air face velocity of 800 FPM. At ITD's less than 70°F, a commercial water-cooled augmentation ammonia condenser is used in parallel with the dry module.

Trane's dry/wet condenser system consists of seven delta assemblies - two 31 ft. long x 9 ft. high panels each. They will operate dry when the ITD is greater than 70°F. When it is less (ambient air temperature exceeding 55°F), the vertical plate fins will be deluged with water to enhance their heat dissipation capability.

The construction of this test facility has been completed and testing will commence in the summer of 1981.

ACKNOWLEDGEMENTS

The program described in this paper was sponsored by the Electric Power Research Institute (EPRI), Contract No. RP 422-2.

Special recognition is given to Messrs. C. F. Gottzmann, F. Notaro and J. B. Wulf (Union Carbide), Mr. G. J. Silvestri (Westinghouse) and Drs. R. W. Zeren and J. Maulbetsch (EPRI) for their efforts in originating and developing the study of the ammonia phase-change dry-cooling concept.

The authors gratefully acknowledge D. J. Webster who was responsible for the design, construction and testing of the pilot plant. Appreciation is also expressed for the assistance of many colleagues in various facets of this particular effort; in particular Messrs. L. R. Niendorf, M. H. Gallisdorfer, T. D. Craig, R. A. McClellan, R. Victor, J. P. Smith and Ms. C. E. McHale.

The authors also wish to acknowledge their colleagues at Battelle (PNL) for helpful information exchange during the test program.

REFERENCES

1. McHale, C. E. Webster, D. J. Jablonka, G. E., Bartz, J. A., New Developments In Dry Cooling of Power Plants, Proc. of the American Power Conference, Vol. 1, pp 673-684. 1979

2. Fricke, H. D., Webster, D. J., McIlroy, K., Bartz, J. A., Heat Transfer Performance of a Dry and Wet/Dry Advanced Cooling Tower Condenser, paper presented at the 19th ASME-AIChE National Heat Transfer Conference, Orlando, Florida, July 1980, ASME Paper No. 80-HT-99.

3. Fricke, H. D., Helenbrook, R. G., McHale, C. E., McIlroy, K., Webster, D. J., Power Plant Waste Heat Rejection Using Dry Cooling Towers, Union Carbide Corp.,Linde Division Interim Report for EPRI Contract, RP 422-2, Tonawanda, NY, December, 1979.

4. Fricke, H. D., Helenbrook, R. G., McHale, C. E., Webster, D. J., Power Plant Waste Heat Rejection Using Dry Cooling Towers, Union Carbide Corp.,Linde Divison Summary Interim Report for EPRI Contract RP 422-2, EPRI-CS-1324, February 1980.

5. Parry, H. L., MacGowan, L. T., Kneid, D. K., Wiles, L. E., Faletti, D. W., Johnson, B. M., Augmented Dry Cooling Surface Test Program: Analysis and Experimental Results, Battelle (PNL) Report No. PNL-2746, Richland, Washington. September 1979.

6. Rosson, H. F., and Meyers, J. A., Chem. Engr. Progr. Symposium, No. 59, 61, pp 190-199, 1965.

7. Braun, D. J., Tokarz, R. D., Johnson, B. M., Allemann, R. T., Braun, David J., Faletti, D. W., MacGowan, L. J., Parry, H. L., Smith, G. C., and Zaloudek, F. R., Comparative Cost Study of Four Wet/Dry Cooling Concepts that Use Ammonia as the Intermediate Heat Exchange Fluid. PNL-2661, Battelle, Pacific Northwest Laboratories, Richland; WA 99352, May 1978.

8. Johnson, B. M., ed. Development of an Advanced Concept Dry/Wet Cooling of Power Generating Plants, Battelle Northwest Interim Report of Research Project RP 422-3 with the Electric Power Research Institute, EPRI-CS-1668, February 1981.

9. Zaloudek, F. R., Brown, L. J., and Allemann, R. T., Advanced Concepts Facility - Measurements and Suggested Test Plan, Battelle Northwest Research Project RP 422-3 with the Electric Power Research Institute EPRI-CS-1530, September 1980.

PB82-228123

STATUS REPORT ON ADVANCED COOLING TOWER PROJECT

R. T. Allemann and B. M. Johnson
Dry Cooling Enhancement Program
Battelle, Pacific Northwest Laboratories
Richland, Washington

J. A. Bartz
Water Quality Control and Heat Rejection Program
Electric Power Research Institute
Palo Alto, California

ABSTRACT

Under the auspices of the Electric Power Research Institute (EPRI) and with contributing work of Union Carbide Corporation, Linde Division, a large-scale test of dry/wet cooling using the ammonia phase-change system, designated the Advanced Concepts Test (ACT), has been constructed at Pacific Gas and Electric Company's Kern Station at Bakersfield, California.

The interest in dry cooling stems from the growing realization that the use of inland water to provide a heat sink for the thermal generation of power cannot continue to increase indefinitely. It is likely that in many locations fresh water will only be used to supplement cooling and will occur through a combination of wet and dry systems.

The test facility described here will be capable of condensing 50,000 lbs/hr of steam from a small auxiliary turbine and will use only 25 percent of the water normally required to reject this heat load in evaporative cooling towers. Two different modes of combining dry and evaporative cooling are being tested. One uses deluge cooling in which water is allowed to flow over the heat exchanger on hot days. The other uses a separate evaporative condenser in parallel to the dry heat exchanger. The design of the cooling system and major components is described, and the technology developed to support the design is summarized. Construction of the project is complete and shakedown and operational testing of subsystems has begun.

Included in the discussion are some details of the cooling tower with both dry and wet/dry surfaces, vapor and liquid piping, deluge and rinse procedure, control, and safety aspects. Technical and experimental backup of some of the design decisions is reviewed. The projected methods of testing and obtaining operational data with a digital data acquisition system are discussed.

1. INTRODUCTION

The Advanced Concepts Test (ACT) Facility has just been constructed at the Kern Station of the Pacific Gas and Electric Company in Bakersfield, California, under the funding of the Electric Power Research Institute (EPRI). The advanced cooling tower project would be a more descriptive name. The Union Carbide Corporation/Linde Division has been working with Battelle-Northwest in carrying forth the conception, design, and construction of this facility. C. F. Braun has provided the detailed design and construction management of the facility.

The system will condense the steam from a turbine, about equivalent to a 10 MW_e turbogenerator, and demonstrate the use of ammonia as a heat-transfer medium between the last stage of the turbine and the air, using alternative types of heat exchangers.

The interest in dry cooling stems from the growing realization that the use of inland water to provide a heat sink for the thermal generation of power cannot continue to increase indefinitely. It is likely that fresh water will only be used to supplement cooling and will occur through a combination of wet and dry systems. This is because using a small amount of cooling water significantly reduces the cost of dry-cooling systems - far greater than the proportionate difference between dry- and evaporative-cooled systems.

Dry cooling of thermal power plants has been the subject of many economic studies and several research programs directed at comparing dry cooling with alternative heat-rejection systems; i.e., once-through, evaporative, and several types of dry and hybrid systems. The research programs have focused on ways to reduce the capital and operating costs of dry cooling, since this method of heat rejection is projected to be more expensive than current (state-of-the-art) conventional ways of cooling power plants.

As a result of early program activities, the water-augmented, intermediate-ammonia system, dry-cooling concept was shown to be potentially more economical to build and operate than other dry cooling concepts. The large-scale Advanced Concepts Test (ACT) Facility project was undertaken to evaluate the technical feasibility of this concept and to provide utilities with the confidence to use the resultant technology for a full-scale demonstration and, eventually, in commercial generation of electricity.

The overall project objective is to develop water-conserving cooling systems that offer the lowest cost alternative to utilities faced with a shortage of water for cooling.

2. SYSTEM DESCRIPTION

The ammonia heat transport system is used because of the high heat transport effectiveness and volumetric efficiency of the phase-change ammonia system in the temperature range of use. Figure 1 schematically shows the temperature of the ammonia as it changes from liquid to vapor in the condenser/reboiler at a constant temperature difference, passes to the air-cooled tower, is condensed by the air cooling, and is cycled back to the condenser/reboiler. The figure shows a parallel diagram for an indirect water-cooling circuit. The flow diagram of the system, shown in Figure 2, includes the first two types of surfaces that are to be tested.

Augmentation by evaporative cooling is also shown in Figure 2. It provides a higher driving force for heat transfer when the air temperature gets very high and greatly reduces the size and cost of the cooling tower.

The evaporative cooling to augment the dry cooling is done at ACT in either of two ways, which will be tested separately:

1) In parallel with the dry heat exchanger: condensing the ammonia in an evaporative condenser (one in which the bare condenser tubes are cooled by water and air flowing simultaneously over the outside surface) manufactured by Baltimore Aircoil. The all-dry heat exchanger being tested is a skived-fin surface developed by Curtiss-Wright (Figures 3 and 4). at full scale, water augmentation would probably be done by a conventional water-cooled condenser and a subsidiary wet tower.

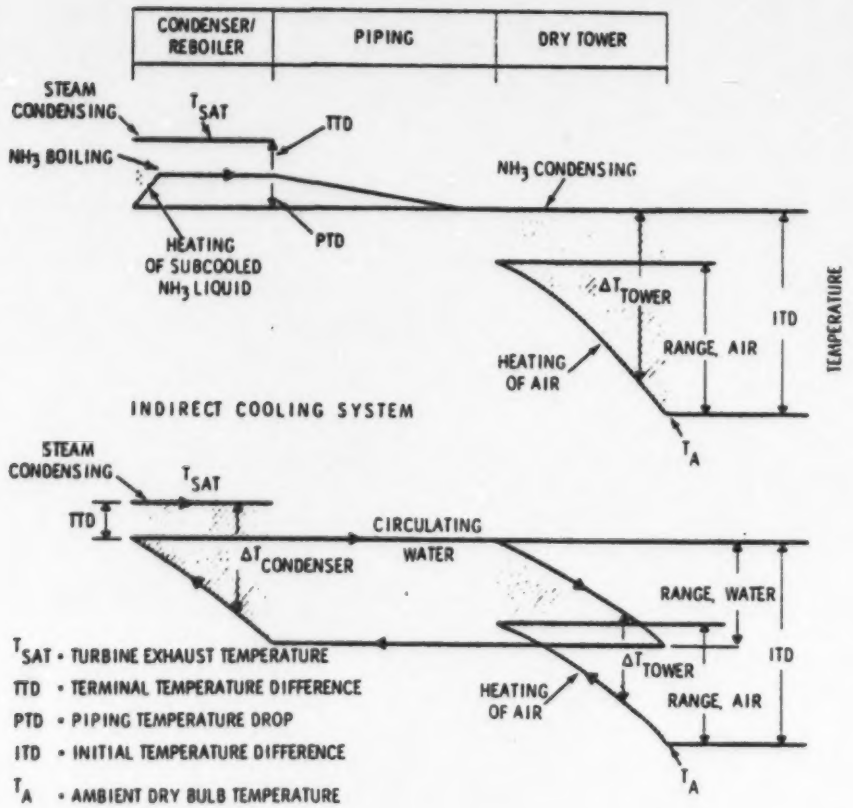

Figure 1. Ammonia Cooling System

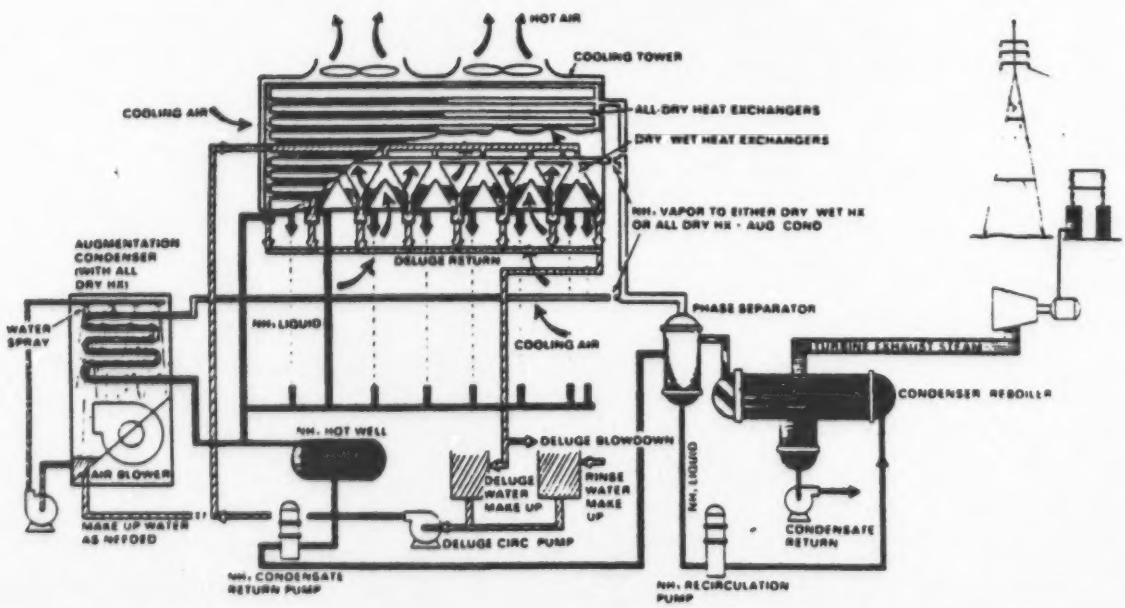

Figure 2. Artist's Sketch and Schematic of ACT Facility

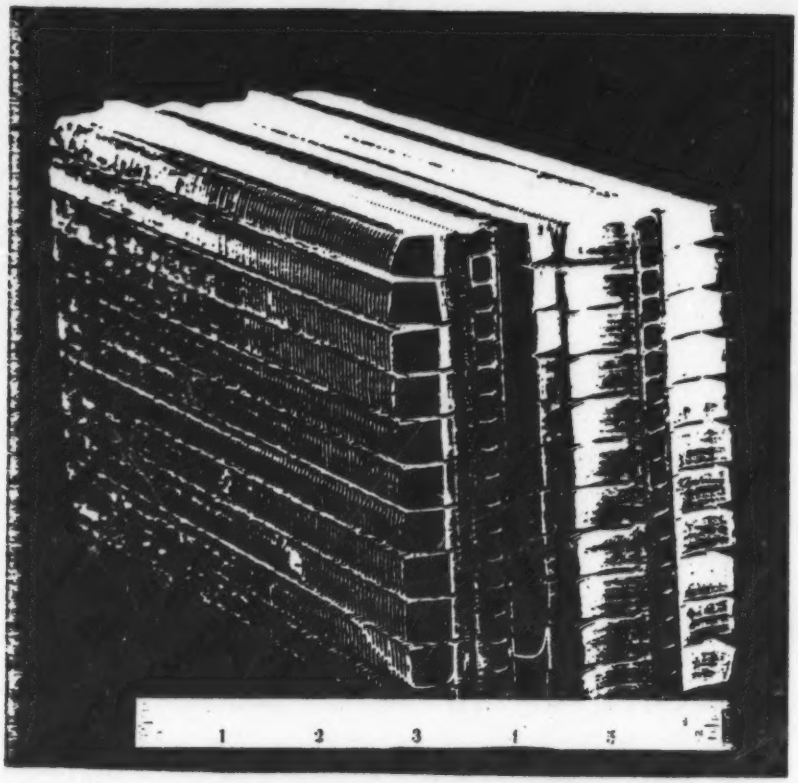

Figure 3. All-Dry Heat Exchanger Surface

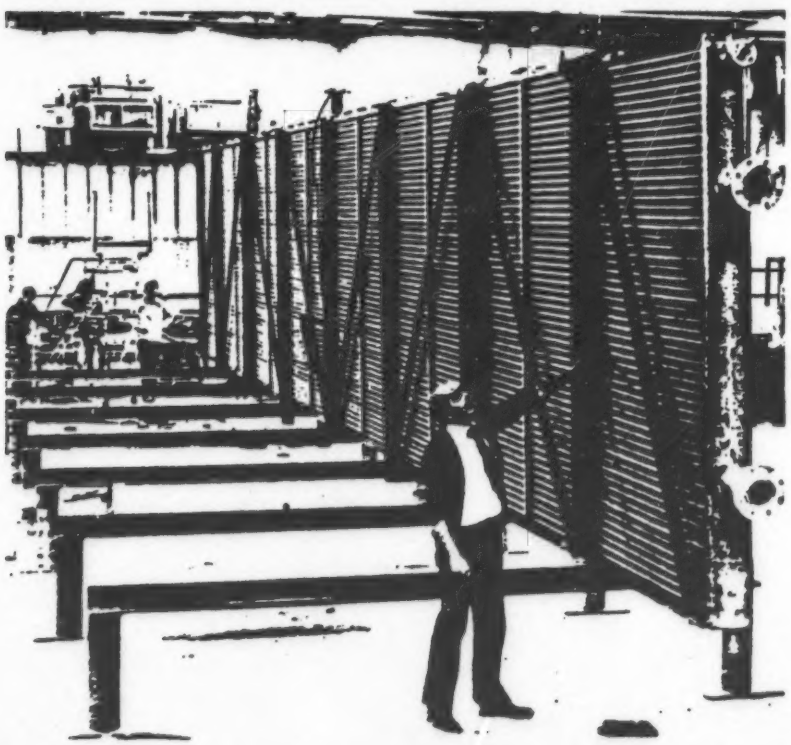

Figure 4. Curtiss-Wright All-Dry Heat Exchanger for the ACT Facility

2) Direct deluge cooling: a portion of the dry heat exchanger surface is covered with a thin film of water so that evaporative and sensible heat transfer occur simultaneously. Only part of the water is evaporated; the rest is recycled. It appears to be a relatively simple and inexpensive way of achieving augmented cooling (i.e., dry/wet cooling). Deluge augmentation is applied to the A-frame arranged heat exchangers built by Trane Company (Figures 5 and 6). Figure 7 is a photograph of the partially completed dry cooling tower, showing where the two types of exchangers are located.

When one of the types of heat exchangers is being tested, the other is isolated by valves on the ammonia lines and by air flow barriers. This flexibility (dual-purpose demonstration) of the ACT tower gives it a complicated appearance, which wouldn't be the case with a final prototype.

The ACT system, as constructed, has the layout shown in Figure 8. The turbine exhaust steam comes from inside the plant building to the steam condenser/ammonia reboiler, and the steam condensate is returned. If ammonia leaks into the condensate, a pH detector will automatically divert the condensate to the drain instead of returning it to the plant. The ammonia vapor is separated from the recycle liquid ammonia and is brought over to the ammonia-condensing heat exchangers mounted in the Hudson Products Corporation cooling tower. The tower has four 16-ft fans for induced flow cooling. The condensed liquid ammonia is returned from the tower hot well to the condenser/reboiler. Storage for anhydrous ammonia is shown.

The system also includes provisions for deluge-water pH control and soft water rinsing. The aqueous ammonia storage tank is present as a vent dump tank only. In case of a leak or overpressurization, the loop ammonia charge can be safely vented into this tank.

Besides the operational controls, the ACT Facility has a data acquisition system (DAS) located in a mobile trailer. This is a computerized digital system for gathering operational data during long periods of testing. The purpose is to obtain data that can be correlated and/or used to verify design equations that have been the basis of the economic calculations.

3. SOME SPECIAL DESIGN ASPECTS

3.1 Water Augmentation

A pilot plant of the ammonia-transport, dry-cooling system has been operated successfully for over three years by Union Carbide Corporation/Linde Division, under the auspices of EPRI. This has been discussed in the preceding paper (Fricke, McElroy and Bartz).

In addition to that work, Battelle has evaluated the relative effectiveness of wet and dry cooling on deluged surfaces by testing in the Water Augmentation Test Apparatus (WATA) [1] at Battelle, Pacific Northwest Laboratories. This apparatus allowed the heat transfer effect of deluge to be studied, as well as the determination of the most effective tilt angles from the standpoint of deluge film hydraulics. In the WATA apparatus (Figure 9) a test heat exchanger is placed in the WATA air flow section and deluge added using various tilt angles, while the heat transfer is measured. Examples of the WATA results, shown in Figure 10 [2] show the relative heat transfer increase by augmentation as plotted versus the transformed driving force based on enthalpy difference. The results from two plate-fin exchangers show that water augmentation increases heat transfer by a factor of 2 to 5, which increases as the heat exchanger and

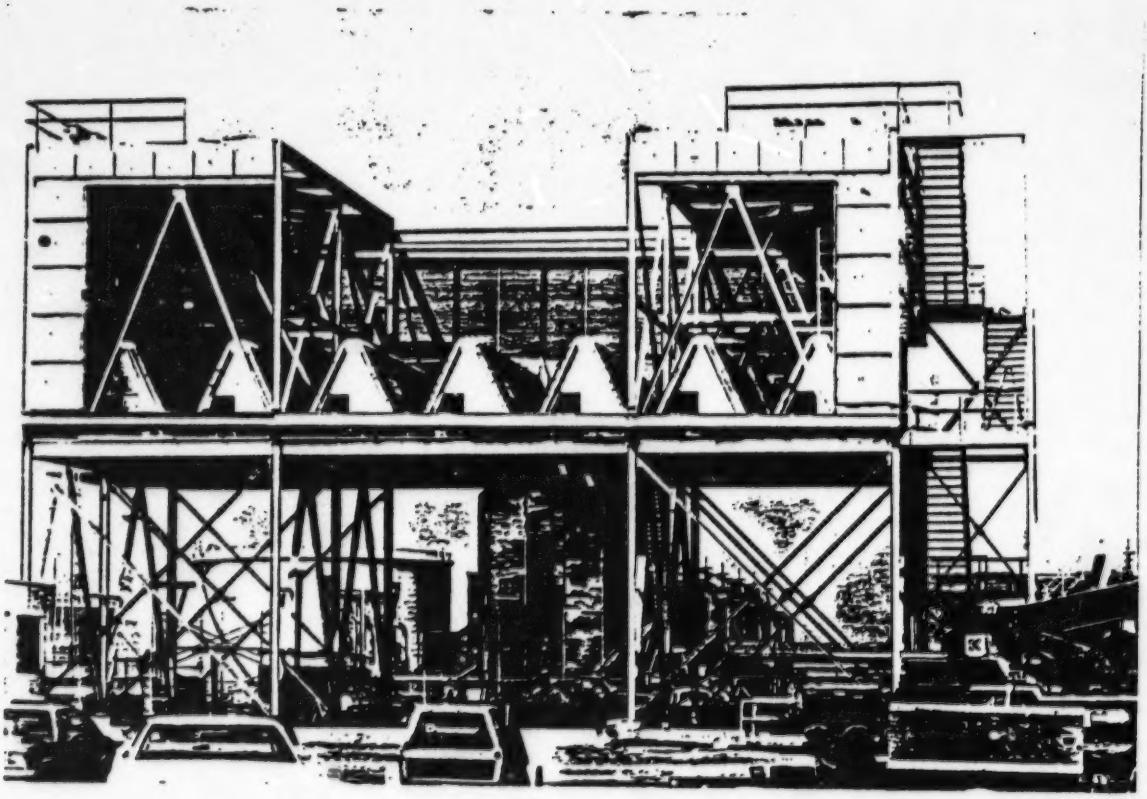

Figure 7. . Partially Built Cooling Tower
at the ACT Facility (November 1980)

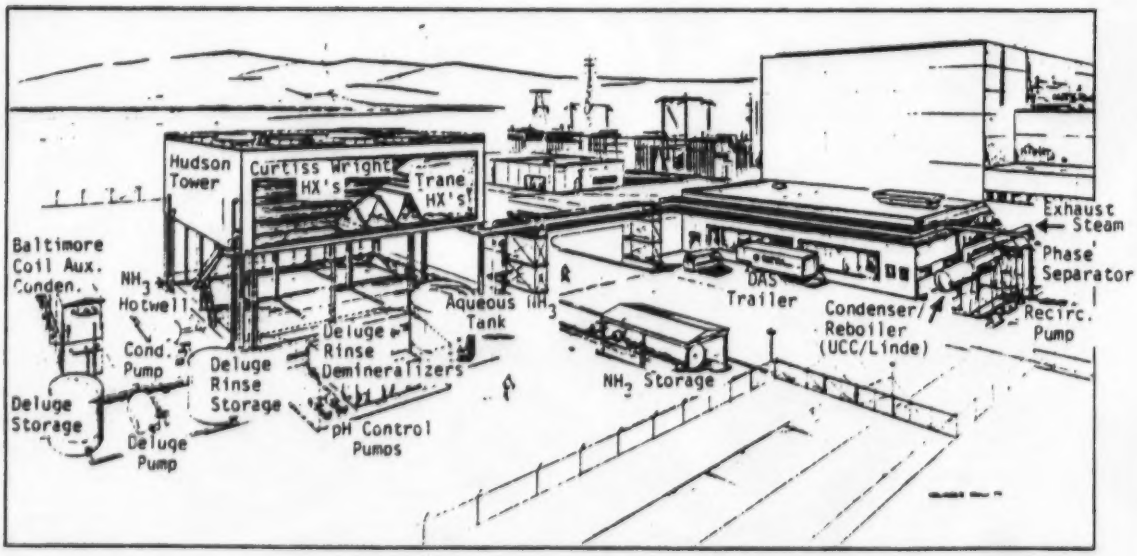

Figure 8. Advanced Concepts Test. Dry Cooling Enhancement Project
PG&E Kern Station, Bakersfield, California

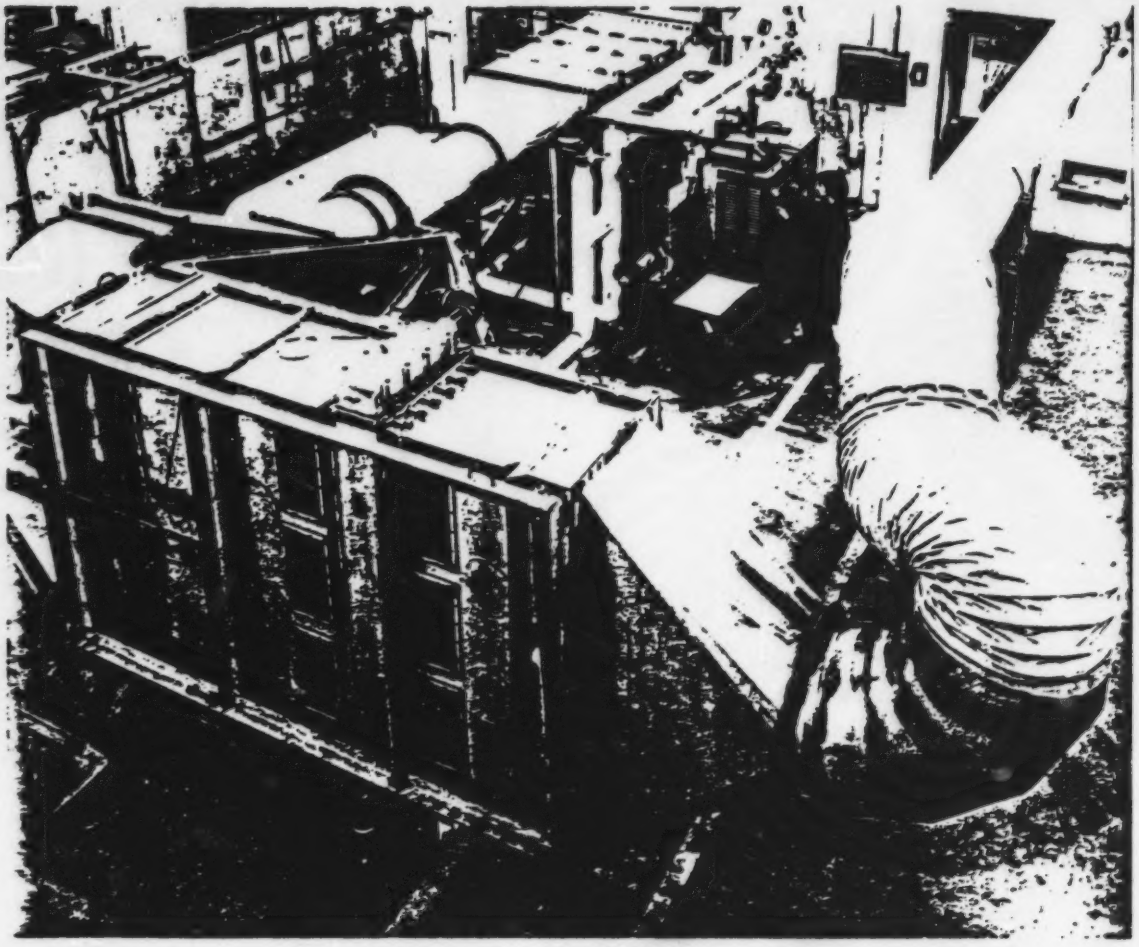

Figure 9. The WATA Loop

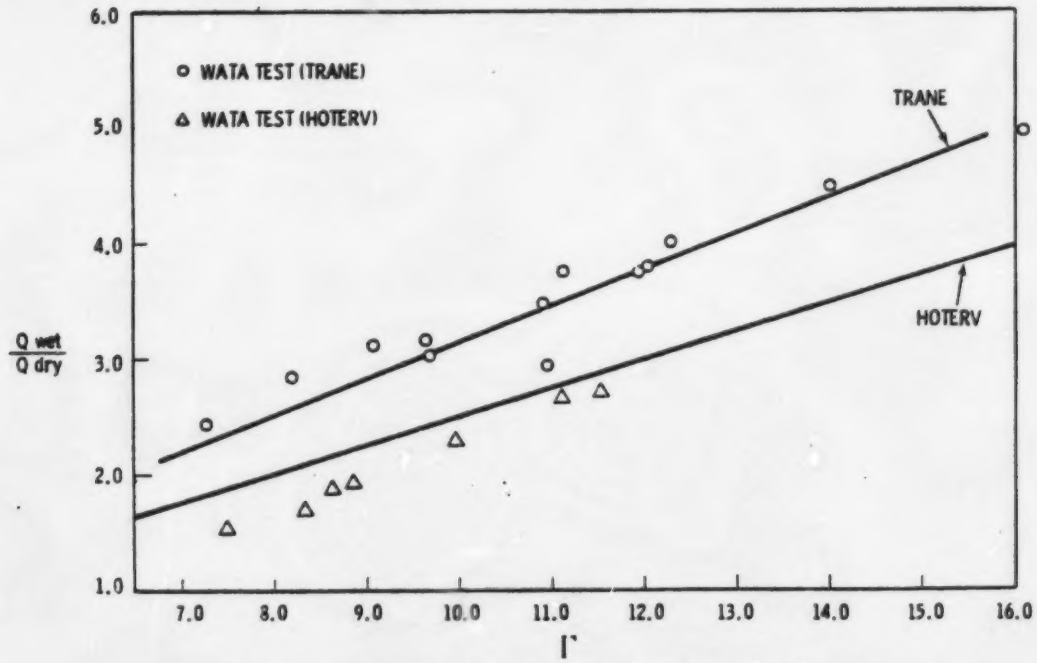

Figure 10. Plot of Heat Transfer Enhancement Ratio Versus Driving Force, Γ

and dry-bulb temperature get higher and the humidity gets lower. This enhancement of cooling can allow an exchanger to be much smaller and still meet the difficult heat rejection condition of hot days.

3.2 Tilt Angle

The angle of the A-frame was also an important design consideration. The angle affects the turning losses and wake effects of the A-frame apex as the air flows upward through them. These, of course, affect the power consumption of the fans and, even more important, the flow distribution through the exchangers. The A-frame angle also affects the total length of the tower. Analytical studies were done at Battelle using the TEMPEST code [3] and 2- and 3-dimensional fluid dynamics code, to evaluate the flow patterns through the A-frames. Figure 11 is an example of the velocity vector plot from TEMPEST.

The flow distribution was also evaluated for the selected A-frames configuration in a water flume at Battelle, using a laser-Doppler anemometer system (Figure 12). The model A-frame was constructed with screens to give the correct loss coefficient for normal flow, and the velocity profiles and losses through the A-frame configuration was evaluated (Figure 13). These showed flow patterns and scaled pressure drop in close agreement with the TEMPEST calculations. The effective loss coefficient for a 50° bundle is ∿1.7 times the flat bundle value. The peak to average flow ratio through the bundle were 1.2.

3.3 A-Frame Orientation and Baffles

An additional design problem studied with the TEMPEST code was the effect of the internal, closed-off A-frames on flow through the side wall exchangers and the effect of the proximity of the fan on uniform flow.

Figure 14 shows a velocity vector diagram from this latter aspect of the study. This type of calculation resulted in a change in the original design of the tower to increase the distance from the exchanger to the fan. The possible improvement in flow by use of fan-entrance baffles was also checked with TEMPEST but showed little improvement (Figure 15).

3.4 Corrosion/Deposition Testing

Aluminum is used in the air-cooled ammonia condenser for ammonia tubes, as well as the cooling fins, and as tubes in the condenser/reboiler. The use of aluminum in industrial situations (condensers and heat exchangers) was reviewed [4, 5] and procedures for successful application were followed. The possible erosion, corrosion, fouling, and deposition aspects are to be evaluated by extensive corrosion samples placed at strategic locations in the facility, as well as by effects on performance. Extensive laboratory studies of corrosion/deposition during deluge cooling have indicated that with careful pH control between pH of 7.4 and 7.8 and with soft water rinsing prior to drying, the deluge system should not experience detrimental corrosion or deposition with the water quality at the Kern site up to a concentration factor of 3 to 4X.

An item of concern is the less-than-ideal location of the dry cooling towers, with respect to the main plant wet cooling towers - the location necessitated by the position of the #1 turbine. The plant cooling towers produce a drift which, in some wind conditions, impinge the dry tower. This may have an effect on deposition, corrosion, and performance that probably would not be typical of a prototypic location. The corrosion/deposition sampling will be important in evaluating the effects of this drift.

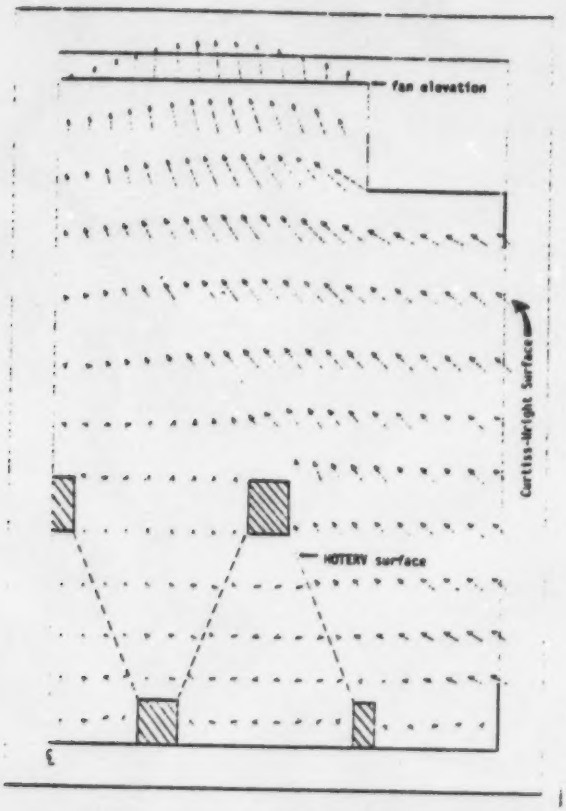

Figure 11. Flow Pattern for Two-Surface Configurations

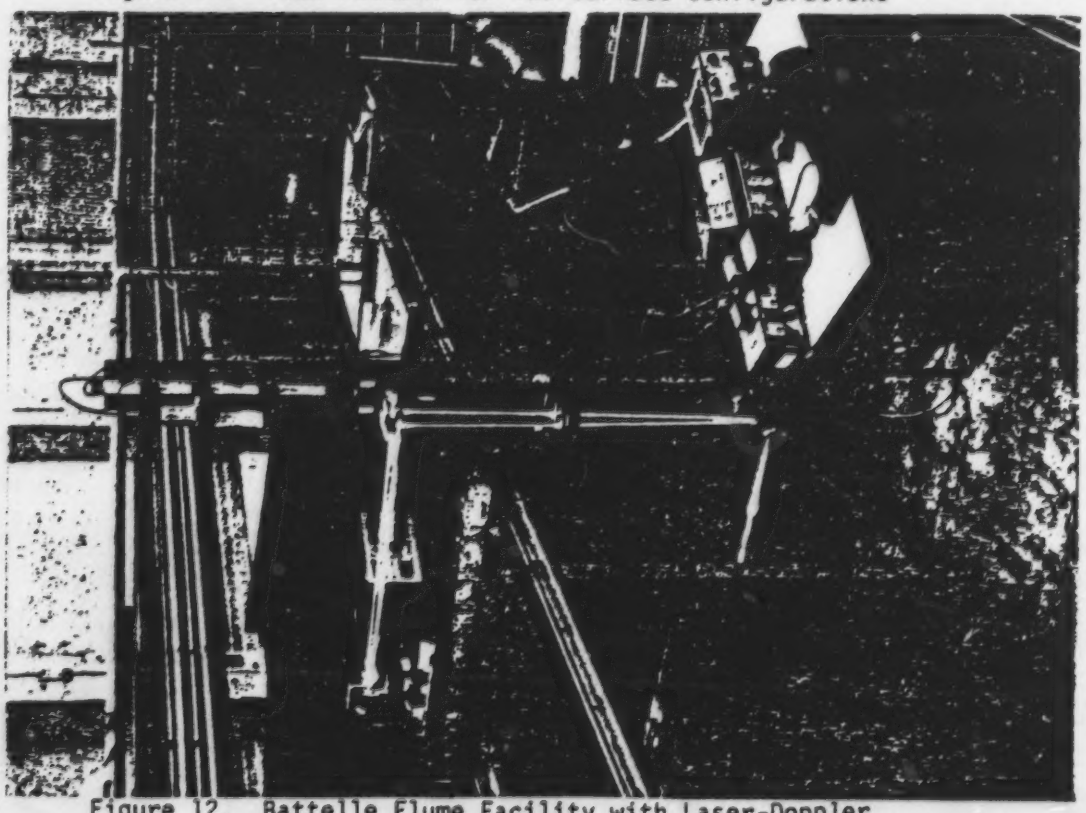

Figure 12. Battelle Flume Facility with Laser-Doppler Used for Flow Modeling Study

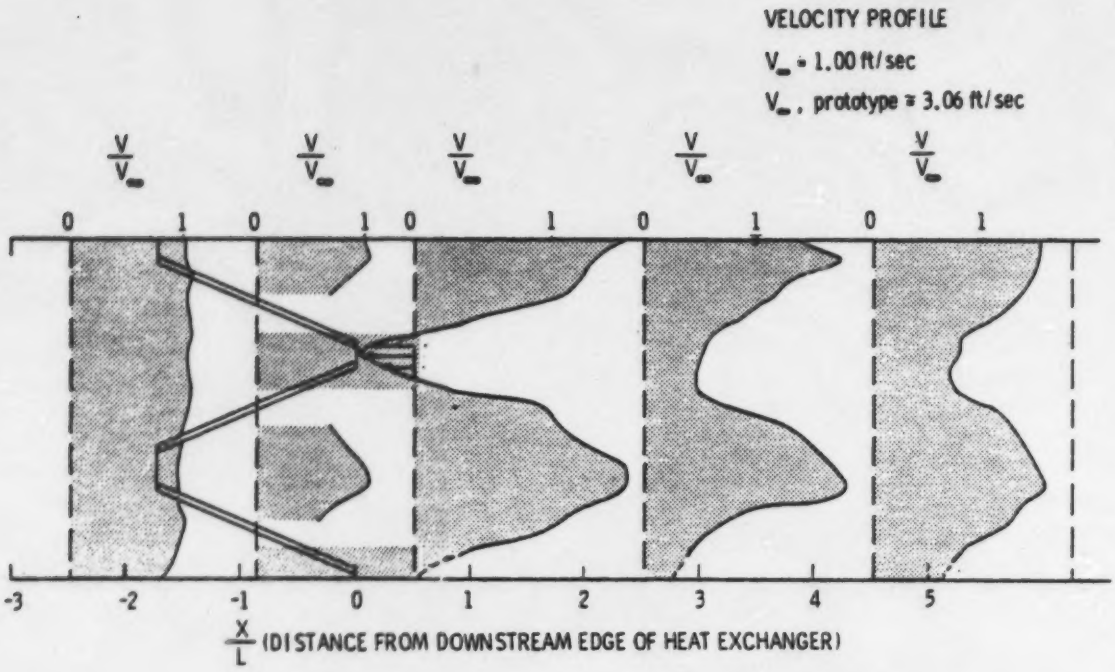
VELOCITY PROFILE
V∞ = 1.00 ft/sec
V∞, prototype = 3.06 ft/sec
V/V∞
0 1 0 1 0 1 0 1 0 1
-3 -2 -1 0 1 2 3 4 5
X/L (DISTANCE FROM DOWNSTREAM EDGE OF HEAT EXCHANGER)

Figure 13. Longitudinal Velocity Profiles near Heat Exchanger

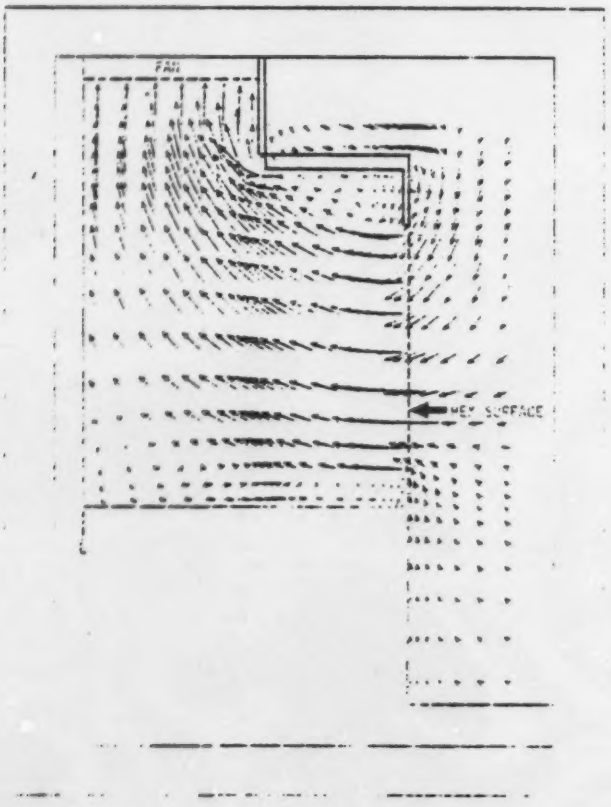

Figure 14. Air Flow within ACT Tower - Without Baffles

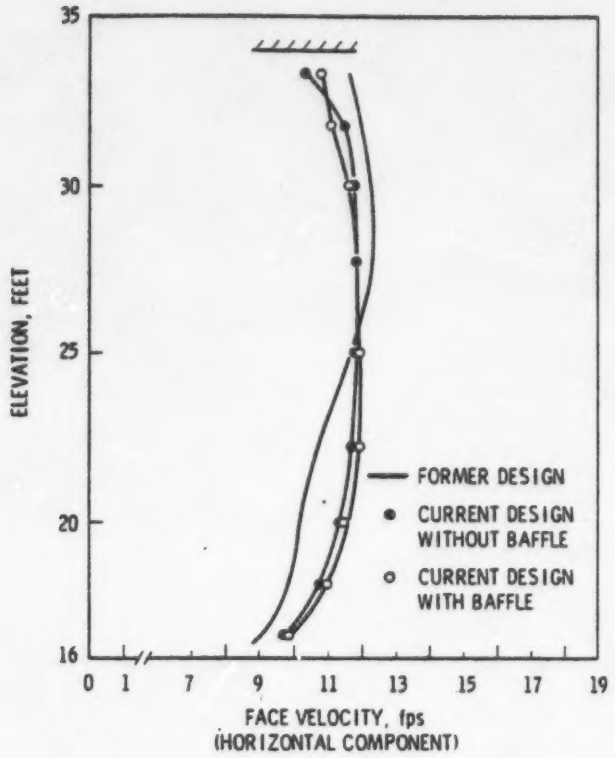

Figure 15. Velocity Distribution through Curtiss-Wright Surface, Present Design

4. INSTRUMENTATION

The instrumentation of the ACT Facility is designed to serve several purposes:

- automatic process control
- manual control
- safety detection
- process alarms
- test data
- field readings

Control and safety functions are independent of the data gathering system, although the data system can present diagnostic information. The system is designed to be normally operated from the main plant control room. Special tests or changeovers will require field valve adjustments so field reading instruments and safety systems and devices (such as fire safety shower use alarms) are included [6].

Data acquisition of up to 240 sensors (currently about 150) is handled by an automatic digital data recording system. Performance values can be calculated almost instantaneously and read or printed out. However, because of the changeability of conditions and the number of variables involved, a statistical

data-reduction and correlation of the data is to be used [7]. The system time-constant will determine how often steady-state/recordable-data conditions will be reached. The test operation will initially take all data and then refine the accuracy "window" to improve the quality of the data as experience with the system is gained. The data acquisition system will produce "quick-look" reports which will show the performance parameters.

5. TESTING PLAN

The ACT Facility is designed to test and demonstrate the ammonia-transport, water-augmentation, heat-rejection concept. Several types of testing are anticipated. In addition to testing the basic performance by passive recording of the data and evaluation of them, the system's operational aspects are to be tested by active changes in control parameters to give an effect that is discernable in spite of the measurement uncertainty. Functional demonstration tests will show how the system responds to changes in loading and plant system changes. Nonstandard condition tests will be run to show the effect of unexpected upsets, such as loss of power, pumps, or control system. Other tests involve calibration as initially and periodically necessary to verify data accuracy.

6. SCHEDULE

The system currently is undergoing a series of operational acceptance test procedures (OATP's) which set up and adjust the operational control systems and instrumentation. Subsequently, there is a series of calibration tests required for the data-gathering instrumentation. These involve such sensors as flow rate meters, fan pitch, pressure sensors, etc., which are used to calculate the heat balances and performance. Due to the first of a kind nature of these tests, they will take some time. As soon as possible, the system will be operated with the dry exchangers, running through a series of passive, active, and functional demonstration tests, before switching over to the wet/dry exchangers.

7. CONCLUSION

The ACT Facility has been designed and built with and through the talents of a large number of people and organizations. The system is built and is now undergoing the operational "shakedown" tests. These will be followed by instrument calibration and first-phase testing by this summer.

ACKNOWLEDGEMENTS

The authors would like to acknowledge the sponsors of this work, the Electric Power Research Institute and the U. S. Department of Energy. The interest and cooperation of Pacific Gas and Electric Company in providing a site for the ACT Facility, as well as technical liaison with and administration of the test location, is gratefully acknowledged. The contributions and expertise of colleagues with the Union Carbide Corporation/Linde Division, who have provided much of the experience in the operation of the ammonia phase-change cooling system, have played a very significant part in the progress of this program. We would also like to acknowledge the design input of the C. F. Braun Company and of the manufacturers of the system components.

REFERENCES

1. H. L. Parry, L. J. MacGowan, D. K. Kreid, L. E. Wiles, D. W. Faletti, B. M. Johnson. Augmented Dry Cooling Surface Test Program: Analysis and Experimental Results. Battelle, Pacific Northwest Laboratories PNL-2746, Richland, Washington, September 1979.

SESSION IV-C

UTILIZATION II

PB82-228131

A REVIEW OF WASTE HEAT RECOVERY TECHNOLOGIES FOR GASEOUS DIFFUSION PLANTS AND OTHER LOW-TEMPERATURE SOURCES

W. P. Teagan, P. C. Mahata, J. Burke
Arthur D. Little, Inc.
Cambridge, Massachusetts, U.S.A.

ABSTRACT

In this paper four technology options have been reviewed applicable for waste heat recovery from large volumes of cooling water of Gaseous Diffusion Plants (a description of which is given later) and similar low-temperature (100-200°F) waste heat sources where flow rate is in the range of 100,000-300,000 GPM. The technology options are: (1) direct heating, (2) temperature augmentation using heat pumps, (3) thermal cooling, and (4) power generation using Organic Rankine Cycle (ORC) engines. The waste heat sources considered are typically hot liquid streams. In this review process the areas covered for each option include technology description and status, system performance, cost implications, and development needs.

1. INTRODUCTION

A program to recover waste heat from four federal facilities, mainly the Gaseous Diffusion Plants (GDP) was initiated in 1977 by the United States Department of Energy (DOE), triggered by the well known oil embargo. The GDPs enrich uranium by repeated compression of uranium hexafluoride gas, thus large volumes of compressor cooling water is required. The GDPs under consideration are located at Portsmouth, Ohio; Oak Ridge, Tennessee; and Paducah, Kentucky. The fourth source under consideration is a nuclear reactor at the Savannah River Plant, South Carolina. Its cooling water flow is also comparable in volume and temperature to those of the GDPs. The waste heat available in these facilities has the potential of energy recovery as high as 0.2 Quad (0.2×10^{15} Btu) per year, which is about 0.25% of total U.S. energy consumption per year; however, the difficulty is that the source temperature is low (about 140-150°F). It is clear that, when the waste heat from these facilities is fully recovered, as much as 36 million bbl of oil can be saved per year.

Four organizations participated in a feasibility study in 1978, and each identified the potential scope and options of heat recovery from one of the federal facilities considered. [1,2,3,4] Subsequently, a review of these four studies was conducted by Arthur D. Little, Inc. which provides management and technical support to DOE on this program, now known as REAP (Residual Energy Application Program).[5] At present the REAP program considers heat recovery not only from the GDPs but also from other sources.

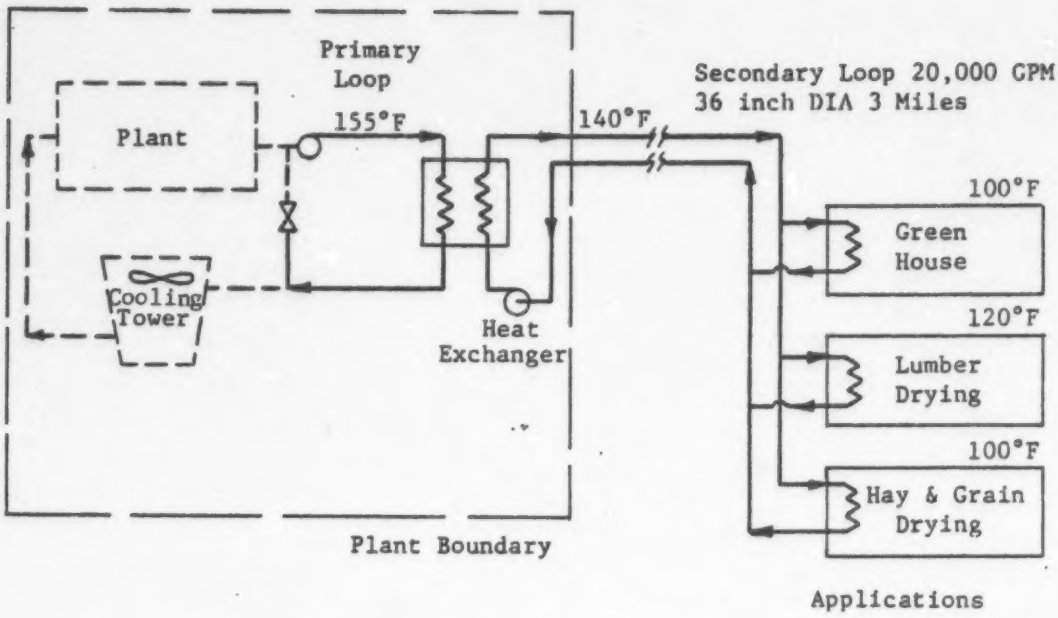

Fig. 1. Schematic Diagram of a Typical Direct Heating Arrangement Using Waste Heat From a Gaseous Diffusion Plant or Power Generating Plant

lake for cooling. Considering the high recovery potential from these types of waste heat sources, the following options have been considered, and some of which are about to be implemented. Another paper describes the overall strategy of these schemes separately.(6)

2. DIRECT HEATING

As shown in Figure 1, a direct heating system utilizing waste heat consists of:

A primary piping loop. This taps into the cooling water (waste heat source), and delivers hot water to an interface heat exchanger and returns the water to the cooling system. The plants, which do not require restriction of containing the primary loop inside the boundary, can provide hot water directly to the end users.

A secondary piping loop. This transports hot water heated in the interface heat exchanger to the end users.

This relatively straightforward system arrangement consists of piping, heat exchangers, and associated pumps and controls. Several applications which have been considered for direct heating included lumber drying, drying alfalfa, hay and grain, greenhouse heating, district heaing, corn wet milling, mushroom house heating, catfish thermal culture, and Malaysian prawn thermal culture. Of these, the first three were determined to be economically attractive for implementation in the Ohio region.(1) Similarly, district heating and fin fish farms were recommended in Tennessee and Kentucky, respectively. Several other applications, such as corn wet milling, might prove to be economical with further

developments in process changes. Table 1 shows some typical direct heating applications indicating their temperature and energy requirements. It is possible that many of these applications can be located near a waste heat source.

Table 1. Examples of Direct Heating Applications Utilizing Low Temperature Waste Heat

Application	Process Temperature	Energy Needs % of Total	Load* Factor
Specific Processes:			
1. Lumber Drying	120°F	100%	0.91
2. Drying Alfalfa, Hay and Corn	100°F	100%	0.17
3. Green House (tomatoes, etc.)	100°F	100%	0.51
4. Finfish Farming	90°F	100%	0.30
5. Meat Packing Plant	140°F	58%	0.23
6. Malt Beverages	140°F	15%	0.82
7. Textile Finishing	140°F 170°F 200°F	16% 10% 3%	0.42 0.42 0.42
8. District Heating	140°F	100%	0.18
9. Corn Wet Milling	130°F	5%	0.96
10. Mushroom House Heating	100°F	100%	0.07
11. Catfish Culture	100°F	100%	0.51
12. Prawn Culture	100°F	100%	0.52
Major Industries:			
1. Lumber	below 200°F	53%	--
2. Food	below 200°F	15%	--
3. Textiles	below 200°F	6%	--

*Fraction of time in a year the process can utilize heat.

Source: References [1], [3]

At this point it is worthwhile looking into the reasons why only a handful of direct heating applications were found to be economically attractive. The principal reasons are:

- Many applications have low load factor,
- Some applicaitons are seasonal in nature,
- Applications such as fish culture might require man-made lakes,
- Locating an application near a GDP site is difficult for some cases, and
- Availability and cost of land might create barriers.

The above barriers are generally true for waste heat sources from power generating plants or process plants. Normally, process applications (corn wet milling, for example) are non-seasonal and have high load factors; however, most of the energy requirement is at temperatures above 200°F.

2.1 Cost

Among the financial factors considered for evaluation of the heat delivery system are capital costs, operating and maintenance (O&M) costs of heat exchangers, pumps, fans, pipes, insulation, ducts and controls, and the cost for both engineering design and installation supervision, as well as skilled labor to install the equipment. The cost of recovered heat (140°F) estimated at the Portsmouth GDP site is about $0.45 per million Btu at the fence. This estimate is based on the cost of primary loop and a life span of 30 years. This is inexpensive compared to the conventional cost of heat ($3-6 per million Btu). As mentioned earlier, other factors play a major role in locating a direct heating application near a GDP. The next option; i.e., temperature augmentation by heat pump makes industrial processes potential candidates for waste heat users, and removes barriers such as seasonality, low load factor, etc.

3. HEAT PUMP SYSTEMS

Heat pumps can boost the temperature of waste heat, thus expanding the range of potential end use applications. These devices can be designed to be compatible with a wide range of source and delivery temperatures--although performance and cost will be dependent on the temperature lift required.

Large heat recovery heat pumps suitable for upgrading waste heat are available in both open and closed versions of the basic vapor compression refrigeration cycle as illustrated in Figures 2 through 4.

Closed cycle heat pumps. These use a working fluid such as R-114 which is kept separate from the process stream with heat exchangers. The closed cycle design can use refrigerants especially tailored to minimize compressor size and cost and can accommodate contaminated streams. The major disadvantage is that the heat exchangers introduce both thermal loss and equipment cost.

Open cycle heat pumps. These designs utilize steam (obtained from flash evaporation of source or process stream) as the working fluid, thereby eliminating the thermal and cost penalty associated with the heat exchangers. A disadvantage is that water has a higher specific volume than

the refrigerants used in closed cycle machines and generally requires more stages of compression, resulting in larger, more costly compression equipment. Two versions exist. In the open cycle, a heat exchanger is used on the source side but not on the process side. In the open-open cycle, no heat exchangers are used. The source water itself is flash evaporated and the vapor is compressed to produce steam. The condensate is not returned, and, therefore, the source water is lost continuously. The limitation is that it may not be feasible to utilize the stream as working fluid if the stream is contaminated.

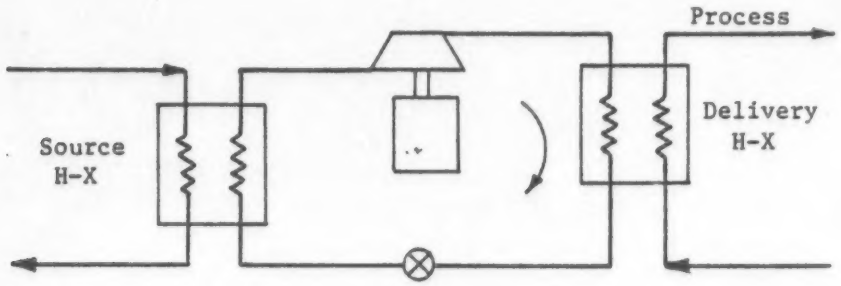

Fig. 2. Closed Cycle Heat Pump

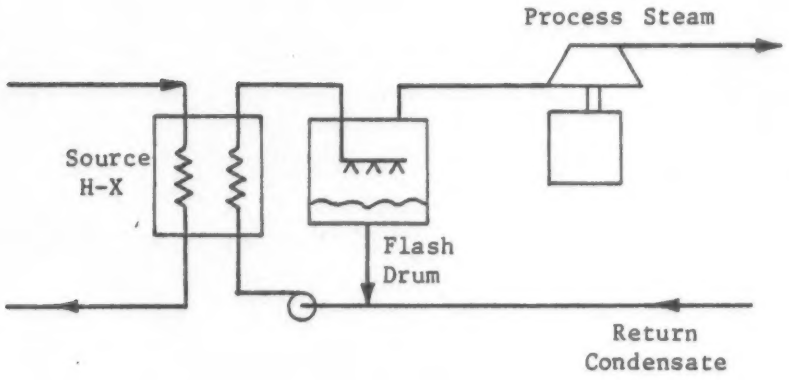

Fig. 3. Open Cycle Heat Pump

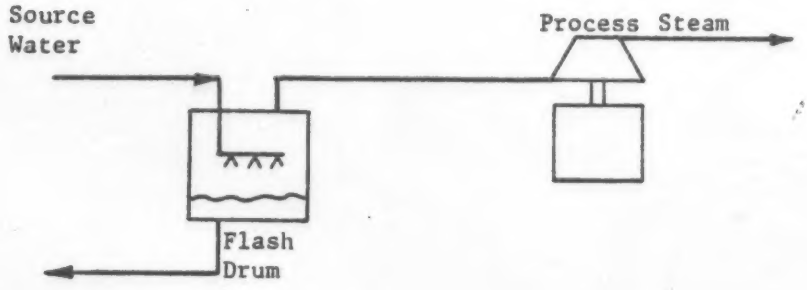

Fig. 4. Open-Open Cycle Heat Pump

Closed cycle heat pumps are currently available as pre-engineered units (the Westinghouse Templifier) for delivery temperatures up to 220°F and in capacities up to approximately 10 x 10^6 Btu/hr at source/delivery temperatures of 130/220°F.(7) Custom design units are available from York for operation between 140°F and 220°F with capacities to 75 x 10^6 Btu/hr and for delivery temperatures to 270°F with reduced capacity.(8) Atlas-Copco Turbonetics, Inc. supplies steam compressors for heat pump applications in capacities up to 44 x 10^6 Btu/hr for delivery temperatures up to and beyond 270°F.(9)

3.1 Technology Status and Issues

In the closed cycle design, maximum delivery temperatures are limited by working fluid stability considerations. R-114, the working fluid used in the Westinghouse Templifier and the lower temperature York custom design units is limited to a delivery temperature of 220°F. Beyond 220°F methanol is the fluid chosen for York custom design equipment. Westinghouse is developing a two stage methanol heat pump for source/delivery temperatures of 212/300°F for the Conservation Solar Division of DOE. However, since methanol has higher specific volume and requires more stages for a given temperature ratio than R-114, this is leading to higher equipment costs. Its use may also pose some hazard problems.

In the open cycle, there is no comparable temperature limit imposed by stability considerations. However, the extremely high specific volume and the large number of stages required for water do result in expensive compression equipment. It is projected that in very large sizes the open cycle design may be comparable in cost to the closed cycle due to the economy of scale in large steam compressors and the relatively little economy of scale of heat exchange equipment. Development activities on open cycle units include MTI and GE contracts funded by DOE for multistage compressors for source/delivery temperatures of 140/250°F(11); an MTI single stage program for temperatures of 190/228°F for the Conservation Solar division of DOE(12); and a Thermoelectron program sponsored by GRI and gas utilities for 212/300°F, with an engine driven rotary screw compressor.(13,14)

The heat pump options discussed above require a compressor drive in the form of either an electric motor or a fuel-fired engine.

Electric motor drive. It is convenient, commercially available, simple and doesn't require on-site fuels. Where the temperature levels are high, and where the local cost of electric power is reasonably low, this may be the best option, and it is the one used in almost all existing installations.

Fossil fuel drive. Either gas turbine, spark ignition natural gas engine, or diesel has the advantage that the engine waste heat will contribute to the process heating; and in some instance, might result in lower total cost per unit delivered heat.

In addition to the open and closed vapor compression cycles discussed above, large absorption systems and chemical heat pumps are also being considered for upgrading waste heat. However, these approaches are still in the very conceptual stage.

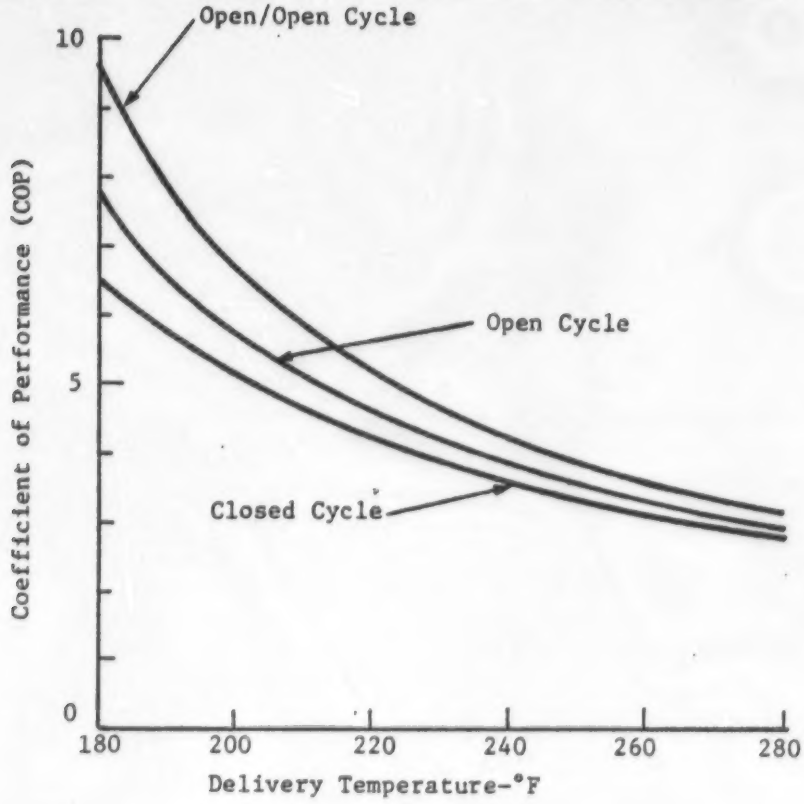

Fig. 5. Variation of Coefficient of Performance of Heat Pumps with Delivery Temperature.

Notes: 1. Heat Pump COP = .60 x Carnot Cycle COP on working fluid temperatures.
2. Source Temperature = 140°F.

3.2 Performance and Cost

The coefficient of performance of a heat pump is dependent on the temperature levels and degree of irreversibility. A good working estimate of COP for the large heat recovery heat pumps of interest can be obtained by assuming a 60% approach to ideal (Carnot) performance based on internal working fluid temperatures and a 10°F temperature differential across the heat exchangers. Typical results are plotted in Figure 5 for an electric driven heat pump, where COP is defined as heat delivered per unit electrical power input.

Typical installed cost per unit heat delivered for closed and open cycles operating between 140°F and 220°F are shown in Table 2.

The economics of upgrading of waste heat by heat pump in any particular installation will be dependent on the equipment capital costs and COPs; the unit energy costs for the heat pump driver, the conventional boiler, and waste heat; as well as the method of financial analysis preferred. As an illustrative sample calculation, Table 3 presents estimates of the cost of heat delivered by a heat pump system operating between 140 and 220°F using the COPs and unit installed costs presented above. All assumptions are stated in Table 3.

Table 2. Cost of Heat Pumps

Description	Closed Cycle (Westinghouse Templifier)	Open Cycle (Atlas-Copco Turbonetics)
Capacity (10^6 Btu/hr)	11	44
Equipment Cost ($000)	147[7]	1060[9]
Installation Factor	2.0	2.0
Installed Cost ($000)	294	2120
Unit Installed Cost ($/$10^6$ Btu/hr)	26,600	48,000

Table 3. Cost of Heat Delivered by Heat Pump in $/$10^6$ Btu

Cycle	Capital and Maintenance Charges	Fuel Cost	Total
Closed	.75	2.80	3.55
Open-Open	1.37	2.26	3.63

Assumptions:

Electricity Cost = 4¢/KWH
20% Capital Recovery Factor
5% Annual Maintenance Costs
100% Utilization Factor
No charge for Waste Heat
140/220°F Source/Delivery Temperatures

For the temperature range, and the assumptions stated above, the cost of delivered heat is essentially the same for the closed and open cycle and in either case compares very favorably with fossil fired boilers. Clearly, the result is very assumption dependent. For instance, increasing the capital recovery factor will increase the delivered heat cost and preferentially penalize the open-open cycle. Likewise, increasing the unit cost of electricity will increase delivered heat cost, preferentially penalizing the closed cycle.

3.3 Development Needs

Development needs are that a closed cycle working fluid should have the favorable thermodynamic and safety characteristics of R-114 combined with higher temperature capabilities. Also, large open cycle steam compressors need to achieve the required economies of scale and take advantage of the relatively thin wall construction possible at low pressure levels. Finally, reliable systems design and cost guidelines are required to better define probable costs for custom design heat pump systems.

4. THERMAL COOLING

Heat actuated equipment can use low temperature waste heat to achieve air conditioning and/or dehumidification. In addition to building climate control, such equipment may have application to a number of industrial processes requiring environmental or process air dehumidification.

4.1 Technology Status

The primary options for thermal cooling and/or dehumidification are as follows:

Absorption refrigerator. These machines represent the most common type of commercially available thermal cooling. Large absorption units, up to several hundred tons, are available as a catalog item for companies, such as Trane, York, and Carrier. The required inlet temperature for this equipment is generally in excess of 200°F. Arkla offers small absorption units (3 and 25 tons) designed for solar cooling with a design inlet temperature of 195°F and operation at reduced capacity possible down to 160°F.(15

Low-temperature Rankine power cycles driven vapor compression cycles. This option, described in the following section, could be utilized to drive conventional vapor compression air conditioning machinery.

Desiccant dehumidification and/or cooling. Such systems utilizing either solid or liquid desiccant may be used to produce dehumidification and/or cooling. Liquid desiccant dehumidifying equipment is available in large sizes from Niagara Blower, Midland Ross Corporation and others. Some types may be consistent with source temperatures as low as 140°F. Solid desiccant equipment, generally requiring somewhat higher regeneration temperatures, is available from Bry-Air, Cargocaire, and others.

Chemical heat pumps. These are in an early stage of development, and are another possible long term option.

4.2 Development Needs

Utilization of waste heat for thermal cooling will be enhanced by absorption or other heat-actuated air conditioning equipment designed for minimum inlet temperature operation consistent with reasonable equipment size and cost. Absorption machines capable of operation at less than 180°F have been developed for solar applications. Equipment capable of operation below 150°F is in development as part of a DOE program.(11)

Also needed is the identification of applications where existing low inlet temperature desiccant dehumidification equipment might be profitably employed either as part of a climate control system or in industrial dehumidification applications.

5. POWER GENERATION USING ORGANIC RANKINE CYCLE (ORC) ENGINES

For all the options discussed earlier, it is essential to locate an application very close to the waste heat source. It has been pointed out that location of an end-user of waste heat near a GDP could be difficult for reasons such as land availability and cost of land, availability of raw materials, regional market for products, and attendant social and institutional issues. To overcome these barriers, the option of power generation from low-temperature waste heat source was considered. The generated electricity could be easily utilized in the plant itself or it could be sold to the utility-grid at a reasonable cost.

Generation of power from waste heat at 150-200°F is possible though the use of organic Rankine cycle power plants. These power plants work under the same principle as the steam power plants. The only difference is that high vapor pressure working fluids are used rather than water to allow for efficient operation at low temperatures. For a power plant with source temperature of 140°F (typical for a GDP) and sink temperature of 80°F, the Carnot efficiency is about 10%. However, the practical Rankine cycle deviates from Carnot cycle due to turbine and pump inefficiencies, non-ideal working fluid characteristics, and heat-exchanger temperature drops.

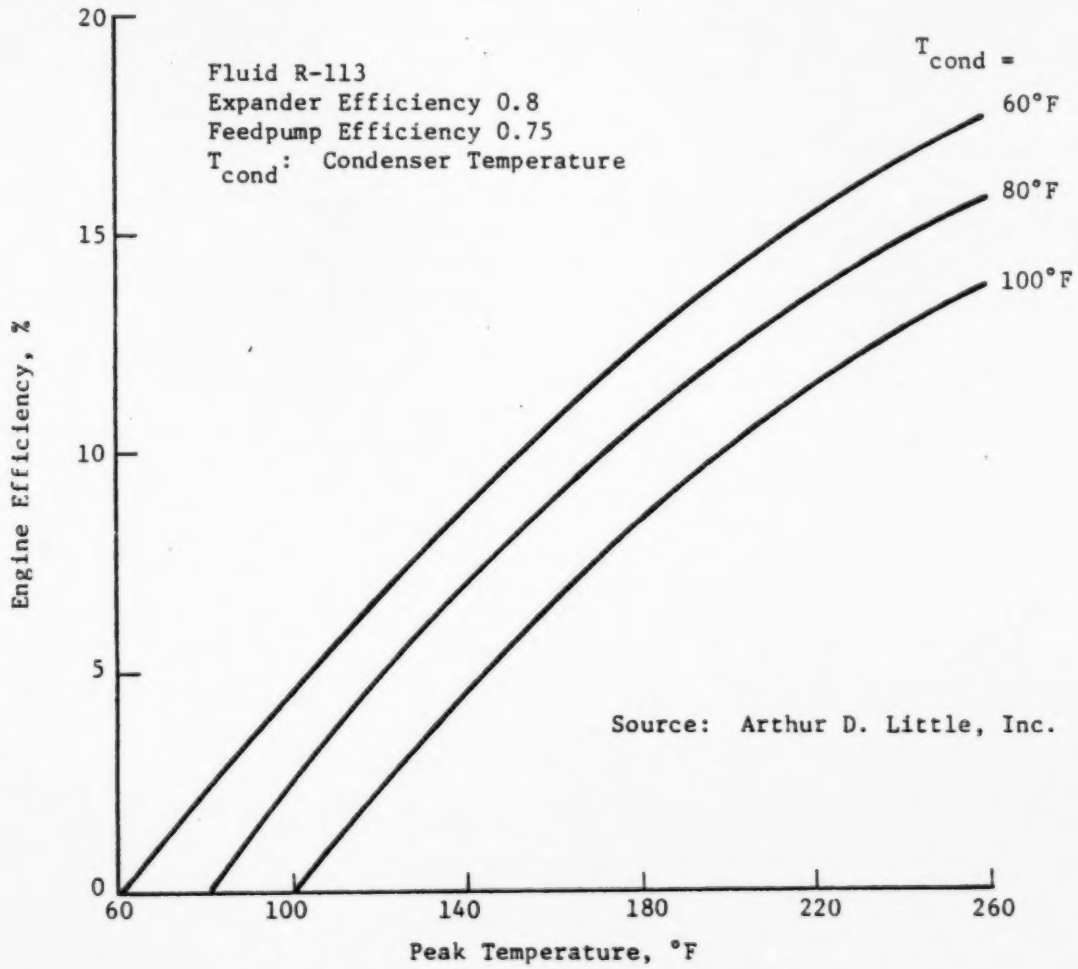

Fig. 6. Rankine Cycle Efficiency - Variation with Peak Cycle Temperature and Condensing Temperature

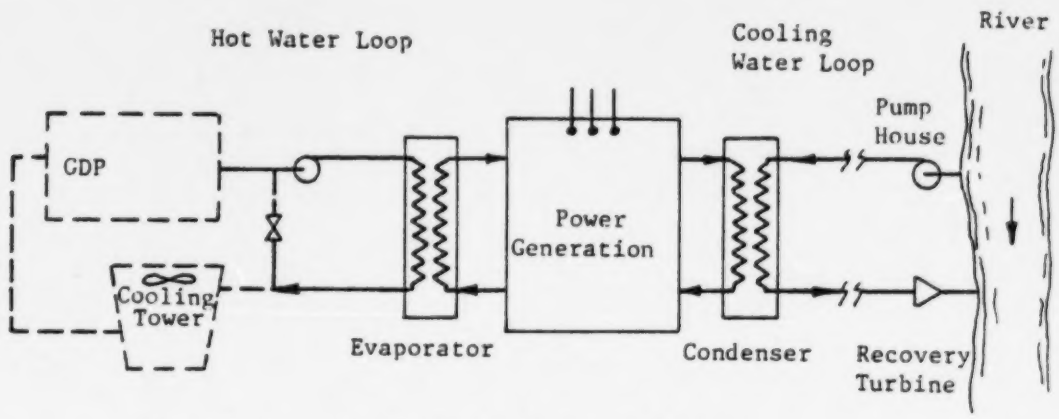

Fig. 7. Power Generation System Using ORC Engines at a Typical GDP Site

Source: References [2] and [3].

Taking these differences into account, the efficiency of a real cycle operating with the waste heat at 140°F is projected to be in the range of 4-6%. The variation of power-plat efficiency with both heat input and heat rejection (condenser) temperature is illustrated in Figure 6. As indicated, the condenser temperature greatly affects performance at low operating temperatures. consequently, wherever possible, relatively cold river water for condenser cooling should be utilized. A general scheme for power generation is shown schematically in Figure 7. The potential of power generation at three GDP sites and at Savannah River plant amounts to about 75 MW.(1-4)

5.1 Technology Status

Table 4 summarizes the major programs in the United States involving the development of ORC engines. As indicated, these engines are being developed for concentrating solar collectors, hot geothermal brines, and Ocean Thermal Energy Conversion (OTEC) power plants. Also shown on Table 4 are the conceptual designs proposed for the REAP program. The working fluids proposed for the REAP program are ammonia, R-500, and R-113. The size range of the REAP systems is 4.5-45 MW, which is larger than any of the systems now operating. Since the heat source for the REAP systems is 140-155°F, this does not correspond exactly to that of the systems under active development. Several studies have shown that there is a considerable amount of reject heat available in industry in the temperature range of 140-200°F which could, in principle, operate a system developed under the REAP program (16). The REAP systems might fill a need in such industrial applications not now being addressed by ongoing programs.

The selection of a working fluid is an important factor in the design and performance of an organic Rankine cycle power system. For example, the use of R-113 results in high cycle efficiency but requires large heat exchangers because of its poor thermal transport properties. The largest difference in performance, however, occurs between the refrigeration fluids and ammonia. Because ammonia has relatively good heat transfer properties, its use results in the lowest-cost system if a single interface heat exchanger is used. However, ammonia is very corrosive to copper, and another isolation heat exchanger may be necessary.

Table 4. Technology Review of Typical Organic Rankine Cycle Engines For Low-Temperature Applications

Organization	Power Output	Source Temperature	Working Fluid
Geothermal:			
Arkansas Power & Light (E)	100 kWe	200°F	Pentane
Republic (East Mesa, CA) (C)	64,000 kWe	335°F	Isobutane
INEL (Raft River) (C)	5,000 kWe	290°F	Isobutane
Barber-Nichols (E)	500 kWe	300°F	Isobutane
Solar Thermal Power:			
I.H. Industries, Japan (P)	25-50 kWe	200°F	R-11
Barber-Nichols (E)	2 kWe	200°F	R-113
Kinetics (Rotary Expander) (E)	5 kWe	200°F	R-114
United Aircraft (C)	3 kWe	200°F	R-113
Solar Ponds:			
Ormat, Israel (E)	150 kWe	200°F	MCB
REAP Program (GDP):			
Bechtel (C)	19,600 kWe	155°F	R-500
Exxon (C)	6,120 kWe	140°F	R-113
Sirrine (C)	4,570 kWe	150°F	Ammonia
ERI (C)	45,000 kWe	140°F	Ammonia
OTEC:			
TRW/Elliot Co. (C)	10,000 kWe	80°F	Ammonia
Applied Physics Lab/John Hopkins Univ. (C)	10,000 kWe	82°F	Ammonia
Lockheed (E)	50 kWe	80°F	Ammonia

C = Conceptual, E = Experimental, P = Production

5.2 Cost of ORC Engines

A comparison of the power plants recommended for GDP applications is given in Table 5. The complete power system comprises three major subsystems; namely, the primary piping loop, the power system, and the cooling system piping. Table 5 identifies each of these cost factors so that their relative importance can be ascertained. The costs of plant i.e., for turbines, generators, internal piping, and pumps are substantial. These costs typically range from $1,230 per kW to $1,830 per kW (1978 estimate). The projections for power system equipment costs at Savannah River is $486 per kW, well below that of the other sites. This relatively low cost projection for the Savannah system results in part from the use of ammonia as the working fluid. In general, the high system costs of Table 5 resulted from the low temperatures of the heat source, which yield low system efficiency. The system costs are very sensitive to

Table 5. Electric Power Generation Systems -- Summary of Costs for Federal Facilities

Description	GDP at Portsmouth OH	GDP at Oak Ridge TN	GDP at Paducah KY	Savannah River Plant SC
Type of Pwr. Gen. Syst. (Rankine Cycle)	R-500 Simple Cycle	R-113 Simple Cycle	NH3 2-Stage Split-cond.	NH3 4-Stage Evap. Cycle
Hot Water:				
flow, GPM	128,000	40,000	31,600	165,000
Temp. Change ^{o}F	25	16.2	27.5	40
Cooling Water:				
flow GPM	293,000	59,600	37,500	1.16×10^{6}
Temp. Change, ^{o}F	10	10	22	7
Net Output, kWe	19,600	6,120	4,570	45,000
Efficiency, %	4.6	6.4	3.6	4.6
Cost of Hot Water Supply $/kWe	50	530	870	523
Cost of Cooling Water $/kWe	720	503	970*	33
Cost of Plant $/kWe	1,830	1,507	1,230	486
TOTAL COST $/kWe	2,600	2,540	3,070	1,042[e]
Cost of Power ¢/kW-hr	5.49[a]	3.03[b]	3.25[c]	2.90[d]

Note: All costs are in 1978 Dollars.

*Same pipe supplies cooling water to other systems.

a. 20 year, 9% interest, equity 50%, load factor 0.9 (7884 hr/yr), 1st year costs are spread uniformly over 20 years.

b. 20 year bond @ 7% interest, 8400 hr/yr operation.

c. 30 year, 8% interest.

d. 11% year, no O&M cost, load factor 0.7 (6130 hr/yr).

e. Engineering, spare parts, and contingency costs are projected to increase total system cost to $1,600 per kW.

Source: References [1] through [4].

variations in temperature levels. For example, a 10°F increase in temperature was projected to decrease system costs by up to 30%.(2) As shown in Table 5 the cost of power from the power plants was estimated to be $.029/kW to $.055/kW (1978). This power cost appears to be competitive as the cost of conventional power increases.

5.3 Development Needs

The technology of ORC engines has been under development for the past 10-15 years. These systems are comprised of components such as heat exchangers, expanders, and pumps which are well understood and often used in industry. As a result, ORC systems and their components have reached a stage where reasonably good performance and reliability could be achieved. Accordingly, there appears to be no major technical barriers to the effective use of these systems by the private sector. In fact, some ORC systems are presently in operation throughout the world today (17, 18).

6. CONCLUSIONS

Finally, it can be said that direct heating is the simplest heat recovery option, and should be utilized wherever possible. Heat pumps are commercially available, and may be suitable in size and temperature range for the GDPs and other applications with some modifications. Regarding power cycles, there appears to be sufficient experience with low temperature operation that systems could be developed by several manufacturers with minimum technical risk. It is not clear, however, that ongoing programs to develop low-temperature heat actuated cooling systems will result in commercially viable equipment.

ACKNOWLEDGEMENTS

The Authors acknowledge the support of the United States Department of Energy, which funded the review of the technology options considered for the Residual Energy Applications Program.

REFERENCES

1. Use of Reject Heat from Uranium Enerichment Gaseous Diffusion Plant at Portsmouth, Ohio, Bechtel National, Inc. Rept. EC-77-C-05-5622, Vols. I and II, San Francisco, California, Oct. 1978.

2. Oak Ridge Gaseous Diffusion Plant Reject Heat Study, Exxon Nuclear Company, Inc., Rept. XN-RT-12, Vols. I through IV, Richland, Washington, Sept. 1978.

3. U.S. Department of Energy Waste Heat Utilization Project for the Paducah, Kentucky, Uranium Enrichment Gaseous Diffusion Plant, J.E. Sirrine Co., Rept. EC-77-C-05-5623, Vols. I and II, Raleigh, North Carolina, Sept. 1978.

4. The Savannah River Plant Low Level Waste Heat Utilization Projects, South Carolina Energy Research Institute, Rept. EC-77-C-09-1021, Vols. I through III, Columbia, South Carolina, Aug. 1978.

5. Utilization of Waste Heat from Federal Facilities, Arthur D. Little, Inc., Rept. EC-77-C-05-5523, Cambridge, Massachusetts, Feb. 1979.

6. D.B. Howard, The DOE Residual Energy Applications Program, Proc. Third Conference on Waste Heat Management and Utilization, 1981.

7. J.A. Siorois, Personal Conversation and Westinghouse Templifier Bulletin TP-1, Feb. 1981.

8. R. Nadler of York Co., Telephone Conversations, Feb. 1981.

9. R. Ingui, Atlas Copco Turbonetics, Telephone Conversations, Feb. 1981.

10. W. Morland, Westinghouse, Telephone Conversation, Feb. 1981.

11. H. Arnold, ORNL, Telephone Conversation, Feb. 1981.

12. Phase I Results Technical Report on High COP Heat Pump System, Mechanical Technology, Inc., Rep., MTI 79TR1, Oct. 1978.

13. R. Sakhuja, et al, Heat Pump Systems for Process Heat Generation, 14th IECEC, Aug. 1979, pp. 1708-1712.

14. R. Sakhuja, ThermoElectron Corp., Telephone Conversation, Feb. 1981.

15. Arkla Application Data: Solaire 36, Form No. SA-41030, Nov. 1976; Solaire 300, Form No. SA-41041, Oct. 1978.

16. H.L. Brown, et al, Industrial Applications Study, Drexel Univ., Report CONS/2862-1, Vols I-IV, Philadelphia, Penn. Dec. 1976.

17. Organic Rankine Cycle Engine Technology in Japan, Galaxy, Inc., Rept. DE-AC03-79 SF 10538, Washington, DC, Oct. 1979.

18. Report on State-of-the-Art and Advanced R&D on Overseas ORC and Rankine Cycle Work in Continental Europe, Galaxy, Inc., Rept. EDE-AC03-79SF10538, Washington, DC, Oct. 1979.

PB82-228149

INDUSTRIAL REFRIGERATION FROM 140°F WASTE HEAT*

Scott J. Hynek
Energy Conservation Division
Foster-Miller Associates, Inc.
Waltham, Massachusetts, U.S.A.

ABSTRACT

Foster-Miller Associates, Inc. has designed and is developing a 20-ton refrigeration system to be powered by the 140°F (60°C) waste hot water that is available at many industrial sites as well as government owned gaseous diffusion plants. It consists of a Rankine cycle driving a reverse-Rankine cycle, integrated in that they share a common working fluid (R-22), a common condenser, and a common crankcase housing the expander and compressor.

1. INTRODUCTION

As the cost of energy continues to rise faster than the cost of machinery, the minimum temperature for economically recoverable waste heat continues to decrease. The Department of Energy, anticipating the day when 140°F water constitutes an exploitable resource, is funding, through the Oak Ridge National Laboratory, the development of several systems to convert 140°F water, which exists in abundance at government-operated gaseous diffusion plants, into process steam or industrial refrigeration. Foster-Miller Associates, Inc. (FMA) has designed and is developing one such system, using an organic Rankine cycle to drive a reverse Rankine refrigeration cycle.

Figure 1 shows how these two cycles are integrated schematically. Both cycles reject heat through the same evaporative condenser, because two smaller condensers with the same cumulative capacity would cost more. Both cycles necessarily use the same working fluid; R-22 was chosen over R-12 because it affords greater capacity per unit displacement in both the expander and the compressor; R-717 was rejected because it is incompatible with the copper windings of the hermetic motor/generator.

---

*Research sponsored by the Office of Coal Utilization, U.S. Department of Energy, under subcontract W-7405-eng-26 with the Union Carbide Corporation

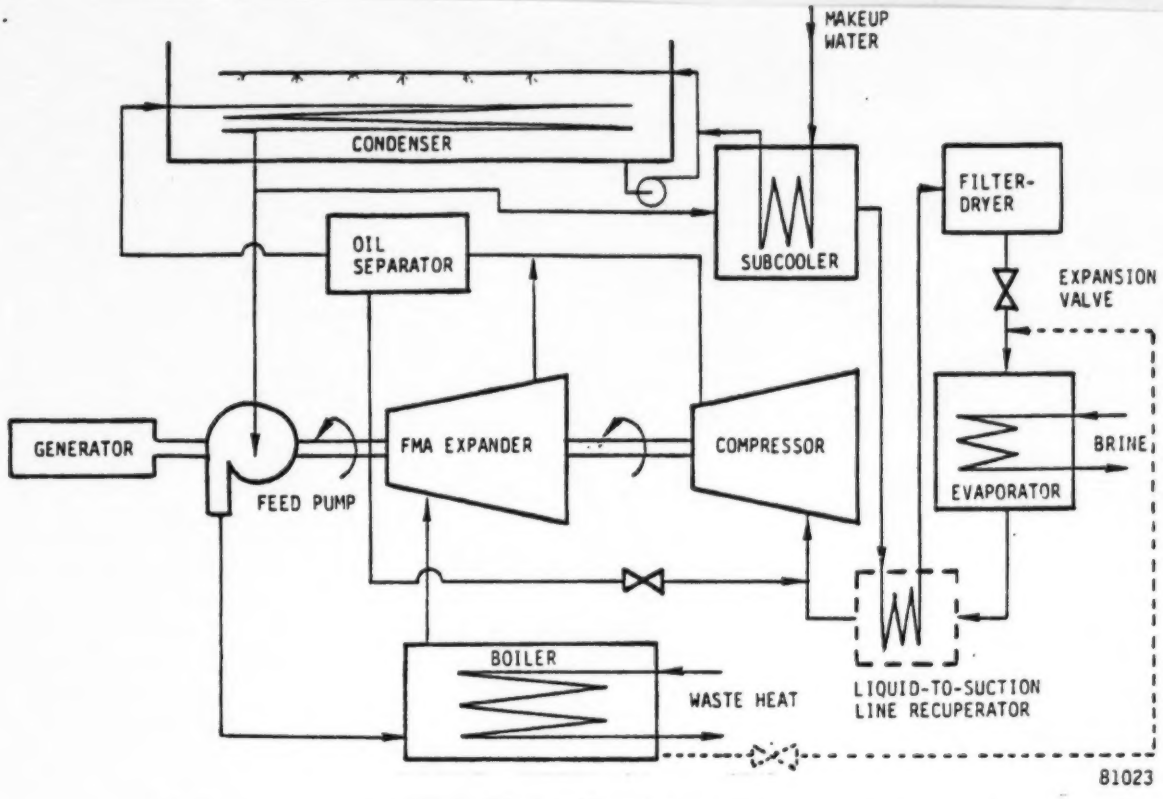

Figure 1. Integrated Rankine-Rankine Refrigeration System Schematic

Figure 2 shows how these two cycles are integrated mechanically. The expander, compressor, boiler feed pump, oil pump, and motor/generator are all contained in a semi-hermetic enclosure. This eliminates exposed shafts and any associated leakage. It also minimizes the number, required effectiveness, and friction of internal shaft seals. The expander and compressor share a crankcase, crankshaft, and lubrication system; this is accomplished by transforming two cylinders of a four-cylinder refrigeration compressor into expander cylinders.

2. CYCLE FEATURES

Certain of the components shown in Figures 1 and 2 deserve further mention.

2.1 Oil Letdown Line

Both the compressor cylinders and expander cylinders contaminate the refrigerant with lubricating oil, most (but not all) of which is returned to the crankcase by the oil separator. The remaining oil moves with the refrigerant as far as the boiler, where it remains dissolved in the liquid phase in an ever-increasing concentration. This concentration cannot be allowed to get

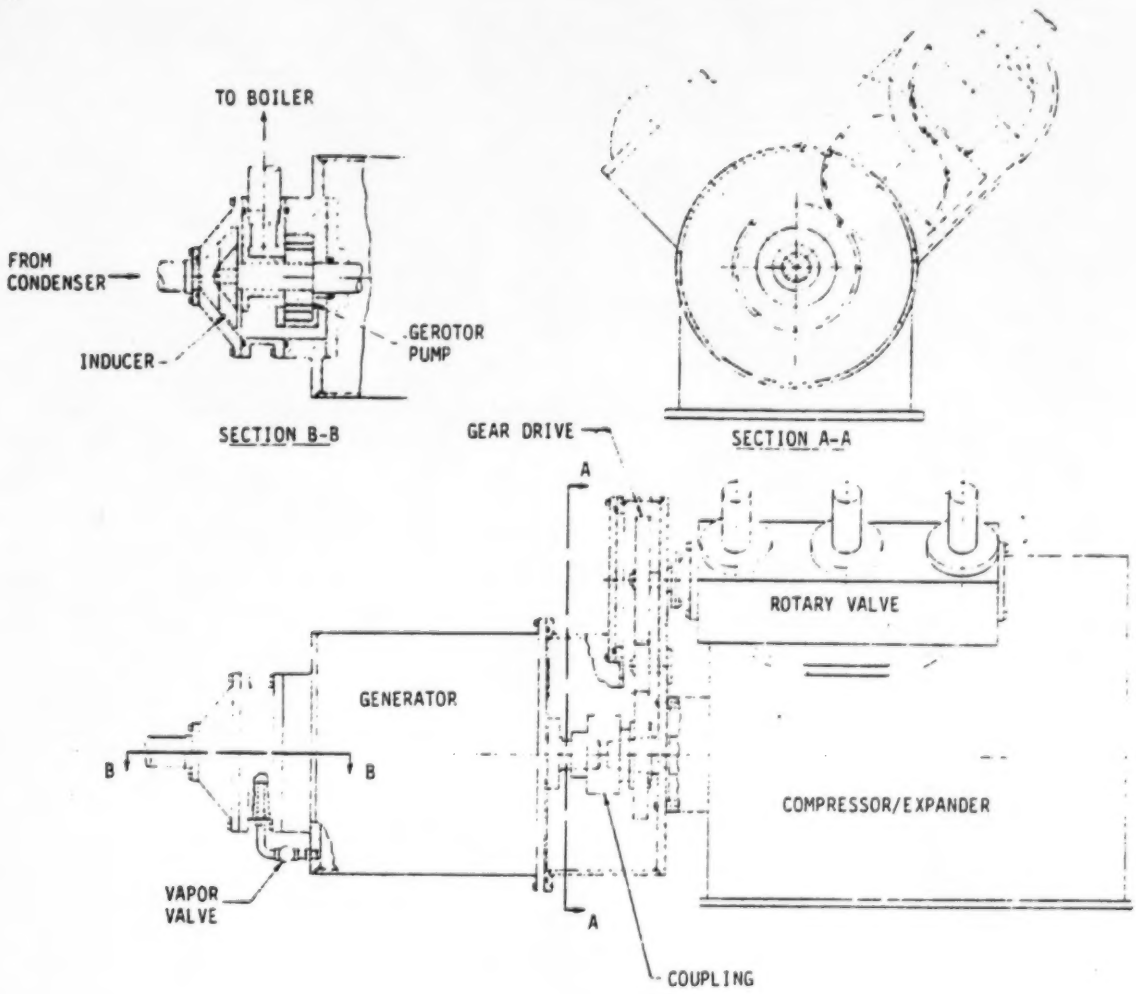

Figure 2. Mechanical Integration of Moving Parts

too high, lest the boiling point of the refrigerant solution be increased. Besides, this oil must eventually be returned to the crankcase.

The oil letdown line (shown dashed on Figure 1) permits the oil-rich liquid to be flashed to evaporator pressure through an expansion valve and returned to the crankcase via the evaporator. The flow rate through this line depends both on the effectiveness of the oil separator and on the maximum permissible oil concentration in the boiler.

2.2 Boiler Feed Pump

The boiler feed pump is a gerotor pump, with 0.0015" axial clearances specially chosen to minimize both backleakage and friction. Because the NPSH required by the gerotor pump can

exceed the available NPSH provided by the condenser subcooling and the static head, it is assisted by a centrifugal inducer shown in Figure 2.

2.3 Refrigeration Effect

The refrigeration effect in the evaporator, and thus the refrigeration capacity of the system, is maximized by subcooling the liquid leaving the condenser. This is accomplished both with a subcooler cooled by the condenser makeup water, and by a liquid-to-suction line recuperator cooled by suction line vapor.

The recuperator is a mixed blessing. Subcooling the liquid line increases the refrigeration effect, but superheating the suction line decreases the volumentric effeciency of the compressor. These effects very nearly cancel each other. However, the compressor needs some suction superheat anyway to protect it against ingestion of liquid; if superheat must be tolerated, then let it buy some refrigeration effect.

3. SYSTEM OPTIMIZATION

The sizes and configurations of the five heat exchangers are selected so as to maximize the overall system's ratio of capacity to initial cost. This capacity/cost ratio and system reliability are the major relevant criteria for judging the system. If the waste heat energy input to the system were assigned significant value, then the overall system efficiency (ratio of evaporator and boiler heat duties) would be significant; however, waste heat is usually considered valueless and is copiously available, so system efficiency matters only insofar as it contributes to the capacity/cost ratio. Operating costs, such as pump and blower power, are to be minimized where possible; however, the typical method of rejecting this waste heat (cooling tower) has comparable operating costs, and it simplifies the optimization process to ignore any differences in these operating costs.

Both cycles are sensitive to the condensing temperature. Table 1 shows that as the condensing temperature rises, the expander power output declines and the compressor power requirement increases. Thus, minimizing the condensing temperature is more important to this system than it would be to an electrically driven refrigeration system. This explains the large size of the condenser, and it explains why an evaporative condenser was chosen. An air cooled condenser rejects heat to the ambient dry bulb temperature, whereas an evaporative condenser rejects to the ambient wet bulb temperature; the difference between dry and wet bulb temperatures is generally significant when compared to the temperature difference that drives this Rankine cycle. A water-cooled condenser with a cooling tower ultimately rejects heat to the ambient wet bulb, but the circulating water loop adds a temperature difference that significantly raises the condensing temperature.

Table 1. - Sensitivity of Power Balance to Condensing Temperature

Condensing Temperature °C (°F)	Expander Output kW	Compressor Input kW	Feed Pump Input kW	Net Power To Generator (From Motor) kW	Balance After Pump And Fan kW
35 (95)	13.0	18.5	1.7	(7.2)	(16.9)
29 (85)	17.7	17.2	2.1	(1.6)	(11.3)
24 (75)	22.2	15.7	2.4	4.1	(5.6)
18 (65)	25.9	13.8	2.7	9.4	(0.3)
13 (55)	29.3	11.6	3.0	14.7	5.0

One approach to the design of this system would be to size the expander to provide sufficient power to drive the compressor when the ambient wet bulb is 80°F, which is exceeded only one percent of the time at the gaseous diffusion plants. Ninety-nine percent of the time the expander would be oversized, and the surplus shaft power would be utilized by the motor/generator, which would act as a motor only when starting plus one percent of the time. This approach would require six expander cylinders to drive two compressor cylinders.

Another approach is to design for an ambient wet bulb temperature that is approximately 20°F lower. This allows two expander cylinders to drive two compressor cylinders. Not only does this cut the total number of cylinders in half, but it allows the boiler to be one-third as large and the condenser to be one-half as large. The motor/generator will need to act as a motor more of the time this way, but it will still function as a generator most of the time.

4. EXPANDER DESIGN

The same low waste heat temperature (140°F) that limits system efficiency also makes possible the straightforward design of the expander. It allows the use of a standard refrigeration compressor crankcase and it allows the use of simple rotary intake and exhaust valves on the expander cylinders.

4.1 Crankcase

The York RS44A compressor was selected. It has four cylinders, each with 3.75 in. bore and 4.5 in. stroke, and operates at 1200 rpm. One feature that makes it attractive to this system is that its discharge is manifolded externally; expander cylinders can be separated from compressor cylinders simply by removing the manifold.

York makes a similar compressor with two-thirds the stroke (3 in.) and three-halves the speed (1800 rpm). Because the piston speed is the same, breathing losses would be the same. The m.e.p. is the same, so friction losses would also remain the same. The slower compressor is more attractive as an expander because its longer storke permits a larger clearance volume, which is necessary to accommodate the expander's valves.

The differential pressure across the piston is limited to 275 lb/in^2. Above this pressure, the connecting rod crank pin bearings become overloaded. The maximum pressure difference will occur across the expander piston, with the boiler pressure above and the evaporator pressure below. Under design conditions (127°F boiler, 15°F evaporator), this pressure difference is 245 lb/in^2. This maximum pressure difference limits the saturated boiler temperature that can be used with R-22 to 136°F (with a 15°F evaporator); boiler temperatures as high as 168°F can be accommodated by using R-12 instead of R-22.

The low temperatures at which the expander operates, together with the low temperature differences between intake and exhaust, together with the low heat transfer coefficients associated with R-22, tend to minimize thermal losses, especially those attributable to cyclic heat transfer. Accordingly, there was no reason to favor a uniflow expander, for its primary advantage is to minimize these losses.

4.2 Rotary Valves

The intake and exhaust valving for both expander cylinders is accomplished by a pair of rotary valves. Both valves are on a single shaft, which is geared to the crankshaft. Figure 3 shows how the valve connects the port in the cylinder head to the intake line, or to the exhaust line, or to neither one, as required.

The free breathing of the rotary valve arrangement is apparent from Figure 4. Because both intake and exhaust functions use the same port to the cylinder, it can be relatively large; the valve open area is 34 percent of the piston area. The flow paths are reasonably straightforward; a flow coefficient of 0.6 was used for the analysis of breathing losses.

Like any rotary valve, this valve requires ample lubrication. This presents no particular problem to this expander. Temperatures are low enough to permit oil lubrication (which is not the case with a steam engine), and the oil is quite compatible with the working fluid. Note in Figure 1 the oil separator that connects to the exhaust of both the compressor and expander cylinders; the expander cylinders contribute more oil to this common exhaust, due primarily to rotary valve lubricating oil.

Lubricating oil is supplied by the compressor's oil pump. The rotary valve requires oil at 300 psig, for the intake fluid is at boiler pressure (285 psig). The compressor's lubrication system is designed to supply oil to the crankshaft at crankcase

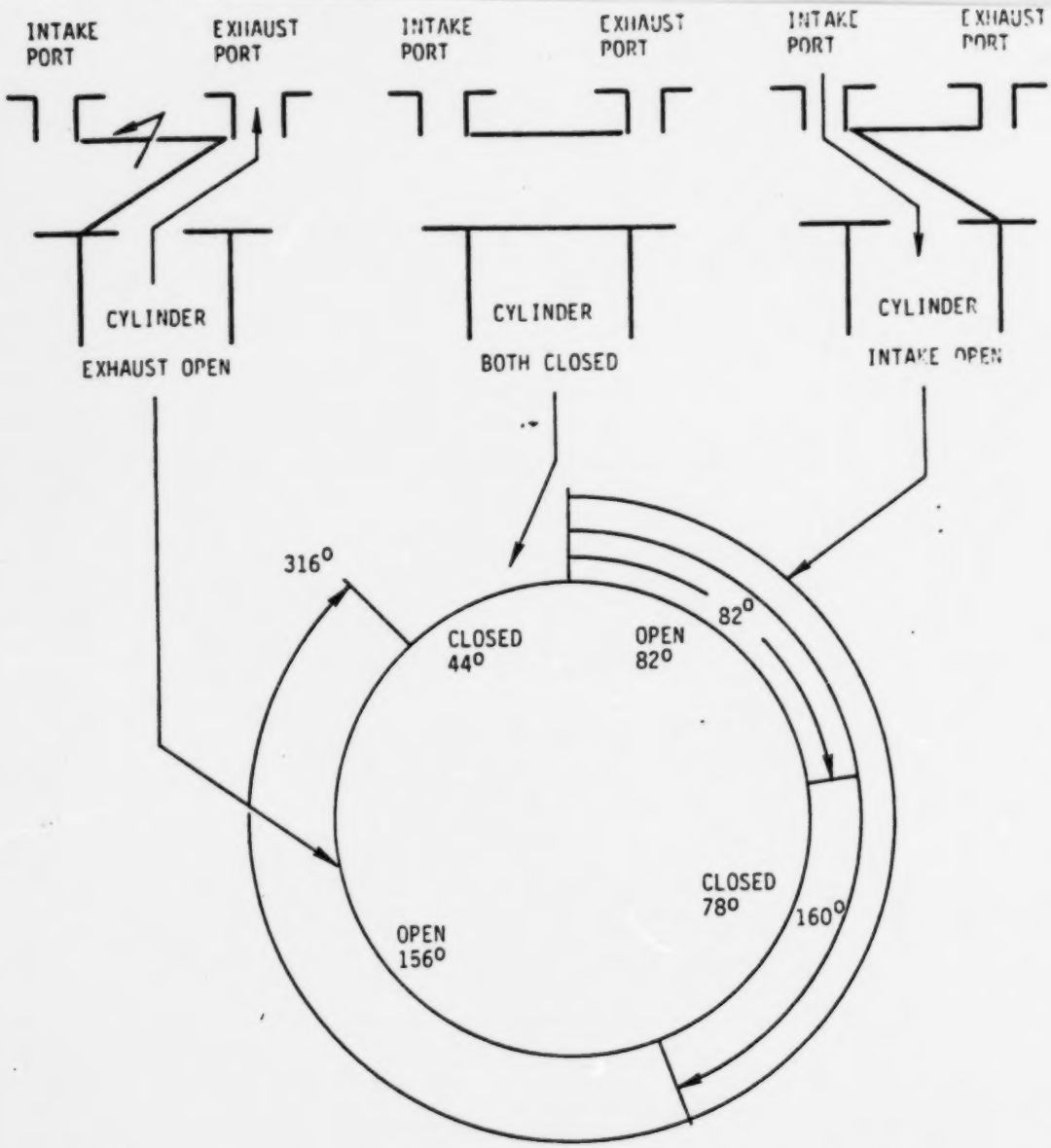

Figure 3. Operation and Timing of Rotary Valve

pressure plus 60 psi, which is less than the rotary valve requires. The lubrication system must be modified (see Figure 5) by blocking one end of the crankshaft and adding a flow restrictor.

The journal bearing surfaces of the rotary valve require tight radial clearances (0.002 in), both to maintain the hydrodynamic film and to prevent leakage. These clearances are possible largely because there is very little differential expansion as the valve warms up to operating temperature.

The efficiency and capacity of a reciprocating expander are quite sensitive to valve timing. Optimum valve timing is a function of inlet and exhaust pressures and of working fluid properties.

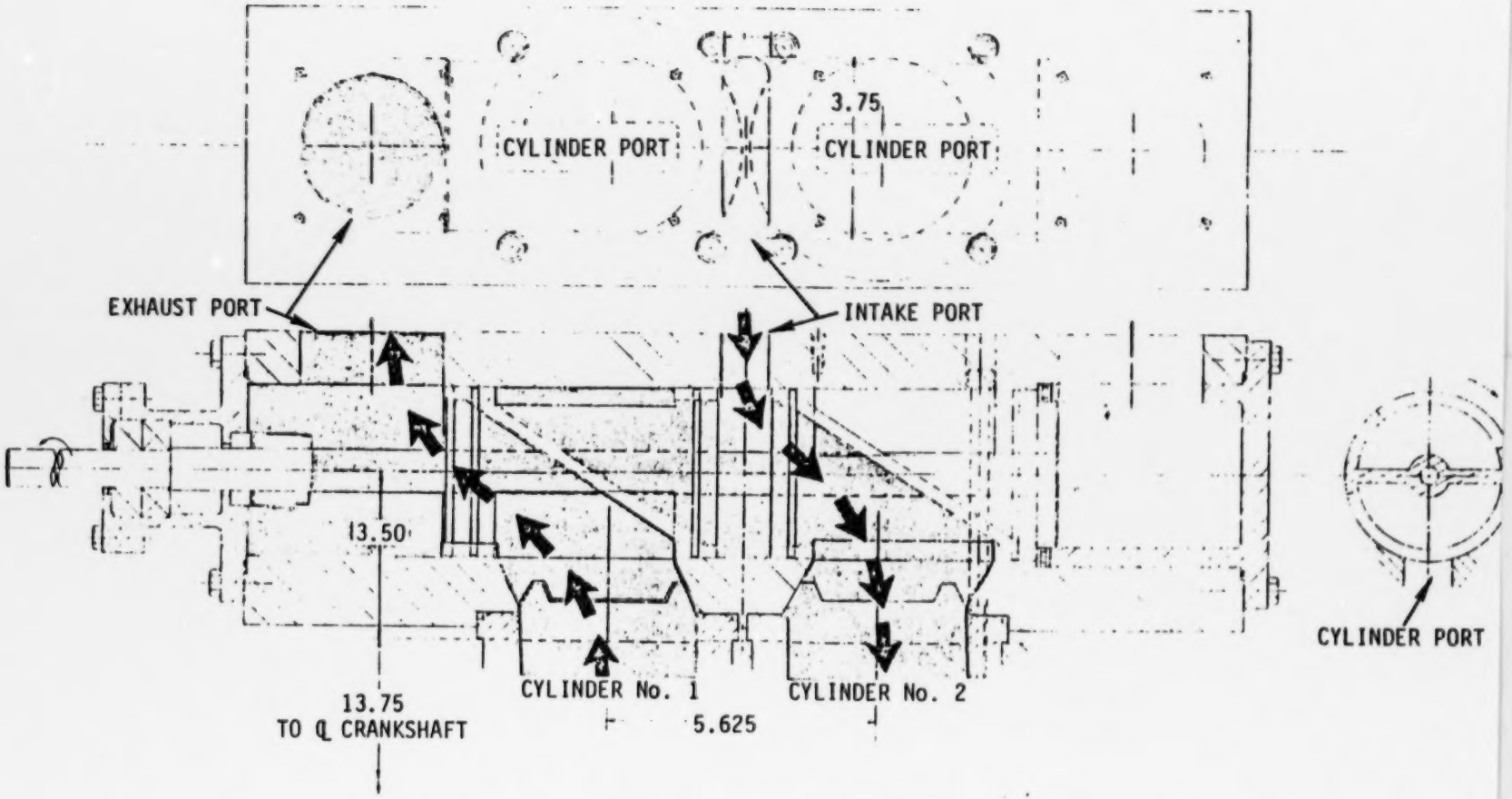

Figure 4. Layout of Rotary Valves, Showing Straightforward Flow Path

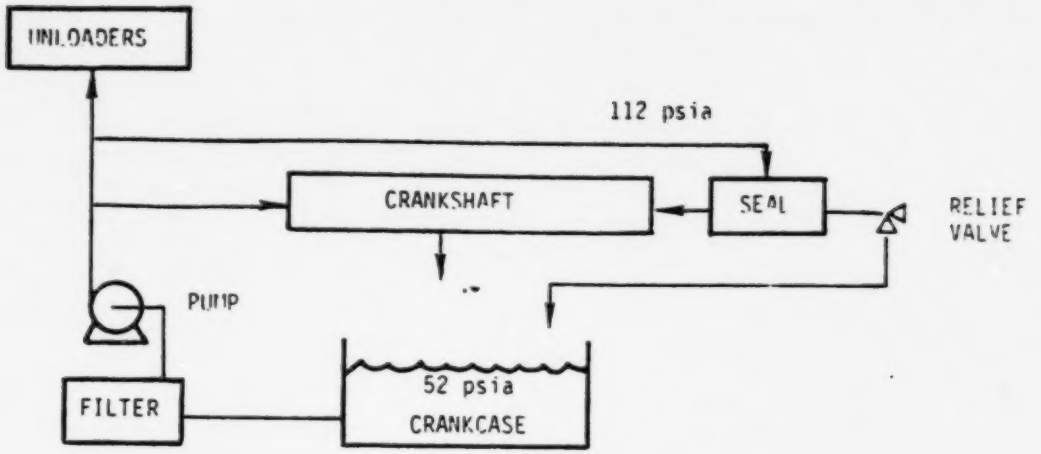

LUBRICATION SYSTEM BEFORE MODIFICATION

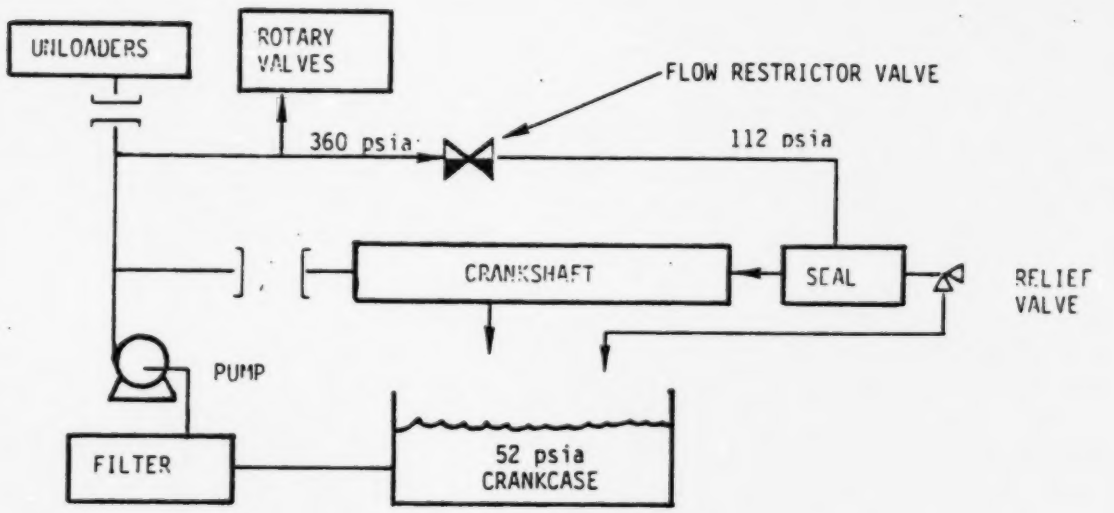

LUBRICATION SYSTEM AFTER MODIFICATION

Figure 5. Modifications to Lubrication System

Ideally, the intake valve should close at a point during the expansion stroke so that at bottom dead center the cylinder pressure equals the exhaust pressure. Similarly, the exhaust valve should close at a point during the compression stroke such that at top dead center the cylinder pressure equals the inlet pressure. These points are easily calculated for the ideal case, which is the isentropic expansion or compression of a perfect gas for cylinder pressure is directly calculable from volume by means of the expression:

$$p\ v^{\gamma} = \text{constant}$$

The *ideal* valve opening points are functions only of intake and exhaust pressures.

However, the *real* case differs form this ideal case because of four factors:

- Inability to open or close valves instantaneously
- Resistance to flow presented by finite flow area
- Heat transfer between working fluid and cylinder walls
- Deviation of working fluid from perfect gas.

All of these factors can be taken into account, but the analysis becomes sufficiently involved to require a computer.

The port angle on the test expander is 33.2 degrees. This means that both the intake and exhaust valve become fully open (or closed) 33.2 crankshaft degrees after opening (or closure) is initiated. When fully open, the valve area is 34 percent of the piston area. Valve area during the opening and closing periods is linear with crank angle.

Flow through the valves is modelled by a finite difference computer program, which keeps track of the mass and pressure inside the expander cylinder. Flow through the valves is proportional to valve open area and to the square root of the pressure difference between the cylinder and the intake or exhaust, as appropriate.

Flow losses present an interesting tradeoff in optimization of valve timing. When they are taken into account, matching pressure inside and outside the cylinders at the end of the stroke is no longer the sole criterion for optimization. Losses through partially open valves depend on the velocity through the valves. A valve that is, say, 50 percent open at the middle of the stroke (when piston velocity is highest) will suffer greater losses than a valve that is 50 percent open later in the stroke. For this reason, efficiencies are maximized with valve closings somewhat later than those that would simply match pressures.

Heat transfer between the cylinder (or piston) and the working fluid can be neglected in this case. Heat transfer coefficients for halocarbons are low, and the temperature differences in this expander are very low. Heat transfer is significant in a steam expander.

R-22 does not behave as a perfect gas. That is, the ratio:

$$\frac{pv}{T}$$

which equals the gas constant for a perfect gas, is not constant. No gas is perfect near the saturation line. Furthermore, saturated R-22 partially condenses when expanded. These discrepancies can be dealt with only by calculating pseudo-perfect gas properties that force the perfect gas equations to fit the property tables.

The computer program can calculate the work per cycle for an expander with a given valve timing. By changing the input valve timing, one can determine the optimum valve timing by maximizing this work.

Figure 6 presents the expander P-V diagram resulting from this computer analysis, together with a tabular comparison of ideal and predicted parameters. This calculation predicted that breathing losses would amount to only 13 percent; by comparison, poppet valves would present a 50 percent breathing loss. Thermal losses are expected to be minimal, for temperature differences are low and thermal transport properties poor. Mechanical losses are expected to be less than those of an internal combustion engine; m.e.p. is comparable, and the expander cylinder environment is less hostile to the lubricating oil.

5. CONCLUSIONS

This Rankine-Rankine refrigeration system maximizes its utility by:

- Operating at full capacity despite variations in ambient wet bulb temperature
- Utilizing off-the-shelf hardware except for the expander's rotary valves and the semi-hermetic housing
- Minimizing breathing losses by a novel valve design.

We hope to operate our demonstration system by the end of this year.

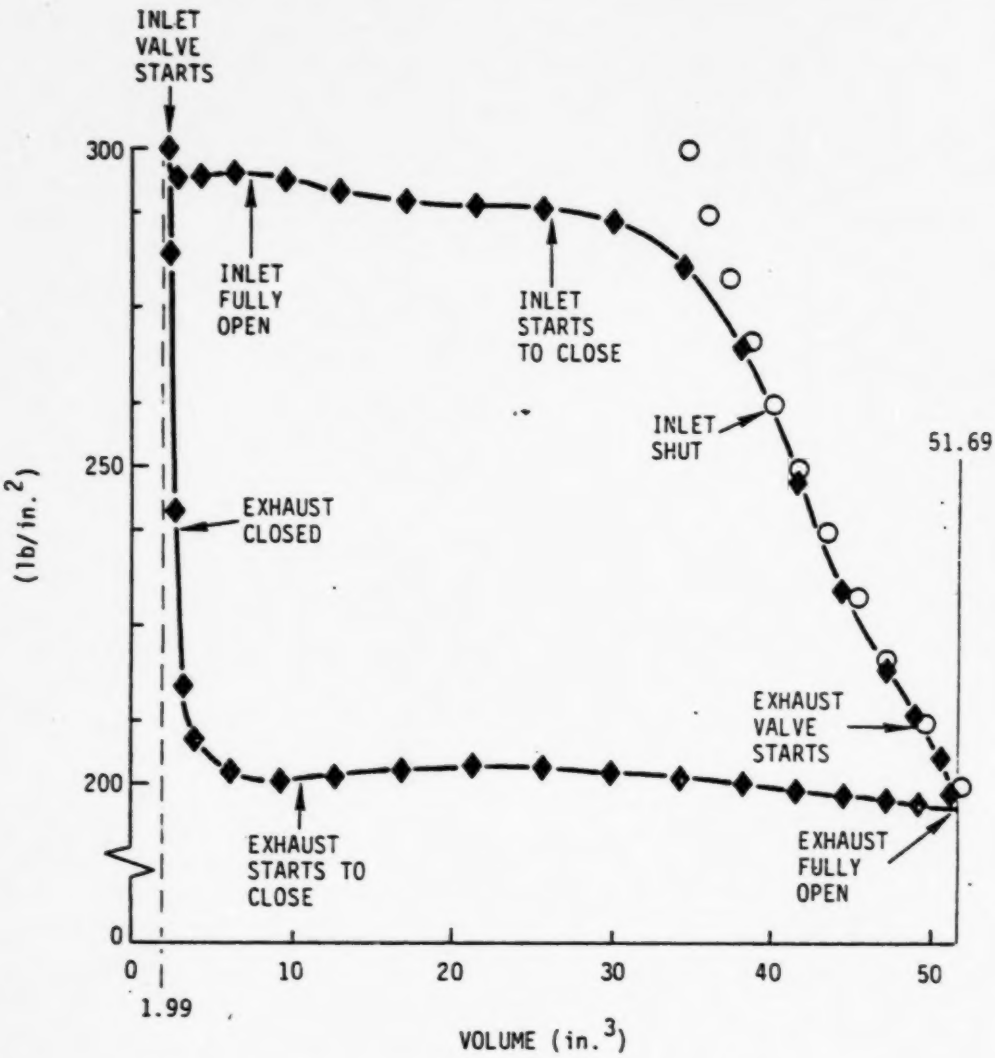

P_1 = 300 lb/in.^{2} T_1 = 127°F

P_2 = 196 lb/in.^{2} T_2 = 95°F

INDICATED MEAN EFFECTIVE PRESSURE - 72.5 lb/in.^{2}

FRICTION MEAN EFFECTIVE PRESSURE - 14.8 lb/in.^{2}

BRAKE MEAN EFFECTIVE PRESSURE - 57.7 lb/in.^{2}

MASS FLOW - 7790 lb/hr

INDICATED EFFICIENCY - 87.2%

BRAKE EFFICIENCY - 69.4%

Figure 6. P-V Diagram From Computer Results

PB82-228156

SOME PROBLEMS IN DESIGNING THE WASTE HEAT POWER STATION OF YOUXI

Dechang Liu, Mingru Zheng
Department of Power Engineering
Huazhong Institute of Technology
Wuhan, Hubei, China

ABSTRACT

Two problems will be analysed and discussed in this paper. They are: (1) unsteady thermal operation condition; and (2) how to meet requires of metallurgical production and electricity generation. Methods for solving above problems are stated too.

1. INTRODUCTION

The First Smeltery of Yunxi at Gejiu in Yunnan Province is a nonferrous metals plant which has many kinds of smelting furnaces, such as reverberatory furnances, melting furnaces and copper blast furnaces. A lot of heat, about 22.4 million kilocalories, was wasted in the smelting process every year. Since water cooling system was used to reduce the temperature great quantity of water and electricity were consumed.

The waste heat generating project of Yunxi involves the construction of 5 waste heat boilers and 2 turbo-generators. Its total capacity is 3.0 MW. The first stage of the project, two boilers and a turbo-generator installed in 1972, have been working well.

2. TECHNOLOGICAL PROCESS OF WASTE HEAT GENERATING

The combustion products from reverberatory furnaces with a temperature of 800-1100^{o}C are conducted into the waste heat boiler, cooled down to 250-300^{o}C, passed through a suction fan, drip washing tower, electrical precipitator and finally vented from a stack. Cool air is supplied to an air preheater by a blower to heat to 180-200^{o}C; the heated air enters the chamber of the reverberatory. Overheat steam, produced by waste heat boiler with 14 kg/cm^{2} and 370^{o}C, drives the turbo-generator unit. Electricity with a voltage raised by a transformer is sent to an electric power system. The schematic of the waste heat generating is shown in figure 1.

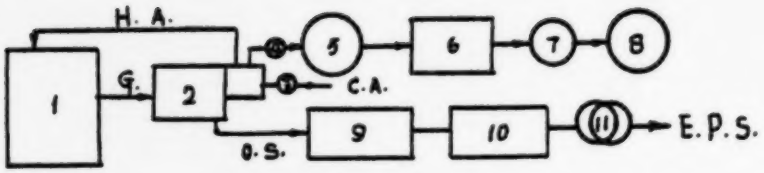

Fig. 1. Schematic of Waste Heat Generating

1 -- Reverberatory Furnace 2 -- Waste Heat Boiler
3 -- Blower 4 -- Suction Fan 5 -- Drip Washing Tower
6 -- Electrical Precipitator 7 --- Main Suction Fan
8 -- Stack 9 -- Turbo 10 -- Generator
11 -- Transformer H.A. -- Heat Air C.A. -- Cool Air
G -- Gas O.S. -- Overheat Steam E.P.S. -- Electric Power System

3. UNSTEADY THERMAL CONDITION OF WASTE HEAT BOILER

Reverberatory furnaces are the heat source of waste heat boilers. The thermal condition of waste heat boilers depends on the thermal condition of reverberatory furnaces. Variation of gas flow, temperature and quantity of gas heat with time in a smelting period of the reverberatory furnace are shown in table 1 and figure 2 - 4,, which were measured before designing the waste heat boiler. From these figures we know that the variation range of gas flow is about 15-18%, the variation range of heat quantity of gas is about 40%.

Table 1. Variation of Thermal Condition of Reverberatory

No.	1	2	3	4	5	6	7	8	9
Time (Min.)	0	42	84	121	164	214	339	382	413
Gas Temp. (°C)	1250	1250	1240	1260	1250	1240	1240	1240	1260
Gas Flow (SM^3/H)	5020	4070	5720	5550	5680	4300	5090	4830	4540
Heat Quantity ($X10^6$ · Kcal/H)	2.32	1.88	2.62	2.58	2.63	1.94	2.33	2.21	2.11

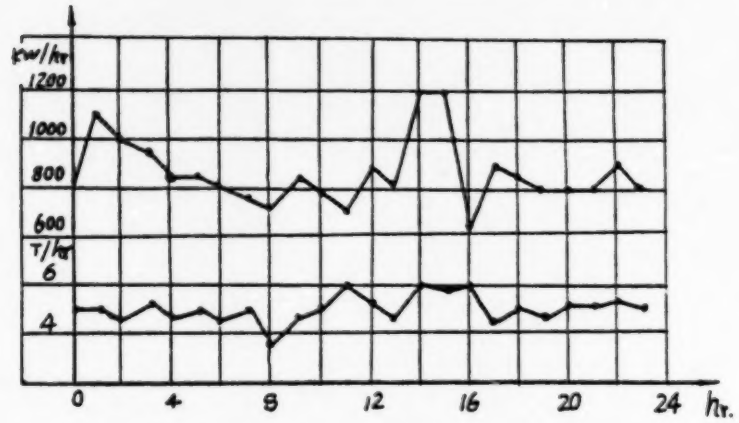

Fig. 6. Variation of Capacity of Boiler and Turbo-Generator

4. DETERMINING CAPACITY AND ARRANGEMENT PATTERN OF BOILER

Reverberatory furnaces supply waste heat boilers with high temperature gas. Exhausted gas from boilers is removed of metal dusts through the electrical precipitator. Determining the capacity and arrangement pattern of boilers should facilitate the tasks of smelting, metal dust collecting and electricity generating.

In determining the capacity of the boiler the following main factors must be considered:

(1). Operation, handling of accidents and equipment maintenance;

(2). Decreasing the resistance drop of gas and air, heat loss and high temperature slagging.

Gas of high temperature is supplied to a waste heat boiler by two smelting furnaces; a boiler capacity is 5 t/hr; semi-outdoor boilers were installed in an elevated position as close to reverberatory furnaces as possible. As a result above mentioned factors were considered practical.

As quality of waste heat boilers is improved and operation experience accumulated, a cooling system of radiant surface can be directly installed in the rising gas ducts of reverberatory furnaces for solving the third factor well mentioned above and strengthening production and increasing heat availability factor.

5. DETERMINING CAPACITY OF TURBO-GENERATOR

In determining capacity of the turbo-generator unit, the thermal condition of smelting furnaces and their yearly operation hours must be considered. The average thermal condition in theory is that smelting furnaces are all in operation at average condition. In such condition the theoretical installed capacity is 4.3 MW.

It is obvious that the unsteady thermal condition of reverberatories influences the thermal condtion of waste heat boilers. The unsteady thermal condition of waste heat boilers is one of important characteristics which must be considered carefully in designing and operating waste heat power station.

The following technical measures have been taken to improve the stability of thermal condition.

(1) Providing a waste heat boiler with two smelting furnaces and staggering their smelting periods can balance the variation range of gas flow and temperature, this to improve the thermal condition stability of waste heat boilers. To fully tap the potentials of waste heat an auxiliary gas path is not designed for regulating the thermal condition of boilers.

(2). 5 t/hr capacity waste heat boilers were converted from 10 t/hr capacity steam boilers with a grate furnace. The water volume of the waste heat boiler, i.e. the stored heat, is twice as much as the steam boiler. As such it can improve the thermal condition stability.

(3). The main steam system is central main piping system. Due to the original layout of the old installations, the new turbo-generator was set up far away from waste heat boilers. The distance between them is about 200 m. The main steam pipe is 200 mm in diameter. As a result the main steam system stores a great quantity of heat, thus to improve the thermal condition of boilers.

Smooth running over the years shows that above mentioned measures play an important role in improving the thermal condition stability. When above mentioned measures can not get the allowed variation range of thermal parameters of waste heat boilers, regulating power controller is the last method.

The variation of thermal parameters of boilers and the capacity of the turbo-generator unit are shown in figure 5-6.

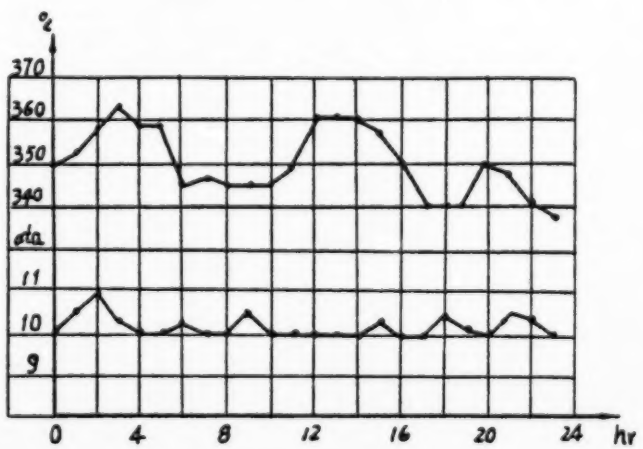

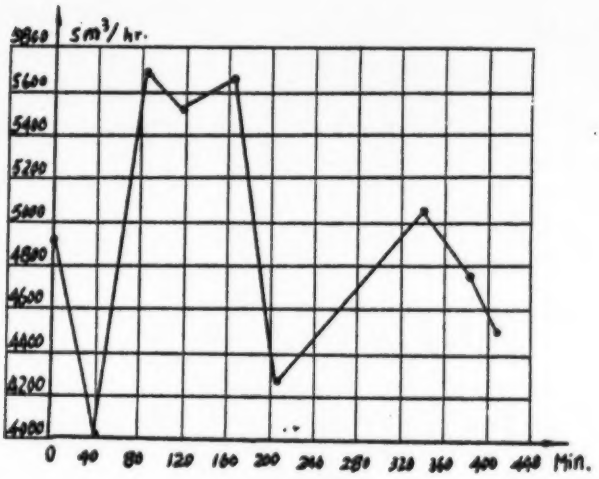

Fig. 2. Variation of Gas Flow of Reverberatory

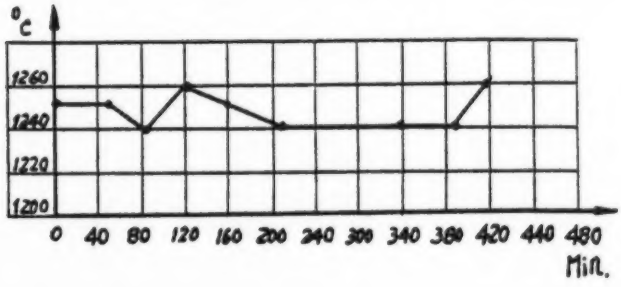

Fig. 3. Variation of Gas Temperature of Reverberatory

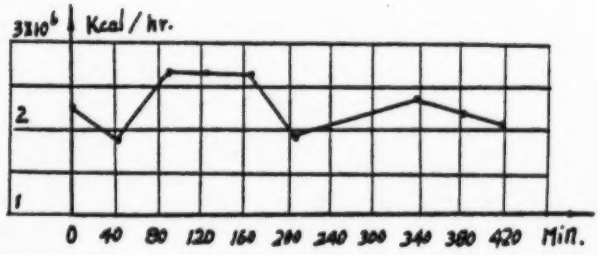

Fig. 4. Variation of Gas Heat Quantity of Reverberatory

The thermal condition is called comprehensive thermal condition after considering operation probability of smelting furnaces. In such condition the installed capacity is 2.9 MW. According to this condition two turbo-generators were chosen in designing waste heat power station.

6. WASTE HEAT GENERATOR AND SMELTING PRODUCTION

The main thermal factors influencing smelting production are air temperature, flow and pressure and vacuum of the furnace chamber. With the air preheater in the tail duct of waste heat boilers, the temperature of heat air can reach 180-200°C. Vacuum of combustion chamber can be met with the installation of suction fan.

The major thermal factors influencing collecting metal dusts are gas temperature, humidity and velocity. After reducing air leakage, keeping the velocity at 0.8 m/sec. and increasing injection of water to get high gas humidity and low gas temperature of 85-80°C, the efficiency of electrical precipitator is about 97-98% when waste heat boilers are running.

7. CONCLUSION

(1). Although the variation of thermal condition of reverberatory is great, the waste heat boiler can be kept operating within an allowed variation range of steam parameters;

(2). Operation practice shows that this kind of technology process of generating electricity is rational and can meet requires of smelting production;

(3). Waste heat generating changes "waste" into the "useful", the yearly saving of standard fuel is about 2100 tons.

PB82-228164

DESIGN OF THE PROPOSED WATTS BAR WASTE HEAT PARK

Charles F. Bowman
and
Robert E. Taylor
Tennessee Valley Authority
Knoxville, Tennessee, U.S.A.

ABSTRACT

TVA has proposed a waste heat park to be located adjacent to the Watts Bar Nuclear Plant. The occupants of the proposed park would be provided with hot water from the nuclear plant's condenser circulating water (CCW) system to utilize a portion of the power plant's waste heat.

Curves are presented here characterizing temperature of the waste heat available in terms of seasonal and diurnal variations for average conditions and high and low extremes. A table shows the frequency distribution of waste heat temperatures for each month of the year based on full load operation of one of the nuclear plant units.

Details of the design of the waste heat distribution (WHD) system inside the security fence of the nuclear plant are also presented. Problems encountered in retrofitting the design of the nuclear plant to include the waste heat piping and valves are discussed.

The paper discusses the conceptual design of the park and how provisions will be made for staged development. The estimated cost of the first stage is presented.

1. INTRODUCTION

A conceptual design and cost estimate has been prepared for the development of the Watts Bar Waste Heat Park to be located adjacent to the Watts Bar Nuclear Plant, consisting of two 1270-MW(e) units located in Rhea County, Tennessee. When completed the park will utilize up to 100,000 gal/min of the nuclear plant's CCW in various heating processes over an area in excess of 400 acres. The Watts Bar site is well suited for this project because it is the first TVA nuclear plant designed to reject its waste heat directly to the environment via natural draft cooling towers operating in a closed cycle. Accordingly, the CCW temperature will never be lower than 93° F at full load operation and will be as high as 130° F during the summer months.

Approximately 14,000 feet of waste heat piping and valves is being installed. A draft environmental impact statement has been issued. A preliminary marketing effort has been performed, and TVA has received

letters of interest from numerous greenhouse operators and several manufacturing firms which can realize significant savings by utilizing the relatively low temperature water available. A cost estimate of the WHD system and other park services has been prepared.

This paper will focus on the salient engineering accomplishments of this project to date: characterization of the waste heat available, the design and installation of the waste heat piping and valves inside the nuclear plant security fence, and the conceptual design of the ultimate park.

2. CHARACTERIZATION OF WASTE HEAT

The waste heat hot water temperature (HWT) is a function of ambient meteorological conditions, unit load, CCW system flow rate, and the way that the cooling tower responds to these variables.

In estimating the temperature of the available waste heat, predictions of ambient meteorological conditions are based upon statistical analysis of data recorded at Chattanooga during the period 1948 through 1973 and the effect of waste heat usage upon HWT was neglected.

The cooling tower performance was estimated using a vendor-supplied approximate mathematical model. Note, however, that the cooling tower contractor recommends not allowing the tower exit temperature to drop below 55° F. This corresponds to a minimum HWT of 93° F at 100 percent load and flow. A manual deicing system in the tower is used to maintain this temperature. The tower performance routine used in this analysis does not include any provisions for determining performance under various manual modes of operation. Instead, a minimum HWT value of 93° F was assumed.

The HWT available when a unit operates at full load under design conditions (tower flow of 410,000 gal/min and tower heat load of 7.8 times 10^9 Btu/hr) is described by Table I and Figures 1 through 5. Table I lists the percent occurence of each HWT value for each of the 12 months. The figures describe typical and extreme HWT patterns.

Figure 1 shows for each month the typical daily minimum (curve A), daily average (curve B), and daily maximum (curve C) values of HWT. Figures 2, 3, 4, and 5 show diurnal variations in HWT for January, April, July, and October, respectively. In each of these four figures, curve A depicts the variation in HWT during the coldest day recorded in that month, curve C depicts the HWT variation during the hottest day, and curve B depicts the average HWT variation.

3. WASTE HEAT PIPING - NUCLEAR PLANT INTERFACE

The decision to make provision for the WHD system in the nuclear plant design came after all of the affected plant features were already installed. Therefore, special problems were encountered while designing and installing the interface between the WHD system and the nuclear plant, since the nuclear plant construction schedule could not be impacted. To further complicate the problem, the site for the waste heat

MONTHLY PERCENT OCCURRENCES FOR EACH TOWER HWT

HWT	JAN	FEB	MAR	APR	MAY	JUNE	JULY	AUG	SEPT	OCT	NOV	DEC
93	4.62	2.96	0.21								0.40	1.59
94	1.88	1.36	0.11								0.26	1.21
95	2.95	1.90	0.28								0.41	1.77
96	3.43	2.46	0.68							0.02	0.80	2.88
97	3.99	3.03	1.15							0.05	1.12	3.76
98	5.10	4.30	2.20	0.06						0.13	1.90	4.86
99	5.57	4.53	2.59	0.28						0.27	3.23	5.43
100	6.55	4.76	3.74	0.50						0.50	4.27	6.01
101	7.07	6.32	5.17	1.01	0.02					0.77	5.18	6.83
102	6.52	6.58	4.92	1.57	0.03				0.03	1.10	5.17	6.54
103	6.66	6.97	5.69	2.17	0.16				0.0	1.42	6.04	7.69
104	5.82	6.81	5.87	2.28	0.28				0.02	1.96	6.75	7.39
105	5.61	6.15	5.30	3.13	0.61	0.02			0.03	2.74	6.35	6.63
106	5.59	6.51	5.97	4.17	0.91	0.05			0.18	3.73	6.43	5.75
107	4.70	5.86	6.43	4.21	1.36	0.11			0.35	4.17	6.30	5.62
108	4.12	5.36	6.35	4.98	1.69	0.07			0.56	4.79	6.35	4.73
109	3.74	4.67	6.88	5.42	2.34	0.17			0.85	5.52	6.12	3.98
110	3.30	3.97	6.59	5.79	2.72	0.28			1.45	5.68	5.47	3.67
111	2.39	3.95	5.74	6.72	3.88	0.45	0.10	0.02	2.05	6.53	4.90	2.82
112	2.43	3.16	4.81	6.40	4.36	1.07	0.14	0.22	2.44	6.52	4.64	2.41
113	2.40	2.65	4.54	7.61	5.96	1.53	0.29	0.54	3.22	7.21	5.00	2.34
114	2.07	2.02	3.72	7.43	6.52	1.86	0.65	0.93	4.01	6.69	3.42	1.83
115	1.54	1.70	3.54	7.40	7.48	3.50	0.90	1.82	6.28	6.77	3.54	1.52
116	1.07	0.92	2.55	6.99	9.05	4.47	1.67	2.86	7.77	7.36	2.60	1.35
117	0.53	0.90	1.99	5.79	8.81	6.58	2.66	3.79	7.94	6.37	1.81	0.71
118	0.29	0.41	1.40	5.06	9.79	9.56	5.21	6.56	9.56	5.62	1.36	0.35
119	0.05	0.11	0.84	4.22	8.14	10.27	7.05	7.49	9.51	4.53	0.67	0.20
120	0.03	0.03	0.44	2.99	6.37	11.52	12.44	11.74	10.33	3.75	0.30	0.04
121			0.18	2.15	7.06	11.76	15.43	14.95	9.92	2.94	0.21	0.01
122			0.11	1.13	5.08	9.98	12.11	11.79	7.02	1.41	0.01	
123				0.42	3.54	8.62	11.29	10.73	6.43	0.80		
124				0.12	2.16	7.01	10.18	9.22	5.01	0.39		
125				0.01	0.88	5.37	9.23	9.03	3.41	0.16		
126					0.28	3.43	6.28	4.84	1.18	0.10		
127					0.04	1.65	2.93	2.41	0.36	0.02		
128						0.49	1.10	0.73	0.09			
129						0.18	0.29	0.21				
130						0.02	0.03	0.07				

Table 1

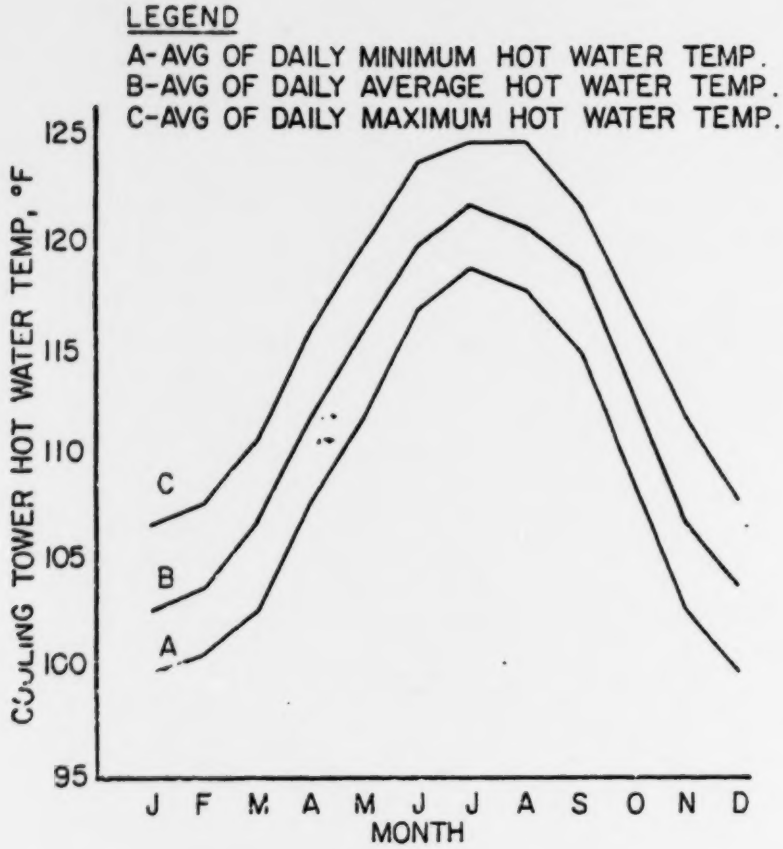

Figure 1 Average Daily Hot Water Temperature

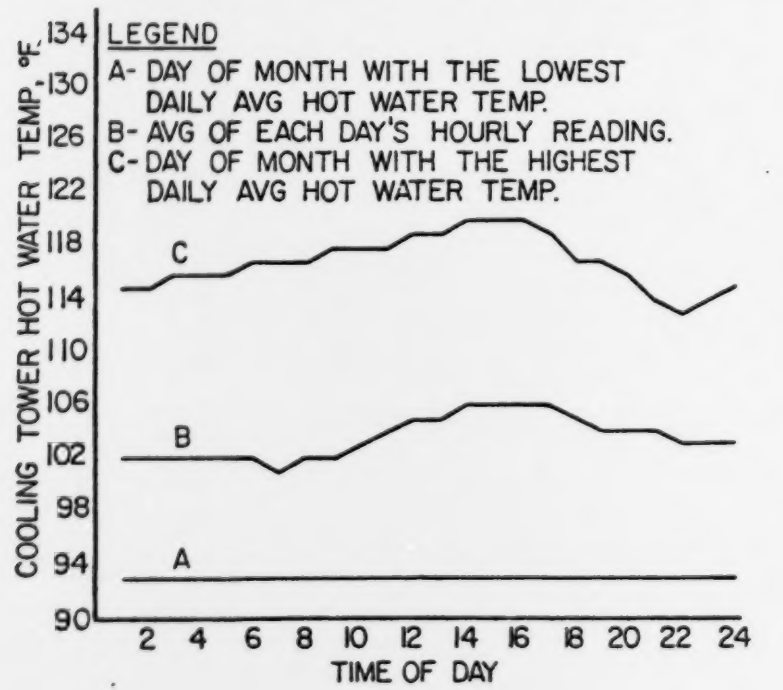

Figure 2 Diurnal Variation in Tower Hot Water Temperature for January

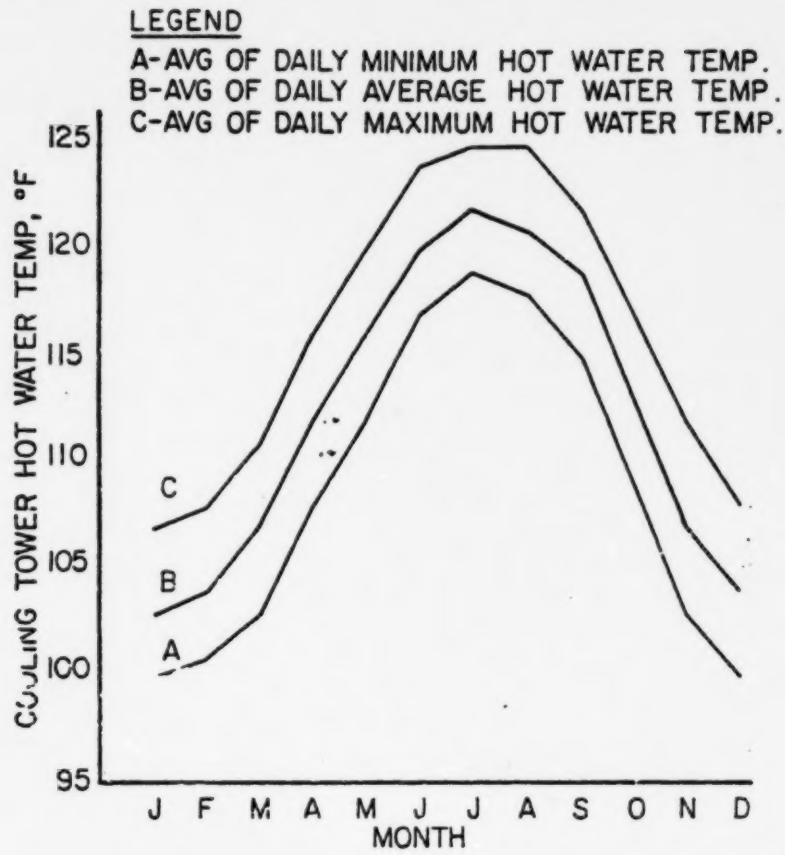

Figure 1 Average Daily Hot Water Temperature

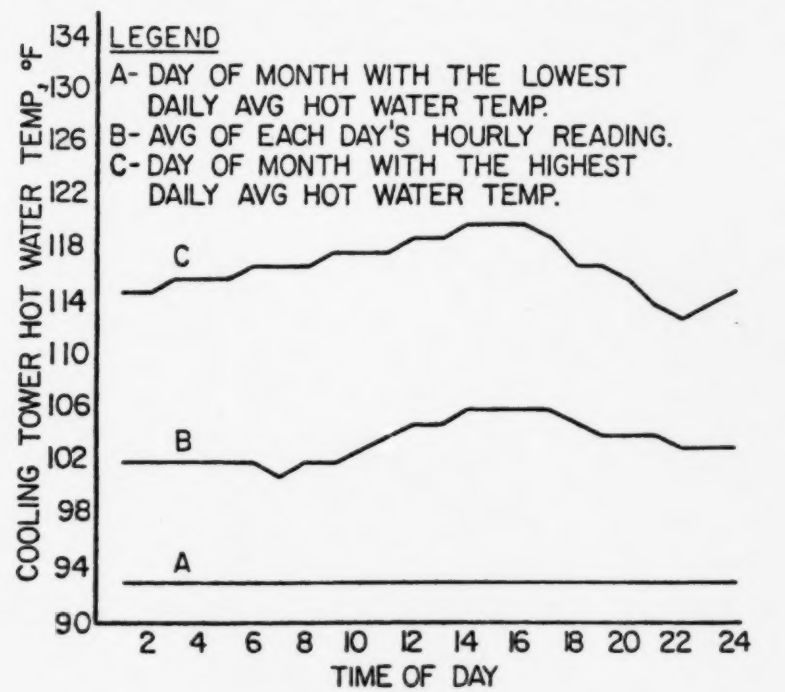

Figure 2 Diurnal Variation in Tower Hot Water Temperature for January

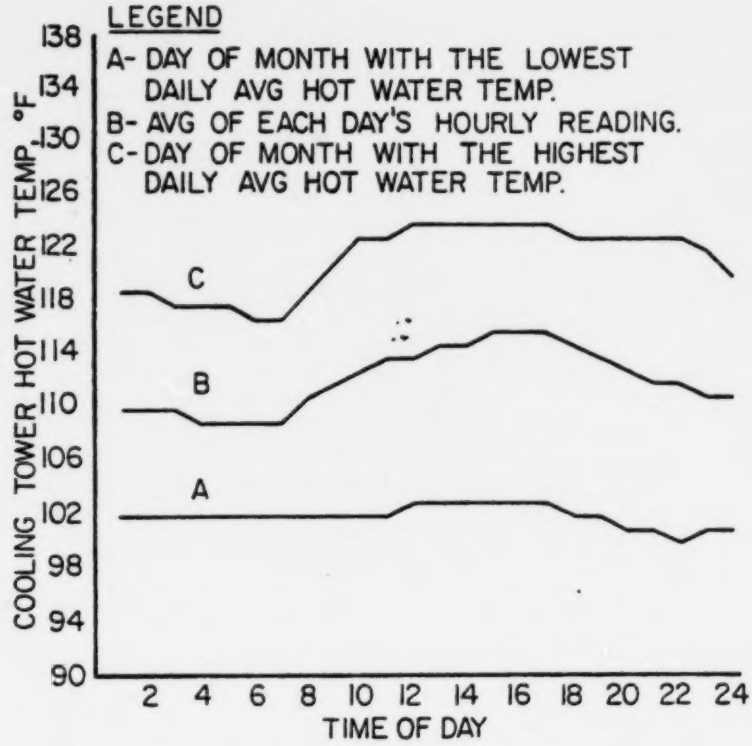

Figure 3 Diurnal Variation in Tower Hot Water Temperature for April

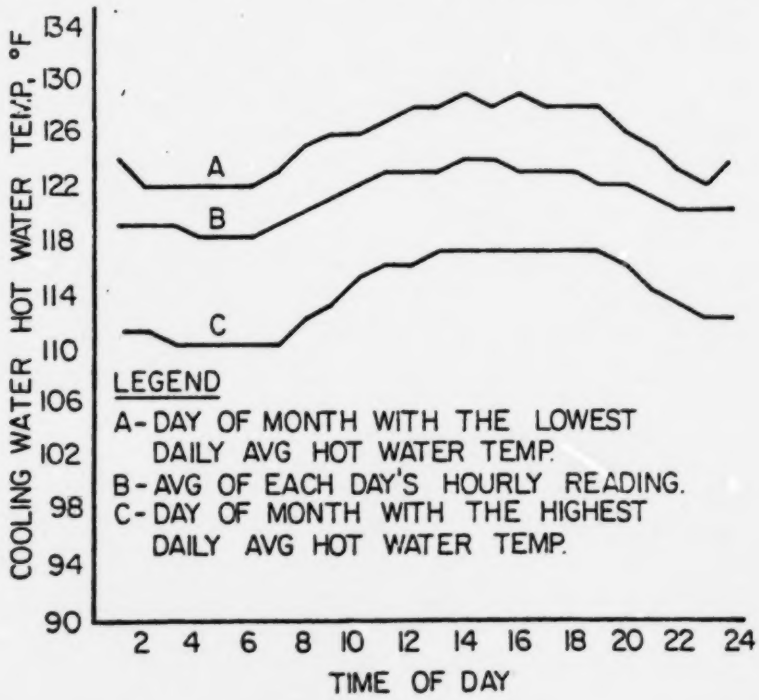

Figure 4 Diurnal Variation in Tower Hot Water Temperature for July

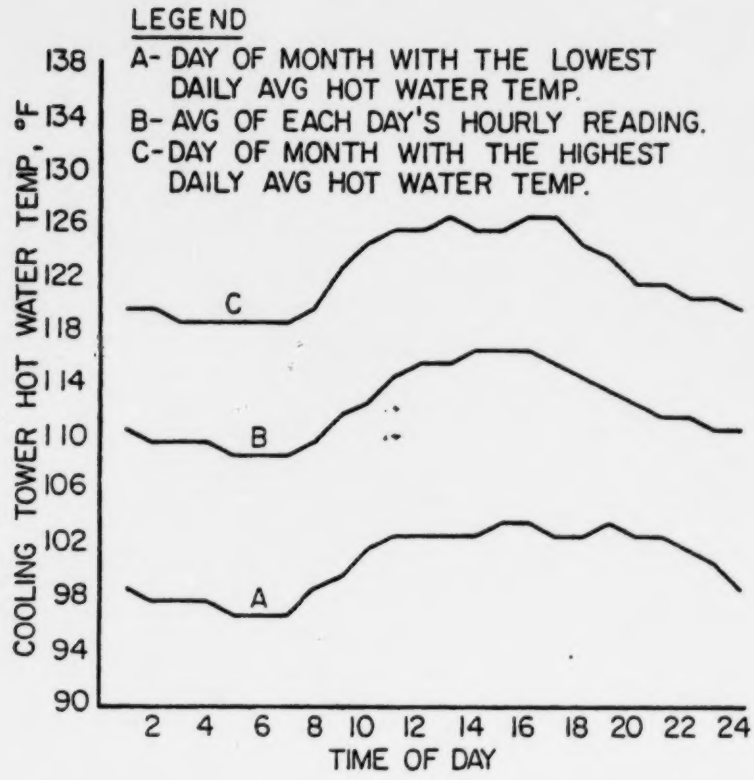

Figure 5 Diurnal Variation in Tower Hot Water Temperature for October

park is on the west side of the nuclear plant, while the cooling towers are located to the east of the plant. Accordingly, the large waste heat supply line and return lines had to be routed around the nuclear plant through an extremely congested yard area. Many of the affected systems were already in operation and were required to support plant construction activity and preoperational testing. In many cases the waste heat piping could be located under the existing features, but this solution required the existing piping and electrical conduit banks to be supported with shoring during construction or to be relocated. In some cases alternative services were provided on a temporary basis while affected systems (such as chemical treatment, lighting, and yard drainage) were taken out of service.

Of special concern was the point where the waste heat piping crossed the safety-related electrical conduit bank that provided power to the essential raw cooling water pumps located in the intake pumping station. In this area, the waste heat piping had to be designed so that its failure would not impact the operation of safety-related equipment. None of these problems proved insurmountable, however, and the waste heat piping has been installed without impacting the nuclear plant construction schedule.

One feature of the plant design that proved very fortunate is the interface between the CCW yard piping, which is concrete pressure pipe, and the piping inside the cooling towers, which is cast-in-place concrete. This transition was found to be of carbon steel pipe of sufficient thickness and length so that the waste heat piping connections

could be readily welded on to the CCW piping. Additionally, a cooling tower bypass line was modified to serve both as a bypass during startup and shutdown of the tower and as a waste heat return line during normal operation. Figure 6 shows the arrangement of the waste heat piping at the interface with the CCW piping. The steel section of transition piping between the CCW yard piping and the cooling tower piping includes two obtuse elbows which are utilized to discourage recirculation. Butterfly valves are provided to isolate the WHD system from the CCW system when required. Only one of the two cooling towers will be used to provide waste heat at any given time.

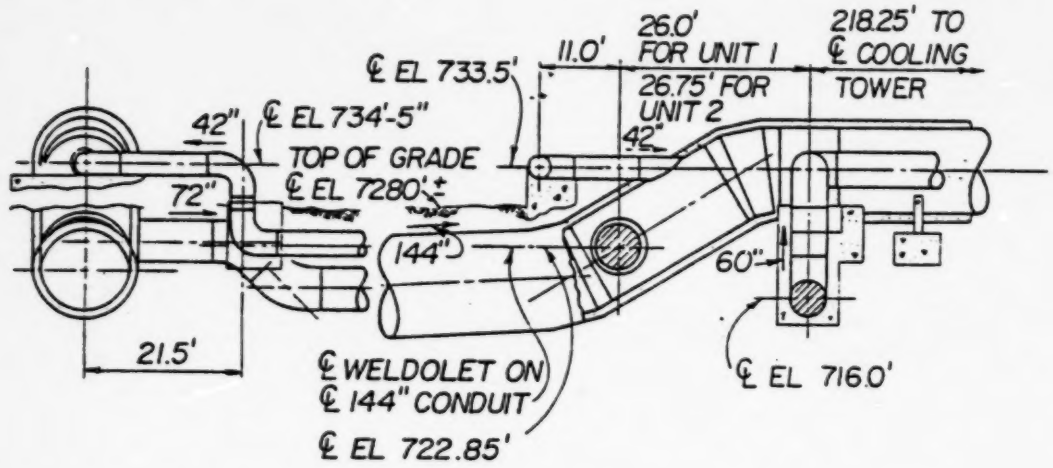

Figure 6 Waste Heat Piping Interface with CCW System

4. CONCEPTUAL DESIGN OF WASTE HEAT PARK

The Watts Bar Waste Heat Park is envisioned as a multi-stage development with completion of the first stage to be concident with that of the last unit of the nuclear plant. Along with the development of the first stage of the WHD system will be the installation of the basic service systems required by the park occupants, including transportation facilities and utilities. Figure 7 shows a conceptual rendering of the park in its ultimate stage of development. A number of approaches at staged development have been considered, and no final decision as to the scope of the first stage has been reached at this time. The approach presented herein appears to be one of the more viable options.

4.1 Waste Heat Distribution System

The WHD system distributes hot CCW to the waste heat user and returns the cooler CCW back to the nuclear plant. The WHD system is the heart of the waste heat park and is particularly critical because of its interfaces with the nuclear plant. Figure 8 shows the flow diagram for the ultimate development of the proposed WHD system based on an assumed mix of park occupants. The design concept makes provision for both those users who reduce the temperature of the CCW by a small amount and return the CCW to the cooling tower for further cooling and those who reduce the CCW temperature to below that coming off the towers and return the CCW to

Figure 7 Proposed Watts Bar Waste Heat Park

the cooling tower basin. Additionally, users may be provided with CCW either by gravity or under pressure if required.

Current plans are for only a portion of the supply pumps and piping to be installed during the initial stage. Only those return pumps and piping for those users which must return the CCW to the cooling tower inlet would be initially provided. However, space will be provided in both pumping stations and electrical services will be sized so that the pumps may be added later. The initial stage of the WHD system would be capable of delivering 28,000 gal/min of CCW to the waste heat user.

4.2 Raw Service Water (RSW) System

A RSW system will be provided to perform various functions such as cooling, makeup, etc. This water would be taken from and returned to the Tennessee River with treatment limited to straining to 1/32-inch and chlorination as required. The system would be designed to provide water at 60 psi with an initial capacity of 7,300 gal/min and an ultimate capacity of 22,000 gal/min by installing additional pumps as required. Space would be provided in the RSW pumping station and electrical service would be sized such that the pumps may be added later.

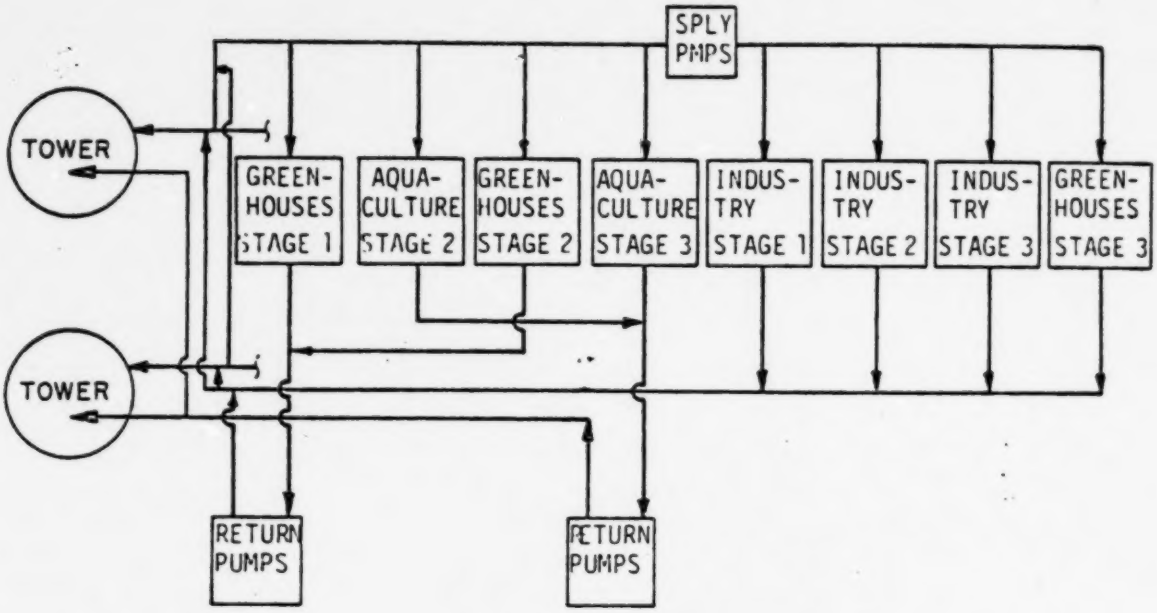

Figure 8 Flow Diagram of Waste Heat Distribution System

4.3 Sanitary Waste Collection and Treatment

A service area will be provided to house the RSW intake, sanitary waste treatment plant, and the potable water plant. Provisions will be made for one 50,000 gallons per day package treatment plant to be added for each stage of development. Both force main with the required lift stations and gravity main sewers will be utilized in the collection system. No provision will be made to handle special industrial wastes.

4.4 Potable Water and Fire Protection System

The potable water and fire protection systems will be combined into one system with makeup from the RSW system. One 100 gal/min packaged water treatment plant would be furnished with each stage of development, and a high pressure pumping system would maintain a level in a 350,000 gallon storage tank located on a nearby hilltop. Hydrants will be located along roads as required.

4.5 Electrical Distribution System

Electrical distribution will consist of a nominal 6.9 kV system, which will supply power to all equipment associated with the WHD system, and a 13.8 kV system, which will feed power to all park occupants and to other park service systems. All electrical distribution will be through underground concrete ducts. Roadway lighting will be provided.

4.6 Site Development

The initial site development will encompass approximately 300 acres with about half in users' lots and the other half used as service and wetland recreation areas and road rights-of-way. Initially, access will be from the nuclear plant access road. Ultimately a separate access will be developed, connecting the park directly with U.S. Highway 68. All main roads will be 24 feet wide with 8 feet wide shoulders. Service roads will be 20 feet wide with 4 foot wide shoulders and surfaced with compacted crushed stone aggregate.

4.7 First Stage Cost

A preliminary estimate of the cost to develop the first stage of the Watts Bar Waste Heat Park is as follows;

WHD System	$26,800,000
RSW System	5,400,000
Sanitary Waste Collection and Treatment System	800,000
Potable Water and Fire Protection system	2,100,000
Electrical Distribution System	3,100,000
Site Development	4,100,000
	$42,300,000

The above costs are in 1983 dollars and include proportioned overhead costs.

5. CONCLUSIONS

Waste heat can be provided from the Watts Bar Nuclear Plant CCW system at temperatures of between 93° F and 130° F. The costs shown do not include operation and maintenance costs and debt service. Based on these projected costs, economic feasibility studies are presently being conducted.

6. ACKNOWLEDGEMENTS

The authors recognize the work of Ebasco Services, Incorporated, who contributed materially to the conceptual design of the Watts Bar Waste Heat Park.

SESSION V A

COOLING TOWER PLUMES

PB82-228172

AN IMPROVED METHOD FOR PREDICTING SEASONAL AND ANNUAL SHADOWING FROM COOLING TOWER PLUMES

R.A. Carhart
Physics - University of Illinois, Chicago Circle
Chicago, Illinois, U.S.A., and
Division of Environmental Impact Studies
Argonne National Laboratory
Argonne, Illinois, U.S.A.

A.J. Policastro
Division of Environmental Impact Studies
Argonne National Laboratory
Argonne, Illinois, U.S.A.

W.E. Dunn
Department of Mechanical Engineering
University of Illinois, Urbana-Champaign
Urbana, Illinois, U.S.A.

ABSTRACT

An improved model developed at Argonne National Laboratory (ANL) for predicting long-term shadowing due to cooling tower plumes is presented, and its assumptions are compared with those used in previous models. The model is based on a method for the selection of representative categories of similar plumes developed by Policastro and Dunn to reduce the large number of meteorological data cases in a season or year at a site to a much smaller number, (about 100) of cases which yield distinctively different plume predictions. Plume predictions for the reduced set of category representative cases are then made with the validated ANL plume model. Full effects of sun angle by time of day and day of the year for the latitude and longitude of the site to be studied are included.

The ANL model yields seasonal and annual isopleths of hours of additional shadowing or isopleths of percentage reduction in total and beam solar energy arriving at the ground on a horizontal surface. Results for two hypothetical sites with 2000 MWe generating capacity are presented, one near Syracuse, New York, and the other near Spokane, Washington.

1. INTRODUCTION

Natural and mechanical draft cooling towers have come into wider use in the past ten years to reduce the thermal impact of electrical energy generation on water bodies. A variety of environmental effects of these towers have been studied, both from the theoretical and experimental viewpoints. One effect which has always been known to occur and has been measured [1,2] in the field is the shadowing of ground areas by the plume. Whether cumulative annual shadowing from a group of cooling towers will have an adverse impact on crop growth in nearby agricultural fields, on solar energy production capacity from neighboring solar collectors or on recrea-

Preceding page blank

tional uses of contiguous lands (e.g. a bathing beach) has yet to be determined.

As with other tower environmental effects, it is desirable to have an inexpensive, easily-usable validated model to predict seasonal and annual plume shadowing at a proposed power plant site in order to make intelligent siting decisions. Since adequate seasonal and/or annual shadowing data are not available, a shadowing model cannot presently be validated. But reasonable models for calculating plume shadowing using validated plume rise methods have been constructed and can be strengthened theoretically. This paper presents an improved model we have developed for predicting seasonal and annual shadowing as part of a larger EPRI-sponsored project to embed the validated ANL plume and drift models in a system of codes for predicting a variety of seasonal and annual cooling tower effects easily.

In Section 2 we review the usefulness of several measures of plume shadowing and discuss two existing methods that hve been developed. In Section 3 we describe the new ANL model approach and give a brief review of the Dunn-Policastro category scheme for associating plume predictions with hourly meteorological data, [3] which is used in the model. Then in Section 4, the model is applied to two hypothetical sites; one near Syracuse, New York; and the other near Spokane, Washington.

2. MEASURES OF SHADOWING AND EXISTING MODELS

2.1 Measures of Shadowing

The first measure of shadowing which has been used in the past is hours of shadow at a given ground location presented on a seasonal or annual basis. This measure has frequently been used by models in carrying out impact studies in a form that determines the shadow's location by assuming that the sun is directly overhead at all hours. This measure is useful if the presence of any shadows at all is known to have a detrimental effect. It will normally include daylight hours when the sky is heavily overcast, however. Thus, it is a conservative measure, as usually employed.

A second measure of visible plume impact which has been used in impact studies and is related to shadowing is hours when the visible plume is overhead, presented on a seasonal or annual basis. Although not a direct measure of shadowing it can be correlated with it to some extent, especially when the assumption that the sun is always overhead is made in many studies. As used by Dunn and Policastro [4] in a study of alternate sites for the Seabrook nuclear power plant in New Hampshire, the measure included both day and night hours. The inclusion of night cases reduces the connection with shadowing, but will yield results which are even more conservative.

The third and last measure of plume shadowing considered here is the actual reduction in solar energy flux on a horizontal surface, presented on a seasonal or annual basis. Previously-used models for plume shadowing have not dealt with actual reduction in

solar energy flux, although all anticipated environmental impacts, except those involving recreational usuage, depend on the change in energy flux. Sunlight is composed of a direct (beam) and a diffuse (scattered) component. A flat plate solar collector accepts both, while a focussing collector accepts mostly the direct component. Vegetation is also able to utilize both components of the sun's energy flux. A natural cloud or plume from a cooling tower will remove only the beam component, and will affect the diffuse component very little. The solar energy flux just beyond the edge of the plume shadow has been measured to be greater than the value if the plume were not there [1,2], presumably due to side-scatter from the visible plume. (This increase has also been noted when natural cumulus clouds are present[5].) We have chosen to predict these two measures of shadowing, percentage reduction in both total and beam solar flux on a horizontal surface, in the ANL model. However, hours of shadowing is an optional prediction which the user can select.

2.2 Methods for Computing Seasonal and Annual Shadowing

The earliest method for computing seasonal or annual cooling tower plume environmental impacts involved making individual plume predictions for each hourly meteorological record. The meteorological data available for impact studies comes either from a National Weather Service ground-level data tape with up to 30 years of data at hourly or three-hourly intervals; or from a Nuclear Regulatory Commission meteorological data tape. The well-known ORFAD model uses this approach. Since a year contains 8760 hourly data records or 2920 three-hourly data records, a highly simplified set of plume and drift models must be used with each hourly case to avoid large computer costs. Validation studies [6] have shown the relative inaccuracy of the ORFAD model, and other highly simplified models.

A better method was developed by Motor Columbus Consulting Engineers in their KUMULUS model [7], based on the philosophy that, except for wind direction, only a limited number of significantly different plumes occur at a particular site. This approach allows use of a validated and more realistic plume model to predict a greatly reduced set of representative plume cases. The categories were established by fixed ranges in relative humidity, temperature and windspeed. A representative set of tower conditions and meteorological data are chosen for each category, and detailed model predictions are made for each category representative. Not all of the 400 resulting categories actually occur at a given site, and experience with KUMULUS has shown the need for no more than about 100-200 categories in practice. In predicting shadowing about 200 cases are used and category representative cases are selected so that their combined windrose equals the seasonal site windrose. The probability of occurence of each category by season is calculated from the hourly data tape records. Then seasonal and annual results for plume length, drift deposition, shadowing and other effects are computed by adding the resulting effect from each category representative prediction weighted by the probabilities. If the effect is directional, such as drift deposition, then the single-case deposition pattern for each category representative is distributed into the proper subsectors for each of the wind directions

in an amount determined by the probability for that wind direction. The angular distribution of shadowing, however, is a simple sum of the patterns which result from each of the category representative cases. In this model the set of meteorological conditions for a category representative is assumed to hold for an entire day largely because the European twice-daily upper-air soundings are used for impact studies by Motor Columbus. The shadow of this single predicted plume is computed at hourly intervals. The plume is assumed to be opaque, and the complex shape of the shadow is considered approximately. This approach includes, then, the effect of variable sun angle. In the Northern Hemisphere, north of the Tropic of Cancer, the shadowing pattern will be shifted toward the north side of the site relative to predicted patterns using the "sun overhead" assumption. (The sun will spend most of the time in the southern sky, tending to cast shadows northward.) Details of additional minor refinements in the KUMULUS shadowing calculations are given in Ref. 7.

3. THE ANL METHOD

In the ANL model we adopt a philosophy similar to that which motivates the KUMULUS method. Our improvements lie in three main areas. First, we define expected categories by selecting ranges in several nondimensional parameters which correlate well with visible plume size. By contrast the KUMULUS method uses categories based on humidity, temperature and windspeed. With their choice of ranges some categories can be shown to contain a wide range of plume lengths [8].

In this ANL model each hourly reading throughout an adequate data acquisition period of from one to five years, (8000-45000 data records), is assigned to a category. (Incomplete records are counted and discarded.) We select a representative hourly record for each category and make a plume prediction with the validated ANL plume model for all of the representative cases, (35-100 in number). The information retained for each category for shadowing calculations includes height of rise of the visible plume above the tower, visible plume length and final plume (temperature) radius.

The second major improvement involves a more realistics representation of the effects of sun angle on shadow location. The ideal method would be to fully map out the shadow for each category representative case, including the actual plume trajectory and radial growth for the sun angles applicable to each hourly reading. However, since one year contains about 4000 daylight hourly records, the computer time needed to carry out this ideal calculation would be prohibitive.

The KUMULUS model avoids this problem by calculating shadows that appear realistic for each representative plume in their category scheme, assuming that the category holds for all hourly meteorological conditions present in a single day. They allow the sun to rise, move across the sky and set, while accumulating hours of shadowing in sectors on the ground as time passes. This method cannot account for possible correlations between wind direction and plume length, nor correlations between certain portions of a season (i.e. certain non-average sun angles) and excessively long or short

plumes.

Although we calculate every hour on the data tape we avoid large computation time by simplifying the shadow geometry, but summing the simplified shadows with the correct sun angles for every hourly reading during the season or year. The plume is approximated by a cylinder of radius (0.7)R, length L and height above the ground $H_T + (0.5)H_p$. The variable R is the final temperature plume radius, L is the visible plume length, H_T is the tower height, and H_p is the final visible plume rise above the tower. (The factors 0.7 and 0.5 were selected as reasonable, conservative values, but have no fundamental theoretical support.) In another geometrical simplification we assign the shadow for a single hour to standard subsectors formed from the intersection of 16 angular rays, (16 wind directions, every 22.5°), with 50 circles, spaced every 0.2 km. out to 10 km. The center of each subsector is checked with a simple algorithm to determine if it lies in the parallelogram shadow. If so, the entire subsector is considered to be shadowed. If not, no shadow is included in that subsector. For individual plume shadow cases this procedure can distort the calculated location of the shadow somewhat. However we have carried out sensitivity tests by further subdividing all subsectors (into 4 and 9 pieces), and we found that the seasonal and annual isopleths change very little.

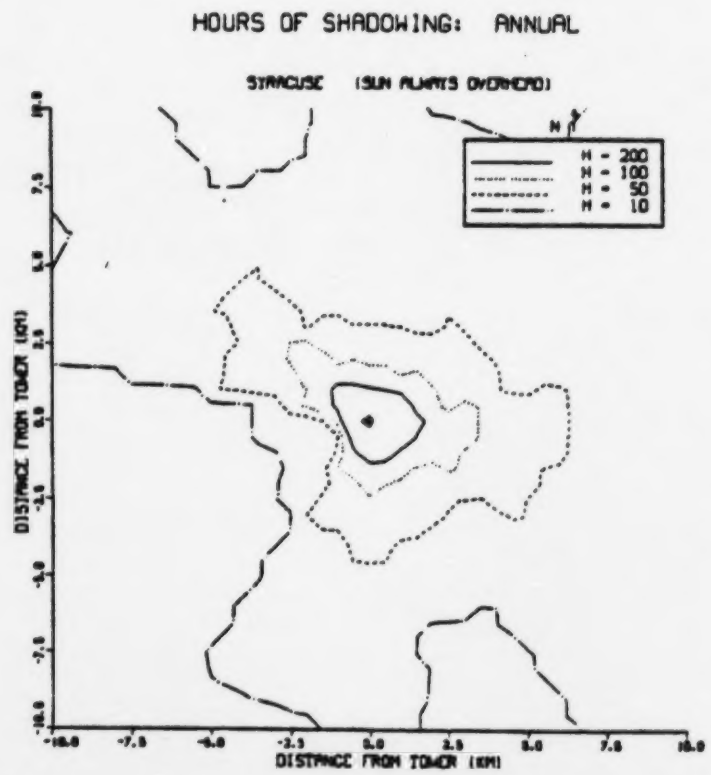

Fig. 1. Annual Hours of Additional Shadow at the Syracuse Site.

In Fig. 1 we show the results of the ANL model run for a year's worth of hourly meteorological data from a hypotnetical site near Syracuse, New York with two 1000 MWe natural draft cooling towers.

The model was run in a user-selected mode which gives annual hours of shadowing with the sun assumed always overhead during daylight hours. Up to 200 hours per year of shadowing are seen to be common within 1 km. of the tower, and 100 hours per year occur at distances of 3 to 4 km. in certain directions, according to this method.

In Fig.2 we show a sample annual calculation [7] done utilizing the KUMULUS model at a site in West Germany. Annual results of 200 hours of shadowing within 1 km. of the towers are seen here; and 100 hours extends at least 4 km. to the northeast. The effects of sun angle seem to be to displace the shadowing pattern to the north of the tower cluster as expected.

Fig. 2. Annual Additional Hours of Shadow at Site Studied with KUMULUS Model.

Figure 3 shows the annual isopleths of percent of daylight hours shadowed with an opaque plume assumed, but with sun angles included. The shift of these isopleths to the northwest compared to those in Fig. 1 shows the sun angle effects for this site. Also, since the 200 hour and 5% isopleths nearly agree (with about 4000 daylight hours per year) a given number of hours of shadow occur over a wider area when the sun angle is included.

Unless the predictions of the KUMULUS model and the ANL model are prepared with the same weather-tape data and then compared, it will be difficult to illustrate the differences in predictions between the methods. And even in that type of comparison, the differences in category selection and the choice of representative cases could mask the differences in shadowing approximation, render-

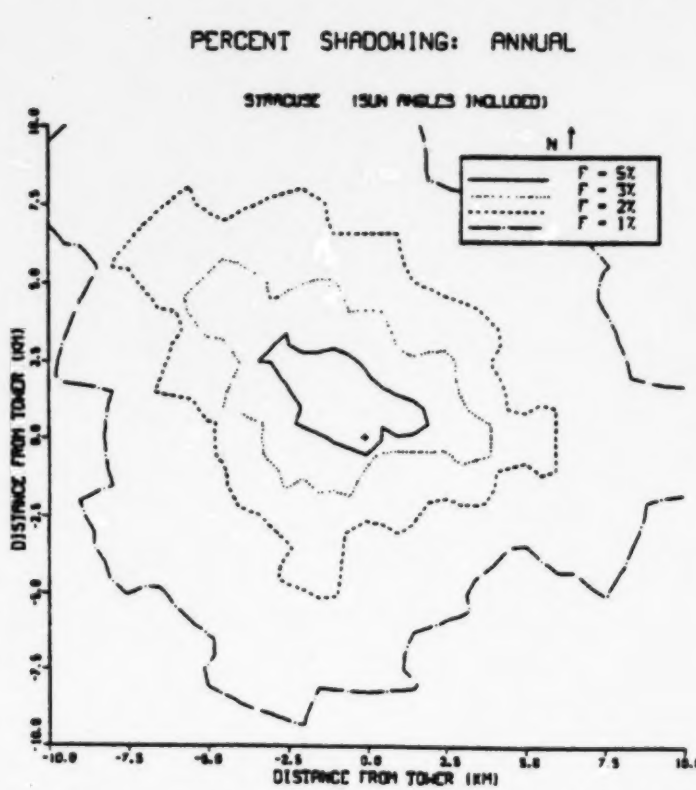

Fig. 3. Annual Percentage of Additional Daylight Hours of Shadow at the Syracuse Site with Sun Angles Considered.

ing the comparison inconclusive.

The third, and most significant, improvement is the calculation of the actual reduction in solar energy flux falling on a horizontal surface, rather than simply "hours of shadow". To predict the average hourly direct and diffuse component of the solar flux near ground level from data contained in commonly-available weather tapes is well beyond the present state-of-the-art. However, in solar energy design work considerable progress has been made in predicting reliable average daily solar energy fluxes [9,10]. Required for a site are the latitude and longitude, the monthly clearness indices, K_i, and the average daily total solar flux on a horizontal surface at sea level for each month of the year, H_i. As a result of the SOLMET program [11] monthly values of K and H are available at about 200 sites across the continental United States, Canada and Alaska. (These values vary smoothly from one site to the next in many parts of the country, which would allow interpolation to most sites.)

Using the formulas of Collares-Pereira and Rabl [9], which are extensions of the work by Liu and Jordan [10], we have defined the average diffuse and direct solar flux on an hourly basis. These hourly fluxes do not represent the actual solar fluxes for that date and hour. But they accurately represent climatological average fluxes for that date and hour. These formulas are well presen-in Ref. 9 and need not concern us here.

The absorbtion of the direct solar beam by the plume is also accounted for by assuming that all rays which intersect the plume pass through a thickness of plume material equal to the diameter. This approximation is clearly conservative, overestimating the energy reduction.

The fraction of direct solar energy absorbed will depend on the liquid water content of the plume, as well as on the path length through plume cloud water droplets. This absorbtion is fairly well known for natural clouds, but the added complexity needed to use these results does not seem justified, given the other approximations we have made and the uncertain accuracy of model predictions of plume liquid water content.

We have chosen, instead, to assume that the visible plume has a standard optical thickness, calibrated from a data case measured in West Germany [1]. The fraction, f, of beam solar energy absorbed in passing through a thickness d of plume material is taken to be

$$f = 1 - \exp(-0.0165d),$$

where d is in meters. The 65m thickness of the visible plume on which the measurements were made absorbed about 65% of the incident beam flux on a horizontal surface at the center of the shadow when the sun was directly overhead, fixing the coefficient 0.0165.

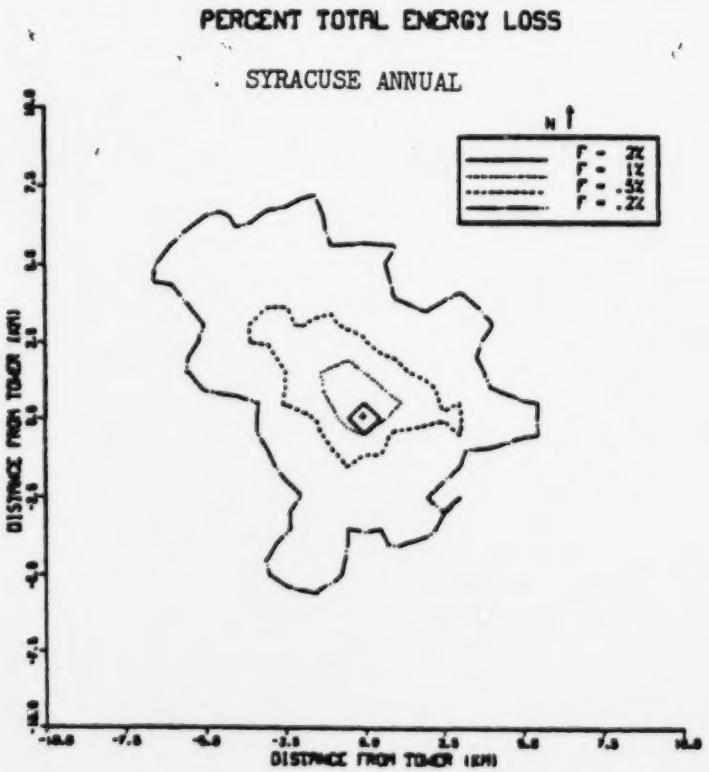

Fig. 4. Annual Percentage of Total Energy Loss at the Syracuse Site.

When these assumptions are combined in the ANL model, we expect the resulting isopleths of percentage reduction for direct and total solar energy deposition to contain the effects of time of day, time of year, plume length and wind direction. We expect the estimates to be conservative, since most of our assumptions overestimate shadowing.

4. RESULTS

The ANL shadowing model has been applied to a hypothetical site with two 1000 MWe natural draft cooling towers near Syracuse, New York, with data for one year from a nearby meteorological tower, and with monthly values of K and H from Syracuse. The plume categories for this site numbered 100. In Fig. 4 we show the annual isopleths for percentage reduction of total horizontal solar energy flux. One should note that the visible plume prediction associated with each hourly reading is the same for Figs. 3, 4, and 5. Within 2 km of the towers no more than 1% of annual total solar flux is lost. This area would normally lie within the plant boundary. The 1% isopleth extends 7.5 km from the towers in Fig. 3 and 3 km from the tower in Fig. 5 in the northwesterly direction, and may cause concern for nearby solar collectors outside the plant boundary, especially if certain seasonal values were higher still in these locations.

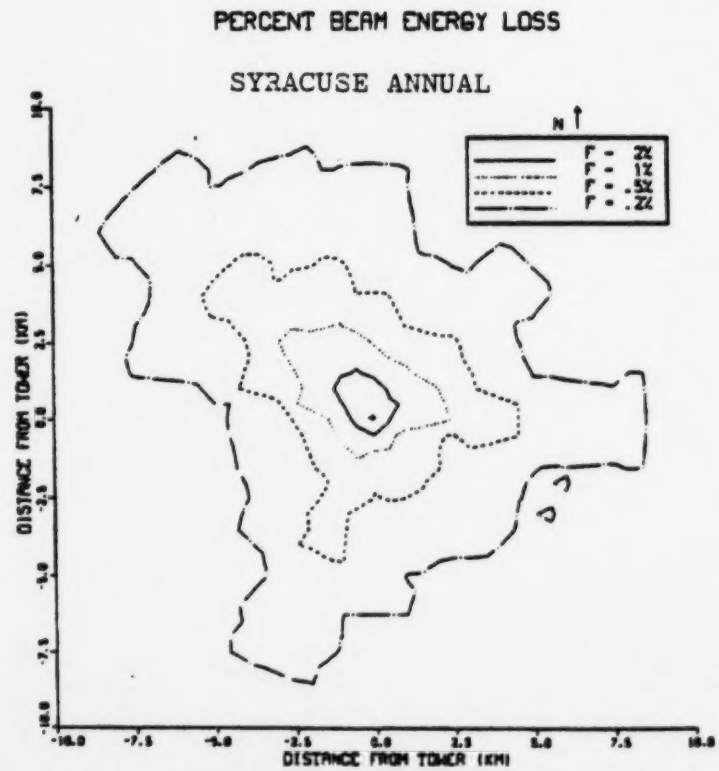

Fig. 5. Annual Percentage of Beam Energy Loss at the Syracuse Site.

We examined a second hypothetical site near Spokane, Washington, to illustrate variations in the prediction of seasonal/annual shadowing as a function of site climatology. Four 500 MWe circular mechanical draft towers were assumed. Although the latitude of Spokane is similar to that of Syracuse, the average humidity is lower. Spokane was one of the SOLMET cities; so that accurate K and H values were available. We were also able to obtain surface weather data covering a five year time span from a nearby airport. Figs. 6 and 7 show the isopleths of percentage reduction for total and direct solar flux at this site averaged over all 5 years of data.

From Fig. 6 one finds that beyond 2 km from the towers, less than 0.5% of the total solar flux is lost, whereas .5% reduction extends 3 to 4 km from the towers at the Syracuse site. Also, from Fig. 7 beyond 3 km from the tower less than 0.5% of the direct (beam) solar flux is lost. The angular distribution of shadowing affords another interesting contrast between the sites. The maximum shadowing occurs to the northwest of the towers at Syracuse, while this maximum occurs to the southwest and northeast of the towers at Spokane.

Finally, we also sought to discover how much the isopleths would change if we used meteorological readings only every three hours at 0300, 0600, 0900, etc. Some meteorological data tapes contain only such three-hourly entries. Also the cost of analysis of

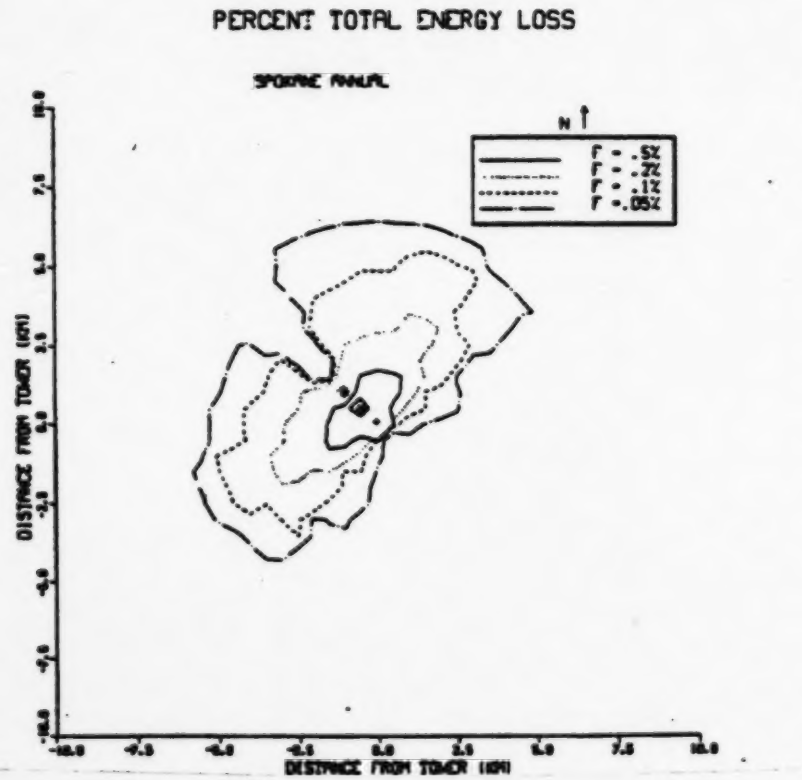

Fig. 6. Annual Percentage of Total Energy Loss at the Spokane Site.

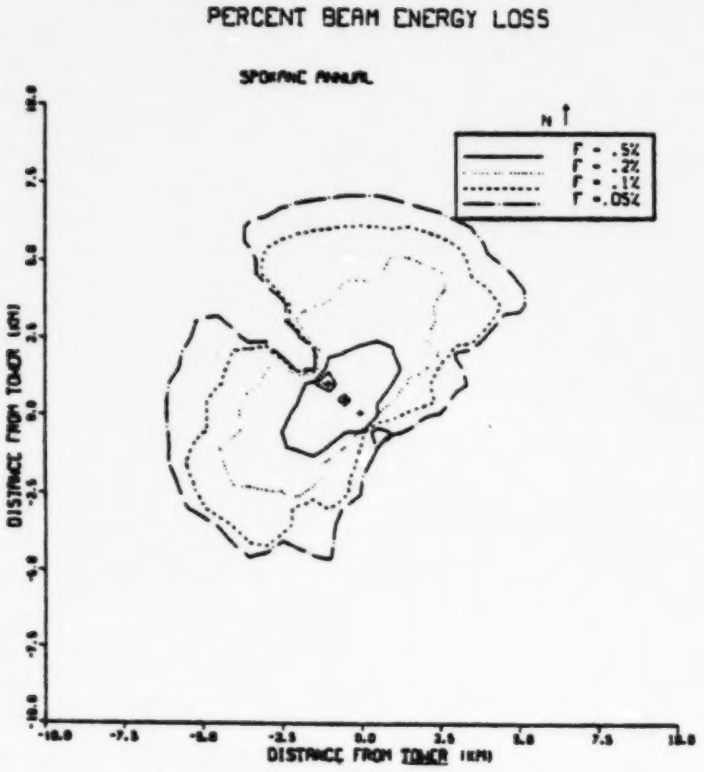

Fig. 7. Annual Percentage of Beam Energy Loss at the Spokane Site.

shadowing effects could be reduced if only every third hourly record were analyzed. We limited this study to the Spokane site, since with five years of data, the omission of 2/3 of the hours seems potentially less serious than with only one year of data.

As we can see from Fig. 8, the percentage of total solar energy flux lost has nearly the same isopleths as in Fig. 6 when all of the hourly values are used. The obvious difference is the absence of the narrow low-shadowing "finger" extending to the northwest of the tower, clearly seen in Fig. 6. A slight inward excursion of the isopleths in this direction can be seen in Fig. 8 , however, which probably represents the remnant of the reduction based on all hours. Apparently, some significant time correlations exist on the order of one or two hours between wind direction, plume length and sun angle. It seems that these correlations are largely washed out when an hourly reading is assumed to hold for three hours at this site. But, since the results of the three-hourly calculation are conservative in this case, one can tentatively conclude that it is sufficient to use eight meteorological records per day, one every three hours, especially for multi-year data acquisition periods.

5. CONCLUSION

At two representative cooling tower sites with 2000 MWe generating capacity in the northern United States we have applied an improved ANL model to calculate annual solar energy flux reduction from the visible plumes. As compared with methods that assume the

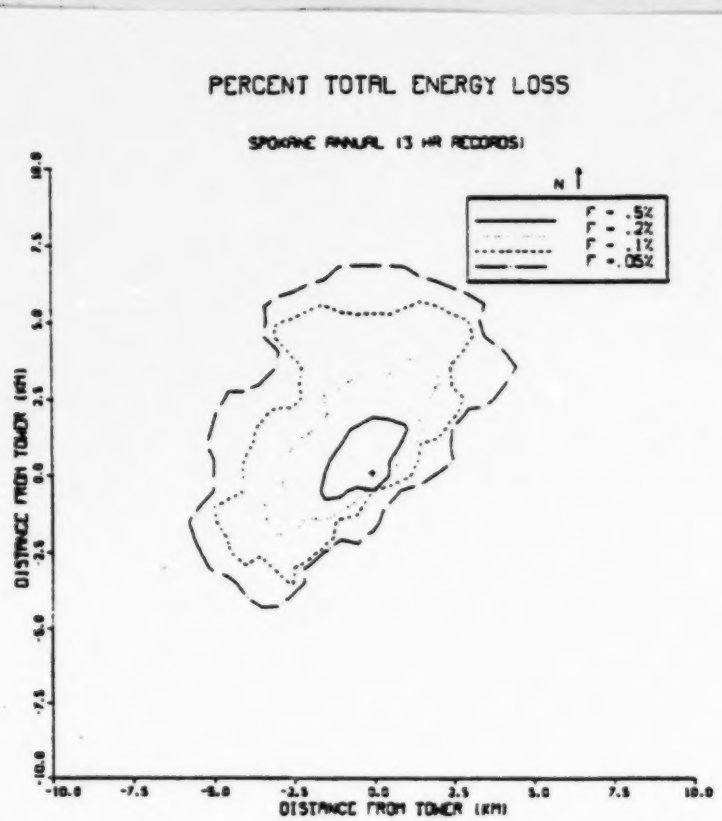

Fig. 8. Annual Percentage of Total Energy Loss at the Spokane Site with Data at 0300, 0600, 0900, etc.

sun is always overhead, the inclusion of sun angle effects shifts the pattern of shadowing intensity in directions characteristic to each site and is more realistic than other methods that assume the sun is overhead. The category scheme used to reduce the distinct predicted plume cases has been strengthened relative to methods based on simple ranges in the meteorological parameters. Sun angle effects are more fully represented in the ANL moedl than in the other models discussed, and the prediction of energy flux reduction (in addition to hours of shadow) affords a more precise measure of plume shadowing.

We have seen at the Syracuse site that 100-200 hours of shadowing would occur mainly within a typical plant boundary (2.5 km from the towers) with the sun overhead assumption. If sun angle effects were included the severity of predicted shadowing increased (1% and 2% isopleths in Fig. 3 ompared to 50 and 100 hour isopleths in Fig. 1) with 100 hours of shadowing occuring over 5 km from the tower. Thus, prediction of hours of shadowing in the model with sun angle effects included is the most conservative method for predicting shadowing discussed in this paper. Maximum shadowing occured to the northwest of the site. Actual energy loss isopleths for the Syracuse site showed less than 1% beam energy reduction beyond 4 km from the towers.

By contrast, at the Spokane site which had lower average relative humidity than the Syracuse site, the solar flux reductions were about one-fourth or one-fifth as high at a given distance from the tower. Consistent with the differences in windrose, the

pattern of shadowing at Spokane had maxima in the northeast and southwest directions, while at Syracuse the dominant direction for shadowing was northwest of the tower. Exclusive of record access time we are able to process 5 years of hourly data with this model on an IBM 370/155 in less than one minute of CPU time.

While similar in their overall features the isopleths produced by limiting meteorological data to 0300, 0600, 0900, etc., lacked some of the fine structure possessed by those obtained utilizing every hourly record. Apparently, changes occurring over 1 or 2 hours are having an effect on the correlations. To investigate this further, we plan to calculate isopleths using the 3-hourly records for a different set of hours on different days, to see if the fine structure of the isopleths can be restored still using a reduced database. Also, we will soon generalize the assumed plume shape to that of a section of a cone perpendicular to its axis. The small radius face will have the tower diameter. The large diameter face will have the final temperature plume radius at disappearance. The shadow of this figure for each predicted plume will then be a quadrilateral, a more realistic shape.

REFERENCES

1. H. Berge, E. King and D. Lorenz, Water Vapor Emissions in the Region of Conventional Thermal Power Station, (Wasserdampfimmissionen in Bereich eines konventionellen thermischen Kraftwerks,) Fortschr.-Ber. VDI-Z., Series 15, No. 6, (1975). (See Figures 3 and 4.)

2. E. Ryznar, An Observation of Cooling Tower Plume Effects on Total Solar Radiation, Atmospheric Environment, vol. 12, pp. 1223-1224, 1978.

3. W.E. Dunn, Predicting the Seasonal and Annual Impacts of Cooling Tower Plumes and Drift, Proc. IAHR Cooling Tower Workshop, San Francisco, CA, Sept. 1980.

4. NRC Staff, Seabrook Alternate Site Study, U.S. Nuclear Regulatory Commission, Docket Nos. 50-443 and 50-444 (1978).

5. M.L. Wesley and R.C. Lipschutz, A Method for Estimating Hourly Averages of Diffuse and Direct Solar Radiation Under a Layer of Scattered Clouds, Solar Energy, vol. 18, pp. 467-473, 1976.

6. A.J. Policastro, R.A. Carhart, S.E. Ziemer and K. Haake, Evaluation of Mathematical Models for Single and Multiple Source Natural Draft Coling Tower Plume Dispersion, U.S. Nuclear Regulatory Commission, NUREG CR 1581, Vol. 1, 1979.

7. H. Fuchs and W. Hofman, A Refined Method to Calculate the Shadowing by Cooling Tower Plumes, Proc. IAHR Cooling Tower Workshop, SAn Francisco, CA. Sept. 1980.

8. Gunter Juersch, German Weather Service Offenbach, 1978 (private communication).

9. M. Collares-Pereira and A. Rabl, The Average Distribution of Solar Radiation - Correlations Between Diffuse and Hemispherical and Between Daily and Hourly Insolation Values, Solar Energy, vol. 22, pp. 156-164, 1979.

10. B.H.Y. Liu and R.C. Jordan, The Interrelationships and Characteristic Distribution of Direct, Diffuse and Total Solar Radiation, Solar Energy, vol. 4, p. 1, 1969.

11. SOLMET Manual, Vol. 2, (Available from the National Climactic Center, Asheville, North Carolina,) 1978.

PB82-228180

COOLING TOWER DRIFT STUDY AT THE OAK RIDGE GASEOUS DIFFUSION PLANT

Shin H. Park
Enrichment Technology Division
Oak Ridge Gaseous Diffusion Plant
Union Carbide Corporation
Nuclear Division
Oak Ridge, Tennessee, U.S.A.

ABSTRACT

The first environmental study of cooling towers at the Oak Ridge Gaseous Diffusion Plant (ORGDP) was conducted in 1973 and provided valuable first hand information on drift from two mechanical draft cooling tower cells; however, the drift percentage of 0.1% measured in that test appeared to be high. Consequently, a drift study was planned and performed in 1978 to define more closely the drift phenomenon of the cooling tower complex. Ten cooling tower cells were involved in this test with drift and ground deposition measurements being performed simultaneously. The average drift percentage measured during this test was much lower at 0.03%, but the downfield deposition measurements of chromium supported the deposition findings of the 1973 study. The results from the 1978 studies exhibited good agreement between the cells and are considered to be more reliable than those obtained in 1973 because of the greater mass of data obtained from a greater number of cells. The results indicate that the sensitive paper method with its large sampling volume provides more reliable source characteristics information than an optical measuring device with a very small sampling volume.

1. INTRODUCTION

The disposal of industrial waste to the atmosphere has become an issue of concern because ever increasing amounts of effluents are being disposed in this manner. The atmospheric response time or time required to dissipate acceptable levels of some of these materials may be short; hours or even minutes, but others may be measured in terms of years.

The operation of water cooling towers provides a means of disposing of waste heat and is a vital part of many industrial processes, including the enrichment of uranium by gaseous diffusion. An advantage of cooling towers is the ability to reject economically large amounts of heat from a Recirculating Cooling Water (RCW) system. A disadvantage is the tendency for some water droplets containing RCW chemicals to be carried from the towers to the environment. The RCW system at the ORGDP contains a zinc/chromium inhibitor for corrosion control. It is this chemical which is being carried in drift from the cooling tower to the environs that has created the need for obtaining reliable drift rate data from the cooling towers. The primary objective of the investigation was the determination of the efflux of chromium to the environs, specifically in the areas where the EPA's guideline for the chromium level is 0.05 ppm.

The 1973 drift study was the first intensive environmental study of large mechanical draft cooling towers. The study extended from December 1972 to July 1973 and consisted of experimental and analytical works by four independent groups. The results of these studies, published by Jallouk, et al[1], was the most comprehensive data on the environmental aspects of the mechanical cooling towers at that time and provided first hand information on the environmental picture at ORGDP.

The drift percentage measurements obtained from the 1973 study were:

	With Optical Measuring System	With Water Sensitive Paper Technique
K-31 Cell 6 (K-31-6)	0.1%	0.028%
K-33 Cell 11G	0.0003%	
K-33 Cell 8G		0.0015%

The large difference in the measurements between K-31 and K-33 is not readily explainable. The mist eliminators in the K-31 cooling tower were slightly damaged, but the general appearance was comparable to the K-33 cooling tower.

This study, therefore, created an incentive to investigate further the drift rate from cooling towers and to compare various measuring techniques with respect to reliability and repeatability as reported by Park, et al[2].

2. 1978 DRIFT STUDY

2.1. Purpose

The drift characteristics of similar cooling towers may be compared but caution must be exercised because the drift fraction is dependent on the physical condition and the operational conditions of the towers. Table 1 shows results of drift studies on mechanical draft towers at ORGDP[1], Turkey Point[3], and New Jersey[4]. Among the towers tested is the Turkey Point cooling tower, a cross-flow cooling tower similar to the K-31 cooling tower; both were built by the same manufacturer. The drift percentage measured on this tower was around 0.00034% compared to 0.028%-0.1% obtained on the K-31 cooling towers. This comparison indicates the drift rate from the K-31 cooling tower is considerably higher than that from the new tower of similar design. However, it is not clear whether such a high drift rate is realistic or if it is due to the over-estimation of drift rate by the measuring technique. The mineral flux from the K-31 cooling towers was also measured with an isokinetic tube (IK). The collection efficiency of the IK tube is better than most drop measuring devices; hence, it was expected that the IK results would be considerably higher than the value obtained by the drop size measuring method. This was not always true, however, and the inconsistencies between the drift rates by the IK method and drop counting method made it more difficult to accept the drift rate results from the cooling towers.

The 1978 drift study was designed and performed in order to resolve some of the inconsistencies of the 1973 study as reported by Park[5]. The goals of the new effort were to determine:

1. A reliable drift rate from the cooling towers at the ORGDP through repeatability of measurements.
2. The attributes of different measuring techniques.

Table 1. Comparison of Tower Characteristics

	ORGDP[1] K-31-6	TURKEY[3] POINT	NEW[4] JERSEY
WATER FLOW RATE, g/sec	2.10×10^5	11.20×10^5	0.47×10^5
AIR FLOW RATE, cfm	5.79×10^5	9.97×10^5	0.70×10^5
L/G	0.67	1.97	1.18
AVERAGE AIR VELOCITY, m/sec	8	11.2	4.4
MANUFACTURER	MARLEY	MARLEY	BALTIMORE AIR
TYPE	CROSS FLOW (Induced)	CROSS FLOW (Induced)	CROSS FLOW (Forced)
YEAR CONSTRUCTED	1951	1974	1970
DRIFT RATE, D g/sec	150-36	3.979	2.3-0.0466
DRIFT FRACTION, Δ, %	0.1-0.028	0.00034	0.003-0.000096
MEDIAN DROP SIZE, $\bar{d}$, μm	175-1000	125	500

3. The effect of operational and physical variations on drift rate.
4. The variation of ground deposition patterns with meteorological conditions.

To achieve these goals, a plan was drafted that called for:

1. Large data sets.
2. The measurement of drop sizes by more than one measuring technique.
3. A comparison of the drift rates obtained by both drop population and mineral flux.
4. Simultaneous measurement of ground deposition with source characterization under various meteorological conditions.

The large data sets would improve the statistical value of the measurements and also provide a check on the repeatability of measurements. These data could then be used to formulate the source characteristics of cooling towers at the ORGDP and validate dispersion models. This analysis was based on the assumption that the operational characteristics and physical condition of the cooling towers at ORGDP did not vary significantly between cells.

2.2 Scope of the Study

Information needed for the study on the environmental effect of the cooling tower includes the drift rate and/or mineral flux rate from the cooling towers. Mineral flux rate may be obtained from the drift rate if the mineral concentration of the droplets in the plume is known, and it usually is assumed to be the same as the basin water. In order to ascertain the validity of this assumption, the mineral flux rate and drift rates were obtained independently. The drift rate can be obtained by counting all the drops in the plume with sensitive papers or optical systems, or physically separating and collecting the drift droplets from the plume. In the 1978 drift study, the droplet spectrum was determined, as well as the drift rate, along with the mineral flux from the cooling tower.

For the source characteristics study, ten fan stacks were chosen. Measurements were conducted at the exit plane of the fan stack of each cell. The exit plane was divided into four equal annular regions. Measurements were conducted along two right angle traverses through the center of the fan stack. There were eight measuring points along each traverse and, therefore, a total of 16 measuring points were used to characterize a source condition. The determination of source characteristics required the following measurements:

1. Velocity.
2. Wet and dry bulb temperatures of the exit air.
3. Droplet distribution.
4. Mineral flux.

These were measured at each measuring point along the traverses. The droplet distribution was measured with two independent measuring techniques over the whole spectrum or a part of the spectrum in order to cross-check the validity of each measuring technique. The two measuring techniques employed in the 1978 drift study were the sensitive paper method and an optical measuring system called the Particulate Instrumentation by Laser Light Scattering System (PILLS).

The mineral flux was measured cumulatively over a radius of the fan stack along the traverse. Hence, four mineral flux measurements were conducted on a fan stack. The mineral flux from the cooling towers was related to the drift rate from the cooling tower to cross-check the measuring technique of the drift rate from the cooling tower.

2.3 Downfield Deposition

The two cooling towers tested (K-31 and K-33) which are separated by about 300 meters are constructed such that all the cells are located along the south-north direction. The dominant wind direction at ORGDP is mainly from the south-west direction. The ground deposition sampling plans were, therefore, developed to collect samples from each cooling tower assuming that the source of the total cooling tower was at the center of each tower. The sampling plans consist of three sampling radii originating from the center of each tower with four to five sampling points along each sampling radii. The sampling radii were started from the north direction and they were at an 11.25° angle as shown in Figure 1. Sampling points along these radii are located at 100 m, 200 m, 500 m, 750 m, and 1,000 m from the cooling tower.

At each measurement, samplers were deployed along any three consecutive radii with two upstream sampling points for background measurements. The two upstream sampling points were located in the SW section of the towers. Therefore, at each measurement, a total of 15 downfield samples along with two upstream samples were used.

The ground deposition measurements at each sampling point consisted of measuring the droplet distribution, the mineral flux deposition, and the airborne concentration of minerals.

The deposition measurement of liquid droplets at various distances from the cooling tower along the prevailing wind direction was necessary to validate the trajectory dispersion model. The deposition was obtained with large sensitive papers which were stained by the droplets.

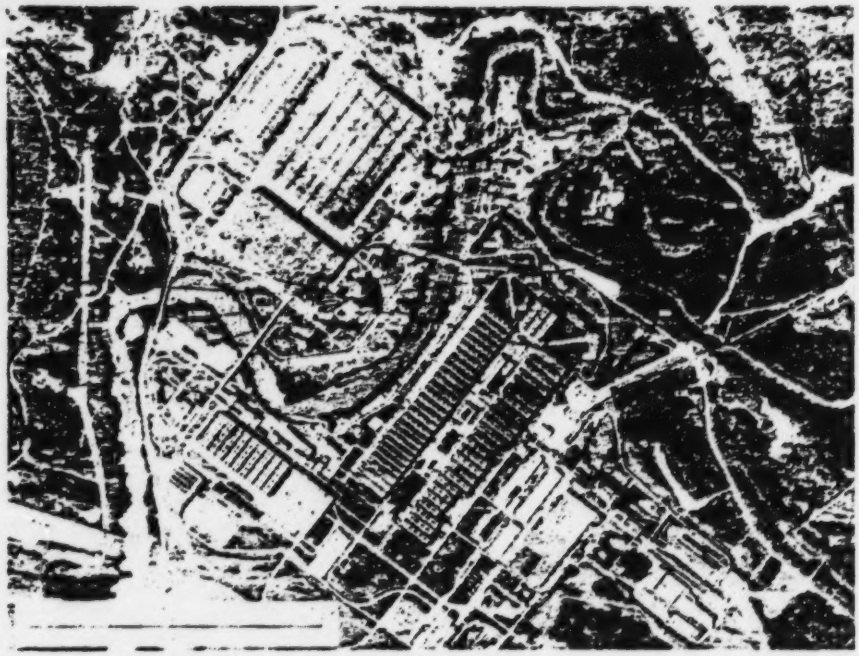

Fig. 1. Ground Deposition Measuring Positions at the ORGDP

Since the droplets fall on sensitive papers, the collection efficiency is 100 percent and the statistical value of the measurements should increase with increased sampling area. A problem associated with this deposition measurement arises when high winds exist and droplets with a horizontal component of velocity fall, creating oblong or elliptical shape.

The mineral residue from the cooling towers were also collected at each ground sampling point with a funnel and bottle assembly. The collection efficiency increases with the opening size of the funnel. Careful handling of the assembly before and after the measurement were necessary to obtain reliable data.

The exposed funnels were washed, scrubbed, and brushed with distilled water to remove all deposition. The rinsed solution in the bottles was then analyzed for mineral content.

The airborne concentration of minerals was measured with the Airborne Particle Samplers (APS). This measurement provided the mineral concentration in the air 1.5 meters above the grade compared to the deposition at a 1/2 meter level by the funnel and bottle assembly.

The meteorological conditions of test days, which are the dominant factors on the dispersion process of drift from the cooling towers, were measured and recorded continuously throughout the study. A 20-meter meteorological tower located 100 meters south of the K-31 cooling tower measured the wind speed and directions as well as the dry and wet bulb temperature.

3. RESULTS

The 1978 drift study was conducted in a ten day period during August and September 1978. The source characteristics of the ten cells were measured simultaneously with the downfield deposition measurements. Since the cell number 6 of the K-31 (K-31-6) cooling tower had been used for the drift study in 1973, it was included in the 1978 drift study. The results of the two tests series have been compared even though the physical and operational conditions of the cell between 1973 and 1978 were not identical. Generally, fill and drift eliminators in all the cells tested had been improved since the 1973 drift study and some of the cells have been equipped with new fan stacks. Cell number 6 of the K-31 cooling tower was equipped with a new 6 foot fan shroud after the 1973 drift study.

3.1 Operating Condition

The operating conditions of the ten cells tested are shown in Table 2 along with the operating conditions of the K-31-6 cooling tower cell in the 1973 drift study. The average heat load of the K-31 cooling tower was about 20 MW per cell compared to 45 MW per cell for the K-33 cooling tower. The heat rejected from the K-31-6 cell was 20 MW during the 1978 drift study compared to 15 MW recorded during the 1973 drift study.

A typical velocity profile is plotted in Figure 2. The velocity profile of the fan shows good symmetry around the fan center with a peak value occurring near the mid point of the fan blade. As shown in the figure, the scatter in the measurements tends to be smaller in the high velocity areas than in the low velocity areas. The measured value near the hub and rim shows widely scattered values. The velocity profile of the counter-flow cooling tower showed wider scattered values near the hub and edge of the fan. The peak value of both cooling tower fans is around 10 m/sec with an average value of approximately 6.5 m/sec. The exit air temperature exhibits a slight variation along the fan traverse with an average value of 37.5°C.

Table 2. Operating Conditions on Cooling Tower Cells Tested

TOWER	CELL NO.	FAN NO.	AIR FLOW RATE CFM	WATER FLOW RATE GPM	L/G	HEAT REJECTED MW
1978 RESULTS						
K-31	5		5.305×10^5	4,400	1.08	22.11
	6		5.130×10^5	4,400	1.09	20.33
	16		5.230×10^5	3,800	0.93	16.49
K-33	9	18	3.136×10^5	3,100	1.26	22.77
	9	17	3.049×10^5	3,140	1.31	24.84
	10	19	3.214×10^5	3,185	1.26	24.78
	10	20	3.221×10^5	3,000	1.19	25.90
	7	13	3.037×10^5	3,000	1.26	21.95
	1	2	3.686×10^5	3,550	1.23	19.69
	1	1	3.429×10^5	3,595	1.23	19.08
1973 RESULTS						
K-31	6		5.79×10^5	3,335	0.67	15.25

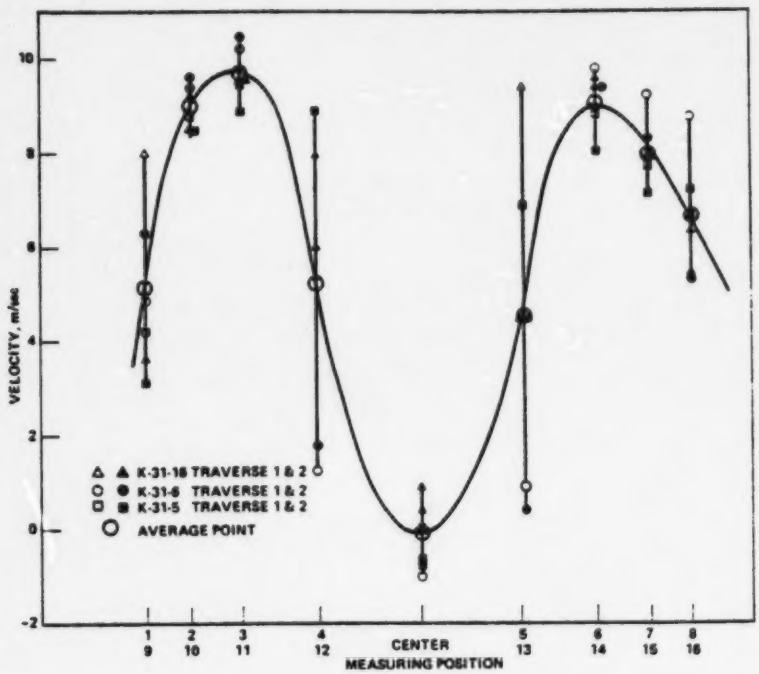

Fig. 2. Velocity Profile of K-31 Cooling Tower Cells Testing

The goals of the 1978 study were to be attained by:

1. Establishing spectrum of droplet sizes with both sensitive papers and PILLS.
2. Comparing the drift rate obtained from the above technique with the results by an isokinetic tube method.

3.2 Source Characteristics

Analysis of the measured data revealed that the PILLS system did not provide reliable results. Hence, the plan to cross-check the droplet size spectrum with the PILLS system was not realized. The drift rates obtained with the isokinetic tube method were compared with those obtained by sensitive paper. The curves representing the drift flux variation with drop sizes for the K-31 and K-33 cooling towers are plotted in Figures 3 and 4.

The agreement of the flux distribution curves is good for the cells tested. The flux distribution curves peak in the 100 to 300 μm diameter droplet size range. The contribution of small droplets to the flux is due to the large number of droplets of small mass. The number of droplets counted in this area promote statistical reliability of drift flux in this size range. But, the drift flux of the larger droplet ranges; namely, droplets larger than about 1,000 μm in diameter, results from a small number of droplets which are generated by the accumulation of liquid on the structural member. These drops, which are occassionally blown off from the structural member, being large in size but few in numbers tend to reduce the reliability of the results. The large deviation of drift flux in the droplet ranges larger than 1,000 μm in diameter was due mainly to these large droplets. The drift flux measurement along two traverses on a cell agree very well in the area where a large number of droplets were counted. But, large deviations occur between the two traverses where the large droplets exist.

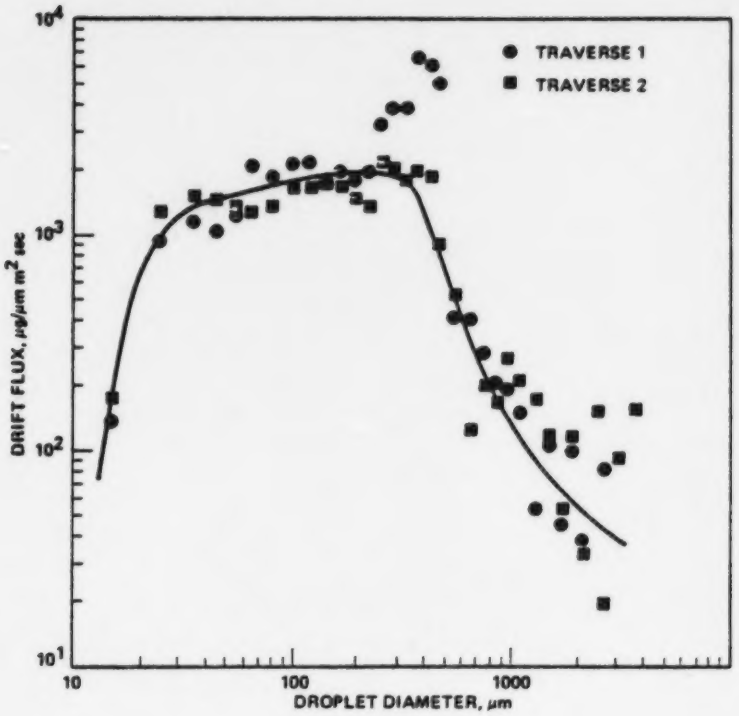

Fig. 3. Variation of Drift Flux With Droplet Size, K-31-6

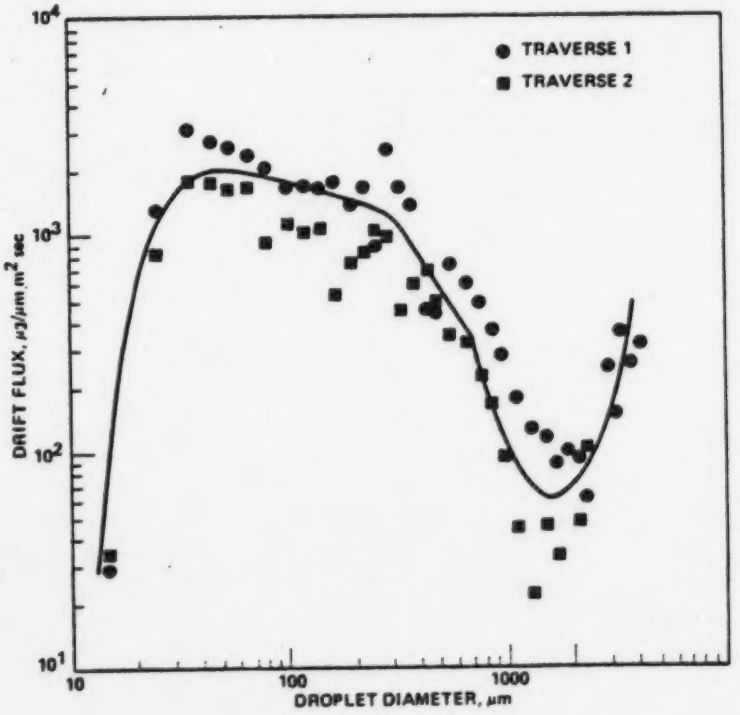

Fig. 4. Variation of Drift Flux With Droplet Size, K-33-1, Fan No. 2

The number density of droplets as a function of diameter is plotted in Figure 5. As had been expected, the number density increased with a decrease in the size of the droplets. This is due to the generation of many small droplets each time a large droplet breaks up. Scriven, et al[6] have studied the droplet break up on fill material and reported that the number of smaller droplets resulted from breaking up of a large drop depended on the initial size of the droplet, flow conditions, and the surface tension of the water. It was expressed as:

$$N(D) \sim \frac{u^2 a^3}{D^2}$$

where u is the impact velocity, a is the radius of the initial drop and D is the diameter of smaller droplets resulting from the break up. N (D) is the number of droplets of size D. If the initial droplets in the cooling tower were assumed to be the same diameter, the number density N (D) would be inversely proportional to the square of the diameter of smaller droplets as:

$$N(D) \sim \frac{1}{D^2}$$

The result of the sensitive paper measurement of the 1978 drift study agreed fairly well with the predicted number density line, in Figure 5, in the range below 500 μm in diameter; the values diverge from this line above 500 μm with the number density decreasing at a faster rate with increasing droplet size. This might be due to a combination of factors such as (1) a decrease in the collection efficiency with increasing droplet sizes and (2) a decrease in the number of larger drops in the plume combined with the short exposure time of the sensitive paper.

The K-31-6 cooling tower tested in 1978 was also compared with that tested in the 1973 test. In the 1973 drift test, the main instrumentation used to generate the drift flux density was an optical measuring system and small sensitive papers. The small sensitive paper measurements were used to supplement the optical measurement system in the small droplet sizes of less than 80 μm in diameter. The results of both studies are plotted in Figure 6 which shows that the drift flux density curve generated in 1973 was roughly an order of magnitude larger than the 1978 study.

The average drift percentages from the 1978 drift study, as calculated by the population method, are shown in Table 3 along with the isokinetic results. Since the sampling efficiency of the isokinetic tube operation is better than 90% for all droplet size ranges, the result obtained by the IK method should be higher and more reliable than those obtained by the sensitive paper method. The results shown in Table 3 confirm this observation.

The degree of difference between the sensitive paper and the IK tube method may be due to the occassional large droplets generated from the structural member of the tower with the accumulation of liquid. The average drift percentages of the towers tested in the 1978 drift study are:

	By Sensitive Paper	By IK Tube
K-31 Cooling Tower	0.019%	0.028%
K-33 Cooling Tower	0.022%	0.033%

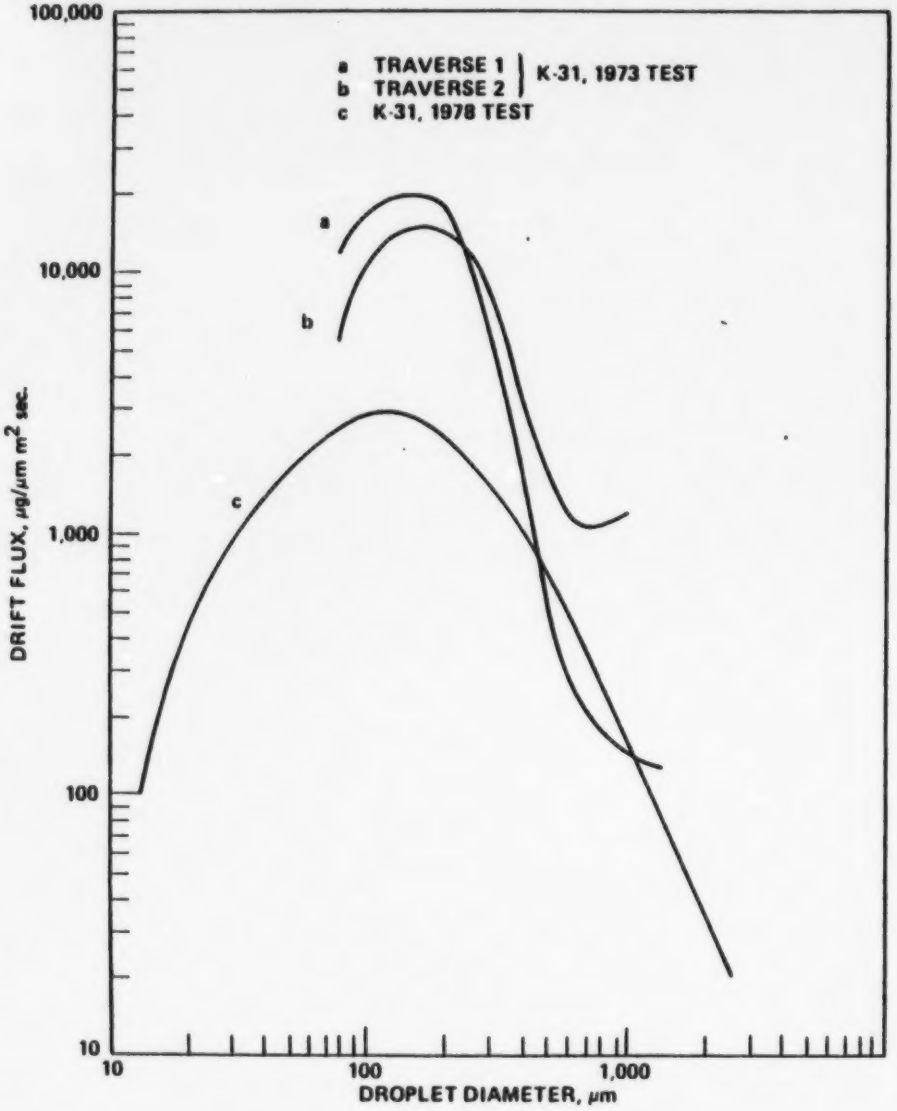

Fig. 6. Drift Flux Variation With Droplet Size

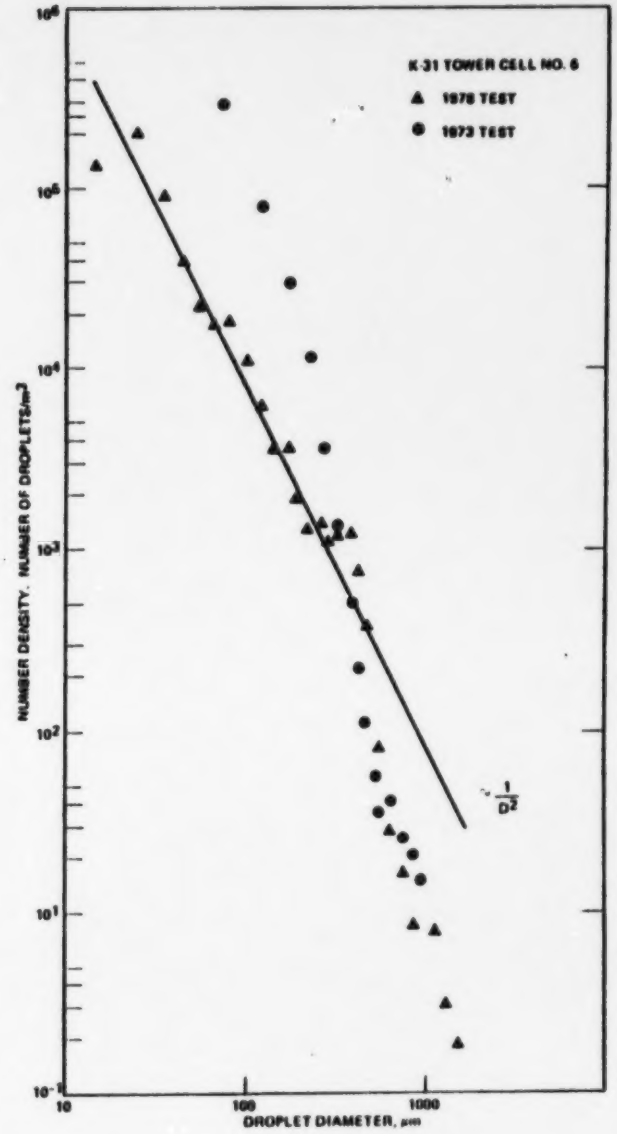

Fig. 5. Variation of Droplet Number Density

Table 3. Drift Percentages of ORGDP Cooling Tower

TOWER NUMBER TOWER-CELL-FAN	DRIFT PERCENTAGE, % 1978 STUDY BY POPULATION METHOD	1978 STUDY BY I.K. METHOD	1973 STUDY BY POPULATION METHOD	1973 STUDY BY I.K. METHOD
K-31-5	0.0195	0.0264		
K-31-6	0.0221	0.0367	0.12[a] 0.028[b]	0.1[a]
K-31-16	0.0155	0.0209		
K-33-1-1	0.0095	0.0152		
K-33-1-2	0.0141	0.0151		
K-33-7-13	0.0332	0.0219		
K-33-9-17	0.0193	0.0415		
K-33-9-18	0.0123	0.0135		
K-33-10-19	0.0460	0.1012		
K-33-10-20	0.0204	0.0221		
K-33-8-16			0.00153[b]	
K-33-6-11			0.000147[a]	0.00055[a]

[a] MEASURED BY ESC
[b] MEASURED BY ATDL

3.3 Downfield Deposition

The major concern of the effect of the cooling towers is the effect of minerals emanated from the cooling towers on vegetation and food chains in the environs of the cooling towers. The drift dispersion pattern has been studied widely over the years. Chen[7] and Polycastro[8] have examined numerous plume dispersion models. Their work indicated that the disagreement between models is as large as a factor of ten, but they were unable to select any single model as being superior to others. This reflects the complexity of the drift dispersion pattern and subsequent modeling in the numerical analysis as well as the lack of good experimental data.

The purpose of downfield deposition measurement in the 1978 drift study were to establish ground concentration variations of minerals around the cooling towers and to generate a large experimental data base for developing a new drift dispersion model or comparing the existing models to select a better performance code for our need.

The downfield deposition measurements were conducted simultaneously with the source characteristics measurements.

The ground deposition measurements were determined from liquid deposition and/or mineral deposition measurement. Besides the ground deposition measurements, airborne concentrations of minerals were also measured 1.5 meters above the grade.

The liquid deposition fluxes measured with sensitive papers, plotted in Figure 7, show that liquid deposition rates of around 300 grams/m^2hr were obtained at stations near the cooling towers compared to 1 to 3 grams/m^2hr obtained at 500 meters distance from the cooling tower. However, the liquid deposition flux obtained at stations within 100 meters of the cooling towers were biased by an occassional plume downwash. The exposure time of the sensitive papers located within 100 meters of the cooling tower was around 5 minutes compared to 2 to 3 hours of exposure time for remote stations. The mass median drop size obtained was 500 μm in diameter near the cooling tower and decreased to around 300 μm in diameter at 600 meters from the cooling tower.

The chromium deposition fluxes measured by two different measuring techniques are plotted in Figure 8. The agreement between the direct measurements of dry minerals which were deposited on the funnel-bottle assembly and those calculated values based on liquid flux measurement is good near the cooling tower. But, the measurements beyond 300 meters indicate more dry minerals are being collected than droplets of drift. This difference is increased further with the distance between the cooling tower and samplers. This could be due to the evaporation of droplets in flight. The measured chromium deposition flux near the cooling tower was about 600 to 700 μg/m^2 day but this was biased by plume downwash. The stations beyond 200 meters distance from the cooling tower were less influenced by the downwash of the plume. The deposition flux of Ca, Mg, and Cr show a similar deposition pattern with distance shown in Figure 9.

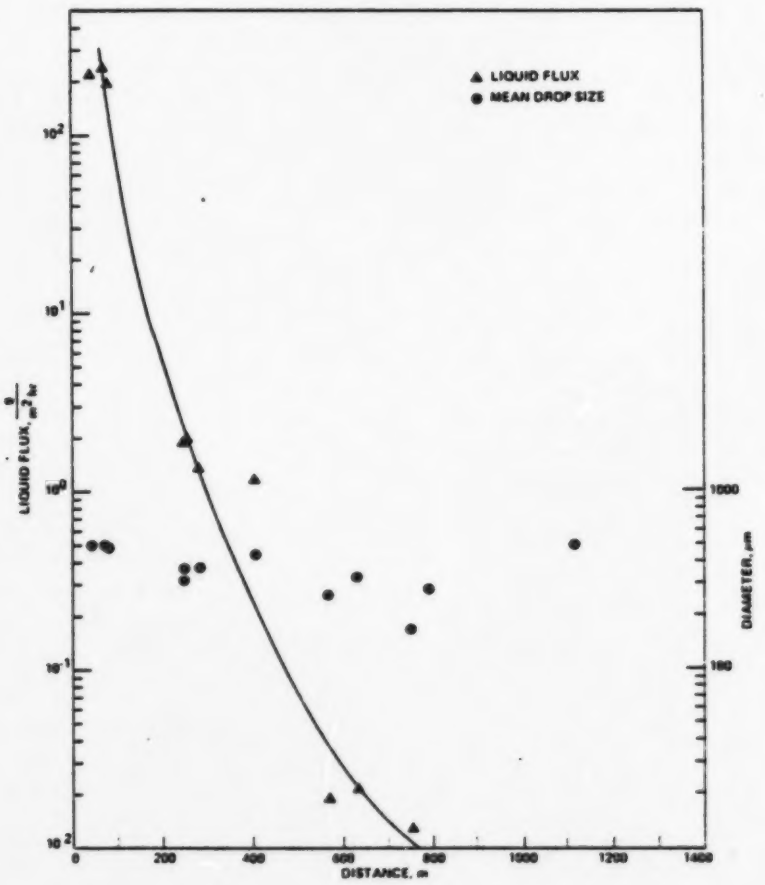

Fig. 7. Variation of Liquid Deposition Flux With Distance From The Cooling Tower, Test Date 8/31/78

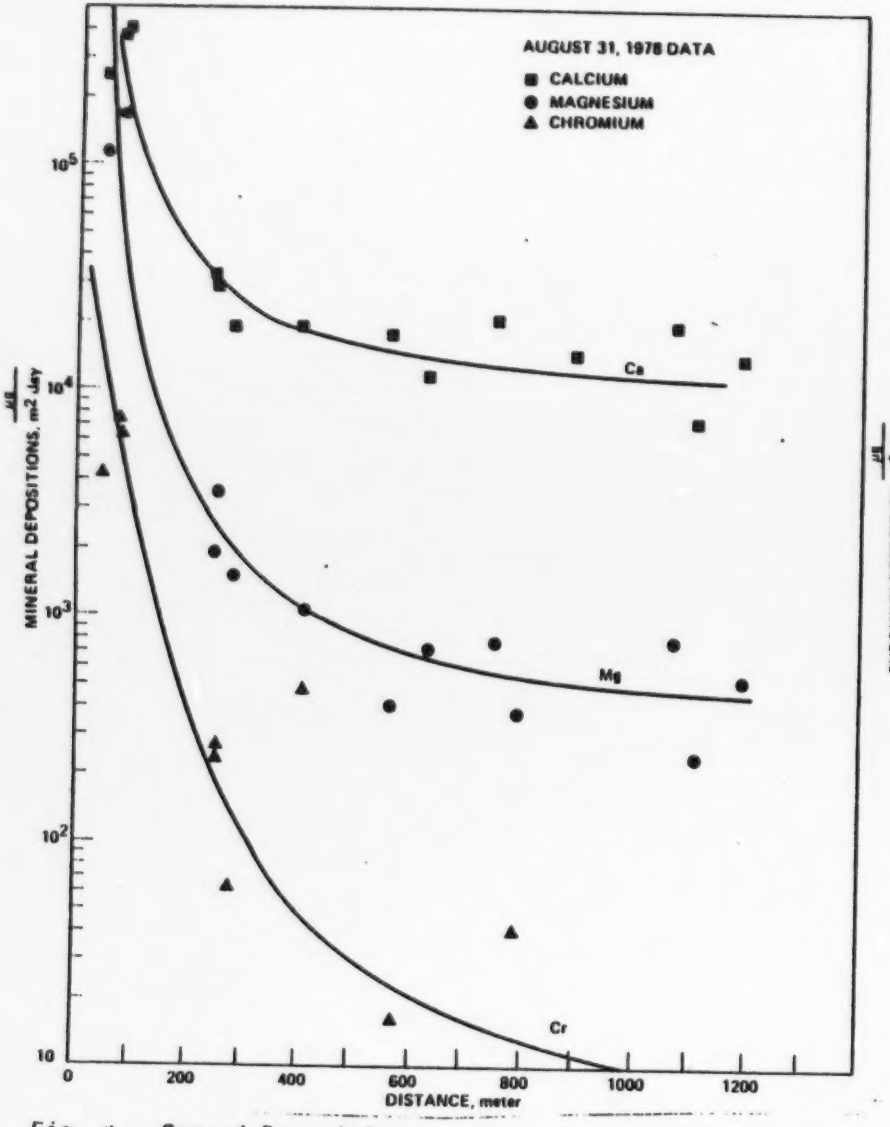

Fig. 9. Ground Deposition Variation of Three Minerals

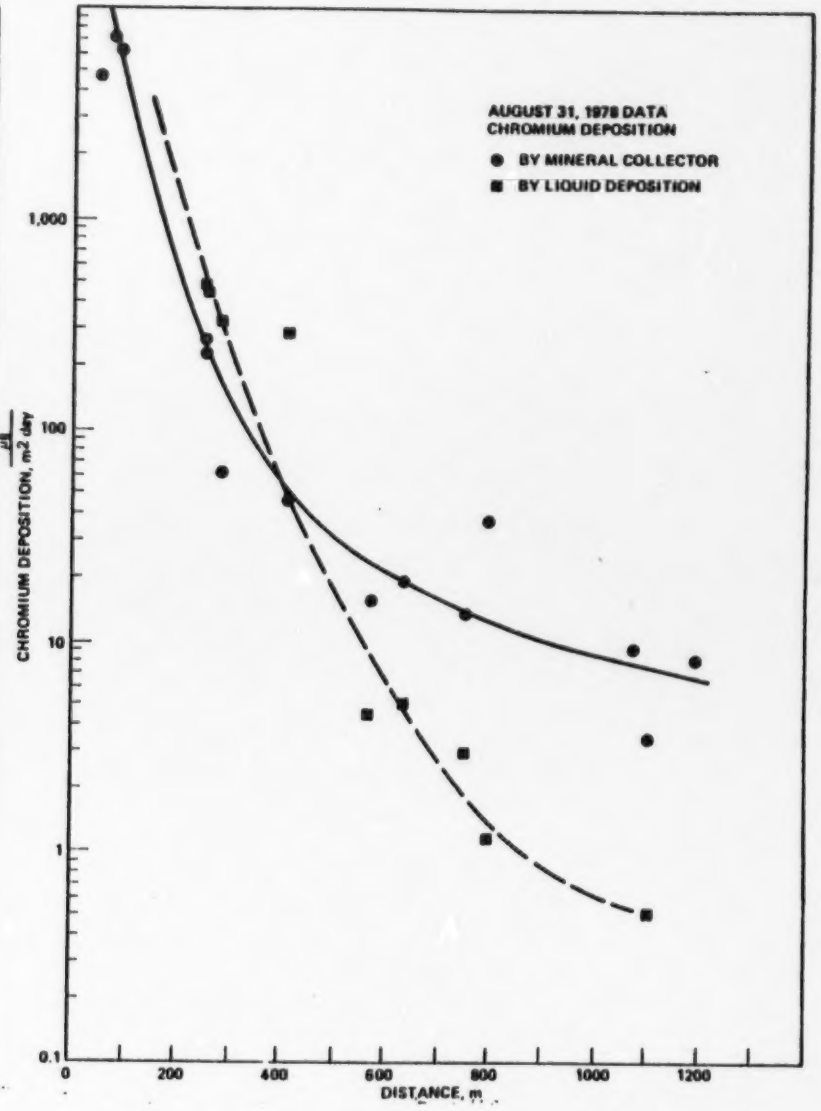

Fig. 8. Chromium Deposition Flux Variation

The difference in magnitude of the measurements of these minerals reflects their concentration in the basin water. The dispersion pattern of the three minerals exhibits a similar deposition outline despite this large difference. The deposition seems to be fairly constant beyond 1,000 meters from the cooling towers. The airborne concentration of chromium measured with rotating filter papers indicate that 2 to 10 ng/m^3 of chromium exists in the air near the cooling towers. The concentration, however, decreases to less than 0.1 ng/m^3 at 500 meters from the cooling tower. The shape of the pattern of airborne concentration of chromium resembles that of ground deposition flux. The airborne concentration measurements were normalized to the product of mean wind velocity and time of exposure. The normalized values along three sampling directions plotted in Figure 10 shows agreement within an order of magnitude between these three directions.

The chromium deposition flux measurements from the 1978 study are plotted in Figure 11 along with the results of the 1973 study; the results of the Environmental Systems Corporation (ESC) and Atmospheric Turbulence Diffusion Laboratory (ATDL) were converted from the drift deposition measurements by sensitive papers while Battelle Northwest's (BNW) result was a direct measurement of chromium deposition. The 1978 measurements seem to agree well with that of BNW in spite of the difference in time of test (meteorological condition difference) and operating condition (source strength difference). The 1978 results are characterized by a much steeper slope with distance than are the results from the 1973 study. This may be attributed partially to poor mist eliminator conditions which resulted in the high drift rate and wider spectrum of droplets experienced by the cooling towers in 1973. Other factors may be due to meteorological conditions which resulted in differences in plume height as well as wind velocities.

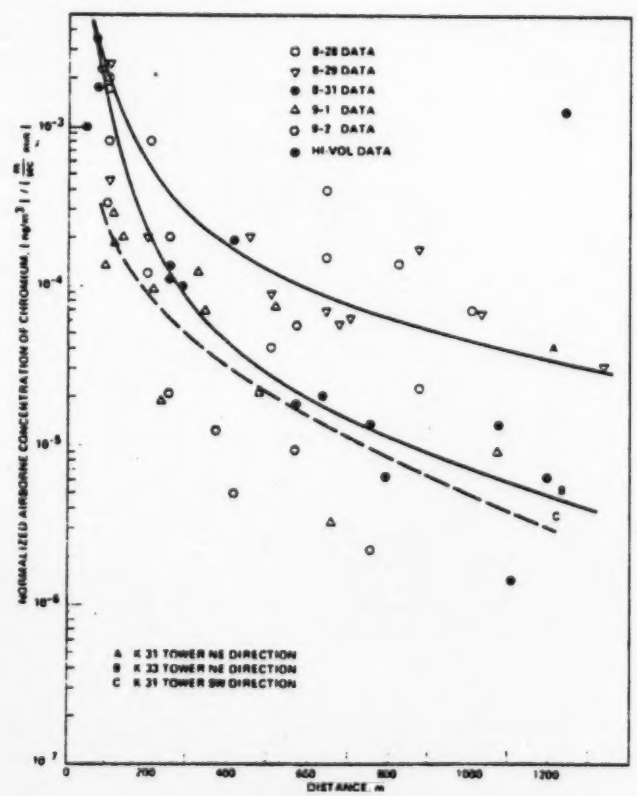

Fig. 10. Variation of Airborne Concentration of Chromium

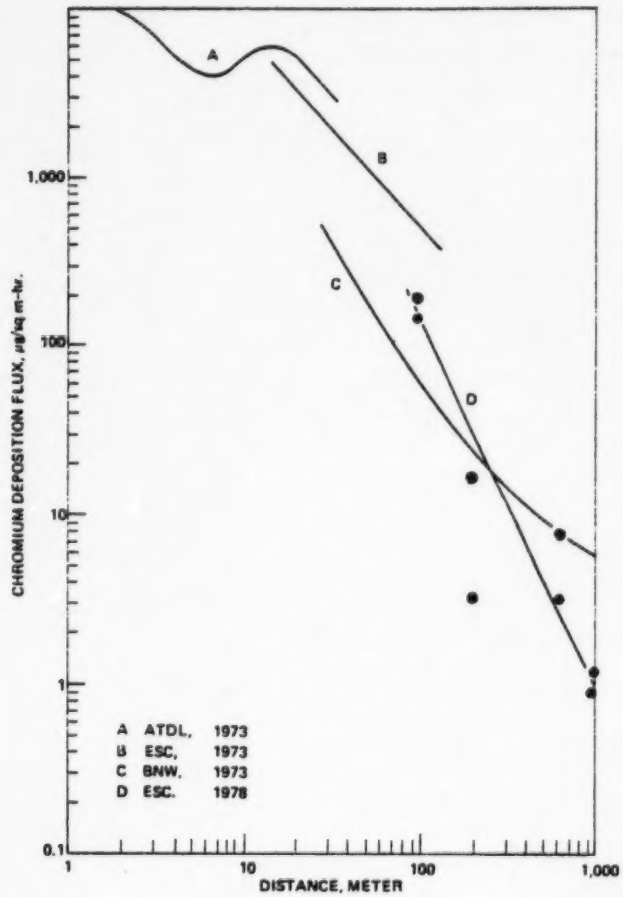

Fig. 11. Variation of Chromium Deposition Flux With Distance

CONCLUSIONS

The drift from the cooling towers at the ORGDP and its subsequent deposition on the ground surrounding the cooling towers has been investigated. Two independent tests were performed with the first conducted in 1973 followed by a more extensive effort in 1978. The 1973 drift study was an exploratory type of study compared to the more extensive and qualitative study conducted in 1978. Some of the results of the two studies; namely, ground deposition of chromium agree fairly well despite differences in cooling tower operating conditions and meteorological conditions. The drift rates measured at the fan stacks, however, differ significantly between studies and between cells. A satisfactory explanation of the differences is difficult since the drift rate of a cooling tower depends on the tower physical conditions as well as tower operating condition. Also, the accuracy of each measuring technique used in these studies varied greatly. The two major techniques employed in these measurements were an optical system in the 1973 study and the sensitive papers method in the 1978 study. The ratio of the sampling volume of the sensitive paper to the optical measurement was 200 to 1 which greatly improved the collection efficiency of the sensitive paper method. The drift flux measurements obtained from the two studies on the K-31 tower are shown in Table 6.

Table 6. Cooling Tower Drift Study at the ORGDP

	Drift Percentage	Measured By
1973 Study	0.1%	PILLS
1978 Study	0.03%	Sensitive Papers

ACKNOWLEDGEMENTS

This paper is based on work performed at the Oak Ridge Gaseous Diffusion Plant operated by Union Carbide Corporation, Nuclear Division for U. S. Department of Energy under contract W-7405 eng 26.

REFERENCES

1. P. A. Jallouk, G. J. Kidd, Jr., and T. Shapiro, Environmental Aspects of Cooling Tower Operation: Survey of the Emission, Transport and Deposition of Drift from the K-31 and K-33 Cooling Towers at ORGDP, Union Carbide Corporation, Nuclear Division, Oak Ridge Gaseous Diffusion Plant, Oak Ridge, Tennessee, 1974.

2. S. H. Park and J. M. Vance, Cooling Tower Drift Study at Oak Ridge Gaseous Diffusion Plant, Symposium on Environmental Effects of Cooling Tower Emission Conference, Proceedings, Cooling Tower Environment 1978, University of Maryland, May 2 to May 4, 1978.

3. G. O. Schrecker and C. D. Henderson, Salt Water Condenser Cooling: Measurements of Salt Water Drift from a Mechanical-Draft Wet Cooling Tower and Spray Modules and Operating Experience with Cooling Tower Materials, Proceedings of American Power Conference, Vol. 28, 1976.

4. R. O. Webb, D. A. Rutherford, and D. W. Cooke, Source and Downwind Cooling Tower Drift Data Acquired at the HUD Jersey City Total Energy Plant, prepared for Energy Division, Union Carbide Corporation, Oak Ridge National Laboratory, October 1977.

5. S. H. Park, Drift Losses from the ORGDP Cooling Towers, Proceedings of 1979 UCC-ND Waste Management Seminar, Union Carbide Corporation, Nuclear Division, Oak Ridge Gaseous Diffusion Plant, Oak Ridge, Tennessee, March 6 and 7, 1979.

6. R. A. Scriven, V. M. Morton, and A. G. Newlands, The Production of Airborne Droplets Below Eliminator Level in Natural Draught Cooling Towers, Atmospheric Environment, Vol. 8, pp. 337, 1974.

7. N. C. Chen and S. R. Hanna, Drift-Modeling and Monitoring Comparisons, Cooling Tower Conference, Houston, Texas 1977.

8. A. J. Policastro, W. E. Dunn, M. L. Breig, and J. P. Ziebarth, The Chalk Point Dye Tracer Study: Validation of Models and Analysis of Field Data, Proceedings of the Second Conference on Waste Heat Management and Utilization, Miami Beach, Florida, December 4 and 6, 1978.

COPYRIGHT NOTICE

BY ACCEPTANCE OF THIS ARTICLE, THE PUBLISHER AND/OR RECIPIENT ACKNOWLEDGES THE U.S. GOVERNMENT'S RIGHT TO RETAIN A NONEXCLUSIVE ROYALTY-FREE LICENSE IN AND TO ANY COPYRIGHT COVERING THIS PAPER.

SESSION V B

GREENHOUSE I

PB82-228198

INDUSTRIAL WASTE HEAT FOR GREENHOUSES

I. J. Crumbly
Fort Valley State College
Fort Valley, GA 31030
U. S. A.

T. G. Brna
U.S. Environmental Protection Agency
Industrial Environmental Research Laboratory
Research Triangle Park, NC 27711
U. S. A.

ABSTRACT

Potential beneficial use of industrial waste heat for the production of bedding plants was evaluated via use of conventionally and warm water heated greenhouses in Fort Valley, Georgia. Each greenhouse was a plastic covered quonset. The waste heat research greenhouse was heated and cooled using simulated warm condenser cooling water, while the control greenhouse had conventional heating and cooling in the 9-month test program. Cultivars of 10 leading ornamental bedding plants, 9 species of foliage plants, and tomatoes (as vegetable bedding plants) were studied for growth rate, survivability, time of flowering, and susceptibility to disease in both greenhouses. Environmental and economic aspects of greenhouse production were addressed as well as horticultural objectives.

No statistically significant difference in growth rate for 7 of 10 ornamental bedding plants and 2 of 8 foliage plants was observed in the two greenhouses. No significant difference in survivability among foliage plants and 8 of 10 ornamental bedding plants was seen in either greenhouse. No diseases were evident in the two greenhouses.

Heating and cooling of the waste heat greenhouse was satisfactory. Environmental control was adequate; at no time was condensation observed on the foliage of plants grown in either greenhouse. Preliminary economics indicate that industrial waste heat can be an attractive alternative to natural gas and fuel oil for greenhouse heating.

1. INTRODUCTION

Energy added to cooling water used in the power plant industry is called waste heat. In the past, the normal procedure has been to discharge cooling water from power plants back into rivers, lakes, and cooling ponds where the energy added is dissipated. To prevent adverse environmental impacts of waste heat and to prevent large water withdrawals associated with harm to aquatic life, the power plant industry now generally uses closed cycle cooling—usually evaporative cooling towers.

The annual quantity of waste heat presently available in the U.S. is approximately 10×10^{18} J (10 quad* Btu), the equivalent to 9×10^{7} m^3 (1.6×10^{9} barrels) of fuel oil [1]. This is slightly less than 20 percent of all the energy used in 1971 and, being a low-grade (low temperature) form of energy, the opportunities to use it beneficially are limited.

*1 quad = 10^{15}

Preceding page blank

Greenhouses require large amounts of energy to maintain adequate temperatures for crop production. The amount of energy required will vary with location, type of greenhouse, energy conservation measures, and crop. In the Tennessee Valley, the annual energy required for greenhouse crop production may exceed 1.3×10^{13} J/hectare (5×10^{9} Btu/acre) and in Minnesota, 1.9×10^{13} J/hectare (7×10^{9} Btu/acre) [2]. The U. S. Department of Agriculture reported in 1974 that 3.3×10^{7} m^2 (3.6×10^{8} ft^2) or 3,320 hectares (8,203 acres) were used for greenhouse space [3]. By conservative estimates, the greenhouse industry has grown by 5 percent each year since 1974 to a current estimate of 4,237 hectares (10,469 acres). If the average energy requirement for greenhouses in the U.S. is estimated as the average requirement for greenhouse production in Minnesota and the Tennessee Valley area, the greenhouse industry uses about 7×10^{6} J (7×10^{12} Btu) annually. Thus, the beneficial use of waste heat for greenhouse heating would entail a significant saving of the fuel equivalent to this annual heating load.

Currently, 30 to 40 percent of the cost of greenhouse crop production is for energy and is increasing, while natural gas and fuel oil supplies are becoming less available for greenhouse heating. Since most greenhouses are heated with natural gas, the present cost for 6.7×10^{16} J (6.4×10^{13} Btu) at \$3.04/GJ (\$3.20/10^{6} Btu) for natural gas exceeds \$204 million annually. Similarly, the cost of the same energy from No. 2 fuel oil at \$6.45/GJ (\$6.80/10^{6} Btu) is over \$433 million. Using waste heat at \$0.96/GJ (\$1.02/10^{6} Btu), the cost of this energy quantity would be \$61.4 million. In addition to conserving fossil fuels, the cost for energy could be reduced by 232% over the use of natural gas or 605% over the use of No. 2 fuel oil if waste heat was used, while at the same time environmental pollution would be reduced through the reduced combustion of fuel.

2. TEST PROGRAM OBJECTIVES AND FACILITIES

2.1 Objectives

The purpose of this study was to investigate the potential beneficial use of industrial waste heat for greenhouse production of bedding plants and foliage plants. The research facilities consisted of a conventional greenhouse and a greenhouse modified to use simulated waste heat.

The major overall objectives were: (1) to test a method of utilizing waste heat, (2) to test the suitability of the waste heat greenhouse environment for the production of ornamental and vegetable bedding crops and foliage plants, and (3) to evaluate the overall economics of the tested system.

2.2 Description of the Research Facilities

The research facilities consisted of two quonset-type plastic greenhouses, each 9.1 m x 21.9 m (30 ft x 72 ft). The plastic covering for each greenhouse consisted of a double layer of 6-mm (0.0024 in.) thick polyethylene plastic. One greenhouse served as a control; the other, as the waste heat research greenhouse.

The control greenhouse was not modified in any manner. It had a climate control system equipped with fans, shutters, plastic convection tube, two natural gas heating units, and controls to provide a suitable greenhouse

environment. Cooling was provided by an evaporative Kool-cel* pad located at one end of the greenhouse and two exhaust fans located at the opposite end of the greenhouse. Heat was supplied by two natural gas heaters with a heating capacity of 1.1×10^8 J/hr (1.05×10^5 Btu/hr). Heated air was disseminated by a fan through a 0.61-m (24-in.) polyethylene convection tube with punched holes to bring about even distribution of heat throughout the greenhouse.

The waste heat greenhouse effected cooling by warm water evaporating from a 4.3 m x 2.7 m (14 ft x 9 ft) Kool-cel pad through which air was circulated by two large exhaust fans. As 0.61 m (2 ft) of the Kool-cel pad is located in the attic plenum, most of the heat from warm water was dissipated in this portion of the Kool-cel pad, so that much of the heat was discharged from the attic before it reached the growing area of the greenhouse. This design of the waste heat research greenhouse permitted the use of warm water during the summer months when the temperature of industrial cooling water, especially from power plants, would be at its highest.

Heating in the waste heat greenhouse was provided by recirculating air through the attic plenum over the Kool-cel pad and/or over the warm-water-heated fin-tube system. The fin-tube system was located 1.2 m (4 ft) downstream from the Kool-cel pad and consisted of two staggered rows of 0.05-m (2 in.) radiation tubes 5.49 m (18 ft) long. The fins on the tubes were 0.1 m x 0.1 m (2 in. x 2 in.). Warm water was pumped through the tubes of the heat exchanger which also aided dehumidification.

Simulated waste heat for the research greenhouse was supplied by a 105 kW electric water heater (boiler). The simulated temperatures of water were based on the average monthly temperatures of effluent condenser cooling water during each month of the year as obtained from the Tennessee Valley Authority's Browns Ferry Nuclear Power Plant in northern Alabama.

The floor in each greenhouse consisted of a concrete walkway 1.2 m (4 ft) wide located in the center of the house with the remaining part of the floor being covered with 0.1 m (4 in.) of gravel.

Figures 1 and 2 are schematic representations of the waste heat greenhouse and control greenhouse, respectively.

3. HORTICULTURAL STUDIES

The horticultural studies began in January 1979 and followed the schedule listed below:

1. January through April 1979, cultivars of the 10 leading ornamental bedding plant crops along with the 2 leading vegetable bedding plant crops were grown in each greenhouse.

2. May through September 1979, cultivars of the leading species of foliage plants and plants adapted for hanging baskets were grown in each greenhouse.

*Trade Mark, ACME Engineering and Manufacturing Corporation

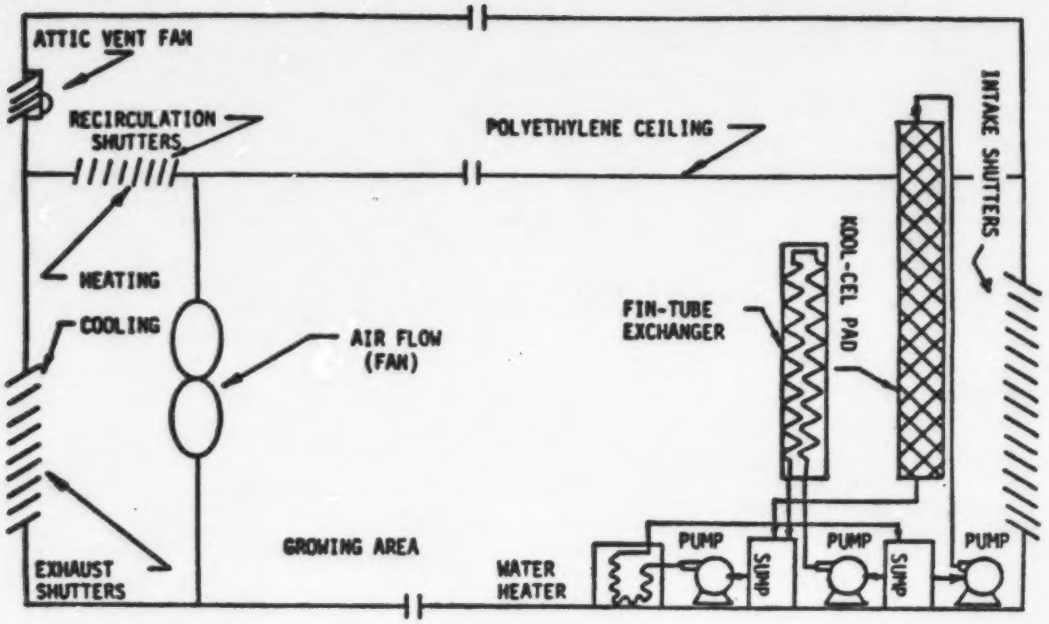

Figure 1. A schematic representation of the waste heat greenhouse.

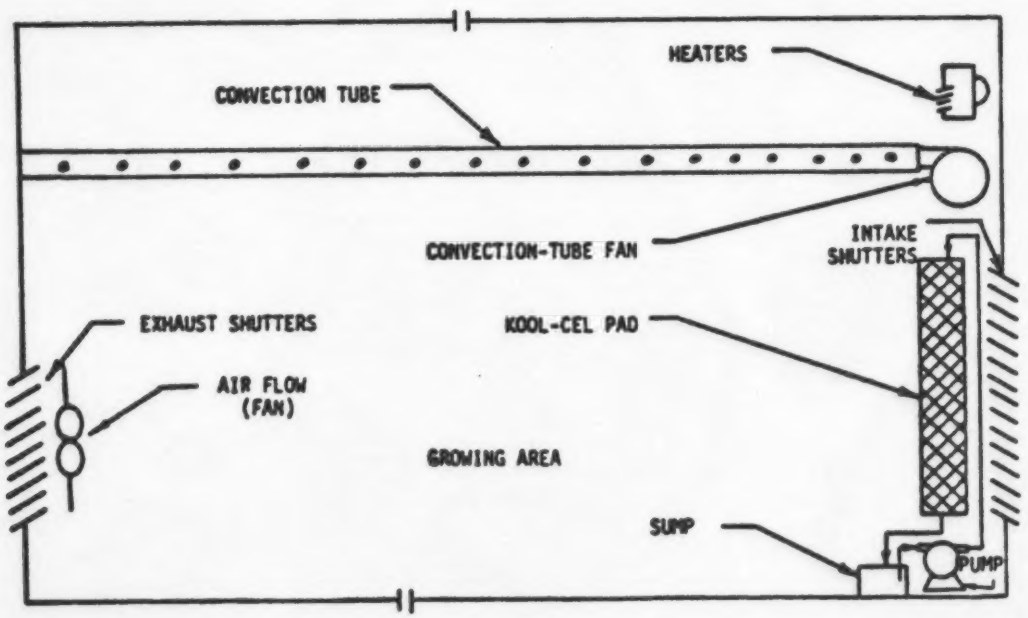

Figure 2. A schematic representation of the conventional greenhouse.

Both the conventional greenhouse and the waste heat greenhouse were operated as commercial-type enterprises, and all parts of the system were evaluated, both from the standpoint of mechanical operation and as a satisfactory structure for plant growth.

3.1 Bedding Plants

All bedding plants were grown from super seedlings obtained from the Ball Seed Company of Chicago, Illinois. Jiffy Mix Plus served as the soil medium.

Seedlings for each species and cultivar were transplanted to cell paks (32/tray), with the exception of geraniums which were transplanted into 0.1-m (4-in.) standard pots. After transplanting, trays and pots for each species were equally divided and half were placed in each of the conventional and waste heat research greenhouses.

Figure 3 depicts the arrangement of the bedding plant species in both greenhouses. The statistical design used for the analysis of variance was the randomized complete block design [4]. A 1.2-m (4-ft) space was placed between each block (replication).

Table 1 depicts the mean dry weight of the whole plant for all species, except peppers. (The pepper seedlings were eaten in both greenhouses by mice.) The growth rate of geraniums, petunias, and verbenas in the conventional greenhouse was statistically greater as compared with the same species grown in the waste heat greenhouse. Although begonias, browallias, coleus, impatiens, marigolds, pansies, salvias, and tomatoes grown in the conventional greenhouse showed a slightly better growth than those grown in the waste heat greenhouse, the differences in growth rates were not statistically significant.

TABLE 1. MEAN DRY WEIGHT (g) OF EIGHT WHOLE PLANTS/REPLICATION, APRIL 1, 1979

SPECIES	DAYS FROM TRANSPLANTING	CONVENTIONAL GREENHOUSE	WASTE HEAT GREENHOUSE
Begonia	50	11.25	10.87
Browallia	48	8.00	6.37
Coleus	49	7.87	6.25
Geranium	47	17.25[a]	13.25[a]
Impatiens	49	12.87	11.37
Marigold	50	14.90	14.00
Pansy	40	11.50	10.25
Petunia	49	17.50[a]	14.87[a]
Salvia	48	13.00	12.25
Tomato	40	17.50	15.30
Verbena	40	13.70[a]	10.37[a]

[a]Significant at the 5% level.

Table 2 compares the number of days required to flower in paks and pots for each species in each greenhouse. The plants grown in the waste heat greenhouse flowered on the average of 7.6 days later than those grown in the

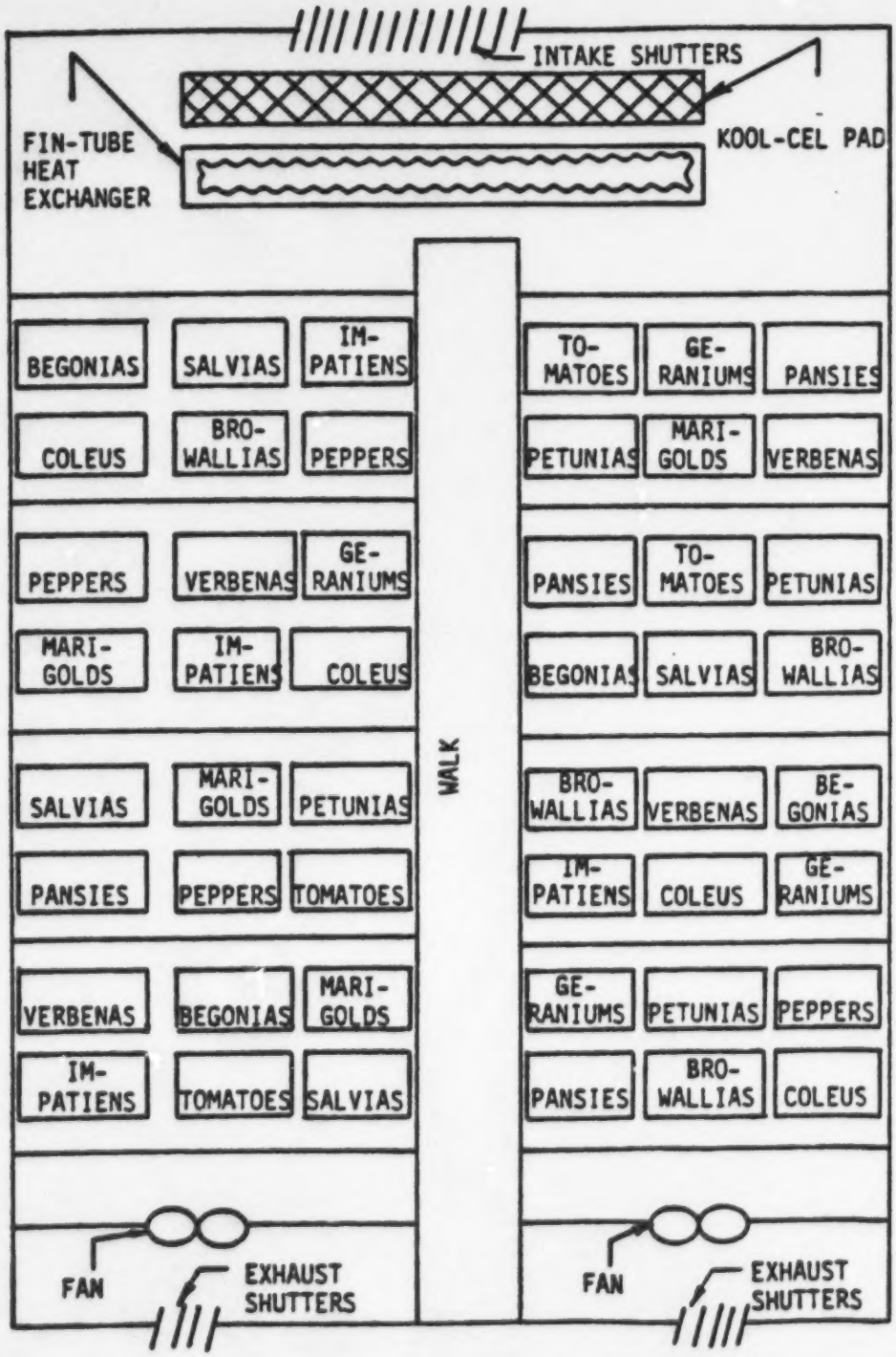

Figure 3. The arrangement of bedding plant species in the waste heat greenhouse.

conventional greenhouse. The greatest difference in flowering was noted in the geraniums which flowered 9 days earlier in the conventional greenhouse. Begonias, browallias, impatiens, and marigolds flowered 8 days earlier in the conventional greenhouse. Pansies, petunias, salvias, and verbenas grown in the conventional greenhouse flowered 7 days earlier than those grown in the waste heat greenhouse. Tomatoes are not listed in Table 2 because tomato bedding plants were sold according to plant size. These plants reached a saleable size in both greenhouses in 4 weeks.

TABLE 2. FLOWERING DATES OF BEDDING PLANTS IN PAKS

SPECIES	CONVENTIONAL GREENHOUSE		WASTE HEAT GREENHOUSE		DAYS DIFFERENCE IN BLOOMING
	TIME FROM TRANSPLANTING TO BLOOM (DAYS)	DATE OF BLOOM	TIME FROM TRANSPLANTING TO BLOOM (DAYS)	DATE OF BLOOM	
Begonia	31	3-13-79	39	3-21-79	8
Browallia	61	4-12-79	69	4-20-79	8
Geranium	79	4-30-79	88	5-09-79	9
Impatiens	33	3-16-79	41	3-24-79	8
Marigold	23	3-05-79	31	3-13-79	8
Pansy	36	3-28-79	43	4-04-79	7
Petunia	39	3-21-79	46	3-28-79	7
Salvia	38	3-20-79	45	3-27-79	7
Verbena	45	4-06-79	52	4-13-79	7

Table 3 shows the survival rate for each species of bedding plants in the conventional greenhouse and the waste heat research greenhouse. Only two species, browallia and coleus, showed a significantly better survival rate in the conventional greenhouse than in the waste heat research greenhouse. Browallia had an 81.0% survival rate in the conventional greenhouse and a 66.0% rate in the waste heat greenhouse. Coleus had an 89.5% survival rate in the conventional greenhouse compared to 78.0% in the waste heat greenhouse. For all other species, the survival rate was not statistically significantly different between the two greenhouses.

TABLE 3. MEAN SURVIVAL RATE BASED ON FOUR FLATS/REPLICATION (128 PLANTS), APRIL 10, 1979

SPECIES	DAYS FROM TRANSPLANTING	CONVENTIONAL GREENHOUSE (%)	WASTE HEAT GREENHOUSE (%)
Begonia	59	95.5	91.7
Browallia	57	81.0[a]	66.0[a]
Coleus	58	89.5[a]	78.0[a]
Geranium	56	98.8	98.4
Impatiens	57	100.0	100.0
Marigold	59	98.7	96.7
Pansy	49	99.2	99.5
Petunia	58	100.0	100.0
Salvia	57	96.2	97.5
Tomato	49	100.0	100.0
Verbena	49	97.5	97.5

[a]Significant at the 5% level.

3.2 Foliage Plants

Foliage plants were grown in both greenhouses from June 1979 through September 1979. Table 4 shows the species and cultivars for both greenhouses.

TABLE 4. SPECIES AND CULTIVARS

SPECIES	TRANSPLANTING DATE
Ardisia humilis	7-14-79
Asparagus meyerii	7-14-79
Begonia Caribbean mix	6-21-79
Dizyotheca elegantissima	6-21-79
Hypoestes sanguinolenta	7-05-79
Philodendron pertussum	7-05-79
Schefflera compacta	7-05-79
Syngonium podophyllum	6-21-79

Foliage plants were also obtained from Ball Seed Company as super seedlings. As all seedlings did not arrive on the same date, transplanting took place from June 12, 1979, through July 14, 1979.

Dry weights were taken August 23, 1979, on Dizotheca elegantissima (false aralia), Ardisia humilis, Begonia Caribbean mix, Syngonium podophyllum (nephthytis green), and Hypoestes sanguinolenta (polka dot plant).

Table 5 compares the mean dry weight for the five species of foliage plants grown in both greenhouses. With the exception of Ardisia humilis, the species listed grew better in the waste heat greenhouse than they did in the conventional greenhouse. Syngonium podophyllum (nephthytis green) grew significantly better in the waste heat greenhouse than it did in the conventional greenhouse.

TABLE 5. MEAN DRY WEIGHT (g) OF AERIAL PLANT PARTS, AUGUST 23, 1979

SPECIES	PLANTS/ REPLICATION	DAYS FROM TRANSPLANTING	CONVENTIONAL GREENHOUSE	WASTE HEAT GREENHOUSE
Dizyotheca elegantissima	10	63	6.38	7.12
Ardisia humilis	10	40	3.74	3.66
Begonia Caribbean mix	10	63	19.72	21.43
Syngonium podophyllum	20	63	34.80[a]	43.70[a]
Hypoestes sanguinolenta	20	63	100.20	92.20

[a]Significant at the 5% level.

The mean dry weight for Asparagus meyerii, Philodendron pertussum, and Schefflera compacta were taken on September 19, 1979. Table 6 shows that Philodendron pertussum grew significantly better in the waste heat research greenhouse than in the conventional greenhouse. Although the growth rates

were not significantly better, both Asparagus meyerii and Schefflera compacta grew better in the waste heat greenhouse than in the conventional greenhouse. These data indicate that foliage plants responded well to the waste heat greenhouse environment.

TABLE 6. MEAN DRY WEIGHT (g) OF AERIAL PLANT PARTS, SEPTEMBER 19, 1979

SPECIES	PLANTS/ REPLICATION	DAYS FROM TRANSPLANTING	CONVENTIONAL GREENHOUSE	WASTE HEAT GREENHOUSE
Asparagus meyerii	10	67	5.13	5.75
Philodendron pertussum	5	76	19.32a	22.60a
Schefflera compacta	5	76	12.45	13.96

[a]Significant at the 5% level.

Table 7 shows the survival rate of each species grown in both greenhouses. In regards to survival rate, the waste heat greenhouse provided an environment equally favorable to that of the conventional greenhouse. As a result of using normal disease preventive practices which were identical for each greenhouse, no evidence of any diseased plants was found.

TABLE 7. MEAN SURVIVABILITY BASED ON 100 PLANTS/REPLICATION, AUGUST 23, 1979

SPECIES	DAYS FROM TRANSPLANTING	CONVENTIONAL GREENHOUSE (%)	WASTE HEAT GREENHOUSE (%)
Dizyotheca elegantissima	63	100.0	100.0
Ardisia humilis	40	100.0	100.0
Asparagus meyerii	40	100.0	100.0
Caribbean mix begonia	63	97.3	96.8
Syngonium podophyllum	63	100.0	100.0
Philodendron pertussum	49	100.0	100.0
Hypoestes sanguinolenta	49	100.0	100.0
Schefflera compacta	49	100.0	100.0

4. GREENHOUSE PERFORMANCE

Histories for temperature and relative humidity were compared for the conventional greenhouse and the waste heat research greenhouse. Temperature was recorded by a hygrothermograph, and the relative humidity was measured with a hand psychrometer. Both temperature and the relative humidity readings were taken on the floor in the center of each greenhouse and on the outside of the greenhouses.

The flow rate of warm water was set at 3.8 m^3/min. (24 gpm) in the waste heat greenhouse. The same flow rate was used for both winter and summer.

The temperature of power plant effluent water will vary according to whether the power plant is operating with a closed cycle or an open cycle cooling system and also according to time of the year. Table 8 shows the temperature of effluent water for both closed cycle and an open cycle cooling at the TVA's Browns Ferry nuclear power plant located in northern Alabama but in reasonable proximity to the test site. As shown in Table 8, the temperature of effluent water will be higher from the power plant operating with closed cycle than from the power plant operating with open cycle cooling.

TABLE 8. AVERAGE MONTHLY TEMPERATURE OF EFFLUENT WATER AT BROWNS FERRY NUCLEAR POWER PLANT LOCATED IN NORTH ALABAMA[a]

MONTH	OPEN CYCLE TEMPERATURE		CLOSED CYCLE TEMPERATURE	
	°C	°F	°C	°F
January	21.30	70.34	43.10	109.58
February	21.80	71.24	43.90	111.00
March	24.40	75.92	45.10	113.18
April	31.30	88.34	47.20	116.96
May	35.80	96.44	49.00	120.20
June	40.60	105.08	50.50	122.90
July	43.10	109.58	51.20	124.16
August	43.20	109.76	51.20	124.16
September	40.60	105.08	49.90	121.82
October	35.70	96.26	47.70	117.86
November	29.10	84.38	45.40	113.72
December	24.40	75.92	43.20	109.76

[a]Earl Burns, TVA, Muscle Shoals, AL. Personal Communication to I. J. Crumbly, October 1978.

In this study, the temperature of water used in the waste heat greenhouse simulated the temperature of effluent water for open cycle cooling throughout the year.

4.1 Heating

During February 1979, the temperature of effluent water under open cycle cooling was 21.8°C (71.2°F) as shown in Table 8. The water used for heating in the waste heat research greenhouse was heated to this temperature. Each greenhouse had the nighttime temperature set at 15.5°C (60°F) and a daytime setting of 21.1°C (70°F).

During a 24-hour period in February, the waste heat research greenhouse maintained an average low night temperature of 12.0°C (53.6°F). In the conventional greenhouse the average low night temperature was 14.1°C (57.4°F). These values corresponded to the average low outside night temperature for this period of 2.6°C (36.7°F) as shown in Figure 4.

It is important to note here that the temperature control box in each greenhouse was located approximately 1.2 m (4 ft) above floor level. However, the hygrothermograph recorded the temperatures at floor level where bedding plants are commonly grown in greenhouses. Temperature stratification is common in greenhouses and is the major reason for the difference between the greenhouse set temperature and the temperatures recorded at floor level.

4.2 Cooling

Both greenhouses were covered with an 80% K-shade cloth to provide favorable light conditions for foliage plants and to aid in cooling. Figure 5 shows the average high temperature for both greenhouses during a hot 4-day period in July using warm water heated to 43.1°C (109.6°F) to cool the waste heat research greenhouse. During this 4-day period, the average high temperature in the waste heat research greenhouse was 30°C (86°F) and 29.4°C (85°F) in the conventional greenhouse. The average high outside temperature covering the same period was 38.6°C (101.5°F). Figure 5 shows hourly cooling for each day during the same 4-day period in July.

5. ECONOMIC STUDIES

Because data were analyzed for only a 9-month period of 1979, the economic projections made herein are of a preliminary nature.

5.1 Projected Cost of Waste Heat

Presently no general conclusions are possible for what waste heat should cost. One suggestion states that waste heat should cost $\$0.19/10^9$ J ($\$0.20/10^6$ Btu) [5]. A more realistic cost might be based on the cost of retrofitting a power plant with a greenhouse heating capability and allocating the cost of retrofitting to the power plant or greenhouse operator, or both. Because each site is expected to have different constraints, the breakeven cost for greenhouse operation is site specific and dependent on the market for greenhouse crops as well as power plant variables.

The investment and operating cost will vary with different sites. However, the Sherco demonstration project near Minneapolis, Minnesota, may serve as a model [6]. For the Sherco demonstration project, the calculated cost (1978$) to deliver the warm water 1,067 m (3,500 ft) to the demonstration greenhouse and return it to the cooling tower the same distance was about $\$0.96/10^9$ J ($\$1.02/10^6$ Btu) per 0.4 hectare (acre) based on the actual installed pipeline cost of about $600,000 for a pipeline flow rate of 15.6 m^3/s (7,000 gpm). Also included in the above cost to deliver the warm water to the greenhouse are the pumping costs at $270/year, chlorination for bacterial slime control estimated to be $550/year, and total operating cost estimated to be $1,500/year per 0.4-hectare (1-acre) greenhouse.

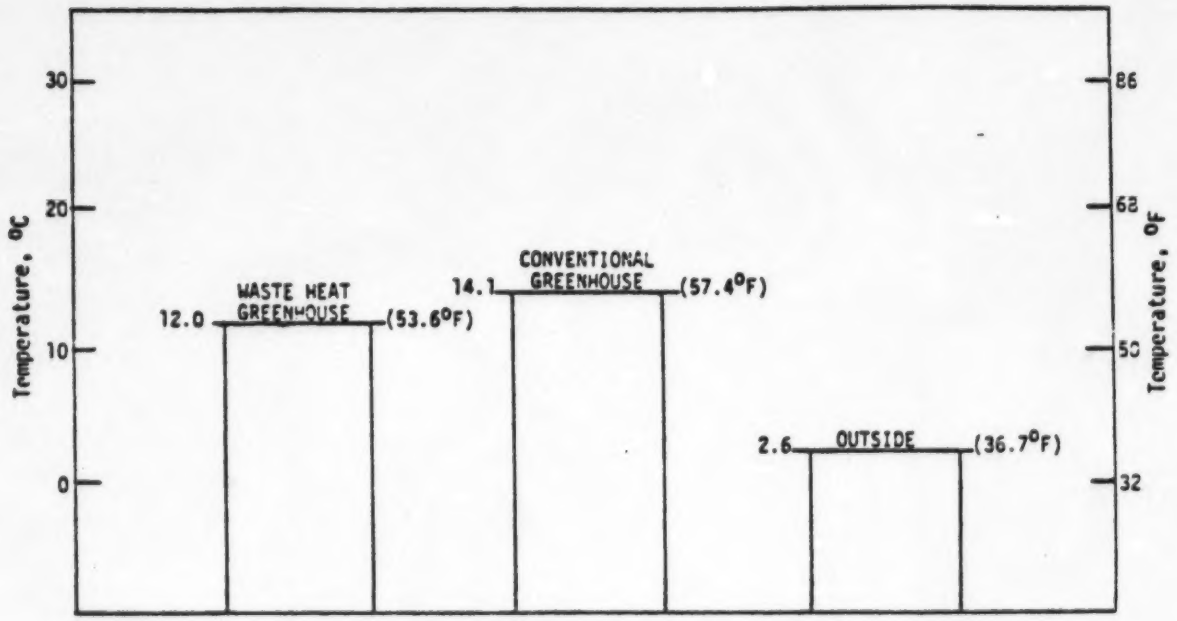

Figure 4. Average low night air temperature from February 1 through February 24, 1979.

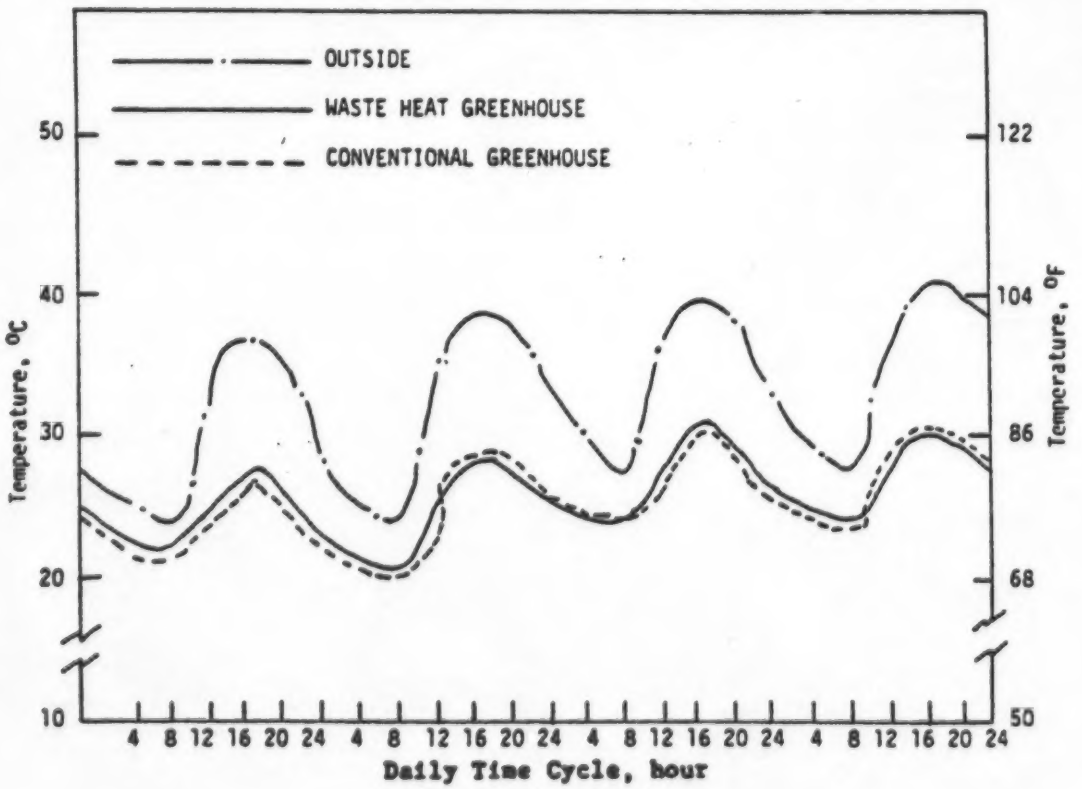

Figure 5. Comparative cooling during 4-day period in July 1979 (waste heat water temperature was 43.1°C (109.6°F)).

5.2 Projected Savings By Using Waste Heat

The number of years required to break even is an important consideration in an economic analysis. Two important factors in determining the number of years required to break even in a waste heat greenhouse operation are the cost of delivered waste heat and the kinds of fossil fuel the waste heat used replaces.

Using actual costs in 1978, the waste heat research greenhouse on an area basis cost about $219,000/hectare ($89,000/acre) more than the conventional greenhouse [7]. With energy prices of $3.04/$10^9$ J ($3.21/$10^6$ Btu) for natural gas and $6.45/$10^9$ J ($6.80/$10^6$ Btu) for No. 2 fuel oil at Fort Valley, Georgia, the approximate annual heating costs using these fuels would be $20,500 and $43,500, respectively, for a 0.4-hectare (1-acre) greenhouse. If the delivered waste heat cost to this greenhouse is $0.96/$10^9$ J ($1.02/$10^6$ Btu) as at the Sherco site [6], the annual savings of waste heat over natural gas would be $14,000 and $37,000 over No. 2 fuel oil. These savings equate to payback periods of 6.4 and 2.4 years, respectively.

It is important to note that inflationary fuel prices and increased fuel costs since 1978 were neglected in computing the above payback periods. Based on past trends, fuel costs are expected to continue increasing and thereby reduce the number of years required to break even using waste heat for greenhouse heating in the future. With the recent lifting of controls on fuel oil prices and the deregulation of natural gas prices expected by 1985 or earlier, the use of waste heat, which is expected to increase in cost at a much slower rate, should become even more attractive for greenhouse heating in the future.

6. CONCLUSIONS

The data included in this report suggest that the growth rate of the bedding plant and foliage plant species studied was not adversely affected by the waste heat greenhouse environment. The plants grown in the conventional greenhouse flowered from 7 to 9 days earlier than those grown in the waste heat research greenhouse. However, this may be insignificant when considering the amount of money saved in fuel cost with waste heat heating. In addition, no diseases were evident in either greenhouse, and this fact is believed to be particularly significant for the high humidity research greenhouse.

The environmental control system for the research greenhouse was adequate. Both heating and cooling were satisfactory with the evaporative pad-warm water system used.

Considering the escalating prices for natural gas and No. 2 fuel oil, the breakeven cost period to heat a greenhouse with waste heat will probably decrease from the 1979 projection of 6 years to 3 to 4 years relative to heating with natural gas and 2 years for heating with No. 2 fuel oil within the next few years.

ACKNOWLEDGMENT

This paper is based on work performed under EPA Grant No. R804499.

REFERENCES

1. C. E. Madewell, L. D. King, Johnny Carter, J. B. Martin, and W. K. Furlong, Progress Report: Using Power Plant Discharge Water in Greenhouse Vegetable Production, Tennessee Valley Authority, Bull. Z-56, Muscle Shoals, AL, Jan. 1975.

2. Burns, Earl R., Robert S. Piles, and Carl E. Madewell, Waste Heat Use in Greenhouses, State of the Art Waste Heat Utilization for Agriculture and Aquaculture. Tennessee Valley Authority Bull. Y-132, Sect. 3, Muscle Shoals, AL, Aug. 1978.

3. Census of Agriculture, U. S. Dept. of Agriculture, Washington, DC, pp. III 38-39, 1974.

4. Steel, Robert G. D. and James H. Torrie. Principles and Procedures of Statistics, McGraw-Hill, New York, 1960.

5. Beall, S. E. Jr., and G. Samuels. The Use of Warm Water for Heating and Cooling Plant and Animal Enclosures, Oak Ridge National Lab. Rept. TM-3381, Oak Ridge, TN, 1971.

6. Boyd, L. L., G. C. Ashley, J. S. Hietala, R. V. Stanfield, and T. R. C. Tonkinson, A Demonstration of Beneficial Uses of Warm Water from Condensers of Electric Generating Plants, U.S. EPA Rept. EPA-600/7-80-099, Research Triangle Park, NC, May 1980 (NTIS Accession No. PB 80-196793).

7. Crumbly, Isaac J., Greenhouse Production of Bedding Plants and Foliage Plants with Industrial Waste Heat. U.S. EPA Rept. EPA-600/7-81-034, Research Triangle Park, NC, March 1981 (NTIS Accession No. PB 81-178279).

PB82-228206

AN UPDATE ON HEATING GREENHOUSES IN NORTHERN CLIMATES WITH POWER PLANT REJECT HEAT

G. C. Ashley, P.E. and J.S. Hietala, P.E.
Ashley Engineering, Inc.
St. Paul, Minnesota 55112, U.S.A.

ABSTRACT

The Sherco Greenhouse Project was a demonstration of the use of electric generating plant waste heat for greenhouse heating. As a result of ten years of research and development, it is now both technically and economically feasible to utilize condenser waste heat for commercial greenhouse heating. Presently three commercial greenhouse operators in Minnesota have put 2.6 acres into production using waste heat from the Northern States Power Company (NSP) Sherburne County Generating Plant located near Minneapolis. The concept has been well received by industry, and there are more than ten similar projects throughout the U.S. and Canada.

While the use of waste heat does not change the total energy consumption of a greenhouse, it substitutes waste or reject heat for the primary energy (natural gas, oil, or propane) that would otherwise have been consumed by the greenhouse. In northern climates this annual energy savings is approximately 10 billion Btu's per acre of greenhouse production. The potential energy savings for the entire U.S. greenhouse industry is estimated at the equivalent of 1,000,000 gallons of oil per day.

1. INTRODUCTION

Power plant waste heat has been used successfully to provide most of the heat energy required by a few large scale commercial greenhouses in Minnesota. Waste heat for this purpose was first sold commercially by Northern States Power Company in 1977. At that time 1.2 acres of commercial greenhouses were built with private financing by individual commercial growers engaged in the production of both floral and vegetable products. These greenhouses were built after and in addition to a successful one-half acre greenhouse demonstration project that was funded by Northern States Power Company, the University of Minnesota, and the U.S. Environmental Protection Agency.

2. SHERCO SITE DEVELOPMENT

Since 1977 the commercial greenhouse acreage at this plant site has expanded to a total of 2.6 acres now in commercial production. In addition, construction is underway for another 1.5 acre expansion, which will bring the total commercial ranges to 4.1 acres by the Fall of 1981.

The original commercial greenhouse operators, who now have four heating seasons of experience using the power plant condenser water for heating, own and operate all of the existing facilities. However, additional strong interest in relocation to the NSP site is being expressed by other Minneapolis area growers who are experiencing unacceptably high fuel costs. In all probability the use of waste heat at this single plant site will expand in the years ahead as these local growers decide to relocate.

The NSP site easily has sufficient waste heat available to service more acres of greenhouses than presently exist in the state of Minnesota. However, the practical size of the present development is on the order of 20 acres, limited primarily by the amount of suitable land located nearby the cooling towers. While it would be possible at the NSP Sherco site to develop a larger land area, this would require some significant additional piping and a massive development is not envisioned in the near future.

3. WASTE HEAT USE

It can probably be safely stated that the large price increases for conventional greenhouse heating fuels is doing as much to foster waste heat utilization development as any other single factor. It appears now that the commercial greenhouse industry is more willing to relocate to take advantage of waste heat than ever before. This interest on the part of the growers is causing the electric utility and other industries to seriously examine the potential for making low grade waste heat available.

For example, the government of Ontario, Canada in conjunction with Ontario Hydro and private businessmen have been very vigorous in the pursuit of large scale waste heat AgriParks. In 1979, the Bruce AgriPark Joint Venture group constructed a one acre productivity test greenhouse at Kincardine, Ontario near the site of the massive Bruce Nuclear Power Development. While the productivity test greenhouse is operating to demonstrate acceptable crop production using simulated waste heat, planning is continuing for the development of up to 150 acres of greenhouses to use either power plant waste heat or industrial waste heat from a planned adjacent industrial park.

In addition to this effort in Ontario, we are aware of similar demonstration projects in Alberta using waste heat from gas pipeline compressor stations; in Ontario using refinery waste heat; and in Saskatchewan using power plant stack gas heat.

In the U.S. there is at least one other power plant site where commercial greenhouses have already relocated to use waste heat. This is the commercial project developed by Pennsylvania Power and Light Company at the Montour Power Plant. Several other utilities in the northern tier states are conducting detailed feasibility studies or research and development projects aimed at commercial use of waste heat. These projects involve power plants located in Wyoming, North Dakota, Minnesota, Illinois, Michigan, New Jersey, and New York.

These projects include both large scale (10 acres and larger) and small scale (less than 10 acres) greenhouse ranges as well as aquacultural and other related activities. One project is considering greenhouses devoted primarily to the production of containerized tree seedlings, while others are considering general floral and vegetable products. Various concepts for waste heat use systems are being studied and developed including heated floors in Pennsylvania and heated roofs in Illinois. Heat pumps and dry and wet heat exchangers are also being studied and developed in some of these projects.

4. ECONOMIC BENEFITS

In the past it was reported that the use of waste heat could be expected to reduce heating costs by about $11,000/acre-yr for a typical double polyethylene greenhouse in Minnesota (reference 1). However, actual operating experience at that time indicated a real savings of only $3,500/acre-yr. Now it is possible to compare the total cost of utilities for the 1978-79 heating season for a waste heat facility to a conventional glass greenhouse. Table I shows a total utility cost difference of nearly $35,000/acre-yr favoring the double poly waste heat greenhouse. Because the comparison is made with a conventional greenhouse that is glass and because the glass greenhouse is somewhat larger than one acre, the adjusted difference is $.30/ft^2 or $13,068/acre-yr.

Because both natural gas and oil prices have increased substantially since the 1978-79 heating season, the economic advantage of waste heat is greater than past experience would suggest. Table II shows the calculated comparative utilities cost to heat a typical double poly greenhouse with conventional fuels or with waste heat. The advantage for waste heat use is from $15,500 to $53,900/acre-yr compared to heating with firm natural gas or No. 2 oil. The actual economic advantage of waste heat today when compared to No. 2 oil, exceeds the advantage that was previously projected for the year 1998. This is due primarily to the fact that the price of No. 2 oil has nearly tripled since 1978.

TABLE I. ENERGY COST HISTORY FOR A WASTE HEAT GREENHOUSE
(1978 - 1979)

MONTH	CONVENTIONAL GREENHOUSE	WASTE HEAT GREENHOUSE
JULY	$ 507	$ 904
AUGUST	484	827
SEPTEMBER	1,253	1,015
OCTOBER	2,503	1,623
NOVEMBER	5,774	1,644
DECEMBER	6,131	1,240
JANUARY	10,508	2,870
FEBRUARY	10,264	2,457
MARCH	7,973	2,239
APRIL	4,814	2,023
MAY	3,327	1,592
JUNE	868	1,149
TOTALS:	$54,406	$19,583

TABLE II. COMPARATIVE UTILITIES COSTS
FOR
PLASTIC COVERED GREENHOUSES
MINNEAPOLIS, MN. PER ACRE BASIS
(FEBRUARY, 1981 FUEL COSTS)

	WASTE HEAT FACILITY	CONVENTIONAL FIRM NATURAL GAS @$3.73/MCF	CONVENTIONAL NO. 2 OIL @$1.06/GAL
FUEL	---	37,300	75,700
ELECTRICITY	12,700	4,000	4,000
SUPPLEMENTAL FUEL[1]	2,600	N/A	---
WASTE HEAT DELIVERY CHARGE[2]	10,500	N/A	---
TOTAL:	25,800	41,300	79,700

[1] Supplemental fuel assumed to be propane @$.62/gal.

[2] Based on current commercial rates at Sherco.

5. DEVELOPMENT PROBLEMS

During the course of development of commercial waste heat utilization, a number of problems have been encountered. The most serious of these have been corrosion and biofouling of piping and heat exchangers, pipeline reliability, and the consumption of supplemental fuel and electric energy to operate the greenhouses.

Biofouling has been successfully controlled by injecting biocides directly into the pipeline networks serving waste heat to the greenhouses. In addition, pipelines are cleaned by "pigging" to reduce build-ups of bioaccumulations. Such cleaning appears to be needed only about every other year at the Sherco site. Greenhouse heat exchangers can be cleaned with normal acid treatments, but none have yet been necessary for scale or bioaccumulation.

Corrosion continues to be a problem with standard steel piping showing significant pitting and deterioration in the original one-half acre greenhouse. The use of all plastic piping in commercial facilities has all but eliminated pipe corrosion problems. However, the greenhouse heat exchangers are subject to corrosion where cast iron or steel headers are used. Copper pipe headered coils are now being used by commercial operators and are apparently resisting any significant corrosion.

During the first year of commercial waste heat service the overall availability was 96.6%, with most of the outage time the result of pipeline failures. Since the 1977-78 heating season, the pipeline availability has been almost 100% and the overall waste heat availability has been greater than 98%. The

early pipeline problems resulted primarily from improper construction and operating procedures that have since been corrected. It appears now that plastic piping as well as cast iron is well suited to the waste heat pipeline application.

Because the waste heat availability has improved, the amount of supplemental fuel usage has steadily decreased with no supplemental heating fuel being required in the 1979-80 heating season. While supplemental fuel usage is expected to vary from year to year, the long term average can be expected to remain about 4% of the annual greenhouse heat needs. (Computer simulations based on condenser log records from other power plants suggest even less supplemental fuel may be needed at base load power plants.)

Another problem can be the amount of electric energy required to operate the waste heat greenhouse heating system, depending upon the cost of electricity and the temperature of the available waste heat. For the commercial greenhouses in Minnesota the cost of electricity is about $8,700/acre-yr to operate the heating system. This relatively high cost results from the fact that the waste heat is generally available at 85-90°F but infrequently above 90°F. The amount of electricity is strongly dependent on the available waste heat temperature and will vary considerably from site to site. If larger, lower cost and practical heat transfer surfaces could be made available for this application, the electric operating cost would be significantly reduced. At present, this an area where further research, development, and demonstration is needed.

6. CONCLUSIONS

The operating experience of commercial growers over the past four years with low temperature power plant waste heat has been good. In addition, the rapid rise in the cost of conventional heating fuels has made the use of waste heat much more attractive as a cost saving measure. This has resulted in the expansion of waste heat use in Minnesota and the development of similar projects in the northern tier states and in Canada. It appears that the use of waste heat for greenhouse heating can and will be expanded to a number of sites throughout the U.S.

REFERENCES

1. G. C. Ashley, J. S. Hietala, and R. V. Stansfield, The Sherco Greenhouse Project: From Demonstration to Commercial Use of Condenser Waste Heat, Proceedings of the Second Conference on Waste Heat Management and Utilization, pp. V-A-16-25, 1978.

SESSION VI A

FISHERIES/AQUACULTURE

Preceding page blank

PB82-228214

STRIPED BASS AND THE MANAGEMENT OF COOLING LAKES

Charles C. Coutant
Environmental Sciences Division
Oak Ridge National Laboratory
Oak Ridge, Tennessee 37830

ABSTRACT

Striped bass, Morone saxatilis, is being introduced to freshwater reservoirs, some of which are used for power plant cooling. The thermal niche of this fish species changes with age and greatly influences its success. Juveniles, which prefer and grow optimally near 24 to 26°C (75-80°F), may thrive in cooling lakes. However, adults, which seek temperatures near 20°C (68°F) and exhibit poor growth and survival above 22°C (72°F), may not survive summer conditions. Striped bass management in cooling lakes should be guided by these thermal requirements.

1: INTRODUCTION

Striped bass is an anadromous fish species native to the east coast of North America that is now being introduced into freshwater reservoirs (for synopses of the species, see [1] and [2]) and highly successful sport fisheries have often developed. Although individuals in freshwater have attained sizes of 23 kg (50 lbs) or more, there have been seasonal die-offs of large fish and poor growth and condition of adults at some sites, which have stimulated careful examination of the species' environmental requirements.

Striped bass management already interacts with power generation. Some reservoirs being stocked with striped bass are used for once-through power plant cooling. Juveniles are being introduced into run-of-river or storage reservoirs already used for cooling, and some closed-cycle cooling lakes have been suggested as sites for striped bass stocking. The compatibility of striped bass with the thermal regimes of cooling lakes is explored in this paper, in order that appropriate fishery management plans can be implemented.

2: THE SPECIES' THERMAL NICHE

Striped bass appear to have a changing thermal niche with age, a fact that greatly influences their success in freshwater environments [3]. A "thermal niche" may be defined broadly as the temperature selected in a thermal gradient after many hours of exposure and the temperature at which growth rate is maximum on unrestricted food ration. These behavioral and physiological criteria generally coincide for fish species that have been studied extensively [4]. Water masses of appropriate temperature constitute

Preceding page blank

an ecological "resource" for a species, in the context of current ecological niche theory [5]. Species are generally most successful in environments where their ecological niche, in this case the suitable temperature range, is amply available.

The thermal niche of a developing striped bass begins near the spawning temperature. It rises rapidly to high temperatures for juvenile growth, then gradually declines as fish mature (Fig. 1). Spawning generally takes place near 18°C (65°F), and available evidence indicates optimal survival and growth of embryos and larvae near this temperature [1,2]. Juveniles, however, grow optimally in and select much higher temperatures -- near 24 to 26°C [6,7]. These physiological and behavioral data, largely from laboratory studies, match the observed spring/summer movement of juveniles of east coast stocks to shallow nursery areas in their native estuaries. Laboratory temperature selection data suggest that preferred temperatures decline as the juveniles grow [7]. Field studies with sonic-tagged subadults in a small Tennessee lake

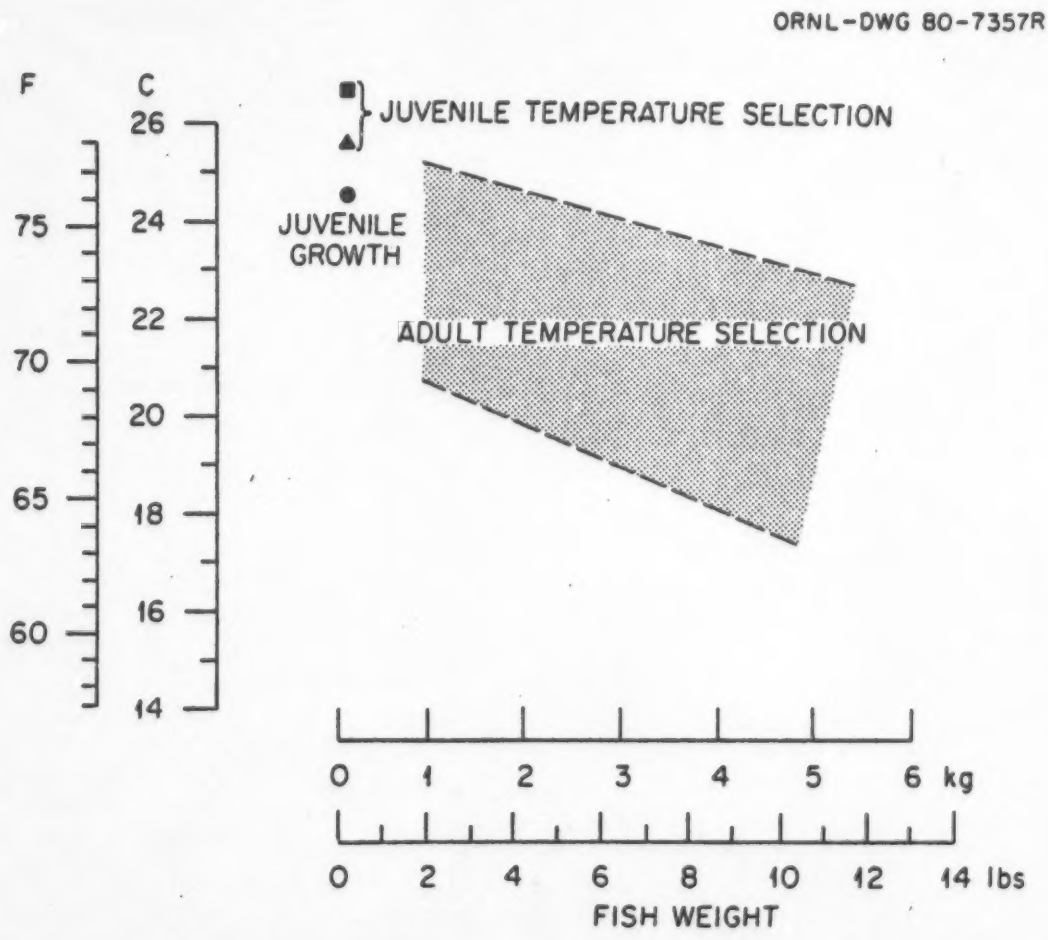

Figure 1. Changing thermal niche with size in striped bass. A-E: Optimal thermal range for growth of embryo, larval and early juvenile stages [1]; ■▲: Temperatures selected by juveniles in laboratory thermal gradients in two studies [7,24]; ● : Optimal growth temperature for well-fed juveniles in laboratory experiments [6]; Shaded: Zone of average temperatures occupied by 40 adults in summer telemetry studies [8,9,10]. Adapted from [3].

showed temperature selection near 22°C (Fig. 2). Adults in Tennessee reservoirs, similarly tagged with temperature-sensing transmitters, generally selected even cooler temperatures -- 18-20°C [9,10]. The requirement of adults for cool, oxygenated waters in summer limited the habitable volume of Cherokee Reservoir, Tennessee, to several small thermal refuges in submerged spring stream channels. The restricted summer habitat appears to have contributed to massive die-offs of adults larger than 4-5 kg (8-10 lbs). In a study just concluded on Watts Bar Rerservoir, Tennessee, the healthy striped bass population exhibited marked seasonal movements related to water temperature [11]. They alternated between autumn-winter-spring habitation of the entire reservoir [temperatures <25°C (77°F)] and summer restriction to two major cool tributaries (Clinch and Little Tennessee Rivers) or a small spring.

This pattern of a size(or age-) dependent thermal niche for striped bass, particularly the intolerance of large fish to warm water, satisfactorily explains many "peculiar" facets of striped bass behavior noted in the scientific literature and in fish management reports. For example, adults have been observed to move upstream toward cool dam tailwaters after spawning rather than move downstream to the ocean when coastal temperatures exceed 26°C [12]. Dam tailwaters seem to attract adults in summer long after the spawning run is over [13]. Summer distribution of adults in Percy Priest Reservoir, Tennessee, consisted of many small "home ranges" that may have been springs [14]. Late summer die-offs are common, but include only large fish [e.g., 15, 16]. In Florida, striped bass grow well as juveniles, but large fish are rarely found [17]. Summer temperatures in most reservoirs across the U.S. are well within the thermal niche range of juveniles, and they thrive in surface waters and coves [e.g., 18].

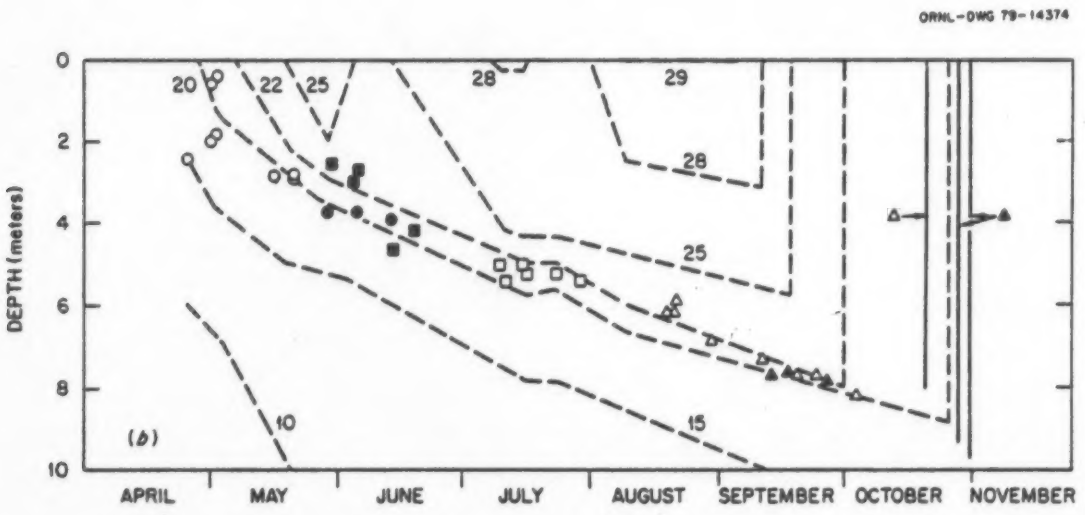

Figure 2. Average temperatures (shown on isotherms) occupied by subadult striped bass [940-2815 g (2-6 lbs)] plotted at the depths where temperatures occurred between April and October 1975 in Lambert Quarry Lake, Tennessee. Isothermal conditions of the epilimnion in late October prevented designating discrete depths (zones that could have been occupied are shown by vertical bars). From [8].

3: ACCESSORY FACTORS

3.1. Dissolved Oxygen

A major impediment to full utilization of thermal zones suitable for adults in summer is availability of dissolved oxygen. Cool temperatures in hypolimnia of lakes are often accompanied by low oxygen levels. This was the case in Cherokee Reservoir [9,10] where fish seemed to occupy dissolved oxygen levels only as low as 2-3 mg/L in order to attain the desired temperatures. Oxygen levels below that point in the main reservoir were avoided, and fish sought refuge in cool springs and spring streams. Because we observed loss of weight, high incidence of bacterial skin infection, and continuous mortalities in the Cherokee fish, we doubt that the 2 mg/L level of dissolved oxygen could be considered satisfactory for a healthy population. A "squeeze" between necessary thermal habitat and available oxygen supplies has been shown to limit available environment for other cool-water species, e.g., the cisco (Coregonus artedii) [19].

The importance of dissolved oxygen to suitable thermal habitat for adult striped bass in summer points to the trophic state of the water as a critical factor for this species. In eutrophic lakes high nutrient levels stimulate high organic matter production (usually phytoplankton) which is followed by oxygen-depleting decomposition in deep (cool) water layers. The cool habitat is then poorly suited for adults. In nutrient poor conditions (oligotrophic) there is little organic matter to decompose, and the cool, deep strata retain enough oxygen in summer to support the adult striped bass at suitable temperatures. Eutrophic lakes can thus be seen as high risk situations for striped bass populations, if a fishery for large sized fish is the objective.

3.2. Food

Clearly, food must be available if fish are to grow and survive. The interactions between a fish's need to seek food and its selection of temperature have been extensively debated with little clear resolution of guiding principles. The bioenergetic demands for food intake would seem to dictate some flexibility in choice of thermal habitat if the fish is to be successful. Some fish species show this flexibility in the form of feeding excursions outside the normal niche breadth, but these seem to occur primarily on the cool side of the thermal niche [20]. Lack of flexibility on the warm side may be related to the physiological causes of rapidly diminishing growth rates above the thermal optimum (see [6]). Even on the cool side, the literature shows some cases of extreme inflexability, e.g., starved bullheads in the Connecticut Yankee discharge canal [21] that apparentaly refused to enter cool water where food was available. Adult striped bass seem to avoid temperatures below about 18.5°C (65°F) [21], but this has not been examined carefully in relation to food availability.

Adult striped bass studied in thermal refuges in Cherokee Reservoir in summer [9,10] appeared to be starving amidst plenty, a circumstance which seems inexplicable except when viewed in the context of thermal niche theory. Fish, collected by electroshocking, from the cool density underflow of Mossy Creek as it entered the reservoir (Fig. 3) exhibited empty stomachs and greatly extended, black-green gall bladders (a symptom of unused digestive capability). Yet there was abundant food in the form of young gizzard shad (Dorosoma cepedianum) in the warm layers above them at 29-32°C (84-90°F).

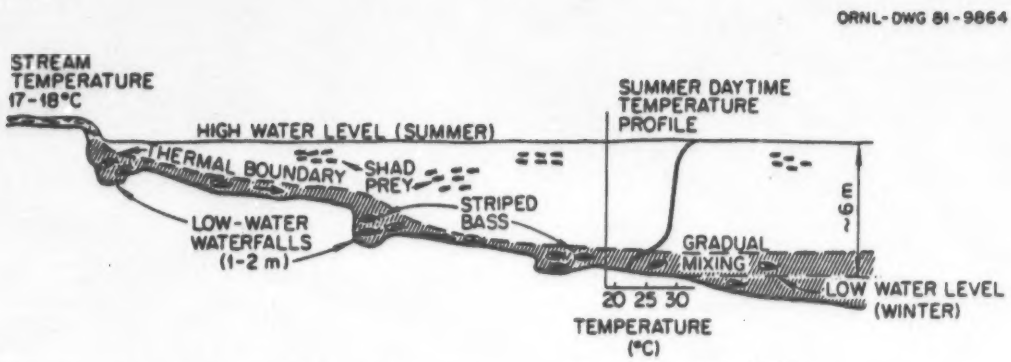

Figure 3. Diagrammatic longitudinal section through Mossy Creek Cove, Cherokee Reservoir, Tennessee, showing density underflow of cool water that constituted a thermal refuge for adult striped bass. Potential prey schooled in warm layers above, but were not utilized. From observations in [9,10].

Bait fish lowered by anglers into the cool underflow invariably caught adult striped bass but the adult bass would not penetrate the sharp thermal gradient to feed on natural schools of prey. From this evidence we conclude that the upper thermal niche boundary for striped bass is extremely inflexible.

4: MANAGEMENT IMPLICATIONS

The implications of these observations for cooling lakes seem clear. In general, lakes with summer temperatures near 24-26°C will provide optimal thermal conditions for growth of juveniles if food resources are available. These temperatures will be increasingly unsuitable as the fish grow, however, and the young fish must move elsewhere for cooler water. Lakes without temperatures below about 22°C in well-oxygenated zones will be unsuitable for adult striped bass larger than about 5 kg.

Cooling reservoirs that can be designed to maintain both warm habitats for juveniles and cool habitats for adults may be successfully managed for striped bass fisheries. Watts Bar Reservoir which we recently studied [11], cools TVA's Kingston Steam Plant, a 1600-MW coal-fired station, yet has a thriving population of large [greater than 14 kg [30 lbs)] healthy striped bass. The principal reason for success appears to be the combination of both extensive warm shallows in coves for juveniles and cool water (<22°C) from the Clinch River tributary (which is fed by a hypolimnetic discharge from upstream Norris Dam) for adults. Even in summer, the warm thermal plume overrides cool water which allows unobstructed passage by adults. In winter, the thermal plume serves as an attractant for mid-sized striped bass and supports a popular sports fishery. The loading factor is also low for this mainstem Tennessee River reservoir. Cherokee Reservoir on the other hand, which receives waste heat from TVA's John Sevier Steam Plant, is eutrophic and has only small thermal refuges [9,10]. Its striped bass population has been plagued by summer mortalities since 1972 when stocked juveniles first reached adult size, and large fish are rare.

Some reduction of suitable adult habitat in summer can actually aid a sports fishery. Thermal refuges serve the necessary function of bringing anglers and fish together. The concentrated fish become a readily harvestable resource, provided the ratio of population size to available thermal refuge

volume is not so high as to induce detrimental crowding causing starvation and disease, as seen in Cherokee Reservoir. Wherever summer thermal habitat is extensive relative to numbers of adult fish, the angler harvest has been low despite a healthy population. For thermal refuges to markedly aid a fishery, the population has to be established long enough for anglers to locate the refuge sites (tracking studies using ultrasonic or radiotelemetry [e.g., 9,10,11] can effectively speed this process). Fishery managers thus have a quantitative goal for establishing stocking rates for each lake based on the size of available adult thermal refuges. They should strive for sufficient adult numbers to induce some concentration in thermal refuges without undue crowding. The appearance of adult mortalities should signal that they have exceeded the lake's summer carrying capacity. The commonly-held belief that juvenile growth rates will be the limiting factor for successful stocking rates is probably not valid for striped bass.

Small, heavily loaded cooling lakes may serve as excellent nursery areas for rapid rearing of juveniles. Current practice for striped bass propagation includes spawning and egg and larval development in controlled hatchery tanks in April and May, followed by rearing to stockable size in heavily fertilized outdoor ponds [K. Cottrell, Eagle Bend Fish Hatchery, Clinton, Tennessee, pers. comm.]. Survival after stocking appears to be highest with the largest juveniles, yet many rearing ponds do not attain optimal growth temperatures of 24-26°C until mid-summer. Waste heat from power generation may thus be used productively in some cooling lakes for enhanced production of large juveniles for stocking elsewhere. The size attainable at these warm temperatures is still unclear, but the average thermal niche appears to have shifted downward to near 22°C by the time the fish have reached about 1 kg (2 lbs) [8]. Production of commercially-marketable striped bass in cooling lakes [22] may be precluded unless the downward shift in thermal niche can be matched by the onset of autumn cooling.

In conclusion, the fishery manager who wishes to use power station cooling lakes for striped bass fisheries needs to carefully answer questions about the annual thermal structure of the water body. Will thermal additions eliminate all water below about 22°C in summer and thus prevent survival and growth of adults? Will overall aquatic productivity be so high that sufficiently cool zones will be deoxygenated? Can thermal refuges for adults be established during critical periods if they are not already available (for example, by diverting spring streams or by pumping cool groundwater)? Can striped bass stocking rates be established so that thermal refuges allow for moderate concentration of adults but are not overtaxed by an expanding group of rapidly-growing juveniles? Can cool-water prey also be stocked which would provide food within the thermal refuges in summer? Will there be extensive areas of shorelines and coves where temperatures will be in the 24-26°C range for maximum growth rate of juveniles? Only by matching the cooling lake to the thermal niche requirements of the fish species can one expect to develop successful populations.

ACKNOWLEDGEMENTS

This research was sponsored by the Office of Health and Environmental Research, U.S. Department of Energy under contract W-7405-eng-26 with Union Carbide Corporation. I thank J. E. Breck and S. W. Christensen for critical review of the manuscript. Publication No. 1760, Environmental Sciences Division, Oak Ridge National Laboratory.

REFERENCES

1. D. T. Westin and B. A. Rogers, Synopsis of Biological Data on the Striped Bass, Morone saxatilis (Walbaum) 1792. Marine Tech. Rept. 67, University of Rhode Island, Kingston, Rhode Island, 1978.

2. E. M. Setzler, W. R. Boynton, K. V. Wood, H. H. Zion, L. Lubbers, N. K. Mountford, P. Frere, L. Tucker, and J. A. Mihursky, Synopsis of Biological Data on Striped Bass, Morone saxatilis (Walbaum), NOAA Tech. Rept. NMFS Circ. 433, FAO Synopsis No. 12T, National Marine Fisheries Service, Washington, D.C., 1980.

3. C. C. Coutant, Environmental Quality for Striped Bass, in H. Clepper (ed.), Marine Recreational Fisheries 5, pp. 179-187, Sport Fishing Institute, Washington, D.C.

4. R. W. McCauley and J. M. Casselman, The Final Preferendum as an Index of the Temperature for Optimum Growth in Fish, European Inland Fisheries Advisory Comm. Symp. 80/E76, 1980.

5. J. J. Magnuson, L. B. Crowder and P. A. Medvick, Temperature as an Ecological Resource, Am. Zool., vol. 19, pp. 331-343, 1979.

6. D. K. Cox and C. C. Coutant, Growth Dynamics of Juvenile Striped Bass as Functions of Temperature and Ration, Trans. Am. Fish. Soc., vol. 110, pp. 226-238, 1981.

7. C. C. Coutant, K. Zachmann, D. K. Cox, and B. Pearman, Temperature Selection by Juvenile Striped Bass in Laboratory and Field, Oak Ridge National Laboratory, Oak Ridge, Tennessee, in preparation.

8. C. C. Coutant and D. S. Carroll, Temperatures Occupied by Ten Ultrasonic-Tagged Striped Bass in Freshwater Lakes, Trans. Am. Fish. Soc., vol. 109, pp. 195-202, 1980.

9. H. R. Waddle, C. C. Coutant, and J. L. Wilson, Summer Habitat Selection by Striped Bass, Morone saxatilis, in Cherokee Reservoir, Tennessee, 1977, Oak Ridge National Laboratory Rept. ORNL/TM-6927, Oak Ridge, Tennessee, 1980.

10. B. A. Schaich and C. C. Coutant, A Biotelemetry Study of Spring and Summer Habitat Selection by Striped Bass in Cherokee Reservoir, Tennessee, 1978, Oak Ridge National Laboratory Rept. ORNL/TM-7127, Oak Ridge, Tennessee, 1980.

11. T. E. Cheek, M. J. Van den Avyle, and C. C. Coutant, Distribution and Movements of Adult Striped Bass, Morone saxatilis, in Watts Bar Reservoir, Oak Ridge National Laboratory, Oak Ridge, Tennessee, in preparation.

12. R. G. Dudley, A. W. Mullis, and J. W. Terrell, Movements of Adult Striped Bass (Morone saxatilis) in the Savannah River, Georgia, Trans. Am. Fish. Soc., vol. 106, pp. 314-322, 1977.

13. D. L. Deppert, The Effect of Striped Bass Predation and Water Quality on the Rainbow Trout Fishery of the Lower Illinois River, M.S. thesis, University of Oklahoma, Norman, Oklahoma, 1978.

14. S. W. Stookesbury, A Biotelemetry Study of the Striped Bass, Morone saxatilis (Walbaum), in J. Percy Priest Reservoir, Tennessee, Tennessee Wildlife Resources Agency Tech. Rept. No. 77-58, Nashville, Tennessee, 1978.

15. J. R. Axon, An Evaluation of Striped Bass Introductions in Herrington Lake, Kentucky Dept. Fish and Wildlife Resources Fisheries Bull. 63, Frankfort, Kentucky, 1979.

16. K. McClosky, Striped Bass Investigations, Report for the Period 5 March 1976 to 29 February 1980, Kansas Fish and Game Commission, Topeka, Kansas, 1980.

17. F. Ware, Investigations of Striped Bass and Morone Hybrids, Florida Game and Freshwater Fish Commission D-J Project, F-32 Final Report, Tallahassee, Florida, 1978.

18. M. J. Van den Avyle and B. J. Higginbotham, Growth, Survival, and Distribution of Striped Bass Stocked into Watts Bar Reservoir, Tennessee, Proc. Annu. Conf. S. E. Assoc. Fish and Wildl. Agencies, vol. 33, pp. 361-370, 1980.

19. P. J. Colby and L. T. Brooke, Cisco (Coregonus artedii) Mortalities in a Southern Michigan lake, July 1968, Limnol. Oceanog., Vol. 14, pp. 958-960, 1969.

20. G. Kromrey, Distribution and Feeding of Pumpkinseed (Lepomis gibbosus) and Black Crappie (Pomoxis nigromaculatus) in a Power Plant Cooling Lake, M.S. thesis, University of Wisconsin, Madison, Wisconsin, 1976.

21. D. Merriman and L. M. Thorpe, The Connecticut River Ecological Study, Am. Fish. Soc. Monogr. No. 1, Bethesda, Maryland, 1976.

22. J. Radovich, Effect of Ocean Temperature on the Seaward Movements of Striped Bass, Roccus saxatilis, on the Pacific Coast, Calif. Fish Game, vol. 49, pp. 191-207, 1963.

23. L. J. Wawronowicz and W. M. Lewis, Evaluation of the Striped Bass as a Pond-Reared Food Fish, Prog. Fish-Cult., vol. 41, pp. 138-139, 1979.

24. J. W. Meldrim and J. J. Gift, Temperature Preference, Avoidance and Shock Experiments with Estuarine Fishes, Ichthyological Associates Bull. 7, Middletown, Delaware, 1971.

PB82-228222

TILAPIA CULTURE IN HEATED EFFLUENTS: ECONOMIC ASPECTS

Robert G. Nelson, Leslie L. Behrends, Edward L. Waddell, Jr., and David W. Burch
Tennessee Valley Authority
Muscle Shoals, Alabama, U.S.A.

ABSTRACT

The Tennessee Valley Authority (TVA) has operated a facility for maintaining tilapia during the winter months for the past two years. The facility is located adjacent to the Browns Ferry Nuclear Plant in north Alabama and consists of six raceways supplied with a total of 1,135 ℓ/min (300 gal/min) of condenser cooling water (CCW) with an average ΔT equal to 14.4° C (26° F). The facility cost about $57,000 to build, including $18,500 for retrofitting an emergency backup system. Monosex hybrid tilapia fingerlings enter the facility weighing 2 to 3 g and are available for stocking at 20 g in ponds after the last frost in April. The existing facility can accommodate 90,000 fingerlings under these conditions but has the capacity to be enlarged to twice the output at only 22 percent additional fixed cost. Internal rate of return on the existing facility in a commercial operation would be about 5 percent; if doubled in size, it would exceed 35 percent.

1. INTRODUCTION

Tilapia culture in temperate climates is limited by the short growing season and lethally low water temperatures in the winter. TVA has long believed that abundant amounts of low-grade waste heat from steam electric generating plants can improve the potential for aquaculture in the Tennessee Valley by removing these constraints. The purpose of this project has been to demonstrate the feasibility of using power plant waste heat to produce tilapia fingerlings (Behrends, et al., 1980) and to make these fingerlings available to farmers in the region for stocking their ponds. A facility was built which uses CCW from TVA's Browns Ferry Nuclear Plant near Athens, Alabama, to overwinter a minimum of 90,000 tilapia fingerlings or enough to stock 8 ha (20 acres) of ponds.

2. DESCRIPTION OF FACILITY

The facility is housed in a double-polyethylene greenhouse measuring 14.6 m by 7.6 m (48 ft by 25 ft). Inside the greenhouse are six raceways, each measuring 3.65 m by 1.2 m by 1.2 m (12 ft by 4 ft by 4 ft). A warmwater delivery system from the power plant supplies CCW at 189 ℓ/min (50 gal/min) to each raceway. The CCW flows directly through the raceways and is discharged into the Tennessee River. More water for blending or emergency supply is available from a 40-m (130 ft) well with a pumping capacity of 227 ℓ/min (60 gal/min). Well water temperature remains near 15.6° C (60° F) year around. Each raceway is supplied with one 1/3-hp aerator.

The facility, as described, was operated during the winter of 1979-80. In February of 1980, a complete shutdown of all three generators at the power plant plus a malfunction in the warning system caused a near-complete kill in the raceways due to lethal low water temperatures. The result was the design and construction of an automatic backup system independent of the alarm system (Waddell, unpublished paper).

The critical factor in a power plant shutdown is the immediate and rapid influx of cold water. To eliminate this problem, a motorized valve on the incoming CCW line was installed. The valve is activated by a thermostat in the first raceway which senses when the water is too cold or too hot and shuts off the CCW. The change in temperature turns on the aerators in each raceway and a high-volume air blower connected to each raceway. The well pump is activated and a gradual exchange of well water begins in the raceways. Finally a propane heater is activated to maintain the greenhouse temperature at 15.6° C (60° F). The backup system operates until it is manually reset. An auxiliary generator provides electricity if power fails.

3. OPERATING PROCEDURE

The overwintering facility was designed to hold up to 2,000 kg (4,409 lb) of fish at the mean maximum CCW temperature occurring in April. This capacity was initially assumed to be equal to 100,000 fingerlings averaging 20 g each. However, different numbers and weights are possible under different conditions of water temperature, flow rate, and fish size.

The fingerlings were assumed to be all-male hybrids produced by crossing female Sarotherodon mossambica with male S. hornorum. Brood stock are allowed to spawn in ponds during the summer and their offspring reach a size of 2 to 3 g by November. Production cost for fingerlings to be overwintered was assumed to be $0.05 each (in 1980 prices). These fingerlings increase their average weight to 20 g by mid-April because of high-quality commercial feed and warm water. About 100,000 fingerlings were stocked in the raceways before the first frost in November; a 10 percent mortality was assumed for the overwintering period.

Two hours of labor were required for feeding and maintenance each day for 200 days. Electricity was used for aeration and lighting. Propane was used only when the emergency backup system was in use. Chemicals for disease treatment and prophylaxis included potassium permanganate, formalin, and terramycin. Harvest and transportation costs included labor for harvesting and for transporting fish to nearby farms. Miscellaneous equipment included nets, buckets, and scales. In the initial analysis there was no charge for CCW.

Fingerlings were to be harvested from the raceways beginning in late April and distributed to fish farms within a 10-county area of north Alabama. The 1980 price of $0.20 each was competitive with delivered prices from other suppliers of tilapia fingerlings in the U.S. Fingerlings were determined to be of sufficient size to reach a marketable food fish size (200 g and above) by the end of a 180-day growing season with good management practices in organically fertilized or fed ponds.

4. INVESTMENT ANALYSIS

Table 1 lists important assumptions used in the analysis. Table 2 lists data on fixed costs and is arranged in the general order in which the items were acquired. The emergency backup equipment accounted for 32 percent of the

capital cost. Table 3 lists variable costs for the first year of operation. Prices were inflated by different factors for different items to give each a short-term (first year) inflation rate and a long-term equivalent rate (see table 1 for inflation rates). Table 4 lists the income statement for each year of the project. At the end of the 10-year period, it was assumed that each of the remaining capital items was sold for its estimated market value at that time (see "end value" in table 4). Internal rate of return (IRR) for the project under these assumptions was projected to be 5 percent. This means that if the owner's cost of capital is less than 5 percent, he will recoup all of his costs from this operation and still make a profit.

While a 5 percent IRR is not an attractive investment during times of high inflation, it must be remembered that the facility as described was designed to demonstrate bio-engineering criteria and to supply a limited number of test farms with tilapia. With relatively minor modifications in design, the facility could achieve a dramatic improvement in profitability. The most obvious of the modifications possible is to increase the capacity of the facility to take advantage of economies of scale. Simply doubling the number of raceways to overwinter 180,000 fingerlings causes the IRR to jump to 35 percent. The reason is that doubling the capacity to twelve raceways only increases capital costs by 22 percent. Cash flow becomes positive in all years, starting at about $2,000 in 1981 and rising to $11,000 by 1990.

There are two cautions. First, it is unrealistic to increase facility size beyond market potential. The infrastructure of growout ponds, processing facilities, and market outlets cannot be expected to expand as a simple response to increased fingerling supply. The industry, however, cannot develop at all without a reliable fingerling supply. Second, it is almost certain that highly profitable enterprises using waste heat from power plants will eventually be charged for the use of this resource. How high the charge is depends on the cost of gaining access to the waste heat (e.g., land and tie-in costs) and the cost of distributing it (e.g., pumping cost). These costs may vary widely from plant to plant and will probably determine the economic feasibility of enterprises using waste heat. At our hypothetical 12-raceway facility, a waste heat charge of $3,000 per year (in 1980 prices, escalated at 2 percent in the first year and 6.5 percent long term) would reduce the IRR to 20 percent.

CONCLUSION

The tilapia overwintering facility at TVA's Browns Ferry Nuclear Plant has demonstrated the bio-engineering feasibility of overwintering considerable numbers of tilapia fingerlings in CCW having an average increase in temperature above ambient of 14.4° C (26° F). Poor reliability of supply of CCW has made necessary more investment in emergency backup equipment to reduce risk of a total loss of stock.

While the existing facility has been used satisfactorily to accomplish the original objectives, it would not provide an adequate return on investment if it were a commercial operation. However, the investment analysis is extremely sensitive to changes in scale and operation. Thus the concept and design warrant further consideration of commercial potential.

REFERENCES

1. Behrends, L. L., J. B. Kingsley, J. J. Maddox, R. S. Pile, J. C. Roetheli, and E. L. Waddell, Jr., Intensive Production of Tilapia Fingerlings in Thermal Effluents, Research Workshop, Summary of Papers, Catfish Farmers of America, p. 42, 1980.

2. Waddell, E. L., Jr., Tilapia Culture in Heated Effluents: Facility Design, Operation, and Evaluation, Unpublished paper.

Table 1

MAJOR ASSUMPTIONS USED IN ANALYSIS OF TILAPIA OVERWINTERING FACILITY

Year built	1980
First year of operation	1981
Length of analysis period	10 years
Downpayment	20%
Long-term borrowing rate	12.5%
Short-term borrowing rate	14%
Years interest paid on loan before operational	0.5
Investment tax credit rate	10%
Method of depreciation	Straight line
Overhead costs	3% of gross revenues
Tax rate schedule used	Corporate
Property tax rate	0.6% of book value
Insurance rate	1.5% of book value

Inflation rates:	Long-Term (%)	First Year (%)
Materials and equipment	7.5	12.0
Wages and salaries	7.5	12.0
Energy prices	11.0	25.0
Revenues	7.5	12.0

Table 2

CONSTRUCTION COSTS FOR TILAPIA OVERWINTERING FACILITY

Item	Purchase Price (in 1980)
Site preparation	10,766
Greenhouse	2,788
Raceways	4,500
Well and pump	1,800
Pressure tank	280
Piping - CCW	2,895
Piping - well	866
Piping - discharge	3,786
Aerators	660
Service main	60
Electrical materials and labor	5,797
Engineering services (initial)	2,980
Construction overhead (initial)	1,209
Heater	350
Generator	5,550
Transfer switch	1,900
Disconnect	138
Air blower	1,225
Starter	294
Electrical equipment	425
Motorized valve	1,000
Blower fittings	542
Thermostat	154
Piping - propane	300
Solenoid	110
Electrical materials	1,654
Labor (installation)	2,635
Engineering services (backup)	1,465
Construction overhead (backup)	710
Total	56,839

Note: Most items include installation except for some pipefitting and electrical work which is included under "Labor (installation)."

Table 3

VARIABLE COSTS FOR TILAPIA OVERWINTERING FACILITY

Item	Units	Cost/Unit (1980 Prices)	Number
3-g fingerlings	each	$ 0.05	100,000
Feed	ton	400.00	5.4
Labor	hours	4.50	400
Electricity	month	10.00	10
Propane	month	20.00	6
Chemicals	misc	200.00	1
Harvest and transportation	delivery	50.00	18
Miscellaneous equipment	misc	200.00	1

Table 4

INCOME STATEMENT BY YEAR FOR TILAPIA OVERWINTERING FACILITY

	1981	1982	1983	1984	1985	1986	1987	1988	1989	1990
Sales	$20,160	$21,941	$23,683	$25,439	$27,230	$29,072	$30,972	$32,940	$34,980	$37,098
Cost and Expenses	27,620	25,279	26,064	26,935	27,660	28,369	28,836	29,756	30,409	31,043
Fingerlings	5,600	6,095	6,579	7,066	7,564	8,075	8,603	9,150	9,717	10,305
Feed	2,419	2,633	2,842	3,053	3,268	3,489	3,717	3,953	4,198	4,452
Labor	2,016	2,194	2,368	2,544	2,723	2,907	3,097	3,294	3,498	3,710
Electricity	125	143	159	176	193	210	227	246	264	284
Propane	150	171	191	211	231	252	273	295	317	341
Chemicals	224	244	263	283	303	323	344	366	389	412
Harvest and Transp	1,008	1,097	1,184	1,272	1,362	1,454	1,549	1,647	1,749	1,855
Miscellaneous Equipment	224	244	263	283	303	323	344	366	389	412
Repair and Maintenance	1,359	1,479	1,596	1,714	1,835	1,959	2,087	2,220	2,357	2,500
Insurance	822	775	727	686	638	595	562	522	485	461
Property Taxes	329	310	291	274	255	238	225	209	194	184
Depreciation	3,517	3,517	3,517	3,551	3,551	3,551	3,319	3,484	3,484	3,484
Interest on Op. Capital	340	367	394	421	449	477	507	538	570	603
Interest on Investment	8,881	5,352	4,979	4,637	4,169	3,642	3,050	2,477	1,747	925
Overhead	605	658	711	763	817	872	929	988	1,049	1,113
Net Income Before Tax	-7,460	-3,338	-2,381	-1,496	-430	703	2,136	3,184	4,571	6,055
Loss Carryover	0	0	0	0	0	-703	-2,136	-3,184	-4,571	-3,075
Federal Income Tax	0	0	0	0	0	0	0	0	0	507
Net Income After Tax	-7,460	-3,338	-2,381	-1,496	-430	0	0	0	0	2,474
Cash Flow	-3,401	-2,808	-2,225	-1,845	-1,091	-484	388	702	1,480	1,636
End Value		30,725								
Internal Rate of Return		5%								

Note: Some figures may not be exact due to rounding errors.

PB82-228230

FISHERIES AND THE DESIGN OF ELECTRIC POWER PLANTS: THE LAKE ERIE EXPERIENCE

Jeffrey M. Reutter, Ph.D.
Charles E. Herdendorf, Ph.D.
Center For Lake Erie Area Research
The Ohio State University
484 West 12th Avenue
Columbus, Ohio 43210, U.S.A.

ABSTRACT

Estimates of annual fish impingement and entrainment at three power plants on the south shore of the Western Basin of Lake Erie have been performed by Ohio State University's Center for Lake Erie Area Research. The Davis-Besse Nuclear Power Plant produces almost 50% more power than the Acme and Bay Shore Power Plants combined, but it impinges less than 0.1% of the fish and entrains less than 1% of the ichthyoplankton the older fossil-fuel plants do. All three plants are in unfavorable locations, as they are situated in areas of high fish densities. However, Davis-Besse has a closed cycle cooling system, off-shore intake, bottom intake, and closed intake canal. All these components appear to contribute to low levels of entrainment and impingement at this facility.

1. INTRODUCTION

Lake Erie is the smallest of the Laurentian Great Lakes, but with the major urban centers of Detroit, Toledo, Cleveland, Erie, and Buffalo dotting its shoreline, more people live around it and utilize its water than any of the others. To service this large population, Lake Erie is surrounded by 18 power plants, 14 of which operate with once-through cooling systems without cooling towers, and many municipal water intakes. These power plants utilize large quantities of water for cooling purposes. The Monroe, Michigan Power Plant, the largest, uses over 1,300,000 gpm, and the eight plants servicing the Cleveland area require over 6,000,000 gpm [1]. The Lake Erie Basin is also a center of industry with over 450 industrial intakes and discharges in the fifteen counties of northeastern Ohio [1].

Lake Erie is also the most biologically productive of the Great Lakes, producing more fish for human consumption each year than are produced from the other four Great Lakes combined. The resurgence of the walleye (Stizostedion v. vitreum) population since 1975 has prompted a 6-fold increase in the charter fishing fleet with approximately 800,000 Ohio anglers fishing Lake Erie and creating a multimillion dollar recreational industry.

This multiplicity of demands upon the resources of the lake is expected to increase by the year 2000 when water shortages are projected for many regions of the country. It is imperative that adverse environmental impacts from the many intakes and discharges be minimized. At the same time, the continued

growth of the area is largely dependent upon a good supply of low-cost power. Therefore, regulations pertaining to the design and siting of water intakes and discharges must be supported with information showing their value and effectiveness. This paper will show the value of cooling water intake and discharge design and siting criteria on Lake Erie, by evaluating entrainment and impingement at three power plants with different intake and cooling system designs located in the Western Basin of the lake. The plants are operated by the Toledo Edison Company. Acme and Bay Shore are coal-fired with once-through cooling systems and intakes on the estuarine portion of the Maumee River (Fig. 1). Davis-Besse is a new nuclear plant with a closed cooling system located on the southwest shore of the lake at Locust Point (Table 1). All data from these plants were collected by The Ohio State University's Center for Lake Erie Area Research.

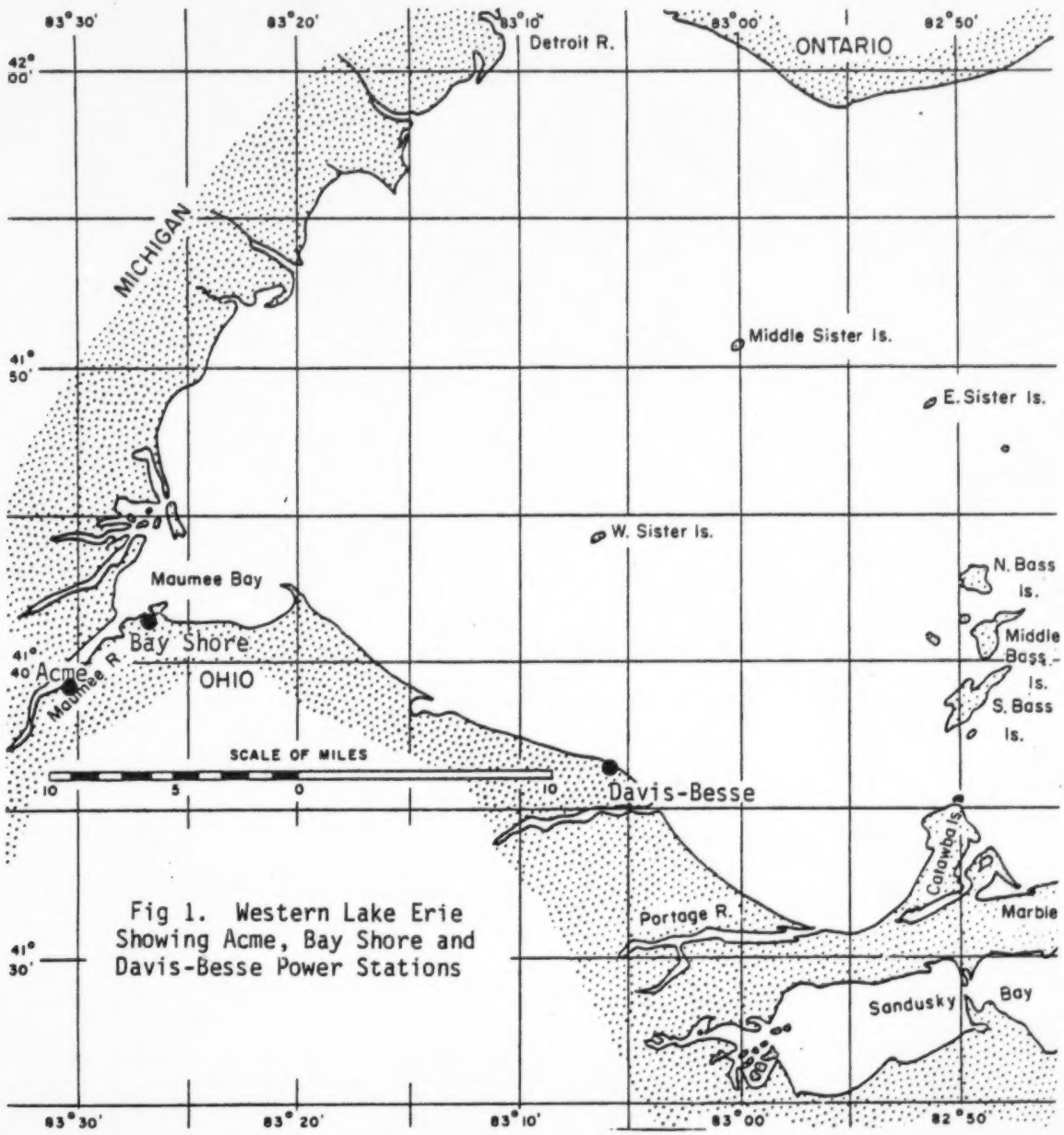

Fig 1. Western Lake Erie Showing Acme, Bay Shore and Davis-Besse Power Stations

TABLE 1. Operating Characteristics of the Power Stations.

PLANT	TYPE	COOLING SYSTEM	PUMPING RATE (GPM)		POWER PRODUCTION (MWe/hr)	
			MAX	MEAN	MAX RATING	MEAN
Acme	Fossil-fuel	Once-through	272,000	172,000	322	104*
Bay Shore	Fossil-fuel	Once-through	518,000	453,000	660	511*
Davis-Besse (Unit I)	Nuclear	Recycled, cooling tower	42,000	21,000	906	872**

*Mean for period 1971-1975

**Projected mean after plant is fully operational

2. PLANT DESCRIPTIONS

2.1. Acme Power Plant

The Acme Power Plant is located in the city of Toledo, Ohio at approximately 41°39'00" N latitude and 83°31'00" W longitude, 3.7 miles upstream from the mouth of the Maumee River (Fig. 1). This plant has five steam electric units with a total rated capacity of 322 megawatts (MW_e). At maximum capacity, 322 MW_e, the plant utilizes cooling water at a rate of 272,000 gpm with an associated heat rise of 15.3°F above ambient. However, this is a peaking plant where the normal load is less than 50 MW_e 40% of the time, less than 100 MW_e 61% of the time, and more than 250 MW_e only 1% of the time. From 1971-1975, the average output was 104.3 MW_e, with a mean temperature rise across the condensers of 9.4°F.

Cooling water for this plant is obtained from the Maumee River. Cooling water enters through a 270-foot inlet canal, traverses the condensers, and is discharged back to the Maumee River through a 760-foot discharge canal to a point approximately 657 feet downriver of the intake. Cooling water traverses a trash rack and one of 6 banks of traveling screens (¼-inch bar mesh) before entering the condensers. Material collected on the traveling screens is washed into a sluiceway and transported to the discharge canal.

2.2. Bay Shore Power Plant

The Bay Shore Power Plant is located on the southern shore of Maumee Bay at approximately 41°41'00" N latitude and 83°26'00" W longitude, near the mouth of the Maumee River (Fig. 1). This is a base load plant with a net summer capacity of 623 megawatts (MW_e) and net winter capacity of 636 MW_e provided by four coal-fired, steam electric units. At a net capacity of 623 MW_e, this plant utilizes 518,000 gpm of water for once-through cooling at a calculated temperature rise of 9.6°F above ambient. Cooling water for the Bay Shore Power Plant is obtained from the Maumee River and after traversing the condensers, is discharged to Maumee Bay. Cooling water enters through a 3,000-foot inlet canal and discharges through a short canal.

The 3,000-foot long intake canal is 250 feet wide and varies in depth from 15 to 20 feet, depending on silt accumulation and dredging frequency. The cooling water traverses a trash rack and one of nine 1/4 or 3/8-inch mesh traveling screens before entering the condenser. Material collected on the traveling screens is washed into a sluiceway and transported to the discharge canal.

2.3. Davis-Besse Nuclear Power Plant

The Davis-Besse Nuclear Power Station is located in Ottawa County, Ohio, at Locust Point on the southwest shore of Lake Erie, about 21 miles east of Toledo. Unit 1 has a net electrical capacity of 906 MW_e and a closed cycle cooling system which dissipates heat to the atmosphere by means of a natural-draft cooling tower, 493 feet high and 415 feet in diameter at its base. Make-up water for cooling purposes is drawn from Lake Erie from a submerged intake crib 3,000 feet offshore through a buried eight-foot diameter conduit to a closed, but uncovered, intake canal (Fig. 2). The canal is approximately 2,950 feet long and terminates at the trash racks of the intake structure. Water is drawn through the intake crib and conduit by gravity. Design capacity for Unit 1 is 42,000 gpm with a resultant approach velocity through the crib ports of 0.25 ft/sec. Cooling tower blowdown is discharged at a point approximately 1,200 feet offshore through a six-foot diameter buried conduit which terminates in a high velocity nozzle to promote rapid mixing. The maximum allowable ΔT is $20^{\circ}F$.

3. METHODS

3.1. Impingement

Acme and Bay Shor[illegible] Impinged fish were collected during a 24-hour period once every seven day[illegible]om September 15, 1976 (September 1, 1976 for Acme) to March 16, 1977 and f[illegible] June 16 to September 15, 1977, and once every four days from March 16 to June 16, 1977. Each 24-hour collection was divided into a 12-hour "night" and a 12-hour "day" collection. Fish were collected by placing a basket (1/4 inch bar mesh) in the sluiceway leading from the traveling screens. This basket was monitored and emptied when full. The percentage of time that the basket was out (being emptied) while the screens were running was recorded. Estimates of the total number of fish impinged were adjusted accordingly. The fish so collected during each 12-hour sampling period were sorted by species and then into size classes or "strata" within each species. This was done to reduce the coefficient of variation of the weights of each species or size class of fish. Based on the coefficient of variation within each size class, the number of fish which had to be weighed and measured (standard length) individually to estimate the mean weight of the fish within that size class to within 10% of the true mean (95% confidence) was determined. The total weight of all fish impinged was determined by actual field measurement. The total weight of each species or size class divided by the mean weight provided the estimate of the number of fish within that species.

This method provided a good estimate of fish impingement on sampling days. These results were converted to a concentration (number of fish/100 cubic meters of cooling water) to estimate impingement on non-sampling days. The mean of the daily concentrations before and after a non-sampling day was multiplied by the flow through the plant on the non-sampling day to estimate impingement on that day.

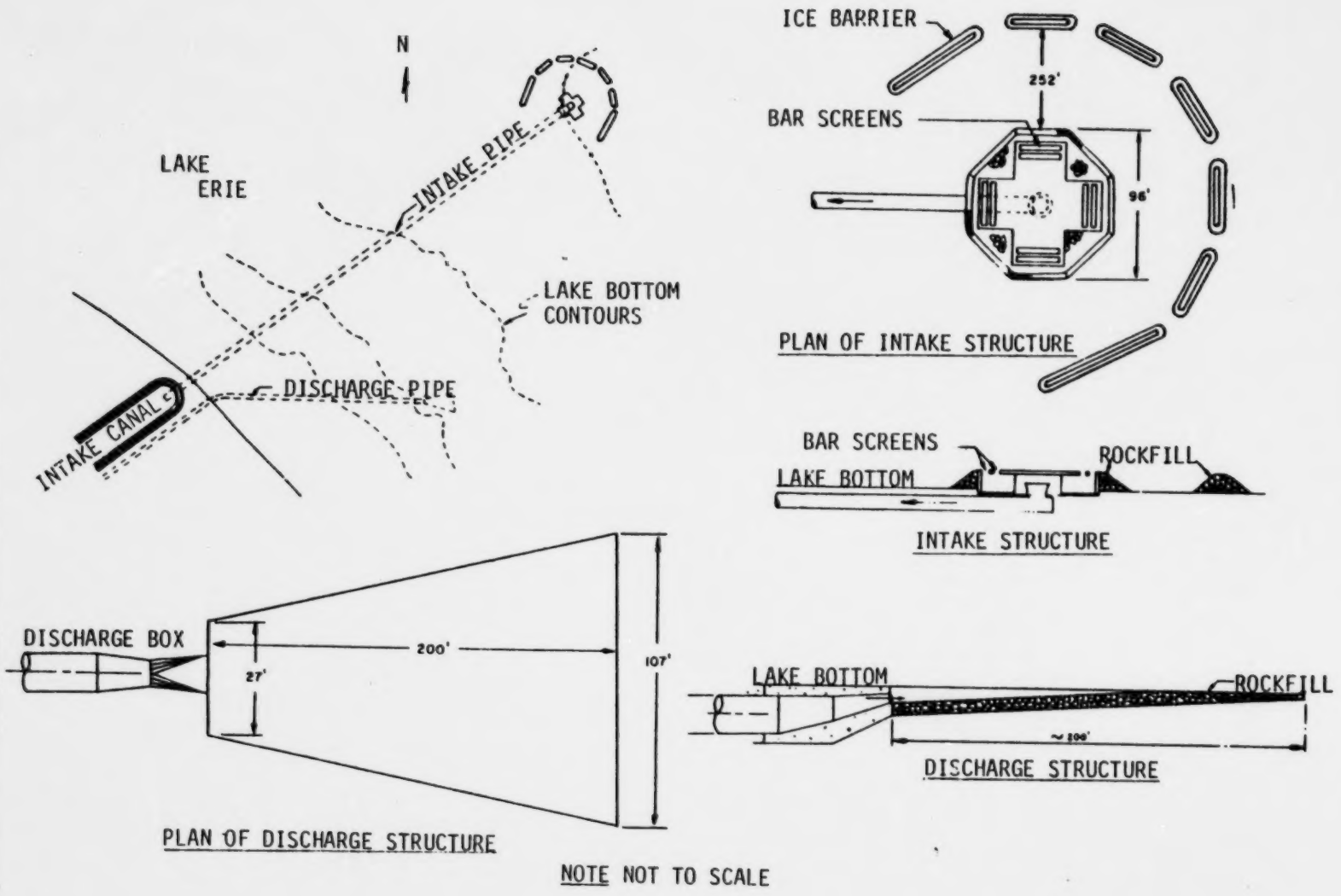

Fig. 2. Intake and Discharge Configuration at the Davis-Besse Nuclear Power Plant.

Davis-Besse. Between January 1 and December 31, 1978 the traveling screens at the Davis-Besse Nuclear Power Station were operated 221 times, while between January 1 and December 31, 1979 the screens were operated 272 times. The date, time, and duration of each screen operation were recorded, even when the impinged fish were not collected. Collections of impinged fish were made on 144 of the 221 screen operations during 1978 and on 134 of the 272 screen operations in 1979 by placing a screen having the same mesh size as the traveling screens (⅜-inch bar mesh) in the sluiceway through which the backwashed material passed. In addition to the information pertinent to traveling screen operation, the total number and total weight of each species and the length and weight of each individual fish were also recorded.

Since the time and duration of every screen operation was known, it was possible to determine the number of hours represented by each collection. From this a rate, fish impinged/hour, was developed and used to estimate impingement on days when samples were not collected.

3.2. Entrainment

Acme and Bay Shore. Two submersible pumps (Kenco model no. 139) were placed in the intake canal in front of the trash racks (one meter below the surface and one meter above the bottom) and operated continuously for a 24-hour period once every seven days from September 1 to September 15, 1976 and June 16 to September 1, 1977 and once every four days from March 16 to June 16, 1977. Each 24-hour period was divided into a 12-hour "night" and a 12-hour "day" collection. The effluent from each pump emptied into a plankton net (50 cm diameter, 0.571 mm mesh) to capture ichthyoplankton. Larvae were identified and categorized by developmental stage (pro-larva, early post-larva, and late post-larva). The ichthyoplankton concentration per unit volume of water was determined by dividing the number of each species and each developmental stage in each collection by the volume of water pumped through the net during that 12-hour collection. The flow rate of each pump was recalculated on each sampling day. The mean of surface and bottom ichthyoplankton concentrations from each period was multiplied by the total flow through the plant during that 12-hour period to obtain the number of larvae and eggs entrained with the cooling water.

The above method provided an estimate of entrainment on sampling days. Mean ichthyoplankton concentrations from several sampling days were averaged and used to estimate entrainment losses on non-sampling days based on the flow through the plant on that day. Variability in these estimates, as evidenced by the confidence intervals, is due to variability in the ichthyoplankton concentrations between sampling periods.

Davis-Besse. Ichthyoplankton entrainment at the Davis-Besse Nuclear Power Plant was computed by multiplying the ichthyoplankton concentration observed at the intake by the intake volume. Ichthyoplankton densities were determined at approximately 10-day intervals from April - August of 1978 and 1979 from four 3-minute, oblique (bottom to surface) tows at 3-4 knots made at night on each date with a 0.75 meter diameter heavy-duty oceanographic plankton net (No. 00, 0.75 mm mesh) equipped with a calibrated General Oceanics flowmeter.

From the above estimates it was possible to determine an approximate period of occurrence for each species and a mean density during that period. For example, during 1978 walleye were not found on April 30 or on June 7 or later. They were present in samples from May 11 and May 21. Therefore, the

period of occurrence was estimated to have been from May 6 (the midpoint between April 30 and May 11) to May 30 (the midpoint between May 21 and June 7). The mean density of walleye during this period was estimated to have been 41.6/100 m^3, computed from the concentration of 79.2/100 m^3 observed on May 11 and the concentration of 4.0/100 m^3 observed on May 21. It was this concentration, 41.6/100 m^3, which was multiplied by the volume of water drawn through the plant from May 6 to May 30.

4. RESULTS

4.1. Impingement

It is estimated that between September 15, 1976 (September 1, 1976 for Acme) and September 15, 1977, 5,729,064 fish of 43 species were impinged at the Acme Power Plant and 17,810,633 fish of 52 species were impinged at Bay Shore (Tables 2 and 3). These estimates do not include fish runs which occurred on seven occasions at Acme and one occasion at Bay Shore. The seven runs at Acme lasted a total of 44.5 hours and impingement an estimated 6,024,060 fish. The run at Bay Shore was less than 12 hours in duration and yielded 506,112 fish. At both plants gizzard shad, emerald shiners and alewives constituted over 99.8% of the fish impinged during runs and over 90% of the fish impinged at all times. At Acme, only three species, gizzard shad, emerald shiner and freshwater drum, represented more than 0.5% of the total number impinged. All fish runs and over 75% of the impingement at Bay Shore and 90% of the impingement at Acme occurred between mid-October and mid-February (Fig. 3).

A total of 6,607 fish of 20 species were impinged at Davis-Besse during 1978, while 4,385 fish of 19 species were impinged during 1979 (Tables 2 and 3). Davis-Besse began commercial operation in August 1977. The plant has not

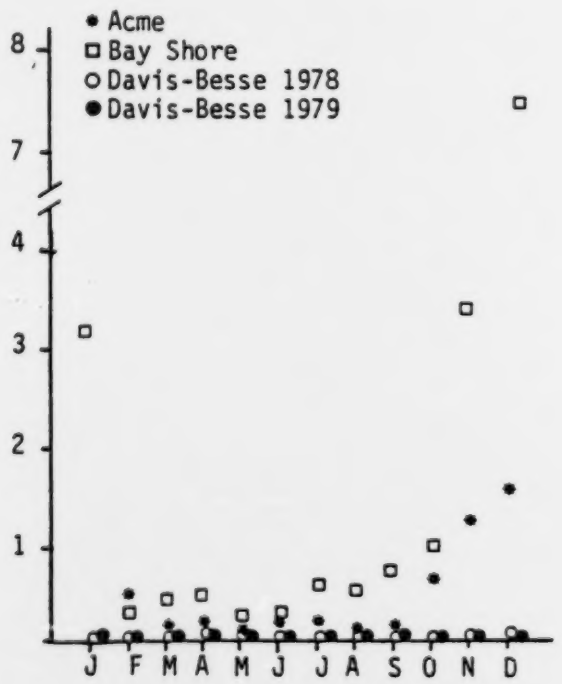

Fig. 3. Millions of Fish Impinged Monthly

TABLE 2. Common and Scientific Names of Fish Impinged and Entrained at the Acme, Bay Shore and Davis-Besse Power Plants.

COMMON NAME	SCIENTIFIC NAME	Acme		Bay Shore		Davis-Besse	
		Ent.	Imp.	Ent.	Imp.	Ent.	Imp.
Alewife	*Alosa pseudoharengus*		*		*		*
Bigmouth Buffalo	*Ictiobus cyprinellus*				*		
Black Bullhead	*Ictalurus melas*		*		*		*
Black Crappie	*Pomoxis nigromaculatus*		*		*		*
Blackside Darter	*Percina maculata*						*
Bluegill	*Lepomis macrochirus*		*	*	*		*
Bluntnose Minnow	*Pimephales notatus*		*		*		*
Bowfin	*Amia calva*				*		
Brindled Madtom	*Noturus miurus*		*		*		
Brook Silversides	*Labidesthes sicculus*				*		
Brown Bullhead	*Ictalurus nebulosus*		*		*		*
Carp	*Cyprinus carpio*	*	*	*	*	*	*
Channel Catfish	*Ictalurus punctatus*	*	*	*	*		*
Channel Darter[a]	*Percina copelandi*				*		
Chinook Salmon	*Oncorhynchus tschawytscha*				*		
Coho Salmon	*O. kisutch*		*		*		
Creek Chub	*Semotilus atromaculatus*		*				
Emerald Shiner	*Notropis atherinoides*		*	*	*	*	*
Fathead Minnow	*Pimephales promelas*		*		*		
Freshwater Drum	*Aplodinotus grunniens*	*	*	*	*	*	*
Gizzard Shad	*Dorosoma cepedianum*	*	*	*	*	*	*
Golden Shiner	*Notemigonus crysoleucas*		*		*		
Goldfish	*Carassius auratus*		*		*		*
Green Sunfish	*Lepomis cyanellus*		*		*		*
Johnny Darter	*Etheostoma nigrum*				*		
Logperch	*Percina caprodes*	*	*	*	*	*	*
Long-nosed Gar	*Lepisosteus osseus*		*		*		
Mooneye[a]	*Hiodon tergisus*		*		*		
Mottled Sculpin	*Cottus bairdi*				*		
Northern Hog Sucker	*Hypentelium nigricans*				*		
Northern Pike	*Esox lucius*		*		*		
Orangespotted Sunfish	*Lepomis humilis*		*		*		
Pumpkinseed	*L. gibbosus*		*		*		*
Quillback	*Carpiodes cyprinus*		*		*		
Rainbow Smelt	*Osmerus mordax*		*	*	*	*	*
Rock Bass	*Ambloplites rupestris*				*		
Sauger	*Stizostedion canadense*		*		*		
Sea Lamprey	*Petromyzon marinus*		*		*		
Shorthead Redhorse	*Moxostoma macrolepidotum*		*		*		
Silver Chub[a]	*Hybopsis storeriana*		*		*		
Silver Lamprey[a]	*Ichthyomyzon unicuspis*		*		*		
Smallmouth Bass	*Micropterus dolomieui*				*		
Spotfin Shiner	*Notropis spilopterus*		*		*		
Spottail Shiner	*N. hudsonius*	*	*	*	*	*	*

TABLE 2 (continued).

COMMON NAME	SCIENTIFIC NAME	Acme		Bay Shore		Davis-Besse	
		Ent.	Imp.	Ent.	Imp.	Ent.	Imp.
Stonecat	*Noturus flavus*		*		*		*
Tadpole Madtom	*N. gyrinus*		*		*		
Threespine Stickleback	*Gasterosteus aculeatus*		*		*		
Troutperch	*Percopsis omiscomaycus*		*	*	*		*
Walleye	*Stizostedion v. vitreum*	*	*	*	*	*	
White Bass	*Morone chrysops*	*	*	*	*	*	*
White Crappie	*Pomoxis annularis*		*		*		*
White Perch	*Morone americana*						*
White Sucker	*Catostomus commersoni*	*	*	*	*	*	
Yellow Bullhead	*Ictalurus natalis*		*		*		
Yellow Perch	*Perca flavescens*	*	*	*	*	*	*

[a]On Ohio's list of endangered wild animals.

operated continuously since that time, but circulating pumps have been operated over 90% of the time, and, as of April 30, 1981, no fish runs were observed. Goldfish was the dominant species impinged, and although numbers were very low, yellow perch constituted a significant portion of the number impinged. As with Acme and Bay Shore, impingement was primarily a cold water phenomenon and young-of-the-year was the dominant age class.

4.2 Entrainment

It is estimated that during the study, 79,492,563 larval fish representing 15 taxa and 178,048,309 fish eggs were entrained at Acme, while 284,717,618 larval fish representing 19 taxa and 426,150,109 fish eggs were entrained at Bay Shore (Tables 2 and 4). At Davis-Besse over a similar period of time, it is estimated that 6,311,371 larvae and 44,278 eggs were entrained during 1978 and 20,620,799 larvae and 101,405 eggs were entrained during 1979. Gizzard shad was the dominant species entrained at all three plants.

5. DISCUSSION

Although the Davis-Besse Nuclear Power Plant produces more power than the Acme and Bay Shore power plants combined. Davis-Besse impinges only 0.05% of the number impinged at Acme and 0.03% of the number impinged at Bay Shore; it entrains only 16.9% of the number of larval fishes entrained at Acme and only 4.7% of the number entrained at Bay Shore; and it entrains only 0.04% of the number of eggs entrained at Acme and only 0.02% of the number entrained at Bay Shore (Fig. 4). Obviously the fact that Davis-Besse has a cooling tower and is not a once-through plant as Acme and Bay Shore are accounts for some of this reduction in impingement and a great majority of the reduction in the entrainment, but the cooling tower reduces the cooling water requirements to 4.6% of Bay Shore's and 12.2% of Acme's, and the impingement losses and total ichthyoplankton (larvae and eggs) losses at Davis-Besse are much less than

TABLE 3. Annual Fish Impingement at the Acme, Bay Shore and Davis-Besse Power Plants in Western Lake Erie.

SPECIES	POWER PLANT	NUMBER IMPINGED	% OF TOTAL	95% CONFIDENCE LOWER	95% CONFIDENCE UPPER
Alewife	Acme	21,412	0.37	15,013	30,539
	Bay Shore	1,375,911	7.73	786,515	2,406,986
	D-B 1978	4	0.06	1	9
	D-B 1979	1	0.02	0	5
Channel Catfish	Acme	3,225	0.06	1,951	5,333
	Bay Shore	20,995	0.12	16,214	27,186
	D-B 1978	3	0.05	1	7
	D-B 1979	0	0.00	0	0.00
Emerald Shiner	Acme	823,791	14.38	554,701	1,223,418
	Bay Shore	3,282,597	18.43	2,147,664	5,017,285
	D-B 1978	991	15.00	636	1,545
	D-B 1979	214	4.88	90	511
Freshwater Drum	Acme	114,152	1.99	90,495	143,994
	Bay Shore	365,779	2.05	271,584	492,697
	D-B 1978	80	1.21	55	114
	D-B 1979	115	2.62	61	218
Gizzard Shad	Acme	4,709,444	82.19	3,306,856	6,706,934
	Bay Shore	11,347,255	63.70	8,698,622	14,802,368
	D-B 1978	391	5.92	201	758
	D-B 1979	162	3.69	95	275
Goldfish	Acme	746	0.01	524	1,061
	Bay Shore	4,471	0.03	3,292	6,073
	D-B 1978	3,299	49.93	2,435	4,468
	D-B 1979	3,449	78.66	2,266	5,248
Rainbow Smelt	Acme	2,644	0.05	1,930	3,624
	Bay Shore	87,374	0.49	62,615	121,923
	D-B 1978	69	1.04	45	107
	D-B 1979	32	0.73	18	55
Spottail Shiner	Acme	15,789	0.28	12,968	19,224
	Bay Shore	212,515	1.19	164,608	274,365
	D-B 1978	15	0.23	9	25
	D-B 1979	9	0.21	5	16
Walleye	Acme	454	0.01	331	623
	Bay Shore	12,187	0.07	9,466	15,690
	D-B 1978	0	0.00	0	0
	D-B 1979	0	0.00	0	0

TABLE 3 (continued).

SPECIES	POWER PLANT	NUMBER IMPINGED	% OF TOTAL	95% CONFIDENCE LOWER	95% CONFIDENCE UPPER
White Bass	Acme	21,549	0.38	17,089	27,174
	Bay Shore	624,078	3.50	467,610	832,902
	D-B 1978	0	0.00	0	0
	D-B 1979	3	0.07	1	12
Yellow Perch	Acme	6,063	0.11	5,153	7,134
	Bay Shore	437,260	2.46	347,626	550,007
	D-B 1978	1,582	23.94	1,082	2,312
	D-B 1979	285	6.50	129	631
Others	Acme	9,795	0.17		
	Bay Shore	40,211	0.23		
	D-B 1978	173	2.62		
	D-B 1979	115	2.62		
TOTAL	Acme	5,729,064	100.00		
	Bay Shore	17,810,633	100.00		
	D-B 1978	6,607	100.00	5,447	8,015
	D-B 1979	4,385	100.00	3,128	6,149

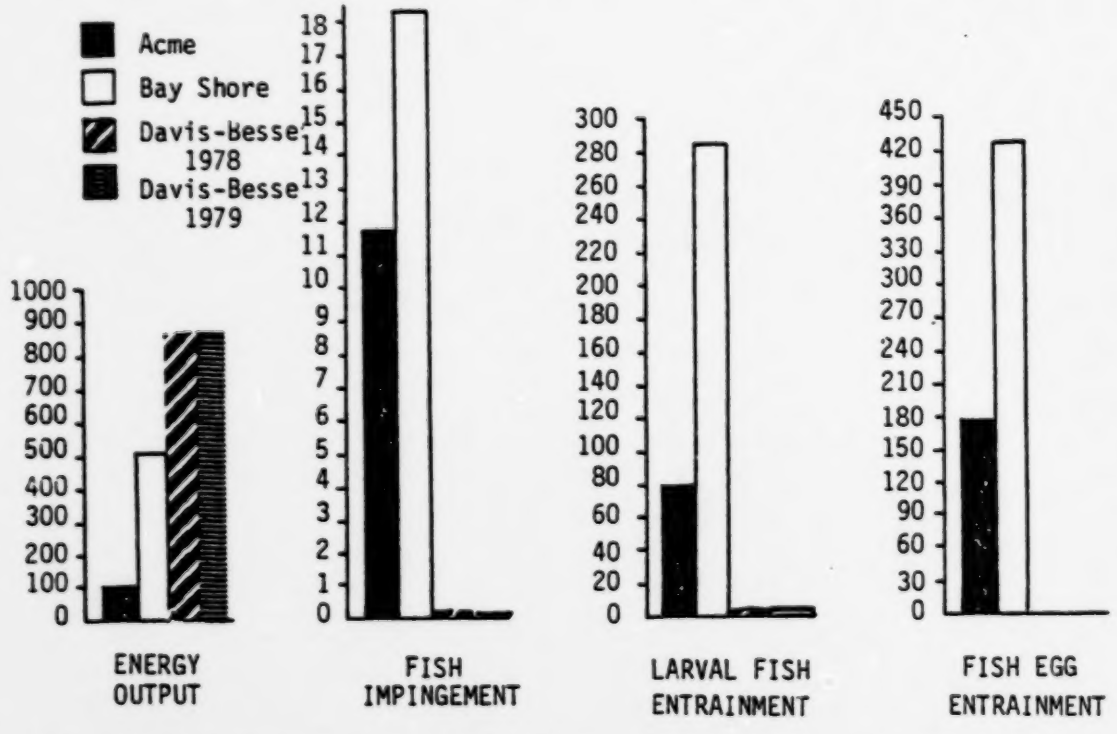

Fig. 4. Megawatts of Power Produced Compared to Millions of Fish Entrained and Impinged.

TABLE 4. Annual Fish Entrainment in Thousands at the Acme, Bay Shore And Davis-Besse Power Plants in Western Lake Erie.

SPECIES	POWER PLANT	NUMBER ENTRAINED	% OF TOTAL	95% CONFIDENCE LOWER	95% CONFIDENCE UPPER
Carp	Acme	1,145	1.44	472	2,774
	Bay Shore	8,252	2.90	4,160	16,368
	D-B 1978	7	0.11	0	27
	D-B 1979	47	0.21	8	86
Channel Catfish	Acme	92	0.12	29	295
	Bay Shore	565.	0.20	165	1,935
	D-B 1978	0	0.00	0	0
	D-B 1979	0	0.00	0	0
Emerald Shiner	Acme	0	0.00	0	0
	Bay Shore	143	0.05	34	595
	D-B 1978	345	5.47	0	1,257
	D-B 1979	6,815	33.06	2,842	10,788
Freshwater Drum	Acme	26,514	33.35	13,382	52,533
	Bay Shore	13,479	4.73	7,373	24,644
	D-B 1978	100	1.58	0	457
	D-B 1979	1,014	4.92	575	1,454
Gizzard Shad	Acme	44,930	56.52	19,516	103,438
	Bay Shore	223,290	78.42	134,750	370,008
	D-B 1978	4,796	76.00	0	13,099
	D-B 1979	10,187	49.41	6,910	13,463
Logperch	Acme	130	0.16	23	738
	Bay Shore	28	0.01	4	173
	D-B 1978	0	0.00	0	0
	D-B 1979	57	0.28	16	98
Rainbow Smelt	Acme	0	0.00	0	0
	Bay Shore	897	0.32	388	2,075
	D-B 1978	95	1.51	0	272
	D-B 1979	763	3.70	471	1,055
Spottail Shiner	Acme	41	0.05	7	247
	Bay Shore	238	0.08	44	1,283
	D-B 1978	16	0.25	0	37
	D-B 1979	38	0.18	0	110
Walleye	Acme	195	0.25	82	462
	Bay Shore	442	0.16	207	943
	D-B 1978	917	14.53	0	11,445
	D-B 1979	42	0.20	22	61
White Bass	Acme	5,778	7.27	2,369	14,365
	Bay Shore	33,108	11.63	13,497	81,216
	D-B 1978	0	0.00	0	0
	D-B 1979	52	0.25	24	79

TABLE 4 (continued).

SPECIES	POWER PLANT	NUMBER ENTRAINED	% OF TOTAL	95% CONFIDENCE LOWER	95% CONFIDENCE UPPER
White Sucker	Acme	33	0.04	12	89
	Bay Shore	674	0.24	249	1,820
	D-B 1978	0	0.00	0	0
	D-B 1979	2	0.01	0	6
Yellow Perch	Acme	14	0.02	3	61
	Bay Shore	2,426	0.85	875	6,728
	D-B 1978	35	0.55	0	91
	D-B 1979	1,595	7.73	1,293	1,897
Others	Acme	621	0.78		
	Bay Shore	1,176	0.41		
	D-B 1978	0	0.00	0	0
	D-B 1979	10	0.05		
TOTAL	Acme	79,493	100.00		
	Bay Shore	284,718	100.00		
	D-B 1978	6,311	100.00		
	D-B 1979	20,622	100.00		
Eggs	Acme	178,048	100.00	53,425	593,375
	Bay Shore	426,150	100.00	239,225	759,133
	D-B 1978	44	100.00	0	185
	D-B 1979	101	100.00	36	167

these figures. Furthermore, adult fish populations near Davis-Besse can be twice that observed at Bay Shore and eight times that observed at Acme [2]. Consequently, the real key to the success of Davis-Besse is in the location and design of the intake.

At Davis-Besse, adult fish densities increased in a shoreward direction, and were only half as great 3,000 feet from shore (where the intake is) as they were 1,500 feet from shore [2]. Consequently, Davis-Besse's off-shore intake is a major advantage over the open shoreline intake canals at Acme and Bay Shore. Furthermore, the fact that these are "open" shoreline canals whereas Davis-Besse's is closed, is also significant, for the open canal causes the many schooling species in Lake Erie (yellow perch, gizzard shad, alewife, emerald shiner) which are following the shoreline to turn and swim into the intakes of the power plants.

The last new design feature of real significance at Davis-Besse is the bottom intake, for bottom ichthyoplankton densities are only approximately half as large as surface densities [2].

In summary, the design features utilized at Davis-Besse, closed cycle cooling system, off-shore intake, closed intake canal, and bottom intake, are effective measures to reduce entrainment and impingement at cooling water intakes in Lake Erie. Siting is also a significant factor in minimizing entrainment and impingement. The authors recommend the Central Basin of the lake for future plant construction because adult fish densities are lower and ichthyoplankton densities along the south shore of Lake Erie decrease very

significantly in an eastward direction [3]. In fact, this reduction is so dramatic that it is the opinion of the authors that in the area east of Cleveland, cooling towers may not be warranted if the plant has an off-shore, bottom intake and a closed intake canal. Furthermore, new plants constructed in this area can anticipate entrainment and impingement levels significantly lower than those of Davis-Besse.

6. CONCLUSIONS

The following power plant design features are very effective at reducing fish entrainment and impingement in Lake Erie: closed cycle cooling system, off-shore intake, bottom intake, and closed intake canal. Due to a significant reduction in fish densities as one leaves the Western Basin and moves eastward, future power plant construction on the south shore of Lake Erie should take place in the area east of Cleveland and no new plants should be constructed anywhere in the Western Basin of the lake. If these suggestions are followed, new plants can be constructed on Lake Erie without harming the valuable and growing fishery.

ACKNOWLEDGEMENTS

The authors wish to express their thanks to Ginger-lyn Summer and Deborah Downey for typing the manuscript, to Cheryl Kimmerline for preparing the figures, and to the entire staff of the Center for Lake Erie Area Research for assisting in sample collection and analysis. We also wish to acknowledge the Toledo Edison Company for funding most of this work and the Ohio Department of Natural Resources and U.S. Fish and Wildlife Service for funding portions of the work on the Davis-Besse Nuclear Power Plant.

REFERENCES

1. M. D. Barnes, J. M. Reutter, C. E. Herdendorf, Lake Erie as an Industrial and Commercial Resource to the Greater Cleveland Area, The Ohio State Univ., CLEAR Tech. Rept. No. 218, Columbus, Ohio, April 1981. 29 p.

2. J. M. Reutter and C. E. Herdendorf, Environmental Impact Appraisal of the Davis-Besse Nuclear Power Station, Unit 1, on the Aquatic Ecology of Lake Erie 1973-1979, The Ohio State Univ., CLEAR Tech. Rept. No. 172, Columbus, Ohio, June 1980. 193 p.

3. J. J. Mizera, Distribution and Entrainment of Larval Fishes in Western and Central Lake Erie, The Ohio State Univ., CLEAR Tech. Rept. No. 215, Columbus, Ohio, February 1981. 225 p.

PB82-228248

ABALONE CULTURE AT A COASTAL ELECTRIC GENERATING STATION

Presented By: J. C. Kelly, N. J. Sevitz and A. Weir, Jr.
Southern California Edison Company
P. O. Box 800
Rosemead, California, 91770, U.S.A.

Presented At: Third Conference on
Waste Heat Management
and Utilization
Eden Rock Hotel
Miami Beach, Florida
May 11 - 13, 1981

Conference Presented By: Department of Mechanical Engineering
University of Miami

Conference Sponsored By: Department of Energy
United States Environmental Protection Agency
Nuclear Regulatory Commission
Electric Power Research Institute
Florida Power and Light Company
School of Continuing Studies
University of Miami

In Cooperation With: American Society of Mechanical Engineers
Miami Section

ABALONE CULTURE AT A COASTAL ELECTRIC GENERATING STATION

J. C. Kelly, N. J. Sevitz and A. Weir, Jr.
Southern California Edison Company
P.O. Box 800
Rosemead, California 91770, U.S.A.

ABSTRACT

The Southern California Edison Company, Research and Development Organization has demonstrated success in several abalone culture projects. These projects are designed to initially produce seed abalone for use in coastal enhancement programs with possible extension into the commercial marketplace with larger sized abalone.

To date one project has successfully reared green abalone (Haliotis fulgens) using thermal effluent water at growth rates exceeding those of animals surveyed in the natural environment. Nearly 9,000 of these animals were used by the California Department of Fish and Game/University of California Sea Grant Coastal Enhancement Program with a few hundred animals given to a Mexican fishing co-operative for experimental transplants in Baja California. Another project was designed to test the feasibility of improving natural resources as a means to mitigate environmental effects through the construction of an artificial reef. The reef was initially planted with tagged kelp (Macrocystis sp) and will be seeded this summer with red abalone (Haliotis rufescens) and pink abalone (Haliotis corrugata), grown at Southern California Edison's Redondo Generating Station.

With all three species, waste heat effluent seawater was employed to accelerate or enhance a part of the hatchery and/or grow out process. Post-larvae, juveniles, and adults have exhibited no indications of unfavorable conditions because of effluent water utilization. Growth curves and culture water temperatures for select species and some life stages are provided in the text. All key culturing was performed by World Research, Ocean Studies Institute [1] and California International Marine Resources [2].

1. INTRODUCTION

The Southern California Edison Company (SCE) has maintained a Thermal Resource Utilization Program in their Research and Development Organization since the early 1970s. This program area has specific projects designed to use waste heat and reject

heat in developing mechanical energy from waste heat engines/turbines as well as enhancing growth rates in crop organisms for aquaculture and agriculture. One of the aquaculture projects is now examining the application of thermal effluent from a coastal generating station to enhance the growth of abalone.

The abalone (Haliotis sp) is a marine mollusk found along the Pacific Coast of North America and is prized as a gourmet seafood item. California Department of Fish and Game records indicate that commercial landings of abalone have decreased while fishing pressure has increased [3]. The declining yield has been attributed to the impact of commercial and sport divers, predation by sea otters, competition from sea urchins, and decrease in available coastal habitats. Its desirability as a seafood and the need to compensate for decreased harvests have targeted the abalone for fisheries management/coastal enhancement work as well as for controlled culture.

SCE has demonstrated through its contractors, World Research and California International Marine Resources, that at least three species of abalone can be cultivated in a laboratory environment and that thermal discharge waters from a once-through ocean cooling system can be used advantageously in support of various life stages of abalone. The three species being cultured are the green abalone (Haliotis fulgens), the pink abalone (Haliotis corrugata) and the red abalone (Haliotis rufescens). These species were selected because of their need in coastal enhancement projects [4] and because of their thermophilic qualities [5] (Figure 1).

2. METHODOLOGY

A small R/D laboratory is situated in the confines of the Redondo Generating Station's facilities. The steam generating station is located on the Southern California coast approximately 16 miles southwest of downtown Los Angeles. Condenser cooling water is drawn in through a capped intake structure located 1200 feet (365 meters) offshore and 30 feet (9 meters) below the surface and is discharged several degrees Celsius above ambient intake waters. The laboratory receives both intake and discharge seawater via individual pump and distribution systems from access openings in the forebays of the plants circulating water system. The delivered seawater is filtered through a high flow-rate sand filter with subsequent filtering down to 5 microns with disposable cartridge filters followed by UV sterilization for the most sensitive early life stages of abalone. Water temperature is regulated via mix valves and experiments are conducted at varying temperatures to determine optimum growth rates for each species and for different life stages of each species.

Broodstock spawning, larval incubation and some of the post-larval rearing utilized acrylic cauldrons, Polyethylene (Nalgene) tanks and small fiberglass round tanks. Round 340 gallon (1300 liter) fiberglass tanks were employed for juvenile rearing while two large rectangular fiberglass tanks served as diatom culture bins and holdings tanks for adult broodstock animals.

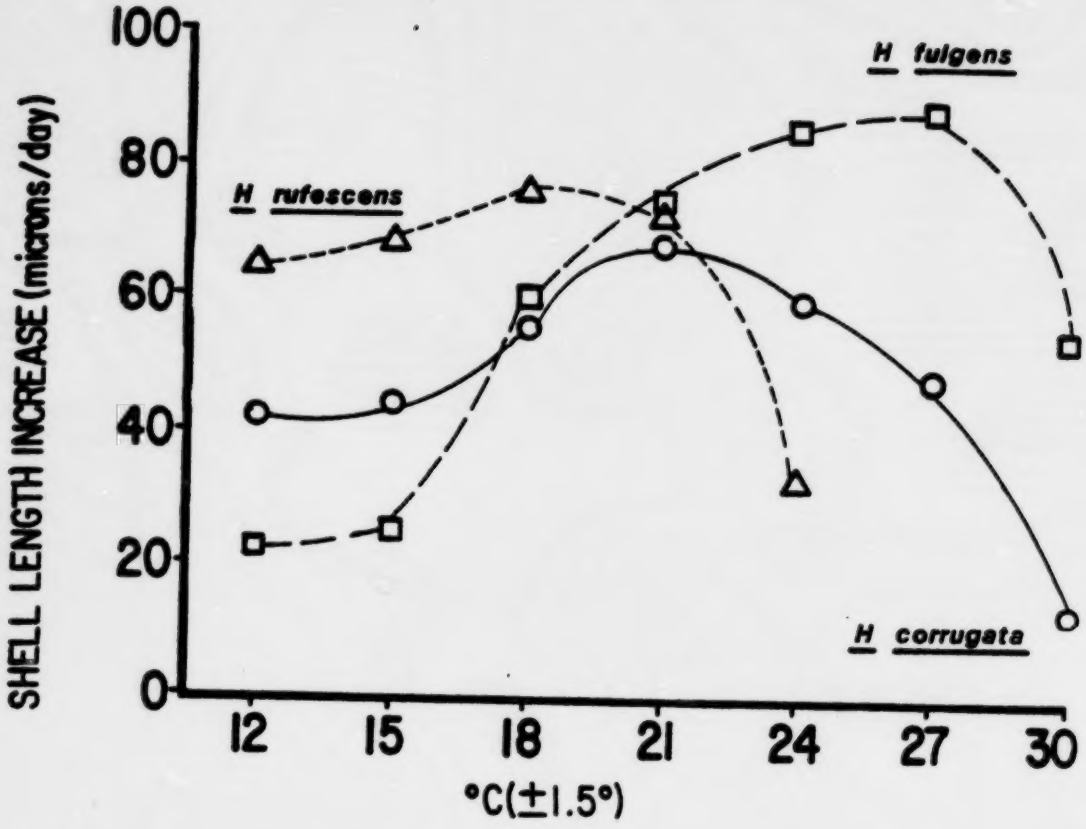

***FIGURE 1** Growth rate of juvenile abalone held for month-long periods at different temperatures. Points are averages for groups of 8 to 15 individuals (Leighton '74)*

Larval and post-larval animals were fed cultured diatoms while juveniles and adults received seaweed (species of Egregia, Macrocystis, Ulva, and Gigartina) collected along the coast. All tanks were housed indoors and either received a natural photoperiod via skylights or artificial photoperiods via natural wavelength lights for experimental work. Each culture tank received its water separately and there were individual drains, hence no seawater was cascaded or shared. Aeration lines with airstones were supplied to each tank and water was continuously exchanged with no recirculation.

3. RESULTS

Broodstock animals were kept in the laboratory throughout the year. All three species of abalone were induced to spawn during all seasons despite the fact that some are naturally refractory during particular seasons. Photoperiod and water temperature appear to be the chief exogenous variables controlling gonadal maturation. Actual spawnings of broodstock animals were induced with hydrogen peroxide [6], hydrogen peroxide and UV-treated seawater, or just UV-treated seawater with good success under all methods. The hydrogen peroxide approach, however, was more controllable and predictable.

Larvae resulting from these spawns were allowed to settle naturally or were induced to settle with GABA (γ - aminobutyric acid) [7]. Again, both methods proved satisfactory, however, the GABA allows more control and predictability in settling and metamorphosis.

Larvae were raised in seawater treated antibiotically with Penicillin G potassium and Streptomycin sulfate. Post-larvae were transferred to large round 340 gallon (1300 liter) tanks. Survivorship from egg to juvenile stages was usually substantially less than the 5 percent often quoted in the literature [8]. Post-larvae were held, effluent water permitting, at species-specific optimal temperatures to achieve good growth rates. Greens (H. fulgens) were held at 20-24°C, pinks (H. corrugata) at 18-22°C, and reds (H. rufuscens) at 16-20°C [5].

The growth of juvenile green abalone (H. fulgens) was assessed experimentally by holding duplicate groups (n = 20) at four temperatures (16°C, 20°C, 24°C and 28°C). The rate of growth was measured over a four-month period and demonstrated a positive correlation between increased temperature and increased growth (Table X). In this experimental regime water flow was not continuous but was changed daily. The 10 liter containers were continuously aerated.

In actual seed production routine the growout water temperature was affected by the availability of heated effluent water resulting in a maintainable temperature range of 18-24°C for green abalone (H. fulgens), 16-22°C for pinks (H. corrugata) and 14-20°C for reds (H. rufescens).

At present, we only have adequate growth data for the green abalone (H. fulgens) as the other two species are more recent additions to the project. The growth data for this species measured over a 20 month period (Figure 2) shows accelerated growth for young juveniles around 5 mm ir size and young adults in the 30 – 40 mm size range. The initial slope, labeled "A" in Figure 2, shows the greatest influence of heated effluent water. The section of the slope labeled "B" in Figure 2 has a decline in growth rate that is attributable to long period of water contamination caused by an offshore dinoflagellate bloom. Intake water carried large quantities of phytoplankton into the filtering system. Algae and associated bacteria films caused minor mortalities (about 320 animals) but had obvious deleterious effects on growth rates.

The last section of the growth curve labeled "C" shows a reduced rate up to 1.5 years and then a retarded growth rate, compared to a naturally occurring population, through the completion of the 20 month observation period.

The attenuated growth of H. fulgens in larger size classes may be attributable to an adult maturation condition. In broodstock conditioning experiments, it was determined [9] that the best conditions for gametogenesis were correlated with the lowest measured somatic growth. Thus, acceleration of overall growth with thermal effluent may decline rapidly as juveniles become capable of gametogenesis. At this time, elevated temper-

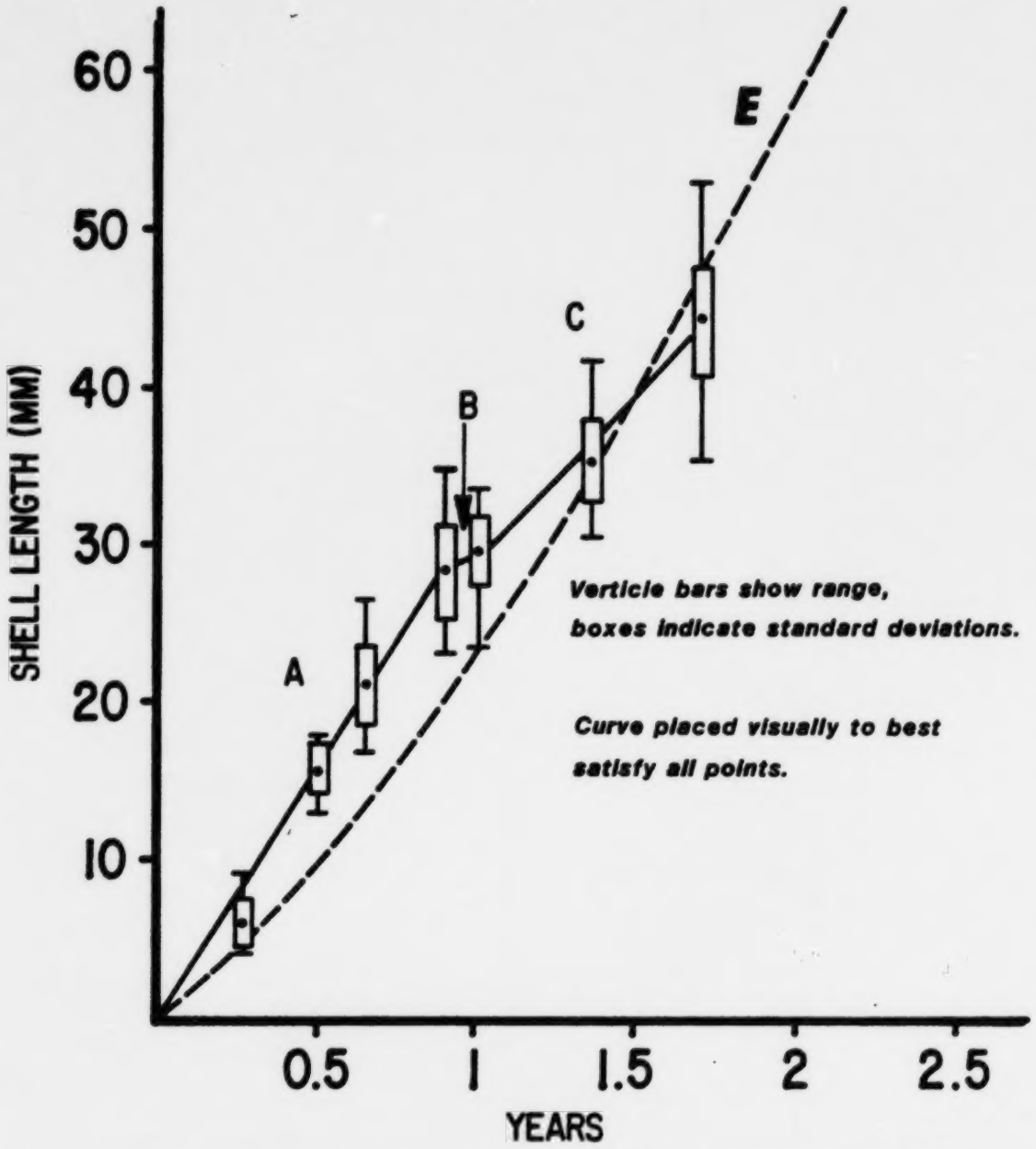

——— Observed growth of juveniles (Apr. 17, '79 spawning) at the SCE Redondo Beach Laboratory.
Segments "A","B" and "C" represent different phases of the growth period as described in the text.

— — — E = Estimates for second year based on field tag-recovery growth (Point Loma shallow water, 12-24° C, 1960-61) (n=26)

FIGURE 2 FIRST YEAR GROWTH IN LABORATORY CULTURED HALIOTIS FULGENS WITH ESTIMATED SECOND YEAR GROWTH BASED ON FIELD OBSERVATIONS (Observations updated Dec. 26, 1980)

atures may inhibit somatic growth and induce gonadal maturation.

The "planting" of young green abalone (H. fulgens) in the Palos Verdes Peninsula area of Southern California has proven very successful. Plants in two different areas in Palos Verdes have resulted in excellent survivorship and continued good growth [10]. Plants of a small number of green abalone (H. fulgens) given to a Mexican fishing co-operative await reportable data; and pink (H. corrugata) and red (H. rufescens) plants on the artificial reef near Camp Pendleton, California are still in preparation.

4. DISCUSSION

The culture of three species of abalone at a coastal electric generating station has had demonstrated success. The advantages of heat afforded by the thermal effluent water of such stations on various life stages of abalone has been shown to be mandatory in a "production" system of abalone. Somatic growth as well as gonadal growth can be accelerated or regulated by control of exposure factors key to broodstock conditioning and opportunistic use of heated seawater. Advances made in the biochemical control of spawning and subsequent settling of larvae have made true production capability more attainable.

The use of a land based growout facility seems to be the only way to achieve the controlled environment necessary for successful accelerated rearing of animals to at least the 40 mm size. Juvenile seed abalone can be planted, in natural or man-made habitats, from at least a 12 mm size, to enhance coastal populations as part of a fisheries management program where accelerated growth is not needed. The chief disadvantage of using heated effluent seawater is that the availability of heat varies seasonally, as coastal ambient waters change temperatures, and daily as the generating station changes its thermal loading (Figure 3). The temperature variability manifests itself in the inability to control production scale culture at optimum growout temperatures and hence temperature ranges must be employed.

The main biological impediment is larval and post-larval attrition. The overall survivorship from fertilized egg to advanced juvenile was 1% or less of estimated spawn figures. Once animals are at least 6 mm their survival seems assured, however, younger stages are not as fortunate. The spread of gametes and larvae in a broadcast breeder, like the abalone, is usually such that heavy attrition can be anticipated, however, any reasonable production system must rely on efficiencies greater than we are presently achieving.

The husbandry of the three species of abalone under investigation is now labor intensive and requires a high degree of technical management to achieve the present level of operation. Although our present abilities in the culture of green and pink abalone is unsurpassed, the need to better understand and standardize routine procedures is necessary to allow skilled personnel the opportunity to tackle obstacles as we continue growout past the 40 mm size range.

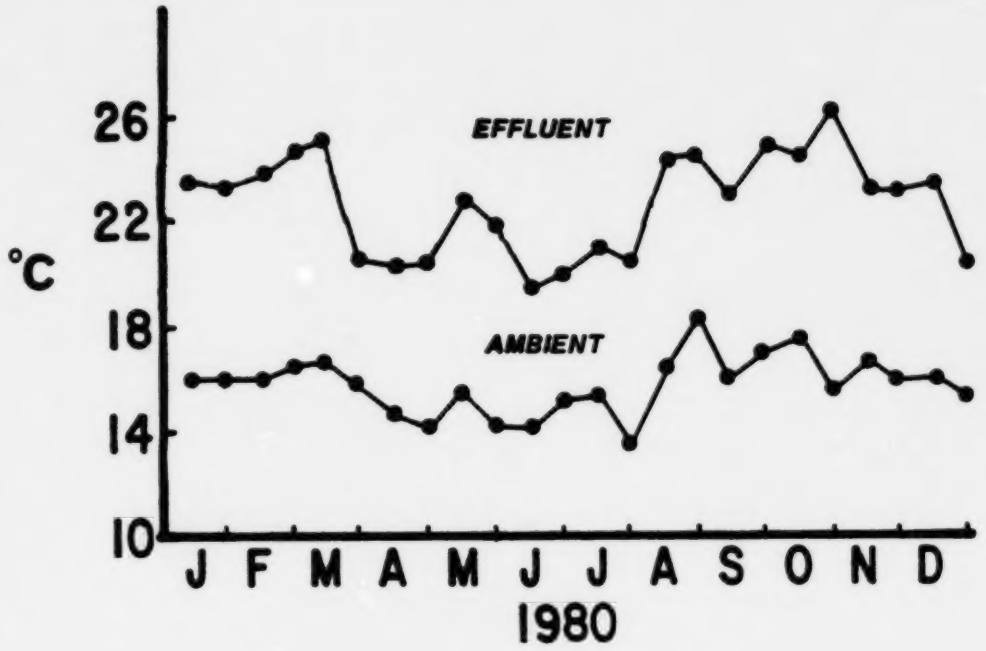

FIGURE 3 Semi-monthly mean temperatures of ambient and effluent seawater delivered to the Redondo Beach SCE Laboratory

5. CONCLUSION & FUTURE DIRECTION

The Southern California Edison Company will continue to support the culture of thermophilic abalone as a part of its Thermal Resource Utilization Program as long as such participation is warranted. The upcoming year will be devoted to streamlining the production of green abalone, to increasing the capability of producing pink abalone and the possible deletion of red abalone from the project. The red abalone has received considerable attention from other culturists and does not require our efforts, except for its use as an experimental animal. We also feel that it is necessary to increase the present growth acceleration, now about 1.6 that of nature [11], to around 2.5 times or greater. Stocking densities and food conversion ratios need to be better defined.

The extension of this project into the commercial marketplace could follow as the natural outcome of successful research. At present we feel satisfied to culture a product, using a part of our thermal resources that would normally be wasted, and to use that product to help enhance our coastline.

Table X

Size Increases for Juvenile Haliotis Fulgens Held at Four Temperatures and Fed a Mixture of Seaweeds for a Period of Four Months

Temperature		Size @ t_0 Group Mean (mm ± SD)		Size @ t_4 mos. Group Mean (mm ± SD)		Increase (mm)	Mean Increase (mm)
	Pair						
16°C	A	13.99	1.94	21.58	2.58	7.59	
	B	13.98	1.99	20.79	2.71	6.81	7.20
20°C	A	13.89	1.78	22.63	2.25	8.74	
	B	13.99	2.33	22.98	3.60	8.99	8.87
24°C	A	14.05	1.87	24.77	2.91	10.72	
	B	13.85	1.99	24.18	3.65	10.33	10.53
28°C	A	13.95	2.19	25.31	1.68	11.36	
	B	13.94	1.87	26.03	2.88	12.09	11.73

REFERENCES

1. Ocean Studies Institute Division, World Research, Inc., 11722 Sorrento Valley Rd., San Diego, CA 91212

2. California - International Marine Resources, Inc., P.O. Box 14343, Santa Barbara, CA 93107
Present Address: Dept. Biological Sciences, University of California, Santa Barbara, CA 93106

3. Burge, R., S. Schultz and M. Odemar. 1975. Draft Report on Recent Abalone Research in California with Recommendations for Management. State of California Resources Agency, Department of Fish and Game. 62 pp.

4. Tegner, M.J., Experimental Abalone Enhancement Program, Proposal Submitted to Sea Grant for the Years 1981 Through 1983. Assistant Research Marine Biologist, Scripps Institute of Oceanography, A-001, La Jolla, California, 92093.

5. Leighton, D. L. 1974. The Influence of Temperature on Larval and Juvenile Growth in Three Species of Southern California Abalones. U.S. National Marine Fish Services, Fish Bull 72(4):1137-1145.

6. Morse, D. E., H. Dunchan, N. Hooker and A. Morse. 1977. Hydrogen Peroxide Induces Spawning in Mollusks, with Activation of Prostaglandin Endoperoxide Synthetase. Science 196:298-300.

7. Morse, D. E., N. Hooker, H. Duncan and L. Jensen. 1979a. - Aminobutyric Acid, a Neurotransmitter, Induces Planktonic Abalone Larvae to Settle and Begin Metamorphosis. Science 204:407-410.

8. Leighton, D. L. 1977. Some Problems and Advances in Culture of North American Abalones (Haliotis). Proceed. First Symposium, Latin American Aquaculture Association, Maracay, Venezuela, November, 1977.

9. Morse, D. E., N. Hooker, and D. L. Leighton. 1981. Control of Reproduction, Larval Development and Metamorphosis in the Thermophilic Green Abalone, Haliotis Fulgens. (In Preparation)

10. Tegner, M. J. 1981. Assistant Research Marine Biologist Scripps Institute of Oceanography, A-001, La Jolla, CA. 92093. Personal Communication.

11. Leighton, D. L., M. J. Byhower, J. C. Kelly, G. N. Hooker and D. E. Morse. 1981. Acceleration of Development and Growth in Young Green Abalone, Haliotis Fulgens, Using Warmed Effluent Seawater. Abstracts: World Mariculture Society Technical Session. Seattle, Washington, March 8-10, 1981.

PB82-228255

TILAPIA CULTURE IN HEATED EFFLUENTS: POTENTIAL FOR COMMERCIALIZATION IN TEMPERATE CLIMATES

L. L. Behrends, D. W. Burch, J. J. Maddox, R. G. Nelson, and E. L. Waddell, Jr.
Tennessee Valley Authority
Muscle Shoals, Alabama, U.S.A.

ABSTRACT

Because the Tennessee Valley is located in a temperate climate, a multi-seasonal approach has been developed for culturing the tropical fish tilapia. During the winter (October-March), temperature of condenser cooling water (CCW) from open-cycle nuclear power plants ranges from 15° to 32° C, and it is ideally suited for overwintering small fingerlings and selected brood stock in raceways. During warmer periods of the year when CCW is too warm for raceway culture, fingerlings are reared to market size in earthen cooling ponds or in farm ponds near the power plant site. Hatchery methods have also been developed for mass production of tilapia and their hybrids. The integrated approach of over-wintering, hatchery production, and growout will be discussed relative to optimal use of heated effluents.

1. INTRODUCTION

The tilapia (Sarotherodon spp.), a diverse group of tropical fish native to Africa and the Middle East, are cultured extensively as food fish in tropical and subtropical countries. Tilapia have several qualities which make them excellent candidates for culture. They grow fast, have good market potential, are relatively resistant to low-oxygen and high-ammonia concentrations, reproduce readily, have few disease problems, and can be cultured both intensively in raceways and extensively in ponds. The most unique and valuable asset of tilapia, however, is their ability to feed on plankton, the base of the food chain in pond culture systems. Thus, instead of requiring a high-protein pelleted diet, tilapia may be cultured on a less costly yet readily available supply of plankton. This is especially valuable since feeding conventional pellets may account for 40 to 60 percent of the operating costs of a fish-farming enterprise. Because of their culture assets, tilapia are considered prime candidates for culture in the United States and other temperate countries (Suffern, 1981) if economical methods can be developed for mass-producing and overwintering selected seedstocks.

1.1. Constraints to Culture in Temperate Climates

Despite the excellent culture characteristics of tilapia, several technical factors prevent development of a wide-scale culture industry in temperate climates. Because tilapia cannot survive in climates where water temperatures are often less than 10° to 12° C for prolonged periods, economical methods must be developed for overwintering seedstocks and broodfish during cooler periods of

the year. A second major problem involves mass production of suitable seedstock (i.e., monosex stocks) for pond culture. Because overwintered tilapia mature and breed at a small size, overpopulation and stunting occur in pond culture which renders the harvest unmarketable. Although methods are available for producing 100 percent male populations via hormone treatment (Shelton, et al., 1978) or hybridization (Mires, 1977), the problem remains that practical and economical methods for mass-producing suitable seedstocks are still not available. Finally, although small isolated studies indicate that tilapia are highly marketable (Suffern, 1981), little work in processing or market development has been done.

1.2. TVA's Development Work

Since the late 1960's, the Tennessee Valley Authority (TVA) has been developing waste heat utilization technologies (Burns, et al., 1980; Hubert, 1980). During the past four years, TVA has been developing the technical criteria required for intensively overwintering tilapia stocks. Related studies have also been conducted on pond fertilization techniques and mass production of suitable seedstocks for pond stocking.

This paper summarizes TVA's research and development work related to the breeding, culture, and overwintering of tilapia. Applied uses of waste heat and its role in development of tilapia culture in temperate climates will be emphasized.

2. PRACTICAL CULTURE OF TILAPIA IN HEATED EFFLUENTS

Several potential benefits may be derived from the use of flowing warm water in raceway and pond culture of tilapia. These include a lengthened growing season, early sexual maturation and spawning, enhanced plankton production, dilution of harmful metabolites, attraction and harvest of tilapia from extensive cooling ponds, and most importantly, the overwintering of culture stocks.

2.1. Overwintering Studies--Prototype Facility (1978-79)

In 1978, a prototype overwintering facility was designed and built at Muscle Shoals, Alabama. The facility, a series of several small raceways (170 ℓ capacity) received a supply of warm water simulating power plant CCW temperatures.

Two raceway culture periods (30 and 32 days in duration) were monitored during the winter of 1978 to determine: (1) growth characteristics of tilapia fingerlings under raceway conditions, (2) changes in water quality as a function of feed rate and water retention time, and (3) the influence of flow rate and aeration on fish density (kg/m^3) and fish-loading rate ($kg/\ell/min$) (Behrends, et al., 1980).

Growth rates of fingerling tilapia were not reduced significantly until average dissolved oxygen concentrations were less than 3 ppm (38 percent saturation, water temperature = 27° C). Based on pH, total ammonia nitrogen, and water temperature, the theoretical un-ionized ammonia concentration (toxic form of ammonia) ranged from 5 to 91 $\mu g/\ell$. When sufficient oxygen was available (>3 ppm), these concentrations of ammonia did not adversely affect growth of tilapia. Final fish densities in the raceways ranged from 27 to 40 kg/m^3 (1.9 to 2.5 lb/ft^3), while final fish-loading rates ranged from 1.2 to 1.7 $kg/\ell/min$ (10 to 14 lb/gal/min).

Based on the 1978 results, a 100,000-fingerling capacity raceway facility was built at the Browns Ferry Nuclear Plant (BFN) near Athens, Alabama.

2.2. Overwintering Facility Design--BFN

The demonstration facility at BFN consists of six fiberglass raceways (3.7 m by 1.2 m by 1.2 m) located inside a 14.6-m by 7.6-m double-polyethylene greenhouse structure; a CCW delivery system capable of providing a maximum of 190 ℓ/min/raceway and a series of redundant backup systems for water flow, aeration, electrical service, and space heating (Waddell, unpublished paper). A deep well with a flow of 230 ℓ/min (≅15° C) is used for blending and as an auxiliary water source during multiple unit shutdowns. Eighteen aquaria (100 ℓ capacity) have also been installed to evaluate spawning characteristics of tilapia as a function of photoperiod and CCW temperatures.

The BFN primarily uses an open-mode cooling system with CCW temperatures averaging 14.4° C above ambient. Effluent CCW temperatures range from 15° C in January to 46° C in August. As a safety feature, the CCW delivery system was retrofitted upstream of the radiological effluent injection site. This measure eliminates the most significant source of radioactivity normally found in liquid effluents from nuclear power plants. Also, condenser cooling water can be supplied to the delivery system from any of the three power production units. This increases reliability of the warmwater source, although not to the extent that backup systems are not required.

2.3. Overwintering Studies--BFN (1979-81)

In mid-October 1979, 70,000 tilapia fingerlings, ranging in weight from 3.0 to 15.0 g, arrived from Auburn University and were stocked into six raceways. Two different species of tilapia, Sarotherodon aurea and S. nilotica were supplied as test species because of their favorable growth rates and relative cold tolerance (Lee, 1979). Growth, survival, and feed conversion values were satisfactory during the winter period. By early February, the fish had increased their initial weight by 250 to 300 percent. Unfortunately, on February 11, 1980 a multiple unit shutdown coupled with an unrelated computer and alarm failure resulted in intrusion of ambient river water and massive mortality of tilapia stocks. The fish were exposed to ambient river water (5° C) for about 18 hours before CCW temperatures rose to preshutdown levels. Complete mortality of the less cold tolerant S. nilotica occurred, while S. aurea, the most cold tolerant of the tilapia species, experienced 95 percent mortality. More tilapia fingerlings were acquired from Florida and reared in the raceways during the remainder of the overwintering period. In mid-April, most of these fingerlings were taken to Auburn University for pond and cage production tests. During the 1980-81 overwintering period, emphasis was placed on overwintering a diversity of broodstock and fingerlings for expanded breeding and pond culture studies respectively. Four stocks of brood-sized tilapia (S. aurea, S. nilotica, S. hornorum, and S. mossambica) and two all-male hybrid strains (S. mossambica ♀ x S. hornorum ♂) and (S. nilotica ♀ x S. hornorum ♂) were successfully overwintered. By early April, the hybrid S. mossambica ♀ x S. hornorum ♂ had increased its initial weight (2.5 g) by 570 percent. Few operational problems were encountered during the 1980-81 overwintering period, due primarily to the adding of several automatic backup systems (Waddell, unpublished paper).

2.4. Tilapia Breeding and Hybridization Studies

Production of all-male tilapia fingerlings by hybridization is advantageous for several reasons. Unwanted reproduction in culture ponds can be avoided if all-male fingerlings are stocked. Also several crosses exhibit hybrid vigor for cold tolerance and growth (Lee, 1979), both significant factors for culture in temperate climates. During 1980, 36 small nylon nets (1.2 m by 1.2 m by 2.7 m, 0.15-cm mesh) were suspended in an earthen pond and evaluated as portable breeding units for producing hybrid tilapia fry (Behrends and Smitherman, 1981). Adult fish (brooders) were stocked into the nets in June, and fry (and eggs) were collected every two weeks for a 6-week period. Three different crosses which theoretically produce 100 percent male offspring were evaluated. Of these, only the female S. mossambica x male S. hornorum cross produced significant numbers of fry. At a stocking rate of 24 brooders (20 females and 4 males), 10,860 fry and fertilized eggs were produced during a 6-week period.

Subsequent net-breeding trials were conducted to quantify the relative ease of producing S. aurea, S. nilotica, S. hornorum, and S. mossambica, and all their hybrids (Behrends and Smitherman, unpublished data).

Breeding studies were continued during the winter of 1980-81 to ascertain the feasibility of inducing tilapia broodstock to spawn early via photoperiod and temperature manipulation. Generally, tilapia will not spawn in north Alabama until late May. However, by late February all four species were exhibiting breeding behavior and spawning occurred in all species by mid-March. Invariably, early spawning occurred only after CCW temperatures were above 24° C and photoperiods were greater than 11 hours. However, our data strongly suggests that temperature was a much stronger stimulus to spawning than photoperiod, as long as the photoperiod was greater than 11 hours. This is a favorable implication for hatchery work at closed-cycle plants where CCW temperatures are much warmer during winter months.

The early spring spawning approach to fingerling production may have advantages over the traditional overwintering approach. Instead of overwintering summer-produced fingerlings, selected groups of broodfish could be overwintered and induced to spawn in early March. Theoretically, for each kg of female broodstock overwintered, 3,000 fry could be produced in the initial spawn, thus increasing the capacity of the overwintering system. More breeding and nursery areas would be required for this operation. Early spring spawning would require that young-of-the-year tilapia reach marketable weight during their first culture season. This procedure remains to be tested.

2.5. Pond Growout of Tilapia

Pond production of tilapia can be accomplished with pelleted feeds, organic fertilizers, or a combination of both. TVA has developed an integrated warmwater aquaculture system for reclaiming valuable plant nutrients from animal wastes which accumulate during livestock feeding in confinement (Behrends, et al., 1980, in press; Behrends, 1980; and Maddox, et al., 1979). During the past five years, experiments were conducted to develop criteria for such a system (figure 1). Results of yield trials indicate that for optimum production of market-sized fish, plankton culture ponds should be fertilized daily during March through October with up to 60 kg/ha/day of fresh swine manure (dry-matter basis). Warm CCW should be directed into the ponds at a rate sufficient to flush them every 10 days. Shorter retention periods (5 days or less) result in less plankton production and hence, less fish production. Longer retention periods (15 days or more), although allowing greater plankton production, also result in less

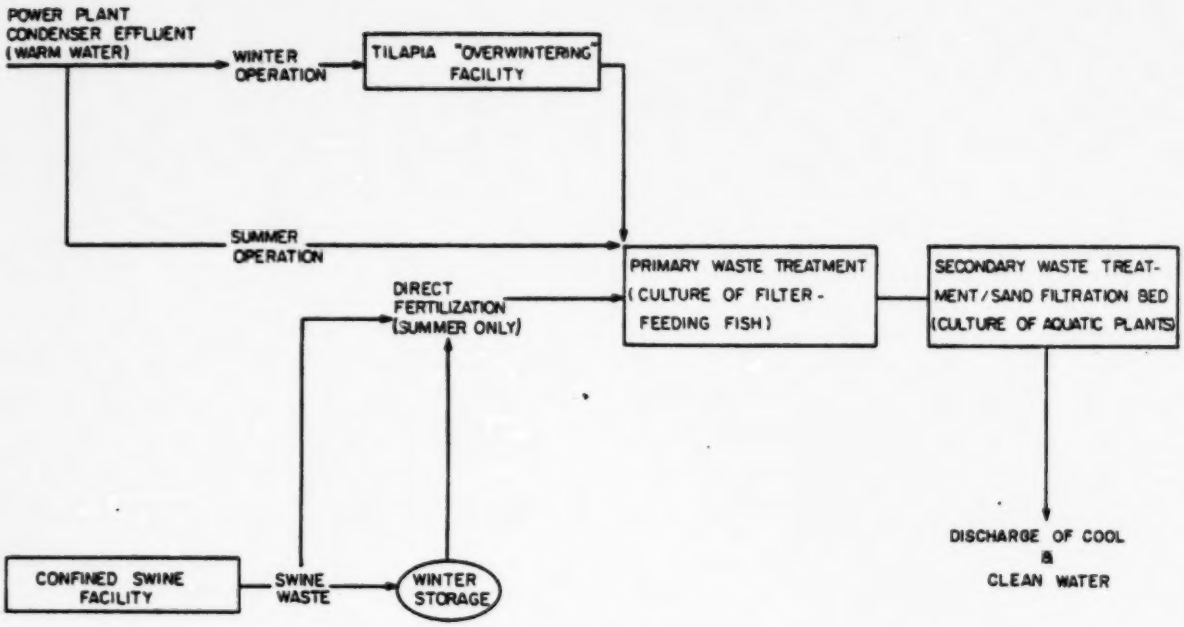

FIGURE 1 BIOLOGICAL RECYCLING OF LIVESTOCK WASTE NUTRIENTS AND ENERGY.

fish production due to the buildup of toxic metabolites, such as ammonia. At a stocking rate of 10,000 to 15,000/ha, production in excess of 6,000 kg/ha is possible during a 6-month growing season (Behrends, et al., in press). Fertility rates and stocking densities have also been developed for static water systems (i.e., no flowing water), and other manure sources (Moav, et al., 1977; Collis and Smitherman, 1978; and Stickney and Hesby, 1977).

Culture ponds can also be used in intensely fed production systems if large volumes of warm water are available to supply oxygen and dilute culture-related metabolites. In Taiwan, tilapia standing crops of near 110,000 kg/ha have been achieved in flowing water ponds with aeration and a nutritionally balanced diet (Lovell, 1980). Intensive pond production systems, although feed intensive, may have application at power plant sites where land may not be available for develment of large extensive production systems.

3. OPTIMIZING USE OF HEATED EFFLUENTS IN TILAPIA CULTURE

One of the most commonly voiced concerns in power plant aquaculture relates to the problem of wide seasonal variation in effluent temperatures. This is especially critical at open-cycle power plants where CCW temperatures may vary as much as 25° to 30° C. Culturally, this problem can be minimized by designing systems to accommodate these large fluctuations in temperature. TVA has proposed adoption of a multiseasonal approach to culturing tilapia which optimizes the use of warm flowing water on an annual basis.

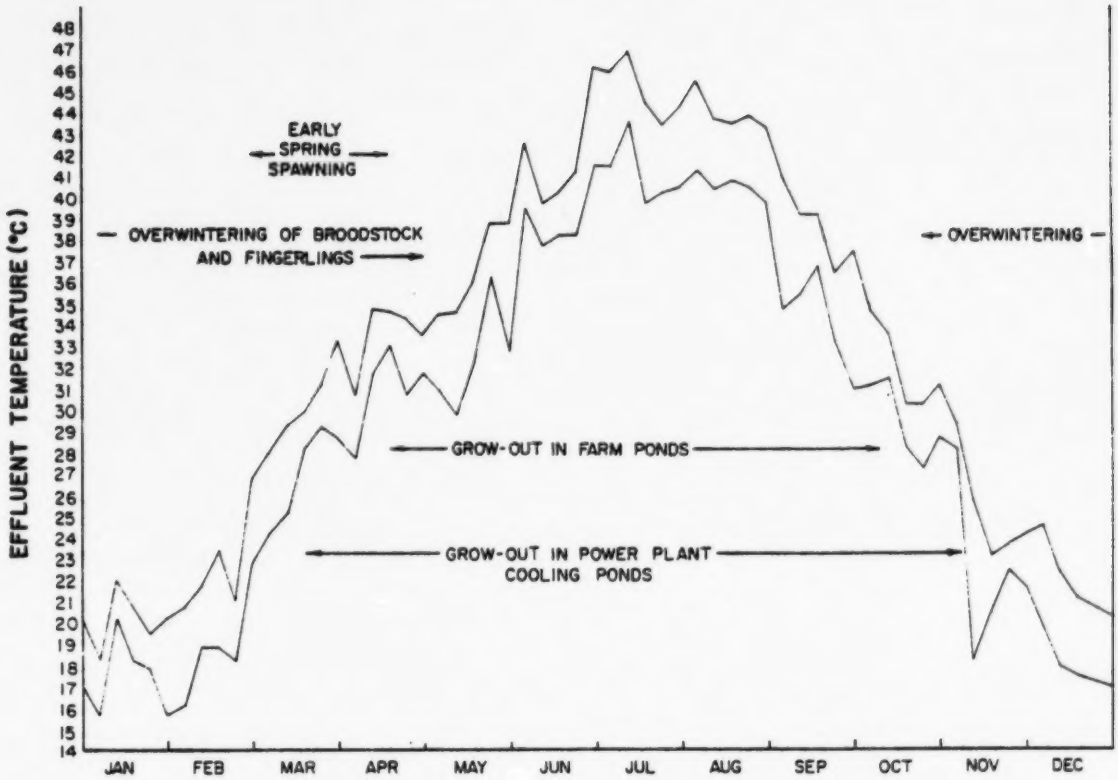

FIGURE 2 BROWNS FERRY CONDENSER EFFLUENT TEMPERATURES AND RELATED TILAPIA CULTURE ACTIVITIES

Figure 2 illustrates the proposed culture activities as they relate to the CCW temperature of BFN. The upper and lower lines represent the mean maximum and mean minimum temperatures respectively. During winter and spring, emphasis will be on hatchery operations and producing stocker-sized fingerlings, while final growout will be performed in ponds during late spring, summer, and fall. Final growout can be performed at the power plant site in appropriately sized cooling ponds or in conventional farm ponds near the power plant site. The farm pond approach has considerable appeal since it has the potential for expanding the land base for tilapia culture to thousands of acres.

CONCLUSION

Although more development work will be required before tilapia culture becomes an aquaculture industry in temperate climates, recent developments in hatchery and overwintering systems will certainly expedite the extension process.

TVA will continue its development work in tilapia culture with an emphasis on extending it from the power plant site to the farm.

ACKNOWLEDGEMENTS

TVA expresses its gratitude to Auburn University's Department of Fisheries and Allied Aquacultures for its cooperation in providing fingerlings and expertise. We also acknowledge John B. Kingsley, Philip W. Barron, and H. Steven Coonrod II for their technical help.

REFERENCES

1. Behrends, L. L., Recycling Livestock Wastes via Fish Culture, Aquaculture Magazine, (7) pp. 38-39, 1980.

2. Behrends, L. L. and R. O. Smitherman, Mass Production of Hybrid Tilapia Fry in Suspended Nylon Mesh Nets, Research Workshop, Summary of Papers, Catfish Farmers of America, p. 62, 1981.

3. Behrends, L. L., J. B. Kingsley, J. J. Maddox, R. S. Pile, J. C. Roetheli, and E. L. Waddell, Jr., Intensive Production of Tilapia Fingerlings in Thermal Effluents, Research Workshop, Summary of Papers, Catfish Farmers of America, p. 42, 1980.

4. Behrends, L. L., J. J. Maddox, C. E. Madewell, and R. S. Pile, Comparison of Two Methods of Using Liquid Swine Manure as an Organic Fertilizer in the Production of Filter-Feeding Fish, Aquaculture (20) pp. 147-153, 1980.

5. Behrends, L. L., J. B. Kingsley, J. J. Maddox, and E. L. Waddell, Jr., Use of Thermal Effluents and Organic Manures to Enhance Pond Production of Freshwater Fish: An Integrated Approach--Part 1, In press.

6. Burns, E. R., L. L. Behrends, J. J. Maddox, C. E. Madewell, D. A. Mays, and R. S. Pile, Agricultural Uses of Power Plant Waste Heat, in L. B. Goss (ed.), Factors Affecting Power Plant Waste Heat Utilization. chap. 1, Pergamon Press, New York, 1980.

7. Collis, W. J. and R. O. Smitherman, Production of Hybrid Tilapia with Cattle Manure and a Commercial Diet, in R. O. Smitherman (ed.), Proceedings of the Symposium on the Culture of Exotic Species, Fish Culture Section, American Fish Society, 1978.

8. Hubert, W. A., Aquacultural Uses of Power Plant Waste Heat, in L. B. Goss (ed.), Factors Affecting Power Plant Waste Heat Utilization, chap. 1, Pergamon Press, New York, 1980.

9. Lee, J. C., Reproduction and Hybridization of Three Cichlid Fishes, Sarotherodon aurea, S. hornorum, and S. nilotica in Aquaria and in Plastic Pools, Ph.D. thesis, Auburn University, Auburn, Alabama, 1979.

10. Lovell, R. T., Feeding Tilapia, Aquaculture Magazine, (7) pp. 42-43, 1980.

11. Maddox, J. J., L. L. Behrends, R. S. Pile, and J. C. Roetheli, Waste Treatment for Confined Swine by Aquaculture, American Society of Agricultural Engineers, Paper No. 79-4077, 1979.

12. Moav, R. G., G. W. Wohlfarth, and G. L. Schroeder, Intensive Polyculture of Fish in Freshwater Ponds, I. Substitution of Expensive Feeds by Liquid Cow Manure, Aquaculture, 10(1) pp. 25-43, 1977.

13. Stickney, R. R., and J. H. Hesby, Water Quality - *Tilapia aurea* Interactions in Ponds Receiving Swine and Poultry Wastes, Proceedings, 8th Annual Meeting World Mariculture Society, pp. 55-73, 1977.

14. Waddell, E. L., Jr., Tilapia Culture in Heated Effluents: Facility Design, Operation, and Evaluation, Unpublished Paper.

15. Suffern, J. S., The Potential of Tilapia in United States Aquaculture, *Aquaculture Magazine*, (6) pp. 14-18, 1980.

SESSION VI B

THERMAL DISCHARGE III

PB82-228263

MATHEMATICAL MODELLING OF THERMAL PLUME INTERACTION AT WATERFORD NUCLEAR POWER STATION

Steve Y. H. Tsai
Division of Environmental Impact Studies
Argonne National Laboratory
Argonne, Illinois 60439

ABSTRACT

The Waldrop plume model was used to analyze the mixing and interaction of thermal effluents in the Mississippi River resulting from heated-water discharges from the Waterford Nuclear Power Station Unit 3 and from two nearby fossil-fueled power stations. The computer program of the model was modified and expanded to accommodate the multiple intake and discharge boundary conditions at the Waterford site. Numerical results of thermal plume temperatures for individual and combined operation of the three power stations were obtained for typical low river flow (200,000 cfs) and maximum station operating conditions. The predicted temperature distributions indicated that the surface jet discharge from Waterford Unit 3 would interact with the thermal plumes produced by the two fossil-fueled stations. The results also showed that heat recirculation between the discharge of an upstream fossil-fueled plant and the intake of Waterford Unit 3 is to be expected. However, the resulting combined temperature distributions were found to be well within the thermal standards established by the state of Louisiana.

1. INTRODUCTION

The Louisiana Power and Light (LP&L) Company is constructing the Waterford Nuclear Power Station, Unit No. 3 (Waterford 3), near the Mississippi River at a point approximately 25 miles (40 km) northwest of New Orleans and approximately 50 miles (80 km) SSE of Baton Rouge, Louisiana (Figure 1). The station is designed to employ a pressurized water reactor to produce a maximum thermal output of 3560 MWt and a maximum net electrical output of 1165 MWe. Because of the low thermal efficiency (32 to 40 percent) of steam-electric power plants, a large amount of waste heat must be disposed. The waste heat produced at Waterford 3 will be removed by a once-through cooling system which will withdraw a design flow rate of 2235 cfs (63.3 m^3/s) from the Mississippi River. The cooling water will be passed through the condenser and various heat exchangers and then returned to the Mississippi River through a surface discharge canal. When the Waterford 3 station is operated at maximum power level, the cooling water temperature rise at the point of discharge will be about 16.1°F (8.9°C).

The discharge of a large quantity of waste heat from the Waterford 3 station into the river raises many environmental concerns regarding possible large-scale modification of the thermal regime of the water body and the resultant potential effects on aquatic ecosystems. These potential effects are of even greater concern because the Waterford 3 station is located near

Preceding page blank

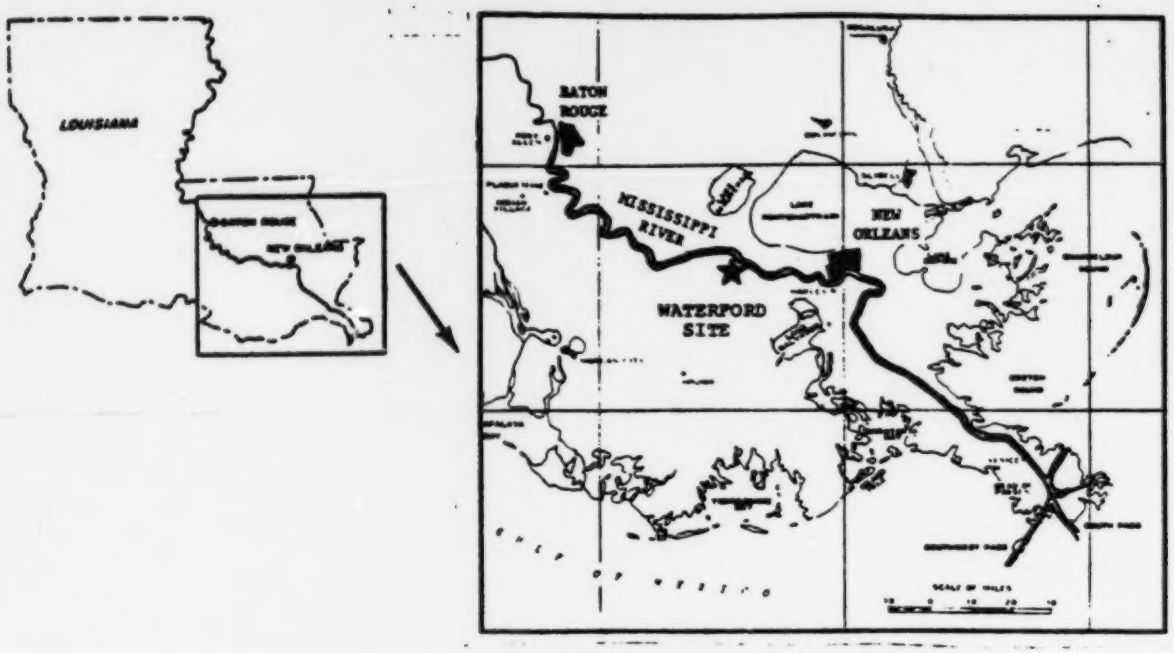

Fig. 1. Map Showing Location of Waterford Nuclear Power Station, Unit No. 3

two existing fossil-fueled power stations (Figure 2). The location of Waterford 3 is approximately 0.5 miles (0.8 km) downstream from the Waterford Units 1 and 2 Station (882 MWe), on the same side of the river, and is almost directly across the river from the Little Gypsy Station (1229 MWe). Depending on river flow conditions and on station operating modes, the thermal plumes produced by the simultaneous operation of all three power stations might interact with one another and create a thermal block that could inhibit the passage of free-swimming and drifting organisms. Furthermore, as indicated in Figure 2, all three stations are located on a river bend. Because of the centrifugal force effect, the river flows around the bend in a complex pattern that can significantly influence the mixing process of the discharged effluents in the river.

The combined thermal plume distributions produced by the operation of all three power stations are required to meet the temperature standards established by the state of Louisiana [1]. The standards specify that for the rivers, the mixing zone is limited to no more than 25 percent of the cross-sectional area and/or volume of flow at any river cross section, and the maximum temperature rise outside the mixing zone is 5°F (2.8°C). Therefore, the objective of this study was to mathematically simulate the merging of the three thermal plumes by considering the river bend effects in order to obtain three-dimensional temperature distributions needed for environmental impact assessment.

2. BASIC EQUATIONS OF THE THERMAL-PLUME MODEL

The Waldrop plume model [2,3] was used to analyze the hydrothermodynamics of the Mississippi River in the vicinity of the Waterford site. This model numerically solves the three-dimensional continuity, energy, and momentum equations for velocity and temperature and includes the effects of the curvature of the river. The following descriptions of the model were abstracted from Reference 3.

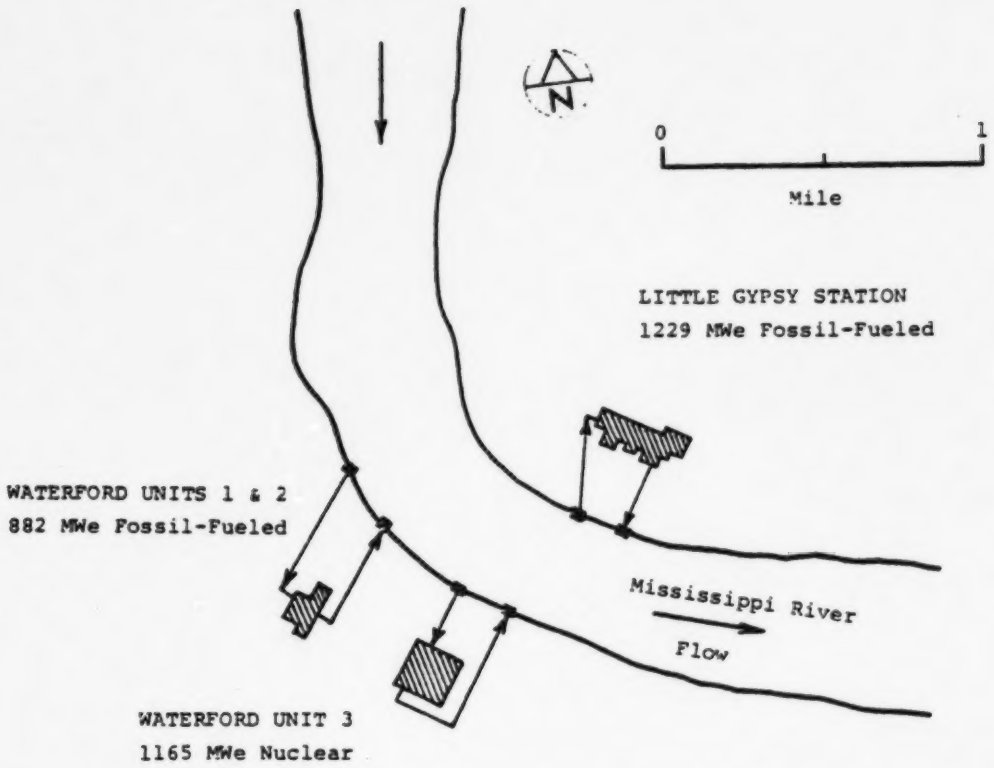

Fig. 2. Relative Location of the Three Power Stations

Assuming that the water is incompressible and that the vertical component of velocity is small, the governing equations of the model in the general orthogonal curvilinear coordinate system are:

continuity equation:

$$\frac{\partial u}{\partial x} + \frac{u}{(R + x)} + \left(\frac{R}{R + x}\right) \frac{\partial v}{\partial y} + \frac{\partial w}{\partial z} = 0 \tag{1}$$

conservation of thermal energy equation:

$$\frac{\partial T}{\partial t} = -\left[u \frac{\partial T}{\partial x} + \left(\frac{R}{R + x}\right) v \frac{\partial T}{\partial y} + w \frac{\partial T}{\partial z}\right] + \alpha_H \left[\frac{\partial^2 T}{\partial x^2} + \frac{1}{(R + x)} \frac{\partial T}{\partial x}\right.$$
$$\left. + \left(\frac{R}{R + x}\right)^2 \frac{\partial^2 T}{\partial y^2} + \frac{Rx}{(R + x)^3} \frac{dR}{dy} \frac{\partial T}{\partial y}\right] + \alpha_V \left[\frac{\partial^2 T}{\partial z^2}\right] \tag{2}$$

x-momentum equation:

$$\frac{\partial u}{\partial t} = -\left[u \frac{\partial u}{\partial x} + \left(\frac{R}{R + x}\right) v \frac{\partial u}{\partial y} + w \frac{\partial u}{\partial z} - \frac{v^2}{(R + x)}\right] - \frac{1}{\rho} \frac{\partial p}{\partial x}$$
$$+ \varepsilon_H \left[\frac{\partial^2 u}{\partial x^2} + \frac{1}{(R + x)} \frac{\partial u}{\partial x} + \left(\frac{R}{R + x}\right)^2 \frac{\partial^2 u}{\partial y^2} - \frac{u}{(R + x)^2} - \frac{2R}{(R + x)^2} \frac{\partial v}{\partial y}\right.$$
$$\left. + \frac{R}{(R + x)^3} \frac{dR}{dy} v + \frac{Rx}{(R + x)^3} \frac{dR}{dy} \frac{\partial u}{\partial y}\right] + \varepsilon_V \left[\frac{\partial^2 u}{\partial z^2}\right] \tag{3}$$

y-momentum equation:

$$\frac{\partial v}{\partial t} = -\left[u\frac{\partial v}{\partial x} + \left(\frac{R}{R+x}\right)v\frac{\partial v}{\partial y} + w\frac{\partial v}{\partial z} + \frac{uv}{(R+x)}\right] - \left(\frac{R}{R+x}\right)\frac{1}{\rho}\frac{\partial p}{\partial y}$$
$$+ \varepsilon_H\left[\frac{\partial^2 v}{\partial x^2} + \frac{1}{(R+x)}\frac{\partial v}{\partial x} + \left(\frac{R}{R+x}\right)^2\frac{\partial^2 v}{\partial y^2} + \frac{2R}{(R+x)^2}\frac{\partial u}{\partial y} - \frac{v}{(R+x)^2}\right.$$
$$\left. + \frac{Rx}{(R+x)^3}\frac{dR}{dy}\frac{\partial v}{\partial y} - \frac{Ru}{(R+x)^3}\frac{dR}{dy}\right] + \varepsilon_V\left[\frac{\partial^2 v}{\partial z^2}\right] \qquad (4)$$

z-momentum equation:

$$0 = -\frac{1}{\rho}\frac{\partial p}{\partial z} - g \qquad (5)$$

where:

x, y, and z are orthogonal curvilinear coordinates as shown in Figure 3; u, v, and w are scalar components of the velocity in x, y, and z directions; t is time; ρ is water density; T is temperature; R is the radius of curvature of the centerline of the river and is a function of y; P is pressure; α_H and α_V are eddy thermal diffusivity coefficients in x and z directions; ε_H and ε_V are eddy viscosity coefficients in x and z directions; and g is acceleration of gravity.

The use of the curvilinear coordinate system permitted a good simulation of the river topography in the vicinity of the Waterford site and rendered an efficient way to include the centrifugal force resulting from the river bend in the governing equations.

The values of ε and α in Equations 2-4 are usually obtained empirically. However, for this study, the horizontal eddy viscosity coefficient, ε_H, was computed by means of Prandtl's mixing length theory. Based on the mixing length equation developed by Yalin [4], ε_H can be expressed as

$$\varepsilon_H = 0.16(D-d)^2\frac{d}{D}\frac{\partial q}{\partial z} \qquad (6)$$

where:

d is the depth below the surface; D is the maximum water depth at the location where d is measured; and q is equal to $\sqrt{u^2+v^2}$.

The horizontal thermal diffusivity, α_H, is related to ε_H by the turbulent Prandtl number, P_t, as

$$\alpha_H = \frac{1}{P_t}\varepsilon_H \qquad (7)$$

For this study, a Prandtl number of 0.75 was assumed.

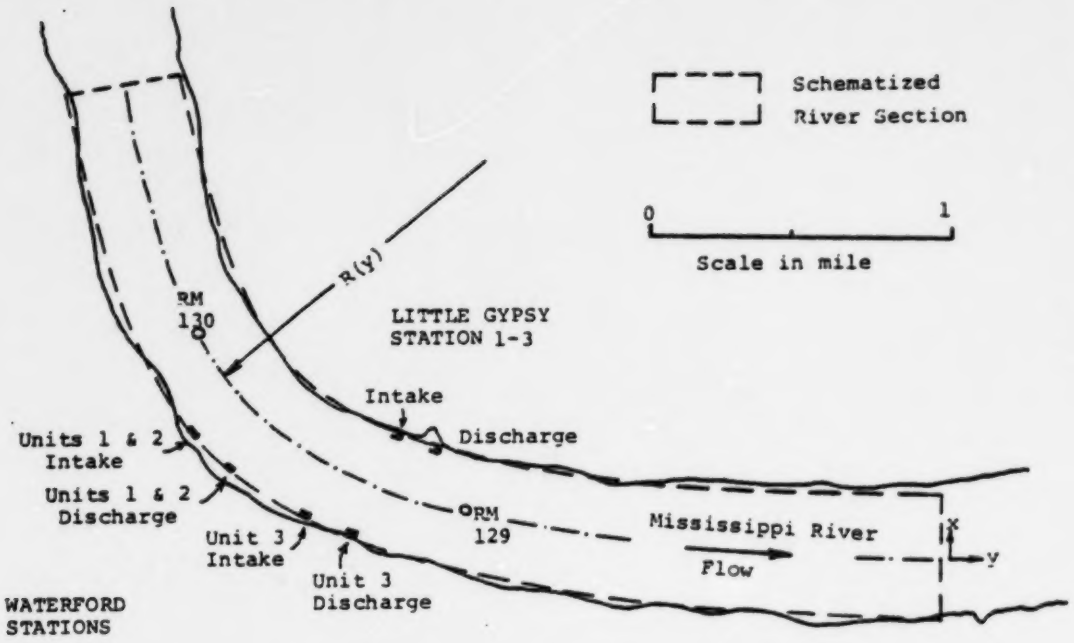

Fig. 3. Coordinate System and Schematized River Section

The vertical viscosity and diffusivity were related to the local horizontal coefficients. Because of the vertical density stratification, the vertical momentum and heat transfer are strongly suppressed [5,6]. This effect was incorporated by Waldrop [2,3] into the model by adopting the empirical damping functions of Munk and Anderson [5] for ε_V and α_V:

$$\varepsilon_V = \varepsilon_H \, (1 + 10R_i)^{-1/2} \tag{8}$$

and

$$\alpha_V = \alpha_H \, (1 + \frac{10}{3}R_i)^{-3/2} \tag{9}$$

where:

$$R_i = - \, (\frac{g}{\rho}) \, (\frac{\partial \rho}{\partial z}) \, (\frac{\partial q}{\partial z})^{-2} \tag{10}$$

Equation 10 is the Richardson Number defined locally from the horizontal flow and vertical density gradient. In this way, the vertical viscosity and diffusivity are attenuated when stratification is present.

Other effects such as wind shear and surface heat transfer were not included in this study.

3. NUMERICAL SOLUTION OF THE BASIC EQUATIONS

The basic equations presented in the previous section were solved numerically by using an explicit finite-difference scheme. The details of the numerical technique can be found in Reference 3 and, therefore, will not be repeated here. The computer program for the Waldrop plume model was originally developed to study the hydrothermodynamics in the streams or rivers where there was only one intake and one discharge. In this study, the program

was modified and expanded to a more generalized fashion such that it was able to accommodate the multiple intake and discharge boundary conditions at the Waterford site.

The schematized river section used in this study extends about 1 mile (1.6 km) upstream from the Waterford 1 and 2 intake location and about 1.5 miles (2.4 km) downstream from the Waterford 3 discharge location (Figure 3). This section was chosen to cover the entire river bend at the Waterford site. A three-dimensional grid network with even spacing of the grid points was placed over the study region. The use of a uniformly-spaced grid pattern was possible because of the stretching transformation of the true spatial coordinates [2,3]. This transformation technique enabled a larger lateral extent to be covered by the grid system, while at the same time retaining finer resolution near the discharge point. A grid spacing of 0.1 was used for each coordinate in the transformed system. The number of grid points used in the x, y, and z directions were 15 by 63 by 12. To ensure computational stability, an incremental time step of one second was used in all numerical calculations.

The computer program, as modified for this study, was run on a CDC 7600 digital computer. The CPU time required to execute 1000 time steps was about 600 seconds. Based on the convergence criteria established in the model, the computed results generally indicated that the solutions became sufficiently close to a steady state after 20,000 time steps.

4. MODEL VERIFICATION

Prior to applying the Waldrop plume model to study thermal plume characteristics in the Mississippi River near the Waterford site, the model was utilized to simulate a river flow condition for which field data had been obtained. On September 9 and 10, 1976, the LP&L conducted temperature surveys in the Mississippi River with both Waterford 1 and 2 and Little Gypsy stations operating. The river flows during the surveys were about 200,000 cfs (5660 m^3/s). The measured isotherms shown in Figures 4 and 5 indicate that although the station discharge and river flow conditions were similar on both days, the extent of the thermal distribution in the river was much less on September 10. This difference was possibly caused by the wind shear effect. There was a 12.3 mph (5.5 m/s) westerly wind on September 9, which would have a large down-river component. On September 10, there was a 6.3 mph (2.8 m/s) southerly wind, which would have a component in the up-river direction. This change in wind speed and direction could have affected the plume dispersion, particular in regions of relatively low river flow (e.g., offshore of the Little Gypsy discharge canal).

As previously mentioned, the effects of wind shear were not considered in this study. Nevertheless, the results of the computed surface temperature isotherms shown in Figures 4 and 5 compare reasonably well with the measured isotherms. Deviations of observed isotherms from calculated isotherms agree qualitatively with the expected effects of wind shear. These data comparisons along with some previous comparisons performed by Waldrop [2,3] provided adequate verification of the model.

5. DISCUSSION OF PREDICTED RESULTS

Numerical results of thermal plume temperatures resulting from the individual and combined operation of Little Gypsy, Waterford 1 and 2, and Waterford 3 stations were obtained for the typical low flow conditions of 200,000 cfs (5660 m^3/s). This flow rate was considered to be the extreme low flow that

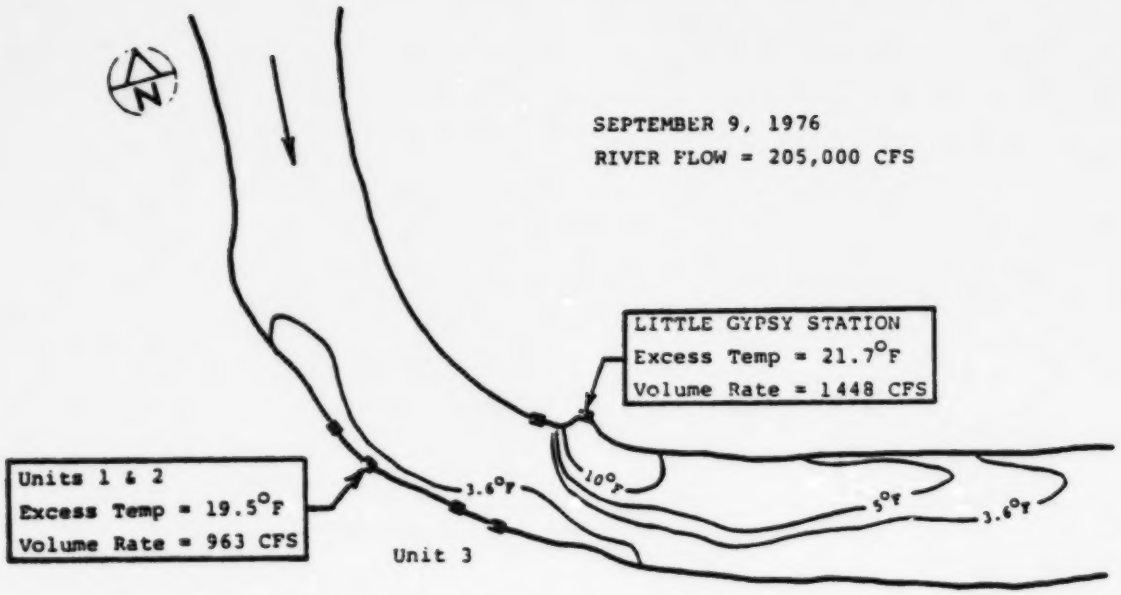

Measured Isotherms

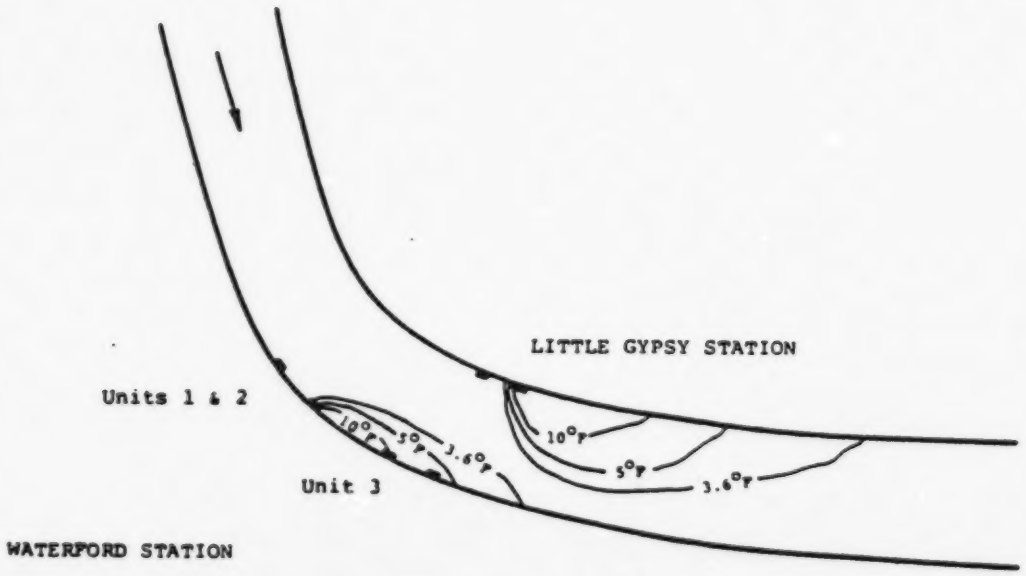

Calculated Isotherms

Fig. 4. Comparison of Measured and Calculated Isotherms, September 9, 1976

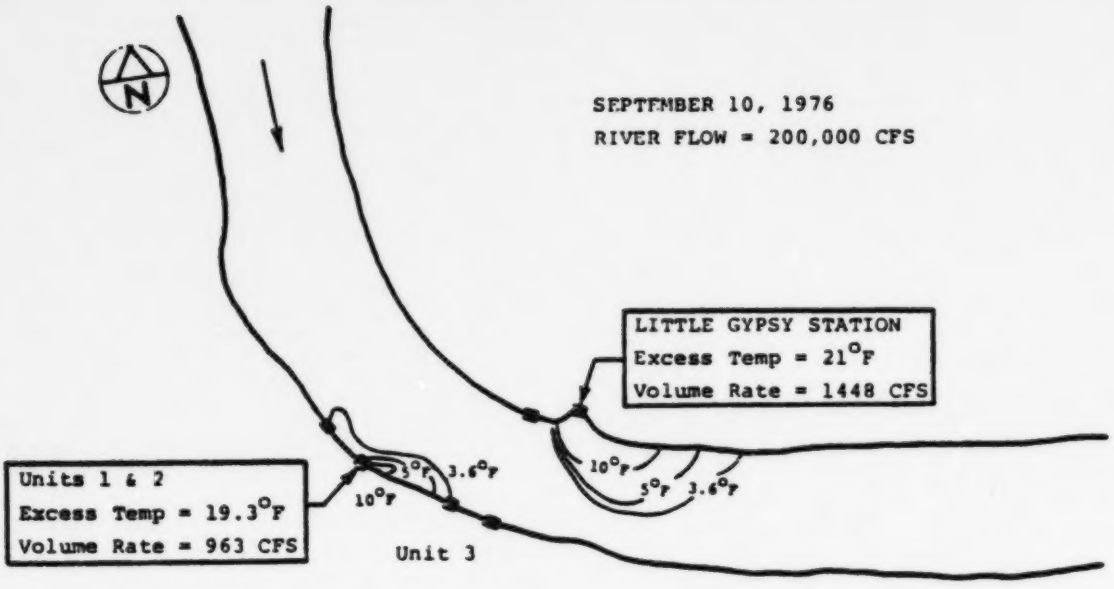

Measured Isotherms

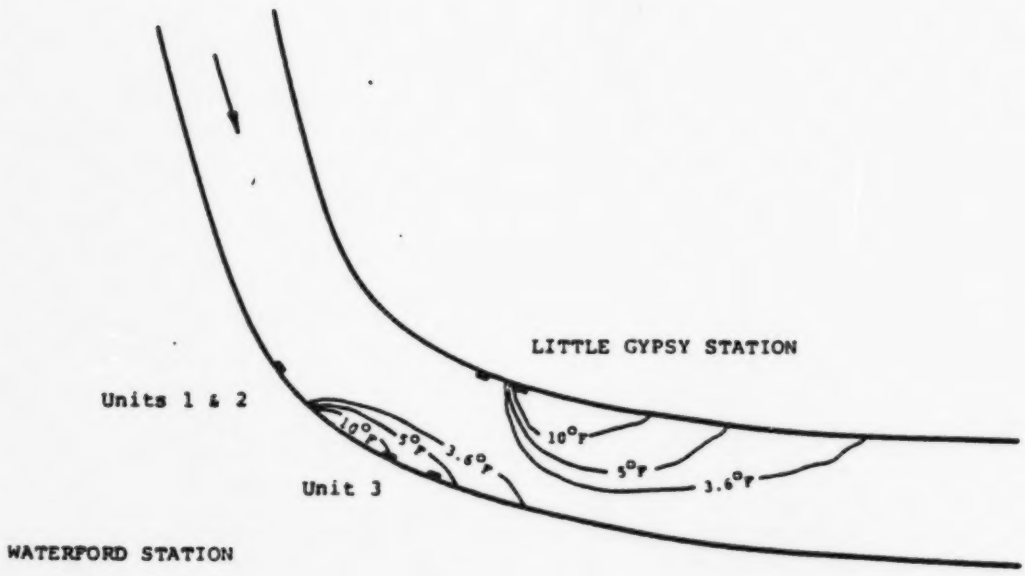

Calculated Isotherms

Fig. 5. Comparison of Measured and Calculated Isotherms, September 10, 1976

would be experienced during the operational lifetime of the Waterford 3 station. For all computations, the three stations were assumed to be operating at maximum power level. The station discharge conditions and the predicted thermal characteristics of 3.6°, 5°, and 10°F (2.0°, 2.8°, and 5.6°C) excess temperature isotherms are presented in Tables 1 and 2. The corresponding surface plumes are depicted in Figures 6 through 10.

Table 1. Station Discharge Conditions for This Study

Operating Station	Discharge Volume Rate (cfs)	Excess Temp. (°F)	Discharge Velocity (fps)
Little Gypsy	1448	21.7	2.4
Waterford 1 & 2	963	19.5	0.1
Waterford 3	2235	16.1	6.1

Table 2. Predicted Thermal Plume Characteristics

Operating Station	Parameter[a] X_m (ft)	Y_m (ft)	Z_m (ft)	A_c/A_T (%)	Vol. (ac-ft)
			3.6°F		
Little Gypsy	1,300	6,600	10.5	3.2	1,250
Waterford 1 & 2	600	4,000	5.6	1.5	560
Waterford 3	1,200	9,600	12.7	4.4	1,650
Combined	1,800	10,800	15.0	11.0	4,680
			5°F		
Little Gypsy	1,100	3,400	6.8	2.2	600
Waterford 1 & 2	400	2,800	3.9	0.8	180
Waterford 3	800	6,600	8.5	3.4	890
Combined	1,800	7,600	10.5	7.3	2,250
			10°F		
Little Gypsy	600	2,200	3.8	0.7	50
Waterford 1 & 2	200	1,500	2.3	0.3	20
Waterford 3	600	3,500	5.1	1.2	85
Combined	1,200	3,900	6.0	2.4	195

[a] X_m = maximum lateral spread; Y_m = maximum longitudinal spread; Z_m = maximum vertical spread; A_c = maximum cross-sectional area for a given excess temperature; A_T = area of the river cross section as denoted in Figure 9; Vol. = volume occupied by excess temperatures higher than that indicated.

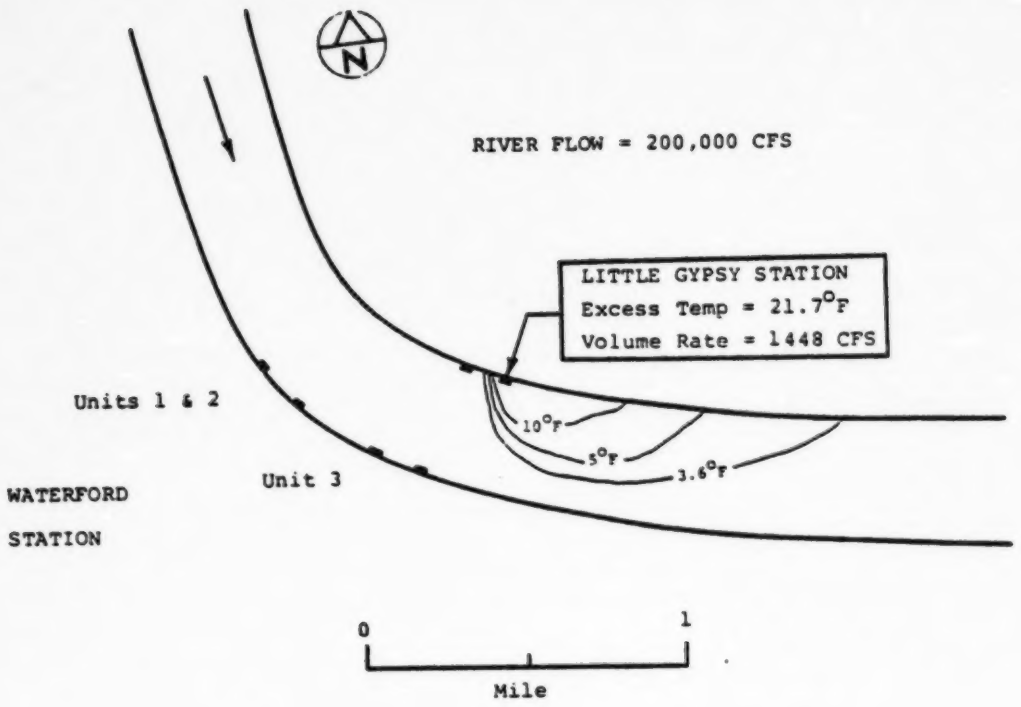

Fig. 6. Predicted Surface Isotherms for the Little Gypsy Station

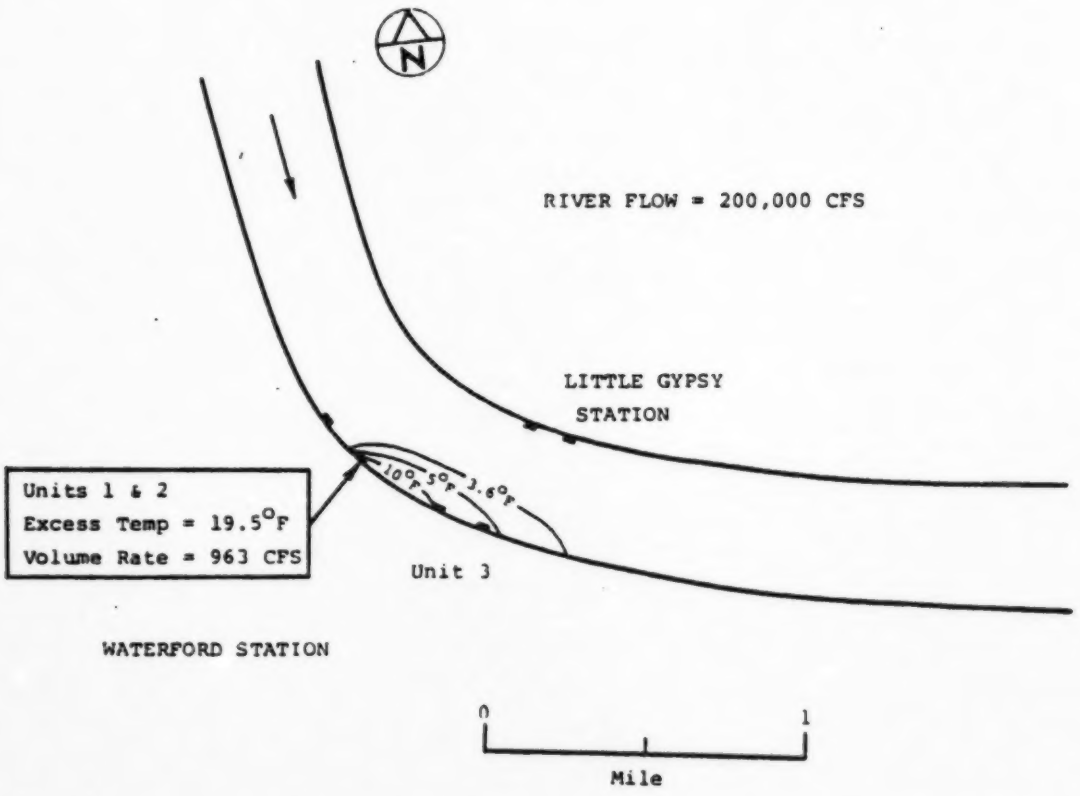

Fig. 7. Predicted Surface Isotherms for the Waterford 1 and 2 Station

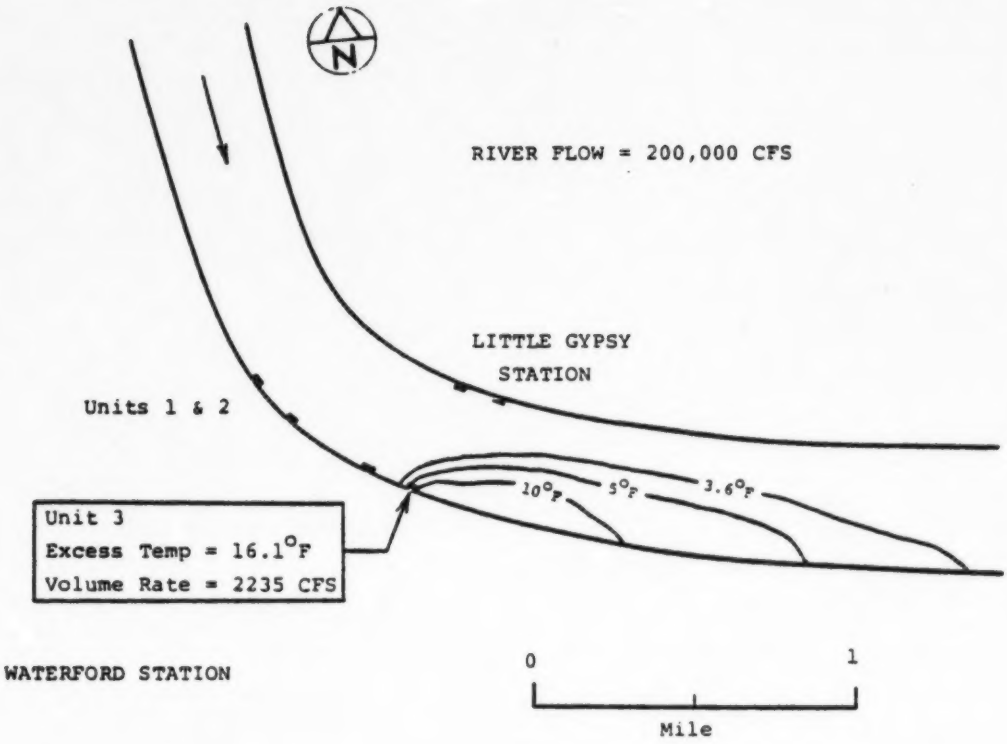

Fig. 8. Predicted Surface Isotherms for the Waterford 3 Station

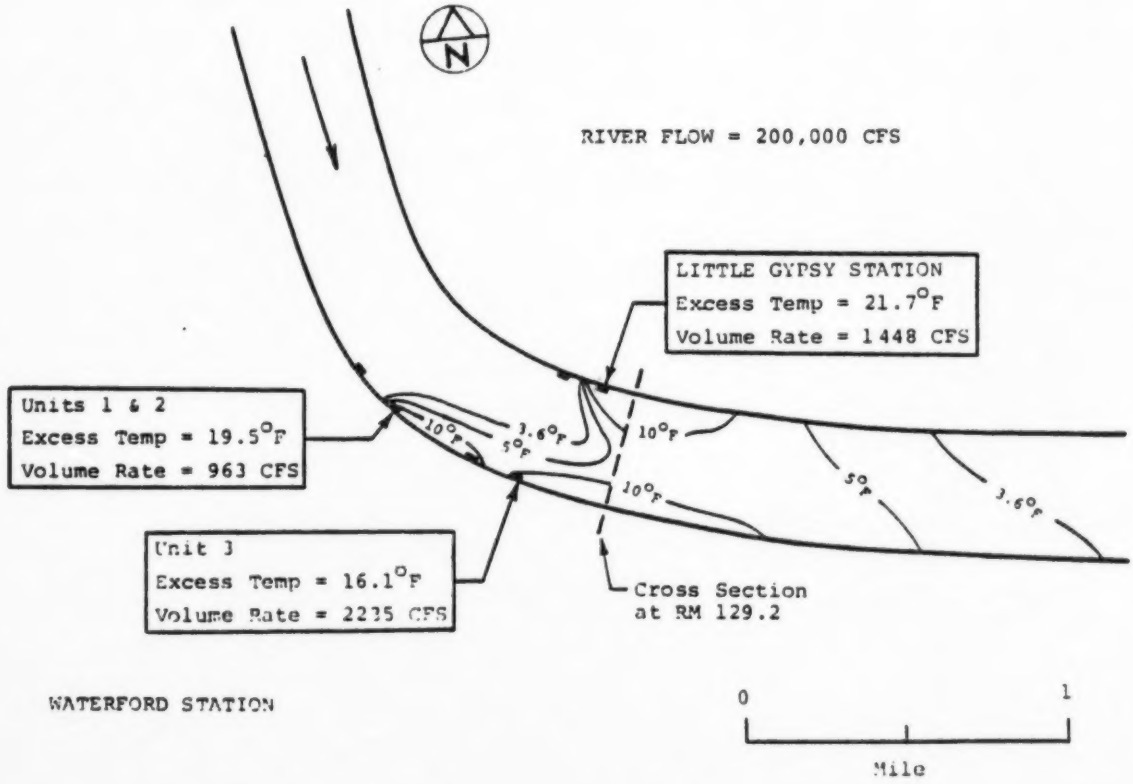

Fig. 9. Predicted Surface Isotherms for the Three Stations Combined

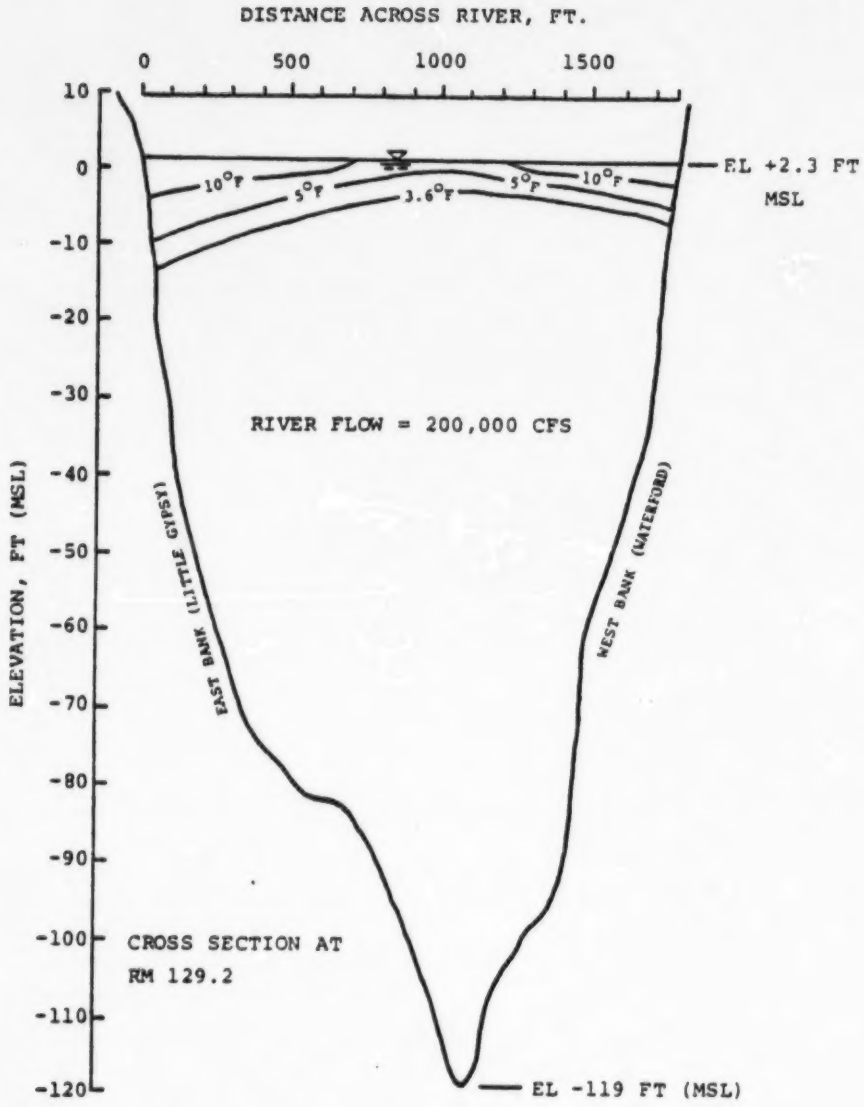

Fig. 10. Cross-Sectional View of Combined Isotherms

For the case with stations operating individually, the results presented in Table 2 and Figures 6 through 8 indicate that the predicted lateral spread of the plume from Little Gypsy station is greater than that from Waterford 3 station, despite the fact that Waterford 3 has a higher discharge velocity. Conversely, the longitudinal and vertical spreads of the plume produced by Waterford 3 are greater than those of Little Gypsy. These plume characteristics are present primarily as a result of the complex flow pattern around the river bend. A major portion of the river flow starts near the Little Gypsy side upstream of the river bend and then bears to the Waterford shore downstream of the river bend. This change of flow direction creates a high river flow region near the Waterford site and a low river flow region offshore of the Little Gypsy station. Consequently, the Little Gypsy surface jet discharge would displace the natural flow and extend itself laterally into the center region of the river whereas the high flow near the west bank of the river would serve to dilute and convect the heated water from Waterford 3 into

downstream portion of the river bend. The Waterford 1 and 2 thermal discharge would affect a smaller portion of the river than the Little Gypsy and Waterford 3 discharges. This is due partly to the low heat-release rate from the Waterford 1 and 2 station and partly to the high river flow rate on the Waterford side of the river.

The characteristics of the combined thermal field as presented in Table 2 and Figure 9 indicate that for typical low river flow conditions, the surface jet discharge from Waterford 3 would interact with the plumes produced by the Little Gypsy and Waterford 1 and 2 stations. Furthermore, the numerical results of the plume temperatures indicate that for the 5°F (2.8°C) isotherm, the combined surface area and volume of all three stations would be about 15 and 35 percent greater than the sums of the individual surface areas and volumes generated by each station. These results are to be expected simply because when individual plumes interfere, they form a single plume with reduced periphery and therefore a diminished ability to entrain ambient water. The combined plume will have to transport a greater distance longitudinally, covering a greater area to entrain sufficient water to reduce plume temperature to 5°F (2.8°C) above ambient.

The combined temperature field as depicted in Figure 9 also shows that heat recirculation between the Waterford 1 and 2 discharge and the Waterford 3 intake is expected to occur. By integrating the water temperature over the entire water column at the Waterford 3 intake, it was calculated that the water with temperature as high as 2°F (1.1°C) above ambient might be swept into the Waterford 3 intake. As the river flow increases, the recirculating tendency of the effluent would tend to be reduced and the plume from the Waterford 1 and 2 station would be expected to hug the downstream shore before it could reach the Waterford 3 intake.

The approximate location of the river cross section, where the combined temperature isotherms occupy the largest cross-sectional area, is denoted in Figure 9. The excess temperature distributions at the cross section are shown in Figure 10. The cross-sectional areas enclosed within 3.6°, 5°, and 10°F (2.0°, 2.8°, and 5.6°C) excess temperature isotherms were computed and the results are shown in Table 2. These results were further examined to ensure that the combined thermal plume distributions produced by the simultaneous operation of all three power stations at the Waterford site would be in compliance with Louisiana water quality criteria [1]. The predicted results indicated that for low river flow conditions, a mixing zone defined by the 5°F (2.8°C) excess temperature isotherm would only occupy a maximum of 7.3 percent of the river cross-sectional area, which is well below the allowable limit of 25 percent. As the river flow increases, the plume distributions on either side of the river would tend to remain separated from each other and the mixing zone area would be reduced.

6. SUMMARY AND CONCLUSIONS

This paper presents the results of an analysis of the mixing and interaction of thermal plumes in the Mississippi River resulting from individual and combined circulating water discharges from the Waterford 3, Waterford 1 and 2, and Little Gypsy power stations. The analysis was performed by using the Waldrop plume model, which numerically solves the three-dimensional equations of continuity, momentum, and energy for velocity and temperature and includes the effects of the river curvature. The computer program of the model was generalized to treat the multiple intake and discharge boundary conditions at the Waterford site and was verified for this study.

Numerical results of thermal plume temperatures obtained for typical low river flow and maximum station operating conditions predicted that the three thermal plumes would interact with one another and that heat recirculation between the Waterford 1 and 2 discharge and the Waterford 3 intake would occur. However, the overall results indicated that the combined temperature distributions would comply with the thermal standards established by the state of Louisiana.

REFERENCES

1. Louisiana Stream Control Commission, Water Quality Criteria, State of Louisiana, 49 pp., 1977.

2. W.R. Waldrop and R.C. Farmer, Thermal Effluents-River Interactions, Proc. XVIth Congress, International Association for Hydraulic Research, Vol. 3, Sao Paulo, Brazil, pp. 221-229, 1975.

3. W.R. Waldrop and F.B. Tatom, Analysis of the Thermal Effluent from the Gallatin Steam Plant During Low River Flows, Tennessee Valley Authority, Rept. No. 33-30, Norris, Tenn., June 1976.

4. M.S. Yalin, Mechanics of Sediment Transport, Pergamon Press, New York, 1972.

5. W.H. Munk and E.R. Anderson, Notes on a Theory of the Thermocline, J. Marine Res., Vol. 7, pp. 276-295, 1947.

6. J.D. Woods, Wave-Induced Shear Instability in the Summer Thermocline, J. Fluid Mechanics, Vol. 32, pp. 791-800, 1968.

ACKNOWLEDGMENTS

The author wishes to thank Dr. W.R. Waldrop and Mrs. Dalpha Stubblefield of the Tennessee Valley Authority for providing the computer program used in this study and for valuable discussions related to the program. Special thanks are due to the author's colleague, Mrs. Dee Wyman, for her excellent editorial work. This study was conducted under the auspices of the Nuclear Regulatory Commission.

PB82-228271

HYDRAULIC MODELING OF THERMAL DISCHARGES INTO SHALLOW TIDAL AFFECTED STREAMS

Howard D. Copp
Professor of Civil Engineering
Albrook Hydraulics Laboratory
Washington State University
Pullman, Washington, U.S.A.

N. S. Shashidhara
Hydraulic Engineer
Ebasco Services, Inc.
New York, New York, U.S.A.

K. R. Wise
Supervisor of Environmental Engineering
Washington Public Power Supply System
Richland, Washington, U.S.A.

ABSTRACT

A thermal-hydraulic model study was conducted to determine whether a submerged, multiport diffuser would induce buoyant plume dispersion that complied with water quality standards established for a tidal reach of river in western Washington state. Certain tide/river flowrate combinations create conditions under which dispersion is least efficient and will require special operations of power plants that create the buoyant plumes. This paper describes model tests of the tidal conditions and plant design specifically for waste heat disposal.

1. INTRODUCTION

The Washington Public Power Supply System is constructing two nuclear fired power plants near Aberdeen, Washington, approximately 20 miles above Grays Harbor, Fig. 1. A natural draft cooling tower will be an integral part of each plant to provide condenser water cooling. Makeup water will be supplied to the towers from a Ranney pumping system; blowdown from the towers will pass through supplemental cooling facilities for temperature reduction before discharging into the Chehalis River. A multiport diffuser will deliver the blowdown water to the river.

Figure 2 illustrates the diffuser design and placement in the river. Blowdown from each power unit's tower will be, nominally, 2,700 gallons per minute or 6.0 cubic feet per second. The diffuser is designed for two unit operation. The diffuser site is subject to mean monthly flowrates varying from 780 cfs in August to over 16,000 cfs in January. River depths vary with position in the stream up to 9.5 ft at about 6,000 cfs, the average annual flowrate, Fig. 2. Velocities at this flowrate average about 2.5 feet per second. The hydraulic characteristics at the diffuser site are subject to tidal influences only at relatively low river flowrates.

The Washington State Department of Ecology has classified the Chehalis River as having excellent water quality. Accordingly, the Washington Water Quality Standards stipulate the following with regard to temperature:

> "...water temperatures shall not exceed 18° Celsius...due to human activity. Temperature increases shall not, at any time, exceed $t = 28/(T + 7)$....

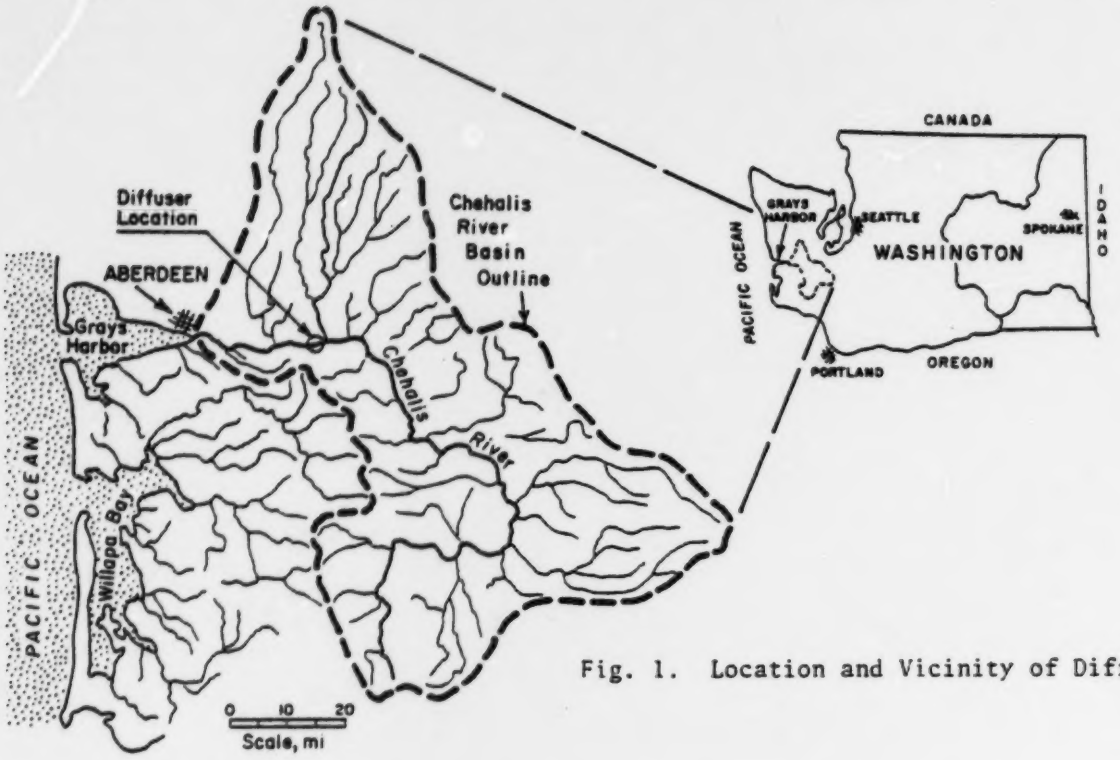

Fig. 1. Location and Vicinity of Diffuser

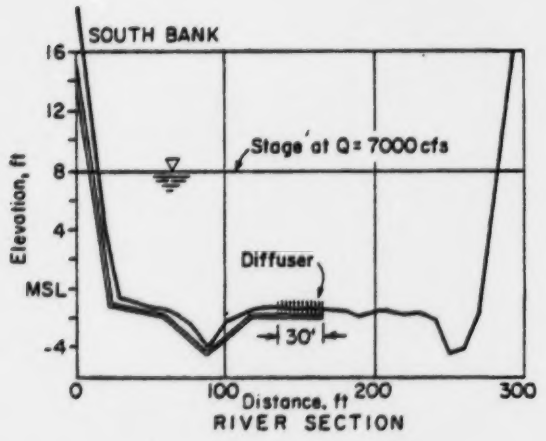

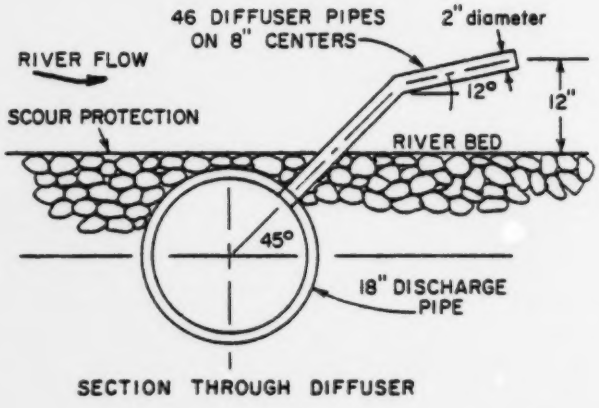

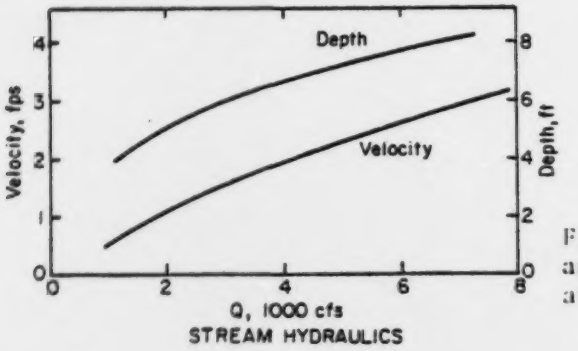

Fig. 2. Diffuser Geometry and River Characteristics at the Diffuser

When natural conditions exceed 18° Celsius...no temperature increase will be allowed which will raise the receiving water temperature by greater than 0.3° Celsius.

For the purposes hereof, "t" represents the permissive temperature change across the dilution zone; and T represents the highest existing temperature in this water classification outside of any dilution zone" (Wash. State Dept. of Ecology, 1977).

Applying these criteria to monthly stream temperatures shown in Column (2) of Table 1 results in the permissible temperatures outside a dilution zone shown in Column (3). In order to comply with the temperature requirements, the difference between diffuser flow temperature and ambient river temperature must be less than those t values or a dilution zone must exist. Anticipated temperatures of the diffuser flow are shown in Column (4); except during May, temperature differentials always exceed the state standards so a dilution zone was proposed.

Numerical models are available to study mixing phenomena in instances similar to this Chehalis River setting and one was used to study this case. The stream velocities, particularly during tides, and the free surface characteristics are not properly treated by the model at more than a short distance downstream from the diffuser ports. The Washington State Energy Facility Site Evaluation Council, which authorizes operation of these two and other power projects, required definitive assessment of thermal loadings. Therefore, a physical model study was undertaken to examine the diffuser performance under a variety of anticipated power plant and river conditions. Warm water plume dispersion was examined in the near vicinity of the diffuser as well as farther removed therefrom to assess diffuser performance in relation to Washington State Water Quality Standards.

Table 1. Water Quality Standards for Temperature

Month	T*/ Outside Dilution Zone (Ambient Temp., T_a) (°C)	Permissible Temp. Rise (°C) $t = \frac{28}{T+7}$	Diffuser Flow Temp., T_j (°C)
(1)	(2)	(3)	(4)
Jan	0.0	4.0	10.3
Feb	1.1	3.5	9.7
Mar	3.9	2.6	8.6
Apr	5.0	2.3	8.9
May	10.0	1.6	10.8
June	11.1	1.5	13.1
July	14.4	1.3	16.1
Aug	15.6	1.2	17.5
Sept	11.7	1.5	18.3
Oct	5.0	2.3	17.5
Nov	4.4	2.5	15.3
Dec	0.6	3.7	12.8

*Values are those which have been exceeded 99% of the time over a 12-year duration record.

2. THE HYDRAULIC MODEL

2.1 Similitude

The hydraulic model used in the study is shown in Fig. 3; it represented a 1,280-ft reach of the river at a scale of 1:12. A detailed discussion of similitude requirements is beyond the scope of this paper.* However, thermal-hydraulic models will simulate prototype mixing phenomena whenever gravitational, viscous, and inertial forces in the model are proportional, one to another, to reflect properly that proportioning in the prototype. This will not necessarily insure that heat transfer processes all will be simulated precisely; transfer through the river surface to the atmosphere, for example, requires atmospheric conditions to be simulated. However, this and certain other processes contribute only in a relatively minor amount to plume characteristics likely to affect stream ecology that were of interest in this study.

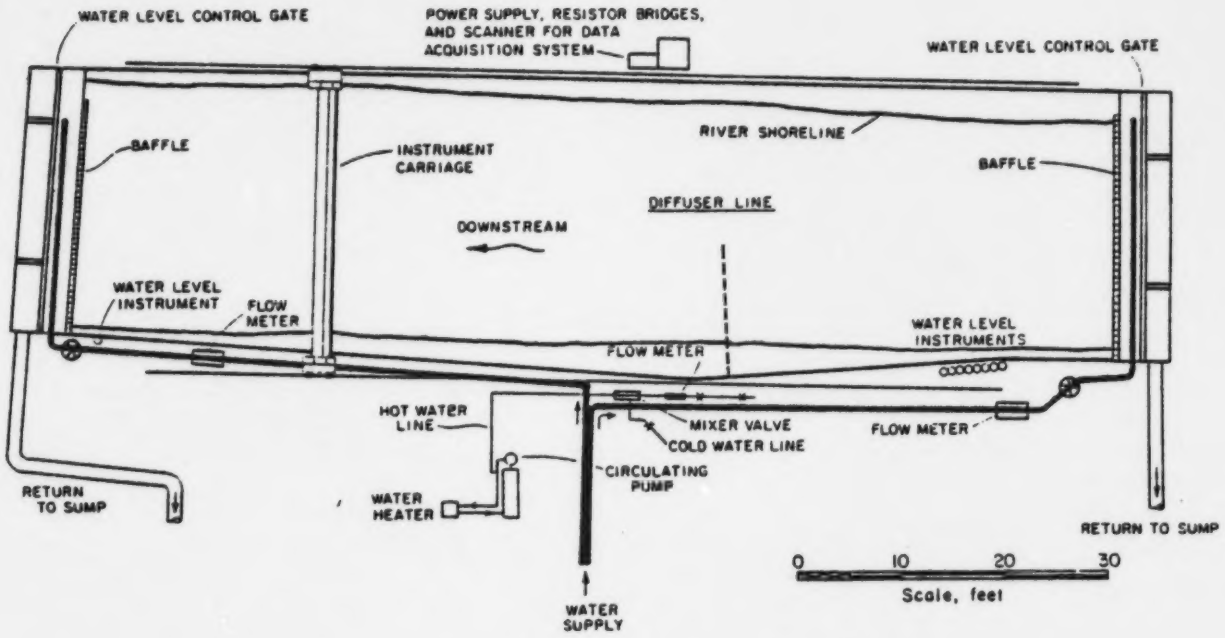

Fig. 3. Hydraulic Model and Apparatus Layout

The densimetric Froude number, F_D, encompasses the gravitational and inertia forces and this was used to simulate diffusion by gravity, i.e.,

$$(F_D)_m = (F_D)_p$$

or

$$\left[\frac{u}{\sqrt{g\frac{\Delta\rho}{\rho}\ell}}\right]_m = \left[\frac{u}{\sqrt{g\frac{\Delta\rho}{\rho}\ell}}\right]_p \qquad (1)$$

*See Koh et al. (1974) for discussions of similitude considerations for thermal-hydraulic modeling.

where m and p refer to model and prototype, respectively, g is the acceleration of gravity, ℓ is a linear dimension, and other parameters are as defined in Fig. 4. Manipulation of Eq. (1) results in

$$u_{j_r} = \sqrt{(g\frac{\Delta\rho}{\rho})_r d_r} \qquad (2)$$

for the diffuser, d being its port diameter and r refers to the ratio of prototype to model quantities.

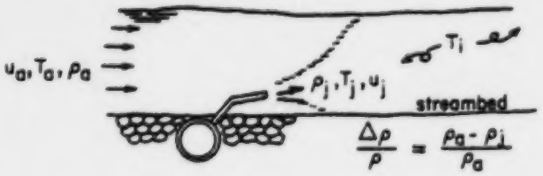

Fig. 4. A Definition Sketch

Turbulent mixing was simulated through the Reynolds number, $\mathbb{R}$. An analytic procedure similar to that above, initiated from $\mathbb{R}_m = \mathbb{R}_p$, results in

$$\mathbb{R}_{j_r} = \frac{u_{j_r} d_r}{\nu_r} \qquad (3)$$

for the diffuser flow. Inserting Eq. (2) into (3)

$$\mathbb{R}_{j_r} = \frac{\sqrt{(g\frac{\Delta\rho}{\rho})_r} d_r^{3/2}}{\nu_r} \qquad (4)$$

where ν is kinematic viscosity.

A value of $\mathbb{R}_{j_r}$ in Eq. (4) can be established from known prototype values and those that earlier research [see, for example, Koh et al. (1974), Jirka and Harleman (1973), and Ackers (1967)] has found appropriate for modeling. $\mathbb{R}_{j_r}$ had to be at least 69 for simulation of the Chehalis River situation. Eq. (4) required a model scale ratio, d_r, of 16 or less. The selected scale ratio of 12 insured fully turbulent flows in the model diffuser and further analyses indicated model streamflows also would be fully turbulent.

Tests were made with the model river in steady state flow, with no river flow (representing transition between ebb and flood flows), and under tidal conditions. Some 250 thermistors measured temperatures in the stream. Test procedures and instrumentation are described in detail by Copp (1979).

2.2 Analysis of Model Test Results

Roberts (1977) suggests two parameters which are useful in evaluating thermal plume dispersion. One is a momentum flux ratio

$$V = \frac{u_a q_a}{u_j q_j} \qquad (5)$$

and the other is a modified densimetric Froude number

$$\mathbb{F} = \frac{u_a^3}{\frac{\Delta\rho}{\rho} g q_j} \qquad (6)$$

where q is discharge per unit width (cfs/ft), and other parameters are as defined earlier. The plume itself can be identified by contour lines of constant values of dilution factors, D.F., where

$$D.F. = \frac{T_j - T_a}{T_i - T_a} \qquad (7)$$

where T is temperature (see Fig. 4). T_i is temperature at any point i in the stream downstream from the diffuser. With T_a and T_i fixed, large dilution factors signify considerable mixing has occurred. Contour "maps" of dilution factors illustrate plume extent and the spatial rate at which mixing occurs.

Model tests of steady state river flows produced empirical relationships between V, F, and the size and location of dilution contours in the form

$$p = kV^m F^n \tag{8}$$

p being contour parameters of area encompassed, distance from the diffuser to the area's centroid, and contour length in the downstream direction, and k, m, and n being constants having unique values for each parameter, p, and for each of three stream depths. Using these relationships, plume extent was mapped for given stream and diffuser flow conditions; Fig. 5 shows one such mapping. The plumes were quite similar, for all steady state flows examined, to that in Fig. 5. Under tidal conditions, u_a varies with time so V and F cannot be used.

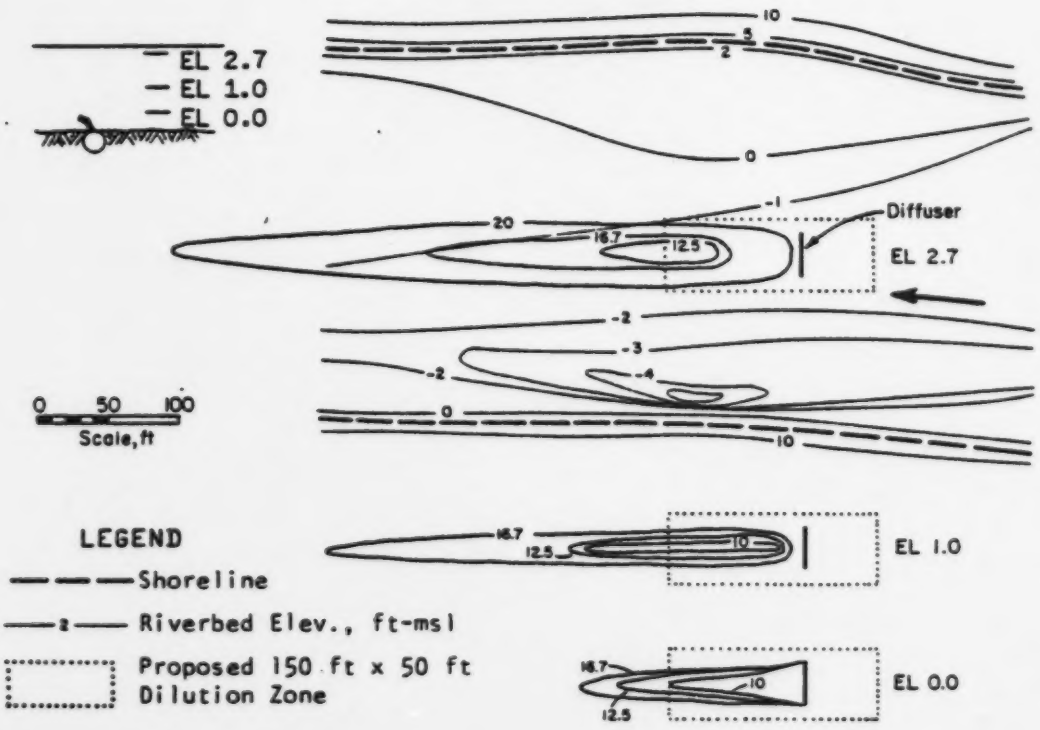

Fig. 5. Dilution Contours for August, Two-Unit Flow
(Q_R = 418 cfs; T_a = 15.6°C [60°F]; Q_D = 12.57 cfs, T_j = 17.5°C [63.5°F])

3. MODEL TESTS OF TIDES

3.1 Selection of Tidal Conditions

Dilution of the plume under stagnation conditions ($u_a = 0$) was significantly slower than under steady state flows and the plume extended over a much broader area because streamflow turbulence did not significantly contribute to entrainment and mixing. Upstream directed river velocities, as would occur when flow reversals exist during tides, may generate more rapid dilution than with stagnation because turbulence would be greater. On the other hand the plume may "fold" back on itself--once during flow reversal at flood tide and a second time when velocities again commence in a downstream direction during ebb tide. Heat "build-up" then might aggravate the dilutions. Several scenarios were hypothesized based on steady state and stagnation model tests. None were entirely useful in assessing plume behavior so model tests of tidal activity were conducted.

Three tidal events were selected for study on the model; these were selected on the basis of joint probability of occurrence of the tide and river flowrate (Ebasco, 1978) and were:

Case	Stream Flowrate at Diffuser Site (cfs)	Tide Amplitude at Aberdeen, Wash. (ft)
1	440	5.6
2	570	4.8
3	700	5.6

These events are indeed rare occurrences. Case 1 has a probability of occurrence of about once in five years. Cases 2 and 3 will occur, on the average, about 1.5 and 3 times per year, respectively.

Various tidal events, including the three cases above, were simulated with a numerical model of gradually-varying, open-channel flow to determine water stages and mean flow velocities at the diffuser location as boundary or operating conditions for the physical model. Figure 6 shows simulated results for the above three cases. The magnitudes and duration of upstream-directed velocities and the duration in which velocities are exceedingly small (between -0.1 and +0.1 fps) were both hypothesized to be significantly influencial in plume dispersion. Consequently the three cases selected for study are those that were felt to create a combination of low streamflow and simultaneous tidal influences representing critical conditions for plume dispersion.

Table 2 shows real time and model river stages and mean velocities for the Case 2 event. Real time data are those determined from the numerical model. Model time is real time divided by $\sqrt{L_T}$ (L_T = model scale = 12) which corresponds to the ordinary Froude Law of Similitude. Model flowrates include quantities entering (or leaving) temporary storage as a result of water level variation. Thus, during flood tide, model flowrates exceed those of real time and during ebb they are less.

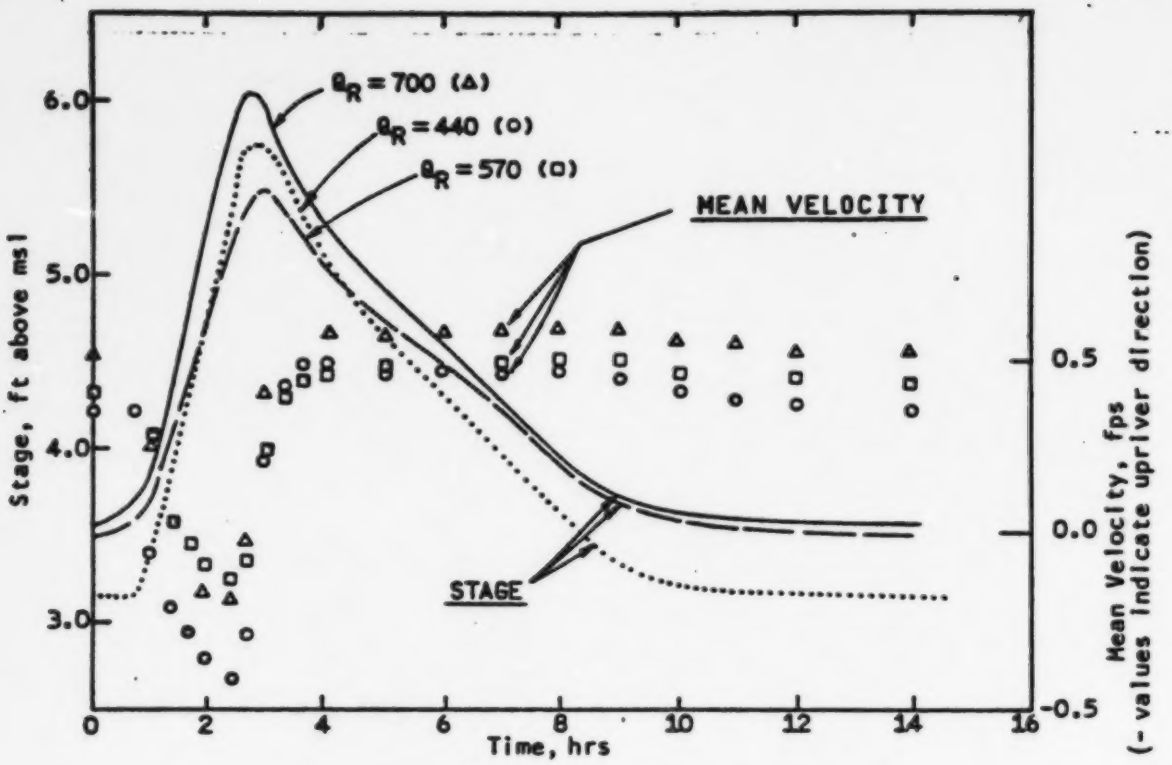

Fig. 6. Tide Characteristics at Diffuser Site

Table 2. Tide Data for Q_R = 570 cfs and a 4.8 ft-msl Tide at Aberdeen (see Fig. 6)

Real Time (hr-min) (1)	Water Surface Elev. (ft-msl) (2)	Net[a] River Flowrate (cfs) (3)	Net[a] Average Velocity (fps) (4)	Model Time (min) (5)	Water Surface Elev. (ft-msl) (6)	Flowrate[b,c] From Upstream (cfs) (7)	Flowrate[b,c] From Downstream (cfs) (8)
0	3.49	571	0.43	0	3.49	571	0
				5	3.50	560	0
				10	3.52	534	0
				15	3.58	507	0
1-00	3.65	359	0.26				
				20	3.80	512	0
				22	3.92	407	0
1-20	4.01	-21	-0.01	23	3.98	367	0
				25	4.12	0	417
1-40	4.36	-15	-0.01				
				30	4.43	0	420
2-00	4.72	-128	-0.08	35	4.74	0	469
2-20	5.09	-223	-0.13	40	5.05	0	513
				45	5.32	0	508
2-40	5.39	-142	-0.08				
				47	5.42	0	334
				48	5.45	0	237
3-00	5.47	444	0.24	50	5.48	164	0
				55	5.41	335	0
3-20	5.34	721	0.40	60	5.28	550	0
3-40	5.18	775	0.44				

[a]Negative values indicate upstream direction.

[b]Values shown are actual river quantities; model quantities are 1/499 times values shown.

[c]Flowrates supplied to the model.

3.2 Test Procedure and Results

Tides were created by varying model flowrate and water surface elevation as shown in Table 2 for Case 2. Diffuser flowrate and temperature were set at predetermined values after which the diffuser flow was diverted into the stream. After about 25 minutes the plume had reached equilibrium; the tide cycle then began. When flood tide commenced (at real time of about 15 minutes for Case 2), flowrate from the upstream end of the model began decreasing. The upstream control gate on the model (see Fig. 3) was raised to prohibit outflow from that end of the model; all outflow passed over the downstream gate which was slowly raised to increase river surface levels as time advanced.

Shortly after upstream-directed river velocities began to occur, flow from the upstream end of the model ceased and that from downstream began increasing. At this time (25 minutes model time for Case 2), the downstream gate prohibited outflow and the upstream gate was slowly adjusted to create appropriate river surface levels. Eventually downstream velocities began to occur again (during ebb tide); accordingly, flow was again introduced from upstream and river levels were maintained by controlling the downstream gate.

Model tests reproduced an abbreviation of complete tides as illustrated in Fig. 6. Approximately 6 of the 14 hours in each case were occupied by essentially steady state flow which did not influence the unsteady state plume dispersion. This is demonstrated later.

Figure 7 illustrates dilution contours at various times during the 5.6 ft-msl tide and river flowrate of 440 cfs. Flood tide velocities here reached nearly 0.5 fps--the highest of the three cases tested. At 1 hour and 10 minutes after onset of the tide, the dilution contours at the diffuser level (EL A) displayed a shape somewhat foreshortened and wider than those in Fig. 5 because upstream-directed river velocities had begun. During the next 15 to 20 minutes, stream velocities forced the plume laterally and upstream; low dilutions were centered around the right end of the diffuser.

At 2 hours and 18 minutes, upstream-directed velocities were at their peak magnitude; this is evidenced by the plume extent near the water surface (EL C). At lower levels, the plume was more confined, however, indicating relatively strong buoyancy, Peak stage was reached at 2 hours and 53 minutes but stream velocities had reversed a second time, i.e., toward downstream again. The plume also reversed its direction a second time. By 3.5 hours, the plume appearance returned to the shape much the same as shown in Fig. 5.

Figure 7 also shows the model tide that was created during the tests. It conforms well with the computed prototype tide. Measured model velocities were at insufficient locations to compute mean values but available data suggests the model velocities conformed exceedingly well with prototype counterparts.

The abbreviated model tide was indeed appropriate since the plume returned to essentially steady state patterns after 3.5 hours. The concern of plume "fold back" proved to be correct but this did not result in extensive heat build-up. Some localized warm spots existed near the diffuser but these were short lived.

The second tidal situation, i.e., 570 cfs stream flowrate and 4.8 ft-msl tide height, produced rather small upstream velocities. Peak magnitudes are less than 0.20 fps; velocities are within the +0.1 to -0.1 fps range for less than one-half hour during the first flow reversal and for about an equal duration during a second reversal. The first reversal occurs at about 1.5 hours time (see Fig. 6). Model tests of these conditions showed that the plume was

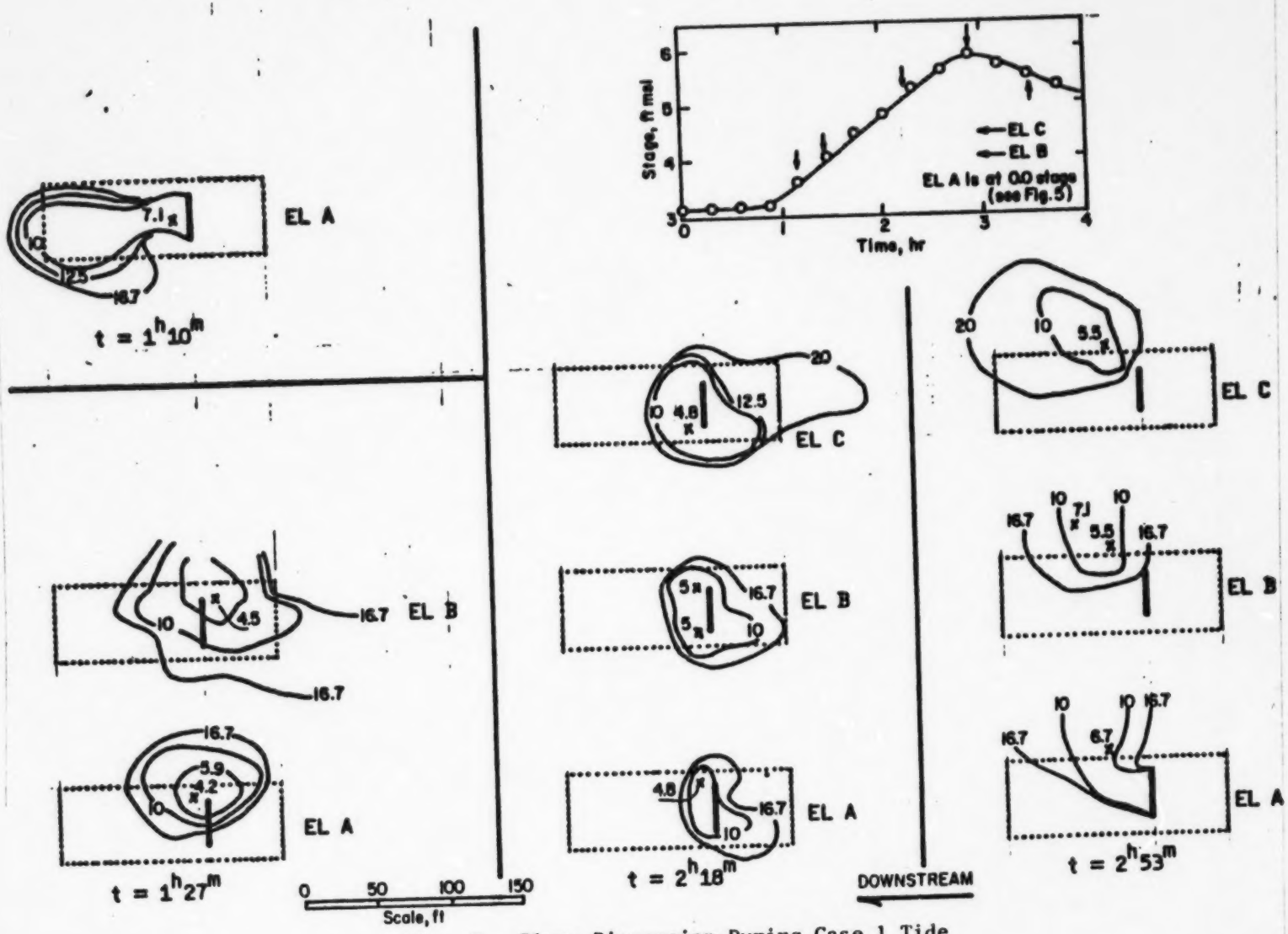

Fig. 7. Plume Dispersion During Case 1 Tide
(Contour numbers are dilution factors.)

affected only slightly during the first 90 minutes. Thereafter, however, the plume began to spread rather widely, Fig. 8.

At 2 hours, the plume spread from shore to shore in surface layers. Relatively warm zones were concentrated near the diffuser. During the next 30 minutes, these zones grew warmer and the plume in surface layers reached its maximum upstream travel. Thereafter, the plume returned to its downstream orientation--reaching steady state conditions after about 3 hours.

The plume spread rather broadly in this case because the velocities were small for some time. Its areal extent and location were much the same as those observed during tests with $u_a = 0$. Localized warm spots occurred here as in the first case and were quite confined near the diffuser.

A tide of 5.6 ft at Aberdeen and 700 cfs river flowrate creates peak stage height higher than either of the other cases but velocities during flood tide, in the upstream direction, are no greater than at the lower flows and the duration when velocities are less than 0.1 fps (in either direction) is least of the three cases.

These conditions began to affect plume dispersion in the surface layers after about 45 minutes. Figure 9 shows the plume thereafter. Near peak tide height, the plume had spread rather widely near the surface--more so than in Case 2. The warmer zone was confined near the diffuser. After about 2 hours and 45 minutes, the plume was confined to definite downstream, middle-of-the-river orientation.

The objective of the model tests was to determine if the diffuser performance would satisfy the water quality standards for temperature. Table 1 shows that $T_j - T_a$ is greater than the permissible temperature rise, t, in all months except May. Consequently, a dilution zone was proposed in which t could exceed those values in Table 1. The dilution zone was 50 ft wide by 150 ft long with 100 of the 150 ft downstream from the diffuser. This zone is shown as a dotted rectangle in Figs. 5. 7, 8, and 9.

Table 3 repeats Table 1 but Column (5) has been added which shows minimum required dilution factors for each month where

$$D.F._{min} = \frac{T_j - T_a}{(T_i - T_a)_{max}} = \frac{T_j - T_a}{t} \qquad (9)$$

Assuming a dilution zone is adopted, dilution factors outside the zone must be greater than $D.F._{min}$ to comply with the water quality standards. October presents the critical condition; if dilution factors of 5.4 or greater occur outside the dilution zone, compliance will be achieved.

All of the anticipated steady state flow conditions will comply with the standards with the dilution zone adopted. However, tidal conditions forced the plume out of the dilution zones during short time intervals when dilution factors were less than 5.4. These occurred at 1 hour and 27 minutes in Case 1 (Fig. 7) and at 2 hours and 46 minutes in Case 2 (Fig. 8). In Case 3 (Fig. 9), a 5.0 dilution factor contour approached the edge of the dilution zone. In each instance, these conditions arose just as flow reversals (either the first or second one) occurred.

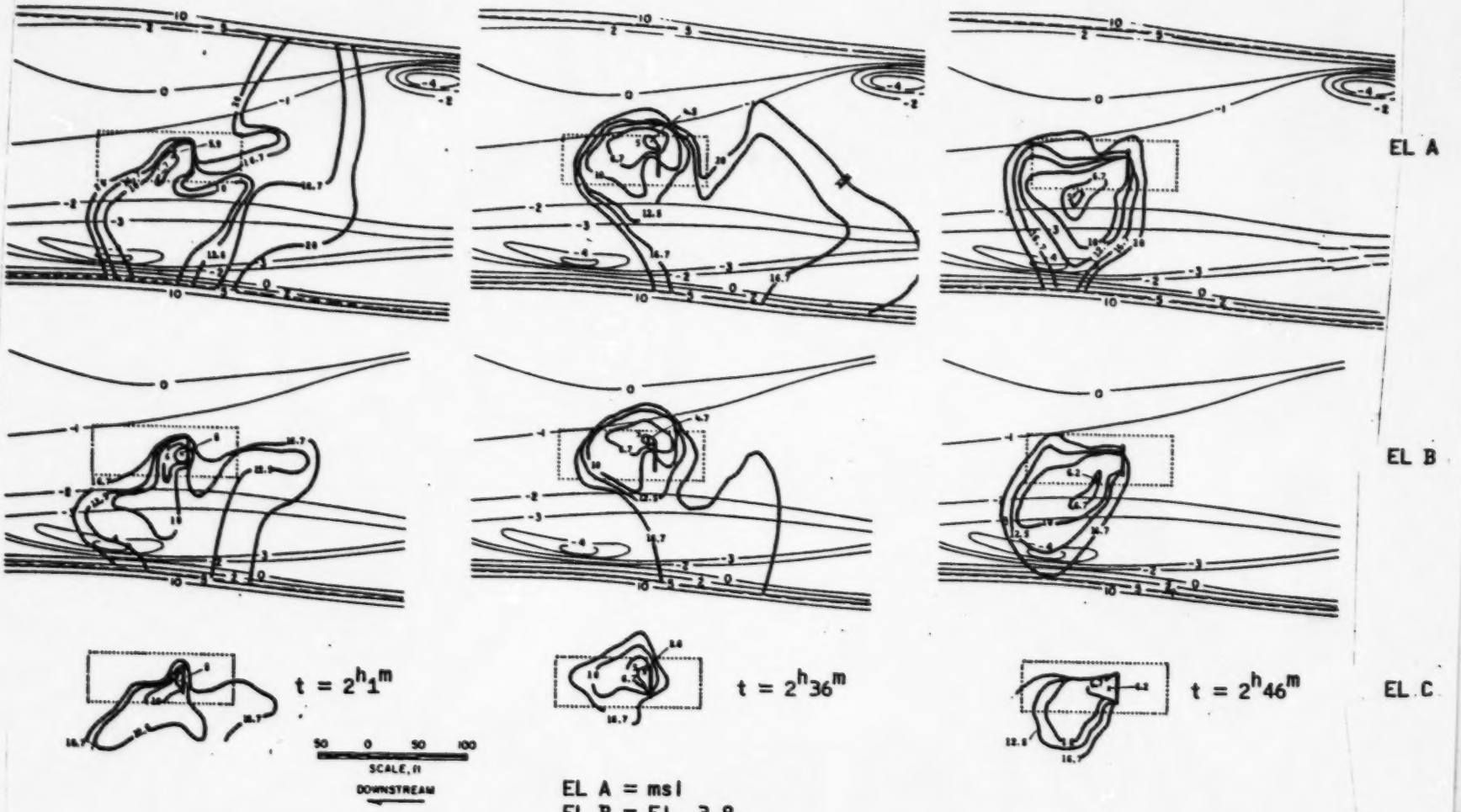

Fig. 8. Plume Dispersion During Case 2 Tide
(Contour numbers are dilution factors.)

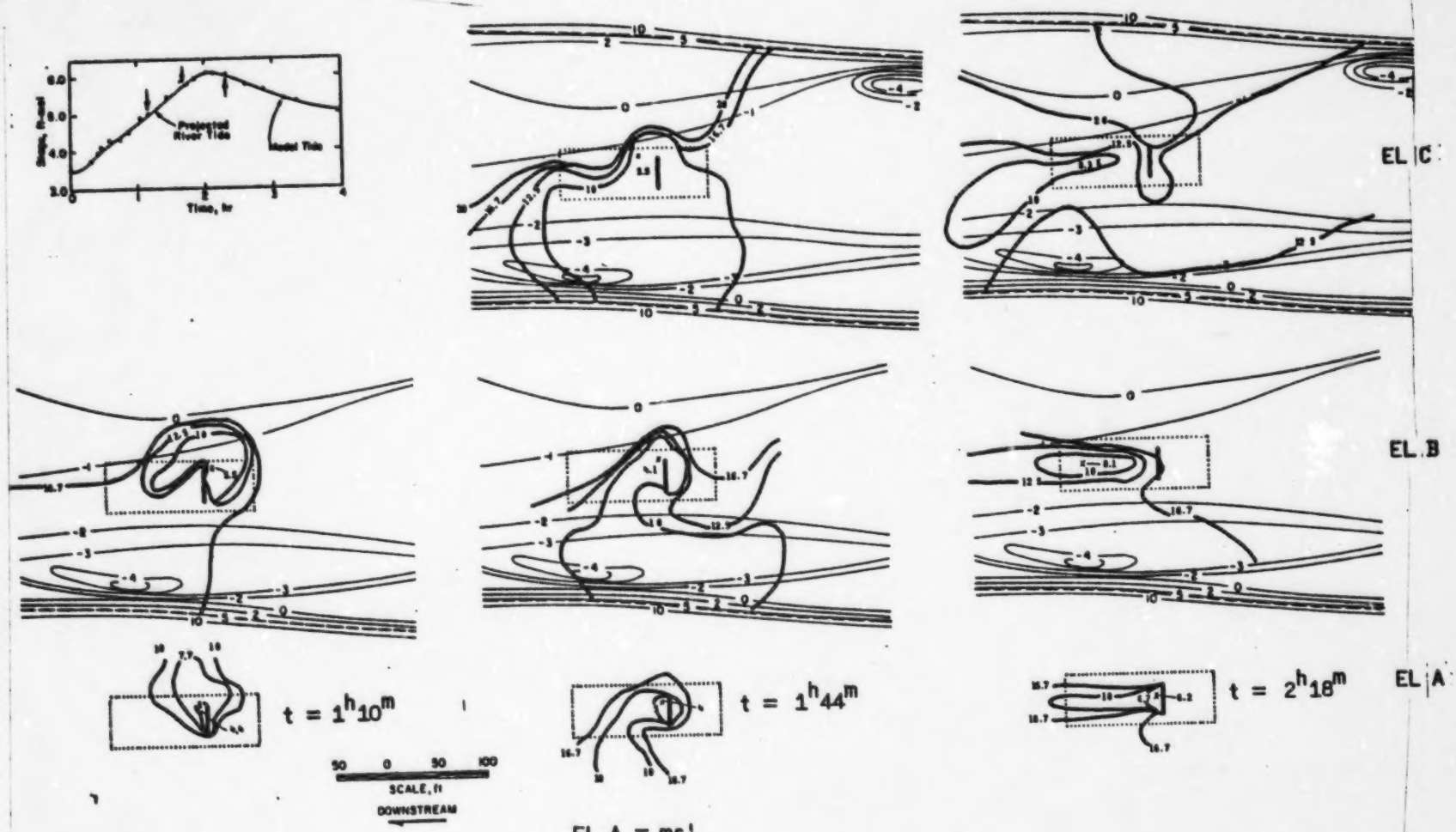

Fig. 9. Plume Dispersion During Case 3 Tide
(Contour numbers are dilution factors.)

Table 3. Dilution Criteria

(1) Month	(2) Ambient Temp., T_a (°C)	(3) Permissible Temp. Rise $t = \frac{2S}{T_a + 7}$ (°C)	(4) T_j (°C)	(5) "Required Minimum" Dilution Factor $\frac{(4)-(2)}{(3)}$
Jan	0.0	4.0	10.3	2.6
Feb	1.1	3.5	9.7	2.5
Mar	3.9	2.6	8.6	1.8
Apr	5.0	2.3	8.9	1.7
May	10.0	1.6	10.8	0.5
June	11.1	1.5	13.1	1.3
July	14.4	1.3	16.1	1.3
Aug	15.6	1.2	17.5	1.6
Sept	11.7	1.5	18.3	4.4
Oct	5.0	2.3	17.5	5.4
Nov	4.4	2.5	15.3	4.4
Dec	0.6	3.7	12.8	3.3

4. MANAGEMENT TOOL APPLICATION

Difficulty sometimes arises in making the transition from scientific study to decision making. In this case, the quasi-judicial administration board, the State Energy Facility Council, was presented with model result reports and expert witness testimony. Council members also visited the laboratory and observed demonstration tests. With the understanding of river behavior provided, the council established discharge permit conditions which considered both the river's fishery resource and the plant's operation.

These conditions required the discharge temperature to be such that the applicable water quality standards for temperature (those referred to earlier) will be complied with at the edge of the dilution zone. Also, when ambient river temperatures are 20°C or less, the temperature of the effluent at the point of discharge is to be 20°C or less and may not exceed the ambient river temperature by more than 15°C. Whenever ambient river temperatures are greater than 20°C, the temperature of the effluent at the point of discharge is to be equal to, or less than, the ambient river temperature.

The dilution zone was permitted with its volume being defined by: a) the water surface and the bottom of the river, b) 50 ft upstream from the diffuser and 100 ft downstream therefrom, and c) 25 ft on both sides of the midpoint of the diffuser. Additionally, discharge flow must cease if the river velocity in the downstream direction drops below 0.3 fps. These creative conditions can be related quite closely to fisheries criteria. The Supply System has responded to the permit conditions with facility changes and acceptance of discharge operation procedures more complex than usual. The cooling tower basins are slightly deeper than normal to provide needed storage to accommodate the river velocity threshold condition. Because the water supply is by Ranney Collectors from an aquifer, the intake water is to be used to cool (counterflow heat exchanger) the discharge.

5. CONCLUSIONS

The hydraulic model proved to be a reliable tool to aid in assessments of diffuser performance and plume dispersion under steady state river flows and unsteady state tidal influences. The model simulated the tidal phenomena extremely well and demonstrated the plume behavior equally well.

Critical dispersion conditions during the tide events occurred immediately after stream velocities reversed their direction as flood tide began as well as during the transition between flood and ebb tide. Velocity magnitudes at these time intervals were insufficient to generate turbulence for mixing or to carry the heat away from the diffuser.

Physical modeling has played an important heat management role in that it not only developed knowledge of physical system behavior but assisted in the presentation of that knowledge in a believable form to the decision maker. A working, believable model was instrumental in developing permit conditions which protect aquatic resources while providing considerable operational flexibility.

ACKNOWLEDGMENT

The authors wish to acknowledge the Washington Public Power Supply System for its assistance in executing the thermal-hydraulic model study which provided the basis for this paper and for its permission to prepare the paper.

REFERENCES

1. Ackers, P., "Modeling of Heated-Water Discharges," Chap. 6 in Engineering Aspects of Thermal Pollution, Vanderbilt University Press, 1969.

2. Copp, Howard D., "Thermal-Hydraulic Model Studies of Buoyant Effluent Discharge Through a Submerged Multiport Diffuser," Tech. Rept. No. HY-2/79, Albrook Hydraulics Laboratory, Washington State University, Pullman, September, 1979.

3. Ebasco Services, Inc., "Hydrological Characteristics and Analytical Modeling of the Chehalis River in the Vicinity of Washington Public Power Supply System Nuclear Projects No. 3 and 5," NPDES Modification Request, Summary Report Appendix A, December, 1978.

4. Jirka, Gerhard and D.R.F. Harleman, "The Mechanics of Submerged Multiport Diffusers for Buoyant Discharges in Shallow Water," Rept. 169, R.M. Parsons Laboratory, Massachusetts Institute of Technology, Cambridge, March, 1973.

5. Koh, Robert C.Y., N. H. Brooks, E. J. List, and E. J. Wolanski, "Hydraulic Modeling Outfall Diffusers for the San Onofre Nuclear Power Plant," Rept. KH-R-30, W. M. Keck Laboratory, California Institute of Technology, Pasadena, January, 1974.

6. Roberts, P.J.W., "Dispersion of Buoyant Waste Water Discharges from Outfall Diffusers of Finite Length," Rept. KH-R-35, W. M. Keck Laboratory, California Institute of Technology, Pasadena, March, 1977.

7. Washington State Department of Ecology, "Washington State Water Quality Standards," December 19, 1977.

PB82-228289

MATHEMATICAL MODELING OF WASTE HEAT DISCHARGE IN LARGE WATER BODIES

Akshai K. Runchal
Analytic & Computational Research, Inc.
Los Angeles, California 90066, U.S.A.

D. Ian Austin
Dames & Moore
Los Angeles, California 90024, U.S.A.

ABSTRACT

This paper presents the mathematical framework, development, validation and application of a mathematical model for simulation of the hydrodynamics and water quality of large-scale water bodies. The model is based upon depth-average shallow water equations and is embodied in two computational modules called TIDAL2 and WQUAL2. The model is applicable to all large-scale, nonstratified, shallow water bodies subject to tidal influences.

The model has been tested using a number of problems with known analytic solutions and using field data. Among the applications of the model, have been the hydrodynamic and thermal modeling of the Persian Gulf, water management study for Kaneohe Bay, Hawaii, hydrodynamic and water quality modeling of St. Johns River near Palatka, Florida and, fresh water influx study in the vicinity of Prudhoe Bay, Alaska. Selected results from these studies are presented.

1. INTRODUCTION

There is an increasing social awareness that the resource 'water' cannot be considered separately from its 'quality'. This awareness is resulting in stricter controls on the disposal of wastes, be they in the form of used water or toxic chemicals. In order to study the existing, and predict future, impacts on the environment of the industrial, urban and agricultural wastes, the need has arisen for large scale numerical models. The present paper describes the mathematical framework of such a model, developed for studies involving large water bodies and illustrates its application in three modeling studies. In two of the studies, the availability of field data allowed extensive model calibration.

2. MATHEMATICAL PRINCIPLES

The mathematical model must describe the hydrodynamics of the water bodies and the characteristics of the parameters defining water quality. Assuming that the water quality has a

negligible influence on the hydrodynamics, an assumption valid except in the case of the most extreme pollution, allows the governing equations of each component to be developed separately. This deccupling is desirable from both mathematical and computational considerations of simplicity and economy. Each component is realized by a computer code, named TIDAL2 and WQUAL2 (Runchal 1978).

The hydrodynamic component of the model, TIDAL2, is based on the depth-averaged shallow water equations (Stoker 1957). These equations make the assumptions of no significant vertical accelerations or vertical stratification, conditions generally met in water bodies such as bays and wide rivers. The governing equations are given by the continuity equation:

$$\frac{\partial \eta}{\partial t} + \frac{\partial (Hu)}{\partial x} + \frac{\partial (Hv)}{\partial y} = 0,$$

and the momentum equations where the equation in the x direction is given by:

$$\frac{\partial u}{\partial t} + \frac{u\partial u}{\partial x} + \frac{v\partial u}{\partial y} = C_w \frac{w^2}{h} \cos\theta - g\frac{\partial \eta}{\partial x} - \frac{1}{\rho}\frac{\partial Pa}{\partial x} + \Omega v - Cf \left|v\right| \frac{u}{h}$$

and an equivalent expression exists in the y direction.

Two auxiliary relations which accompany the above equations are:

$$\eta = H - h \quad , \text{ and}$$

$$C_w = C_2 + C_3 \, (\text{MAX} \, (0., \, (1 - W_o/W)^2))$$

The notation used in the above equations is as follows:

C_1	is a bottom stress coefficient;
C_W, C_2, C_3	are wind stress coefficients;
g	is the coefficient of gravitational acceleration
h	is the depth of water below a horizontal datum plane;
H	is the total depth of water;
P_a	is the atmospheric pressure;
t	is the time coordinate;

u.v	are the "depth-averaged" horizontal velocity components in the directions of x and y respectively;
W	is the wind velocity;
W_o	is a reference wind velocity;
x,y	are a set of mutually orthogonal coordinates in the horizontal directions;
η	is the departure of the water surface measured positive upwards from the datum plane;
ρ	is the mass density of water;
Ω	is the Coriolis parameter; and
θ	is the direction of wind measured from the positive direction of x towards the positive direction of y.

The governing equations for the water quality parameter Q are the vertically integrated time dependent mass balance equations. Q may represent temperature, salinity or the concentration of a pollutant. The governing equation is given by:

$$\frac{\partial(HQ)}{\partial t} + \frac{\partial(HuQ)}{\partial x} + \frac{\partial(HvQ)}{\partial y} = \frac{\partial(HD\partial Q)}{\partial x}\frac{}{\partial x} + \frac{\partial(HD\partial Q)}{\partial y}\frac{}{\partial y} + m'Qs$$

where

H	is the depth of water;
m'	is the local volumetric inflow rate of water per unit surface area of the bay (such as that resulting from rainfall);
S	is the local volumetric load rate from sources (such as that resulting from inflow streams and sewers);
t	is the time coordinate;
u,v	are the horizontal velocity components in the x and y directions, respectively;
x,y	are a set of mutually-orthogonal horizontal coordinates;
D	is the diffusivity coefficient for the property Q; and
Q	is the water quality parameter (N,P or S) in appropriate units.

This equation is a satisfactory approximation to reality for water bodies where the effects of thermal or density stratification are not predominant. In any case, even though the variation of the water quality parameters with depth are not predicted by the model, it will provide a reasonably accurate picture of the average values should such variation exist.

The numerical technique used to solve both sets of equations is a nodal point integration (NPI) scheme, more commonly, though rather inaccurately, labeled as an Intergrated Finite Difference (IFD) scheme. In respect of its temporal integration, the scheme similar to that used by Leendertse (1970); Runchal (1974 & 1977) has described the modification and improvement made to the scheme. It is a space-staggered, split-time-level, semi-implicit scheme which is particularly efficient and economical when using long term integration.

The shallow water equation are solved for surface displacement, , and water velocities, u and v. Boundary conditions of either velocity or water level may be used. The velocities obtained from TIDAL2 are used with suitable boundary conditions in WQUAL2 to solve for the water quality parameter Q. Variable grid spacing allows higher resolution to be obtained in regions of special interest.

3. MODELLING STUDY, KANEOHE BAY, HAWAII

3.1 Purpose of Study

Kaneohe Bay, situated on the north-east coast of the Hawaiian island of Oahu, is a region of major urban and light industrial development. The impact of this development on the quality of the water in the bay under various land use scenarios was the subject of a study undertaken by the U.S. Army Corps of Engineers. The scenarios included high and low projected population growth, the influence of various storm run-off and bathymetric modifications to the bay. Water quality in the bay was characterized by the levels of total nitrogen, total phosphorous and salinity.

3.2 The Site

The study region is shown in Figure 1. A barrier reef separates the bay from the ocean and is cut by two navigation channels, a 30 foot deep navigation channel at the northern end and a 10 foot deep sampan channel at the southern end. A fringing reef forms the southeast basin. Water depths in the bay range from 10 to 50 feet with the shallower depths predominating.

3.3 The Model and Calibration And Predictions

For the purpose of model calibration, a 30 day field study was mounted to collect current and tidal data. The location of

the six current meters and the tide recorder are shown on Figure 1. Additional intensive short term studies were mounted to track drogues released during high and slack tides, to record the movement of dye releases for diffusion coefficient estimation, and to measure salinity fluctuations.

Two days, each representative of the prevailing wind conditions, were selected as the calibration test cases. The tidal data was used for the boundary condition required by TIDAL2. Parametric studies showed that a friction coefficient of 0.01 and a 7.5 minute tidal phase lag from one to the other end of the offshore boundary were optimum. A comparison of predicted versus measured data is shown in Figure 2. The comparison showed good agreement with a tendency to underpredict the current speed. Considering the uncertainties in the measured input data and the use of a single wind value rather than the locally varying value this tendency is understandable. Further details of the calibertion effort are available in U.S. Army Corps of Engineers (1977).

The three land use scenarios of present, high future and low future growth were each studied under steady state and storm runoff conditions. The volume flux vectors for average tide and wind conditions shown in Figure 3 are representative of the plots produced by TIDAL2 for the various conditions. A salinity time history and isoquants of tide-averaged total phosphorous are shown respectively in Figures 4 and 5. It was found that high growth rate would only produce significant increases in total N and total P in the southern part of the bay. 50 year storms would produce significant increases in total N and total P and decreases in salinity for a number of days under existing conditions. Currents were found to be previously tidal driven with only minor wind effects and little stratification. Details of these predictions are available in USACE (1977) and Runchal (1978).

4. MODELLING STUDY, ST. JOHN'S RIVER, FLORIDA

4.1 Purpose of Study

As part of a proposal by the Seminole Electric Cooperative Inc. to build a 1200 Megawatt coal-fired electric generating plant, a study to investigate the impact of cooling water and dissolved solids on the St. John's River was conducted. The emphasis of the study was on the impact of blowdown discharge with feasibility studies of alternative cooling water discharge systems as a second objective.

4.2 The Site

The study area consists of an approximately 8-mile reach of the St. John's River near Palatka, Putnam County, Florida, (Figure 6). The river is tidally influenced at the point-of-discharge (POD) to the extent of full flow reversal. It is approximately 6000 feet wide and varies in depth from a few feet to 15 feet with the average depth being on the order of

10 feet. USGS maintains a river gauge station near the town of Palatka, gauge G in Figure 6, which indicates an average flow of 0.2 fps and a maximum flow of approximately 1 fps.

4.3 Calibration Studies

Four current meters and staff gauges were installed at the sites shown in Figure 6 for one week to provide calibration data for the numerical model. Adverse weather conditions did not allow a complete week of records to be obtained. However, the field data did allow considerable cross-checking of the numerical results. Boundary conditions of velocity on the 'upstream' free boundary and stage heights on the downstream boundary were used in the hydrodynamic model. The coefficient of bottom friction was varied from 0.00 to 0.03. Figure 7 shows the model results versus measured results at gauge Station B (see Figure 6) using a coefficient of bottom friction of 0.01. The agreement is very good and is typical of the agreement found at other gauge stations.

4.4 Simulations

The principal objective of the study was to predict the increase in water temperature and Total Dissolved Solids (TDS) in the vicinity of the POD. For this purpose a number of extreme and average scenarios were selected from historic tidal data. These scenarios included consistent upstream oscillatory and consistent downstream flows. The oscillatory flow (MAF) is potentially the worst case as there is minimum flushing at the POD. By making the assumptions of no surface heat loss and calm wind conditions, conservative results were assured.

The finite difference grid used in the studies is shown in Figure 6. The grid is refined near the POD for greater accuracy. Figure 8 shows the predicted temperature contours at ebb tide for the MAF case. The ambient water temperature for this case is 87°F.

The study predicted that the thermal impact of once-through discharge order the work flow and ambient conditions created a temperature rise in excess of 2°F for two miles downstream of the POD. Once through cooling with a topping tower reduced the figure to 1°F while blowdown discharge with 5% excess temperature reduced the area affected to approximately 50 feet.

5. MODELLING STUDY, PRUDHOE BAY, ALASKA

5.1 Purpose of Study

This study was conducted to assess the relative impact of a number of causeway extension design options upon the salinity and local circulation patterns near Prudhoe Bay, Alaska. The

options included a straightforward extension of the existing structure and the construction of an offshore island. The historic, "no causeway" and existing causeway situations were modeled to provide a datum. In addition the influence of a breach in the existing causeway was analyzed.

5.2 The Site

Prudhoe Bay is located on the coast of the Beaufort Sea, west of the mouth of the Sagavanirktok River and east of the Kuparuk River which flows into Simpson Lagoon, (Figure 9). The existing causeway extends 7,500 feet offshore to the 10 foot depth contour. Approximately one mile west of the tip of the causeway a 40-mile barrier island chain begins, creating Simpson Lagoon which has depths of 3 to 7 feet. The coastal region is frozen from October to May when the spring runoff begins. The ice then retreats to the limit of the year-round offshore pack ice. The above mentioned rivers are the only two with significant flows and extended discharge period and therefore have a major influence on local salinity. Because of the pack ice, waves are generally less than one foot. Tides in the region have a range less than 0.8 feet in height. However, the predominately east-northeast winds can cause water level changes of up to 3.2 feet (Spight 1979).

Calibration of the numerical model was not possible due to the lack of local data. However as the study was intended to be comparative rather than absolute, calibration was not of major importance.

5.3 Simulations

Four wind conditions, representing the average and storm winds from the two predominant directions, and two river discharges, representing the spring runoff and low flow average conditions were selected to be the scenario variables for each causeway geometry. Since the primary purpose of the analysis was a comparative study, other parameters such as bottom friction and the dispersion coefficient were held constant.

The discretization grid is shown in Figure 9. A number of sea boundary conditions were applied due to the difficulty caused by the lack of field data. It was found however that the influence of boundary conditions did not extend to the region of interest indicating that local wind and oceanographic effects are dominant.

A quadratic wind stress term, similar in form to that of bottom friction, was applied; the drag coefficient C_D was calculated from the work of Wilson (1960). The wind stress coefficient was calculated from the work of Wilson, Keulegan (1951) and Van Dorn (1953).

Results from the study are shown in Figures 10 and 11. Figure 10 shows the current vectors resulting from high flow

river discharge and Figure 11 the salinity differences created by these conditions relative to the existing causeway.

The study predicted that in the easterly wind conditions the extension of the causeway would cause an increase in salinity in Simpson Lagoon on the same order as the construction of the existing causeway, approximately 2 to 4 ppt. The offshore island has a minimal effect on existing salinity values while Prudhoe Bay was insensitive to changes in wind and causeway modifications.

CONCLUSIONS

The mathematical model of TIDAL2 and WQUAL2 is able to provide acceptable predictions of the behavior of a nonstratified, shallow water body of water for practical decision making relating to resource management, engineering analysis and environmental impact. The model has been widely tested and applied to a range of problems.

Although the model is a powerful tool it cannot be applied without being aware of a number of numerical and physical considerations. The numerical considerations primarily relate to the time step and grid size chosen. Because only one value of water column depth is specified per grid-cell, the model simplifies the complex bathymetry in terms of rectangular prisms. Thus, all specific bathymetric features less than the grid size are either ignored or grossly approximated.

There are also some practical considerations which, though not being limitations of the model, may yet limit the validity of the predictions. The TIDAL2 and WQUAL2 are a set of very general and comprehensive models. Ideally, a very detailed and sophisticated level of input is needed. This relates to the initial and boundary conditions, time histories of the flow rates and pollutant loads, the tidal and current history at open ocean boundaries and, surface winds, diffusivity and bottom-friction coefficients throughout the field of computation. Almost always, for any practical application, these inputs to the required detail and reliability, are not available. Thus, simplifying assumptions need to be made and these, in turn, limit the quality of the model predictions. This fact is of considerable importance both in comparing the predictions with the field data and in relating the predictions to the likely behavior of the water body.

ACKNOWLEDGEMENTS

The bulk of the work described above was performed at Advanced Technology Group, Dames & Moore under AKR's guidance. The assistance and encouragement (in alphabetical order) of Philippe Bardey, Billy Hall, Jim Hendrickson, Hyung-Sik Kim, Roger Schlueter and Geri Segal are gratefully acknowledged.

REFERENCES

1. A.K. Runchal, Mathematical Study of a Large Water Body, Proc. Symp. Technical, Environmental, Socioeconomic and Regulatory Aspects of Coastal Zone Management, ASCE, pp. 1897-1916, 1978.

2. J.J. Stoker, Water Waves, Interscience Publishers, New York, 1957.

3. J.J. Leenderste, A Water Quality Simulation Model for Well-mixed Estuaries and Coastal Seas: Volume 1, Principles of Computation, Rand Corporation, RM-6230-RC, 1970.

4. A.K. Runchal, A Computer Program for Tidal Studies: TIDAL, Dames and Moore ATG/TR/3, 1974.

5. A.K. Runchal, A Hydrodynamic and Water Quality Model for Large Water Bodies, Dames and Moore ATG/TR/5, 1977.

6. USACE, Kaneohe Bay Urban Water Resources Study: Computer Modeling U.S. Army Engineer District, Honolulu, Hawaii, 1977.

7. T.M. Spight, Prudhoe Bay West Dock Extension: Synthesis of Environmetal Studies 1974-1978, Woodward Clyde Consultants, Anchorage, Alaska, 1979.

8. B.W. Wilson, Note on Surface Wind Stresses Over Water at Low and High Speeds, Journal of Geophysical Records, Vol. 65, No. 11, pp. 3377-3382, 1960.

9. G. Keulegan, Wind Tides in Small Closed Channels, Research Paper 2207, National Bureau of Standards, U.S., 1951.

10. W.G. Van Dorn, Wind Stresses on an Artificial Pond, Journal Marine Research, Vol. 12, pp. 216-249, 1953.

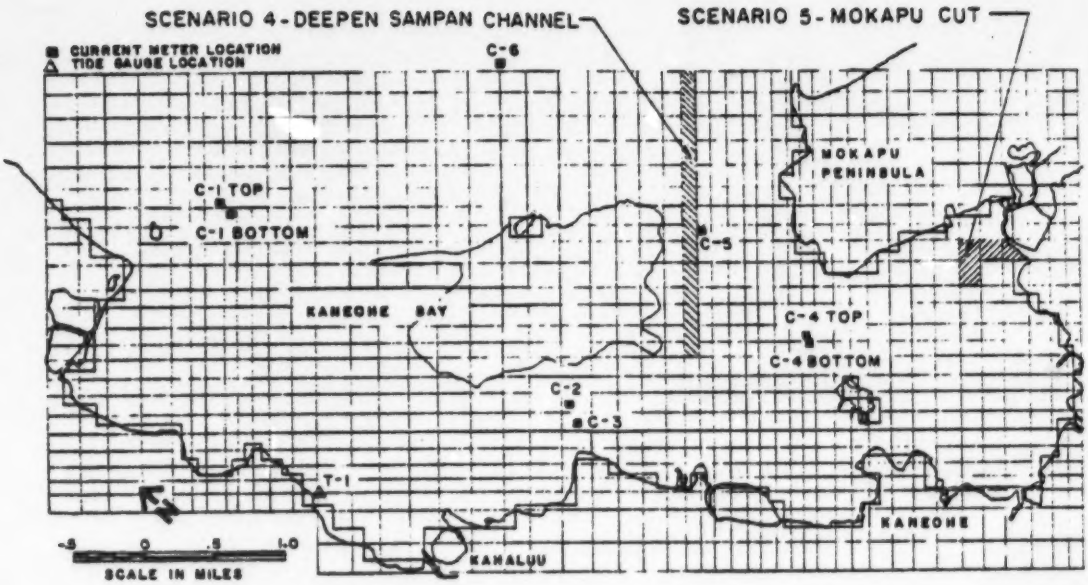

FIG. 1 THE TIDAL2 AND WQUAL 2 GRID FOR KANEOHE BAY STUDY

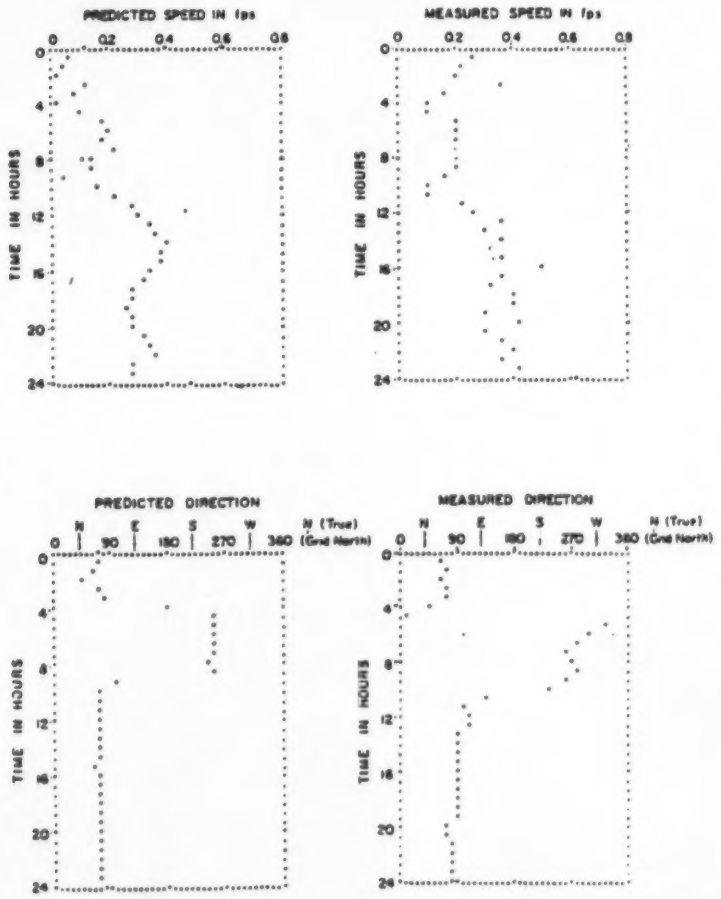
PREDICTED SPEED IN fps
MEASURED SPEED IN fps
0 0.2 0.4 0.6 0.8
TIME IN HOURS
0 4 8 12 16 20 24
PREDICTED DIRECTION
MEASURED DIRECTION
N E S W N (True)
0 90 180 270 360 (Grid North)

FIG. 2 COMPARISON OF PREDICTED AND MEASURED CURRENTS FOR CURRENT METER 1B ON 28 OCT. 76

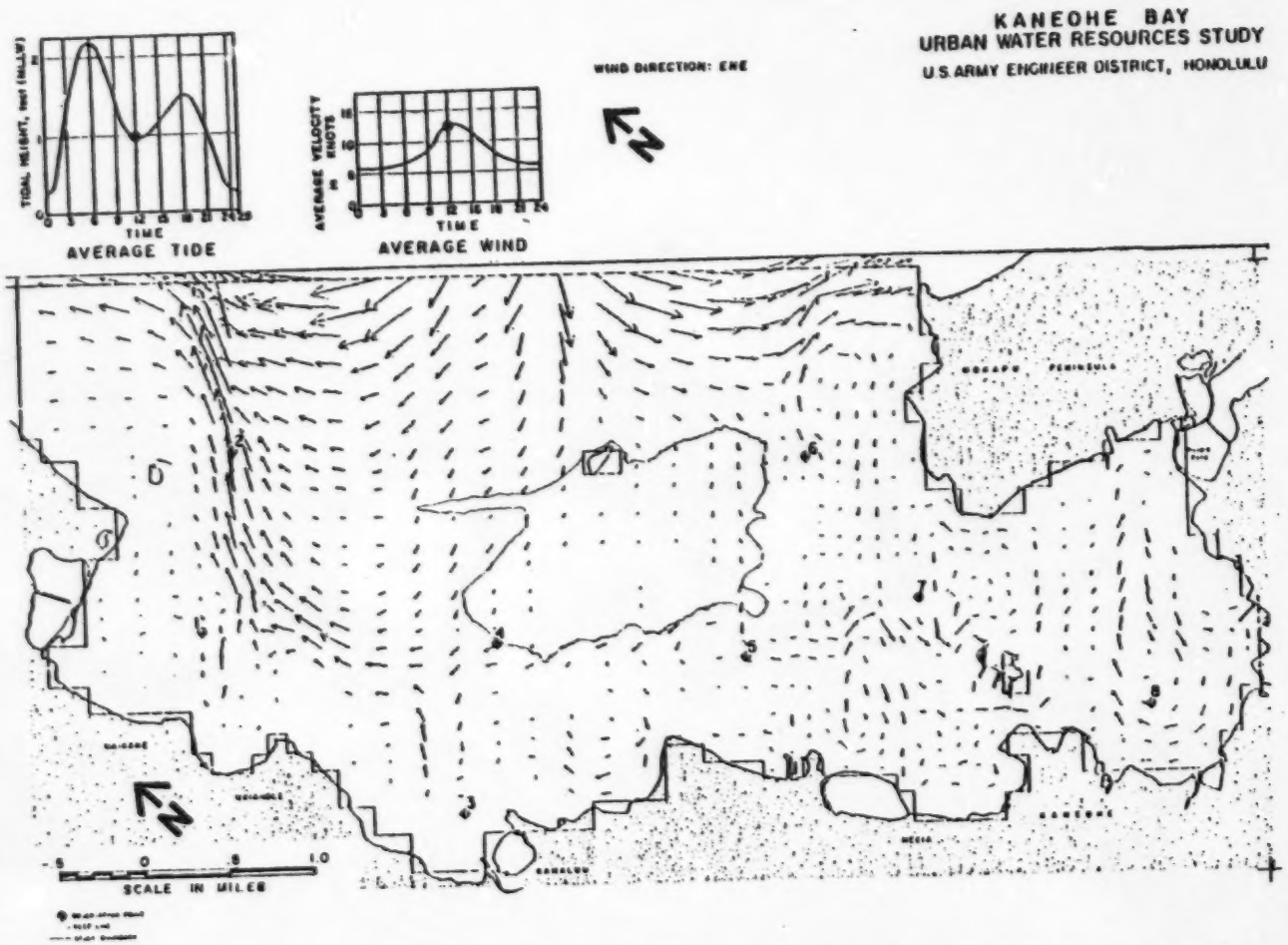

FIG. 3 VECTORS OF VOLUME FLUX FOR THE AVERAGE TIDE AND WIND CONDITIONS (TIME: 12.00)

FIG. 4 SALINITY TIME HISTORY AT OBSERVATION POINT NO. 3

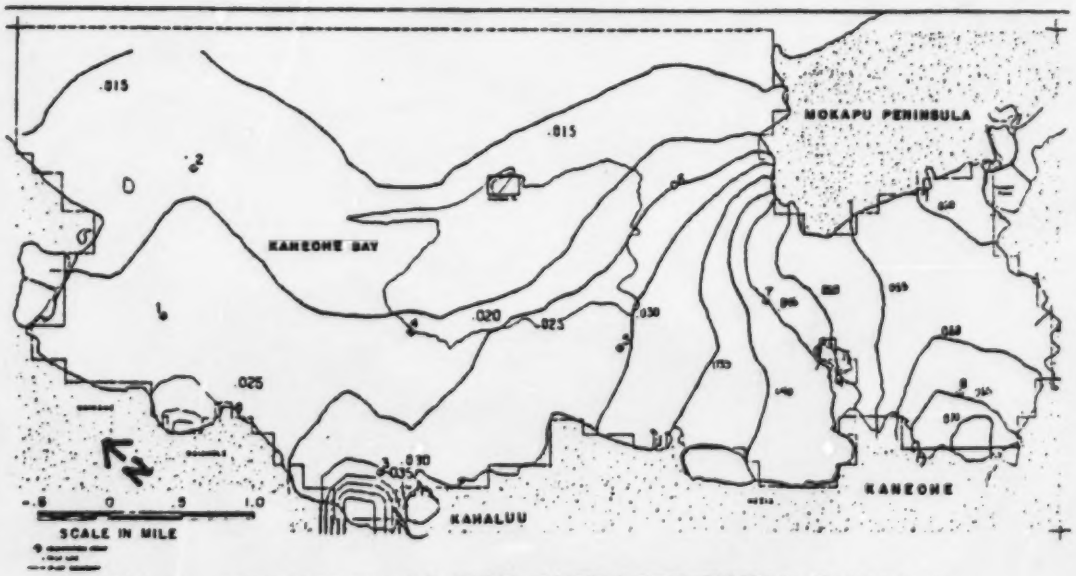

FIG. 5 ISOQUANTS OF TIDE-AVERAGED TOTAL P IN Mg/L
FOR EXISTING LAND USE SCENARIO - STEADY STATE

PB82-228297

EFFECTS OF MODEL DISTORTION ON THE NEAR-FIELD BEHAVIOUR OF THERMAL SURFACE DISCHARGES

D. Hoogendoorn and A. Quist
Delft Hydraulics Laboratory
Delft, the Netherlands

ABSTRACT

Hydraulic modeling of cooling water problems involves contradictory scale requirements. Therefore it is a common practice to apply separate models for near-field and far-field phenomena. The near-field model must be undistorted in order to reproduce the momentum affected region around the cooling water outfall. Heat recirculation through the intake is being investigated in a far-field model, covering a large area where heat transfer through the water surface is important. In order to reproduce this heat transport properly far-field models require airconditioning facilities or distorted scales.
The investigations described here were started to define conditions where near-field phenomena will still be reproduced correctly in a distorted far-field model.
The tests have been done for surface discharges from a rectangular outfall for shallow conditions. Main parameters that have been varied are: the bottom slope in front of the outfall, the discharge densimetric Froude number and the aspect ratio of the outfall.

1. INTRODUCTION

Hydraulic far-field modeling is most valuable for the majority of the investigations of the thermal impact and heat recirculation associated with hydrothermal discharges. For two reasons hydraulic far-field models should be distorted. The first practical reason is to limit the horizontal dimensions of the hydraulic model, whereas vertical dimensions must be chosen large enough to fulfil turbulence requirements. The second, more principle reason is to reproduce the heat exchange with the atmosphere correctly. In undistorted scale models this heat exchange is too large, in spite of the fact that the exchange coefficient in laboratory halls will be somewhat lower than prototype heat exchange coefficients.
A consequence of scale distortion is that near-field effects, e.g. thermal plume characteristics of the cooling water discharge, in principle cannot be reproduced without scale effects. To avoid this problem a separate undistorted near-field model would be needed. This model must preferably be operated simultaneously with the far-field model in order to include interaction between near-field and far-field by transferring the results of each model to the other one.
To avoid this difficult and expensive approach it is attractive to find conditions where separate modeling of the near-field and the far-field is not necessary. The purpose of the present model study is to determine those discharge conditions which allow scale distortion of the near-field, or to determine how

the near-field phenomena are affected by scale distortion [1].
This study does not pretend to cover a wide range of parameters but is limited to those conditions which often occur in cooling water problems and which seem promising with respect to acceptability of scale effects. Although this approach is not a fundamental one, it is expected that the results add valuable information to the scarce data of earlier publications for practical use in hydrothermal modeling.

2. RESULTS OF PREVIOUS INVESTIGATIONS

Although a number of investigators executed experiments on surface discharges only few of them investigated the influence of scale distortion on thermal plume characteristics.
Häggström [2] investigated the effects of scale distortion by theoretical and numerical analyses and by analysis of published results of laboratory experiments. His general conclusion is that scale effects increase with increasing discharge densimetric Froude number i.e. with inertia forces becoming stronger compared with buoyancy forces. For discharge densimetric Froude numbers smaller than 2 scale effects can be neglected.At larger discharge densimetric Froude number scale distortion results in too small a decrease in centre-line temperature, too small a plume thickness and too large areas within the isotherms.
In case of the presence of ambient velocities Häggström concluded, using numerical models, that plume direction changes too slowly, so the warm water will flow out too far from the shore.

Häggström's conclusions are valid for the deep water case. Any influence of the bottom geometry will in principle increase the reproducibility of the thermal plume characteristics in case of scale distortion, because vertical entrainment - which is the main parameter affected by scale distortion - will be reduced in shallow water conditions.
A promising support is found in a study of Safaie [3], which indicates that the thermal plume separation point in case of a sloping bottom is not sensitive to scale distortion.

Liong [4] investigated the effects of distortion on buoyant jets in a cross flow for the two-dimensional and the three-dimensional case. His experiments were executed with a horizontal bottom of the ambient water. The ambient water depth was equal to the discharge channel depth for the two-dimensional case and to three times the discharge channel depth for the three-dimensional case. Liong distinguished different scale effects for the entrainment region and the stable region.
For the two-dimensional case the centreline temperature decreased too slowly in the entrainment region but the decrease in the stable region was found to be correct.
Furthermore Liong found too small a plume thickness, too large a plume width and too large areas within the isotherms. The centreline trajectory was found to be independent of the distortion ratio.
For the three-dimensional case the centreline temperature decreased too slowly in the entrainment region but decreased too fast in the stable region. The plume thickness, the plume width and the areas within the isotherms for $\Delta T_c/\Delta T_o > 0{,}3$ were found to be too large. For values of $\Delta T_c/\Delta T_o < 0{,}3$ the areas within the isotherms were too small. The centreline trajectory was found to intrude slightly further from the coast with increasing distortion ratio. In general Liong concluded that the above described scale effects were less severe than expected from theoretical computations.

3. TEST SET-UP

In the near-field the spread of warm water is governed by jet diffusion, which can be divided into vertical and horizontal entrainment and by buoyancy spread. Of these processes the horizontal entrainment and the buoyancy spread can theoretically be reproduced correctly in a distorted model [2]. The effects of distortion in the near-field are thus dependent on the reproduction of the vertical entrainment. Reproduction of vertical entrainment is less important if this parameter is small. This will be the case under one of the following conditions:

- At small aspect ratio's
- If the densimetric Froudenumber is small buoyancy effects are strong compared with inertia forces, which results in weak vertical entrainment
- Shallow water will limit the supply of water needed for dilution from vertical entrainment.

The test set-up of the present study is based upon promising conditions with respect to the acceptability of scale effects. On the other hand the parameters were chosen in view of common practical conditions. Shallow water conditions are often present if coastal discharges are concerned. Therefore the undistorted reference bottom slope was chosen at 1:80. Discharge densimetric Froudenumbers up to 3,9 were used. The aspect ratio's varied between 10 and 3,3. Smaller aspect ratio's are rare for coastal discharges. The maximum distortion ratio of r = 4 covers a lot of far-field model distortions but not all. However, the limited model basin depth and water heating capacity did not allow to test larger distortion ratio's.

4. EXPERIMENTAL EQUIPMENT

The experiments were performed in a 5 x 10 m^2 basin shown in Figure 1. It was equiped with boundaries for the adjustment of an ambient cross-flow. However all tests have been done without ambient currents. The sloping bottom of the basin was insulated with polystirene plates to avoid heat loss. The water level in the basin was controlled with an adjustable weir. The water depth in the basin was measured with a fixed point gauge located near the cooling water discharge point.

Because of the limited dimensions of the test basin and the absence of ambient currents the test duration was limited from the moment that the heated water discharge started until the moment the plume reached the opposite basin wall. The moment of reaching the opposite basin wall could be determined by adding dye to the heated water discharge.

The heated water discharge structure (Figure 2) was located at the centre of the shallow long side of the basin. It was oriented perpendicular to the coast line and had a rectangular cross-sectional shape. The channel width b_o was adjustable from 0 to 0,2 m. The bottom level of the discharge channel was equal to the ambient water depth at the coast line.

The heated discharge was supplied from three electrical heating boilers with a total capacity of 25,5 kW. With a control valve the temperature difference ΔT_o between ambient and heated water was adjusted. The flow rate of the heated water was measured with a rotameter.

Temperatures were measured with 75 thermistors at different locations and depths in the basin. Because of the absence of ambient currents the cooling water plume was symmetrical to the axis of the discharge channel, so temperatures have only been measured in one half of the plume. The data collection was achieved with a Philips PM 2400 data logging system. Temperatures were measured at 0,5 cm below the water surface, at half depth and at 0,5 cm above the bottom.

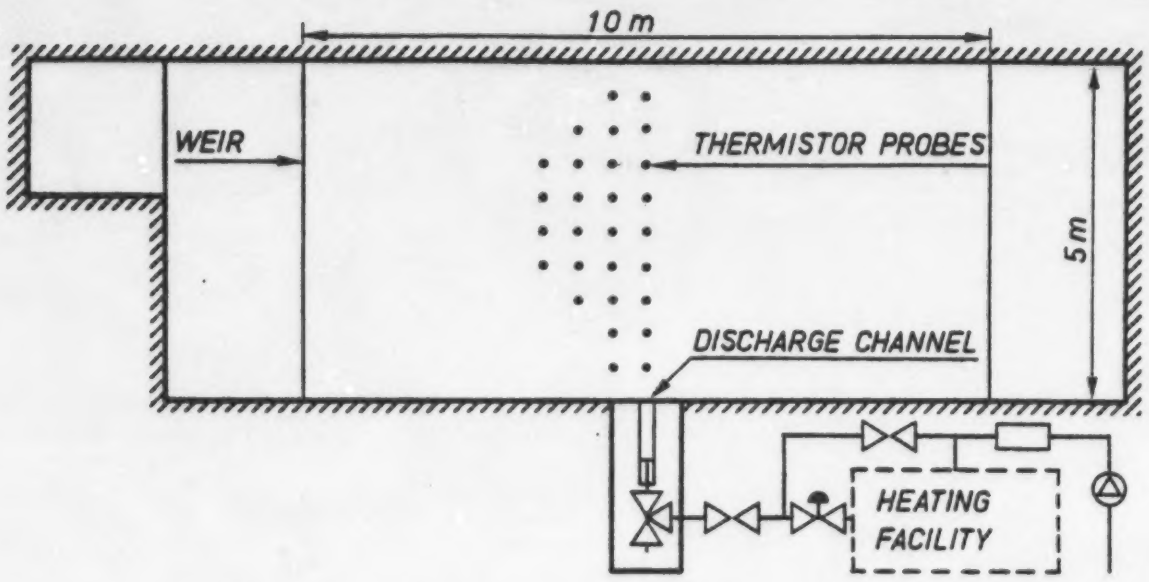

FIGURE 1 PLAN VIEW OF THE MODEL BASIN

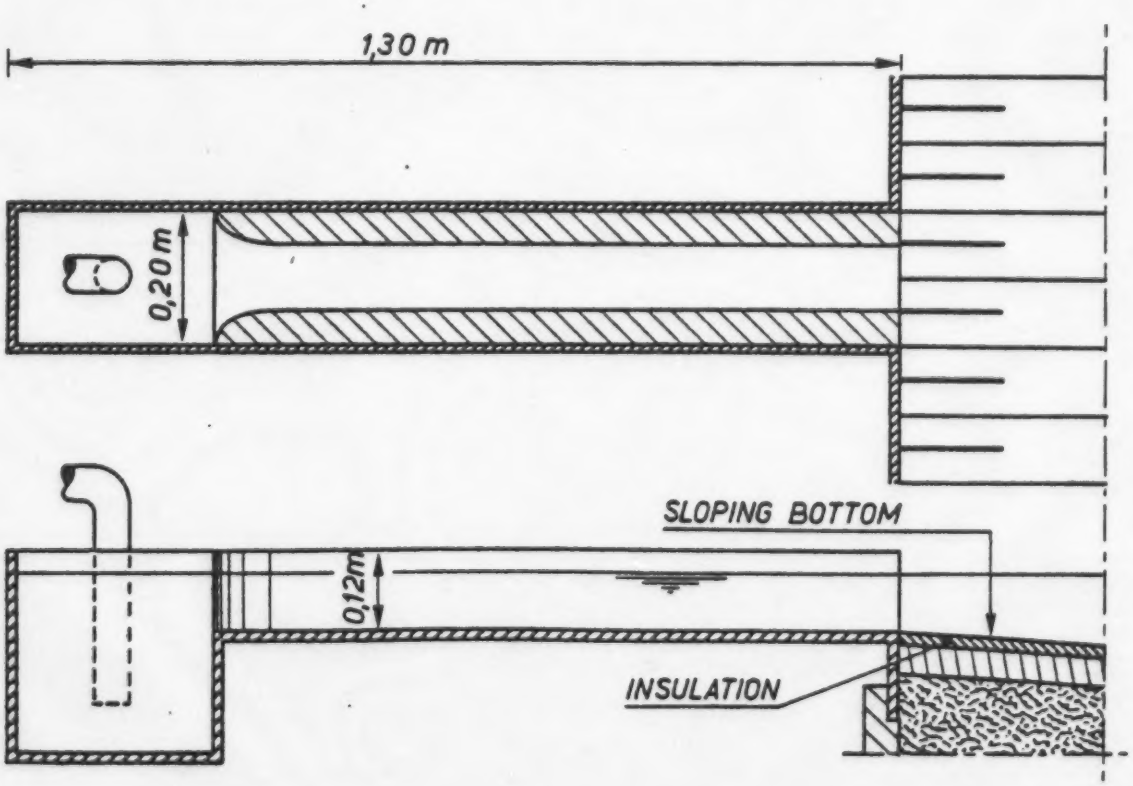

FIGURE 2 SHAPE OF THE DISCHARGE CHANNEL

During each run the propagation of the front of the plume was photographed.

5. MEASURING PROCEDURE

Before starting a run the water level in the basin was adjusted with the weir. The ambient water temperature was determined by scanning all the thermistors in the ambient water and averaging the measured values. During each run the ambient water temperature was checked with one thermistor located in a part of the basin outside the heated plume.
Before the start of a run the heated water was discharged to a dummy reservoir. By turning a two-way valve one could change the direction of the flow into the discharge channel. At that moment the discharge channel was empty while a valve at the end of the discharge channel prevented the ambient water to enter the discharge channel. After turning the two-way valve the discharge channel was filled with heated water. At the moment the water level in the discharge channel became equal to the ambient water level, the valve at the end of the discharge channel was removed and the run started. This moment was taken as $t = 0$.
After starting a run the temperatures in the plume were registrated each full minute until the front of the plume reached the opposite wall of the basin.
After finishing a run the basin was emptied and flushed during half an hour before starting a new run.

6. TEST PROGRAM

All runs were carried out with stagnant ambient water. Besides the distortion ratio r the parameters varied were the discharge densimetric Froude number $Fr_{d.o}$ and the aspect ratio A_r.
For both the densimetric Froude number and the aspect ratio three different values have been used. The values of the discharge densimetric Froude number were 1,3, 2,6 and 3,9 while the values of the aspect ratio were 3,3, 5 and 10. Due to small variations in h_o and $\Delta\rho/\rho_o$ the actual discharge densimetric Froude number and the aspect ratio differed slighty from the above given values. The temperature difference ΔT_o between heated water and ambient water was about 10^oC while the ambient water temperature was about $16,5^oC$.
During the test program the actual temperature difference varied from 9,7 to $11,3^oC$ and the actual ambient water temperature varied from 16,1 to $17,3^oC$.
The Reynolds number Re for all runs was sufficiently large to guarantee turbulent flow conditions according to the criterion developed by Ungate [5].
The test program is presented in Table I. Nine tests have been done with a bottom slope of 1:80 ($I = 0,0125$). These tests are the reference tests of the undistorted situation (runs 01 through 09). Nine tests have been done with a distortion ratio of $r = 2$ (runs 11 through 19) and nine tests have been done with a distortion ratio of $r = 4$ (runs 21 through 29).

7. RESULTS

Because vertical entrainment is expected to be the parameter which is most sensitive to scale distortion, it is usefull to analyse this effect separately. This is possible by comparing runs with identical $Fr_{d.o}$ and identical actual aspect ratio's A_a but with different bottom slopes. Therefore, we compare the following pairs of runs:
With $A_a = 5$ runs 02/11, 05/14 and 08/17 and with $A_a = 2,5$ runs 12/21, 15/24 and 18/27. Figure 3 shows the results with $A_a = 2,5$.
From this comparison the following conclusions can be drawn.
For $A_a = 2,5$ and bottom slopes of 1:40 and 1:20 the commencement of the centre-

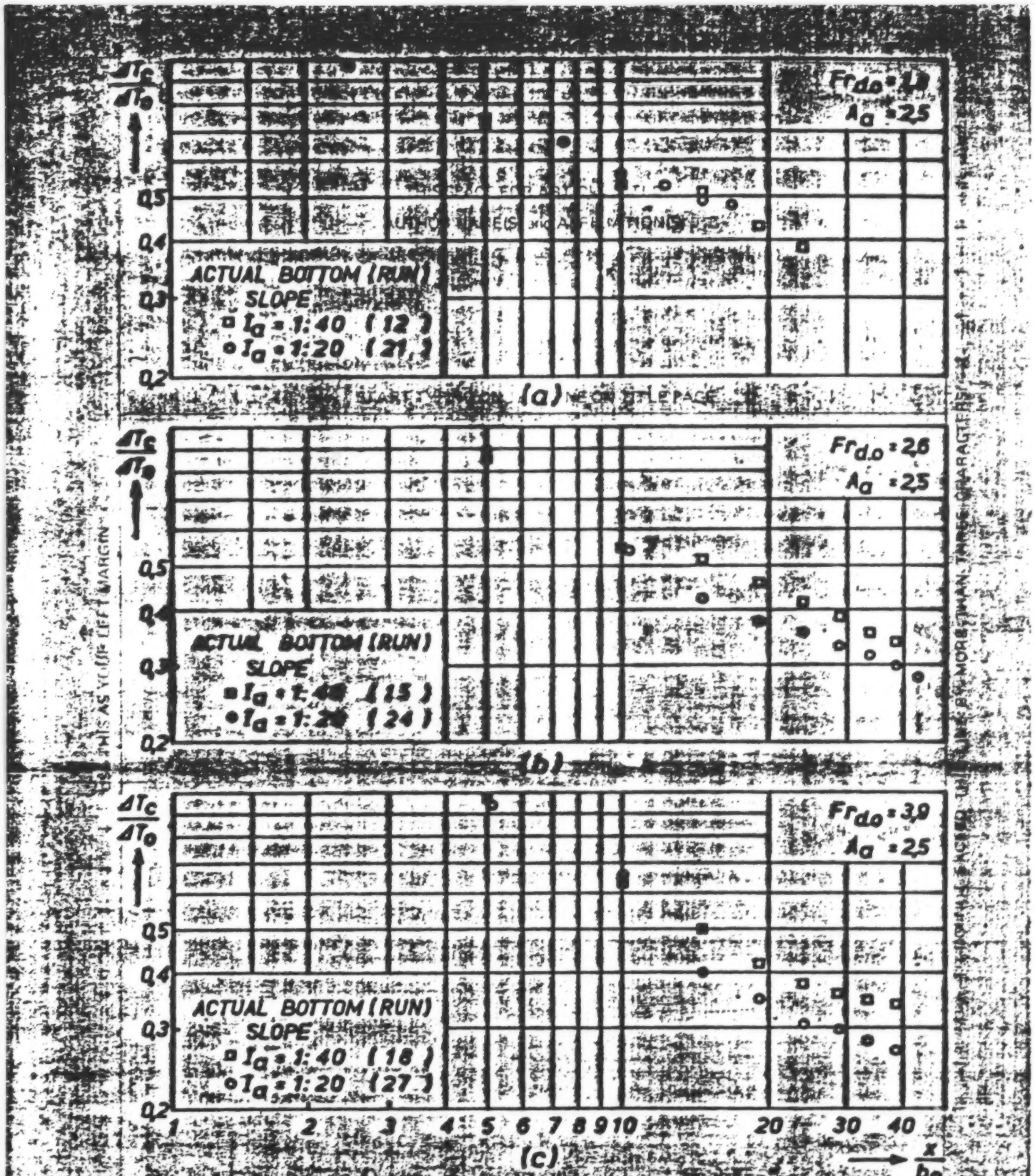

FIGURE 3 EFFECT OF THE BOTTOM SLOPE ON THE CENTRELINE TEMPERATURE DECAY FOR DIFFERENT Fr_{do}-VALUES

Reproduced from best available copy.

line temperature decay depends on $Fr_{d.o}$. Increasing $Fr_{d.o}$ gives an increase of the distance where the plume separates from the sloping bottom. The temperature decay curves for $Fr_{d.o}$ = 1,3 are identical for both bottom slopes. For $Fr_{d.o}$ = 2,6 and 3,9 the effect of stronger vertical entrainment due to an increased bottom slope starts at about x/b_o = 10.
For A_a = 5 and bottom slopes of 1:80 and 1:40 the centre-line temperature decay starts at about x/b_o = 2,5, independent of the discharge densimetric Froude number. For $Fr_{d.o}$ = 1,3 and 2,6 centre-line temperature decay curves are identical. For $Fr_{d.o}$ = 3,9 the decay starts to show differences at x/b_o = 5, with a stronger decay for the 1:40 bottom slope.

We now proceed to the complete analysis of effects from scale distortion.Therefore nine triplets of runs are compared: runs 01/11/21, 02/12/22, etcetera.

7.1. Centre-line temperature decay

The effect of scale distortion on the centre-line temperature decay is more complicated than the above described effect of changing the bottom slope only. Scale distortion reduces also the actual aspect ratio A_a. The effect of the increased h_o is that the influence of vertical entrainment on ΔT_c starts at larger x/b_o. So close to the discharge ΔT_c is too large under distorted conditions. Further away ΔT_c is reduced too much because the steeper bottom allows the lower layer to deliver water for vertical entrainment more easily. This effect is illustrated clearly in Figure 4c.
Figure 4 shows the runs with $Fr_{d.o}$ = 2,6 illustrating the effect of the aspect ratio and Figure 5 shows the runs with A_r = 5, illustrating the effect of the discharge densimetric Froude number.

All runs with $Fr_{d.o}$ = 1,3 show no noticeable scale effects, because the vertical entrainment is small. The runs with $Fr_{d.o}$ = 2,6 and 3,9 give substantial scale effects for A_r = 10. Here the centre-line temperature decay starts at the same distance from the outlet but from this start the distorted runs show too fast a temperature decay. With A_r = 5 this effect is slightly compensated since the temperature decay in the distorted cases starts further away from the outlet. For A = 3,3 scale effects are noticeable both close to the outlet and far from the outlet, with reversed sign. The results indicate that for smaller aspect ratio's increase of the discharge densimetric Froude number might reduce scale effects.

7.2. Plume thickness and width

Measurement of temperatures at the surface, half depth and bottom does not allow to define the thickness of the plume accurately. Measurements at half depth indicate that in some runs distortion creates a slight decrease of the plume thickness. Measurements near the bottom show that the length of the bottom attachment zone depends mainly on the discharge densimetric Froude number. Significant differences between different distortion ratio's were not found.
Photographs of the propagation of the front do not show significant effects of scale distortion on the shape of the plume. Surface temperatures outside the centre-line of the plume show no scale effects as long as the centre-line temperature shows no scale effects. In cases where distortion causes too fast a centre-line temperature decay temperatures outside the centre line are too low as well, resulting in too small areas within isotherms.

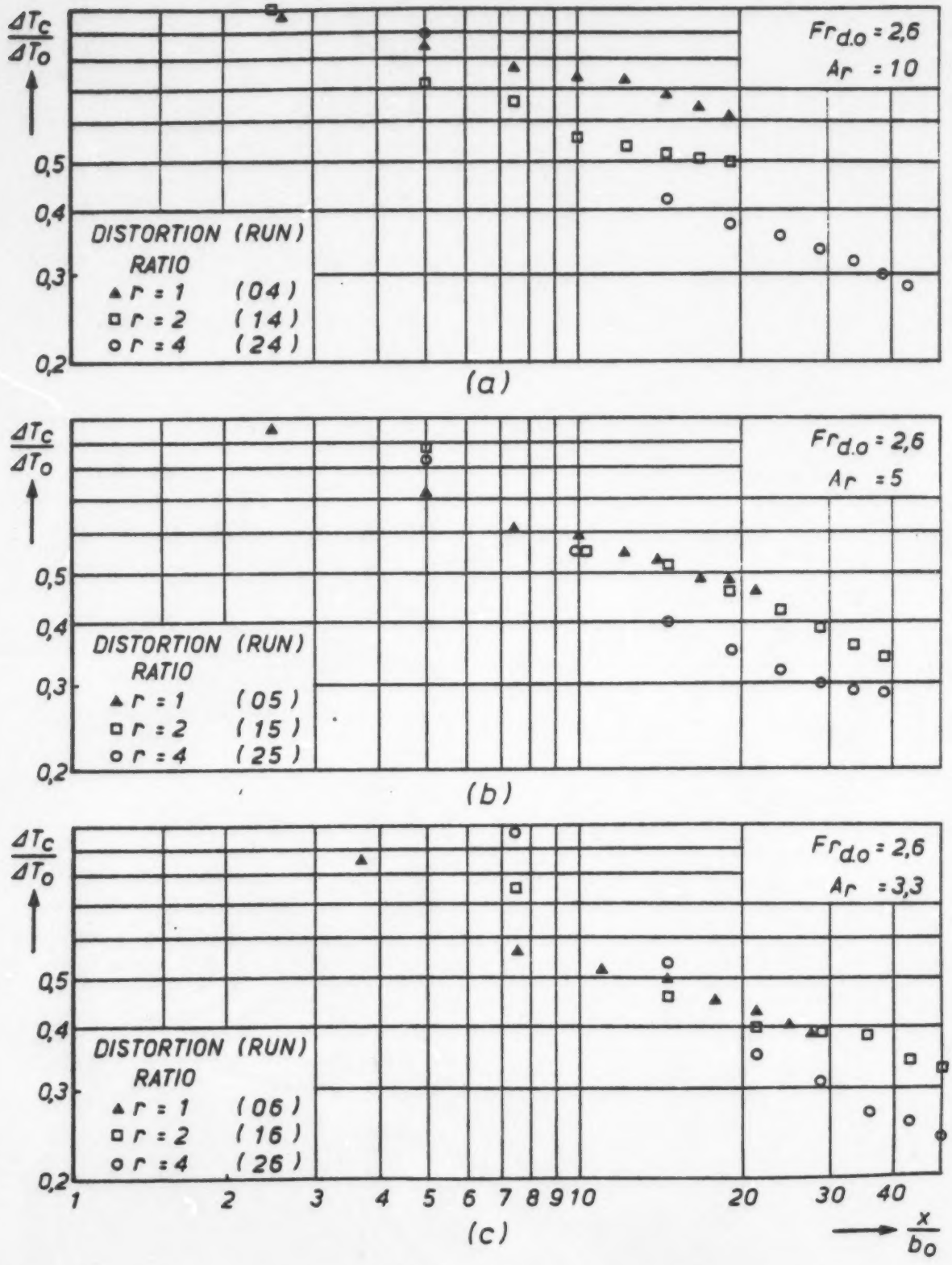

FIGURE 4 EFFECT OF DISTORTION ON THE CENTRELINE TEMPERATURE DECAY FOR DIFFERENT A_r - VALUES

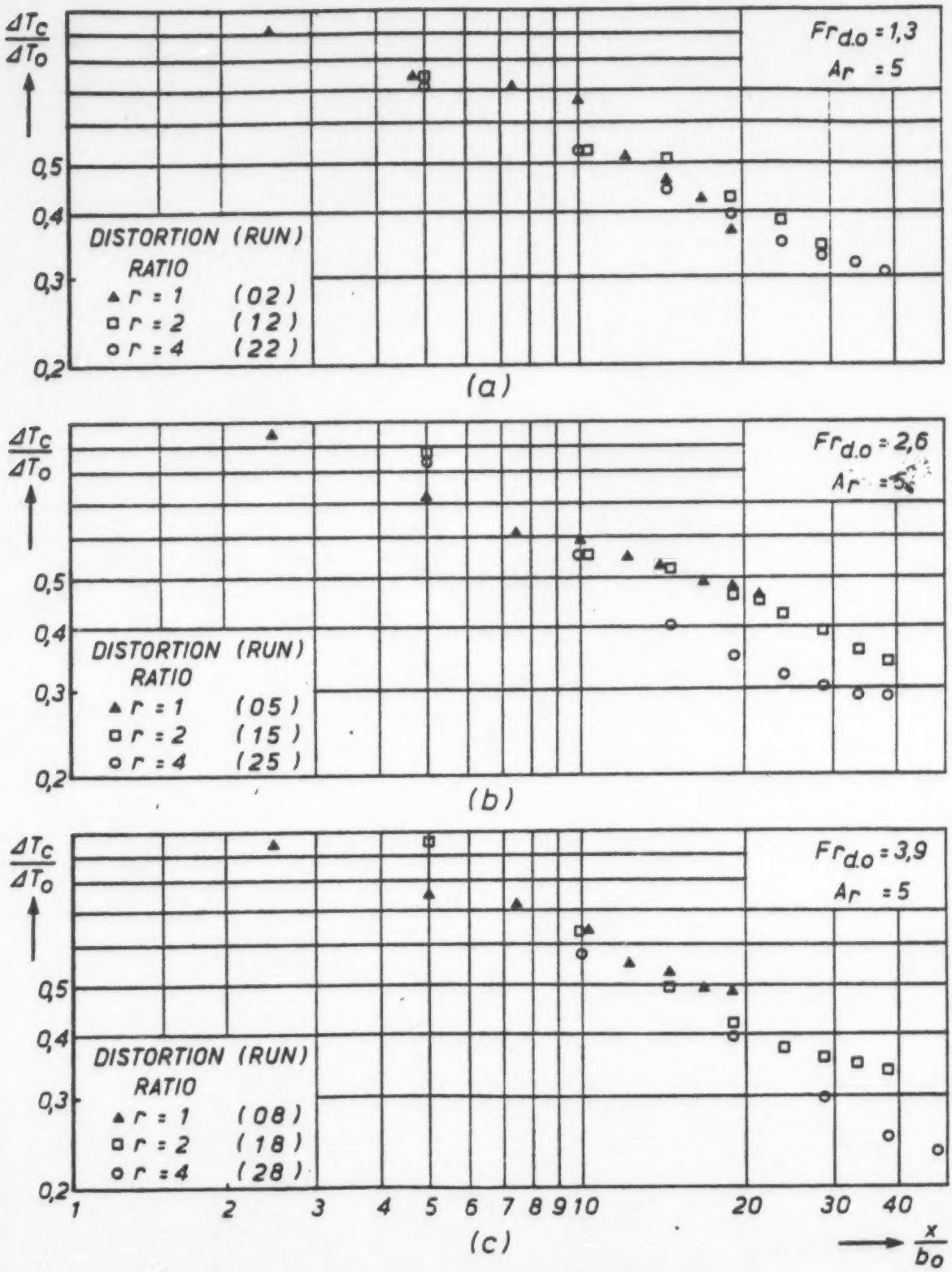

FIGURE 5 EFFECT OF DISTORTION ON THE CENTRELINE TEMPERATURE DECAY FOR DIFFERENT $Fr_{d.o.}$ - VALUES

8. CONCLUSIONS

Vertical entrainment is the main parameter which is sensitive to scale distortion. Since literature already shows that in deep water conditions the centre-line temperature decay will be too small in distorted models, shallow water conditions were investigated. The effect of shallow water with a bottom slope of 1:80 is that vertical entrainment is reduced, resulting in centre-line temperature decays which start at greater distance, but which are too large if scale distortion is applied. These effects compensate each other in some cases.
For a discharge densimetric Froude number of 1,3 distortion ratio's up to r = 4 are applicable independent of the aspect ratio of the outlet. Probably higher distortion ratio's are applicable as well.
For a discharge densimetric Froude number of 2,6 a distortion ratio of r = 2 is applicable for aspect ratio's smaller than $A_r = 5$.
For a discharge densimetric Froude number of 3,9 a distortion ratio of r = 2 is applicable for aspect ratio's smaller than $A_r = 3,3$.

REFERENCES

1. Hoogendoorn, D. and Quist, A.Effects of model distortion on the near-field behaviour of thermal surface discharges. Delft Hydraulics Laboratory, Delft, the Netherlands, report S93, April 1981.

2. Häggström, S. Surface discharge of cooling water, effects of distortion in model investigations. Report series A:3. Dept. of Hydraulics, Chalmers Univ. of Technology, Götenborg, Sweden, 1978.

3. Safaie, B. Mixing of horizontal buoyant jet over sloping bottom. Techn. Rep. HEL 27-4. Hydr. Eng. Lab., Univ. of California, Berkeley, California, July 1978.

4. Liong, S.Y. Effects of vertical distortion on thermal hydraulic modeling of surface discharges. Univ. of Iowa, Iowa, May 1977.

5. Ungate, C.D. Temperature reduction in a submerged vertical jet in the laminair-turbulent transition. M.S. Thesis, Dept. of Civil Eng., Massachusetts Institute of Technology, Cambridge, Mass., 1974.

LIST OF SYMBOLS

A	= aspect ratio = b_o/h_o	-
b_o	= full width of the discharge channel	m
$Fr_{d.o}$	= discharge densimetric Froude number = $v_o/\sqrt{\frac{\Delta\rho}{\rho_o} g h_o}$	-
g	= acceleration of gravity	m/s^2
h_o	= water depth in the discharge channel	m
I	= bottom slope in the receiving water body	-
q	= heated water discharge	m^3/s
r	= distortion ratio (ratio between horizontal and vertical length scales)	-
Re	= Reynolds number = $v_o \times 4R_h/\nu_o$	-
R_h	= hydraulic radius	m
T_a	= ambient water temperature	^oC
ΔT_c	= plume centreline excess temperature	^oC
ΔT_o	= temperature difference between heated water at the discharge point and ambient water	^oC
v_o	= discharge velocity	m/s

x	= distance along the centreline of the plume	m
ρ_o	= density of ambient water	kg/m^3
$\Delta\rho$	= density difference between ambient water and heated water	kg/m^3
ν	= kinematic viscosity	m^2/s

subscripts
r : refers to reference tests (distortion ratio r = 1)
a : refers to actual parameter value

run	r	$Fr_{d.o}$	q	b_o	h_o	A_r	T_a	T_o	I_a	R_e
			x 10^{-3} m^3/s	x 10^{-2} m	x 10^{-2} m		°C	°C		
01	1	1,2	0,11	20	2,1	9,5	16,9	10,8	0,0125	1818
02	1	1,2	0,31	20	4,2	4,8	17,0	10,7	0,0125	4366
03	1	1,2	0,21	13,3	4,1	3,2	16,7	10,8	0,0125	3907
04	1	2,3	0,22	20	2,1	9,5	16,4	11,3	0,0125	3636
05	1	2,5	0,62	20	4,2	4,8	17,1	10,0	0,0125	8732
06	1	2,5	0,43	13,3	4,2	3,2	17,1	10,1	0,0125	7926
07	1	3,5	0,33	20	2,1	9,5	16,6	11,2	0,0125	5455
08	1	3,7	0,93	20	4,2	4,8	16,9	9,9	0,0125	13099
09	1	3,7	0,62	13,3	4,2	3,2	17,1	10,0	0,0125	11429
11	2	1,2	0,31	20	4,2	9,5	16,0	10,3	0,0125	4366
12	2	1,3	0,16	10	4,1	4,9	16,1	10,8	0,025	3516
13	2	1,4	0,11	6,7	4,0	3,3	16,0	10,5	0,025	2993
14	2	2,5	0,62	20	4,2	9,5	16,0	9,7	0,025	8732
15	2	2,5	0,31	10	4,1	4,9	16,0	10,3	0,025	6813
16	2	2,5	0,21	6,7	4,1	3,2	16,0	10,7	0,025	5638
17	2	3,7	0,93	20	4,2	9,5	16,0	9,9	0,025	13099
18	2	3,9	0,47	10	4,1	4,9	16,0	10,0	0,025	10330
19	2	3,8	0,31	6,7	4,1	3,2	16,2	9,9	0,025	8322
21	4	1,3	0,88	20	8,1	9,9	16,1	10,1	0,05	9724
22	4	1,3	0,44	10	8,1	4,9	16,0	10,4	0,05	6718
23	4	1,2	0,29	6,7	8,1	3,3	16,0	10,7	0,05	5066
24	4	2,5	0,31	10	4,1	9,8	16,0	10,1	0,05	6813
25	4	2,6	0,88	10	8,2	4,9	16,1	10,0	0,05	13333
26	4	2,6	0,59	6,7	8,0	3,3	16,1	10,4	0,05	10396
27	4	3,9	0,47	10	4,1	9,8	16,0	9,8	0,05	10330
28	4	4,0	0,24	5	4,0	5,0	16,0	10,5	0,05	7385
29	4	3,8	0,89	6,7	8,1	3,3	16,1	10,5	0,05	15546

Table I Test program

PB82-228305

MATHEMATICAL MODELS FOR POWER PLANT WASTE HEAT DISCHARGE

P.G. Kharche and P.C.K. Variyar
Tata Consulting Engineers
Bangalore 560 052
INDIA

ABSTRACT

In waste heat discharge systems, the warm water may be floated at the surface so as to aid heat dissipation to the atmosphere while cold water is drawn from below the epilimnion of the water body. However, the warm water may recirculate before complete heat dissipation depending on various factors such as meteorological conditions, relative locations of intake and outfall, outfall velocity, etc..

Mathematical models have been developed to analyse the flow and temperature patterns so as to aid in deciding the suitability of a water body as a heat sink, relative locations of outfall and intake and extent of temperature rise at intake on enhancement of existing power plant capacity. One and two dimensional models are used to analyse essentially three dimensional problems.

This paper describes the mathematical formulation and the associated computer programmes having a special feature like interactive facility. The advantages and limitations of the present method of solution are also furnished.

1. INTRODUCTION

Power plants reject low grade heat to the cooling water circulated in the condenser, which is drawn from the cooler layers of a water body. The hot discharge is floated over the surface of the water body in order to obtain a higher surface temperature for better heat dissipation to the atmosphere, unless prevented by restrictions on the level of thermal pollution.

In most practical cases, the water body is stratified, with a vertical temperature variation in which the lighter hot fluid lies above the denser cold fluid. However, for large energy complexes using existing environmental interfaces, cooling water flow rates are massive enough to create flow fields in the water body. These flow fields may overcome the natural barrier

caused by temperature stratification and result in recirculation of warm water into the intake, lowering the power plant efficiency. Consequently, the intake and outlet are to be designed so as to keep the disturbance to the thermocline at a minimum. Other related problems include determination of flow and temperature fields in an extended water body (such as a river) from an existing power plant, so as to decide the location of a new power plant.

For analysing such heat discharge problems, mathematical models have been developed to simulate the energy exchange at the surface and the thermal behaviour of the water body. Since the phenomenon is complex, a number of models have been developed to understand various aspects and to determine the influence of various parameters. These have shown that the complex, three dimensional problem can be studied by means of one and two dimensional models using interactive graphic facilities to enable quick interpretation of results. This paper reports extension of basic work reported in [1]. Physical concepts which are discussed in [1] are briefed below prior to the description of mathematical models.

2. PHYSICAL CONCEPTS

2.1 Energy Exchange At The Surface

The surface temperature of a water body is dependent to a large extent, on the thermal energy exchange mechanisms of the surface layer with the environment.

The mathematical representation of the surface energy exchange mechanisms such as solar radiation, atmospheric radiation, back radiation from the water surface, convection, evaporation have been considered in formulating the models [1, 2, 3].

2.2 Water Body Behaviour

The first step in studying thermal discharges from power plants, is to simulate and analyse the natural cycle of the water body. Most water bodies, such as lakes, are stratified due to the energy transfer at the surface. The depth of the lighter or hotter fluid, termed as the 'epilimnion' is an important parameter as it affects flow patterns and for a stratified lake, it is around 3 - 5 meters [1].

The thermal response of a water body has also been studied and it has been found [1] that stabilisation of temperature distribution takes several days. Thus average values of ambient parameters such as solar radiation, cloud cover, relative humidity, temperature, wind velocity, etc., over significant duration of time should be taken into account while simulating the surface energy exchange mechanisms in both the steady state and transient models described below.

3. MATHEMATICAL MODELS

Point, one and two dimensional models have been developed to analyse the phenomenon of thermal discharges into water bodies. These models can be used to determine the temperatures and velocities at points of interest, such as at the power plant intake. They may be used individually for certain special situations, but in cases where the phenomenon is essentially three dimensional, they have to be used in combination.

3.1 Point Model

The point model computes the energy transfer per unit surface area, given the parameters like solar radiation, cloud cover, ambient temperature, wind velocity and relative humidity. This model can thus be used to determine the equilibrium surface temperature of the natural water body, the average temperature rise due to heat rejection and the effect of the various ambient parameters on the surface temperature [1] . These results can be used to give an important guideline for the rating of the power plant that may be planned on a given water body, and the anticipated effects at various seasons of the year.

3.2 One Dimensional Models

Physically one dimensional (1-D) model represents the circumstance, when the small dimensions of the water body, or strong lateral mixing in a large water body, results in uniform conditions in two dimensions, with variation only in the third. This third dimension is taken as horizontal in the 1-D horizontal model and as vertical in the 1-D vertical model. The equations representing these models are given in [1] .

The transient 1-D vertical model can be used to determine the vertical temperature profile in the water body. It can thus be used to determine the depth of the epilimnion at specified ambient conditions, the transient effects due to fluctuations in ambient conditions, and the rise in the average intake temperature. The model is particularly applicable for water bodies of small surface area. The use of this model could be extended to large water bodies also by determining the flow pattern from the two dimensional models, with the area for averaging derived on the above basis.

The one dimensional model considers the stratification of the water body, through the naturally generated stratification resulting from heat transfer mechanisms and a turbulent eddy diffusivity (ϵ_H) varying with depth. In general, the water body is fully mixed in winter and stratified in summer as it gains energy. A fully mixed region arises at the top as the lake starts losing energy in autumn. In the model, this region is computed taking into account the instability due to

the upper layers being cooled. The energy is distributed to an isothermal top layer, which increases in depth with time, till the waterbody is fully mixed in early winter.

The 1-D horizontal model is used for determining the temperature profile of a water body such as a river or channel, whose length is very large compared to width, and also for ascertaining the extent to which the thermal influence of a power plant extends downstream. The results of this model for various heat rejection rates, showing the decrease in temperature of the discharge with distance from the outfall is shown in Fig. 1. The figure indicates the horizontal separation required for negligible recirculation. It also indicates the heat rejection rate permissible for a water body of a given dimension.

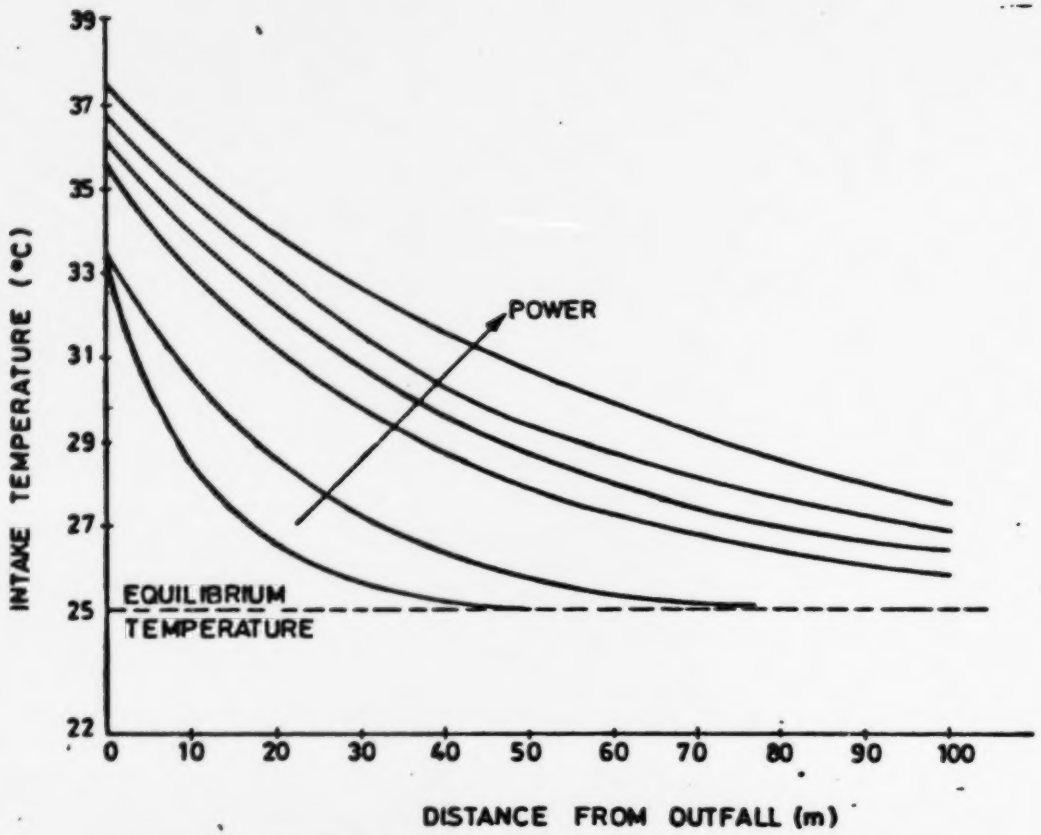

FIG.1. ONE DIMENSIONAL HORIZONTAL MODEL. EFFECT OF HEAT REJECTION ON TEMPERATURE DISTRIBUTION

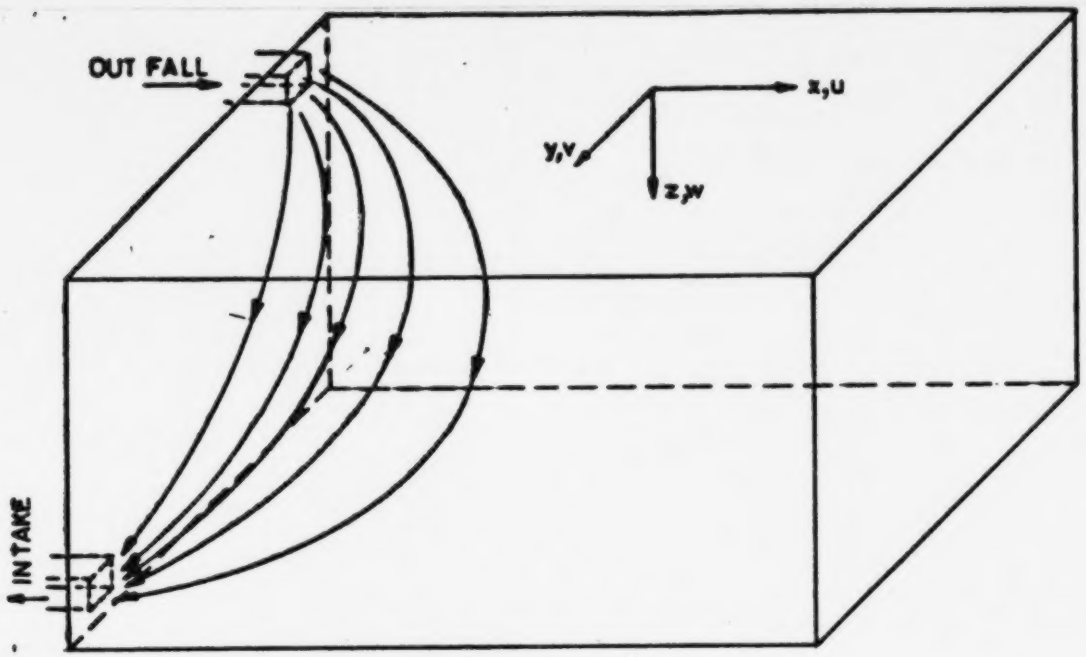

FIG.2. A SIMPLIFIED VERSION OF THE FLOW PATTERN

3.3 Two Dimensional Models

Consider the simple physical system, for heat rejection shown in Fig. 2. The intake and outfall are located arbitrarily, separated in both the vertical and the horizontal planes. In a real situation, configuration of the water body would be arbitrary and complex. The problem may be viewed as a combination of a horizontal flow and a vertical flow as depicted in Fig. 2. [4] . The two dimensional (2-D) horizontal model simulates the horizontal flow and the 2-D vertical model simulates the vertical flow. The two dimensional models assume complete mixing in one direction. The 2-D horizontal model is characterised by averaging over a finite depth, whose magnitude is determined from the vertical model study; as it varies with the flow velocities and the intake/outfall locations. In many cases of interest it may be close to the vertical distance between the intake and outfall [4] .

The governing equations for this flow are:

$$u\frac{\partial u}{\partial x} + v\frac{\partial u}{\partial y} = \epsilon M\left(\frac{\partial^2 u}{\partial x^2} + \frac{\partial^2 u}{\partial y^2}\right) - \frac{1}{\rho}\frac{\partial p}{\partial x} \quad (1)$$

$$u\frac{\partial v}{\partial x} + v\frac{\partial v}{\partial y} = \epsilon M\left(\frac{\partial^2 v}{\partial x^2} + \frac{\partial^2 v}{\partial y^2}\right) - \frac{1}{\rho}\frac{\partial p}{\partial y} \quad (2)$$

$$u\frac{\partial t}{\partial x} + v\frac{\partial t}{\partial y} = \epsilon H\left(\frac{\partial^2 t}{\partial x^2} + \frac{\partial^2 t}{\partial y^2}\right) + \frac{Q}{\rho c_p \Delta z} \quad (3)$$

The above equations are solved by the stream function concept, eliminating pressure in the first two equations and obtaining the velocity field, which is then fed into third equation for obtaining the temperature field.

In the vertical 2-D model, important parameters such as the vertical separation of the intake and outfall locations, the stratification effect and the buoyancy effect due to temperature difference between the outfall and the ambient are considered.

For the vertical model, averaging is done over the transverse distance, the value of which is to be determined from the flow spread as obtained from the horizontal model. In both the vertical and horizontal models, averaging implies adjustment of flow velocity so as to obtain given heat input and flow rate into the water body. For steady state conditions, equations (1) to (3) become:

$$u\frac{\partial u}{\partial x} + w\frac{\partial w}{\partial z} = \epsilon M\left(\frac{\partial^2 u}{\partial x^2} + \frac{\partial^2 u}{\partial z^2}\right) - \frac{1}{\rho}\frac{\partial p}{\partial x} \quad (4)$$

$$u\frac{\partial w}{\partial x} + w\frac{\partial w}{\partial z} = \epsilon M\left(\frac{\partial^2 w}{\partial x^2} + \frac{\partial^2 w}{\partial z^2}\right) - \frac{1}{\rho}\frac{\partial p}{\partial z} + g\beta\,(t - te) \quad (5)$$

$$u\frac{\partial t}{\partial x} + w\frac{\partial t}{\partial z} = \epsilon H\left(\frac{\partial^2 t}{\partial x^2} + \frac{\partial^2 t}{\partial y^2}\right) \quad (6)$$

These equations are coupled together through the temperature 't' due to the buoyancy effect and must be solved simultaneously.

The buoyancy effects in the vertical model are represented by a buoyancy parameter which is given by:

$$B = \frac{g\beta\Delta t}{U^2/l^2} = \frac{Gr}{Re^2} \tag{7}$$

In the governing equations for both horizontal and vertical models, it can be easily shown that for large R_e, the viscous or diffusion terms become smaller. This leads to the inviscid approximation, which gives the governing equation for flow as:

$$\nabla^2\psi = 0 \tag{8}$$

For low R_e, the inertia terms are small and the equations become linear, obtained as:

$$\nabla^2 \nabla^2\psi = 0 \tag{9}$$

For the two models, the average velocities obtained may be employed to determine the appropriate governing equations. In the mixed region, where neither approximation is valid, the full equations at given R_e must be solved. For the averaged velocities generally found in the vertical model equation (9) is valid.

The flow and temperature fields, shown as stream lines and isotherms respectively, for a horizontal two dimensional model using the inviscid approximation and with the intake and outfall at opposite ends are shown in Fig. 3. The same problem has been analysed with the vertical two dimensional model and the results are shown in Fig. 4. By analysing a particular case with both the models the temperature rise at the intake can be determined.

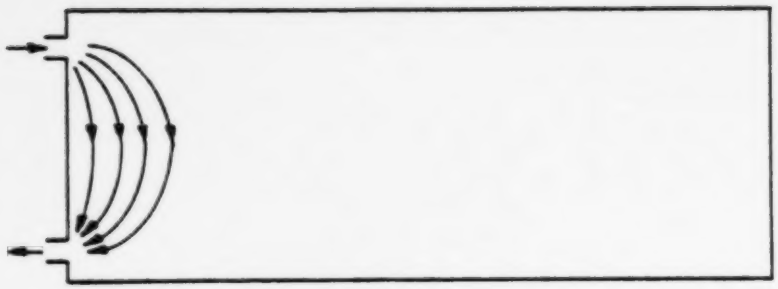

FIG. 3(a). HORIZONTAL

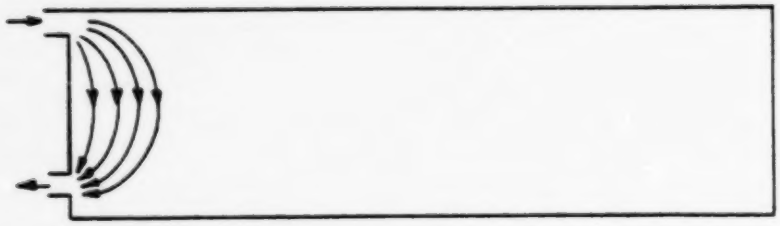

FIG. 3(b). VERTICAL

FIG. 3. THE PROBLEM VIEWED IN TERMS OF TWO DIMENSIONAL, HORIZONTAL AND VERTICAL FLOWS

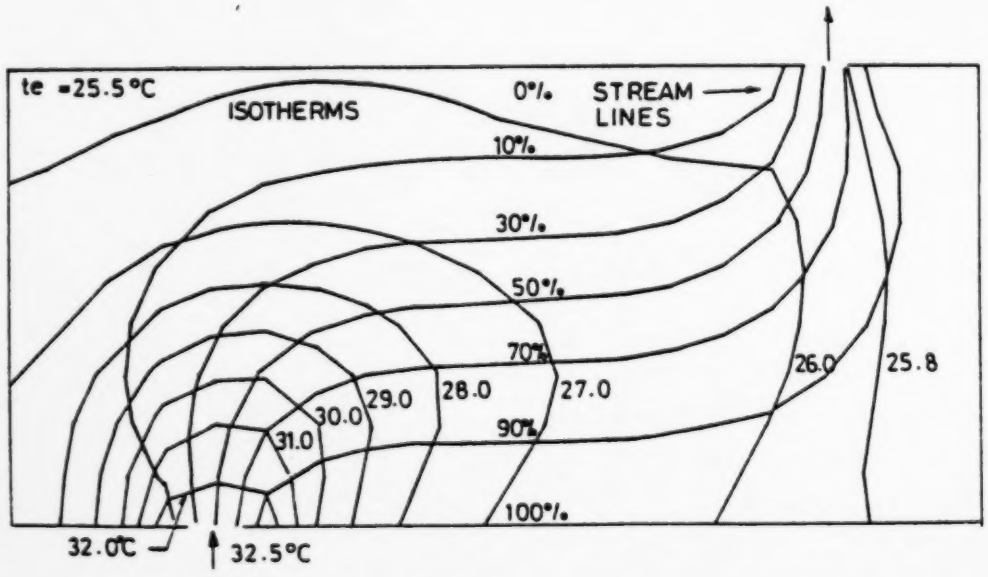

FIG. 4. HORIZONTAL TWO DIMENSIONAL MODEL. VELOCITY = 10^{-3} m/s DEPTH = 2.5 m. OUTFALL TEMP. = 32.5°C.

4. COMPUTER PROGRAMS

Computer programs have been developed to represent the point, 1-D horizontal, 1-D vertical, 2-D horizontal and 2-D vertical models. Both steady state and transient dynamics can be analysed using these models.

A graphic routine has been developed which can be used with the 2-D models to display stream lines and isotherms on a CRT screen (or plot on plotter). In the 2-D horizontal model, the coordinates of the corner points of an equivalent polygon are used for representing the boundary of the water body. All computations at a node are performed only after ascertaining that it is within the boundary of the water body. The coordinates of the intake and outfall can be interactively changed, enabling various locations to be tried out during the analysis. Similarly, the depth of the outfall and intake can be interactively changed for the vertical model.

5. PROCEDURE FOR USING THE MODELS

In some special cases, the various models can be used individually, as stated in the corresponding sections. However, in most practical cases, where the flow pattern is essentially three dimensional, the models have to be used in combination to obtain the temperature profile.

For example, in a particular case, the point model is used with the given weather conditions to obtain natural equilibrium water temperature over the year. The 1-D vertical transient model is used to determine the natural vertical temperature profiles over the year. The 2-D horizontal model is next used with the best intuitive/logical location of intake-outfall and the physical depth of outfall to give an estimate of the spread of the flow field. This information and the total heat rejected is used with the 1-D vertical transient model to give the 'worst' weather conditions over the year. These conditions are then used with the 2-D vertical model to give the value of the inlet temperature. Typical results are shown in Fig. 5. The intake-outfall configurations are then altered and various alternatives studied with each case being analysed by both vertical and horizontal models to give logically consistent results.

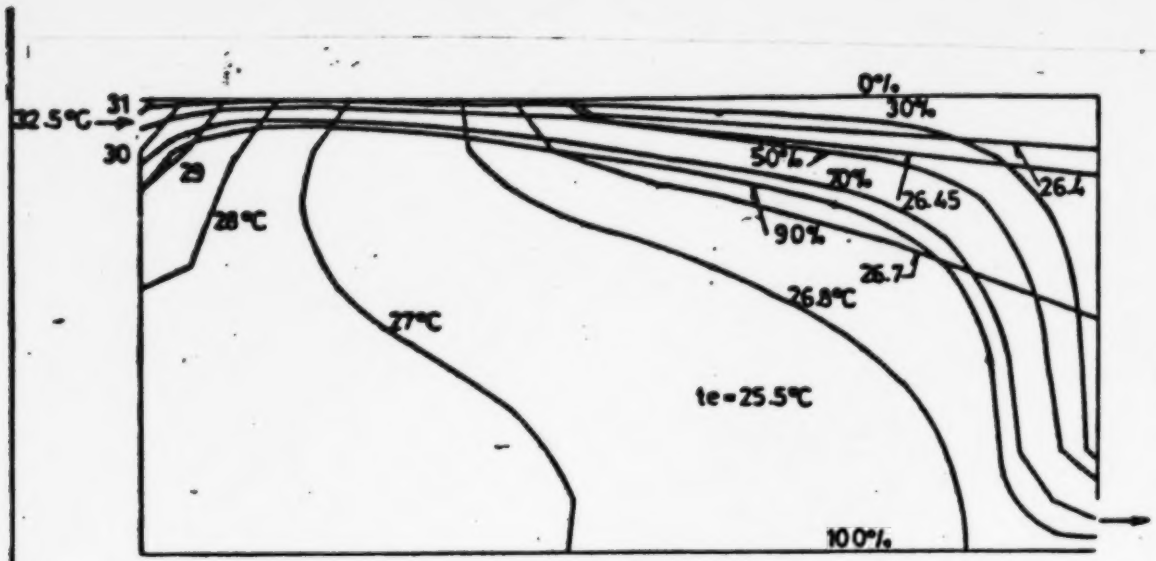

FIG.5. VERTICAL 2D MODEL. HEIGHT OF OUTFALL=1m
$\varepsilon M = 10^{-3} m^2/s$ $Bf = 10^{-3}$ $\varepsilon H = 1.8 \times 10^{-3} m^2/s$

6. CONCLUSIONS

A series of models have been developed to analyse thermal discharges into water bodies. The approach followed is to analyse the complex three dimensional phenomenon with a relatively simple one and two dimensional models so that the result can be interpreted and related to the physics of the actual case. Use of interactive graphics facilitates this procedure.

These models serve as an effective tool in the design of thermal discharges into water bodies as the effects of various parameters such as location of intake and outfall, outfall and intake velocities, etc., on the temperature distribution can be determined. The extent of recirculation to be expected in a particular case can also be estimated.

ACKNOWLEDGEMENTS

The authors wish to acknowledge the help rendered by Dr. Y. Jaluria, Indian Institute of Technology, Kanpur, India. We would also wish to place on record our sincere thanks to the management of Tata Consulting Engineers for their kind permission to publish this paper.

NOMENCLATURES

B	=	buoyancy parameter
Cp	=	specific heat, Kcal/Kg - ^{o}C
E	=	acceleration due to gravity, m/sec^{-}
Gr	=	Grashoff number
l	=	height of the out fall, m
p	=	pressure, Kg/m^{2}
Q	=	heat gained, $Kcal/m^{2}$ - sec
Re	=	Reynolds number
t	=	temperature, ^{o}C
U,V,W	=	Velocity components in X, Y, Z directions respectively, m/sec
β	=	coefficient of thermal expansion of water
ρ	=	density, Kg/m^{3}
ψ	=	stream function
ϵH	=	eddy diffusivity
ϵM	=	eddy viscosity

REFERENCES

1. Variyar, P.C.K., Mehta, S.I. and Jaluria, Y., Mathematical models for analysing heat rejection from power plants to a water body. Presented at 4th National Conference of Heat Transfer, India, 1978,

2. Anderson, E.R. Energy budget studies, water loss investigation, Lake Hefner studies, Goel Survey, U S Dept. of Interior, Washington D.C., 1954.

3. Rapnael, J.M., Prediction of temperature in rivers and reservoirs, ASCE J. of Power Division, pp 157-181, July 1962.

4. Jirka, G.H., Abraham, G. and Harleman, D.R.F., An assessment of techniques for hydrothermal prediction, Report prepared for Nuclear Regulatory Communication, Report No. PB-250509, Nat. Tech. Inf. Service, USA, 1975.

Reproduced from best available copy.

SESSION VII A

GREENHOUSE II

Preceding page blank

PB82-228313

GREENHOUSE HEATING SYSTEM DESIGN AND ECONOMICS FOR WASTE HEAT UTILIZATION

D. M. Stipanuk and R. E. Friday
Department of Agricultural Engineering
Cornell University
Ithaca, New York

B. Chezar
Power Authority of the State of New York
New York, New York

ABSTRACT

Three distinct categories of waste heat are discussed. These categories are low temperature (32-80°F), moderate temperature (80-130°F), and high temperature (over 130°F). If a moderate temperature source is used the sizing of the heat delivery system to provide less than 100% of the greenhouse design heating load from waste heat can result in substantial cost savings. Several new innovations in greenhouse heating (heated porous concrete floors, plastic panel heat exchangers and low operating power fan coil units) are discussed which offer the designer of heating systems options which are suitable for various applications.

1. INTRODUCTION

Within the past five years a substantial number of experimental and commercial waste heat greenhouse operations have been undertaken. The earliest major commercial waste heat operation in the U.S., the Northern States Power (NSP) greenhouse in Minnesota, continues to exhibit growth in the acreage at its location., Recently, Pennsylvania Power and Light (PP&L) has begun supplying waste heat to a 2.75 acre greenhouse in Pennsylvania and several Canadian ventures have either begun or are in the planning stages. The Power Authority of the State of New York (PASNY) is currently preparing bid documents for the initiation of a waste heat greenhouse at their Astoria 6 (New York City) plant.

An excellent overview of many aspects of waste heat utilization has been presented by Goss et al. (1980). This discussion deals quite extensively with the concerns of both the waste heat supplier and the user and included legal and contractual considerations. Since the subject of Goss et al. was the general topic of waste heat a great deal of detail on the topic of waste heat for greenhouses was not included.

Work at Cornell funded by the PASNY and the New York State Energy Research and Development Authority (NYSERDA) has resulted in several design recommendations for waste heat greenhouses. In addition, several new heating system options have been researched which appear to broaden the options available to prospective waste heat greenhouse developers.

Preceding page blank

2. GREENHOUSE HEATING REQUIREMENTS

The initial sizing of a greenhouse heating system requires information regarding the peak heating load of the greenhouse. Several factors must be considered when evaluating the peak heating load of the greenhouse. Among the factors which are important are:

1. The heat loss characteristics of the greenhouse structure.

2. The indoor (greenhouse) and outdoor (ambient) design temperature for the greenhouse.

While the size (BTUs/HR) of the greenhouse heating system is dictated by the values listed above, the annual heating needs (BTUs) of the greenhouse are based for the most part on the total Heating Degree Days (HDDs) for the proposed greenhouse location.

Table 1 lists recommended design heat loss values ("U" values) for various types of greenhouses. These values have been developed by the National Greenhouse Manufacturers Association. As can be seen from Table 1, the heating requirements for a glass greenhouse will be substantially higher per ft^2 than for a double-layer plastic greenhouse.

The indoor design temperature for the greenhouse is somewhat dependent upon the type of crop which will be grown. Table 2 lists the recommended daytime and nighttime greenhouse temperatures for several common greenhouse crops. Since the grower may wish to change crops during the lifetime of the greenhouse the heating system may be sized for a relatively high indoor temperature to allow for this option. The outdoor design temperature selected is generally from the ASHRAE Handbook of Fundamentals. A median of annual extremes value may be used, especially if the coincident wind velocity term in the winter months is high.

A factor which complicates a detailed analysis of annual greenhouse heating needs is the solar gain of the greenhouse during the day. Peak heating needs are generally assumed to occur at night so the solar term is not a problem in sizing the system. However, it is not particularly simple to estimate the overall solar contribution to the greenhouse. Albright (1978) reported on a test period in which 56% of the recorded HDDs occurred at night (6 p.m. to 8 a.m.) while 71% of the total auxiliary heat was required at night. For a climate such as Ithaca, New York, it is likely the daytime hours contribute about 25% of the auxiliary heating while the nighttime hours contribute the remaining 75%.

3. WASTE HEAT SOURCES

S. Brown in Goss et al. (1980) presents an excellent overview of the various types of power plant condenser cooling water discharges and the temperature levels involved. In addition to the large quantities of heat discharged in the condenser cooling water of power plants there are a number of other smaller power plant discharge sources which are often mixed with the cooling water. These include various oil coolers, condensate discharges and miscellaneous other sources such as the water used for the cooling of multistage air compressors. Industrial plants may also have heated discharge streams varying in quantity and temperature depending on the nature of the production process.

Waste heat streams for potential greenhouse heating can generally be classified most conveniently based on the temperature of the streams. For the purpose of discussing the use of waste heat for greenhouse heating the most convenient categories of waste heat are high temperature (above 130°F), moderate temperature (80 to 130°F) and low temperature (32 to 80°F). The exact limits of the various categories are somewhat arbitrary, particularly in the transition from moderate to high temperature waste heat.

3.1 High Temperature Waste Heat

High temperature waste heat (above 130°F) is not readily available from electric power stations in any of the normal cooling water streams. Access to a high temperature waste heat source from a power plant will generally require access to the steam system of the power station with a possible reduction in the MWHR production. Given the high value of the MWHRs produced and the concern for the quality of the steam it is unlikely a waste heat greenhouse will have access to the steam cycle.

High temperature waste heat is more likely to be available from such sources as boiler or furnance stack gases or emissions. A study for NYSERDA (1978) indicated the amount of industrial waste exhaust energy produced in New York State each year was 68 x 10^{12} BTU. This is the energy equivalent of 480 million gallons of fuel oil. Table 3 summarizes the results of the survey done for NYSERDA of industrial waste heat sources in New York State.

Use of a high temperature waste heat stream for greenhouse heating does not require the use of unusual heating systems. Assuming the waste heat stream can be made available in the form of high temperature water, a conventional pipe heating system (pipes around the perimeter and in the gutter area or under the benches) can be used to heat the greenhouse. The high temperature waste heat source is the most desirable waste heat source. It is likely such sources will also be valuable to the industrial plant producing the waste heat. It is more likely the greenhouse will have to compete with the manufacturing plant for the "rights" to utilize the high temperature waste heat source. This may mean the industrial plant will place a relatively high charge for the discharged heat.

3.2 Moderate Temperature Waste Heat

Moderate temperature waste heat (80 to 130°F) may be readily available from some electric power generating stations. The availability of moderate temperature waste heat is most likely at power plants having cooling towers, cooling lakes or cooling channels. Power plants with once through cooling systems are not likely to have cooling water discharge temperatures consistently in the moderate temperature range during the winter months. This will be particularly true for power plants in the northern portion of the United States or Canada, areas where the greenhouse industry could substantially benefit from waste heat utilization due to cold ambient temperatures.

The primary attention to date to the use of moderate temperature waste heat sources has been directed at the use of the condenser cooling water from electrical power stations using cooling towers (NSP and PP&L, for example). The investigation of other sources of moderate temperature heat has been relatively slight. New York State, with slightly less than 10% of the population of the United States and about 400 acres of commercial greenhouses has no

electric power generating stations with cooling towers. Other states are expected to have similar "problems" regarding waste heat.

Discussions with the engineering staff of PASNY regarding the possibilities of waste heat utilization at the Astoria 6 power station (a 825 MW oil fired unit with once through cooling located in the Astoria section of Queens in New York City) resulted in the identification of several potential moderate temperature waste heat streams. Among the sources identified were the main turbine lube oil cooling water, the closed cooling water system, and the condensate from the steam used to heat oil at the adjacent oil tank farm. While none of these sources has the quantity of heat present in the condenser cooling water, the amount of a heat in some of the sources is substantial. For example, the turbine lube oil cooling water removes in excess of 12×10^6 BTUs per hour from the lube oil. This source is available whenever the power plant is operating and does not vary with unit load. This is a major advantage.

Use of moderate temperature waste heat as a source for greenhouse heating poses several design problems. The relatively low temperature of the waste heat source means the temperature difference between the greenhouse air temperature and the heat source is relatively low (typically 30-40°F). In order to deliver the required greenhouse heating, the heat exchange mechanism between the waste heat and the greenhouse must either have a large surface area and/or utilize fans to increase the heat transfer coefficient between the air and the waste heat. If the surface area of the exchanger is increased the cost of the exchanger may also increase. If the exchanger becomes too large it may interfere with light levels in the greenhouse and reduce production. If the fan power consumption reaches very high levels the cost of operating the fans may prove to be a significant cost item somewhat offseting the savings of switching to a waste heat source.

3.3 Low Temperature Waste Heat

Low temperature waste heat (32-80°F) is available from many sources. Once through cooling systems on electrical generating plants in the northern U.S. will typically have cooling water exit temperatures in this range during the winter months. Table 4 lists the cooling water exit temperatures which are typical of the Astoria 6 power plant during the heating season. Use of water at these temperatures directly as a source of heat from greenhouses is not possible except under very unusual circumstances. Walker (1978) has proposed spraying this water over the surface of the greenhouse to reduce the heating load in the greenhouse. While this concept would appear to have some merit, the results of the studies performed by Walker at an Illinois Power Co. plant have not yet been released.

Other sources of low temperature waste heat exist beside the cooling water discharge from electric power plants. Lanz (1978) reported on the use of waste water treatment plant effluent as a waste heat source. He indicated this effluent was at a low temperature of 64°F in January and peaked at a high value of 88°F in July. This stream averaged a flow rate of 38×10^6 gallons per day (over 1.5×10^6 gallons per hour). Lanz used a heat pump to elevate the temperature of the waste heat to 160°F so it could be used for space heating.

The use of a water-to-water heat pump at Astoria was studied. The results of the study indicated the heat pump would have substantial investment and operating costs which would adversely affect the feasability of this means of waste heat utilization. Only if a very high priced alternative were the

only option would the heat pump waste heat combination prove attractive. This result led to the investigation of the presence of other heat sources at Astoria which were at a higher temperature. The result of this investigation was the suggestion to use the turbine lube oil cooling water, a moderate temperature source.

3.4 Reliability and the Need for Backup

The reliability of the waste heat source is a very key issue in assessing the viability of a waste heat application. Assuming the annual maintenance outage of Astoria is scheduled in either the early fall or the late spring (summer is not possible due to the high summer load of New York City) it is likely Astoria will not be available for about 10% of the heating season due to unscheduled maintenance (10% of the Heating Degree Days). Because of this problem it is necessary to have a 100% backup system. PP&L has elected to provide the grower with a coal fired boiler rather than connect the greenhouse to the second unit at the site. This decision was made because of the cost of the additional connection. At Astoria, steam is available to serve as a backup source.

It may be desirable for the backup heating system to be able to interface with the heat delivery system for the waste heat. In this way additional investment for a backup heat delivery system can be avoided.

The operation of the backup greenhouse heating system during a power outage may be important. Waste heat systems which require substantial amounts of power for heat delivery, such as fan coil systems and especially heat pump systems, may be subject to potential disaster during prolonged electrical outages in sub-freezing weather. Standby power systems to operate the fan coil systems may not be prohibitively expensive. It is estimated no grower could afford the standby power system needed to operate the heat pump delivery systems. Several hundred KW of standby power per acre would probably be required for the heat pump systems. The heated floor system and the plastic panel heat exchanger discussed later in this report will have relatively small operating power and probably could be supplied with a standby power system at a reasonable cost.

4. GREENHOUSE HEATING SYSTEMS SUITABLE FOR WASTE HEAT UTILIZATION

Depending on the temperature of the waste heat source, there are various heating systems which may be suitable for utilization of waste heat for greenhouse heating. Among these systems, pipe delivery, fan coils, heated floors and plastic panel heat exchangers appear to be leading options. The first three are in commercial use at the present time. The plastic panel heat exchanger is a recent development at Cornell University which appears to have promise for both conventional and waste heat greenhouse heating.

4.1 Pipe Delivery

If a high temperature waste heat source is available it is quite probable the grower may consider the use of a pipe heating system. In these systems pipes are placed around the perimeter of the greenhouse, in the area under the gutters and, possibly, in the area under the benches. Langhans (1980) contains a discussion of the details of such a heating system.

The sizing of a pipe delivery system for a high temperature waste heat greenhouse is not significantly different than it would be for a conventional greenhouse with a boiler source. Since the pipe system would also serve as a means of delivering the backup/auxiliary heat there is no reason to be concerned about the means of delivering the backup heat. The backup/auxiliary heat will be at a temperature near that of the waste heat source so the heating capacity of the system will be approximately the same whether the heat source is waste heat or backup/auxiliary. No significant additional waste heat delivery costs will be incurred by the grower since the size and cost of the heat delivery system in the greenhouse will be approximately the same as for a conventional greenhouse.

4.2 Fan Coil Delivery

Fan coil heat delivery might be chosen when a moderate temperature waste heat source was available. It could also be chosen for a high temperature waste heat source. However, the differences in the cost of the fan coil units and the operating power required for a moderate temperature versus a high temperature source would be very large.

Table 5 summarizes capacity, operating power and unit cost data for three fan coil delivery options. The hot water data was taken from specification sheets. The McQuay LSL - 217 coil is currently in use at the NSP waste heat greenhouse. The Modine coil is a prototype developed by Modine specifically for use in a waste heat greenhouse. The Modine coil is the coil recommended by Cornell for the PASNY waste heat greenhouse. Several interesting differences exist between moderate temperature fan coil units and high temperature fan coil units. High temperature fan coil units (designed for use with 200°F hot water or steam) have an initial cost of about $2,600 per 10^6 BTU/HR of capacity. Moderate temperature coils have an initial cost of $20 to $25,000 per 10^6 BTU/HR of capacity. This is obviously a significant increase in cost resulting in a substantial increased investment in heating system capacity for a moderate temperature system.

The moderate temperature fan coil units also require substantially more fan power to deliver their heat than do the high temperature coils. A typical high temperature coil requires about 2 HP of fan power per 10^6 BTU/HR of capacity. A moderate temperature coil such as the McQuay unit requires 24 HP per 10^6 BTU/HR of capacity. The Modine coil requires 12 HP of fan coil power per 10^6 BTU/HR of capacity.

Moderate temperature fan coil capacity can be significantly affected by changes in the greenhouse temperature, the temperature of the water supplied to the fan coil and the flow rate of the water through the fan coil. An increase in the greenhouse temperature reduces the temperature difference between the greenhouse air and the moderate temperature water entering the fan coil. The rate of heat transfer from the fan coil unit is approximately proportional to the temperature difference between the moderate temperature water entering the coil and the greenhouse air.[1] Therefore, if the greenhouse is operated at 60°F and the moderate temperature heat source temperature drops from 100 to 95°F, the capacity of the fan coil units drops to 87.5% of its value with a 100°F source temperature. Similarly, if the temperature of the moderate temperature heat is raised from 100 to 105°F, the

[1]The heat transfer rate is actually proportional to the log mean temperature difference.

capacity of the fan coil unit will be 112.5% of its value at the 100°F source temperature. A similar but opposite change in the fan coil capacity occurs for increases or decreases in the greenhouse air temperature.

Since the moderate temperature fan coil capacity can be significantly increased by supplying it with hot water, the fan coil can serve as a peaking system for greenhouse heating. When operated in this manner the moderate temperature fan coil has its capacity effectively doubled or tripled by connecting it to a source of high temperature heat such as a boiler. Use of the moderate temperature coil in this manner can result in a significant reduction in the capital investment for a fan coil heating system using moderate temperature waste heat. The Astoria example later in this paper illustrates this .

Fan coil units can readily serve as a delivery means for backup or auxiliary heat should the waste heat source be unavailable. No additional investment in a backup heat delivery system is necessary if fan coil units are present. Some sort of backup heat source (a boiler) will be necessary as well as some means of switching the fan coils to the boiler. One advantage of being able to use the fan coil units as a means of backup heat delivery is the lack of a need to install additional heaters in the greenhouse.

4.3 Heated Floors for Greenhouses

Two primary means of supplying greenhouse heating needs via heated floors are currently in commercial use. The first of these uses pipes embedded in the soil comprising the greenhouse floor. This system contributes a portion of the heating needs at the NSP greenhouse. The second version of a heated floor system is the porous concrete floor developed at Rutgers University. This system may exist in three forms: a flooded floor, a piped floor or a combination of the two.

The use of pipes embedded in the soil comprising the greenhouse floor has been studied rather extensively. Heat transfer from the pipes to the floor and hence from the floor eventually to the greenhouse is negatively affected by the drying out of the soil near the pipes, and by losses to the soil below the pipes. It may be desirable to insulate the area below the pipes to avoid non-useful heat loss from the pipes. Roller (1980) reported on heat transfer rates from buried pipes to various types of soils. The maximum rate of heat transfer reported by Roller was about .56 BTU/HR - ft^2 - °F. He reported the floor was estimated to be able to supply 36% of the annual heating needs of a greenhouse located in Wooster, Ohio if a source of 35°C water were available.

Use of soil heating may be desirable when crops are grown on or in the soil. Roller reported significantly decreased growing times (improved productivity) for lettuce grown in heated soil. The overall contribution of the heated soil system to the heating load is relatively slight due to the relatively poor heat transfer between the pipes and the floor.

Roberts (1980) of Rutgers reported heat transfer data for heated porous concrete floors. These systems use either pipes embedded in the floor with warm water circulated through the pipes or a flooded floor with the water about 3 inches below the top of the floor or a combination of the two where the heated water is circulated through pipes in a flooded floor. Heat transfer rates for the porous floor systems are significantly better than for soil heating only. Table 6 compares heat transfer rates for the two methods of floor heating. Table 6 includes a "breakeven" temperature for the floor

heating systems. The "breakeven" temperature is the temperature at which the loss rate from the floor equals the loss rate from a double-poly greenhouse.

The heated floor systems are most suitable for waste heat applications with essentially no limit on the quantity of waste heat. In these circumstances the water serving as a heat source can be circulated quickly resulting in a relatively small temperature drop in the water and a high mean temperature for the floor. This will result in higher overall rates of heat transfer to the greenhouse. PP&L reports a 9-10°F temperature drop in the heated porous floor system at their Montour site. This is 5°F less than the 15 degree drop which is typical of the value for fan coil design. When limited quantities of waste heat are available (a limited GPM at a fixed temperature) the maximum use of this waste heat will require a greater temperatue drop. While this can to some degree be accomplished by slowing the flow rate of the water through the floor this will also mean the floor will operate at a lower mean temperature. Operation of the floor at a lower mean temperature will decrease the heat transfer capacity of the floor and therefore its potential contribution to the annual heating needs of the greenhouse.

4.4 Plastic Panel Heat Exchangers

An experimental greenhouse heating system has been developed at Cornell University using plastic panels for both heat delivery and as bench tops. The plastic panels used are sold commercially as solar swimming pool water heaters. The panels consist of 4' x 10' sheets of plastic with integral flow channels connected to headers at each end. Water is circulated into one of the headers, flows through the flow channels in the sheets and exits at the other header. An excellent overview of these panels is provided by Madsen (1981).

It was anticipated the plastic panel heat delivery system would have the following advantages over competing systems for moderate temperature waste heat delivery:

1. Provide bottom heat for bench grown crops.

2. Have heat transfer relatively unaffected by the presence of a crop since both sides of the panel contribute to its heating ability.

3. Require relatively little heat delivery pump or fan power.

4. Have a portion of its cost offset by the bench top material replaced.

5. Be modular, easily installed by the grower and easily repaired or replaced.

6. Offer the possibility of increased overall heat transfer by fan assist under the panels.

Greenhouse testing of the panels has been underway at Cornell since the winter of 1980-81. Table 7 summarizes preliminary heat transfer data. Assuming a greenhouse has a heat loss rate of 1.2 BTU/Ft^2 - HR - °F based on floor area and the design temperature difference for the greenhouse location is 60°F, a maximum heating capacity of 72 BTU/Ft^2 will be required. Assuming a very modest bench to floor ratio of 50%, the design heat transfer rate per

ft^2 of bench will be 144/BTU-Ft^2. Assuming a 30°F temperature difference between the water in the panel and the greenhouse (i.e. 90°F water and a 60°F greenhouse) the required heat transfer rate is 4.8 BTU/HR - Ft^2. This value is within the range of heat tranfer possible from the panels with fan assist.

Plant research using the panels indicates no plant growth problems have been observed with mums for mat temperatures in the range of 90 to 100°F. Sustained operation of the mats at higher temperatures resulted in a decreased growth rate for the mums. It is expected no plant growth problems should exist if the mat is operated below 100°F.

If the plastic panels are purchased commercially in large volumes they should be available for \$2 - \$4 per ft^2. The cost of a plastic panel heating system should be comparable to that of a fan coil system but with only a fraction of the operating energy since fan operation under the panels will only occur during very cold ambient. The panels may cost somewhat more than a floor heating system. However, the panels have the capability of delivering 100% of the heating needs of the greenhouse. No investment in additional heat delivery capacity will be needed if the panels comprise the bench tops in the greenhouse and fans are placed under benches.

5. GREENHOUSE HEAT DELIVERY SYSTEM SIZING - ASTORIA AS AN EXAMPLE

During the analysis of heating system options for the Astoria site two greenhouse heat delivery system sizing criteria were developed for moderate (and possibly low) temperature waste heat installations. These criteria are summarized below:

Recommended Sizing Criteria for Moderate Temperature Waste Heat Delivery Systems
1. Sizing of the greenhouse heat delivery system for 100% of the greenhouse design load from waste heat is a sub-optimal choice resulting in unwarranted capital investment.
2. Selection of a waste heat source based on its ability to provide 100% of the design heating load of a greenhouse is an unduly restrictive criteria resulting in the exclusion of economically viable waste heat sources.

The first sizing criteria, that of sizing the greenhouse heat delivery system for less than 100% of the peak heating load of the greenhouse, is a result of the distribution of greenhouse heating requirements. Table 8 lists the nighttime heating degree hours for Newark, New Jersey. The design ambient temperature for a greenhouse at Newark would be about 7°F.

Using a fan coil delivery system as an example, the relative performance of heat delivery systems sized to provide less than 100% of the design load for a greenhouse can be compared. Table 9 summarizes the results of an analysis for Astoria of various design options. A fan coil option which is sized for 80% of the peak heating needs of a greenhouse is capable of providing 99% of the annual heating needs of the greenhouse from waste heat.

Table 10 relates the financial aspects of the data in Table 9. The 80% design option results in first year costs which are \$4,500 less per acre than a 100% waste heat case. This is a 20% reduction in the first year costs.

Table 11 extends the results of Table 10 to include a 10 year discounted cash flow analysis of various heat delivery system sizing options. The 80% design case has a present worth of $22,300 less than the 100% waste design case for a 19% savings.

The high cost of fan coil delivery systems and the relatively short period of time during which the full capacity of a 100% design waste heat delivery system is used results in an economic optimum at some design other than 100%. The exact design optimum will vary from installation to installation depending on the cost of the backup heat. A cost of backup of $8/MMBTU, as is used in one of the examples, will favor a lower design value for the fan coil capacity. A higher cost of backup, such as the $16/MMBTU used in the other example, will favor a higher fan coil design value. The reliability of the waste heat source may also influence the economic design optimum.

The second sizing criteria is somewhat a result of the first although they are separable. If the design heating load of the greenhouse (and values within 20% of this load) are incurred during a relatively small percentage of the year, a waste heat source which has available only a fraction of the design heating load of a greenhouse may still be a viable (economical) waste heat source. The Astoria unit is an example of this.

The identified moderate temperature waste heat source at Astoria is the turbine lube oil cooling water. This source is available at about 100°F with a flow rate of 350 GPM. If this water were to be cooled to the 60°F greenhouse air temperature (perfect heat exchange) a maximum of 7 MMBTU/HR of heat would be available. This would appear to be only capable of meeting the heating needs of 2.3 acres of greenhouse. This source would appear to have a very limited potential to supply the heating needs of the 3 acres reserved for waste heat greenhouses at Astoria.

Using the same computer model used to evaluate the sizing design criteria for fan coils discussed previously, the potential of using the 350 GPM source discussed above was evaluated. Sizing the heat delivery system at about 83% of the design heating load, the 350 GPM source was able to supply 92% of the annual greenhouse heating load for 3 acres from waste heat. Given the assumptions used in the computer program this value is probably a conservative estimate of the potential of the waste heat source.

Ashley (1979) reported an investment in moderate water temperature pipelines at NSP of $35 - $40,000 per acre. PP&L recently invested $700,000 in a pipeline for 30 acres and opted to forego an additional $300,000 to connect a second unit for backup. Assuming these costs are to some extent proportional to the % of the design load to be supplied from waste heat, the scaling down of the % of the design load to be supplied from waste heat could reduce the cost of such pipelines. This approach could substantially reduce the high initial cost of waste heat ventures. This may help to reduce the reluctance of potential waste heat suppliers to enter into such agreements. More study is needed of this approach in terms of design and overall economics before definitive guidelines can be given. The concept appears to have significant potential for improving waste heat economics.

6. CONCLUSIONS

The development of a moderate temperature fan coil unit by Modine Manufacturing can reduce the operating power of these units. In areas with high electric costs this may be a very attractive option.

The use of plastic panel heat exchangers as a means of supplying greenhouse heating needs has promise. The primary benefits of this method are the high heat transfer rates achieved with little fan power and the ease with which a grower could install such a system. Control of the heat is also relatively easy. The panels should offer yet another option to the designer of a waste heat greenhouse.

The design of greenhouse heating systems using moderate temperature waste heat sources can benefit economically by an analysis of the distribution of the heating degree days for the potential location. If fan coil units are selected as the means of providing heat a significant reduction (20% or more) in the installed cost of the fan coil system can be achieved by sizing these systems for less than 100% of the design load of the greenhouse from waste heat. It is possible a comparable savings may also exist for a similar sizing method for the waste heat delivery pipelines.

REFERENCES

1. L. D. Albright, et al., Experimental Results of Solar Heating a Brace Institute Style Greenhouse, 3rd Annual Conference on Solar Energy for Heating of Greenhouses and Greenhouse-Residence Combinations, Fort Collins, Colorado, 1978.

2. G. C. Ashley, Heating Greenhouses in Northern Climates with Power Plant Reject Heat, HORTSCIENCE, Vol. 14(2), 1979.

3. L. Barry Goss, ed., Factors Affecting Power Plant Waste Heat Utilization, Pergamon Press, New York, 1980.

4. R. W. Langhans, Greenhouse Management, Halcyon Press, Ithaca, New York, 1980.

5. R. W. Lanz, Heat Recovery and Utilization for Green Bay's Waste Water Treatment Facility, Proceedings of the Second Conference on Waste Heat Management and Utilization, University of Miami, Coral Gables, Florida, 1978.

6. P. Madsen and K. Goss, Report on Non-Metallic Solar Collectors, Solar Age, January, 1981.

7. W. J. Roberts and D. R. Means, Floor Heating of Greenhouses, Paper 80-4027, American Society of Agricultural Engineers, San Antonio, Texas, 1980.

8. W. L. Roller and D. L. Elwell, Waste Heat for Soil Heating in Greenhouses, Paper 80-4032, American Society of Agricultural Engineers, San Antonio, Texas, 1980.

9. P. N. Walker, "Surface Heating Greenhouses with Power Plant Cooling Water," Transactions of the ASAE, Vol. 21, No. 2, 1978.

Table 1. Recommended "U" Values of Various Types of Greenhouses

Greenhouse Type	"U" Value (BTU/HR - FT^2 - °F)[1]
All metal (tight glass house)	1.20
Wood houses (glass)	
Good tight houses	1.09
Fairly tight houses	1.23
Loose houses	1.36
Fiberglass Covered Wood Houses	1.05
Fiberglass Covered Metal Houses	1.11
Plastic Covered Metal Houses (single layer)	1.11
Plastic Covered Metal Houses (double layer)	.78

[1]For a 60° temperature difference and wind speed less than 15 mph.

Sources: Greenhouse Management, J. J. Hanan, W. D. Holley and K. L. Goldsberry. Springer-Verlag, New York, 1978.
The Greenhouse Climate Control Handbook, Acme Engineering & Mfg. Corp., Muskogee, OK, 1978.

Table 2. Recommended Greenhouse Temperatures

Crop	Daytime Temperature	Nighttime Temperature
Chrysanthemum	65-70°F	60°F
Poinsettia	70	63
Rose	70-75	60

Source: Greenhouse Management, J. J. Hanan, W. D. Holley & K. L. Goldsberry, Springer-Verlag, New York, 1978.

Table 3. High Temerature Industrial Waste Heat in New York State

Source (Temp. - °F)	Annual Waste Heat (10^{12} BTU/YR)
Boiler (300 - 600)	28
Drying (100 - 150)	16
Furnace: 600	5
800	1
1000	8
1100	3
1200	7
Total:	68

Source: Low Level Heat Recovery Application in New York State, NYSERDA Report 78-16, Albany, NY, 1978.

Table 4. Astoria 6 Discharge Cooling Water Temperatures

Date	Discharge Water Temperature	Time
11/ 1/78	60°F	2 AM
11/15/78	59	2 AM
12/15/78	61	11 AM
1/ 2/79	47	2 AM
1/31/79	39	4 AM
2/15/79	35	5 AM
3/ 1/79	38	11 PM
3/14/79	40	3 AM
4/ 1/79	43	6 AM

Table 5. Fan Coils - Comparative Data

Fan Coil Type	Capacity (BTU/HR)	Fan H.P. per 10^6 BTU/HR	Unit Cost ($ per 10^6 BTU/HR)[1]
Hot (200°F) Water	224,000	2.2	$ 2,600
McQuay LSL-217	207,131[2]	24	19,300
Modine Prototype	126,000[2]	12	25,400

[1] 1981 $ excluding installation.
[2] Water Δ T = 14.8°F. Inlet water temp - Inlet air temp = 30°F.

Table 6. Floor Heating Heat Transfer Values

Description	"U" Value (BTU/HR - Ft^2 - °F)	"Breakeven" Ambient[3]
Flooded Floor (porous)[1]		
Bare	1.55	21°F
Flats	.90	39
Embedded Pipe[1] (6" spacing) Bare Floor (porous)	.74	42
Heated Soil[2]	.56	46

[1] Roberts (1980); [2] Roller (1980)
[3] Ambient air temperature at which floor loss rate = greenhouse loss rate for a greenhouse temperature of 60°F and 90°F water temperature.

Table 7. Heat Transfer Data for Plastic Panel Heat Exchangers

Mode of Operation	Approximate "U" Value (BTU/HR - FT^2 - °F)[1]
Bare Panel	2.4
Dense Potted Plant Canopy (148 CFM Fan)	4.3
Dense Potted Plant Canopy (296 CFM Fan)	5.1

[1]Based on Bench area, In glass greenhouse.

Table 8. Nighttime Heating Degree Hours (4:30 PM - 8:30 AM) at Newark, New Jersey

Temperature Range (°F)	Hours of Occurrance	Degree Hours (65°F Base)	%	Degree Hours (60°F Base)	%
60-64	533	1,599	2	-	-
55-59	497	3,976	4	1,491	2
40-54	484	6,292	7	3,872	6
45-49	462	8,316	9	6,006	9
40-44	519	11,937	13	9,342	13
35-39	597	16,716	19	13,731	20
30-34	465	15,345	17	13,020	19
25-29	276	10,488	12	9,108	13
20-24	170	7,310	8	6,460	9
15-19	93	4,464	5	3,999	6
10-14	44	2,332	3	2,112	3
5- 9	15	870	1	795	1
0- 4	2	126	<1	116	<1
Totals	4,157	89,771		70,050	

Source: Engineering Weather Data, U. S. Dept. of the Air Force, AFM-88-29, July 1978.

Table 9. Fan Coil Sizing at Astoria

% of Design Heating Load from Waste Heat	100	90	80	70	60
Installed Fan Coil Capacity (MMBTU/HR)	3.0	2.7	2.4	2.1	1.8
% of Annual Heating Load From Waste Heat	100	100	99	96	92

Table 10. First Year Heating Cost (Incl. Capital Investment) for Various Fan Coil Design Levels for a One Acre Greenhouse

	% of Design Load from Waste Heat				
	100[1]	90	80	70	60
Number of Fan Coils[2]	24	22	19	17	14
Fan Coil Investment[2]	$115,200	$106,000	$91,200	$81,600	$67,200
Annualized Fan Coil Cost (@ 20%/year)	23,000	21,200	18,200	16,300	13,400
Peaking Fuel Cost (@ $8/10^6 BTU)	0	60	300	1,200	2,400
Peaking Fuel Cost (@ $16/10^6 BTU)	0	120	600	2,400	4,800
Annualized Fan Coil	23,000	21,260	18,500	17,500	15,800
Plus Peaking Fuel Cost	23,000	21,320	18,800	18,700	18,200

[1]Heating system sized to provide 100% of greenhouse design heating load. In this analysis assumed to be 3 x 10^6 BTU/HR. Annual usage assumed to be 4 x 10^9 BTU.
[2]Using Modine coil, see Table 5, 126,000 BTU/HR per unit; $3,200 per coil plus 50% for installation.
[3]$8/$10^6$ BTU peaking fuel
[4]$16/$10^6$ BTU peaking fuel

Table 11. Discounted Cash Flow Analysis of Fan Coil Design Options

	% of Design Load from Waste Heat				
	100	90	80	70	60
Present Value:[1]					
@ $8/MMBTU[2] Auxiliary	$116,700	$107,200	$94,400	$ 94,000	$ 91,400
@ $16/MMBTU[2] Auxiliary	116,700	107,800	97,400	106,000	115,400

[1]1981 $, Fan coil investment plus auxiliary fuel.
[2]1981 fuel cost escalated 20% per year

All analyses for 10 year period; 20% per year fixed charge rate include maintenance and depreciation; 20% discount rate.

PB82-228321

GREENHOUSE HEATING OPTIONS: CAN WASTE HEAT COMPETE?

Richard E. Friday and David. M. Stipanuk
Department of Agricultural Engineering
Cornell University, Ithaca, New York

Gerald B. White
Department of Agricultural Economics
Cornell University, Ithaca, New York

ABSTRACT

This paper reports on a discounted cash flow analysis of the costs of waste heat greenhouse systems and more conventional heating alternatives. The annual equivalent of the ten-year heating, structure and startup costs for selected representative waste heat utilization systems, source temperatures and reliabilities are estimated. These costs are compared with the annual costs of continuing to heat an existing greenhouse with conventional fuels. They are also compared with the annual equivalent heating costs of a thermal night curtain system installed in an existing greenhouse and an existing greenhouse converted to a coal heating system.

1. INTRODUCTION

Waste heat has been touted as being either a free or cheap source of heat for greenhouses for over a decade. At Cornell University, we have collected more than 15 loose leaf notebooks, numerous pamphlets and several books of material reporting on research and demonstration projects dealing with various aspects of waste heat utilization for greenhouses. Much of the research and development work has taken place in the United States, but we also know of waste heat greenhouse studies and demonstrations that have been located in at least twelve other countries.[1]

We believe that sound economic analysis is a good place to start in assessing the future of waste heat greenhouses. But this greenhouse heating alternative can not be examined in isolation. What alternatives should waste heat greenhouse installations be compared to? Waste heat greenhouses will have to be built as completely new installations. Most waste heat analysis has been based on the implicit assumption that the relevant alternative is a new conventional greenhouse structure heated with fuel oil. This may not be the most valid comparison.

If the greenhouse industry is expanding, or if substantial amounts of the existing greenhouse acreage are being replaced each year, new waste heat greenhouses could be compared to new conventional structures heated by conventional means. If waste heat greenhouses compared favorably, they could provide the expansion facilities in the greenhouse industry. While we do not know exactly what the total heated greenhouse acreage is in the United States, the information in Figure 1 on national trends of greenhouse production

[1] Belgium, Canada, Czechoslovakia, England, France, Hungary, Ireland, Netherlands, Sweden, Scotland, U.S.S.R., West Germany.

Figure 1. United States Greenhouse Production Area in Selected Crops, 1975-1980.

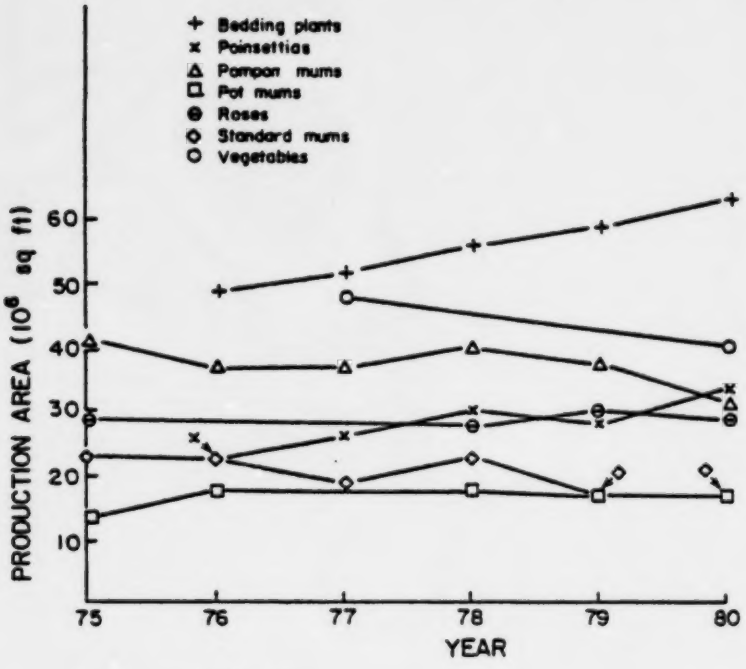

Sources: (1) (2)

devoted to selected major greenhouse crops is instructive [1]. Of the seven major crops shown, only bedding plants and poinsettias have exhibited any consistent increase in greenhouse production area in recent years. Both are very seasonal crops. This lack of expansion implies the possibility that, with current yields and product prices, the gross returns from many greenhouse crops are not large enough to cover the growing costs plus both the heating costs and the costs of a new structure. If this is true, growers with a committed investment can continue to operate in the short run as long as they can cover variable costs, but when the facilities become worn out or obsolete, investment in new facilities is not attractive. Such a trend can be seen in the greenhouse vegetable industry, in which a recent survey estimated that the producing area has declined by more than 15% in just three years [2]. In the traditional production center of Ohio, the trend was even more dramatic with a 45% decline in the greenhouse vegetable production area in the same three years.

One possible conclusion is that, in large parts of the United States, waste heat greenhouses will not be able to grow appreciably in the very near future simply because they are cheaper than the combined heating and structural cost of a new conventional greenhouse. Instead they may have to be so inexpensive to build and operate that they will actually replace substantial amounts of existing conventional greenhouses.

In reality the owners of existing greenhouse facilities have other options. The construction of a new waste heat facility capitalizes many of the greenhouse costs and requires a commitment for a number of years in order to justify those costs. A grower with an existing greenhouse, however, has the option of making a decision whether to continue or not each year. Fixed

costs such as depreciation and interest on existing facilities are not relevant to the decision. The economically optimal decision is to adopt waste heat technology when the additional operating cost of continuing to use the existing facility for one more season is higher than the average annualized cost of building and operating a waste heat facility. The owner of an existing facility also has a number of heat conservation and alternative fuel options that are now commercially available. For a smaller investment than is required for a waste heat facility it is possible for an existing facility to use a less expensive fuel or to use substantially less fuel.

2. GOALS

The primary goal of this analysis is to estimate the annual equivalent cash flow (AECF) of the total ten-year heating, structural and start-up costs for selected alternative waste heat utilization systems designed to use an 85°F waste heat source with a 95% reliability.[2] In addition, costs are estimated for one of the more viable waste heat systems operated over a range of waste heat source temperatures from 65-95°F and with a reliability of 80% and 95%.

The annual equivalents of the total heating, structural and start-up costs for the waste heat systems are then compared with the annual operating costs of heating an existing greenhouse with a conventional heating system using fuel oil or natural gas.

Finally, the annual equivalents of the waste heat system costs are compared with the annual equivalents of the additional investment and operating costs associated with the following types of modification of existing conventional greenhouse heating systems:

a) The installation of a thermal night curtain insulating systems in anexisting greenhouse structure with a conventional heating system;

b) The conversion of an existing greenhouse structure to a coal fueled heating system.

3. METHODOLOGY

The goals of this analysis involve the comparison of a large number of widely differing heating alternatives. For simplification, the analyses of heating systems presented in this report were based on partial budgets. Only heating costs and costs made necessary by a particular heating system were included. Costs and returns which were assumed to be the same for the alternative heating systems were not included. It was assumed that climate factors, greenhouse temperatures, cropping systems and receipts were the same for each alternative heating system. Costs associated with prior investment in existing conventional facilities were not included. New investment in greenhouse structures and heat exchangers required to make use of waste heat were included. In existing conventional greenhouse structures, only the additional investment required to install heat conservation modifications was included.

---

[2]The waste heat source is available for 95% of the heating hours.

The alternative heating systems being compared are characterized by widely differing mixtures of capital investment and annual operating costs. In order to make the comparisons of alternative heating systems as comprehensive and meaningful as possible, the cost for each alternative heating system was first formulated as a flow of estimated after-tax expenses. Only in this way could the effects of tax depreciation and investment tax credits be included. Ten-year flows were used to spread out investment costs. Selected costs, including fuels, were allowed to increase at a more rapid rate than inflation. Where only annual operating costs were counted, as in the case of continued operation of existing conventional installations, costs for a single year were also analyzed.

Each ten-year flow was then converted with an appropriate discount rate to an equivalent present value of the flow. The value of a dollar spent today is higher than the value of a dollar spent tomorrow because it can be used for immediate consumption or to earn more than a dollar in the future. Alternative heating systems must be compared in terms of what they would cost at the same point in time. Discounting makes the value of future costs comparable to current costs by correcting for the effects of inflation, risk and the time value of money. If a discount rate is chosen which accurately reflects the values of these variables as perceived by the grower, discounting a flow of heating costs should result in a present value to which the grower is indifferent when compared with the flow of future costs.

The discount rate is usually based on the cost of capital for investment. Because the cost flows being discounted in this case were after-tax costs, the discount rate used in the analysis was also adjusted for the marginal income tax rate. This is because income tax affects the after-tax cost of capital to the grower (3).

The last step necessary before direct comparisons could be made between heating system cost flows with different time horizons was the conversion of the present values of the cost flows to an annual equivalent cash flow (AECF) (3). The lump sum present value of the total heating cost for each alternative was expanded to a flow of equivalent real annual costs which, when discounted with an inflation-free discount rate, would yield the original present value. Using the inflation-free discount rate to obtain the annual equivalent from the present value removes the effect of inflation so that the equivalent is expressed in constant dollars. The real annual equivalent cash flows for alternative heating system costs can then be compared directly to each other. In particular, the use of AECF makes it feasible to compare the cost of waste heat greenhouses with the alternative of continuing to heat an existing greenhouse with conventional fossil fuels for an additional year.

4. DESCRIPTION OF THE SYSTEMS

4.1. Greenhouse Structure and Heating Requirements

The costs for all cases have been estimated for a one acre greenhouse structure of gutter-connected design with a double polyethylene covering. It was assumed that, in all cases, the greenhouse would be maintained at a minimum night/day air temperature regime of 60°/70°F. All cases were modelled for a hypothetical location with a climate representative of lower New York State/Long Island/northern New Jersey. Climatological data from Newark, N.J. [6] was used because it was disaggregated into the number of hours at each

Table 1. Assumed Values for the Analysis.

GREENHOUSE STRUCTURE & HEATING REQUIREMENTS	
Greenhouse size	1 acre
Geenhouse design	double poly, gutter connected
Min. design air temp	+11°F
Surface area/floor area	1.33
Min. greenhouse night temp	60°F
Min. greenhouse day temp	70°F
Greenhouse "U" value	.8 BTU/hr•ft^2•°F
Design max. heat loss	2.3x10^{6}BTU/hr•acre
Night heating degree hrs	70,052/yr
Night heat/total heat	75%
Annual heat loss/acre	4,250x10^{6}BTU/acre•yr
ECONOMIC PARAMETERS	
Utility prices	
Propane	$.69/gal
Natural gas	$.40/therm
Fuel oil (#2)	$1/gal
Coal	$62./ton
Electricity	$.05/kWh
Price increases	
Coal	15%/yr
All other fuels	18%/yr
Electricity	12%/yr
Pipeline capital recovery	fixed
All other costs	8%/yr
Pipeline (pump) capital recovery rate	20%/yr(25%/yr)
Marginal income tax rate	33%
Investment Tax Credits	
Structures	10%
Waste heat equipment	10%
Coal equipment	20%
Night curtain pulling system	10%
Night curtain fabric	3.33%
Depreciation methods	
Greenhouse structures	SL, 10 yrs
All equipment	DDB, 7 yrs
Discount rate (cost of capital)	
Nominal	15%
Real	7%
ALL WASTE HEAT SYSTEMS	
Distance to waste heat source	3,500'
Greenhouse area served by pipeline	10 acres
Qty. of waste heat available	unlimited
Maximum pipeline pressure drop	.5psi/100'
Propane heat content	93,000 BTU/gal
Propane combustion efficiency	75%
FAN COIL WASTE HEAT	
Unit specifications	
Heat exchange capacity with 30° ΔT (entering water temp. -entering air temp.)	207,000 BTU/hr• unit
Water flow	28 gpm/unit
Water ΔT (entering water-exit water)	15° F
Fan HP	5 HP/unit
POROUS FLOOR SYSTEMS	
Heat Transfer Rate	
Flooded porous floor	1.45 BTU/hr•ft^2•°F
Piped porous floor	.67 BTU/hr•ft^2•°F
Water temperature drop through the floor	5°F
Pipe spacing	12"
HEAT PUMP/PARTIAL FAN COIL	
Heat pump capacity	100 tons
Heat pump average COP	7.0
Heat pump water pressure drop	15 psi
CONVENTIONAL HEATING SYSTEMS	
Natural Gas Hot Water	
Heat content	100,000 BTU/therm
Combustion efficiency	75%
Heating system electricity use	5.0 kw/10^6 BTU
Oil Forced Air	
Heat content	139,000 BTU/gal
Combustion efficiency	65%
Heating system electricity use	9.0 kw/10^6 BTU
MODIFIED CONVENTIONAL SYSTEMS	
Night Curtain/Oil Heat	
Nighttime fuel savings	50%
Annual fuel savings	38%
Fabric life	5 years
Coal Conversion	
Coal type	anthracite
Heat content	13,000 BTU/lb.
Combustion efficiency	70%
Additional maintenance labor	600 hr/acre•yr
Heating system electrical use	4.0 kw/10^6 BTU

ambient temperature and because Newark was close to the Astoria waste heat site that was being studied in New York City as part of this project. Further assumptions about the greenhouse structure and its heat loss characteristics are summarized in Table 1.

4.2. Waste Heat Systems

The investment and operating costs were estimated for representative one acre waste heat greenhouses connected by pipeline to the cooling towers of a hypothetical power plant located 3,500 feet away. The pipeline and related pumps were sized to provide sufficient water to meet the greenhouse heat exchanger design requirements for 10 acres of greenhouses. It was assumed that multiple pumps would be installed in the pipeline so that staged pumping, based on the greenhouse heat requirements, could be utilized. Pumping electricity requirements assumed that 25% more water was pumped than was actually required to meet the greenhouse usage. The power plant itself was assumed to provide cooling water at a constant 85°F with a 95% reliability. The partial fan coil systems were later recalculated for 65°F, 75°F and 95°F source temperatures and one case was estimated for an 80% reliability. An inexpensive propane unit heater backup system was included in all waste heat cases to supply heat during the outage periods. Other assumptions about the waste heat systems are listed in Table 2. Three basic types of waste heat delivery systems were modelled. This was not meant to be an inclusive list. Other types of heat exchangers could have been included but were not, either because of problems associated with them (high humidity with evaporative pads) or because they had not yet been sufficiently tested for performance (plastic panel heat exchangers).

Fan coil. This design was based on the performance and cost characteristics of the McQuay fan coil heat exchangers that are in actual use in the first one acre commercial greenhouse at the Northern States Power waste heat greenhouse site (7)(8). Performance specifications and updated March 1980 prices were obtained from the manufacturer. For the purposes of this analysis, it has been assumed that the heat exchange capacity and the water temperature drop of these units would vary in direct proportion to changes in the temperature difference between the entering water and the desired greenhouse temperature. A sufficient number of fan coil units was included to provide 100% of the greenhouse design heat loss and the necessary pipeline and pumps were sized accordingly.

Partial fan coil. This system was based on exactly the same units as the system just described. The only difference is that the number of fan coil units was reduced so that they were only able to provide a maximum of 70% of the normal greenhouse design heat loss. Propane fuel burned in the backup heating system served as a supplemental heat source. The scaling down of the primary heat exchanger system substantially reduced the investment cost but only minimally increased conventional fuel requirements. According to calculations made from detailed degree hour information, the 70% design would still be able to supply 96% of the total annual heat requirements.

Because the partial fan coil design turned out to be an economically desirable waste heat system, costs for this design were later recalculated for three other waste heat source temperatures (95, 75 and 65°F). The original 85°F case was also re-estimated assuming a waste heat reliability of only 80%, such as might be encountered at a single-unit power plant.

The 65°F source temperature reduced the heat exchange capacity of the fan coils so much that a centrifugal water-to-water heat pump was incorporated into this design to increase the temperature of the water available to the fan coils to 85°F. The heat pump was sized to provide sufficient heated water for a 70% design fan coil complement.

Flooded porous concrete floor/fan coil. This system is based on a Rutgers University design for a low temperature heat exchanger built into the floor of a greenhouse. The system was originally designed for use with warmed water supplied by solar collectors. A waste heat greenhouse that utilizes a variation of this heat exchanger design has recently been constructed by a commercial grower at a power plant site in Pennsylvania.[3]

The design details of the flooded porous floor system have been described in various papers (9)(10). In general, a special greenhouse floor is constructed which consists of four layers. A vinyl swimming pool liner is laid over polystyrene board insulation. The liner is filled with 6-9" of gravel with provisions made for flowing warm water through it. The entire floor is coverd with a 3" cap of porous concrete to form a firm surface. The porous concrete is made with aggregate, cement and water but no sand.

This analysis assumed that heat transfer takes place from the warm water in the floor to the greenhouse air at a rate of 1.45 BTU/Hr.•ft^2•°F (9). This heat transfer rate has been verified by more recent experiments at Rutgers University as being within the range for a bare porous floor (11). Covering the floor with pots or flats reduces the heat transfer rate substantially. Therefore, this analysis is only strictly valid if crops grown on benches are assumed.

At the assumed heat transfer rate, the bare porous floor in this analysis would be able to supply 62% of the assumed greenhouse hourly heat loss when provided with an 85°F waste heat source. This floor design would provide 93% of the annual heat requirements if there were 100% waste heat reliability. A sufficient number of fan coil units identical to those already described were included in the design to make up the remainder. Because the floor system was assumed to reduce the water temperature by only 5°F, the fan coils were designed to utilize the warm water coming out of the floor. Pipeline and pumps, therefore, were sized to handle only the flow rate required for the operation of the floor.

Piped porous concrete floor/fan coil. In this design, also developed by Rutgers University, loops of thinwall polyethylene pipe that carry warm water are embedded in a porous concrete floor (12). This floor heating system is less expensive to construct than the flooded porous floor because less material is required and there is no need for a waterproof liner. It is also a less efficient heat exchanger. Variations of this design have been installed commercially as a supplement to conventional greenhouse heating systems, especially with crops that are commonly grown on the floor.

Based on our interpretation of the early test results, this analysis assumed a heat transfer rate from the floor of .67 BTU/Hr.•ft^2•°F (12). This is based on the difference between the average water temperature in the floor and the greenhouse air temperature. More recent published results from Rutgers University show a somewhat lower heat transfer rate (11). Heat exchange from a floor covered with flats or pots is even less.

[3] The Montour plant owned by Pennsylvania Power and Light.

For the design used in this analysis, the piped porous floor was calcuated to be able to provide up to 29% of the design greenhouse heating load with a waste heat source of 85°F. A floor operating at this level could supply 60% of the annual heat requirement if the waste heat source were perfectly reliable. A sufficient number of fan coil units were included in the total design to provide waste heat capability for 100% of the design greenhouse heating load. As with the flooded floor version, the fan coil units were assumed to utilize warm water as it came out of the floor.

4.3. Conventional Heating Systems

Of the many combinations possible, two types of existing conventional greenhouse heating systems were chosen for which to evaluate operating costs. One system was composed of a natural gas boiler and associated heat exchangers installed in an existing plastic greenhouse. A second system used #2 fuel oil in individual forced air unit heaters in an existing plastic greenhouse structure. Operating costs estimated for each system included fuel, heating system electricity, and repairs, taxes and insurance on the heating system equipment.

The operating costs for each conventional system were estimated for a single year (1980/81) and also over a period of ten years. For the ten year cases, fuel and electricity costs were assumed to increase more rapidly than the assumed rate of inflation.

4.4. Modified Conventional Heating Systems

Two of the possible modifications to existing greenhouses that are most likely to be considered as alternatives to waste heat greenhouses were analyzed. Both were assumed to be applied to an existing double plastic structure. The first option involved retrofitting a thermal night curtain into an existing double plastic structure equipped with forced air oil heat. A single layer, aluminized curtain with a motorized pulling mechanism of a type that is commercially available was chosen. The investment and operating costs were estimated over a ten year period. The costs considered included the night curtain investment and fabric replacement costs; repairs, taxes and insurance on the night curtain and heating system equipment; and some operating labor for the night curtain. No allowance for crop yield reductions caused by possible shading from the night curtain was made in this analysis. In reality, shading losses can be signifcant. A methodology for dealing with this factor and its implications have been discussed elsewhere (4) (5).

A different modification involved the conversion of an existing hot water heating system in an existing double plastic greenhouse to a coal boiler (13). Substantial investments in a completely new boiler, stoker, fuel and ash handling equipment and boiler room modifications were assumed. A representative mid-1980 Long Island price for low sulfur Pennsylvania anthracite coal was used to ensure that environmental regulations could be met. Estimates of the additional labor required and the repair, property tax and insurance costs associated with the heating equipment were included. Costs were calculated over ten years with annual increases in prices.

5. ASSUMPTIONS AND SOURCES OF DATA

Selected assumptions about the site, economic parameters and characteristics of the alternative systems considred are presented in Table 1. The estimated before-tax investment costs and first year annual operating costs are summarized for each alternative system in Table 2. Investment costs were estimated for the spring of 1980 and operating costs were based on what were expected to be typical prices for the 1980/81 heating season. The prices and rates of increase that were used can be found in Table 1. All investments were assumed to have zero salvage value at the end of the ten year period.

Estimates of the investment required for each system were made based on a variety of sources, including manufacturers, greenhouse suppliers and construction cost estimating publications (14). For the fan coil and heat pump costs, updated March 1980 prices were obtained from the manufacturers. Installation costs for these items were assumed to be 50% of the equipment costs. In order to estimate the cost of the flooded floor system, the material requirements described in published reports were updated to March 1980 prices. The installation labor component was established at 75% of the materials cost, which agrees well with the ratio contained in the 1977 cost breakdown of constructing a large demonstration installation (10). The

The estimates for all waste heat greenhouses include the cost to install equipment was included. The costs of the polyethylene cover, benches and repairs, property taxes and insurance on the structure were not included because they were assumed to be the same as for the existing conventional systems. The 1980 cost of the installed greenhouse structure was placed at $\$4/ft^2$ of floor area based on published estimates [15] and the average of three estimates received for a greenhouse structure at the Astoria waste heat site. The cost of the heating system was included separately for each alternative. A one-time startup cost of \$30,000/acre was included during the first operating year of all waste heat systems.

For the purposes of this analysis, the marginal income tax rate was set at 33%. All costs were converted to present value with an after-tax discount rate of 10% (equivalent to 15% before tax). Real annual equivalent cash flows were obtained with an inflation-free after-tax discount rate of 4.67%.

6. RESULTS

6.1. Alternative Waste Heat Delivery Systems

Three major types of waste heat systems were modelled under comparable assumptions. In each case, the waste heat delivery system was assumed to be sized for the full design heat load of the greenhouse. Under these assumptions, there is surprisingly little difference among the after-tax real annual equivalent costs for the three types of delivery systems (Figure 2). The fan coil option seems to enjoy a small cost advantage with an AECF of \$41,200. However, the most expensive option is only eight percent more expensive at \$44,700/year. These differences are not especially significant in the total context of operating a greenhouse. Preliminary sensitivity analysis has shown that changes in the assumed values of several variables, including the cost of capital and the price of electricity, can easily change the ranking of the cost of the three delivery systems.

Table 2. Estimated Investment and First Year Annual Operating Costs for Alternative Waste Heat, Conventional and Modified Conventional Greenhouse Heating Systems.[1-2]

System	Investment Costs[3] ($/acre)		First Year Annual Operating Costs ($/acre/year)				
	Heating Equipment[4]	Greenhouse Structure and Startup[5]	Pipeline[6]	Repairs, Taxes, Insurance[7]	Greenhouse Electricity[8]	Pipeline Electricity	Fuel
FULL DESIGN WASTE HEAT							
Fan Coil	107,000	204,000	5,900	4,300	5,700	1,000	2,100
Flooded Porous Floor/ Fan Coil	149,600	204,000	8,200	5,100	1,300	2,200	2,100
Piped Porous Floor/ Fan Coil	156,900	204,000	5,900	5,700	3,600	1,300	2,100
PARTIAL FAN COIL WASTE HEAT							
Temperature Reliability							
85°F 95%	83,900	204,000	4,800	3,400	5,700	800	3,800
85°F 80%	83,900	204,000	4,800	3,400	4,900	700	9,600
95°F 95%	66,500	204,000	4,800	2,700	4,100	500	3,800
75°F 95%	123,100	204,000	7,100	4,900	11,500	2,300	3,800
65°F 95%	141,900[9]	204,000	4,900	5,600	14,000	900	3,800
CONVENTIONAL HEATING							
Natural Gas Hot Water	-	-	-	3,000	1,100	-	22,800
Oil Forced Air	-	-	-	1,400	1,900	-	47,000
MODIFIED CONVENTIONAL HEATING							
Night Curtain/Oil Heat	-	76,200[10]	-	4,900	1,400	-	29,500[11]
Coal Conversion	79,400[12]	30,000[13]	-	3,400	900	-	18,200[14]

[1] See Table 1 for assumptions.
[2] All costs are before income taxes.
[3] Installed costs.
[4] All waste heat systems include a propane backup heating system ($21,500).
[5] All waste heat cases include startup costs ($30,000). Structure costs exclude cost of polyethylene covering and benches.
[6] Includes pipeline capital recovery, repairs, property taxes and insurance.
[7] For heat exchanger, heat pump, night curtain and coal tem only. conversion investments only.
[8] Waste heat delivery system or conventional heating system only.
[9] Includes heat pump ($58,000).
[10] Night curtain fabric and pulling system costs. Fabric ($21,800 assumed to be replaced after 5 years.
[11] Includes $500 for additional labor.
[12] New coal stoker, boiler and fuel handling equipment.
[13] Boiler room modifications and coal storage facilities.
[14] Includes $3,000 of additional heating system labor.

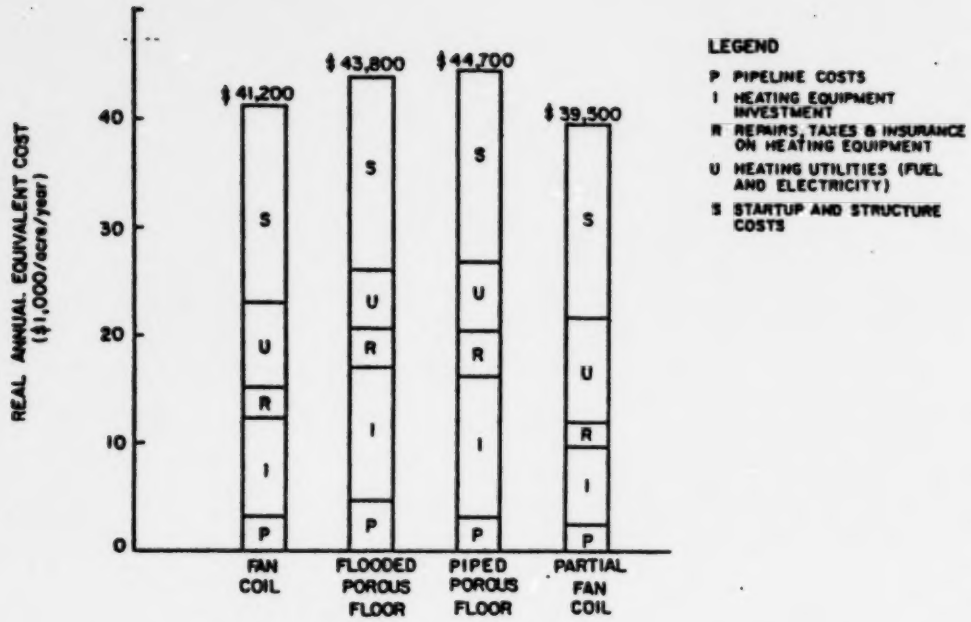

Figure 2. After Tax Real Annual Equivalent Heating, Structure and Startup Costs for Alternative Waste Heat Greenhouse Systems with an 85 F Source and 95% Reliability.

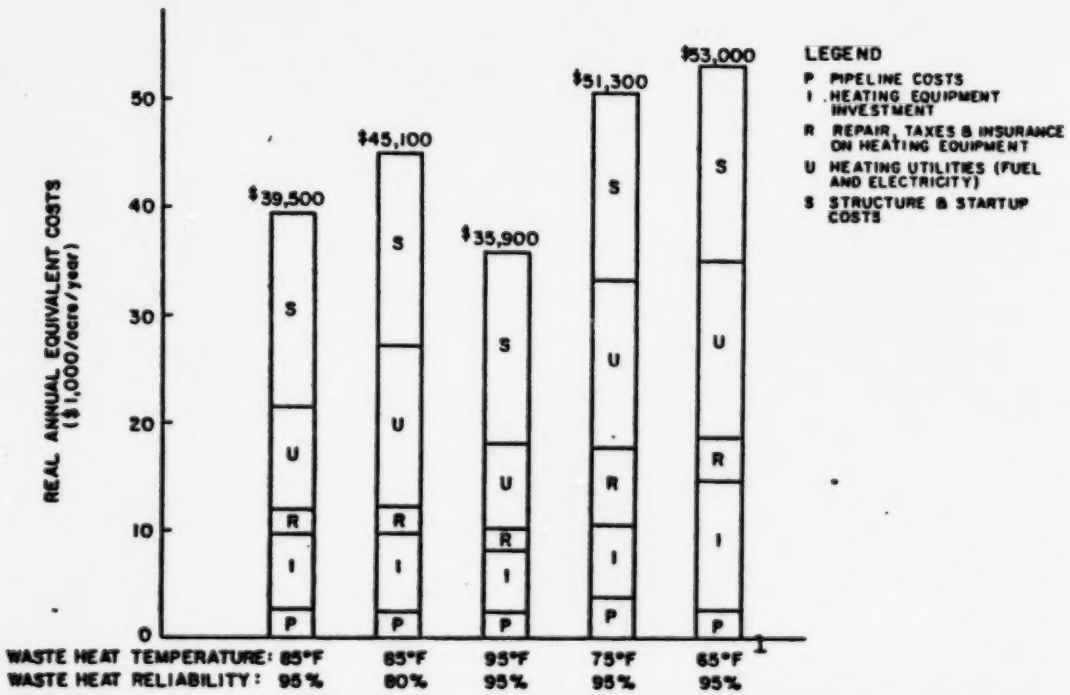

Figure 3. After Tax Real Annual Equivalent Heating, Structure and Startup Costs for Partial Design Fan Coil Waste Heat Greenhouse System with Alternative Source Temperatures and Reliabilities.

[1] Design includes heat pump.

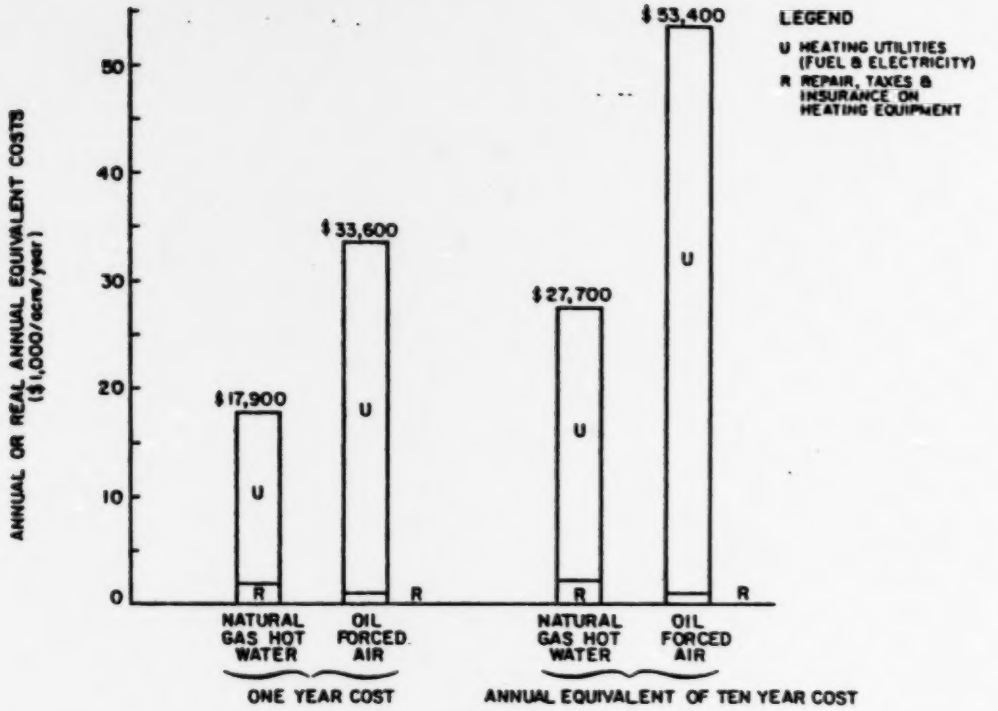

Figure 4. After Tax Annual Operating Costs for Conventional Greenhouse Heating Systems in Existing Double Plastic Structures.

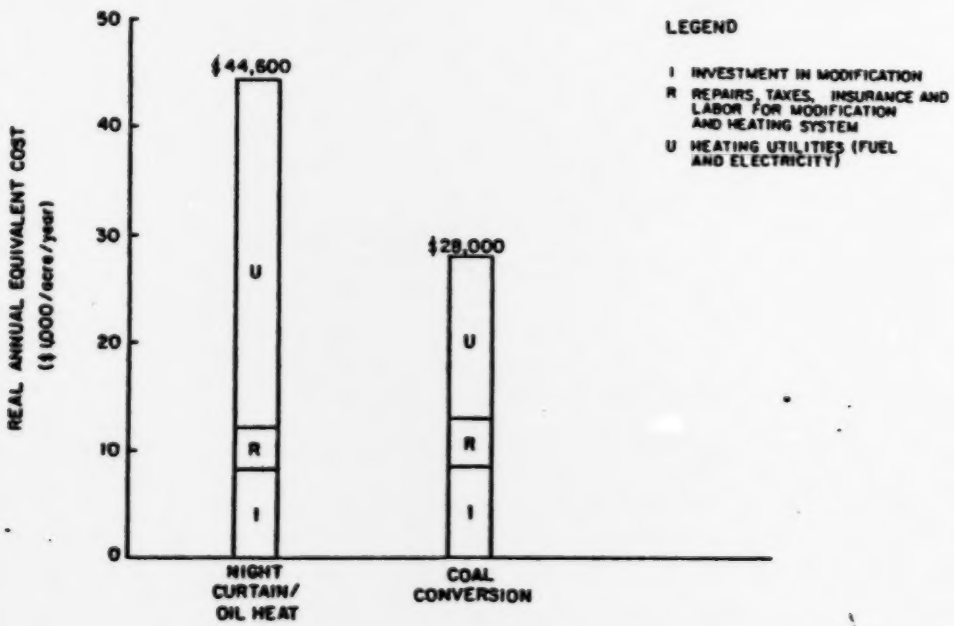

Figure 5. After Tax Real Annual Equivalent Heating Costs for Modified Conventional Heating Systems in Existing Double Plastic Structures.

There were also several factors that were left out of this generalized analysis that could be to the economic benefit of the warm floor systems. Fan coil units that use waste heat are bulky and either occupy or shade valuable grenhouse floor space. Fan coil units in waste heat applications also are very noisy. Greenhouses heated with warm porous floors are extremely quiet and the warm floor may be conducive to worker comfort and productivity. For certain crops, a warm porous floor could also be used as a growing surface that substitutes for conventional raised benches and makes possible a high ratio of cropping area to floor area. There is even the possibility that growing crops on the warm floor will make it possible to lower the air temperature somewhat. However, covering the floor with crops also substantially reduces the heat transfer from the floor.

It is more direct to make comparisons of the same type of heat delivery system designed for different levels of capacity. There is some benefit to intentionally undersizing expensive waste heat delivery systems as shown by the partial fan coil case. Preliminary sensitivity-analysis has shown that the savings would have been even greater in this example if the delivery system had been further reduced to 50% or 60% of the design level. Although only a fan coil comparison is presented here, similar savings can also be realized for the porous floor/fan coil cases. This is because porous floor heat exchangers are, by their nature, limited to providing less than 100% of the greenhouse heating load under most conditions. A reduction in the capacity of these systems usually would involve eliminating part of the supplemental (fan coil) heat exchanger capacity.

6.2 Effects of Source Temperatures and Reliabilities

The partial fan coil system that appeared to have the lowest annual equivalent cost under the original assumptions was then recalculated for three different waste heat source temperatures (65°, 75° and 95°F) as well as for one other level of waste heat reliability (80%) at the original 85° temperature. The results are presented in Figure 3.

Comparison of the results for the four cases where the reliabilities are the same but the source temperatures are different illustrates a conclusion that is often overlooked. What may seem to be small differences in the source temperature can make substantial differences in the total cost of heating a greenhouse with waste heat. The reason is that the rate of heat transfer from a given heat exchanger is approximately proportional to the temperature difference between the greenhouse temperature and the temperature of the waste heat source. When the waste heat temperature approaches closely (within 5 or 10°F) the desired greenhouse temperature, it is somewhat more economical to use heat pumps to increase the temperature difference to a more usable level.

Of the four waste heat temperatures presented, the lowest cost alternative (95°F source, 95% reliability) is indicative of what might be found at a very high quality power plant waste heat site (a base loaded, multiple unit plant that utilizes recirculating cooling towers). Much more typical of the power plant sites available is a plant with once-through cooling. The most expensive waste heat option in Figure 3 (using a 65°F source) would be an optimistic version of this case.

Comparison of the first two cases in Figure 3 illustrates that the reliability of waste heat sources can also have a significant effect on the

cost of waste heat usage. Although not illustrated here, a combination of a low temperature and unreliable waste heat source is especially detrimental to the economic viability of waste heat greenhouses.

6.3. Comparison of Waste Heat Systems with Existing Conventional Greenhouses

Both the ten-year annual equivalent operating cost and the one-year operating cost for continuing to operate two types of conventional heating systems in plastic houses are summarized in Figure 4. For each type of fuel, the annual equivalent cash flow derived from ten years of operating the conventional system is much higher than the annual operating cost for a single additional year. This is because of the assumed increase in conventional fuel prices over time. There is also a large difference between the two types of heating systems. The annual operating cost of the natural gas hot water system in this example is a little more than 50% of the annual operating cost of the fuel oil system.

The very wide spread in annual operating costs for conventional heating systems illustrate why it is so difficult to compare waste heat systems to the continued operation of conventional heating systems. Depending on the conventional system used as the base case, it is possible to come to the conclusion that all, or none, of the waste heat installations examined here are capable of replacing existing conventional greenhouses. All of the waste heat systems have an annual equivalent cash flow that is less than the annual equivalent cash flow for heating a conventional plastic greenhouse with fuel oil over ten years. However, this does not necessarily mean that the time for extensive waste heat installations had yet arrived in 1980 if the alternative of continuing to heat an existing greenhouse one year at a time with fuel oil is allowed. The single year annual cost for doing this was still less than the annual equivalent cash flow for any of the waste heat systems considered and growers still have the year-to-year option of continuing with their existing facilities.

Whether natural gas heating costs are considered in terms of a ten-year annual equivalent or only the current year, they are substantially less than the annual equivalent costs for all of the waste heat installations considered. This has different implications in an area like New York State, where it is estimated that only 8% of the existing greenhouse acreage is heated by natural gas [16], than for an area like Ohio and Ontario where as much as 60% of the existing greenhouse acreage is heated with natural gas.

6.4. Comparison of Waste Heat Greenhouses with Existing Modified Conventional Greenhouses

The AECF heating costs for modifying existing plastic greenhouse structures to conserve heat or to convert to a less expensive fuel in Figure 5 can be compared with any of the waste heat alternatives in Figure 2 or 3. The AECF for a thermal night curtain installed in an existing plastic structure with forced-air oil heat is more expensive than many of the waste heat cases in this analysis. However, it is still a less expensive option than building a waste heat greenhouse using an unreliable or low temperature waste heat source.

The AECF of converting an existing hot water heating system in an existing plastic structure to coal compares very favorably with all of the waste heat cases when the cost of a new greenhouse structure is included in

structure along with the coal heating system, coal apparently can compete with some of the more expensive waste heat alternatives. This conclusion is supported by the fact that there have been a large number of coal conversions initiated at existing greenhouses in portions of the eastern U.S. during the past year.[4]

7. CONCLUSIONS

While a large number of conclusions could be drawn from such a generalized analysis, the following selected conclusions are among the more important:

1. While different types of waste heat delivery systems are quite different in the mixture of investment and operating costs, there appear to be several types of delivery systems that are roughly comparable in total annual cost. The actual selection of a waste heat design will depend on a number of factors, including the character of the waste heat source, the type of crop being grown, the price of electricity and the cost of capital. Perhaps the most important factor will be grower preference.

2. There are significant economies to be achieved by intentionally sizing the waste heat delivery systems to handle only a portion of the maximum greenhouse heat load.

3. Waste heat source temperatures and reliabilities are important determinants of the total cost of waste heat greenhouses. Where a choice of waste heat sources is available, there will be an incentive to develop the higher temperature and more reliable sources first.

4. Where the options are available, the use of natural gas in existing greenhouses and the conversion of existing central heating systems to coal represent major competition for new waste heat installations.

5. The cost of a new greenhouse structure and associated startup costs represent a large portion of total waste heat greenhouse costs. Therefore, whether waste heat greenhouses are able to compete depends largely on whether their costs are compared to the cost of constructing new greenhouses with conventional heat or if they instead are compared to the costs of operating or modifying existing greenhouse facilities.

6. Under the right conditions, waste heat greenhouses are an economically viable alternative at the present time. Where available, they will be an attractive option to constructing new greenhouses with more conventional heating systems. Waste heat greenhouses will replace existing facilities first where the proposed waste heat source is reliable and available at 95°F or above, and where natural gas and coal are not economically available.

---

[4] It is reported that more than 50 coal conversions have been carried out or initiated during the past year on Long Island alone.

7. In areas where greenhouse acreage is not substantially expanding, where the waste heat conditions are less than ideal or where competition from natural gas and coal are strong, it may take time to attract a large acreage of greenhouses to a particular site. However, waste heat cost estimates usually assume that the waste heat auxillary facilities will be fully utilized from the day of their installation and their cost can be spread over the full complement of greenhouses. Underutilization of waste heat facilities would eventually result in higher per acre costs than were used in this analysis.

REFERENCES

1. Crop Reporting Board, Floriculture Crops, SpCr 6-1, USDA, 1975-1980.

2. Greenhouse Update—1980, American Vegetable Grower, vol. 28(11), pp. 58-61+, November 1980.

3. R. D. Aplin, G. L. Casler and C. P. Francis. Capital Investment Analysis Using Discounted Cash Flows, Grid, Inc., Columbus, Ohio, 1977.

4. G. R. Fohner and G. B. White. The Economics of Movable Interior Blankets for Fuel Conservation in Greenhouses. Agric. Econ. Res. 80-2, Department of Agricultural Economics, Cornell University, Ithaca, New York, 1980.

5. G. B. White, G. R. Fohner and L. D. Albright, The Economics of Movable Interior Blankets for Greenhouses, Amer. Soc. of Agric. Eng. Paper No. 80-4030, ASAE, St. Joseph, Michigan, June 1980.

6. U. S. Dept. of the Air Force, Engineering Weather Data, Air Force Manual 88-29, July 1978.

7. G. C. Ashley, Heating Greenhouses in Northern Climates with Power Plant Reject Heat, HortScience, vol. 14(2), pp. 155-160, April 1979.

8. L. L. Boyd, A. M. Flikke, R. V. Stansfield, G. C. Ashley and J. Hietala. Use of Waste Heat from Electric Generating Plants for Greenhouse Heating, Amer. Soc. of Agr. Eng. Paper No. 77-4531, ASAE, St. Joseph, Michigan, 1977.

9. D. R. Mears, W. J. Roberts, J. C. Simpkins and P. W. Kendall, The Rutgers Solar Heating System for Greenhouses, Amer. Soc. of Agr. Eng. Paper No. 77-4009, ASAE, St. Joseph, Michigan, 1977.

10. D. R. Mears, W. J. Roberts and P. W. Kendall, Development of a Greenhouse Solar Heating Demonstration, Amer. Soc. of Agr. Eng. Paper No. 78-4512, ASAE, St. Joseph, Michigan, 1978.

11. W. J. Roberts and D. R. Mears, Floor Heating of Greenhouses, Amer. Soc. of Agr. Eng. Paper No. 80-4027, ASAE, St. Joseph, Michigan, 1980.

12. W. J. Roberts and D. R. Mears, Floor Heating of Greenhouses, Cooperative Extension Service, Rutgers University, New Brunswick, New Jersey, January 1979.

13. V. Ball, Energy: Fuel Outlook '81, Grower Talks, vol. 44(2), pp.1-23, June 1980.

14. R. S. Godfrey (ed.), Building Construction Cost Data, Robert Snow Means Company, Duxbury, Massachusetts, 1980.

15. J. W. Bartok, Comparative Cost of Greenhouse Construction, Agricultural Engineering SEG-35 (Revised), University of Connecticut Cooperative Extension Service, Storrs, Connecticut, 2 p., 1980.

16. R. A. Pellerin, E. D. Markwardt and R. K. Koelsch, Greenhouse Energy Survey, Agricultural Energy Conservation Program, Cooperative Extension, Agricultural Engineering Department, Cornell University, Ithaca, New York, 1979.

PE82-228339

MONTOUR WASTE HEAT GREENHOUSE PROJECT

Robert P. Johnson, Pennsylvania Power & Light Company, Allentown, PA

Kenneth G. Bryfogle, Jr., Bryfogle's, Inc., Muncy, PA

Dr. David R. Mears, Rutgers University, New Brunswick, NJ

Thomas O. Manning, Solar Engineering Group, Princeton, NJ

1. ABSTRACT

In 1979 Pennsylvania Power & Light, in conjunction with Bryfogle's, Inc., initiated a program to construct greenhouses to be heated with warm water discharged from PP&L's Montour coal-fired generating station at Washingtonville, Pennsylvania. In early 1980, detailed planning for the project was undertaken and specifications for the greenhouse heating system were prepared by the Department of Agricultural Engineering at Rutgers University. Construction on the 2.75-acre greenhouse was initiated in June, 1980; and in early December the facility was connected to a 20-inch warm water pipeline. The greenhouse is now fully operational and was used to finish off a crop of Christmas poinsettias and for full production of the spring holiday crops.

2. INTRODUCTION

2.1 Rationale for the Demonstration of Waste Heat Floriculture

In producing electricity, a steam electric generating station rejects a large quantity of low level heat through a cooling system designed to remove heat from the backend of the steam turbines. By locating next to an electric power plant, a greenhouse operator can use this reject heat to warm the greenhouse in place of fuel oils commonly used in many parts of the country.

Presently, billions of gallons of fuel oil are used each year to heat commercial greenhouses at a consumption rate in north-central Pennsylvania of up to two gallons per year for every square-foot of growing area. The heating bill accounts for a half to two-thirds of the cost of a flower and is an expense the grower has no control over. Increased oil prices and the inefficiency associated with the many old greenhouse ranges in the Northeast have made it possible for growers in South America and Canada to capture a large percentage of the flower and pot plant business in this region.

It is obvious that the economic impact of imported flowers has had a serious effect on the greenhouse industry, and the trend will continue at a rapid pace unless something can be done. The solution lies in well-managed, highly energy-efficient greenhouse complexes with low level reject heat utilization. This, unfortunately, has been a largely undeveloped process with only one other commercial demonstration facility in the United States located at Northern States Power's Sherburne Power Plant in Minnesota.

Additional demonstration facilities were needed to determine the specific regional problems, develop lower cost and more energy-efficient heating systems, fine-tune the heating requirements, test new energy-saving products, and educate and familiarize other growers with low level heating equipment.

2.2 Historical Perspective

Bryfogle's, Inc., in conjunction with PP&L, has been operating such a facility since December 1, 1980 at PP&L's Montour Steam Electric Station. The path leading to this first installation was difficult at times and has required some extraordinary and cooperative efforts from a number of organizations, individuals, lending institutions, and government agencies.

Back in 1973, before the oil embargo, Ken Bryfogle, President of Bryfogle's, Inc., came to PP&L to discuss the possibilities of heating a greenhouse with some of the power plant reject heat. Several schemes were studied carefully; but with heating oil at less than 20 cents per gallon, no scheme looked worthwhile.

After the embargo, PP&L and the Pennsylvania Science and Engineering Foundation had a renewed interest and worked together with another area grower to develop a plan. The Northern States Power project was already started by then and was studied for possible application at Montour. The grower was concerned about the high electric cost of moving air and water through the large heat exchangers that are used at NSP. PP&L came to the conclusion that another replication of the NSP system was of marginal benefit to PP&L unless it was commercially viable to the grower. The grower backed out of the project for several reasons; state budgetary problems removed PSEF's possible contribution to the project, and the project came to a halt.

Discussions with Bryfogle had continued on and off through this period, but efforts to secure loans or grants were stymied.

In 1979, however, Bryfogle lost some growing area due to floods, and an Appalachian Regional Commission grant was secured through the efforts of SEDA-COG, a regional planning and development organization that serves an 11-county area in north-central Pennsylvania and specializes in planning for and securing funds for local projects. Also, during the same period, the Rutgers warm floor heating system, under development since 1976, had emerged on the scene, and was being demonstrated successfully in solar applications at Rutgers and at a commercial greenhouse in New Jersey. The combination of these items, along with several other achievements, broke the log jam of stumbling blocks.

2.3 Present Status

Bryfogle's Montour greenhouse now consists of 2.75 acres. Even without the weather stripping and heat conservation systems completed, Bryfogle held satisfactory nighttime temperatures with -14°F and thirty mile winds outside. Growing appears to be better than in his conventional greenhouses, as does employee comfort because of the warm floor. Auxiliary energy consumption is almost nil, and no problems have been encountered in the first five months of operation. A Christmas poinsettia crop was finished off at Montour, a full crop of pot mums and lilies was grown for the spring holidays, and the houses are now full of vegetable starts and bedding plants for the early

summer markets. Under present conditions, it would seem likely that significant savings are possible, and that growing may be carried on competitively with warmer climates.

2.4 Future

PP&L hopes to expand the project to the full capacity of the 20-inch pipeline installed to deliver the warm water. The pipeline and site may support from 20 to 40 acres of greenhouses, depending on the results of the present project and some energy management plans being considered. Bryfogle has some preliminary expansion plans; and PP&L will be encouraging other growers to take part at Montour.

It is our hope that the effort put into this project will ease the institutional, financial, and technological restraints for future waste heat greenhouse development at Montour as well as other utility sites.

3. PROJECT DESCRIPTIONS

3.1 Power Plant

PP&L is an investor-owned electric utility serving central-eastern Pennsylvania with an installed generating capability of 6,500,000 KW. PP&L provides electricity for about one million customers and has a service territory that covers nearly one fourth of Pennsylvania's 45,000 square miles. The Montour Power Plant is located on a 1,200-acre site near the town of Washingtonville, 25 miles southeast of Williamsport (see the map, Figure 1). The plant has two 800,000 KW units fueled with bituminous coal from western Pennsylvania. The two units were placed in operation in 1972 and 1973. Each of the units has its own 370-foot high natural draft cooling tower, designed and constructed by the Marley Company. The Montour site is made up of generally flat farm land, and is located 12 miles from the West Branch of the Susquehanna River. Plant make-up water is piped through a 42-inch diameter pipeline from that river.

The greenhouse site is located on PP&L property 3500 feet from the Unit 1 cooling tower. The land is leased to Bryfogle under a long term lease with renewable options.

The warm water pipeline consists of 20-inch supply and return pipelines buried a minimum depth of three feet. The pipe is a high density polyethylene Drisco ™ Pipe.

3.2 Greenhouse Design

The greenhouse complex is made up of 20 gutter-connected 210 x 28-foot bays for a total growing area of 2.75 acres. The structural framework is prefabricated aluminum weighing approximately 1.3 pounds per square foot of house. The roof is an energy-efficient, double-layer, air-inflated polyethylene, and the perimeter walls are covered with treated, translucent, fiberglass panels. An overhead energy blanket is being installed to further improve the thermal efficiency and to provide photoperiod control. The greenhouse was designed and constructed by PolyGrowers, Inc. - a Bryfogle-owned company.

The design principles for the Montour greenhouse heating system evolved from research conducted at Rutgers University in 1976 on solar heated greenhouses. A commercial demonstration project at Kube Pak Garden Plants, Inc. in Allentown, New Jersey was built in 1977 to test the concepts developed by Rutger's research in a full-scale facility. During the 1978-79 heating season, detailed performance data from the Kube Pak Greenhouse was evaluated. During the same period, data was also collected from a smaller greenhouse at the Public Service Electric and Gas Mercer Generating Station. This prototype was designed to use condenser discharge water as a heat source, in order to evaluate the feasibility of this concept incorporating the features of solar greenhouses constructed at Rutgers.

In order to design the greenhouse heating systems, it was found necessary to evaluate a number of potential designs over an entire heating season. The heating load is determined by outside temperature, and the heat provided depends upon the temperature of the warm water from the utility which is also variable. Therefore, a number of alternative heating system designs were evaluated by computer simulations. Data on the heat transfer characteristics of the floor heating system were obtained from the solar greenhouse research program. Weather conditions and water temperatures were taken from actual records of the operation of the Montour Power Plant.

The components of the Montour greenhouse heating system can be divided into three general categories: warm water heat distribution system, energy conserving features, and backup heat. See Figures 2 through 8.

The design for extracting heat from the warm water incorporates two independent components. The floor system is both storage and primary heat exchanger for the greenhouse. The floor is constructed of a biocide-treated vinyl swimming pool liner filled with gravel, which is flooded with water, and a cap of porous concrete. The porous concrete forms a heat exchange surface and a firm floor which allows excess irrigation water to drain. The water and the gravel provide thermal storage and are heated by the condenser discharge water flowing through loops of polyethylene pipe embedded in the gravel. Details of the floor are shown in Figure 4.

A pair of 1-1/4" finned pipes located underneath each gutter serve as the secondary heat exchangers. The condenser discharge water flows through these pipes when the heat coming from the porous concrete floor is not sufficient to meet the heating demand.

The backup heating system consists of two boilers, one oil-fired and one which may be fired with either oil or coal. Hot water from these boilers may be pumped through an additional finned pipe located underneath each gutter when needed. The water temperature in these pipes is modulated using a mixing valve to help maintain uniform air temperatures. An additional heat exchanger is located in the water flume along the west wall of the greenhouse so that the backup system (fossil fuel) can be used to maintain floor water temperature when necessary. The backup heating system is designed to carry the greenhouse heating load when the power plant is not operating, and to provide supplementary heat when the primary and secondary exchangers on the water heat system cannot provide all the heating requirements. Figures 2 and 3 are schematic representations of the various heating systems.

The warm floor heating system used in the Montour greenhouse has many features which improve greenhouse environmental and growing conditions.

Porous concrete floors have been used by many growers who grow directly on the floor because they provide a firm surface, reduce weed problems and allow excess water to drain, thereby eliminating problems associated with no drainage and reducing humidity in the greenhouse. The floor provides uniform air temperature and warm root zones. The thermal storage feature ensures that greenhouse air temperatures will not fall below freezing overnight in the event of a system failure or during times when the power plant is shut down for a few hours.

The major problem in utilizing waste heat in greenhouses is providing sufficient heat transfer capacity with the heating components. The curtain insulating system reduces the magnitude of this problem by decreasing the greenhouse heating load; however, preliminary results have shown that very little supplemental heat is required without the curtains, even at sub-zero temperatures. The curtain drive system can also be used to provide summer shading if required, or alternatively, photoperiod control when necessary. The curtain system is shown in Figure 4.

Greenhouse cooling is accomplished with the aid of another innovative concept from Rutgers University. Each of the twenty 210 x 28 foot wide bays has two vent fans in the east wall to exhaust air. The inlet on the west wall consists of a window opening which is about three feet from top to bottom and runs the entire width of the 28 foot bay. This 3' x 28' panel, or window, is hinged at the top and is pushed out at the bottom using rack and pinion drivers. The vent windows in five adjacent bays are hooked together and operate as a single unit. Thus a section of five greenhouse bays, 210-feet by 140-feet, is ventilated with a total of ten fans drawing air through a 140-foot window.

The control system for this five-bay zone senses the greenhouse temperature and modulates the fan operation and window opening accordingly. The system is designed to maintain an optimum high air velocity through the opening, which insures good mixing of cold incoming air with the greenhouse environment.

3.3 Data Acquisition

PP&L and Bryfogle's have an extensive instrumentation and data acquisition program planned. Due to the urgency of completing the greenhouse and the heating system, the installation of this system has fallen behind schedule and is being installed too late to provide us with the comprehensive data we would like to have had during this first heating season.

PP&L's overall objective is to provide a microcomputer-based instrumentation system capable of providing the information needed to evaluate the greenhouse design, establish environmental control strategies, and to optimize the design of any future installations.

To accomplish this, an instrumentation system capable of monitoring 128 inputs is being developed by the Solar Engineering Group of Princeton, New Jersey.

4. PROJECT CONSTRUCTION

The Montour waste heat greenhouse was placed in service using power plant reject heat on December 1, 1980. The construction of this 2.75-acre complex and the design and construction of the 3500 foot pipeline was completed in only five and one half months.

Initial site development work was begun in mid-June, 1980 with site clearing and leveling. The land sloped from north to south and required quite a bit of work to get the 560 foot length as level as required for the flooded-floor heating system. After site preparation was completed, the boring of the holes for the vertical greenhouse members was begun on about June 24. All 275 posts were in place and set in concrete by July 18.

The construction of the warm floor heating system was the next item on the critical path and was begun on July 28, 1980 with placement of the 20 mil. vinyl liner that is designed to contain the water within the floor. Over three acres of vinyl were put down in 30 by 210-foot strips. The strips were overlapped and joined with adhesives to form one continuous water-tight barrier under the entire 2.75 acres. A 1/8-inch layer of DuPont Microfoam was placed on the vinyl to protect the liner from puncture.

The next major step in the operation was the placement of the 3/4 inch black poly pipe on the Microfoam. The pipes are spaced about one foot apart for the entire 560 foot length, requiring almost 24 miles of pipe. The pipe was delivered in precut 210 foot rolls to speed the laydown process. As pipe placement progressed along the length of the greenhouse, workers followed several bays behind pouring the eight-inch layer of gravel over the poly pipe. This was accomplished with a large crane and material handling bucket. Pipe laydown was started on about July 28, and both the pipe and the gravel were completely in place within about 12 days (August 8, 1980). The gravel supports the porous concrete floor and forms the water space for the under-floor pool. Irrigation piping and electrical conduit were installed in the floor in the period from August 8 to August 25, 1980, and the floor was ready for the porous concrete cap.

The porous concrete was poured starting on August 25 and was completed on September 5, 1980. As work on the floor progressed, PolyGrowers started work on the greenhouse roof structural members. By September 22, 1980 the roof structure was completed, and half of the greenhouse had the double-layer polyethylene covering in place. The heating contractor was working on the overhead heating system and back-up boiler installation. The electrical work was in progress.

PP&L had completed the pipeline design, had the required materials on site, and started pipeline construction at about this time.

By October 9, the remaining greenhouse roof material was in place and the side and end walls were being put up. At this point, Bryfogle was concentrating on closing in one half of the greenhouse and completing the overhead construction so that a crop of poinsettias could be transferred from Bryfogle's Muncy facility. These poinsettias were started in Muncy from cuttings. As they grew, the size of the pots and the required spacing between the pots increased to the stage that Bryfogle's would soon be unable to accommodate the entire crop at Muncy. By October 14, construction of the north half was far enough along to start the transfer of crops to Montour.

The first back-up boiler was hooked up to the overhead fin tube during the week of October 20, 1980, and the poinsettia crop was in its new home.

Work on the coal boiler, waste heat piping headers and tie-ins, electrical wiring, heat blanket system, irrigation, and ventilation systems was active at this time.

Heat was applied to the floor system for the first time during the week of November 10, 1980. This was accomplished with the back-up boiler floor heat exchanger loop in the west flume. The system worked very well and proved that the back-up boiler's heat could be effectively transferred to the floor.

The greenhouse waste heat piping to the floor system was completed and pressure tested on November 24. PP&L's 20-inch pipeline from the power plant was completed, flushed, pressure tested, and placed in service on November 26, 1980. The 100-foot long tie line between the greenhouse and the 20-inch line failed its pressure test on November 26, requiring some additional thrust block work. This work was completed by Monday, December 1, 1980, and power plant reject heat was sent through the greenhouse for the first time.

5. FINANCIAL PERSPECTIVE

5.1 Greenhouse Costs

The cost of Bryfogle's Montour greenhouse complex was $1,212,000. This includes site preparation, service building, and back-up heating, all sized for the present greenhouse and future expansion. The additional cost associated with the low level waste heat system is difficult to break out since some of the work involved in the floor heating system would be required in conventional construction. Also, the additional cost factor will be largely determined by what type of greenhouse is used for comparison, since many greenhouse operators are now starting to add porous concrete floors with embedded plastic pipe for floor warming with fossil fuel boilers as the heat source. The cost data for this prototype greenhouse are being analyzed to determine the realistic additional cost of the waste heat system and to determine where these costs may possibly be reduced in future construction.

The financing of the greenhouse was accomplished with the aid of a $357,000 grant from the Appalachian Regional Commission, a $300,000 low-interest loan from the Pennsylvania Industrial Development Authority, and bank loans totaling about $500,000.

5.2 Fees and Charges

In order to move ahead with an almost untried design and a greenhouse located 15 miles from his headquarters, certain advantages were given to Bryfogle to reduce the risk. It was felt that it would take two winters to prove out the design and complete the analysis of the system, so there will be no charge for warm water during that period. The charge levied for warm water following the first two years was negotiated prior to construction of the pipeline and was based on recovering the cost of PP&L's capital investment plus operating expenses and allowed profit. No additional pumping energy is required on PP&L's part, and only a small amount was added for

pipeline maintenance. The fee calculation was based on the capital carrying charge on the estimated $400,000 pipeline, divided evenly over an assumed 15 acres that the pipeline could ultimately serve. The fee was set at $5,000 per acre per year.

The final installed cost of the pipeline was $700,000, due in part to a larger pipe size, deeper trench, a labor shortage, and some difficulty digging in the power plant area. Based on the actual cost, it is anticipated that future development by other growers will cost slightly more than the $5,000 being charged to Bryfogle's. The fee will remain constant through the life of the greenhouse. Therefore, in place of rising fuel bills, the greenhouse heating cost is comprised of a warm water fee and an increased capital investment in the heating system. Both of these costs, however, are fixed over the life of the greenhouse.

An important objective of the planned data acquisition and performance analysis program described earlier is to determine what improvements can be made in the design and management of the system to increase the acreage that can be supported by a given pipeline, thereby reducing the per-acre pipeline charges. Preliminary observations of system performance indicate that substantial reductions in water requirements per acre are possible.

Land is leased under a long term arrangement with renewable options out to 40 years. The land rental is $25 per acre-year and is subject to escalation tied to the Consumer Price Index.

6. GREENHOUSE PERFORMANCE

The power plant's warm water has been delivered to the greenhouse at temperatures ranging from 90°F to 115°F with the weighted average at about 100°F. The temperature drop in the 3500 foot supply pipeline has been less than two degrees even with the present low flow velocity in the oversized pipeline. This may be due in part to the insulating qualities of the boiler bottom ash used as the select backfill around the piping.

The temperature drop between the greenhouse supply and return points has been 9° to 10°F. The system was designed for a 10°F drop. The temperature of the soil in pots on the floor seems to remain fairly constant at 68° to 70°F with the floor heating system on. However, determination of this effect of the water temperature on the heat transfer in the floor will not be known in detail until the full instrumentation system is in place, and data for a heating system has been analyzed.

In the fall of 1980, a crop of 30,000 poinsettias was finished off in the Montour greenhouse after getting started in Bryfogle's Muncy facility. The backup heating system was used until December 1, at which time the final hookup was made to the warm water line from the generating station. Satisfactory greenhouse temperatures have been maintained without the use of backup heat whenever the power plant is operating, even without the curtain insulation system operating. On two occasions in December, when outside temperatures fell below -15°F, the greenhouse was maintained at 54°F or higher. On one of these occasions, the backup heating system had failed and could not be used. The storage capacity of the floor maintained the greenhouse at acceptable levels overnight. Bryfogle feels that the poinsettias finished on the warm floor at Montour had significantly better plant development than those that remained in the conventional greenhouse at Muncy.

FIGURE 1
PP&L SERVICE TERRITORY (LIGHT SHADING)
AND THE
MONTOUR WASTE
HEAT GREENHOUSE

PP&L supplies electric service to a population of 2,309,000 people in a 10,000 square mile area in 29 counties of central eastern Pennsylvania.

* Under Construction

MONTOUR WASTE HEAT GREENHOUSE

SCHEMATIC REPRESENTATION – SYSTEMS SHOWN PARTIALLY & NOT TO SCALE

	SYSTEM	SOURCE	DESCRIPTION
A	FLOOR HEATING LOOPS	POWER PLANT	MAIN SOURCE OF HEAT – 3/4" BLACK POLY PIPES EMBEDDED IN THE FLOOR, SEE FIG 4 , CIRCULATE PLANT WATER THROUGH THE FLOOR POOL.
B	WASTE HT OVERHEAD FIN TUBE	POWER PLANT	2" COPPER w/ALUM FIN TUBE ; 2 UNDER EA GUTTER. POWER PLANT WATER CIRCULATES OVERHEAD TO PROVIDE TOUCH-UP TEMP CONTROL AND SNOW MELT CAPABILITY. SEE FIG. 6
C	POOL CIRCULATION	POWER PLANT BACK-UP	CIRCULATION OF UNDER FLOOR POOL, FIG. 7 , FOR EVEN HEAT DISTRIBUTION. PUMP IN S.W. FLUME DISCHARGES WATER IN EAST FLUME. PERF. PIPES ALLOW LENGTH-WISE MOVEMENT.
D	BACK-UP OVERHEAD FIN TUBE	BACK UP BOILER	1 1/4" COPPER/FIN TUBE ; ONE UNDER EA. GUTTER – FOR BACK-UP HEAT AND EMERGENCY SNOW MELTING. SEE FIG 8
E	BACK-UP FLOOR HEATING	BACK-UP BOILER	STEEL HEAT EXCHANGER SUBMERGED IN THE WEST FLUME. USED IN CONJUNCTION WITH THE POOL WTR CIRC. SYSTEM TO SUPPLY BACK-UP HEAT TO FLOOR. SEE FIG. 7

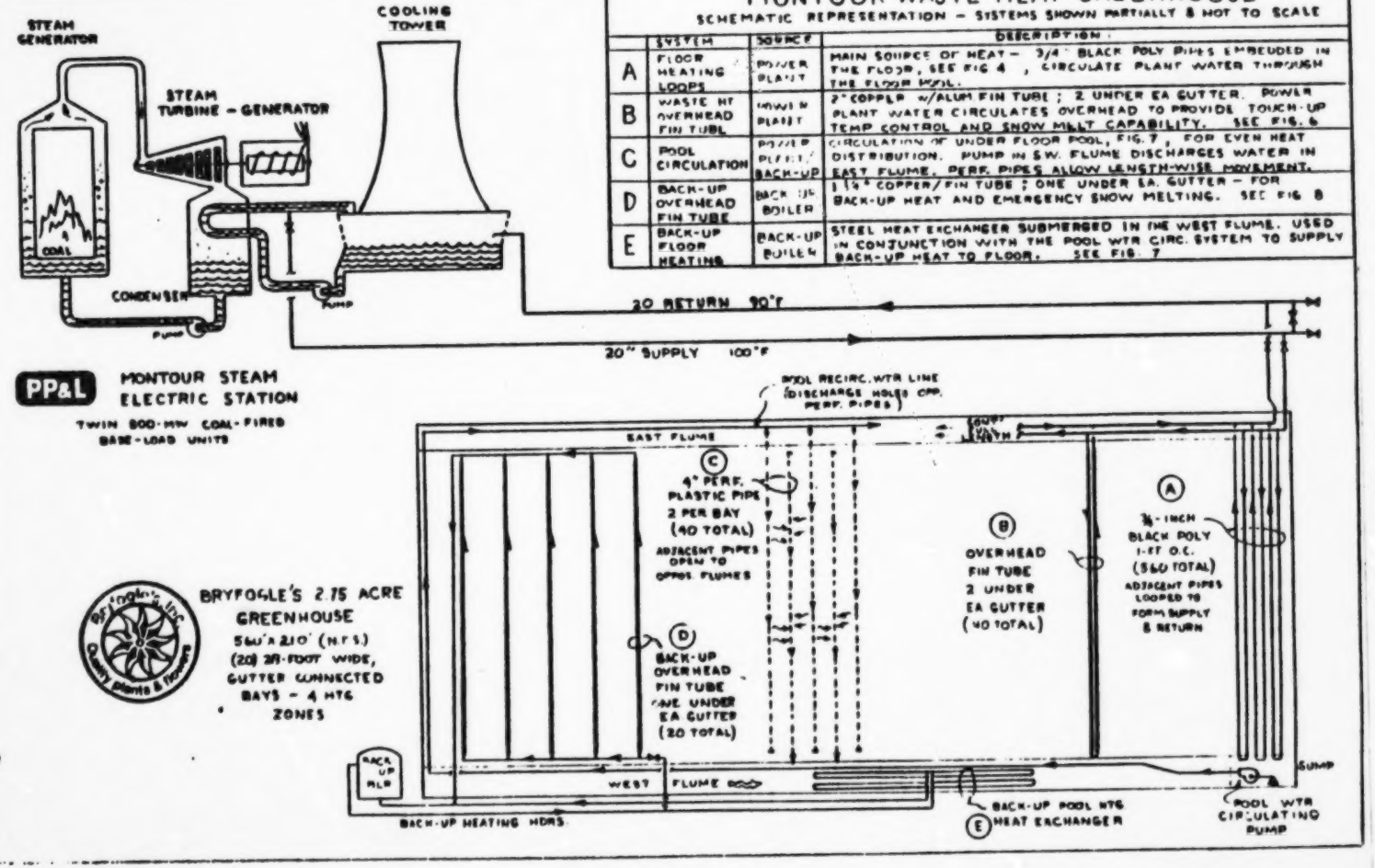

FIGURE 2

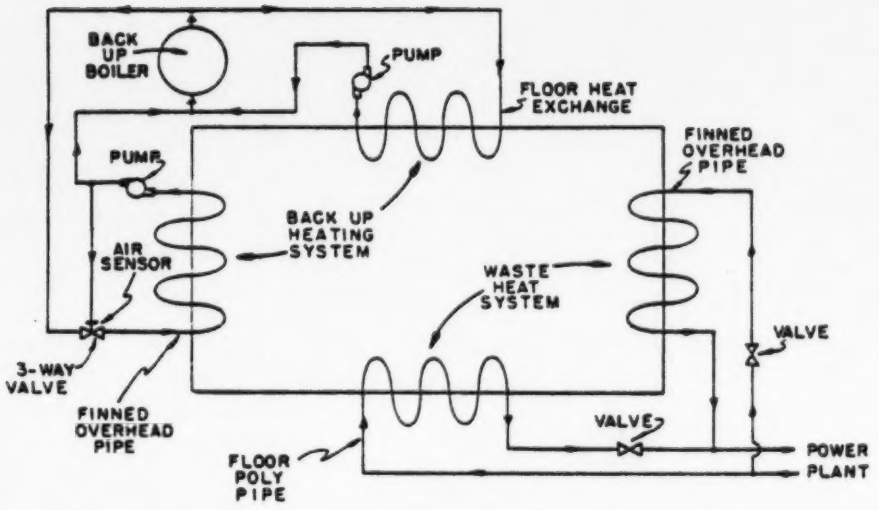

SCHEMATIC LAYOUT OF WASTE HEAT AND BACK UP HEATING SYSTEMS

Figure 3

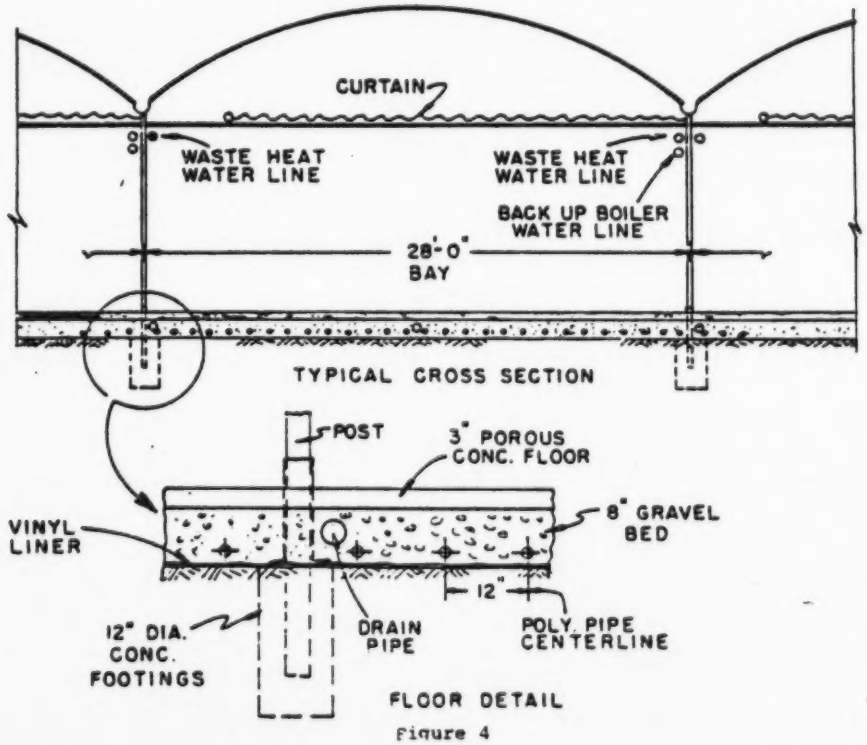

Figure 4

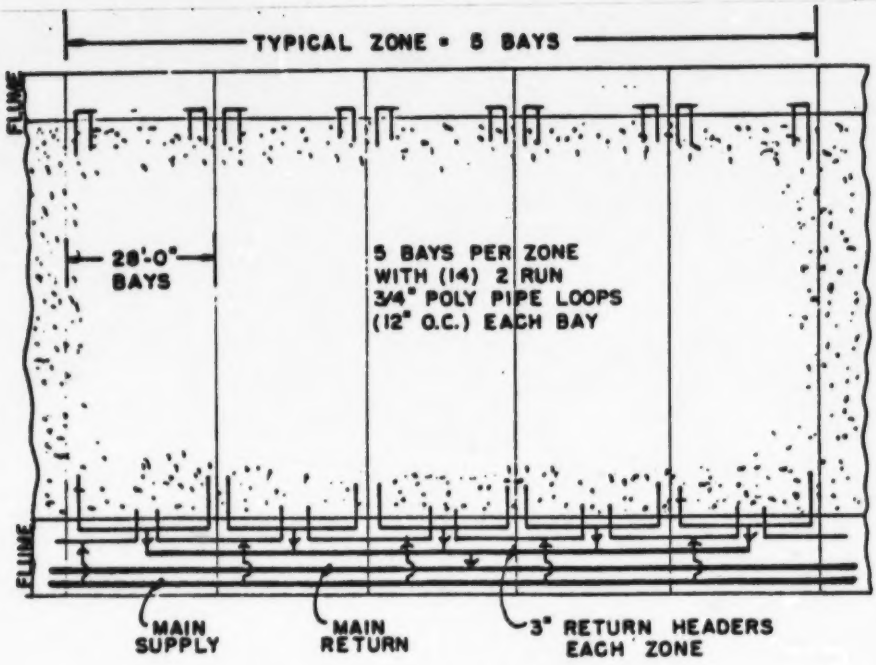
TYPICAL ZONE = 5 BAYS
FLUME
28'-0" BAYS
5 BAYS PER ZONE WITH (14) 2 RUN 3/4" POLY PIPE LOOPS (12" O.C.) EACH BAY
FLUME
MAIN SUPPLY
MAIN RETURN
3" RETURN HEADERS EACH ZONE

WASTE HEAT FLOOR HEATING SYSTEM

Figure 5

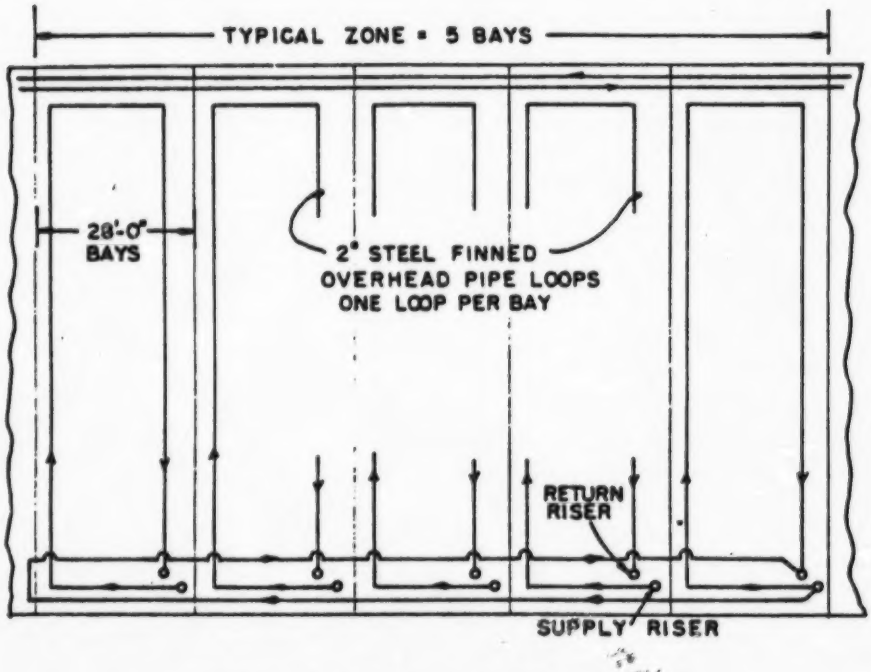

WASTE HEAT OVERHEAD FINNED PIPE HEAT SYSTEM

Figure 6

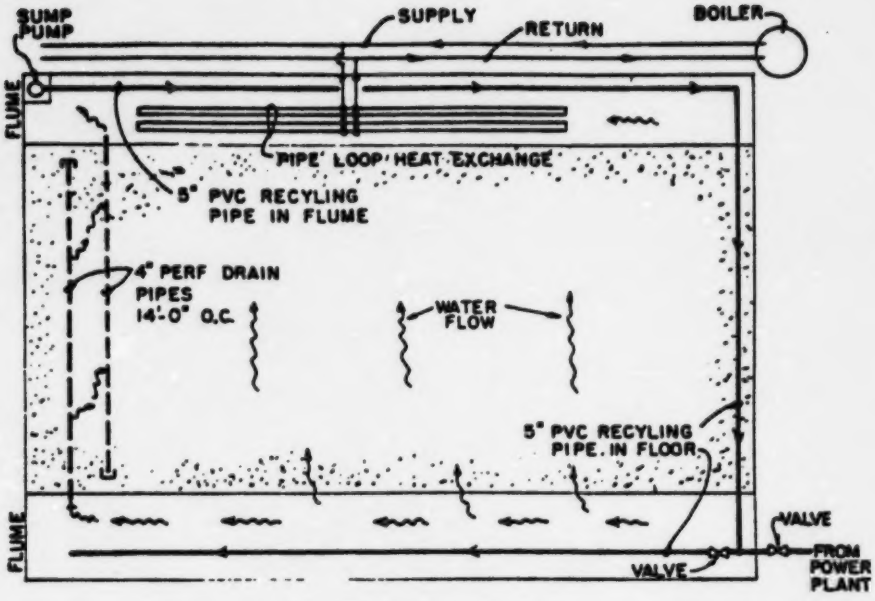

BACK-UP FLOOR HEATING SYSTEM
Figure 7

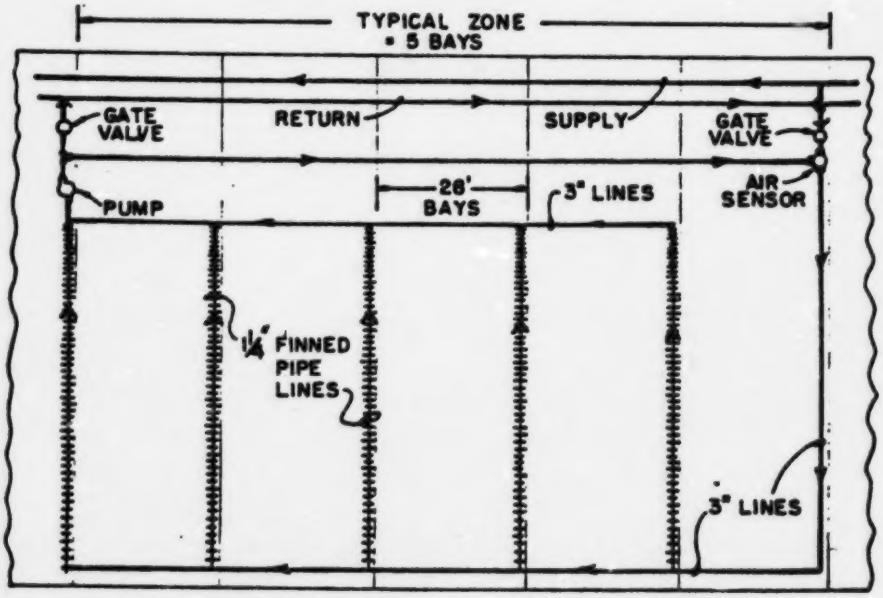

BACK-UP OVERHEAD PIPE HEAT SYSTEM
Figure 8

SESSION VII B

THERMAL DISCHARGE IV

Preceding page blank

PB82-228347

ASSESSMENT OF MODELS USED TO PREDICT EVAPORATIVE WATER LOSS AT COOLING IMPOUNDMENTS

E. E. Adams, K. R. Helfrich, A. L. Godbey and D. R. F. Harleman
R. M. Parsons Laboratory for Water Resources and Hydrodynamics
Massachusetts Institute of Technology
Cambridge, Massachusetts 02139, U.S.A.

ABSTRACT

Variability of predicted evaporation from heated water bodies was investigated in this paper. Accurate short term water temperature and meteorological data, available from two cooling impoundments, were used as the basis for comparison, calibration, and verification of the predictive accuracy of ten evaporation equations. In order to capture relevant spatial and temporal scales characteristic of cooling impoundments and therefore evaporation, a dynamic hydrothermal model was employed in the study. Results lead to a heirarchy of variability in predicted water loss.

1. INTRODUCTION

Cooling impoundments can offer a number of advantages over cooling towers for dissipation of waste heat. Among them are an increase in net efficiency of power production, thermal inertia which reduces short term fluctuations and water storage capability. A major disadvantage is, however, a lack of confidence in the ability to predict various aspects of their hydrothermal performance and consumptive water use. Because evaporative mass loss is usually the major component of cooling impoundment water consumption and evaporative heat flux is one of the dominant terms in the energy budget governing impoundment water temperatures, an increase in confidence means that an improved understanding of evaporation from cooling impoundments is necessary.

Prediction of evaporation in cooling ponds is more difficult and less certain than predicting natural evaporation from unheated water bodies. This is in part due to the elevated water surface temperatures which characterize heated impoundments. This increase in water surface temperatures may lead to local instability where buoyant free convection becomes important. Evaporation models developed for natural water bodies generally do not perform well when applied to heated water bodies presumably for this reason [1]. Additionally, few reliable data sets from heat-loaded conditions are available with which to calibrate/verify evaporation equations. It is the objective of this paper to assess the accuracy of various models used to predict evaporation from heated water bodies.

2. EVAPORATION EQUATIONS

Under realistic atmospheric conditions evaporation from an open body of water is dominated by turbulent processes. This turbulent transport of water

Preceding page blank

vapor is given by

$$E = \rho_a \overline{w'q'} \qquad (1)$$

where E = evaporative mass loss rate; ρ_a = density of moist air; w' = vertical velocity fluctuation; and q' = specific humidity fluctuation. Eq. (1) as an analytical tool is not readily useful. However, use of dynamic similarity arguments leads to an empirical evaporation of the form [2]

$$E = f(W_z)(e_s - e_z) \qquad (2)$$

where e_s is saturated vapor pressure at water surface temperature; e_z is vapor pressure of the air at some prescribed height z; and $f(W_z)$ is an empirical function of wind speed at elevation z. In practice, evaporation may depend upon other parameters such as local stability, fetch length, etc. In general we can write

$$E = E(W_z, T_s, T_z, \text{ relative humidity, stability, fetch, } \ldots)$$

Notice that Eqn. (1) gives evaporation only at a point over the water surface, but Eqn. (2) is usually extrapolated to give evaporation integrated over some water surface area.

Presently we have identified over 100 evaporation equations of various forms. Several other listings of equations are available [1,3,4]. A complete listing would not be useful as many equations are slight variations of each other. Based upon functional representation, usually the form of $f(W_z)$, it is possible to group the equations under several headings. For the present purposes the equations were grouped into one of three categories: Dalton law type, modified Dalton law and stability dependent equations.

Dalton law equations take the form

$$f(W_z) = a + bW_z$$

where a and b are empirically determined constants. Modified Dalton law equations are similar except that some dependence, often the wind speed, is changed slightly, say

$$f(W_z) = a + bW_z^{\alpha}$$

where α is some constant not equal to one. The stability dependent equations generally take the form

$$f(W_z) = f(W_z, \text{stability}).$$

The stability dependence may take several forms; the most common is some dependence upon free convection often parameterized by the air-water temperature difference.

Ten equations, representing all three categories were selected in order to examine the variability of predicted evaporation from heated water bodies. Table 1 lists these equations along with references and comments. Information most pertinent to this investigation includes whether or not the equation was developed for use on heated water bodies, what data if any it was originally calibrated with and what type of data (location, etc.) is needed to use the equation properly.

Table 1: Evaporation Equations

Name and Ref.	Equation*	Units	Calibration or Testing	Location of Met. Variables	Comment
Lake Hefner (LH) [5]	$17W_2(e_s-e_2)$	BTU/ft^2-day mph mmHg	natural lakes	bulk of pond measurements at 2 meters height	Dalton Law
Ryan-Harleman (RH) [1]	$(22.4(\Delta\theta_v)^{1/3}+.14W_2)(e_s-e_2)$	BTU/ft^2-day mph mmHg	heated impoundments	bulk of pond measurements at 2 meters height	stability dependent
Kimsha-Donchenko (RD) [6]	$(61+1.47\Delta\theta+13.3W_2)(e_s-e_2)$	BTU/ft^2-day mph mmHg	thermally loaded streams	bulk of pond measurements at 2 meters height	stability dependent
Brady, Graves and Geyer (BGG) [7]	$(70+W_2^2)(e_s-e_2)$	BTU/ft^2-day mph mmHg	heated impoundments	bulk of pond measurements at 2 meters height	Modified Dalton Law
Harbeck (H) [8]	$\frac{24.2W_2}{A^{0.5}}(e_s-e_2)$	BTU/ft^2-day mph mmHg acres	natural lakes	bulk of pond measurements at 2 meters height	Dalton Law fetch dependence
Goodling, Sill and McCabe (GSM) [9]	$(25.1(\Delta e)^{1/3}+\frac{690W_2}{R_L^{0.2}})(e_s-e_2)$	BTU/ft^2-day mph mmHg	none	bulk of pond measurements at 2 meters height average fetch length	stability and fetch dependent
Weisman (W) [10]	$a(\frac{x_o}{z_o})^{-n}u_*(e_s-e_2)$	see ref.	none	Same as above	stability and fetch dependent
Argonne (ARG) [11]	$\frac{K^2W(q_s-q_a)}{(\ln(z/z_w)-\psi_m)(\ln(z/z_o)-\psi_m)}$	see ref.	heated impoundments	local boundary layer measurements for all variables. This study used bulk measurements at 2 meters.	stability dependent
Meyer (M) [12]	$(80+10W_2)(e_s-e_2)$	BTU/ft^2-day mph mmHg	natural lakes	bulk of pond measurements at 2 meters height	Dalton Law
Throne (T) [13]	$(67+17W_2)(e_s-e_2)$	BTU mph mmHg	heated impoundments	Same as above	Dalton Law

*see references for complete definition of variables

3. EVALUATION OF EQUATIONS

3.1 Pond Modeling

Evaluation of evaporation formulae performance on cooling impoundments is more difficult than for natural water bodies. This is due primarily to the larger spatial and temporal variability in water temperatures caused by plant loading and complicated hydraulic characteristics. Natural lakes by comparison exhibit less of these variabilities in water temperatures. For these reasons the bulk energy budget approach often used in calibration/verification of evaporation equations is not very useful. The bulk approach is typically used on a time scale longer (≈ weekly at the shortest) than cooling impoundment temporal flucutations. Also the bulk approach does not consider spatial variations in water surface temperature and therefore evaporation. Hydrothermal models, on the other hand, provide a useful tool for indirectly "measuring" evaporation (with an energy budget) and for calibrating formulae. Examples of hydrothermal model use for these goals are given by [14,15,16]. Additionally, these models are necessary to accurately predict future evaporation from cooling impoundments.

In principle a model should be 3-D and transient but because of numerical and economic considerations this is not feasible for studies where long time frames (e.g., 10 years say for water consumption) are often necessary. At the other end of the spectrum are the simple steady state models. They, however, shortcut many of the physically relevant characteristics such as transient non-linear meteorology and spatial detail. Clearly, an intermediate level of sophistication is necessary—one which meets both spatial and temporal detail and computational efficiency objectives. For this study the model MITEMP [16] was chosen. It facilitates the modeling of cooling impoundments in a numerically 1-D framework yet at the same time preserves the essential spatial structure and transient response characteristic of a cooling impoundment. Use of the full non-linear surface heat transfer formulations is also possible.

MITEMP is based on a classification scheme [17] that depends upon three parameters: the thermal loading ϕ (MW_t/acre); the relative pond depth expressed by the "pond number" P; and the horizontal aspect ratio L/W. The pond number is defined as

$$P = \left(\frac{f_i Q_o^2}{4\beta \Delta T_o g H^3 W^2} D_v^3 \frac{L}{H}\right)^{1/4} \qquad (3)$$

where L = pond length along the flow path, W = flow path width (W = A/L), A = pond surface area, H = average pond depth, Q_o = condenser flow rate, ΔT_o = condenser temperature rise, D_v = volumetric dilution produced by entrance mixing, f_i = interfacial friction factor, β = coefficient of thermal expansion and g = gravitational acceleration. Figure 1 emphasizes the usefulness of the pond number in classifying the vertical structure of a cooling impoundment. At one extreme are vertically fully mixed ponds ($P \geq 1$) and at the other are ponds which show increasingly stronger vertical temperature gradients ($P \to 0$).

Figure 2 shows the classification scheme upon which MITEMP is based and the role of the three parameters in defining the pond structure. Four categories of pond structure are available. For our work, though, only the three pertaining to heat loaded conditions ($\phi \geq 0.2$ MW_t/acre) are of interest. For $P < 0.5$ the "deep" cooling pond model is used. For $P \geq 0.5$ the one layer or "shallow" cooling pond models are used. Because of later applications to specific data sets

only the two one-layer models will be discussed.

If L/W is large the hydrothermal structure of a shallow pond will be predominantly one dimensional and longitudinal dispersion will be the dominant mixing process. The governing equation for pond temperatures is

$$\frac{\partial T}{\partial t}(x,t) + U\frac{\partial T}{\partial x}(x,t) = E_L\frac{\partial^2 T}{\partial x^2}(x,t) - \frac{\phi_n}{\rho c H}(x,t) \qquad (4)$$

with boundary conditions

$$UT(o,t) - E_L\frac{\partial T}{\partial x}(o,t) = U\,T_o(t) \qquad \text{at } x = 0$$

and (5)

$$\frac{\partial T}{\partial x}(L,t) = 0 \qquad \text{at } x = L$$

where $T(x,t)$ = cross-sectionally averaged temperatures, U = cross-sectionally averaged velocity Q_o/WH, x = longitudinal distance, t = time, $T_o(t)$ = inflow temperature, E_L = longitudinal dispersion coefficient, $\phi_n(x,t)$ = net surface heat transfer to the atmosphere comprised of net solar radiation, longwave atmospheric radiation, back radiation, evaporation and conduction (non-linear analysis), ρ = density of water, c = specific heat of water. The boundary conditions insure conservation of thermal energy. See Figure 3. The main parameter required to describe the hydrothermal structure is the dispersion coefficient, which may be estimated approximately from Fischer's analysis [17,18], and fine tuned in accordance with measurements. This helps eliminate uncertainty in predicted evaporation caused by incorrect modeling of the hydrothermal structure.

For L/W < 3 to 5 the hydraulic structure is dominated by recirculating flow. See Figure 4. The temperature in each flow zone (jet and return) is describable by equations (4) and (5) which are applied to each zone separately. With recirculating flow the dispersion coefficient does not play a major role in describing the hydrothermal characteristics. The dilution factor D and the area ratio q are more important. Again correct specification of these parameters can reduce uncertainty in predicted evaporation.

Reexamination of Figure 1 indicates that for 0.5 < P < 1.0 vertical temperature gradients are observed. Since the "shallow" pond models are formulated for depth-average temperature we have made modifications to compute the surface heat exchange based on an elevated temperature which reflects the effect of vertical stratification. Using Figure 1 as a guide a pond average vertical temperature gradient as a function of pond number is found. Considering this vertical temperature gradient to be linear the basic heat transport equation (4) is not altered except that the surface heat flux ϕ_n is evaluated at a temperature $\overline{\Delta T}_v/2$ above the depth averaged temperature calculated by the model.

In addition to hydrothermal structure other terms in the pond energy balance must be modeled accurately. In the following analysis of specific data sets all terms except the computed atmospheric radiation were either measured or computed to a reasonable degree of accuracy ($\pm$ 5-10% or better). For computing atmospheric radiation the relation given by Swinbank [19] and modified for cloud cover effect by Geiger [20] is used in the model. It is the cloud cover effect which causes the most uncertainty. Ryan and Harleman [1] state that the accuracy for clear skies is $\pm$ 5% but for cloudy conditions it is probably much worse. We estimate errors of $\pm$ 15% or larger are possible due both to the cloud cover correction to the equation and the ambiguous definition and inaccurate measurement of cloud cover.

3.2 Data Sets

To evaluate evaporation formulae one must have good field data. Several excellent studies of evaporation from natural lakes were conducted by the U.S.G.S. in the 1950's [5,21]. This data is not useful for our present purposes because natural water bodies differ from cooling impoundments in several important ways previously mentioned. Because of these differences it is evident that equations used on heated water bodies must be calibrated/verified using data from heated water bodies.

Availability of this type of data is very limited. Several data sets exist [1,7,22] but they do not lend themselves to dynamic analysis or are not in a form which is readily available. Two data sets which are attainable include Dresden cooling pond [23] and Powerton cooling pond [24]. Both are perched impoundments designed specifically for waste heat disposal and are located in Illinois.

Both data sets contain detailed information on plant operating characteristics (i.e., flow rate, inflow and outflow water temperatures), primary meteorological variables, and pond water temperatures reported in 1 hour averages (converted to 3-hour averages for analysis with MITEMP). The Dresden data is from 9/12/75 to 10/31/75. The meteorological variables were measured on site with the exception of solar radiation which was measured at Argonne National Laboratory (40 miles away) and cloud cover which was reported from Chicago O'Hare Airport, about 100 miles away. The Powerton data covers the period 8/1/76 to 8/31/76. All meteorological variables were measured at the NWS station in Peoria, Illinois (20 miles away) except for solar radiation which was measured on site.

3.3 Analysis with Dresden Data

The Dresden data was chosen for the initial evaluation of the predictive accuracy and calibration of the different equations. Both data sets are of comparable quality to allow dynamic simulation. Dresden pond, however, has a better defined thermal structure. Uncertainty in predicted evaporation and subsequent calibration should be reduced.

Dresden has a total surface area of 1275 acres and consists of three compartments in series which are separated by internal diking and constrictions. The flow path is about 33,000 ft. and the average depth is 10 ft. The plant flow rate and condenser temperature rise are nearly constant at 1800 cfs and 15° F during the period of investigation. The pond number for Dresden is calculated to be 0.9. Along with large horizontal aspect ratios for each compartment the hydraulics are predominantly vertically mixed and longitudinally dispersive. Field measurements [23] verify this assessment; thus Dresden was modeled as three vertically mixed longitudinally dispersive ponds in series using MITEMP. No account for vertical temperature gradients has been undertaken as the field data indicated very slight gradients ($\overline{\Delta T}_v \lesssim 1^\circ$ F) on average.

The deviation of predicted station intake temperatures (pond outlet temperatures) from the corresponding measured temperatures is an indication of the predictive accuracy of each equation assuming the pond hydraulics are well modeled and that all other energy inputs or outputs are accurately represented. The energy input from the plant is specified using measured station discharge temperature and flow rate. Two measures of the deviation between model and measurement were computed. One was the mean error of the predicted

vs. measured intake temperatures. The other was the variance (or standard deviation) of the predicted vs. measured intake temperature about the mean error. The mean error indicates if too much or too little total heat loss is occuring and the standard deviation indicates, to some degree, how well the formulas respond to shorter term variations in meteorological conditions. After computing the mean error, standard deviation and total predicted water loss, each equation was calibrated to the Dresden data by adjusting the factor α in

$$E = \alpha f(W_z)(e_s - e_z)$$

until the mean error was zero.

Prior to actual analysis of the equation predictions the hydraulic structure (dispersion coefficient) was calibrated. Initial estimates of dispersion coefficients were made for each pond compartment based on Fischer's analysis [17,18]. Then, using the Lake Hefner equation, the dispersion coefficients were changed by a constant fraction of the Fischer value (E_{L_F}) until the shape of the predicted longitudinal temperature profiles matched the shape of the measured profiles. This procedure was used because the shape of the temperature profile is predominantly a function of the dispersion coefficient, while the actual water temperatures are predominantly a function of the surface heat transfer (e.g., evaporation). Using this approach a value of 0.25 times the Fischer relationship was determined to best represent the hydraulic characteristics of Dresden Pond and was used in subsequent model calibration/verification. Because there was a range in the values of E_L (between 0 and 0.50 E_{L_F}) which gave satisfactory longitudinal temperature profiles when compared to the measured data, some uncertainty is associated with the chosen value of E_L. This uncertainty translated to an uncertainty of $\pm$ 3% in α calibrated for zero mean error between predicted and measured intake temperatures using the Lake Hefner equation. This result is representative of all the equations.

Table 2 contains the predictions for the 50 days of data from Dresden Pond. The average water loss rates and mean errors between predicted and measured intake temperature ranged from 18.7 cfs to 25.3 cfs and -3.68° F to +0.94° F (α = 1.0 for all equations). The average predicted water loss rate was 21.9 cfs. The spread, 1/2(High-Low)/average, was about $\pm$ 15%.

The variability in evaporative loss rate is quite a bit less than that observed when evaporative mass loss is computed for each equation using the average meteorological conditions and average measured water temperature at Dresden during the 50-day period. (T_s = 78° F, T_a = 55.5° F, relative humidity = 68%, W_2 = 6.9 mph.) Using this single set of conditions (referred to as static condition) the spread about the average value is $\pm$ 28%. The reduction in the variability of water loss predictions between the dynamic calculations ($\pm$ 15%) and the static calculations ($\pm$ 28%) can be attributed to two factors: feedback between temperatures and evaporation and the effect of averaging over variable atmospheric conditions. Along similar lines it is noted from Table 2 that, on average, the percentage change between calibrated and uncalibrated water loss was only 68% of the calibrated adjustment to the wind speed functions (α).

To further characterize the feedback between evaporation and water temperatures associated with the dynamic model we ran a hypothetical case using the Dresden Pond configuration and meteorological conditions in a closed cycle mode of station operation in which the station condenser rise ΔT_o was specified rather than the actual temperatures. In this situation the predicted water loss rates for all non-calibrated equations (α = 1.0) exhibited a spread about the average value of $\pm$ 3.6%, much lower than the previous two cases. This

Table 2: Equation Predictions at Dresden

Equation	Mean Intake Error α=1.0 (^{o}F)	Std. Dev. (^{o}F)	Water Loss Rate (cfs)	Calibrated α for Dresden	Mean Intake Error (^{o}F)	Std. Dev. (^{o}F)	Water Loss Rate (cfs)
1 (LH)	0.94	0.91	18.7	1.11	0	0.95	20.1
2 (RH)	-2.22	1.11	23.0	0.79	0	1.07	19.8
3 (RD)	-3.58	1.28	25.0	0.69	0	1.20	19.8
4 (BGG)	0.01	0.94	20.1	1.00	0	0.94	20.1
5 (H)	0.98	0.92	18.7	1.11	0	0.95	20.1
6 (GSM)	-1.44	1.28	21.9	0.86	0	1.31	19.9
7 (WB)	-2.56	1.06	23.6	0.76	0	0.95	19.9
8 (ARG)	-0.46	1.34	21.0	0.95	0	1.29	20.3
9 (M)	-1.57	1.28	22.0	0.85	0	1.33	19.8
10 (T)	-3.68	1.12	25.3	0.69	0	1.07	19.9
Average = -1.36^{o}F			21.9 cfs	0.88			20.0 cfs
Spread = $\pm$ 2.33^{o}F			$\pm$ 15%	$\pm$ 0.21			$\pm$ 1.3%

Table 3: Equation Predictions at Powerton

Equation	Mean Intake Error α=1.0 (^{o}F)	Std. Dev. (^{o}F)	Water Loss Rate (cfs)	Calibrated α for Dresden	Mean Intake Error (^{o}F)	Std. Dev. (^{o}F)	Water Loss Rate (cfs)
1 (LH)	3.04	1.04	23.7	1.11	0.91	0.94	26.5
2 (RH)	-0.62	1.14	29.2	0.79	0.17	1.10	27.4
3 (RD)	-1.87	1.22	31.1	0.69	0.16	1.18	27.3
4 (BGG)	1.79	1.14	25.4	1.00	1.04	1.06	26.7
5 (H)	3.13	1.04	23.6	1.11	1.22	0.94	26.3
6 (GSM)	-0.50	1.22	29.1	0.86	-0.46	1.18	28.3
7 (WB)	-0.32	1.07	28.9	0.76	0.84	1.03	26.5
8 (ARG)	1.50	1.01	26.2	0.95	0.81	0.98	26.7
9 (M)	-0.38	1.20	28.7	0.85	-0.05	1.17	27.6
10 (T)	-2.05	1.05	31.5	0.69	0.29	1.03	27.2
Average = 0.37^{o}F			27.7 cfs	0.88	0.49^{o}F		27.0 cfs
Spread = $\pm$2.59^{o}F			$\pm$ 14%	$\pm$ 0.21	$\pm$ .84^{o}F		$\pm$ 3.7%

suggests a heirarchy of probable uncertainty in water consumption estimates. Static calculations based on fixed meteorological and water temperature data give the most variability whereas calculations using a dynamic model operating in closed cycle mode are quite consistent regardless of evaporation equation used. Table 4 summarizes these results.

3.4 Analysis with Powerton Data

To assess the consistency of the calibrations performed with the Dresden data a similar analysis with the Powerton data was performed. Powerton, though, presented a more difficult modeling job. It has a total surface area of 1442 acres and consists of three compartments of approximately equal size. Based upon the average plant flow rate and temperature rise a pond number of 0.5 was computed. The horizontal aspect ratio for each compartment is low suggesting recirculating flow in each. Powerton was modeled as three shallow recirculating compartments in series with a correction for the vertical temperature gradient predicted from the pond number. With the computed pond number and average condenser temperature rise Figure 1 gave $\overline{\Delta T}_v = 4^o$ F which agreed well with the field data on a pond average basis.

Further specification of the hydraulic structure was possible using the dilution and area factors defined in Figure 4. The dispersion coefficient was set at $0.25 \times E_{LF}$. By comparing initial simulations with field data and using results of previous studies of Powerton [17] values for the area and dilution factors for each compartment were set. Sensitivity studies showed that a 10% change in the dilution factor caused a 6% change in α adjusted for zero mean error. This gives slightly more uncertainty in the evaporation due to hydraulic characteristics than observed at Dresden, but due to the increased complexity at Powerton this was expected.

The results for the uncalibrated ($\alpha = 1.0$) and Dresden-calibrated equations are shown in Table 3. As would be expected all ten calibrated equations performed much better at Powerton when compared to the uncalibrated results at Dresden or Powerton. The spread of the water loss estimates for the calibrated equations is $\pm$ 3.7% about a mean of 27.0 cfs. By comparison the non-calibrated equations had a spread of $\pm$ 14%. See Table 4. The calibrated equations which performed best (measured by mean error) were the Meyer equation, the Ryan-Harleman equation, the Rimsha-Donchenko equation and the Throne equation. The last three equations were developed specifically for heated water conditions while the Meyer equation was originally developed for natural situations.

4. SUMMARY AND CONCLUSION

Due to the large spatial and temporal variations in water temperatures which characterize cooling impoundments a hydrothermal model which captures the relevant space and time scales must be used to calibrate/verify evaporation equations as well as to (later) perform water loss calculations.

In this study ten evaporation equations (see Table 1) were evaluated on complete data sets from Dresden and Powerton cooling ponds using the model MITEMP. Results of these comparisons are provided in Tables 2 and 3. As expected, generally better agreement--both before and after calibrations--was obtained using those equations which were developed specifically for heated ponds. However, specific recommendations regarding which of the equations are most suitable, and conclusions regarding the absolute accuracies, should be delayed until more testing with data sets from different geographical locations is undertaken.

Table 4: Summary of Variability of Water Loss Predictions

Situation	Spread about average
Static calculation, uncalibrated	± 28%
Open cycle simulation at Dresden, uncalibrated	± 15%
Open cycle simulation at Powerton, uncalibrated	± 14%
Closed cycle simulation at Dresden, uncalibrated	± 3.6%
Open cycle simulation at Powerton, calibrated at Dresden	± 3.7%
Open cycle simulation at Dresden, calibrated at Dresden	± 1.3%
Closed cycle simulation at Powerton, calibrated at Dresden	± 1.3%

Table 4 summarizes the variabilities of predicted water loss for different computational situations. Greatest variability among equations (± 28%) was found when the uncalibrated equations were used under static conditions of specified meteorology and water temperature data. This variability is reduced when the equations are calibrated (using one data set) before application (to the second data set), and when the simulations are performed in a dynamic mode with coupled calculations of temperature and evaporation. Thus the range of predicted evaporation rates for equations calibrated at Dresden and used at Powerton for closed cycle dynamic calculations was only ± 1.3%. The strong feedback between evaporation and pond temperature is a major reason for reduced variability suggesting additional motivation for the use of a dynamic hydrothermal model to compute pond evaporation. Even if only approximate water loss estimates are required, the coupling suggests that these estimates should be based on anticipated water temperatures which reflect the evaporation equation used to compute water loss.

It is important to recognize that the variabilities reflected in Table 4 represent the relative accuracy of the various equations under different predictive conditions and not the absolute accuracy of the equations. Uncertainty in the latter is a function of uncertainty in the other heat flux terms, especially shortwave solar and longwave atmospheric radiation.

REFERENCES

1. P. Ryan and D.R.F. Harleman, An Analytical and Experimental Study of Transient Cooling Pond Behavior, R.M. Parsons Laboratory, Technical Report No. 161, MIT, 1973.

2. P.E. Eagleson, Dynamic Hydrology, McGraw-Hill, New York, 1969.

3. P.P. Paily, E.O. Macagno and J.F. Kennedy, Winter Regime Surface Heat Loss from Heated Streams, Iowa Inst. of Hydraulic Res., Report No. 155, 1974.

4. W.O. Wunderlich, Heat and Mass Transfer Between a Water Surface and the Atmosphere, Engineering Lab., Tenn. Valley Authority, Lab. Report No. 14, 1972.

5. M.A. Kohler, Lake and Dam Evaporation in Water Loss Investigations-Lake Hefner Studies, USGS Prof. Paper 269, 1954.

6. V.A. Rimsha and R.V. Donchenko, The Investigation of Heat Loss from Free Water Surfaces in Wintertime, (in Russian) Trudy Leningrad Gosub. Gidrol. Inst. 64, 1957.

7. K.D. Brady, W.L. Graves and J.C. Geyer, Cooling Water Studies for Edison Electric Institute, Proj. No. RP-49-Surface Heat Exchange at Power Plant Cooling Lakes, The Johns Hopkins Univ., 1969.

8. G.E. Harbeck, A Practical Field Technique for Measuring Reservoir Evaporation Utilizing Mass-Transfer Theory, USGS Prof. Paper 272-E, 1962.

9. J.S. Goodling, B.L. Sill and W.J. McCabe, An Evaporation Equation for an Open Body of Water Exposed to the Atmosphere, Water Resources Bulletin, Vol. 12, No. 4, 1976.

10. R.N. Weisman, Comparison of Warm Water Evaporation Equations, Jour. Hyd. Div., ASCE, Vol. 101, No. HY10, November 1975.

11. B.B. Hicks, M.L. Wesely and C.M. Sheih, Eddy-correlation Measurements over a Cooling Pond with Limited Fetch, 1974 Annual Report of Radiological and Environmental Res. Div., Argonne Nat. Lab., ANL-75-60 Part IV, 1975.

12. A.F. Meyer, Evaporation from Lakes and Reservoirs, Minnesota Resources Comm., St. Paul, Minn., June 1942.

13. R.F. Throne, How to Predict Cooling Lake Action, Power, pp. 86-89, September 1951.

14. H.E. Jobson, Canal Evaporation Determined by Thermal Modeling, Symposium on Modeling Techniques, Waterways, Harbors and Coastal Engineering Div. of ASCE, p. 729, September 1975.

15. A.M. Mitry and B.L. Sill, A Model for Prediction of Evaporative Heat Flux in Large Bodies of Water, Proc. of the Second Conf. on Waste Heat Mgnt. and Util., pp. VII-B-109 to 123, December 1978.

16. K.H. Octavio et al., Mathematical Predictive Models for Cooling Ponds and Lakes-Parts B and C, R.M. Parsons Laboratory, Technical Report No. 262, MIT, 1980.

17. G.H. Jirka et al., Mathematical Predictive Models for Cooling Ponds and Lakes-Part A, R.M. Parsons Laboratory, Technical Report No. 238, MIT, 1978.

18. H.B. Fischer, The Mechanics of Dispersion in Natural Streams, Jour. Hyd. Div., ASCE, Vol. 93, No. HY6, June 1969.

19. W.C. Swinbank, Longwave Radiation from Clear Skies, Quarterly Jour. of the Roy. Met. Soc., Vol. 89, July 1963.

20. R. Geiger, The Climate Near The Ground, Harvard Univ. Press, Cambridge, Mass., 1965.

21. G.E. Harbeck et al., Water Loss Investigations: Lake Mean Studies, USGS Prof. Paper 298, 1958.

22. W. McMillan, Cooling from Open Water Surfaces: Final Report Part 1: Lake Trowsfynydd Cooling Investigation, NS/SSD/RR/1204/73, North Western Region Scientific Services Division, CEGB, September 1973.

23. NUS Corporation, Temperature Distribution in Dresden Cooling Pond, 1976.

24. NUS Corporation, Temperature Distribution in Powerton Cooling Pond, 1976.

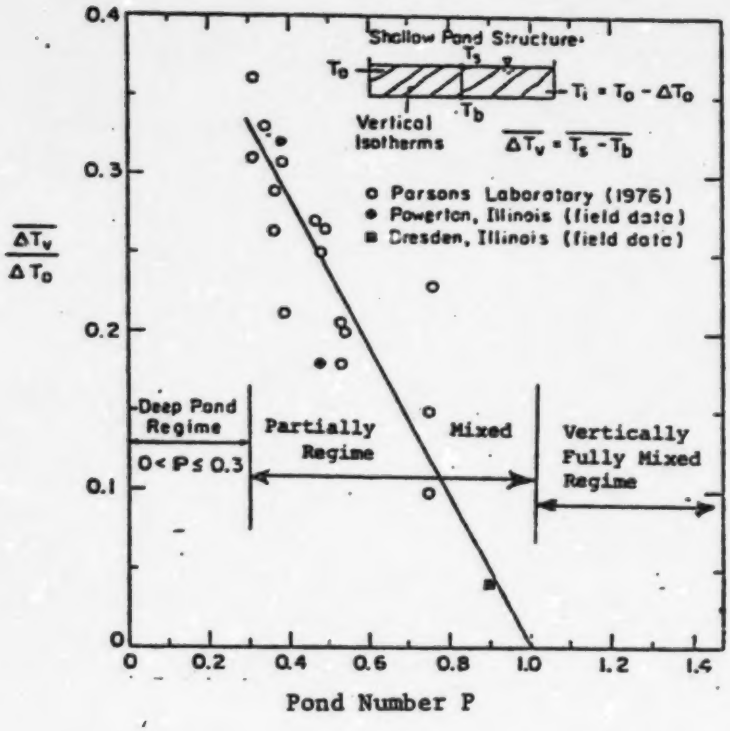

Figure 1: Relation Between Vertical Temperature Gradient and Pond Number P. (from [17])

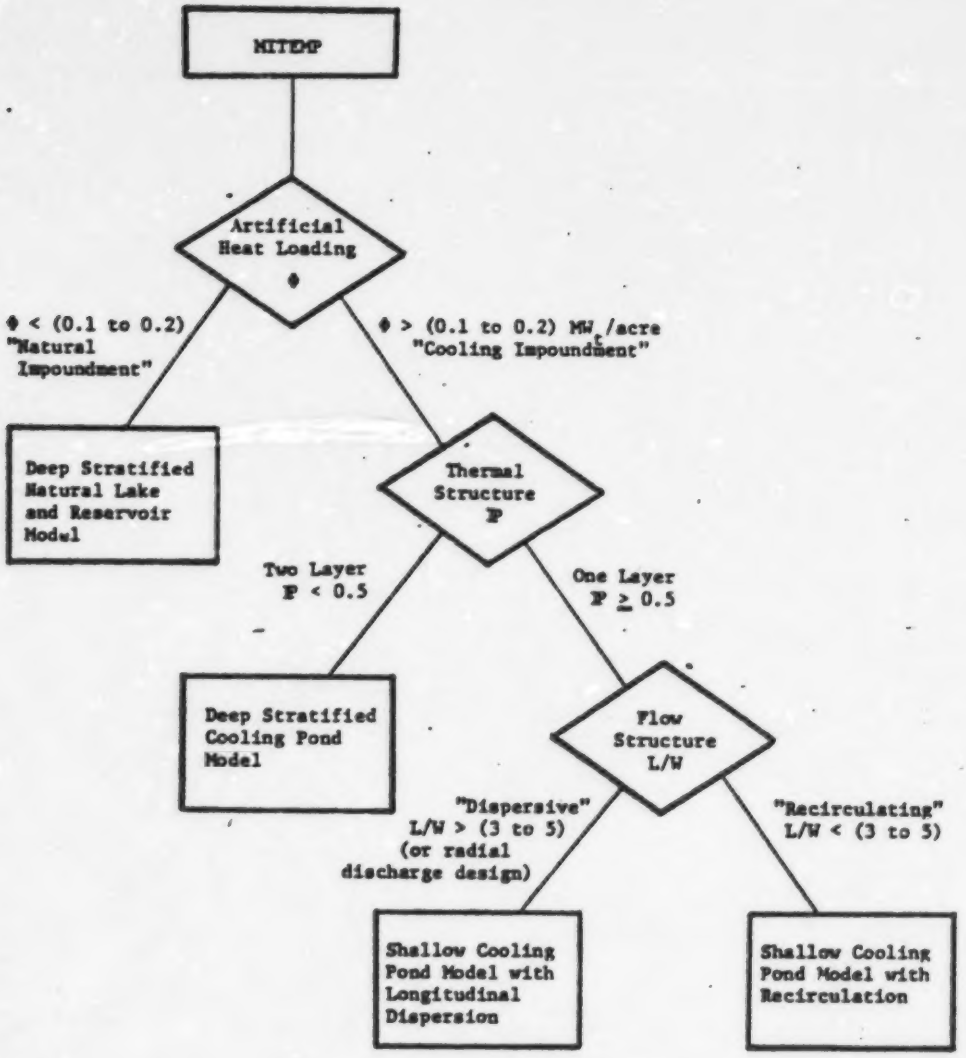

Figure 2: Hierarchical Structure and Decision Tree for MITEMP.

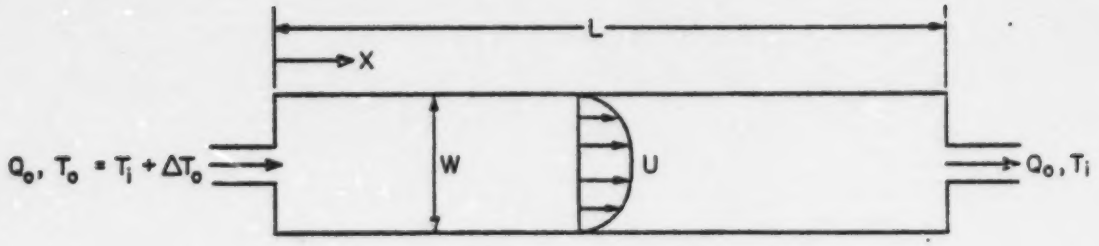

Figure 3: Plan View of Shallow Cooling Pond with Longitudinal Dispersion (Depth = H).

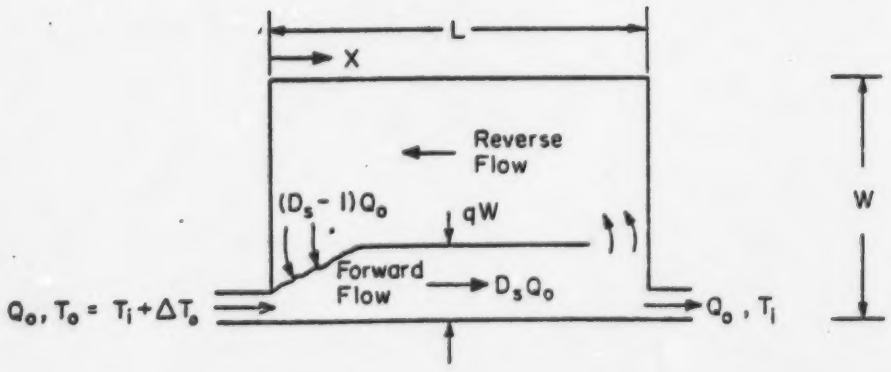

Figure 4: Plan View of Shallow Cooling Pond with Lateral Recirculation (Depth = H).

PB82-228354

USE OF NON-SITE SPECIFIC WIND SPEED DATA IN PREDICTING LAKE TEMPERATURES AND EVAPORATION

A. M. Mitry
Design Engineering Department
Duke Power Company
Charlotte, N.C.

B. L. Sill
Civil Engineering Department
Clemson University
Clemson, S.C.

ABSTRACT

Analyses are presented to determine the sensitivity of lake temperature and evaporation predictions to errors in wind speed input. Such errors occur when data from a remote meteorological station is used to make temperature and evaporation predictions for large water bodies such as stratified lakes. For the present study, temperatures are computed with a previously validated analytical model [1, 2]. Resulting temperatures are used in an energy balance for the lake to calculate evaporative heat flux [3]. Three wind speed functions f, of differing forms are used in the analysis to link the wind speed W to lake temperature. Results indicate that evaporation predictions using the additive forms of the wind speed functions ($f = a_o + a_1 W$, $f = a_o + a_2 W^2$, with a_i constants) are less sensitive to wind speed errors than predictions using the form $f = a_1 W$. It is shown that combining the analytical model of ref. 1 with the additive f's result in only a $\pm$ 5% change in annual evaporation predictions for a $\pm$ 30% error in wind speed.

INTRODUCTION

There are many occasions when water temperature or evaporation predictions must be made on lakes for which there is no site specific meteorological data. In these instances, data from the nearest meteorological station (usually an airport) is typically employed. Depending on the relative locations of the airport and lake, the input wind speed data necessary to make predictions can be in error, with differences of $\pm$ 10% not uncommon. As a result, it is important to know if these errors will prevent satisfactory results when combined with an analytical model. To properly answer this question, it is useful to trace the manner in which the wind speed fits into the ultimate prediction of lake temperature and evaporation.

The distribution of energy within a water body is accomplished differently in different models [1, 4]; however all must supply a surface energy flux boundary condition. This is often done with a modified form of Newton's law of cooling in which the surface energy transfer rate q_s, is proportional to the difference in the water surface temperature T_s and an "equilibrium temperature" T_e, or

$$q_s = -K'(T_s - T_e) \qquad (1)$$

where K' is the surface heat exchange coefficient. The portion of q_s due to evaporative heat flux (q_e) at the surface is often taken as

$$q_e = f(e_s - e_a) \tag{2}$$

with f the "wind speed function" dependent on wind speed, and e_s and e_a the saturated and ambient water vapor pressures respectively. From a knowledge of these fluxes and the short wave (q_{sw}), long wave (q_{lw}); and back radiation (q_{br}) energy fluxes, both K' and T_e can be calculated respectively [4]

$$K' = 1.30 + f(b + .142)\frac{cal}{m^2\ s\ ^oC} \tag{3}$$

$$T_e = \frac{(q_{sw} + q_{lw}) + f(bT_d + .142T_a) - 73.3}{K'}\ (^oC) \tag{4}$$

In these expressions, q has the units of $cal/m^2/s$, T_d and T_a the dew point and dry bulb temperatures are in ^oC and b is given by

$$b = \frac{134,000}{(T^*)^2}\ Exp\ (17.62 - \frac{5300}{T^*})\ \frac{mmHg}{^oC} \tag{5}$$

where

$$T^* = \frac{T_s + T_d}{2} + 273\ (^oK) \tag{6}$$

Thus the surface energy flux q_s, depends on the wind speed function through Eqs. (3) and (4). As a result, different wind speed functions as well as different wind speeds will alter calculated values of K' and T_e and ultimately predictions of lake temperature and evaporation.

To demonstrate the variability in f's proposed by a number of researchers, Table I gives a summary of 14 functions. All are of the form

$$f = a_o + a_1W + a_2W^2\ \frac{Cal}{m^2\ s\ mmHg} \tag{7}$$

with the coefficients a_o, a_1, and a_2 given in Table I. Three of these expressions (nos. 3,4, and 14) were used in the analysis presented below. They were selected as representative of the widely different forms in use and certainly different f's will yield somewhat different results. However, it is felt that the three functions used are adequate to demonstrate the effect of errors in wind speed since they vary nearly encompass the maximum and minimum values of f for all wind speed used.

ANALYSIS

Water Temperatures:

The analytical model used here for water temperature prediction has been presented in earlier papers [1, 2] and verified with the field data

from Cayuga Lake, New York [1], and Lake Belews, N.C. [3]. The analysis used in developing the model will be briefly outlined; the basic equations are

$$\rho C_p \frac{\partial T}{\partial t} = -\frac{\partial}{\partial Z}(q + q_r) \quad \text{in } 0 \leq Z \leq H \tag{8}$$

$$T = T_s(t) \quad \text{in } 0 \leq Z \leq h(t) \tag{9}$$

$$T = T(Z,t) \quad \text{in } h(t) \leq Z \leq H \tag{10}$$

Here T and T_s are the water body and surface temperatures respectively, t is time, Z the vertical coordinate meadured downward from the surface, and q and q_r the turbulent and radiative heat fluxes respectively. Also ρ is the density, C_p the specific heat, h the thermocline depth and H the total depth of the water body. A dimensionless temperature Θ, and coordinate η are defined as

$$\Theta(\eta) = \frac{T_s - T}{T_s - T_H}, \quad \text{in } h(t) \leq Z \leq H \tag{11}$$

$$\eta = \frac{Z - h}{H - h}, \quad \text{in } h(t) \leq Z \leq H \tag{12}$$

The radiative heat flux, q_r was treated by solving the equation of radiative transfer over the entire depth of the body of water for a plane parallel, absorbing, emitting, isotropically scattering gray medium with azimuthal symmetry. Appropriate radiation boundary conditions were established and the Marshak boundary condition approximation was applied. Zeroth* and first** moments of the energy equation were taken. As a result, two coupled, first order, non-linear ordinary differential equations were obtained and a computer program, based on the Runge Kutta method was developed to solve them for the determination of T_s and h and hence T.

Among the input data required to run the program, are values for the equilibrium temperature T_e, and the surface heat exchange coefficient K' which are obtained with the use of equations 3 and 4. Examination of the resulting values indicated that the annual variation of T_e and k' could be represented well by sinusoidal relations as reported by Sundaram et al [12, 13] for any lake. These are

$$T_e = \bar{T}_e + \Delta T_e \sin(\Omega t + \phi_1) \tag{13}$$

$$K' = \bar{K}' + \Delta K' \sin(\Omega t + \phi_2) \tag{14}$$

where $\bar{T}_e$ and $\bar{K}'$ are average values, ΔT_e and $\Delta K'$ are half the annual variation, $\Omega = 2\pi/365$, t is the time in days and ϕ_1 and ϕ_2 are phase angles dependent upon conditions from which the computations begin.

*Integrate equation (8) from Z = 0 to Z = H.

**Multiply equation (8) by Z and then integrate from Z = 0 to Z = H.

The surface temperatures predicted by the model along with T_e and K' are then used in the calculation of evaporative heat flux q_e.

Evaporative Heat Flux:

Applying an energy balance to a body of water leads to [3]

$$q_e = \frac{1}{1 + B} (q_{sw} + q_{lw} - q_{br} - q_s) \tag{15}$$

where B, the Bowen ratio is given as [4]

$$B = \frac{0.142}{b} \frac{T_s - T_a}{T_s - T_d} \tag{16}$$

Also

$$q_{sw} = \text{specified from meteorological data (or calculated)} \tag{17}$$

$$q_{br} = 73 + 1.30\ T_s(^{\circ}C) \tag{18}$$

$$q_{lw} = 1.24 \times 10^{-13}(Ta + 273)^6(1 + 0.172C^2) \tag{19}$$

where C is the cloud cover in tenths, q has the units of $cal/m^2/s$, and all temperatures are in $^{\circ}C$.

It has been established [3] that the calculation of q_s is insensitive to choice of f so long as the proper wind speed is used. As a result, surface temperatures (and thus q_{br} and q_s) are predicted with confidence, thus allowing an accurate prediction of evaporation which also is relatively insensitive to choice of wind speed function. However, the present study examines only the effect of wind speed errors with respect to choice of the wind speed function selected.

Wind Speeds and Wind Speed Functions:

As mentioned above, three f's were selected for testing the effect of wind speed errors on lake surface temperature and evaporation predictions. Field data computed from monthly average meteorology at Greensboro, N.C. for the period 1949-1970 were used as correct input. The calculation procedure was as follows:

a) Each wind speed function was used to determine monthly average values for equilibrium temperature, T_e, and heat exchange coefficient K'. Values of $\overline{T}_e$, ΔT_e, ϕ_1, $\overline{K}'$, $\Delta K'$ and ϕ_2 were then determined so that T_e and K' were expressed in the sinusoidal forms of equations (13) and (14).

b) T_e and K' were then used, along with other field data, as input to the analytical model to compute water temperatures and evaporative heat flux. This procedure was carried out using a range of wind speeds. The purpose of this study was to evaluate the sensitivity of various wind speed functions to errors in wind speed as reflected in evaporation calculations. Thus since the monthly average wind speeds for Greensboro vary little ($\pm$ 20% maximum) through the year, the annual

average values of wind speed were used in calculation of evaporation. This provides the most straightforward means of evaluating wind speed function sensitivity.

RESULTS

Field data that correspond to Greensboro, N.C. were used as input parameters for the analytical model in the form

$$T_a = 14.50 + 10.69 \sin(\frac{2\pi}{365} t - 1.141), \ ^{o}C$$

$$T_d = 8.19 + 10.56 \sin(\frac{2\pi}{365} t - 0.683), \ ^{o}C$$

The incident solar radiation was expressed by the relationship

$$I = 3645.73 + 205.86 \sin(\frac{2\pi}{365} t - 0.683), \ kCal/m^2/day$$

The semi-empirical relation between the shear stress τ_s, at the surface, and the wind speed given by Munk and Anderson [7] was used to evaluate the friction velocity w^*, and the minimum temperature during spring homothermy was assumed to be 5.83 ^{o}C as obtained from measurements on lakes in the Greensboro, N.C. vicinity. The absorption and scattering coefficients for water and the particles in suspension were assumed to be 1.017 m^{-1} and 2.06 m^{-1} respectively, and the depth of the lake was taken as 30.48 m.

Calculated surface temperatures for several wind speeds are given in Table II for the three wind speed functions studied. For the present sensitivity analysis, the annual average wind speed of 3.44 m/s is the proper value and changes in temperature from those at this speed will be examined. As would be expected, predicted surface temperatures are somewhat higher (1-5^{o}C) if an error in wind speed reduces the value used. For positive errors (higher speeds) the reverse is true and temperatures are under predicted (1-3^{o}C) for May-September. However, temperatures are overpredicted for the remaining months (October-April). Examination of Table II indicates that the additive forms tested in the model ($f = a_o + a_1 W$, $f = a_o + a_2 W^2$) generally give better results than the form $F = a_1 W$.

Annual evaporation (in m) predictions are shown in Fig. 1, again for the three wind speed functions tested. It is here that the difference in function type is most apparent. All the f's give similar values at the correct wind speed of 3.44 m/s. These results of about 1.18 m/yr agree well with annual evaporation measurements of 1.02 m/yr [8] and 0.96 m/yr [9] given for the Greensboro vicinity. This agreement indicates that the use of yearly average wind speed values as opposed to daily or monthly values is not extremely critical. As the wind speed is changed, predictions for the $f = a_1 W$ type vary much more rapidly than for the additive forms. In fact a $\pm$ 30% variation in W produces only a $\pm$ 5% change in evaporation predictions using the additive type functions. However the same changes in W give a 15% change in evaporation prediction using the $f = a_1 W$ form. Even in the worst case however, the percent change in predicted evaporation is much less than the percent change in wind speed.

It is a straightforward matter to compare the evaporation changes using the model described above with the changes which occur if Eq 2 is used directly to compute evaporations with erroneous wind speed data. For the simple $f = a_1 W$ form of the wind speed function, evaporation is directly proportional to wind speed so that a $\pm$ 30% error in wind speed translates directly into a $\pm$ 30% error. The additive forms give approximately a $\pm$ 20% evaporation change for the same error in wind speed. When this is compared with a 5% change using the analysis above, the advantage of the model becomes quite clear.

SUMMARY

The results of this study may be summarized very simply; for the two types of wind speed functions tested, the additive form is generally least sensitive to errors in wind speed input data. In other words, if non-site specific wind data is used in predictions of lake temperature and evaporation, it is expected that the results would be more accurate if an additive type wind speed function was employed rather than the simple $f = a_1 W$ type. It is particularly important for evaporation predictions to use the additive form in combination with an analytical model such as the one described above. The degree of sensitivity to wind speed errors is important since meteorological data is not routinely acquired on most lakes.

TABLE I
SUMMARY OF SELECTED WIND SPEED FUNCTIONS*
OF THE FORM $f=a_o+a_1w+a_2w^2$ Cal/s/m^2/mmHg

f No.	a_o	a_1	a_2	ref
1	2.20 - 3.45	.49 - .77	-	4
2	-	.84	-	10
3	2.20	-	.11	11
4	-	.91	-	4
5	-	1.26	-	5
6	-	.91	-	4
7	1.22	.77	-	4
8	2.10	.77	-	4
9	1.91	.56	-	4
10	1.91	.91	-	4
11	2.35	-	.16	5
12	1.47	.70	-	5
13	$.62\Delta T_v^{1/3}$	.91	-	4
14	$.78\Delta e^{1/3}$	$48.4/Re_L^{.2}$	-	6

*Wind speed w is in m/s measured at a height of 8m

$e = e_s - e_a$

T_v = virtual temperature ^oC

Re_L = Air Reynolds number based on fetch length L and the free stream velocity

TABLE II

SURFACE TEMPERATURE PREDICTION RESULTS (^{o}C)

FOR SEVERAL WIND SPEEDS

	W = 2.24 m/s			W = 3.44 m/s			W = 4.47 m/s		
f no.	3	4	14	3	4	14	3	4	14
Month									
J	8.2	8.8	8.2	7.4	7.5	7.7	6.4	6.4	10.0
F	6.8	7.5	7.0	5.8	5.9	6.2	11.7	11.7	9.9
M	7.0	7.6	7.2	6.8	7.1	6.4	11.0	11.0	13.4
A	11.7	11.7	11.7	11.4	11.4	11.4	11.0	11.0	14.2
M	23.0	24.3	22.7	18.9	19.0	19.2	16.3	16.3	24.0
J	27.3	29.2	27.2	24.7	24.9	24.7	22.0	22.0	24.3
J	29.3	30.7	28.5	26.7	26.8	26.6	24.7	24.7	21.9
A	27.7	28.7	26.6	25.6	25.7	25.3	24.3	24.3	17.9
S	23.5	24.4	22.6	22.1	22.2	21.8	21.4	21.4	13.9
O	18.5	19.3	17.8	17.7	17.7	17.5	17.3	17.3	10.5
N	13.9	14.6	13.4	13.3	13.4	13.2	13.3	13.3	7.5
D	10.4	11.1	10.3	10.0	10.1	10.2	9.6	9.6	13.5

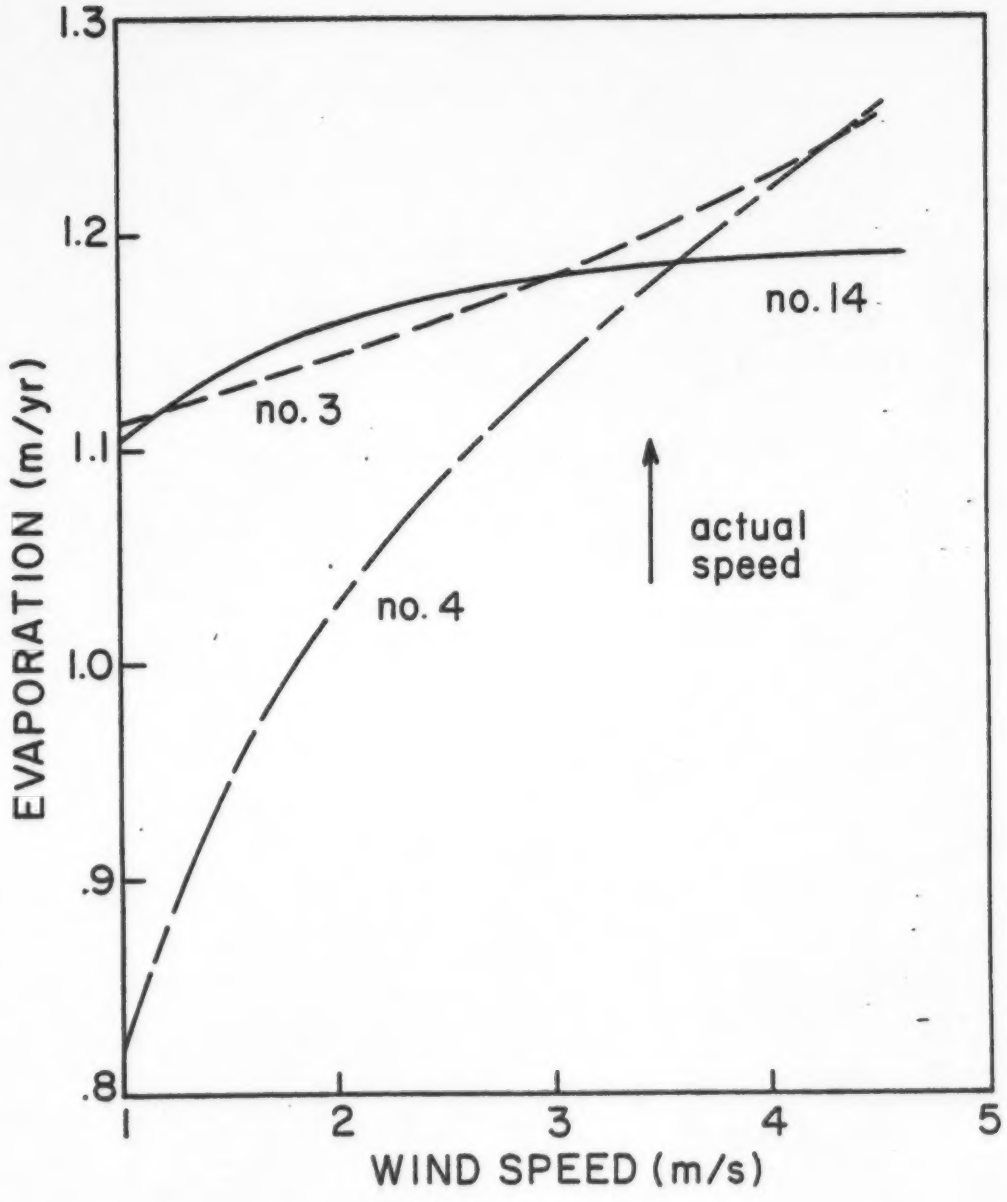

Fig. 1 Effect of errors in wind speed on annual evaporation predictions for three types of wind speed functions (nos. 3, 4, 14 Table I).

REFERENCES

1. A. M. Mitry and M. N. Ozisik, One-Dimensional MOdel for Seasonal Variation of Temperature Distribution in Stratified Lakes, International Journal of Heat and Mass Transfer, Vol. 19, pp. 201-205, 1976.

2. A. M. Mitry and M. N. Ozisik, A Two-Dimensional Time Dependent Model for Seasonal Variation of Temperature Distribution in Stratified Lakes, Letter in Heat and Mass Transfer, Vol. 3, pp. 475-484, 1976.

3. A. M. Mitry and B. L. Sill, A Model for Prediction of Evaporative Heat Flux in Large Bodies of Water, Proceedings, Second Conference on Waste Heat Management and Utilization, Univ. Miami, December, 1978.

4. P. J. Ryan and D. R. F. Harleman, Analytical and Experimental Study of Transient Cooling Pond Behavior, Ralph M. Parsons Laboratory, Dept. of Civil Engineering, Report No. 161, Massachusetts Institute of Technology, Cambridge, Mass., Jan. 1973.

5. J. E. Edinger, D. K. Brady and J. C. Geyer, Heat Exchange and Transport in the Environment, Report No. 14, Electric Power Research Institute Research Project RP-49, Johns Hopkins University, Baltimore, Maryland, Nov. 1974.

6. J. S. Goodling, B. L. Sill and W. J. McCabe, An Evaporation Equation for an Open Body of Water Exposed to the Atmosphere, Water Resources Bulletin, Vol. 12, No. 4, Aug. 1976.

7. W. H. Munk and E. R. Anderson, Notes on the Theory of Thermoclines, Journal of Marine Research, Vol. 7, pp. 276-295, 1948.

8. J. J. Geraghty, D. W. Miller, F. Van der Leeden and F. L. Troise, Water Atlas of the United States, Water Information Center Publication, Port Washington, NY, 1973.

9. W. L. Younts, G. L. Giese, and E. F. Hubbard, Evaporation From Lake Michie, North Carolina, 1961-1971, U.S. Geological Survey Water-Resource Investigation, pp. 38-73, 1973.

10. Water-Loss Investigations: Lake Hefner Studies, Technical Report, U.S. Geological Survey Professional Paper 269, U.S. Government Printing Office, 1954.

11. D. K. Brady, W. L. Graves, Jr., and J. C. Geyer, Surface Heat Exchange at Power Plant Cooling Lakes, Edison Electric Institute Research Project RP-49, Report No. 5, The Johns Hopkins University, Baltimore, Maryland, Nov. 1969.

12. T. R. Sundaram and R. G. Rehm, Formation and Maintenance Of Thermoclines In Stratified Lakes Including The Effect Of Plant Thermal Discharges, AIAA Paper, No. 70-238, 1970.

13. T. R. Sundaram and R. G. Rehm, The Effects Of Thermal Discharges On The Stratification Cycle Of Lakes, AIAA Paper No. 71-16, 1971.

PB82-228362

COOLING POND PERFORMANCE AND RIVER IMPACT DUE TO CYCLIC DAILY POWER GENERATION

Y. J. Tsai and W. Yow
Stone & Webster Engineering Corporation,
Boston, Massachusetts

ABSTRACT

Hydrothermal analysis for the heated effluents of the Tracy Plant of Sierra Pacific Power Company was performed to evaluate the cooling pond performance and predict the temperature distributions in the Tracy cooling pond and the Truckee River. Because of the distinct flow characteristics in both the cooling pond and the river, two different temperature prediction models, each characterizing its own distinctive features, have been used in the study. The predictions in the cooling pond were carried out by a transient two-dimensional hydrothermal model, while the temperature distributions in the river were predicted by use of a two-dimensional steady state dispersion model. Prior to the analysis, a field survey was conducted to determine the existing thermal patterns in the river and to supply information for the evaluation of the rate of intake heat recirculation. The field survey results were used to calibrate and verify mathematical models developed for prediction of the temperature distributions in the river and the cooling pond under maximum plant operating conditions.

1. INTRODUCTION

The Tracy Plant of Sierra Pacific Power Company consists of three oil-burning power generation units with capacity in MW of each unit being 53, 83 and 110, respectively. This paper presents hydrothermal analyses performed for the condenser cooling water system which existed prior to July 1977. Since that time, a complete closed-loop cooling system has been employed without any water being discharged from the plant into the Truckee River [1].

The condenser cooling water supplies for Units 1 and 2 were taken from the Truckee River at the plant site. Unit 1 had a once-through cooling system. The heated water from Unit 1 condenser system was discharged back to the river at about 200 ft downstream of the intake area. Unit 2 used a cooling pond for supplemental cooling. The heated effluents from Unit 2 were released to the pond, where a great portion of the heat load was dissipated to the atmosphere by surface heat transfer. The remaining heat loads in the pond were then released to the Truckee River. Unit 3 utilized a cooling tower as a cooling device which formed a closed-loop cooling system.

The Tracy cooling pond is a man-made shallow pond with a surface area of approximately 30 acres for heat dissipation to the atmosphere. From April through December of each year, the pond was regulated in such a way

that the outlet gate was closed when Unit 2 was in operation; the gate was opened to release water to the river only when the unit was not in operation. This type of ponding arrangement allowed more heat to be dissipated from the pond surface. Furthermore, the staggered schedule of pond release and plant operation would eliminate any heat recirculation through the intake to the condenser system. This paper discusses the analysis of the hydrothermal characteristics in the cooling pond due to the heated effluents from Unit 2 and the impact of cooling pond thermal discharge on the river for the operating conditions prevailed prior to July 1977.

Because of the distinct flow characteristics exhibited in both the cooling pond and the river, two different temperature prediction models, each characterizing its own distinctive features, have been used in this study. The predictions in the cooling pond are carried out by a transient two-dimensional hydrothermal model; the temperature distributions in the river are predicted by use of a two-dimensional steady state dispersion model.

2. COOLING POND TEMPERATURE PREDICTION

Operational experiences of the Tracy cooling pond show that the water temperature in the pond is vertically mixed with temperature decay in the general direction of flow. No thermal stratification has been observed mainly due to the shallowness of the pond. The average pond depth is 7 ft and the lateral dimension of the pond normal to the flow path is about 500 ft. This physical configuration is ideal for the application of a vertically integrated two-dimensional mathematical model. A transient model with finite difference approach was adopted for cooling pond temperature simulation.

2.1 Mathematical Model

The basic partial differential equations that describe the transient phenomena in a two-dimensional model consist of the equations of continuity, momentum, and heat flow. These equations are shown in a Cartesian coordinate system with x- and y- directions on the horizontal plane as follows:

$$\frac{\partial \eta}{\partial t} + \frac{\partial}{\partial x}\left[u(h+\eta)\right] + \frac{\partial}{\partial y}\left[v(h+\eta)\right] - S = 0 \qquad (1)$$

$$\frac{\partial u}{\partial t} + u\frac{\partial u}{\partial x} + v\frac{\partial u}{\partial y} = -g\frac{\partial \eta}{\partial x} - \frac{1}{\rho}\frac{\partial P_a}{\partial x} + fv + \frac{\tau_{w,x} - \tau_{b,x}}{\rho(h+\eta)} \qquad (2)$$

$$\frac{\partial v}{\partial t} + u\frac{\partial v}{\partial x} + v\frac{\partial v}{\partial y} = -g\frac{\partial \eta}{\partial y} - \frac{1}{\rho}\frac{\partial P_a}{\partial y} - fu + \frac{\tau_{w,y} - \tau_{b,y}}{\rho(h+\eta)} \qquad (3)$$

$$\frac{\partial}{\partial t}(h\Delta T) + \frac{\partial}{\partial x}(uh\Delta T) + \frac{\partial}{\partial y}(vh\Delta T) = \frac{\partial}{\partial x}\left(h K_x \frac{\partial \Delta T}{\partial x}\right) + \frac{\partial}{\partial y}\left(h K_y \frac{\partial \Delta T}{\partial y}\right) + \frac{W}{\rho C_p} - \frac{K\Delta T}{\rho C_p} \qquad (4)$$

Where η is the wave height and h is the mean depth; u and v are velocity components in the x- and y- directions, respectively; S is a source or sink; g is the gravitational constant; Pa is the atmospheric pressure; f is the Coriolis parameter; Γw and Γb are shear stresses at the water surface and at the bottom, respectively; Kx and Ky are the diffusivities in the x- and y- directions, respectively; K is the surface heat exchange coefficient; Cp is the specific heat of water, W is the heat source or sink per unit area; and t is time.

Equations 1 through 3 constitute a hydrodynamic model which may be solved simultaneously for the three unknowns, u, v, and η by use of appropriate boundary conditions. The instantaneous flow patterns and the water level fluctuation as obtained from the hydrodynamic model are then used in conjunction with Equation 4 to predict temperature rise from known heat sources. This latter stage of analysis is also called the thermal model.

Appropriate boundary conditions are required for solutions in both the hydrodynamic and the thermal models. Since land boundary is the only type of boundary existing in a cooling pond, the boundary condition in the hydrodynamic model specifies that the velocity component normal to the land boundary be zero. The boundary condition in the thermal model requires that heat flux across the boundary be zero. The condenser discharge and the pond outlet discharge are the source and sink which have already been included in the basic equations.

The basic equations, 1 through 4, must be placed in finite difference forms before they can be used for a problem solution. The Alternate Direction Implicit Method has been successfully used to obtain the numerical solution for the hydrodynamic model [2,3]. The finite difference equations are presented in a space-staggered grid system and the numerical computations are carried out at a double time-step operation. In the first operation, the values of the dependent variables η, u, and v are obtained by a scheme which is implicit in η and u and explicit in v. Then, in the second operation, the values of the unknowns are obtained by a scheme which is implicit in η and v and explicit in u. This multi-operational method used in the solution of the finite difference equations offers an advantage of guaranteed stability in numerical solution. Once the solution to the hydrodynamic model has been obtained, the thermal model as shown in Equation 4 can also be solved in a similar manner by using the space-staggered alternate direction implicit finite difference scheme. The detailed procedures to obtain solutions for both the hydrodynamic and thermal models have been discussed in Reference 3.

In utilizing the mathematical models, a collection of square cells with average water depth is used to represent the cooling pond. A grid system of 16 by 23 covering the entire area of the pond is used. The size of the cell is 75 ft and is determined by the required accuracy of the results and the cost of computer time. The model boundary of the pond is chosen to closely approximate the prototype geometry including the center dividing dike. The grid's layout of the cooling pond is shown as the base map for Figure 5.

2.2 Measurements and Model Prediction

Field survey case. A field survey was conducted to measure the water temperatures in the cooling pond outlet and in the Truckee River [4]. The observed water temperature at the cooling pond outlet was 6°F higher than the ambient water temperature, which is the river water temperature upstream of the discharge outlet without the influence of the plant heat discharge.

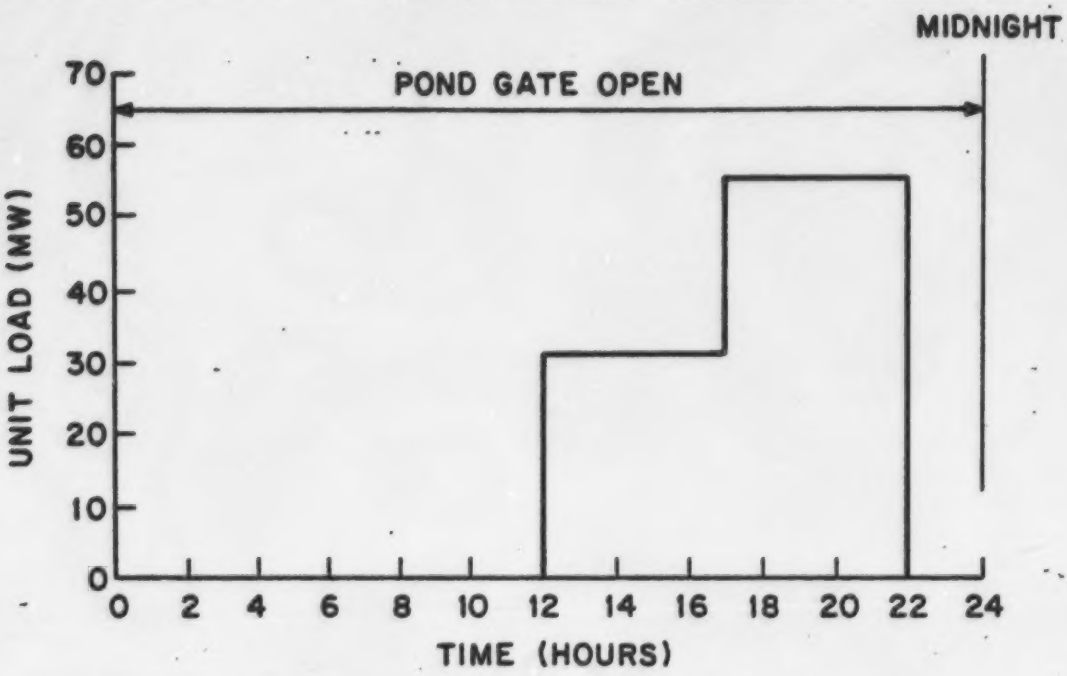

Fig. 1 Daily Load Pattern of Unit 2, Field Survey Case

Prior to and during the survey period, Unit 2 was operating on a daily cycle represented by the pattern shown in Figure 1. When the unit load was low in the beginning of the daily operation, only one circulating water pump was used, but both pumps were used when the unit load was increased. The condenser flow rates for one- and two-pump operation were 42 and 72 cfs, respectively. The recorded condenser outlet temperatures were 20°F higher than the ambient temperature for both operating conditions. The cooling pond outlet gate was wide open during the survey period. Based on the recorded meteorological data during the survey, the surface heat exchange coefficient was determined to be 120 Btu/°F-day-ft^2.

The model was solved in two separate steps. In the first step, the hydrodynamic model was run to obtain the flow patterns and the water level fluctuation in the pond. The data were stored in a computer disk ready to be used for the thermal model. In the second step, the thermal model was run to obtain the temperature pattern throughout the whole pond. Zero temperature rise was specified as the model initial condition. The temperature gradually built up to a level which was governed by the surface heat exchange and the boundary conditions. The results of the simulation for a few daily cycles are shown in Figure 2. In this figure, the upper plot shows both the condenser flow rate and predicted cooling pond outlet flow rate in cfs versus time in hours. The lower plot presents the predicted cooling pond outlet temperature rise in °F versus time in hours. It can be seen that the cooling pond discharge temperature rise reaches 6°F, which matches the measured values in the survey.

Maximum daily load operation. The Tracy cooling pond was operated in a ponding mode in all months of the year except January, February, and March. In this arangement, the pond outlet gate was closed between 10:00 in the morning and 12:00 midnight when Unit 2 was running, as shown in Figure 3. The gate opened after midnight when the unit was shutdown. This mode of pond operation would allow condenser heat effluents to be detained longer in the pond, and consequently, permit more heat to be dissipated to the atmosphere.

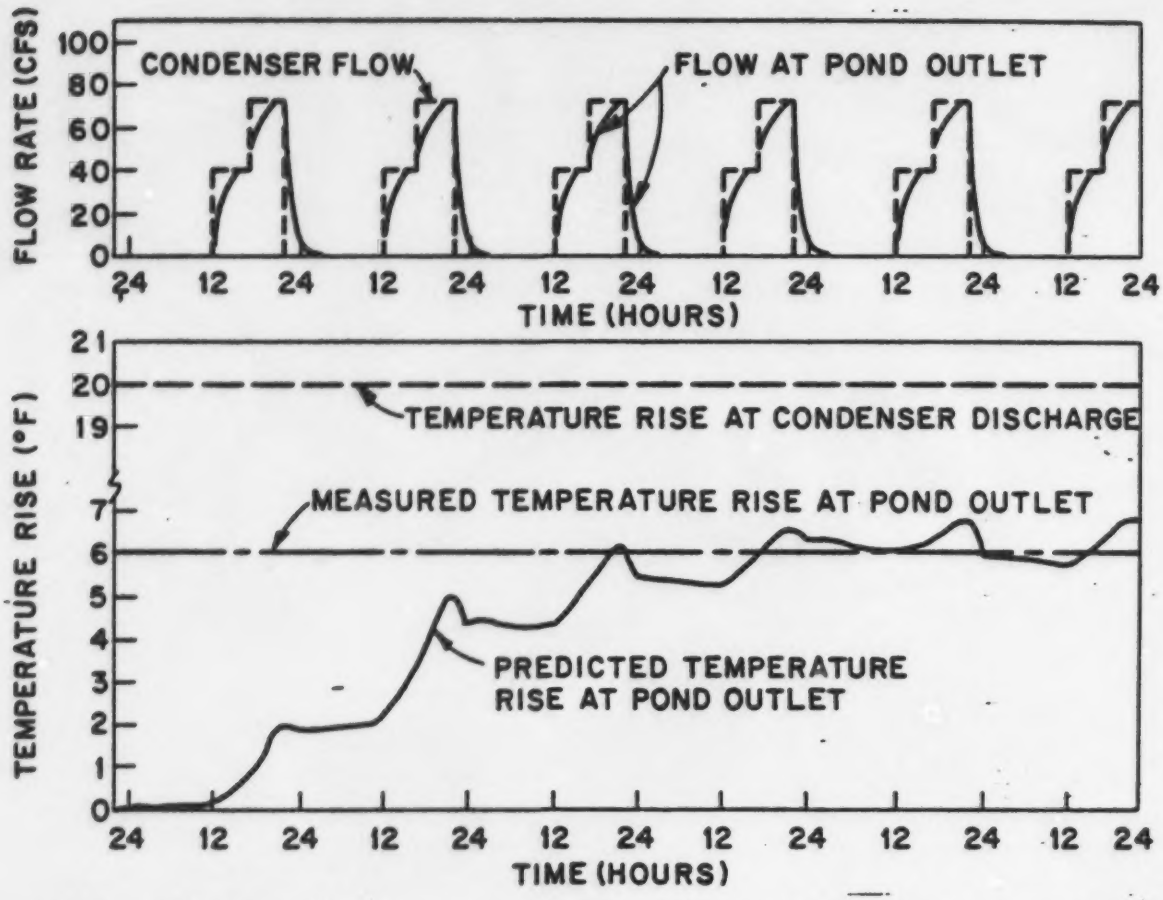

Fig. 2 Flow Rate and Temperature Rise in Cooling Pond, Field Survey Case

The maximum generation load pattern of Unit 2 is shown in Figure 3. The circulating water pumps deliver 42 cfs during lower plant output and 72 cfs during higher plant output, resulting in a net condenser temperature rise of approximately 29°F for both operating conditions. The surface heat exchange coefficient and eddy diffusivity in the cooling pond during summer are 160 Btu/°F-day-ft^2 and 0.108 ft^2/sec, respectively.

By using the two-dimensional hydrothermal model described previously, the predicted temperature rises at the cooling pond discharge are shown in Figure 4. The condenser discharge and the cooling pond outlet flow rate as determined in the hydrothermal model are also shown in Figure 4. The typical isotherm configurations throughout the cooling pond are shown in Figure 5, which represents the conditions at 9:00 pm when the plant was operating at the maximum generating capacity with the gate closed.

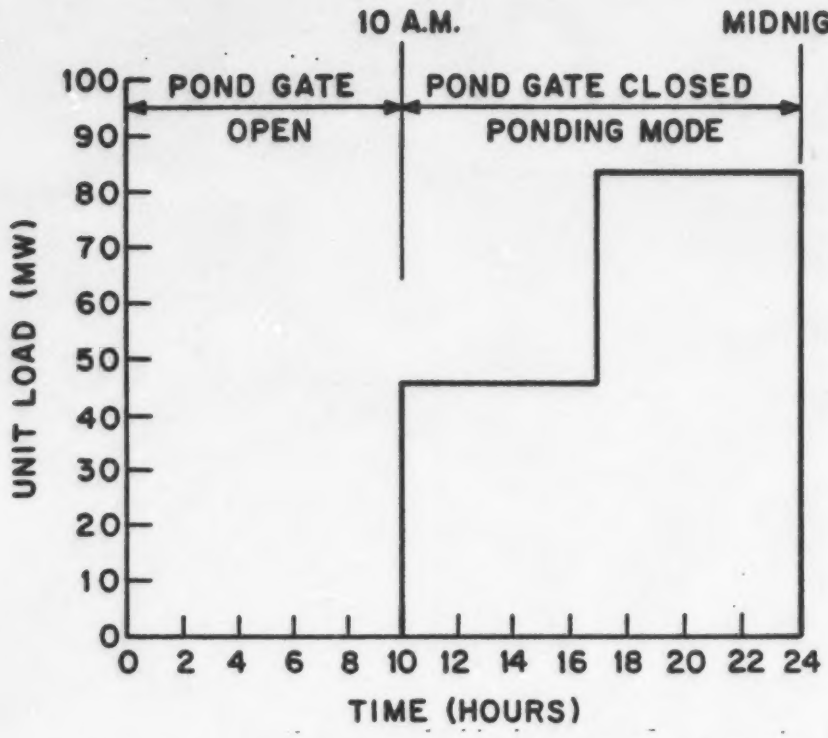

Fig. 3 Maximum Daily Load Pattern of Unit 2

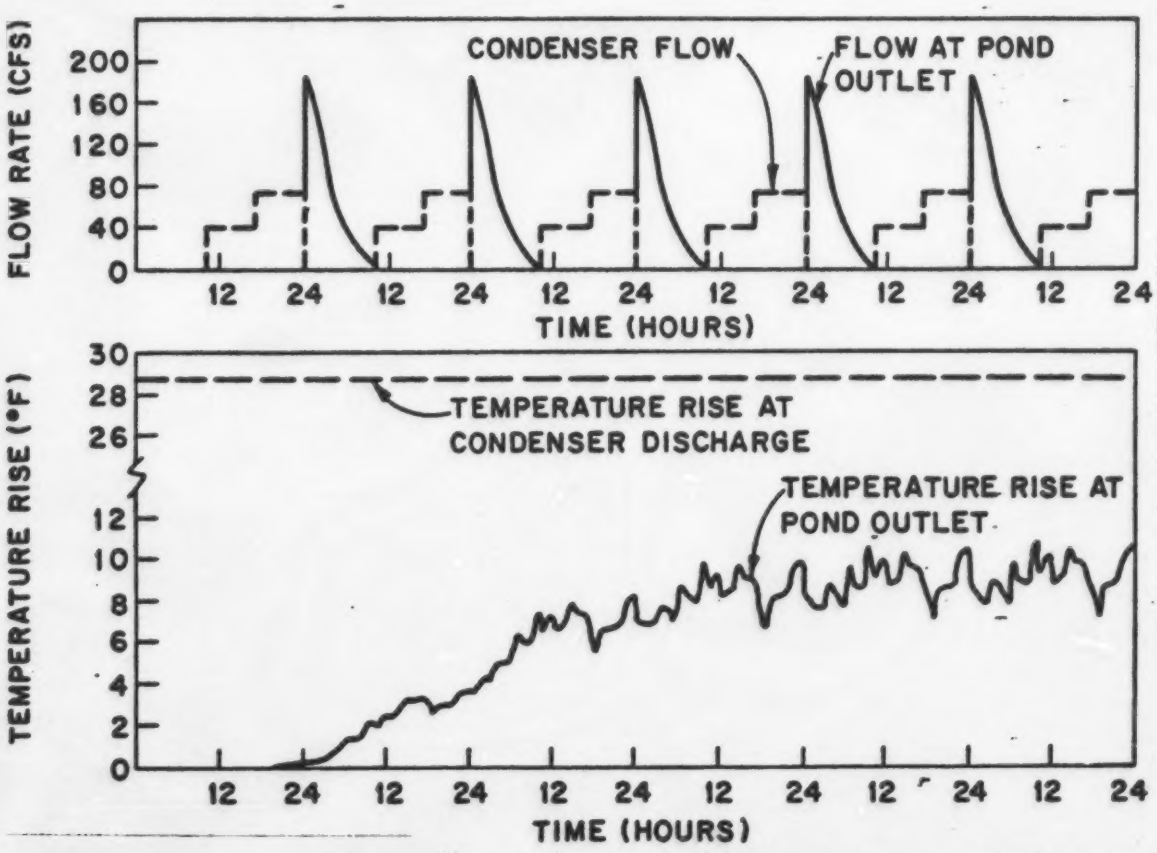

Fig. 4 Flow Rate and Temperature Rise in Cooling Pond, Maximum Daily Load Operation

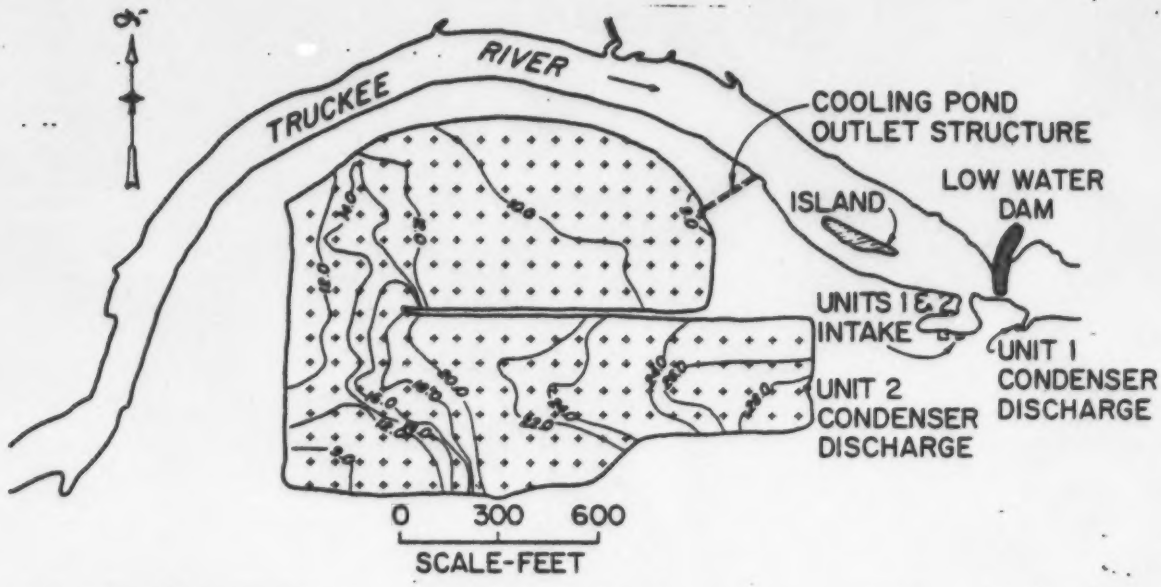

Fig. 5 Isothermal Map of Cooling Pond at 9 pm, Maximum Daily Load Operation, Temperature Rise in °F

3. RIVER TEMPERATURE PREDICTION

The width of the Truckee River reach along the Tracy Plant area is approximately 150 ft with an average water depth of 5 ft at normal river flow. Because of the turbulence and shallowness of the river, the heated effluents discharged from the outlets would mix vertically without thermal stratification. The heated cooling water would mix with the river flow and attach to the shoreline with fairly steep lateral temperature gradient. The highest temperature was observed along the shoreline with temperature decay normal to the flow toward the opposite shore. At a further downstream distance, the cooling water eventually would mix fully with the river flow across the river section. A steady state, vertically averaged, two-dimensional model with analytical solution was adopted for this river temperature simulation purpose.

3.1 Mathematical Model

The basic partial differential equation that describes the heat dispersion phenomena in a steady uniform current is:

$$\frac{\partial}{\partial y}\left(-K_y \frac{\partial \Delta T}{\partial y}\right) + u \frac{\partial \Delta T}{\partial x} + K\Delta T = 0 \qquad (5)$$

in which ΔT is the temperature rise; u is the velocity along the x- direction; K_y is the lateral diffusivity; and K is the surface heat exchange coefficient. Although Equation 5 applies to a uni-directional flow field, the temperature gradients extend both the x- and y- directions in the horizontal plane. The equation is basically a heat conservation equation with the assumption that longitudinal dispersion is negligible. This assumption is justified by the fact that the dispersion of heat in the x-direction is very small compared with the advection of heat in the same direction.

Boundary conditions are required in order to obtain a solution for Equation 5. One of the boundary conditions is the source condition which is specified by a rectangular plane source with a thickness extending to the depth of the river and a breadth, b, in the y- direction. This rectangular source is placed in the vertical plane at $x = 0$. In a river model, a boundary condition specifying that no heat flux takes place across the river banks is also required.

For a river of width w, the dispersion in the lateral direction is usually bounded by the banks. Using the method of image, one obtains the solution to Equation 5 applied to a finite domain being bounded in the lateral direction as follows [5]:

$$\Delta T = \frac{1}{2}\,\Delta T_o \exp(-Kx/u) \sum \left\{ \operatorname{erf}\left[\frac{-(2nw + y_e - y) + b/2}{2} \sqrt{\frac{u}{K_y X}} \right] - \operatorname{erf}\left[\frac{-(2nw + y_e - y) - b/2}{2} \sqrt{\frac{u}{K_y X}} \right] + \operatorname{erf}\left[\frac{-(2nw - y_e - y) + b/2}{2} \sqrt{\frac{u}{K_y X}} \right] - \operatorname{erf}\left[\frac{-(2nw - y_e - y) - b/2}{2} \sqrt{\frac{u}{K_y X}} \right] \right\} \qquad (6)$$

where y_e is distance between the center of the plane source and the shoreline, ΔT_o is the initial temperature rise at the source plane.

Equation 6 was developed by several investigators [5,6] and has been applied successfully to the diffusion of sewage effluent in an ocean and heated water discharges in rivers.

3.2 Measurements and Model Prediction

Field survey case. The predictions of the temperatures in the Truckee River by using Equation 6 are compared with the measurements in the field surveys. The measured isotherms in the river developed by Unit 1 heat discharges are shown in Figure 6. Temperature rises are shown relative to the ambient water temperature. Temperature predictions based on Equation 6 are made to simulate the survey conditions. The measured temperature rise in the river at the vicinity of Unit 1 discharge was 18.5°F. The river velocity during the survey was 0.9 ft/sec. In the analysis, the heated discharge equivalent to a plane source 30 ft wide by 5 ft deep was placed at the exit of the Unit 1 discharge channel normal to the river current. This plane source was used to account for all the heat input from both the Unit 1 effluents and those released from the pond. A lateral diffusivity of 2 ft^2/sec was used in the model. The predicted isotherms are also shown in Figure 6. The measured and predicted temperature rises at the south bank of the river versus distance from the discharge channel are shown in Figure 7. It can be seen that the model prediction is in good agreement with the field measurement.

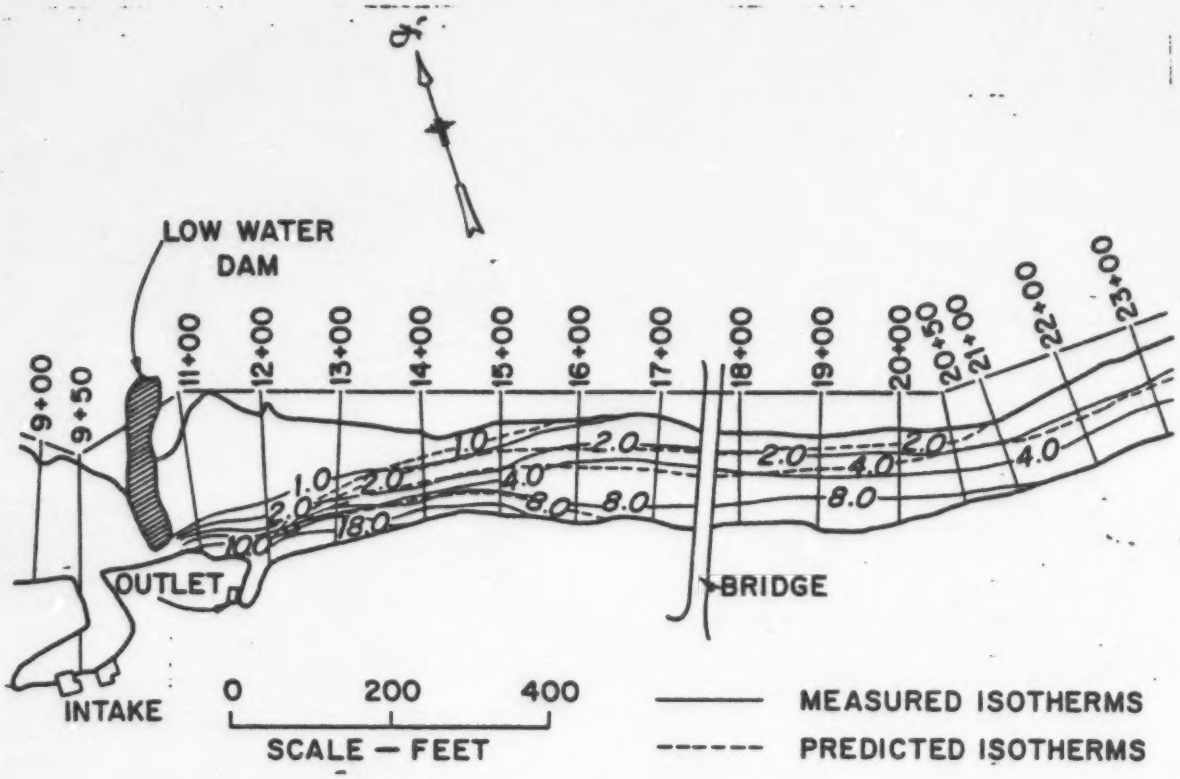

Fig. 6 Predicted and Measured Isotherms in Truckee River with Unit 1 Operating, Temperature Rise in °F

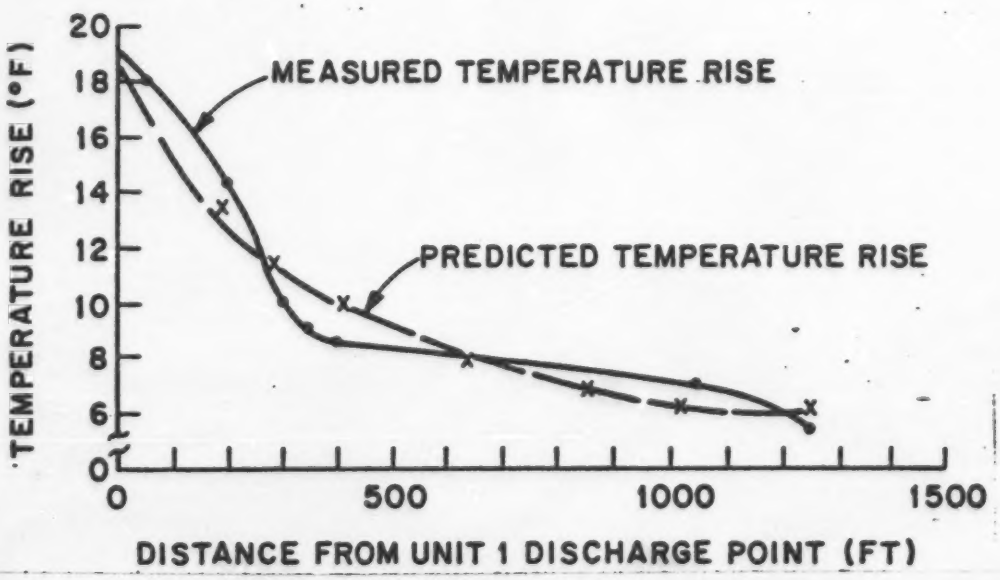

Fig. 7 Measured and Predicted Temperature Rises in the River along South Bank versus Distance

Maximum daily load operation. The mathemathical model described in Section 3.1 is used to predict the temperature rises in the Truckee River during the maximum capacity of plant operations in the summer for the cooling system existing prior to July 1977.

The analysis determines the isotherm pattern in the river when the cooling pond outlet gate was opened just shortly after midnight. According to the simulation from the cooling pond model, the discharge flow rate into the river at the time the gate was opened is 185 cfs. The temperature of the released water was 11°F above natural water temperature. This quantity of heat input to the river could be represented in the model by a 100-ft-wide by 6-ft-deep heat source at the outlet structure, placed in a direction normal to the river current. Based on a river flow of 400 cfs, the predicted temperature distributions in the Truckee River are shown in Figure 8. This temperature rise pattern exists only for a short time period and represents the worst possible impact on the river. It is assumed that Unit 1 was not operating when the cooling pond outlet gate was opened. Consequently, isotherms in the river were contributed solely by the heat discharges from the pond.

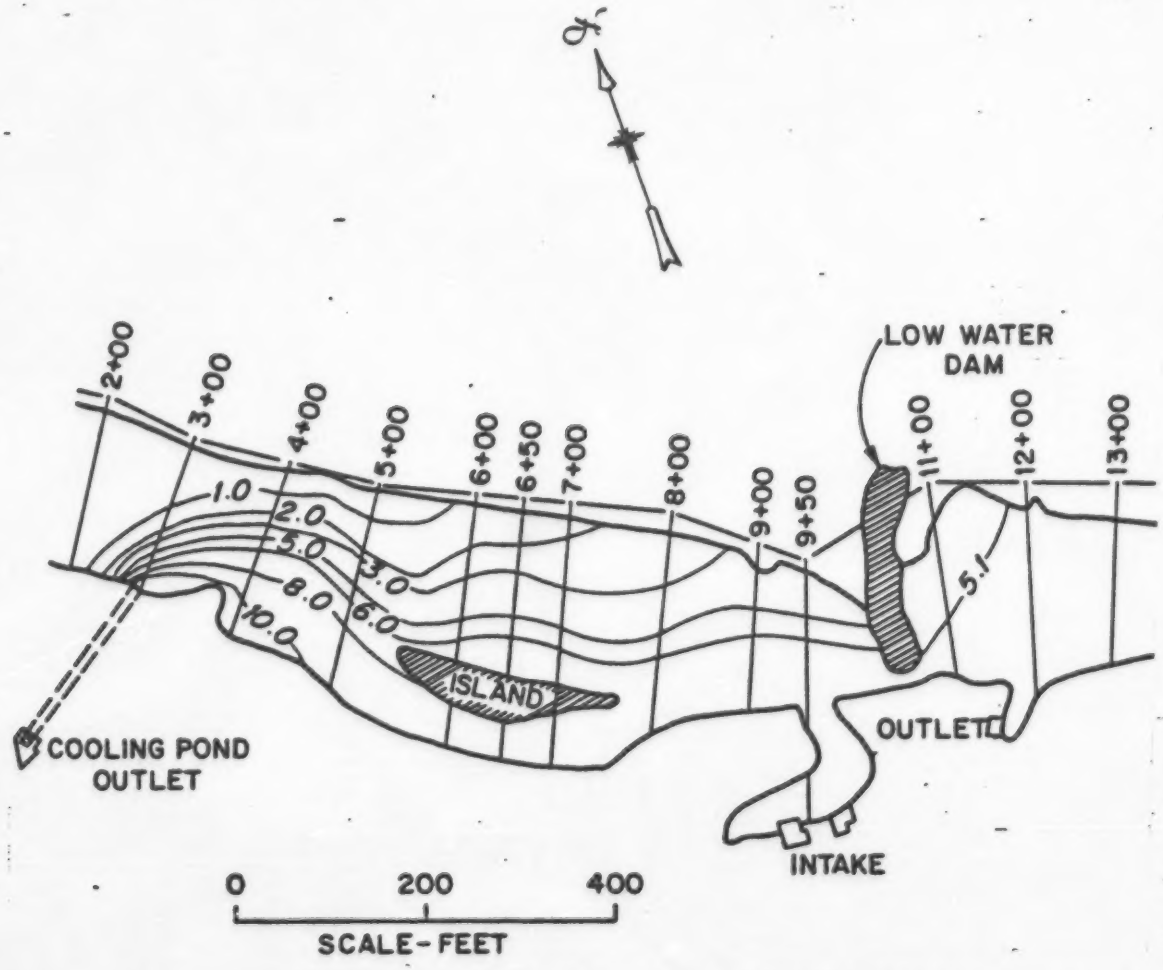

Fig. 8 Predicted Isotherms in Truckee River, Maximum Daily Load Operation, Temperature Rise in °F

4. CONCLUSIONS

A cooling pond with a surface area of approximately 30 acres was used to supplement the heat dissipation before being discharged into a river. This arrangement effectively reduced the thermal load on the river. The thermal performance of the cooling pond and thermal impact on the river due to transient heat load and cooling water flow were successfully analyzed by means of mathematical modeling. A two-dimensional transient hydrothermal model for the cooling pond and a two-dimensional steady state dispersion model for the river were calibrated and used in tandem to analyze the cooling pond performance and the thermal impact on the river. The model results compared very favorably with data obtained from the field measurements. These models were then used to determine the maximum impact conditions on the river for two different modes of pond operation: a continuous release in winter, and a ponding arrangement in the remainder of the year.

REFERENCES

1. Montgomery, W., An Innovative Solution to Environmental Regulations, PCEA Meeting, San Francisco, CA, March 13, 1980.

2. Leendertse, J. J., Aspect of a Computational Model for Long Period Water Wave Propagation, The Rand Corp. Report RM 5294-PR, 1967.

3. Tsai, Y. J. and Chang, Y. C., Two Dimensional Transient Hydrothermal Mathematical Model, Proc. First World Congress on Water Resources - Water for the Human Environment, Vol. IV, pp. 76-88, 1973.

4. Stone & Webster Engineering Corporation, Hydrothermal Analysis for Tracy Plant, Sierra Pacific Power Company, August 1975.

5. Harleman, D. R. F., Transport Processes in Water Quality Control, Civil Engineering Department, MIT, Cambridge, Massachusetts, 1970.

6. Brooks, N. H., Diffusion of Sewage Effluent in an Ocean Current, Proc. First International Conf. on Waste Disposal in the Marine Environment, Pergamon Press, pp. 246-267, 1960.

PB82-228370

HEAT REJECTION FROM COOLING WATER OF A THERMAL POWER PLANT BY RECIRCULATION IN WATER BODY

A.K. Agrawal and Dr.Manohar Prasad
Department of Mechanical Engineering
Indian Institute of Technology, Kanpur-208016(INDIA)

ABSTRACT

The experimental results show that there is feasibility of determination of heat-transfer to environment in terms of a single parameter, the pond number, which can be obtained in terms of inlet flow rate, temperature, intake position geometry of water body etc. Present experimental investigation provides that intake from the upper layer yields higher temperature compared to lower side intakes. Pond number is more in case of bottom intake as compared to top intake yielding less short circuiting between discharge and intake waters.

A lake has been simulated by a tank of capacity about 1,36,000 ml. This has been selected such that for hot water flow rate of 50 to 350 ml/min, it serves as a huge reservoir. Various discharge and intake positions are selected. From experimental study it has been found that hot water should be discharged at top and drawn out from an intake made at about half of the depth.

1. INTRODUCTION

Thermal efficiency of large or super power plants lie in the range of 38 to 45%. It implies, therefore that for 1 MW of power generation heat-equivalent to about 1.5 MW isrejected to the cooling water which, in turn, is either discharged into a huge natural water body such as a lake, a river, an ocean or recycled through a cooling tower. When water is discharged into one end of a reservoir, heat transfer is accomplished by heat and mass interaction between the free water surface and the surrounding air. The cool water is then supplied steadily to the condenser from another end. The relative distance between discharge and intake points governs the achievement of desired cool water temperature. The optimum distance between the two ends depends upon the economic survey, in that cost of canal construction, its maintenance expenditures and pumping cost together with plant efficiency variations due to cooling water temperature changes should be considered.

Cooling towers bring about small improvement in thermal efficiency as a result of lower condensing temperature. The economical gain accrued from the narginal improvement in the thermal efficiency is too small to neutrilize the additional installation, maintenance and operating costs. As a result cooling towers prove to be uneconomical, [1] and it is suggested to use it as a helper mode, in big or super power plants.

Tremendous amount of heat rejection to water bodies elevates their temperatures as well as of the ambient air, due to formation of a plume over the free surface. In cold countries increased temperature can be gainfully exploited for fisheries since maturity period of fish reduces considerably at higher temperatures (upto around 15 C). [2] . Growth of some fishes is also enhanced at around 15 C [3] . On the other hand hot countries are adversely affected by the heat disposal. The elevated temperature causes thermal pollution of water and atmosphere. The inhabitants put serious objections to it because of ecological imbalance, affected aquatic life etc.

The warm water from the power plant is either discharged at the surface of the water body or through submerged jets deep into it. The latter permits absorption of heat in the large volumes at the cost of low heat-dissipation to surrounding air [4] . So in large power plants warm water is generally discharged at the surface [5] .

Discharged water at the surface initially tries to spread in both horizontal and vertical directions. But buoyancy forces acting upwards, reduce vertical entrainment [6] . Therefore, the warm water jet expands more in the horizontal direction, providing wider warm surface for the heat and mass interaction with the surrounding atmosphere.

The analysis of thermal behavior, of a water body becomes extremely complex due to most unpridictable fluctuations in temperature and humidity conditions of atmosphere, wind velocity and its direction etc. Few models of temperature distribution and system analysis have been given by various authors [6,7,8,9].

In the present work the object is to get generalized expressions for the distance between discharge and intake points. The experimental results are in favour of intake below the top surface, since intake at top yields higher temperature. The paper also provides method to determine heat rejection to atmosphere by convection, evaporation and radiation from the free surface of the water body, in terms of pond number. When water is discharged at top, a warmer and a cooler layers are formed in the water body. The pond number is the ratio of warmer surface layer thickness to the average depth of the water body [10] .

2. ANALYSIS

The energy balance for the water body can be written as ;

$$P\,(1-\eta_{th})\times 3600 = \dot{m}_w\,(T_i - T_o) = Q_s + Q_n \qquad (1)$$

or,

$$\dot{m}_w\,c_p\,(T_i - T_o) = \int_A\int (h_c + h_r)\,\Delta T \cdot dA + \int_A\int h_d\,(w_s - w_a)\,\Delta h \cdot dA + \int\int\int c_p\,\rho\,\Delta T' \cdot dV \qquad (2)$$

where

Q_s : Surface Heat-Transfer; kJ/h

Q_n : Heat Accumulation in the water body ; kJ/h

P : Power Plant Output ; kW

η_{th} : Thermal Efficiency of Power Plant

$\dot{m}_w$: Rate of water circulation ; kg/h

T_i , T_o : Discharge and Intake Temperatures of Water: C

h_c, h_r : Convective,and Radiative heat-transfer coefficients kJ/m^2-h-C

h_d : Mass diffusion coefficient; kg/m^2.h

w_s, w_a : Specific humadity of saturated air and atmospheric air

A, V : Free surface area and volume of water body

ΔT : Temperature difference at surface $(T_s - T_a)$; C

$\Delta T'$: Temperature difference of any element $(T_{element} - T_a)$; C

T_a : Ambient Temp. ; C

C_p : Specific heat of water body ; kJ/kg-C

ρ : Density of water ; kg/m^3

The above equation requires the information of various quanties like, convective, radiative heat-transfer coefficient, mass diffusion coefficient,temperature distribution inside the body etc. for various atmospheric conditions. So the actual determination becomes very difficult. However, some correlations based upon statistical analysis of a particular location can be made available.

3. EXPERIMENTAL SET-UP

It comprises a tank of size 570 X 570 X 425 mm deep, fabricated from 12.7 mm thick perspex sheet. Holes for discharge (A) and intakes (B) were made as shown in fig. 1. The tank as well as the pipes were insulated with thermocole to minimize heat loss to surroundings. The only heat interaction between the system and surroundings occurs through the free water surface because the heat loss through the remaining surfaces is kept below 1% of the heat input to the tank by warm water discharge.

The calibrated rotameters and copper constanton thermocouples were used to measure water flow rates and temperatures at various locations (250 volume elements) in the tank, respectively. The water at controlled temperature from an ultra-thermostatic bath was first pumped to a constant head device. This arrangement ensured the steady flow rate of warm water, through the rotameter, placed between constant head device and the tank. Similar arrangement was made for the intake. Discharged and intake flow rates were kept the same so as to maintain a constant level in the water tank.

The water discharge was varied from 50 to 300 ml/min. The temperature difference of warm water to the atmosphere was varied from 10 to 25°C. Wind velocity was negligibly small and the relative humidity of atmosphere varied from 55 to 65% during the experimental period.

4. EXPERIMENTAL RESULTS

4.1 Effects of Discharge Conditions

The variation of pond number (IP) with flow rates for various operating temperatures is shown in Fig. 2. It is seen than when the intake is from the top, the penetration is less as compared to intake from the bottom. This seems to be due to different density gradients. However, in this case

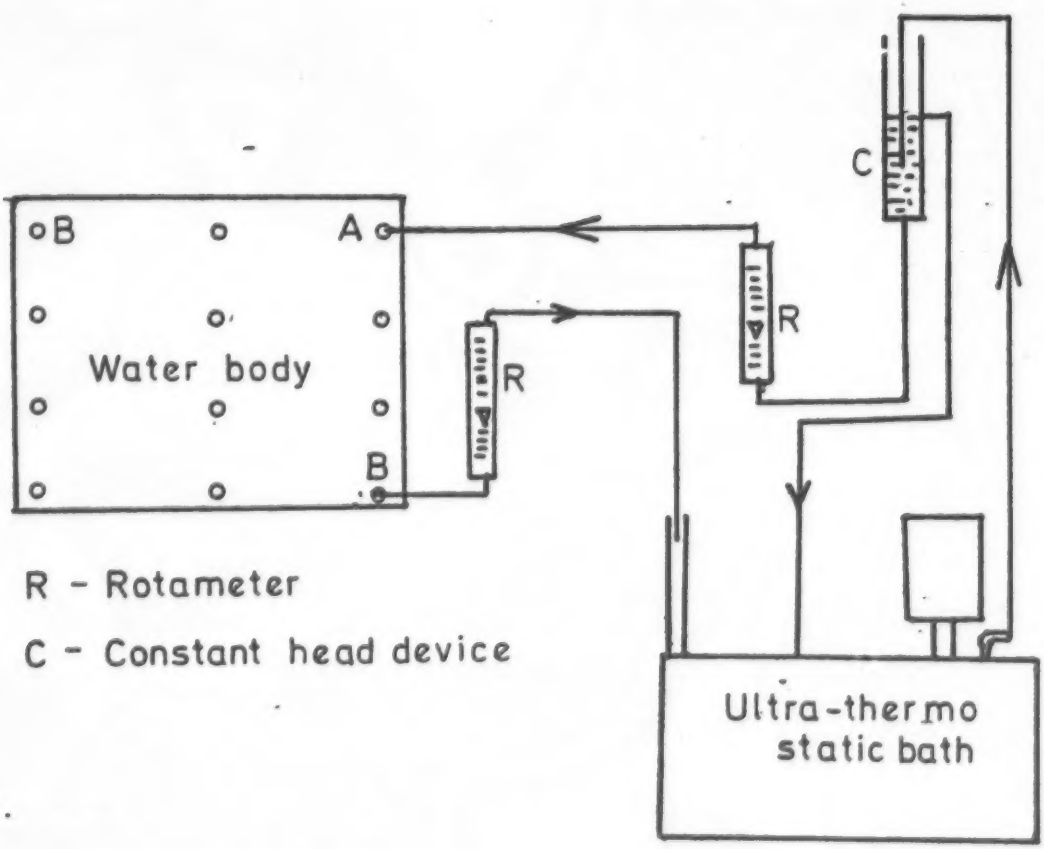

Fig. 1. Experimental set-up.

the intake temperature is higher. The variation of intake temperature for different discharges for various positions of intake is shown in Fig. 3. Evidently, the higher the discharge rate, the larger is the intake temperature. As such a lower discharge is desirable to get lower intake temperature.

As the discharge temperature increases, the penetration increases when the intake is from the bottom. This contradicts the one reported in [10] . It seems that layers get thermally affected in the long run even though the buoyancy forces act upwards.

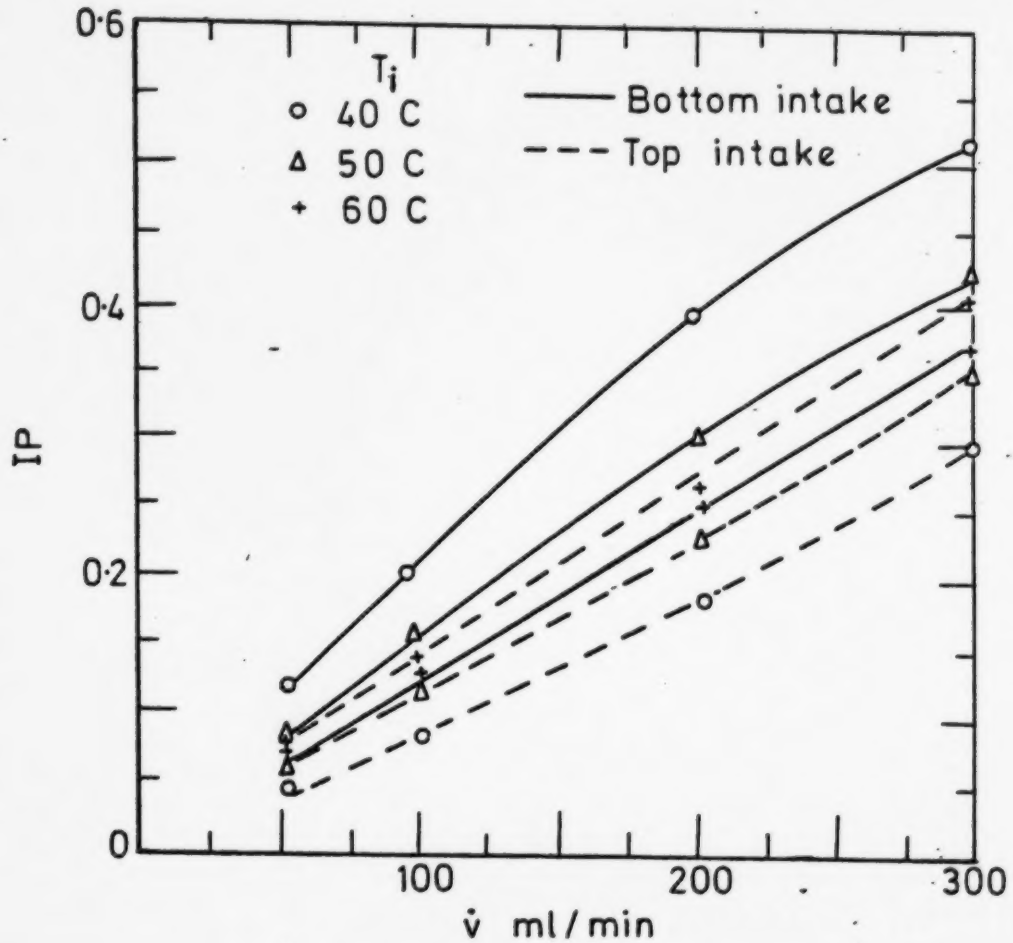

Fig. 2. Variation of pond number with discharge conditions.

4.2 Heat Rejection To Surroundings

To determine heat transfer to surroundings, by convection, evaporation and radiation, the backward calculations were done using Eq. (2). The heat accumulation was calculated from the temperature readings and the volume integral. The net heat input to the tank by warm water was found from :

$$Q_{net} = 0.99 \times 10^{-6} \dot{v}\, t\, (T_i - T_o)\, C_p \,. \qquad (3)$$

where

$\dot{v}$: Volume flow rate ; ml/min

t : Time ; min.

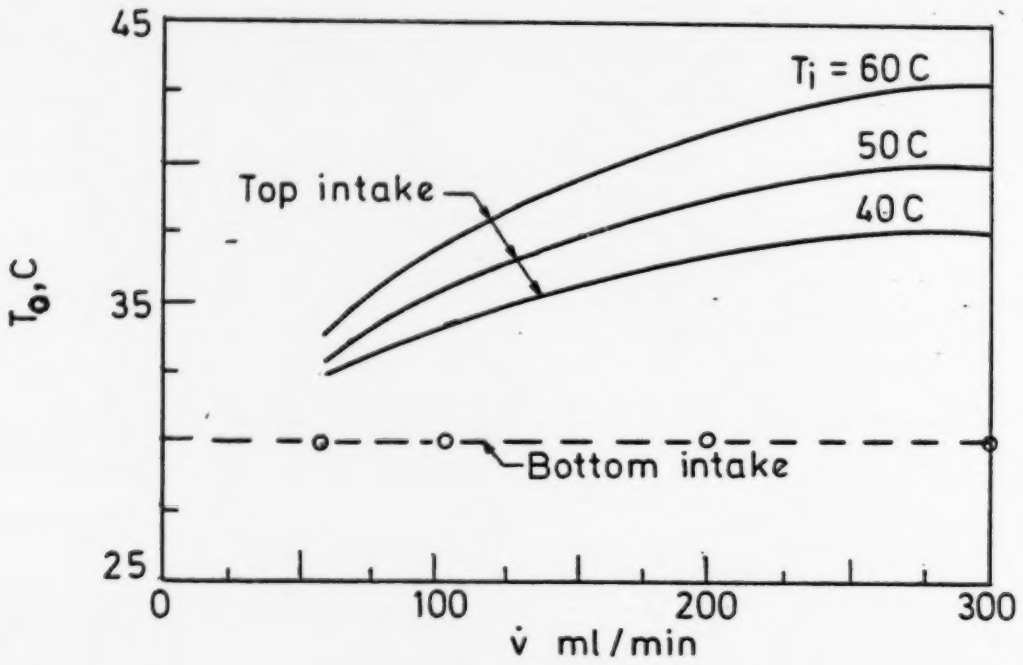

Fig. 3. Variation of intake temperatures with discharge conditions.

The factor 0.99 has been introduced to account for the heat loss through the insulated surface which remains within 1% of total heat input.

From Eq. (1 and 3) :

$$Q_s = Q_{net} - Q_h \qquad (4)$$

Now Q_s can be written in the functional form as :

$$Q_s = f\ (T_i, T_o, \dot{v}, A, T_{wb}, T_{db}, d) \qquad (5)$$

where,

T_{wb}, T_{db} : Wet-bulb and dry-bulb temperatures of surrounding air ; C

d : Distance between discharge and intake points ; m .

Since pond number depends upon those parameters which influence Q_s, it is desirable to correlate the dimensionless heat transfer ($\bar{Q}$) as :

$$\bar{Q} = Q_s/Q_{net} = F\ (IP) \qquad (6)$$

The experimental results have been used to find out a correlation between $\bar{Q}$ and pond number. It gives :

$$\bar{Q} = 0.6732\ IP^{0.225} \qquad (7)$$

within $\pm$ 15% .

Further experimental work is in progress to cover wider range of application aiming at development of engineering correlations.

5. CONCLUSIONS

(a) The heat transfer to environment is possible to correlate in terms of pond number. In the present work, satisfactory correlation of experimental data has been found.

(b) The pond number increases with increasing discharge temperature and discharge if intake is at the bottom. Similar behaviour has been found even for intake at top, yielding pond number of smaller magnitude.

(c) The ratio of heat rejection to surrounding to the net heat input to water body is correlated in terms of pond number.

6. ACKNOWLEDGEMENTS

Thanks are due to Mr. P.N. Misra and Mr. P.N. Sharma for the help rendered by them in fabrication and carrying out experimental work.

REFERENCES

1. W.L. Harper and W.R. Waldrop, An Operational Procedure for Predicting the Most Economical Use of Condenser Cooling Modes, Waste Heat Management and Utilization, Vol. 1, pp. 501-512, 1979.

2. C.N. Hodges, H. Jenson and C.O. Hodges, Waste Heat Use in Controlled Environmental Greenhouses, Beneficial Uses of Thermal Discharges, New York State Department of Environmental Conservation, Sept. 1970.

3. W.J. McNeil, Heated Water From Generators Presents Fish Culture Possibilities, The American Fish Farmer and World Agriculture News, Vol. 1, No. 11, Oct. 1970.

4. S. Ostrach, J. Prahl and T. Tong, The Discharge of a Submerged Buoyant Jet Into a Startified Environment, Waste Heat Management and Utilization, Vol. 2, pp. 1513-34, 1979.

5. A. Zukauskas, Warm-Water Spreading in Cooling Ponds of Steam Power Plants, Heat-Transfer and Turbulent Buoyant Convection, Vol. 1, pp. 139-57, 1977.

6. J.J. McGuirk and W. Rodi, Calculation of Three-Dimensional Heated Surface Jets, Heat-Transfer and Turbulent Buoyant Convection, Vol. 1, pp. 275-88, 1977.

7. G.H. Jirka, G. Abraham, R.R. Harleman and R.M. Parsons, Lab. Report No. 21, Deptt. of Civil Engg., M.I.T., U.S.A., July 1975.

8. S. Lee, S. Sengupta, C. Tasai and H. Miller, Three-Dimensional Free-Surface Model for Thermal Discharge, Waste Heat Management and Utilization, Vol.3, pp. 1615-34, 1979.

9. A.W. Miller, Jr. and R.L. Street, Surface Heat-Transfer From a Geothermally Heated Lake, Waste Heat Management and Utilization, Vol. 3, pp. 1907-26, 1979.

10. K.D. Robinson, R.J. Schafish and G. Cemougis, A System Approach to Biologicaland Thermal Considerations in Cooling Lake Analyses, Waste Heat Management and Utilization, Vol. 1, pp. 153-74, 1979.

PB82-228388

NUMERICAL SIMULATION OF THE THERMAL DISCHARGE FOR OCONEE POWER PLANT INTO LAKE KEOWEE

S. Sinha, E. Nwadike, S. Sengupta and S. Lee

Department of Mechanical Engineering
University of Miami, Coral Gables, Florida 33124
U. S. A.

Understanding the environmental impact of hot water discharge from the condenser of a steam power plant is of considerable importance in helping to preserve aquatic life and also the overall efficiency of the power plant. In recent years, with improvement of computing facilities, different types of mathematical models have been developed to predict such effects. The present work involves the prediction of thermal dispersion using a three dimensional numerical simulation model. The area of interest is Lake Keowee in South Carolina which is located about 40 km west of Greenville and was made from 1968 through 1971 by damning the Little River and Keowee River. At present it constitutes the Keowee Toxaway Complex of Duke Power Company. The lake has two arms connected by a canal and has three power plants on it; the Oconee Nuclear power plant which takes its condenser cooling water from the lower arm and discharges it into the upper arm; Jocassee pumped storage station which is located at the extreme end of the upper arm and uses Lake Keowee as its lower reservoir and the Keowee-hydro station which is located adjacent to the Oconee nuclear power station and uses Lake Keowee as its higher level reservoir. Lake Keowee has a full pond elevation of 243.8 above mean sea level, full pond volume of 1.18×10^9 m^3, a mean depth of 15.8m, an area of 74 km^2 and a shoreline of about 480 km. A map of Lake Keowee is shown in Figure 1.

The mathematical model used is a three dimensional Rigid Lid model which is used to predict the three dimensional velocity and temperature distributions in the vicinity of the heated discharge from Oconee nuclear station. The model formulation is based on Sengupta and Lick (1974) and it essentially solves the three dimensional momentum, continuity and energy equations subject to the rigid lid (horizontal free surface), hydrostatic and Boussinesq approximations. Vertical stretching, originally adopted by Sengupta and Lick (1974) is used to handle uneven bottom topography.

An explicit finite difference scheme is used for the solution of the equations. Due to the Rigid Lid assumption, the Courant-Lewy-Fredrichs condition for surface gravity waves is eliminated but the surface pressure ceases to be atmospheric. A predictive Poisson's equation is obtained for the 'rigid lid' pressure by vertically integrating the horizontal momentum equations and they are solved by a successive over relazation method at each time step.

For verification purposes the temperatures and velocities were measured with infrared photography by overflying NASA aircraft and current meters.

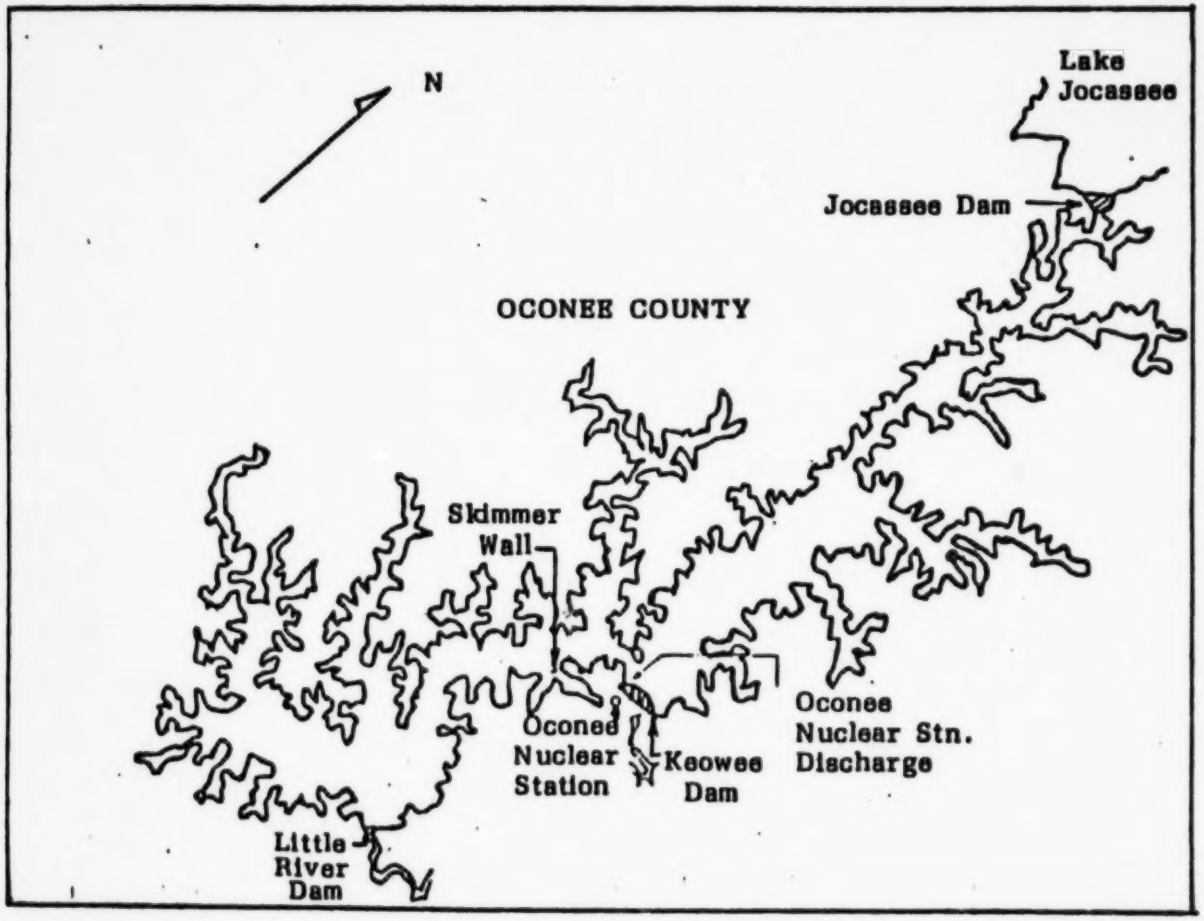

Figure 1. Lake Keowee

The ground truth data, infrared digicolor photographs, temperatures and flow rates through the three power plants (supplied by Duke Power companies monitoring stations) together with meteorological data (air temperature, windspeed, humidity and solar radiation) constituted the entire data base.

A total of two cases were simulated for Lake Keowee.

Case 1. Preliminary and Archival Runs.

These cases were primarily executed for the purpose of selecting b.c.s., initial condition and to test the behavior of the model when incomplete and/or arbitrary data are used. Various runs were made to investigate the effects of surface wind shear stress and bottom topography. Archival data was used to test the model and the results compared well.

Case 2. Summer and Winter Runs.

The annual cycle of a cooling lake can be divided into two, namely a heating season and a cooling season. Hence the predictive accuracy of the model was verified fore these two seasons. For simplicity of simulation the bottom of the domain was cut off at a depth of 16 meters since the previous data showed very little activity below this depth.

Data was obtained through in site measurements, power plant discharge data, meteorological data and remote sensing.

The days selected for simulation were Aug. 24 and 25, 1978 (summer) and Feb. 27 and 28, 1979 (winter). Comparisons were made between the measured and predicted surface isotherms and velocities within the domain. The simulation was carried out on an hourly basis and comparisons were made only at those hours where all the needed data were available simultaneously.

The surface isotherm comparison is excellent for the summer runs. The shapes the isotherms were found to be similar. However the values of the temperature on two comparing isotherms varied slightly. Nevertheless the root mean square error between measured and predicted valves, were found to be within 0.55°C.

The winter runs represent simulations when the cooling season is in full swing. The comparison in this case also proved to be good. The root mean square accuracy between measured and predicted isotherms was found to be within 0.82°C.

Both in summer and winter simulations the following characteristics were found:

a) The main driving forces responsible for determining the shape of the isotherms are the ambient temperature, discharge temperature and flow through Jocassee pumped storage station

b) Only the surface velocities get affected by the wind.

ACKNOWLEDGMENTS

This work was supported by a contract from the National Aeronautics and Space Administration (NASA-KSC) and the Environmental Protection Agency (EPA-RTP).

The authors express their sincere gratitude for the technical and managerial support of Mr. Roy A. Bland, the NASA-KSC project manager of the contract, and the NASA-KSC remote sensing group. Special thanks are also due to Dr. Theodore G. Brna, the EPA-RTP project manager, for his guidance and support of the experiments, and to Mr. S. B. Hager, Chief Engineer, Civil-Environmental Division, and Mr. William J. McCabe, Assistant Design Engineer, both from the Duke Power Company, Charlotte, North Carolina, and their data collection group for data acquisition. The support of Mr. Charles H. Kaplan of EPA was extremely helpful in the planning and reviewing of this project.

REFERENCES

1) Duke Power Co. "Oconee Nuclear Station Thermal Plume Study" 1978.

2) Duke Power Co. "Oconee Nuclear Station Thermal Plume Study" 1979.

3) Duke Power Co. "Oconee Nuclear Station Environmental Summary Report, 1971-1976" 1976.

4) Freeman, N. G., Hale, N. G., Danard, M. B. "A Modified Sigma Equations Approach to the Numerical Modelling of Great Lakes Hydrodynamics". J. Geo. Res., Vol. 77, No. 6, 1972.

5) Haq and Lick, W. "The Time-Dependent Wind Driven Flow In A Constant Depth Lake" Presented at the 16th Conference on Great Lakes Research, Huron, Ohio 1973.

6) Sengupta, S. and Lick, W. "A Numerical Model for Wind Driven Circulation and Temperature Fields in Lakes and Ponds", 1974. FTAS/TR-74-98.

7) Sengupta, S., Lee, S. S. and Bland, R., "Numerical Modelling of Circulation in Biscayne Bay," Presented at the 56th Annual Meeting of the American Geophysical Union, 1975. Appeared in Transition of the American Geophysical Union, June, 1975.

8) Sengupta, S., Lee, S., and Mathavan, S. K. "Three Dimensional Numerical Model for Lake Belews" 1977. NASA Contract NAS10-9005.

9) Sengupta, S., Lee, S., Nwadike, E. V., "Verification of One-Dimensional Numerical Model at Lake Keowee", 1980. NASA Contract NAS10-9410.

10) Sengupta, S., Lee, S., Nwadike, E.V., Sinha, S.K. "Verification of Three-Dimensional Rigid Model at Lake Keowee". 1980. NASA Contract NAS 10-9410.

11) Wilson, B. W., "Note on Surface Wind Stresses Over Water at Low and High Wind Speeds", Journal of Geophysical Research, Vol. 65, No. 10, 1960.

12. Young, D., Liggett, J. S., Gallagher, R. H., "Unsteady Stratified Circulation In A Cavity" J. of Engineering Mechanics Div. ASCE, Dec. 1976.

SESSION VII C

ENVIRONMENTAL EFFECT

PB82-228396

LIFE HISTORY CHARACTERISTICS AND PHYSIOLOGICAL TOLERANCES OF *TEREDO BARTSCHI*, A SHIPWORM INTRODUCED INTO TWO TEMPERATE ZONE NUCLEAR POWER PLANT EFFLUENTS.

K. Elaine Hoagland
Lehigh University
Bethlehem, Pennsylvania, U.S.A.
and
Academy of Natural Sciences
Philadelphia, Pennsylvania, U.S.A.

ABSTRACT

Teredo bartschi Clapp (Bivalvia: Teredinidae), a tropical and subtropical marine wood-borer, has been introduced into the heated effluents of the nuclear generating stations at Oyster Creek, New Jersey, and Millstone, Connecticut. Allozyme studies show that the introduced populations are closely related to *T. bartschi* from Florida, but they have less genetic variation. The Oyster Creek population has undergone 3 crashes during station outages, each time followed by an outbreak when the heated effluent returned. *T. bartschi* tolerates higher temperatures than the 2 native temperate species, *T. navalis* and *B. gouldi*. However, it survives poorly below 11° C. *T. bartschi* has life history characters that give it both a high rate of increase and good competitive ability. It has a very short generation time and matures at a small size. It has not replaced the native species where it has been introduced. Its survival is unpredictable due to temperature fluctuations, and its populations are patchy due to lack of a planktonic larval stage.

1. INTRODUCTION

Two nuclear power plants located in the Western Atlantic temperate zone have provided highly favorable environments for the proliferation of wood-boring bivalves ("shipworms", family Teredinidae). Both have once-through cooling systems that release heated saltwater effluents. The Oyster Creek Nuclear Generating Station on Barnegat Bay began operating in December, 1969, and a shipworm outbreak was discovered in the vicinity of the heated effluent in 1971 (Turner, 1974a). Much has been written documenting the relationship between the operation of the generating station and the shipworm outbreak (Hoagland & Crocket, 1979; Hoagland *et al.*, 1980; Richards *et al.*, 1980). The species initially present were *Teredo navalis* Linnaeus and *Bankia gouldi* (Bartsch), both native to Barnegat Bay. In August of 1974, 2 non-native species, *Teredo bartschi* Clapp and *T. furcifera* von Martens, were discovered (Turner, 1974b). Turner identified them primarily on the basis of the shape of the pallets and the type of larval development. *T. bartschi* became a serious pest in the heated effluent and soon was found in the intake area, Forked River (Hoagland & Turner, 1980). *T. furcifera* spread into Barnegat Bay but disappeared during one of the prolonged outages of the generating station and has not returned.

Although no large shipworm outbreak has been recorded at the Millstone Nuclear Generating Station near Waterford, Connecticut, *Teredo bartschi* was discovered there in 1975. The only sympatric teredinid is *T. navalis*.

Preceding page blank

was removed: a "monthly" panel that was deployed the previous month, a "yearly" panel that was deployed 12 months before, and one of the 12 "cumulative" panels that had been deployed in May. Using X-rays of each panel as aids, the animals were dissected from the wood, identified, measured, examined for brooded larvae in the gills, and counted. The number of empty burrows representing dead shipworms was estimated.

Specimens of *Teredo bartschi, T. navalis, and Bankia gouldi* from Barnegat Bay, New Jersey and from Millstone, Connecticut were collected in wood panels, dissected out while still alive, and frozen in Tris tissue buffer. Specimens of *T. bartschi, Bankia fimbriatula,* and the pholad *Martesia striata* from Florida were similarly obtained and prepared. The specimens were electrophoresed using the horizontal starch-gel method within 9 months of collection, following the procedures in Hoagland & Turner (1981). Twenty-one enzyme loci were analysed; allele frequencies for each locus were recorded. Calculations of genetic identity and distance (Nei, 1972) were made, in order to determine similarity of the populations of *T. bartschi.* The other species were analysed so that the genetic distances between populations and species could be calibrated. The amount of genetic variation within each population was assessed using standard indices of heterozygosity (H) and percent polymorphic loci (P) described by Selander (1976).

Populations of *Teredo bartschi, T. navalis, and Bankia gouldi* from Oyster Creek were maintained in the laboratory at 22±2 °/₀₀ salinity and 15-22° C for use in physiological studies and to observe reproduction. Temperature and salinity preferences of adults were delineated by observing changes in the siphon activity of several individuals as the variable under study was gradually changed. At least one panel was held under constant conditions and observed as a control.

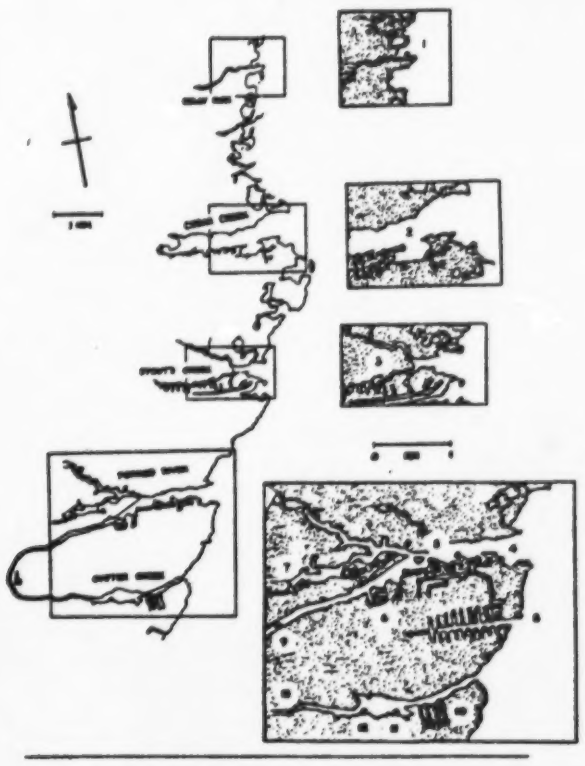

Fig. 2. Locations of stations 1-13 in Barnegat Bay and adjacent creeks.

Responses of *T. bartschi* pediveligers to salinities of 2, 5, 10, 20, 30, and 40 °/₀₀ were recorded every 20 minutes for 4 hours at 18° C. Each salinity condition was established with artificial seawater in a finger bowl containing 10 pediveligers and a sliver of presoaked white pine. The categories of behavior recorded include various swimming and crawling patterns and the extent to which the shells were open. Animals were gradually acclimated to the final salinity of the experiment.

Lower salinity tolerances for the three species from Barnegat Bay were estimated by lowering the salinity 2-3 °/₀₀ a day over a period of weeks until a change in behavior of the adult shipworms was observed (Hoagland *et al.*, 1980). Long-term experiments were performed at the salinities at which behavioral changes were observed in the preliminary experiments (Hoagland & Crocket, 1980). These salinities were 12 °/₀₀, 9 °/₀₀, 6 °/₀₀, and 3 °/₀₀. Upper salinity tolerances were delineated in a similar manner; the salinity was increased 1-2 °/₀₀ per day. The temperature was 20-24° C for these experiments. When behavioral changes and mortality were noted, the salinity was held constant for several days. Control panels for the salinity experiments were held at 20-24° C and 22 °/₀₀.

Upper temperature tolerances were tested by holding the salinity constant at 22 °/₀₀. Daily observations were made as the temperature was raised by 1°C per day. A control panel was maintained at 24° C. The panels were returned to 25° C and observed for several more days when significant mortality was observed. Preliminary estimates of lower temperature tolerance of *T. bartschi* have been determined by placing *T. bartschi* adults in an outdoor salt water system over the winter months at 22 °/₀₀ salinity and observing the siphon activity and production of frass (wastes and wood fragments), compared with *T. navalis*. Further details of the above experiments, including sample size, exact schedule of temperature and salinity changes, and methods of maintaining the cultures, are in Hoagland *et al.*, 1980, Hoagland & Crocket, 1980, and Hoagland & Crocket, 1981.

3. RESULTS AND DISCUSSION

3.1 Shipworm populations

The abundances of the shipworm species in Oyster Creek over the years of study are shown in Table 1. The population of *T. bartschi* exploded in the summer and fall of 1974, 1978, and 1979 when the heated effluent was present during winter and early spring. The population was severely reduced in 1976-1977 and 1980 when there were prolonged outages covering substantial parts of the months January-April. Dredging of Oyster Creek occurred in early 1979. It had the effect of reducing the adult population of *T. bartschi*, but had little effect on the size of the year class recruited the next summer and fall, which was the largest reported.

The 12 wood panels submerged in the effluent of the Millstone Nuclear Generating Station from June to November, 1980, yielded only 24 specimens of *Teredo bartschi*, 16 of which were in a single panel. There were 51 specimens of *T. navalis* altogether in the 12 panels.

The responses of the native species to fluctuations in the thermal effluent have not been as dramatic as that of the introduced species. However, the presence of *Teredo bartschi* may have reduced the populations of native species in Oyster Creek. Panels removed from Oyster Creek on August 24, 1975, contained about 10 *Bankia gouldi* and hundreds of *T. bartschi*, whereas in a panel removed from station 6 in Forked River, there were 35 specimens of

B. gouldi and no other species. *T. navalis* has never been the major element of the Oyster Creek teredinid fauna, but is usually present at a density of 1 to 2 per panel. It was affected by the outages of the generating station in 1976-1977, and took longer to recover than did *T. bartschi*.

TABLE 1

AVERAGE NUMBER OF SHIPWORMS PER PANEL IN OYSTER CREEK, CUMULATIVE PANELS SUBMERGED IN MAY OF EACH YEAR

Date Removed	*T. bartschi*	*B. gouldi*	*T. navalis*	Major Station Outages
1972 Oct.	0	7	1	May 1-June 20
Nov.	0	8	1	
1973 Oct.	0	21	0	April 14-June 4
Nov.	0	14	0	September 8-October 5
1974 Oct.*	>500	10	1	April 13-June 29
Nov.*	>500	>10	0	
1975 Oct.*	>500	>20	0	February 4-February 29#
Nov.*	no panel			March 29-May 26#
1976 Oct.	0	3	0	Dec. 27,1975-March 11,1976#
Nov.	0	4	0	
1977 Oct.	0	3	0	April 23-August 4#
Nov.	5	3	0	
1978 Sept.	625	2	0	September 16-December 8
Oct.	480	2	0	
Nov.	439	1	0	
1979 Sept.	640	4	1	May 2-May 31
Oct.	1,000	3	1	
Nov.	400	1	2	
1980 Sept.	0	4	1	January 5-July 19#
Oct.	162	2	1	
Nov.	300	3	1	

* Counted from X-rays
\# Prolonged winter and early spring outages

In shipworm population studies at Millstone, Connecticut, researchers have consistently found small populations of *T. bartschi* (Battelle Columbus Laboratories, 1979). The lack of large populations is probably due to the colder ambient temperature and the very limited supply of wood substrate in the Millstone effluent.

The distribution of *Teredo bartschi* in Barnegat Bay corresponds exactly to the geographical limits of the thermal effluent, which are from Waretown to Forked River (Figure 1). First found in Oyster Creek, *T. bartschi* next appeared at Bayside Beach Club (station 8) between Oyster Creek and Forked River. After the outages in 1976, we did not find *T. bartschi* at all, but a few specimens were reported near our station 12 in Oyster Creek by Richards *et al.* (1976). In late 1977, we found a few *T. bartschi* at station 12. In

1978, after the effluent had been present for a full winter and spring, *T. bartschi* first reappeared in significant numbers at station 12. By February it was found at station 11 as well. In July, it reached station 10. By August it had spread to Bayside Beach Club, and in November it had reached the mouth of Forked River itself (station 4).

In February, 1979, we recorded *T. bartschi* at station 6 in a lagoon off Forked River for the first time. In August, 1979, it was found at station 5 near the branching point of Forked River. Finally, in November, 1979, *T. bartschi* was recorded at the mouth of Waretown Creek (station 14). It had been tentatively identified there once before, in 1975 by R. D. Turner (personal communication).

In the 1980-81 shipworm season, following the January 5-July 19 outage, *T. bartschi* appeared late; settlement did not begin until September and large populations were not present until November (Fig. 3). Specimens were first found alive only at station 12. Then in November, they reappeared at station 8. In March, they reappeared at stations 10 and 11. There may be some small source of heated water, such as a pipe carrying waste water, entering Oyster Creek near station 12 that provides a refuge for the subtropical species.

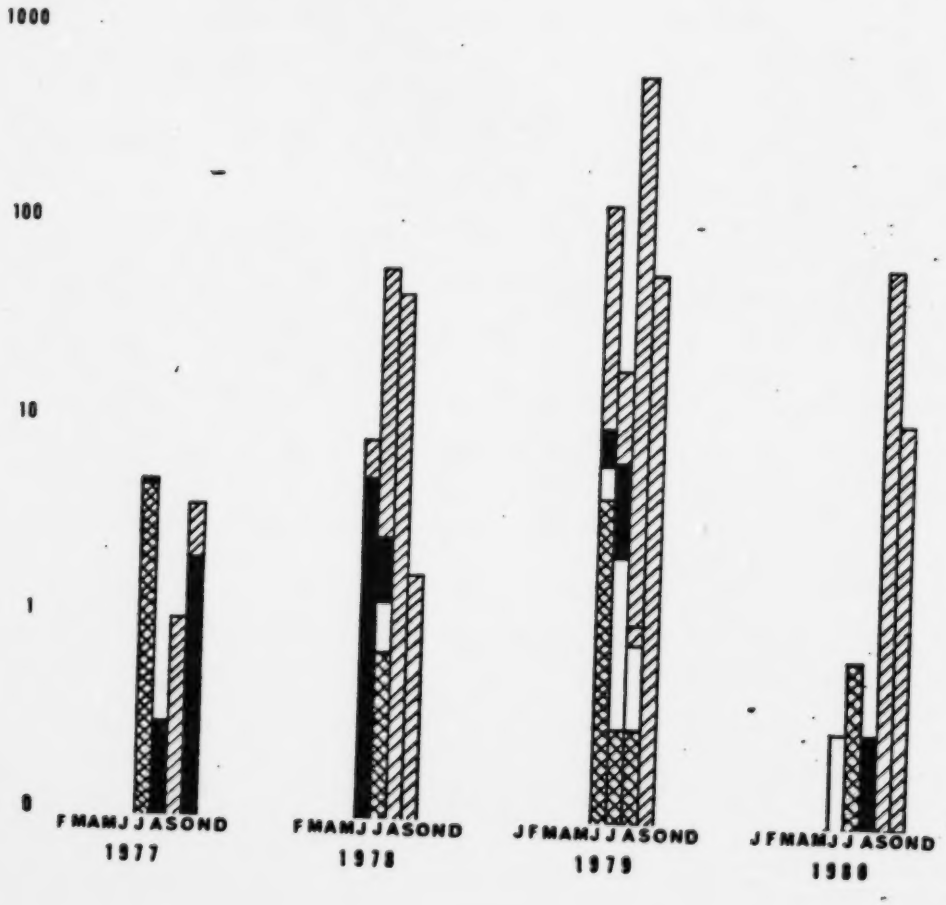

Fig. 3. Numbers of Shipworms Settling per Wood Panel each Month in Oyster Creek, 1977-1980. Log scale.

Although animals brooding larvae have been found at all the above stations, densities greater than 8 per panel have been found only at Bayside Beach Club (station 8) and the mouth of Waretown Creek (station 14). *Teredo bartschi* is not established independent of the Oyster Creek population at the other stations. The general pattern of migration implicates recirculation of the thermal effluent into Forked River in establishing the range of the introduced species. The migration has gone outward from a reservoir population at station 12.

The larvae of *Teredo bartschi* develop in brood pouches in the gills before being released as crawling and swimming young known as pediveligers. In contrast, *T. navalis* broods for a shorter time, releasing straight-hinge stage veliger larvae that must spend several weeks feeding in the plankton. *Bankia gouldi* does not brood at all but releases eggs that develop in the plankton. Pediveligers of *T. bartschi* obtained from specimens collected in Oyster Creek have remained unmetamorphosed for as long as 25 days before successfully entering wood in the laboratory. Therefore they probably have considerable ability to disperse under natural conditions.

The percentages of individuals that were brooding young when taken from test panels are shown in Table 2. There is a higher frequency of brooding in *Teredo bartschi* than in *T. navalis* (overall, about 35% versus 15%). Despite a smaller number of offspring per brood, ~10^3 versus 10^5 or more in *T. navalis*, *T. bartschi* has a high reproductive effort. In July 1978, 28% of *T. bartschi* in panels submerged for only two months were already brooding young while only 9 specimens out of hundreds of *T. navalis* found in Barnegat Bay were brooding. The smallest specimen of *Teredo bartschi* carrying young was 4 mm long, while the smallest brooding specimen of *T. navalis* in Barnegat Bay was 16 mm long. Therefore *T. bartschi* has a shorter generation time than *T. navalis*. Because it can mature at a very small size, it is not as affected

TABLE 2

THE PERCENTAGES OF THE POPULATIONS FOUND TO BE BROODING YOUNG
A dash indicates no specimens were collected.

	Teredo bartschi		*Teredo navalis*	
Date Removed	Oyster Creek	Elsewhere	Oyster Creek	Elsewhere
1978				
June	25	0	0	19
July	20	0	-	50
August	26	-	0	11
September	39	0	0	1
October	34	0	-	1.5
November	26	75	-	0.6
December	38	69	0	0
1979				
January	37	100	0	0
February	25	58	0	0
March	22	-	0	0
April	10	-	0	0
May	0	-	-	67
June	86	-	100	29
July	18	-	25	15
August	45	21	60	10
September	71	100	100	25
October	61	56	0	11
November	50	44	0	0
December	36	38	0	0

by crowding as the larger species that mature more slowly. The maximum length of *T. bartschi* found in Oyster Creek is 132 mm; that of *T. navalis* is 360 mm, while that of *Bankia gouldi* is 450 mm.

The high percentage of *T. bartschi* that have hermaphroditic gonads compared with the native shipworms (Richards *et al.*, 1980), the size and age at which eggs are produced by *T. bartschi*, and the high frequency of brooding individuals in populations of *T. bartschi* suggest that it is a simultaneous hermaphrodite. In fact, some individual test panels dissected have contained 100% brooding individuals. The high percentage of brooding individuals of *T. bartschi* give it a high intrinsic rate of increase (r). If the species is capable of simultaneous hermaphroditism, it would have a reproductive advantage over other species, since the effective population size of a hermaphroditic population is larger than that of a protandrous population. It has been assumed since the work of Coe (1941) on *Teredo navalis* that all teredinids are protandrous hermaphrodites, but the sexual systems of *T. bartschi* and many other species have not been examined rigorously. Recently, some evidence has been presented to suggest hermaphroditism and self-fertilization in some species of shipworms (Eckelbarger & Reish, 1972).

The brooding of young in nearly every month does not mean that young are released and settle successfully in every month. Settlement of *Teredo bartschi* in Oyster Creek is highly seasonal. But there is the potential for release at almost any time if external conditions are favorable. Most of the larvae held over winter are near or at the pediveliger stage. In the laboratory, *T. bartschi* releases larvae all year long when maintained at 22 $\pm$ 2 $^{o}/_{oo}$ and at temperatures from 15° C in winter to 25° C in summer. Specimens of *T.bartschi* collected at Ft. Pierce, Florida in October, 1979 and November, 1980 contained pediveliger larvae. Likewise, specimens from Millstone, Connecticut, contained larvae when collected in November, 1980.

The settlement period for *Teredo bartschi* in Oyster Creek is longer than that for either of the native species (Figure 3). In 1978, *T. bartschi* settled before the native species by one month. An animal settling in mid-June can easily mature and produce offspring that themselves release pediveligers in October. Therefore, a piece of wood often contains three generations if it was deployed in May and removed in November. The size frequencies of the shipworms in November cumulative panels are consistent with this three-generation model.

T. navalis pediveligers settle from late June to October, but very few individuals settling in July or August reproduce before the next summer. Therefore a panel removed in November contains one to two generations. *Bankia gouldi* usually undergoes a single settlement per year, from late June to August. Like that of *T. navalis*, its settlement is not as dense as that of *T. bartschi*, because the larvae are dispersed during their planktotrophic development.

Survivorship is difficult to quantify because of overlapping generations and difficulty in counting empty shipworm burrows and identifying their former occupants. All species of Teredinidae suffer heavy winter mortality in Barnegat Bay, especially in years when there is heavy settlement during the summer. The specimens collected in any one piece of wood include few age classes because destruction of wood is so rapid; mortality occurs when the wood begins to fall apart and exposes the shipworm tubes. Macroscopic predators in Oyster Creek include the polychaete *Nereis succinea* and the flatworms *Euplana gracilis* and *Stylochus ellipticus*. Based on size, growth rates, and rates of wood destruction, I estimate that the average *Bankia gouldi* in Barnegat Bay lives two to three years. Most individuals of *Teredo bartschi* and *T. navalis*

TABLE 3

THE PERCENTAGE OF TEREDINIDAE SURVIVING THE WINTER IN OYSTER CREEK
A dash indicates fewer than 5 specimens collected.

Panel Deployed	Panel Removed	Outage	*T.bartschi*	*T.navalis*	*B.gouldi*
May, 1976	March, 1977	—	—	100%	83%
May, 1977	June, 1978	4/23-8/4 '77	70%	—	--
May, 1978	March, 1979	9/16-12/8 '78	<2%	--	100%
May, 1979	March, 1980	5/2-5/31 '79 1/5-7/19 '80	<1%	<1%	70%
May, 1980	March, 1981	1/5-7/19 '80	100%	13%	100%

live only 9 to 18 months, and most of those that survive the winter settled in the fall. In our panels, both *Teredo* species suffer heavy winter mortality, while *Bankia gouldi* does not (Table 3). Mortality appears to be higher when the creek is dredged or the generating station shuts down for the months of January to April, as in 1977-78. Unfortunately, the winter outages followed heavy summer sets of *T. bartschi*, so the two effects cannot be separated in our analysis of mortality. The surviving year-old specimens of *T. bartschi* reach lengths of 80-132 mm. They have a disproportionate genetic influence on the next generation, because individuals produce eggs in proportion to their size.

The size of the population of *Teredo bartschi* in Oyster Creek is controlled by the number of surviving adults (related to temperatures during winter and severity of wood destruction), the date when the water reaches temperatures high enough to allow release of pediveligers in summer, and the water temperatures in summer that control the rate of growth and development of the shipworms. For example, the outage in 1980 caused very high mortality of *T. bartschi* by March, 1980 (Table 3). The delayed warmup of Oyster Creek postponed release of pediveligers. But finally, when they were released in September during a period of high water temperature, the population expanded rapidly (Table 1).

3.2 Population genetics

The introduction of *Teredo bartschi* to Oyster Creek was accompanied by an almost total loss of genetic variability, assuming that the founder population came from Florida or at least was genetically similar to the population from Florida that I have used as a control (Table 4). Bottlenecks in 1976-77 and 1980 have prevented the reintroduction of genetic variation through accumulation of mutations that Nei *et al.* (1975) have demonstrated is possible. The specimens collected in Oyster Creek in 1979 and Fall, 1980, were genetically identical and strongly support the theory that the population underwent a bottleneck and was not reintroduced in the Fall of 1980. The Connecticut population of *T. bartschi* is nearly as monomorphic as that from Oyster Creek, showing the importance of the initial founder effect as compared with later bottlenecks. The levels of polymorphism in the species used for comparison are typical of other marine invertebrates (Selander, 1976).

TABLE 4

GENETIC VARIATION IN POPULATIONS OF *TEREDO BARTSCHI* AND SOME OTHER TEREDINIDAE, CALCULATED FROM GENE FREQUENCY DATA DETERMINED ELECTROPHORETICALLY

	Percent Polymorphic Loci, P	Heterozygosity, H
T. bartschi, Florida	35	.008
T. bartschi, New Jersey	10	.004
T. bartschi, Connecticut	10	.000
T. navalis, New Jersey	55	.069
T. navalis, Connecticut	55	.150
B. gouldi, New Jersey	70	.133
F. fimbriatula, Florida	55	.138
M. striata, Florida	65	.146

The genetic distances between the taxa (Table 5) leave no doubt that the two introduced populations are closely related to *Teredo bartschi* in Florida, and that all three populations belong to the same species. The genetic distances separating the three populations are too similar to distinguish between the possibilities that *Teredo bartschi* was introduced from Florida to Connecticut by way of Oyster Creek and that the two northern populations represent separate introductions. The Florida and New Jersey populations are more similar at 2 loci, the Florida and Connecticut populations are more similar at 3 loci, and the Connecticut and New Jersey populations are more similar at 5 loci. The similarities of the populations from Connecticut and New Jersey are due to fixation of common alleles, while the similarities of the New Jersey and Florida populations are due to unique alleles in the Connecticut population.

TABLE 5

NEI'S GENETIC DISTANCES BETWEEN TAXA COMPARED ELECTROPHORETICALLY, BASED ON 21 ENZYME LOCI

	T.b. Fla.	*T.b.* Conn.	*T.n.* N.J.	*T.n.* Conn.	*B.g.* N.J.	*B.f.* Fla.	*M.s.* Fla.
T. bartschi, N.J.	0.123	0.109	0.798	0.907	0.823	0.705	1.326
T. bartschi, Fla.		0.086	0.745	0.867	0.956	0.896	1.375
T. bartschi, Conn.			0.821	0.833	0.940	0.867	1.340
T. navalis, N.J.				0.251	0.684	0.845	1.326
T. navalis, Conn.					0.667	0.998	1.123
B. gouldi, N.J.						0.500	0.837
B. fimbriatula, Fla.							1.457
M. striata, Fla.							

3.3 Physical characteristics of the environments and physiology of *Teredo bartschi*

The thermal effluent in Oyster Creek has a ΔT of between 4 and 12° C, depending on the time of year, level of operation of the generating station, and number of dilution pumps operating. In July and August, the water temperature often exceeds 30° C. In July, 1973, 37.2° C was recorded in Oyster Creek. However, by the time the effluent has traveled to the mouth of Waretown Creek or Forked River, the ΔT is usually reduced to 1-2° C. In January and February with the plant operating, the temperature in Oyster Creek is usually 3-5° C above the ambient temperature of -1 to 0° C.

The salinity of both Forked River and Oyster Creek has been elevated and made constant, due to the pumping of circulation and dilution water from Barnegat Bay. The range of salinity in Oyster Creek since 1976 has been 12.5 - 28.0 °/₀₀, except in 1979 when it was as low as 7.5 °/₀₀. The salinity in the bay itself is 8.0 at creek mouths to 30.0 °/₀₀ at Long Beach Island.

In the area of Ft. Pierce, Florida, where *Teredo bartschi* has been found, the annual temperature and salinity ranges are approximately 12-31° C and 10-30 °/₀₀, respectively (D. Mook, personal communication). In the Millstone, Connecticut, thermal effluent, the temperature and salinity ranges are 2-25° C and 28-33 °/₀₀, respectively (D. Morgan, personal communication).

Temperature tolerance experiments show that adult *Teredo bartschi* at 22 °/₀₀ can survive over the range 11-35° C, while the native New Jersey teredinids withstand 0-30° C (Table 6). Salinity tolerance limits were similar for adults of all three species. Greater than 50% of the specimens were active over the range 7-45 °/₀₀ at 20-24° C in experiments lasting 60 days. Pediveligers of *T. bartschi* were swimming or crawling over the salinity range 5-35 °/₀₀ at 20-22° C. Signs of osmotic stress occurred between 5 and 10 °/₀₀. More detailed results can be found in Hoagland *et al.*, 1980, Hoagland & Crocket, 1980, and Hoagland & Crocket, 1981.

The upper salinity limit for all the teredinids examined is far above that reached in Oyster Creek or Barnegat Bay, New Jersey. The distribution of all three species in Barnegat Bay and its tidal creeks is consistent with the laboratory finding that 7 °/₀₀ is the lower limit for these species. Because the thermal effluent in Oyster Creek exceeds 30° but not 35° C during the summer, mortality of the native species, but not *Teredo bartschi*, is expected.

TABLE 6

RESULTS OF TEMPERATURE TOLERANCE EXPERIMENTS

	T.bartschi	*T.navalis*	*B.gouldi*
The Point (°C) at which 50% of the Individuals Become Inactive			
Upper temperature	35	30	29,30*
Lower temperature	12	9	9
The Point (°C) at which Mortality Reaches 50%			
Upper temperature	#	30	29,30
Lower temperature	10	#	-1

* Two separate experiments
\# No experiment performed

The lower temperatures in Oyster Creek during winter are expected to cause mortality of *T. bartschi* even when the thermal plume is present. The selective pressure on the introduced populations to adapt to a lower minimum temperature must be very great, if only a few of the most tolerant individuals survive every year.

4. Conclusions

Genetic data confirm that *Teredo bartschi* has been introduced into the thermal effluents at Oyster Creek, New Jersey, and Millstone, Connecticut. The data on temperature tolerances confirm that *T. bartschi* is adapted to a warmer temperature regime than are *Bankia gouldi*, the species native to New Jersey, and *T. navalis*, the species native to both New Jersey and Connecticut. *Teredo bartschi* is genetically impoverished due to founder effects plus small population size in Connecticut and bottlenecks in New Jersey. However, monomorphism in the soluble proteins is not correlated with narrow physiological tolerances. There is a possibility that strong selective pressures, as evidenced by high adult mortality under temperature stress, could drive the introduced populations of *T. bartschi* to become better adapted to cold temperatures. In that case *T. bartschi* could spread more widely in the cold temperate region.

Although *Teredo bartschi* has built up very large populations in Oyster Creek almost to the exclusion of the native species, it has not become a major element in Barnegat Bay and has not replaced the native species. It has the classical characteristics of a successful introduced, "opportunistic" species. These are a high rate of increase (r), high rate of survival of larvae, broad physiological tolerances, ability to hold brooding larvae over the winter, and hermaphroditism. *Teredo bartschi* is a good competitor in any one piece of wood because it has a shorter lifespan, reproduces at a smaller size, and hence can withstand crowding better (have a higher carrying capacity) than the native species. Its long reproductive season gives the potential for more reproductive events per year than occur in the native species. However, it is unable to dominate an entire area for any length of time, because its population structure is inherently patchy in time and space. Patchiness is caused by the lack of planktonic larval dispersal plus heavy winter mortality. Even if *T. bartschi* evolved greater tolerance to low temperature, it probably would not out-compete the native species because of the niche differences associated with differences in life history. It does, however, increase damage to wooden structures in those places where several species co-occur.

The population size of *Teredo bartschi* in Oyster Creek and Forked River tracks the operation of the Oyster Creek Nuclear Generating Station. Because the introduced population of *T. bartschi* is geographically restricted to the thermal plumes of the two power plants, this species is a good indicator of shipworm damage caused by the two plants.

Control of *Teredo bartschi* must be attempted when the populations are small, such as in winters when the generating stations are refueling and the effluent is absent. Known residual populations such as the one at station 12 in Oyster Creek should be removed at that time. Driftwood should be removed whenever it is observed in thermal effluents. All wooden boats entering thermal effluents should be examined and treated for shipworms to prevent further introductions of exotic species and to prevent spread of existing ones.

ACKNOWLEDGEMENTS

Much of the field work was done in collaboration with R. D. Turner; she supplied data for the years 1971-1974 and confirmed identifications of the shipworms. L. Crocket, M. Rochester, J. Selman, J. McKinley, J. Harms, and G. Böhlke provided technical assistance. The manuscript was read by G. M. Davis, M. Itzkowitz, and R. D. Turner. Funding was provided by the U. S. Nuclear Regulatory Commission and a Fleischmann Foundation grant to the Wetlands Institute, Lehigh University. Laboratory facilities were made available by G. M. Davis, Academy of Natural Sciences.

REFERENCES

1. Battelle Columbus Laboratories, Annual Report on a Monitoring Program on the Ecology of the Marine Environment of the Millstone Point, Connecticut Area to Northeast Utilities Service Company, Section A: Exposure Panels. Rept. 14892, 1979.

2. W. R. Coe, Sexual Phases in Wood-Boring Mollusks, Biol. Bull., vol. 81, pp. 168-176, 1941.

3. K. J. Eckelbarger and D. J. Reish, A First Report of Self-Fertilization in the Wood-Boring Family Teredinidae (Mollusca: Bivalvia), Bulletin of the Southern California Academy of Sciences, vol. 71, pp. 48-50, 1972.

4. K. E. Hoagland and L. Crocket, Analysis of Populations of Boring and Fouling Organisms in the Vicinity of the Oyster Creek Nuclear Generating Station. Annual Progress Report, Sept. 1, 1977-Aug. 31, 1978. NTIS #NUREG/CR-0634, 1979.

5. K. E. Hoagland and L. Crocket, Ecological Studies of Wood-Boring Bivalves in the Vicinity of the Oyster Creek Nuclear Generating Station, June 1-Aug. 31, 1980. Report to the U. S. Nuclear Regulatory Commission. NTIS #NUREG/CR-1855, 1980.

6. K. E. Hoagland and L. Crocket, Ecological Studies of Wood-Boring Bivalves in the Vicinity of the Oyster Creek Nuclear Generating Station, Sept. 1-Nov. 30, 1980. Report to the U. S. Nuclear Regulatory Commission. NTIS #NUREG/CR-1939, 1981.

7. K. E. Hoagland, L. Crocket, and R. D. Turner, Ecological Studies of Wood-Boring Bivalves in the Vicinity of the Oyster Creek Nuclear Generating Station, Sept. 1, 1979-Feb. 28, 1980. Report to the U. S. Nuclear Regulatory Commission. NTIS #NUREG/CR-1517, 1980.

8. K. E. Hoagland and R. D. Turner, Range Extensions of Teredinids (Shipworms) and Polychaetes in the Vicinity of a Temperate-Zone Nuclear Generating Station, Marine Biology, vol. 58, pp. 55-64, 1980.

9. K. E. Hoagland and R. D. Turner, Evolution and Adaptive Radiation of Wood-Boring Bivalves (Pholadacea). Malacologia, in press, 1981.

10. M. Nei, Genetic Distance between Populations. American Naturalist, vol. 106, pp. 283-292, 1972.

11. M. Nei, T. Maruyama and R. Chakraborty, The Bottleneck Effect and Genetic Variability in Populations, Evolution, vol. 29, pp. 1-10, 1975.

12. B. R. Richards, C. I. Belmore, R. E. Hillman and J. Maciolek, Woodborer Study Associated with the Oyster Creek Generating Station. Annual Report for the Period December 1, 1978 to November 30, 1979, Jersey Central Power & Light Co., Duxbury, Mass., Feb. 29, 1980.

13. B. R. Richards, A. E. Rehm, C. I. Belmore and R. E. Hillman, Woodborer Study Associated with the Oyster Creek Generating Study. Annual Report for the Period June 1, 1975 to May 31, 1976 to Jersey Central Power & Light Co., Duxbury, Mass., Nov. 30, 1976.

14. R. K. Selander, Genic Variation in Natural Populations, in F. J. Ayala (ed.), Molecular Evolution, pp. 21-45, Sinauer Associates, Sunderland, Mass., 1976.

15. R. D. Turner, In the Path of a Warm, Saline Effluent. American Malacol. Union Bull. for 1973, vol. 39, pp. 36-41, 1974(a).

16. R. D. Turner, Report on Panels Removed August 27, 1974 from Oyster Creek, Stout's Creek, and Holly Park. Harvard University, Cambridge, Mass., September, 1974.

PB82-228404

IMPACT OF SALINE AEROSOL DRIFT FROM BRACKISH WATER COOLING TOWERS ON CROPS AND SOILS

Charles L. Mulchi, James A. Armbruster and D. C. Wolf
Department of Agronomy
University of Maryland
College Park, Maryland 20742 U.S.A.

ABSTRACT

The effects of saline aerosol emissions from a brackish water, natural draft cooling tower at Chalk Point, Maryland, on crops and soils were investigated over the period 1973 through 1979. The study included: (a) investigations of crop productivity, chemistry of foliage samples from crops, and examinations of changes in soil chemical parameters in permanent research sites located at 1.6, 4.8 and 9.6 km distances from the operating tower, and (b) simulation saline aerosol drift studies on corn and soybeans over five growing seasons.

No significant changes occurred in sodium, chloride or metabolic index values in foliage samples from either corn or soybeans after the cooling tower became operation. Grain yields for corn were significantly lower after the tower began operations but the reductions were associated with below normal amounts and distribution of rainfall. Significant changes were observed in the soil chemical parameters (soil pH, extractable P, Na and electrical conductivity) investigated. None of the changes could be associated with salt emissions from the cooling tower. The changes observed could be associated with increases in soil acidity possibly related to acid forming substances released from the power plant.

Regression analyses of yield data vs. salt deposition rates produced linear relationships for both crops. Corn and soybean yields were described by the relationships $Y_c = 97.9 - 1.94X$ and $Y_{sb} = 103.5 - 1.73X$, respectively, where X equaled the rate of salt deposition (kg/ha/wk) and yields (Y) were expressed as % of non-treated controls. Regression analyses were also performed on leaf sodium, leaf chloride, and metabolic index values for both crops vs. salt deposition rates and between these three chemical parameters and yields.

1: INTRODUCTION

The construction of cooling towers on electrical generating units has accelerated in recent years in response to thermal pollution regulations which have forced electric power utilites to seek alternatives to once-through cooling systems. The expansion of electric power generation in the United States has been particularly notable along inland coastal regions. The circulation of brackish water within a cooling tower causes the creation of saline aerosol droplets which become entrained in the air stream thus subject to escape from the tower as drift. The quantity of saline aerosol drift from a wet cooling tower is dependant upon the salinity of the water supply, the tower concentration factor, circulation rate and the efficiency of the tower drift eliminators to trap aerosol particulates (1,2,3). The height of the cooling tower, the updraft velosity of the tower and the meteorological parameters of the region governs the dispersal of salts on surrounding terrain (3).

Several articles which addressed the potential ecological impact of wet cooling towers have been published within the past decade (1,4,5,6,7); however, the number of case studies on the effects of saline aerosol emissions on crops, soils, and native vegetation near operating towers have been limited (8,9,10,11,12,13,14). Cooling tower emissions other than saline aerosol droplets have been examined for their environmental effects. The impact of drift containing chromium and zinc (15,16) and sulfate (17) emissions from freshwater cooling towers have been reported. Freudenthal, et al. (6) surveyed the literature concerning the emissions of pathogenic and toxic substances from cooling devices. These reports suggest that the impact of wet cooling towers on the environment could occur through a variety of ways depending on the chemical makeup of the cooling tower and biological composition of the areas adjacent to the towers.

Several research groups have examined the response of a wide range of plant species to simulated saline aerosol drift from cooling towers (11,14,18). The work described in this report was part of a comprehensive investigation of the Unit No. 3 cooling tower in operation at the Chalk Point Generating Station in Maryland. The general objectives of this research were to: a) determine the foliar salt tolerance of field grown corn and soybeans and to associate changes in leaf chemistry with changes in crop productivity, b) compare results from drift simulation studies with information on corn and soybeans grown at twelve research sites near the Chalk Point Generating Station and c) examine the changes in the chemical properties of soils surrounding the Chalk Point Generating Station after the brackish water cooling tower began operations.

2: MATERIALS AND METHODS

2.1. Foliar Salt Tolerance Studies

Field experiments with foliar salt applications to corn and soybeans were conducted from 1973 to 1977 on a Monmouth fine sandy loam soil at the University of Maryland's Tobacco Experimental Farm near Upper Marlboro, Maryland. The same cultivars of corn, 'Pioneer 3369A,' and of soybeans, 'York,' were used in all experiments. The experimental plots

were fertilized and limed according to soil test recommendations each year with NH_4NO_3, ordinary superphosphate, K_2SO_4, and dolomitic limestone. The foliar salt treatments in 1973 were applied one time per week; however, the 1974-1977 treatments were applied as salt spray mists 5 days per week using a self-propelled sprayer at weekly salt deposition rates which varied from 0 to 22.2 kg/ha/wk. A ground speed of 8 km/hr was utilized for all spray treatments. The treatments were initiated after plant establishment and continued for 8 weeks. The salt source in 1973 and 1974 was NaCl; however, the 1975, 1976 and 1977 studies utilized brackish water from the Unit No. 3 cooling tower at Chalk Point with total dissolved solid concentrations which averaged 11.3, 20.0 and 26.2 PPT, respectively. In all experiments, spray booms were adjusted to approximately 0.5 m above plant tops. Nozzles (Conejet TX1SS, Agrotec Inc., Salisbury, MD) were used which delivered a hollow cone spray pattern of saline aerosol droplets which averaged 100 microns size range, comparable to the mass median diameters of droplets being emitted from the Unit No. 3 cooling tower at Chalk Point (2,19). A randomized, complete block design with four treatment replications was used in all experiments. Experimental units were four plant rows 7.6 m in length and spaced 102 cm apart. Treatments were applied to the two center rows, and the outside rows served as border rows to reduce drift contamination. Corn and soybean plants were thinned to plant populations of approximately 50,000 and 330,000 plants/ha, respectively. Corn leaf samples were collected at tasseling and soybean leaf samples were collected at flowering from the two treatment rows. Entire leaves from 6 to 8 plants per plot was excised at the point of ear attachment on corn and the entire leaf canopy was removed from 12 soybean plants per plot. The foliage samples were rinsed in deionized water, oven-dried at 60 C for 72 hours, then ground in a Wiley mill to pass a 1 mm screen. After digestion of the plant tissue by a $HClO_4$-HNO_3 technique, the samples were analyzed for P, K, Ca, Mg, and Na with a five-channel autoanalyzer. Chloride in the plant tissue was analyzed by potentiometric titration with $AgNO_3$ employing a chloride specific ion electrode (20). The leaf elemental data were used to calculate metabolic index values for the plant tissue by equation 1 (21). Grain

$$\text{Metabolic Index} = \frac{\% P + \% K + \% Ca + \% Mg}{\% Na + \% Cl} \qquad [1]$$

yields were determined on 6.1 m of the two center plot rows for each crop and all yields were corrected to 12.5% moisture.

Data for the individual parameters were examined annually for statistical significance ($p < 0.05$) using procedures outlined for a randomized complete block design (22). At the completion of the series, means from the five individual studies for a given parameter were combined using procedures outlined for polynomial regression analyses (19). Polynomial regression analyses were conducted for leaf sodium and chloride contents, metabolic index and yields vs. salt deposition rates for the two crop species. The yield data were expressed as percent of non-treated controls. Polynomial regression analyses were also performed on yields vs. leaf sodium, leaf chloride and metabolic index values for the two crop species.

2.2. Cooling Tower Salt Drift Monitoring Study

A field crop and soils monitoring study to examine salt drift

deposition from the Chalk Point Generating Station, operated by the Potomac Electric Power Company and located in southern Maryland, was established in 1973 (10,25). The installation contains two coal-fired 330 MWe units (Units No. 1 & 2) which employ once-through cooling, and two oil-fired 660 MWe units (Units No. 3 & 4) which utilize natural draft cooling towers. Brackish water (3-14 PPT total dissolved solids) from the Patuxent River is circulated in the cooling towers and is used in wet-scrubbers in the two larger furnace stacks. Intermittent operation of Unit No. 3 was initiated in April, 1975 and Unit No. 4 is scheduled for operation in the 1980's. The maximum rate of drift loss from each cooling tower was set at 0.002% of the circulation rate of 990,000 liters/min (2,11,25).

A network of 12 monitoring sites was established in 1973 surrounding the power plant (Fig. 1). Sites were located at approximately 1.6, 4.8, and 9.6 km in the north, east, south, and west directions from the plant. The 0.16 ha sites were subdivided for agricultural species, botanical species, and soils research. Three five-row plots each of corn ('Pioneer 3369A') and soybeans ('York') were planted annually from 1973 to 1978. Individual plots were 7.6 m long with row spacings of 102 cm. All plots were fertilized according to soil test recomendations for each soil type with fertilizer materials as discussed in the foliar salt tolerance experiments. Weeds were controlled by a combination of mechanical cultivations and the application of preemergence herbicides

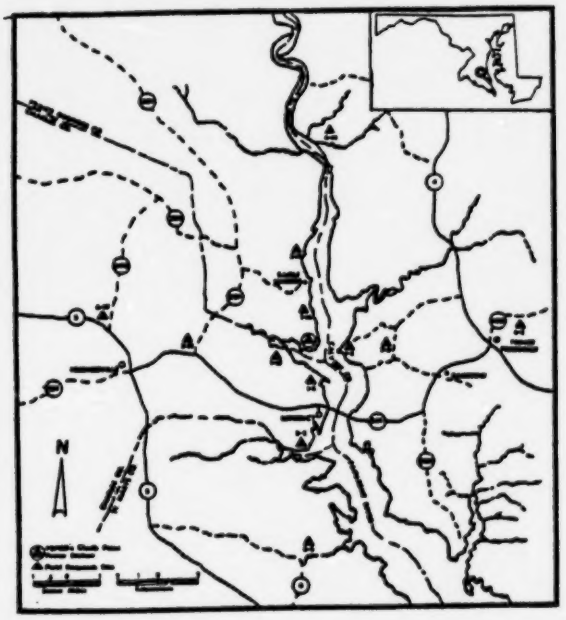

Figure 1. Location of twelve permanent monitoring sites used for crops and soils investigations of the effects of saline aerosol drift from the natural draft brackish water cooling tower at Chalk Point, Md.

at recommended rates. Foliage samples were collected and analyzed as previously described. Grain yields were determined on 6.1 m lengths of the three center rows of each plot and corrected to 12.5% moisture.

Crops data collected in 1973 and 1974 were considered as baseline. Statistical comparisons were conducted between baseline data and combined postoperative data of 1975 through 1978. All data were tested for homogeneity of variance (23). A factorial design analysis of variance with three factors: monitoring period, distance, and direction from the power plant, was conducted on all data (22). Mean separation was accomplished using procedures discussed by Duncan (24).

Soil samples were collected each year from areas 9 m x 9 m in size at each of the 12 research sites (Fig. 1) which were maintained as undisturbed soils research plots over the study period. The soils research plots were subdivided into nine 3 m x 3 m sectors and core samples from 0-15 cm depth were analyzed for soil reaction (pH), extractable P and Na, and electrical conductivity (E.C.) in the Soil Testing Laboratory at the University of Maryland, College Park, Maryland, employing autoanalyzer methods. Statistical analyses were conducted on the soils data to determine if significant changes had occurred in the individual parameters over the monitoring period. A factorial design with distance, direction and time was utilized. Least significant differences (LSD) values were calculated for each parameter where significance was found at $p < 0.05$ (22).

3: RESULTS AND DISCUSSION

3.1. Tolerance to Foliar Applied Salts

The response of corn and soybean plants to saline aerosol mist treatments were somewhat varied from year to year depending on the salt application rates and environmental conditions during the growing seasons. However, the interval between initiation of the mist treatments and the first symptom appearance was consistantly shorter for soybeans than corn which suggest that juvenile soybean plants are more susceptible than juvenile corn plants to airborn salt. Foliar injury from saline aerosol treatments on juvenile soybeans typically occurred first on younger leaf tissue as cuppings of leaf margins, extensive interveinal chlorosis and necrotic lesions along the margins. As the soybean plants matured, the symptoms were more prominant on the older leaves in the lower portions of the canopy giving the plants a drought-stressed appearance (9). Foliar injury from saline aerosol treatments on corn was exhibited primarily on fully expanded leaves. Tip portions of the more mature corn leaves displayed massive chlorisis with intermittent interveinal chlorosis extending back from the tips thus producing a speckled appearance. As the corn plants matured, the amounts of chlorotic tissue progressively increased with each succeeding leaf and the chlorotic areas on the older leaves became necrotic. Thus, with regards to general symptom development, salt injury symptoms on corn became progressively more pronounced with plant age, whereas, the soybeans appeared to recover from early injury and displayed only minor evidences of foliar injury on the upper portions of the canopy after eight weeks of treatments.

3.2. Uptake of Foliar Applied Salts

The application of foliar salts induced significant differences in sodium and chloride contents in leaves collected from all studies involving both crops conducted over the five-year period. Summaries of the chloride uptake relationships in the corn and soybean leaf samples obtained from the five studies are listed in Table 1. The chloride levels in control plants averaged 0.20 and 0.06% for corn and soybeans, respectively. At very low salt deposition rates, the rates of chloride buildup in corn and soybean leaves appear similar. With progressively higher salt deposition rates, the patterns for chloride accumulation in the two crop species differed. The rate of chloride accumulation appeared to decline in corn with progressively higher salt deposition rates whereas the rates of chloride accumulation in soybeans appeared to increase with an increase in salt deposition rates up to about 14 kg/ha/wk then rapidly declined with subsequent increases in salt deposition. Experimental conditions and/or the types of salt sources utilized influenced the patterns for chloride accumulation in both crops. The 1976 data for corn were excluded from the regression analyses for chloride due to wide variability in plant growth and productivity among the plots in the study. Total precipitation amounts for the months of June and August, 1976 were 66 and 52%, respectively, below the long term average monthly values for the region.

Summaries of the sodium uptake relationships in corn and soybean leaves from the five investigations are also shown in Table 1. Means for control plants not exposed to saline aerosol mist treatments were similar for both species and averaged approximately 0.10 and 0.09% for corn and soybeans, respectively. From an overall perspective, the response for sodium uptake in corn per unit salt deposition was approximately twice that for soybeans. The sodium data for corn conformed to a linear relationship ($r = 0.94$) whereas the sodium data for soybeans conformed to a nonlinear relationship ($r = 0.88$) with progressively higher sodium contents with increased salt deposition rates.

The impact of salt deposition on the metabolic index values are summarized in Table 1 for corn and soybeans. Significant reductions in metabolic index values were observed in all five studies involving both crop species with increased salt deposition rates. Metabolic index values for corn plants not exposed to saline aerosol mist treatments averaged 10.6 whereas the average metabolic index value for control soybean plants was 30.8. Very low salt deposition rates produced faster reductions in the metabolic index values in soybeans than in corn. The rates of reduction in metabolic index values at high rates of salt deposition appeared similar for the two crop species. Correlation coefficients (r) for metabolic index values (Table 1) for both crops suggest that the results were influenced by factors such as environmental conditions and salt sources. However, the data for each individual study appeared to conform to the overall relationships quite well considering the number of influencial factors present in each study. These general relationships could be quite useful in attempting to assess the general impact of saline aerosol drift on these two crop species, especially in areas near operating cooling towers where no absolute control plants would be possible without artificial means to exclude the saline aerosol drift.

Table 1. Summary of regression analyses of leaf sodium, leaf chloride, metablic index values and yields of corn and soybeans vs. salt deposition rates.

Parameter	Corn		Soybeans	
	Mathematical Relationship	Correlation Coefficient (r)	Mathematical Relationship	Correlation Coefficient (r)
Na (%)*	$\hat{Y}_c = 0.099 + 0.024X$**	0.94	$\hat{Y}_{sb} = 0.086 + 0.011X + 0.0006X^2$	0.88
Cl (%)*	$\hat{Y}_c = 0.20 + 0.07X - 0.001X^2$	0.95	$\hat{Y}_{sb} = 0.059 + 0.073X + 0.004X^2 - 0.0004X^3$	0.95
Metabolic Index	$\hat{Y}_c = 10.61 - 1.52X + 0.085X^2$	-0.84	$\hat{Y}_{sb} = 30.8 - 8.86X + 1.42X^2 - 0.06X^3$	-0.72
Yields (%)***	$\hat{Y}_c = 97.9 - 1.94X$	-0.93	$\hat{Y}_{sb} = 103.5 - 1.73X$	-0.90

* Leaf Na and Cl expressed on dry weight basis.

** X equals salt deposition rate in kg/ha/wk.

*** Yields expressed are % of non-treated controls.

The background saline aerosol drift for the region in which these studies were conducted would be expected to be typical of the levels found in a broad range of coastal environments. The range in salt deposition values for the region was 6.6 to 70.1 mg/m^2-month for sodium and 8.6 to 179.4 mg/m^2-month for chloride and the average monthly sodium and chloride deposition rates for the region over the period spanned by the investigation were 27.9 mg/m^2-month and 55 mg/m^2-month, respectively (11). Rainfall sodium and chloride values average 0.51 ppm and 1.13 ppm, respectively, which were consistant with values previously reported (26).

3.3. Impact of Foliar Applied Salts on Grain Yields

Relationships summarizing the impact of the saline aerosol treatments on grain yields for corn and soybeans in the five investigations conducted over the 1973-1977 growing seasons are included in Table 1. Yields of both crop species were found to be significantly ($p < 0.05$) reduced by the treatments (0 to 22.2 kg/ha/wk) imposed during the 1973 and 1974 studies. The treatments (0 to 6.6 kg/ha/wk) imposed in the 1975-1977 studies were designed to simulate conditions which have been projected as being representative of salt depositional patterns for regions adjacent to brackish water cooling towers (2,19). The yield results from both crops most appropriately fit linear relationships. The correlation coefficients for both sets of data indicate some variability in the results which could be attributed to variation in environmental conditions as previously discussed. However, considering the range of environmental conditions under which the studies were conducted and the variations in treatments imposed, correlation coefficients (r) of -0.93 for corn and -0.90 for soybeans support the general conclusion that saline aerosol drift from cooling towers could cause substantial impacts on the productivity of there two crops, especially at high salt deposition rates. At very low salt deposition rates, similar to the 1975-1977 studies, there was greater impact on corn than on soybeans. Considering that the intercept ($a = 97.9$) was very close to the theoretical intercept value of 100 for zero salt deposition on corn, salt deposition rates as low as 2 kg/ha/wk could induce yield reductions in corn of approximately 5%. For soybeans, salt deposition rates greater than 3 kg/ha/wk were required to reduce yields below the controls and some 5 kg/ha/wk were required to reduce yields by 5%. Therefore, it would appear that productivity in corn would be impacted to a greater degree by saline aerosol than in soybeans over a broad range in salt deposition rates.

Considering the improvements in the technology for controlling salt emissions from cooling towers and the concern for minimizing environmental impact near emission sources, it would be highly unlikely that salt deposition rates in excess of a few kg/ha/wk would be observed outside the immediate environment of the power plant (2,3). As a practical matter, yield reductions of perhaps 5 to 10% would be the maximum amounts one would anticipate even under the most adverse conditions. From the results in these studies, one would conclude that soybeans would be a more logical choice than corn for agricultural production near emission sources for saline aerosols.

3.4. Predicting Yield Losses Near Saline Aerosol Emission Sources

Using the available data regarding leaf sodium and chloride contents, metabolic index values and yields expressed as percent of controls, mathematic relationships were determined for predicting yield losses from corn and soybeans under the influence of saline aerosol drift (Table 2). The relationships which exhibited the highest correlation coefficients for both crops involved linear relationships with leaf chlorides. For corn, the relationship predicts a 35.5% reduction in yield for plants which exhibit tissue chloride contents of 1.0% on a dry weight basis. Soybean plants which contain 1.0% chloride in the leaves would have yields reduced 20% below control plants. The relationships between tissue sodium contents and yields of both crops appear comparable to those involving chloride. Corn and soybean plants exhibiting 1.0% sodium would be projected to have yields reduced approximately 64 and 58%, respectively, below yields for control plants not exposed to saline aerosol drift. The use of metabolic index values to predict yield losses in corn and soybeans would be comparable to the use of either sodium or chloride contents for corn but more variable than either element for use on soybeans. The use of metabolic index values appear to have no major advantage over either sodium or chloride alone for predicting yield losses in corn and soybeans.

The data from which the relationships shown in Tables 1 and 2 were obtained represented single cultivars of corn and soybeans grown under several environmental conditions and salt sources. Considering that different cultivars of the same species will most probably vary in their abilities to accumulate sodium or chloride, there may be some variability in the accuracy of the relationships shown for general use among cultivars of corn and soybeans. Further studies would be necessary to establish the utility of these relationships over a wide range of cultivars and environmental conditions. Considering that the productivity of corn and soybeans can be affected by a wide range of environmental and cultural parameters, perhaps the greatest utility of the relationships shown in Tables 1 and 2 would be to eliminate salt deposition as a causal factor in certain situations, especially if sodium and chloride levels in the impacted vegetation were within typical baseline values cited in the present studies.

3.5. Impact of Saline Aerosol Emissions from Chalk Point on Corn and Soybeans

The results in Table 3 summarize the leaf sodium, chloride and metabolic index values and yield data for corn and soybeans which were grown at 12 research sites near the Chalk Point Generating Station over the period 1973 through 1978. With respect to changes in leaf chemistry, there were no significant changes in either crop for leaf sodium and chloride contents or metabolic index values after the brackish water cooling tower began operations. There were very slight increases in sodium levels in soybeans and increased chloride levels in both species after Unit No. 3 began operating. However, there appeared to be a rather uniform distribution of the salts throughout the region with the results being very close to background for both crops (11). The metabolic index data confirmed the sodium and chloride results with trends for lower index values appearing for soybeans only. The quantities of salts emitted from Chalk Point during the 1975-78 growing

Table 2. Predicting corn and soybean yields from the leaf sodium, leaf chloride and metabolic index values.

Impact Parameter (X)	Corn Yields (Y_c)** Mathematical Relationship	Corn Yields (Y_c)** Correlation Coefficient (r)	Soybean Yields (Y_{sb})** Mathematical Relationship	Soybean Yields (Y_{sb})** Correlation Coefficient (r)
Cl (%)*	Y_c=105-35.5X	-0.91	Y_{sb}=104-20X	-0.79
Na (%)*	Y_c-102-63.7X	-0.81	Y_{sb}=105-57.9X	-0.79
Metabolic Index	Y_c=58.8+7.3X-0.32X^2	0.86	Y_{sb}=67.2+4.9X-0.21X^2	0.56

* Leaf sodium and chloride contents expressed on a % of dry weight basis.

** Yields of corn and soybeans are based on % of non-treated controls.

Table 3. Effect of saline aerosol emissions from Chalk Point on corn and soybean leaf tissue sodium, chloride, metabolic index values and grain yields at three distances from the power plant before and after Unit No. 3 operations.

Monitoring Period	Corn				Soybean			
	Distance, Km			Monitoring period mean	Distance, Km			Monitoring period mean
	1.6	4.8	9.6		1.6	4.8	9.6	
	% Na				% Na			
Baseline ('73-'74)	0.10a*	0.10a	0.10a	0.10a**	0.09a*	0.09a	0.09a	0.09a**
Postoperation ('75-'78)	0.10a	0.09a	0.09a	0.09a	0.10a	0.10a	0.10a	0.10a
	% Cl				% Cl			
Baseline ('73-'74)	0.14a	0.17a	0.18a	0.16a	0.06a	0.07a	0.06a	0.06a
Postoperation ('75-'78)	0.17a	0.19a	0.20a	0.19a	0.05a	0.10a	0.08a	0.08a
	Metabolic Index				Metabolic Index			
Baseline ('73-'74)	15.7a	13.7a	12.3a	13.9a	32.3a	28.2a	30.0a	30.1a
Postoperation ('75-'78)	13.6a	13.0a	13.2a	13.2a	30.7a	26.8a	28.3	28.5a
	Grain yield, kg/ha				Grain yield, kg/ha			
Baseline ('73-'74)	8078a	7664a	8310a	8009a	2144a	2092a	2317a	2182a
Postoperation ('75-'78)	6322b	6642b	7025b	6724b	2466a	2045a	2196a	2055a

* Distance means within and between monitoring periods followed by the same letter are not significantly different ($p < 0.05$).

** Monitoring period means across all distances followed by the same letter are not significantly different ($p < 0.05$).

seasons were of such low magnitude that the tissue sodium and chloride levels in crops growing at or beyond 1.6 km remained unchanged. The yields of corn observed during the 1975-78 growing seasons were significantly below the yields observed during 1973-74. From the leaf chemistry results, the reduction in corn yields appear to be caused by factors other than salt emissions. The reduction in corn yields observed after the brackish water cooling tower began operation appear to be related to rainfall amounts and distribution. Soybean yields generally show less variation than corn yields during periods of mild moisture stress.

3.6. Impact of Saline Aerosol Emissions From Chalk Point on Soil Chemical Parameters.

The results in Figure 2 summarize information regarding four

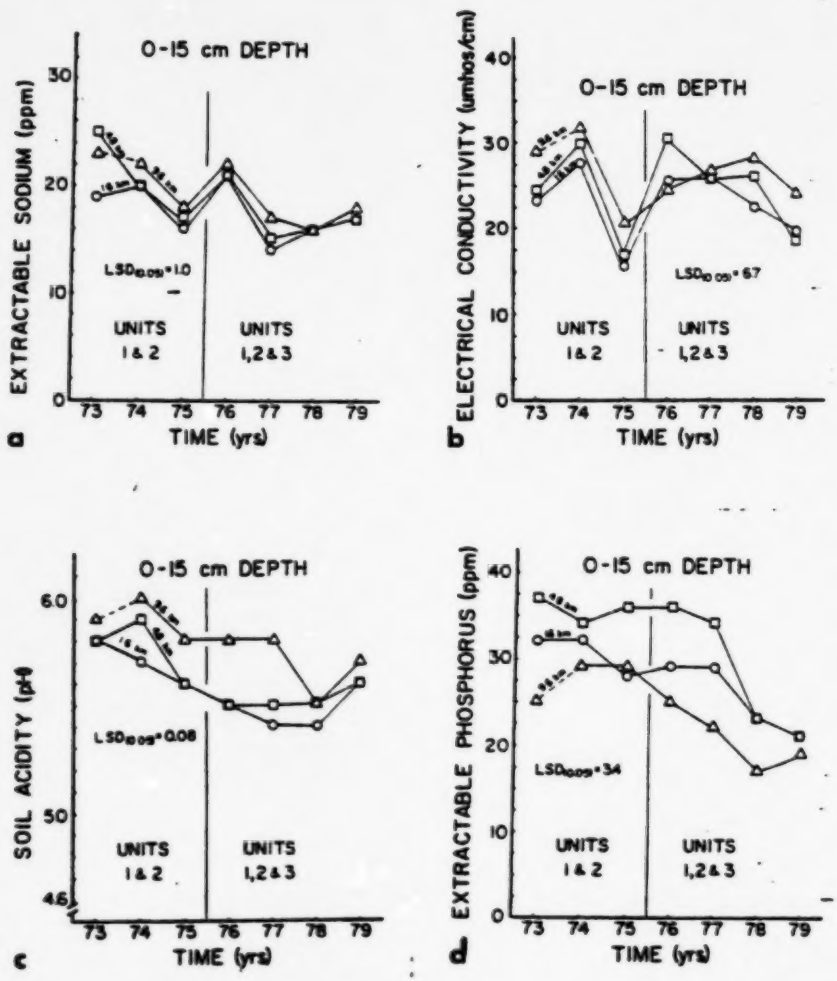

Fig. 2. Changes in soil chemical parameters in samples collected from 0-15 cm depth from sites located within 1.6, 4.8 and 9.6 km distances from Chalk Point, Md., over the period 1973 through 1979: (a) extractable sodium, (b) electrical conductivity, (c) soil acidity and (d) extractable phosphorous.

chemical parameters determined in soil samples collected from 0-15 cm depth at twelve research sites near Chalk Point. The results illustrate changes in the means averaged over the four sites within the 1.6, 4.8 and 9.6 km radii from the Chalk Point facility over the period May, 1973, through May, 1979. Since Unit No. 3 at Chalk Point did not become fully operational until July, 1975, this allowed three sampling dates prior and four sampling dates after the brackish water cooling tower began normal operations. The LSD values reported in each graph can be used to compare means for the three distances within the same sampling date or changes in means within a given distance across sampling dates.

Extractable sodium. The levels of estractable Na in the soils near the Chalk Point Generating Station are summarized in Fig. 2a. Although the results were significantly different at $p < 0.05$, there was a general trend for lower levels of extractable Na with time at all three distances. The initiation of Unit No. 3 operations after the May, 1975, sampling date appears to have had no effect on Na levels in the soil. These results suggest that the quantities of rainwater percolating through the soils were sufficient to prevent a general buildup of Na in the soils in the region. The general downward trends for sodium suggest that the amounts of Na supplied in fertilizer materials prior to the establishment of the monitoring sites were in sufficient amounts to elevate the levels of extractable Na in the soils. After the fertilizer additions were haulted in the spring of 1973, the soils appear to be returning to lower equilibrium levels for Na.

Electrical conductivity (E.C.). The changes in E.C. values, a measure of the total salinity of the soils, near the Chalk Point Generating Station with time are summarized in Fig. 2b. These results show very wide year to year variation, especially for 1975, prior to initiation of Unit No. 3 operations. Since there were only minor differences among the soils at the three distances in terms of their overall drainage characteristics, small differences in total salinity were expected. As observed in the previous section regarding Na, there appears to be a gradual decline in the E.C. with time which suggest that the practice of supplying fertilizer materials before monitoring was initiated perhaps elevated the total soil salt levels. Since 1973, the soils have been returning to their natural equilibrium levels with regards to total salts. The changes at 9.6 km appear similar to those at 1.6 km which suggest that the Unit No. 3 cooling tower has had no appreciable impact on the salinity of the soil at or beyond the distance of 1.6 km.

Soil acidity (pH). The results in Fig. 2c summarize changes in the soil acidity over time with increased distance from the Chalk Point Generating Station. There were significant changes in soil acidity at all three distances from the power plant over the seven years of monitoring. There were general declines in soil pH values showing increased acidity levels at all distances prior to Unit No. 3 operations. The declining pH values were characteristic of agricultural soils which had been previously managed with liming materials to reduce the effects of soil acidity on crop productivity (28). The rate of pH shift would be influenced by the overall buffer capacities of the soils and the amounts of hydrogen ions interacting with the soil solutions. Under normal farming operations, certain types of fertilizers such as sulfur and ammonium sulfate and other hydrogen ion suppliers cause the soil pH values to decrease. Also, crop residues undergoing

decomposition release organic acids in the soils. Acid materials are also applied to the soils via rainfall and the overall topic of acid rainfall has commanded a great deal of attention in very recent months. Therefore, the observation of a general decline in soil pH would be expected from these soils since each of the research sites, except 1-N, were established within areas under active management for crop production.

The impact of emission from Chalk Point, especially sulfur and nitrogen oxides, on rainfall acidity has been investigated (29,30). Rainwater pH values as low as 4.0 have been observed in the vicinity of Chalk Point during the periods which coincided with the present studies. Rainfall pH values observed during the pre Unit No. 3 monitoring phase averaged 5.65±0.75 during 11/75 - 4/75. After Unit No. 3 became operational, rainfall pH values averaged 5.29±0.72 during 7/57 - 4/76, 5.28±0.66 during 5/76 - 3/77, and 5.76±0.64 during 4/77 - 10/77. The continuous impact of rainfall with acidity levels comparable to those cited above on soils with a low buffer capacity or cation exchange capacity, such as the light textured soils near the Chalk Point facility, could induce the progressive declines in soil pH observed in Fig. 2c.

Extractable phosphorus. The results in Fig. 2d illustrate the changes in the concentrations of extractable phosphorus observed in soils with increased distance from Chalk Point over the period May, 1973, through May, 1979. Significant declines were observed in the phosphorus concentrations with time at all three distances. The declines were initiated prior to Unit No. 3 operations; however, the rate of change observed at the 4.8 and 9.6 km sites appeared to increase after Unit No. 3 became operational. The progressive decreases in extractable phosphorus observed in Fig. 2d can be related to several factors. As evidenced by the soil pH results in Fig. 2c, the progressive decrease in soil pH provided an environmental for the rapid fixation of the extractable phosphorus by various metal ions which were (a) being deposited in more soluble forms in the rainfall and dustfall (27) and (b) the general increase in the availability of metals such as Fe, Al and Mn in soils with the decrease in soil pH. The fixation of the phosphorus by such metals is caused by the formation of less soluble forms. The H_2PO_4 ion will also react with hydrous oxides of these elements thus further reducing the levels of available phosphorus (28).

ACKNOWLEDGEMENTS

This research was sponsored by the Maryland Department of Natural Resources - Power Plant Siting Program and coordinated through the Water Resources Research Center of the University of Maryland, College Park, Maryland. Statistical services were provided by the Computer Science Center of the University of Maryland, College Park, Maryland. Appreciation is extended to Dr. John Foss, Professor of Soil Science at the University of Maryland, for his assistance in classifying the soils at the research sites.

REFERENCES

1. Roffman, A., et al., The State of the Art of Saltwater Cooling Tower for Steam Electric Generating Plants, USAEC Report WASH 1244, Westinghouse Electric Corp., Feb. 1960.

2. Davis, E. A., Environmental Assessment of Chalk Point Cooling Tower Drift and Vapor Emisssions, Md. Dept. of Natural Resources Power Plant Siting Program, PPSP-CPCTP-28, 1979.

3. Israel, G. W. and T. J. Overcamp, Drift Deposition Model for Natural Draft Cooling Towers, Cooling Tower Environment - 1974, ERDA Symposium Series, CONF-740302, pp. 614-628, 1975.

4. Hindawi, I. J., L. C. Raniere and J. A. Rea, Ecological Effects of Aerosol Drfit from a Saltwater Cooling System, USEPA, Ecological Research Series, EPA-600/3-76-078, 1976.

5. Nicholas, G. W. and D. M. Sopocy, Evaluation of Cooling Tower Environmental Effects, Combustion, Vol. 46, pp. 34-41, 1974.

6. Freudenthal, H. D., J. E. Rubinstein and A. Uzzo, Effects of Pathogenic and Toxic Materials Transplanted via Cooling Device Drift, Vol. 1. Technical Report, USEPA, EPA-600/7-79-25/a, pp. 208, 1979.

7. Edmonds, P. R., H. A. Roffman and R. C. Maxwell, Some Terrestrial Considerations Associated with Cooling Towers Systems for Electric Power Generation, Cooling Tower Environment - 1974, ERDA Symposium Series, CONF-740302, pp. 393-407, 1975.

8. Wienenfeld, R. P., L. R. Hossner and E. L. McWilliams, Effects of Evaporative Salt Water Cooling Towers on Salt Drift and Salt Deposition on Surrounding Soils, J. Environ. Qual., vol. 7, pp. 293-298, 1978.

9. Mulchi, C. L. and J. A. Armbruster, Effects of Salt Spray on the Yield and Nutrient Balance of Corn and Soybeans, Cooling Tower Environment - 1974, ERDA Symposium Series, CONF-740302, pp. 379-392, 1975.

10. Mulchi, C. L., D. C. Wolf, J. E. Foss, J. A. Armbruster, C. R. Curtis and G. Israel, Potential Environmental Effects Associated with Brackish Water Cooling Towers at Chalk Point, Maryland, Environmental Chemistry and Cycling Processes, DOE Symposium Series 45, CONF-760429, pp. 329-346, 1978.

11. Mulchi, C. L., D. C. Wolf and J. A. Armbruster, Cooling Tower Effects on Crops and Soils - Post Operational Report No. 4, Md. Dept. of Natural Resources - Power Plant Siting Program, PPSP-CPCTP-29, pp. 215, 1979.

12. Curtis, C. R., T. L. Lauver and B. A. Francis, Foliar Salt in Native Vegetation: Seasonal Variation, Environ. Pollut., vol. 12, pp. 69-80, 1977.

13. Lauver, T. L., C. R. Curtis, G. Patterson and L. W. Douglas, Effects of Saline Cooling Tower Drift on Seasonal Variations of Sodium and Chloride Concentrations in Native Perennial Vegetation, Cooling Tower Environment - 1978 - A Symposium on Environmental Effects of Cooling Tower Emissions. Md. Dept. of Nat. Resources - Power Plant Siting Program, PPSP-CPCTP-22, pp. 1-49-64, 1978.

14. Francis, B. A., Effects of Simulated Cooling Tower Drift on Woody Species, Md. Dept. of Nat. Resources - Power Plant Siting Program, PPSP-CPCTP-17, pp. 69, 1977.

15. Taylor, F. G., Jr., L. K. Mann, R. C. Dahlman and F. L. Miller, Environmental Effects of Chromium and Zinc in Cooling-Water Drift. Cooling Tower Environment - 1974, ERDA Symposium Series, CONF-740302, pp. 408-426, 1975.

16. Parr, P. D., F. G. Taylor, Jr. and J. J. Beauchamp, Sensitivity of Tobacco to Chromium from Mechanical Draft Cooling Tower Drift, Atmos. Environ., vol. 10, pp. 421-423, 1976.

17. Rochow, J. J. Measurements and Vegetation Impact of Chemical Drift from Mechanical Draft Cooling Towers, Environ. Sci. and Tech., vol. 12, pp. 1379-1383, 1978.

18. McCune, D. C., D. H. Silberman, R. H. Mandl, L. H. Winstein, P. C. Freudenthal and P. A. Giardina, Studies on the Effects of Saline Aerosols of Cooling Tower Origin on Plants, J. of Air Poll. Control Assoc., vol. 27, pp. 319-324, 1977.

19. Israel, G. W., T. J. Overcamp, and W. J. Pringle, A Method to Measure Drift Deposition from Saline Natural Draft Cooling Towers, Atmos. Environ., vol. 11, pp. 123-130, 1977.

20. LaCroix, R. L., D. R. Keeney, and L. M. Walsh, Potentiometric Titration of Chloride in Plant Tissue Extracts Using the Chloride Ion Electrode, Soil Sci. Plant Anal., vol. 1, pp. 1-6, 1970.

21. Button, E. F., Metabolic Index as a Diagnostic Tool in Tree Health Determination, Conn. Dept. of transportation, Bureau of Highways, Highway Res. Record No. 355, pp. 6-8, 1969.

22. Snedecor, G. W. and W. G. Cochran, Statistical Methods, 6th ed., Iowa State Univ. Press, Ames, Iowa, 1967.

23. Cochran, W. G., The Distribution of the Largest of a Set of Variables as a Fraction of their Total, Ann. Engenics, vol. 11, pp. 47-52, 1941.

24. Duncan, D. B., Multiple Range and Multiple F Tests, Biometrics, vol. 11, pp. 1-42, 1955.

25. Pell, J., The Chalk Point Cooling Tower Project, Cooling Tower Environment - 1974, ERDA Symposium Series, CONF-740302, pp. 88-127, 1975.

26. Jung, C. E. and P. E. Gustafson, On the Distribution of Sea Salt Over the United States and Its Removal by Precipitation, Tellus, vol. 9, pp. 88-127, 1975.

27. Mastradone, P. J., Trace Metal Deposition on Agricultural Crops Near the Chalk Point Generating Station, Md. Dept. of Natural Resources - Power Plant Siting Program, PPSP-CPCTP-33, 1979.

28. Buckman, H. O. and N. C. Brady, The Nature and Properties of Soils, 6th ed., The Macmillan Co., New York, 1961.

29. Li, Ta-Yung and H. E. Landsberg, Rainwater pH Close to a Major Power Plant, Atmos. Environ., vol. 9, pp. 81-88, 1975.

30. Mulchi, C. L., D. C. Wolf and J. A. Armbruster, Cooling Tower Effects on Crops and Soils - Post Operational Report No. 3, Md. Dept. of Nat. Resources - Power Plant Siting Program. PPSP-CPCTP-23, pp. 98, 1978.

PB82-228412

SECTION 316(b) AND MODELING OF ICHTHYOPLANKTON ENTRAINMENT

D. S. Vaughan
Environmental Sciences Division
Oak Ridge National Laboratory
Oak Ridge, Tennessee 37830

ABSTRACT

Section 316(b) of the Federal Water Pollution Control Act Amendments of 1972 requires the use of "best technology available for minimizing adverse environmental impacts" due to operation of intake systems by cooling water users such as steam electric power plants. One significant form of impact resulting from cooling water use is entrainment mortality of ichthyoplankton. Two basic modeling approaches were used to assess the impacts of ichthyoplankton entrainment, the "equivalent adult" method and age-structure models. Various assumptions and conventions associated with the equivalent adult method, which can lead to a serious underestimate of the potential loss of adults, are discussed. Possible methods for partially correcting some of these biases are suggested. The age-structure modeling approach suffers from fewer sources of bias than does the "equivalent adult" method, and provides a means for assessing long-term impacts of entrainment on fish populations. However, because of the difficulty in estimating density-dependent coefficients, ranges of estimates of long-term impacts on fish populations should be obtained.

1: INTRODUCTION

The Federal Water Pollution Control Act Amendments of 1972 (Public Law 92-500) prohibits the discharge of any pollutant into a water body unless authorized by permit. Section 316(b) of this Act requires the use of "best technology available for minimizing adverse environmental impacts" due to operation of intake systems by cooling water users such as steam electric plants. The U.S. Environmental Protection Agency interprets Section 316(b) to indirectly require closed-cycle cooling [1]. Closed-cycle cooling (e.g., cooling towers) will reduce the need for cooling water by approximately an order of magnitude. Entrainment is a major type of adverse impact that steam electric plants have on the aquatic environment and, in particular, on fish populations [2]. Fish drawn into the cooling water intakes of steam electric plants, and small enough to pass through the debris screens, are entrained in the condenser cooling system. Ichthyoplankton less than approximately 50 mm in length are usually susceptible to entrainment. The fraction of live fish entrained that are killed is known as entrainment mortality. In addition to a multitude of site-specific entrainment studies, both the accuracy [3] and precision [4] of entrainment mortality estimates have been examined.

Three competing sources of stress can result in entrainment mortality: (1) thermal, (2) biocidal, and (3) physical. A rapid rise in temperature occurs during passage through the condenser tubes, with a "maximum excess" temperature attained at the downstream ends of the tubes. Exposure to this maximum excess temperature continues during passage through the discharge system of the steam electric plant and is followed by decreasing excess temperature as an organism is carried through the thermal plume following discharge to the cooling water body [5]. Biocides such as calcium and sodium hypochlorite are sometimes used intermittently to control fouling organisms in the intake structures and condenser tubes [6]. Physical stresses experienced by entrained organisms include mechanical buffeting, acceleration, shear forces, and abrupt changes in hydrostatic pressure [7]. In addition, the concurrent effect of these three sources of stress can lead to an additional (synergistic or supra-additive) mortality beyond that predicted by separate assessment of the three causes of mortality [2].

This paper compares and contrasts two modeling approaches used to predict the effects of entrainment mortality on fish populations. First, the "equivalent adult" methodology is presented, emphasizing assumptions and conventions common to its use, as well as potential sources of biases or inaccuracies that result in errors in the estimated loss to the adult population. Some corrections to this methodology are suggested which will partially offset sampling and other biases. Second, an age-structure approach, which suffers from fewer biases than the "equivalent adult" method, is outlined. Biases resulting from this approach, and the problem of incorporating density-dependent mechanisms, are briefly discussed.

2: EQUIVALENT ADULTS METHODOLOGY

2.1. Introduction

A simple technique for estimating the number of adult fish that would have been produced if ichthyoplankton (fish eggs, larvae, and young juveniles) not been entrained was proposed by Horst [8] and modified by Goodyear [9]. However, as indicated below, various assumptions and conventions associated with this technique can lead to considerable inaccuracies (or biases) in estimates of the potential loss to adult population, and thus, it should be used only when it is not possible to use alternative methods because of lack of data.

2.2. Model Description

Horst [8] sets the loss to the adult population due to entrainment equal to the number of eggs, larvae, or juveniles entrained times the survival from the egg, larval, or juvenile stages, respectively, to the age when the fish species reaches sexual maturity. This method assumes that the population is in equilibrium and that an average female produces just enough eggs to replace herself. A sex ratio of one-to-one is often assumed.

Equations (13) through (16) in Horst [8] were used to derive the following equations for eggs,

$$N_a = S_e \cdot N_e = N_e \cdot (2/F) \quad , \qquad (1)$$

for larvae,

$$N_a = S_\ell \cdot N_\ell = N_\ell \cdot [2/(S'_e \cdot F)] \quad , \tag{2}$$

and for juveniles,

$$N_a = S_j \cdot N_j = N_j \cdot [2/(S'_e \cdot S'_\ell \cdot F)] \quad , \tag{3}$$

where N_e, N_ℓ, and N_j are the numbers of eggs, larvae, and juveniles entrained, respectively; N_a is the number of equivalent adults (at age of first maturity); S_e, S_ℓ, and S_j are the fractions normally surviving in the absence of entrainment from egg, larval, and juvenile stages to the age of first maturity, respectively; S'_e and S'_ℓ are the fraction surviving the duration of the egg and larval stages, respectively; and F is a measure of lifetime fecundity of a typical breeding pair.

Little insight is provided by this technique into long-term effects on fish populations, because it does not consider any compensatory mechanism which might partially offset losses over several generations. However, this technique also implicitly assumes that a reduction in adults in one generation does not reduce the number of spawning adults in future generations. This feedback mechanism in a real population would cause the impact due to a steam electric plant to become more severe with time (in the absence of compensation). Thus, results should only be used to provide very rough estimates (within an order of magnitude at best) of the potential severity of entrainment impact by a cooling water system.

2.3. Sources of Bias

Several sources of bias often overlooked in applications of the equivalent adult technique in 316(b) demonstrations [10] include estimation of daily concentration, gear avoidance, age of entrained life stages, partially identified or unidentified ichthyoplankton, and expected lifetime fecundity.

Pyne [11] showed that the maximum likelihood estimator of the average daily concentration, D, for n separate samples from Poisson-distributed organisms, collected with varying volumes, is

$$D^* = \sum_{i=1}^{n} N_i / \sum_{i=1}^{n} V_i \quad , \tag{4}$$

where N_i is the number of ichthyoplankton found in V_i m^3 of water strained in the i^{th} sample. In some 316(b) demonstrations, the daily concentrations of an ichthyoplankton life stage are calculated from

$$D' = (1/n) \cdot \sum_{i=1}^{n} D_i \quad , \tag{5}$$

where $D_i = N_i/V_i$ is the concentration observed in each sample during a day of sampling. In all likelihood, $D^* \neq D'$, although one estimate is not consistently larger or smaller than the other. Both estimators under assumptions of normality are biased (Ref. [12], Problem 35), but the bias for D' is n times the bias for D*. Furthermore, if one assumes that the sampling error for the volume is very small with respect to the sampling error for the counts and that the sampling error for the volume can be ignored, then both estimators are unbiased. However, in this case the variance of D* is still less than the variance of D', and thus D* is the preferred estimator.

A simple means for obtaining the annual entrainment estimate (E) for a life stage of a fish population can be calculated from the mean density (D_j^*) by

$$E = \sum_{j=1}^{r} D_j^* \cdot Q_j^* \quad , \tag{6}$$

where $Q_j^* = 86400 \cdot Q_j \cdot A_j$, the number of seconds in a day is 86400, Q_j is the average flow rate (vol/s) at the intake sampling station during each of the r sampling periods, and A_j is the number of days over which the average daily concentration and flow rate are applicable. Errors in estimating the average daily concentration will lead to errors in estimating the total number of entrained ichthyoplankton.

The problem of gear avoidance by ichthyoplankton, and the resultant underestimation of their abundance, has been addressed [13-18]. The use of night samples instead of day and night samples may partially compensate for the avoidance capability of ichthyoplankton when the avoidance behavior is sight-dependent, but may introduce error when true densities vary on a diel basis. This method does not compensate for net extrusion of eggs or smaller larvae, which would have an effect on abundance estimates similar to that of gear avoidance. Leithiser et al. [19] demonstrated that for cooling water velocities of 40 cm/s or less, a 1.0-m net was less efficient than a high volume pump, based on night samples. Their data indicate that a 1.0-m net was only 79 to 85% as efficient as a high volume pump. Hence, even after using night samples to correct for gear avoidance, considerable error in estimates of ichthyoplankton abundance may remain.

A significant source of bias from this technique results from "within stage" differences in egg, larval, and juvenile survival. Younger eggs, larvae, or juveniles have a lower probability of survival to adult stage than do older eggs, larvae, or juveniles, respectively. A rough correction for the larval stage can be made when that stage is divided into protolarval, mesolarval, and metalarval stages [10]. Knowledge of the age of distribution of entrained larvae (and eggs and juveniles) is critical because an individual juvenile is more likely to survive to the adult stage than an individual metalarva, and a single metalarva is more likely to survive to the adult stage than a single mesolarva. Although most ichthyoplankton entrained will be eggs and protolarvae, most of the potential loss to the adult population may result from the entrainment of less abundant older larvae and juveniles [9]. Horst's [8] method, as commonly applied, assumes that all ichthyoplankton entrained have just entered their particular life stage and have the whole life stage ahead of them with all its potential sources of mortality. By dividing the larval stage into three substages (protolarvae, mesolarvae, and metalarvae), this source of bias can be partially reduced.

Ignoring the egg stage for the moment, larvae and juveniles can be defined in terms of "equivalent protolarvae" as follows [10]:

$$N_p = E_p + \frac{E_m}{S_m'} + \frac{E_t}{S_t'} + \frac{E_j}{S_j'} \quad , \tag{7}$$

where N_p is the number of "equivalent protolarvae" resulting from entrained protolarvae (E_p), entrained mesolarvae (E_m), entrained metalarvae (E_t), and entrained juveniles (E_j). The survival to the three older stages from the protolarvae stage are given by S_m', S_t', and S_j', respectively.

Another approach to correcting for this source of bias would be to assume exponential mortality during the life stage and calculate the expected age of an individual larvae ($\bar{t}$) [20]:

$$\bar{t} = \frac{(1/p) - \exp(-p \cdot d) \cdot [d + (1/p)]}{1 - \exp(-p \cdot d)} \quad , \tag{8}$$

where d is the duration of the life stage in days, and p is the daily instantaneous mortality rate. The expected survival for an "average" individual of a life stage would then be given by

$$S^* = \exp(-p^* \bar{t}) \quad . \tag{9}$$

This expected survival (S^*) would then be used in place of the survival from the start of the life stage to the adult stage [S_e, S_ℓ, or S_j in Eqs. (1) through (3)].

Because some of the partially identified (to family and genus level), unidentified, or unidentifiable ichthyoplankton might belong to one of the species under study, a means of dealing with these ichthyoplankton in the model should be considered. The simplest method would be to distribute the partially identified ichthyoplankton proportionally among the identifiable species that fall within the genus or family level. Next the unidentified and unidentifiable ichthyoplankton should be distributed proportionally among all of the species, taking into account the distribution of partially identified ichthyoplankton from the previous step. This approach assumes that the partially identified and unidentified ichthyoplankton do not belong to any species for which immature individuals have not been described and which therefore constitute a separate taxon. If the various species (or sizes within a species) are differentially susceptible to sampling destruction, then the potential for introducing additional error is present.

The final source of bias to be discussed in this section concerns the fecundity term (F) which appears in Eqs. (1) through (3). Horst [8] defines F as "the fecundity of a breeding pair during their life." This definition has been open to varied interpretations. One approach has been to simply sum the female fecundity over all the mature age classes. This approach will significantly overestimate the lifetime female fecundity, since no adjustment has been made for adult mortality. Overestimating F will lead to an underestimate of S_e, S_ℓ, and/or S_j, as well as of the number of "equivalent adults" lost due to entrainment. Goodyear [9] suggests the following for estimating F:

$$F = \sum_{i=a}^{k} P_i \cdot S_i \cdot F_i \quad , \tag{10}$$

where a is the age of first maturity (or recruitment to the adult population), k is the oldest age class in the population, P_i is the fraction of females that are mature in age class i, S_i is the survival probability from recruitment to age class i, and F_i is the average fecundity of mature females of age class i.

2.4. Discussion of "Equivalent Adult" Method

Adjustments have been suggested to Horst's [8] "equivalent adult" method to correct for several sources of potential bias. In general, the greatest

effect (increase in impact projected) results from correcting for the age of the entrained ichthyoplankton. Two additional sources of bias may also tend to underestimate the losses as "equivalent adults." First, sorting efficiency is generally assumed to be 100%. If a sorter does not pick out all of the fish in a sample, then the estimated number of ichthyoplankton entrained will be low. Second, any entrainment occurring before or after the ichthyoplankton sampling season will also lead to an underestimate of the number of ichthyoplankton. Incorporating these adjustments with the "equivalent adult" method will frequently lead to an increase in impact estimates (e.g., Ref. [10]).

3: AGE-STRUCTURE APPROACH

3.1. Introduction

An alternative approach to assessing the effects of entrainment on fish populations is a full-scale life-cycle or age-structure approach. Unlike the "equivalent adult" method the entire population is considered. However, more detailed data are required, including (1) early life stage survival rates (egg, larval, and juvenile life stages), (2) age-class-specific fecundity per female, (3) age-class-specific sex ratios, (4) age of onset of sexual maturity, (5) proportion of mature females per age class, and (6) annual adult mortality by age class.

The age-structure model is subject to many of the same biases as the "equivalent adult" method, including the estimation of daily concentration of entrained ichthyoplankton, gear avoidance, and partially identified or unidentified ichthyoplankton. Calculating a conditional power-plant mortality rate, however, circumvents the problem of determining the age of an entrained life stage, while the age-structure formulation removes the necessity for estimating an expected lifetime fecundity. Furthermore, the age-structure model automatically reduces the population fecundity with time as future population levels are reduced. Intrinsically, the model allows for changes in age-structure with time. Finally, it is possible to include density-dependent functions for survival or fecundity terms to represent compensatory (or even depensatory) mechanisms.

3.2. Model Structure

The Leslie matrix or age-structure model was developed independently by Bernardelli [21], Lewis [22], and Leslie [23]. The Leslie matrix, M, was originally conceived as time-invariant and density-independent, projecting the age structure of a population, N, through time, t, most often in increments of one year. Thus

$$N(t+1) = M \cdot N(t) \quad , \tag{11}$$

where $M = \{a_{ij}\}$ is the Leslie matrix such that

$$a_{ij} = \begin{cases} B_j, & \text{for } i = 0 \\ S_j, & \text{for } i = j+1 \\ 0, & \text{otherwise} \end{cases} \quad , \tag{12}$$

and N(t) and N(t+1) represent the population age structures at times t and t+1, respectively. The last age class reproducing, or final age class considered, is denoted by k. The first row of M, given by B_j, contains measures

of the fecundity by age class j (j=0,1,...,k-1), while the subdiagonal elements of M, given by S_j, contain the annual survival rates for age class j (j=0,1,...,k-2). If N(0) is some initial population age structure, then the population age structure at any time t can be found by repeated application of Eq. (11); i.e.,

$$N(t) = M^t \cdot N(0) \quad . \tag{13}$$

Leslie [23] worked from the basic life table to determine the matrix elements. He defined B_j as "the number of daughters born in the interval t to t+1 per female alive aged j to j+1." He proceeded to define B_j operationally so as to spread the production of eggs over the duration of one time unit. Emlen [24] implicitly assumed that egg production occurs over a short duration of time immediately prior to the end of each time increment by setting

$$B_j = S_j \cdot m_{j+1} \qquad (j=0,1,\ldots,k-1) \quad , \tag{14}$$

where m_j is the number of eggs produced per individual in age class j. An alternate definition of B_j has been used [25-27]:

$$B_j = S_0 \cdot m_j \qquad (j=1,2,\ldots,k) \quad . \tag{15}$$

The expression given by Eq. (15) for fecundity implicitly assumes that egg production occurs over a short span of time immediately following the start of each time increment.

Vaughan and Saila [28] present an equation for determining the fraction of eggs which survive to the start of age class 1, S_0, based on Eq. (14), i.e.,

$$S_0 = \frac{\lambda}{m_1 + \sum_{i=1}^{k-1} \left[\left(m_{i+1} / \lambda^i \right) \left(\prod_{j=1}^{i} S_j \right) \right]} \quad , \tag{16}$$

where λ is the maximal eigenvalue of the Leslie matrix. When $\lambda = 1$, the population is at equilibrium. A similar equation can be derived for a population using the fecundity measure in Eq. (15) and the method described in Vaughan and Saila [28], i.e.,

$$S_0 = \frac{\lambda}{m_1 + \sum_{i=2}^{k} \left[\left(m_i / \lambda^{i-1} \right) \left(\prod_{j=1}^{i-1} S_j \right) \right]} \quad . \tag{17}$$

Note that Eqs. (16) and (17) are equal for all values of the maximal eigenvalue and will produce the same estimates for S_0. These estimates were used in the "equivalent adult" method to obtain estimates of survival from a given life stage to age class 1, when survival in the earlier stages are known.

3.3. Outline of Approach

Basically, this approach requires data input at one of two possible starting points. The first starting point requires both an estimate of the number of eggs, larvae, and/or juveniles entrained; the natural conditional mortality rates for these early life stages; and an estimate of the sexually mature population size. The natural conditional mortality rate is that fraction of the initial number of eggs, larvae, or juveniles produced that would

die as a result of natural causes (i.e., non-cooling water system causes) during that year or duration of the life stage. The second starting point requires only an estimate of the power-plant conditional mortality rates for the egg, larval, and juvenile life stages resulting from cooling water entrainment. This estimate might be obtained from an hydrodynamic-type model or empirically (e.g., the empirical transport model of Boreman et al. [29]. In either case, the approach requires general life history data consisting of age-specific mortality, fecundity, fraction mature, and sex ratio.

Given estimates of the total number of entrained ichthyoplankton, one may attempt to bracket the true impact on a population by using a range of estimates at each step. A range of corrections can be used to represent imperfect gear efficiencies. For example, assuming a gear efficiency of 0.5 for the larval stage, one can divide the initial entrainment estimates for larvae by 0.5 to obtain a corrected estimate.

Ricker [30] defines the exploitation rate of a population as the fraction of the initial population removed by man during a specified time interval. Dividing the corrected entrainment estimate for a given life stage (egg, larval, or juvenile) by the total annual production of that life stage provides an estimate of the power-plant exploitation rate. Total annual production of a life stage (egg, larval, or juvenile) can be obtained by multiplying the total mature population by the average fecundity per mature female and then by the survival rate up to the start of the life stage under consideration.

While passing through a given life stage, an organism is exposed to competing sources of mortality, i.e., natural vs entrainment. Hence, obtaining an estimate of the power-plant conditional mortality rate for each entrained life stage is necessary. Barnthouse et al. [31] describe an iterative method for obtaining the power-plant conditional mortality rate for a life stage from the power-plant exploitation rate and natural conditional mortality rate for the given life stage. This conditional mortality rate represents the fraction of the initial number of a life stage produced that would be killed by entrainment if no other causes of mortality were operating. Thus the probability of surviving entrainment (1 - power-plant conditional mortality rate) is independent of the probability of surviving natural sources of mortality (1 - natural conditional mortality rate). An overall power-plant conditional mortality rate, m, can be obtained from life-stage-specific, power-plant conditional mortality rates (m_e, m_l, and m_j for the egg, larval, and juveniles stages, respectively) as follows

$$m = 1 - (1-m_e)\ (1-m_l)\ (1-m_j) \quad . \tag{18}$$

The product of the two survival rates (natural and power plant) yields the probability of survival when both natural and power-plant entrainment mortalities are present together, i.e.,

$$S_{op} = S_o \cdot (1-m) \quad , \tag{19}$$

where S_{op} is the fraction of age class 0 ichthyoplankton surviving both natural and entrainment sources of mortality.

The density-independent Leslie matrix model can be used to project a population forward 40 years (the assumed average lifetime of a steam electric plant) with and without the power-plant conditional mortality rate. The difference in the projected population sizes are then compared (i.e., percent

population reduction after 40 years). Finally, impact factors can be developed for a range of hypothesized power-plant conditional mortality rates. The 40-year impact factor can be defined as the ratio of the fractional loss to a population after 40 years to the power-plant conditional mortality rate. The impact factor is, to a large extent, a function of that age class most important to a population in terms of egg production. The later in the life cycle of a population this age class occurs, the lower the range of impact factors will be.

3.4. Discussion of Age-Structure Approach

Given the availability of necessary data, an age-structure modeling approach based on life-history data provides a better technique for assessing the long-term impacts of steam electric plants on fish populations. This approach is especially useful since the impacts are not uniform over the entire life span of the individual. The approach suffers from some of the same biases as the "equivalent adults" technique, including estimation of daily concentration, gear avoidance, and partially identified or unidentified ichthyoplankton. However, several sources of bias present in the equivalent adult method are avoided by using the age structure approach. The most serious of these sources of bias, age of the entrained life stages, is avoided in the age-structure approach by calculating the power plant conditional mortality rate. The age-structure approach, instead of calculating an "expected lifetime fecundity," uses fecundity values for each mature age class. Furthermore, a feedback mechanism is inherent in the age-structure approach, which allows the reduction in adults in one generation to reduce the number of spawning adults in future generations, and permits long-term, in addition to short-term, estimates of impacts on fish populations.

The major problem in lending realism to age-structure modeling is concerned with the controversial issue of density-dependence [32]. Although populations in their natural state normally respond in a compensatory manner, populations under large stresses can respond in a density-independent, or even depensatory, manner resulting in a population "crash" [33]. Density-dependent mechanisms can be incorporated into an age-structure model, but estimates of realistic coefficients which express the amount of compensation are difficult, if not impossible, to obtain. Ranges of values for the density-dependent coefficients were used to modify long-term potential impacts to fish populations [20,34]. The equivalent adult method can not be adjusted to allow for compensatory mechanisms.

4: CONCLUSIONS

Two methods for assessing the impact of cooling water systems on fish populations due to entrainment mortality were explored. The "equivalent adult" method requires relatively little data, but is subject to serious biases. The greatest bias results from assuming all eggs, larvae, or juveniles have just entered that life stage at the time of entrainment. The age-structure approach is subject to fewer biases, but requires more data. In addition, the age-structure approach allows one to assess long-term impacts on fish populations. This approach is especially useful when impacts are not uniform over the entire life span of the organism. The latter method can be used to address the problem of incorporation of density-dependent mechanisms in developing and bracketing realistic long-term predictions of fish population dynamics, though estimates of the density-dependent coefficients are extremely difficult to obtain.

ACKNOWLEDGEMENTS

The author wishes to thank Drs. S. M. Adams and G. F. Cada for their careful reviews of the manuscript. Research was supported by the Minnesota Pollution Control Agency and the U.S. Environmental Protection Agency, Region V, under interagency agreement 40-650-77 (Task Order No. ORNL/EPA-V8) with the U.S. Department of Energy under contract W-7405-eng-26 with Union Carbide Corporation. Publication No. 1759, Environmental Sciences Division, Oak Ridge National Laboratory.

REFERENCES

1. G. S. Milburn and G. C. Ginsberg, Regulatory Developments in Section 316(b), in L. D. Jensen (ed.), Fourth National Workshop on Entrainment and Impingement, pp. 11-20, Ecological Analysts, Inc., Melville, New York, 1978.

2. J. Boreman, L. W. Barnthouse, D. S. Vaughan, C. P. Goodyear, S. W. Christensen, K. D. Kumar, B. L. Kirk, and W. Van Winkle, Entrainment Impact Estimates for Six Fish Species Inhabiting the Hudson River Estuary, vol. 1, Impact of Entrainment and Impingement on Fish Populations in the Hudson River Estuary, ORNL/NUREG/TM-385/V1, Oak Ridge National Laboratory, Oak Ridge, Tennessee, in press.

3. J. Boreman and C. P. Goodyear, Biases in the Estimation of Entrainment Mortality, in L. D. Jensen (ed.), Issues Associated with Impact Assessment: Proc., Fifth National Workshop on Entrainment and Impingement, Ecological Analysts, Inc., Sparks, Maryland, in press.

4. D. S. Vaughan and K. D. Kumar, Detectability and Precision of Estimates of Entrainment Mortality of Ichthyoplankton, ORNL/NUREG/TM-435, Oak Ridge National Laboratory, Oak Ridge, Tennessee, in press.

5. J. R. Schubel, C. C. Coutant, and P. M. J. Woodhead, Thermal Effects of Entrainment, in J. R. Schubel and B. C. Marcy, Jr. (eds.), Power Plant Entrainment: A Biological Asesssment, chap. 2, Academic Press, New York, 1978.

6. R. P. Morgan, II, and E. J. Carpenter, Biocides, in J. R. Schubel and B. C. Marcy, Jr. (eds.), Power Plant Entrainment: A Biological Assessment, chap. 3, Academic Press, New York, 1978.

7. B. C. Marcy, Jr., A. D. Beck, and R. E. Ulanowicz, Effects and Impacts of Physical Stress on Entrained Organisms, in J. R. Schubel and B. C. Marcy, Jr. (eds.), Power Plant Entrainment: A Biological Assessment, chap. 4, Academic Press, New York, 1978.

8. T. J. Horst, An Assessment of Impact Due to Entrainment of Ichthyoplankton, in S. B. Saila (ed.), Fisheries and Energy Production, pp. 107-118, D. C. Heath and Co., Lexington, Massachusetts, 1975.

9. C. P. Goodyear, Entrainment Impact Estimates using the Equivalent Adult Approach, Tech. Rep. USFWS No. FWS-OBS-78/65, 1978.

10. S. M. Adams, D. S. Vaughan, S. G. Hildebrand, and K. D. Kumar, An Approach to Ecological Assessment of Power-Plant-Intake [316(b)] Related Issues: The Prairie Island Case, ORNL/TM-7421, Oak Ridge National Laboratory, Oak Ridge, Tennessee, 1981.

11. D. A. Pyne, On the Comparison of Two Binomial or Poisson Populations When Sampling Units are Nonhomogeneous, Tech. Rept. No. 246, Dept. of Mathematics, The Johns Hopkins University, 1976.

12. Des Raj, Sampling theory, McGraw-Hill Book Co., New York, 1968.

13. H. Bjorke, O. Dragesund, and O. Ulltang, Efficiency Test on Four High-Speed Plankton Samplers, in J. H. S. Blaxter (ed.), The Early Life History of Fish, pp. 183-200, Springer-Verlag, Berlin, 1974.

14. D. Schnack, On the Reliability of Methods for Quantitative Surveys of Fish Larvae, in J. H. S. Blaxter (ed.), The Early Life History of Fish, pp. 201-212, Springer-Verlag, Berlin, 1974.

15. G. I. Murphy and R. I. Clutter, Sampling Anchovy Larvae with a Plankton Purse Seine, Fish. Bull., vol. 70(3), pp. 789-798, 1972.

16. M. A. Kjelson, Estimating the Size of Juvenile Fish Populations in Southeastern Coastal-Plain Estuaries, in W. Van Winkle (ed.), Assessing the Effects of Power-Plant-Induced Mortalities on Fish Populations, pp. 71-90, Pergamon Press, New York, 1977.

17. M. A. Kjelson and D. R. Colby, The Evaluation and Use of Gear Efficiencies in the Estimation of Estuarine Fish Abundance, in M. Wiley (ed.), Estuarine Processes, vol. II, pp. 416-424, Academic Press, New York, 1977.

18. P. M. McGroddy and R. L. Wyman, Efficiency of Nets and a New Device for Sampling Living Fish Larvae, J. Fish. Res. Board Can., vol. 34, pp. 571-574, 1977.

19. R. M. Leithiser, K. F. Ehrlich, and A. B. Thum, Comparison of a High Volume Pump and Conventional Plankton Nets for Collecting Fish Larvae Entrained in Power Plant Cooling Systems, J. Fish. Res. Board Can. vol. 36, pp. 81-84, 1979.

20. D. S. Vaughan, An Age Structure Model of Yellow Perch in Western Lake Erie, in D. G. Chapman and V. F. Gallucci (eds.) Quantitative Population Dynamics, International Cooperative Publishing House, Fairland, Maryland, in press.

21. H. Bernardelli, Population Waves, J. Burma Res. Soc., vol. 31, pp. 1-18, 1941.

22. E. G. Lewis, On the Generation and Growth of a Population, Sankhya, vol. 6, pp. 93-96, 1942.

23. P. H. Leslie, On the Use of Matrices in Certain Population Mathematics, Biometrika, vol. 33, pp. 183-212, 1945.

24. J. M. Emlen, Ecology: An Evolutionary Approach, Addison-Wesley, Reading, Massachusetts, 1973.

25. G. J. Paulik, Studies of the Possible Form of the Stock-Recruitment Curve, Rapp. P.-V. Reun. Cons. Perm. Int. Explor. Mer, vol. 164, pp. 302-315, 1973.

26. A. L. Jensen, Leslie Matrix Models for Fisheries Studies, Biometrics, vol. 30, 547-551, 1974.

27. T. J. Quinn, II, The Use of Leslie-Type-Age-Structure Models for the Pacific Halibut Population, in D. G. Chapman and V. F. Gallucci (eds.), Quantitative Population Dynamics, International Cooperative Publishing House, Fairland, Maryland, in press.

28. D. S. Vaughan and S. B. Saila, A Method for Determining Mortality Rates Using the Leslie Matrix, Trans. Am. Fish. Soc., vol. 105(3), pp. 380-383, 1976.

29. J. Boreman, C. P. Goodyear, and S. W. Christensen, An Empirical Transport Model for Evaluating Entrainment of Aquatic Organisms by Power Plants, Tech. Rep. USFWS No. FWS/OBS-78/90, 67 pp., 1978.

30. W. E. Ricker, Computation and Interpretation of Biological Statistics of Fish Populations, Fisheries Research Board of Canada Bull. No. 191, 1975.

31. L. W. Barnthouse, D. L. DeAngelis, and S. W. Christensen, An Empirical Model of Impingement Impact, ORNL/NUREG/TM-290, Oak Ridge National Laboratory, Oak Ridge, Tennessee, 1979.

32. J. T. McFadden, An Argument Supporting the Reality of Compensation in Fish Populations and a Plea to Let Them Exercise It, in W. Van Winkle (ed.), Assessing the Effects of Power-Plant-Induced Mortalities on Fish Populations, pp. 153-183, Pergamon Press, New York, 1977.

33. C. P. Goodyear, Assessing the Impact of Power Plant Mortality on the Compensatory Reserve of Fish Populations, in W. Van Winkle (ed.), Assessing the Effects of Power-Plant-Induced Mortalities on Fish Populations, pp. 186-195, Pergamon Press, New York, 1977.

34. K. W. Hess, M. P. Sissenwine, and S. B. Saila, Simulating the Impact of the Entrainment of Winter Flounder Larvae, in S. B. Saila (ed.), Fisheries and Energy Production, pp. 1-29, D. C. Heath and Co., Lexington, Massachusetts, 1975.

PB82-228420

RNA/DNA RATIO IN TROPICAL FISH EXPOSED TO THERMAL DISCHARGES IN RANA PRATAP SAGAR LAKE

P.R. Kamath, K.G. Warughese, P.V. Vyas and R.P. Gurg
Environmental Studies Section
Health Physics Division
Bhabha Atomic Research Centre
Bombay 400 085, India.

ABSTRACT

Changes in RNA content in cells without alteration in DNA have been observed under environmental stress in organisms. RNA/DNA ratio has come to be used as an indicator of growth in fishes, as the ratio reflects the changing environmental conditions.

Laboratory investigations were conducted in aquaria under controlled temperatures with fingerlings of L. rohita to relate RNA/DNA ratios with thermal exposure. Body weights and RNA/DNA ratios were determined in muscular tissue at different increases in temperature and exposure periods.

The observations show that under controlled exposures and in confined environment, the ratios reflect response to thermal stress when the temperatures are high. Under optimal conditions, RNA/DNA ratio corresponds to increase in body weight.

The difficulties of direct application of the ratio to indicate growth rate in fish under field conditions are discussed.

1. INTRODUCTION

Changes in RNA countent in the cells without alteration in DNA has been reported under adverse environmental conditions in liver tissue from a loss of basophilic cytoplasmic granules [1]. It is also known that lipid phosphorous and RNA - phosphorous may change without DNA - phosphorous content being altered by fasting or refeeding. The amount of DNA per nucleus in somatic cell does not show significant variation with change in nutritional conditions. The changes in RNA content of cells are primarily attributed to loss or gain of RNA in microsomes.

The ratio of total RNA to DNA in tissue has come to be used as an indicator of growth in fishes. A comparison of RNA/DNA ratio and Liver - somatic index (Liver to Body weight ratio) as indicators of growth rate and energy storage has been made by Bulow [2]. RNA/DNA ratio determinations have been found to conform to changing conditions in the environment and habits. Spigarelli has determined [3] RNA/DNA ratios in Coho salmon

during high feeding on forage fishes, followed by tremendous growth rate in summer months, just prior to spawning migrations in late fall. The ratios increase during the period of growth and fall when feeding ceases and energy is expended in upstream migration and gamete production.

Variations in environmental parameters affecting changes in RNA, other than growth factors alone, come in the way of applying RNA/DNA ratio for assessing thermal effects in fishes. The variables are : size and age of individuals in the population, species variation, acclimation temperature, non-uniform distribution of nutrients and dissolved oxygen and varying residence time in stratified waters. There is therefore a need to study the changes in RNA/DNA ratio in fishes under controlled thermal exposures. A laboratory investigation was carried out on fingerlings of Labeo rohita placed in aquaria, maintained at steady temperatures and uniform environmental conditions in the media.

The studies presented here were conducted in the Environmental Survey Laboratory at the site of the Rajasthan Atomic Power Station. The temperature increase in receiving waters at the outfall in the Rana Pratap Sagar Lake [4] was found to range between 2 - 2.5°C above that of ambient waters upstream. The Lake is located in the region of widely varying diurnal and seasonal temperatures and the waters are distinctly stratified with a strong thermocline in the season following winter.

2. EXPERIMENTAL

2.1 Equipment

The equipment consists of two glass aquaria tanks (75 cm x 45 cm x 20 cm) filled upto 40 cm with raw lake water. The first aquaria, the ambient tank, represents the temperature t_o °C of the lake epilimnion waters, changing gradually from morning to night and on successive days of the run. The second aquaria, the heated tank, contains an immersion heater, to raise the temperature of water, connected with a cut out relay to maintain the desired temperature. The two aquaria tanks are electronically connected such that, as the temperature of water varies in the ambient tank, the heater tank continues to maintain the designated increase above the ambient (t_o °C plus).

2.2 Exposure Conditions

20 fingerlings of Labeo rohita (local : Rohu) were placed in each tank. The temperature of the heated tank was maintained at designated increase of 2,3,4 and 6°C above that in the ambient, taken as t_o °C. The increase in wet weight (g) and RNA/DNA ratio in muscular tissue were determined at zero time (start), and intervals of 5,10 and greater than 10 days of exposure. The waters were agitated by bubbling air and dissolved oxygen (DO) content checked with dip DO meters. 5-6 ppm DO was present throughout the duration of the experiment. The D.O. increased to 7-8 ppm when oxygen was bubbled instead of air (Table 2). Temperature of water was uniform throughout because of agitation, free fish movement and confinement. The fishes were fed daily with balls of rice bran mixed with oil cake.

2.3 Analytical

Three fishes were removed from each tank at scheduled intervals and left in air. They were wiped dry in folds of filter paper and the wet weight determined.

Soft epaxial tissue was collected from the fishes after removal of skin and bones. 5 g of the soft tissue was defatted in a blender with chloroform - methanol - ether (1 min) and squeezed free of solvents, air dried and then ground to fine powder (- 40 mesh).

30 mg of dry defatted tissue was suspended in 3 ml 5 % trichloracetic acid (TCA) solution in thick walled 15 ml conical centrifuge tubes and heated in a boiling water bath for 30 min. The TCA extract was centrifuged, separated and made to a known volume. Standard RNA and DNA solutions were made similarly in 5 % TCA solution. RNA was determined by orcinol reaction and absorption measurements made at 660 mμ. DNA was similarly determined using diphenylamine and measurement of absorption at 600 mμ [5]. Estimation of DNA and RNA was made in TCA extract by comparison with standard RNA and DNA solutions. Correction for DNA reaction with orcinol was also made using std DNA solution. The observations are presented in Tables 1 and 2.

Table 1

Seasonal Variation in RNA/DNA ratio - fish, L. rohita

(air bubbling)

Season and Temperatures	Zero day		Fifth day		Tenth day	
	Wet wt. g	RNA/DNA	Wet wt. g	RNA/DNA	Wet wt. g	RNA/DNA
Sept. 1980						
t_o (32°C)	10.6	9.2				
t_o + 2°C (34°C)			11.2	7.16		
(34°C)			11.7	7.40		
t_o + 4°C (36°C)					11.7	6.35
Nov. 1980						
t_o (24°C)	2.71	1.8				
t_o + 3°C (27°C)			5.6	3.8	5.6	3.04
t_o + 6°C (30°C)			4.5	3.5	7.6	3.2
Dec. 1980						
t_o (22°C)	14.6	7.2				
t_o + 2°C (24°C)			14.3	8.4		
t_o + 8°C (30°C)			14.9	7.9		

Table 2

Variation in RNA/DNA ratio of L. rohita with daily change in temperature of water (oxygen bubbling)

Season & Temperature	Zero day		Fifth day		Tenth day		10 days	
	Wet wt. g	RNA/ DNA	Wet wt. g	RNA/ DNA	Wet wt. g	RNA/ DNA	Wet wt. g	RNA/ DNA
February 1981								
t_o (18°C)	16.9	6.1	21.6	7.6	18	7.3	15.9	7.5
			t_o 18°		t_o 22°		t_o 24°	
t_o + 3°C			20.6	8.7	20.1	10.2	18.4	8.2
t_o + 6°C			20.8	7.4	20.2	7.36	15.6	5.6

3. DISCUSSION

The results presented in Table 1 show that in a confined space with uniform increase in temperature of the aquatic media there is increase in RNA/DNA ratio in the fingerlings of L. rohita when the temperatures are in the range 24-27°C. At 30°C and above the increase in weight may be attributed to increase in skeletal weight, other tissues and lipids in the absence of a corresponding increase in RNA/DNA ratio. In the beginning of winter (Nov. readings) when the t_o values range from 24-27°C, there is a doubling of body weight and values of RNA/DNA ratio in 5 days. The t_o + 6°C and t_o + 8°C readings in Table 1, show that at 30°C L. rohita shows signs of thermal stress under sustained exposure conditions. Under field conditions, L. rohita escapes thermal stress by moving out of thermal plumes or dipping into the hypolimion where cooler waters are available.

The experimental conditions (Table 2) are relatively more favourable for survival and growth because oxygen is bubbled through and daily temperatures are also gradually varying. The increase in body weight at 27°C however is not spectacular. At 30°C (t_o + 6°C) the body weight and RNA/DNA fall with long residence under stress.

It would appear from the study that the RNA/DNA ratios can be good indicators of growth or stress to fish, when the stresses are not severe. Field observations are necessary to confirm that the reduction in RNA/DNA reflects thermal exposures when other factors affecting growth are present. Other parameters that may influence change in ratio are - age, species variation and feeding habits of fish.

REFERENCES

1. J.N.Davidson, The Biochemistry of the Nucleic Acids, Methuen and Co. Ltd. London. P-107, 1968.

2. Frank I. Bulow, C.B. Coburn and Charles S. Cobb., Comparisons of two Blue gill populations by Means of the RNA/DNA Ratio and Liver - Somatic Index. Trans American Fisheries Society, USA, 107 (6) 799-803, 1978.

3. S.A. Spigarelli and P.R. Harbach, Preliminary use of RNA-DNA ratios to estimate recent growth of Lake Michigan Fishes. Radiological and Environmental Research Division (ANL, Argonne) Annual Report ANL-8060 P-156, 1973.

4. P.R. Kamath, R.P. Garg, I.S. Bhat and P.V. Vyas, Measurement and Evaluation of Thermal Effects in the intermixing zone at low Power Nuclear Station outfall., Third Waste Heat Management and Utilisation Conference, Miami Beach, Florida, Dec. 4-6, 1978.

5. F.J. Bulow, RNA-DNA Ratios as indicators of recent growth rates of a fish. J. Fisheries Res. Board, Canada 27:2343-2349, 1970.

WORKING SESSION W-1

ECOLOGICAL EFFECTS

PB82-228438

ECOLOGICAL EFFECTS ASSESSMENT - REQUIREMENTS VS. STATE-OF-THE-ART

D. H. McKenzie
J. M. Thomas
L. L. Eberhardt
Ecological Sciences Department
Pacific Northwest Laboratory
Richland, Washington, U.S.A.

ABSTRACT

Much of the legislation and regulations that are applicable to environmental impact assessments indicate that ecosystem effects should be addressed. Review of current applications and approaches often indicates that individual organism effects are quantitatively addressed. Quantitative population level effects are rarely considered. Ecosystem level effects, if addressed, are only on a qualitative basis. The paper addresses the areas of: current program objectives, establishing regulations, quantitative methodologies, the roles of biomonitoring data and simulation modeling, attempts to predict future effects and mechanisms for improvement. Areas for development of improved methodology are developed within each of these areas that could increase the quantitative content of environmental inputs to decision-makers.

1. INTRODUCTION

In 1969, Congress instituted the National Environmental Policy Act (NEPA). Simply stated, its goal was to require a systematic evaluation of potential environmental damage which might result from federal agency activities. It was intended as a planning tool for government evaluation on project alternatives having the potential for environmental damage. The interpretation of NEPA by courts and regulators, instituted by concerned "environmentalists" has resulted in ecological impact assessment requirements for the electric power industry in particular.

In a reaction to the Calvert Cliffs Decision (1971) the former Atomic Energy Commission issued revised regulations. Those regulations greatly influenced the environmental monitoring programs currently used to assess the environmental impact of nuclear, as well as non-nuclear, electric power plants. Since 1971, regulations devised to protect the environment have proliferated and it is not surprising that there are jurisdictional overlaps and redundancies in the current regulations. Those relevant to the electric utility industry at the federal level include NRC's guidance on ecological matters, EPA's regulations based on FWPCA (as amended in 1972), and particulars of the Coastal Zone Management Act (NOAA) and the Water Resources Planning Act (Water Resources Council). Portions of the Fish and Shellfish Coordinating Act (Interior Department) and Endangered Species Act have resulted in additional regulatory influence. Additional regulations including many on thermal effluents have been imposed by some states.

Preceding page blank

Both historically and currently the electric power industry collects considerable amounts of data in an attempt to comply with the foregoing regulatory requirements and the intent of NEPA. Reviews of nuclear power plant monitoring data and environmental statements have concluded that defensible quantitative statements about the existence of impacts cannot be based on the collected data (Adams et al., 1977, Gore et al., 1977, Murarka et al., 1976). Some of the factors contributing to the lack of quantitative statements from these studies were attributable to the manner in which the monitoring program was conducted. However, the state-of-the-art in ecology and resource management indicates that quantitative assessments at the ecosystem level (where NEPA's intent is directed) cannot be made (Ghiselin, 1978). Van Winkle (1977) points to several limitations imposed on impact assessments at the population level: the general inability to quantify compensatory capabilities; large, uncontrollable and unpredictable natural variations; uncontrollable effects from other sources of impact; incompatible time frames for decision-making; and the manifestation of impacts in ecological components with long generation times. Thus, regulatory intent and ecological knowledge have not been compatible on a population level, a lower level of complexity than the ecosystem. As a result, present impact assessments depend heavily on experience and ecological judgements (Thomas and McKenzie, 1979).

Because ecological assessment studies are being conducted under the NEPA mandate and field data collected must contribute to the decision-making process, monitoring programs should address tractable questions. The electric power industry has devoted considerable resources to collect data and produce reports on the ecological effects of power generation. We believe that these resource allocations will continue into the foreseeable future. The aggregate dollar amount spent per year may exceed the ecological research budgets of most federal and state agencies. The magnitude of this resource commitment makes it imperative that many relevant questions be addressed in an organized way. For example:

Are the results obtained relevant to NEPA or other postulated objectives?

Have monitoring objectives been adequately and appropriately defined?

Are useful scientific results produced?

Do monitoring data obtained under the current system provide direction for solving problems or bring the state-of-the-art closer to meeting the intent of NEPA?

Can current resource allocations be changed so resulting data are more useful to regulators and also contribute to scientific needs?

These questions are raised in order to initiate a reevaluation of the state-of-the-art of impact assessments at power plant sites. Failure to address such questions on a scientific basis has resulted in conflicts between science and regulatory requirements, even though environmental statements are being written and power plants licensed. For example, though the intent of NEPA requires an assessment of ecosystems effects, in situ individual organisms effects are usually addressed in practice. Often, when effects at the population level are studied, inappropriate methodology has been used (Thomas et al., 1978, Gore et al., 1979, Fritz et al., 1980). Assessment of ecosystems effects are generally beyond scientific state-of-the-art.

Additional problems which have resulted from current procedures are: (1) ecologists conducting monitoring studies are unable to study crucial questions because regulations or custom often dictate data collection on non-critical ecosystem components; (2) no integration of monitoring objectives takes place; and (3) regional effects are generally not considered. As a result, highly educated and skilled participants as well as managers of monitoring programs can become frustrated, and their work may be judged as routine by peers. In this paper, as an approach to obtaining such solutions, we address the following areas:

Current assessment programs and their objectives

Problems in establishing regulations

Need for modified or new quantitative methods

Role for biomonitoring data

Role of simulation modeling

Predictors of future effects

Need for regulatory changes

Within each of these areas we develop positions that are relevant to thermal effluent impacts as well as the broader aquatic impacts of concern to the electrical industry, such as impingement, entrainment, toxic substances and acid rain impacts. Our objective is to focus the attention of the scientific community on these areas, to facilitate a reevaluation of ecological assessment methodology, and to initiate a program to reduce the conflict between regulatory intent and ecological knowledge.

2. THE CURRENT SITUATION

From an ecologist's viewpoint, environmental monitoring has and will cost staggering sums. These expenditures have been undertaken because of requirements set forth by regulators (interpretation of NEPA), because of intervenor

actions, consultant advice, concern for the company's image on environmental issues which may lead to expensive operating or construction delays. Most of the data resulting from such studies have been reported in semi-annual reports which reside in company files or regulatory agency storage. As such, these data are not easily accessible, and are seldom evaluated; nor do they appear to be used. The apparent return to the expenditures has been the occasional completion of quality scientific research and compilation of data generally not reliable for decision-making purposes. In some cases, we suspect a negative environmental image is fostered.

An aquatic monitoring program usually consists of several loosely linked sampling programs that collect data during a preoperational phase, usually two or three years, and an operational phase, often three or more years. Typical ecosystem components sampled are water chemistry, phytoplankton, zooplankton, benthos, ichthyoplankton, and fish communities. Sampling stations are usually established in a near- and far-field zone, rarely exceeding a few kilometers from the plant site. Monthly or quarterly collections are made at each station and the organisms identified to a lowest practical taxon. Data summaries and interpretations are usually presented for "important" fish species and for dominant species or taxa in other trophic levels. When attempted, rigorous hypothesis testing usually identifies the obvious (i.e., temporal and spatial differences in organism densities), and provides results that are nearly as difficult to interpret as the original data. Interpretation of these data is generally left to a "qualified" ecologist, who must evaluate data on individual organisms and develop an information (e.g., population, community, ecosystem) synthesis to evaluate ecosystem impacts.

A continuation of the current procedures will result in additional major expenditures without noticeably different returns. Moreover, those conducting field studies will continue to have difficulty relating to their scientific peers because of the routine nature of monitoring and environmental managers will continue to be frustrated. Part of the reason for the continuation of the current situation is that an organized, comprehensive and scientific appraisal has not been made of the realistic possibilities in ecological effects assessments. Field data collected must be evaluated for its adequacy in meeting the intent of regulations and in forming the basis for choosing policy alternatives. We believe that improvements are needed and can be attained. Since monies will be committed to monitoring studies, then realistic, credible scientific information on ecological impacts of the construction and operation of electric power plants must be generated if any change is to come about. To enhance credibility, results should be available in the open, i.e., peer reviewed, scientific literature.

We believe that an innovative program incorporating basic and applied research with field demonstrations is needed to help bring about more meaningful and scientifically acceptable monitoring programs. A national, organized and planned research program could result in monitoring approaches that would enhance the reliability of environmental information available to decision-makers intent on complying with NEPA.

3. PROBLEMS IN ESTABLISHING REGULATIONS

A recent article by Reynolds (1980) traces the development of current regulations associated with power plant cooling systems. Reynolds contends that current regulations and guidelines have led to cooling system policies that do not appear to represent an appropriate balance of environmental risks. For example, the thermal and chemical regulations and guidelines were developed primarily from laboratory results for individual organisms, i.e., toxicity tests. Such an approach rests on the hypothesis that protecting the individual organism protects the ecosystem. While it is likely that hypothesis is true, successful standards and regulations undoubtedly depend upon selecting the appropriate "indicator" organism. Such attempts to project laboratory toxicity results to field situations are replete with difficulties (Thomas, 1979).

We believe (Thomas, 1979) that the current state of understanding in ecological theory, quantitative methodology, and the ability to conduct field "experiments" severely hampers regulators in devising "scientifically based" standards. In fact, considerable judgement and concomitant use of safety factors often must be employed, resulting in standards and regulations which often appear overly conservative (Reynolds, 1980). A coordinated program of laboratory and field research accompanied by appropriate quantitative evaluation of resulting data and the judicious use of simulation models, could lead to more realistic standards and operating procedures for electric power plants. Such research cannot be solely laboratory oriented. Crosschecks of results in actual ecosystems must be obtained to validate laboratory data because changes in water volumes, interactions, feedbacks, compensation, and inter/intra species biomass relationships, as well as age class phenomena, can affect natural systems. Crosschecks in ecosystems where perturbation levels are currently near or at existing standards may be a good place to begin development of methodology to compare laboratory effects data with observed changes in ecosystems.

4. THE NEED FOR MODIFIED OR NEW QUANTITATIVE METHODS

In order to assess the environmental effects of construction or operation associated with power plants, improved quantitative tools are necessary because:

> Assessments using data from monitoring programs, as now conducted, presume that data analysis can be accomplished using traditional methods of statistical analysis.
>
> Current methods of population census are limited, costly and result in extremely wide confidence limits.
>
> Lack of data, knowledge and methodology prevents devising reliable stock-recruitment models, particularly for earlier life stages.
>
> The nature of population regulation is uncertain.

The use of laboratory data in field settings requires field estimates of crucial parameters (e.g., population sizes, survival rates).

The integration of species-specific information into a test(s) of community or ecosystem level hypotheses cannot be accomplished within a meaningful statistical framework.

Innovative ways to circumvent these limitations can lead to more cost-effective quantitative assessments of the effects of activities at power plant sites.

Our experience has led us to a particular approach in designing environmental impact studies where the main goal is to test the impact hypothesis. Briefly, the basis is that of employing paired (matched) control and "impact" stations, for which baseline data are obtained in a preoperational period. Impacts are evaluated in terms of a shift in the ratio of the paired stations after power plant operation begins. The underlying rationale is that most effects extraneous to plant operation (e.g., weather) are likely to operate on a spatial scale large enough to affect both members of the paired set; hence, any shifts in the ratio would probably be associated with impacts of the generating station. What is done, in effect, is to attempt to substitute repeated observations over time for replication. A brief accounting of the method appears in Eberhardt (1976); some applications are in Thomas et al. (1978) and Skalski and McKenzie (1981).

The basic idea described above has been discussed at considerable length in a book by Green (1979). He advocates the use of a baseline (preoperational) period in which stations in both the zone of impact influence and control zones are observed, followed by a further series of observations after the impact source becomes active. He does not, however, use matched stations, but instead recommends random location of the individual stations in study areas selected in and out of the impact zone. A logical, but unfortunate consequence of this approach, is that the statistical analysis must depend on the test of interaction in an analysis of variance model. With the exception of a test devised for a particular form of interaction (Tukey's Test), such an analysis of variance is invalid without true replications.

Conceivably, Green's approach could be carried out in a manner such that only a first order interaction must be evaluated. A more common approach in the literature dealing with impact evaluation is one in which second and third order interactions are involved. The problems in handling such data have been discussed in Thomas et al. (1978), and McCaughran (1977).

Four assumptions are usually postulated as a basis for the analysis of variance. As is well-known, they are not mutually exclusive. Also, as Scheffe (1959) points out, routine testing of assumptions can have quite unsatisfactory effects on the inferential procedures associated with the analysis of variance. The preferred procedure is one of establishing validity of the assumptions (or, more practically, that they are met to a reasonable approximation). This is done by extensive testing over sizeable sets of data of the kind considered appropriate for the particular studies to be analyzed. Such tests should be conducted.

Normality of errors is one assumption required by analysis of variance

procedures. Many approaches, including our own, utilize a logarithmic transformation to meet this assumption. However, assumption of lognormality needs to be evaluated, even though it can be rejected for many sets of data on the basis that the observations are discrete, rather than continuous. Thus, the use of alternate models such as the Poisson log-normal should be considered.

Homoscedasticity or equal variance is another assumption needing evaluation. Scheffe's tests for homoscedasticity could be used when the hazards associated with Bartlett's test are evident. However, Scheffe's test may be unsatisfactory with small samples, so evidence again points to the need for large-scale testing, rather than routine tests. In addition, other, more recently developed tests could be considered. Statistical independence of errors is one of the more critical issues in choosing the kinds of analyses that seem feasible with impact data. Various tests for serial correlation could be used in initial explorations of data, and degree of correlation and its consequences should be evaluated. Undoubtedly, some investigation of the vexing problem of outliers would be needed in this context. The assumption of additivity is a problem when dealing with interactions as a key issue in methods to study the impact hypotheses. We suspect that the evaluation of additivity would be one of the more difficult problems to deal with because there are few "balanced" sets of data available for the circumstances we regard as essential for a workable design.

The meaning of "replications" normally encountered in impact studies is uncertain and needs investigation. Most of the current analyses regard repeated samples taken at nearly the same site and same time as replicates. One view is that these are replicate samples (Green, 1979) but not replicates in the sense of an experimental design. It may be necessary to look more carefully at the kinds of models that are considered appropriate. If the spatial-temporal behavior of the biota is regarded as following some sort of process-model, then it may indeed be feasible to consider taking replicate observations on that process. Some deliberate experimentation may be needed on this point, inasmuch as the interpretation considered here requires independent sampling, almost never done in practice.

The role of transformations has been pointed out in conjunction with assumptions above, but it is listed here as a separate category for emphasis. It seems self-evident that the issue of replications would necessarily interact with any approach to transformations. We believe that a careful appraisal of transformations in two-way tables with one observation per cell may be needed. One simple approach could be to use the methods proposed by Cressie (1978). The station pairs method would then concern univariate analyses. However, there may be a need to do research on multivariate analysis, inasmuch as certain outcomes of any evaluation of designs could lead in that direction, both through analysis of vectors of random variables and in the use of auxiliary variables in regression or analysis of covariance techniques.

Comparisons of estimates of population abundance are another source of uncertainty in environmental assessment studies. Typically, the techniques used in electric utility environmental assessment programs for monitoring fish populations were adopted from fish and wildlife census techniques developed by resource managers. Though they were developed with the objective of providing descriptive data on the demographics of animal populations, and may be very helpful in estimating population parameters for models, they are not very helpful in detecting impact (McKenzie et al., 1979). Seber (1973) presents

a comprehensive review of useful techniques for estimating animal abundance. However, only two references (Chapman, 1951; Chapman and Overton, 1966), contain a limited description of quantitative techniques for comparing abundance estimates. Evaluation of impact implies that at least four abundance estimates be compared, i.e., control and treated populations from preoperational and operational periods.

Two different methods have generally been used to provide estimates of animal abundance. The principal method has been to use indices as an indirect measure of abundance, where the index is a count or other measurement (i.e., catch-per-unit-effort) assumed to be directly related to population size. The majority of electric utility monitoring programs are based on this procedure. The second method involves obtaining estimates of absolute animal abundance. Estimates obtained by either method are sometimes followed by attempts to compare population levels statistically.

Another quantitative approach to impact assessment is that of linear regression. In those circumstances where an established gradient of some sort is associated with the source of impact, it may be expected that regression techniques would provide adequate evidence of impact. An example is provided by studies of thermal effects on benthic organisms. Various technical problems may need to be considered (errors in the independent variable, nonlinear responses, etc.), but the inferential problems do not seem difficult. However, factors coincident with distance from source (depth gradients, currents, fertility) can confound interpretation (Thomas et al., 1978).

Yet another quantitative approach could be based on the analysis of covariance. Covariance techniques may be appropriate in designs in a number of ways, and it is anticipated that several prospects need to be evaluated. One prospect is to use the "baseline" (preoperational) data as a covariate in comparing operational data on exposed and control sites. A critical issue in design is whether or not errors in successive observations taken over time can be considered independent. If the errors are serially correlated, there may be advantages in using regression analysis due to the usual robustness of regression. However, flexibility is thus sacrificed, so an advantageous approach may well be one that blends regression and the analysis of variance, e.g., the analysis of covariance.

5. ROLE FOR BIOMONITORING DATA

We have found (Thomas et al., 1981) that biomonitoring data have been and will be (under programs funded by DOE, NSF, EPA) collected to document changes in population abundance. These data will be taken to manage for sustained yields, to verify compliance with regulatory directives, and to obtain estimates of normal population abundance and cycles for research purposes. Little has been done with such long-term data sets in terms of attempting to imply cause and effect when population changes are noted. Other than inference by correlation, it appears that little can be done, since biomonitoring studies are usually not designed in a statistical sense. Observed changes can be brought about by compensation, indirect effects, direct mortality, interactions and environmental variables. Thomas et al. (1981), however, have proposed that biomonitoring data can serve to test laboratory results against long-term historical trends.

The purposes of biomonitoring studies are generally not the same as for impact assessment monitoring (i.e., to "detect impact" if it exists). However, in instances where long-term data are available for ecosystems unimpinged by activities of industry, observed changes may be accompanied by plausible and perhaps quantifiable (even though by correlation, modeling or comparisons with laboratory data) explanations for those changes may then be applied in other, similar systems. Plausible examples of concern to the electric utility industry include transmission systems (i.e., effects of right-of-way and high voltage transmission), acid rain and power plants sited on reservoirs.

6. ROLE OF SIMULATION MODELS

The major modeling application in ecological impact assessment has consisted of attempts to predict environmental effects and changes associated with the power plant operation. Reviews have shown that these models are heavily focused on physical processes (hydrodynamic modeling), contain scanty information on biological details and rationale, are sensitive to processes for which very little, if any, quantitative information exists (i.e., compensation, predator/prey relationship), and cannot be expected to predict impacts reliably (Swartzman et al., 1978). Our assessment of the role that modeling has played suggests that models have been overemphasized for prediction and inadequately used as heuristic tools.

The state-of-the-art of simulation modeling and modeling experience suggests that models may have more appropriate roles. For example, modeling could serve as a framework for conceptualizing the ecosystems and impact mechanisms. When establishing what and when to sample and designing monitoring programs, models can aid in focusing on the processes and lead to more explicit objectives and rationales. An additional role that has not received much attention but has potential is that of providing inductive evidence for evaluating the plausibility of impact. Hypotheses about the direction and potential magnitude of change can be systematically evaluated within a rigorous scientific process. Identification of processes and parameters that appear to control ecosystem responses to industrial operations could potentially provide input to the engineering design and operations which could reduce impacts. Those suggested changes for the role of models in impact assessment have recently been published (Thomas and McKenzie, 1979).

7. PREDICTORS OF FUTURE EFFECTS

One of the most difficult problems the electric utility industry has had to address (Indian Point Nuclear Power Plant is the most notable example) has been assessment of effects on future aquatic populations. In the absence of any acceptable methodology for conducting these studies (due to the state-of-the-art in field and quantitative ecology and simulation modeling), we have proposed a plan to address the question (Thomas and McKenzie, 1979). These workers found that results from studies at a single site will generally not be conclusive from a quantitative point of view, apparently in agreement with the recent work of Fritz et al. (1980).

Because considerable research appears to be needed, we earlier proposed a process for conducting power plant monitoring studies which allows an orderly progression of research directed toward the questions of changes in future

populations due to power plant operations. The assessment of ecological effects is not restricted to electric power producers; the problems are universal in ecology. The ideas presented by Thomas and McKenzie (1979) are subject to debate and the plan contains aspects which need to be tested at a power plant site. A partial demonstration of the plan's feasibility can be found in the methods and conduct of monitoring programs at Connecticut Yankee and Indian Point. Since one advantage of the plan is that utilities can terminate monitoring in a known time under certain conditions, a demonstration of the plan's usefulness may be warranted. This could avoid both continuing monitoring costs (assessed to ratepayers in the case of power plants) and allow research efforts at power plant sites to be directed toward questions of population ecology that will fulfill the intent of NEPA.

8. NEED FOR REGULATORY CHANGE

Since industry is required to assess the environmental impact of their activities, they should attempt, as groups, to seek changes in unrealistic and unproductive approaches and methods. Such changes must be based upon a decision to evaluate current approaches and seek enhanced methods which represent advances in the state-of-the-art of ecological assessments. Improved quantitative methodology followed by analysis of a large body of operating experience could aid in evaluating, in general, the environmental risk associated with the variety of cooling system alternatives. The mechanisms for changing regulations so that improved approaches and methods will be incorporated are unclear because of competing jurisdictions and special interests of many concerned groups (i.e., environmentalists, intervenor groups, industry, consultants, etc.). Understanding of this "legal arena" and the mechanism, data, and evidence needed to produce change will involve the interaction of legal specialists and environmental scientists in a well-conducted, scientifically-based test case. Applied and theoretical research conducted at selected sites and directed toward specific questions could serve as one way to develop such a case.

9. CONCLUSIONS

Concerns for environmental quality and the inability to test and evaluate crucial hypotheses quantitatively contributed to current requirements in ecological effects assessments. Current cooling system approaches, data collection programs and ecological effects assessments reflect these factors. Over a decade of experience provides the basis for a timely review and evaluation of current practice. The magnitude of economic and environmental resources being committed to cooling system alternatives mandates that the decision-making process result in as many optimal choices as possible. In addition the resources being devoted to environmental data collection and interpretation provide considerable motivation for providing meaningful input to the decision-making process. We maintain that the input should be as quantitative and as free from subjective content as is reasonably possible. An alternative viewpoint suggests that the past several decades of experience be considered but a first step with the current task that of designing a second step.

ACKNOWLEDGEMENTS

Work performed under Contract DE-AC06-76RLO-1830 for the Nuclear Regulatory Commission, Division of Safeguards, Fuel Cycle and Environmental Research, Related Services Agreement TD 0782, Environmental Protection Agencies' Environmental Research Laboratory, Corvallis, Oregon under Related Services Agreement TD 1124, and the Department of Energy.

REFERENCES

Adams, S. M., P. A. Cunningham, D. D. Gray, K. D. Kumar, and A. J. Witten. 1977. A critical evaluation of the nonradiological environmental technical specifications, Vol. 1, Program Description, Summary and Recommendations, Oak Ridge National Laboratory, Oak Ridge, TN., ORNL/NUREG/TM-69, pp. 50.

Chapman, D. G. 1951. Some properties of the hypergeometric distribution with applications to zoological censuses. Univ. of Calif. Public. Stat. 1:131-160.

Chapman, D. G. and W. S. Overton. 1966. Estimating and testing differences between population levels by the Schnabel estimation method. J. Wildl. Manage. 30:173-180.

Cressie, N.A.C. 1978. Removing nonadditivity from two-way tables with one observation per cell. Biometrics 34:505-513.

Eberhardt, L. L. 1976. Quantitative ecology and impact assessment. J. Environ. Manage. 4:27-70.

Fritz, E. A., R. J. Rago and I. R. Murarka. 1980. Strategy for assessing impacts of power plants of fish and shellfish populations, U. S. Fish and Wildlife Service, Biological Services Program, National Power Plant Team, FWS/OBS/34, pp. 68.

Ghiselin, J. 1978. Environmental reports for the Nuclear Regulatory Commission: Guidelines thwart sound ecological design. FORUM, Env. Management 2:99-111.

Gore, K. L., J. M. Thomas, L. D. Kannberg and D. G. Watson. 1977. Evaluation of nuclear power plant environmental impact prediction, based on monitoring programs. Summary and recommendations. BNWL-2153, NRC-1. Pacific Northwest Laboratory, Richland, WA.

Gore, K. L., J. M. Thomas and D. G. Watson. 1979. Quantitative evaluation of environmental impact assessment, based on aquatic monitoring programs at three nuclear power plants. J. Environ. Manage. 8:1-7.

Green, R. H. 1979. Sampling Design and Statistical Methods for Environmental Biologists. John Wiley and Sons. New York, NY.

McCaughran, D. A. 1977. The Quality of Inferences Concerning the Effects of Nuclear Power Plants on the Environment in: (W. Van Winkle, ed.) Assessing the Effects of Power-Plant-Induced Mortality Fish Populations, pp. 365-372. Pergamon Press, New York, NY.

McKenzie, D. H., K. S. Baker, D. H. Fickeisen, R. M. Metzger and J. R. Skalski. 1979. The application of fisheries management techniques to assessing impacts, Pacific Northwest Laboratory, Publ. No. NUREG/CR-0572, U. S. Nuclear Regulatory Commission, Washington, D. C., pp. 82.

Murarka, I. P., A. J. Policastro, A. J. Ferrante, and G. J. Marmer. 1976. An evaluation of environmental data relating to selected nuclear power plant sites: a synthesis and summary with recommendations. Argonne National Laboratory, Argonne, IL., ANL/EIS-8, pp. 23.

Reynolds, John Z. 1980. Power Plant Cooling Systems; Policy Alternatives, Science 207 (4429):367-372.

Seber, G.A.F. 1973. The Estimation of Animal Abundance. Charles Griffin and Co., London, pp. 506.

Scheffe, H. 1959. The Analyses of Variance. John Wiley and Sons. New York, NY.

Skalski, J. R. and D. H. McKenzie. 1981. A design for aquatic monitoring programs, ms. accepted, J. Environ. Manage.

Swartzman, G., R. Deriso and C. Cowan. 1978. Comparison of simulation models used in assessing the effects of power-plant-induced mortality on fish populations. Publ. No. NUREG/CR-0474, Nuclear Regulatory Commission, Wash., D.C.

Thomas, J. M., J. A. Mahaffey, K. L. Gore and D. G. Watson. 1978. Statistical methods used to assess biological impact at nuclear power plants. J. Environ. Manage. 7:269-290.

Thomas, J. M. and D. H. McKenzie. 1979. A proposal for assessing biological effects of power plants on fish populations. Fisheries 4:23-27.

Thomas, J. M. 1979. Problems in quantitative effects assessments based on biological and ecological laboratory studies - Western North America Regional Meeting of the Biometrics Society, Los Angeles, CA. June 26-28, 1979.

Thomas, J. M., D. H. McKenzie and L. L. Eberhardt. 1981. Some limitations of biological monitoring. Ms. accepted Environment International.

Van Winkle, W. 1977. Conclusions and recommendations for assessing the population-level-effects of power plant exploitation: the optimist, the pessimist, and the realist. in: (W. Van Winkle ed.) Assessing the Effects of Power-Plant-Induced Mortality on Fish Populations. pp. 365-372. Pergamon Press, New York, NY.

WORKING SESSION W-2

MATHEMATICAL MODELLING

PB82-228446

COMMON PROBLEMS IN MODELING OF THERMAL PLUMES IN AIR AND WATER

Anthony J. Policastro
Division of Environmental Impact Studies
Argonne National Laboratory
Argonne, Illinois 60439

William E. Dunn
Department of Mechanical and
Industrial Engineering
University of Illinois
Urbana, Illinois 61801

ABSTRACT

This paper identifies several important problems in the development of one-dimensional mathematical models for vapor plume dispersion and thermal discharges in water. One-dimensional integral models provide a reliable means of identifying modeling problems since they are relatively free of computational difficulties, rely on simple mixing relationships, are easy to use, and permit extensive model/data comparisons.

Cooling tower plumes are characterized by high buoyancy, high crossflow-to-exit velocity ratios, potential downwash conditions, and the potential for phase changes during dispersion. The three basic problems in modeling cooling tower plumes are (a) difficulties in determining the proper balance between buoyancy and momentum transfer processes due to the highly buoyant nature of the plumes, (b) the treatment of tower downwash effects of additional bending and dilution, and (c) the too strong feedback of thermodynamic effects into plume dynamics.

In contrast, thermal plumes in water are characterized generally by moderate buoyancy effects and low-to-moderate ambient currents. Important practical problems occur due to the site-specific effects of bottom, surface, and shoreline interaction, possible irregular discharge geometries, and transient effects. Problems in these areas are illustrated by examining three typical sites for which extensive application of surface discharge models have been made.

In effect, the models for thermal discharges in water have the same fundamental problems as do the cooling tower plume models (difficulty with highly buoyant plumes, empirical treatment of simple boundary interferences, etc.) but to a lesser extent. However, surface discharge models suffer greater practical, site-specific problems (irregular bottom and shoreline, transient effects, etc.). The problems most common to cooling tower and thermal plume models relate to the treatment of buoyancy and the interaction with boundaries.

1. INTRODUCTION

This paper identifies several basic problems in the modeling of buoyant jets drawing on experience in both the modeling of cooling tower plumes and the modeling of thermal discharges in water. Whenever possible, available

Preceding page blank

remedies to the problem are identified, although these remedies may not be wholly satisfying from a fundamental viewpoint.

Our discussion will focus on one-dimensional ("integral") models which represent the most common approach to plume modeling. Examining the theory and performance of the integral models is the best way to identify basic modeling dilemmas, because these models are free of numerical complications and employ fairly simple mixing relationships with relatively few parameters. In a sense, integral models represent an attempt to fit available data on macroscopic plume behavior without attempting to describe the physics on a microscopic level. Thus, the integral models enable one to study the scaling relationships inherent in the data. Moreover, one-dimensional models are easy to use for parametric studies and permit extensive model/data comparisons.

We will first discuss cooling tower plumes, inasmuch as these are relatively free flows with essentially identical discharge configurations from site to site. Cooling tower plumes thus approach free circular buoyant jets with most modeling problems related to the high amount of buoyancy, the high crossflow to exit velocity ratio and, to a lesser extent, the multi-component nature of the plume.

Thermal plumes in water typically exhibit site-specific problems related to factors such as (a) discharge geometry, (b) bottom shoreline or surface interactions, (c) transient effects, (d) complex currents, etc. We will consider three sites for which model performance has been evaluated and attempt to examine the major mechanisms inadequately or incorrectly treated by the available models. These site-specific problems add to the basic problems of modeling buoyancy and crossflow phenomena as noted above.

2. PROBLEMS IN MODELING COOLING TOWER PLUMES

Cooling tower plumes are characterized by high buoyancy (initial densimetric Froude number less than 1), high cross flow to exit velocity ratios (typically, $0.5 < U_o/W_o < 3.0$), the importance of stabilizing layers which cap plume rise, buoyancy and wake induced vortex patterns, pressure forces induced by the tower wake and important thermodynamic effects under certain sets of atmospheric conditions. These factors distinguish cooling tower plumes from other types of buoyant jets including cooling water discharges.

The one-dimensional or integral models employ conservation equations for momentum, energy and total water written in terms of a one dimensional coordinate system along the plume centerline. Fluxes are usually characterized in terms of the centerline velocity, temperature and water content and the local radius of the plume. In combination with a mixing law and a psychrometric relation, the conservation equations yield a set of ordinary differential equations which are then integrated as an initial-value problem from the tower exit. The details of model development for many of the models available in the literature may be found in references 1-4.

Table 1 summarizes comparisons of 15 models with 39 sets of data on observed visible plume rise and length taken at 6 different sites in the United States and Western Europe. Notably, the models which perform the best overall have been extensively calibrated with all or part of this data base. The fact that no model can accurately predict all cases is partially due to inaccuracies in the data (mostly in the meteorological input), but also is a reflection of the fact that the models cannot be adequately fit to all the data and still retain reasonable values of the fitting coefficients. A closer

Table 1. Performance statistics for fifteen models for the prediction of single tower natural-draft visible plume rise and visible plume length.

VISIBLE PLUME RISE

Model	N_2	N_5	N_F
Slawson-Wigley	17	30	0
Slawson (Closed Form)	20	32	0
Weil	16	32	0
Frick	16	37	0
Winiarski-Frick	31	37	0
Winiarski-Frick (1977)	24	37	0
ORFAD	5	11	27
Hanna	30	38	0
Tsai-Huang (Stone & Webster Engr. Corp.)	24	32	0
Lee-Batty	19	32	1
Lee (NUS)	29	38	0
Calabrese-Halitsky-Woodard (Pickard-Lowe-Garrick Inc.)	18	29	8
Stephen-Moroz	24	35	0
Saame	17	36	2
Orville	23	35	0
KUMULUS	27	35	1
ANL	30	35	0

VISIBLE PLUME LENGTH

Model	N_2	$N_{2.5}$	N_5	N_F
Slawson-Wigley	7	11	24	0
Slawson (Closed Form)	13	19	27	0
Weil	5	7	19	0
Frick	3	4	15	0
Winiarski-Frick	23	27	33	0
Winiarski-Frick (1977)	14	20	30	0
ORFAD	0	0	2	17
Hanna	21	23	27	11
Tsai-Huang (Stone & Webster Engr. Corp.)	19	21	28	6
Lee-Batty	8	14	24	2
Lee (NUS)	5	7	21	2
Calabrese-Halitsky-Woodard (Pickard-Lowe-Garrick Inc.)	13	19	27	8
Stephen-Moroz	16	18	23	13
Saame	11	19	28	2
Orville	20	23	32	0
KUMULUS	27	30	33	1
ANL	23	30	37	0

Notes: N_2 is the number of times the prediction is within a factor of 2.

$N_{2.5}$ is the number of times the prediction is within a factor of 2.5.

N_5 is the number of times the prediction is within a factor of 5.

N_F is the number of failures of the model in 39 data sets.

examination reveals that certain anomalies exist which pose modeling challenges. In fact, the most successful models use one or more controversial assumptions, i.e., assumptions which enable the model to be calibrated against the data but which are of uncertain physical soundness. We shall consider three such areas of controversy, but first let us place these assumptions in proper perspective among the numerous other assumptions used in a typical one-dimensional model.

Among the least controversial assumptions are the boundary-layer approximation, the Boussinesq approximation, the use of a Morton-Taylor-Turner entrainment hypothesis for simple cases, the use of parametric profiles in calculating fluxes and the assumption of equilibrium thermodynamics. The boundary-layer approximation treats diffusion in the principle direction of flow as negligible in comparison with advection. The Boussinesq assumption states that density differences need only be considered in so far as they influence buoyancy; elsewhere, density may be taken as a constant property of the material. The assumption that mixing is proportional to the centerline velocity as advanced by Morton, Taylor and Turner [5] has been verified for nonbuoyant jets and a similar result was found for pure plumes. Thus, in these two extremes, the validity of this analysis appears to be valid. The use of similarity profiles to express the fluxes in terms of centerline values and a jet or plume radius is much more open to question; yet, in most cases, one is able to reformulate the equations directly in terms of fluxes thereby lessening the significance of the particular profile assumption which is made. Finally, the use of equilibrium thermodynamics simply refers to the assumption that water vapor instantly condenses at supersaturation, which we know is only approximately correct. High degrees of supersaturation seem unlikely however, given the large number of condensation nuclei in the normal atmosphere. Wigley [6] has discussed the question of equilibrium thermodynamics in detail.

Somewhat more uncertain are assumptions concerning the region of flow establishment, the existence of differential spreading rates, and the effects of ambient turbulence. The region of flow establishment is much different for a cooling tower plume than for either a heated water discharge or a nonbuoyant jet. In most analyses, this region is either ignored completely or inadequately treated. The existence of different spreading or mixing rates for momentum, energy and total water is supported by the measurements of George et al. [7] and Nakagome and Hishida [8]. Their data indicate that for densimetric Froude numbers typical of cooling tower plumes, the spreading rate of temperature is roughly 10% less than that of momentum (although at higher densimetric Froude numbers, the reverse appears to be true.) Ambient turbulence will certainly affect dispersion of the plume, particularly once shear-induced mixing has fallen off. Although these effects have received little attention, ambient turbulence is probably the mechanism limiting the length of the longest visible plumes and is probably an important consideration for this reason alone.

The most significant issues in terms of obtaining a model which gives reliable predictions over the full range of available data include achieving the proper balance between buoyancy and momentum, the treatment of tower downwash, handling large cross-flow-to-exit velocity ratios and obtaining the proper mixing coefficients for complex cases such as those involving plume merging. We shall examine in more depth the first three of these.

2.1 Balance Between Momentum Transfer and Dilution Mechanisms

If the same mixing is assumed for momentum, energy, and vapor, then the resulting model cannot be simultaneously calibrated against dilution and trajectory data. Models that tend to correctly predict trajectory will, in

turn, over-predict dilution, all else being equal. Similarly, models that predict dilution well will yield plumes that tend to rise too high. To illustrate this effect in a situation where it occurs due to cross flow (occasionally identified as the root cause of the problem), consider Figure 1. Here plots are given of vertical velocity data (usually only available indirectly through the observed trajectory) and dilution data along the plume centerline for a discharge into stagnant ambient for an initial densimetric Froude number of 0.55. These data were taken in a hydraulic laboratory model of a cooling tower discharge by Electricite De France, [9]. Consider, as an example, the prediction of the Winiarski-Frick model, which appears to do quite well in dilution predictions but clearly overpredicts vertical velocities more than a diameter above the exit plane. Good performance in both cases is possible only if either the bent-over plume assumption is utilized (i.e., acceleration to the cross flow velocity is made instantaneous) or differential spreading rates (larger than observed experimentally) are used, or, for best results, both of these assumptions are invoked simultaneously. The reasonableness of these assumptions is presently unknown.

2.2 Treatment of Tower Downwash Effects

The wake behind the cooling tower structure affects the plume in two ways. First, the increased pressure difference between the upwind and lee sides of the tower exerts a force on the plume which can bend the plume trajectory below the exit plane. Second, wake turbulence enhances mixing and dilution. Although uncommon, buildings upwind of a cooling tower may also affect plume behavior.

Figure 2 illustrates the effects of tower downwash on plume length. Here, the distance to achieve a dilution ratio of 0.1 is plotted against k, the crossflow to exit velocity ratio, for a fixed initial densimetric Froude number of 0.8. These data, again taken in a hydraulic laboratory model, reveal that the distance to a given dilution increases to a maximum for $k \approx 1.7$ and then begins to decline. Only the ANL model, which includes an empirical treatment of downwash, exhibits a trend similar to that of the measurements. Unfortunately, available data do not fully parameterize the variation of downwash effects with all relevant variables.

2.3 Treatment of Plume Thermodynamics

Under most atmospheric conditions, the exact treatment of plume thermodynamics has little impact on plume predictions. However, in about 10-20% of the cases which exist at most sites, both trajectory and plume length predictions are very sensitive to the thermodynamic analysis. Our study has shown that use of the equilibrium assumption across the entire plume cross section greatly exaggerates the importance of thermodynamic factors. This effect is illustrated in Figure 3 in which even the over-dilution characteristic of the Weil model is insufficient to offset the impact of phase change energy release which yields an extremely long plume. On the other hand, the treatment of total water as a passive tracer without condensation heating of the plume prevents proper prediction of the very longest plumes.

Methods which are used to sidestep this problem include (a) use of a smaller spreading rate for the water in the plume as compared with momentum (in some cases, even smaller than for temperature, an assumption which is probably more doubtful), (b) use of Gaussian-type profiles to reduce the radius of the region with condensed liquid water, (c) reduction of the effective latent heat of vaporization in the belief that some of the energy release

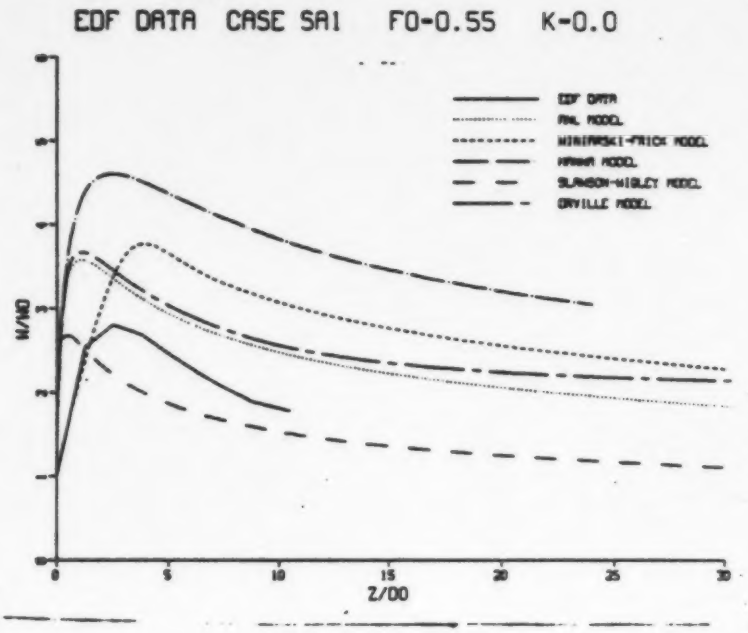

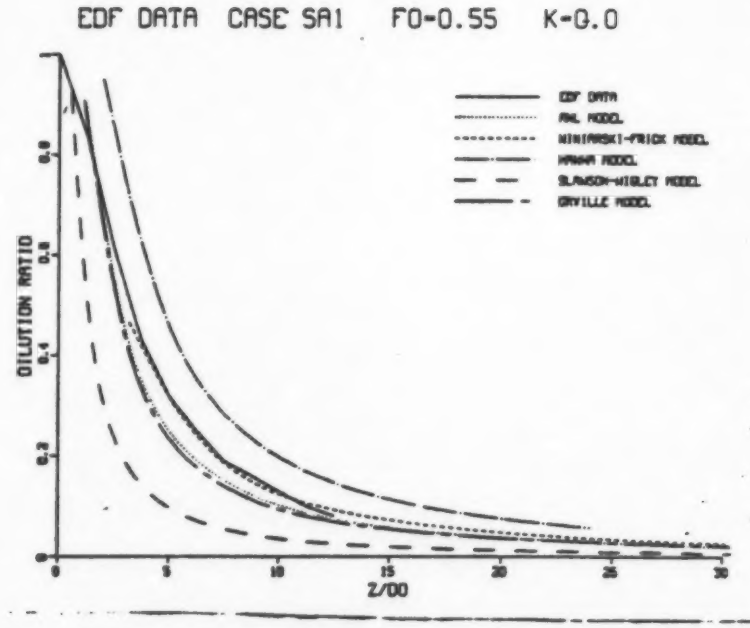

Fig. 1. Comparisons of predictions of ANL, Winiarski-Frick, Hanna, Slawson-Wigley, and Orville models to EDF laboratory data...Case SA1, F_o = 0.55, k = 0.0...(top) centerline velocity, (bottom) centerline dilution.

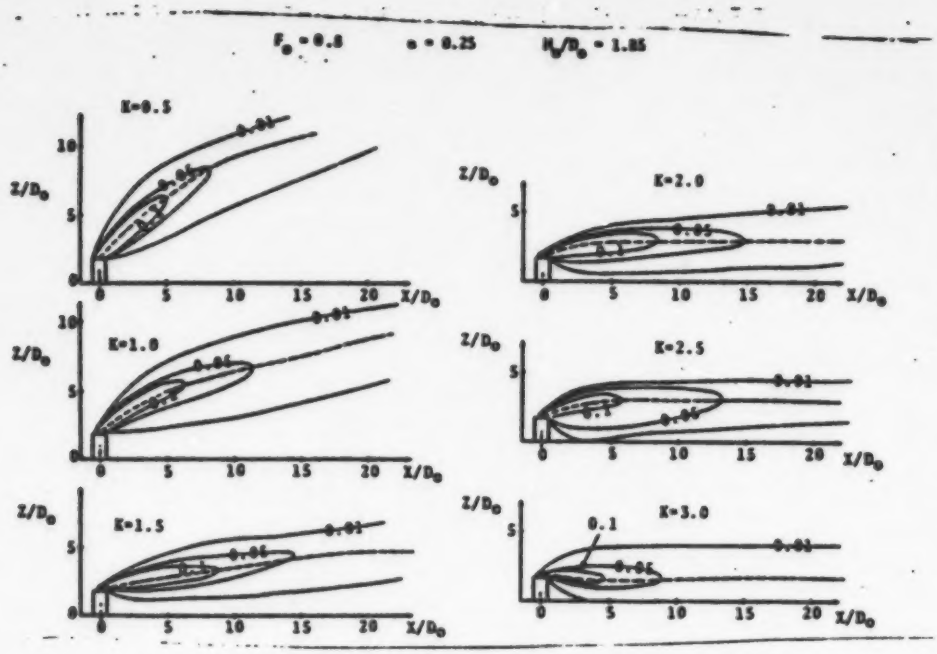

Fig. 2a. Parametric laboratory study of isoconcentration contours for a natural-draft cooling tower plume ... variation in k.

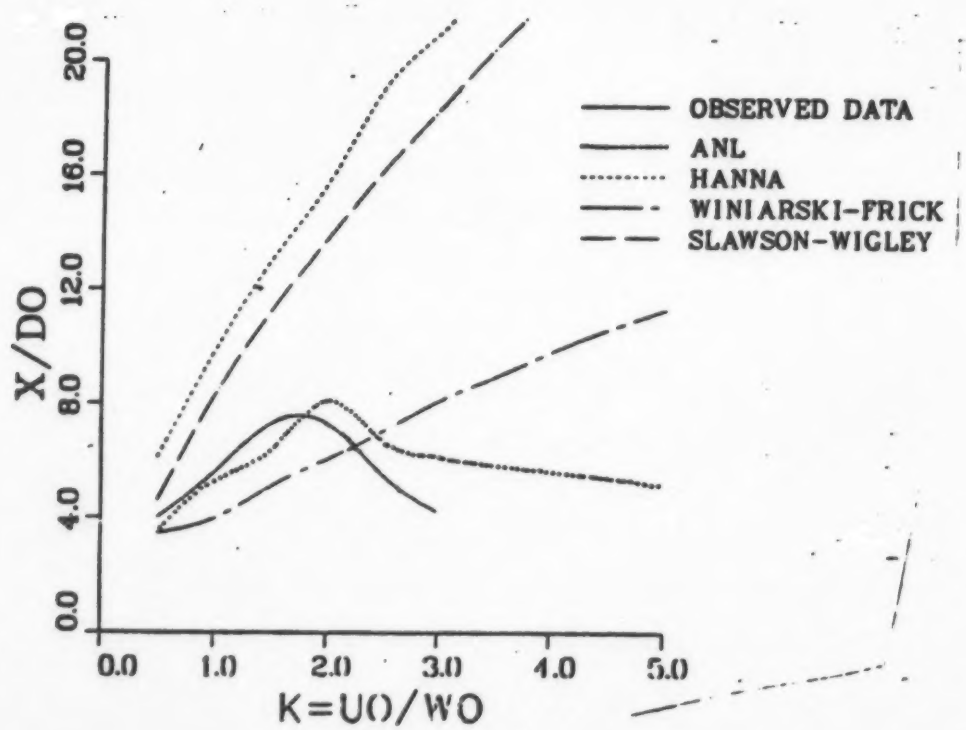

Fig. 2b. Variation of downwind distance X/D with k for the centerline location where the concentration excess ratio $\Delta c/\Delta c_o = 0.1$ ... EDF data and predictions of ANL, Hanna, Winiarski-Frick and Slawson-Wigley Models.

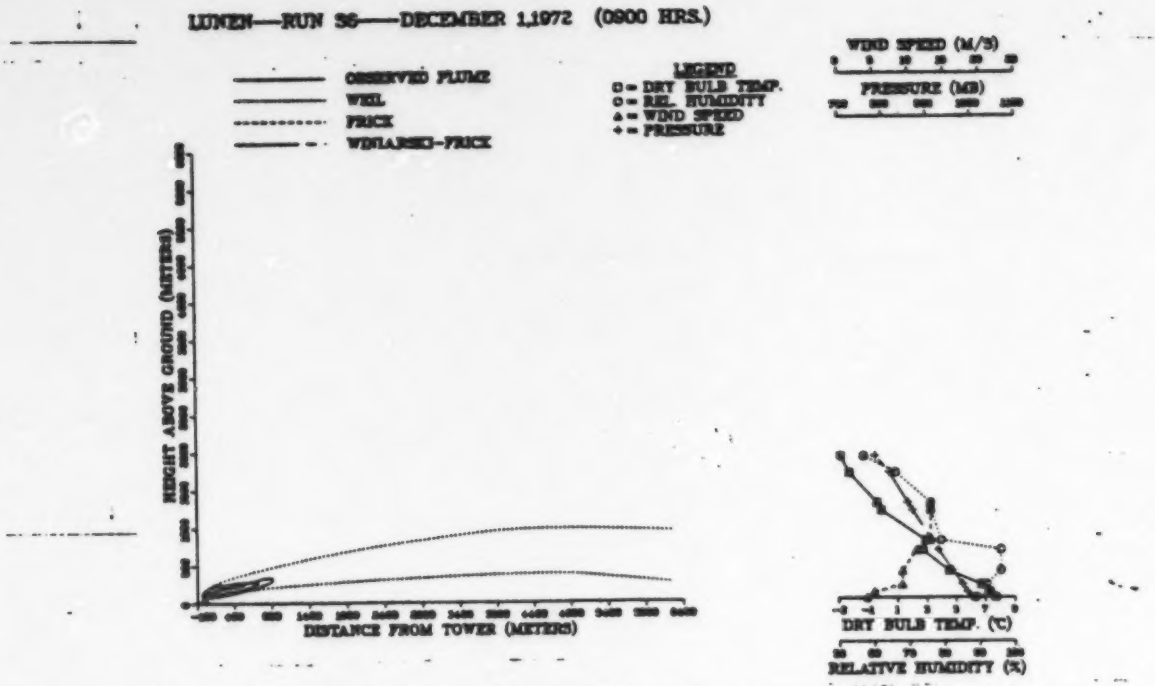

Fig. 3. Comparison of plume-model predictions of Weil, Frick, and Winiarski-Frick to observed visible-plume outline at Lunen: December 1, 1972 (0900 Hrs.)

goes into the turbulent and rotational motion of the plume and (d) the use of a rate equation for condensation in place of equilibrium thermodynamics. The validity of these alternatives is unknown at present.

3. PROBLEMS IN MODELING THERMAL PLUMES IN WATER

Boundary interference can be important under certain conditions for cooling tower plumes (high winds or large buildings upwind of the tower), yet it is seldom the dominant factor in plume dispersion. Such is not the case for thermal plumes in water. Moreover, cooling water discharges typically have less relative buoyancy and experience much smaller relative crossflows due to a higher exit velocity. Discharge configurations are highly variable and may be quite different from that assumed in the development of available models.

Deep water submerged discharges are similar in many respects to the cooling tower plumes discussed in the previous section. For shallow water discharges, the confining nature of the surface and bottom often overshadow buoyant jet development in the classical sense. Under certain conditions, the plume may mix vertically, completely filling the water depth. Discharges made at the shoreline may be forced against the shore by the current, producing long sinuous shorebound plumes. Transient currents produced by tidal influences or rapidly changing winds can also be significant considerations for plume modeling. To illustrate how these factors manifest themselves in the practical application of thermal plume models, we shall examine the results of model data comparisons from 3 sites.

3.1 Pilgrim Plant

The Pilgrim Plant on Cape Cod Bay is beset by strong wind effects, tidal and wind induced currents, bottom and shoreline interference with the plume, the presence of a very low densimetric Froude number at high tide, and a free overall discharge at low tide. Figure 4 illustrates the shoreline and bottom contours in the vicinity of the discharge; it may be observed that two shoals extend out from the shoreline, one on each side of the discharge. Typical high and low tide plumes are illustrated in Figures 5 and 6, respectively. Notably, low tide plumes are characterized by significant bottom interaction due to low water levels and higher effective densimetric Froude Numbers. In contrast, high tide plumes are characterized by buoyancy limited vertical mixing and relatively little bottom contact. Somewhat surprisingly, these two extremes yield statistically similar plumes in terms of surface isotherm areas, a common means of characterizing cooling water plumes.

Figure 7 compares predictions of the Pritchard model with the aggregate observational data from the Pilgrim plant, plotted without regard to tidal stage. As can be seen, the high tide predictions are reasonable and are, perhaps, on the conservative side. The low tide predictions, however, greatly overestimate plume dispersion due to a failure to consider the cutoff of vertical mixing by the bottom. Thus, the dominant mechanism at low tide is omitted from consideration. More details of the Pilgrim study are given by Dunn et. al. [10].

3.2 Kewaunee Plant

The 540 MWe Kewaunee Plant is located north of a small promontory on the western shore of Lake Michigan. The lake bottom in the area has a gradual slope of 1/100. The Kewaunee plumes may be divided into three broad categories: 1) northward, in which case the plume is sheltered by the promontory; 2) lakeward, in which case the plume moves offshore under the influences of discharge momentum; and 3) southward, in which case the plume interacts strongly with the promontory.

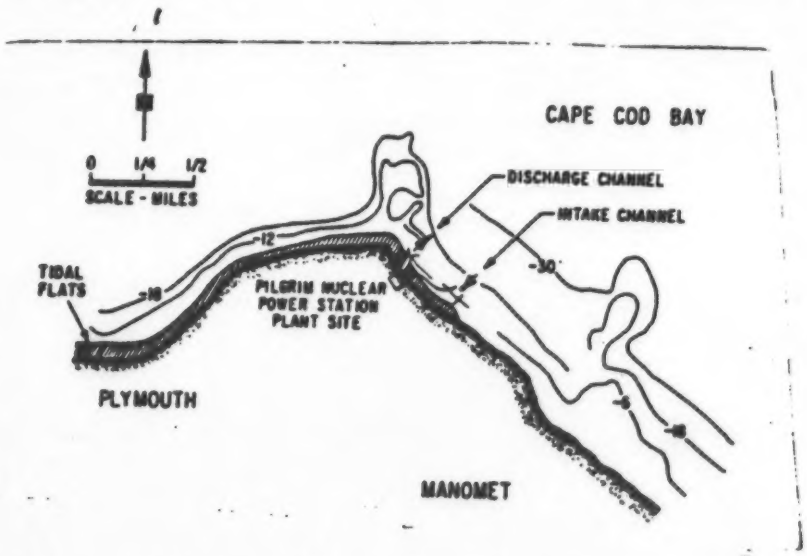

Fig. 4. Schematic View of the Pilgrim Nuclear Power Station Site.

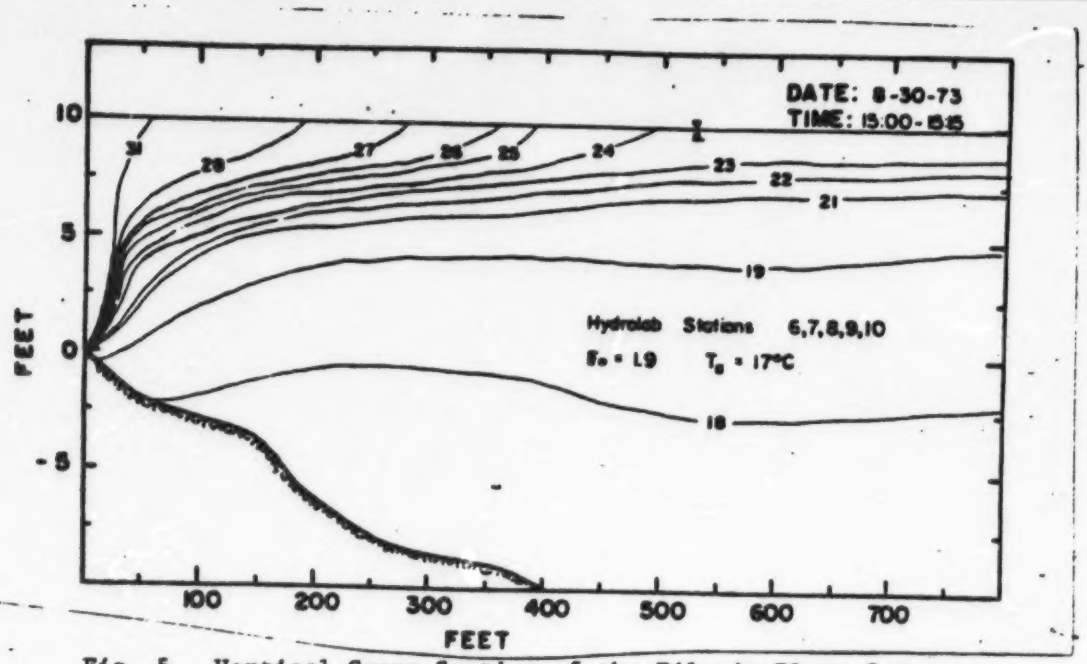

Fig. 5. Vertical Cross Section of the Pilgrim Plume for an Initial Densimetric Froude Number of 1.9.

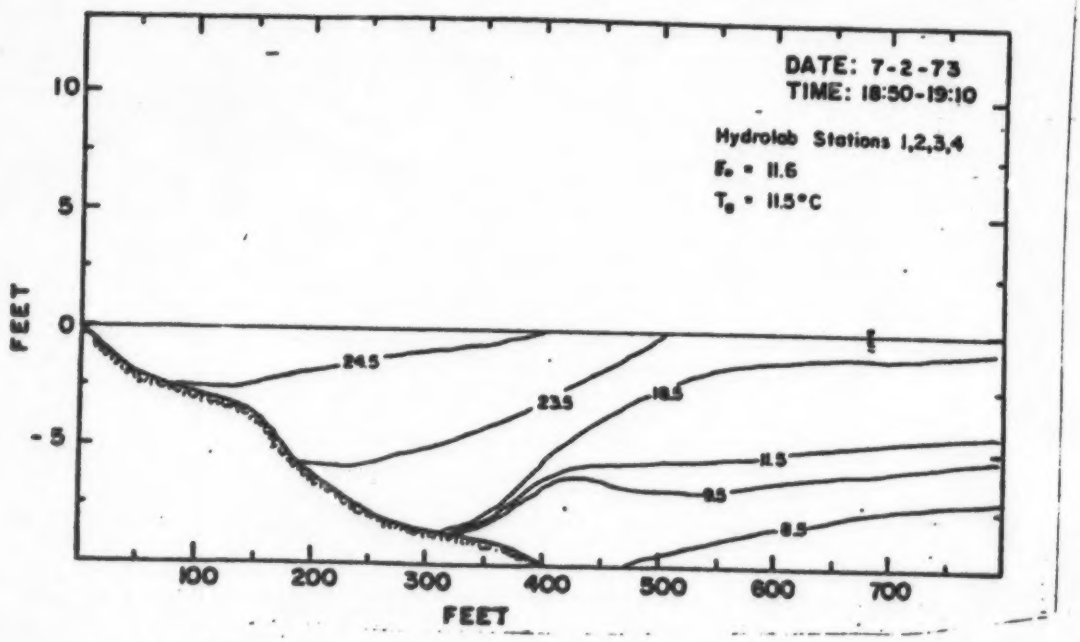

Fig. 6. Vertical Cross Section of the Pilgrim Plume for an Initial Densimetric Froude Number of 11.6.

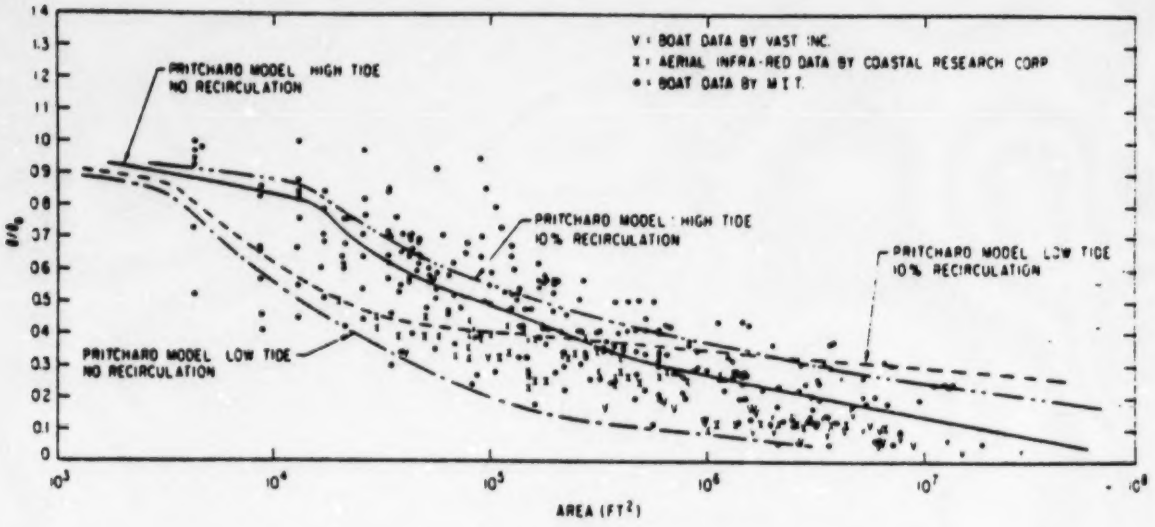
V = BOAT DATA BY VAST INC.
X = AERIAL INFRA-RED DATA BY COASTAL RESEARCH CORP
• = BOAT DATA BY M.I.T.
PRITCHARD MODEL HIGH TIDE NO RECIRCULATION
PRITCHARD MODEL HIGH TIDE 10% RECIRCULATION
PRITCHARD MODEL LOW TIDE 10% RECIRCULATION
PRITCHARD MODEL LOW TIDE NO RECIRCULATION
AREA (FT²)

Fig. 7. Comparison of available data from the Pilgrim Plant with selected Pritchard model predictions.

Figure 8 shows 3 comparisons of the Pritchard model predictions of the isotherm area against the observed values. The first comparison is for the model as originally formulated, from which we may observe a tendency for the model to underpredict the areas of the smaller isotherms and overpredict the areas of the larger ones. The second comparison reveals a small improvement when the additional effects of lake level are included. The third result shows the significant improvement possible when the model is modified and recalibrated to better incorporate site dependent factors. We must emphasize, however, that a model so calibrated for a single specific site should be used very cautiously in application to different sites. The work done at the Kewaunee site is discussed in depth by Murarka et al. [11].

3.3 Zion Plant

The Zion Nuclear Power Plant has two 1085 MWe units which also discharge from the Western shore of Lake Michigan through two box-like submerged discharge ports located 760 ft. off shore. Each structure has 14 outlet louvers 7 feet wide and 3 ft high. Owing to the rapid mixing between adjacent individual louvered slots, each discharge may be approximated as a rectangular slot 3 ft high and 75 feet long. The two slots, in turn, are oriented at 45° and 135° with respect to the north shore. Although the top of the discharge is 8 ft below mean lake level and the bottom of the discharge rests on the lake bottom, the discharge mixes vertically very quickly after exiting the discharge structure and fills the complete water depth. Thus, the Zion discharge is, in fact, more like a traditional surface discharge than a traditional submerged discharge such that application of a submerged discharge model would be unadvised. Other complicating factors include recirculation to the intake, reentrainment of the plume during current reversals and stratification in the ambient.

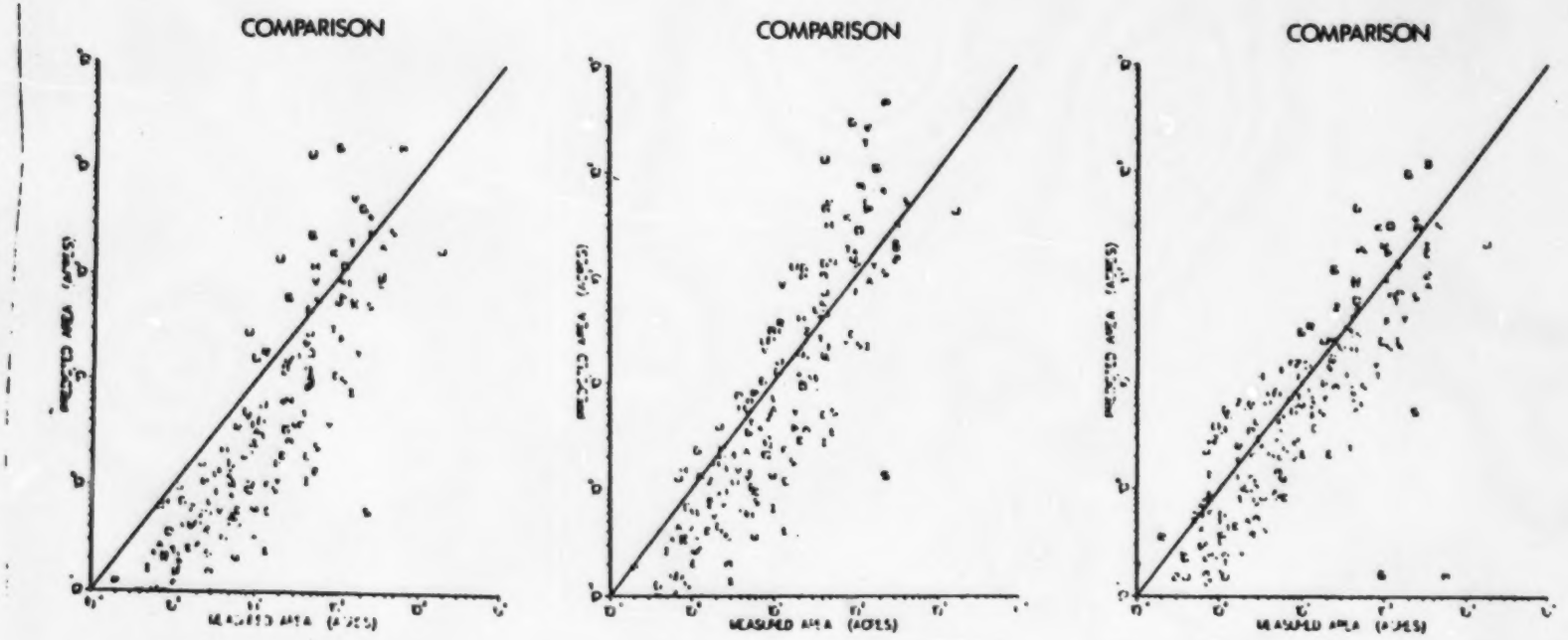

Fig. 8. Conglomerate plot of model/data comparisons to surface isotherm areas for Versions 1, 2, and 3 (left, middle, right, respectively) of Paily Model.

Figure 9 shows a comparison of preoperational predictions with measured surface isotherm areas. As may be observed, predictions can be improved significantly by including bottom interaction and re-entrainment as shown by the curved labeled "corrected." The work done at the Zion Site is discussed in depth by Mararka et al. [12].

4. CONCLUSIONS

Despite many years of research in the area of buoyant jet modeling, fundamental problems exist in our understanding of the basic physics of plume dispersion. Two of these fundamental problems common to plumes released into water and into air are the correct treatment of buoyancy and the handling of boundary interactions. Modeling discharges from cooling towers is relatively free of site specific problems since the receiving media and the discharge geometry is quite similar at all sites. By contrast, thermal discharges of cooling water exhibit many site specific problems relating to bottom shoreline and surface interaction, irregular discharge geometry, etc.

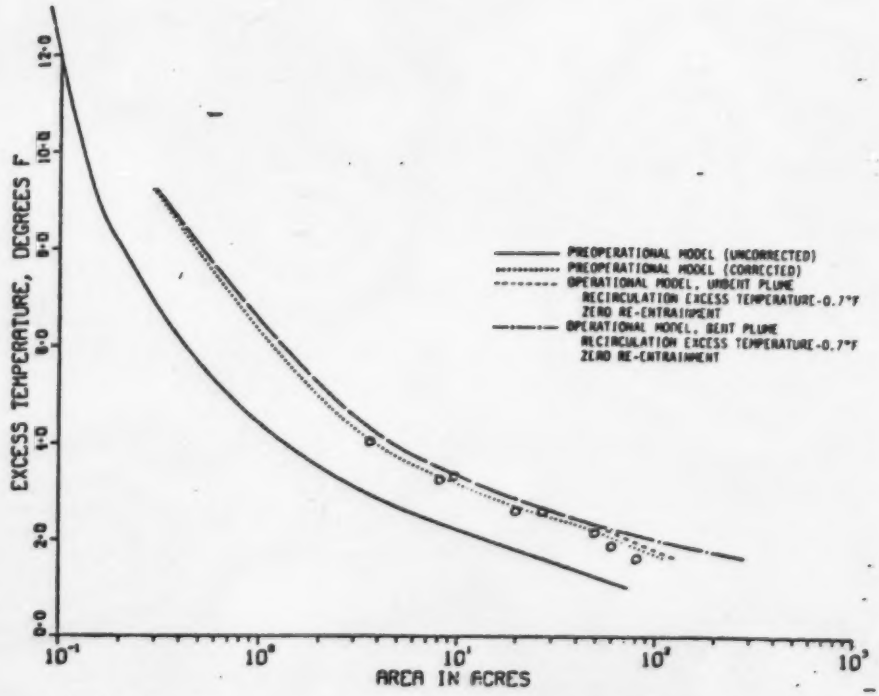

Fig. 9. Comparison of Pritchard Model predictions to Zion surface area data for December 9, 1973--unstratified conditions.

REFERENCES

1. A.J. Policastro, R.A. Carhart, S.E. Ziemer and K. Haake, Evaluation of Mathematical Models for Single and Multiple Source Natural Draft Cooling Tower Plume Dispersion, Division of Environmental Impact Studies, Argonne National Laboratory, U.S. Nuclear Regulatory Commission, NUREG CR 1581, Vol. 1, 1979.

2. A.J. Policastro, W.E. Dunn, M.L. Breig, J.P. Ziebarth, Evaluation of Mathematical Models for Characterizing Plume Behavior from Cooling Towers. Vol. 2. Salt Drift Deposition from Natural Draft Cooling Towers, Division of Environmental Impact Studies, Argonne National Laboratory, U.S. Nuclear Regulatory Commission Report NUREG/CR-1581, February 1979.

3. W.E. Dunn, S.K. Cooper, and P.M. Gavin, Evaluation of Mathematical Models for Characterizing Plume Behavior from Cooling Towers. Vol. 3. Plume Rise from Mechanical Draft Cooling Towers. Department of Mechanical and Industrial Engineering, University of Illinois at Urbana, U.S. Nuclear Regulatory Commission Report NUREG/CR-1581, December 1979.

4. R.A. Carhart, A.J. Policastro, and S. Ziemer, Evaluation of Mathematical Models for Natural-Draft Cooling-Tower Plume Dispersion. Atmospheric Environment. May 1981.

5. B. Morton, G. Taylor, and J. Turner, Turbulent Gravitational Convection from Maintained and Instantaneous Sources, Proc. of Royal Society of London, Ser. A. Vol. 234, pp. 1-23, 1956.

6. T.M.L. Wigley, Condensation in Jets, Industrial Plumes and Cooling Tower Plumes, Journal of Applied Meteorology, Vol. 14, p. 78-86, February 1975.

7. W.K. George Jr., R.L. Alpert, and F. Tamanini, Turbulence Measurements in an Axisymmetric Buoyant Plume, Basic Research Department, Technical Report 22359-2. RC-B-53, Faculty Mutual Research, Norwood, Massachusetts, January 1976.

8. H. Nakagome and M. Hishida. The Structure of Turbulent Diffusion in an Axisymmetric Thermal Plume. IN: Turbulent Buoyant Convection. Proceedings International Center for Heat and Mass Transfer. Dubrovnik, Yugoslavia. pp. 361-372, August 1977.

9. P.L. Vollet, Study of Jets in Transverse Currents and in Stratified Environments, Doctoral Dissertation, Curie University, Paris, France, February 1977 (in French).

10. W.E. Dunn, A. Policastro, and R.A. Paddock, Surface Thermal Plumes: Evaluation of Mathematical Models for the Near and Complete Field, Argonne National Laboratory, ANL/WR-75-3, Part One (June 1975), Part Two (August 1975).

11. I.P. Murarka, J. Ferrante, A. Policastro, and E. Daniels, An Evaluation of Environmental Data Relating to Selected Nuclear Power Plant Sites, The Kewaunee Nuclear Power Plant Site, Division of Environmental Impact Studies, Report ANL/EIS-1, Argonne National Laboratory, August 1976.

12. I.P. Murarka, A. Policastro, E. Daniels, J. Ferrante, and F. Vaslow, An Evaluation of Environmental Data Relating to Selected Nuclear Power Plant Sites, The Zion Nuclear Power Plant Site, Division of Environmental Impact Studies, Report ANL/EIS-5. November 1976.

WORKING SESSION W-3

UTILIZATION

PB82-228453

COGENERATION - A STATUS REPORT OF THE DEPARTMENT OF ENERGY INDUSTRIAL PROGRAM

Alan J. Streb
Acting Director
Industrial Programs
Department of Energy
Washington, D.C. 20585

ABSTRACT

Industrial Cogeneration saves energy because low heat rate byproduct power displaces high heat rate central station power. Maximum energy savings occur if the power byproduct of the cogeneration system is maximized. Maximum saving of critical fuels occurs when the cogeneration system is fuel flexible. Most industrial cogeneration systems which have been installed to date employ extraction steam turbine systems. To a lesser extent gas turbines and diesel machines have been used. Although steam turbine systems can use any common fuel, they are relatively inefficient in cogeneration because the steam extracted for process use competes directly with power production. On the other hand, gas turbine and diesel engines deliver power more efficiently but as currently applied to cogeneration, they require the use of more critical fuels (oil and gas).

The Department of Energy (DOE) cogeneration program seeks to encourage the development of cogeneration and reorient its implementation toward systems which offer larger overall energy savings - with emphasis on savings of critical fuels. The program contains two basic elements. They are technology development and market stimulation.

Accurate knowledge of the degree to which cogeneration has already developed and the magnitude of the remaining opportunity is essential to the development of a rational national plan. The DOE effort to characterize the potential cogeneration opportunity seeks to provide this knowledge. In the past, aggregate energy service demands of various industrial sectors were used as the basis for projections of potential capacity. As part of the DOE industrial cogeneration program, a much more sophisticated model has recently

Preceding page blank

been developed which examines energy service demands on a process-specific basis and relates the processes to specific industrial plants. Coupled with a newly tabulated inventory of existing systems, the model, thus, enables the projection of cogeneration potential which includes estimates of the size and number of systems within each industrial sector. A preliminary analysis of national cogeneration potential development based on this new model is presented in the paper.

INTRODUCTION

The principal industrial energy demands are in the form of steam or process heat. Frequently, the industrial thermal process utilizes only a small fraction of the thermodynamic availability of the input energy source (see Figure 1). The balance of the availability is lost. Maximum energy efficiency is realized when availability loss is minimized. It is often possible to couple one industrial process with a complementary process to minimize this loss. Complementing one industrial process with another is known as energy cascading. Where it is impractical to cascade industrial processes it may be possible to couple the process with a heat engine. Complementing an industrial process with a heat engine is called cogeneration. In this context, the mechanical or electrical power produced by an industrial cogeneration system is a byproduct of the process, which may or may not match the power demands of the industrial plant.

Topping cycle cogeneration systems utilize thermal energy at high temperatures to produce power, then utilize the lower temperature exhaust to satisfy process thermal demands. To derive maximum benefit from topping cycle cogeneration, conversion system technologies must be available which can be closely matched to the specific thermal demands of low temperature industrial processes. Because the nature of the thermal demands varies considerably, a variety of energy conversion system technologies are required. A maximum degree of fuel flexibility is also desirable.

Bottoming cycle cogeneration systems are coupled with high temperature industrial processes to utilize the waste heat from the process to generate power. Because industrial waste heat varies substantially in temperature and volume, a range of waste heat engine technologies and equipment sizes are required to efficiently capture this potential resource.

The total potential for industrial cogeneration, in terms of energy savings, is a function of the industrial thermal requirements which are compatible with cogeneration and the mix of technologies which are used to meet the thermal requirements. High power to thermal output ratio conversion systems will deliver large quantities of byproduct power and, because cogenerated byproduct power is produced at a low heat rate in comparison to conventional power production, those systems which maximize power output will usually deliver the greatest energy savings. The actual energy savings which result from cogeneration are, therefore, highly dependent on the selected technology mix and on the degree of market penetration.

The overall DOE program, therefore, contains two thrusts - technology development and market stimulation. The technology development thrust seeks to remove technological obstacles to the acceptance of fuel flexible efficient systems. The market stimulation activity seeks to identify viable opportunities and to develop mechanisms to encourage acceptance.

Energy conversion system technologies are available today which enable cogeneration to satisfy much of the industrial thermal energy demand. A summary of the characteristics and developmental status of a number of alternative topping and bottoming cycle alternatives are shown in Tables IA and IB respectively. Approximate values of the conversion efficiency are presented for each system. Three descriptive parameters - power to thermal ratio, effective heat rate and savings per process thermal unit — have been developed and are described in Table I. The values of these parameters for each of the conversion systems are given in the tables.

Significant variation exists in conversion efficiency of topping cycle conversion systems and, as a result, in their specific energy savings. If energy savings were the only consideration, gas turbine and diesel systems would be the obvious first choice. The current ability to burn coal and process residuals is a compelling argument however, which favors the choice of steam turbine systems.

Advances in technologies such as externally fired gas turbines, coal slurry burning diesels and Stirling engines will combine the fuel flexibility advantage of steam turbines with the performance advantages of gas turbine and diesel engines. In the short term coal or industrial wastes should be used in those industrial applications with which they are compatible. In these installations, steam turbine cogeneration systems will be used. When industrial residuals are not available, or when coal cannot be used in any event because of site limitations, serious consideration should be given to petroleum or gas fueled cogeneration, which can maximize energy savings and decrease overall petroleum or gas consumption.

The practice of bottoming cycle cogeneration has not yet developed on a large scale. Bottoming cycle cogeneration requires low temperature conversion systems which have limited commercial availabilty. This limitation will be quickly overcome when the viability of the market becomes more certain. Development is progressing on several candidate conversion system technologies identified in Table IB. Technical feasibility has been demonstrated on all of the candidates In the near term, economic considerations are more important than conversion efficiency since power in any magnitude is more valuable than the low grade waste heat source. Field trials are in progress but economics must be improved before any substantial demand will develop.

The DOE industrial cogeneration technology development activity includes component development and industrial integration engineering and testing of those systems which fall outside the range of conventional proven practice and which offer some significant advantages with respect to improved energy use efficiency.

The DOE component development program consists of RD&D activities designed to expedite the commercial readiness of advanced cogeneration technologies. The primary objective is to accelerate the introduction of technologies in the industrial sector to achieve savings in oil and natural gas through fuel switching and improved conversion efficiency. This effort addresses completely new technologies for cogeneration applications such as organic Rankine bottoming cycles as well as major advancements in existing technologies to achieve improved efficiency and fuel flexible systems such as externally fired Brayton cycle engines.

Gas turbine technology occupies an important position in the DOE cogeneration component development program. Work is underway in both open and closed cycle systems. The principal project is the development of a high temperature gas turbine fired with the low BTU gas product of a coal gasifier and operated

in a combined cycle system. One of the key aspects of this project is the development of advanced cooling concepts such as film and transpiration cooling, and water/steam cooling turbine blades and nozzles. Projects are also underway dealing with combined closed cycle gas turbines, and with externally fired open cycle gas turbine components, both of which enable direct operation with coal and other alternate fuels. Another project which has been initiated is the assessment of the feasibility of burning coal directly in diesel engines. In the latter project, coal is delivered in a slurry with oil or water as the vehicle. The coal-water slurry approach is particularly interesting because it eliminates the need for oil as a fuel and increases the specific power output of the engine. A test engine has operated for short periods of time on both the coal-oil and coal-water slurry fuel systems.

Another DOE component development program focuses on the recovery of relatively high grade industrial waste heat by employing bottoming cycle systems. Work is in progress on both Rankine and Brayton cycle machines. Concentration has been placed on the development of organic Rankine engines because of the potential for high efficiency over the range of temperatures commonly found in industrial waste streams. Small engines have been built and operated successfully. More work is needed to broaden available size range and to increase flexibility with respect to waste stream temperatures.

Acting under the assumption that it is necessary to demonstrate satisfactory performance of advanced technologies in an industrial environment before industry will readily accept those technologies, DOE has initiated three projects which support the industrial integration of systems which depart from conventional practice. These projects are heavily cost-shared by the host industry. Currently, there are two topping cycle projects - a high-back pressure steam turbine system and a residual oil-fired low speed diesel system. The high-back pressure steam turbine cogeneration system demonstration is being installed in a textile mill. It consists of a coal fired boiler providing steam to a steam turbine. This turbine operates at an unusually high-back pressure of 225 psi. This exhaust steam is delivered to a 225 psi manifold that provides process steam for the plant. The system provides 4 MW of electricity and 135,000 lbs/hr of steam. There are no emission problems, the exhaust contaminants are controlled by a bag house and the State environmental permit has been received. The overall energy use efficiency is greater than 77 percent. Projected energy savings for this one unit are 289 x 10^9 BTU/yr (or 50,000 bbl/yr oil equivalent). The savings are in coal at the plant, and in coal, oil and nuclear at the utility. The savings lead to a DCF return on investment (ROI) on the generation components capital cost of 20 percent. A low speed diesel cogeneration system is being developed for a pharmaceutical plant. It consists of a ten cylinder unit that produces 23.3 MW of electricity, 160,000 lb/hr of 225 psi steam and 260,000 lb/hr of hot water. It is an unusual arrangement in that the diesel exhaust is reburned in the supplementary fired waste heat boiler. The maximum plant electricity demand is 23,000 KW resulting in a small surplus of power available for delivery to the utility grid. The system is very efficient, its overall calculated efficiency, giving effect to the electricity, steam and hot water produced, is in excess of 87 percent. This one unit is projected to save 225,000 bbl/yr of the residual oil it uses for fuel, over conventional generation of heat and power. The savings resulting from the decreased fuel and electricity costs provide a DCF ROI of 19 percent. The emissions are within the Federal Ambient Air Quality Standards and a Prevention of Significant Deterioration (PSD) permit has been approved by the Environmental Protection Agency. The preliminary design has been prepared and approved, the large components (diesel, generator, and boiler) are on order and the detail design is being completed. Installation will be completed in the summer of 1982 and a one-year evaluation period is

planned. In addition, the DOE is also supporting one bottoming cycle demonstration project which involves a number of adaptations of an organic Rankine waste heat engine system to a variety of industrial applications. These units will utilize waste heat from hot process streams or exhaust gases and produce electricity for in plant use or delivery to the utility grid. In the present configuration they provide 600 KW electrical; development is underway to increase the output of this engine to 750 KW. Initial installations are planned for a container plant and a cement kiln. Three existing development units are installed and operating, a fourth is being installed.

MARKET STIMULATION

The market stimulation activity has encompassed numerous projects. Case studies were conducted which examined several existing cogenerators to develop an understanding of the conditions which lead to the original investment decision and to document their experience in operating such systems. The results of these efforts documented in Reference 1 confirm that cogeneration systems can be totally compatible with industrial process operations and provide sufficient benefit in terms of avoided purchased power cost to justify continued operations. However, one case was found which was something less than a satisfactory experience; in which unanticipated operational costs resulted in financial losses eventually forcing abandonment of the system.

The Industrial Cogeneration Optimization Program (ICOP) consisted of a second set of very detailed case studies which examined a range of potential cogeneration sites. The primary objective of this effort was to identify the method for selecting the system configuration or configurations which would yield maximum energy savings and simultaneously yield a reasonable return on investment for each of the cases studied. Potential impediments resulting from conflicting regulations were identified and discussed. The most significant general conclusions resulting from this effort were - "that with present and projected energy prices, the coal fired steam turbine was the only commercially available power generation system which provided a rate of return in excess of the threshold for most of the plants under consideration. There were several cases where due to special circumstances, primarily where the local utility used large amounts of oil or gas, use of combustion turbines, even though they used premium fuels, provided large net savings of oil or gas."

Perhaps the questions most frequently asked regarding cogeneration relate to the potential for development. Just how much power could be cogenerated and what contribution could be made to improve energy used efficiency? Under DOE sponsorship, a study entitled "The Potential for Cogeneration Development in Six Major Industries by 1985," referred to hereafter as the "Six Industry Study" (Reference 2) was conducted by Resource Planning Associates to provide answers to this question. Estimates of cogeneration potential were made based on a gross examination of the steam demands in six major industrial sectors (chemicals, petroleum refining, paper, steel, textiles, and food). Steam demands which were not technically compatible with cogeneration were eliminated from consideration. Such eliminations were made when steam demands for certain processes were small, were transient in nature or were expected to decline as a result of anticipated process modifications. Steam demands which passed the technical test were then examined for economic acceptability. It was assumed that technically compatible cogeneration opportunities would be developed by industry to the same extent as any other discretionary investment which produces a comparable return. Historical evidence was used to develop the relationship between the return on various investment opportunities available

to an industrial sector and the degree to which the industry had made such investments. Combining this information with estimates of return-on-investment for various cogeneration systems produced an estimate of the extent to which the cogeneration system would be developed for a particular application in a particular industrial sector. Aggregation of all of the technically and economically viable applications in all of the sectors yielded the estimate of total potential for cogeneration. Projections were made for future years by considering the anticipated growth in each of the industries. The effect of various Government policy initiatives such as tax incentives, loan guarantees and regulatory relief were also examined by considering the likely effect of these actions on the return on investment. In a sequel to the basic study, consideration was also given to the effect of the adoption of high power to thermal ratio cogeneration technologies which would yield higher output of byproduct power than the traditional practice and, therefore, offer greater potential savings. The bottom line conclusion of the effort was that cogeneration could contribute between 40,000 MW and 120 000 MW of new capacity by the year 2000 and save between 1.6 and 4.0 quadrillion BTU of energy per year. The large range of the estimates were attributable to the possible range of acceptance of the non-conventional cogeneration practice, the incentives provided by the Government for such investments, and the extent to which surplus power could be absorbed by the local utility companies. Much useful information emerged from this effort. The study provided insight into the Government policies which would most effectively encourage cogeneration investments and the technical directions which cogeneration should take if energy savings were to be maximized. Accordingly, the Six Industry Study had a strong influence on the composition of the DOE cogeneration program.

Although the Six Industry Study provided much useful information, a much more detailed examination was needed to provide a more accurate and detailed characterization of existing as well as potential capacity. For example, it is obviously useful to know the numbers and sizes of systems already in place, the numbers and sizes of potential systems, and the distribution of potential capacity by State and electrical service region.

In 1980 a comprehensive detailed study was initiated to collect and compile this data. This study entitled "Targeting of Cogeneration Opportunities at the Plant Site" (TOCOPS) is being performed by General Energy Associates with the assistance of the International Cogeneration Society. The compilation and characterization of existing cogenerators is being assembled by examining data available from their connected utilities and a very comprehensive commercial data base. Development of the initial existing cogeneration data base has been completed and is now being validated through the utilities and industries associated with the specific systems. Results to date are in close agreement with independent evaluations of electrical capacity. Approximately 7300 MWe are connected to the utility nets around the country and it is estimated that there is an additional 1600 MWe which are not grid connected. Over 475 installations of electricity producing units have been identified and there are undoubtedly many more not grid connected. In particular, there is little knowledge of the numbers of direct shaft power units that may be installed in the process industries. Industrial cogeneration's contribution toward meeting the present electrical requirements of the Nation exceeds 47 billion kilowatt hours.

The major objective of the TOCOPS effort is to determine the potential for cogeneration on a plant by plant basis. This determination is being made by utilizing a General Energy Associates data base called the Industrial Plant Energy Profile (IPEP). IPEP was developed by combining a process encyclopedia developed under DOE sponsorship with industrial trade association data on major

plants as illustrated in Figures 2A and 2B. The process encyclopedia is a compilation of material and energy balances for 108 major industrial processes. It describes the nature volume, and conditions of all streams flowing through each process. An example is shown in Figure 3. The industrial trade association data provides the location of and process equipment data on approximately seven thousand major plants and provides information relative to the volume and types of product produced at each plant. The combination of the encyclopedia and the plant file enable estimation of the character and magnitude of all process streams. Thus, on a plant by plant basis, IPEP can be employed to estimate the steam and process heat requirements as well as the temperature and magnitude of waste heat streams. TOCOPS uses these results as shown in Figure 2B to determine those which are compatible with cogeneration and employs the characteristics of candidate cogeneration systems to estimate the magnitude of byproduct power production and energy savings potential. Adjustments are made in the estimates in those cases where cogeneration systems are already in place with known characteristics. Economic tests are applied to potential systems to ensure that the system meets the required investment criteria which would likely be imposed by the owner. Aggregation of estimated potential for all of the plants result in overall estimates of national potential for cogeneration. Because estimates are developed on a plant by plant basis, aggregations can also be made by locality, SIC code and powerplant size.

Work is progressing and will be complete late in 1981. At the time of this writing, preliminary results are available and reveal some interesting market features. Figures 4 and 5 shows the total potential number of installations and cogeneration power by industrial sector. It is no surprise that the majority of the opportunities are found in chemical, refining and pulp and paper. The chart also shows the systems already in place represent a very small fraction of the total potential. Figure 6 shows total number of systems by system size It is interesting to note that most of the potential systems are in the size range less than 5 MW but that there is also a significant cluster in the 10-20 MW range. Although most of the potential systems by number are in the small size ranges, most of the potential power generation is in the range from 20 to 50 MW as shown in Figure 7. Figure 8 shows the cumulative power cogenerated versus plant size. This illustration shows that the potential for cogenerated power is currently 50 000 MW based on aggregation of data from existing U. S. industrial plants. As industrial production grows the potential for cogeneration will also grow. Based on an anticipated growth of 5 percent per year, the potential for cogeneration will reach approximately 120,000 MW by the year 2000. This preliminary estimate is in good agreement and tends to confirm the results of the Six Industry Study. If this level of cogeneration were to be developed by the year 2000, it would produce energy savings of over 4 quadrillion BTU's annually relative to the energy required to generate the same power at central station powerplants. The remaining work on this study is to crosscheck the estimates against the results obtained in selected interviews and rationalize any differences that are revealed. The potential for cogeneration will then be reported by industrial sector, geographic location, utility service region and system size.

CURRENT NATIONAL ACTIVITY

The recent market activity for cogeneration equipment has been mixed, with most equipment manufacturers reporting few specific cogeneration unit sales. One major manufacturer however reports that his back pressure and extraction steam turbine unit sales are up by 50 percent. The majority of the manufacturers report a lot of interest and requests for information but that most clients are delaying commitment. The expressed reasons for this un-

willingness to commit are the present economic situation, the potential changes to the Fuel Use Act and the Natural Gas Policy Act and uncertainty over the new rates resulting from the Public Utility Regulatory Policies Act (PURPA). These issues are slowly being resolved. Industrial purchasers will always opt to put their available capital in product improvements or production capacity rather than a cogeneration installation when perceived returns are approximately equal. But the return on investment for cogeneration is improving. Incremental new capacity for cogeneration at present, based on recent experience, should be 700 - 1200 MWe per year. The most recent reports (Reference 3) indicate that 774 MWe will be added in 1981. With the backed-up demand as reported by the several manufacturers, the annual sales should rise dramatically when the restraining factors, real and imagined, are removed.

The national benefit is clear, the attractiveness of cogeneration is improving - the opportunity for cogeneration is now.

MAJOR CONCLUSIONS

- Cogeneration can yield significant national energy savings.
- Cogeneration system installation as projected by two demonstration projects can provide acceptable return on investment.
- The majority of power generated will be from units in the 10 - 50 MW electrical size.
- The largest number of potential systems are in the size range below 5 MW electrical.
- The present market activity is slow but appears to be ready to increase dramatically in the near future when several constraints are removed.

REFERENCES

1. Industrial Cogeneration, Report # 6, Project Overview and Synthesis, Jack Faucett Associates, Argonne National Laboratory Contract #31-190-38-4834, May 1980.
2. The Potential for Cogeneration Development in Six Major Industries by 1985, Resource Planning Associates, Cambridge, Massachusetts, NTIS Report # HCP/M60172-01/2, December 1977.
3. New Generating Capacity: When, Where, and By Whom, Power Engineering, Vol. 85, Number 4, April 1981.
4. Industrial Cogeneration Optimization Program, Arthur D. Little, C-82467, DOE/CS/05310-1 and DOE/CS/05310-01, January 1980.
5. Industrial Cogeneration Optimization Program, TRW, Inc., CONS-4300-T1, September 1979.
6. Guidelines for Developing State Cogeneration Policies, Resource Planning Associates, HCP/M 8688-01, April 1979.

Figure 1

UTILIZATION OF THERMODYNAMIC AVAILABILITY

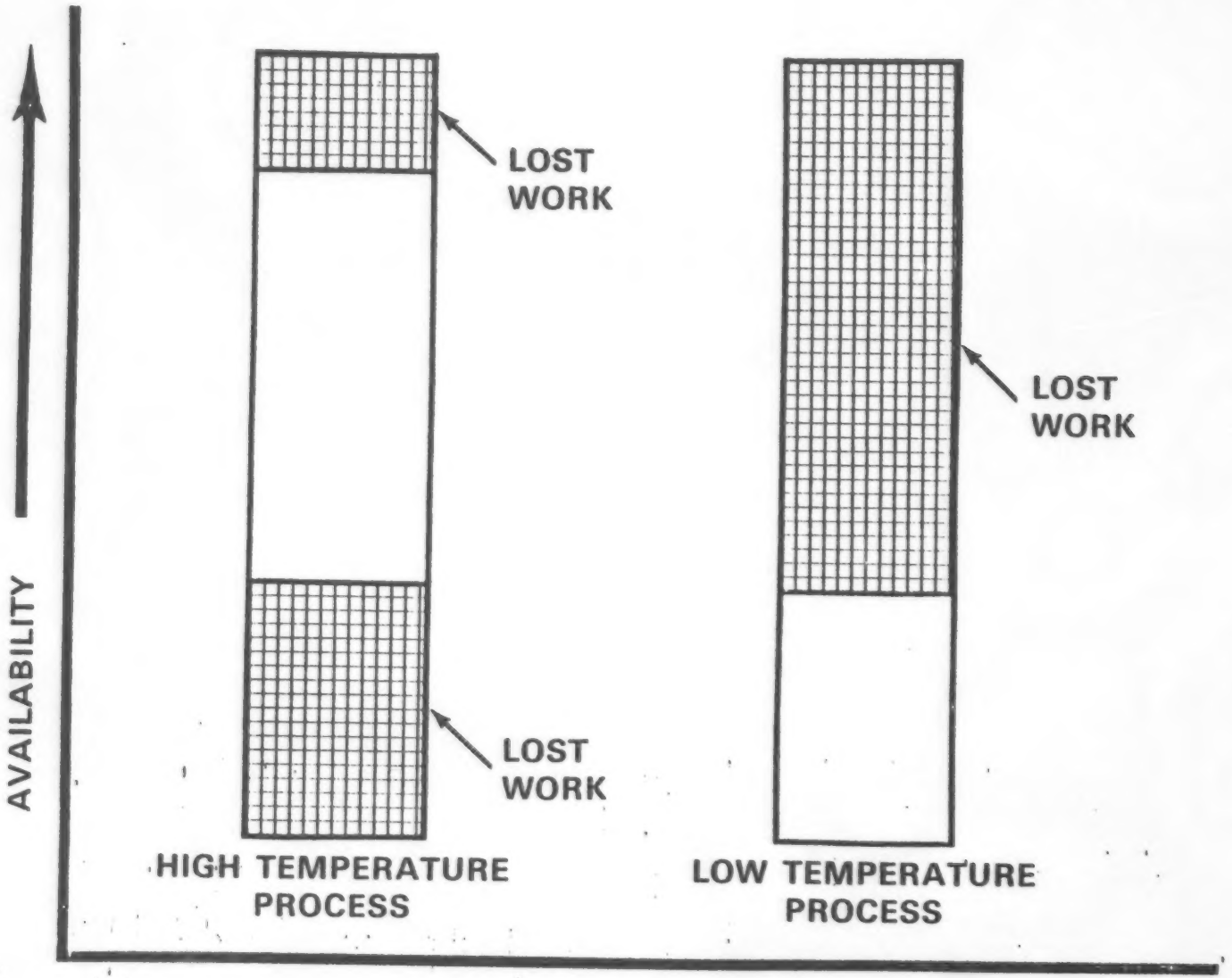

M-3-681

Figure 2A

Approach to General Energy Associates Industrial Plant Energy Profile Data Base (GEA/IPEP)

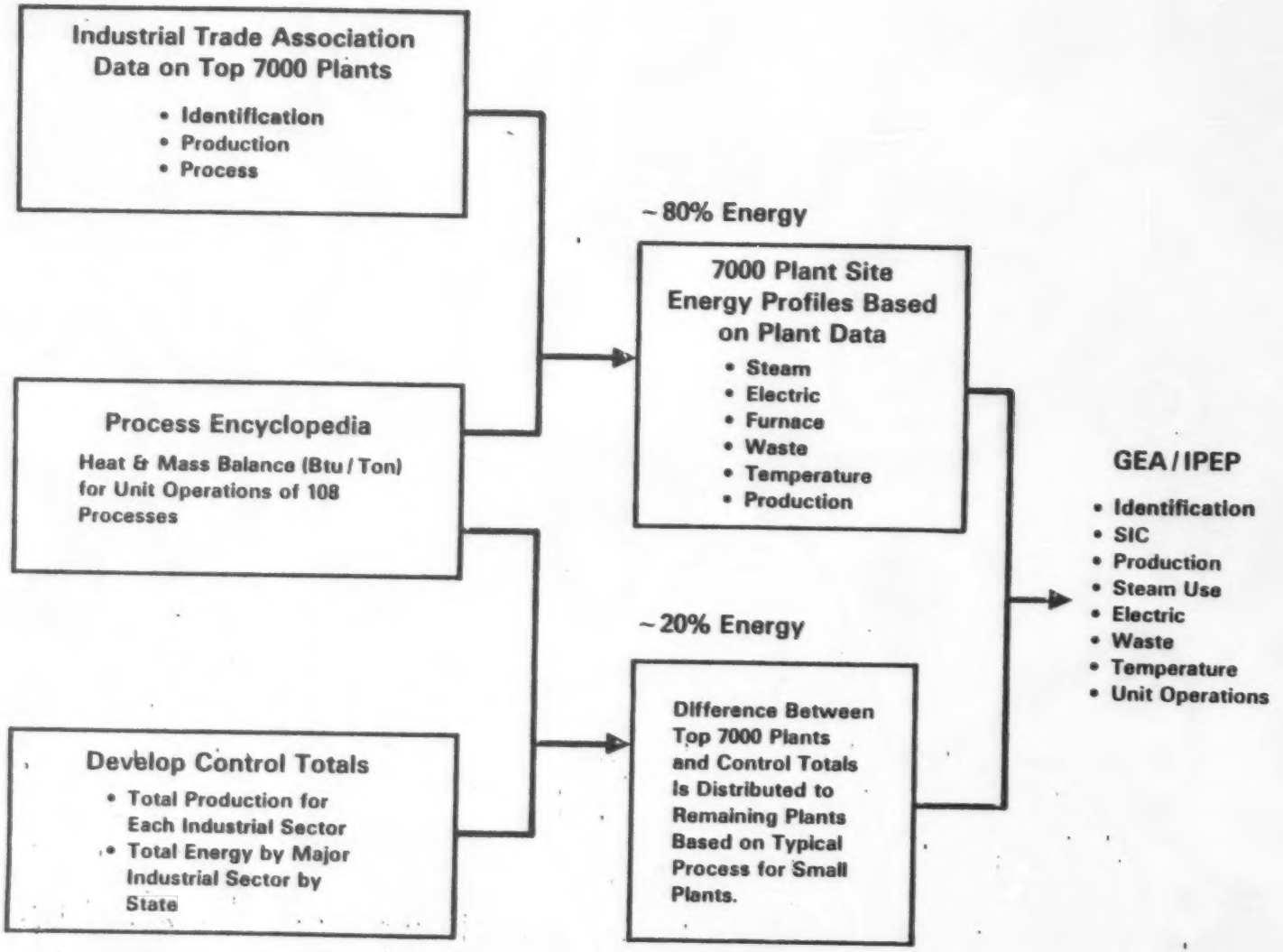

W-3-682

Figure 2B

COGENERATION PROGRAM METHODOLOGY (TOCOPS)**

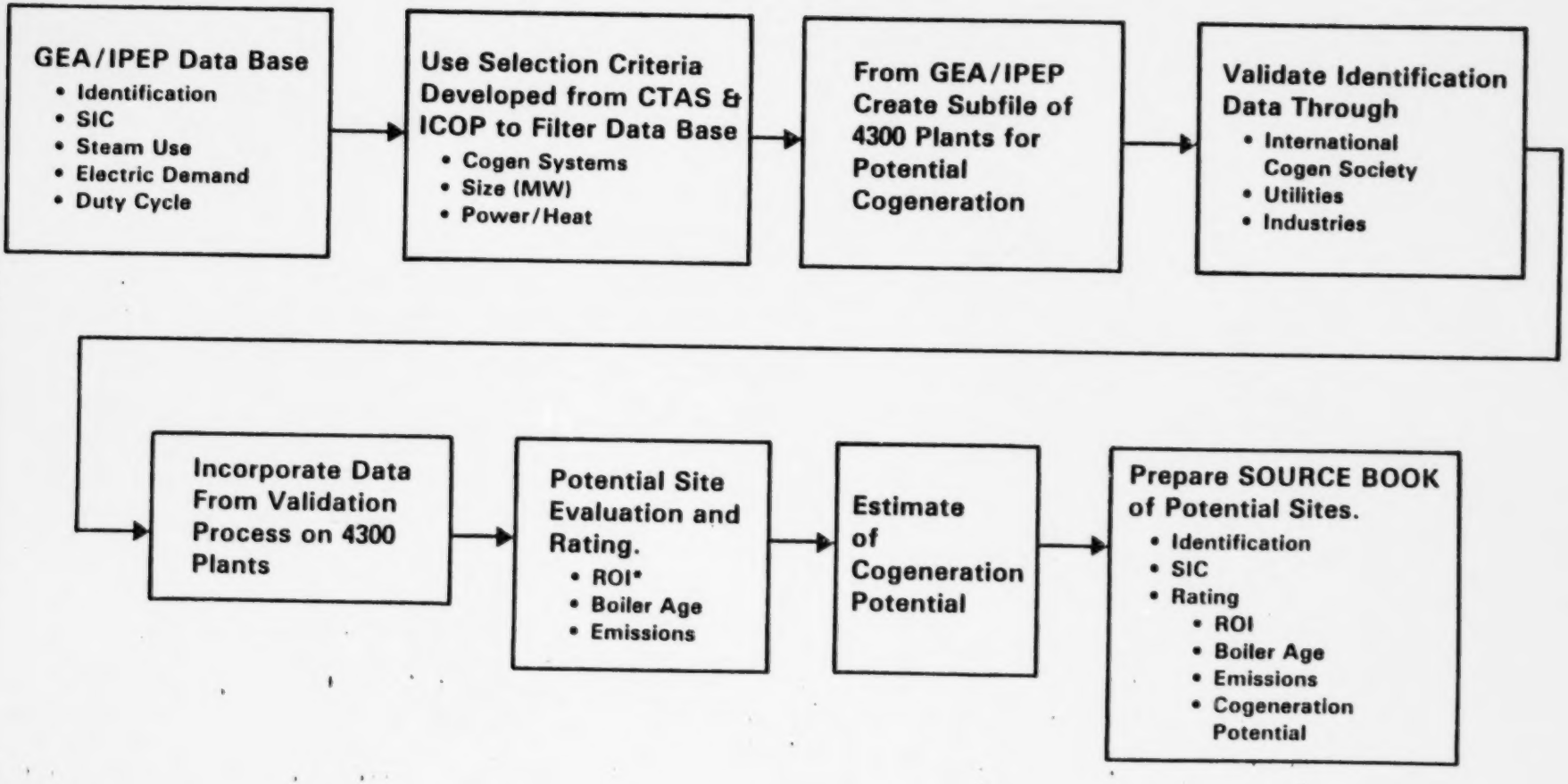

W-3-683

*Must pass minimum value.

**(Targets of Cogeneration Opportunities at the Plant Site)

Figure 3A

SIC 2812-1 Alkalies and Chlorine ($NaOH$, Cl_2 — Diaphragm Cell) Process Flow

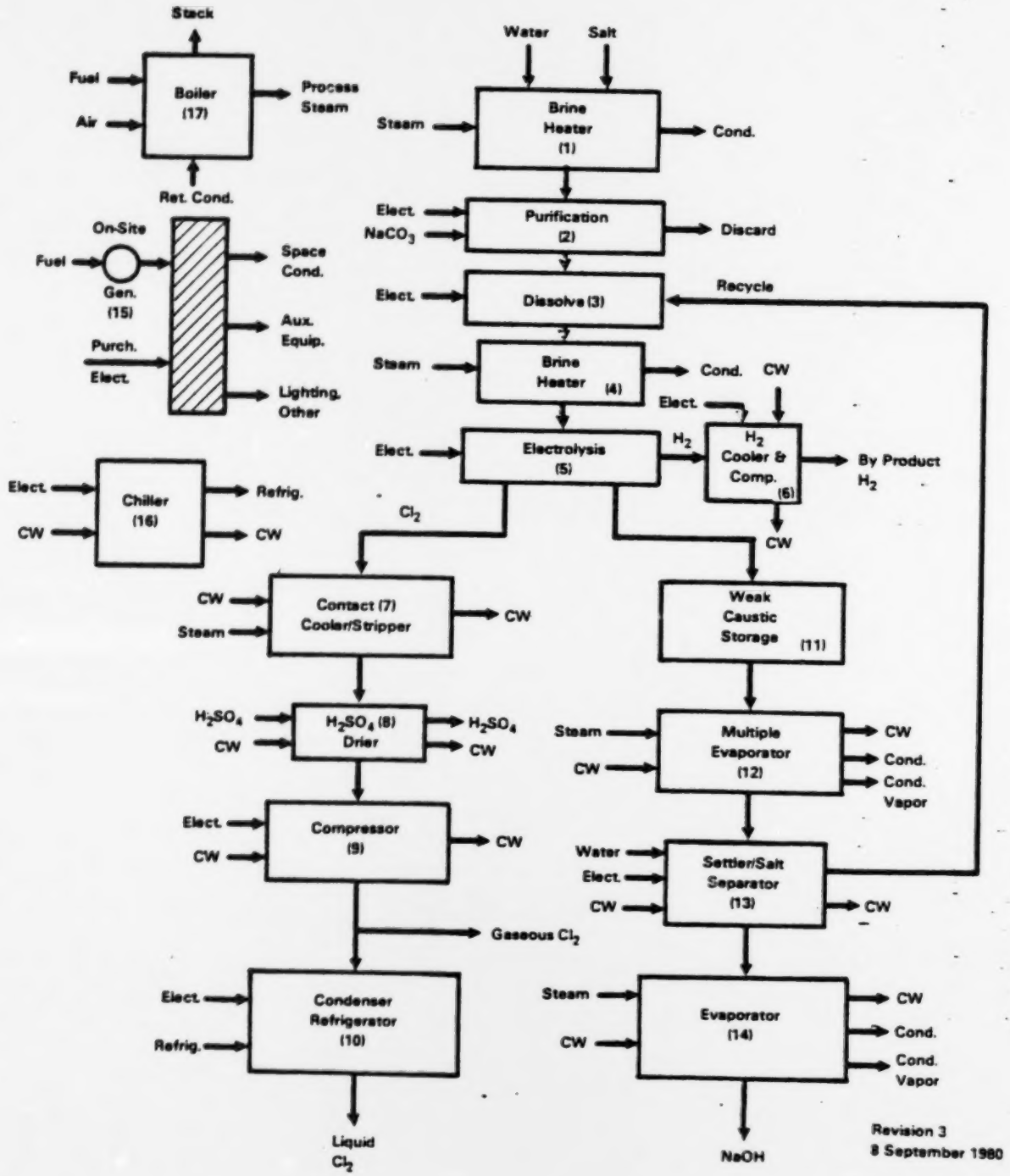

Figure 3B

Industry 28121: Alkalies and Chlorine

Unit Operation			Inlet				Outlet			
No	Description	Temp (F)	Flow	Temp (F)	Mass (Lb)	Energy (Btu)	Flow	Temp (F)	Mass (Lb)	Energy (Btu)
1	Brine Heater	160	Salt	75	3 000	0 0	Brine	160	16 000	1185 0
			Water	75	13 000	0 0	Cond	180	1 200	150 0
			Steam	350	1 200	1410 0	Loss			75 0
2	Purification	130	Brine	160	16 000	1185 0	Brine	130	16 000	785 0
			CM Treat	75	0 060	0 0	Sludge	130	0 060	5 0
			Electric			10 0	Loss			405 0
3	Salt Dissolver	130	Brine	130	16 000	785 0	Brine	129	16 300	780 0
			Salt	75	0 300	0 0	Loss			20 0
			Electric			15 0				
4	Brine Heater	160	Brine	129	16 300	780 0	Brine	160	16 300	1210 0
			Steam	350	0 500	600 0	Cond	180	0 500	60 0
							Loss			110 0
5	Electrolysis	190	Brine	160	16 300	1210 0	Cl Gas	190	2 020	400 0
			Electric			4500 0	H_2 Gas	190	0 030	10 0
			Endotherm			2700 0	Caustic	190	14 250	1500 0
							Loss			1100 0
6	Cooler	75	H_2 Gas	190	0 030	10 0	H_2 Gas	75	0 030	0 0
			CW	75	0 560	0 0	CW	95	0 560	11 0
			Electric			1 0				
7	Cooler	100	Cl_2 Gas	190	2 020	400 0	Cl_2 Gas	100	1 020	25 0
			Water	75	16 500	0 0	WW	115	17 900	695 0
			Steam	350	0 400	500 0	Loss			180 0
8	Drier	75	Cl_2 Gas	100	1 020	25 0	Cl_2 Gas	95	1 000	5 0
			H_2SO_4	75	0 060	0 0	H_2SO_4	95	0 080	5 0
			CW	75	0 500	0 0	CW	95	0 500	10 0
							Loss			5 0
9	Compression	75	Cl_2 Gas	95	1 000	5 0	Cl_2	75	0 320	0 0
			CW	75	1 750	0 0	CW	95	1 750	35 0
			Electric			35 0	Cl_2 Gas	75	0 680	0 0
							Loss			5 0
10	Condenser	50	Cl_2 Gas	75	0 320	0 0	Cl_2 Liq	50	0 320	50 0
			Refrig	20		110 0	Loss			60 0
11	Evaporators	220	Caustic	190	14 250	1500 0	NaOH Liq	180	4 600	350 0
			Steam	350	3 000	3500 0	Cond	180	3 000	375 0
			CW	75	140 000	0 0	Cond Vpr	180	9 600	1011 0
							CW	95	140 000	2964 0
							Loss			300 0

Figure 4

Existing and Potential Site Profile (Preliminary 3-15-81)

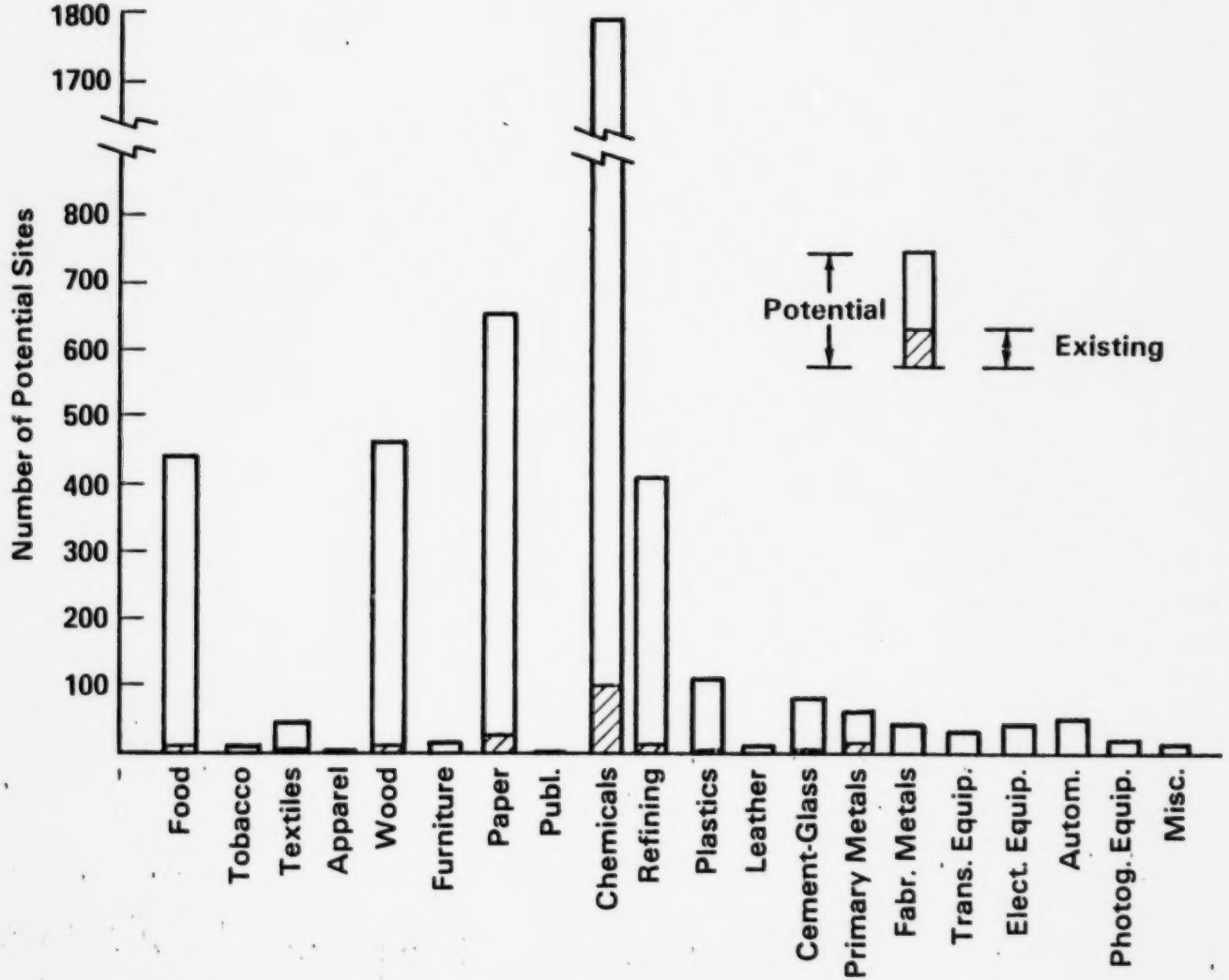

W-3-686

Figure 5

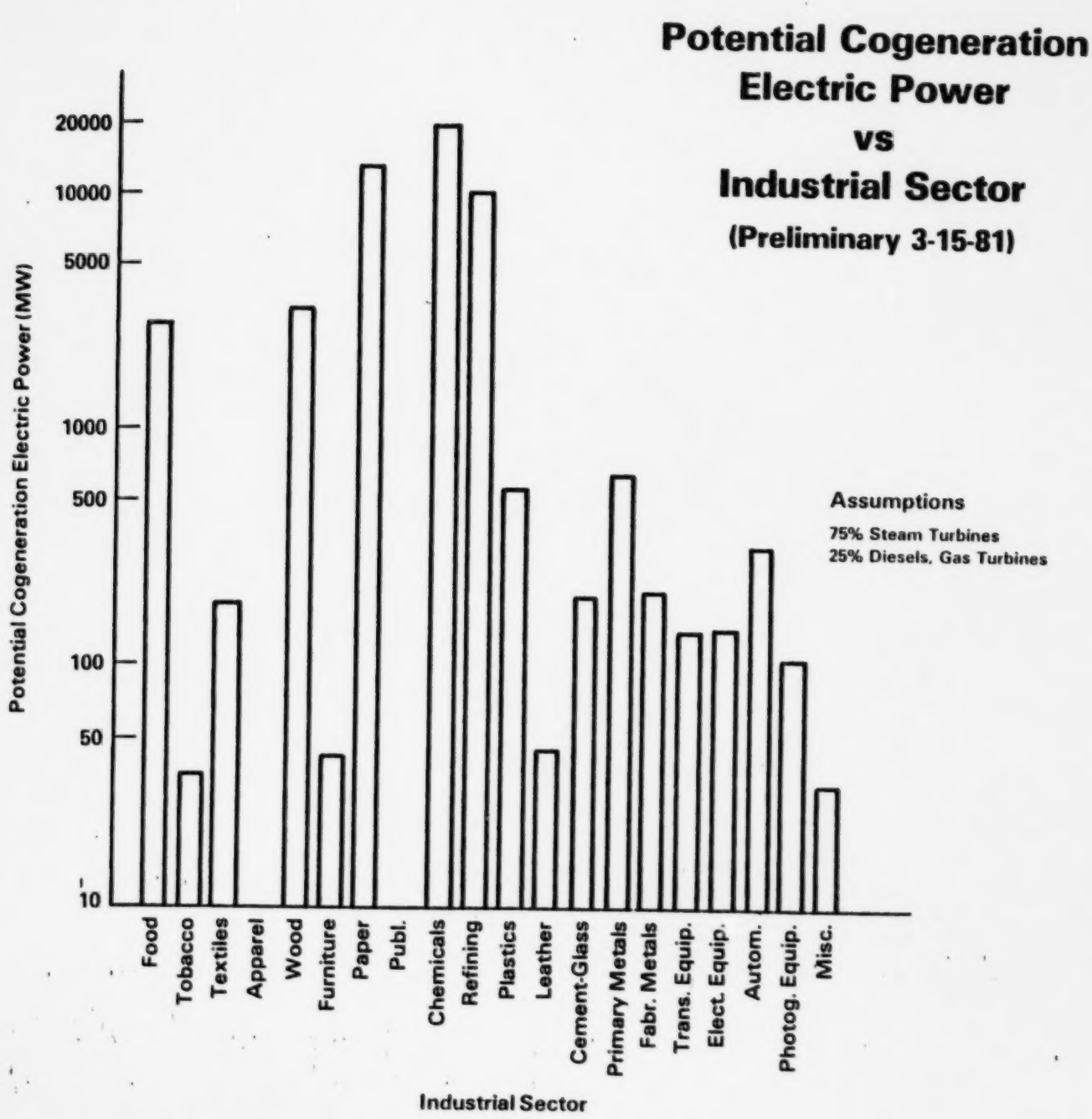

W-3-687

Figure 6

Number of Potential Cogeneration Plant Sites vs Cogeneration System Size

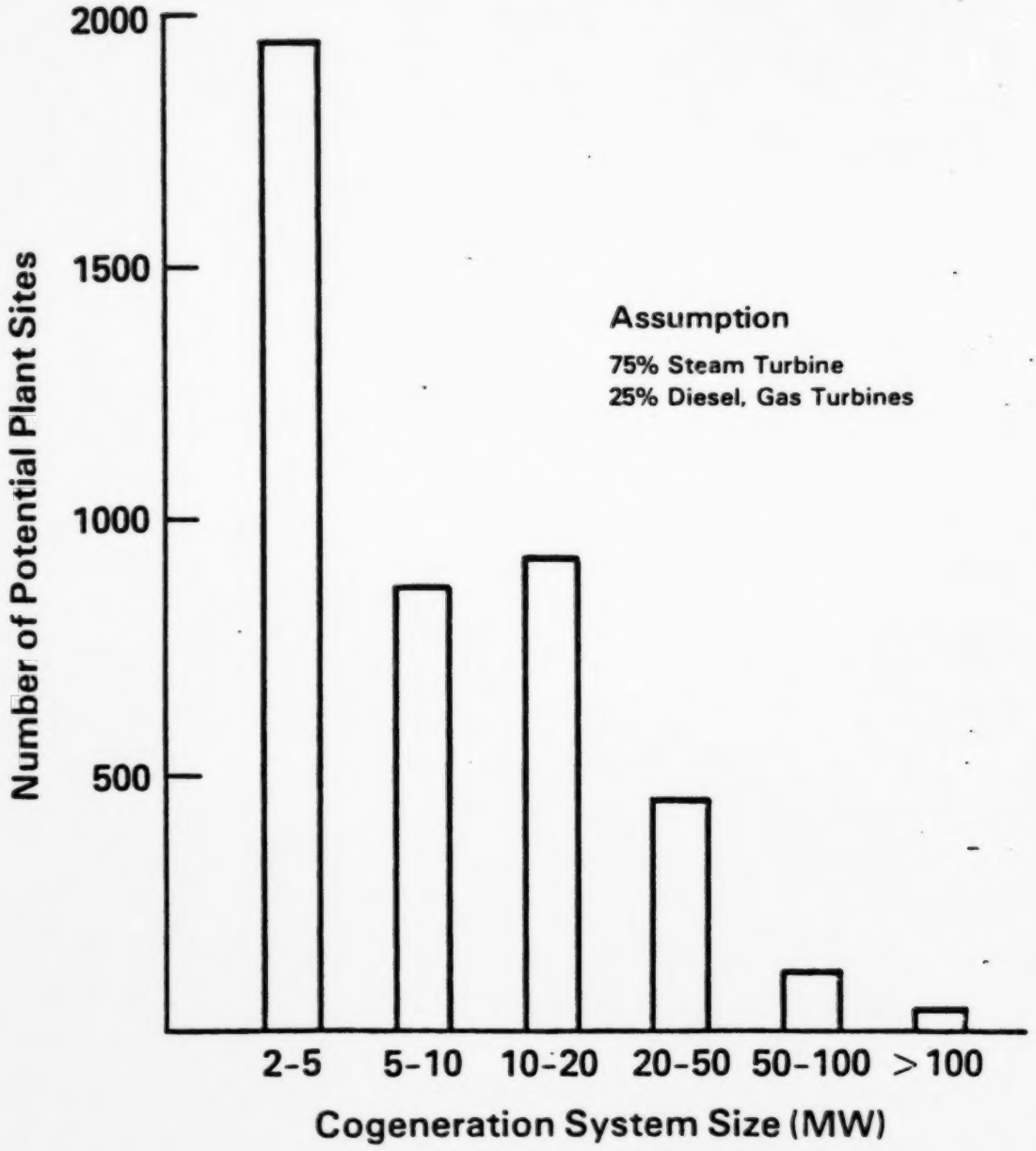

W-3-688

Figure 7

Potential Cogeneration Electric Power vs System Size

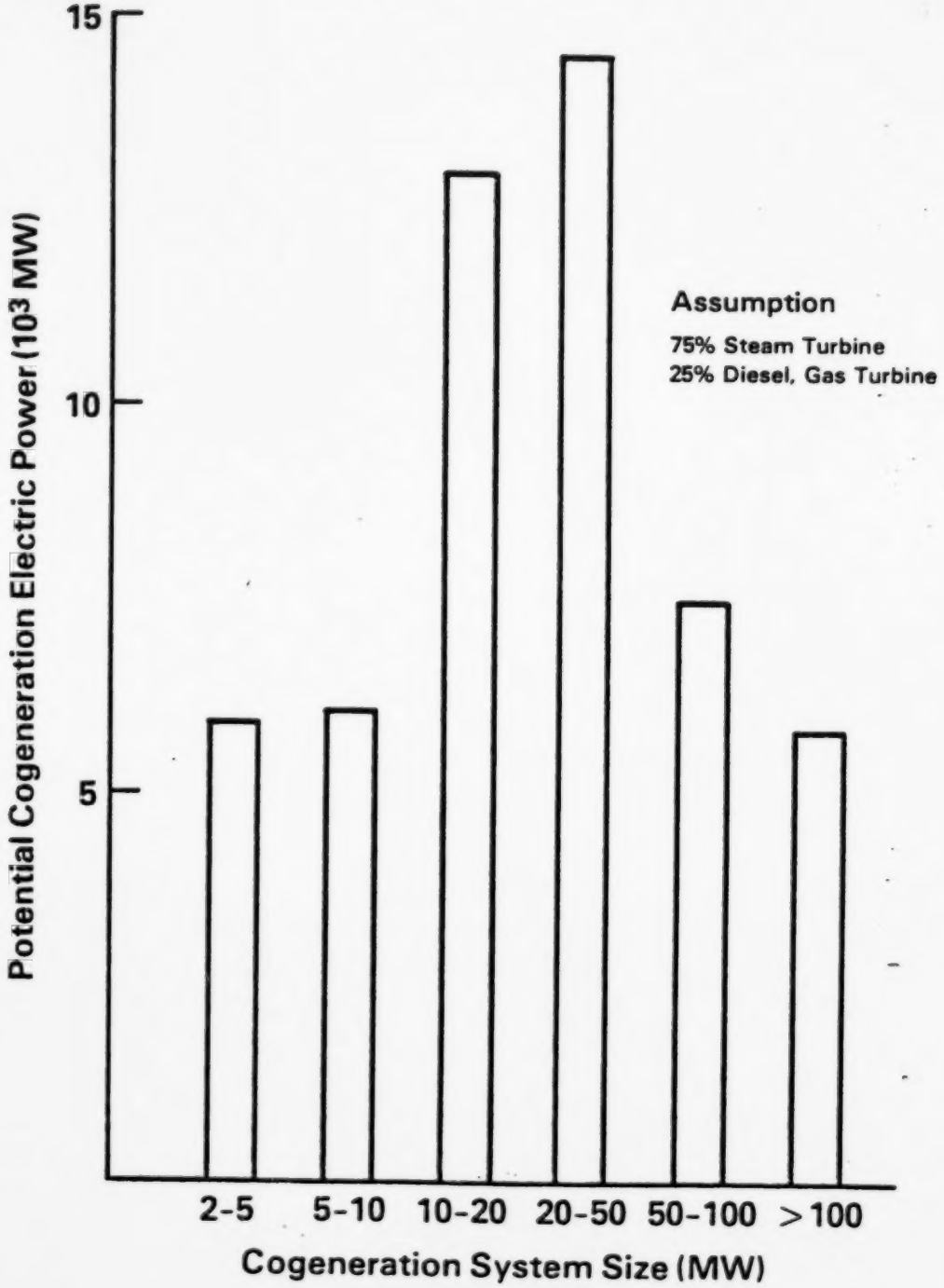

W-3-689

Figure 8

Cumulative Potential Cogeneration Electric Power (MW) vs Cogeneration System Size

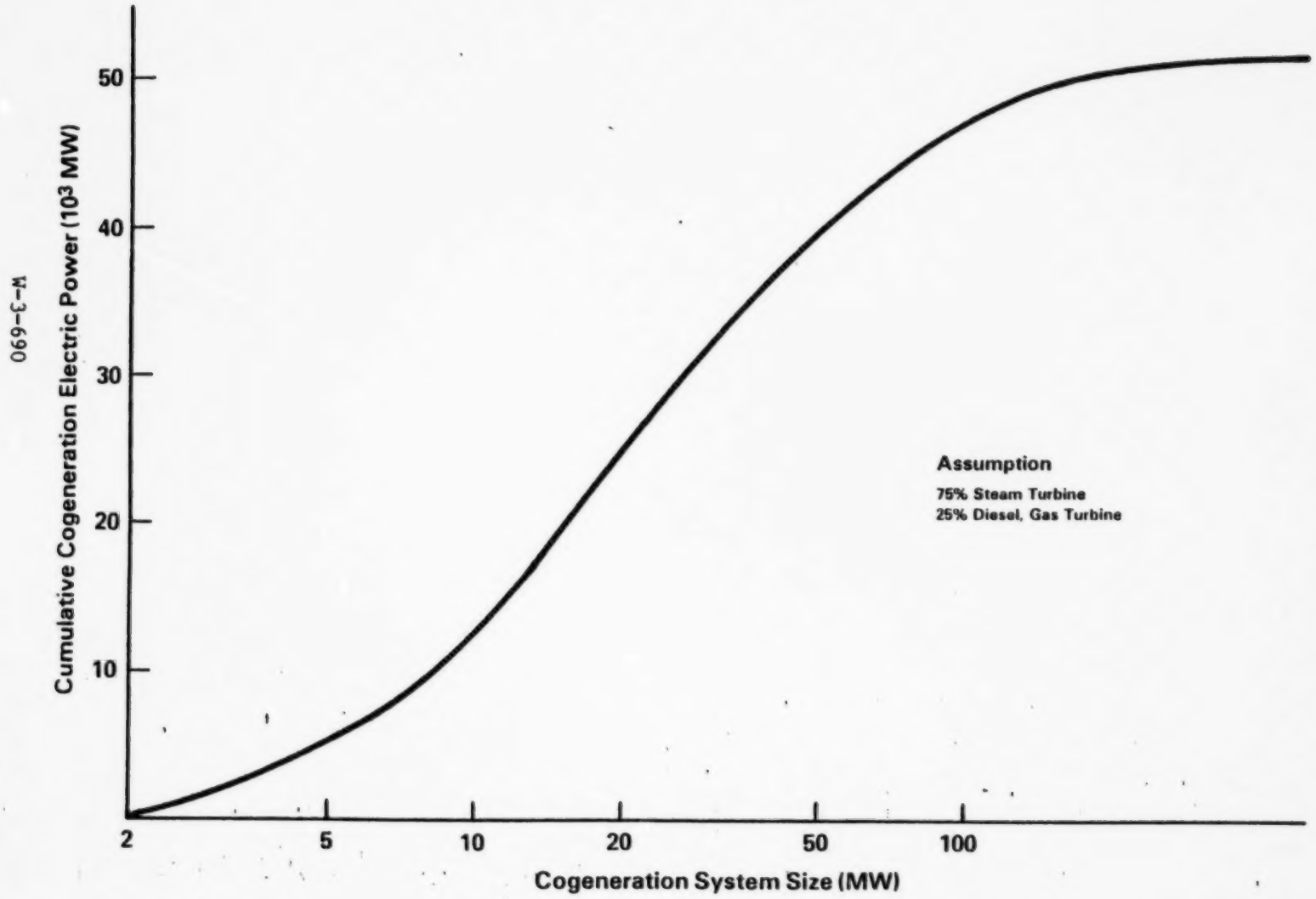

W-3-690

Table 1A

TOPPING CYCLE TECHNOLOGY STATUS

TOPPING CYCLE CONVERSION TECHNOLOGY	TECHNOLOGY STATUS[1]	FUEL FLEXIBILITY						OUTPUT THERMAL ENERGY FORM	CONVERSION EFFICIENCY %[2]	POWER THERMAL[3] kw-Hr 10^4 BTU	EFFECTIVE HEAT RATE[4] BTU /kw-Hr	ENERGY SAVING PER[5] PROCESS THERMAL UNIT BTU/BTU
		GAS	LIGHT DISTILLATE	HEAVY PETROLEUM	PETROLEUM RESIDUALS	COAL	WOOD & PROCESS RESIDUAL					
STEAM TURBINE – BACK PRESSURE	A							STEAM 200psi	13	43	4,300	.24
DIESEL – WASTE HEAT BOILER	A							STEAM 200psi	35	342	5,550	1.68
GAS TURBINE – WASTE HEAT BOILER	A							STEAM 200psi	30	209	5,100	1.10
GAS TURBINE – PROCESS HEATER	A							PROCESS HEAT 800°F	30	140	4,200	.87
DIESEL – SLURRY FUEL WASTE HEAT BOILER	C							STEAM	35	342	5,500	1.68
GAS TURBINE – EXTERNAL FIRING WASTE HEAT BOILER	C							STEAM	25	163	5,600	.78
STIRLING – WASTE HEAT BOILER	C							STEAM	35	342	5,500	1.68

1 TECHNOLOGY STATUS
- A - MATURE TECHNOLOGY - EQUIPMENT REGULARLY MANUFACTURED
- B - MATURE TECHNOLOGY - EQUIPMENT CAN BE BUILT TO ORDER
- C - TECHNOLOGY STILL UNDER DEVELOPMENT

2 CONVERSION EFFICIENCY

$$\frac{\text{NET WORK OUTPUT}}{\text{TOTAL FUEL INPUT}} \left[\frac{\text{BTU}}{\text{BTU}}\right]$$

3 POWER TO THERMAL ENERGY RATIO

$$\frac{\text{NET ELECTRICAL ENERGY OUTPUT}}{\text{USEFUL THERMAL ENERGY OUTPUT}} \left[\frac{\text{kw Hr}}{10^4\ \text{BTU}}\right]$$

4 EFFECTIVE HEAT RATE

$$\frac{\text{TOTAL FUEL INPUT - FUEL REQUIRED FOR USEFUL THERMAL OUTPUT}}{\text{NET ELECTRICAL ENERGY OUTPUT}} \left[\frac{\text{BTU}}{\text{kw Hr}}\right]$$

5 ENERGY SAVINGS

(UTILITY HEAT RATE - EFFECTIVE HEAT RATE) POWER TO THERMAL ENERGY RATIO $\left[\frac{\text{BTU}}{\text{BTU}}\right]$

Table 1B

BOTTOMING CYCLE TECHNOLOGY STATUS

BOTTOMING CYCLE CONVERSION TECHNOLOGY	TECHNOLOGY STATUS	FUEL FLEXIBILITY						INPUT THERMAL ENERGY FORM	CONVERSION EFFICIENCY %	POWER/THERMAL kw-HR/10^6 BTU	EFFECTIVE HEAT RATE BTU/kw-HR	ENERGY SAVINGS PER PROCESS THERMAL UNIT BTU/BTU
		GAS	LIGHT DISTILLATE	HEAVY PETROLEUM	PETROLEUM RESIDUALS	COAL	WOOD & PROCESS RESIDUAL					
SUBATOMSPHERIC BRAYTON	C							PROCESS EXHAUST 1200°F	11	32	0	.34
STEAM TURBINE	B							PROCESS EXHAUST 1000°F	16	47	0	.49
ORGANIC RANKINE	B/C							PROCESS EXHAUST 800°F	16	47	0	.49

SESSION VIII-A

THERMAL DISCHARGE V

Preceding page blank

PB82-228461

CASE STUDY OF THE AL KHOBAR COOLING WATER INVESTIGATION

Peter Mortensen, Andrew McCowan and G.S. Rodenhuis
Danish Hydraulic Institute, (DHI)
DK-2970 Horsholm, Denmark

ABSTRACT

A large power and desalination plant is planned constructed at Al Khobar in Saudi Arabia. The proposed plant consists of three units each supplying 500 MW to the power network, and a similar amount of power to a desalination plant. The overall cooling water requirement is 200 m^3/s with a warm up range of 6^oC. Salinity increase in outlet is about 2.3 o/oo. In this paper it is summarized how the cooling water system was analysed by the combined use of physical and mathematical models, calibrated and verified from field data. This approach was selected because of the very complicated physical conditions with combined effects of the surplus temperature and high salinity of the outfall jet, and extremely complex hydrodynamic conditions.

The study included extensive field investigations, recirculation management, environmental impact evaluation, hydraulic optimization of outlet structures, calculation of hydraulic transients in the cooling water system and various other aspects.

1. INTRODUCTION

The site for the Al Khobar power and desalination plant is located approximately 10 km south of Al Khobar city at a point on the Gulf Coast called Al Aziziyah.

The plant is planned for future extensions up to three units, each with the capacity to produce 190.000 m^3/day of product water by multistage flash distillation and at the same time generating enough electric power to allow 500 MW to be fed to the transmission grid. During summer approximately 200 m^3/s of cooling water will be discharged during normal operation, with its temperature increased about 6^oC and its salinity increased 2.3 o/oo above the intake temperature and salinity.

The design of the cooling water system should be based on the requirement that recirculation of the cooling water was kept within tolerable economic and operational limits. Further should be included a study of the environmental impact of the discharge of heated water and brine and the possible influence from this on the selection of the optimal layout.

Oceanographic and environmental studies were carried out in order to provide a basis for the selection of the optimal location of intake and outlet.

Preceding page blank

Main emphasis in this paper is laid upon a presentation of the hydraulic studies. In consequence of the complicated hydrographic conditions and the small scale interaction in the near field between intake and outlet, the study was based on a combined use of physical and mathematical models, calibrated and verified from field data.

A numerical model of the type employed in the present studies, is limited in its description of integrated values over water depth and of a computational grid with a certain discrete mesh size. It cannot therefore, describe in detail the conditions in the area immediately around the outfall and between outfall and intake, the so-called "near-field". Therefore two physical model studies were carried out to supplement the mathematical models for the details in the "near-field". In order to keep the options for the selection of layout open, these studies were carried out as "parameter studies", in which all important parameters such as intake/outlet alternative, number of plant units in operation, canal length, load case and tidal flow were varied.

Two main alternative layouts of the intake/outlet system were considered. In Fig. 1 the layouts are sketched. In alternative A the intake is located offshore, connected by a culvert below seabed to an onshore pumphouse. Outlet located onshore, constructed as an overflow weir. In alternative B the intake is located onshore, protected by a breakwater which at the same time serves to provide a stilling basin for sediment. Outlet offshore, with a culvert below the seabed.

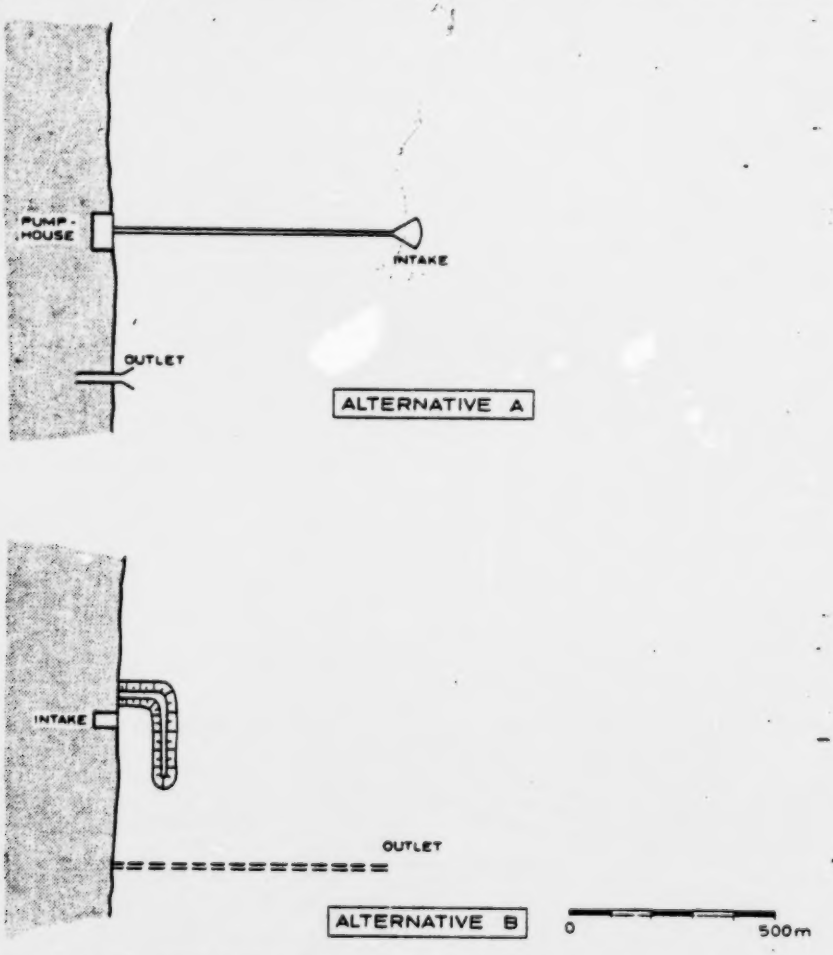

Fig. 1 Layouts for Alternatives A and B with Intake, resp. Outlet Channel perpendicular to the Coast.

Several modifications of alternative A and B were included in the study.

2. FIELD INVESTIGATIONS

The field investigations included a long term measurement program covering a period of 18 months with two intensive survey periods of 2 months' and 1 month's duration.

The measurement program included current recordings and profilings at several locations, water level recordings, temperature and salinity measurements, tracer studies, bottom sampling and suspended sediment sampling, wind and wave recordings, and bathymetric surveys.

The collected data formed the basis for construction and calibration of physical and mathematical models and determination of dispersion coefficients to be used in the mathematical transport-dispersion model.

3. MODEL STUDIES

Physical and mathematical model studies were carried out in order to determine the distribution of heated water and brine discharged into the sea by the planned Al Khobar power and desalinition plant. Environmental studies have been carried out to assess the impact of such discharges on the marine environment and to establish the effects the marine conditions can have on plant operation.

Mathematical model studies were initiated immediately at the start of the contract in order to quickly give a first approximation of the heat-fields and salinity fields to be expected for Alternative A and B and for different culvert lengths. The computations used an uncalibrated model and average tide conditions. This gave very important information for the following detailed model studies.

The physical model studies included two different sets of tests:

Tests in a so-called "near-field" model, in which only the outlets were included, and tests in a so-called "interaction" model where both intakes as well as outlets were included.

To include regional accumulation effects a far-field mathematical model was used. The model consisted of a hydrodynamic stage and a transport-dispersion stage.

3.1 Physical Models

The near-field model was the first model being studied. A scale model of the sea bottom and the coast line in the vicinity of the outfall structure was built in a 35 x 26 m test facility. A linear scale of 1:40 was applied such that model covered approximately 600 m coastline on either side of the outfall structure and approximately 900 x 600 m sea bottom.

The data collecting, measuring of temperature, salinity and currents were made from a rack moving through the plume. The set-up is sketched in Fig. 2.

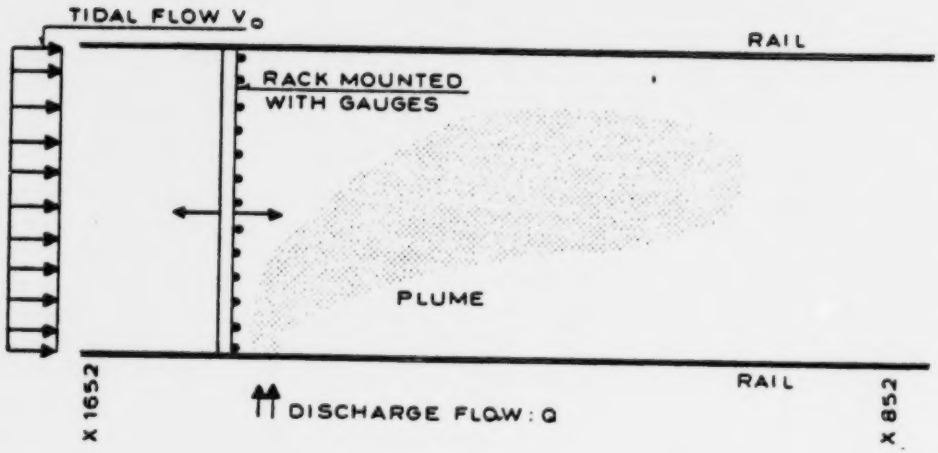

Fig. 2 Definition Sketch of Recording Set-Up.

Gauges were mounted on the rack with a distance corresponding to 32 m in prototype, allowing temperature and conductivity (salinity) to be measured in three levels: 1 m above the seabed (lower level), 1 m below the surface (upper level) and at mid depth.

Tidal flow velocities from 0 to 1 m/s, prototype values were reproduced. Cooling water discharges were produced using heating equipment able to provide a continuous supply of water with a very precise excess temperature in the range Δt = 0-15°C, and discharges in the range of 0-20 l/s (0-200 m^3/s prototype).

Furthermore, it was possible to add saline water into the discharge to produce the correct density differences in relation to the ambient water.

In the model various shapes of the outfall weir of Alternative A were tested in order to establish the hydraulically optimal form. Further, the distribution of the excess heat and brine in the sea in the immediate vicinity of the outfall was investigated for the Alternative A outlet and Alternative B outlet under different tidal flow conditions, for different loadcases and for different number of plant units in operation. The results were also used to guide the approximation of the near-field distribution of heat and salinity in the mathematical models.

With the shape of the outfall determined in the near-field study, extensive tests for Alternative A and B were carried out in an "interaction" model to establish the risk of direct recirculation for various lengths and angles to the coast of culvert, various loadcases and different number of plant units in operation.

The model was constructed to a linear scale of 1:80. The tests were carried out with varying tidal flow and with a measuring technique similar to the near-field model but with the gauges fixed in a grid.

In the tests were determined the degree of possible direct recirculation between intakes and outfalls. The main conclusions of the tests were in general that culverts perpendicular to the coast gives a lower maximum excess temperature at the intakes than a layout with angled direction of intake culverts. Further the tests gave the excess temperature variation at the intake as

function of culvert length. For same culvert length Alternative B gave a smaller degree of direct recirculation than Alternative A.

3.2 Mathematical Models

The results of the physical near-field models were examined closely to ensure that these effects of the near field, were introduced into the far field mathematical models in a reasonable manner. In this way it is possible to place confidence in the calculation of indirect recirculation due to accumulation of excess temperature and salinity in the far field.

The hydrodynamic conditions in the project area are very complex, with the relatively shallow area between Saudi Arabia and Bahrain forming a sill between the deeper water of the Gulf and the Dawhat Salwa. The tidal wave entering from the Gulf is heavily damped and distorted as it passes over this sill.

The sill which is made up of shallows, channels and reefs, provides a greater resistance to ebb flows at low water than to flood flows at high water. This "pumping" effect generates net drift currents at the plant site as the Dawhat Salwa gradually fills or empties. Net currents induced by evaporation and the circulation around Bahrain also affect the accumulation of excess heat and salinity at the plant site.

Correct reproduction of these regional phenomena was therefore important for the study of indirect recirculation effects. For this to be possible it was necessary to establish boundary conditions for the local models as part of the larger overall system.

Initially the "Dawhat Salwa" model (shown in Fig. 3) available from a previous study of the Saudi Arabia-Bahrain Causeway was considered for this purpose. However, the open northern boundary of this model is located close to the amphidromic points for the diurnal components of the tide in the Gulf. This results in large variations in phase of these components along the boundary, which could not be accurately described by the existing schematization of the model boundary.

Further it was difficult to obtain adequate water level data along the northern boundary. Therefore it was decided to gencrate the boundary data for the Dawhat Salwa model by direct simulation of the entire Gulf area using DHI's Gulf Model.

In all, four hydrodynamic models with successively finer grids focussing onto the project area were used. The locations of these models are shown in Figs. 3 and 4, and brief descriptions are given below:

Gulf Model: 8000 m grid

The Gulf model was developed as an internal research project at DHI and was specifically designed to provide suitable boundary data for more local models. The model topography is based on Admiralty Charts 2847 and 2837, supplemented by finer scale charts in the complex reef areas along the western and southern coastlines. Boundary data are determined from predicted tides at two secondary tidal stations at either side of the Strait of Hormuz, and the model was calibrated against predicted tides at various locations throughout the Gulf.

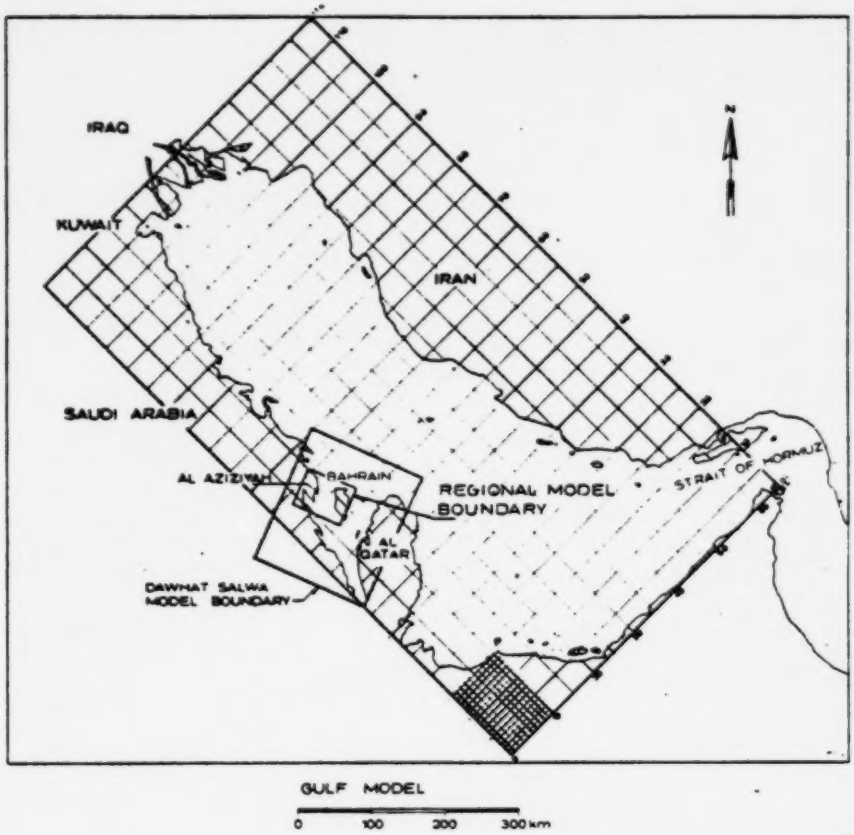

Fig. 3 Gulf Model, Dawhat Salwa Model and Regional Model.

Dawhat Salwa Model: 3000 m Grid

This model is based on the original coarse grid model used in a previous study and covers the entire region of the Dawhat Salwa to its entrance in the Gulf. For the present project, boundary data were transferred by time and space interpolation from the results obtained in the Gulf model.

Regional Model: 740 m Grid

This model was based on the fine grid Dawhat Salwa Model. The rather unusual grid size (740.8 m to be precise) comes from the metric conversion of 0.4 nautical miles which was the grid size originally specified in the Causeway study. Boundary data for this model were transferred from the results of the Dawhat Salwa Model.

Local Model: 247 m Grid

This model was set up to provide a detailed description of the hydrodynamics in the project area to be used as input data to the transport-dispersion model. The boundaries of the local model coincide directly with grid lines in the regional model and the grid size is refined by an integer factor of 3.

Intake and outlet spacings investigated in the local model are therefore multiples of 246.93 m (the resulting grid size) i.e. 494 m, 741 m, 987 m and 1235 m.

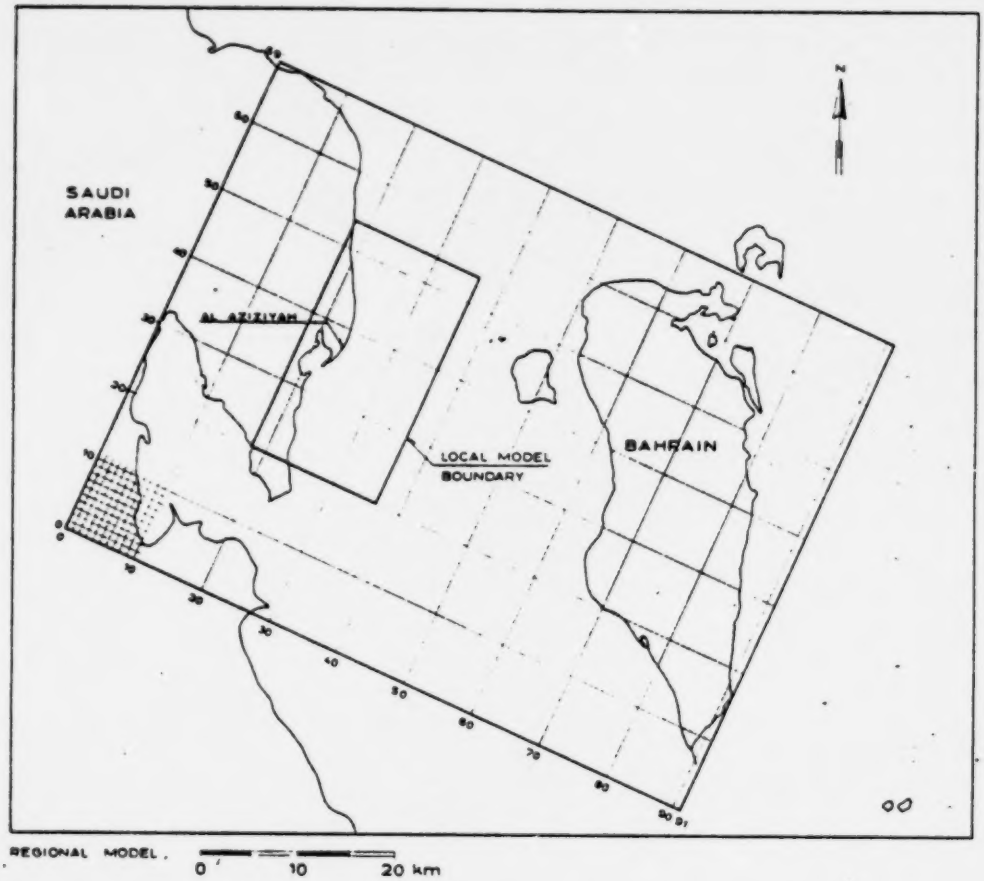

Fig. 4 Regional Model and Local Model.

Transport-Dispersion Model

A single local transport-dispersion model was sufficient to adequately describe the movements of the excess temperature and salinity fields which would arise from operation of the proposed plant. This model was based on the local hydrodynamic model and used the same grid and topography.

For every time step, water levels and velocities computed in the hydrodynamic model are used as input data at each corresponding grid point of the transport-dispersion model. The hydrodynamic input data includes regional effects such as net drift currents from the successive transfer of boundary data originating from the overall hydrodynamic simulation of the Gulf. In this way the effects of regional phenomena will be included in the excess temperature and salinity fields calculated in the "local" transport-dispersion model.

The procedure required for making a typical model run, is outlined in Fig. 5 below.

The mathematical models discussed above were set up using the hydrodynamic and transport-dispersion stages of DHI's System 21 /1/.

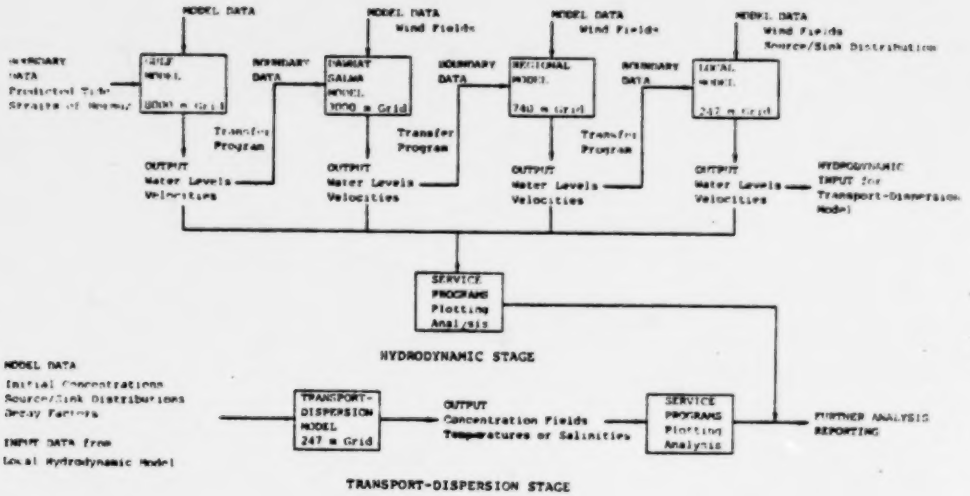

Fig. 5 Typical Sequence Involved in a Full Model Run.

The vertical integration of the equations used in S21HD and S21TD assumes the flow to be well mixed, with velocity and concentration profiles uniform over the depth. The vertical salinity and temperature gradients are generally very small. Additionally, the increase in salinity and increase in temperature of the cooling water will combine to reduce the differences in density between the outfall discharge and its receiving waters. Except in the immediate vicinity of the outfall, the assumption of full vertical mixing was therefore considered reasonable.

The hydrodynamic models were calibrated and verified against water level and current measurements taken during the intensive field survey. A six day period covering spring tide conditions was used for calibration. A similar period of neap tide conditions was used for verification.

The principal requirements for any transport-dispersion model, is that the hydrodynamic input data be sufficiently correct and that the model is capable of using this input to accurately transport concentrations without introducing significant numerical dispersion. Further it was secured that the source distribution in the transport-dispersion model reproduced the near-field effects revealed in the physical models, in the most realistic way. A detailed discussion of the importance of the source distribution in transport-dispersion models with a certain discrete grid size is given in /2/.

Dispersion coefficients used in the transport-dispersion model were calculated on the basis of intensive dye tracer investigations. With the calculated dispersion coefficients the transport-dispersion model was checked by simulating two selected dye tests. The degree of spreading of the dye patch obtained in the model showed that the calculated dispersion coefficients were reasonable.

3.3 Recirculation

For comparing and optimizing the intake and outlet channel lengths for Alternative A and B all tests were carried out under actual tidal conditions. As comparison period was chosen two tidal cycles between neap and spring tide. Fig. 6 shows envelopes of maximum and mean excess temperatures occuring during the comparison period for one intake/outlet situation.

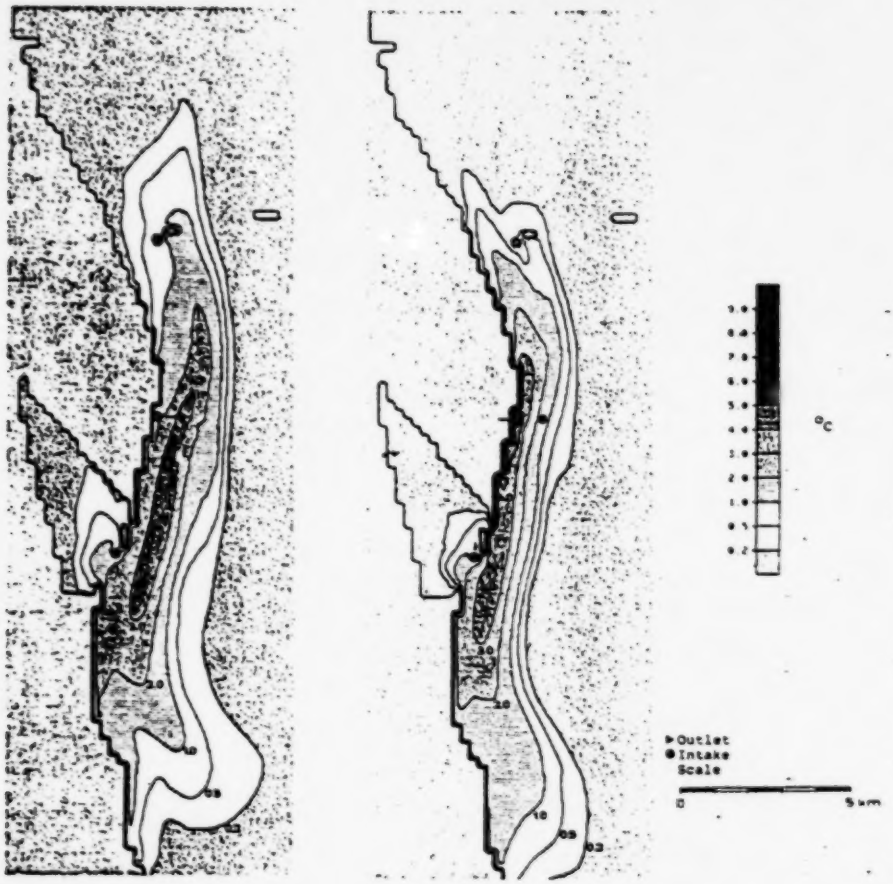

Fig. 6 Envelopes of Maximum and Mean Excess Temperatures Alternative A - 700 m.

Typical characteristics of the intake excess temperature are shown in Fig. 7. The direct recirculation is shown added to the far-field indirect recirculation, raising its peak values. Results of the interaction physical model tests reveal a 50-60% direct recirculation for Alternative A, 450 m i.e. a peak value of 50-60% of the discharge excess temperature. It should be noted that the addition of direct and indirect recirculation provides a conservative upper value. For culvert length of 700 m and longer, and for Alternative B the direct recirculation is only very small, i.e. 0.1-0.2°C.

The statistical characteristics of the intake excess temperature variations were evaluated with due consideration to: Tidal conditions, background sea temperature, wind speed, operational conditions, plant layout, culvert length. For this purpose a 15 days' design period was constructed.

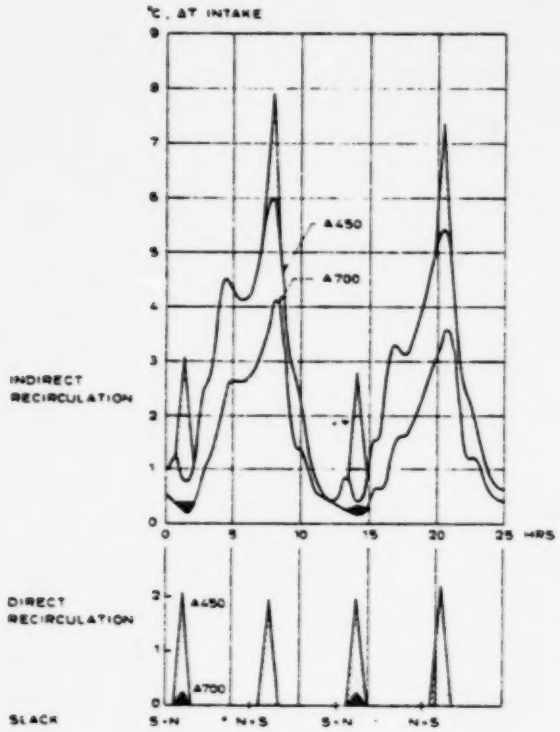

Fig. 7 Direct and Indirect Recirculation for A, 450 m and A, 700 m.

4. RECIRCULATION MANAGEMENT

Preference of one intake/outlet alternative over another depends on the criterion against which the alternative is judged. Therefore the advantage or disadvantage of Alternative A, against B was analysed using various criteria.

After these analyses a final judgement must be made, giving a certain weight to each of the criteria employed. To do this requires insight into the operational characteristics of the plant, costs of certain alternative constructions, as well as an insight in the program and investments for future extensions.

For most of the criteria employed it was found that a specific tendency between Alternative A and B applies regardless of the length of culvert. So, for most of the criteria employed one may first select the alternative and then select the length.

For one criterion however, this procedure is not applicable. When employing an optimum criterion of plant efficiency loss versus construction cost, the optimal length should be computed and then for this length the total cost. Then the total cost obtained for each alternative should be compared.

Below are given examples of applicable criteria.

In Fig. 8 are shown comparisons between Alternative A and B under different temperature exceedance criteria.

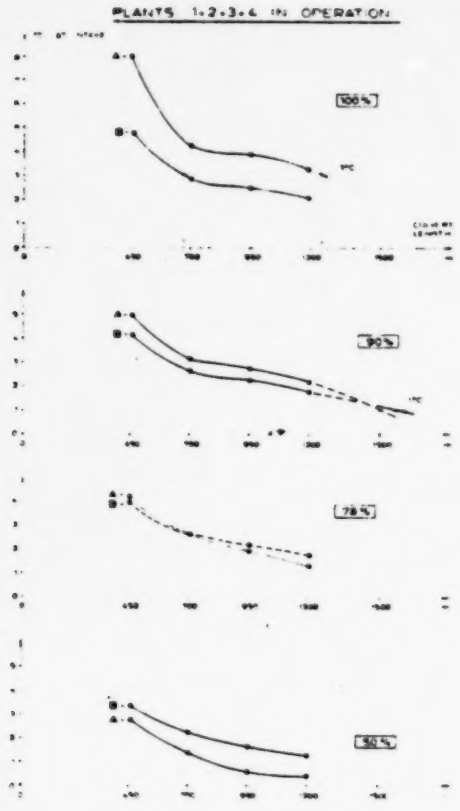

Fig. 8 Comparison Alternative A and B under Temperature Exceedance Criterium. During the percentage or time indicated, ΔT intake is less than the temperature indicated by the curve.

From Fig. 8 it can be seen that whereas the 100% and 90% lines for Alternative A are above those for Alternative B for all culvert lengths considered, the reverse becomes true for the 50% lines. Thus between 90% and 50% some cross-over must take place.

For a 700 m culvert length this cross-over point was found to be, $\Delta T \leq 2.6^{\circ}C$ during 78% of the time for all plants in operation.

Thus it could be stated that:

1. For 700 m culverts the excess temperature which is not exceeded during 78% of the time will be the same for both Alternative A and Alternative B.

2. For culverts less than 700 m the excess temperature which is not exceeded during 78% of the time will be greater for Alternative A than for Alternative B.

3. For culverts greater than 700 m the excess temperature which is not exceeded during 78% of the time will be lower for Alternative A than for Alternative B.

A very relevant measure of performance is the sum of the excess temperature over a certain period. This gives a certain "degree.hrs" quantity. For a comparison period of 25 hrs this quantity has been determined for Alternative A and B and plotted in Fig. 9.

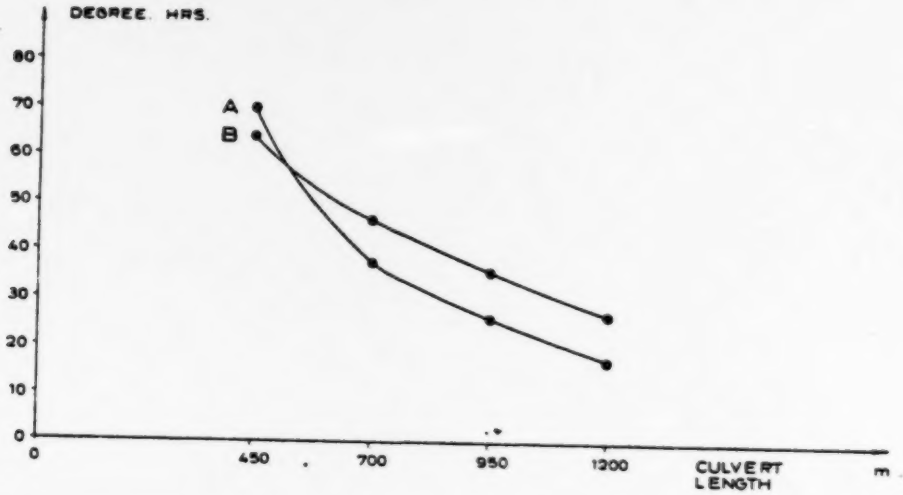

Fig. 9 Comparison of Alternative A and B for the Sum of Excess Temperature over 25 hrs - the "Degree.Hrs" criterion.

In general the objective of recirculation management is to minimize the sum of construction and plant operation costs and possible damages to the aquatic environment. The applicability of this principle is shown in /3/.

In this case study it was obvious that the spacing between intake and outfall has decisive importance for the overall economy of the plant. By providing a small distance between intake and outfall, construction costs are kept low at the expense of a more or less permanent reduction of the plant's efficiency due to the associated higher degree of recirculation. On the other hand, a very large spacing may impose unnecessarily high costs of construction which may not be justified by the associated gain in terms of plant efficiency.

An optimization analysis can only be carried out with insight into the operational characteristics of the plant as well as knowledge of the program and investments for future extensions. This has not been terminated so far.

For illustrative purposes an optimization has been carried out using simplified cost functions. An optimum culvert length was calculated at nearly 1300 m for both alternatives but with smallest loss of efficiency with Alternabive A.

5. HYDRAULIC DESIGN

Hydraulic design analyses have been carried out for intake structures, culverts and outfall structures. The design criteria were determined according to a situation which has a probability of occurrence once/50 years.

Based on physical model tests the outfall structure was designed to distribute the flow evenly over the width of the overflow and to discharge the cooling water with so small a momentum as possible.

Transient flow conditions in the intake cooling water system were investigated, including design of measures to control the flow conditions.

6. CONCLUSIONS

The case study has shown that at the moment physical and mathematical models in combination constitute an optimum tool in studies of recirculation of cooling water. Complicated hydrodynamic conditions and intake/outlet interaction demand this approach in final design studies.

Further it is demonstrated how variations in design parameters easily can be tested in the models and provide the basis for the optimization of the cooling water system. It is shown that preference of one intake/outlet alternative over another is greatly dependent of the criterion against which the alternative is judged.

ACKNOWLEDGEMENT

The work reported here was commissioned by Hyundai Construction Company of South Korea. Hyundai as a member of a consortium of companies is in contract with the Saline Water Conversion Corporation, SWCC of Saudi Arabia. Fichtner Consulting Engineers, of Stuttgart, W. Germany, are the SWCC's consultant on the project. Hyundai and Fichtner have participated in discussions of all principal aspects of this study and DHI gratefully acknowledges their active role. We would like to express our appreciation to SWCC, who kindly allowed this work to be reported.

REFERENCES

1. Description of System 21, March 1979, Danish Hydraulic Institute.

2. Rodenhuis, G.S. and Kroszynski, U.: Numerical modelling in Cooling Water Circulation Studies: Techniques, Principle Errors, Practical Applications. Conf. on Wast Heat Management and Utilization, Florida, 1977.

3. Schrøder, H.: Selection of Alternative Coastal Locations. Conf. on Waste Heat Management and Utilization, Florida, 1977.

PB82-228479

REMOTE-SENSING STUDY OF MESOSCALE MIXING PROCESSES OFF SAN ONOFRE NUCLEAR GENERATING STATION

Robert S. Grove
Research and Development
Southern California Edison Company
Rosemead, California, 91770, U.S.A.

Choule J. Sonu
Tekmarine, Incorporated
Sierra Madre, California, 91024, U.S.A.

ABSTRACT

Turbulent energy in the ocean, which is manifest in the form of mesoscale eddies, has been receiving increasing attention in recent years. This paper investigates possible effects of coastal mesoscale and sub-mesoscale eddies as they are generated and move through the Southern California Bight. Sudden quantum changes in sea water temperatures and currents in the oceanographic records from the San Onofre Nuclear Generating Station (33°22.5'N and 117°32.5'W) may be at least in part attributed to the advection of such eddies. A sequence of 1980 TIROS-N satellite thermal imagery forms the basis of this analysis. In addition, historical coastal temperature data from the National Ocean Survey stations are subjected to statistical analysis to aid in segregating data dependence on annual and seasonal cycles as well as longshore distributions of distinct or persistent temperature patterns. Both the remote sensing data and historical records indicate strong evidence of eddy interaction in the nearshore zone and a local influence of coastal upwelling. The study of coastal power plant effluent dispersion will benefit from further refinement of these eddy and upwelling mixing concepts.

1. INTRODUCTION

The objective of this paper is to present a Lagrangian view of coastal oceanography with reference to the Southern California Bight. From a discharger's point of view, it is important not only to recognize physical and biological nearshore processes as a function of time, but also as a function of space. The Lagrangian view emphasizes the spatial relationships and is particularly relevant in areas where a significant degree of alongshore variability is expected in currents and water mass characteristics. Such situations exist in the Southern California Bight where eddies, gyres and local circulations resulting from irregular coastline configurations appear to interact with complex water mass distributions associated with regional and local upwelling.

In contrast, existing methods of water current and tem-

perature analysis at a coastal power plant rely mostly on the Eulerian approach; that is, using a few moored current meters and temperature sensing devices in and near the predicted plume area. From these fixed point records many statistics can be generated, yet this approach leads to quite speculative hypotheses on the possible roles of internal waves, thermocline fluctuations, storm cycles, tidal currents, and the role of mesoscale and submesoscale eddies. Consider the temperature record taken offshore of San Onofre in the summer of 1980 (Figure 1). Rapid ambient temperature fluctuations of up to 4°C, with periods of four to seven days, are occurring (the San Onofre Nuclear Generating Station was not in operation during this period) and the amplitude of these high frequency changes is similar to the historical low frequency seasonal changes. No simple explanation of the driving forces involved in this rapid succession was evident in the San Onofre data collected at the time.

2. COASTAL OCEANOGRAPHY – EDDIES AND UPWELLING

The coastline configuration and related nearshore topography are both the generators and recipients of two dominant coastal oceanographic phenomenon, eddies and upwelling.

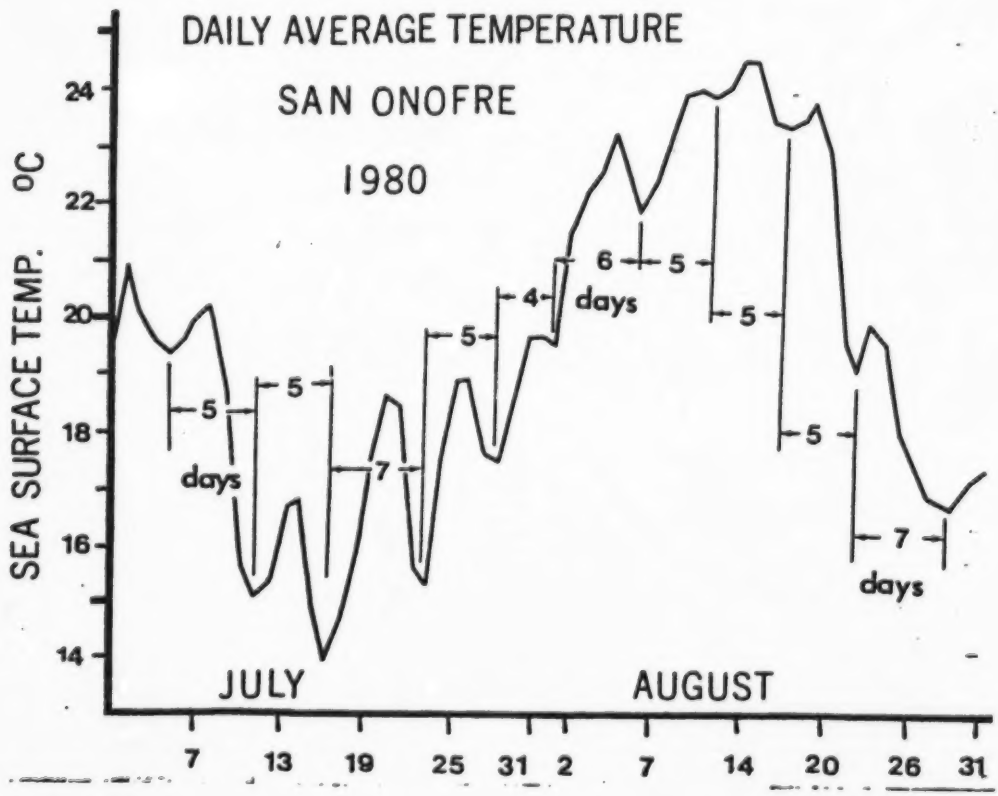

Figure 1. Example of abrupt near-surface ambient water temperature changes offshore of San Onofre Nuclear Generating Station.

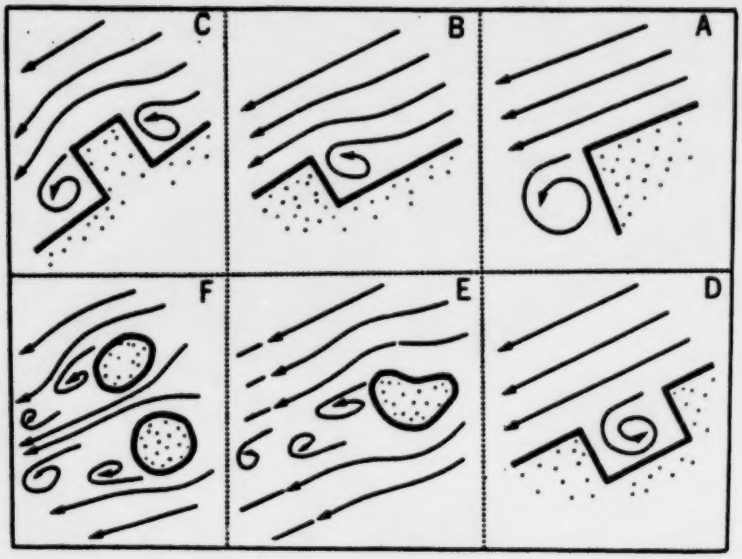

Figure 3. Schematic illustration showing various eddies formed at irregular shoreline discontinuities.

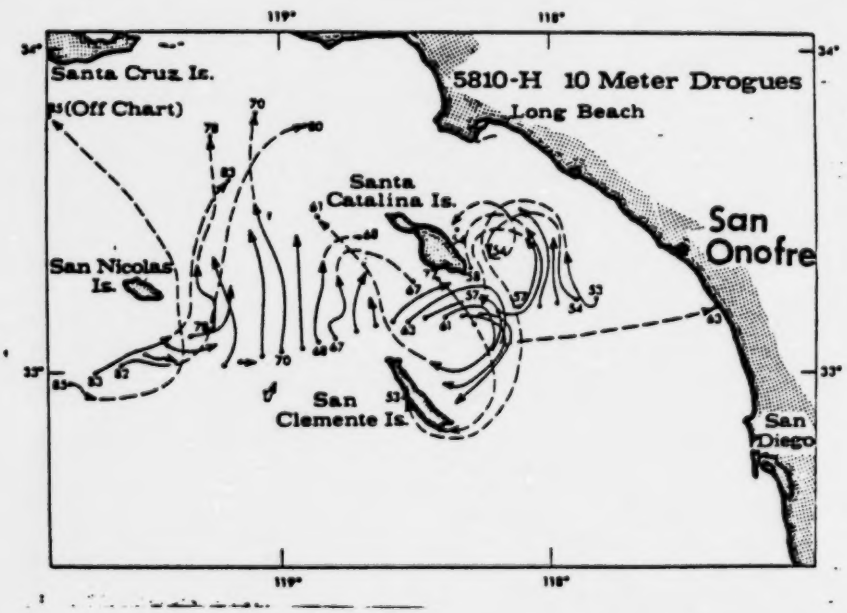

Figure 4. Typical eddies in the Southern California Bight, 23-27 October 1958, solid lines denote the paths of the 10 m deep drogues, dotted lines connect the last surveyed position with the location of final recovery. From SIO Report 62-67, 1962, Fig. 1, p. 3.

a simple computation as to how a vortex (or eddy) is formed by offshore islands is made. This computation is based on the general rule that under most ranges of Reynolds numbers the Strouhal number is about 0.2 for a stable von Karman vortex

street. The computation shows in the case of a circular island of a diameter of 10 km:

Impinging Current (Knots)	Number of Vortices Formed per day
0.2	2
0.4	3
0.6	5
0.8	7
1.0	10

Also, these vortices move at a speed approximately 70% of the ambient current.

2.2 Upwelling

Upwelling also takes place along the coastal boundary. Upwelling is a phenomenon associated with the effect of the sloping bottom rather than the effects of the plain-view shoreline configuration. Figure 5 is a satellite infrared image that shows the dynamics involved in coastal motions and reveals the nearshore colder waters upwelling. Upwelling is also associated with submarine canyons. Colder bottom waters can be found to use the submarine canyons as conduits, driving up the canyons, emerging in the coastal zone at the canyon heads to replenish surface waters driven offshore by longshore winds. An isolated instance of this phenomenon was investigated off of Newport Beach (Stevenson and Gorsline, 1956). Cold water surface patches formed at the head of the Newport Submarine Canyon (Figure 6). These patches tend to persist for extended periods (days) and subsequently move along the coast as distinct masses.

2.3 Interaction of Upwelling and Eddies

The cold water welling up at the coast can be readily entrapped in the forming eddies, and once this happens, the cold water masses would form a progressing group of isolated patches. Some of these would remain captive at locations of coastal irregularities, and some would drift away with the ambient current (such as in Figure 6). The stronger the wind, the stronger the upwelling and the more frequent the eddy formation, thus the coupling processes would be accelerated.

The passage of von Karman vortices can be estimated given that the average coastal surface current in the Southern California area is 15 cm/sec. (0.3 knots) and assuming an eddy size of 20 km in diameter:

Eddy speed: 15 x 0.7 = 10 cm/sec. (0.2 knots)

Distance between eddies: 40 km

Time between successive eddies: 4.6 days – 5 days

Duration of cold spell during each passage: 2 days

Figure 5. TIROS-N satellite infrared image showing the dynamics involved in coastal water motions and revealing nearshore up welling, cooler temperature water is lighter, warmer temperature water is darker shading.

3. THE COUPLING PROCESS – SATELLITE IMAGERY

In order to more fully investigate the coupling effects of eddies and upwelling, with the intention being to isolate areas of optimum mixing along the coast for heated effluent dispersion, Southern California Edison in 1980 began a cold-water eddy analysis using TIROS-N satellite imagery. The satellite program represents a powerful tool to accomplish the resolution of these

4. A dominating expansion of the cold water front is evident by March 31, 1980 after the March 19-20 warm water expansion period decays.

A further investigation to the last point above reveals that a meteorological front is passing through the area during this March 19-21 period. From the weather satellite GOES, a picture from March 19, 1980 shows that warm wind from the south is developing and driving warm water north, with a low pressure center and cold front further off the coast and to the north, which in turn would cause the suppression of upwelling in the study area. By March 26 the cold front is passing through the Bight as evidenced by the cloud pattern on this day in the TIROS-N sequence (Figure 7b). Behind, the cold front winds from the north are again engaging the regional upwelling and driving the southerly extent of the warmer waters out of the area. In conclusion, coastal waters appear to respond in a very sensitive manner to synoptic (that is, 4 or 5 day) weather cycles.

4. INTEGRATING HISTORICAL SEA SURFACE DATA

In parallel to the satellite assessment of upwelling and eddy coupling, an analysis of historical sea surface temperature data was initiated. Sea surface temperatures from National Ocean Survey Data were obtained at 13 stations in Southern California covering over two decades (SIO, 1955-1978). Monthly average temperatures were established. The data is presented as a function of both time and space (Figure 8). For the purposes of this analysis a graphic eigen analysis is presented.

Gross patterns of seasonal temperature changes are apparent. Temperatures at the southerly stations steadily increase into summer. Temperatures at the northerly stations seem under the influence of upwelling as the seasons progress from winter, which marks the seasonal warming trend. Therefore, the northerly-southerly gradient extends and then recedes back over the year.

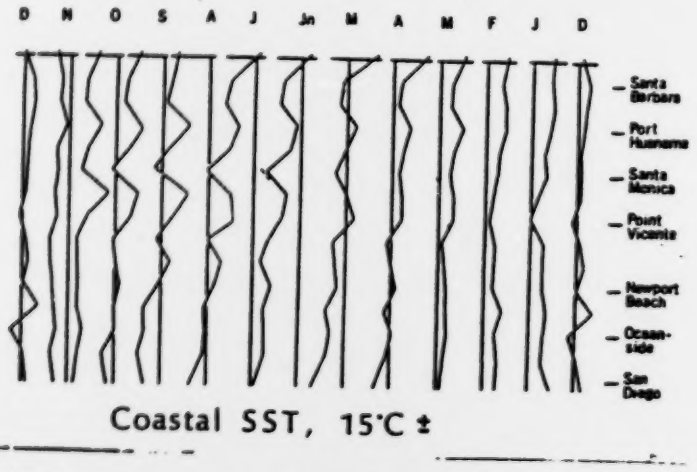

Figure 8. Surface water temperature data, monthly averages at 13 Southern California stations, National Ocean Survey, 1955-1978.

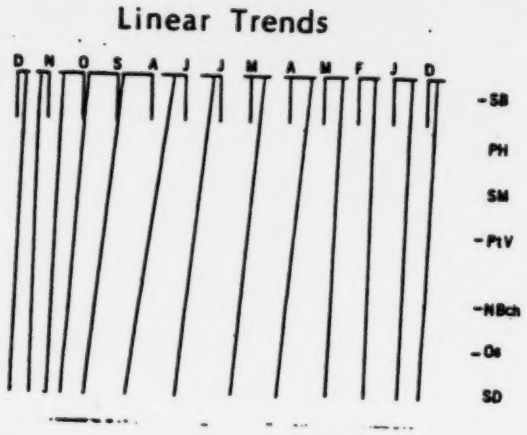

Figure 9. Linear trends of the surface water temperature data from Figure 8.

It can be concluded then, that over a distance of less than 400 km very intensive dynamics are influencing the temperature structure.

From the original data, the linear trend can be isolated (Figure 9). This clearly portrays the southerly warming/cooling and northerly damped seasonal trends.

Then, subtracting the linear trend from the original data, the non-linear trend emerges (Figure 10). It can now be seen that rather consistent shapes appear seasonally in the curves in certain areas. The lines are straight in winter and demonstrate consistent modes in the summer. The arrows indicate temperatures at areas that are consistently suppressed. The suppressions increase through summer, suggesting the possible seasonal effect of upwelling. It is happening at locations such as Point Vicente, which is in the lee of a point, and remembering the mechanics of eddies (Figure 3a), this would be a prime condition for the initiation of upwelling.

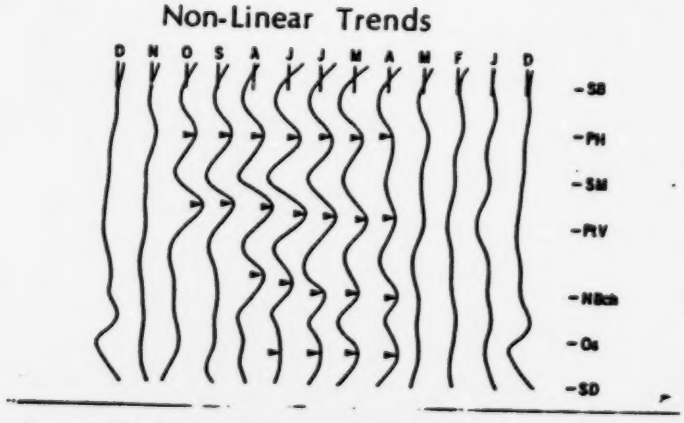

Figure 10. Non-linear trends of the surface water temperature data from Figure 8.

But Port Henueme and Newport Beach do not have points or capes nearby. This apparent contradiction can be explained by looking for other influential features and remembering that upwelling in these areas is the probable response to the nearby submarine canyons. The submarine canyon brings cold water to the coastal area as surface waters move offshore.

5. CONCLUSION

Understanding the passage of massive and distinct water masses through the Southern California Bight, with a better idea of type, frequency, scale, and extremes is of vital concern to environmental management of the use of these coastal waters for thermal effluent dispersion. Hopefully, these new tools we have started to use will create beneficial vantage points to excel the study of mixing along the Southern California coast.

Further, this initial assessment of the March 1980 TIROS-N satellite pictures and historical surface temperature information leads to the hypothesis that surface waters in the Southern California Bight may be mixing and turning over much more rapidly than previously described in studies such as Jones, 1971 that calculates Bight-wide water residence time of 3 months.

REFERENCES

1. SIO Report 62-27. 1962. Results of current measurements with drogues, 1958-61. Scripps Inst. Oceanog., University of California.

2. Stevenson, R. E. and D. S. Gorsline. 1956. A shoreward movement of cool subsurface water. Trans. Amer. Geophys. Un. 37:553-57.

3. Jones, James H. 1971. General circulation and water characteristics in the Southern California Bight. Southern California Coastal Water Research Project. SCCWRP TR101.

4. Frei, Werner. 1977. Image enhancement by histogram hyperbolization. Computer Graphics and Image Processing 6, 286-294.

5. SIO Reports. 1975-1978. Surface water temperatures at shore stations, United States West Coast. Reference number 57-28, 60-27, 61-14, 62-11, 63-17, 64-6, 65-9, 66-8, 67-9, 68-22, 69-14, 70-26, 71-23, 72-62, 73-15, 75-8, 77-12, 78-5, 78-16, 79-9. Scripps Inst. Oceanog., University of California.

PB82-228487

COMBINED EFFECTS OF CITY AND COOLING TOWER HEAT RELEASE ON THE THERMAL STRUCTURE AND VELOCITY FIELD OF THE LOWEST AIR LAYERS OF THE ATMOSPHERE

D. Haschke
Swiss Federal Institute for Reactor Research
Würenlingen, Switzerland
and
C.A. Jacobs and J.P. Pandolfo
The Center for the Environment & Man, Inc.
Hartford, CT 06120, U.S.A

1. INTRODUCTION

The investigation of possible mesoscale climatic effects of rejecting large amounts of waste heat into the atmosphere by means of natural draft cooling towers has been the purpose of the project CLIMOD, which was started in 1976. In parallel with an extensive field program, which was undertaken to get in situ measurements of meteorological variables, a theoretical program of mesoscale boundary layer simulation was carried out.

Meteorological considerations led to a characterization of so-called critical regional weather situations, which were considered to be sensitive to anthropogenic modification on the regional scale. One such critical weather situation was an anticyclonic high pressure winter situation with a strong elevated inversion. The effect of cooling towers and city heat release on the thermal structure of the lowest air layers during such a weather situation is discussed in this paper.

2. REGIONAL TOPOGRAPHY

The area which was taken for the simulation is shown in Figure 1. It shows the upper Rhine Valley between the Swiss city of Basel in the west and the mouth of the river Aare just outside the east boundary. The topography as produced by computer graphics is shown in Figure 1. It is smoothed due to the 3 km x 3 km horizontal grid resolution used in the model and gives a good representation of the actual topography, retaining the important features and neglecting sub-grid scale characteristics. The highest elevation in the simulated topography is about 900 m above sea level, the lowest about 250 m above sea level. The area extends 60 km in the E-W direction and 21 km in the N-S direction. Four types of subsurface were used for the simulation according to the prevalent land use in each 3 km x 3 km grid square centered on each horizontal mesh point (station):

- urban
- suburban
- rural
- forest.

The relevant physical parameters of each surface type are listed in Table 1.

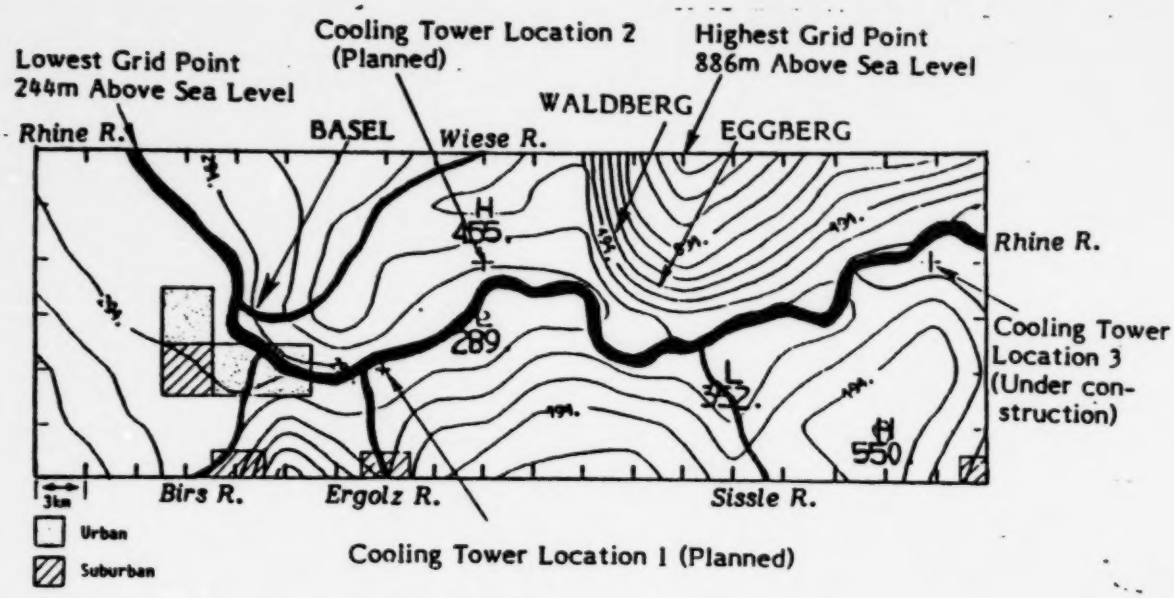

Figure 1. Topography for model simulation.

TABLE 1

Physical Parameters of Surface Types Used in Model Simulation

		Station Type			
Parameter	Unit	Rural	Forest	Suburban	Urban
Short Wave Albedo	---	.25	.10	.23	.20
Roughness Length	cm	~3.0	~12.0	~15.0	~50.0
Evaporation Parameter	---	.30	1.0	.10	.05
Sensible Heat Release	W cm^{-2}	0.0	0.0	2.5×10^{-3}	5.0×10^{-3}
Soil Thermal Diffusivity	$cm^2\ s^{-1}$	.008 wet .004 dry	.008	.01	.02

3. WEATHER SITUATION

The case study was performed for an anticyclonic situation which was observed during the period December 14 to December 21, 1977. The center of a high pressure system is approximately over central Europe and moves slowly to the east, where it remains fairly stationary during the latter part of the period. The Swiss plateau, i.e., the basin between the Swiss Alps and the Jura is filled with cold, foggy air up to heights of about 600 to 800 m above ground. Above , there is slight advection of dry warm air from the SW. Cold air flows to the northeast from the Swiss plateau into the Rhine Valley, which is also fog covered in its eastern portion almost to cooling tower location 2 on Figure 1, further to the west are clear, but hazy skies. Due to the warm and dry air overflowing the "cold air lake" a strong and persistent elevated inversion is formed which effectively limits the dispersion of waste heat and pollutants to the air layers below the inversion, i.e., to the air layers up to about 400 to 500 m above ground.

4. PLANETARY BOUNDARY LAYER (PBL) MODEL

The PBL model used for the simulations is extensively described in (1) and (2). Various recent applications of the model are described in (3), (4) and (5). The model is mathematically and physically based on the Eulerian conservation equations for momentum, heat, water vapor, salinity, and air and water pollutants, and is subject to a set of interface and boundary conditions necessary for physical and mathematical consistency. The model is capable of examining the transport and diffusion process in the air-land or air-water planetary boundary layer. The principal processes parameterized are boundary-layer turbulence in stratified (humidity, salinity, and temperature dependent) conditions, cloud-dependent radiative heating, and for a set of vertical grid points which contain an air-water interface, mixing due to wind-generated waves on the interface. In its present version, the horizontal diffusion in the model is incorporated through a strongly and implicitly diffusive finite-difference scheme for the horizontal advection terms--viz., upwind differencing. Terms representing other transport and diffusion processes are explicitly included in the differential equations. The vertical transfer processes are simulated on a relatively fine grid (i.e, of the order of meters to tens of meters) in the lowest portion of the modeled volume, whereas the horizontal grid spacing is of the order of a few to hundreds of kilometers.

Although the model in its most general form simulates three-dimensional space (x,y,z), more specialized experiemnts may be carried out using grid configurations of one (z only) or two (x,y or y,z) spatial dimensions. For convenience, the form that the model assumes during a simulation becomes a matter of exercising options built into the model. The one-and two-dimensional forms require less execution time because of fewer grid points. Therefore, a choice of a grid configuration can be made considering the economic factors and the space and time scales necessary to describe the phenomena which are to be simulated. The model uses the same equations for the one-two- and three-dimensional forms, except that appropriate terms (i.e., the horizontal gradients of the dependent variable in the one-dimensional version) are specified rather than predicted.

5. MODEL INPUT

5.1 Meteorological Input:

Meteorological soundings were available for a 7-day period starting December 14, 1977 at cooling tower location 1 (see Figure 1) and mostly at hourly or bi-hourly intervals. These local soundings normally reached heights of 500 to 600 m above ground, but occasionally extended to 1100 m above ground. To construct an initial field of meteorological variables, temperature, wind, and humidity from the 11 hr (Local Standard Time) sounding on December 18, 1977 were taken. This sounding extended to 1000 m above ground, and was supplemented with values taken from the noon sounding of the Swiss Weather Office at Payerne for the layers above 1000 m.

Boundary conditions for the meteorological variables have to be specified both at the top and bottom surface of the modeled volume, as well as at the lateral surfaces. On the top surface, temperature, wind and humidity were kept constant during the simulation period. The bottom surface was taken at 0.50 m below ground level and the temperature was kept constant there. Lateral boundary conditions are fairly compli-cated due to the complex physics involved in this case and had to be derived by an iterative process. The gradients for temperature and velocity thus obtained at the inflow boundaries are shown in Figure 2. The height dependence of $\partial T/\partial y$ was estimated using the thermal wind equations. The large negative value of $\partial T/\partial y$ between 400 and 600 m above ground is due to the transition of the large-scale flow from generally S-W aloft, to S-E and E in the air layers near the ground. The shape of $\partial T/\partial x$ between 0 and 400 m above ground gives cold advection for air flowing into the region from the east and simulates the cold air inflow from the Swiss plateau. The values for $\partial T/\partial x$ have been chosen in order to reproduce the observed temperature profile in the region.

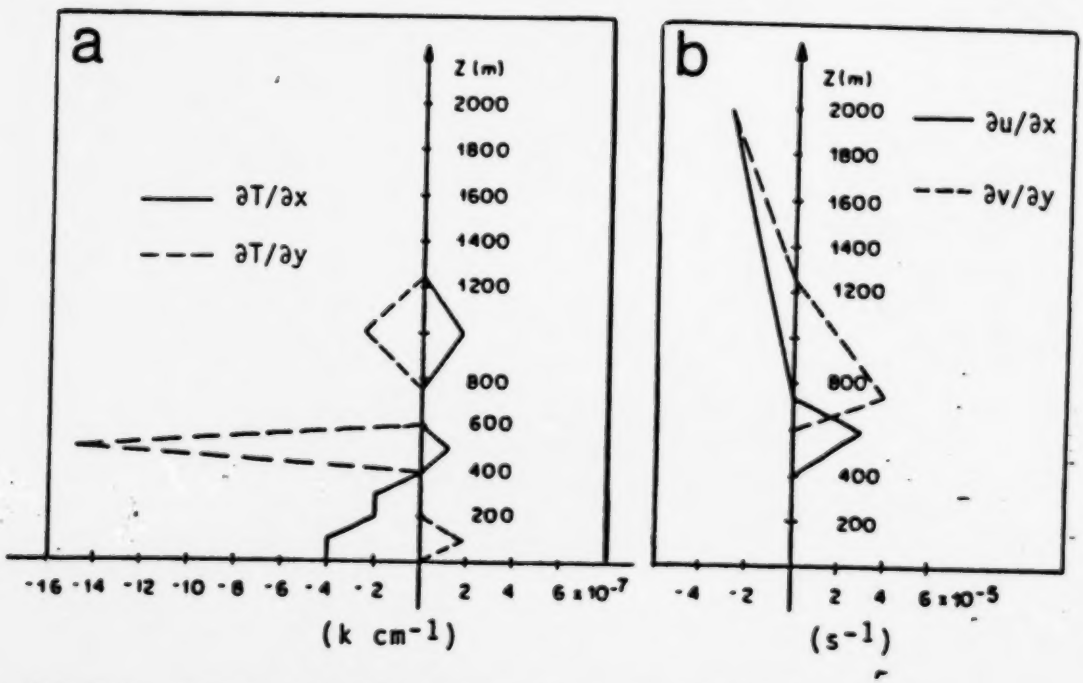

Figure 2. Boundary conditions at the lateral inflow boundaries. a) Temperature gradients; b) Velocity gradients (divergence).

The values for $\partial u/\partial x$ and $\partial v/\partial y$ define the synoptic scale divergence and are chosen to simulate the typical high-pressure downward motion associated with the simulated weather situation of about 1 to 2 cm s^{-1} . Simulation results indicated that a downward motion of this order of magnitude was necessary to maintain a stable elevated inversion in agreement with observations.

5.2 Anthropogenic Input:

It consists mainly of surface physical specifications related to the urban and suburban areas as shown in Figure 1. The sensible heat release was assumed 50 W m^{-1} for urban and 25 W m^{-1} for suburban areas. The physical properties of the subsurface were taken as listed in Table 1.

Furthermore, two strong elevated point energy sources (e.g., dry cooling towers) were inserted at cooling tower location 1 (2000 Mwth) and cooling tower location 2 (4000 Mwth) with a source elevation of 300 m above ground (see Figure 1). Dry cooling towers emitting only sensible heat were used, because regional scale effects should show more clearly than with wet cooling towers of equal power. (5)

6. SIMULATION RESULTS*

6.1 Two-dimensional Results:

To give a general idea about the simulated weather situation, some results of a two-dimensional x-z simulation are presented. Figure 3 shows a comparison between simulated and observed vertical temperature profiles above cooling tower location 1 (station 7) and above a city station (station 2) to the east. The strong temperature inversion of about 10 °C, starting at about 200 m above ground up to about 600 m above ground is clearly visible. This inversion remains stable for about 96 hours. A shallow air layer which is influenced by the underlying surface extends up to 100 m above ground, and is about 2 °C warmer over the city station than over the rural station.

Figure 4 compares observed and calculated winds 24 hours after start of simulation. It shows that general wind directions and velocities can be predicted with reasonable accuracy.

* Acknowledgment is made to the National Center for Atmospheric Research, which is sponsored by the National Science Foundation, for the computing time used in this research.

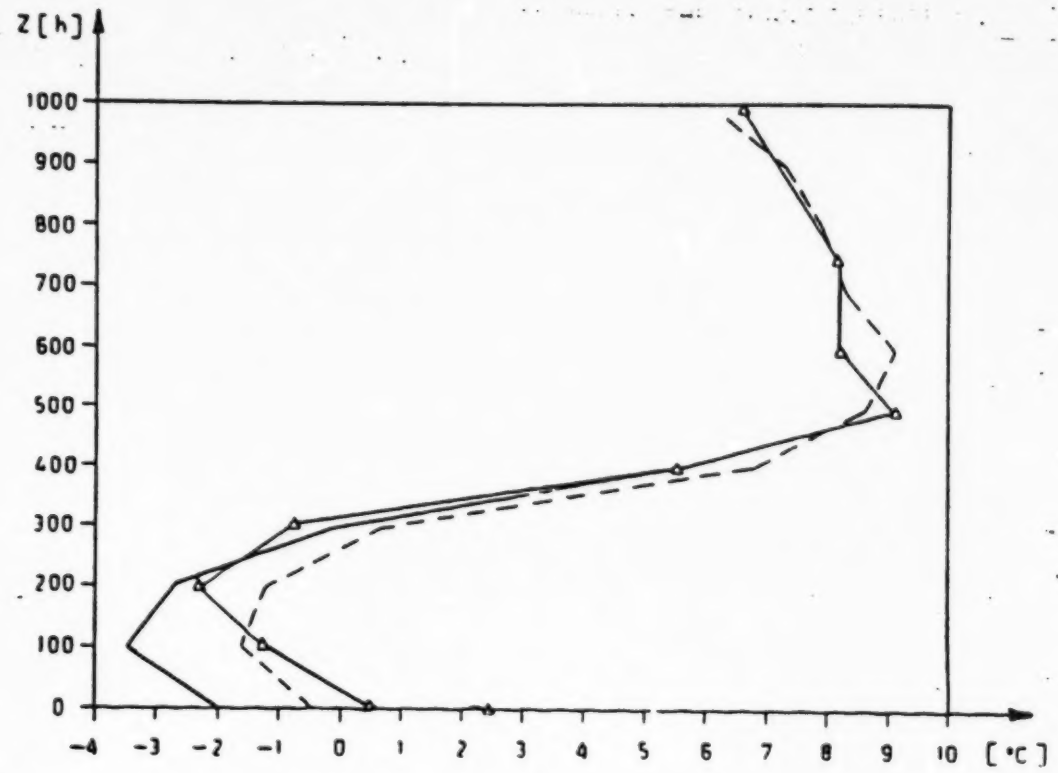

Figure 3: Comparison of calculated and observed Temperature Profiles, 24 hours after start of simulation; Dec. 19, 1977, 11 a.m. Observed (dashed line); calculated, rural station 7 (solid line); calculated, city station 2 (solid/symbol).

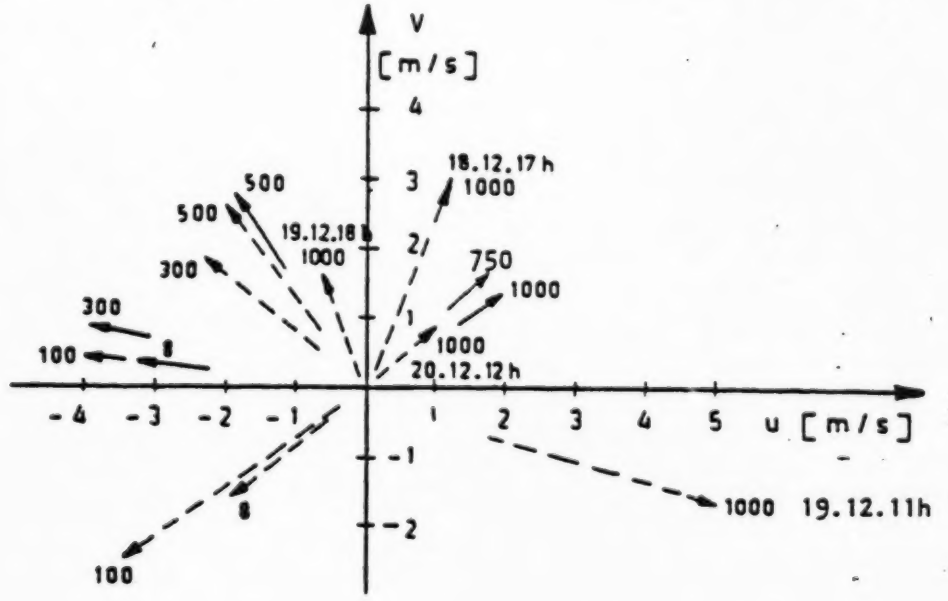

Figure 4: Observed and calculated winds, 24 hours after start of simulation; Dec. 19, 1977, 11 am. ——→100 calculated, - - -→100 observed } 100 m above ground

START TYPING ON THIS LINE OF ALL PAGES OTHER THAN TITLE PAGE

Figure 5 gives a comparison between observed and calculated temperatures over a 24-hour simulation period and at four different height levels. The 600- and 500-m level is in the inversion and shows no diurnal variation. At the 300-m level the model predicts a diurnal temperature variation which is, however, not clearly supported by observations. The observations show temperature increases of two and more degrees for height increases of about 50 m and indicate that a 100-m vertical resolution as used by the model is probably not sufficiently detailed for this transition layer. The 2-m level shows a typical clear but hazy winter diurnal temperature variation which is well-supported by the observations.

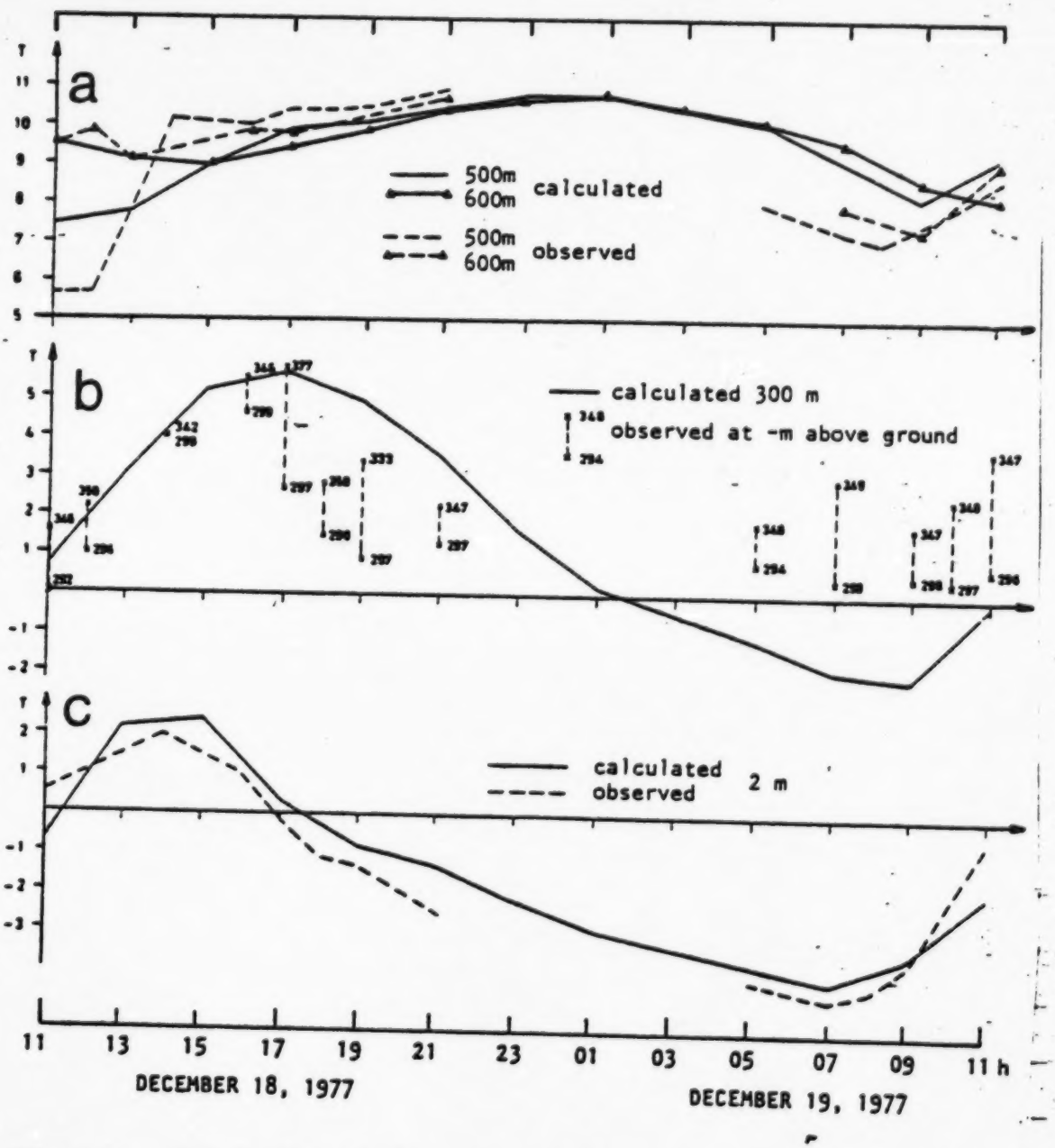

Figure 5: Time series of observed (dashed lines) and calculated (solid lines) temperatures at four different height levels: a) 600 m and 500 m above ground; b) 300 m above ground; c) 2 m above ground.

6.2 Three-dimensional Simulation Results:

On Figure 6, temperature differences between the case with city and cooling tower heat release and the control run case with no anthropogenic heat release are shown. Temperature fields are presented at seven height levels, i.e., at 8 m, 16 m, 32 m, 100 m, 200 m, 300 m and 400 m above ground and after eight hours of simulated time. The effect of the city heat release is clearly visible in the lowest three levels. The magnitude of the heat island is of the order of about 1 °C, the area with more than 0.5 °C temperature increase is about 10 to 12 km in diameter. Its shape depends on the prevailing winds and extends, therefore, more to the S-W. Small temperature effects of the order of 0.1 °C to 0.2 °C extend over fairly large areas. The 100-m level shows a general warming of about 0.3 °C but no city heat island effect can be seen. This can be understood from the simulated temperature profile in Figure 3, which indicates a general increase in stability at that level and above, which prevents further vertical transport of heat, thereby limiting the city influence to heights below 100 m above ground.

At the 300-m level, which is the assumed source height for the cooling tower heat release, the temperature effect of those strong point sources is clearly visible. The temperature increase is of the order of about 0.5 °C in the area close to the cooling towers and about 0.3 °C in an area of about 15-km diameter. It is interesting to note that due to the strong inversion, the 400-m level is not influenced by the cooling tower heat release, whereas the 200-m level shows warming. Furthermore, it is noted that there is no apparent interaction between city heat island and cooling tower heat release.

Figure 7 is a plot of the build-up of the city heat island. It can be seen that the city heat island builds up immediately after startup to values of about 0.2 to 0.3 °C and remains there for about 3 hours. Then the 8- and 16-m level starts to warm because of the increase in atmospheric stability due to the increased late afternoon radiation cooling, and another 3 hours later the 32-m level starts warming rapidly due to a local breakdown of atmospheric stability. Around 7 p.m., there is a brief decrease in temperature at the 8- and 16-m level which corresponds to an increase in the 100-m level and indicates a short and local decrease in stability (thermal bubble). After about 10 hours of simulated time, all levels approach approximately constant temperatures.

Figure 8 shows the temperature effect due to cooling tower operation. The 300-m level (source height) shows a relatively constant warming of the order of about 0.5 to 0.6 °C, warming in the 200-m level is (except for a period of about 3 hours, from 6 to 8 p.m.) much smaller. Temperature effects in the 400-m level are both slightly positive and negative, i.e., both cooling and warming have been found, which indicate the possibility of waves caused by the cooling tower heat release in these very stable layers.

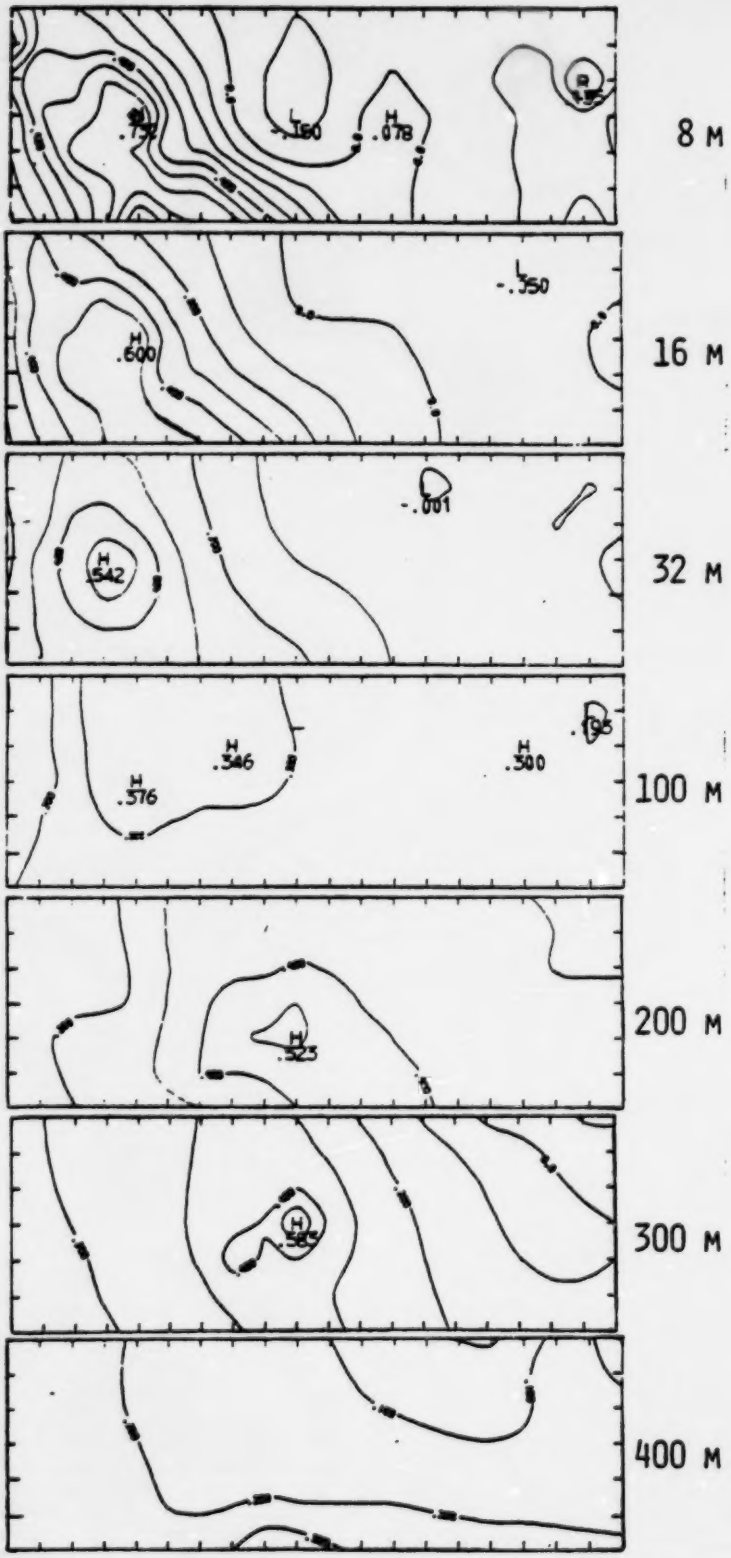

Figure 6: Temperature effect of city and cooling tower heat release, December 18, 1977, 7 p.m. (8 hours after start of simulation). Plots show temperature differences (degrees celsius) with anthropogenic heat release versus a control run without anthropogenic heat release for 7 height levels above ground. The topography and cooling tower locations are shown in Figure 1.

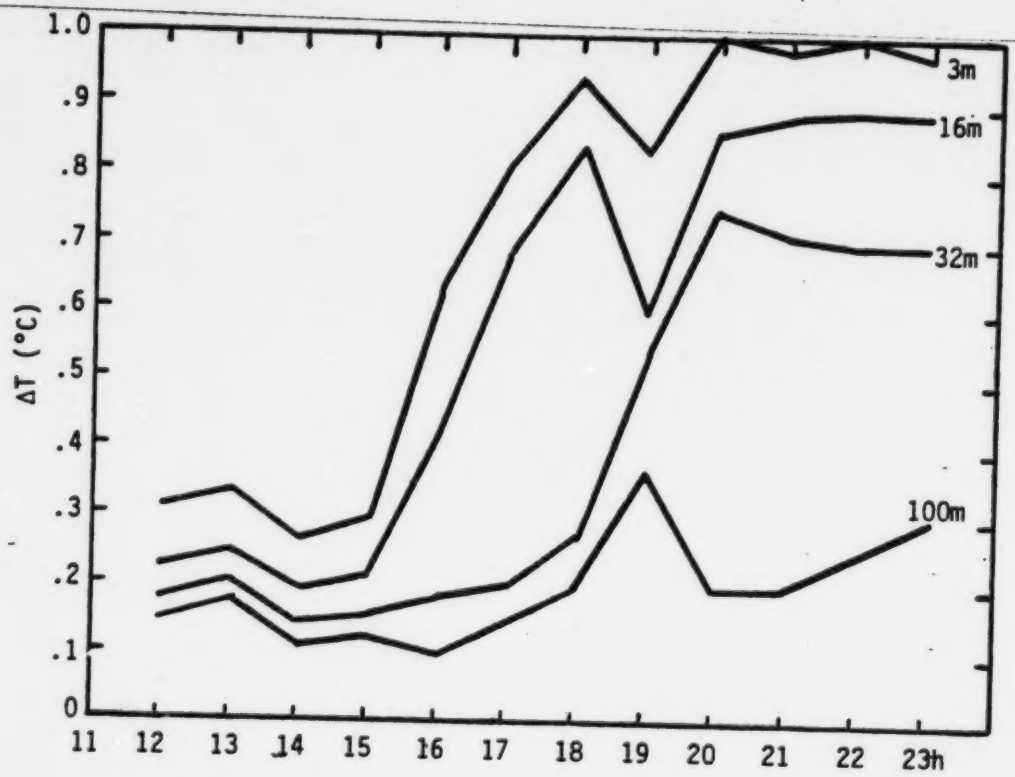

Figure 7: Temperature increase in the city heat island 8 m, 16 m, 32 m and 100 m above ground; December 18, 1977, 11 a.m. to 11 p.m.

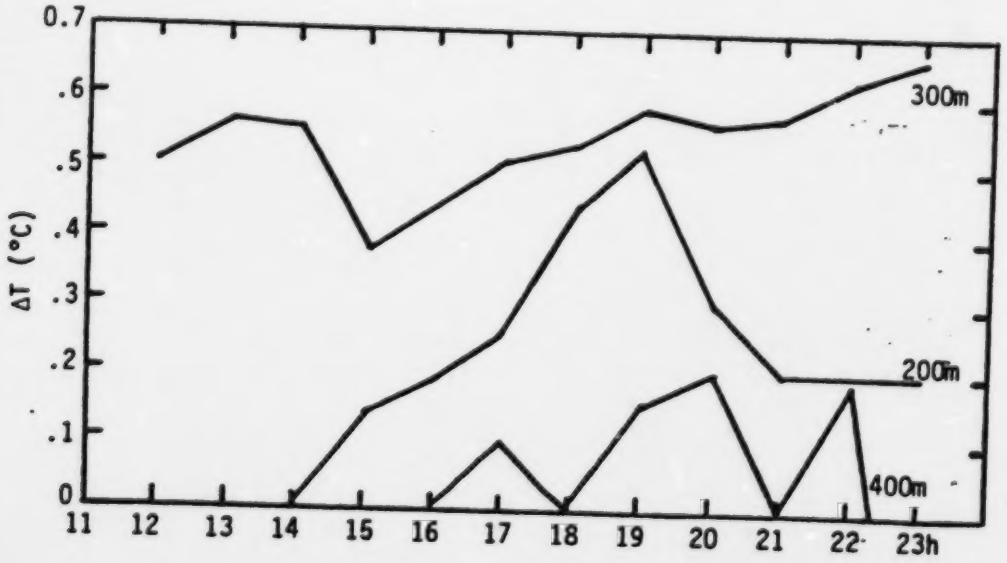

Figure 8: Temperature effect of cooling tower operation, 200, 300 and 400 m above ground; December 18, 1977, 11 a.m. to 11 p.m.

SUMMARY AND CONCLUSIONS

The effects of anthropogenic heat release from a city and cooling tower in an anticyclonic winter situation with strong inversion conditions are simulated using a physically complete mathematical model of the planetary boundary layer. It is shown that in very stable atmospheric conditions the city heat island extends up to heights of about 100 m. Results indicate that cooling tower heat is not diffused vertically but only advected horizontally under extremely stable conditions and that the cooling tower plumes do not interact with the neighboring city heat island.

REFERENCES

1) Jacobs, C. A. and J. Pandolfo, 1974: A Description of a General Three-dimensional Numerical Simulation Model of acoupled Air-water and/or Air-land Boundary Layer. CEM Report 4131-509a.

2) Pandolfo, J. P. and P. S. Brown, 1980: A gravity wave problem with the upstream difference method. J. Comp. Phys., 37:2, 141-150.

3) Atwater, M. A., 1977: Urbanization and pollutant effects on the thermal structure in four climatic regimes. J. Appl. Meteor., 16, 888-895.

4) Pandolfo, J. P. and C. A. Jacobs: Computer simulation of meso-scale meteorological effects of alternative waste-heat disposal method. Proc., 2nd Waste Heat Management and Utilization Conference, Miami Beach, FL, December 4-8, 1978.

5) Haschke, D., F. Gassmann, C. A. Jacobs and J. P. Pandolfo: Computer simulation of mesoscale meteorological effects of waste heat disposal through cooling tower. EPRI - Cooling Tower Workshop, San Francisco, 1981.

SESSION VIII-B

UTILIZATION III

PB82-228495

ENERGY APPLIED SYSTEMS TEST FACILITY

F. J. McCrosson, P.W. Yngve and F. H. Zander
South Carolina Energy Research Institute
Columbia, South Carolina, 29201, U.S.A.

ABSTRACT

This paper presents a design and operation preview of the proposed Energy Applied Systems Test (EAST) Facility. The EAST Facility is one element of the U.S. Department of Energy Residual Energy Applications Program (REAP), which has a two-fold goal: to recover large quantities of residual energy at Federal nuclear facilities and to stimulate waste heat recovery in the private sector. To help meet this goal, the proposed EAST Facility will provide development and confidence testing for industrial scale heat pumps, absorption chillers, and Rankine-cycle power generation systems. The facility, to be located at the Savannah River Plant (SRP) in Aiken, South Carolina, will be government-owned and contractor-operated. A competent technical staff will assist both the equipment developer and the end user in the development, testing, and commercialization of the equipment. Completion of design and construction are scheduled for mid-1982 and mid-1984, respectively.

1. INTRODUCTION

The proposed Energy Applied Systems Test (EAST) Facility will provide unique capabilities for testing residual energy recovery systems for waste streams in the 100-1000°F range. The facility will eventually allow testing heat pumps with outputs as large as 100 million Btu/hr and power generation systems of 4-5 MWe. Initially, however, it will be used for testing smaller scale systems of 5-25 million Btu/hr and 0.5-2 MWe.

The government-owned, contractor-operated facility will probably be located near one of the nuclear production reactors at the Savannah River Plant (SRP) in Aiken, South Carolina, where it can draw from the reactor's large flow of heated water. Equipment developers and manufacturers will have access to flexible facilities for long-term, third-party confidence testing. The facility will not have a regulatory role.

This paper describes the overall scope and capabilities of the EAST Facility. Design requirements are being prepared and will go to the designer at the end of May 1981. During June and July, amendments to the requirements will be prepared after discussions with the designer, potential users of the facility, and potential users of the test equipment. Please contact one of the authors if you wish to take part in these discussions.

2. BACKGROUND

In 1977-1978 the U.S. Department of Energy (DOE) evaluated the feasibility

Preceding page blank

of using large quantities of low-grade heat dissipated at four nuclear facilities. (1) One of these facilities was the Savannah River Plant, which produces nuclear materials in Aiken, South Carolina (2); the others were gaseous diffusion plants located in Tennessee, Kentucky, and Ohio. (3,4,5) Collectively, the four facilities reject .28 quads annually in the form of 130-165°F water effluent. (1 quad = 10^{15} Btu)

DOE concluded that immediate implementation of direct-use options such as greenhouse operations and lumber and grain drying could result in significant energy recovery at these facilities. Even with full implementation of all practical direct-use options, however, most of the residual energy would go unused. Thus, there is a need to use heat pump and power generation systems for converting the large quantities of reject heat to steam and electricity, which have much broader applications.

The power generation systems considered for the Federal facilities were based on the Rankine-cycle principle. These systems generate their power from the heated water. Individual systems would have outputs in the range of 5-45 MWe. Although systems for nearly similar temperature ranges have been under development for the Ocean Thermal Energy Conversion Program (6) and the Geothermal Energy Program (7), no systems directly apply to the Federal facilities. Likewise, the heat pumps for the Federal facility applications are considerably larger than industrial heat pump systems now on the market. They also call for significantly higher output temperatures than now possible in the commercial units.

DOE's Residual Energy Application Program (REAP), of which the EAST Facility is a part, grew out of those 1977-1978 studies. The objectives of REAP are to:

- conduct realistic feasibility experiments to recover residual heat energy in real world environments;
- effectively use residual energy from the three DOE gaseous diffusion plants and the SRP production reactors; and
- conduct ongoing technology development and system R&D activities that focus on the effectiveness of components, subsystems, and systems.

These objectives for the total REAP program aim at the single overall goal of achieving optimum usage of available residual energy within the private sector. The objectives of the EAST Facility are to:

- perform research and development on heat energy recovery and conversion equipment as required;
- establish high confidence in system performance, system availability, and system operating, maintenance, and material costs; and
- provide a national competence in technologies required for the installation and operation of heat recovery systems.

3. RESIDUAL ENERGY RESOURCE

The potential for residual energy recovery and use in the United States is very large. About 30% of the energy we consume now dissipates to the environment (8), and very little is recovered. Yet, the technologies (heat pumps and power generation systems) that offer the greatest potential for recovering

large quantities are currently available. The need for government involvement in this program arises because the rate of return on investment for heat recovery systems typically makes them marginally competitive with other investment alternatives available to the private sector. Also, these systems frequently carry a higher risk, primarily because of uncertainty in the short- and long-term reliability.

Figure 1 gives estimates of annual residual heat at the four DOE facilities and in the utility and industrial sectors. The numbers include only the more easily recovered forms of residual energy and do not include product heat losses. Estimating the accuracy of the numbers for the industrial sector is difficult because individual plants in the same 4-digit Standard Industrial Classification (SIC) can vary greatly. The South Carolina Energy Research Institute is now studying the potential for waste heat recovery in South Carolina. Preliminary results confirm the general conclusions of the Drexel University study (10) upon which the industrial numbers in Figure 1 are based. At the more specific 4-digit SIC level and for individual plants, there are notable differences from the generalized flow and temperature characterizations at the 2-digit SIC level in the 1978 Drexel study. For example, hydraulic cement plants are characterized by 650°F exhaust in the Drexel studies, whereas the two wet process plants in South Carolina are in the 400-450°F range, and the exhaust temperature of the one dry process plant is even lower. These lower temperatures significantly reduce the attractiveness of power generating bottoming cycles, especially since these systems typically cool the exhaust only to about 300°F to avoid heat exchanger corrosion. On the more positive side, contaminated process water in SIC-22, Textile Mill Products, is categorized at 120°F in the Drexel study. Textile finishing plants account for most of this water. In South Carolina, a textile state, we have found the contaminated process water in cotton and cotton blend finishing plants is frequently 175°F or more, and hence more attractive for recovery.

Categorization of the sizes of heat recovery equipment required for industry is even more difficult because size requirements vary so much from plant to plant within the same industry. Also, to categorize a plant by a single residual energy source can be misleading. In the finishing plants, for example,

	ANNUAL RESIDUAL ENERGY, 10^{12} BTU/YEAR			
	Liquid			Gaseous
	95-120°F	130-160°F	170-200°F	300-1000°F
Four DOE Facilities[9]		280		
Industry[9,10]	1100	1680	155	3710
Utilities				
• Base-Load[9] (Wet cooling towers)	2800			-
• Gas Turbines & Diesels[11]				70

Figure 1. Residual Energy By Sector and Temperature

the contaminated process streams from individual operations are frequently segregated and are not amenable to tapping at one location. Nevertheless, we have generally estimated the sizes needed in the United States. We based the estimates, given in Figure 2, on work performed for us by United Technologies Research Center. (9)

Predicting penetration of the technology into the marketplace is still more difficult because it depends on such factors as the performance of the equipment, industry's perception of the merit of the equipment, even on the Middle East situation. We included our estimates for the penetration factors in Figure 2. They could be in error by a factor of three or more, but they do illustrate how an estimate is required before we can determine the ultimate size of the market at equilibrium. Our estimate for the size of the market is in Figure 3. At today's prices, the installed heat pump and power generation equipment at equilibrium would be worth $5 billion.

Of equal importance is the sharpness of the rise in the S-shaped curve that typically categorizes the sales of equipment from start to market equilibrium. Our studies indicate that if the EAST Facility shortened the time to achieve market equilibrium by just one year, the monetary value of the energy saved would be 70 times the cost to build and operate the facility for five years. (12)

4. SYSTEMS

We anticipate that the heat pumps tested in the EAST Facility will have capacities up to 100-200 million Btu/hr and the power generation systems, capacities up to 4-5 MWe output. After testing, these systems would become the principal components of large Central Energy Management Systems (CEMS) to supply steam and electricity to an industrial park at a Federal facility. The CEMS steam and electric output would be sized to provide the optimum mix for the industries in the park.

Figure 4 illustrates schematically the dual-fluid, Rankine-cycle heat pump proposed by United Technologies Research Center for a CEMS at Portsmouth, Ohio. In this concept, R-11 (freon) vapor is generated at 130°F in a horizontal flooded-type evaporator by the heat recovered from the 150°F waste stream. The vapor is compressed in two stages by centrifugal compressors directly driven by a gas turbine engine. The flow then condenses in a condenser/boiler where steam is generated at 250°F and 34 psia. A two-stage compressor then produces steam with a 300°F saturation temperature. The hot exhaust gases from the gas turbine driver are directed into a residual-heat boiler capable of producing steam

	Heat Pump Capacity (10^6 BTU/Hr)			Power System Capacity (MWe)		
	95-120°F	130-160°F	170-200°F	130-160°F	170-200°F	300-1000°F
DOE Facilities		100-200		4-5		
Industry	10-30 (.50)	30 (.50)	100 (.30)		1-2 (.30)	1-2 (.60)
Utilities	100-200 (.20)					1-2 (.60)

Figure 2. Estimated Heat Pump/Power Generation System Sizes (Market Penetration Factors in Parentheses)

Type Unit & Size Range	Temperature of Residual Energy 95-120°F	130-160°F	170-200°F	300-1000°F	Total
Heat Pumps					
• 10-30 x 10^6 BTU/hr	1600	850			2450
• 100-200 x 10^6 BTU/hr	200		10		210
Power Generation Systems					
• 1-2 MW			20	1600	1620

Figure 3. Number of Units in Private Sector at Market Equilibrium

at 300°F or higher. An economic evaluation of this system showed that a before-tax return on investment of 20% is possible with a system output of 25 million Btu/hr. Systems above 100 million Btu/hr will result in a before-tax return on investment of 30% or greater. To install and test a system sized for 100 million Btu/hr will require an 80-by-70 ft. space 25 ft. high.

The selection of each system element is critical to the economic attractiveness of any project and is dependent on many factors which are specific to each site. For example, the major design considerations for the system shown in Figure 4 are the cycle configuration, the working fluid, and the driver. United Technologies Research Center chose a closed cycle because the working fluid is confined in a closed loop, therefore allowing a greater choice of fluids which can optimize the process. The working fluid (R-11) was selected on the basis of its performance, its ability to maintain smaller, lower cost components and its relative low cost when compared to other options. United Technologies Research Center selected the gas turbine drive since a portion of the heat content of the high temperature exhaust gas can be recovered to augment the heat pump output. In comparison, an electric motor driving a heat pump with a coefficient of performance (COP) of 3 will give an overall COPF of 1.0. COPF, the coefficient of performance based on primary fuel input, is equal to the ratio of the heat output from the heat pump to the heat content of the primary fuel used. The gas turbine driver will result in a COPF of $\sim$ 1.3 for the same example.

The dual-pressure, Rankine-cycle power plant proposed by United Technologies Research Center is shown schematically in Figure 5. The two-stage ammonia cycle employs an intermediate heat exchanger to isolate the ammonia from the process water, and it rejects heat to a mechanical draft cooling tower. The intermediate loop water (at 146°F) flows successively through high- and low-pressure ammonia evaporators and an ammonia feed heater. The evaporators are large, vertical, natural circulation boilers with water flowing through the tubes. In the high pressure evaporator, the ammonia vaporizes at a temperature of 125°F and a pressure of 308 psia. In the low pressure evaporator, the ammonia vaporizes at a temperature of 110°F and a pressure of 243 psia. Vapor from both evaporators flows to separate radial inflow turbines which, in turn, drive ac generators producing about 4.25 MWe net power. Cooling water at 67°F pumps through the condenser and returns to the cooling tower at 77°F. The required waste stream flow rate for this system is 22,550 gpm. The cooling water flow is 72,000 gpm. The system will require an 80-by-110-ft. space 57 ft. high.

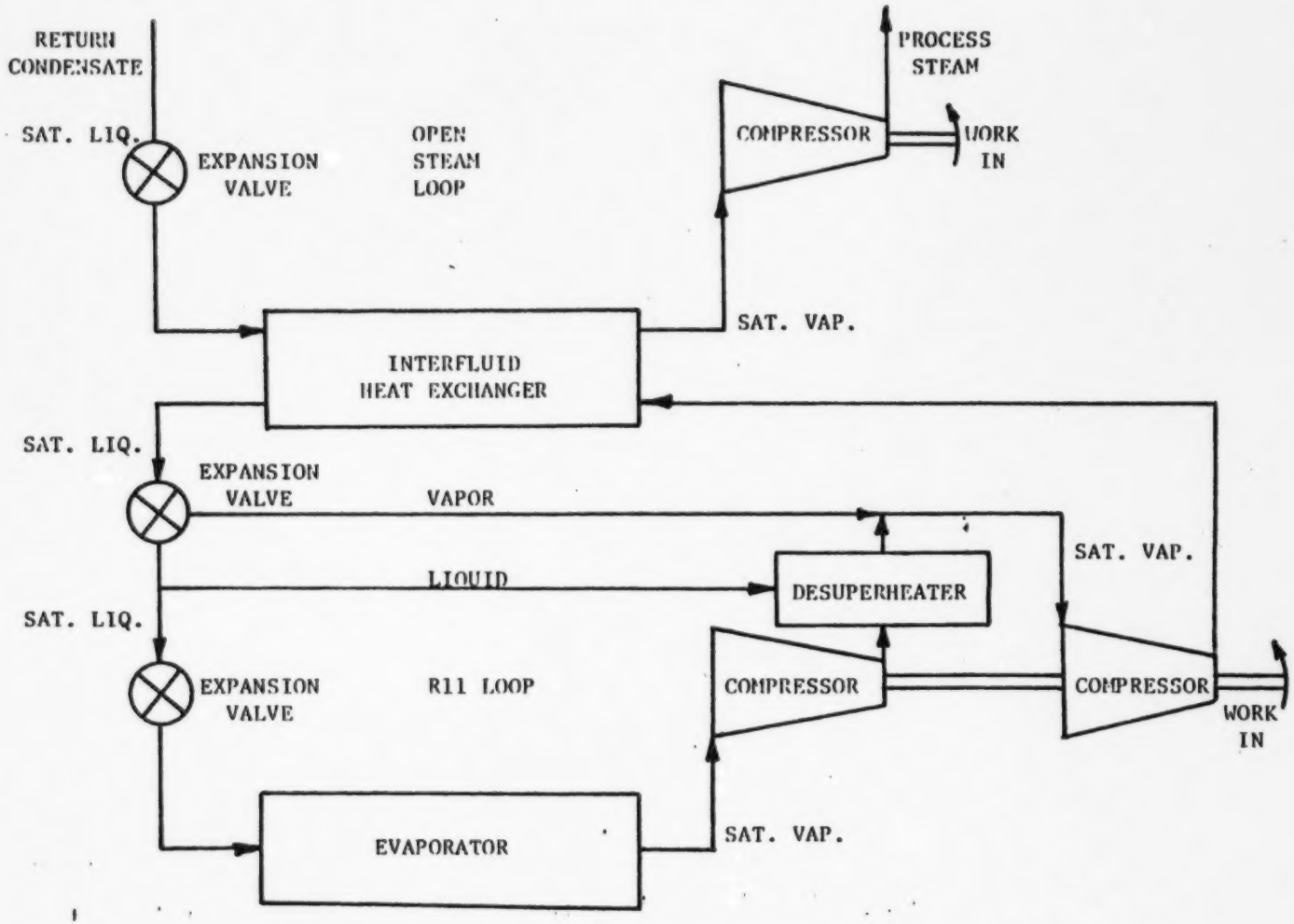

Figure 4. Dual-Fluid, Rankine-Cycle Heat Pump

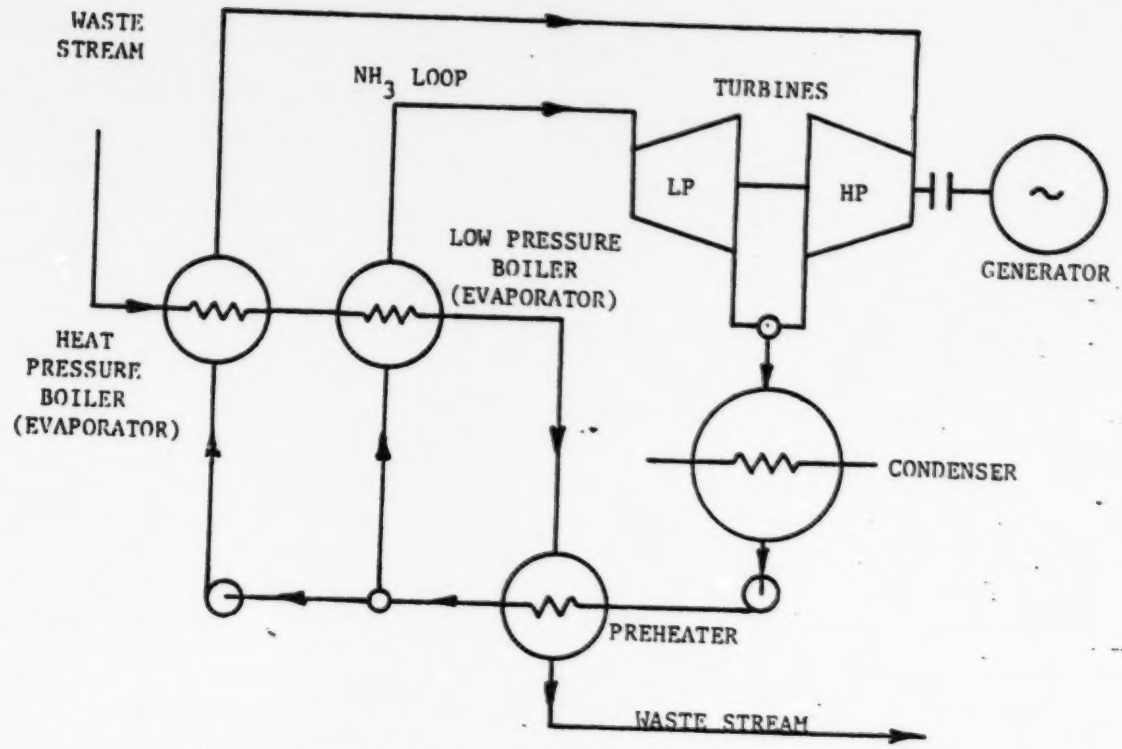

Figure 5. Dual-Pressure Rankine-Cycle Power Plant

As in the case of the heat pump, the selection of particular elements is very site specific. For the system in Figure 5, the major design considerations were the number of evaporation stages, the overall system size, and the working fluid. Two evaporation stages were selected because their use resulted in an increase of 35% greater power and a reduction in the overall installed cost/kw by about 16%. On a $/kw basis, the system size apparently is not a factor in the size range of 2-30 MWe. The working fluid (ammonia) was selected for its thermodynamic properties, chemical stability, operating temperature range, non-flammability, availability, and cost.

As Figure 3 indicated, most of the heat recovery applications in the industrial sector will involve smaller heat pumps and power generation systems than those proposed for the CEMS. A primary role of the EAST Facility will be to test 5-25 million Btu/hr heat pumps and 0.5-2 MWe power generation systems to confirm specified levels of confidence associated with systems performance in commercial environments. We anticipate both open and closed cycle systems, as well as a diversity of potential drivers for the heat pump compressor. The facility will also test absorption chillers with cooling capacities in the 200-300 ton range. The testing for power generation systems will include high-temperature gaseous waste streams (200-1000°F) and low-temperature liquid streams (< 200°F). Figure 6 illustrates a high-temperature power generation system developed by Mechanical Technologies Incorporated. The EAST Facility space required to test this system, which has an output of 4.17 MWe, will be a 100-by-40 ft. area 40 ft. high.

5. TEST PROGRAM

EAST Facility testing of the heat pump and power generation systems (Figures 4 and 5) would require 15 months and 11 months, respectively.

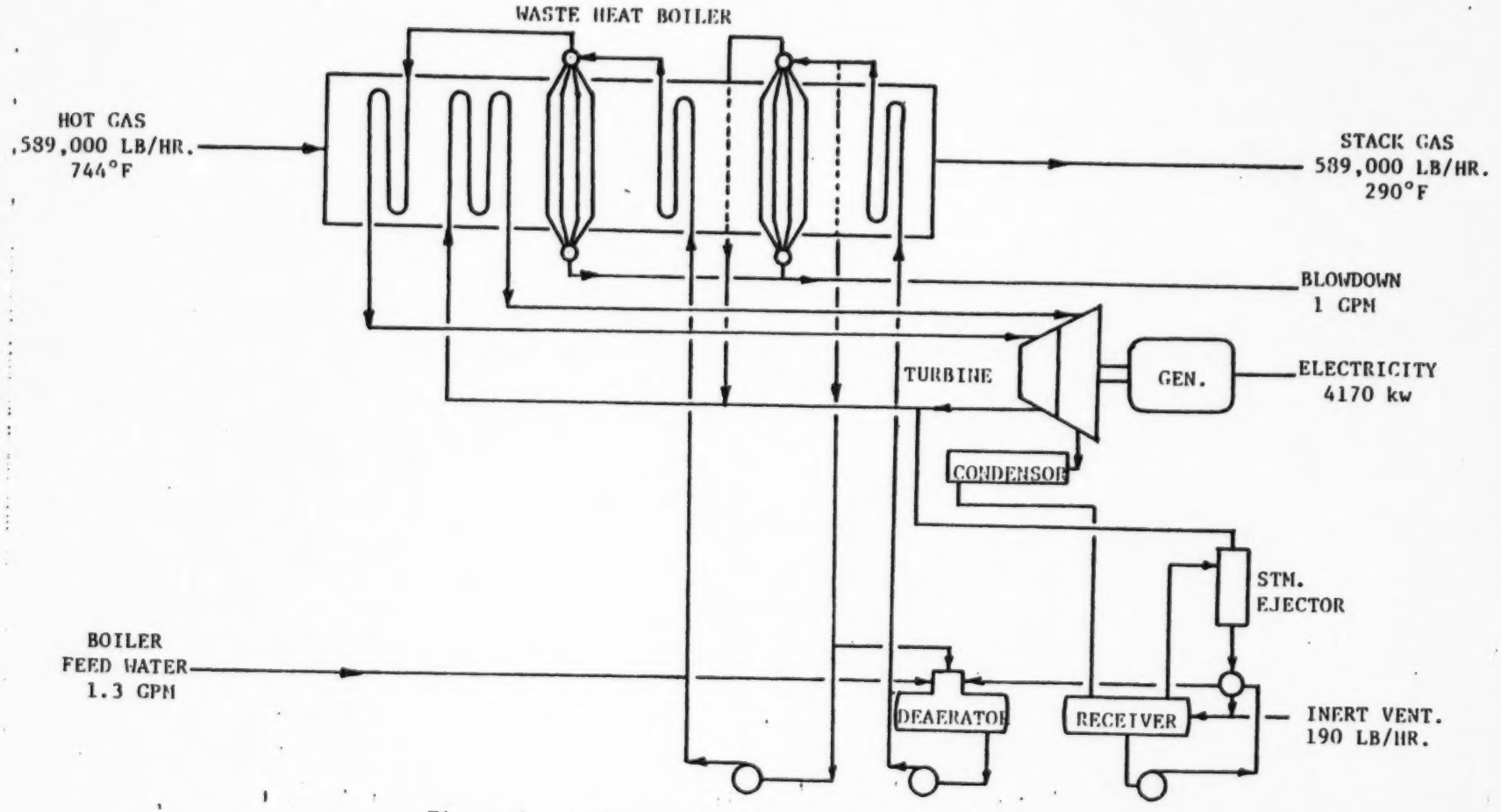

Figure 6. High-Temperature Power Generation System

Initial system checkouts, green running, performance evaluation, and endurance testing would follow installation of the heat pump system. Checkouts include working fluid subsystem leak tests and instrumentation calibrations. Green running involves limited operations of gradually increasing temperature and power levels and monitoring of critical components (e.g., compressor) and critical test parameters (e.g., engine vibration level). Performance evaluation covers a wide range of operating levels to characterize the behavior of each major component and to profile the overall system performance. Temperature, pressure, and flow rate measurements in and out of each heat exchanger would help to define heat transfer coefficients, pressure loss characteristics, and adiabatic efficiencies of the compressors and the gas turbine driver. With these data, we could identify needs for changing or adjusting control devices. Endurance testing would consume about 4000 hours. Critical subsystems/components and associated test data would be monitored for degradations of performance. For example, reductions of the heat transfer coefficient or increases of pressure loss may indicate some heat exchanger fouling; excessive vibration may indicate some bearing wear; and periodic analyses of working fluid samples may provide early signs of contamination or decomposition.

Working fluid leak checks, instrumentation calibrations, transient testing, performance evaluation, and endurance testing would follow installation of the electrical power generation system. Transient testing includes cyclical start-up, shutdown, and load dropping to characterize control stability, system response rates, and other behavior; it would require about one month of the overall testing period. Performance and endurance testing would measure and profile the system's power conversion efficiency for most of the effluent and cooling water conditions expected at the Federal facility end-use site. Many activities related to heat pump system testing also apply to this system.

For these two large systems, we expect the overall periods of test conduct to include some EAST-team-monitored developer testing followed by some developer-team-assisted independent testing by EAST personnel. The latter efforts would include reliability testing to determine availability and maintainability of the system.

Testing for the smaller systems (capacities less than 25 million Btu/hr for heat pumps and 2 MWe for power generation systems) will be less developmental in nature and more concerned with confidence or reliability. Testing will focus on

- performance within specified ranges of input and output conditions, including deteriorating conditions;
- flexibility (performance explorations beyond specified ranges of input and output conditions);
- operability and controllability;
- maintainability, with respect to normal maintenance/repair; and
- normal/accelerated time to failure (encompassing various failure and degradation mechanisms).

In focusing on these factors, the EAST Facility will pursue product testing well beyond the bounds of product demonstration and will provide test results generated by an independent, disinterested third party.

Rigorous definitions of failure, accept/reject criteria, ground rules for test conduct, and methods for data analysis will be included in test

planning so that expectations are clearly defined and misunderstandings between the customer and EAST personnel are prevented. Specified test objectives will be based on:

- establishing performance characteristics and limits;
- verifying performance characteristics with respect to environmental conditions;
- qualifying system/subsystem/component life expectancy, mean time between failure (MTBF), mean time to repair (MTTR), human factors, and safety;
- quantifying confidence levels for system/subsystem/component life expectancy, MTBF, MTTR, human factors, and safety; and
- verifying equipment characteristics of importance to operations/maintenance personnel.

To meet these objectives, the EAST Facility will obtain test data from manufacturers, developers, vendors, and users and from engineering evaluations to establish a predictive reliability data base. At a minimum, data will consist of audits covering equipment developmental activities such as specifications, component selections, and all aspects of component/subsystem/system testing by the developer, including stress testing. Data should include the results of developer's environmental studies and failure modes, effects, and criticality analyses to confirm estimates of MTBF and MTTR.

Data collected through EAST will be combined with the established reliability data base using Bayesian techniques to develop confidence statements of MTBF, MTTR, availability, etc. Through comparison of predicted to determined reliability/maintainability values, critical components will be identified for special evaluation.

6. FACILITY DESIGN CONSIDERATIONS AND SCHEDULE

The facility will be built in two phases. The first phase will provide a three-bay core area for testing heat pumps with outputs up to 25 million Btu/hr, high- and low-temperature power generation systems with .5-2 MWe outputs and absorption chillers with 200-300 ton capacities. In the second phase, an expanded area will allow simultaneous testing of a greater number of the systems or individual developmental testing of the larger size systems proposed for the CEMS.

As an example of requirements for the expanded facility, the following are the specifications associated with the heat pump test bay:

- Test Bay Size and Location: 80 ft. wide, 70 ft. deep, 25 ft. high, indoors or outdoors.
- Waste Stream Inputs

  Water: 10,000 gpm at 150°F, standard pressure; lesser flow rates at 200°F and/or 100 psia.

  Steam: 50,000 lb/hr at 200°F, 20 psia.
- Working Fluid Storage and/or Treatment

Water Storage: 5000 gallons at 70°F.

Freon (R-11) Storage: 2500 gallons at 70°F.

Steam Generation: As necessary to directly heat feedwater.

- Electrical Power Input: 600 Kilowatts, 480 volts, 3 phase, ac.
- Cooling Water Input: 10,000 gpm at 70°F, standard pressure.
- Test Instrumentation: Up to 200 channels needed for system/subsystem monitoring/control and data acquisition/processing/recording.
- Computer: Required.
- Safety and Environmental Control: Freon leak detection/monitoring, safety inspection, Freon fire control and fume protection, standard power plant fire protection and emission monitoring, effluent quality monitoring.

The expanded facility will have capacity for testing heat pumps up to 100 million Btu/hr output and power generation systems up to 5 MWe. The corresponding flow requirements for the facility would then be 45,000 gpm of heated water and 100,000 gpm of cooling water. In tests involving smaller systems, these flows would allow simultaneous testing of three to four heat pumps of 10 million-50 million Btu/hr capacity and a similar number of power generation systems in the 1-2 MWe range. With a distribution and control system, there could be varying flow input conditions, cycling, intermixing, and distribution of these hot and cold streams. There would also be supplemental heating for the streams.

Figure 7 shows the schedule for design, construction, and operation of the EAST Facility.

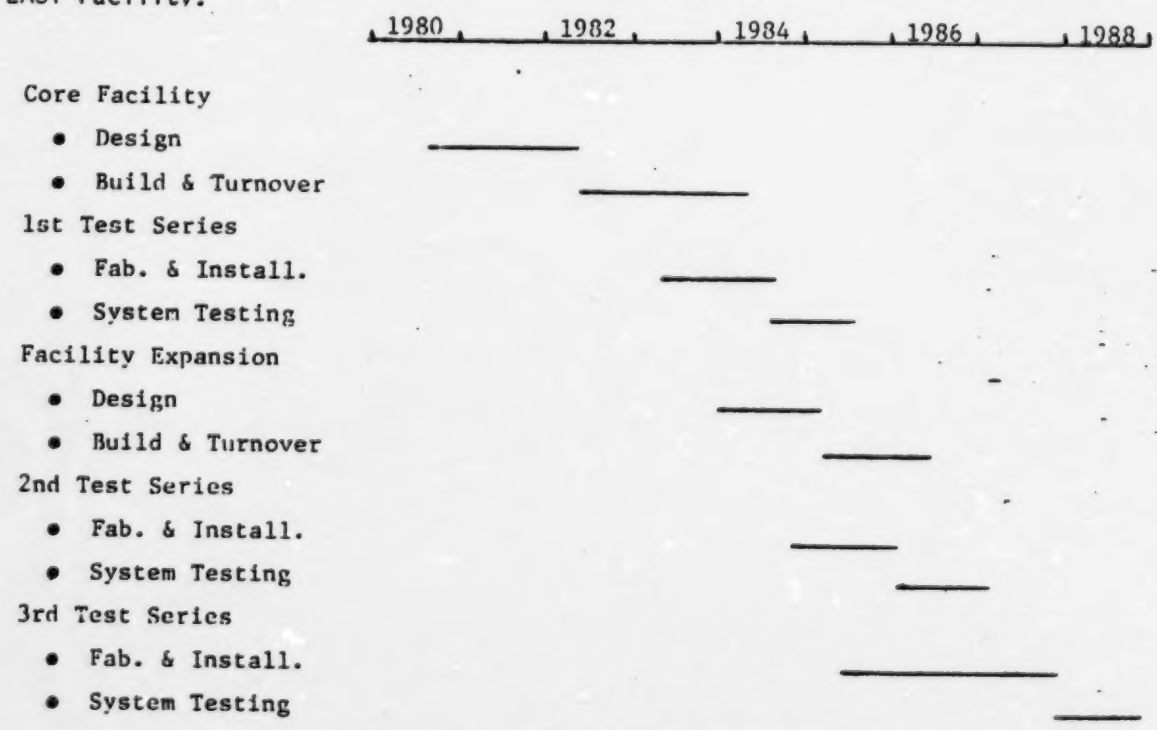

Figure 7. EAST Facility Schedule

7. CONCLUSIONS

According to our estimates in Figure 3, industrial-scale heat pumps could save approximately .4 quads per year at market equilibrium. Rankine-cycle power generating systems could save a similar amount. The heat pump energy savings is the difference between the energy required to generate steam in an 80% efficient boiler and the energy required by a heat pump with a COP of 3 that is driven by a gas turbine or diesel. The Rankine-cycle power generation systems were compared to 33% efficient power plants.

The EAST Facility will help achieve those energy savings by providing exploration, development, application, and confidence tests. The facility may be used in three major modes:

- government-owned test articles, government-funded tests;
- privately owned test articles, government funded tests; and
- privately owned test articles, privately funded tests.

Variations of these modes will be considered individually and may include jointly funded tests, partial government ownership, ownership by a department other than DOE, EAST-initiated tests, and others.

Design of the first phase, core facility is scheduled for a mid-1982 completion. Construction has an 18-month schedule with turnover in mid-1984.

ACKNOWLEDGEMENT

The information contained in this paper was developed during the course of work under Contract DE-AC09-77ET 12866 with the U.S. Department of Energy.

REFERENCES

1. Utilization of Waste Heat from Federal Facilities, prepared under U.S. Department of Energy Contract EC-77-C-05-5523 by Arthur D. Little, Inc., February, 1979.

2. The Savannah River Plant Low Level Waste Heat Utilization Project, Report prepared for U.S. Department of Energy by South Carolina Energy Research Institute, DOE/EC/1021-1, November, 1978.

3. Oak Ridge Gaseous Diffusion Plant Reject Heat Study, Final Report prepared for U.S. Department of Energy by Exxon Nuclear Company, Inc., Vols. I through IV, September, 1978.

4. U.S. Department of Energy Waste Heat Utilization Project for the Paducah, Kentucky, Uranium Enrichment Gaseous Diffusion Plant, Final Report prepared by J.E. Sirrine Co., Vols. I and II, September, 1978.

5. Use of Reject Heat from Uranium Enrichment Gaseous Diffusion Plant Portsmouth, Ohio, Final Report prepared for U.S. Department of Energy by Bechtel National, Inc., Vols. I and II, October, 1978.

6. Proceedings of the Fifth Ocean Thermal Energy Conversion Conference, a World-wide Survey of the Design and Operation of Geothermal Power Plants, DOE/RA/28320-1, January, 1980.

7. Ronald Di Pippo, (ed.), Geothermal Energy as a Source of Electricity, a World-wide Survey of the Design and Operation of Geothermal Power Plants, DOE/RA/28320-1, January, 1980.

8. J. Neal, A Waste Heat Utilization Program, Proceedings of the Second Conference on Waste Heat Management and Utilization, Miami Beach, Florida, II-3, December, 1978.

9. Systems Analysis Report, Part of a Systems Test and Evaluation Study for the Residual Energy Applications Program, prepared under U.S. Department of Energy Contract DE-AC09-77ET-12866 by the South Carolina Energy Research Institute, DOE/ET/12866-3, October, 1980.

10. Industrial Applications Study, prepared under U.S. Department of Energy Contract E (11-1) 2862 by Drexel University, HCP/T2862-01, March, 1978.

11. Monthly Energy Review, DOE/EIA-0035/9 (79), September, 1979.

12. Support & Integration Report, Part of a Systems Test and Evaluation Study for the Residual Energy Applications Program, prepared under U.S. Department of Energy Contract DE-AC09-77ET-12866 by the South Carolina Energy Research Institute, DOE/ET/12866-6, November, 1980.

SESSION IX-A

UTILIZATION IV

PB82-228503

THE POTENTIAL FOR WASTE HEAT UTILIZATION RESULTING FROM THE USE OF POTABLE WATER SUPPLIES AS COOLING WATER PRIOR TO TREATMENT

R. H. Ramsey, III, R. D. Bowersock, L. V. Urban, J. H. Strickland, and R. M. Sweazy
Water Resources Center
Texas Tech University
Lubbock, Texas, U.S.A.

ABSTRACT

The study concept was examined on the assumption that electricity is the primary product produced by the utility and that outlet temperatures from the condenser could be in a range of from 90° to 120°F. The effects of elevated water temperature on water treatment processes and the probable water temperature profile exhibited in a municipal system were investigated. The heat loss model showed that only slight decreases in water temperature would be experienced in the larger transmission and distribution mains. Greater heat losses would occur in the smaller distribution mains and customer service lines; there would still, however, be an increase in water temperatures so that the amount of energy needed to heat water would be reduced. A questionnaire sent to residents in seven southwestern cities gave a 73% favorable response for implementation of the concept. It was determined that most of the detrimental environmental impacts could be mitigated by the utilities through proper system design and management.

1. INTRODUCTION

The feasibility of using municipal water supplies prior to treatment, as condenser cooling water was examined in a study conducted at Texas Tech University [1]. In this concept, portrayed on Figure 1, raw water from the municipal supply source would be transported to a storage reservoir located adjacent to the energy generation facility. Water would be piped from this reservoir to the condenser of a generating unit or, if the water supply is large enough, to the condensers in a power plant. A once-through cooling system supplied with the inflow water to the municipal treatment plant would be used. If other units were on a closed cycle system using cooling towers, no pipe connections between the units would be allowed. The hot water outflow from the condenser would be piped to a storage reservoir located adjacent to the municipal water treatment plant; from here it would be drawn, treated, and distributed to water consumers. The principal objective was to determine whether the concept would have beneficial economic effects on the public utility which subsequently treats and distributes this water and on the user of the warmed water.

Preceding page blank

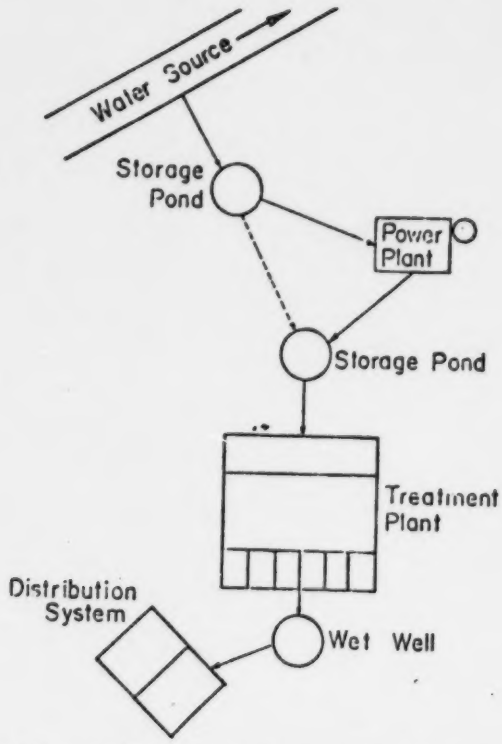

Figure 1. Flow Pattern for System Concept.

2. POTENTIAL BENEFITS FROM SYSTEM IMPLEMENTATION

In this section the potential benefits that can be realized by the electric and water utilities and their customers will be examined.

2.1 Electric Utility

The competition for scarce water supplies is intensive in many parts of the country. Use of large volumes of cooling water in energy generation facilities creates conflicts with other demands. Only a single acquisition strategy may be open to utilities in some localities whereas in others several alternatives may be feasible from a physical, technological, economic, and legal basis. Such alternatives include:

- Purchase of water rights
- Initiation of application procedures for appropriation of water from local sources.
- Location, obtaining, and importation of water from other areas to the use site.
- Reclamation of wastewater.

These strategies all involve considerable costs to utilities just for obtaining and transporting water to the generating facility. The use of potable water supplies as cooling water can reduce costs for acquisition and transport. Generating facilities are normally located close to the load centers. Potable water

is also required in these load centers. Water that is being transported to meet public needs can be routed through the power generating facility with much less cost than would result from employing one of the other alternatives cited above.

The water use requirements in the urban area will dictate the amount of water that will be available for use by the utility. The quantity in some cases may be enough to supply only one boiler unit whereas in others there will be enough to supply the whole installation. Exit temperatures from the condenser may be higher than those allowed in once-through systems discharging back into the aquatic environment. Table 1 shows the quantities of water and the potential cooling capacity for various condenser exit temperatures. The inlet temperature of 80°F corresponds to that of average summer conditions. Generally, water requirements by the public are at their highest levels during the summer period. This allows large quantities of water to be available for cooling. Both water needs and water temperatures decrease during other periods of the year. But cooler inlet water temperatures provide greater heat capacity per unit volume of water.

The system concept provides once-through cooling which can be accomplished at a lower cost than other cooling water management systems [2]. Because of limited physical availability of water and/or the cost of implementation associated with the strategy, it may well be necessary that the water used will need to be recirculated through the system. Additional costs to the energy producer in the form of cooling towers, pumps, piping, and water treatment would be incurred. Water must be treated to minimize biological growth, to prevent foaming, and to maintain a desired pH level. Water quality thus deteriorates due to increased constituent concentration caused by evaporation during cooling as well as by the addition of chemicals to condition the water. The quality deterioration may necessitate that "boiler blowdown" be treated prior to its release to area streams or be disposed of on-site.

TABLE 1

Energy Output From Various Water Treatment Rates for an Input Water Temperature of 80°F

Water Treatment Rate (MGD)	Water Temperature at Condenser Outlet (°F)				
	85	90	100	110	120
10	4.5*	9.0	18.0	27.2	36.2
25	11.3	22.6	45.3	67.9	90.5
50	22.6	45.3	90.6	135.8	181.0
100	45.3	90.5	181.1	271.6	363.0

* Electric energy output in megawatts

Note: ' cooling water is to carry away 45% of heat energy produced
' stack losses are 15% of heat energy produced
' Electricity generated at 40% thermal efficiency

By providing warm water to the consumer the utility can reduce its energy output requirement. If 5.68 kWh of electric energy are saved per home per day in raising the temperature of water to 150°F from 100°F rather than from 62.5°F, this would represent a saving of 18.35 kWh of thermal energy which need not be generated if electricity is delivered to the residence with an efficiency of 31%. For one thousand homes, the savings in fuel consumed at the plant would be approximately eleven barrels of oil per day. The saving to a utility in fuel costs and in installed generating capacity to provide the 5680 kWh of power required for heating water during the daily activity period in one thousand homes and the savings in cooling water management costs for either an alternative once-through system or a closed cycle system using an evaporative method can be significant.

2.2 Water Utility

Benefits from elevated water temperatures will occur in water treatment operations. In normal operations, a treatment plant adjusts to the temperature regimes of the raw water entering the plant. These, in turn, depend on source characteristics. Surface waters from lakes and rivers, for example, have seasonal temperature variations occurring over a span of several tens of degrees. Waters from underground sources exhibit fairly constant temperatures at all times.

The treatment facility incorporates features designed to accommodate low temperature regimes. Operational or structural measures are used to prevent icing or freezing of system components so that treatment can continue during extended periods with temperatures below freezing. Also, the rates of chemical reaction and of settling of suspended particles is slower in colder water. These two factors generally determine the sizing of the treatment reactors. Normally, little concern is expressed by the designer for water temperatures outside of the probable low water temperature regime. Plant management, however, will require information on the frequency distribution of cold temperatures because of the effects on chemical use and treatment efficiency.

Laboratory studies. These were made to determine effects on alum-floc sedimentation, adsorption of organics by powdered activated carbon (PAC), rapid sand filtration, and disinfection over the range of 30°C to 60°C. These treatment methods were chosen for study because little is known about their behavior at elevated temperatures and because they represent the major portion of capital investment and operation costs in a conventional water treatment plant. The findings of the laboratory studies for the first three treatment methods are discussed below. The experimental studies on disinfection at high temperatures are still in progress.

Sedimentation. The effect of temperature on the coagulation and sedimentation of an alum-bentonite floc was investigated by means of the jar test. The procedure was performed at each of the four test temperatures --- 30°, 40°, 50°, and 60°C --- at alum concentrations of 0.0, 1.0, 5.0, 10.0, and 20.0 mg/l. Optical density (OD) readings were made at specified time intervals after completion of the slow mix phase in the jar test. Figure

2 shows the effects of temperature on the OD readings using an alum concentration of 5 mg/l. Table 2 summarizes the data obtained in this phase and shows the minimum alum concentration to reduce floc turbidity by at least 90% in a specified time interval for the test temperature. The tests run at 0.0 mg/l of alum showed the effects of temperature on viscosity of water which is, in turn, important in the rate and extent of settling.

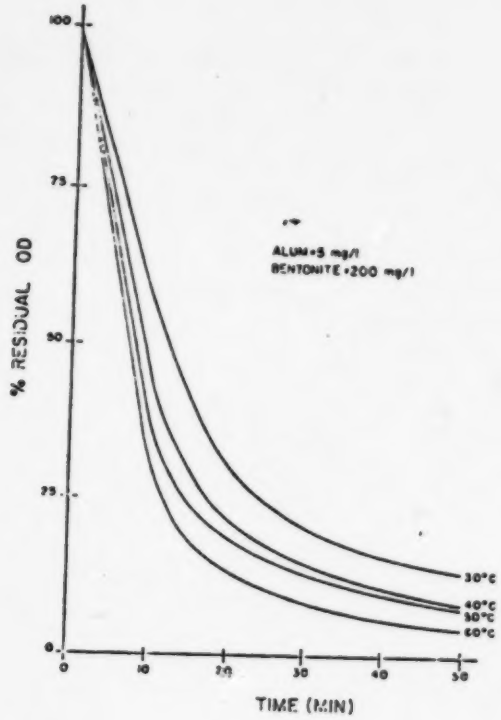

Figure 2. Effect of Temperature on Sedimentation.

TABLE 2

Minimum Alum Concentration in mg/l Required to Reduce Floc Turbidity by at Least 90%

TEMPERATURE	TIME (min)				
	10	20	30	40	50
30	-	10	10	10	10
40	-	10	10	5	5
50	20	10	5	5	5
60	20	10	5	1	0

Adsorption. The jar test was used to study the effects of temperature on adsorption of organics by powdered activated carbon (PAC) in the presence of bentonite and alum. The adsorbable organic used was methyl organge. Optical density

measurements were made. Figure 3 illustrates the effects of temperature on the adsorption of methyl orange by PAC in the presence of 1 mg/l of alum and 200 mg/l of bentonite. Similar results were obtained using 0.0, 5.0, 10.0, and 20.0 mg/l of alum, indicating that PAC rather than the floc was responsible for the major portion of color removal.

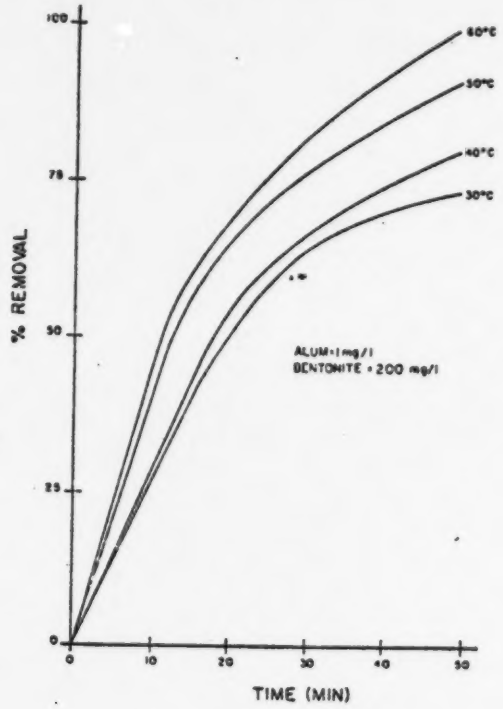

Figure 3. Removal of Methyl Orange by Powdered Activated Carbon at Various Temperatures.

Filtration. In municipal water treatment, filtration is the unit operation in which water is passed through a porous medium to remove suspended solids remaining in the water after sedimentation. A test column 2.7 cm in diameter and 50.8 cm in height was prepared for each run. The columns were standardized and those having a hydraulic conductivity of 70 ± 1 ml/minute were used in the test. The columns were then loaded at a rate of 0.1 m^3/minute/m^2 with an influent solution containing floc from 10 mg/l alum in a solution of 100 mg/l of bentonite at the test temperature. Temperature was found to have little effect on floc size since OD varied by less than 0.02 OD units between experiments.

At specific intervals, head loss was read and the effluent volume was collected and measured. The filtration experiments were run at the two extreme temperatures, 30° and 60°C, and a median temperature of 45°C. Figure 4 shows the effect of temperature on a sand column receiving flow at a constant head. Each isotherm represents the normalized data from at least three separate test runs.

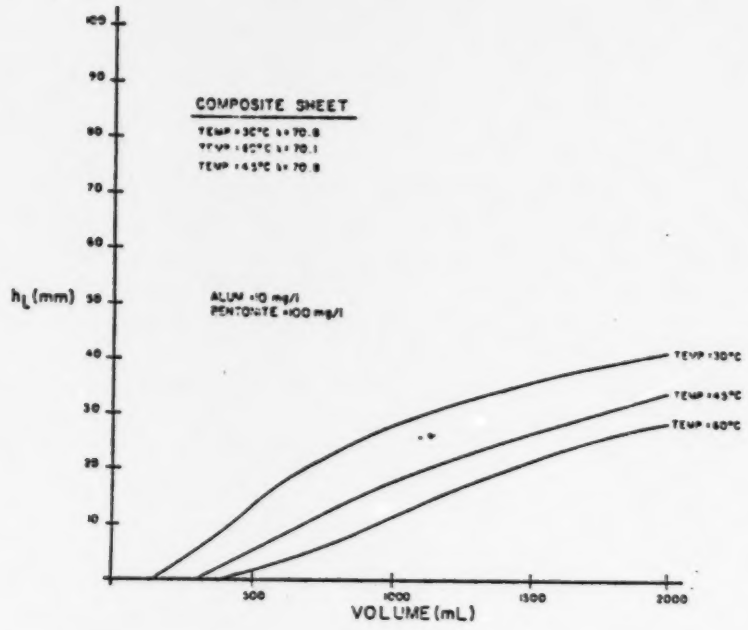

Figure 4. Head Loss Profiles of Temperature Effects on Contact Filtration of an Alum Floc.

Impact of high temperatures on water treatment. For the three water treatment operations evaluated in the study, elevated temperatures appear to have a beneficial effect. However, these experiments were designed to facilitate ease and accuracy of measurements and not to model precisely the conditions in a water treatment plant.

Warmer temperatures in the water would allow increases in the overflow rates in sedimentation basins. Therefore, the required basin volume would be less in the construction of new plants. If the concept were to be implemented in an existing plant, the treatment capacity of the existing basins would be increased considerably. As an example, using standard sizes of alum floc to calculate settling velocities at 10°C and 50°C, a 690% increase in velocity would occur over the 40°C temperature span.

Adsorption studies indicate that increased organic removal may occur at elevated temperatures. In a PAC system removing dissolved organics from potable waters this would appear to be beneficial.

The column studies show that for the particular system used, head loss is less for a given volume of water at the higher temperatures. Since the loading rates to the sand filter would be the same at each temperature, the length of filter runs could be increased in treatment plant operation. This effect may be enhanced at the higher temperatures because of increased sedimentation efficiency.

2.3 Water Utility Customers

Heat losses that would occur in a municipal water system supplied with warm water were investigated by means of models that examined losses in water treatment and in the distribution system. The results showed that, in all seasons, the slope of the temperature profile is mild throughout the treatment plant and in the large transmission and distribution mains. Position of consumers in the distribution grid would have an important effect on their water temperatures.

Water quality customers are supplied through an interconnected pipe network of which the design is based upon the location of existing customers and of the anticipated growth. Through hydraulic analysis, the pipes in the grid and supporting appurtenances such as pump stations and distribution storage are sized to meet the design flow demands at various points in the service area. Flow in the network occurs when a pressure differential is developed between the high pressure in the distribution system and the lower pressure at the point of use by the customer.

In periods of high use, such as the interval from 6 a.m. to 8 a.m., flows in the transmission and distribution lines are generally in the direction determined in the design analysis --- with possible exceptions in some of the smaller distribution mains. In the smaller mains, changes in flow direction may occur because of the storage capacity in the pipe and the demands of the consumers which occur episodically along the length of the main.

Since the goals of municipal water supply are to provide a pathogen-free water in the necessary amounts whenever required and wherever located in the system, flow reversals are not at present significant. However, in the case of the transport of heated water, the number of flow reversals, the use rates of water, and other factors that determine the time a water molecule remains in the system would become important. Water use patterns, soil conditions, location in the pipe grid, and ambient weather conditions interact to determine the temperature of water available for each customer in the system. Usage values; being affected by lifestyle or business type of the customer, number of people in the household or employed in the business, season of the year, day of the week, and time of day; vary greatly among consumers. Soil type, temperatures and moisture conditions can affect the rates of heat flow from the pipe to the soil. The location of the customer within the network will determine the availability of warmer water to him. Water users located close to major transmission or distribution mains will have better access to warmer water than will other users. Also, use sites closer to the water treatment plant will obtain warmer water than sites located further away because flow rates will be higher and therefore the rate of renewal will be faster.

A heat loss model was developed and evaluated for use in the study by assuming an example treatment distribution system exhibiting a specified hourly use rate for the maximum daily demand. An additional use pattern was developed to illustrate what would happen under winter conditions when use rates were

less. Treatment levels in the latter case were reduced to 50% of maximum daily rates and flows in the distribution systems would be 66% of the maximum daily rate. Table 3 shows the temperature conditions in the test system that would result under maximum use conditions for the weather that existed on December 21, 1977 in Lubbock, Texas. Table 4 shows the diurnal temperature regime in the distribution main at the end of the system when the inlet temperature was 110°F at the water treatment plant. The water in the service line to the household (beyond sample point 17) would be colder than that in the 4-inch main. However, the amount of water stored in the service line is small. For example, a 0.75-inch I.D. pipe stores one gallon of water per 43.6 feet of pipe. The greater the use of water in a time period, the greater the chance of receiving warm water within the household.

TABLE 3

Diurnal Temperature Range Exhibited in 50 MGD Example Municipal Water System for Different Inlet Water Temperatures for Weather Conditions in Lubbock, TX on Dec. 21, 1977

Sample Point	Description	Inlet Temperature				
		45°	90°	100°	110°	120°
(1)	Exit from Raw Water Storage	44.5-45.1	88.5-89.6	98.1-99.5	107.7-109.3	117.1-119.1
(2)	Exit at Flocculation Basin	44.3-45.2	87.9-89.4	97.4-99.3	106.7-109.1	115.9-118.7
(3)	Exit at Sedimentation Chamber	43.7-45.4	85.9-88.9	94.9-98.6	103.7-108.2	112.2-117.5
(4)	Exit at Filter Unit	43.3-45.6	84.5-88.5	93.2-98.1	101.6-107.6	109.7-116.7
(5)	(4) + 2600' of 45" pipe	43.3-45.6	84.5-88.5	93.2-98.1	101.6-107.6	109.6-116.7
(6)	(5) + 2600' of 30" pipe	43.3-45.6	84.4-88.5	93.1-98.1	101.5-107.6	109.6-116.7
(7)	(6) + 2600' of 27" pipe	43.3-45.6	84.4-88.5	93.1-98.1	101.5-107.6	109.5-116.6
(8)	(7) + 2600' of 24" pipe	43.3-45.6	84.3-88.5	93.0-98.1	101.4-107.5	109.4-116.6
(9)	(8) + 2600' of 24" pipe	43.3-45.6	84.2-88.4	92.9-98.0	101.2-107.5	109.3-116.5
(10)	(9) + 2600' of 20" pipe	43.3-45.6	84.1-88.4	92.7-98.0	101.1-107.4	109.1-116.4
(11)	(10) + 2600' of 20" pipe	43.3-45.6	83.9-88.3	92.5-97.9	100.8-107.3	108.8-116.3
(12)	(11) + 2600' of 18" pipe	43.4-45.6	83.5-88.2	92.0-97.7	100.3-107.2	108.2-116.0
(13)	(12) + 2600' of 10" pipe	43.4-45.5	81.0-87.3	89.0-96.6	96.7-105.9	104.1-114.2
(14)	(13) + 2600' of 8" pipe	43.4-45.5	77.9-86.1	85.1-95.2	92.2-104.2	98.9-111.9
(15)	(14) + 1300' of 8" pipe	43.5-45.4	73.6-84.4	80.0-93.1	86.2-101.7	92.1-108.4
(16)	(15) + 1300' of 6" pipe	43.5-45.3	70.4-82.9	76.0-91.3	81.5-99.6	86.8-105.6
(17)	(16) + 1300' of 4" pipe	43.6-45.3	67.9-81.1	73.1-89.9	78.1-98.0	32.9-103.4

Note: Ground temperature is approximately 44° F at depth of four feet.

TABLE 4

Diurnal Temperature Regime at Final Outlet in Example Distribution System for Maximum Flow Day and Average Day at Inlet Temperature of 110°F Using Weather Conditions at Lubbock, Texas on 21 December, 1977

Time	°F for Maximum Flow	°F for Average Flow
0300	78.1	59.5
0600	82.4	64.1
0900	95.1	81.5
1200	94.8	81.1
1500	93.8	79.7
1800	94.4	80.4
2100	96.2	83.4
2400	89.3	72.8
Average	90.7	75.6

The temperature variations in the test system were less for dates examined in other seasons. For an inlet temperature of 100°F at the water treatment plant, the following daily variations occurred on the test dates listed.

DATE (1977)	DIURNAL TEMPERATURE RANGE (°F)
March 21	91.0 - 98.7
June 21	95.4 - 99.7
September 21	94.6 - 100.4
December 21	73.1 - 89.9

The value of 100.4°F in September is due to the increase caused by insolation. The heat imput received in open reactors was transmitted to the rest of the system. Examination of the data showed that the impact of solar radiation during the early afternoon hours overrode use rate in the system for all the inlet temperature rates in June and all but the 120°F inlet temperature on the March and September dates.

Benefits of the warmer water at the consumer use point are two-fold. Energy costs in heating water are reduced and the amount of hot water used may be reduced. The latter benefit results from two factors: less water is run waiting for an acceptable water temperature for use, and less water is required to bring it to the desired blend temperature.

Estimates of the amount of hot water used in homes vary. For a family of four, estimates range from 50 gallons per day [3] to approximately 115 gallons per day [4]. For other family sizes, one-third of water consumption is reckoned to be hot water [5]. The energy required for residential hot water heaters has been estimated to range from 20-25% of the total fuel use in the household [6]. Potential impact on household energy use and annual cost for water heating were investigated for the system concept. The kilowatt hours of electricity used to heat 50 gallons of water per day to different outlet temperatures from the level of annual water temperatures at sample point 17, with and without the study concept, were determined. The annual costs were determined from the daily use requirements. Using the

average annual water temperature of 62.5°F and a hot water outlet temperature of 150°F, the daily use for heating hot water was 13.2 kWh and at $0.05 per kWh the annual cost was $240.90. Employing the concept and with outlet temperatures at the condenser of 90°, 100°, 110°, and 120°F, the results at the household were respectively 10.21 kWh/d and $186.33 per year; 8.48 kWh/d and $154.76 per year; 7.41 kWh/d and $135.23 per year; and 6.26 kWh/d and $114.24 per year.

Two factors would indicate that reductions of hot water use are possible. If warmer water were available at the faucet, then no hot water might be needed to provide water at an acceptable temperature. Also when warmer water is desired at the faucet, less hot water will have to be used in producing water at the desired temperature.

3. POTENTIAL PROBLEMS FROM SYSTEM IMPLEMENTATION

In this section, the primary problems associated with implementation of the study concept are discussed.

3.1 Institutional Problems

The study concept impacts three user groups: the electrical utility, the water utility, and the customers of the utilities. Implementation into a working system will depend upon a favorable reception by each of the three groups. This, in turn, will depend on how each group views the benefits obtained from concept implementation. If savings in capital and operational costs would occur it can be expected that the utilities would favor the use of the concept if other circumstances were favorable. These would include such considerations as new facilities being needed by one or both utilities, construction sites for such facilities, and suitable transmission infrastructures for water or power being available or planned.

The consumers, with their many individual concerns, introduce additional complexity in the determination of the acceptability of the concept. Their evaluations of the benefits the utilities receive in comparison to the benefits or costs that the customer will experience will determine the feasibility of implementation. The problem of public acceptance is especially difficult when choices are to be made about a new product, idea or practice which will affect everyone in a consuming public once a decision is reached. Real and imagined problems take on a significance often not warranted by facts because of the importance that individuals attach to the topic. Concern for the health of their families, pets, and plants; damage to material; or the inconveniences caused by the changed temperature conditions can create insurmountable problems for implementation of the concept.

To determine its acceptability, a letter briefly outlining the concept and listing some advantages and disadvantages was sent out to a test population in seven cities in Arizona, Colorado, New Mexico and Texas. A postcard was enclosed to record a yes-or-no reply. Replies were received from 86 of the 329 letters delivered --- a 26.1% response rate. Overall, approval was

received from 63 (73.3%) and rejection from 23 (26.7%).

A variety of comments were received from 36 of the 86 respondents. Of the 21 comments received accompanying the 63 favorable responses, 10 could be considered as conditional responses where acceptance would be contingent on further clarification. It is evident from the high percentage of respondents (41.2%) who took the time to write a comment that the system concept would become a much discussed issue in an area where implementation were to be proposed.

Other "concerned parties", in addition to the three user groups who must favor the concept, include numerous government agencies that monitor and oversee activities of the electric and water utilities. Through examination of plans, proposed practices, or existing operations, these agencies determine whether standards are violated and thus actively exert controls on implementation of new technology.

Professional organizations aid in the development and setting of standards of practice and performance. Activities in the form of meetings, conferences, and publications provide a forum whereby members evaluate the utility of new technology in light of organizational goals. Implementation of new technology is enhanced if it meets approval or doomed if it fails to.

3.2 Technological Problems

The use of heated water can cause problems downstream from the electrical utility. These can be grouped as problems associated with the water itself or in the conveyance system for the water. In the former category, the heating of water will cause increased rates of chemical and biological activity. For irreversible reactions this means that an increase in temperature will cause a final product to be formed in a shorter time span; for reversible reactions, temperatures influence both the time to reach equilibrium and the balance at equilibrium. Taste and odor producing substances are more noticeable due to increased solubility. Biological activity may double or triple over a 10°C temperature rise. Growth rates may be affected and the organisms which can survive at high temperatures may have wider distribution throughout the system.

Increased water temperatures in the conveyance systems can cause difficulty in areas where plastic pipe is used. The plastic pipe in common use in distribution systems has an upper temperature limit of 100°F because of its thermostability characteristics. Many points in a system could have temperatures greater than this. More thermostable plastics or other materials must be utilized when this concept is considered if maximum energy savings are to be gained. Moreover, plastic materials now normally utilized in water meters and other plumbing fixtures can be damaged by the use of warm water in the systems.

In normal distribution systems, the temperature regime of the ground and pipe change gradually over the year. The expansion of pipe materials and perhaps other phenomena associated with possible wide ranges in temperatures diurnally will need

further investigation.

4. ENVIRONMENTAL IMPACT ANALYSIS OF SYSTEM CONCEPT

It is recognized that a municipality contemplating the use of water outlined in this report is unlikely to become involved in the Environmental Impact Statement (EIS) process. However, it is also recognized that an examination of the environmental implications in an EIS format can be extremely beneficial in weighing the "pros and cons" of the proposal and other alternatives. The project staff, therefore, examined the environmental consequences of the proposed arrangement from an EIS perspective, incorporating both biophysical and socioeconomic environmental aspects.

Both positive and negative environmental impacts were found to accompany the implementation of the proposed system of using municipal water supplies, prior to treatment, as condenser cooling water. Some of the negative impacts have already been alluded to in the previous section on technological problems. On the whole, in this preliminary study the proposed concept was found to offer several positive benefits. Additional studies, however, would be necessary to substantiate these findings.

Most of the adverse impacts identified in the EIS phase may be avoided through the selection and control of the flow rate in the system, thereby controlling the temperature of the water entering the distribution system. If higher temperatures are desired in the system, avoidance of temperature sensitive materials (certain plastics) may be necessary.

Comparison of the proposed concept with other alternatives available to electric utilities showed that the proposed system eliminates many undesirable features of the others by incorporating energy recovery, multiple use of a valuable resource, and the elimination of thermal impacts to water ecosystems. Environmental gains will continue throughout the life of the project. Economic benefits will occur in the form of smaller energy charges for the consumer and reduced cost of power generation, pumping, and water treatment for the utility. Additionally, implementation of the proposed system would have definite, positive impacts on the irreversible and irretrievable commitment of energy and water resources. Since waste heat would be recovered, fuel consumption associated with domestic water heating would be reduced significantly.

5. CONCLUSIONS

The results of the study showed that the use of potable water supplies for cooling in a once-through system for thermal power generation prior to the treatment and distribution of water in a municipal system is both feasible and compatible in locations where cooling water supplies are limited, electric power needs are increasing, and municipal water flows are adequate. Decreased volumes of cooling water and simplified facilities for its management are possible in once-through systems when water temperatures at the condenser outlet are increased over those allowed when cooling water is returned to a water course.

The elevated water temperatures at the water treatment facility will increase the rates of chemical reactions, increase the solubility of chemicals used in treatment, and decrease the amounts of chemicals required to produce an acceptable level of treatment. These factors will reduce the operational costs for water treatment. The decreased viscosity of the warmer water will permit the utilization of smaller sedimentation units. This, in turn, will reduce the capital and amortization costs of water treatment facilities.

The amounts of energy received as heated water will depend on the location of the consumer in the system. In all seasons, however, the slope of the temperature profile is mild throughout the treatment plant and in the larger transmission and distribution mains. The water temperatures in a municipal treatment and distribution system where the concept was employed could be controlled by the water utilities through design and management of treatment and storage facilities. This would allow mitigation of unfavorable impacts caused by elevated water temperatures at the point of use.

Further research is needed to determine the impacts on materials currently utilized in water system facilities due both to elevated water temperature and to daily cycling of water temperatures between an elevated level caused by warm water flowing in the conduit and the lower extremes corresponding to the ground temperature. Additional work needs to be instigated to determine the effects on irrigating plants with warmer water. Moreover, a public education program must be developed for use in areas where implementation of the concept is contemplated.

ACKNOWLEDGMENTS

The research from which this report was derived was financed in part by Matching Grant No. 14-34-0001-9135 between the United States Department of the Interior, Office of Water Research and Technology and in part by Texas Tech University. Sincere appreciation is extended to these organizations, and their support is gratefully acknowledged. Special thanks go to Mrs. Raynell Keller and Dr. George Whetstone for their assistance in preparing this paper.

REFERENCES

1. Ramsey, R.H.; Bowersock, R.D.; Urban, L.V.; Strickland, J.H.: and Sweazy, R.M., Feasibility Study to Determine the Practicality of Using Potable Municipal Water Supplies as a Source of Condenser Cooling Water for Power Generating Facilities. Final Report to Office of Water Research and Technology, August 1980.

2. Hill, P.G., Power Generation. Cambridge: MIT Press, 1977.

3. Hand, J., Home Guide to Solar Heating and Cooling. New York: Book Division, Times Mirror Magazines, Inc. 1978.

4. Bailey, J.R.; Benoit, R.J.; Dodson, J.L.; Robb, J.M.; and Wallman, H. A Study of Flow Reduction and Treatment of

Wastewater from Households. Water Pollution Control Research Series; 11050FKE 12/69.

5. Anderson, B. Solar Energy, Fundamentals in Building Design. New York: McGraw Hill Book Company, 1977.

6. Jarmul, S. The Architect's Guide to Energy Conservation. New York: McGraw Hill, 1980.

RENOVATION AND REUSE OF COOLING TOWER BLOWDOWN USING WASTE-HEAT DISTILLATION

PB82-231408

D. M. Burkhart
Southern California Edison Company
Rosemead, California, 91770, U.S.A.

W. Chow
Electric Power Research Institute
Palo Alto, California, 94303, U.S.A.

H. H. Sephton
University of California, Berkeley
Berkeley, California, 94804, U.S.A.

ABSTRACT

Initial testing of a 190 m^3/day (50,000 gallon/day) prototype waste heat vertical tube foam evaporation plant for the renovation of cooling tower blowdown has been completed. Using turbine exhaust steam (40-55°C) as an evaporative heat source, about 98% of the blowdown was recovered as a distillate. The blowdown volume was thus reduced by about 50-fold and a distillate was produced which was of nearly boiler makeup quality.

1. INTRODUCTION

In the last decade, there has been a definite swing away from "once-through" cooling of steam-electric power plants to alternative cooling methods. This has been accelerated by environmental concerns over both water conservation and thermal pollution of the waterways. The current trend for power plant cooling system design now favors evaporative cooling towers.

Unfortunately, the use of cooling towers has created its own list of problems; among them being the disposal of large volumes of saline waters, known as blowdown, and the consumption of fresh water.

Depending on the quality of the plant water supply, plant cooling towers typically can operate at cycles of concentration ranging between 2 and 10. As an example, neglecting drift losses, a tower operating at seven cycles of concentration creates a requirement to blowdown one-sixth of the tower's evaporation losses in order to maintain steady-state operation at that concentration. By 1985, forecasts for total volumetric blowdown for utility cooling towers within the United States project an excess of one billion gallons per day [1]. The disposal of this blowdown in some locales can be difficult from a regulatory and/or political standpoint in addition to being very expensive.

With predictions of water supply shortage in the arid Southwest and some other sections of the country as early as 1990, uses of fresh water have become competitive and politically

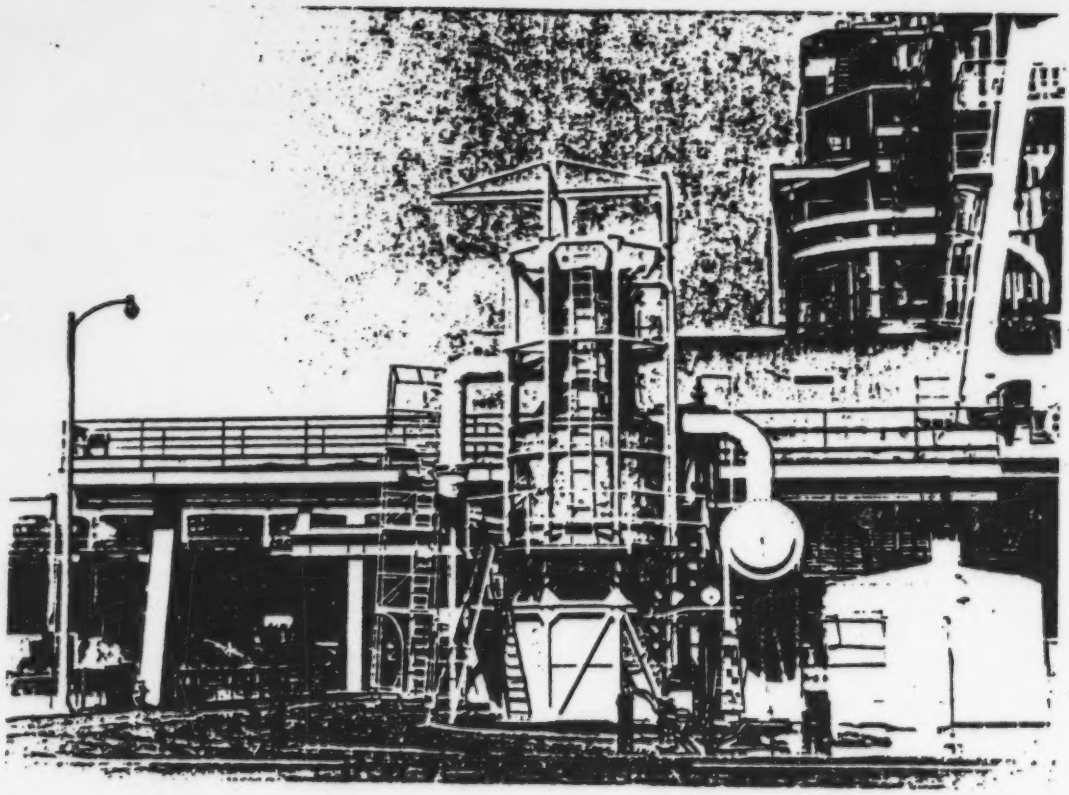

Figure 1. WH-VTFE plant is shown adjacent to the Unit 4 condenser and steam turbine at the Etiwanda Generating Station.

sensitive. This creates a situation where water for power plants becomes less available and more expensive to obtain. Eventually, increasingly severe conditions will compel utilities to less feasible and more costly alternatives which may include procuring agricultural lands simply for their water rights.

However, the development of a new technology gives promise of an economical solution to these two problems [2]. The technology discussed here, Waste Heat Vertical Tube Foam Evaporation (WH-VTFE), reduces the volume of blowdown to approximately one-fiftieth of its original while recovering 98% of the blowdown as a high quality, reusable distillate.

Testing of this process has been underway for more than a year at the Southern California Edison Company's (SCE) 330 MWe Etiwanda Generating Station Unit 4. The installed test plant is seen in Figure 1. The test plant, a 190 m^3/day (50,000 gallon/day) prototype, is being tested under the sponsorship of the Electric Power Research Institute, U.S. Environmental Protection Agency, Office of Water Research and Technology, Envirotech Corporation, and SCE.

2. PROCESS DESCRIPTION

The actual process for WH-VTFE is very simple as can be

seen in Figure 2. The blowdown is injected into the continuously circulating evaporator feed. The blowdown is heated and a portion evaporated as it passes through the vertical tube foam evaporator (VTFE) tubes. The vapor is removed and condensed and is then available for reuse by the station. The remaining blowdown is recirculated except for a small portion (less than 10%) which is removed in order to control the level of concentration. This stream is then injected into the smaller evaporator-crystallizer (EC) for final concentration. The decision to use two stages of evaporation is a function of the degree of concentration required and is purely economic. All concentration could be achieved in one stage, but because the boiling point is elevated as the brine is concentrated, it becomes more economical to use an additional stage at high concentrations.

The heat for evaporation is provided by turbine exhaust steam, hence the term "waste heat." After the steam is condensed in the evaporator, the condensate is returned to the steam turbine condenser. Heat transfer on the steamside of the evaporator tubes is enhanced by the use of double-fluted tubes having a steam condensation coefficient about five times greater than that of a smooth tube.

On the blowdown (brine) side the evaporation coefficient is increased by a factor of four to six by the introduction of a foamy flow regime. Foamy flow refers to the addition of a few parts per million of a surfactant (detergent) to the

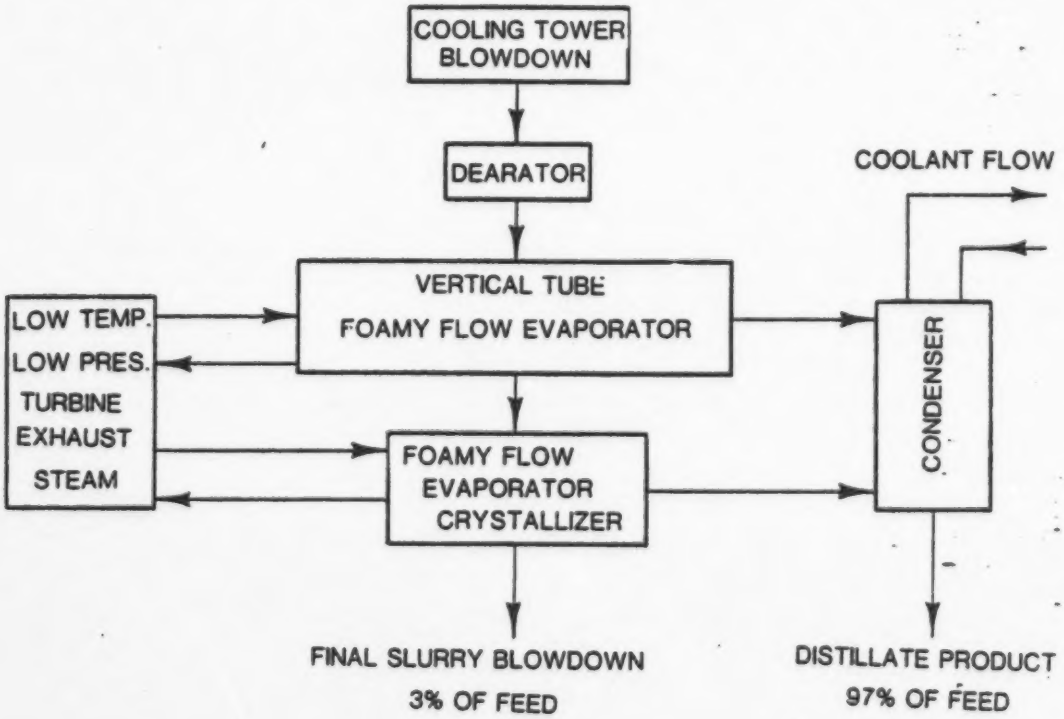

Figure 2. Simplified flow diagram illustrates the WH-VTFE process.

evaporator feed to act as a foaming agent and dispersant. The foamy flow through the tubes provides a thin-film, a wiped film or an agitated thin-film mechanism which increases the local heat transfer coefficient from the tube wall to the liquid phase. Simply, the foamy bubbles passing through the tubes continually wipe the surface of the tubes clean, allowing the surface to be constantly replenished with a fresh supply of liquid. The enhanced heat transfer permits the economic use of the low grade heat (40-55°C) available from the turbine exhaust.

3. INSTALLATION OF TEST FACILITY

One of the interesting aspects of this test was the actual integration of the test facility with the generating station. The location of the facility was, to a degree, fortuitous with all required hook-ups (steam, water, electrical) being located within 100 feet. The main concern with the installation was protection of the generating station from upsets due to the test facility.

Because steam is taken from the main condenser, loss of vacuum was the major concern. To defend against this, three protective measures were taken. First, the steam valve from the main condenser to the evaporator is controlled from the Unit 4 control room, allowing the operators to insure the integrity of the system before opening the valve. The other two protective measures are designed to either prevent the steam valve from opening or close it immediately. One is a differential pressure

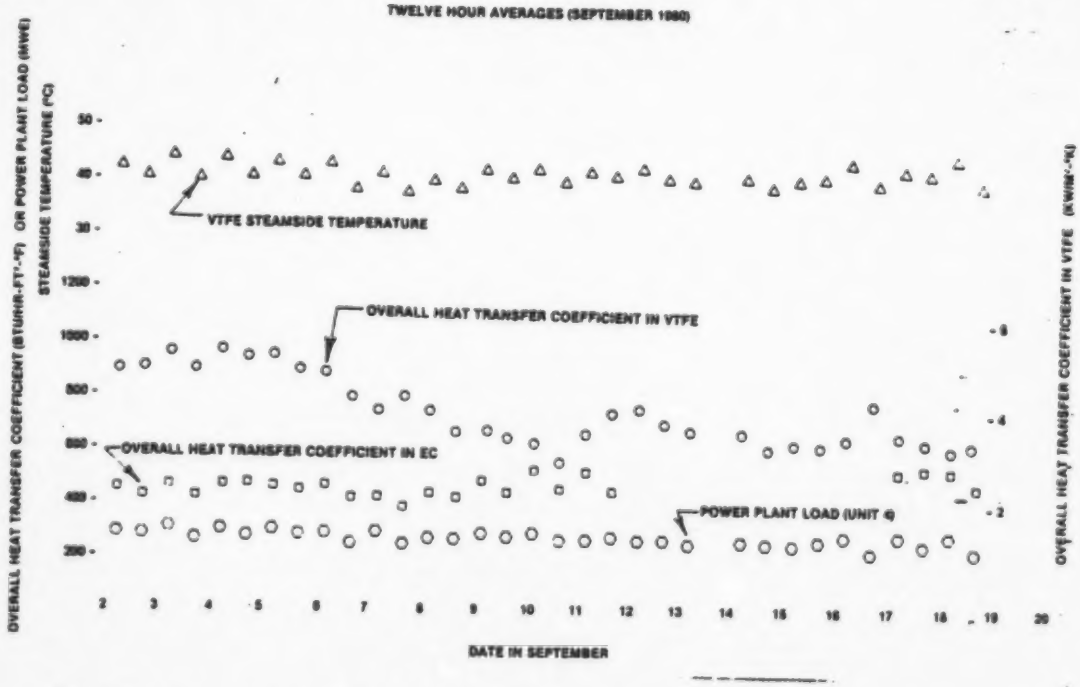
TWELVE HOUR AVERAGES (SEPTEMBER 1980)
OVERALL HEAT TRANSFER COEFFICIENT (BTU/HR-FT²-°F) OR POWER PLANT LOAD (MWE)
STEAMSIDE TEMPERATURE (°C)
OVERALL HEAT TRANSFER COEFFICIENT IN VTFE (KW/M²-°K)
VTFE STEAMSIDE TEMPERATURE
OVERALL HEAT TRANSFER COEFFICIENT IN VTFE
OVERALL HEAT TRANSFER COEFFICIENT IN EC
POWER PLANT LOAD (UNIT 4)
DATE IN SEPTEMBER

Figure 3. Data obtained during the first continuous operation test.

switch which indicates reverse flow in the steam line (catastrophic failure of the evaporator), and the other is a pressure switch set to trip on a sudden rise of condenser pressure.

4. DISCUSSION OF TEST

Following initial start-up, shakedown testing, and parametric testing of the plant, a continuous operation test of 400 hours duration was completed. During that test, a marked reduction in heat transfer performance of the main vertical tube foam evaporator (VTFE) was observed (see Figure 3).

During subsequent examination, it was found that obstruction of the feed distribution orifices, caused by wood slivers (cooling tower debris) and salt crystals, had occurred. The maldistribution of the feed created a situation where some tubes were starved for flow and ran dry, with calcium sulfate scaling in the VTFE and silica deposits in the EC as the result. To mitigate this problem, after cleaning the tubes, a stainless steel wire mesh screen was installed over the orifice plate above the VTFE distillation tube bundle.

Following this, the plant resumed continuous operation testing. Figure 4 shows the test data obtained over a 21-day period in summary form. All the significant data obtained during this period were averaged to provide the 12-hour-averaged data plots shown. Actually, test data were taken every 30 minutes, so that each plotted point represents the average value from about 24 individual test results. Data were thus

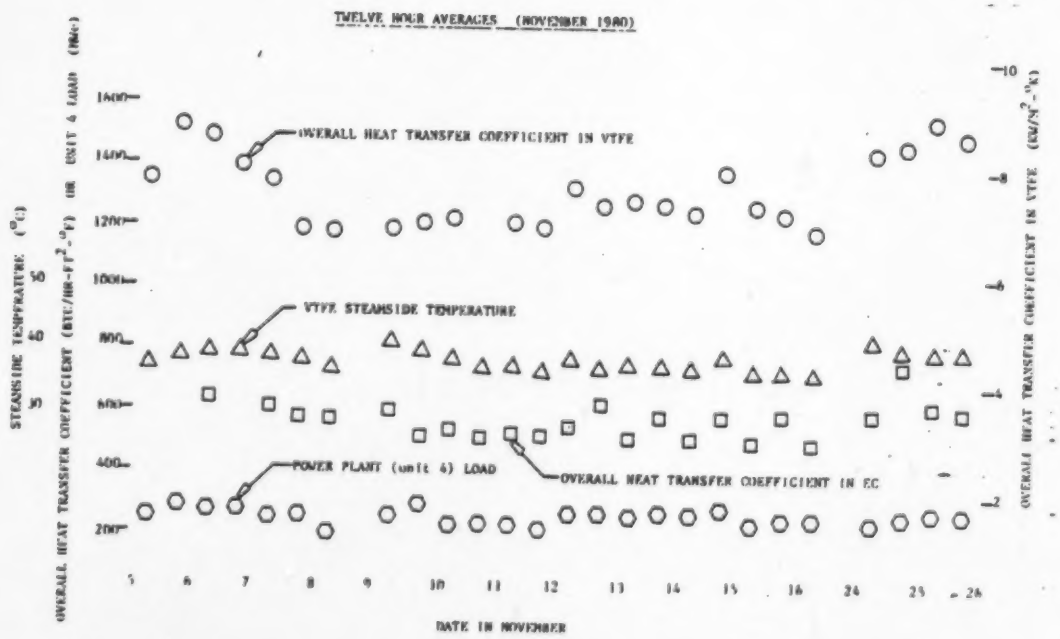
TWELVE HOUR AVERAGES (NOVEMBER 1980)
OVERALL HEAT TRANSFER COEFFICIENT IN VTFE
VTFE STEAMSIDE TEMPERATURE
POWER PLANT (unit 6) LOAD
OVERALL HEAT TRANSFER COEFFICIENT IN EC
DATE IN NOVEMBER

Figure 4. Data obtained during the second continuous operation test.

plotted for the averaged VTFE and EC heat transfer performances, the steamside temperature (turbine exhaust steam) and the power (MWe) production for Unit 4 of the Etiwanda Generating Station. The latter was rather unsteady during this test period due to a problem with steam control to the turbine of Unit 4; this problem finally necessitated a shutdown of this unit for about a week for repairs. The WH-VTFE facility was maintained on standby operation during this time to resume full operation as soon as turbine exhaust steam would become available. Full vacuum and recirculation of the VTFE and EC brine slurries were maintained at all times. In a similar manner, the WH-VTFE facility remained in operation during the daily and weekly cycling typical of most power plants as they respond to the changing demand for power by industrial and residential customers.

Performance of the WH-VTFE plant was completely successful during this follow-on test phase. About 98% of the blowdown was recovered as a distilled water having total dissolved solids (TDS) of about 5 mg/l, with the residual slurry having a TDS of about 220,000 mg/l. The heat transfer coefficient of the VTFE, in which 92 – 97% of the evaporation occurred, ranged between 5700 to 9100 Watts/m^2-°C (1000-1600 Btu/hr-ft^2-°F) in proportion to the turbine exhaust temperature. The EC heat transfer coefficient ranged between 2800 and 3400 Watts/m^2-°C (500-600 Btu/hr-ft^2-°F) due to the elevated boiling point of the saturated brine from which sodium sulfate and sodium chloride crystallized continuously during evaporation.

It is apparent from the averaged data plotted in Figure 4, that the heat transfer performance level depended upon the

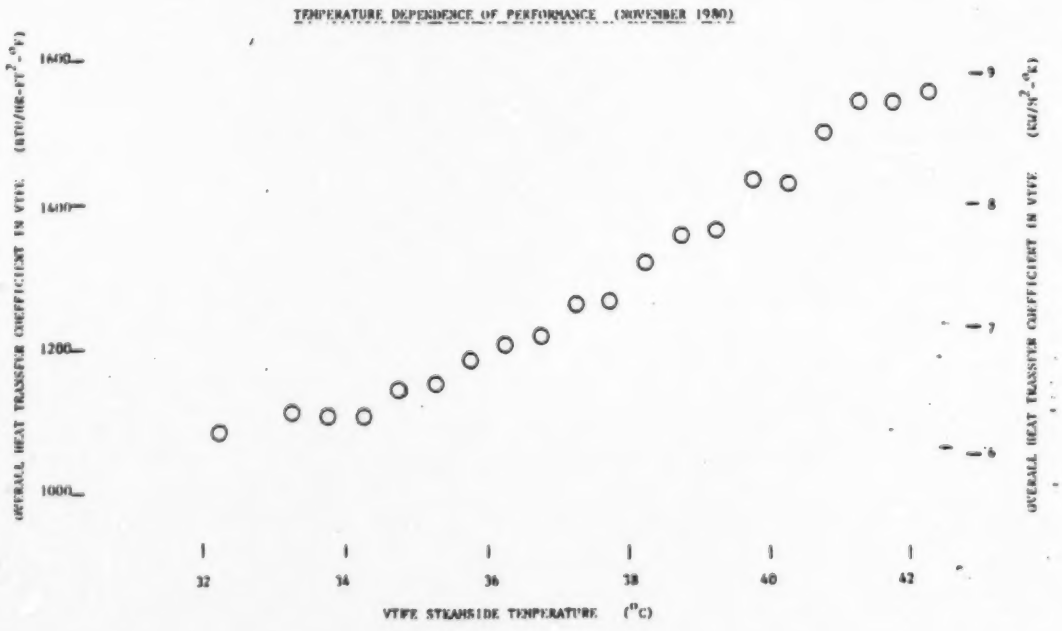

Figure 5. Plot of data demonstrating dependence of VTFE heat transfer performance upon steamside temperature.

steamside temperature and the power plant load (MWe). This relationship was more clearly shown in Figure 5 by plotting the averaged VTFE performance as a function of the steamside temperature for this entire test period. A proportional relationship is clearly shown, nearly linear for steamside temperatures above 34°C. This relationship underscores one advantage of enhancement of the heat transfer performance by induced foamy flow or VTFE. The higher steamside temperatures provide increases in ΔT and higher heat fluxes which in turn improve or intensify foaminess which increases the VTFE coefficient, U. In typical non-foamy vertical tube evaporators the U-value tends to diminish at increased ΔT-values [3].

No degradation of heat transfer performance was noted during this test and, at its completion, the tubes were again examined for scaling. The tubes were found clean except for a fine powder residue which was easily wiped off.

5. CONCLUSION

Several conclusions may be drawn from the results of the initial testing:

1. Adequate temperature differences exist within the heat rejection system of a steam-electric power plant to drive a WH-VTFE process.

2. A valuable distillate is recoverable from a power plant waste product (blowdown), thus reducing environmental impact and conserving water.

3. Blowdown volume may be reduced as much as 50-fold through the use of WH-VTFE. This has great significance when zero discharge is a consideration.

Based on these encouraging results, a six-month continuous operation test is being planned to prove out the long-term operability of the process.

REFERENCES

1. Fluor Engineers, Desalting Plans and Progress: An Evaluation tion of the State-of-the-Art and Future Research and Development Requirements, Office of Water Research and Technology, Jan. 1978.

2. H. H. Sephton, Desalination by Vertical Tube Foam Evaporation Utilizing Power Plant Waste Heat, Proc. of the Seventh International Symposium on Fresh Water from the Sea, Vol. 1, pp. 263-271, 1980.

3. R. P. Hammond, L. G. Alexander, H. W. Hoffman, Oakridge National Laboratories, Performance Characteristics of Advanced Evaporator Tubes for Long-Tube Vertical Evaporators, Office of Saline Waters, R&D Progress Report #644, Jan. 1971.

PB82-228511

WASTE-HEAT DESALINATION OF SEAWATER FOR BOILER FEED

H. H. Sephton
Envirotech-Sephton Development Center
Emeryville, California, U.S.A.

S. J. Senatore
EBASCO
New York, N. Y., U.S.A.

ABSTRACT

A novel evaporation process has been developed during the past decade that provides a substantial increase in the productivity rate (capacity) of vertical tube evaporators. This process, vertical tube foam evaporation, has been well defined in a series of pilot plants and has been field demonstrated at a power plant site for the desalination of cooling tower blowdown. The energy for evaporation used in this demonstration was turbine exhaust steam, of essentially zero value. Based on this demonstration a design and cost estimates have been prepared for using waste-heat desalination to convert seawater into boiler feed. This waste-heat vertical tube foam evaporation (WH-VTFE) plant had a design capacity of 151 cubic meters (40,000 U.S. gallons) per day of distillate. Since this evaporation plant augments the capacity of the power plant condenser it improves the turbine efficiency and provides a saving in fuel.

1. INTRODUCTION

The vertical tube foam evaporation (VTFE) development during the past decade responds well to the continued increase in fuel costs. It provides enhanced evaporation rates to either reduce the capital cost of evaporation equipment or the energy required for this process; consequently, it provides increased flexibility for an optimization of overall or annual cost savings. The power plant exhaust steam has essentially zero value; as used here in conjunction with VTFE, this provides for substantial savings in annual costs. In this application, the evaporator performs a service to the power plant by acting as a final condenser. The turbine exhaust condensate is returned to the power plant after evaporating a comparable amount of seawater in the VTFE. This new vapor is condensed into fresh water of high quality in a surface type condenser cooled with seawater and similar to but smaller than the power plant condenser.

A waste-heat vertical tube foam evaporation (WH-VTFE) plant was designed and its costs estimated based on two recently proven developments (1,2,3):

a. Vertical tube foam evaporation (VTFE) of seawater

into distilled water at low temperatures.

b. The field operation of a WH-VTFE prototype plant of 151 m^3 (50,000 U.S. gpd) capacity at the Southern California Edison power plant site at Etiwanda, utilizing turbine exhaust steam as the only energy to drive the evaporation process, converting 97% of the cooling tower blowdown feed to useful distilled water and a slurried-salt residue of 3%, with heat rejection to the power plant coolant.

These demonstrations opened up a new opportunity for low-cost desalting of both seawater and industrial wastewater at power plant sites. The only energy requirements of the WH-VTFE process is to pump liquids and for deaeration, at approximately 10 kWh per 1000 gallons of product. This compares with the 50 to 90 kWh/1000g required by alternative processes. Moreover, the WH-VTFE plant would provide high-quality water of about 5mg/liter (5 ppm) of total dissolved solids (TDS). This would reduce the cost of ion-exchange polishing to provide boiler-feed quality water significantly.

Another potential saving provided by the WH-VTFE process results from the fact that the power plant turbine exhaust pressure is thereby reduced. This is the consequence of the additional condensation area provided by the VTFE condenser. The increase in turbine efficiency thus provided can reduce fuel consumption substantially. It was estimated that this 151 m^3 per day WH-VTFE plant would reduce the fuel consumption of a 37 MWe coastal power plant by $40,000 to $80,000 per year, based on literature data (4). This potential saving could approximate the capital cost of the evaporation plant when capitalized over the life of this plant.

2. WH-VTFE PROCESS ASPECTS

2.1. Fow Diagram

A simplified flow diagram for this proposed facility is shown in Figure 1; this includes a vacuum deaerator, a downflow VTFE and its condenser as the main components. The feed for the WH-VTFE plant is taken from the heated seawater coolant, and the concentrated blowdown brine would be returned to this flow for remixing and rejection to the ocean. The feed is acidified for decarbonation and is deaerated by cascading it over a packed bed inside an evacuated vessel. The deaerated feed is pumped into the VTFE recycle brine. This brine is maintained at constant salinity and volume by means of a conductivity monitor and a level controller, and is continuously recycled to the top of the VTFE unit for distribution to the distillation tube bundle through an orifice plate. Chemical additions to this brine include measured flows of a surfactant (foaming agent) and an oxygen scavenger (sodium sulfite). An anti-foaming agent may be added to the blowdown or the foaming agent may be recovered by foam flotation (5) for recycle into the VTFE brine. The VTFE vapor is condensed in the seawater-cooled condenser maintained under full vacuum. The distillate is pumped out to atmospheric

pressure, and its flowrate and quality (conductivity) monitored. Turbine exhaust steam is condensed under vacuum on the shell-side of the VTFE tube bundle; its quality and flowrate are monitored and it is then returned to the power plant condenser hotwell.

The turbine exhaust pressure is reduced because of the condensation of some (6 to 10 percent) exhaust steam in the VTFE bundle that is maintained at a pressure lower or equal to that of the power plant condenser. The power plant condensation area for turbine exhaust steam is thus enlarged by the VTFE. The condenser of the VTFE facility is operated at a pressure lower than that of the power plant condenser.

2.2. Feed Pretreatment

The feed for the evaporation plant is to be taken from the power plant coolant blowdown flume: Seawater having a temperature of about 95°F and an H_2S content of up to about 10 ppm would be adjusted to a pH of about 4.5 by the automatic addition of sulfuric acid. Hydrogen peroxide would be added in 100% excess of the H_2S content and the feed retained in a fiberglass vessel for 15 minutes to permit oxidation to elemental sulfur precipitates, to be removed by filtration. The excess H_2O_2, air, oxygen and non-condensible gases are then to be removed in a vacuum deaerator vessel as the feed cascades downward over a packed bed. The pH of the deaerated feed would be automatically adjusted by the addition of NaOH to a pH of 6.8. The addition

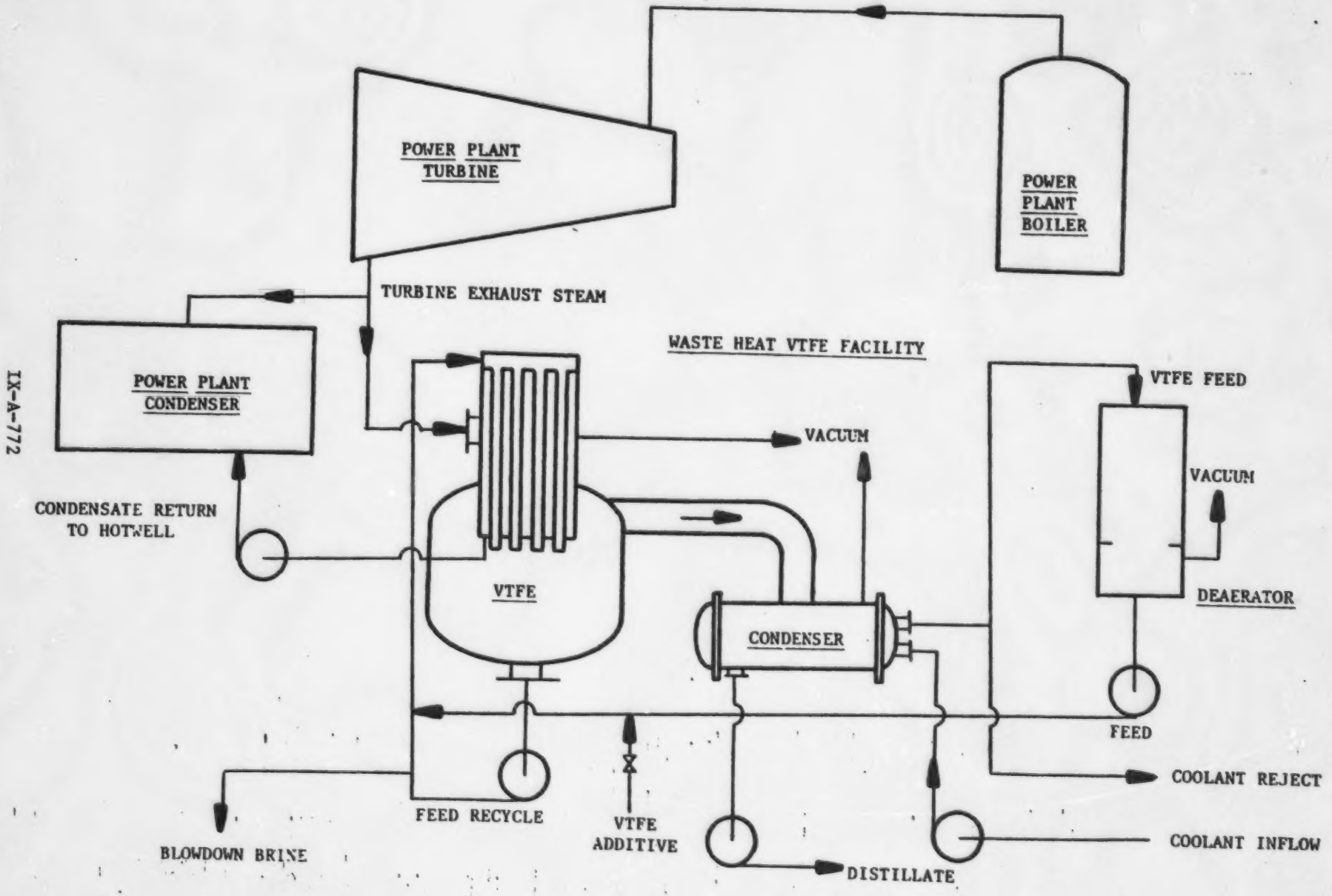

IX-A-772

FIGURE 1: FLOW DIAGRAM FOR WASTE-HEAT VERTICAL TUBE FOAM EVAPORATION OF SEAWATER

of an oxygen scavenger (Na_2SO_3) and surfactant at a concentration of about 50 ppm would complete the pretreatment of the feed.

2.3. General Design Criteria

The process conditions for the purpose of the WH-VTFE design were as follows:

a. Turbine exhaust steam temperature to be 115°F, at saturation, free of non-condensibles and foreign materials.

b. Seawater coolant available at 78°F and 5 psig at 4000 gpm.

c. Plant coolant seawater available at 95°F, for use as VTFE feed.

d. Electrical power for operating pumps, instruments, controls and lighting.

e. Product flowrate to be 40,000 gpd and of a quality not to exceed 10 ppm (mg/liter) of total dissolved solids.

f. WH-VTFE blowdown and coolant to be discharged to the existing power plant coolant discharge flume.

g. Plant design to include all feed pretreatment facilities needed.

2.4. WH-VTFE Process

The objective of the VTFE process is to evaporate the liquid from a foamy annular layer flowing over a heat transfer surface, with the vapor released flowing as a separate phase over the foamy layer and in shear-flow interaction with it. This mechanism can provide up to a sixfold enhancement of the local heat transfer coefficient at the brine-side tube surface (1,6). As a consequence, the overall heat transfer coefficient, or the evaporator productivity rate (capacity) is substantially increased. The temperature driving force for evaporation (ΔT) can therefore by much lower than in conventional vertical tube evaporation (VTE). Consequently, a significant part of the turbine exhaust flow (waste-heat) from at least some pre-existing power plants could be utilized for desalting before its rejection to the coolant. In the case of future power plants, the feasibility of producing substantial quantities of distilled water is apparent; the condensation of turbine exhaust steam in VTFE condensers would replace part of, or augment the usual water-cooled condenser capacity and provide desalination at apparently reasonable cost. As an alternative to a surface condenser for distillate production, a barometric condenser may be used; in this case the vapor produced by WH-VTFE is directly condensed into the power plant coolant and dilutes it.

3. WH-VTFE DESIGN

3.1. Interface with the Power Plant

The integrity and performance of the power plant low pressure turbine and condenser has to remain unimpaired by the WH-VTFE with adequate failsafe precautions. This condition was met by providing a special, vacuum-tight butterfly valve for waste steam flow, with automatic control and provision for override or shut-down from the power plant control room. This valve would be shut tight automatically if at any time the pressure in the VTFE shell-side would not be lower than the pressure in the power plant condenser by a margin preset on a differential pressure monitor. It could also be shut tightly within thirty seconds by throwing an electrical contact in the control room. This control system was also used satisfactorily at Etiwanda. The VTFE facility would automatically adjust to any alteration in or shutdown of waste steam flow. A 0.91 m (36-inch) butterfly valve incorporating a spherical disc seal, actuated eccentrically by pivoting around an offset shaft and providing a non-wearing continuous-contact circle when closed, was used (Jamesbury, Wafer-Sphere valve) for waste steam control.

3.2. Design of the WH-VTFE and Condenser

The design of this plant is similar to that of the existing prototype plant now operating on cooling tower blowdown at the Southern California Edison Company power plant near San Bernardino, and reported in the preceding paper at this Conference. Several papers have been published on the design and operation of the prototype plant (2,3). The design of the WH-VTFE plant of 40,000 gpd capacity was based on the following criteria:

a. The design performance would be in excess of 40,000 gpd of distilled water of 5 ppm of TDS when the turbine exhaust steam is available at 115°F (15,000 pounds per hour) and coolant of 79°F at 3,000 gpm. The expected performance would be in excess of 60,000 gpd of distilled water with steam at 120°F (22,000 lb/hr) and coolant at 4500 gpm. The product water quality should be better than 10 ppm of TDS.

b. The construction materials to be used are consistent with best practice: Stainless steels (Types 316L and 304L) are used in brine-contact areas and for the main liquid-transfer pumps and brine transfer pipes, a fiberglass-epoxy pipe (0.5M dia.) is used for coolant transfer, a 1M stainless steel butterfly valve capable of vacuum-tight shut-down is used for steam control, and a similar 0.5M valve for coolant control.

c. Vertical tube evaporators for seawater distillation have been in use for many years in the Caribbean (St. Croix, St. Thomas), Netherlands and elsewhere. These are multieffect plants operating over a temperature range including a low of 120°F and a high of 220°F. Most of their operating problems have been related to corrosion/erosion and scaling in the high temperature effects. The present design is for a low-temperature, single-effect system that has been successfully demonstrated recently with a system closely similar to this

design operated under the more challenging process conditions of scale-free operation with seed-slurry evaporation at much higher feed concentrations.

The WH-VTFE design coefficients used for this plant were conservative because it would have been the first commercial plant and it was designed while the field test program at Etiwanda was still in an early phase. It is now apparent that carbon steel vessels should be considered in view of the very low corrosion rates observed at Etiwanda; in addition, the design performance could be 50 percent higher than those used in the present plant, to provide significant reduction in heat exchanger tube cost.

The prototype WH-VTFE plant is shown in Figure 2 as it is presently being demonstrated at the Southern California Edison (SCE) power plant site at Etiwanda. Several papers have been published on the design of this plant and on estensive distillation tests conducted with it in Richmond, California, using seawater as feed (2,3). The present design was based directly on this prototype and on these tests as well as extensive earlier development work of VTFE for seawater distillation (6). The total capital cost of all equipment items for the 151 m^3 WH-VTFE plant for seawater conversion amounted to $650,000. An additional $100,000 is estimated as the cost of site work and erection including startup.

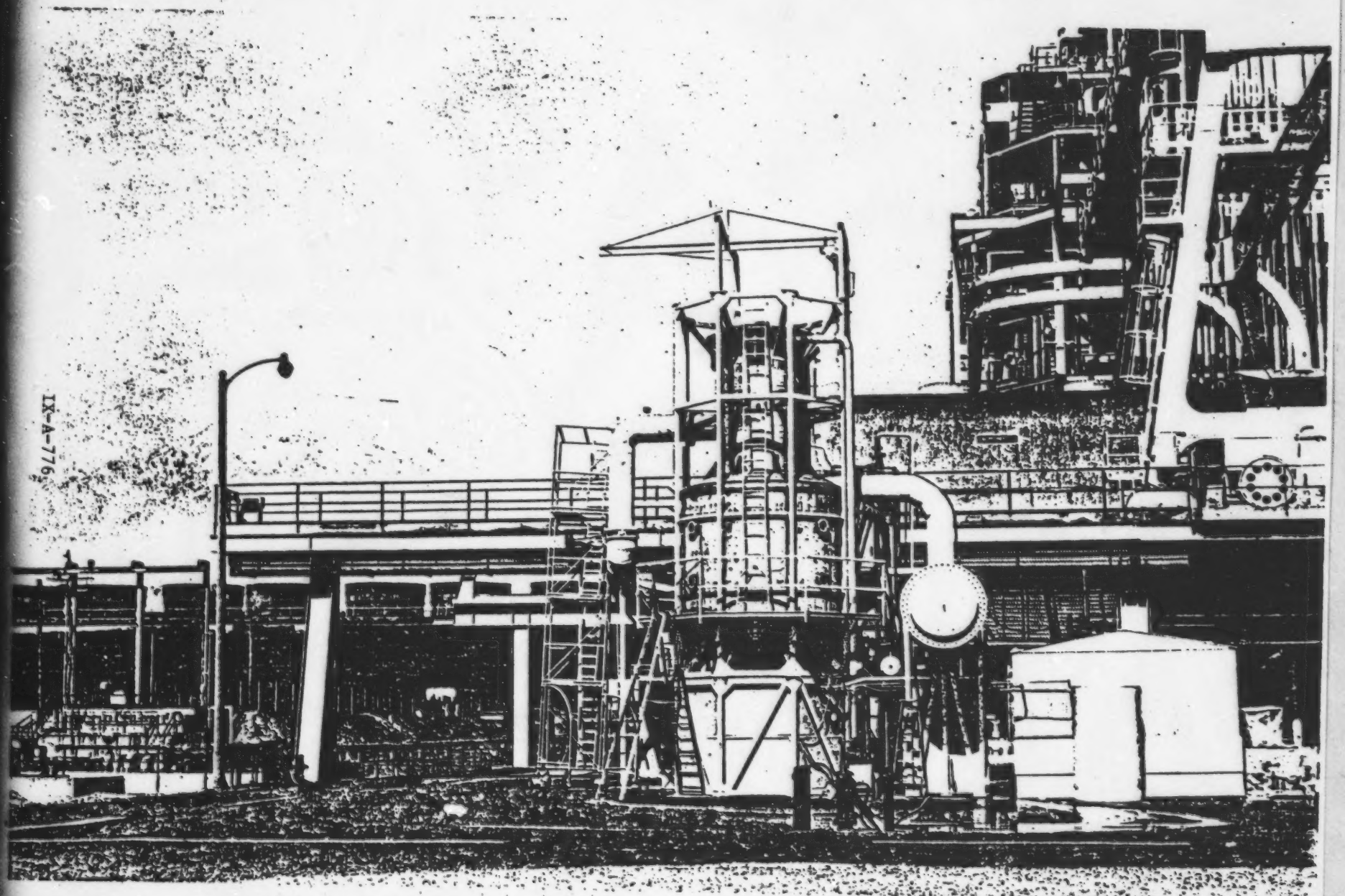

FIGURE 2: PROTOTYPE WASTE-HEAT VERTICAL TUBE FOAM EVAPORATOR AT SCE POWER PLANT

4. DISCUSSION

This 151 m^3 (40,000 U.S. gpd) WH-VTFE facility was designed for retrofitting to a 37 MWe thermal power plant to provide distillate for boiler feed after ion exchange polishing, using seawater contaminated with hydrogen sulfide as feed. This facility would utilize about 6 percent of the turbine exhaust steam (WH) to drive the evaporation process, improving the turbine efficiency significantly. A complete design and cost estimation were carried out, based on data and information obtained with the closely similar prototype shown in Figure 2.

The WH-VTFE concept appears promising and responsive to the continued increase in the cost of fuel. Power plant exhaust steam as used in this facility has an esentially zero value. The foamy flow evaporator (VTFE) provides an enhanced heat transfer performance during evaporation of the seawater feed during downflow through vertical distillation tubes as a foamy layer. This mode of flow is imposed after the addition of about 30 mg of a selected surfactant per liter of seawater feed, and by the process conditions applied. The overall heat transfer coefficient of evaporation is thereby maintained above 6800 W per m^2-^oC (1200 Btu per hr-ft^2-^oF), about 50 percent higher than in conventional VTE (3). The VTFE process thus provides a relatively high evaporation rate, even at waste-heat temperatures and with low-energy driving forces (ΔT). In addition, the surfactant additive provides a significant advantage as a dispersant, helping to keep the evaporator surfaces clean. The additive used is biodegradable and recyclable, and is selected from commonly used industrial surfactants.

The capital cost (without contingency and fees) of this WH-VTFE facility was estimated at $750,000. Based on a capital recovery factor of 8.88% (8% for 30 yrs.) the capital and operating costs would be $81,600 per year. Assuming a water production rate of 14.6 million gallons per year and an annual operating and maintenance of 2% of the plant capital cost, the cost of water without energy charge is $1.48 per m^3 ($5.6 per 1000 gals.). The calculated water cost for larger plants of this type, based on an equipment size/cost exponent of 0.6 to 0.75, ranged downward to between $0.26 to $0.53 per m^3 ($1 to $2 per 1000 gals.) for a WH-VTFE plant of 11,325 m^3 ($3x10^6$gals.) per day capacity.

5. CONCLUSIONS

It is apparent that the WH-VTFE should provide a competitive alternative for producing distilled water or boiler feed from seawater at coastal base-loaded power plant sites that have a high availability factor.

6. ACKNOWLEDGEMENTS

The design and construction of the prototype plant was sponsored by a grant from the Environmental Protection Agency. The test operations with this WH-VTFE facility were co-sponsored

by the Electric Power Research Institute, the U.S. Office of Water Research and Technology, the Southern California Edison Company and Envirotech Corporation.

The authors are especially indebted to their colleagues at ESDC and EBASCO for assistance with the design and cost calculations.

REFERENCES

1. H. H. Sephton, Interface Enhancement Applied to Evaporation of Liquids, U. S. Patent No. 3,846,254, and corresponding foreign patents, 1974.

2. H. H. Sephton, Vertical Tube Evaporation for Fresh Water Production Using Power Plant Waste Heat, Desalination, vol. 31, pp. 187-195, 1979.

3. H. H. Sephton, Desalination by Vertical Tube Foam Evaporation Utilizing Power Plant Waste Heat, Proceedings of the International Symposium on Fresh Water from the Sea, vol. 1, pp. 262-271, 1980.

4. L. S. Marks, Mechanical Engineers' Handbook, 8th Edition, pp. 9-52, McGraw-Hill, New York, 1978.

5. E. Valdes-Krieg, C. Judson King and H. H. Sephton, Removal of Surfactants and Particulate Matter from Seawater Desalination Blowdown Brines by Foam Fractionation, Desalination, vol. 16, pp. 39-53, 1975.

6. H. H. Sephton, New Developments in Vertical Tube Evaporation of Seawater, Proceedings of the Fifth International Symposium on Fresh Water from the Sea, vol. 2, pp. 279-287, 1976.

PB82-228529

IMMISCIBLE LIQUID CYCLE IN LARGE SCALE MEDIUM TEMPERATURE WASTE HEAT RECOVERY

Bryce M. Burnside
Visiting Professor
Mechanical and Aeronautical Engineering Department
Carleton University
Ottawa, Canada

ABSTRACT

Application of the immiscible liquid cycle to extraction of heat from waste gases at initial temperatures of 250-350°C is described. Between 5 and 18% more heat can be extracted by the cycle than the conventional steam cycle. The plant envisaged is simple and of conventional design and is capable of development to more efficient operation. Formulae are presented to enable designers to make a preliminary assessment of the cycle.

1: BACKGROUND

Political and economic considerations continue to dictate the efficient use of fuel and by the same token the utilisation of waste heat to the maximum possible advantage. With fuel costs rising faster than inflation in many countries it should be possible for designers to contemplate more elaborate plant while still maintaining traditional capital: running cost ratios. Waste heat takes many forms. This paper concentrates on the retrieval of heat from waste or exhaust gases. Many such sources exist particularly as prime mover exhausts or in chemical processes. There are a number of ways in which these waste heat sources can be used but attention here will be directed to upgrading to work by Rankine cycles.

If the temperature of the gaseous source is high enough the dual pressure steam cycle [1] with LP turbine steam admission permits very effective recuperation. For example a gas turbine exhaust at 513°C can be reduced to 110°C stack temperature at a cycle efficiency of about 31% using this cycle. At lower waste gas temperatures, however, the effectiveness of this cycle and of the simple Rankine cycle with superheat is reduced because of the combined effect of increased wetness in the LP stages of the turbine and the poor match of heated fluid to heating gas.

These facts are well known and the use of pure organic fluids [2] or miscible aqueous/organic systems [3] has been proposed to improve the efficiency of heat recovery. Such remedies probably represent the best thermodynamic solution to heat recovery from gases at moderate temperatures. However, there has been reluctance among manufacturers to adopt such schemes in large scale heat recovery partly because of doubts about fluid stability and external shaft sealing problems. The miscible Fluorinol 85 system [3] seems less subject to these objections than pure organic systems although a sealing problem remains.

The author [4] has pointed out that the use of aqueous organic systems, immiscible in the liquid phase reduces the shaft sealing problems to the same level as in conventional steam plants. Water and steam seals only may be used. Any change in the working fluid composition which results is easily rectified because of the immiscibility of organic liquid and water. Further, the very stable alkanes, which on their own have unsuitable thermodynamic properties, can be used. A number of immiscible liquid cycles can be devised [5], [6] to match heat extraction from gaseous heat sources. For example, high temperature open cycle gas turbine exhausts at over 500°C are better matched by the dual pressure steam/immiscible liquid cycle than by the conventional steam/steam dual pressure cycle [6]. This cycle uses steam only at the high temperature end and an immiscible liquid combination at the stack end where the matching to cooling exhaust gas is most important. Unlike arrangements suggested in the past this dual pressure cycle has no expensive closed heat exchanger between HP and LP sections. It is capable of operating at any top temperature suitable for the steam cycle with similar shaft sealing problems. In these respects it is superior to pure organic cycles or miscible liquid cycles in which the organic and steam are not readily separated.

At lower gas temperatures the simple immiscible liquid cycle with LP deaerator heater has an even greater advantage over the corresponding steam cycle [5] due to the very wet turbine expansion and poor matching of the latter cycle. For example 13% more work can be obtained from a gas stream at 350°C using the immiscible liquid cycle [5]. In the original concept the deaerator heater in this cycle was a liquid heater. In this paper the characteristics of the immiscible liquid cycle with LP boiler deaerator heater is investigated. Further, the possibility of reducing the condenser cooling water requirement by cooling the non-eutectic condensing section of the condenser with condensate is discussed.

2: NOMENCLATURE

A	turbine annulus area, m^2
h	specific enthalpy, kJ/kg
m	kg fluid/kg gas, boiler
M	kg fluid/kg gas, deaerator
q	dryness fraction deaerator inlet
Q_R	heat rejected, condenser, kW
t	temperature, °C
T	temperature, K
x	mass fraction boiler
y	mass fraction deaerator
Δt	pinch point temp. difference
η	efficiency

Subscripts

1-12	vapour cycle state points
A-X	gas states
c	condenser
d.pt.	dew point state
eut	eutectic
et	regenerator vapour exit
ew	eutectic steam
L.P.	low pressure
s,w	steam, water
wf	water fraction of liquid

3: THE CYCLE

The cycle and its matching diagram are shown in figures 1 and 2. From the

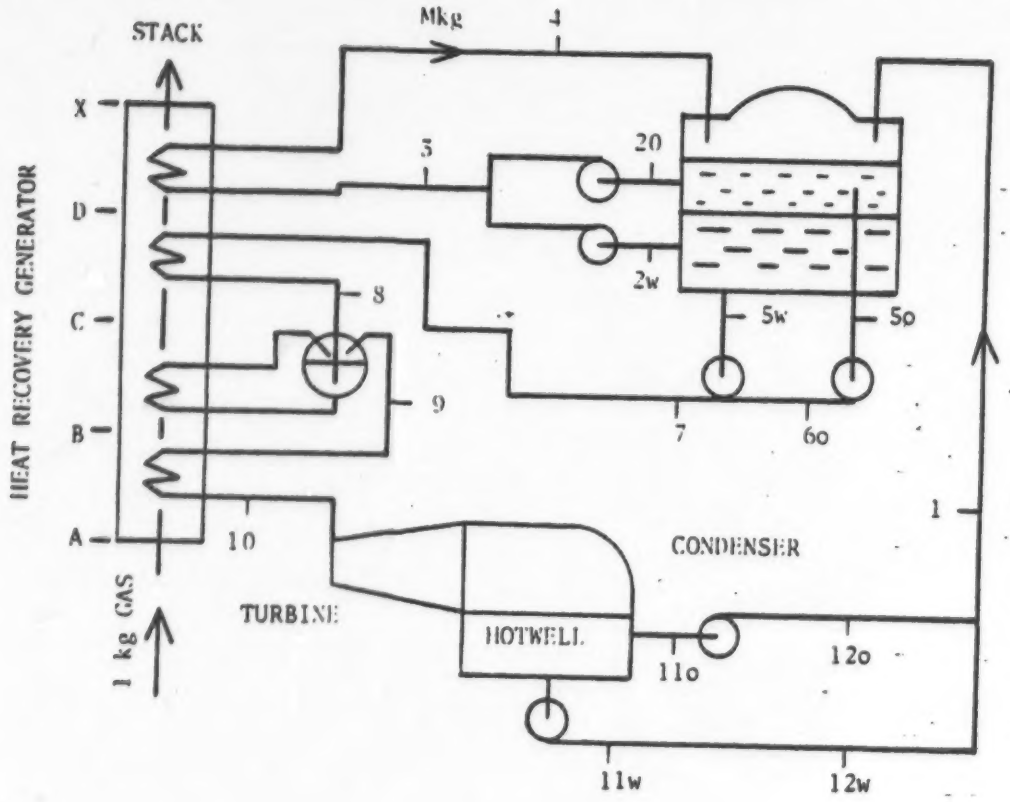

FIGURE 1

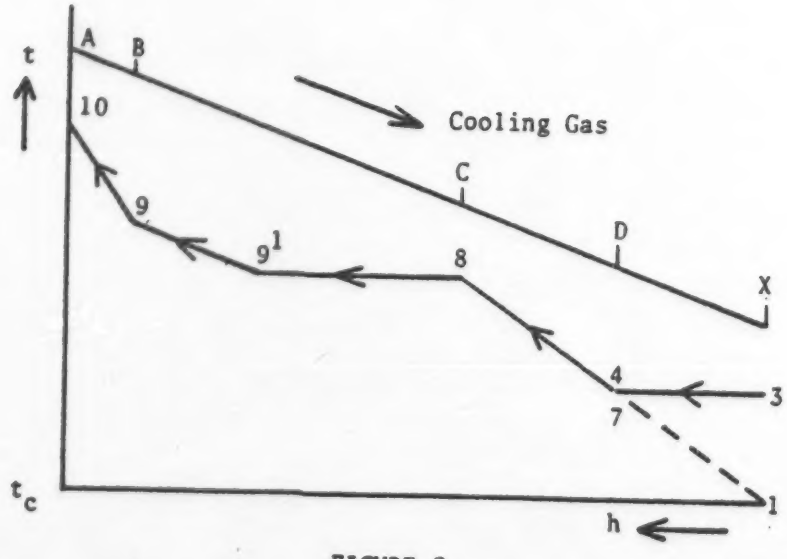

FIGURE 2

IX-A-781

deaerator the liquids are pumped in predetermined proportion, x_w, through the economiser, 7-8, before boiling, 8-9 and superheating, 9-10. The steam fraction of the mixed vapours expanding in the turbine is always high enough to ensure completely dry conditions. The upper limit is a compromise between good matching between working fluid and gas temperatures in the heaters and the eutectic composition which gives the lowest possible condensing temperature [7]. After condensation and liquid separation the liquids are returned to the deaerator where they are raised to the eutectic temperature by the condensation of eutectic vapour returning from the LP boiler, 4. The water fraction of the two phase liquid circulated through the LP section, 3, is y_w and the dryness fraction returning to the deaerator, 4, is q. The ratios of working fluid to gas flow in the HP and LP sections of the heat recovery generator are m and M respectively.

Organic pump external shaft seals are supplied with water from the water feed pump delivery. The turbine external seals are supplied with steam generated in an auxiliary circuit in the heat recovery generator from water originating in the drum or at the water pump delivery.

Pinch points in the cycle are at inlet to HP and LP boilers on the working fluid side, figure 2. Because of the requirement to maintain a reasonable level of water fraction, x_w in the HP circuit there is effectively only the one pinch point - in the HP section.

4: CYCLE ANALYSIS

4.1 Matching cycle to heating gas supply

General expressions for the relations between parameters of the cycle were obtained based on the following principle assumptions,

(i) No pressure drops in the heat exchangers.
(ii) All components other than the heat exchangers are adiabatic.
(iii) Circulating pump but not feed pump work is ignored.
(iv) Waste gas has constant specific heat (1.047 kJ/kgK).

The analysis and other assumptions are set out in appendix 1. The calculations, which involved a number of iterations, were handled by computer.

Assuming a deaerator pressure of 1 bar and a maximum fluid temperature of 250°C (t_{10}) all the parameters of the cycle were evaluated for the three binary systems, steam/nonane, steam/octane and steam/heptane for a range of HP pressures and for condenser temperatures 30-50°C. The HP pinch point temperature difference was set at 30K and the LP value at not less than 30K. The calculations were performed for entering gas temperatures between 250 and 350°C. Superheat temperature t_{10} was kept at least 50K below the gas temperature.

The constraints on cycle parameters are evident in figures 3 - 5. Figure 3 shows the relation between cycle pressure and L.P. pinch point temperature difference and steam mass fraction, x_w, for fixed gas inlet temperature and condenser temperature. At fixed Δt_{LP}, x_w rises steeply with falling p_H. There is advantage in operating at $x_w = x_{eut\ c}$, the eutectic mass fraction of steam at the condenser pressure. Then all the condensation takes place at the lowest possible cycle temperature and there is no diffusion resistance to mass transfer in the condenser. Also, x_w is not then much different from the eutectic value in the boiler which simplifies the boiling process although, in removing the section 8 - 9, figure 2, in that process it increases irreversibility of

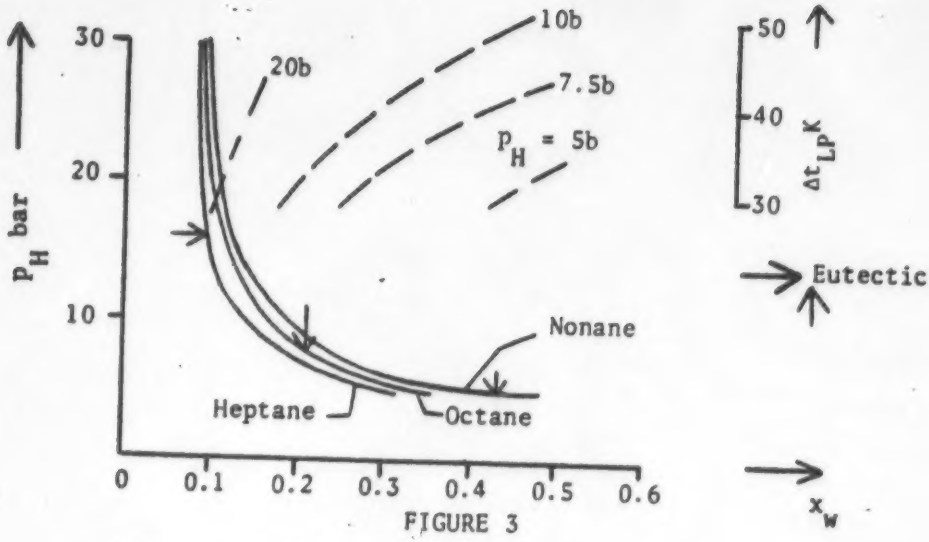

FIGURE 3

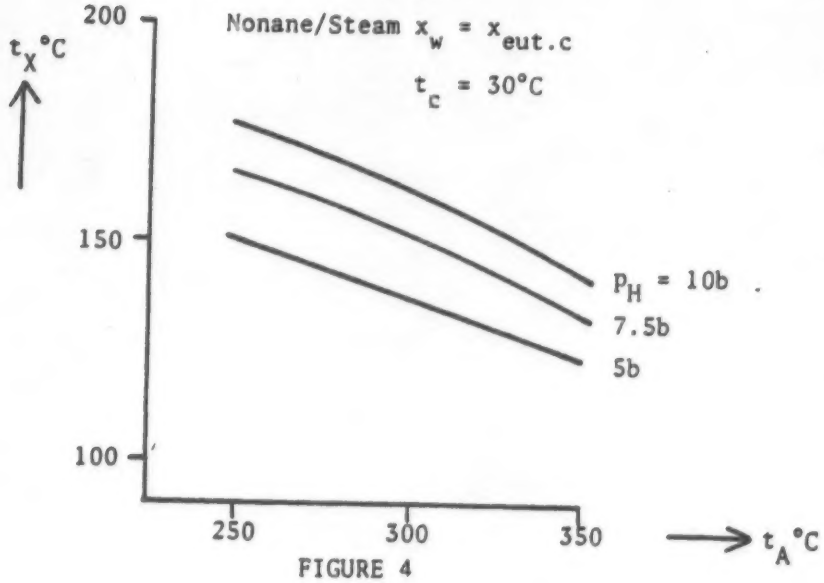

FIGURE 4

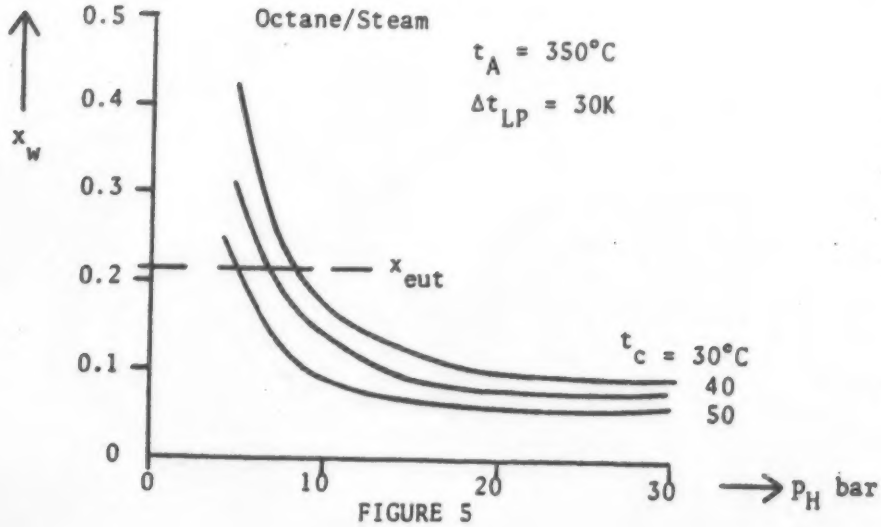

FIGURE 5

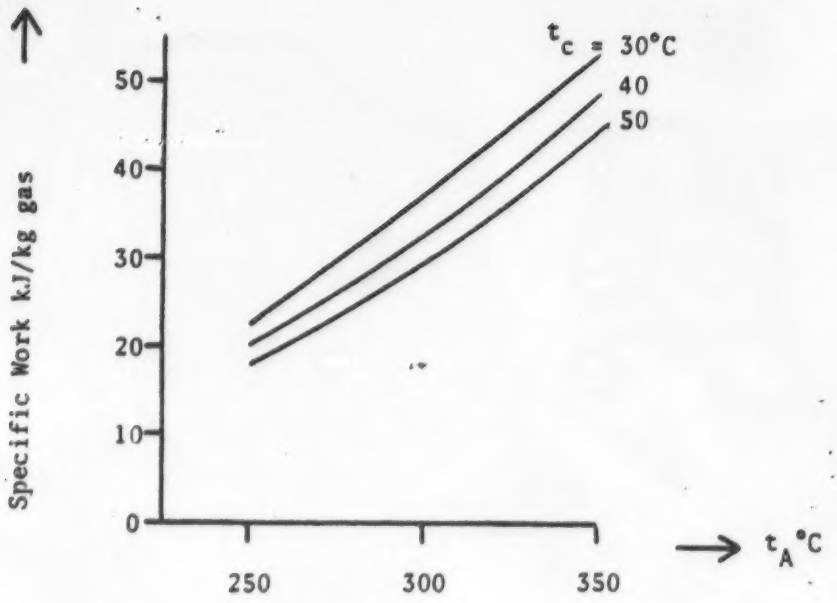

FIGURE 6

the boiling. The dashed curves in figure 3 show that an increase in Δt_{LP} permits the use of a higher boiler pressure at given x_w. Although this results in better HP matching it increases the stack temperature. A compromise is required here. It is also evident from figure 3 that because the eutectic mass fraction x_w decreases with decrease in organic molecular weight a higher boiler pressure is possible with steam/heptane than with steam/nonane. However, the slope of the dew line on the temperature - entropy diagram is also important - if the molecular weight of organic is too low a superheated turbine exhaust may result or the difference between dew point and eutectic temperatures in the condenser may be large [7].

Figure 4 shows the effect of gas inlet temperature, t_A, on stack temperature for three different boiler pressures and for $x_w = x_{eut\ c}$. The curves are drawn for the nonane/steam system. As expected the match is more difficult as t_A falls and the lower the pressure the lower the stack temperature. In figure 5 the effect of condensing temperature on the optimum cycle pressure, p_H, is shown for a fixed Δt_{LP}. The curves, which are drawn for the octane/steam system, show that a lower condenser temperature allows a higher boiler pressure for fixed x_w and in particular for $x_w = x_{eut\ c}$.

4.2 The turbine expansion

The above has been concerned with optimizing matching between gas and working fluid, in other words with maximising the fluid to gas ratio, m. Combining this with high turbine efficiency leads to the desired high specific work output. A principle advantage of the immiscible liquid cycle is the possibility of a completely dry turbine expansion. Thus there are no wetness losses which reduce considerably the efficiency of the steam turbine at these

conditions. The lower x_w the higher the molecular weight of the fluid and the drier the expansion. If the turbine exhaust condition is just dry at the eutectic condition, $x_w = x_{eut\ c}$, the optimum specific work per kg of gas will be obtained.

As an example table 1 shows the turbine exhaust conditions for steam/nonane with the eutectic compositions corresponding to condenser temperatures of 30 and 50°C - 43 and 41% steam respectively. Values are for two inlet pressures p_H = 5 and 10 bar each for the two inlet temperatures t_{10} = 250 and 200°C corresponding to gas supply temperature $t_A \geq 300$°C and $t_A < 300$°C respectively. The proportion of the expansion in the superheat region, $\Delta h_{dry}/\Delta h$, is satisfactory for the higher inlet temperature at both condenser temperatures but 8% and 16% of the expansion is in the wet region for t_{10} = 200°C at t_c = 50 and 30°C respectively. Further the exhaust is excessively superheated at t_{10} = 250°C

Condenser temperature 30°C				
t_{10} °C	250	250	200	200
p_H bar	10	5	10	5
$(\Delta h_{dry}/\Delta h)$%	100	100	84	97
$((h_{out} - h_{sat})/\Delta h)$%	4	18	-	-
Condenser temperature 50°C				
t_{10} °C	250	250	200	200
p_H bar	10	5	10	5
$(\Delta h_{dry}/\Delta h)$%	100	100	92	100
$((h_{out} - h_{sat})/\Delta h)$%	17	37	-	9

Table 1. Turbine expansions steam/nonane ($x_w = x_{eut\ c}$, η_s = 0.86)

especially at the higher condenser pressure. The expansion can be made drier by reducing the mass fraction of steam, x_w. There are two ways of doing this. The same organic can be used which raises the dew point temperature at exhaust above the eutectic temperature. This raises the average temperature of heat rejection and hence lowers the cycle efficiency. It is also possible to use the steam/octane mixture which has a lower eutectic steam mass fraction - 21% at 30°C condensing temperature. When the turbine exhaust is excessively superheated the solution is to increase x_w. Again this can be done either by decreasing the nonane content or by changing to decane/steam which has a eutectic steam mass fraction of 68%. The former is preferred since the jump in $x_{eut\ c}$ in going from nonane to decane is likely to lead to wet turbine conditions and to poor matching of cycle to cooling gas.

Table 2 shows the revised fluid compositions required for just dry turbine exhausts where the eutectic compositions of table 1 lead to wet or very superheated conditions. Lower pressure, more superheated inlet conditions and high condensing temperature require the greatest increase over eutectic compositions. For example the 250°C, 5 bar inlet, 50°C condensing conditions require a 65% steam mixture - about the decane/steam eutectic value - with consequent poor cycle - gas matching. The steam content may be reduced by increasing the pres-

sure. In the last two columns of table 2 nonane and octane/steam x_w are compared. As might be expected they are about the same and about mid-way between the eutectic compositions of the systems.

t_{10} °C	250	250	250	200	200	200
t_c °C	30	50	50	50	30	30
p_H bar	5	10	5	10	10	10
Organic	NON	NON	NON	NON	NON	OCT
x_w	0.55	0.52	0.65	0.34	0.30	0.34

Table 2. Fluid composition - just dry expansions (ηs = 0.86).

4.3 Immiscible liquid cycle performance

Figure 6 shows the specific work output of the cycle as a function of gas supply and condensing temperatures. Corresponding cycle constants are recorded in table 3. Maximum fluid temperature was limited to a conservative 250°C although the stability of nonane should permit operation to 300°C without significant degradation. Other than this the temperature difference $t_A - t_{10}$ was set at 50K. Since fluid steam content was chosen, tables 1 and 2, for completely dry expansion, the turbine efficiency has been set high.

Δt_{pinch} K	30
c_{pm} kJ/kg K	1.047
η_s	0.86
η_{pump}	0.70
Max. t_{10} °C	250
Min. p_H bar	5
Organic	nonane

Table 3. Cycle constants.

5: STEAM CYCLE PERFORMANCE COMPARISON

5.1 Specific work output

Assuming the same conditions, Table 3, but maintaining only a 50K temperature difference $t_A - t_{10}$, the immiscible liquid and steam cycle outputs were compared. The results are shown in figure. 7. Steam turbine expansions, especially at the lower gas supply and condensing temperatures, were very wet. Wetness losses were calculated assuming 1% reduction in stage efficiency for each

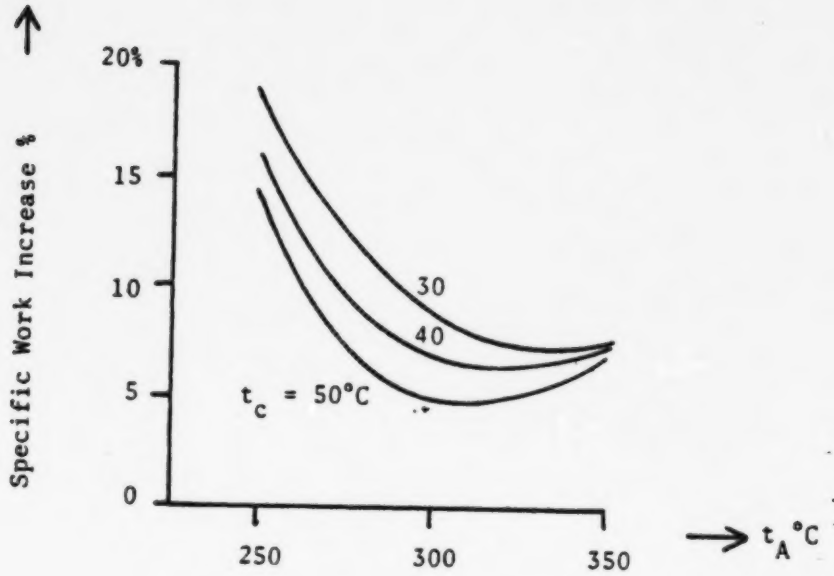

FIGURE 7

percentage average wetness in a stage [8], based on the "dry" efficiency assumed for the mixed vapour turbine, Table. 3. The proposed cycle shows improvement ranging from about 5 to 18% in work output per kg gas compared with the

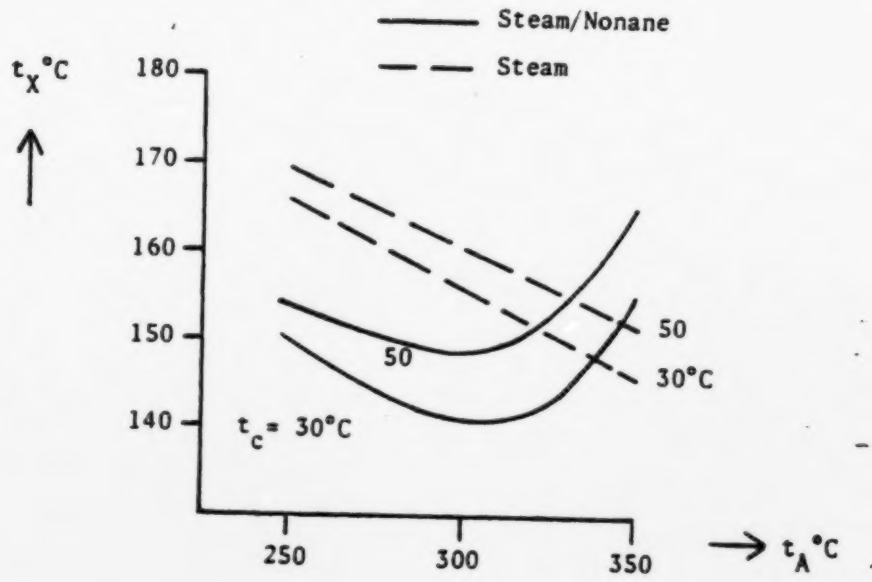

FIGURE 8

steam cycle. Greatest advantage is obtained at the lowest gas supply temperature and the lowest condensing temperature. Under these conditions the steam cycle is at the greatest disadvantage with highest wetness losses and accentuated matching irreversibilities.

The shape of the Figure 7 curves is strongly influenced by the imposed "just dry" expansion conditions. It should be emphasized that this is not necessarily the condition for maximum specific work output but a practical compromise to avoid the regenerator which is required [3] if that condition were desired. The minimum on the $t_c = 50°C$ curve, for example, corresponds to $x_w = 0.65$. This high value, Table 2, was necessary to avoid excessively superheated turbine exhaust. In other schemes [3] where high organic content aqueous miscible systems are used better matching is achieved but regeneration is required.

Boiler pressures were chosen to maximize work output. At $t_A = 350°C$ the optimum $p_H = 15$ bar. In all other cases including the steam cycle the optimum $p_H = 5$ bar, the lowest pressure considered. Stack temperatures are compared in figure 8. At $t_A = 350°C$ less of the enthalpy of the gas is used by organic than steam cycle. The specific work improvement comes from improved cycle efficiency due to the higher optimum boiler pressure of the organic cycle. At lower gas supply temperatures the better work output results partly from higher organic turbine efficiency due to increased wetness in the steam turbine and partly from increased enthalpy extraction from the gas. In all cases the stack temperature is high enough to avoid gas condensation problems - at least for low sulphur content gas - especially since the lowest liquid temperature in the economiser is the eutectic temperature of nonane at 1 bar, 94°C.

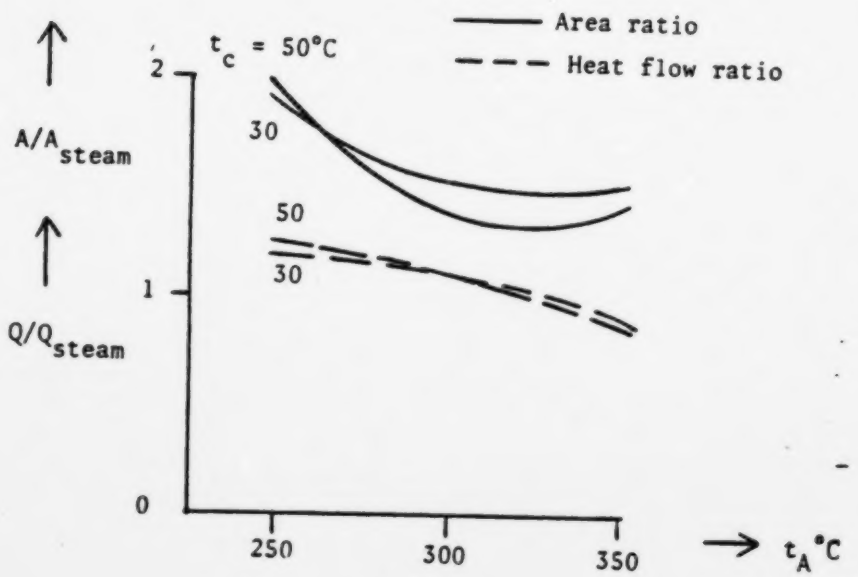

FIGURE 9

5.2 Condensing surface area

Condensing organic vapours requires greater surface area than condensing steam for the same heat rejection mainly due to their much lower liquid thermal conductivity. When condensing vapours of immiscible liquids channelling flow condensation of the two liquid components occurs and the heat transfer coefficient is the liquid volume fraction weighted mean of the Nusselt film values for each component. Assuming about the same level of drainage and vapour velocity effects and that heat transfer resistance of cooling water boundary layer and condensing film are about the same, the steam and immiscible liquid cycle condensing surface areas required were calculated, Figure 9. At t_A = 350 and 300°C about half as much condensing surface is required and at t_A = 250°C nearly double that for steam. The heat rejected by the two cycles varies much less so that the cooling water requirement in the worst case, t_A = 250°C, t = 50°C of the organic cycle is 20% greater than for steam.

5.3 Heat recovery generator

In the vapour generator the main heat transfer resistance is envisaged to be on the gas side as usual. The biggest departure from steam generator conditions is in the economiser section where in the worst case, t_A = 250°C about 53% more heat transfer occurs with a reduction in log mean temperature difference of about 5%. However preheat is only 10% of the total heat transfer in the vapour generator.

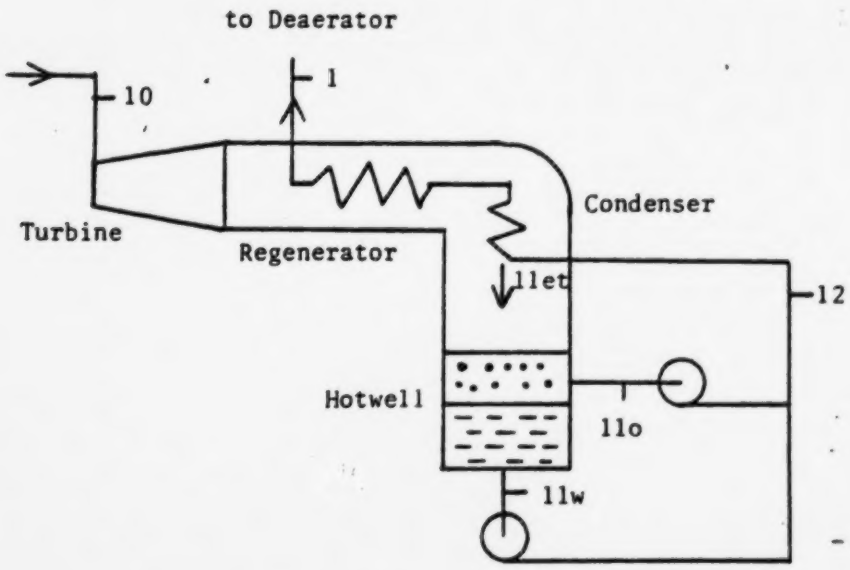

FIGURE 10

5.4 The turbine

Specific work comparisons between steam and immiscible liquid cycles assumed that it is possible to design a mixed vapour turbine with the "dry" efficiency of the steam turbine. For this to be possible the mixed vapour turbine must be of the same conventional design with the same level of stage loading and compressibility effects. It is not reasonable to expect to make use of the lower enthalpy drop in the immiscible liquid cycle to reduce the number of stages since this inevitably involves high Mach numbers in a fluid with lower sonic velocity than steam. The problems may be illustrated by comparing turbine duties for the t_A = 350°C, t = 30°C cycles of figure 7. Table 4 shows the main parameters. Volume flows of the mixed vapour turbine

Turbine	Nonane/steam	Steam
$\Delta h_{overall}$	427	688
$\dot{V}_{in}/\dot{V}_{steam}$	0.265	-
$\dot{V}_{out}/\dot{V}_{steam}$	0.786	-
a/a_{steam}	0.7	-
Pressure ratio	299	118

Table 4. Turbine duties

are lower than steam particularly at inlet because of the higher optimum boiler pressure. The t_A = 250 and 300°C cycles of figure 7, whose boiler pressures are 5 bar, do not have this peculiarity. Due to the lower sonic velocity in nonane/steam the axial velocities are lower for the same level of compressibility effects off-setting the lower volume flow somewhat. Roughly speaking stage enthalpy drops of only $(0.7)^2$, or about half that of the steam turbine can be accommodated. Allowing for the lower overall enthalpy drop about 25% more stages are required in the mixed vapour turbine. For the same stage loading, $\Delta h/U^2$, the blade speed must be reduced by about 16%. If the RPM is the same, a lower mean diameter turbine with more stages, lower stresses and of conventional design emerges. Precautions against moisture damage are unnecessary and sealing is conventional with steam buffer external shaft seals.

6: DISCUSSION

A major advantage of the immiscible liquid cycle in the form proposed above, figure 1, is its simplicity and, apart from rotating seal steam paths and controlling the water mass fraction to the economiser, its requirement for only conventional design. The liquid flow control may be based on turbine exhaust temperature which is held just above the dewpoint at the condenser pressure by varying the proportions of water and nonane liquid supplied to the two phase liquid economiser. Rotating shafts on turbine and nonane feedpump require buffer steam or water seals. An auxiliary boiler heated by the gas stream and fed from the water feedpump is necessary for this because the turbine vapour contains nonane. Another possibility is to extract water from the boiler drum followed by evaporation in an auxiliary boiler. Water for the or-

ganic pump seals can be tapped direct from the water feedpump. Since the liquids are immiscible no problems are created by steam from seals leaking into the working fluid since make-up or removal of liquid after condensation is a simple matter.

The author emphasizes that the improvement in performance provided by the cycle recommended here is only the first of a number of ways of further exceeding the steam cycle output. In the past, improvement in performance of steam cycles which involved plant complication has been a gradual process. Operating experience of each modification was obtained before proceeding to another. The simple immiscible liquid cycle, figure 1, is presented as the first stage in such a process - a process likely to be accelerated by rising fuel costs.

An obvious first improvement is to raise the maximum superheat temperature to 300°C. The alkanes are extremely stable compounds and in the present context breakdown should be no more severe than for the pure compound in an inert atmosphere at the same temperature. Any degradation products are not corrosive even in the presence of water. The worst effect which could occur is the presence of small amounts of hydrogen in the condenser which can be removed with other non-condensable gases in the usual way. Unlike other proposals [3] the organic contains no halogens in the presence of water, a combination which manufacturers might be reluctant to use in expensive large scale power plant because of the corrosive effects in the event that free halogens should appear in the degradation products.

Restricting the amount of superheat at turbine exhaust has a deleterious effect on matching of the cycle leading to water mass fractions as high as 65%, table 2. Matching can be improved dramatically using lower steam mass fractions but this has the effect of reducing cycle efficiency due to the raised average temperature of heat rejection. Thus although much more heat is extracted from the gas more of it is rejected expensively in the condenser. This effect can be removed of course by introducing a regenerator [3] into the cycle, heating the feedwater by means of the desuperheating steam in a closed heater. A free choice of x_w can be made to best suit the cycle matching without decreasing the overall efficiency. In the immiscible liquid cycle better matching infers lower x_w and for optimum performance steam/octane with its lower eutectic water content, $x_{eut\ c} = 0.21$, is preferred. Figure 10 shows the regeneration modification to the cycle of figure 1. The cycle analysis is summarised in the Appendix. If x_w is not equal to $x_{eut\ c}$ some regeneration can take place in the condenser itself between the vapour leaving the regenerator at just above the dewpoint temperature and the condensate at the eutectic temperature. This has the effect of reducing the cooling water requirement in the condenser. Since the heat exchange is within an existing heat exchanger the heat transfer surface need only be increased by an amount consistent with the extra diffusion resistance to heat transfer caused by condensing above the eutectic temperature.

At this stage, however, the simpler cycle for which results have been presented, due to its almost conventional design, is more likely to be accepted. With the above modifications it is capable of the performance which has been presented by other researchers [3] for miscible aqueous systems with the advantage of greater fluid stability and easier correction of fluid composition. Further the possibility of changing fluid composition readily during operation has some advantages for part load operation.

7: CONCLUSIONS

The simplest version of the immiscible liquid cycle applied to the extraction of heat from waste gases at moderate temperatures has been presented. This cycle has been analysed and compared with the conventional steam cycle. The following conclusions have been reached

(i) The plant is simple and of almost conventional design

(ii) The working fluid is very stable with harmless degradation products and the maximum temperature is only 250°C.

(iii) Between 5 and 18% more work can be extracted from waste gases at temperatures between 250 and 300°C.

(iv) The turbine design can be conventional with an entirely dry expansion.

(v) No regenerator is required.

(vi) Steam and water external seals only are required and immiscibility of the liquids simplifies rectification of fluid composition.

(vii) Sensitive control of fluid flows may be based on turbine exhaust temperature.

(viii) The cycle is capable of improved performance, once established in practice, by increasing superheat temperature and by adding regeneration.

(ix) On the negative side: more condensing surface is required.

Formulae have been presented to provide designers with enough information to make preliminary calculations.

8: ACKNOWLEDGEMENTS

The author expresses thanks to Carleton University, Ottawa, Canada, for providing computing facilities and for typing the manuscript.

9: REFERENCES

1. R. Coats, Gas Turbines in Combined Cycles, Repowering and Combined Heat and Power Production, John Brown Engineering (Clydebank) Ltd., Rept., British Energy Exhibition, Peking, June 1979.

2. J.P. Bindon and A.D. Carmichael, A Preliminary Assessment of the Combined Gas Turbine and Vapour Turbine Engine, Jl. Inst. Fuel, vol. 41, pp.28-36, 1968.

3. D.T. Morgan and J.P. Davis, High Efficiency Decentralised Power Generation Utilising Diesel Engines coupled with Organic Working Fluid Rankine-Cycle Engines operating on Diesel Reject Heat", Thermoelectron Corp., Rept. TE4186-27-75, Nov. 1974.

4. B.M. Burnside, The Immiscible Liquid Binary Rankine Cycle, Jl. Mech. Eng. Sci., vol. 18, pp.79-86, 1976.

5. B.M. Burnside, Bottoming Gas Turbine Electric Plant by Immiscible Liquid Cycles, Jl. Eng. for Power, vol. 102, pp.951-956, Oct., 1980.

6. B.M. Burnside, Dual Pressure Steam/Immiscible Liquid Cycles for Gas Turbine Exhaust Heat Recovery, A.S.M.E. Gas Turbine Conference, Houston, Texas, Paper 81-GT-55, March, 1981.

7. B.M. Burnside, Research Note: Temperature-Entropy Diagrams of the Immiscible Liquid Binary Cycle, Jl. Mech. Eng. Science, vol.19, pp.131-132, 1977.

8. B.M. Burnside, A Professional Exercise in Applied Thermodynamics, Intl. Jl. Mech. Eng. Education, vol. 8, pp.25-32, 1980.

APPENDIX 1. CYCLE ANALYSIS

Figure 1 cycle.

In addition to assumptions (i) - (iv) of the main text the following simplifying assumptions were made

(a) Steam to seal losses were ignored
(b) Mixtures of steam and organic vapours were assumed to be ideal mixtures of real gases.
(c) The two phase liquid leaving the HP economiser was at the eutectic temperature.
(d) No vapour was bled from the drum for deaerator heating.

Applying heat balances to the deaerator and each section of the heat exchanger and after some reduction the following relation for x_w, the mass fraction of steam in the vapour expanding through the turbine, is obtained.

$$\frac{h_A - h_c}{h_c - h_x} = \frac{h_{10}(x_w) - x_w h_{8w} - (1 - x_w)h_{8o}}{x_w(h_{8w}-h_{6w}+h_{5w}-h_{12w}) + (1 - x_w)(h_{8o}-h_{6o}+h_{5o}-h_{12o})} \qquad (1)$$

Gas enthalpies h_c and h_x are fixed by the pinch point temperature differences $t_c - t_8$ and $t_x - t_3$, figure 2 and the other pure fluid enthalpies by the pressure levels in condenser, deaerator and HP boiler and feedpump work. x_w is the only unknown in (1) but it appears implicitly in $h_{10}(x_w)$ the turbine inlet enthalpy. The turbine inlet temperature, t_{10}, is an independent variable and a Newton-Raphson iteration in (1) is required to calculate x_w at fixed t_{10}. The fluid: gas mass flow ratios in HP and LP circuits are then given by

$$m = (h_A - h_c)/(h_{10} - x_w h_{8w} - (1 - x_w)h_{8o})$$

and

$$M = m(x_w.(h_{5w} - h_{12w}) + (1 - x_w).(h_{5o} - h_{12o}))/(h_4 - h_3)$$

Key enthalpies in the calculations are

$$h_8 = x_w h_{8w} + (1 - x_w)h_{8o}$$

and

$$h_q = h_{d.pt.}(p_H, x_w).$$

The dryness fraction, q, of fluid entering the deaerator from the LP boiler is related to the overall H_2O mass fraction, y_w, water mass fraction in the liquid, y_{wf}, and the steam mass fraction in the eutectic vapour, x_{ew}, by mass conservation.

Hence

$$y_{wf} = (y_w - q.x_{ew})/(1 - q)$$

This equation implies the permissible range of dryness fraction, q,

For $y_w > x_{ew}$

$$0 < q < (1 - y_w)/(1 - x_{ew})$$

or $y_w < x_{ew}$

$$0 < q < y_w/x_{ew}$$

The vapour : gas flow ratio in the HP section and the stack temperature, t_x, are not affected by the composition of fluid in the LP boiler. Typically, therefore, the LP boiler hot line composition was assumed eutectic vapour only in the calculations.

Figure 10 cycle.

The solution is similar. Equation (1) is replaced by

$$\frac{h_A - h_c}{h_c - h_x} = \frac{h_{10}(x_w) - x_w h_{8w} - (1 - x_w)h_{8o}}{[x_w(h_{8w}-h_{6w}+h_{5w}-h_{12w}) + (1 - x_w)(h_{8o}-h_{6o}-h_{5o}-h_{12o})-h_{11}(x_w,t_{11}) + h_{11et}]} \quad (2)$$

h_{11et} the dewpoint enthalpy at exit from the vapour side of the regenerator is calculated as follows

$$t_{11et} = t_{12} + \Delta t$$

where Δt is the regenerator cold side temperature difference. x_{11et} is obtained by iterating in

$$t_{11et} = t_{d.pt.}\ (p_c,\ x_{11et})$$

Then

$$h_{11et} = h_{d.pt.}\ (p_c,\ t_{11et})$$

In (2), therefore, x_w is the only unknown but it appears implicitly in h_{10} and h_{11}. Iterative calculation is required to obtain it. m and M are then found as in the figure 1 cycle.

PB82-228537

THE FUNCTION OF CHAINS IN THE TRANSFER OF LOW GRADE HEAT IN ROTARY KILNS.

M.C. Patterson, F.D. Moles and B.G. Jenkins
Fuels and Energy Research Group,
Department of Chemical Engineering,
University of Surrey, Guildford, Surrey, England.

ABSTRACT

A brief introduction to cement manufacturing has been given and the process energy requirements have been discussed with regard to areas of possible waste heat recovery. A case study has shown that significant energy savings can be made in the least energy efficient, wet, process of manufacture by reduction of feed moisture content and by improved design of heat transfer inserts in the drying zone. It has also been shown that utilisation of low grade heat within the kiln is more thermally efficient than waste heat recovery external to it.

The functions of chains in rotary kilns, from impressions gained within the cement industry, have been discussed and a brief description of a pilot scale kiln chain rig given. A summary of the results from this investigatory rig has been presented, and their context explained.

1. INTRODUCTION

Cement is manufactured by two main routes, wet or dry, depending on which historical or economic constraints apply. Developed from these routes are two more processes, semi-wet and semi-dry (Fig. 1).

The cement industry has for many years utilised the enthalpy of its product clinker to preheat secondary air for combustion, and to dry fuel on coal fired plants. It is also common practice in the dry process for waste heat from the kiln exit gases to be used for raw materials drying and process steam requirements. However, the exit gas temperature from long wet kilns is considerably lower than that required for effective waste heat recovery, except perhaps for the production of low pressure steam or hot water. The poor specific fuel consumption of the wet process kiln compared to the semi-wet, semi-dry and dry installations, is not a result of the starting moisture content of the raw materials, but is related to the enormous quantities of water required to produce a suitable kiln feed slurry.

Thus, in wet process kilns, the most energy intensive, it is more thermally efficient to reduce fuel usage by minimising the kiln back-end gas enthalpy losses rather than attempt to recover waste heat external to the kiln. The choice of new plant is now, of course, biased away from the wet process, but hundreds of wet kilns exist and many will be in operation for years to come. The capital outlay required to convert long wet kilns to semi-wet or dry is

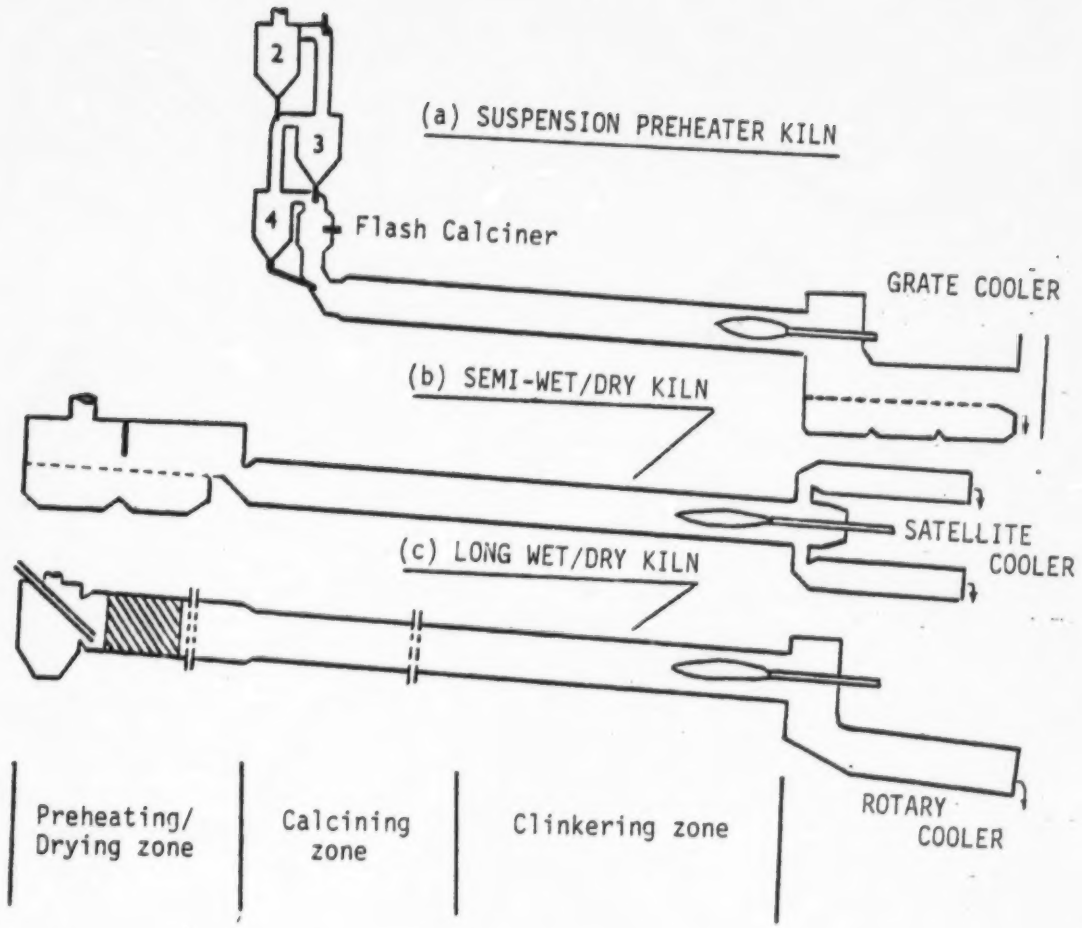

Fig. 1. Types of Cement Kiln and Cooler used in the Manufacture of Portland Cement

high and the payback time is long. The wet process, obsolete or not, is here to stay for at least another decade.

Sometime in the late 1930's the output of wet process rotary kilns was substantially increased by the introduction of steel chains in the feed end, where raw material drying occurs. By the mid 1950's, the introduction of very much larger kilns in the Industry brought about a change in chain design to spirally hung systems, because these not only required less maintenance but improved output. During the forty years that chain systems have been in use in the Industry, neither the drying, heat transfer, dust collection, nor material transport functions of such systems have been thoroughly understood, still less investigated. Whilst some problems have been solved by trial and error methods, for example by even density chain systems, the theoretical reasons for these successes have not been appreciated. There are many, often conflicting views on chaining kilns; some of these have a valid scientific basis, but others are rule of thumb, based on years of observation.

In an effort to remedy this situation, a programme of investigation was

initiated in 1974 in the University of Surrey's Chemical Engineering Department. The work, which was sponsored by two cement manufacturers, involved the fabrication of various physical models to study both the aerodynamics and heat transfer characteristics of chain zones. In addition a mathematical model of the system was developed as an aid to better design.

2. BRIEF INTRODUCTION TO THE PORTLAND CEMENT MAKING PROCESS

Cement is made by pyro-processing a mixture of finely ground calcareous minerals, such as chalk and limestone, and argillaceous materials, such as shale and clay. The mixture is heated to approximately 1450°C to produce a clinker, and the latter is ground to a fine cement powder to which a small amount of gypsum is added to control the setting time. By mixing the cement with gravel, sand and water, concrete is produced.

2.1 The Wet Process Route

Cement slurry is pumped into the uppermost section of a long inclined rotary kiln, which is rotated at between 0.75-2.5 rpm. In the drying section of such kilns, chains are hung in curtains or festoons to act as heat exchangers between the hot combustion gases and the wet slurry; these chains also act as dust collectors and as aids to material transport [1], [2], [3]. The raw material leaves the drying section with a moisture content of typically 6-8 wt. % and then passes into the calcining zone.

In the calcining zone, carbon dioxide dissociates from the feed and is carried away by the kiln gases which pass countercurrently across the bed material. Throughout this zone, the rate controlling step of calcination takes place as the feed is heated to temperatures greater than 900°C.

The calcined material finally enters the burning zone of the kiln where it attains its sintering temperature of approximately 1260°C and starts to flux. A partial phase change to liquid gradually takes place, allowing the free lime and silica contained in the bed materials to combine to form tricalcium silicate (C_3S). At temperatures of approximately 1450°C, almost all of the free lime combines to complete the clinkering process. A delicate balance exists in this zone between the completion of clinkering and the risk of overburning of the sintered material, and it is this balance which determines the final product strength and the clinker grindability.

2.2 Product Energy Requirements

Figure 2 shows heat balances, in the form of Sankey diagrams, for typical examples of small wet (100 tonne/day) and large dry (1400 tonne/day) process kilns calculated from extensive data of kiln operation over a considerable time interval [4].

The immediate difference between the two processes is the much higher energy requirement of the wet process, which is almost entirely accounted for in the exit gas enthalpy (62% of the fuel, compared to 7% for the dry process). This is due to the large volume of water evaporated from the slurry, which has a high latent heat of vaporization.

Thus, although the exit gas temperature is lower for the wet process (276°C) than the dry (316°C), significant energy savings can be made in the wet process

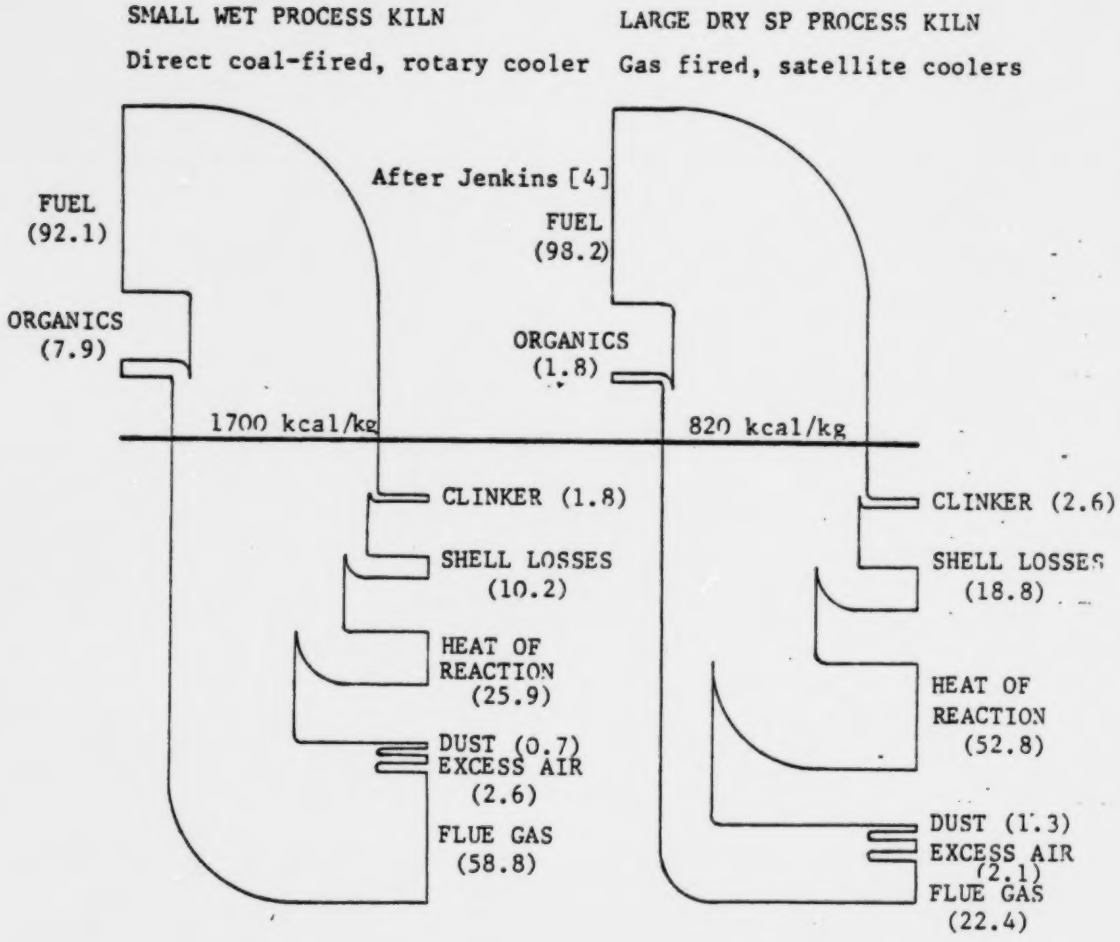

Fig. 2. Heat Balance (Sankey diagrams) comparing a Traditional Small Wet Process Kiln with a Large, Modern, Dry Process Kiln with Suspension Preheater

by a reduction in the feed moisture and improved design of heat transfer inserts in the drying zone. A 1% reduction of feed moisture content will produce a 1.1% fuel saving in a wet process kiln, and increase the kiln capacity by 1.5% [4], [5].

Small quantities of additives can be incorporated into the raw material to reduce the moisture content of the slurry to a minimum level at which it can still be handled and transported through the kiln itself. Moisture contents as low as 28 wt. % have been achieved, the limit being the point at which dust losses from the system become unacceptable. Additives have been the subject of extensive research, and for each particular raw material the type and quantity of additive has to be determined experimentally.

In Table 1, the fuel consumption of the long wet process kiln is compared to other cement manufacturing methods to illustrate the enormous fuel savings that can be made in converting from wet to dry process with, for instance, a

TABLE 1 Fuel Consumption Figures for Different Cement Manufacturing Processes

	(kcal/kg)	
	Typical	Best*
Wet process kilns		
long kiln	1650	1050
short kiln and calcinator	1300	-
Grate process kilns		
semi-wet kiln	1000	850
semi-dry kiln	950	800
Dry process kilns		
long kiln	1300	900
suspension pre-heater and short kiln	875	750

* Data from more than one source

suspension preheater. However, the capital cost of such conversions is very high and the payback time is long; often the decision is taken to utilise as much existing plant as possible by shortening the rotary kiln and using an external (pre-)calcining/drying unit. A recently reported conversion from long wet to dry process with precalcining preheater cost $56 million at 1980 prices [6].

Reducing the moisture in the kiln feed by filter pressing produces substantial gains in fuel economy; this is often negated by the cost of an external unit, such as a Lepol Grate or other preheater which requires extra maintenance and control in addition to capital expenditure. Clearly the economic merits of conversion have to be carefully studied for each individual case.

2.3 Recovery of Waste and Low-grade Heat

There are two main areas in the cement kiln process where waste heat can be recovered:

(i) From the clinker product as it cools from 1400°C to ambient
(ii) From the flue gases at 500°C to their acid dew point.

Invariably, whatever the cement making process, the air used to cool the clinker is utilised as preheated secondary air for combustion, typically up to temperatures approaching 800°C. In coal-fired kilns, some of this air is

drawn off to dry coal in the milling plant; in oil fired plants waste heat is used to preheat the fuel oil.

In dry process kilns, the flue gas enthalpy is sometimes utilised to dry the raw meal before it is fed into the suspension preheater tower. However, it has previously been shown by Weber [7] that the waste heat can be utilised only down to the exit gas temperature of the drying plant, and that the efficiency of utilisation (η) is highly dependent on the inlet gas temperature (Fig. 3). Below gas temperatures of 400°C, the heat utilisation potential shows a sharp decline. Similar findings have been reported by Brooks and Gray [8] in studies on open-hearth furnace waste heat boilers.

Weber [7] has also shown that the heat consumption for drying raw cement material decreases with higher drying gas temperature (Fig. 4), and he concluded from this theoretical work that it is more economical to use auxiliary heat for raw meal drying than to use low temperature kiln exit gases for this purpose. The practical implications of this theory are borne out by dry process cement making experience, where waste heat alone (ex-clinker coolers) is sufficient for raw material drying only where the moisture content of the latter is less than 6-8 wt. %. An auxiliary supply of heat is required for raw materials containing greater levels of moisture.

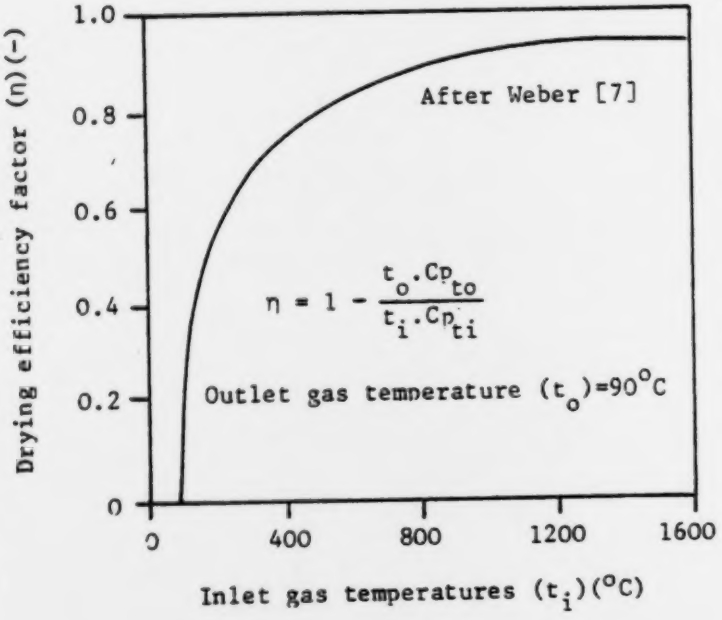

Fig. 3. Drying Efficiency Factor (η) as a Function of inlet gas temperature.

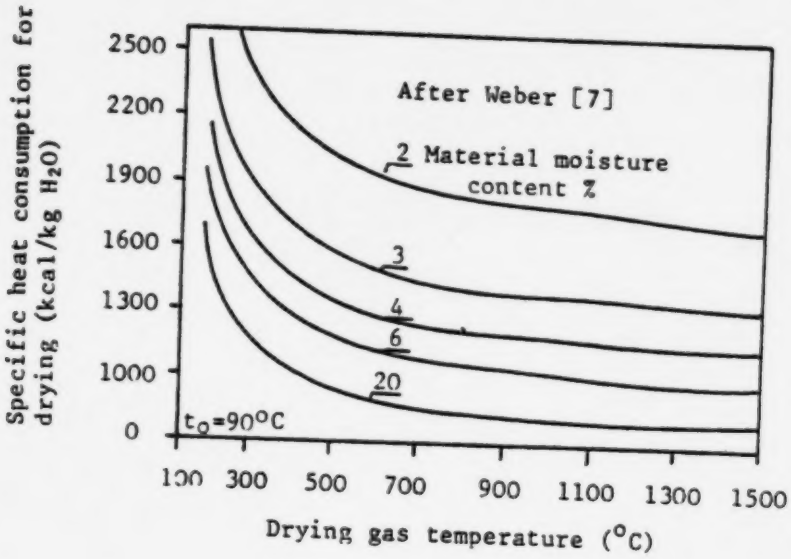

Fig. 4. Specific Heat Consumption for Raw Material Drying as a Function of Gas Temperature and Material Moisture Content

In the case of the long wet process kiln, with its generally lower back end gas temperatures, Weber's conclusions [7] give a clear indication that it is thermally inefficient with regard to waste heat recovery by this means. In the past, external feed preheaters and spray dryers have been used as an integral part of the wet process, but their success is very much dependent on raw material properties. Unlike internal heat exchange inserts, such external units have the advantage that their operation is independent of kiln rotational speed, but they are prone to air inleakage which can cause the gas temperature to fall below its dew point.

3. THE ROLE OF KILN CHAIN SYSTEMS IN WET PROCESS KILNS

3.1 Background to Chain Systems

Sometime in the early 1930's, chains were first hung in the drying zone of a wet process kiln in Northern France to improve the heat consumption and to increase clinker production. These chains were suspended from the inside of the kiln shell, and as the kiln rotated, they absorbed heat from the flue gases and transferred it to the much cooler cement slurry [1]. In this section of the paper, an attempt has been made to describe the impressions gained by the cement industry of the role of chains through various private publications, and also by discussions with those people within the Industry who have collected practical know-how over many years of experience.

3.2 The Function of Kiln Chain System

The duty of a chain system is complex, and depends on the state of the raw material in the zone being considered, as well as the manner in which the kiln is operated.

Dust kilns. In a dust kiln, the residual moisture in the feed is completely driven off, and the chains are allowed to crush the friable solid. Part of the dust so produced leaves the kiln with the exit gas stream and is collected for re-introduction to the kiln, either at the burner end by insufflation, or at some position along the kiln shell. Larger kilns (greater than 2.5 metres internal diameter) tend to be dust kilns, whereas smaller kilns are almost invariably of the nodule type [9]. Because most large, wet process kilns have, or will be converted to semi-wet or dry operation in the near future, the role of chains in the nodule kiln has been discussed.

Nodule kilns. This type of kiln differs from the dust kiln in that the raw slurry, which may have a moisture content anywhere between 28-44 wt. %, is converted into a uniform nodular solid containing 6-8 wt. % water at the exit from the chains. The strength and size of these nodules should be such that they can withstand the thermal shock and mechanical attrition of their passage along the kiln.

Chain systems. The chain zone can be likened to a massive countercurrent heat exchanger in which one of the fluid streams gradually changes state from a Non-Newtonian dispersion to an intractable puggy mass, and finally emerges as a granular solid. Depending on the degree of water evaporated from the slurry, the gas flowrate will also alter along the kiln axis as more water is driven off. Although some semblance of steady state conditions may be achieved axially, transient heat transfer prevails as the chains and the kiln shell wall enter and leave the gas and solid streams.

Slurry properties. Further complications arise in that the rheological nature of the slurry is strongly influenced by the composition and the degree of grinding of the raw materials, the moisture content of the chalk/clay mixture, and the age of the slurry itself. The slurry viscosity and moisture content will also change dramatically as cement dust is recombined with the wet charge [10].

Kiln drying zone. It follows that a kiln drying zone must be tailored to the particular needs of the raw material to be processed and the required clinker production rate. Dust losses from the kiln exit gases are minimised by the wet-film filter properties of the chains when coated with slurry. If, however, too dense a chain curtain is installed at the back end of the system, the raw material is likely to spill back over the dam ring. On the other hand, insufficient chain density at the back end of the kiln will cause less heat to be removed from the combustion gases, resulting in elevated flue gas temperatures and correspondingly high heat losses from the large volume of process gases associated with the wet process kiln.

Convective heat transfer. The low temperatures and high flowrates of the gases in the cold end of the drying section cause convection to be the dominant mechanism of heat release from the gas. The drying and heat exchange rates within the chain system will vary with the surface area of wet slurry in contact with the moving gas stream, and hence with the rate at which fresh surface is exposed. The size and shape of each chain link, and whether or not the link is liable to clog, determines the surface area of slurry carried by a length of hanging chain, and also the heat carried into the slurry from the gas [11].

Therefore the area and mass densities of installed chain will influence the overall evaporative effect of the system.

Puggy state. During its passage through the drying zone, the moisture in the slurry is evaporated and the slurry enters its puggy region, in which it shows a tendency to ball up and become a heavy, unmanageable mass which sometimes clings to the chains and to the kiln shell [11]. In this region, the chains must be sufficiently heavy to crush these mud rings and to transport the material along the kiln. Failure to do so can result in surging which adversely affects product output and quality [12].

Nodulization. At the hot end of the chain zone, the charge is changed into a rolling, nodular bed, having different heat transfer characteristics from the other two zones [10]. No longer can the chains be wetted, nor can they pick up and expose the sticky material to the gas stream as they had in their previous role as heat exchange inserts. In this zone, radiation from the chains and the kiln shell becomes more significant at gas temperatures higher than 400°C. The nodular charge renews the surface area exposed to the gas stream by solids mixing caused by the rotation of the kiln. The heat from the chains, the walls and the rolling material surface is dissipated by solids convection into the core of the solids bed.

Limitations on chain quantity. If this section of the chain zone is too long for the amount of moisture to be removed from the slurry, then dust is likely to be raised as the nodules become too brittle to survive the action of the chains [2], [13]. In the case of a chain zone being extended too far into the calcining zone, the radiation and high gas temperatures in this region cause high wear rates as the chains literally burn away.

4. INVESTIGATION INTO HEAT AND MASS TRANSFER IN CHAIN ZONES

4.1 System Aerodynamics

A 1/30th geometric scale model was used to study the aerodynamics of the chain zone using isothermal modelling techniques. Initial tests using a rotated water model with flow tracer elements indicated that the fluid velocity through the chain banks is less than that through the tunnel left below the hanging chains, and that kiln rotation has no apparent effect on the flow patterns of the fluid stream.

Air modelling techniques using hot wire anemometry have shown that the axial gas velocity across a gravel charge representing the slurry bed is up to 20 percent higher than that through the chains themselves.

Both techniques have demonstrated that the chains offer significant resistance to the fluid stream and are effective as flow straighteners to the gas stream.

4.2 Mathematical Model

A mathematical model, using iterative procedures, has been developed in order to predict the performance of kiln chain systems for a range of process conditions [14].

Predictions from the model require reliable and accurate data from real kiln systems. However, there is little published literature concerning the

heat transfer characteristics of chains in rotary kilns, and virtually none describing the internal mechanisms of heat transport. Previous analysis of unsteady state heat transfer in rotary devices is limited, and is non-existent in the case of flexible heat exchange inserts (i.e. chains). The estimation of heat transfer coefficients and the nature of their relationship to the gas flowrate is of fundamental importance in the design and imporvement of chain systems.

4.3 Pilot Scale Kiln Chain Rig

In order to generate the required heat and mass transfer data, a pilot scale model has been constructed in the University's Department of Chemical Engineering, based on a typical three spiral-start chained section. The model comprises a 0.3 m internal diameter cylinder through which furnace flue gases from an auxiliary-fired furnace pass over (preheated) raw cement slurry. The 1 m long chain zone is housed within this cylinder. Gas temperatures of up to 800°C can be obtained over a range of gas and solids flowrates, and at kiln rotational speeds of 0.2-4.5 rpm.

The transient response of the chain tip and selected locations on the kiln shell wall has been monitored by flexible miniature thermocouples. Inflexible, sheathed thermocouples have been used to measure gas and solids temperatures along the length of the model by halting the model rotation and allowing thermal equilibrium to be attained with the probe either in the solids or in the gas stream. In the case of wet slurry, the film coating on the thermocouple was allowed to dry before the reading was taken.

5. RESULTS OF EXPERIMENTAL INVESTIGATION

The technological and operating problems of the wet process have inevitably been related to the non-Newtonian nature of kiln feed slurry and the wide variability of its physical properties. These properties also vary with the degree of grinding of the raw materials and the period of storage of the chalk/clay mix. These are the main reasons for the difficulty in analysing the heat transfer and material transport characteristics of the wet part of the drying zone in such kilns.

The results summarised in this paper are based on the heat transfer to a raw cement slurry of non-Newtonian (Pseudoplastic) nature over the moisture content range 38-50 wt. %. Because of properties peculiar to raw cement slurry, the critical moisture content range 26-34 wt. % moisture does not lend itself to small scale physical modelling, slurry becoming an intractible solid mass between these limits.

Investigations are currently being carried out into the heat transfer to the dry, granular solid in the hotter section of kiln chain zones, where pre-calcining may take place. Subsequent investigations aim to examine the novel practice of feeding chain systems with a filter pressed, solid feed of moisture content 17-18 wt. %. This "dry" data will enable the mathematical model mentioned in section 4.2 to be applied to full scale predictions of kiln chain performance from first principles.

5.1 Summary of Results

The values of heat transfer and drying rate coefficient over the range of

conditions studied are summarised in Table 2.

Table 2. Summary of Kiln Chain Model Heat Transfer and Drying Rate Coefficients		
	Value range	
Gas : Chain H.T.C.	1 - 85	(kcal/hm^2 ^{o}C)
Gas : Wall H.T.C.	10 - 104	
Gas : Slurry H.T.C.	2 - 19	
Slurry : Chain H.T.C.	20 - 275	
Slurry : Wall H.T.C.	80 - 225	
Overall H.T.C.	2 - 16	
Overall drying rate coefficient	0.2 - 1.8	(kg/hm^2)
Slurry mass flowrate	200 - 410	(kg/h)
Gas Reynolds Number range	2000 - 50,000	(-)

The effects of kiln rotational speed on bed loading and feed residence time were found to be significant even though a slurry bed dam ring had been installed to regulate the solids bed depth. Correction factors were applied to the theoretical areas of chain and wall in the gas and solids in order to compensate for these effects.

Gas side heat transfer. The gas:wall heat transfer coefficients (Fig. 6) are of the same order as those quoted by literature [15] and have been correlated to yield the equation:

$$Nu_{gw} = 0.58\ Re^{0.686} \qquad \ldots\ldots\ldots (1)$$

where Nu_{gw} = Nusselt Number (gas:wall coefficients) based on inside diameter of kiln tube;

Re = Gas Reynolds Number, same basis. Value range 2000-50,000.

Comparison of the slurry to gas, chain and wall heat transfer results with the limited data available from literature has proved disappointing [16]. The gas side heat transfer coefficients are less than half the corresponding slurry side values, and the gas to chain coefficient is more highly dependent on the gas flowrate than is the analogous gas to wall coefficient. The gas:chain heat transfer (Fig. 5) is summarised by the equation:

$$Nu_{gc} = 3.08 \times 10^{-19}\ Re^{4.33} \qquad \ldots\ldots\ldots (2)$$

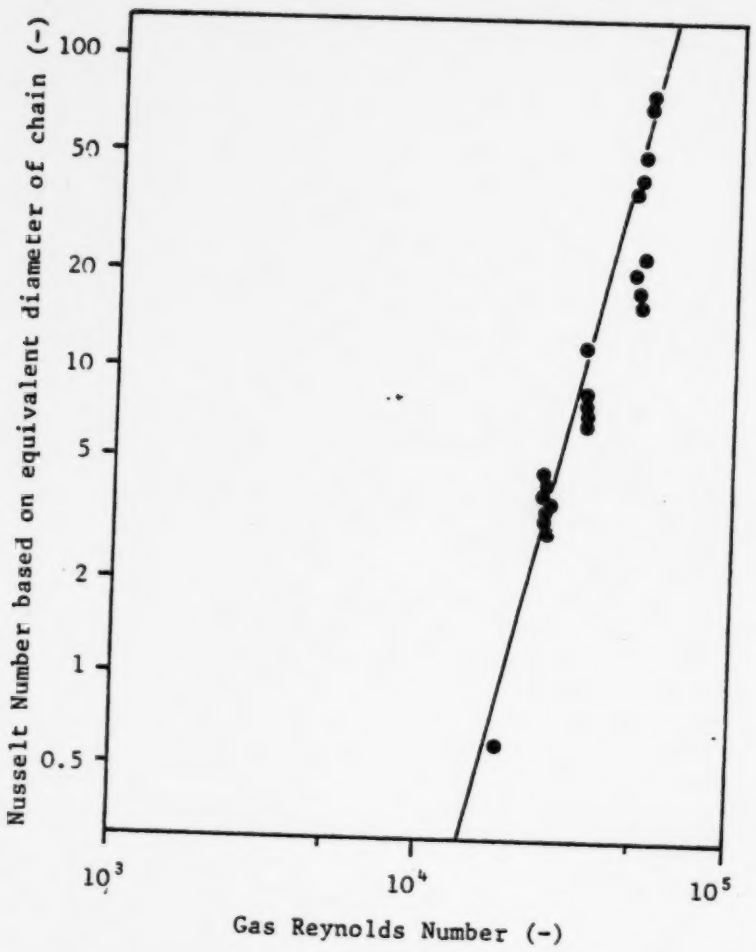

Fig. 5. Relationship between Nusselt and Reynolds Dimensionless Groups (Gas:Chain)

where Nu_{gc} = Nusselt Number (gas:chain coefficient) based on equivalent diameter of chain.

Gas side heat transfer is the rate controlling function, indicating that the chains are the predominant factor in heat transfer by merit of their large surface area.

Slurry side heat transfer. An increase in kiln rotational speed beyond 1 rpm increases, in an exponential manner, the heat and mass transfer coefficients between the slurry and the internal heat exchange surfaces. Slurry:wall, and slurry:chain heat transfer coefficients are of the same order.

The overall effect of kiln rotational speed is insignificant, as shown by the values of the overall heat transfer coefficient which are independent of kiln speed over the range investigated. This lends further support to the supposition that gas side heat transfer is the rate controlling factor, since the slurry side coefficients increase dramatically with rotational speed.

Drying rate coefficients. The gas and slurry flowrates have a positive effect

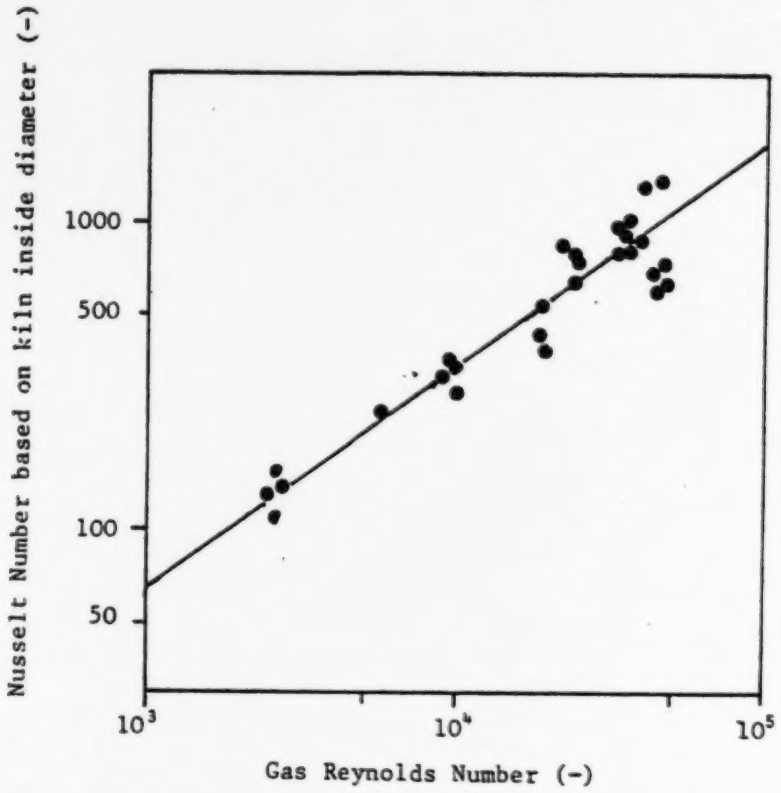

Fig. 6. Relationship between Nusselt and Reynolds Dimensionless Groups (Gas:Walls)

on the slurry drying rate coefficient, and the values of the latter compare favourably with published literature concerning kiln drying zones [17]. Kiln rotational speed has no apparent effect on the drying rate coefficient.

5.2 Application of Results

Using a simplistic model of a slurry-wetted drying zone of a wet process kiln operated under low load conditions, predictions have been made of the effect of variations in chain surface area on the kiln exit gas temperature. A three spiral start system has been modelled, using heat and mass transfer coefficients evaluated for each gas flowrate from data measured on the kiln chain model.

It can be seen from Figure 7 that a 5% reduction in chain surface area from a design value of 3738m^2, results in an increase of exit gas temperature of up to 10^{0}C. Because of the abrasive nature of raw cement slurry, chain wear is inevitable; frequently, whole chain lengths become detached from their hangers, and are carried into the burning zone. The resultant loss of internal area for heat and mass transfer causes less heat to be removed from the exit gases and hence increases back end enthalpy losses.

The predictions also show that the exit gas temperature is strongly

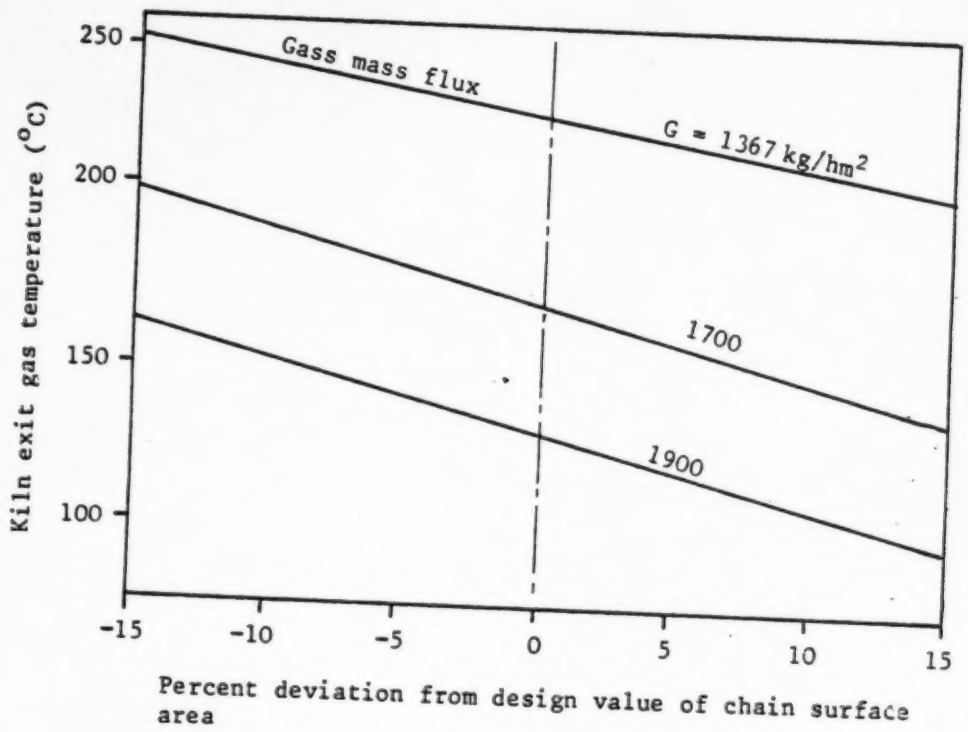

Fig. 7. Predicted Effects of Chain Surface Area on Kiln Exit Gas Temperature for a Range of Gas Flowrates

dependent on gas flowrate, an increase in gas mass flux reducing the exit gas temperature. This is due to the influence of the gas flowrate on the gas:chain heat transfer coefficient, which greatly increases the transfer of heat to the chains at higher gas throughputs. The result of this velocity effect is lower exit gas temperatures, even though disproportionately more heat must be removed from the flue gases to achieve this aim.

For a kiln fired on high quality coal, a 12°C reduction in exit gas temperature results in a 1% saving in fuel.

CONCLUSIONS

1. It is more thermally efficient to internally utilise the enthalpy of the exit gases from wet process kilns, rather than attempt external waste heat recovery. Significant energy savings can be made in the wet process by a reduction in the feed moisture content and by improved design of heat transfer inserts in the drying zone.

2. A 1% reduction of feed moisture content will produce a 1.1% fuel saving in a wet process kiln and increase the kiln capacity by 1.5%.

3. Gas side heat transfer is the limiting factor in the transfer of heat in kiln drying zones. The gas side coefficients are less than half the correspond-

ing slurry side values, and the gas to chain coefficient is more highly dependent on the gas flowrate than is the analogous gas to wall coefficient.

4. An increase in kiln rotational speed increases the individual heat transfer and drying rate coefficients between the slurry and the internal heat exchange surfaces, but the overall effect of kiln speed is insignificant.

5. Chain surface area is the most important operational variable controlling heat transfer in wet process kiln drying zones. Computer predictions have shown that the exit gas temperature is dependent on the area of chains available for heat transfer, a 5% reduction in chain surface resulting in up to 10°C increase in exit gas temperature, depending on the gas flowrate. A 12°C reduction in exit gas temperature results in a 1% fuel saving.

ACKNOWLEDGEMENTS

The authors wish to express their gratitude to Rugby Portland Cement Company Ltd. for awarding a research fellowship to allow this investigation to be undertaken. They would also like to thank Blue Circle Industries and Aberthaw and Bristol Channel Cement Company Ltd. for their cooperation in providing comprehensive data on the operational performance of their kilns.

The authors are indebted to the technicians of the Department of Chemical Engineering for the construction and development of the experimental rigs, as well as Mr. A.H.J. Tate and Mr. B. Carter for their guidance in computer programming.

REFERENCES

1. Anon., Die Schlammtrocknung der Fellner & Ziegler AG zur Verkesserung der Wärmewirtschaff in Nassdrehöfen, Zement, Vol.4, pp. 41-42, 1934.

2. H.R. Norbom, Wet or Dry Process Kiln for Your New Installation, Rock Products, Vol. 71, pp. 92-98, May 1974.

3. W.R. Dersnah, Chain System Installations in Cement Kilns, Part 1, Pit and Quarry, Vol. 48, pp. 94, 96-99, 104, 134, Nov. 1956.

4. B.G. Jenkins, Heat Transfer in Rotary Cement Kilns, Ph.D. thesis, Univ. of Surrey, Guildford, Surrey, 1976.

5. W.H. Duda, Cement Data Book, 2nd Ed., pp. 355-366, MacDonald and Evans, London, 1977.

6. G.D. Staublin, Charlevoix's Conversion and Flash Calcining Experience, Int. 16th Cement Seminar, Rock Products, Chicago, Ill., Dec. 1980.

7. P. Weber, Utilisation of Waste Heat from Dry Process Kilns, Zement Kalk und Gips Spec. English Ed., Vol. 5, pp. 214-221, 1967.

8. S.H. Brooks and F.A. Gray, Availability and Economic Recovery of Waste Heat in Iron and Steel Works, Proc. 2nd Symp. Waste Heat Recovery, Inst. Fuel, Bournemouth, 1961.

9. P.J. Mullinger, Private Comminication, Univ. of Surrey, Nov. 10th, 1980.

10. W.R. Dersnah, Chain System Installations in Cement Kilns, Pit and Quarry, Vol. 48, pp. 119-122, Dec. 1956.

11. W.E. Drayton, Know Your Kiln's Chain System, Rock Products, Vol. 69, pp. 88-89, 126, May 1972.

12. E. Burke and G. Field, Problems of Heat Transfer from Flames in the Cement Industry, 1st Flames in Industry Symposium, Inst. Fuel, London, Oct. 1957.

13. H. Gygi, Thermodynamics of the Cement Kiln, Proc. 3rd Symp. (Int) Chemistry of Cement, paper 21, London, pp. 750-789, 1952.

14. M.C. Patterson, B.G. Jenkins and F.D. Moles, Unpublished work, Univ. of Surrey, Guildford, Surrey, 1980.

15. W.H. Perry, Chemical Engineers Handbook, 4th Ed., McGraw Hill, New York, 1969.

16. S.H. Tscheng and A.P. Watkinson, Convective Heat Transfer in a Rotary Kiln, Canadian Jnl. Chem. Eng., Vol. 57, pp. 433-443, 1979.

17. P. Weber, Heat Transfer in Rotary Kilns with Due Regard to Cyclic Processes and Phase Formation, Zement Kalk und Gips Spec., English Ed. Wiesbaden, Bauverlag GMBH, 1963.

MOTOR COLUMBUS
CONSULTING ENGINEERS INC.
BADEN/SWITZERLAND

PB82-228545

Third Conference on Waste Heat Management and Utilization

Miami Beach, Florida
(May 11 - 13, 1981)

PROCESS STEAM LINE FROM THE GOESGEN NUCLEAR POWER STATION TO THE CARDBOARD INDUSTRY AT NIEDERGOESGEN, SWITZERLAND

Author: I. Daglio
Motor-Columbus
Consulting Engineers Inc.
CH-5401 Baden/Switzerland

Summary :

The process steam at a medium-size cardboard factory in Niedergösgen, a town near the Gösgen nuclear power plant site, was previously produced by boilers with heavy fuel oil burners which used to cause considerable pollution of the environment. A logical solution was to transfer process heat from the Gösgen power plant, only 1.75 km away.

ATEL, the Aare-Tessin Electricity Company, commissioned Motor-Columbus as general contractor to design and build a steam supply from the Gösgen nuclear power plant to the Niedergösgen cardboard factory. That was the first instance of using nuclear heat for industrial purposes in Switzerland.

In cardboard production out of waste paper, 2.6 to 2.7 tons of process steam per ton of paper are needed for the drying process alone. While it is not possible to reduce the steam consumption of the cardboard machinery as such, there are two ways of reducing production costs, in order to keep prices within competitive limits:

(1) By increasing the availability of the cardboard production plant

(2) By using a low-cost, reliable steam supply

In 1978/79 Motor-Columbus was entrusted with the design, construction and commissioning of a 1.75 km long steam pipeline from the Gösgen nuclear power plant to the Niedergösgen cardboard factory, acting as a general contractor. Construction started in September 1978; at the end of 1979 the pipeline went into commercial operation.

Heat Extraction

The heat for the cardboard factory is extracted through an evaporator from the live steam line between the reactor and the high-pressure turbine. This has the advantage that the process heat supply and the electric power generation plant can operate independently of each other.

Pipeline Layout

Within the power plant boundaries the pipeline had to be laid in man-sized energy transport tunnels due to special inspection and maintenance obligations towards the power plant operator. Along the natural course of the Aare river the pipeline was laid above ground using the Pipe Track System which is largely prefabricated. The industrial areas to the north of the Aare river were crossed by means of underground through ducts. These ducts are used for normal traffic loads. The curved section along the industrial railway, where the pipeline supports allow longitudinal and transverse displacements, is a novelty. In a widened through duct, this system allows for thermal expansion.

The steam pipeline has an overall length of 1,750 m and has been laid as follows:

- Open, in the power house	100 m (5 %)
- In man-sized tunnels	360 m (21 %
- In through ducts	470 m (28 %)
- Open	820 m (46 %)

During normal operation no drain water condensates develop. The condensates forming during start-up (about 8,000 l) are either conducted to the cooling tower cup or collected in basins and carried off to the open or collected in the cardboard factory, depending on the place where they originate.

Commissioning

For putting the installation into service, the following load cases were tested:

- Feed-Water pipe hydraulic pressure transients
- Water shortage in the condensate tank at the cardboard factory
- Feed-water pump switch off at full load
- Full load cutoffs of steam as well as of feed-water
- Radioactivity increase
- Live steam isolation
- Safety valve blow-off at the power plant and at the cardboard factory.

Steam Condition Control, Activity Monitoring

Control of the steam condition at the evaporator outlet in the nuclear power plant is achieved by means of a throttle in the feed-water line and a level control in the evaporator. The pressure in the steam line acts as a control signal. A remote control system between the heat consumer and the heat producer is not necessary due to the inherent stability of this control system.

The radioactivity of the process steam is continuously monitored by means of a measuring station at the evaporator outlet. It will automatically interrupt the steam supply before the J-131 activity reaches a preset limit value.

Temperature and Pressure Monitoring

Temperature and pressure of the steam are measured and recorded at each end of the steam pipeline. Comparison of the recorded values allows a continuous supervision of operating conditions and of the quality of the thermal insulation of the steam pipeline.

Financial Savings

The steam produced in the nuclear power plant costs less than that produced in the cardboard factory's own heavy fuel oil fired boilers, in spite of the considerable distance. In additon, the personnel of the factory heating plants becomes available for other duties. Also, the nuclear plant supply is basically more reliable.

Reducing Environmental Impact

Each day 60 tons of heavy fuel oil were burned in the cardboard factory. This oil contained between 900 to 1,000 kg sulphur dioxide which was emitted into the atmosphere with the fumes. On days with unfavourable wind direction these fumes used to disturb the densely populated near-by areas. There was a strong suspicion that the irregular leaf growth observed in the surrounding forests was due to the cumulated ecological impact in the atmosphere.

The modern energy transport installation at Gösgen is an important contribution to the protection of the environment and it provides a reliable energy supply. In addition, the primary energy resources are better utilized due to the cogeneration. It is therefore not surprising that this project was actively supported by everybody concerned.

Project Data

Steam line, nominal width 350:

- Pipe dimensions	Ø 355.6 x 8.0 mm
- Material	seamless steel pipe St 35
- Rated pressure	25 bar
- Operational pressure	13 bar
- Design pressure	19 bar
- Water test pressure	24 bar
- Operational temperature	194 - 222 °C
- Design temperature	230 °C
- Design steam throughput	22.2 kg/s = 80 t/h
- Steam velocity	34.5 m/s

Feed-water line, nominal width 150:

- Pipe dimensions	Ø 168.3 x 4.5 mm
- Material	seamless steel pipe St 35
- Rated pressure	40 bar
- Operational pressure	24 bar
- Design pressure	26 bar
- Water test pressure	40 bar
- Operational temperature	106 °C
- Design temperature	110 °C
- Design feed-water throughput	22.5 kg/s = 81 t/h
- Feed-water velocity	1.13 m/s

Insulation :

Steam pipe:

- Insulation thickness 150 mm: 100 mm slag shell, 50 mm slag wool mat with aluminum lining, 1.0 mm aluminum sheething

Feed-water pipe:

- Insulation thickness 70 mm: 70 mm slag wool shell, covered by 0.8 mm aluminum sheeting

High pressure feed-water pumps:

- Number	2
- Type	centrifugal pumps
- Stages	4
- Speed	2,900 rpm
- Motor capacity	55 kW
- Pumping head	21.4 bar
- Throughput	13.9 kg/s

At parallel operation:

- Pumping head	21.9 bar
- Throughput	2 x 11.3 kg/s

MOTOR COLUMBUS
CONSULTING ENGINEERS INC.
BADEN/SWITZERLAND

FIG. 1

LAYOUT OF THE PROCESS STEAM PIPELINE

Scale: 1 : 7500

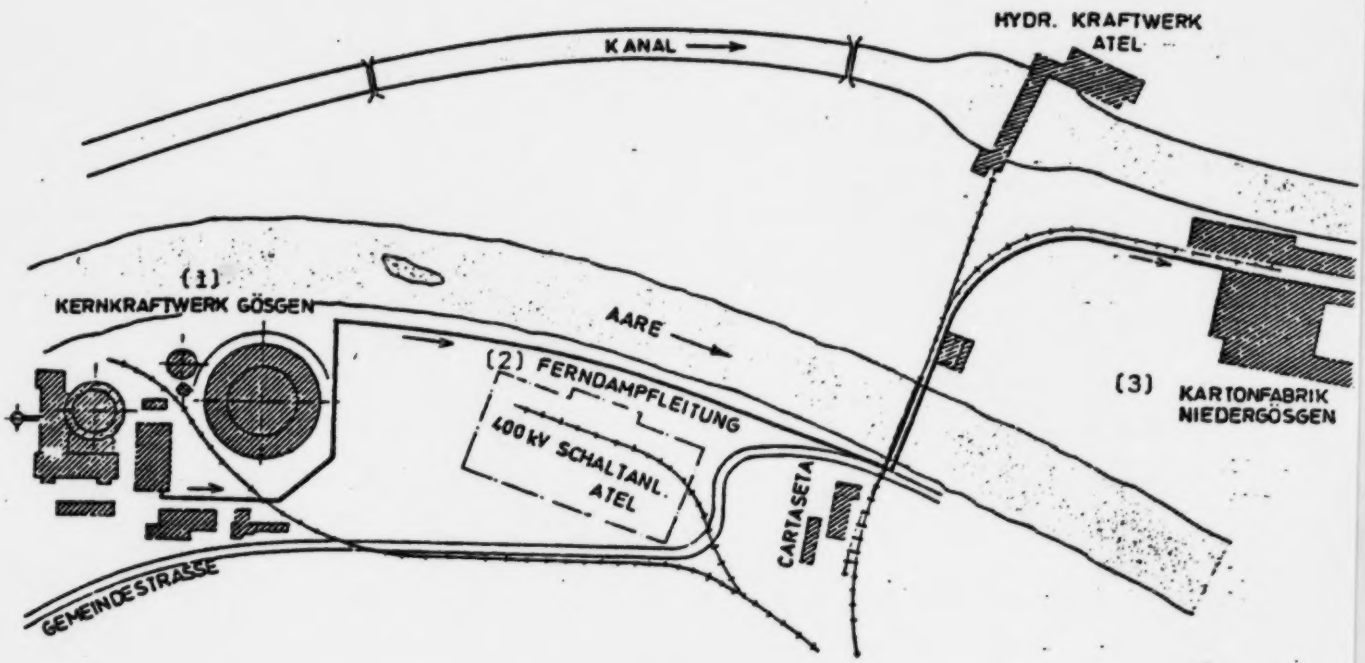

LEGEND:

(1) Goesgen nuclear power plant

(2) Process steam pipeline

(3) Cardboard factory Niedergösgen

MOTOR COLUMBUS
CONSULTING ENGINEERS INC.
BADEN/SWITZERLAND

FIG. 2

SCHEMATIC OF THE COMBINED NUCLEAR POWER AND STEAM GENERATING PLANT

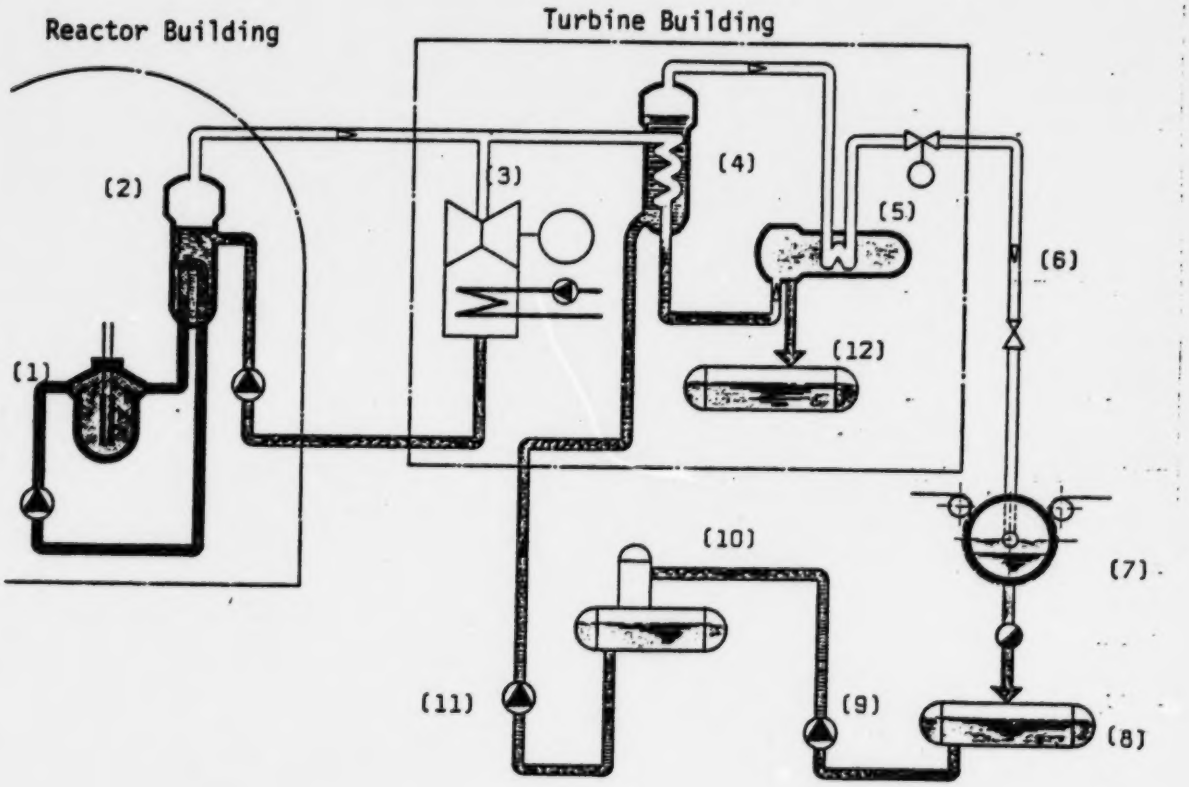

LEGEND:

(1) Reactor pressure vessel
(2) Reactor steam generator
(3) Steam turbine with alternator
(4) Process steam generator (evaporator)
(5) Superheater
(6) Steam pipeline (1.75 km)
(7) Paper machine
(8) Process steam condensate tank
(9) Low pressure condensate pump
(10) Deaerator
(11) High pressure condensate pump
(12) Power plant condensate tank

MOTOR COLUMBUS
CONSULTING ENGINEERS INC.
BADEN/SWITZERLAND

FIG. 3

SCHEMATIC OF THE PROCESS STEAM GENERATION

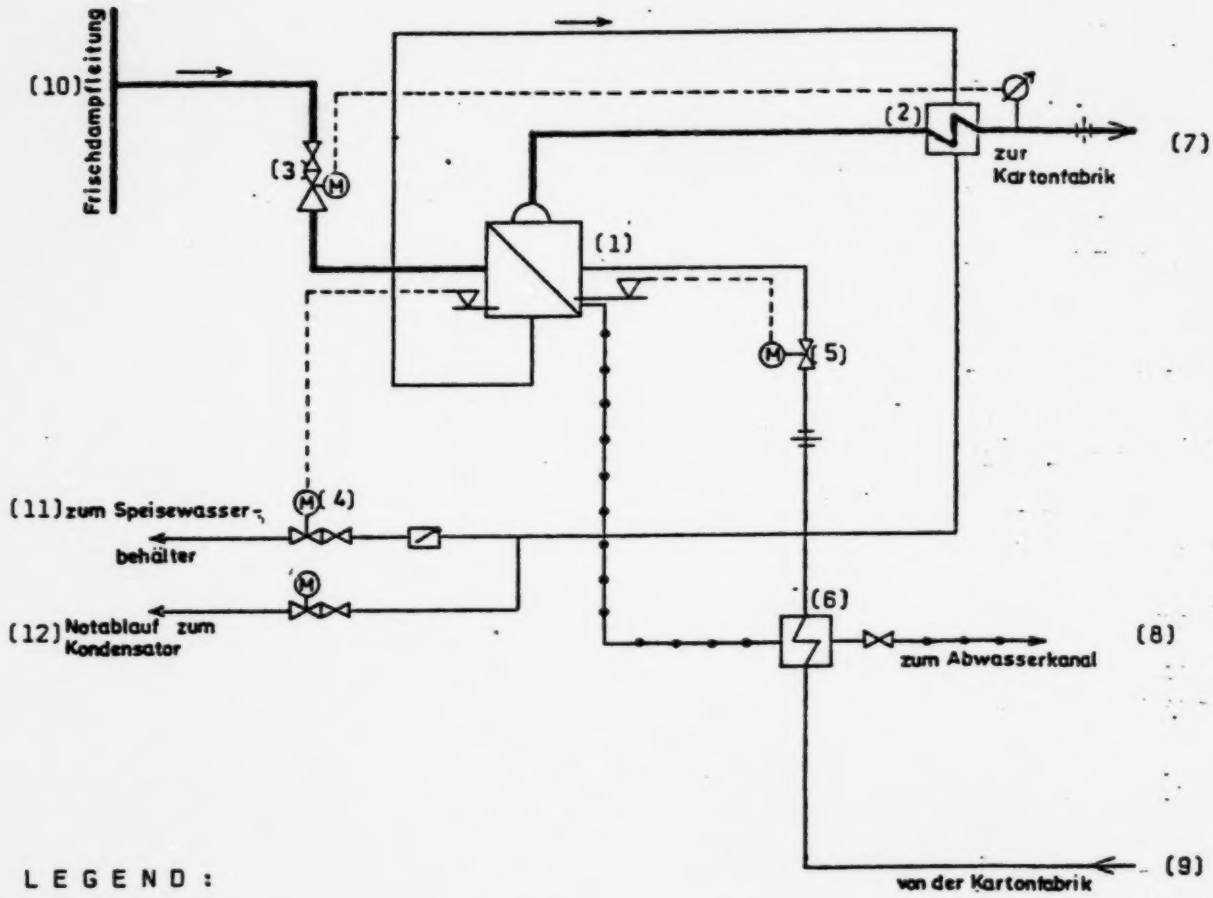

L E G E N D :

(1) Evaporator

(2) Superheater

(3) Pressure reducing station

(4) Heating steam drain outlet-control station

(5) Evaporator inlet-control station

(6) Blowdowncooler

(7) To the cardboard plant

(8) To the water treatment plant

(9) From the cardboard plant

(10) Live steam line

(11) To the feedwater tank

(12) Emergency drain to the condenser

SESSION IX-B

THERMAL DISCHARGE VI

PB82-228552

FINITE ELEMENT MODELING OF A COMPLEX EMBAYMENT SYSTEM

Donald P. Galya
Paula M. Colangelo

Stone & Webster Engineering Corporation
Boston, Massachusetts

ABSTRACT

In a preliminary feasibility study for a new coal-fired electric generating station at Boston Edison Company's Edgar Station site, three candidate diffuser locations in the Hingham-Hull-Quincy embayment system were evaluated for their suitability as waste heat disposal sites. A pair of two-dimensional, time-dependent, finite element models, CAFE-1 and DISPER-1, were selected for this purpose. CAFE-1, a hydrodynamic model, was used to simulate water surface elevations and vertically averaged velocities in the embayment system. DISPER-1, the companion dispersion model, was used to predict far-field temperature distributions resulting from the waste heat discharged at each of the three candidate sites. During the course of the study, DISPER-1 was modified to allow the use of a spatially variable dispersion coefficient. This modification provided a more realistic simulation of dispersion processes in the complex embayment system and solved stability problems that had developed during application of the model.

1. INTRODUCTION

In the present study, a pair of two-dimensional finite element models, a hydrodynamic model and a dispersion model, were applied to predict impacts related to thermal discharges in the complex embayment system composed of Hingham Bay, Hull Bay and Quincy Bay. This embayment system is shown in Figure 1. Three candidate diffuser locations, shown in Figure 1, were evaluated for their suitability as waste heat disposal sites. This effort was part of a preliminary feasibility study for a new coal-fired electric generating station at Boston Edison Company's Edgar Station site.

In the course of the study, stability problems were encountered during the application of the dispersion model. These problems were resolved by using a spatially variable dispersion coefficient. This also resulted in a more physically realistic representation of the dispersion processes in the study region. Therefore, while a homogeneous dispersion coefficient can usually be used to obtain satisfactory results in dispersion studies employing two-dimensional numerical models, complex hydrodynamic systems may require the use of a spatially variable dispersion coefficient, which will more accurately represent the dispersion process and may aid in reducing numerical instability.

© Stone & Webster Engineering Corporation (1981)

Preceding page blank

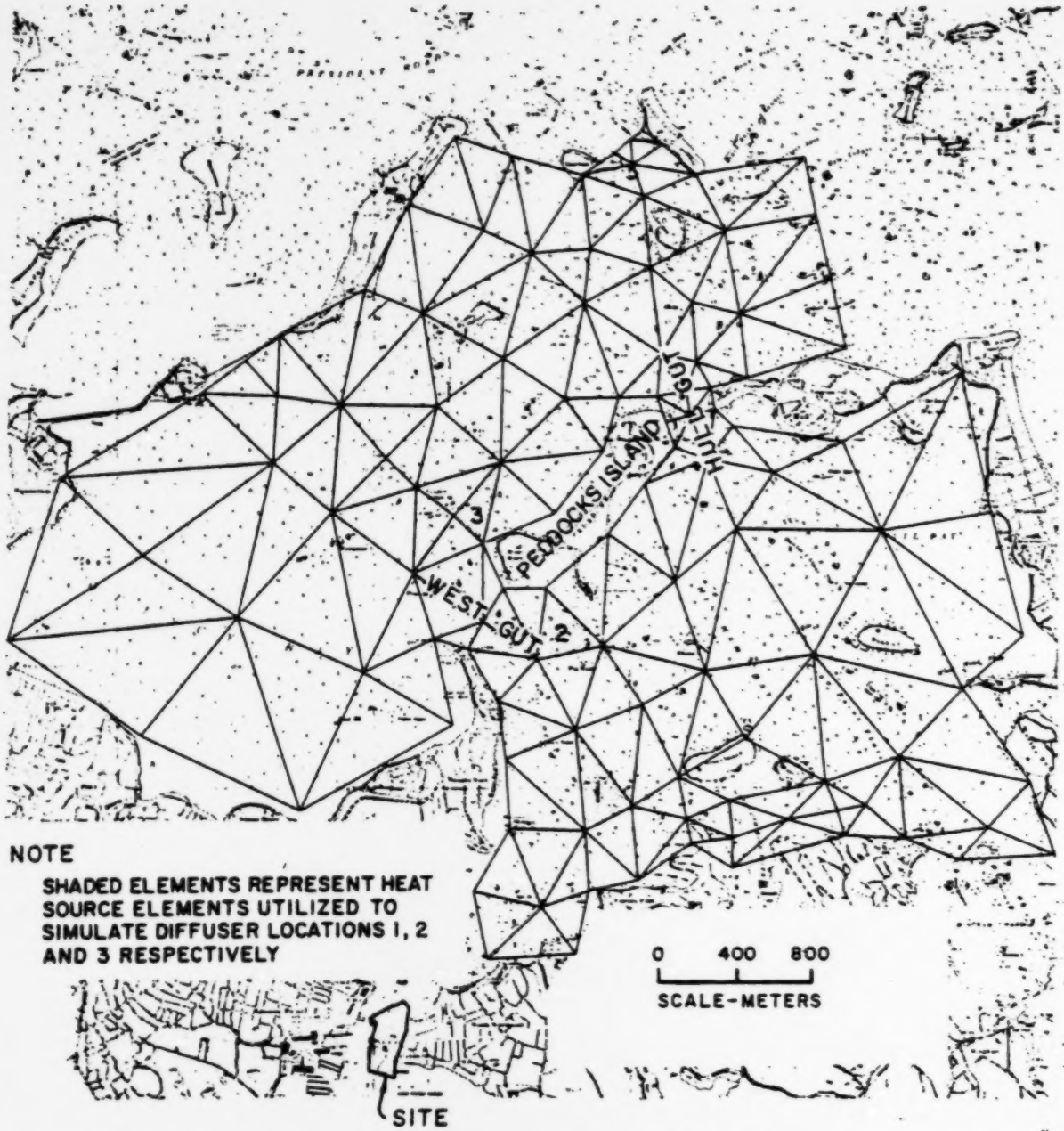

FIGURE 1
FINITE ELEMENT GRID AND STUDY AREA

2. MODELS USED

The models used in this study, CAFE-1 and DISPER-1, are two-dimensional, time-dependent models that were developed at the Massachusetts Institute of Technology[1,2]. These models have been successfully applied in several dispersion studies[2,3].

CAFE-1 is a hydrodynamic model that uses input parameters such as study area geometry, bottom roughness, and boundary tidal fluctuations in solving the vertically integrated equations of conservation of mass and momentum. The output from CAFE-1 consists of tidal heights and vertically integrated velocities within the region of computation.

DISPER-1 is a dispersion model used in the present application to predict temperatures above ambient (ΔT) due to the introduction of a source of heat. DISPER-1 accepts input parameters such as study area geometry, dispersion coefficient, atmospheric heat exchange coefficient, and temporally varying values of water velocity and depth at grid points within the solution field. The model employs these parameters in solving the vertically integrated form of the convective diffusion equation.

Both CAFE-1 and DISPER-1 employ the finite element method to solve the basic equations mentioned above. The finite element method provides a high degree of solution accuracy compared to other numerical methods while permitting great flexibility in the expression of geometry, boundary conditions and input parameters. In employing the finite element method, the study area is subdivided into an array of discrete elements. The finite element array developed for a study region is determined primarily by the geometry of the area and the objectives of the study. In particular, geometric constraints dictate that smaller elements must be used in narrow, channelized regions. Also, if the objective is to examine the dispersion of a discharged substance as in the present study, resolution of the grid should be greater in the vicinity of discharge than at locations where concentrations (or temperatures) and gradients are small. The finite element array developed for use in the present study is shown in Figure 1.

3. INITIAL MODEL APPLICATION

3.1 CAFE-1

Boundary conditions employed in this application of CAFE-1 are of two types, open ocean boundaries and fixed land boundaries (see Figure 1). At the four open ocean boundaries, tide data were prescribed in terms of tidal amplitude and tidal period. For the fixed land boundaries, an impermeable land condition was assumed.

Eddy viscosity values, bottom friction factor values, and the time step for initial runs were estimated from guidelines given by Wang and Connor[1]. Depths for the grid system were obtained from National Ocean Survey Nautical Charts[4]. The depth at each node was determined from chart values in the vicinity of each node.

Initial attempts to obtain results from CAFE-1 were hampered by stability problems. The source of the instability was located in the areas of Hull Gut and along the southern border of Peddocks Island. The reasons for the instability were determined to be rapid changes in element size in the area of Hull Gut and large variations in depths from node to node at both locations. The problem in Hull Gut was resolved by increasing the size of the elements and correspondingly decreasing the depth to maintain similarity of cross-sectioned area and flow. Water depths at nodes along Peddocks Island were modified to minimize abrupt

changes while maintaining the character of the bottom topography. In addition, bottom friction factors at the problem locations were increased slightly to damp oscillatory wave formation.

The CAFE-1 model was calibrated using Tide Table data[5] and NOAA tidal current charts[6] for Boston Harbor. Tidal period and elevations from the Tide Tables were specified at the open boundaries. Bottom friction factor values in various elements were adjusted so that predicted current velocities agreed well with corresponding NOAA[6] measurements. The results obtained from the calibration effort are presented in Figure 2. The results from this effort subsequently were used as input to DISPER-1.

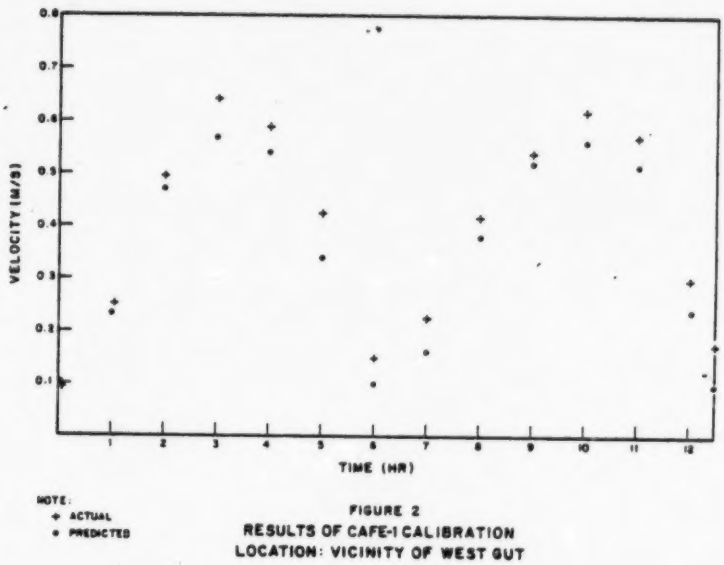

FIGURE 2
RESULTS OF CAFE-1 CALIBRATION
LOCATION: VICINITY OF WEST GUT

3.2 DISPER-1

Input parameters to DISPER-1 included velocity and water level data from CAFE-1, a boundary condition ΔT of zero degrees at the open boundaries and a surface heat transfer coefficient of 100 Btu/ft^2 °F day. Three separate runs were made, one for each of the three candidate diffuser sites under consideration. Heat at the rate of 5.08 x 10^9 Btu/hr was introduced to the system via a source element in the vicinity of the diffuser location under consideration.

In the absence of a dye survey in the study region, the value used for the dispersion coefficient must be based on engineering judgment. Initial attempts were made to run DISPER-1 with a homogeneous, isotropic dispersion coefficient of 30 m^2/sec, a value which had been found to yield satisfactory results in previous studies in Massachusetts Bay[7,8,9]. These attempts were thwarted by stability problems, the source of which were determined to be located around the regions of Hull Gut and West Gut.

Two test cases were run in order to determine the reason for the instability. For the first case the advective transport was eliminated by setting the velocities equal to zero. In the second case, the dispersion coefficient was increased by an order of magnitude, to

300 m^2/sec. Both cases resulted in stable (though somewhat unrealistic) solutions. This indicated that the stability criterion[7]

$$E/(U\Delta S) > 1/2$$

where

E = dispersion coefficient
U = velocity
ΔS = grid size

was being violated at some point during the computation. Hand calculation of values of $E/(U\Delta S)$ confirmed this.

Examination of the stability criterion indicated that there were three possible pathways to improve the computational stability: a) increasing the dispersion coefficient; b) decreasing the velocity; and c) decreasing the grid size.

Increasing the dispersion coefficient throughout the grid did yield a stable solution; however, the value had to be increased to 300 m^2/sec in order to do so. This value, while realistic for portions of the study region, was judged to be too high for the large embayment areas. This resulted in an unrealistically high dispersion of the discharged heat and thus, non-conservative results. Reformulating the grid to provide more resolution by using smaller elements in the problem areas was considered but was not done because of the amount of time that would have been required. Furthermore, reductions of mesh size of an order of magnitude would have been required. Therefore, it was decided that the best method within the time available to obtain fairly realistic results that tended to be on the conservative side (due to reduced advection) was to rerun the models, generating reduced velocities by CAFE-1, and using those velocities and a dispersion coefficient of 30 m^2/sec as input to DISPER-1.

4. FINAL APPLICATION

4.1 CAFE-1

In this application of CAFE-1, the same input parameters were used as in the initial application except that the tidal amplitude at the open ocean boundaries was reduced by approximately 40 percent. This resulted in velocities approximately 40 percent lower than the original values predicted by the average tidal simulation. The attenuated velocity field for the maximum flood and maximum ebb portions of the tidal cycle are shown in Figures 3 and 4, respectively.

4.2 DISPER-1

The final application of DISPER-1 took place in two phases. In the first phase, the model was run with inputs of a homogeneous dispersion coefficient of 30 m^2/sec and the attenuated velocities predicted by CAFE-1. This case ran longer than the case with the unattenuated velocities but still became unstable before a converged solution was reached.

FIGURE 3
VELOCITY DISTRIBUTION AT MAXIMUM EBB

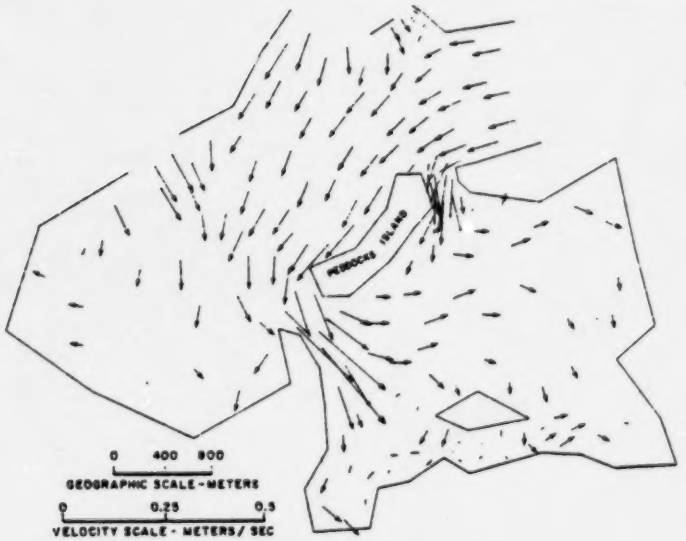

FIGURE 4
VELOCITY DISTRIBUTION AT MAXIMUM FLOOD

Rather than reduce the velocities still further, to what would have been an unrealistic level, it was decided that a different approach would be taken. Reformulating the grid was again considered at this point in the study but was not implemented because in order to meet the stability criterion it would have been necessary to reduce the size of the elements by an order of magnitude. However, as the problem areas were located near areas of flow constriction where horizontal velocity gradients were high, it was not only acceptable but more realistic to

use a much higher dispersion coefficient in those areas. This was true because the exceptionally high horizontal velocity gradients could not be resolved adequately by the grid. To compensate for this effect, the application of a subgrid scale eddy diffusivity coefficient (ε) was appropriate. Christodoulou et al[7] propose using Equation 1 to estimate ε.

$$\varepsilon = L^2 \sqrt{\phi} \qquad (1)$$

where $$\phi = 2\left(\frac{\partial \bar{u}}{\partial x}\right)^2 + 2\left(\frac{\partial \bar{v}}{\partial y}\right)^2 + \left(\frac{\partial \bar{u}}{\partial y} + \frac{\partial \bar{v}}{\partial x}\right)^2$$

$$L = 0.17 \sqrt{A}$$

$\bar{u}$, $\bar{v}$ = vertically averaged velocities of x, y coordinates, respectively

A = area of element

Application of Equation 1 near the channel areas indicated that it was physically realistic to increase the dispersion coefficient to 300 m^2/sec in those areas. With Equation 1 as a physical guideline and the stability criterion as a check on solution stability, values of dispersion coefficient then were developed for the entire grid.

The values developed varied from 300 m^2/sec in elements in and adjacent to the channel regions, to 30 m^2/sec in the wide open areas of Hingham, Hull, and Quincy Bays. DISPER-1 was modified so that it was able to accept and use a spatially variable dispersion coefficient. Application of the modified version of DISPER-1 with a spatially variable dispersion coefficient successfully produced a stable, realistic temperature solution. The temperature fields obtained at low water slack for each of the diffuser locations are presented in Figures 5, 6, and 7.

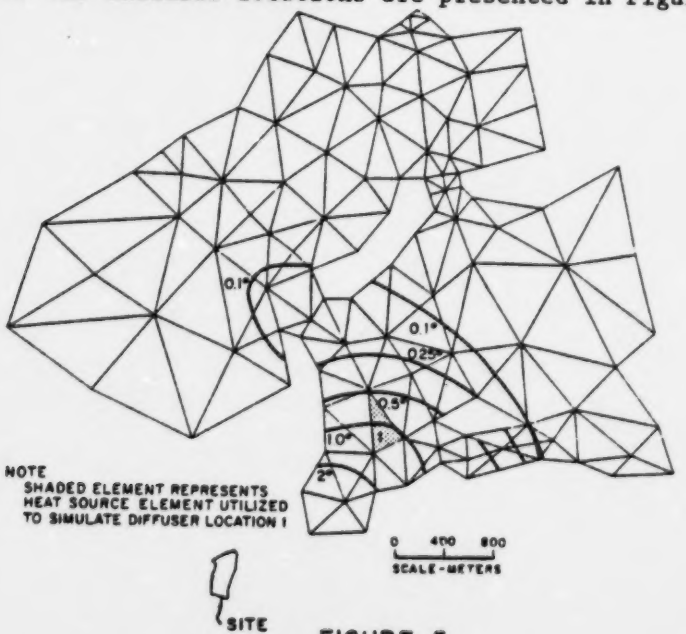

FIGURE 5
ΔT (°F) ISOTHERMS FOR DIFFUSER LOCATION 1 AT LOW WATER SLACK

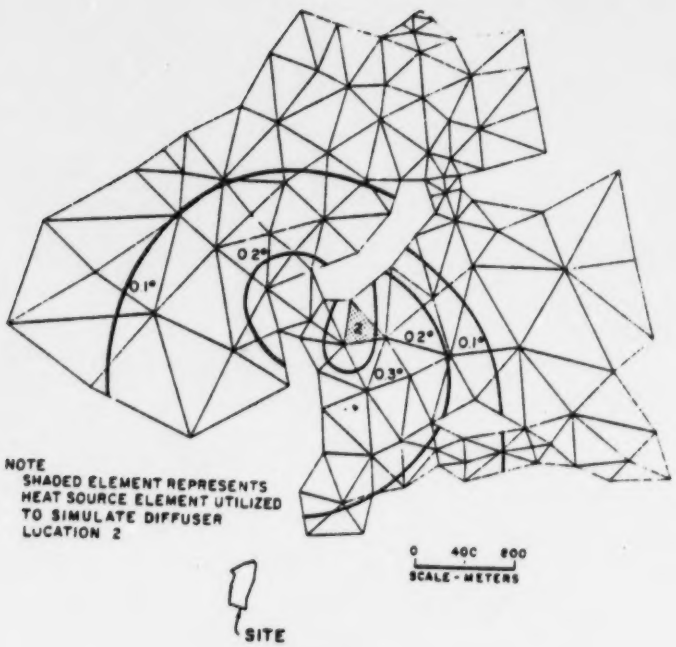

FIGURE 6
ΔT (°F) ISOTHERMS FOR DIFFUSER
LOCATION 2 AT LOW WATER SLACK

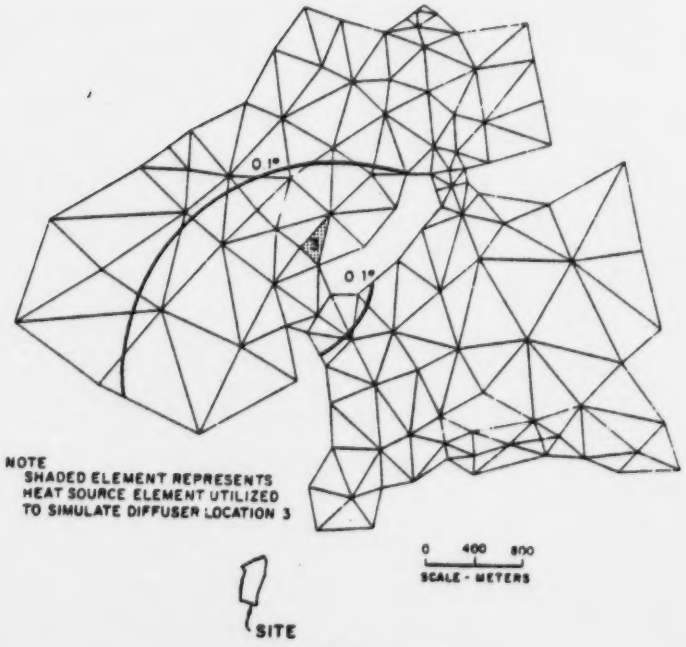

FIGURE 7
ΔT (°F) ISOTHERMS FOR DIFFUSER
LOCATION 3 AT LOW WATER SLACK

5. CONCLUSION

While success has been achieved in the past[2,3] with the use of a homogeneous dispersion coefficient in the application of the finite element model DISPER-1, the experience gained in the present study indicates that this may not be adequate for complex hydrodynamic systems. In these systems, differences in the type of flow regimes may result in a significant variation in dispersion throughout the study region. In addition, the grid system itself may play a role in the spatial variation of the dispersion coefficient. This will occur if the grid does not resolve completely the horizontal velocity field. In these areas, it is physically realistic to adjust the dispersion coefficient from element to element to account for this effect. Thus, in applications of the DISPER-1 model to complex hydrodynamic systems, consideration should be given to using spatially varying values of dispersion coefficient. This will result in a more realistic simulation of the system and may aid in reducing numerical instability.

REFERENCES

1Wang, J.D. and Connor, J.J., Mathematical Modeling of Near Coastal Circulation, Technical Report No. 200, R.M. Parsons Laboratory for Water Resources and Hydrodynamics, Massachusetts Institute of Technology, Cambridge, Massachusetts, 1975.

2Leimkuhler, W.F., et al, Two-Dimensional Finite Element Dispersion Model, Proc. Symp. on Modeling Techniques, Modeling 75, San Francisco, California, 1975.

3Mangarella, P.A., Thermal Impact Modeling in San Francisco Bay, Proc. Specialty Conf. on Conservation and Utilization of Water and Energy Resources, San Francisco, California, 1979.

4National Ocean Survey, NOAA, Bathymetric Chart Number 13270, 43rd edition, U.S. Department of Commerce, 1979.

5National Ocean Survey, NOAA, Tide Tables High and Low Water Predictions: East Coast of North and South America, U.S. Department of Commerce, 1979.

6National Ocean Survey, NOAA, Tidal Current Charts: Boston Harbor, Fourth Edition, U.S. Department of Commerce, 1977.

7Christodoulou, G.C., et al, Mathematical Modeling of Dispersion in Stratified Waters, Technical Report No. 219, R.M. Parsons Laboratory for Water Resources and Hydrodynamics. Massachuetts Institute of Technology, Cambridge, Massachusetts, 1976.

8Pagenkopf, J.R., et al, Circulation and Dispersion Studies at the Pilgrim Nuclear Power Station, Technical Report No. 210, R.M. Parson Laboratory for Water Resources and Hydrodynamics, Cambridge, Massachusetts, 1976.

9Pearce, B.R. and Christodoulou, G.C., Application of a Finite Element Model for Coastal Waters, Proc. XVI International Association of Hydraulic Research Congress, Sao Paulo, Brazil, 1975.

SESSION IX-C

MANAGEMENT & REGULATION

Preceding page blank

PB82-228560

REGULATORY REQUIREMENTS FOR THERMAL DISCHARGES AND DEMONSTRATION OF COMPLIANCE

N.S. Shashidhara
Envirosphere Company
A Division of Ebasco Services Incorporated
Two World Trade Center
New York, New York 10048, U.S.A.

ABSTRACT

The Clean Water Act (ACT) prohibits thermal discharges into public waters without a permit and attempts to control thermal discharges through one of the following approaches: Effluent Limitations or Section 316 (A) Demonstrations and Water Quality Standards. Effluent limitations are intended to control pollutants (under the ACT heat is considered a pollutant) through controlling their discharge from particular sources. Water quality standards, on the other hand, attempt to control water pollution through controlling the concentration of pollutants allowed in a waterbody. Section 316 (A) of the ACT allows variance from any such limitations if the discharger can demonstrate that such limitations are more stringent than necessary to assure the protection and propagation of a balanced indigineous population of shellfish, fish and wildlife in and on the body of water into which the discharge is to be made.

To ensure non contravention with these regulatory requirements as well as to demonstate that compliance is maintained prediction of the effects of thermal discharges as well as monitoring of thermal plume in the receiving water body (RWB) is required. Methods of predicting or demonstrating compliance with these regulatory requirements will be discussed in this paper. Criteria for demonstration of the conformity of predictive models and prototype results are also included. Case studies will be used to provide insight into "problem areas" associated with compliance demonstration and these studies can serve as one basis for recommending guidelines for future compliance demonstrations.

1. INTRODUCTION

The permits and certifications which are required for Power Plant construction and operation under the Clean Water Act are:

- Section 401 Certification
- Section 402/National Pollutant Discharge Elimination System (NPDES) Permit
- Section 404 Permit/Rivers and Harbors Act Permit

Clean Water Act Section 401 certification requires that a proposed new source must obtain a certification from the State in which the discharge will occur. This certification is intended to ensure that discharges from the source will comply with the federal ACT and state water requirements. No

Preceding page blank

Federal permit can be issued until this is obtained. One certification can be used for all Federal permits. Section 402 of the ACT provides for the creation of a NPDES permit program. The section authorizes and directs the Adminstrator to issue a permit to all point source discharges into navigable waters only after assuring that the applicable effluent standards and water quality standards will be complied with. EPA (and under some conditions the State) issues both a construction and operation stage NPDES permit for a new plant. NPDES permit application requires demonstration of compliance with effluent limitations, state water quality standards and (if desired) a 316 (A) thermal variance demonstration. Section 404 (Corps of Engineers) permit does not deal with thermal discharges directly and hence is not discussed here.

Water quality standards contain three major elements: The use to be made of the navigable waters; criteria to protect these uses and an antidegradation statement to protect existing high quality waters from degradation by the addition of pollutants. Water quality standards consider size and nature of the RWB (surface or ground water), seasonal effects, type of species in the RWB, water use, etc.

A review of the (i) July 1980 USEPA Publication(1) "Water Quality Standards Criteria Digest" and (ii) monitoring requirements of several states that require demonstration of compliance shows that the language of permits generally read as*:

1. The areal extent of ___^{o}F isotherm of temperature rise shall not exceed a mixing zone of ___ acres,

2. The maximum temperature rise after a reasonable mixing with RWB, either at the surface or at the bottom, shall not exceed ___^{o}F,

3. The maximum temperature (absolute) after a reasonable mixing shall not exceed ___^{o}F, and

4. The temperature at the point of discharge (POD) shall not exceed either ___^{o}F above the RWB temperature or a maximum of ___^{o}F.

Generally, at the pre-operational stage, mathematical and/or physical model studies are performed to predict thermal discharge effects. Similarly, at the post-operational stage field surveys are performed to verify the predictions made earlier and to amend the results, if needed. Utilizing the results of these studies, compliance with permit requirements is demonstrated.

2. METHODS FOR DEMONSTRATING COMPLIANCE

2.1 Mathematical Models

The principle advantage of mathematical modeling for temperature prediction is the fact that it can be applied to different plant design, operation and ambient conditions. Disadvantages, however, are that most mathematical models provide comparatively little physical insight. Also, there are certain fundamental physical (input) parameters which must

---

*Since the numerical limits stipulated in the regulatory requirements differ from case to case, these limits have been omitted to avoid confusion.

be obtained either from field or physical model studies and incorporated in the mathematical model.

Different types of mathematical models for both surface and submerged discharges into different types of receiving waters (lakes, rivers, oceans, estuaries and cooling ponds) are discussed in references 2 and 3. Models can be grouped into (1) integral (2) differential-numerical (3) phemenological, and (4) subchannel balancing method. Exhibit 1 represents components of a mathematical model approach for demonstrating compliance at the design or conceptual engineering stage. In the application of modeling, it is essential for the user to understand required input data for modeling and limitations of the model itself. Ambient data (flow, velocity, bathymetry, temperature, dispersion characteristics and meteorological conditions) has to be properly evaluated. Plant related data includes discharge structure design, velocity, excess temperature, different operational modes and discharge conditions.

At the post-operational stage, when a mathematical model is utilized for thermal plume evaluation, the model has to be first calibrated with appropriate plant design, operation and ambient conditions. Once calibrated with actual field data, the model can be applied to other seasonal/operational conditions. A typical flow diagram for calibrating a model is shown in Exhibit 2. This exhibit shows the calibration procedure for a plant located beside a river between two Gaging Stations, Station 1 and 2.

2.2 Physical Hydraulic Models

Unlike mathematical modeling, physical models can include complicated geometry, flow and boundary conditions for site specific situations. Physical modeling serves several purposes: (a) Quantitative estimates of plume temperature and flow characteristics, (b) provides qualitative visualization of plume and flow characteristics, (c) provides better understanding of the phenomenon influencing the plume behavior and (d) provides a better visual demonstration for the laymen. Restrictions for physical modeling, however, are (a) generally more expensive than mathematical modeling (b) more time consuming (c) one single physical model cannot model both near and far field regions of the plume.

Prior to the construction and operation of physical models it is best to conduct a preliminary evaluation of the plume utilizing mathematical models. This will provide some measure of the plume temperature, velocity and extent and assist the modeler in choosing model scale and dimensions for the model basin. Physical modeling requires that meaningful relations be established between model and prototype. It is generally impossible to simulate all the phenomena which occur in a prototype in a single model and hence a judicious selection has to be made as to which physical processes are considered more important than others. Sometimes coupling of mathematical models (for jet mixing region and transient far field region) and physical models (for near field region) seems like an optimum approach. The schematics of physical model study and parameters influencing the plume are presented in Exhibit 3.

2.3 Field Surveys

As part of various environmental licensing documents, a utility is required to submit a planned post-operational monitoring program. However, inorder to assess the impact of thermal discharges a baseline (pre-operational) monitoring is also required. Objective of these

pre-operational studies are to establish a basis for post-operational compliance with water quality standards.

The pre-operational survey has been as short as few months and has gone as long as 3 to 4 years. The monitoring activities generally cover bathymetry, temperature and current measurements at two or three depths, diffusion/dispersion measurements (Dye/Drogue), water quality, meteorological parameters, tide/wave observations etc. A thorough examination of available literature should definitely be a part of the survey. The emphasis at the pre-operational stage is to provide input for modeling, design, siting criteria and generally define base line conditions.

Post-operational monitoring is oriented towards assessment of plant induced changes and demonstration of compliance. In this sense, it has a more narrow but specific focus than pre-operational survey. However, the monitoring effort is more difficult and involved because evidence of operational impact will have to be conclusively documented and regulatory compliance proven. Greater monitoring emphasis should be placed in those portions of an RWB (such as shorelines, bottom, mixing zone, etc) where measureable impact is expected . Monitoring should envelope all affected volumes of the waterbody down to the point where the temperature differential is about $1^{o}F$. As before, measurements of bathymetry, temperature and currents, meteorological parameters, and water quality are made. However, because of its regulatory implications temperature monitoring becomes the primary issue. Depending upon the permit requirements, Triaxial mapping (Boat Survey) and/or aerial infrared scanning methods are frequently employed for plume temperature definition and mixing zone compliance. Selection of a particular monitoring program depends on the approach to be used in verifying a discharge system's performance and demonstrating compliance. For example, for water quality standards which require measurements a certain distance below the water surface or on the bottom, infrared scanning method maybe less satisfactory. One real problem during the post-operational survey lies in the definition and determination of "ambient temperature".

Triaxial survey methods provide three dimensional thermal picture. In this case, the spatial resolution is determined by boat transects. To obtain an acurate mapping of a meandering thermal plume and "hot spots" (maximum surface temperature) the field survey team is faced with a dilemma of obtaining data over a short enough period of time to justify synopticity and yet perform enough number of transects to clearly identify the plume and its boundaries.

Speed of data acquisition (i.e synopticity) and extent of aerial coverage makes infrared scanning superior to triaxial method. The application of infrared surveys is restricted to surface area and skin temperature measurements and does not provide three dimensional features. Furthermore, water surface layer and atmospheric influences may distort the plume picture making infrared scanning as only a qualitative tool[4]. Envirosphere surveys have indicated that when suitable ground truth information is utilized infrared survey results compare favourably with those from Triaxial mapping.

3. CASE STUDIES

3.1 Case Study: One

At the request of a utility company, Envirosphere Company, performed combined triaxial mapping and airborne infrared scan surveys. The purpose was to verify compliance of thermal discharges from an ocean diffuser with applicable regulations. The regulations required that the surface areal extent of ___ ^{o}F isotherm of temperature rise (i.e., ISOTHERM AREA) shall not exceed a mixing zone of _____ acres.

The scope of the study included a field monitoring program, performed under known plant operating conditions, and verification of the mathematical models previously used for the design of the diffuser system. The field surveys included definition of ambient conditions, mapping of temperature distribution at three water depths and airborne infrared thermal imagery. Verification of the mathematical models involved predictions of ISOTHERM AREAS and comparison with corresponding results from the field measurements.

Upon completion of the field program the following data were processed: (i) moored thermographs and current meter data, (ii) data from each near and far-field survey and (iii) infrared imagery for the overflights.

Analysis of the data revealed that the natural conditions at the time of the survey were quite complex and showed significant temporal and spatial variations. These variations reflected possible effects of the inlets along the coastline, upwelling and downwelling phenomena, solar heating, and large scale offshore currents andwarm streams. The ISOTHERM AREA (whose area was required for compliance demonstration) was completely masked by the horizontal temperature variation in the local natural environment. In such cases, the plume and ISOTHERM AREA were delineated by a minimum temperature boundary as shown in Exhibit 4. In this exhibit (from the triaxial survey) the plume boundary could be identified by a pocket of cold water enclosed by the isotherms between the plume axis (arrows in the exhibit) and warm water along the shore. The pocket of cold water was separated from a trough of cold water further to the north by a warm water ridge extending seaward. The seaward boundary of the plume only partially separated the plume from warm ambient waters offshore. The ISOTHERM AREAS obtained from infrared scanning (Exhibit 4) compared favorably with those obtained from triaxial mapping. During the field survey, whenever a strong horizontal temperature stratification was present, the ISOTHERM AREA was found to be significantly smaller compared to those cases when the ambient was nearly isothermal. The ISOTHERM AREAS demonstrated compliance with regulations. Mathematical models (integral and phenomenological techniques, particularly) were found to conservatively overestimate the area whenever the ambient was non-isothermal. Thus proper calibration of the model with results from field data became an essential part of the compliance demonstration.

3.2 Case Study: Two

In the second case, where the discharge was through a submerged diffuser, the maximum surface temperature rise (or the 'hot spot' temperature rise) was not to exceed _____ ^{o}F.

A demonstration of compliance was performed using a triaxial survey. Whenever thermal mapping of the near-field is involved, high resolution of measurements is needed because of the rapid rate of change of temperature due to turbulent jet entrainment and large thermal gradients in small distances. Vertical temperature profiles were also measured (at several depths and several points in and out of the plume zone) using thermistor probes and a deck readout unit.

Preliminary surveys showed that the position of the 'hot spot' varied from instance to instance. This, in addition to strong jet induced velocities and extreme horizontal and vertical temperature stratifications suggested that the use of permanently moored (in-situ) instrumentation would not be suitable for 'hot spot' temperature measurements. During the survey one boat transect intersected the boil spot to observe the peak surface temperature. The triaxial survey provided a high density of temperature measurements to define the plume and the hot spot temperature.

Upon completion of the survey a comparison of the results from mathematical models (integral techniques) and field survey was made. It was found that if an assumption of isothermal ambient field is made (i.e. 70°F in the example, below), then the predicted results would be considerably higher than the field data (i.e. 78°F vs 73°F). On the other hand, when the representative temperature that is entrained into the discharge plume was incorporated (item ii) the predicted and the field results compared well.

The following example illustrates this point:

(i)	Jet Discharge Temperature:	95°F
(ii)	Representative Temperature of Entrained Water	66°F
(iii)	Surface Temperature:	70°F
(iv)	Actual Discharge Temperature Rise:	29°F
(v)	Predicted Results	
	-hot spot temperature rise:	8°F
	-hot spot temperature with reference to item iii:	78°F
	-hot spot temperature with reference to item ii	74°F
	-hot spot temperature rise for regulatory compliance:	4°F
(vi)	Measured Results	
	- Measured hot spot temperature:	73°F
	- hot spot temperature rise for regulatory compliance:	3°F

After the mathematical model validity was demonstrated, the model was used for other operating/ambient conditions.

3.3 Case Study: Three

In this situation for a coastal site (once-through cooling plant) the regulations required that all temperature standards be met at the discharge point, i.e. no allowance of mixing zone for thermal discharges was to be provided. It was demonstrated that these regulations could not be met even by utilizing a closed cycle cooling system.

State regulations related to thermal mixing zones can be classified into four categories: (i) Explicit provision for mixing zones, (ii) Implicit provision for mixing zones, (iii) Mixing zones not discussed or implied and (iv) Explicit exclusion of mixing zones. That is, some state regulations indicate that the mixing zone concept as applied to thermal discharges is not a viable approach and have specifically excluded its use in order to achieve water quality standards. Some other state regulations indicate that such 'explicit exclusion' apply to all RWB's while some others refer to specific RWB's. The July 1980 EPA publication[1] on 'Mixing Zones' indicates that "If no such zone is recognized by a State, then waters must meet the criteria at the point of discharge."

For the plant considered in this case study, which is situated adjacent to a coastal body of water the regulations did not allow any mixing zone. The plant site was considered optimum for once through cooling from all other considerations (discharging at an offshore distance of about 1500 to 2000 feet). On behalf of the utility, Envirosphere Company held meetings with regulatory agencies and conducted public workshops to discuss topics such as: (i) Purpose of a mixing zone, (ii) Definition of significant adverse environmental impact, (iii) Economic quantification of biological impacts, (iv) Site Specific (or Case Specific) monitoring requirements, (v) Related Case Histories, (vi) Feasibility of closed cycle cooling to meet the state water temperature standards, and (vii) Cost-benefit analysis.

It was shown in these meetings why the regulations related to heated discharges should include allowance for mixing zones. It was demonstrated that (i) Even with a change in plant design to a more expensive closed cycle cooling system (tower or spray system) discharging about one to two percent of the plant's waste heat as blowdown, the regulations could not be met, (ii) the national policy goals/attitudes with respect to the concept and application of mixing zones (delineated in three documents, which are familiarly called the Green, Blue and Red Books - see Appendix one) advocates and is consistent with the use of mixing zones, (iii) the technological "tools" are available to develop the data and information essential to the decision making process, (iv) That mixing zones have been successfully used without significant adverse environmental effect across the country, and (v) the agencies should consider taking the formal position that the mixing zone concept should be considered applicable to the discharge of heat on a case-by-case basis. The allowance and size of the mixing zone would be determined upon demonstration that no significant adverse environmental effects would result and in consideration of alternatives available and the costs and benefits associated with each.

As a result of all these considerations presented by Envirosphere Company, the regulatory authorities modified the discharge permit to include a mixing zone.

3.4 Case Study: Four

In this case, the discharge temperature or the temperature outside a designated mixing zone was not to exceed _____°F. But it was observed that the ambient temperature, even in the absence of plant discharges had exceeded the stipulated temperature.

In order to comply with this regulation in a strict sense would mean 'zero discharge' (at a considerable economic penalty) during those times when the RWB temperature equals or exceeds that stipulated in the standards. Conventional methods of cooling could not produce the sufficiently low discharge temperatures. Other schemes such as (a) dilution (b) discharging blowdown into a ground water acquifer were also considered.

Dilution scheme was not found to be a suitable alternative because,

(i) dilution of the discharge with water which already has reached the limiting temperature would not help in meeting the standards, (ii)cost of pumping increases, (iii) mechanical stress and thermal shock increase, and (iv) impingement loss increases.

Discharging blowdown into a ground water aquifer was also found not feasible since the discharged water would eventually reach the RWB after a certain time lag (2 to 3 months) and temperature would not decay enough to meet the standards applicable at the time when the ground water plume would enter the RWB.

The utility company then obtained a variance from applicable water quality standards by (i) demonstrating to the permitting authorities that the RWB reaches limiting temperature conditions infrequently, (ii) demonstrating no adverse environmental impact and economic hardship, and (iii) demonstrating that they had considered best of all available approaches to control thermal discharges.

4. CONCLUSIONS

Based on the experience gained from actual studies (analytical and physical model studies and field monitoring programs) criteria for demonstration of (i) model vs prototype conformity and (ii) compliance with regulatory requirements have been developed and presented in this paper. These considerations can lead to (i) a refinement and augmentation of water quality standards and (ii) formulations of procedural guidelines for compliance demonstration.

APPENDIX - ONE

National policy goals/attitudes with respect to the concept and application of mixing zones are delineated in three documents which are familiarly called the "Green Book", the "Blue Book" and the "Red Book". With respect to the mixing zone concept, it is interesting to note the different approaches taken over a period of some ten years.

The Green Book took a somewhat passive approach towards the concept of mixing zones, whereas the Blue and Red Books have addressed the concept

directly. More specifically, the Green Book suggests in the section entitled "Zone of Passage" that

> "...any barrier to migration and the free movement of the aquatic biota can be harmful in a number of ways... (Therefore) it is essential that adequate passageways be maintained at all times for the movement or drift of the biota... It is recognized, however, that certain areas of mixing are unavoidable... The shape and size of mixing areas will vary with the location, size, character, and use of the receiving water and should be established by proper administrative authority... (However), mixing should be accomplished as quickly as possible through the use of devices which insure that the waste is mixed with the allocated dilution water in the smallest possible area."

The approach in the Blue Book is significantly different as represented in the following direct quote:

> "A mixing zone is a region in which a discharge of quality characteristics differ from those of the receiving water is in transit and progressively diluted from the source to the receiving system. In this region water quality characteristics necessary for the protection of aquatic life are based on time-exposure relationships of organisms. The boundary of a mixing zone is where the organism response is no longer time-dependent. At that boundary, receiving system water quality characteristics based on long-term exposure will protect aquatic life."

Subsequent to this definition, the Blue Book formally recommends that:

> "To avoid potential biological damage or interference with other uses of the receiving system, it is recommended that mixing zone characteristics be defined on a case-by-case basis after determination that the assimilative capacity of the receiving system can safely accommodate the discharge taking into consideration the physical, chemical, and biological characteristics of the discharge and the receiving system, the life history and behavior of organisms in the receiving systm and desired uses of the waters."

The definition in the Red Book is:

> "A mixing zone is an area contiguous to a discharge where receiving water quality may neither meet all quality criteria nor requirements otherwise applicable to the receiving water. It is obvious that any time an effluent is added to a receiving waterway, where the effluent is poorer in quality, there will be a zone of mixing. The mixing zone should be considered as a place where wastes and water mix and not as a place where effluents are treated."

In essence, the recommendation of the Red and Blue Books are that site-by-site analysis be undertaken in full view of prevailing local situations. This national policy position is not inconsistent with the position that is advocated in the paper.

REFERENCES

1. Water Quality Standards Criteria Digest. A Compilation of State/Federal Criteria U.S.E.P.A. July, 1980.

2. W.E. Dunn, A.J. Policastro, and R.A. Paddock, Surface Thermal Plumes: Evaluation of Mathematical models for the Near-and complete Field. Argonne national Laboratory. ANL/WR-75-3, Illinois 1975

3. G.H. Jirka, G. Abraham and D.R.F. Harleman, An Assessment of Techniques for Hydrothermal Prediction. R.M. Parsons Laborotory, Report No. 203, Mass. inst. Tech. July 1975

4. J.V. Tokar, Hydrothermal and Chemical Monitoring at Nuclear Power Plant Sites: An Overview, Argonne National Laboratory, July 1974.

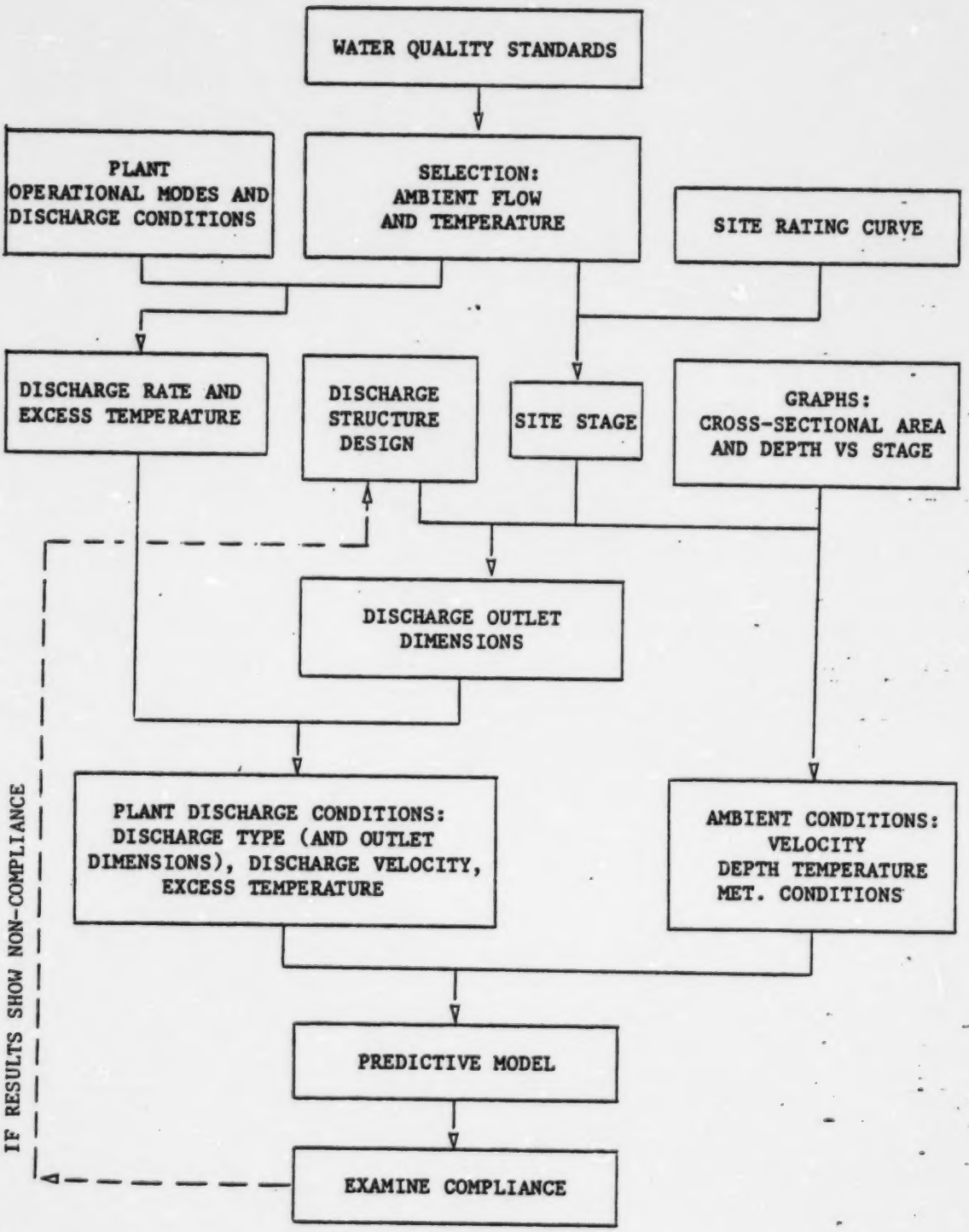
WATER QUALITY STANDARDS
PLANT OPERATIONAL MODES AND DISCHARGE CONDITIONS
SELECTION: AMBIENT FLOW AND TEMPERATURE
SITE RATING CURVE
DISCHARGE RATE AND EXCESS TEMPERATURE
DISCHARGE STRUCTURE DESIGN
SITE STAGE
GRAPHS: CROSS-SECTIONAL AREA AND DEPTH VS STAGE
DISCHARGE OUTLET DIMENSIONS
PLANT DISCHARGE CONDITIONS: DISCHARGE TYPE (AND OUTLET DIMENSIONS), DISCHARGE VELOCITY, EXCESS TEMPERATURE
AMBIENT CONDITIONS: VELOCITY DEPTH TEMPERATURE MET. CONDITIONS
PREDICTIVE MODEL
EXAMINE COMPLIANCE
IF RESULTS SHOW NON-COMPLIANCE

TYPICAL FLOW DIAGRAM: INPUT DATA FOR PREDICTION

EXHIBIT 1

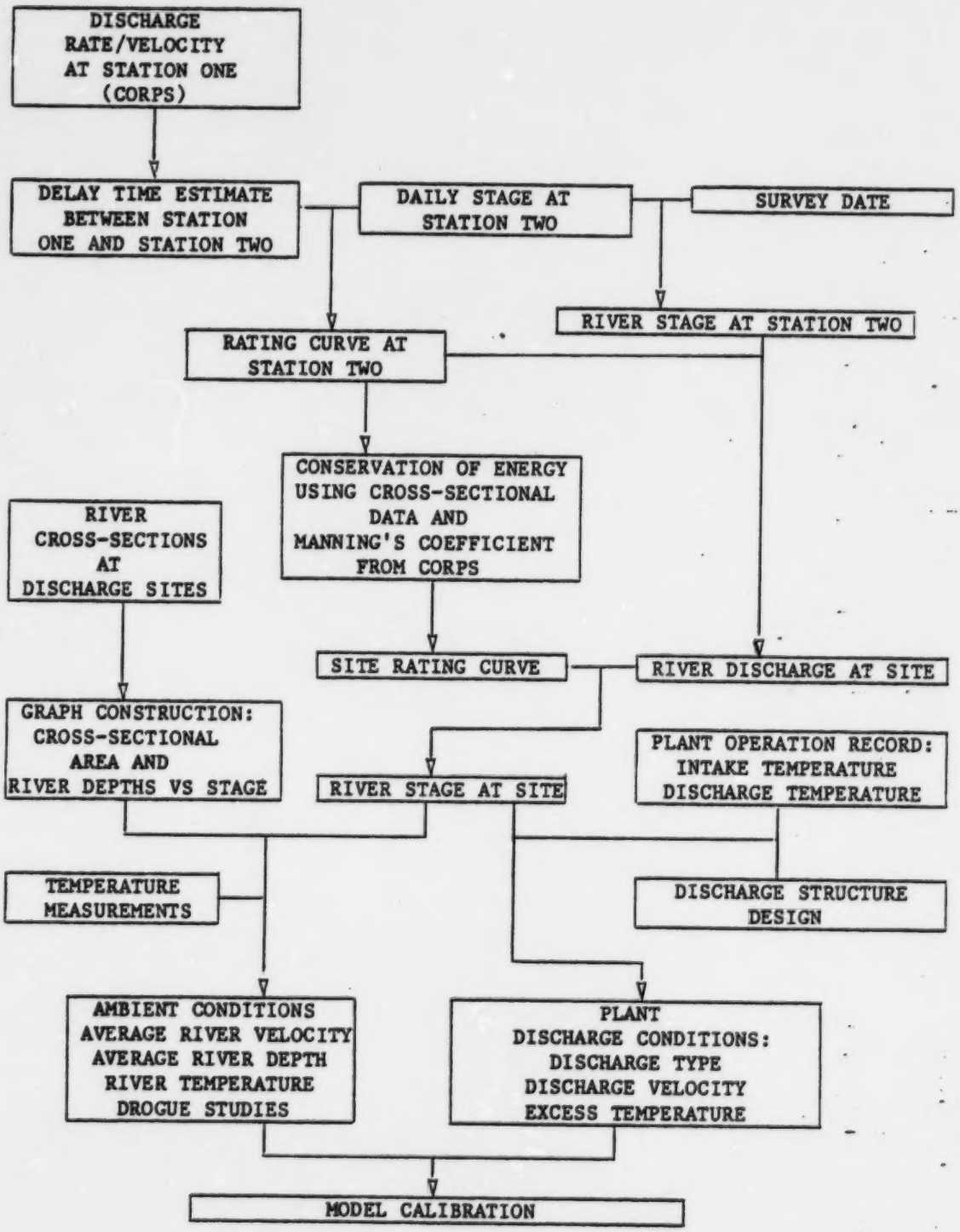
DISCHARGE RATE/VELOCITY AT STATION ONE (CORPS)
DELAY TIME ESTIMATE BETWEEN STATION ONE AND STATION TWO
DAILY STAGE AT STATION TWO
SURVEY DATE
RIVER STAGE AT STATION TWO
RATING CURVE AT STATION TWO
CONSERVATION OF ENERGY USING CROSS-SECTIONAL DATA AND MANNING'S COEFFICIENT FROM CORPS
RIVER CROSS-SECTIONS AT DISCHARGE SITES
SITE RATING CURVE
RIVER DISCHARGE AT SITE
GRAPH CONSTRUCTION: CROSS-SECTIONAL AREA AND RIVER DEPTHS VS STAGE
PLANT OPERATION RECORD: INTAKE TEMPERATURE DISCHARGE TEMPERATURE
RIVER STAGE AT SITE
TEMPERATURE MEASUREMENTS
DISCHARGE STRUCTURE DESIGN
AMBIENT CONDITIONS AVERAGE RIVER VELOCITY AVERAGE RIVER DEPTH RIVER TEMPERATURE DROGUE STUDIES
PLANT DISCHARGE CONDITIONS: DISCHARGE TYPE DISCHARGE VELOCITY EXCESS TEMPERATURE
MODEL CALIBRATION

FLOW DIAGRAM: INPUT DATA
COMPUTATIONS FOR MODEL CALIBRATION

EXHIBIT 2

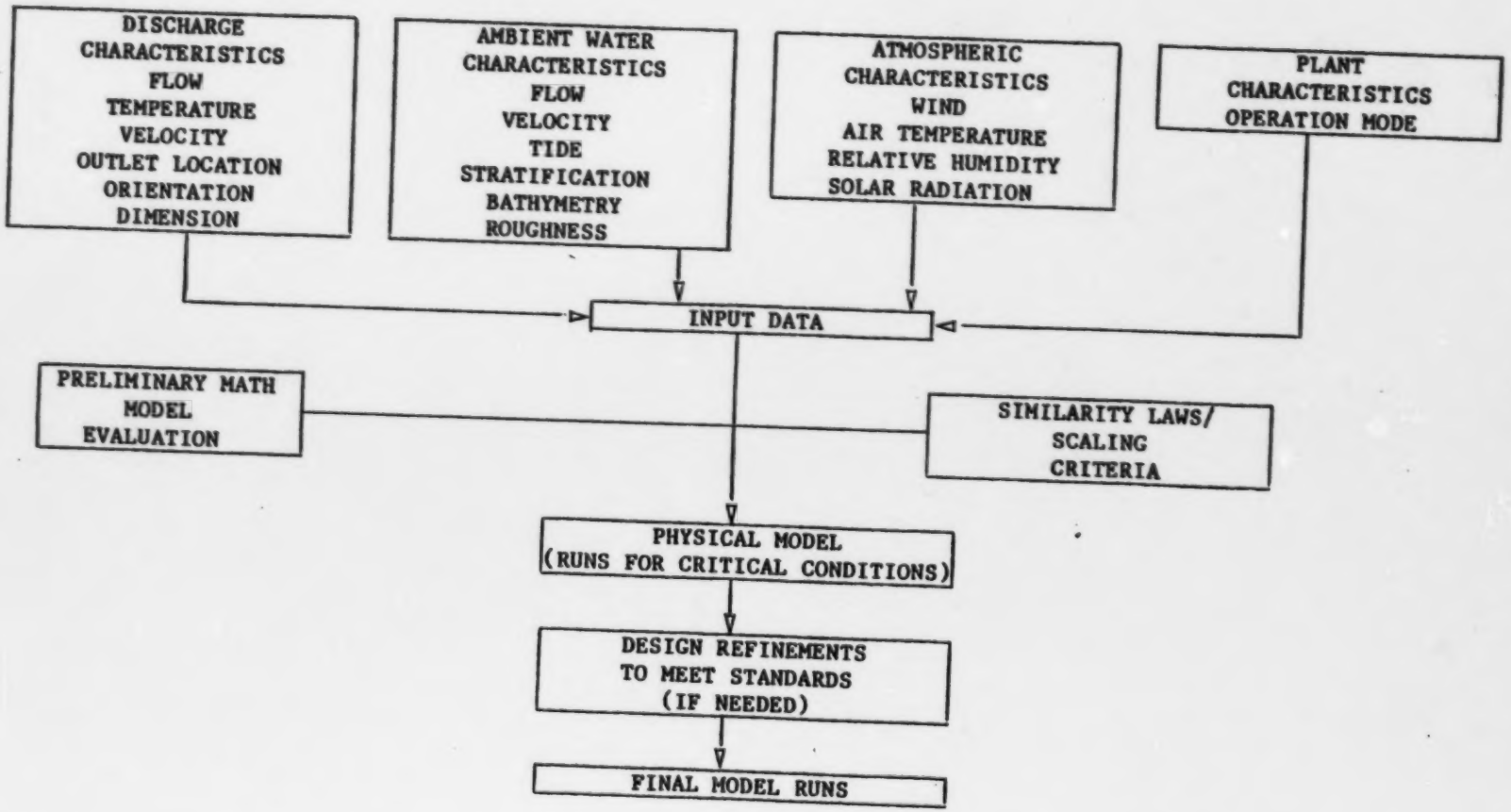

TYPICAL FLOW DIAGRAM: PHYSICAL MODEL STUDY

EXHIBIT 3

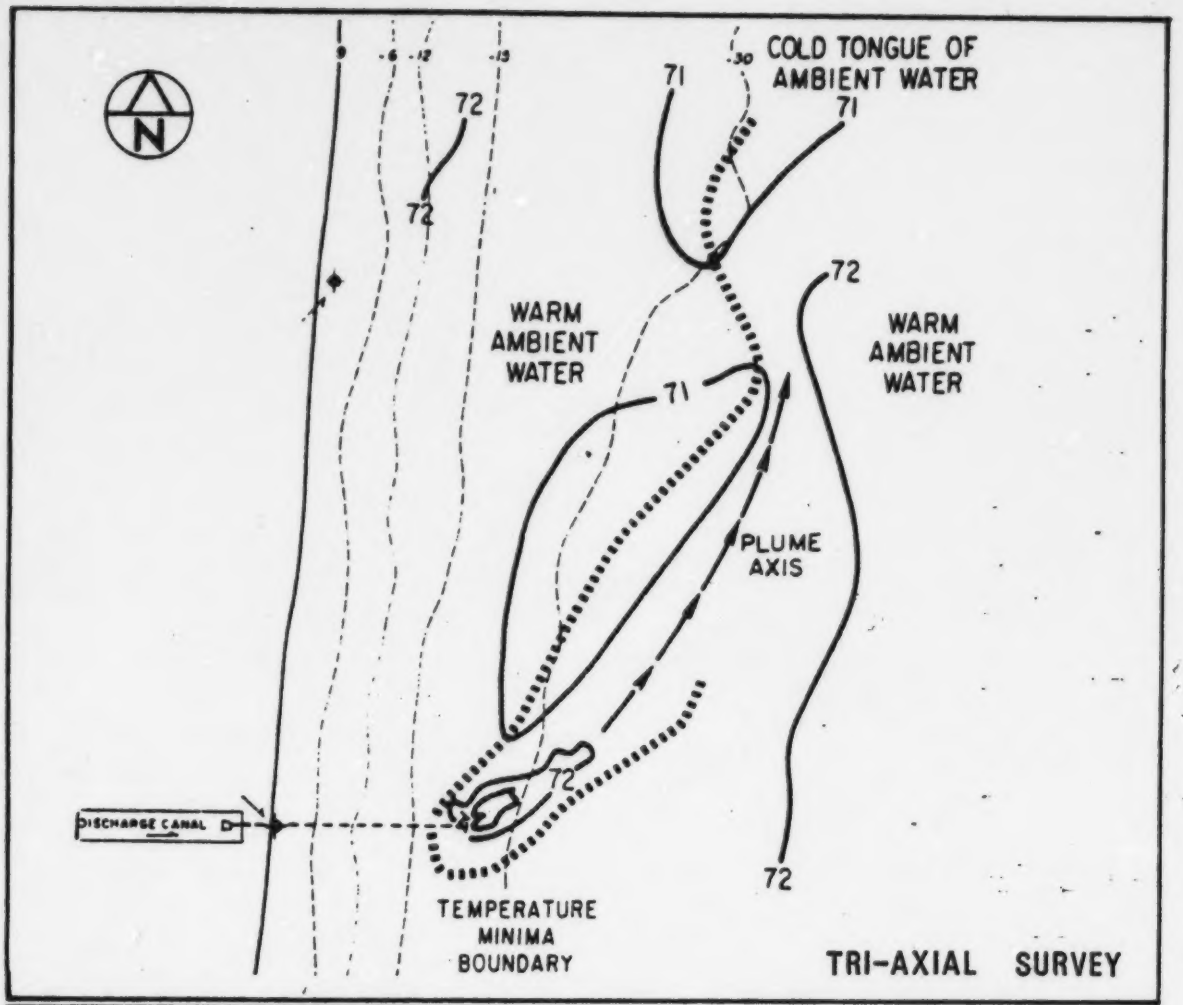

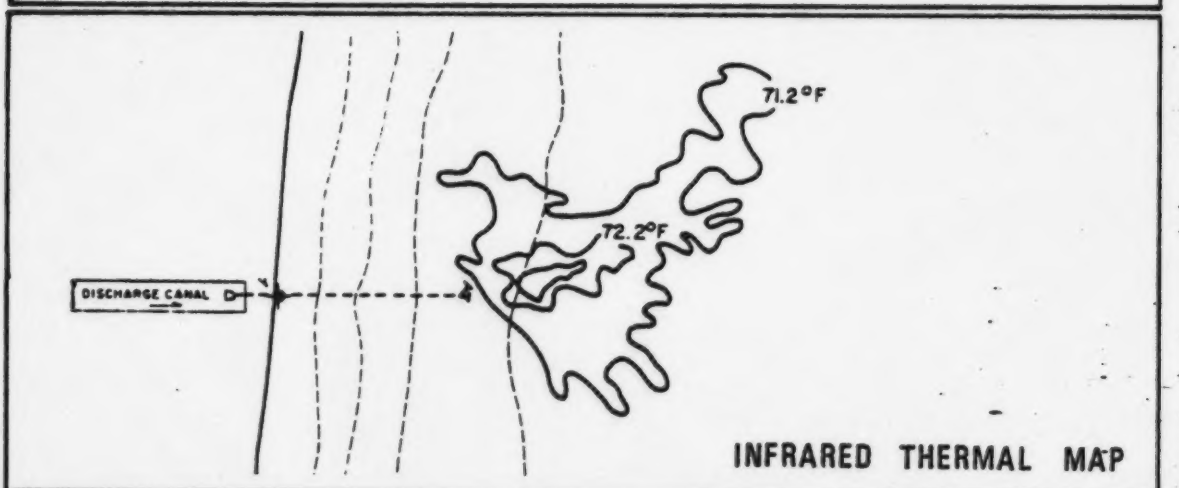

OCEAN DISCHARGE STUDY

FAR-FIELD ISOTHERMS

EXHIBIT 4

PB82-228578

MANAGEMENT OF WASTE HEAT FROM THERMAL POWER PLANTS AS RELATED TO RISING COST OF FUEL

Dr Miodrag M. Mesarović
Thermal and Nuclear Power Plants Dept.
ENERGOPROJEKT Corporation
Belgrade, Yugoslavia

ABSTRACT

Rising costs of fuel have very serious economic, social and political implications, requiring an energy policy based primarily on energy savings. Waste heat management in thermal power plants is one of the numerous means to do so. This report presents an overall analysis of waste heat management through selection of sites and cooling systems for thermal power plants, combined heat and electricity production, as well as an optimum cold end parameters for varying fuel costs. Case studies include low grade coal, lignite. A conclusion is drawn that the rise of fuel cost imply, as an optimum, more costly equipment in order to reduce its detrimental effects on the plant economy.

1. INTRODUCTION

The world is now faced with the energy shortage and a rapid growth of fuel costs, as well as with crucial choices in the energy field, which have very serious economical, social and even political implications. It is therefore of prime importance to establish a strong energy policy, which makes use of all the possibilities offered by the nature, including, first of all, energy savings. However, neither the "first" energy crisis of 1973/74 did influence world energy habits, nor did that numerous energy studies which forecast emergence of a future energy situation. (Such a situation already begun in 1979 by another steep rise of oil prices, usually refered to as the "second" energy crisis). Thus, in most cases, neither the energy savings, nor new energies (the readiest and the most important of which is nuclear energy) have experienced the development as called by the situation.

Therefore, the oil, that helped development of the industrialized countries, now contributes heavily to the inflation problems in many of them. The high oil prices are even more burdensome to the developing countries. Although it is generally recognized that continuing high oil prices (fig. 1) may accelerate growth of nuclear power both in industrialized and developing countries, oposing factors such as reduced overall energy demand, environmental considerations and unwillingness of the public to accept a rapid proliferation of nuclear plants, may tend to ameliorate the rate of growth.

Electric power industry is still, to the extent of 50 to 90% of its capacity, a conversion industry turning into electricity energy of fossil fuels (which have alternative energy uses), but in future it will use uranium (which has no alternative energy uses) leaving fossil fuels for other purposes. However, fossil fueled electric power plants still provide the bulk of electric energy and, although their capacity will decline in percent of total capacity, it is projected to increase substantially by the end of century. Consequently, the electric power industry, based on the stations utilizing less than 40% of the heat input would be badly hit if it continues to depend upon such increasingly expensive fossil fuel (fig. 1a). It is, therefore, obvious that the importance of another fossil fuel, coal, is growing again, and some countries have made progress in converting oil fired power stations to coal (ironically, some of these have previously been converted from coal to oil). However, the price of coal is rising as well, irrespective of its quality (fig. 1 b shows the price index of low grade coal such as lignite, for example).

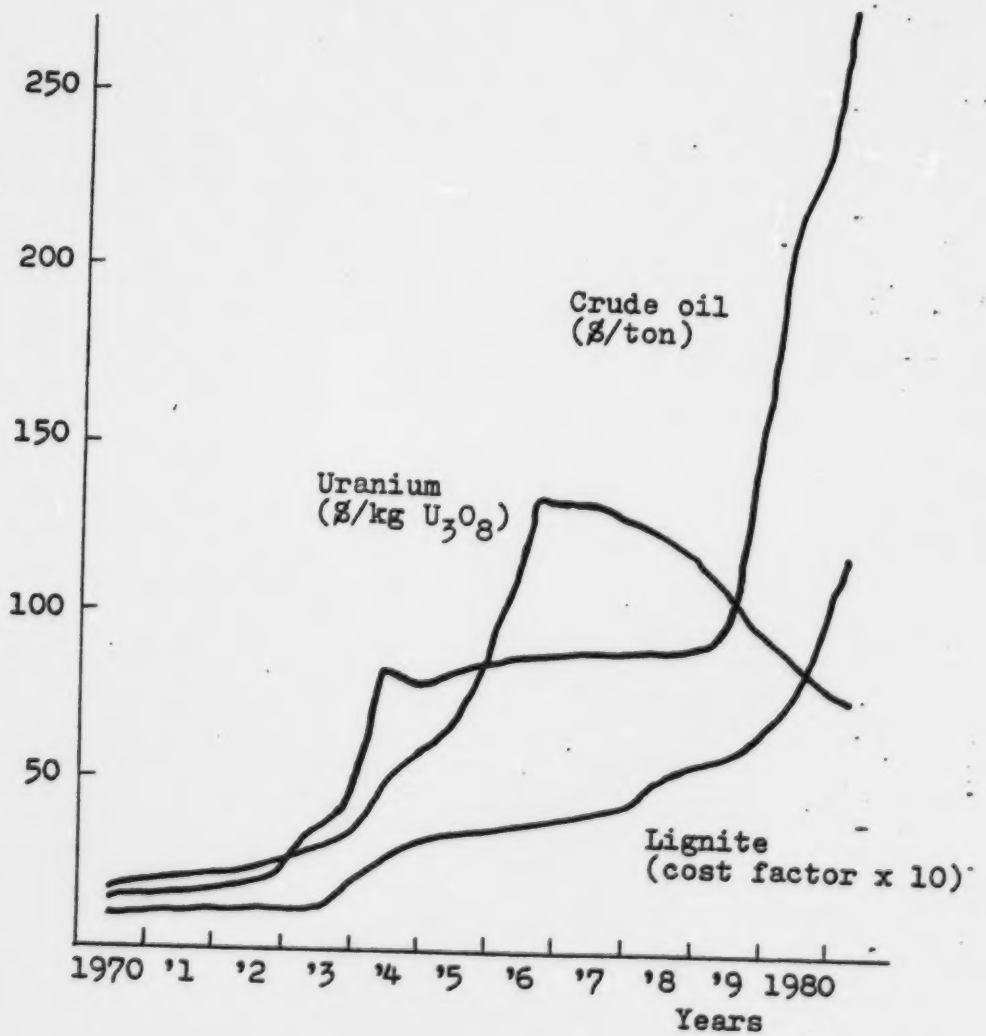

Fig. 1. Costs of Fuels History

Current prices of uranium are decreasing, as shown in fig.1c, and may even drop as low as 60 $ per kg of U_3O_8 before rising again. This is due to the fact that demand of nuclear fuel has diminished (leading to an oversupply) as a consequence of recent cancellations or defferals of nuclear power plant projects. Fuel costs are less significant as an element in electricity price for nuclear compared to conventional stations, and, consequently, the rise of prices of fossil fuels has greatly increased economic incentive to adopt nuclear generating capacity and, at the same time, to achieve greater price stability. Moreover, the widespread distribution of abundant resources of uranium (at costs no longer a limiting factor) offers the prospect of reduced vulnerability to interruption of supplies.

2. WASTE HEAT MANAGEMENT FROM ELECTRICITY PRODUCTION

2.1. Amount of Waste Heat

Thermal power plants are based on the steam cycle, in which the steam, produced at high temperature and pressure in the boiler or reactor, is expanded through the steam turbine, giving up energy which drives generator to produce the electricity. At the exhaust of the turbine, the steam is condensed before being returned (to the boiler or reactor) for a repetition of the cycle. A large amount of heat, known as waste heat, is given up to the cooling water in the condensing process.

The amount of waste heat is related to the type and efficiency of the plant. In the most efficient fossil fired plant, only about 40% of the energy contained in the fuel is converted to the electricity, about 15% is lost in the plant (through the stack and in the ash), so that at least 45% of the energy input is discharged as waste heat. Nuclear power plants with thermal reactors have even lower efficiencies, only about 33%, approximately 5% is lost in the plant, so that waste heat constitutes more than 60% of the heat input. This means that the waste heat from nuclear power plants is 1.4 to 1.5 times that from fossil fired plants of the same size, [1]. (Advanced reactor concepts, fast breeders and high temperature reactors are expected to reach the efficiencies of the fossil fired plants).

Obviously, due to rise of fuel costs, it is a strong economic incentive to maximize the energy conversion, thus reducing the waste heat. The reduction of waste heat should be as much as possible, or rather, as economically feasible; since higher efficiencies require more expensive equipment, it is possible to optimize the level of waste heat by applying a cost-benefit approach. Bearing in mind the rise of fuel costs and an enormous portion of heat wasted to the cooling water, one may conclude that the solution of the problem lies in drastic reduction of the waste heat. However, due to obvious limitations imposed by the nature of the steam cycle itself, total possible savings are relatively small.(Even such, they are of great importance in electricity generation economy, as will be demonstrated latter in this report). One of the most efficient methods of reduction of waste heat is achieved by dual purpose plants for combined production of electricity and heat for different industrial applications and/or district heating. In such plants the waste heat is reduced by a factor of 3 to 5, fig.2.

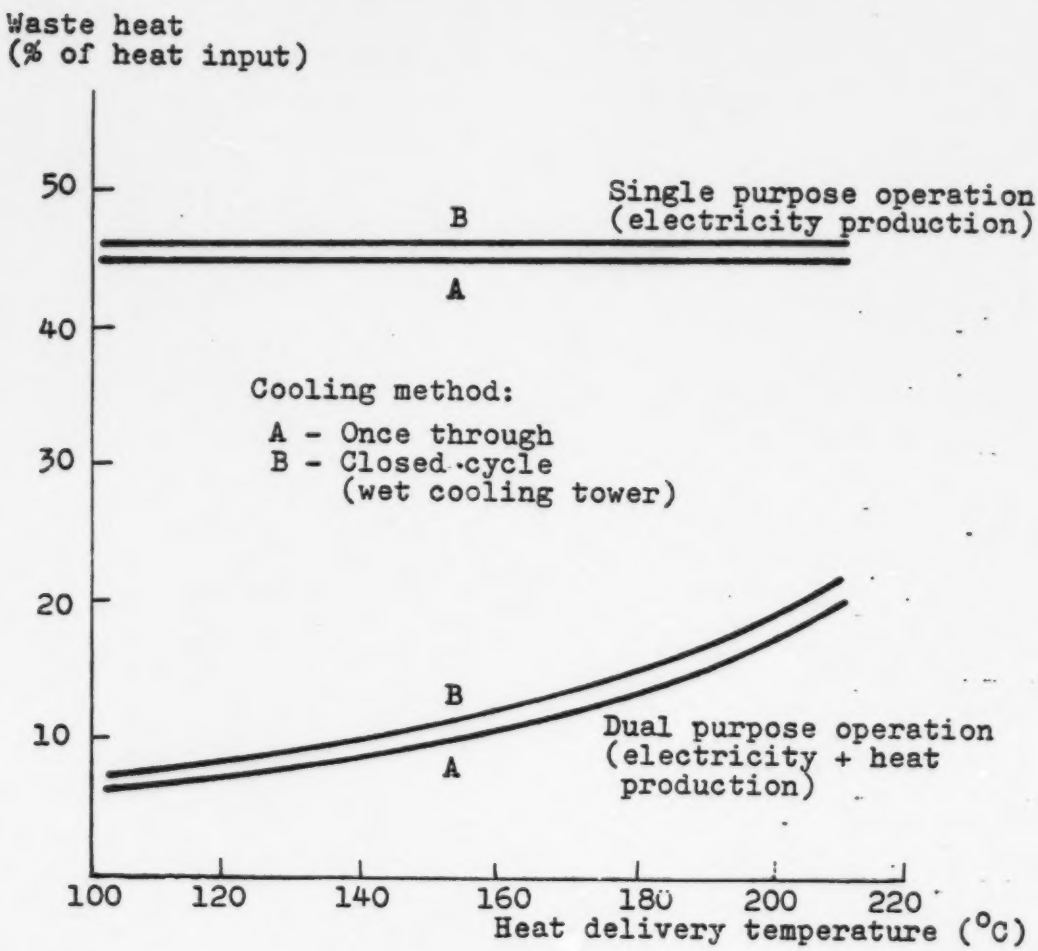

Fig. 2. Waste Heat from Fossil Fired Dual Purpose Plant as related to Cooling Method and Hot water Delivery Temperature

2.2. Methods of Dissipation of Waste Heat

One of the major problems involved in implementing the power plants is the choice of their cooling systems to transport the waste heat to the environment. As the least expensive and most efficient alternative, once-through cooling has been the historically prefered cooling method. With once-through cooling system applied, the lowest condensing temperatures and highest efficiencies are achieved. Therefore, the once-through cooling system provides the most efficient utilization of turbine heat input, since the steam can expand to a low exhaust pressure and produce more useful work, thus minimizing the waste heat.

Due to increase of capacity of thermal power plants and thermal pollution control regulations, the possible sites with once-through cooling are becoming limited, thus requiring the adoption of supplementary methods to reject waste heat from future power plants such as cooling lakes, spray ponds and cooling towers. These future trends have an important effect on waste heat management and plant efficiency, requiring different turbine designs. The use

of these supplementary cooling systems does not economically permit similar efficient operation and consequently is more vulnerabby rising costs of fuel.

From the standpoint of low capital cost and high plant efficiency, the most favored closed cycle cooling system is the evaporative (wet) cooling tower, with either a mechanical or natural draft. All of the waste heat rejection takes place within the cooling tower, where most of the heat is dissipated by evaporating a portion of circulating warm water, while the remaining heat is lost by sensible heat transfer to the air [2]. From the economic point of view, natural draft cooling towers are more expensive, while mechanical draft cooling towers consume more energy. By the rise of unit sizes and water costs simultaneously with fuel cost, mechanical draft cooling became less convenient than natural draft cooling.

One particular problem with wet cooling towers is the make-up water, which is necessary to compensate the various water losses in the cooling circuit (evaporation losses, drift and blowdown), which amount 2.4 l/kWh in fossil fired plants to 3.3 l/kWh. All of these wet tower problems may be eliminated through the use of dry cooling towers. In dry type of cooling tower the cooling water never comes in direct contact with the air and all of the waste heat is rejected through fin tube exchangers. Thus, there are no evaporative losses which would require make-up water. (Another type of dry cooling system, known as an air cooled condenser, would condensate steam directly, inside the fin tubes). However, equipment costs for this type of cooling is several times greater than for wet cooling. Also, the higher condensing temperatures, causing a higher turbine capability loss, make dry cooling even more unatractive.

Since dry bulb temperatures are higher than wet bulb temperatures, the dry cooling system is forced to reject waste heat to higher temperature sink. Compared to wet cooling systems, this results in higher turbine exhaust pressures, poorer plant performance and higher replacement energy costs through the year. The performance of the dry cooling system is particularly poor (compared to wet cooling system) during peak temperature periods and results in both capability and replacement energy cost penalties, fig. 3. (If high exhaust pressure turbine designs are used to reduce the hot day capacity deficit, higher heat rates are incurred during the remainder of the year).

2.3. Energy and Capability Losses and Siting of Thermal Power Plants versus Fuel Cost

Since closed cycle cooling systems would force turbines to operate at higher exhaust pressures, there would be an energy and capability loss resulting in additional capital and fuel expenditures compared to once-through cooling systems. Energy and capability losses have two components: losses due to turbine derating through increased turbine exhaust pressure and losses due to increased increased auxiliary power requirements (pumping and fan drives). Since nuclear power plants reject larger quantity of waste heat, they experience greater energy and capability losses than conventional power plants. With wet cooling towers, energy

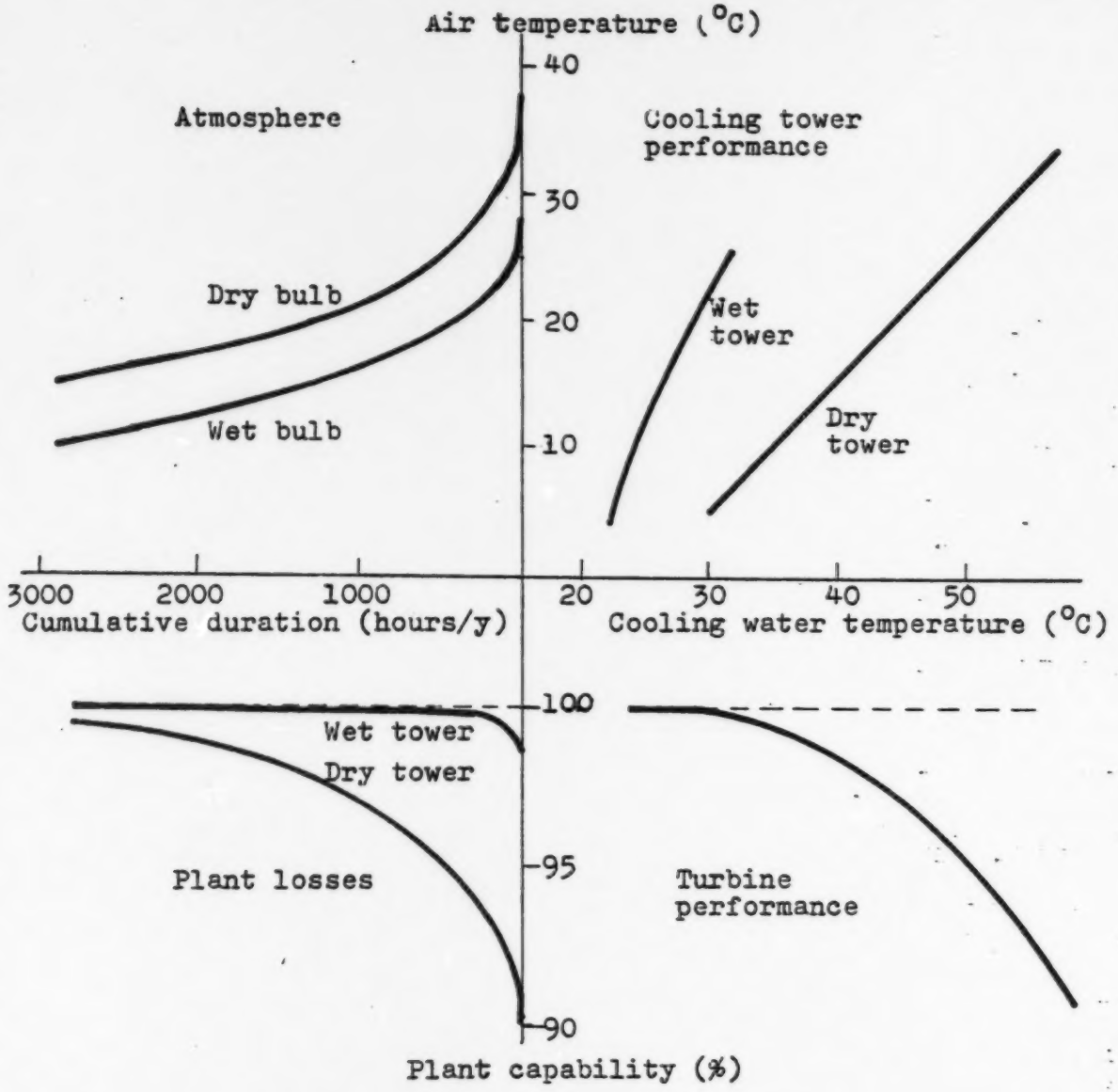

Fig. 3. Closed Cycle Cooling Performance Curves

losses are approximately 1.7 to 2.0% for fossil fired plants and 3% for nuclear plants, while capability losses 2.5 to 3% and 5%, respectively. With dry cooling towers these losses are much greater, exceeding 10% for nuclear plants.

Obviously, by the rise of fuel costs, the energy and capability losses play an increasing role in the plant design and the site selection. Economic consequences of these losses are so important that even distant cooling water sources which enable once-through cooling became very attractive. This is the case even if fossil fired plants are considered (which have much lower energy and capability losses than nuclear plants), when enormous quantities of low grade coal such as lignite of L.H.V. 6000 to 8000 kJ/kg appear economically feasible to be transported to the sites where

once-through cooling is possible. Break-even distances of such sites from the coal mines increase with rising costs of fuel. This is demonstrated in fig. 4 by assuming energy losses only, transportation of lignite (6000 kJ/kg) by railroads, electricity transmission back (alternatively). Increase of equipment costs was assumed as well.

Evidently, the break-even distances increase with rising the fuel costs, particularly if dry cooling towers are considered and if capability losses are accounted for (in fig. 4 only energy losses are taken into account). Thus, the waste heat management problem and the rise of fuel costs might cause an increase in projected movement of coal, which is of particular concern since coal is viewed as an energy source in the 1990's. On the other hand, athough future movement of coal (all transportation networks included: railroads, highways, barges, truck, slurry pipelines) would increase both on the international and local scale, the rise of its prices would force electric utilities to produce heat and electricity in dual purpose plants, thus introducing an additional siting criterion (represented by drastic reduction of the waste heat and by an expensive heat transportation to the load center). This is due to the facts that the waste heat in combined heat and electricity producing cycles diminishes the energy and capability losses (compared to these of electricity producing cycle) and that break-even distances of transporting heat to the load center increase with rising prices of fuel oil, as shown in fig.5.

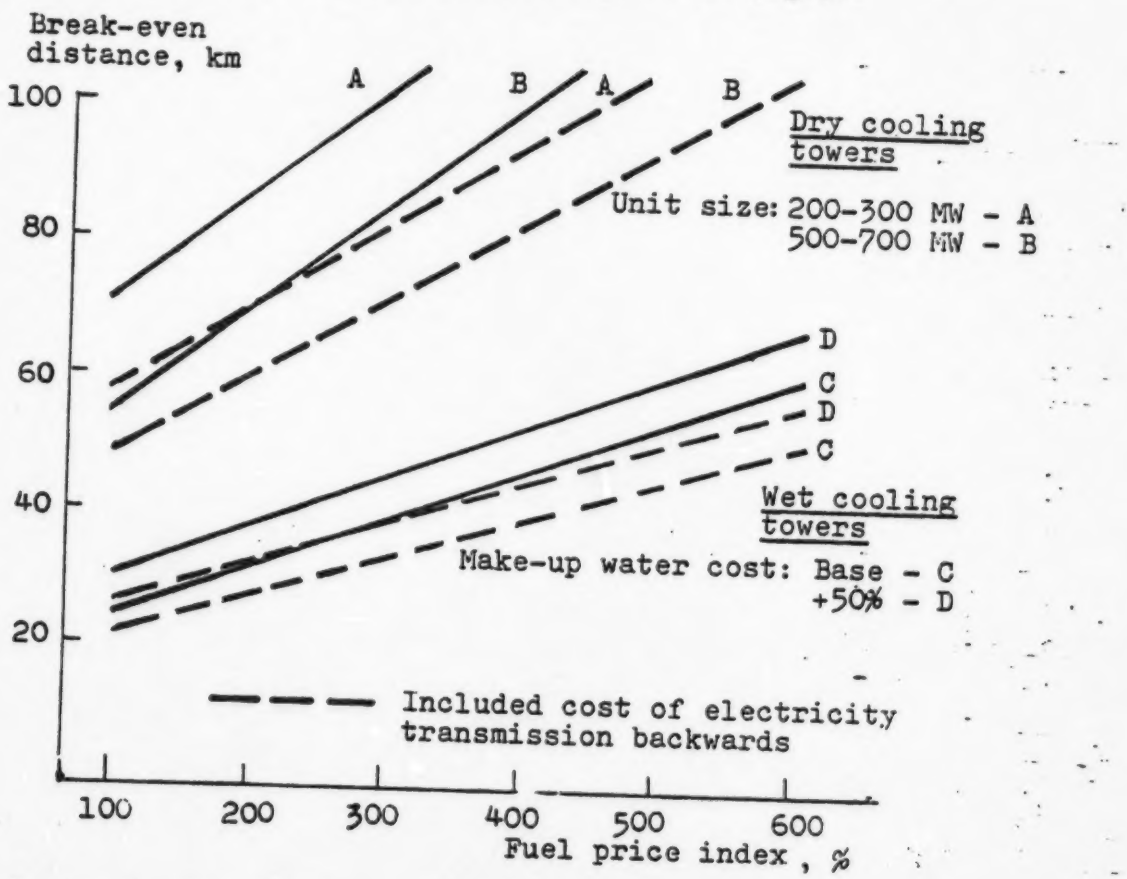

Fig. 4. Break-even Distance of a Site with Once-through Cooling

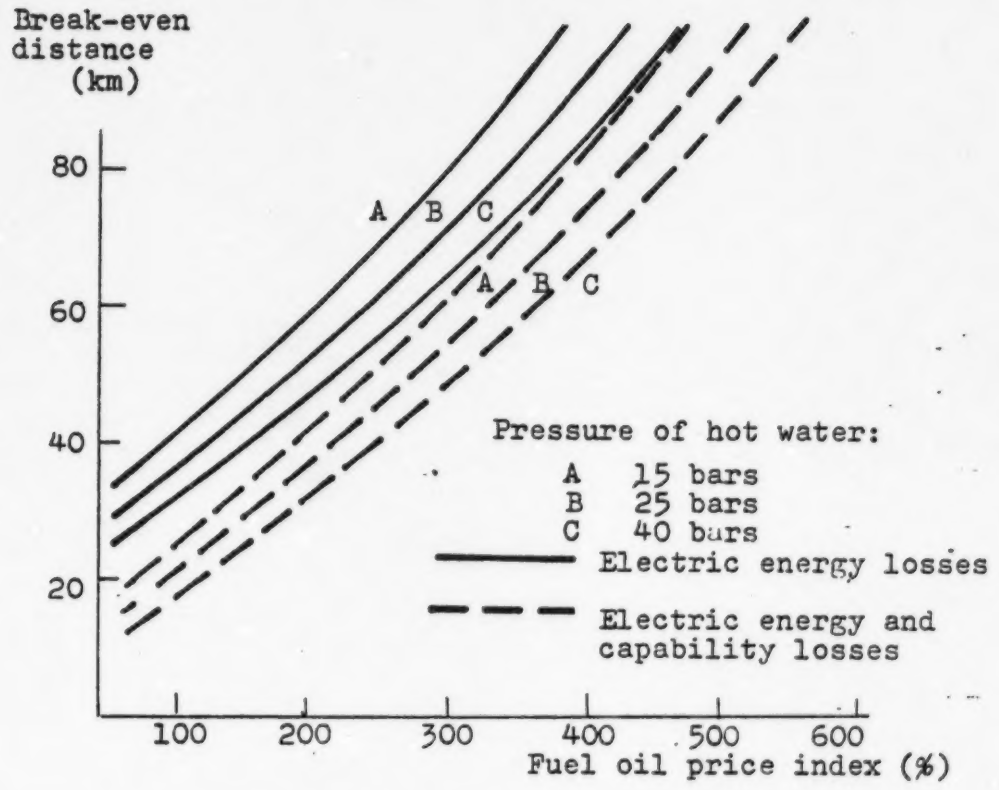

Fig. 5. Break-even Distances of Hot Water Transport from Dual Purpose Plants vs Fuel Oil Price

It is obvious that such dual purpose plant is of great environmental concern not only due to reduced quantity of waste heat, but also due to reduced air pollution in urban centers to which the heat energy is supplied to replace its local production by conventional means. By applying a cost-benefit approach, it may be easily demonstrated that the rise of fuel costs enables the heat from dual purpose plant to serve an increased portion of the heat load, thus minimizing the effective energy supplied by local peaking power plants.

From figs. 3 and 4 it is evident that capability losses with dry cooling are much more sensitive to fuel costs. Consequently, the application of wet cooling towers instead becomes economically feasible even if cost of make-up water is very high. As dry cooling towers are limited in size to 200 to 300 MW at present with a tendency of reaching unit sizes of 500 to 700 MW, both alternatives are taken into account. Calculations made with present cost estimates for wet and dry cooling towers in lignite fired steam electric plants show that break-even costs of make-up water are increasing in proportion to the fuel cost rise, as shown in fig. 6. Wet cooling towers are more economical below and dry cooling towers above the break-even line drawn for a given unit size of dry cooling tower. As a consequence, management of waste heat by the use of dry cooling towers could hardly be justified, even if their specific costs have been reduced, due to ever increasing fuel costs.

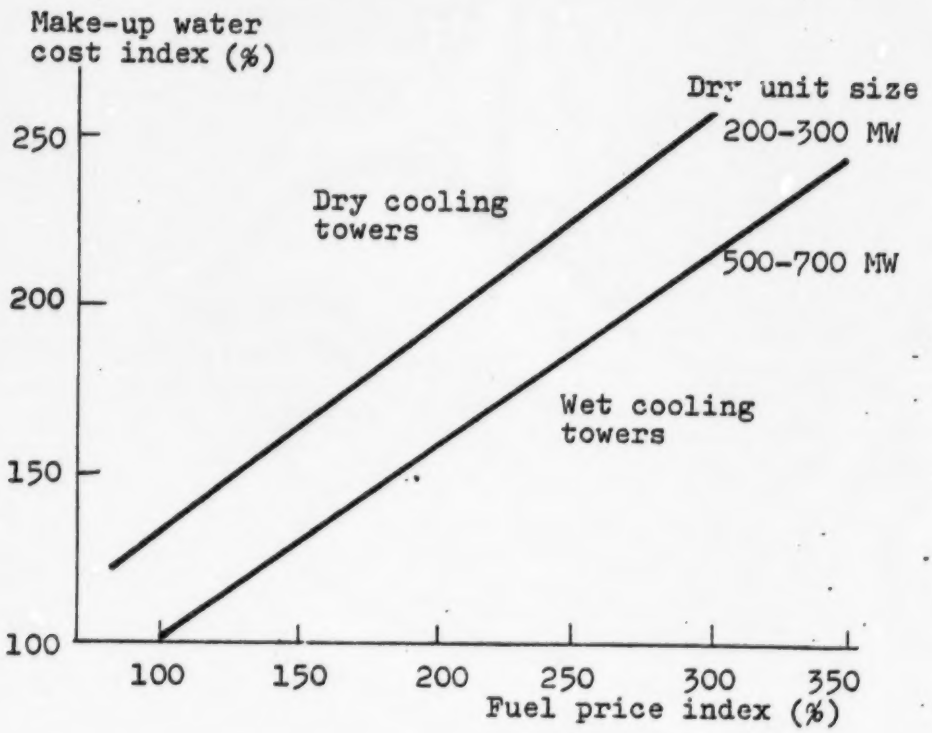

Fig. 6. Break-even Costs of Make-up Water vs. Fuel Price

2.4. Optimizing "Cold End" of Thermal Power Plants with Reference to Rising Cost of Fuel

Because of the expected increased application of wet cooling towers and other supplementary devices to reject the waste heat, very exact methods were found necessary to conduct a complete and accurate cost analysis for selecting (as a system) the most economic combination of turbine, condenser and waste heat sink. This analysis includes load duration curves, weather data as well as fuel and water costs plus many other economic factors over the plant operating life.

Turbine with longer last row blades produces more power than one with shorter blades at lower exhaust pressures and less power at higher exhaust pressures. When wet cooling towers are used, turbine exhaust pressures can range enormously, depending upon the choice of tower design. Thus, there is no obvious conclusion as to which turbine design is the best economic choice and therefore many other factors must be taken into consideration. These include capital costs for the turbine and cooling system, penalties for auxiliary power, make-up water costs, fuel costs, as well as cost of money, taxes, depreciation and other pertinent factors.

The steam condensing temperature is usually 3 - 6°C higher than the warmed water temperature leaving condenser. This difference is known as "terminal temperature difference", TTD. Optimum TTD is reduced when the fuel costs rise, as shown on fig. 7. This means an increased surface (and cost) of condenser, to cope with detrimental effects of high fuel costs on the overall plant economy.

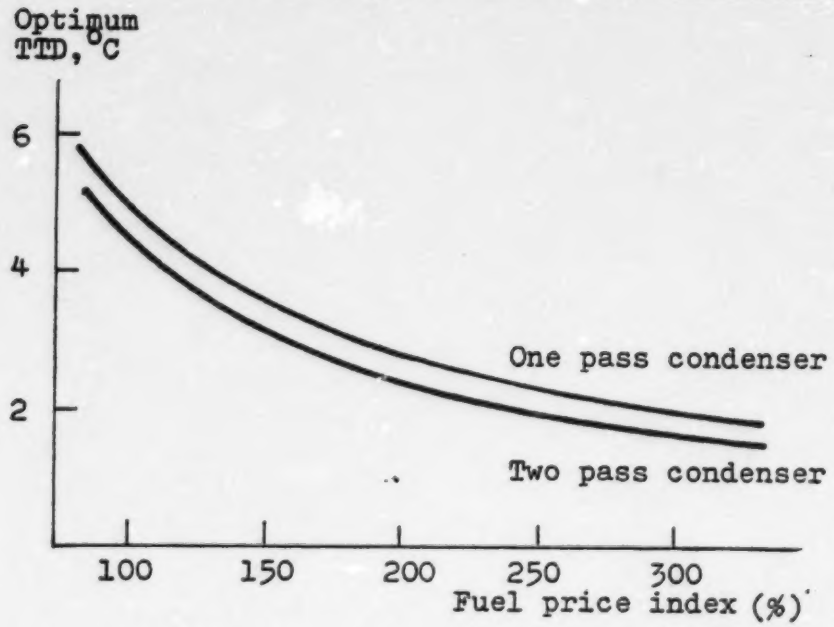

Fig. 7. Optimum Condenser TTD versus Fuel Price

Wet cooling tower design is determined by its cooling range (difference between the warm water temperature leaving the condenser and the cold water temperature leaving the cooling tower) and approach temperature (difference between the cold water temperature leaving the cooling tower and the ambient wet bulb temperature). While the cooling range determines the flow of cooling water through the condenser, the approach temperature determines the temperature of the heat sink. From fig. 8 it is evident that, for a given cooling range (12°C) and TTD (4°C), optimum design approach temperature is lower as the fuel costs rise. The same applies to the exhaust steam temperature. Economically optimum design cooling range is also decreasing as the fuel cost rises, as shown on fig. 9 for different design approach temperatures.

It comes out from the above analysis that optimum design parameters of a thermal power plant with closed cycle cooling are approaching those of a plant with once-through cooling as the fuel costs rise. Evidently, the cost-benefit approach applied to the optimum design of the plant's "cold end" (low pressure turbine, condenser, cooling tower, piping, cooling water pumps) showed that the best economic choice would lead to lower exhaust pressures, close to the values achieved by once through cooling, the more so as the cost of fuel would be higher. This means that the waste heat must be reduced as much as economically feasible and rejected to the environment at temperatures of the sink determined by the optimum parameters of the plant's "cold end" as a system.

Naturally, to achieve such a goal with present rates of the increase of fuel prices on the world market, more costly equipment are necessary. This is due to the fact that the price of turbine is increasing with lowering the exhaust steam pressure, the price of condenser is increasing both with reducing the cooling range and reducing the terminal temperature difference (TTD), the price

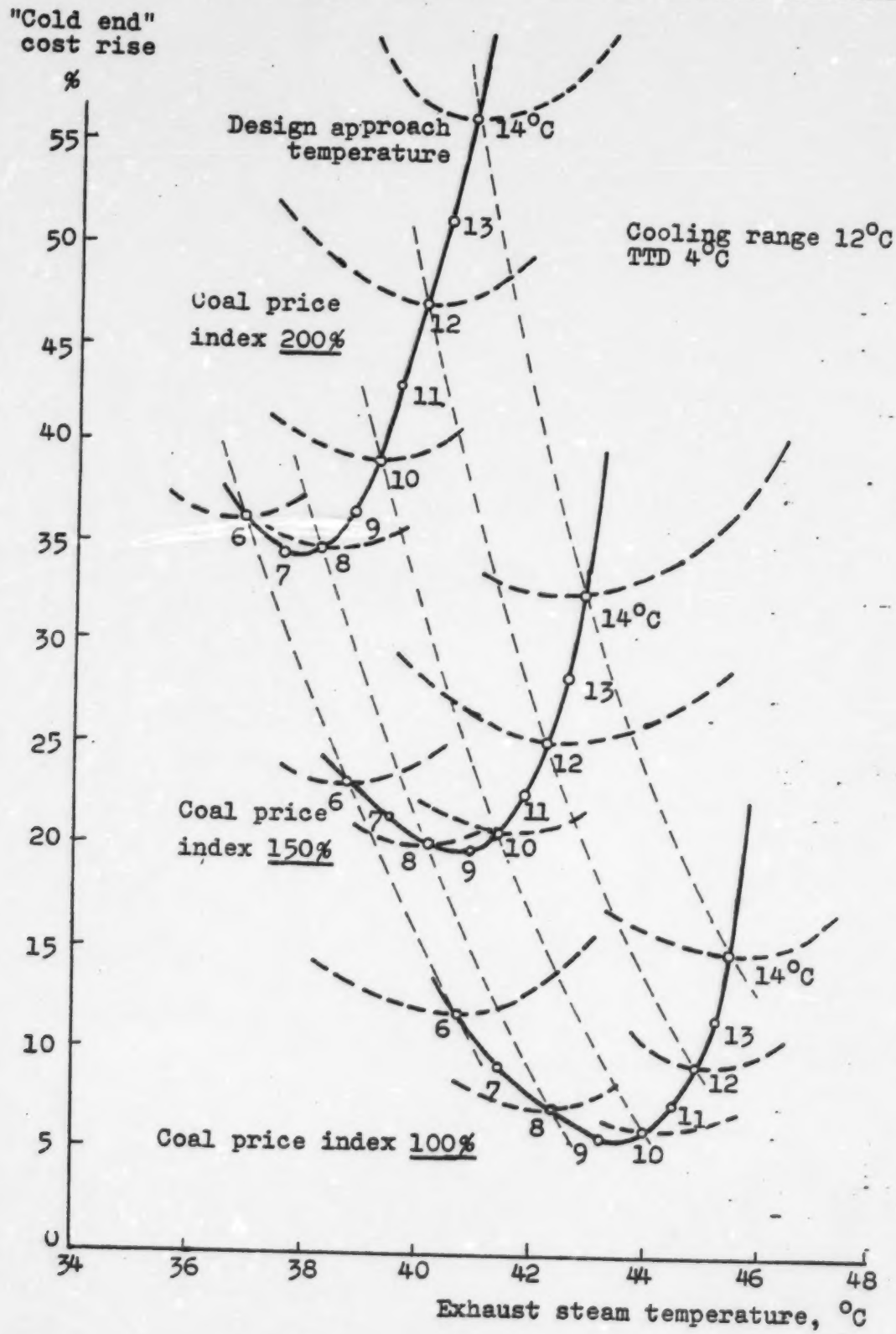

Fig.8. Optimum Design Approach Temperature and Exhaust Steam Temperature versus Fuel Price

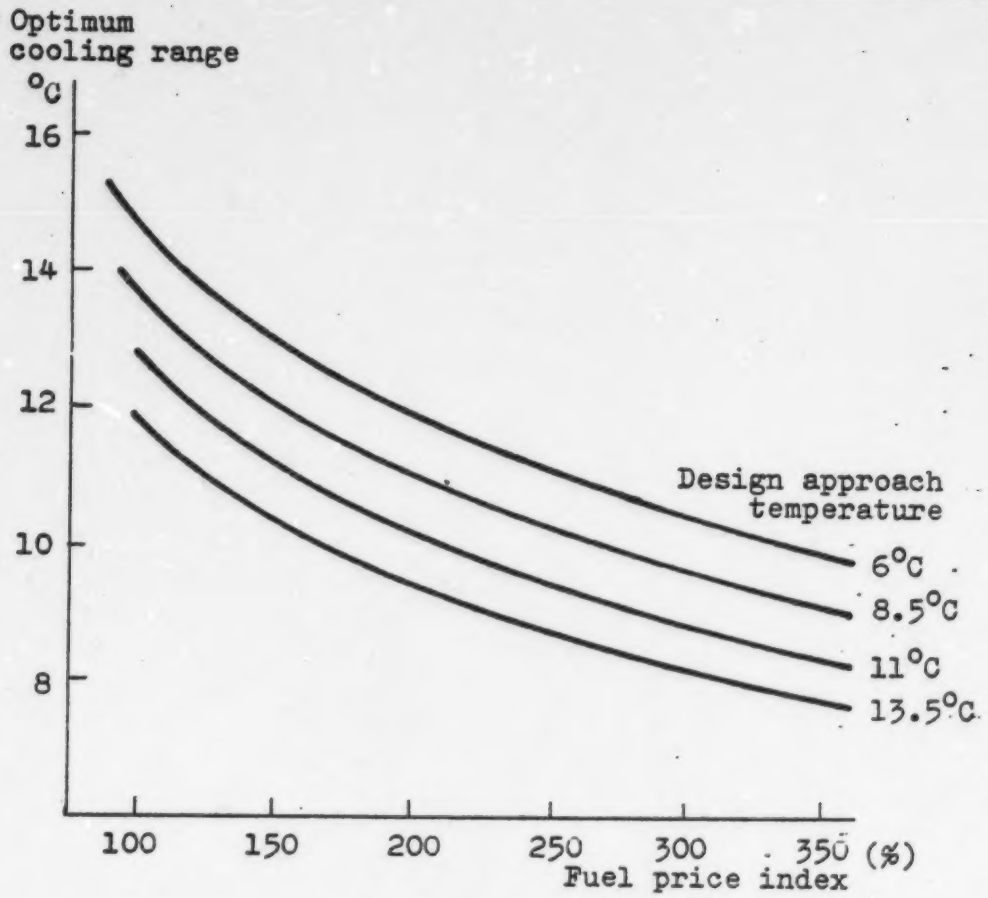

Fig. 9. Optimum Cooling Range versus Fuel Price

of wet cooling tower is increasing both with reducing the cooling range and with reducing the approach temperature, the prices of pumps and piping are increasing with increasing the cooling water flow, since all of these trends were found to be economically optimum when the fuel cost rises. Therefore, in order to reduce the unavoidable energy generating cost penalties in power plants with closed cycle cooling (relative to once-through cooling), these plants must have an optimum combination of the turbine, condenser, pumps, piping and cooling tower, whose performances would require more costly equipment as the fuel costs rise. Fig. 10 shows the estimated increase in particular equipment costs, as a result of their adjustment to achieve optimum performances in conformity with fuel costs during the plant lifetime.

Thus, the rising cost of fuel impies more expensive equipment of a thermal power plant, which means further increase in the energy generating costs. However, such an increase is much less than it could be expected in a plant without an optimum "cold end" in relation to the fuel cost during its lifetime. An optimum "cold end" leads finally to the dimensions of the cooling system for waste heat management, which give the lowest energy generating cost with a given cost of fuel.

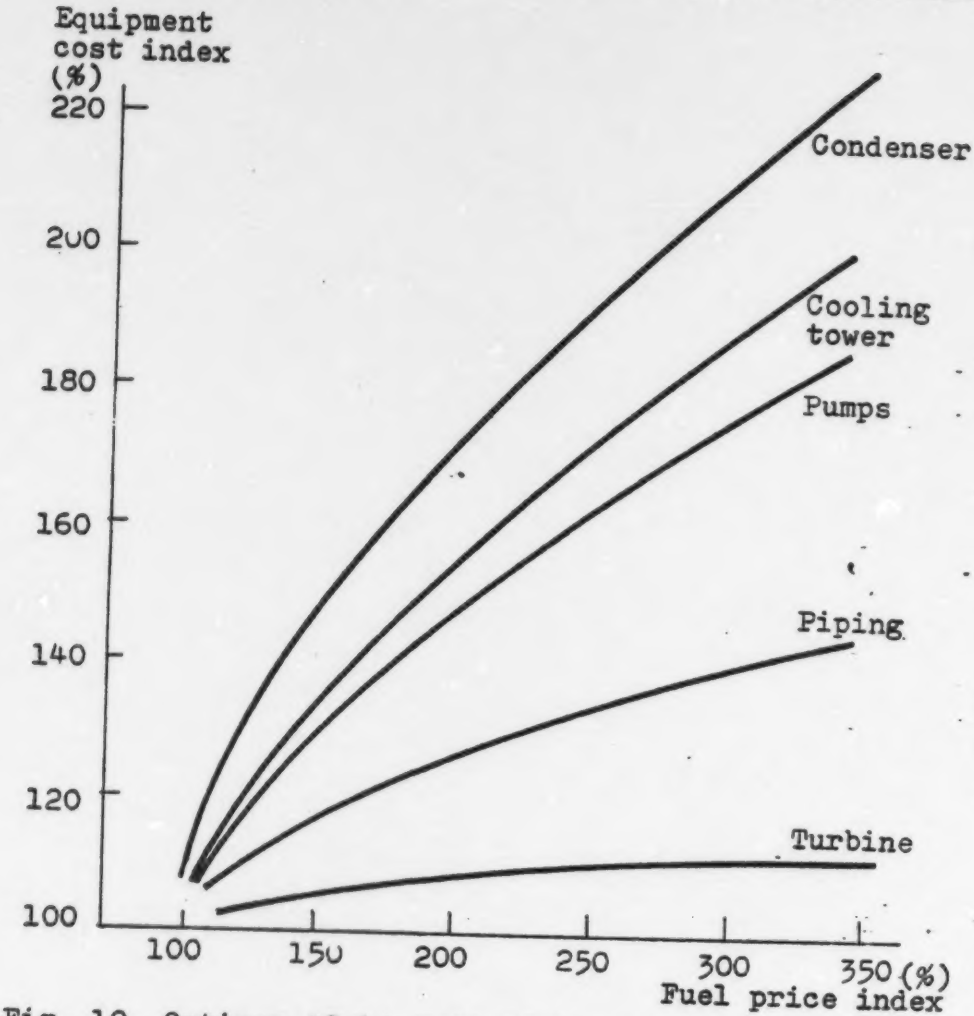

Fig. 10. Optimum "Cold End" Equipment Costs versus Fuel Price

3. CONCLUSION

Waste heat from thermal power plants represents a very large portion of the total heat input: approximatelly 45% in fossil fired plants and over 60% in nuclear. Therefore, its dissipation to the atmosphere (as an ultimate heat sink) from the surface of water body (once-through cooling) or directly by the closed cycle cooling (wet or dry cooling towers) plays an important role in the overall plant economy, the more so as the cost of fuel rises. By it, the sites where once-through cooling is applicable became competitive even if far from the alternative site with closed cycle cooling, particularly if make-up water is scarce or expensive. The competitiveness of dry cooling towers is greatly decreased by the high costs of fuel.

The growing concerns over environmental protection and energy savings give rise to the importance of dual purpose plants for a combined heat and electricity production, by which the overall efficiency is greatly increased and consequently the waste heat qua-

ntity reduced. The rise of fuel costs makes it economically attractive to apply such a source for urban heating and industrial purposes even if far away from the load centers.

Energy generating costs are greatly affected by the rise of fuel prices, not only for the reason of fuel expenditures, but also for the reason of more costly equipment which have to be introduced in order to maximize the efficiency of the plant. In such a way, an optimum "cold end" of a thermal power plant with closed cycle cooling would approach the conditions of once-through cooling, thus minimizing the quantity of waste heat and moderating severe consequences of rapid growth of fuel costs.

REFERENCES

1. M. Mesarović, Waste Heat Disposal from Steam-Electric Plants with Reference to the Stochastic Nature of some Environmental Conditions and Thermal Pollution Control Regulations, Proc. Symp. Environmental Effects of Cooling Systems at Nuclear Power Plants, IAEA 187/25, pp. 311-330, 1975.

2. M. Mesarović, ARARAT - a Computer Code for Thermal Design of Cooling Towers, Nucl. Engng Design, Vol. 24, No. 1, pp. 57-70, 1973.

PB82-228586

REGULATORY ASPECTS OF WASTE HEAT MANAGEMENT AND UTILIZATION

William A. Anderson, II
1850 K Street, N. W.
Washington, D. C. 20006

ABSTRACT

The need for rational management and utilization of waste heat is undeniable. Yet conflicting governmental policies have resulted in regulatory constraints that often foreclose rational solutions. Effluent limitations and water quality standards under the Federal Water Pollution Control Act restrict use of surface waters, including cooling lakes, for waste heat management. Other regulatory constraints, including provisions of the Clean Air Act Amendments of 1977, may preclude the use of evaporative cooling towers under some circumstances due to salt-drift emissions. Waste heat utilization schemes involving clusters of industrial facilities will also encounter environmental regulatory constraints. Provisions of both the Air Act and the Water Act will limit industrial concentration in any given locality. Thermal aquaculture may be possible under governing EPA regulations only in blowdown streams from closed-cycle systems. Concentrated contaminants in these blowdown streams may make the produce unmarketable. Federal Energy Regulatory Commission rules promulgated last year, however, aim to remove some regulatory barriers facing cogenerators.

1. INTRODUCTION

The topic of this conference is of pressing social concern. This concern is evident in the environmental restrictions on waste heat disposal and in the growing realization of the practical need to use, not waste, this energy. Reliance on these secondary energy resources will conserve primary energy resources and reduce the total pollution load associated with meeting increasing energy demand. Certainly, the need for rational management and utilization of waste heat energy has never been greater. And this need will not diminish. But is rational management and utilization a "pipe dream?" Do current regulatory constraints foreclose many feasible options?

This paper considers selected regulatory aspects of, first, rational management of waste heat and, second, of potential uses of waste heat. The emphasis is on management.

We will see that the environmental pressures for control are not necessarily consistent with rational management. And some of the more feasible schemes for using waste heat would encounter such severe regulatory obstacles that their potential is unlikely to be realized.

The dichotomy between management and utilization is somewhat artificial. Each affects the other. The management scheme in a particular situation will often determine what uses may be feasible. Similarly, any effective use of waste heat is one means of managing it. So the line between the two is not bright. For purposes of this discussion, however, "management" may be simply defined as what you do with waste heat when you want only to get rid of it. "Utilization" is when you want to do something with it before you get rid of it.

2. MANAGEMENT

2.1. Definitions

In order to discuss rational management and regulatory constraints, it is necessary first to define the terms. We begin with management. It may be defined simply as the mechanism or system for the dissipation of waste heat to the atmosphere. Management of waste heat in steam-electric power generation may involve use of surface waters or of some mechanical devices, such as a cooling tower, as an intermediate medium through which to dissipate the waste heat to the atmosphere. There may be competing objectives in management. Utility companies seek a low-cost way to get rid of waste heat in a manner that is environmentally acceptable. The regulators typically seek an environmentally acceptable way that is not prohibitively expensive.

What is rational management? In my view, rational management must be that method of dissipation that is the least resource-intensive. The resources of concern must be viewed broadly. They encompass capital resources, environmental resources, and energy resources. A management system that consumes additional energy in order to dissipate waste heat is rational only if there are commensurate savings in environmental resources. One that consumes environmental resources may not be rational unless there are compensating or offsetting savings in capital or energy resources.

A regulatory constraint is a requirement imposed by statute or rule to perform or refrain from some specific act, or to do it only in a particular way. In this context, we are concerned with three general types of constraints:

-- direct restrictions on thermal discharges, e.g., technology-based effluent limitations;

-- indirect restrictions on thermal additions, e.g., water quality standards for temperature; and

-- ancillary restrictions on activities that are a necessary concomitant of a particular waste heat management scheme.

We will consider the implications of each of these for waste waste heat management.

2.2. Direct Restrictions on Thermal Discharges: Effluent Limitations

The Federal Water Pollution Control Act, as amended, 1/ requires all existing discharges of heat to navigable waters to attain effluent limitations reflecting "best available technology economically achievable" by July 1, 1984. Water Act § 301(b)(2)(A), (F). New thermal discharges must comply with standards of performance based on application of the "best available demonstrated control technology, process, operating methods, or other alternatives." Water Act § 306(a)(1). For convenience, I will refer to both of these requirements as the "BAT requirement." These requirements are applied to individual facilities in discharge permits without which discharges are not allowed. Water Act §§ 301(a), 402. Pursuant to this statute, the Federal Environmental Protection Agency (EPA) published regulations to define the BAT requirements for thermal discharges. 2/ EPA based its regulations on the premise that BAT must remove heat atmosphere prior to discharge to navigable waters. So its regulations required closed-cycle cooling, principally evaporative cooling towers, for all larger, newer steam-sources. The regulations severely limited new uses of cooling lakes. 3/

I understand that evaporative cooling towers dissipate 97 to 98 percent of the waste heat load directly to the atomsphere and discharge the remainder in blowdown. They require only 10 percent or so of the intake water necessary for once-through operation, and thus yield incidental benefits in siting flexibility and in reduction of impingement and entrainment of aquatic organisms.

But evaporative cooling towers are costly in terms of both capital and energy consumption. Table 1 below summarizes the results of a recent study by the Stone & Webster Engineering Corporation for the Utility Water Act Group. 4/ The costs shown

TABLE 1

THE COST OF CLOSED-CYCLE COOLING SYSTEMS 5/

(EXCLUDING INTEREST AND ESCALATION DURING CONSTRUCTION)

System	Cost ($/KW-July 1977)		% Energy Loss		% Capability Loss	
	Nuclear	Fossil	Nuclear	Fossil	Nuclear	Fossil
Retrofit						
Mechanical Draft Cooling Tower	40.57	27.64	4.2	1.3	4.5	2.3
Natural Draft Cooling Tower	50.65	34.50	3.0	1.0	4.9	2.8
New Units						
Mechanical Draft Cooling Tower	15.46	10.53	2.2	0.7	2.9	1.5
Natural Draft Cooling Tower	20.84	14.19	1.9	0.6	3.2	1.8

for existing and new units are installed capital costs in dollars per kilowatt of electrical capacity, normalized to July 1977 dollars. They do not include, for example, energy penalties or replacement capacity. The cost figures represent the average of costs reported in studies on thirty retrofit installations and thirty-five new unit installations, normalized to July 1977 dollars. Retrofitting a hypothetical, typical 1,000 megawatt fossil unit would cost $28-35 million; retrofitting a nuclear unit, from $40-50 million. And retrofit systems would impose energy penalties of from 1 to 4.2 percent of the total energy output of the unit over its useful life. So cooling towers represent a somewhat extreme instance of using capital and energy resources to dissipate waste heat. Other studies for the Utility Water Act Group show that this method of managing waste heat also consumes more water through evaporation than alternative means, particularly use of cooling lakes.6/

Is this cooling tower requirement for BAT consistent with rational management? As noted above, rational management must consider total resource use. EPA made no conscientious, systematic effort to determine whether the savings in environmental resources justified the capital cost or energy consumption of its regulations. While the Act contains in § 316(a) a case-by-case variance mechanism, it is based solely on a demonstration of the absence of significant adverse effects in the aquatic environment. Section 316(a) does not, for example, take into account capital cost, energy use, or water consumption. Thus, while it may prevent the most irrational results, it cannot ensure the optimum resource use that should be the touchstone of rational management of waste heat.

The United States Court of Appeals for the Fifth Circuit knocked down EPA's closed-cycle cooling rules for power plants, largely because the Agency did not consider whether the rules would result in tangible environmental benefits. 7/ Since the court's decision in July 1976, EPA has not repromulgated BAT regulations for thermal discharges from any point source category. In the absence of any effective EPA regulations defining BAT, these requirements have been determined on a case-by-case basis. EPA is expected, however, to promulgate new regulations for thermal discharges within the next year.

2.3. Indirect Restrictions: Water Quality Standards

The Water Act also requires compliance with water quality standards established under state law. See Water Act §§ 301(b)(1)(C), 303. Water quality standards for temperature, in contrast to effluent limitations, do not directly limit the amount of heat discharged. They typically set maximum permissible absolute temperatures and limits on temperature increases above ambient. Compliance is ordinarily required at the edge of a mixing zone which may be delineated in terms of surface area, cross-section, and, on flowing streams, percentage of river flow. Typical temperature standards for estuaries set an allowable temperature increase of 1.5°F during summer months and 4.0°F during the remainder of the year. 8/ In other water bodies, the Mississippi River, for example, typical standards set a maximum allowable temperature for each month of the year.

In theory, water quality standards are based on a rough cost-benefit analysis at the state level. Ideally, this balancing judgment occurs when the state designates a particular use for the stream segment or water body in question. The state can then draw on water quality criteria information provided by EPA to determine the level of water quality necessary to support the designated use. In practice, the designated use often reflects more a federal EPA policy than a conscious or reasoned state judgment. And the specific temperature criteria are too often set without adequate consideration of local ambient conditions. In several cases I have handled, historical temperature records showed that natural ambient temperatures equalled or exceeded the temperature standards prescribed for a stream. When ambient river temperatures equal the standard, of course, any addition of waste heat would cause a theoretical violation, even though the temperature increase may not be measurable beyond the mixing zone.

Water quality standards have had a greater practical effect on waste heat management than have technology-based effluent limitations. All of you are probably aware of one or more instances in which temperature standards have required the installation of closed-cycle cooling or of some helper system to dissipate part of the waste heat prior to discharge. In other cases, these standards have required installation of high-velocity offshore diffusers to meet surface area restrictions on mixing zones. In my experience, these water quality standards for temperature are seldom set or applied in consideration of a full resource-use analysis. It is quite likely -- I would say unavoidable -- that these standards have led to waste heat management that is not rational.

The regulations that EPA published in 1979 to overhaul the central permit system under the Clean Water Act, the National Pollutant Discharge Elimination System (NPDES), contained an anomolous provision that would have led to even less rational results. In some cases, cooling towers or other mechanical cooling systems have been installed to ensure compliance with water quality standards under extreme ambient conditions. Temperature standards may require operation of cooling towers, for example, only during summer months. EPA's NPDES regulations however, contained a provision that would have required continous, year-round operation, regardless of ambient conditions. To its credit, in the 1980 version of these regulations, EPA clarified this provision to the effect that such systems need only to be operated when necessary for compliance with permit conditions. 40 C.F.R. § 122.7(e) (1980). But then, in a classic display of bureaucratic slight-of-hand, the Agency said in another provision (40 C.F.R. § 122.60(a)(2)) that treatment systems, such as cooling towers, may be "by-passed" only for essential maintenance -- even if the diversion results in no violation of permit limitations. Unlike the water quality standards themselves, this provision cannot be justified even in theory. During much of the year, it would result in treatment for treatment's sake. In my judgment, this is the antithesis of rational management.

2.4. Ancillary Restrictions

In addition to the primary constraints represented by effluent limitations and water quality standards, many other regulatory requirements may place constraints on waste heat management. These include regulation or restriction of new consumptive uses of freshwater, restrictions designed to protect downstream flows or to prevent salt-water intrusion, regulations or restrictions on construction of surface impoundments and, surprisingly, provisions of the Clean Air Act, as amended in 1977. Other regulatory constraints that are generally less significant may nonetheless be important in a particular case. These include noise and zoning ordinances, other land use planning restrictions, regulations governing historic and scenic preservation, and regulations governing structure height within the vicinity of airports. Any of these regulatory constraints may foreclose or affect waste heat management options.

Restrictions on new consumptive uses of freshwater may effectively preclude waste heat dissipation systems such as cooling towers that rely heavily on evaporation. In some areas, such as the Susquehanna River basin, consumption of fresh water by cooling tower evaporation must be offset by additional upstream storage for augmentation during low flow. In other areas, flow-maintenance requirements may preclude construction of on-stream impoundments or withdrawal of makeup for off-stream cooling reservoirs. Such restrictions would foreclose use of surface impoundments for waste heat management. In addition, construction of a dam to impound waters classified as navigable under FWPCA would require many permits and approvals, including a permit under § 404 of the Act from either the Corps of Engineers or the state.

Air quality regulations also impose constraints on waste heat management alternatives. Some state agencies have applied general limitations on particulate emissions to cooling tower drift. These restrictions are primarily a concern at existing or planned cooling tower installations using saltwater makeup. To date, the principal effect of application of particulate emission limitations has been to impose engineering constraints on design or operation of the cooling tower facilities. The Clean Air Act Amendments of 1977, especially the provisions for prevention of significant deterioration (PSD) and for "trade-offs" in nonattainment areas, may lead to substantially greater constraints on retrofit or new cooling tower installations.

The PSD provisions of the 1977 Amendments require a preconstruction review of all new or modified major emitting facilities in areas where the ambient air quality standards are presently being attained. The purpose of this review is to ensure that increased emissions above a baseline concentration do not exceed the allowable increment in affected air quality control regions. This restriction is in addition to the requirement to use "best available control technology" (BACT). Major emitting facilities are defined as those within specified industrial categories -- including the most energy-intensive industries such as chemical process plants -- fossil-fuel-fired power plants, that have the potential to emit more than 100 tons per

year of a regulated pollutant. Facilities not within one of the specified industrial categories are "major emitting facilities" only if they have the potential to emit 250 tons per year of a regulated pollutant. Suspended particulate matter is a regulated pollutant under the Act. If cooling tower drift is treated as particulate matter, a question that may depend on state classifications, construction of cooling towers using high salinity makeup may trigger PSD review. As a practical matter, new industrial facilities in attainment areas will be subject to PSD review in any event. It is in retrofit situations where PSD review triggered by cooling tower installation is likely to have the greater impact. Whether the "triggering" particulate emission rate is 100 tons per year or 250 tons per year will depend upon whether the cooling tower is treated as a separate source or as part of the facility it serves.

In the first phase of PSD permitting, only very large cooling tower installations would be severely constrained by allowable PSD increments if only the tower drift emissions are charged against the increment. If, however, total particulate emissions from the facility are charged against the increment once PSD review is triggered by a tower installation, the increment limits may preclude use of towers using high salinity makeup. Similarly, as portions of the allowable increment are consumed by construction of major emitting facilities, the constraints on cooling tower construction would become more severe. Thus, PSD review may operate as a constraint on waste heat management in situations where cooling towers would be the rational solution.

In areas of the country where ambient air quality standards for particulates are not being attained, implementation of the nonattainment provisions of the Clean Air Act would similarly constrain cooling tower use if drift is regulated as particulate emissions. Construction of cooling towers in these areas would be contingent upon offsetting reductions in existing particulate emissions. As a consequence of these Clean Air Act provisions, increased efficiency of drift eliminators, operation of towers at lower cycles of concentration, or use of freshwater makeup may be important considerations for cooling tower installations at coastal sites.

EPA Administrator designate Anne Gorsuch, in accordance with the Reagan Administration's intention to reduce unnecessary regulatory restrictions, has indicated that amendments to the Clean Air Act may be forthcoming. Although neither Gorsuch nor the Administration has specified just what changes will be made, it is possible that waste heat utilization may be increased by relaxed restrictions.

3. UTILIZATION

At this time, one set of regulations truly aim at encouraging waste utilization through the vehicle of cogeneration. But many of the same regulatory constraints that affect waste heat management will also affect waste heat utilization. In addition, other regulatory constraints, including public utility rate regulation and food and drug laws, may come into play depending upon the particular use of waste heat involved. We will con-

sider in turn some regulations that would impinge on various cogeneration arrangements and on thermal aquaculture as examples of potential uses of waste heat.

3.1. Thermal Aquaculture

Use of waste heat to enhance production of fish and shellfish in aquaculture projects is an interesting prospect. Oysters and catfish are among the species that have been commercially cultured in thermal discharges from power plants. Feasibility studies and the experience in other countries, particularly Japan, indicate substantial potential for thermal aquaculture of other species of fish and shellfish. But regulatory constraints will, in all likelihood, prevent realizing this potential.

Aquaculture projects in navigable waters are governed by § 318 of the Clean Water Act. Aquaculture projects confined to artificially constructed ponds or runs may not be subject to § 318, although EPA's definition of "navigable waters" is so broad that exclusion from coverage is doubtful. In any event, discharges from an aquaculture project to navigable waters are subject to regulation as point source discharges under the Act. Pursuant to § 318, EPA has established regulations providing guidelines for issuance of permits or discharges to aquaculture projects. These regulations limit the allowable size of a designated project area and impose restrictions on the "migration of pollutants" from the area. In order to issue a permit for a discharge to an aquaculture project, the EPA Regional Administrator must make a series of determinations. Importantly, he must determine that "migration of pollutants" from the project area will not violate water quality standards or effluent limitations that would be applicable to the supplier of the pollutant. Mixing zone provisions of water quality standards apply to approved projects. In addition, the migration of pollutants from the aquaculture project may not exceed the discharge allowable under effluent limitations applicable to the supplier of the pollutant. If EPA's revised effluent limitations for thermal discharges from power plants, for example, require closed-cycle cooling, the heat that "migrates" from a thermal aquaculture project must not exceed the amount of heat that would be discharged from a closed-cycle cooling system. In short, aquaculture projects would be allowed only with closed-cycle cooling systems. The concentration of potential contaminants in closed-cycle cooling systems, however, may make the blow-down discharge unsuitable for use in aquaculture.

Food and drug laws will also govern deleterious substances other than radioactivity. Heavy metals concentrated in receiving water may well be subject to regulations or prohibition. The outlook, therefore, is not bright for aquaculture.

3.2. Cogeneration

Cogeneration has been broadly defined as the coincident generation of steam and electricity. There are generally two types of systems: (1) topping cycle, in which turbine exhaust steam is used to provide heat for industrial processes, and

(2) bottoming cycle, in which process heat or steam is then used to generate electricity. Cogeneration has the potential to increase the thermal efficiency of fossil power plants from roughly 33 percent to 80 percent in some applications. The potential for energy savings is obvious. But until recently, a lack of regulatory incentives curbed the potential success of cogeneration ventures. New regulations, however, aim at an aggressive encouragement of cogeneration.

Section 210 of the Public Utilities Regulatory Policies Act (PURPA) of 1978 required the Federal Energy Regulatory Commission (FERC) to set rules to encourage cogeneration and small power production. These rules, promulgated last year, aim at breaking down three barriers that previously plagued would-be cogenerators and small power producers. First, nothing generally required utilities to purchase electric output from a cogenerator. Second, some utilities allegedly charged discriminatorily high rates for back-up service to cogenerators. Third, cogenerators that did provide electricity to a utility ran the risk of falling under state and federal regulations as electric utilities. Let us focus for a moment on the regulations affecting cogeneration.

A February 25, 1980 final rule requires electric utilities to buy electric energy and capacity available from qualifying cogenerators at a rate that reflects the costs the utility can avoid by obtaining energy and capacity from the cogenerator rather than generating it themselves or buying it from other sources. This final rule also requires electric utilities to furnish electric energy to qualifying facilities "on a nondiscriminatory basis . . . just and reasonable . . . and in the public interest." 18 C.F.R. § 292.304 (1980). The qualifying facilities may also request certain types of service to supplement, or back up, their own facilities' generation. The electric utility must provide this service on request.

A supplementary rule, promulgated March 20, sets forth criteria and procedures necessary to obtain "qualifying status." A facility can gain certification without specific FERC action. An optional procedure is available too, when necessary, specifically to award qualifying status.

A cogeneration facility, with the exception of new diesel cogeneration facilities, may be a qualifying facility by fulfilling two requirements. Like the small power producer, not more than 50 percent of the equity interest in the facility can be held by an electric utility, by a public utility holding company or by a person holding a major interest in a electric utility. 18 C.F.R. § 292.203(b). Unlike the small power producer, the cogeneration facility must meet the operating and efficiency standards delineated in 18 C.F.R. § 292.205.

Rules implementing the Natural Gas Policy Act of 1978 (NGPA) establish another valuable incentive for cogenerators. Natural gas used by a "qualifying cogeneration facility" (i.e., one that meets the above PURPA requirements) is exempt from incremental pricing provisions in the NGPA. 18 C.F.R. § 292.205(c). The requirements for "qualifying" facilities may

be waived, however, if the FERC considers that a facility's significant energy savings warrant such action. 18 C.F.R. § 292.205(c).

A representative of FERC's General Counsel stated that 50 facilities now qualify as of May 1980. Approximately 25 percent of these submitted self-qualifying notices, and 75 percent applied for qualification through the optional procedure. The FERC rules do seem to encourage -- indeed, in some instances to demand -- interconnection between utilities and qualifying cogenerators. The California Public Utilities Commission levied a $7.2 million per year rate penalty on Pacific Gas & Electric Company for "failing to accommodate and preserve cogeneration." 9/ The FERC estimates that the 1980 regulations will provide approximately 12,000 Mw of capacity by 1995.

With the exception of new diesel cogeneration facilities, an environmental assessment prepared by FERC declared that the 1980 rules will not significantly affect the environment. Other environmental regulations, however, do affect the ease with which a cogenerator may operate.

The feasibility of large-scale bottoming-cycle cogeneration projects depends heavily on clustering of industrial facilities around a central generating station. Provisions of both the Clean Air Act and the Clean Water Act, however, may effectively preclude such clustering in the future. The Clean Air Act's greatest impact, of course, will be on coal-fired central stations. PSD and nonattainment provisions will make it difficult to locate large industrial facilities in close proximity to one another, if they are major emitting sources of controlled pollutants. In addition to regulating sulfur oxide and particulate matter, the Air Act's PSD provisions direct EPA to promulgate PSD regulations for HC, CO, photochemical oxidants, NOx, and lead. Two or more sources of the same pollutant may have difficulty locating close to one another in many parts of the country. The siting difficulties will be even more severe in nonattainment areas, although the potential for offsets may be greater in those areas since they are frequently already heavily industrialized. Under the Water Act, waste load allocations designed to implement water quality standards may impose analogous restrictions on the location of major new sources of water discharges.

Health and safety regulations impose significant constraints on the potential secondary uses of nuclear-generated steam. Use of nuclear-generated steam in the processing of food, drugs, or cosmetic items or ingredients is subject to special constraints under provisions of the Federal Food, Drug & Cosmetics Act regulating adulterated substances and "additives." One provision prohibits subjecting food or food products to radiation, 21 U.S.C. § 342(a)(7), unless the FDA issues a regulation supporting the exposure. The so-called "Delaney Clause" prohibits "additives" that have been found to cause cancer upon ingestion by man or animal. Under this provision, nuclear-product steam cannot be used in food processing if there is any reasonable probability of exposure to radioactivity.

4. CONCLUSION

Regulatory constraints that arise from conflicting governmental policies often thwart the use and management of waste heat. Economic incentives seem to be doing the most to encourage utilization. The importance of carefully husbanding our energy and other resources calls for further examination of regulations to determine how they may be modified to encourage rational management and utilization of waste heat.

REFERENCES

1. 33 U.S.C. §§ 1251, et seq. (Supp. II 1978) (hereinafter cited as the Water Act). Citations in this paper are to sections of the Water Act rather than to the United States Code.

2. 39 Fed. Reg. 36186, 36200-01 (1974, codified at 40 C.F.R. §§ 423.13(l), 423.15(l) (1977)).

3. Compare 40 C.F.R. § 423.13(l)(3) with § 423.15(l)(2) (1977).

4. Stone & Webster Engineering Corp., Report on the Capital Costs of Closed-Cycle Cooling Systems, in Thermal Control Cost Factors, submitted to U.S. EPA by the Utility Water Act Group (June 1978).

5. Stone & Webster Engineering Corp., Report on the Capital Costs of Closed-Cycle Cooling Systems, Tables 1-2 and 1-4 (May 1978).

6. Espey, Huston & Associates, Inc., The Use of Surface Water Impoundments for Cooling of Steam-Electric Power Stations in Cooling Impoundments, submitted to U.S. EPA by the Utility Water Act Group (June 1978).

7. Appalachian Power Co. v. Train, 545 F.2d 1351 (4th Cir. 1976).

8. E.g., Envir. Rep. 736: 0502 (Del. Stream Quality Criteria).

9. Arnold Nadler, FERC's New Cooperation Rules, Public Power, vol. 38, p. 45, 1980.

SESSION X-A

UTILIZATION V

PB82-228594

WASTED LATENT HEAT RECOVERY FROM LOW TEMPERATURE GASES

Dr. Yen-Hsiung Kiang, P.E.
Trane Thermal, Process Division
The Trane Company
Conshohocken, PA 19428, U.S.A.

ABSTRACT

In industrial plants, a possible waste heat source is uncondensable gases saturated with water vapor. An example of this type of waste heat source is the scrubber exhaust gases. Considering that the latent heat of water is 550 Kcal/kg, for every kilogram of water vapor lost through the stack, 550 Kcal is lost. To recover the latent heat, it is necessary to condense the water vapor in the presence of non-condensables. This presents an unusual but interesting heat transfer problem. The purpose of this paper is to present the partial condensation heat recovery technology and its applications. The application of the basic technology to gases other than air-water mixture will also be discussed.

1. INTRODUCTION

In industrial plants, a possible waste heat source is gases saturated with water vapor. Considering that the latent heat of water is 550 Kcal/kg, for every kilogram of water vapor lost through the stack, 550 Kcal is lost. To recover the latent heat, it is necessary to condense the water vapor in the presence of noncondensables.

The water content and recoverable heat of saturated air is illustrated in Figure 1. The recoverable heat for each degree of temperature cooled for the mixture is presented in Figure 2.(1)

The heat in the water saturated air can be recovered through a shell and tube heat exchanger (Figure 3). The low temperature heat can be used in vacuum evaporation, water heating, and evaporator and boiler feedwater heating. The major drawback in this system is the low temperature, which limits the application.

Preceding page blank

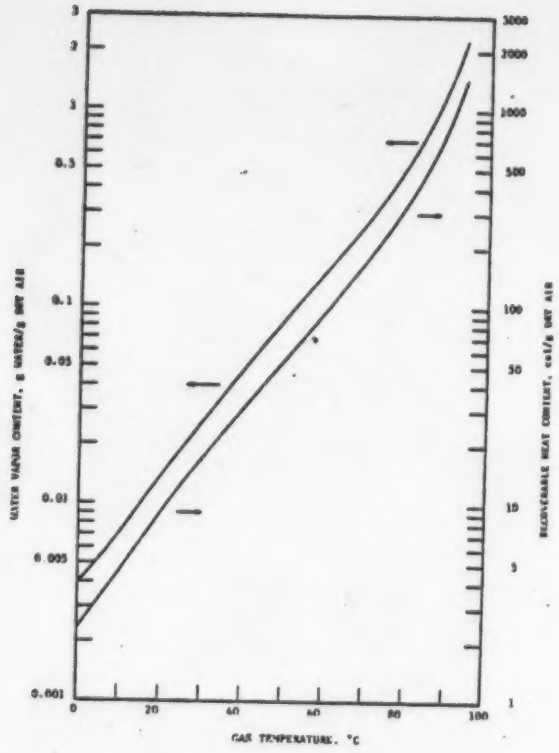

Fig. 1 - Property of Saturated Air

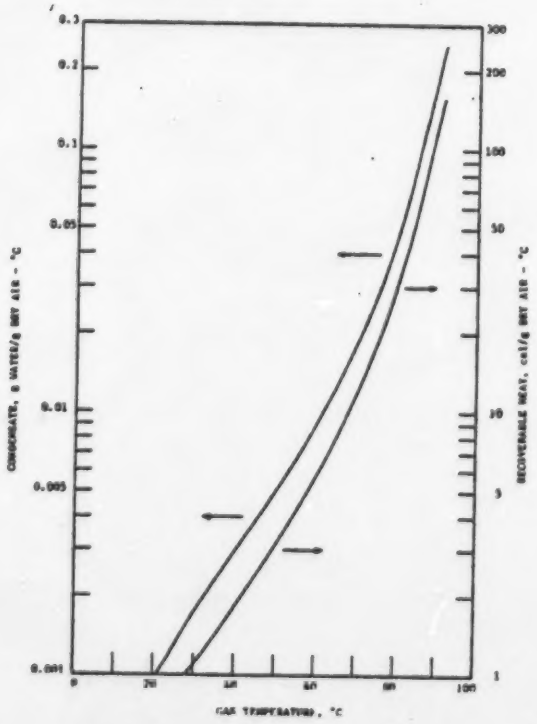

Fig. 2 - Heat Recovery of Saturated Air

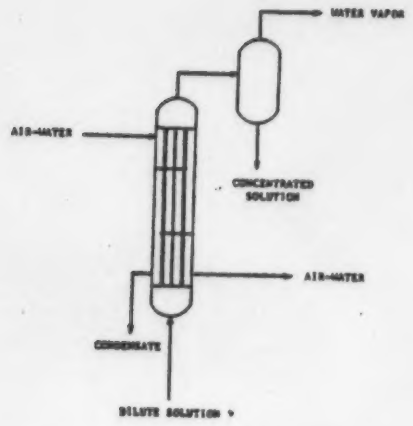

Fig. 3 - Surface Condenser

The wasted heat can also be received through direct contact condenser, Figure 4. In this type of application, the heat can only be used to heat water. Also, the contamination of the hot water stream must be considered.

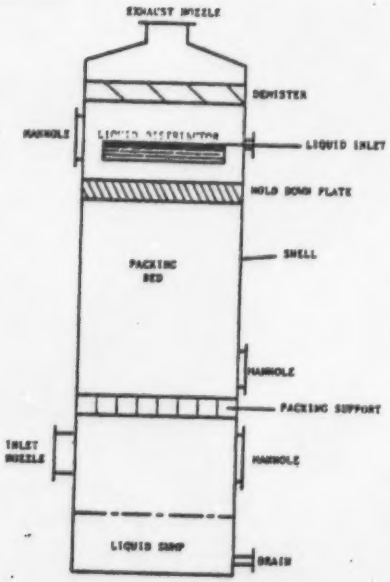

Fig. 4 - Packed Tower Condenser

2. HEAT TRANSFER

There are two types of condensers for recovery of waste heat from water saturated gases: the surface condenser and the direct contact condenser. The heat transfer aspect of both types of equipment is discussed below.

2.1 Surface Condenser

The design of a surface condenser for the condensation of vapors from a mixture of vapors with noncondensing gases presents several very unusual conditions and complications in heat transfer not encountered in the condensation of pure vapors or in the cooling or heating of homogeneous fluid streams. In the condensation of vapors from their mixture with noncondensing gases, the properties of the gas stream vary greatly as the water vapor is removed. Also, the condensation of the vapors depends upon the mass transfer of water vapor molecules as well as heat transfer.

A condensing heat transfer model is shown in Figure 5. The heat transfer process contains four sections: the liquid film, the tube wall, the condensing film, and the gas film. A stepwise trial and error method can be used to determine the heat transfer coefficient and heat transfer surface as proposed by Colburn and Hougen[2].

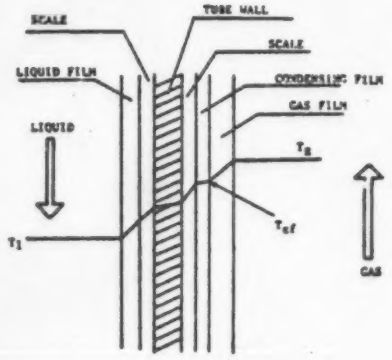

Fig. 5 - Condensing Heat Transfer Model

Due to the complexity of the heat transfer process, no conventional method of calculating mean temperature differences based on terminal conditions is applicable. The true average temperature difference between the heating and cooling fluids may be greater than the temperature difference as defined at either end of the exchanger. As has been shown by Colburn and Hougen, the conventional defined mean temperature difference may give a surface area which is 50% higher than required for heat transfer.

The typical heat transfer requirement is illustrated by the following system. A shell and tube heat exchanger is used to cool an air stream, saturated with water vapor, from 95 to 40°C by heating water from 20 to 60°C. Gas passes through the shell side, with water side velocity at 1.2 m/sec. and dry air flow rate at 1270 kg/hr.

Figure 6 shows the heat transfer rate at different gas temperatures along the exchanger. Figure 7 presents the clean overall coefficient. The overall coefficient for a condensing system is much higher than for a gas-liquid system, which is approximately 25 cal/cm^2-hr-°C. The heat transfer area requirement is shown in Figure 8. The condensing film surface temperature and the temperature difference at each point are presented in Figure 9. Based on terminal temperature, the logarithmic mean temperature difference is 27°C; however, the actual mean temperature difference, the average of the point temperature difference, is 35°C. A detailed discussion on this subject is

available from Reference 1.

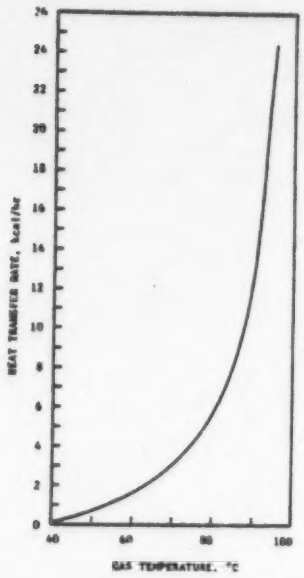

Fig. 6 - Heat Transfer Rate

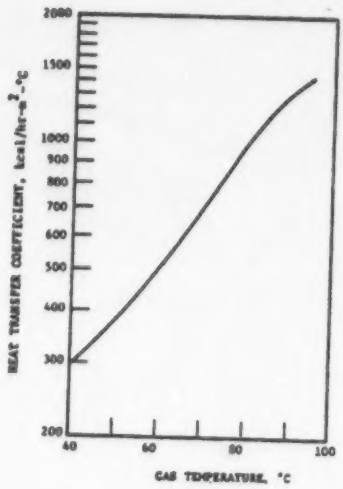

Fig. 7 - Heat Transfer Coefficient

2.2 Direct Contact Condenser

In the waste latent heat recovery application, the condensation of water vapor occurs during the heat transfer operation. Total heat transfer in the direct contact condenser includes gaseous sensible heat transfer, Q_g, as well as the heat of condensation. The overall heat transfer coefficient may be defined as

$$\frac{1}{U_a} = \frac{1}{h_{ea}} + \frac{1}{\alpha(h_{ga})} \frac{Q_g}{Q}$$

where Q is the total heat transferred, h_{ga} is the gas side heat transfer coefficient. Both h_{ga} and h_{ea} are functions of equipment used, as well as the properties of the gas and liquid. The coefficient α is defined as

$$\alpha = \frac{C_o}{1 - e^{-C_o}}$$

where the constant C_o is defined as

$$C_o = \frac{N_A C_{gA}}{(h_{ga})V}$$

where N_A is the rate of condensation of water, C_{gA} is the heat capacity of water vapor, and V is the heat transfer volume.

Gas-to-liquid heat exchangers are usually classified as differential stage or equilibrium stage units. In the differential stage unit, there are always temperature driving forces for heat transfer. In the equilibrium

stage unit, gas and liquid are separated when they are in equilibirum with each other. The differential stage units are available as spray towers, baffle columns, and packed towers. The equilibrium stage units are available as tray towers, venturi contactors, and spargers. A detailed discussion of all the equipment is presented in Reference 1.

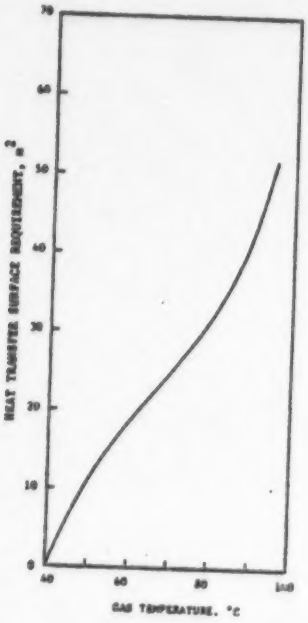

Fig. 8 - Heat Transfer Surface Temperature

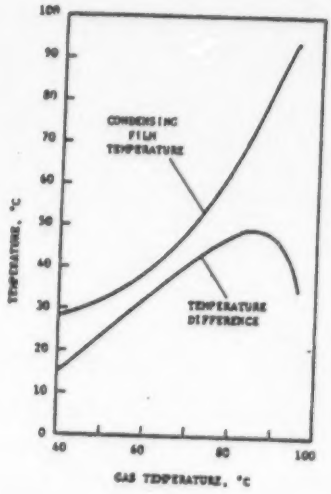

Fig. 9 - Temperature Difference in Partial Surface Condenser

3. LIMITATIONS

3.1 Surface Condenser

Wet environments require critical material selection to provide heat exchanger design. It is necessary to know the composition and constituents of the mixed vapors. When vapor streams are water, air, and hydrogen chloride mixtures, the material for the heat exchanger is limited to tantanlum or non-metallic materials, such as graphite. When the vapor streams contain chloride salts, use of stainless steel will result in stress cracking. It is advisable to use a higher alloy, such as Carpenter 20, titanium, or Hastelloy. For phosphoric acids and sulfuric acids, Hastelloy is also a good choice.

Low temperatures present other difficulties in applying this technology. The low temperature dictates that waste heat must be recovered on site. In most cases, besides waste concentration, exchangers are usually used as hot water heaters, boiler and evaporator feedwater heaters.

3.2 Direct Contact Condenser

The major disadvantage of direct contact condensers are the application and contamination. Because of the condensation of water vapor, the direct contact condenser can only be applied to water heating systems. Contamination of the water to be heated may prove to be detrimental. For example, combustion flue gases usually contain carbon dioxide, nitrogen oxides, and sulfur oxides. Direct heat transfer between the gas and water usually results in dissolution

of these acids into water. Thus, the application of this type of heat recovery system must be analyzed individually.

4. APPLICATIONS

4.1 Waste Incineration Application

This technology has been applied successfully in waste incineration systems. A system developed by Nittetu Chemical Engineering Ltd. of Japan is illustrated in Figure 10 (1,3).

This system is developed to reduce waste disposal cost for metal-bearing wastes which will form low melting point compounds. The basic system is shown in Figure 10. The incinerator is to be operated at a temperature at which the alkali compounds will be in the molten state. The exhaust gases from the quench tank will be saturated with water vapor at a temperature between 85 to 95°C.

The shell and tube heat exchanger is designed to partially condense the water vapor and recover the waste heat. The heat exchanger can be used to preconcentrate waste liquids, thus saving disposal costs. It can also be used as a heat source for process plant use. This design keeps the metallic compound in a molten state, and only small, nonsticky particles will be able to reach the heat exchanger. Field operation data show that fouling of the exchanger is small.

Large savings of auxiliary fuel (up to 80%) have been achieved when using these systems to preconcentrate aqueous wastes(4). The Sub-X® tank serves as both a quench and particulate removal device. Only particulates of sizes smaller than 2 micron will pass through the quench tank, and because of the condensed water washing on the surface of the exchanger, most of the particle buildup will be washed out.

4.2 Waste Water Treatment Application

The Aluminum Company of America has also developed a device, shown in Figure 11 (5,6). Its primary use is to concentrate wastewater. The wastes are pumped into the top of the exchanger and dispersed in a large volume of pressurized air. The waste-air mixture passes downward through the tubes where it is heated by a hot air-water vapor mixture on the shell side. As the temperature increases, the air is humidified with water vapor from the wastes. To increase the temperature for maximum humidification, low pressure steam is used on a portion of each tube length. The air absorbs a large amount of pure water vapor, and the waste-air mixture discharges from the tubes. This mixture of air and water vapor is separated from the excess liquid wastes.

The air-water vapor mixture is then conducted through a bypass line to the shell side, where the mixture is cooled by the waste-air mixture inside the tube. This cooling results in partial condensation of the water vapor. The remaining air-water vapor mixture then passes through an air or water cooled condenser to collect the remaining water vapor.

Approximately 2 g of waste can be treated for each gram of low pressure steam used. The heat from the vapor condensed and from the mixed waste products is available for space heating purposes. It is estimated that more than 80% of the heat in the steam can be recovered with proper arrangements.

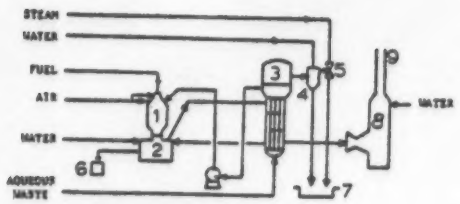

Fig. 10 - Salty Waste Incineration System:
(1) incinerator
(2) quench tank
(3) evaporator
(4) condenser
(5) steam ejector
(6) salt tank
(7) water tank
(8) venturi-separator
(9) stack

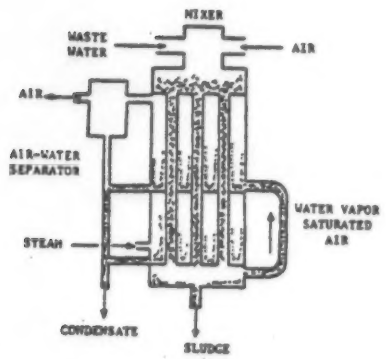

Fig. 11 - Brine Concentrator/Heat Recovery System

4.3 Multiple Effect Evaporator

The system described in Figure 12 is a direct multiple effect evaporation system (7,8). The system starts by contact of the hot flue gases with water in a venturi scrubber. The sensible heat in the flue gases is transferred into the water vapor. The flue gas exhaust from the venturi scrubber is saturated with water vapor. The latent heat in the water vapor is then recovered in a countercurrent tower to condense the water vapor. The heat in the condensates and cooling water is then used as the heat source in a vacuum evaporator.

4.4 Waste Heat Recovery Application in Citrus Process

A simplified process flow diagram for a citrus plant is illustrated in Figure 13 (9). In this process, a juice concentrator uses waste steam from the molasses evaporator as the heat source. Plant steam is used in the molasses evaporator to concentrate the molasses. The peel is dried through a "fire dryer" to about 8% moisture. The dryer uses hot gases from a furnace to dry the peel by direct contact of the gases with the peel. Traditionally,

all fire dryers were directly vented to the atmosphere. The exhaust gases were usually hot and contained some moisture. An ideal location to recover this waste heat is in the molasses evaporator, replacing plant steam.

The system can then be modified as illustrated in Figure 14. To maximize energy efficiency, the fire dryer exhaust is modified so that its exhaust gas is saturated with water vapor and at its adiabatic end point, approximately 90°C. A surface condenser partially condenses the water vapor and is used as the molasses evaporator.

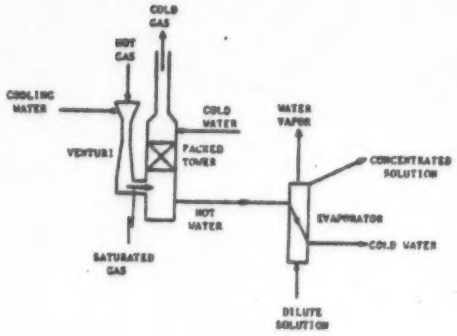

Fig. 12 - Direct Multiple Effect Evaporation System

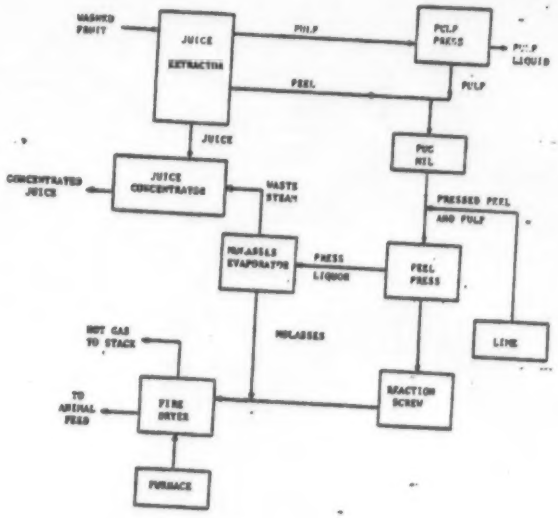

Fig. 13 - Schematic Program of a Conventional Citrus Processing Plant

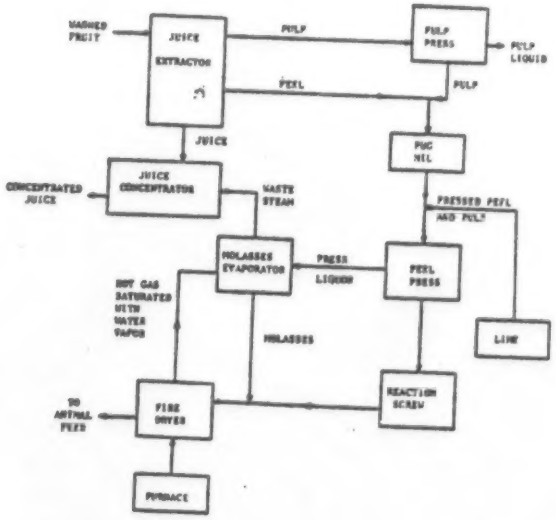

Fig. 14 - Waste Heat Recovery Schematic of a Citrus Processing Plant

5. CONCLUSION

Applying partial condensers to recover waste heat is an area long ignored by industry. By careful screening, there are thousands of potential heat sources which can be recovered through this technology. As an example, if an air stream is saturated with acetone and benzene, and there is a requirement of heating a liquid stream from -20 to 40°C, the arrangement in Figure 15 not only will recover the latent heat of acetone and benzene, which is approximately 120 Kcal/kg, but also will reduce the hydrocarbon emissions in the air stream. Another added advantage is that by properly dividing the heat exchanger, the unit can be used as a fractionation tower to recover different fractions of acetone-benzene mixture.

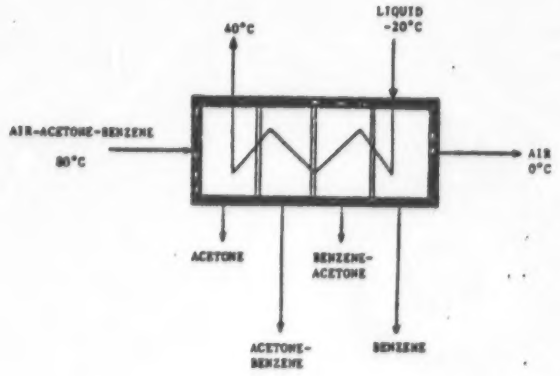

Fig. 15 - Condensing Fractionating Heat Exchanger

REFERENCES

1. Kiang, Y.H., "Waste Energy Utilization Technology", Marcel Dekker, 1981.
2. Colburn, A.P. and Hougen, O.H., Ind. Eng. Chem.,26, 11, p. 1178, 1954.
3. Kiang, Y.H., Chem. Eng. Progr., 72, 1, p. 71, 1976.
4. Kiang, Y.H., AIChE Symposium Series (Water-1978), 75, p. 46, 1979.
5. Industrial Heating, p. 32, July 1975.
6. Industrial Water Eng., p. 3, March/April 1975.
7. Farin, W.G., Pulp and Paper, p. 98, August 1975.
8. Farin, W.G., Chem. Eng., 83, 6, p. 100, 1976.
9. Kreider, K.G. and McNeil, M.B., "Waste Heat Management Guide Book", National Bureau of Standards Handbook 121, Washington, D.C., 1977.

ECONOMIC EVALUATION OF COMPETING INDUSTRIAL WASTE-HEAT RECOVERY TECHNOLOGIES

PB82-228602

Paul J. Grogan
Integrated Assessments and Policy Evaluation Group
Energy and Environmental Systems Division
Argonne National Laboratory
Argonne, Illinois, U.S.A.

Harry L. Brown and Bernard B. Hamel
General Energy Associates, Inc.
1106 Winding Road Drive
Cherry Hill, New Jersey, U.S.A.

ABSTRACT

The economics of conventional waste-heat-recovery technologies and fluidized-bed heat exchangers were analyzed according to their applications and potential market shares in the industrial sector. The performance parameters and costs of these technologies were based upon existing information. Data on available waste energy in industry, and the waste-heat temperatures, were based upon the Industrial Plant Energy Profile (IPEP). This model, available through General Energy Associates, Inc. (GEA), contains plant-energy information from approximately 400,000 industrial plant sites in the country. These sites represent the bulk of the U.S. industrial manufacturing capacity. Based on this information, the available waste energy from each of the industrial sectors was determined by major unit operation. Each of the competing heat-recovery technologies, both conventional and fluidized-bed, was applied to the waste streams. Energy savings and payback periods were determined on the bases of waste-heat source and plant size. Conventional heat exchangers showed a significant number of applications with paybacks of less than one year. The fluidized-bed systems had a limited number of such applications.

1 INTRODUCTION

Interest in waste-heat-recovery technologies, generated by escalating industrial fuel prices, has led to increases in the availability of energy-conserving processes and devices in the marketplace. Each technology has characteristics which make it well suited to specific industrial applications. One of the newer energy-recovery technologies that competes against established methods and products is a fluidized-bed system of waste-heat recovery. This report describes the extent to which fluidized-bed waste-heat recovery (FBWHR) can compete economically with conventional methods of waste-heat recovery. Included is a discussion of technical and economic characteristics of three existing heat-recovery methods, as well as a discussion of the total potential for recovering waste heat in the industrial sector. The economic attractiveness of each heat-recovery technique, using the simple payback as an investment criterion, is examined for a number of applications. In an effort to forecast which devices will most likely be implemented at particular kinds of plant sites, market shares are allocated to the various technologies on the basis of their respective payback periods.

This study utilizes information and data bases developed by General Energy Associates (GEA), including the Industrial Plant Energy Profile (IPEP) data base. From these sources, the available waste energy and the performance factors and costs of three conventional heat-recovery technologies were obtained.[1,2] Similar basic information on three fluidized-bed designs was developed from literature sources.[3-7] Based upon this information, competing heat-recovery technologies, including the FBWHR designs, were analyzed for various applications within the industrial sector. Twenty industries were selected for analysis from the Standard Industrial Classification (SIC). Table 1 identifies the industries represented by the SIC codes.

The current study is part of a larger study of fluidized-bed technology conducted by Argonne National Laboratory (ANL) for the Office of Industrial Programs of the Department of Energy (DOE). The objectives of the larger study are to determine critical factors affecting heat-recovery performance of fluidized-bed technology, promising industrial applications, and areas of technical uncertainty. These determinations are meant to provide DOE with information for its research, development, and demonstration efforts in the fluidized-bed heat-recovery area. The other three parts of the ANL study of FBWHR technology are as follows:

- A technical analysis of FBWHR,[3]
- A market evaluation of the acceptability of the technology,[8] and

Table 1 The 20 SIC Categories Analyzed for Waste-Heat Characteristics

SIC	Designation
20	Food and kindred products
21	Tobacco products
22	Textile mill products
23	Apparel, other textiles
24	Lumber and wood products
25	Furniture and fixtures
26	Paper and allied products
27	Printing and publishing
28	Chemicals, allied products
29	Petroleum and coal products
30	Rubber, misc. plastic products
31	Leather, leather products
32	Stone, clay, glass products
33	Primary metal industries
34	Fabricated metal products
35	Machinery, except electric
36	Electric, electronic equipment
37	Transportation equipment
38	Instruments, related products
39	Misc. manufacturing industries

- An assessment of the environmental control capabilities of the technology.[9]

The three waste-heat-recovery technologies considered in this study, and against which the fluidized-bed technology is compared, are:

- Economizers. These gas-to-liquid heat exchangers recover energy from exhaust gases to heat liquids. They are typically used to increase boiler efficiency by preheating feedwater.
- Waste-heat boilers. These heat exchangers are used to recover energy from gaseous sources and generate steam.
- Recuperators/regenerators. These gas-to-gas heat exchangers are used for such purposes as preheating combustion air to improve combustion efficiency. They may also be used to heat air or gases supplied to other processes.

2 APPLICATION OF FLUIDIZED-BED TECHNOLOGY TO THE RECOVERY OF WASTE HEAT

A fluidized bed enhances the heat-transfer coefficient on the gas side (external side) of a heat exchanger by promoting turbulence in the neighborhood of the tube banks. This type of heat exchanger has potential advantages in applications where relatively small temperature differences exist between the two heat-exchanger fluids. As shown in Fig. 1, a gaseous waste stream flows in a vertical direction across a horizontal row of finned tubes. The bed material is held in the vicinity of the tube rows by a distributor plate when no gas is flowing.

The effectiveness of fluidized beds for increasing heat-transfer rates of submerged heat-exchange surfaces has been known for many years. Relative to conventional heat exchangers, enhancement ratios as high as 25 times for a fluidized bed have been measured.[3-9] Experimental liquid-fluidized-bed heat exchangers have also been built and have demonstrated enhancement ratios of two. The claim is made for both gaseous and liquid fluidized beds that fouling due to contamination in the fluid stream is prevented by the scouring of the particles in the bed. The principal near-term application of fluidized-bed exchangers is expected to be as water heaters and waste-heat boilers.

In this study, the fluidized-bed technology has been considered for the following three applications:

- Steam generation to provide 100 psig steam from feedwater at 60°F;
- Thermal fluid heating to raise the temperature of a gaseous stream from 400°F to 500°F; and
- Liquid heating to raise the temperature of water from 140°F to 180°F.

The technical performance characteristics and parameters for the fluidized-bed system were based on the information presented in Refs. 6 and 7.

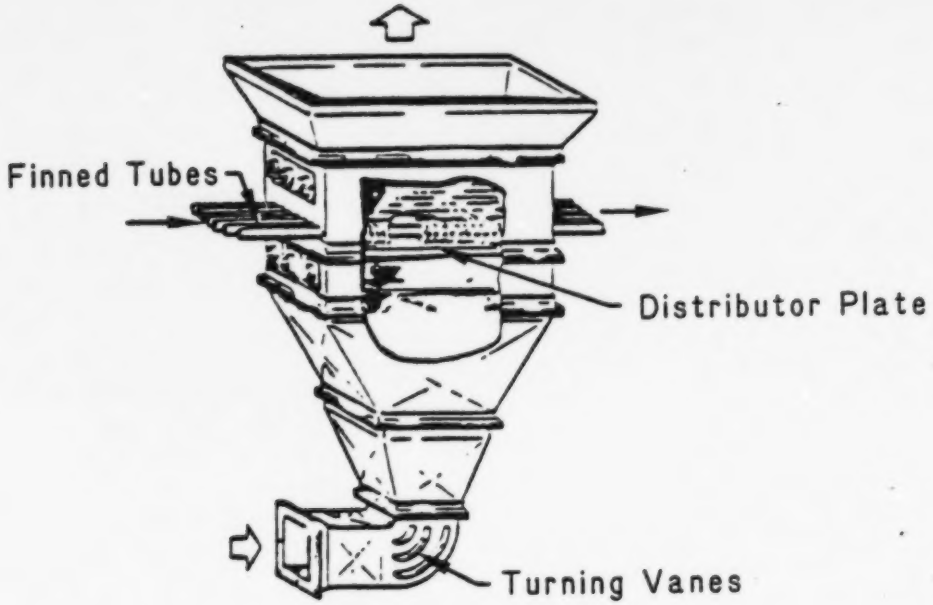

Fig. 1 Fluidized-Bed Heat Exchanger

3 DESCRIPTION OF THE GEA/IPEP MODEL

The methodology developed in constructing the GEA Industrial Plant Energy Profile (IPEP) melds a variety of data streams into a coherent data-management system. The IPEP approach is based on the premise that the fundamental unit of energy use in the industrial sector is the individual industrial plant site. With this premise in place, and an estimating methodology established, a data system has been created that allows different levels of aggregation. In this way the uncertainties, errors, and inaccuracies associated with any aggregate figures can be clearly shown to be attributed to the individual plant estimates. Rather than beginning with aggregate data -- with its uncertain origins -- and then disaggregating to end-use and process levels, the IPEP approach builds up from the plant level.

The basic data tool of the IPEP is the Dun & Bradstreet plant list for the U.S. This contains company name; number of employees; sales; four-digit SIC classification code; and address at the state, county, and 5-digit zip code level for more than 400,000 manufacturing establishments. The IPEP took into account number of employees, sales and 4-digit SIC for a specific plant site; to these data it added a detailed process/product data base and extensive plant-specific data obtained from trade associations. The Census of Manufacturer's Data was then used, as control sums at a plant's most local level, to modify all estimates so that local considerations are taken into account. In developing this approach, a cornerstone has been the plant-specific trade-association data available for more than 4500 plant sites -- this allows accurate estimates of process energy use for plants that represent more than 65% of national energy use.

4 ECONOMICS OF HEAT RECOVERY

The adoption of any heat-recovery technology by an industrial user will primarily depend on the economic attractiveness of the investment. Other factors such as capital availability, environmental concerns, and reliability of the equipment may be considered -- but a firm's eventual decision is usually based on a comparison of the project's economic return against some minimally acceptable investment criterion. One such investment criterion is the payback period, and it is used in this report to analyze the economic attractiveness of competing heat-recovery technologies. Selection of technology based on payback analyses introduces some uncertainty into the decision-making process because of economic inaccuracies associated with use of the payback period. These inaccuracies are explained by the omission of discount rates, inflation, depreciation, and other economic parameters from an investment analysis. Use of the payback period for investment analysis is simple, however, and is considered useful for screening purposes or when uncertainty exists in the data.

The basic model for determining economic payback of conventional heat exchangers and a fluidized-bed heat exchanger is based upon the following factors.

TIC = total installed cost ($),

OM = annual maintenance and operating costs ($/yr),

TS = annual cost savings from energy recovery ($/yr),

CF = cash flow for a given year ($/yr),

I = integral number of years from 1980 base year -- for 1985, for example, I = 5, and

J = payback period (no. of years).

These factors are incorporated into the formulation

$$CF = (1.12)^{I-1} (TS - OM)(0.5)$$

where

1.12 = yearly inflation rate of 12%, and

0.5 = tax rate.

From this analysis, a given technology's payback period -- the period of time in years it takes that technology to pay back the total costs associated with its installation -- may be determined as follows:

$$\sum_{I=1}^{J} CF \geq TIC$$

Thus the sum of the cash flow every year is assessed until the sum is greater than or equal to the total installed cost. That year (J) represents the payback period.

5 EQUIPMENT COST ESTIMATES

Equipment and installation costs were taken from a number of sources. The following information was used as the basis for the results presented in Sec. 6.

5.1 Tubular Cross-Flow Heat Exchanger

The basic source of cost information was Fig. 2. In addition to that information the following factors were included.

- A 30% inflation from 1978 to 1980,
- A 2.5 multiplying factor for steel tubes, and
- A 2.0 multiplying factor for installation cost (Ref. 1).

The final cost equation is

$$\text{Cost } (\$/ft^2) = 188.1(A)^{-0.26}$$

where

A = heat-exchanger external tube-surface area (ft^2).

5.2 Plate-Fin Heat Exchanger

The basic source of cost information was also Fig. 2. The following factors were also included.

- A 30% inflation from 1978 to 1980, and
- A 2.0 multiplying factor for installation costs (Ref. 1).

The final cost equation is

$$\text{Cost } (\$/ft^2) = 9293(A)^{-0.603}$$

where

A = heat-exchanger total heat-transfer area, which is two times outer or inner area (ft^2).

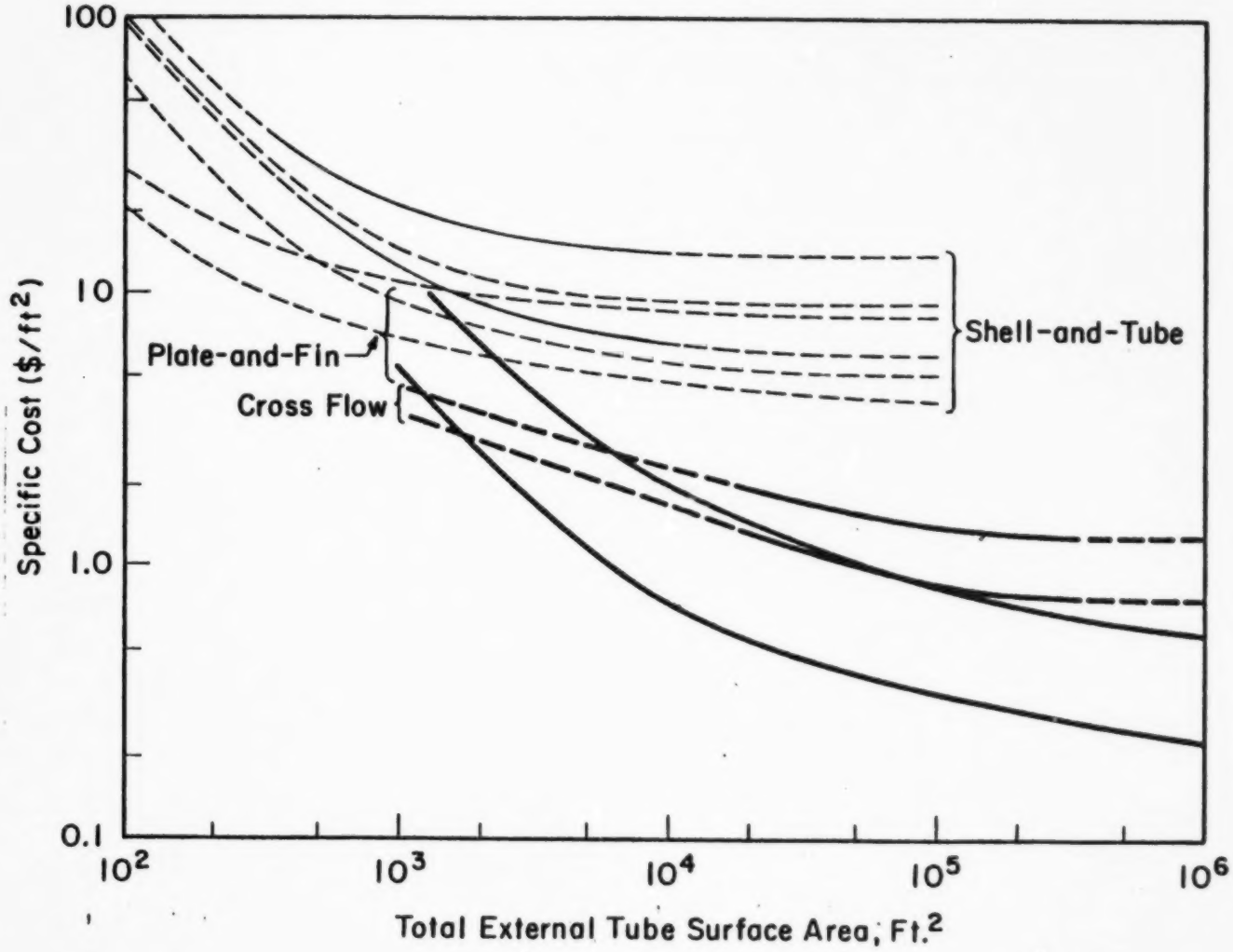

Fig. 2 Heat Exchanger Costs

5.3 Shell-and-Tube Heat Exchanger

Figure 2 was again used for the basic cost information applicable to this exchanger. For this particular unit, curve Number 5 was used from Fig. 2. In addition the following factors were included.

- A 30% inflation from 1978 to 1980,
- A 1.2 cost multiplier for boilers, and
- A 2.0 multiplying factor for installation cost (Ref. 1).

The final cost equations are

$$\text{Cost } (\$/ft^2) = 4575(A)^{-0.696} \quad \text{(for an area } <2000\ ft^2)$$

$$\text{Cost } (\$/ft^2) = 50.39(A)^{-0.103} \quad \text{(for an area } >2000\ ft^2)$$

where

A = heat-exchanger external tube-surface area (ft^2).

5.4 Operation and Maintenance Costs

The operation and maintenance costs for the cross-flow, plate-and-fin and shell-and-tube heat exchangers were based on Fig. 3. These costs are based on a semiannual cleaning and a 30% inflation from 1978 to 1980. The final cost equation is

$$\text{OM costs } (\$/yr) = 0.259(Q)^{0.566}$$

where

Q = heat-transfer rate (Btu/hr) for the heat exchanger.

5.5 Fluidized-Bed System for Steam Raising

The basic source of cost information for this technology was Fig. 4. In addition, the following factors were included.

- A 15% inflation from 1979 to 1980, and
- A 2.0 multiplying factor for installed costs.

The final cost equations are

$$\text{Cost } (10^3\$) = 3.468M + 41.89 \text{ for } M < 22.4$$

$$\text{Cost } (10^3\$) = 2.645M + 60.38 \text{ for } M > 22.4$$

where

M = waste-gas mass-flow rate (10^3 lb/hr).

The operation and maintenance cost for all FBWHR systems was based on a surcharge of 10% on equipment costs.

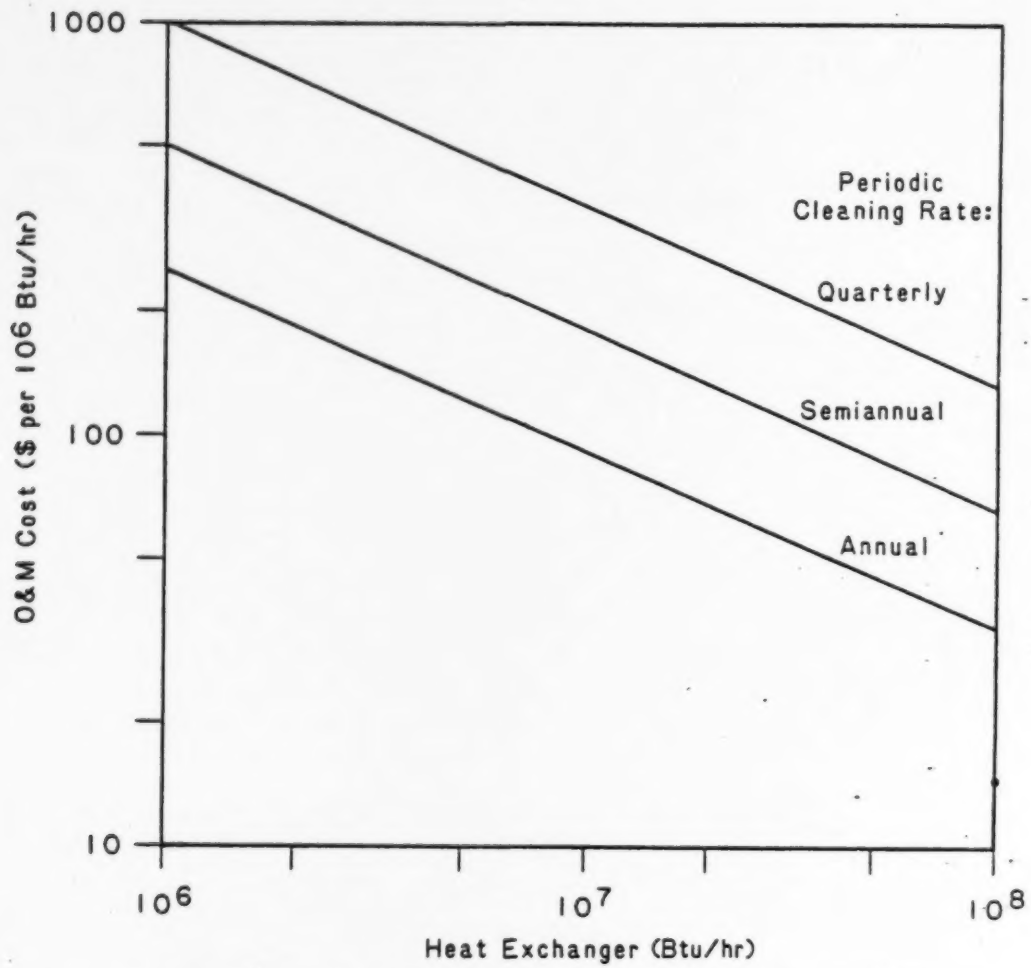

Fig. 3 Annual Operating and Maintenance Costs for Cross-Flow, Plate-Fin, and Shell-and-Tube Heat Exchangers, in 1978 Dollars (Source: Ref. 1)

5.6 Fluidized-Bed System for Thermal Fluid Heating

The basic source of cost information was curve B of Fig. 4. Other factors included are:

- A 15% inflation from 1979 to 1980, and
- A 2.0 multiplying factor for installation costs.

The final cost equations are

$$\text{Cost } (10^3\$) = 2.698M + 22.36 \text{ for } M < 22.4$$

$$\text{Cost } (10^3\$) = 2.645M + 23.58 \text{ for } M > 22.4$$

where

M = waste-gas mass-flow rate (10^3 lb/hr).

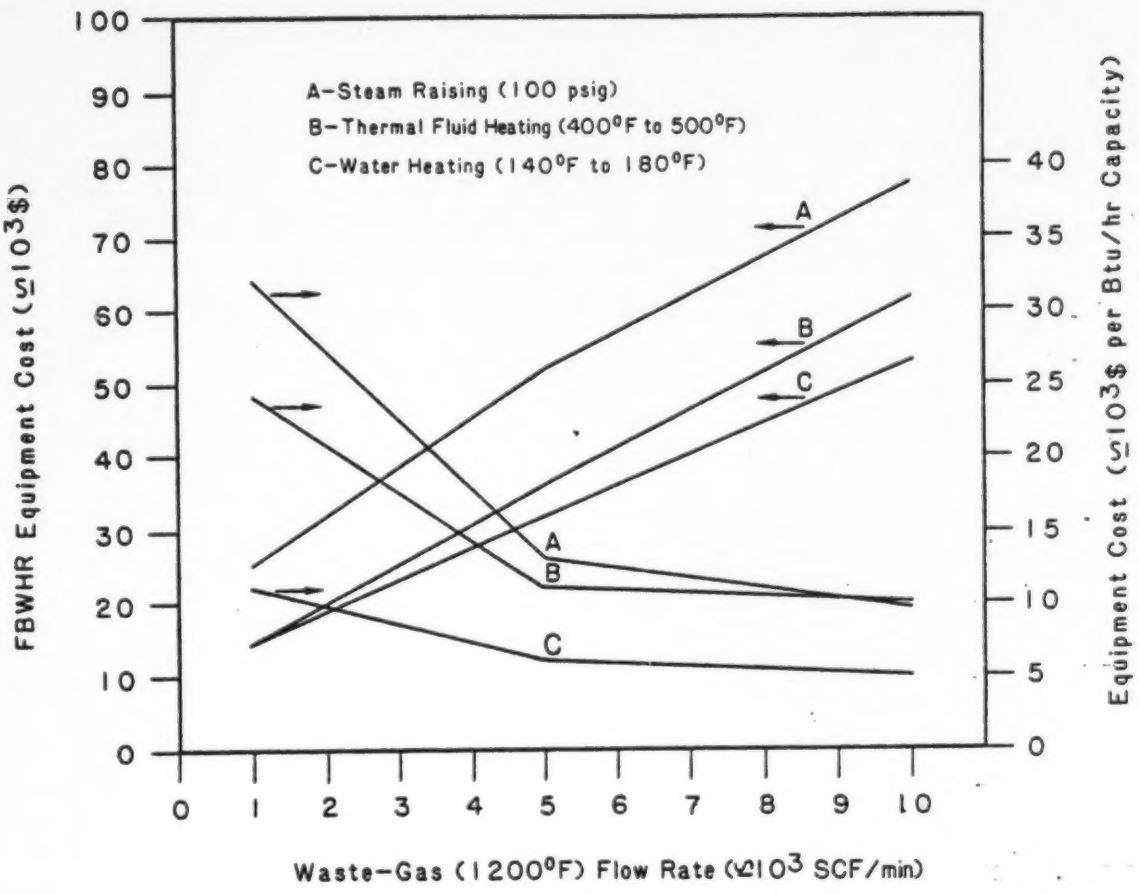

Fig. 4 Cost of Fluidized-Bed Equipment

5.7 Fluidized-Bed System for Water Heating

The source of information for these costs was curve C from Fig. 4 In addition, the following factors were included;

- A 15% inflation from 1979 to 1980, and
- A 2.0 multiplying factor for installation costs.

The final cost equation is

$$\text{Cost } (10^3\$) = 2.215M + 24.54$$

where

M = waste-gas mass-flow rate (10^3 lb/hr).

6 CONCLUSIONS

Technical and economic descriptions of waste-heat recovery technologies contained in previous sections are analyzed here to indicate the nature and

extent of the potential market for each of the alternatives. The sources of waste heat -- by unit operations in a variety of industries -- are presented in Table 2. In the table, unit operations (e.g., boilers, dryers, furnaces, reactors) are presented with a waste-heat temperature range. The total waste energy available from these unit operations within each two-digit SIC sector is also given. The information presented in Table 2 is the input information for the subsequent market-share analyses.

In this study 62 unit operations are considered covering a waste-temperature range of 200°F to 2000°F. A review of Table 2 points out the large amount of waste energy associated with boilers and in SIC 20, 26, 28, 29, 32, and 33.

In Ref. 10, energy savings and payback periods for each application are presented for three generalized plant sizes. For the sake of brevity, these paybacks are not reproduced here but can be found in Appendix B of Ref. 10. The plant sizes are:

- Small, meaning fewer than 50 employees;
- Medium, meaning 50 to 500 employees; and
- Large, meaning more than 500 employees.

The results of the payback analysis for conventional technology indicate:

- Economizer payback periods range from one to three years.
- Recuperator/regenerator payback periods range from two to 22 years, with a significant number of applications having a payback period of less than 10 years.
- Waste-heat-boiler payback periods range from one to seven years, with a significant number of applications having a payback period of less than three years.

Results for fluidized-bed technology are less optimistic:

- Payback periods for the hot-water heating application range from one to 25 years, with most applications less than five years.
- Payback periods for the fluid-thermal heating application range from two to >25 years, with a significant number of cases not applicable. The applications appear limited.
- The fluid-thermal heating application from two to >25 years, with a significant number of cases not applicable. The applications appear limited.

Table 2 Available Waste Energy in Industry

SIC[a]	Source of Waste Energy, by Unit Operation	Temp. Range (°F)	Waste Energy (10^{12} Btu/Yr)
20	Boiler	400-500	110.0
	Charcoal regenerator furnace	800-1000	0.7
	Dryer	300-500	12.7
	Dryer	500-800	36.7
21	Boiler	400-500	11.2
22	Boiler	400-500	8.1
	Dryer	300-500	18.9
23	Boiler	400-500	4.0
24	Boiler	400-500	7.2
	Dryer	300-500	63.2
25	Boiler	400-500	4.0
26	Boiler	400-500	137
	Kiln dryers	200-400	219
27	Boiler	400-500	10.2
28	Boiler	400-500	282.5
	Dryers	<200	8.7
	Dryers	200-600	11.3
	Kiln	200-600	40.7
	Kiln	1000-1200	17.0
28	Reactor	300-600	30.4
	Reactor	1000-1200	63.7
	Reactor	1200-1600	43.6
29	Boiler	400-500	133.2
	Distillation column	800-1000	103
	Distillation column	1000-1200	144.2
	Alkyl unit	400-600	61.8
30	Boiler	300-500	22.6
	Curing oven	200-400	17.9
	Drying unit	<200	14.2
	Dryer	200-400	9.9
	Molding unit	200-400	23.3
31	Boiler	300-500	2.2
32	Boiler	300-500	2.3
	Dryer	300-500	40.8
	Kiln	400-600	25.8
	Kiln	800-1200	220.3
	Heat-treating furnace	800-1000	3.5
	Annealing furnace	1000-1200	23.4
	Melting furnace	1200-1400	45.8
	Curing ovens	600-800	4.4
32	Forehearth	1200-1400	13.1
33	Boiler	400-700	43.9
	Furnace	300-500	299
	Furnace	500-1000	331
	Furnace	1000-1500	340
	Furnace	>1500	88.0
34	Boiler	400-500	3.0
	Heating furnace	300-500	35.2
	Heating furnace	1500-2000	25.5
35	Boiler	400-500	31.3
	Heat-treating furnace	1800-2000	4.7
	Dryer	500-1000	21.7
36	Boiler	400-500	27.5
	Dryer	300-500	1.5
37	Boiler	400-500	18.9
	Dryers	300-500	43.5
	Furnaces	>1500	55.1
38	Boiler	400-500	8.6
	Dryers	300-500	7.6
39	Boiler	400-500	2.8
	Dryer	300-500	2.1
	Curing oven	500-1000	2.5

[a]Categories are identified by industry names in Table 1.

From this assessment, the fluidized-bed system appears to compete reasonably for the hot-water heating application, specifically in those cases where the payback is less than one year and therefore corresponds to the payback period of conventional heat exchangers. A step-by-step comparison would show that application to SICs 28, 29, 32, and 33 for specific applications may be favorable for large plants. Paybacks for the fluidized-bed applications rise at a much faster rate than do those of conventional systems, as a smaller and smaller plant is approached.

In making a detailed market assessment concerning competing technologies, many factors must be considered. These factors (some of which were mentioned earlier) include the following:

- Technology cost,
- Payback,
- Energy savings,
- State of art of the technology,
- Industry investment criteria,
- Environmental factors,
- Actual plant conditions,
- Number of manufacturers and distributors,
- Extent of time equipment has been on market,
- General installation and operating experience, and
- Government incentives.

Of course some are more important than others, and additional ones may be added to the list for specific types of plants.

Recognizing these factors, a simplified approach has been taken to assess competing market potentials. The approach assumes that for each market segment (industry SIC and plant size), the waste-heat-recovery technology selected for implementation by the plant would be the one with the shortest payback period. For the market-share analysis, the recoverable waste heat was divided among the technologies equally when the payback periods were equal. A five-year payback was used to screen economical applications from the complete set of plants sizes and industries appearing in Ref. 10. Despite the simplified approach, the consistency of the analysis provides an insight that may not be obtainable from in-depth case studies.

A comparison of conventional heat-recovery technologies indicates economizers will capture a majority of the waste-heat-recovery market. Table 3 lists the amount of waste heat available by industry for each equipment type. Economizers and conventional waste-heat boilers account for nearly all the economic applications, capturing 58% and 42% of the waste-heat-recovery market respectively. Recuperators do not appear to be economically competitive when compared against other heat-recovery options for the applications considered in this analysis.

Table 3 Conventional-Technology Market Shares by Industry[a]

SIC	Waste Heat Available	Economizer	Waste-Heat Boiler	Recuperator
20	160	67	-	-
21	11	3	2	-
22	27	12	-	-
23	4	1	-	-
24	70	33	-	-
25	4	1	-	-
26	356	99	24	-
27	10	4	-	-
28	498	161	61	-
29	442	126	128	8
30	88	12	-	-
31	2	1	-	-
32	379	119	137	-
33	1102	310	328	-
34	64	20	7	-
35	58	26	3	-
36	29	12	-	-
37	118	39	21	-
38	16	6	-	-
39	7	2	-	-
TOTAL	3445	1054	711	8

[a] 10^{12} Btu/yr.

A look at the market for conventional heat-recovery technology by plant size indicates that conventional waste-heat boilers are most economical for and capture the biggest share of the large-plant market. (See Table 4.) Economizer market shares are roughly equal for the medium and large plants. As one might expect, the large and medium plants represent the major part of the waste-heat-recovery market, despite the larger number of small plants in some industries.

The same methodology used to determine market shares for conventional heat-recovery technology was used to estimate FBWHR market shares. Market shares for the fluidized-bed economizer in major energy-consuming industries with potential applications are shown in Table 5. The results indicate that the fluidized-bed economizer could capture approximately 27% of

Table 4 Conventional-Technology Market Shares by Firm Size[a]

Firm Size	Economizer	Waste-Heat Boiler	Recuperator
Small	145	51	-
Medium	484	182	-
Large	425	478	8
TOTAL	1054	711	8

[a] 10^{12} Btu/yr.

the economizer market. Similar conditions exist in the waste-heat-boiler market.

Estimates of the market for FBWHR equipment presented here appear optimistic in light of industrial decision-making processes. New technology, with some degree of technical or economic uncertainty associated with it, is sometimes required to meet stricter investment hurdles relative to conventional technology. Put another way, many users would rather pay a cost premium for using existing technology than switch to a new technology that appears to be more attractive on a purely economic basis. Because of resistance to new technology -- even though, in this case, fluidized-bed units provide effective economic competition for conventional heat-recovery equipment -- the FBWHR market share is likely to be less than the data presented here would indicate. Attainment of that share is also likely to take longer than would be likely for a conventional technology. The unique FBWHB characteristics not presented here, however (see Refs. 3 and 5), give it advantages for certain specific applications.

Table 5 Fluidized-Bed-Economizer and Conventional-Economizer Market Shares[a]

SIC	Conventional Economizer	Fluidized-Bed Economizer
20	67	-
26	123	-
28	194	30
29	180	62
32	122	49
33	438	155
37	39	21
TOTAL	1163	317

[a] 10^{12} Btu/yr.

REFERENCES

1. *Waste Heat Energy Recovery Technologies Evaluation and Assessment*, prepared by United Technologies Research Center for the U.S. Department of Energy, contract EY-76-S-02-2862 to Drexel University, Philadelphia, Pa. (Sept. 1979).

2. *Energy Analysis of 108 Industrial Processes*, Drexel University, U.S. Department of Energy contract E(11-1)2862, Philadelphia (June 1979).

3. Vogel, G.J., and P.J. Grogan, *Application of Fluidized-Bed Technology to the Recovery of Waste Heat*, Argonne National Laboratory Report ANL/CNSV-TM-34 (Aug. 1979).

4. Cole, W.E. and M. Suo, *Waste Heat Recovery: Waste Heat Recovery With Fluidized-Beds*, Chemical Engineering Progress (Dec. 1979).

5. Cox, D., et al., *Potential Industrial Applications for Fluidized-Bed Waste Heat Recovery Systems*, MITRE Corp. report MTR-79W00468, McLean, Va. (Dec. 1979).

6. Literature from Granco Equipment Co., Grand Rapids, Mich.

7. *Energy Conservation for Industry*, Compatible Systems Corporation literature, River Forest, Ill.

8. Grogan, P.J., F.T. Campos, C.L. Fey and N.P. Klein, *A Preliminary Market Assessment of Fluidized-Bed Waste-Heat Recovery Technology*, Argonne National Laboratory Report, in press (June 1980).

9. Vogel, G.J., and P.J. Grogan *A Description of Emission Control Using Fluidized-Bed, Heat Exchange Technology*, Argonne National Laboratory ANL/CNSV-TM-64 (June 1980).

10. Grogan, P.J., B.B. Hamel, H.L. Brown, and M.J. Koluch, *Economic Analysis of Industrial Waste-Heat Recovery: Fluidized-Bed Technology vs. Three Conventional Alternatives*, Argonne National Laboratory Report, in press (April 1981).

PB82-228610

HEAT RECOVERY FROM TURBINE EXHAUST GAS

G. HESSE
GEA - POWER COOLING SYSTEMS, INC.
SAN DIEGO, CALIFORNIA, U.S.A.

ABSTRACT

Three alternatives of increasing the fuel efficiency of simple cycle gas turbine installations are discussed in this paper: (1) recuperated cycle, (2) combined cycle, and (3) recuperated cycle combined with heat recovery. The same level of fuel efficiency can be achieved with any one of the alternatives, however, at different levels of capital investment. For the recuperated system which has the lowest capital cost, guide lines are provided for its optimum selection.

1. INTRODUCTION

Stationary gas turbines are most often operated as simple cycle machines to drive generators, compressors or pumps. The thermal efficiency of such gas turbines ranges normally between 20 and 30%. The low efficiency can be tolerated as long as the fuel is inexpensive or where the turbines operate at low annual plant capacity factors, as in peak-loaded electric generating units. The rapid increase in fuel costs dictates however, a change with regard to the overall cycle efficiency requirements. The first step in this direction is the installation of recuperators on small and medium size industrial type gas turbines. For aircraft derivative gas turbines or for very large industrial type gas turbines the choice is often combined cycle operation. A further alternative which is being considered more and more frequently is to recover heat for process or various other heating requirements from turbine exhaust gas either in separate installations or in combination with recuperators.

2. SIMPLE CYCLE

The simple cycle which requires the lowest capital investment has been used in the past for most gas turbine installations. Its schematic is shown in Figure 1. For simplicity the gas turbine is shown as a single shaft engine whereas two shaft engines are more common. In most cases the fuel efficiency is around 25%. Turbines of a more modern design have efficiencies in the range of 30%. However, cycle efficiency below 20% is also not uncommon for small gas turbines.

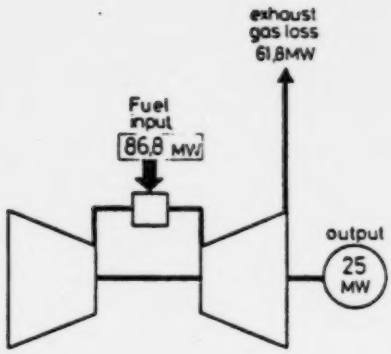

$$\eta = \frac{25}{86,8} = 28,8\%$$

Figure 1.
Frame 5 - Gas Turbine,
Simple Cycle.

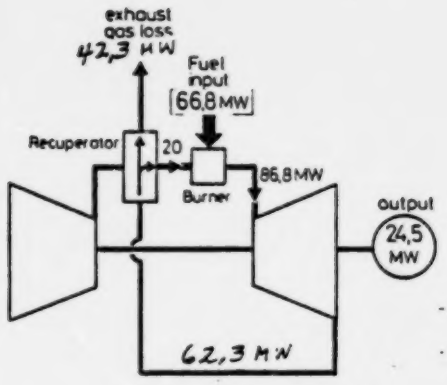

$$\eta = \frac{24,5}{66,8} = 36,7\%$$

Figure 2.
Frame 5 - Gas Turbine
with Recuperator (84%).

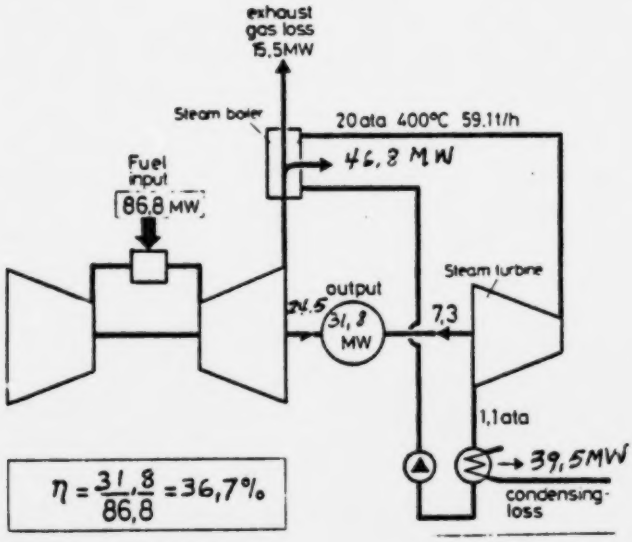

$$\eta = \frac{31,8}{86,8} = 36,7\%$$

Figure 3.
Combined-Cycle with
Frame 5 - Gas Turbine
and 7.3 MW Steam Turbine.

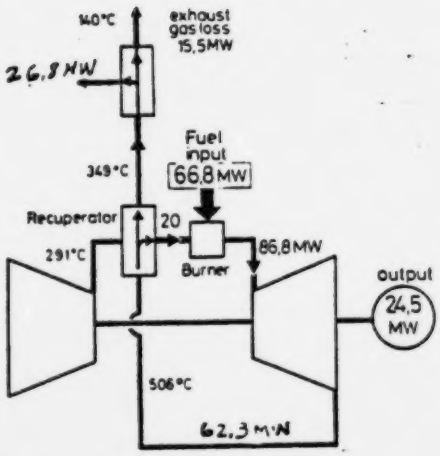

$$\eta = \frac{24,5}{66,8} = 36,7\%$$

Figure 4.
Frame 5 - Gas Turbine with
Combined Recuperator (84%)
Plus Waste Heat Boiler.

3. RECUPERATED CYCLE

Gas turbine recuperators extract heat from the exhaust gas and preheat the compressed air before it enters the combustor. As a result the fuel consumption can be reduced by 25% or more, increasing the cycle efficiency by up to 10 points of efficiency and more in extreme cases. The major application for recuperated gas turbines (as shown in Figure 2) to date has been in gas pipe line compressor stations. The function of the compressor stations is to increase the gas pressure which is the driving force for transporting the natural gas through the pipe line. Gas turbines being used as prime movers for the pipe line compressors extract their fuel directly from the gas pipe line. It is obvious that the use of recuperators on gas pipe line compressor stations means less fuel is consumed to move more gas through the pipe line. Using the parameters listed below for a natural gas pipe line the increase in pipe line capacity can be calculated to be 2.6%.

Length of pipe line	: 1,500 miles
Pipe line through put, base loaded	: 1 billion standard cubic feet/day
Number of compressor stations	: 25
Power requirement at each station	: 18,000 HP
Difference in heat rate between simple cycle and recuperated cycle, assuming an 85% effective GEA recuperator	: 2,400 $\frac{BTU}{HP\text{-}HR}$
Heat value	: 1,000 $\frac{BTU}{FT^3}$

$$\text{Capacity increase} = \frac{25 \times 18{,}000 \times 2{,}400 \times 24}{1{,}000 \times 10^9} \times 100 = 2.6\%$$

4. COMBINED CYCLE

To increase the overall thermal efficiency of a gas turbine installation the hot exhaust gas can be utilized to generate steam to drive a steam turbine. In case of a gas turbine power plant the steam turbine would be used to generate electric power. Both the gas turbine and the steam turbine can be connected to the same generator shaft as shown in Figure 3, or the steam turbine can drive a separate electric generator. Combined cycle power plants of this kind are well known.

As an example the City of Braintree, Massachusetts operates an 85 MW combined cycle power plant designed for 37% thermal efficiency [1]. Nearly 24% (20 MW) of the total station power output is generated by the steam turbine generator.

A 200 MW combined cycle plant is scheduled to start operating in 1981 at the Chugach Electric Association Beluga Power Plant in Alaska. 60 MW or 30% of the power will be generated by the steam turbine. The steam is generated using the exhaust gas from two 70 MW gas turbine generator sets.

In the case of smaller size gas turbines being used for compressor drives on gas pipe lines (normally rated up to 30,000 HP) there are the options of either using the additional steam turbine power to increase the compressor capacity of the pipe line or to generate electric power.

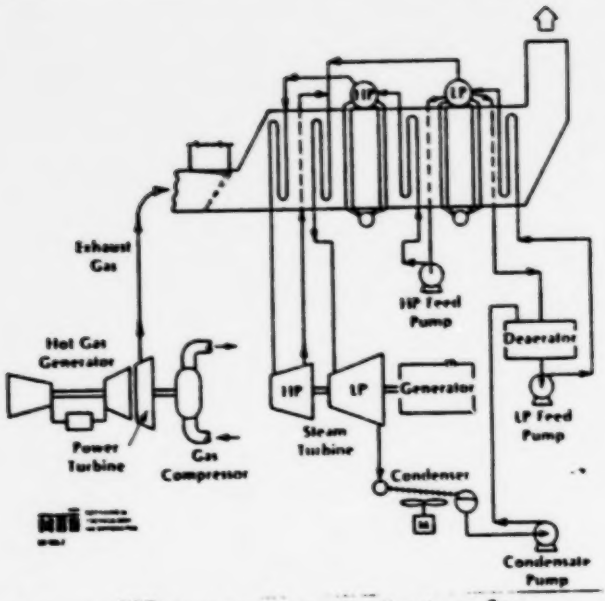

Figure 5. Combined-Cycle System for Gerber Compressor Station

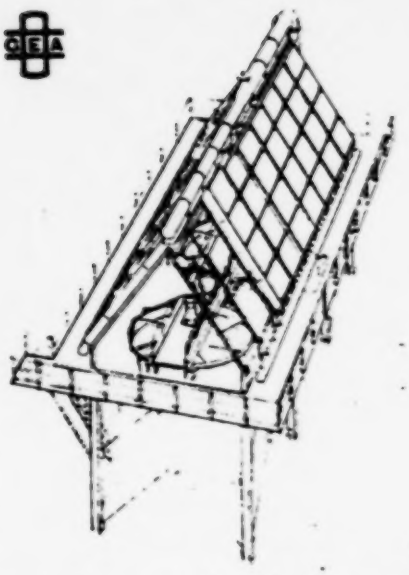

Figure 6. Air Cooled Steam Condenser

For the cogeneration plant now under construction at Pacific Gas and Electric Company's Gerber Compressor Station, the selection was to generate electric power. Figure 5 shows the schematic of the total system [2]. The exhaust gas from the originally installed 12,500 HP gas turbine, which is the prime mover for the pipe line gas compressor, will be ducted through a waste heat boiler. The steam generated in two separate loops at different pressure will drive the turbine generator set and generate 4 MW of electric power. The thermal efficiency of the gas turbine is 25.3%. Adding the steam cycle results in thermal efficiency of 36.1% for the combined cycle plant.

The installation of a combined cycle plant designed as a compressor drive system and using an aircraft derivative gas turbine, site rated at 5,529 HP is described in [3]. The thermal efficiency of 29% for the gas turbine has been increased to 40% for the combined cycle.

A characteristic feature of most combined cycle plants is the air cooled steam condenser as shown in Figure 6, which permits installation of new plants or retrofitting of existing simple cycle gas turbines at sites with limited or no cooling water available.

5. RECUPERATED CYCLE WITH HEAT RECOVERY

As opposed to recuperated cycles and combined cycles the heat recovery from turbine exhaust gas has not been utilized to any great extent. Besides the lack of incentive due to historically low fuel costs, the amount of heat contained in the turbine exhaust gas is so large that finding a user for it in close proximity to the gas turbine has been a major problem. One viable solution to this problem is to combine the recuperated cycle with a heat recovery unit or waste heat boiler as shown in Figure 4.

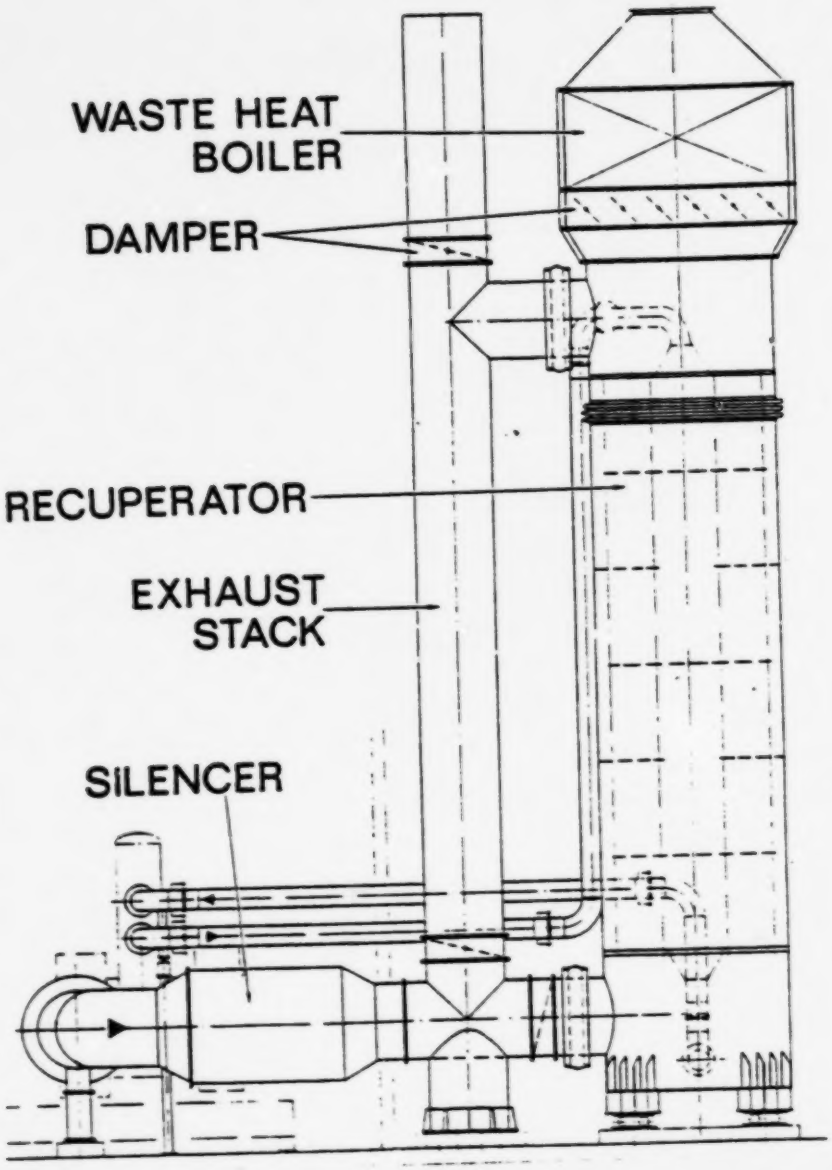

Figure 7. Combined Recuperator and Waste Heat Boiler

Since the temperature level for most heat requirements is much lower than the exhaust gas temperature, the exhaust gas is first ducted through a standard GEA recuperator before it enters the heat recovery unit. The effectiveness of the recuperator is selected such that just enough heat remains in the exhaust gas to cover the requirements set by the heat recovery unit.

The heat recovery unit is normally built from carbon steel fin tubes. Therefore, the extent of heat recovery is limited by a minimum exhaust gas temperature of 280° F out of the heat recovery unit in order to avoid corrosion as a result of acid condensation.

The recovered heat can be used for many applications such as hot water for process or general heating applications, process steam or heating of dryers. Combined recuperator and heat recovery units as described and shown in Figure 7 are in operation in connection with G.E. Frame 3 size gas turbines rated at 10 MW. The recuperator effectiveness is 81%. The heat recovery unit is heating water pressurized to 85 psig which is being used for the central heating

station of the City of Lemgo. The water at a flow rate of 660 GPM is heated from 140° F to 266° F, which is equivalent to a heat flow of 12.2 MW.

For the use on offshore oil drilling platforms there are combined recuperator heat recovery units under construction which in addition to the 80% recuperator effectiveness provide also a flow of glycol water mix heated from 200° F to 300° F.

Other systems for 25 MW size gas turbines, providing process heat for a refinery are being designed at this time.

6. ECONOMIC CONSIDERATIONS

A comparison of the three alternatives for recovering heat from the same type of gas turbine (Frame 5) shown in Figures 2, 3, and 4 makes it obvious that the thermal efficiency can be raised in all three cases to the same level of 36 to 37%. Since the operating costs are dominated by the fuel cost it appears that the three systems are about equal with respect to the operating cost. However, a comparison of the capital investment for the three systems shows a clear advantage for the recuperated system, closely followed by the combination of recuperator and heat recovery unit. The capital investment for the combined cycle system is far higher than the recuperated cycle, particularly when used with small gas turbines.

To further demonstrate the economic advantage of the recuperated cycle an example is presented further below, which is based on a Frame 3 size gas turbine. The cycle parameters are listed in Table 1. For the economic evaluation the current market price of 1.0 million dollars for the complete recuperator system and \$5.0/1,000 FT^3 of natural gas have been applied. Based on the differential heat rate and turbine power output the fuel savings for the 85% recuperated cycle are 34,350 FT^3/HR which is worth \$171.75 per hour of operation. The savings in fuel cost as a function of month of operation are shown in Figure 8, in which the number of hours of operation per year is the parameter. Also shown in Figure 8 is the initial capital investment with and without a 15% interest charge. For simplification, the interest has not been compounded and no interest has been credited to the savings in fuel cost. In addition, no escalation for the fuel cost has been considered which adds to the conservatism of the evaluation. It should also be mentioned that a recuperator system as described in this paper is essentially maintenance free. Therefore, the savings in fuel cost are net savings in operating cost. Assuming 8,000 hours of operation per year, Figure 8 shows that the capital investment is payed back by the fuel savings in less than 9 months. Considering the 15% interest charge on the investment the pay back time increases by one month. Recovering the capital investment in less than a year certainly is an exceptionally good business result.

The evaluation as shown is very simple and it can easily be adjusted for price escalation or for gas turbines differing from the one being used in this example. To optimize the recuperator effectiveness for a given application, Figure 9 provides the relative price of the recuperator system as a function of effectiveness and also for two different values for the pressure drop. An increase in pressure drop will result in a reduced turbine power out put. If the actual pressure drop influence is not known for a given turbine, it can be assumed that a one percent increase in pressure drop reduces the turbine power between 1.0 and 1.4 percent.

TABLE 1

COMPARISON BETWEEN SIMPLE CYCLE AND RECUPERATED CYCLE OPERATION FOR A FRAME 3 SIZE GAS TURBINE (ISO-CONDITION, AMBIENT AIR TEMPERATURE 59° F).

1. SIMPLE CYCLE

Turbine Power Output	:	13,680 HP
Air side Pressure Drop	:	4 IN W.C.
Gas side Pressure Drop	:	10 IN W.C.
Heat Rate	:	10,096 BTU/HP-HR
Fuel Consumption	:	133,200 FT^3/HR
Thermal Efficiency	:	24.9%
Fuel	:	Natural Gas
Heat Value of Fuel	:	1,037 BTU/FT^3

2. RECUPERATED CYCLE

Turbine Power Output : 13,320 HP (1)

Recuperator Effectiveness	Heat Rate	Fuel Consumption	Fuel Savings		Thermal Efficiency
%	BTU/HP-HR	FT^3/HR	FT^3/HR	%	%
75	8,048	103,370	29,830	22.4	31.3
80	7,872	101,100	32,100	24.1	32.0
85	7,696	98,850	34,350	25.8	32.7

Note (1): Loss of 2.6% power compared to simple cycle due to higher pressure drop of recuperated cycle. Recuperator total static pressure drop: 3.5%

Cost for an 85% recuperator system, including piping, foundations, erection and insulation (1981): $1,000,000
Cost for natural gas : $5.00/1,000 FT^3

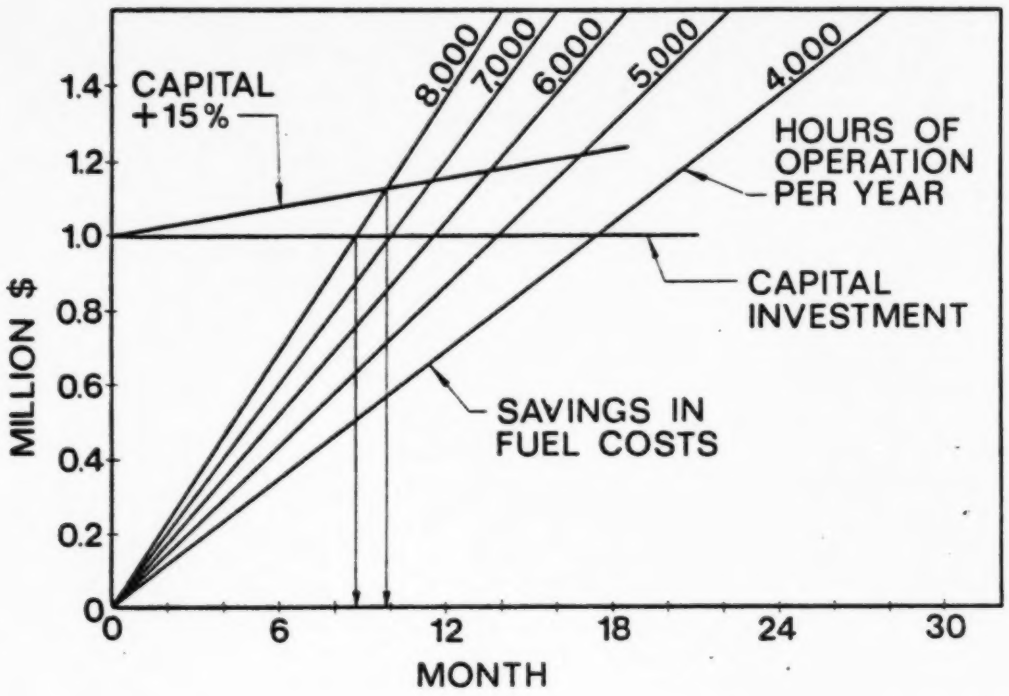

Figure 8. Amortization Time for Recuperator Installation.

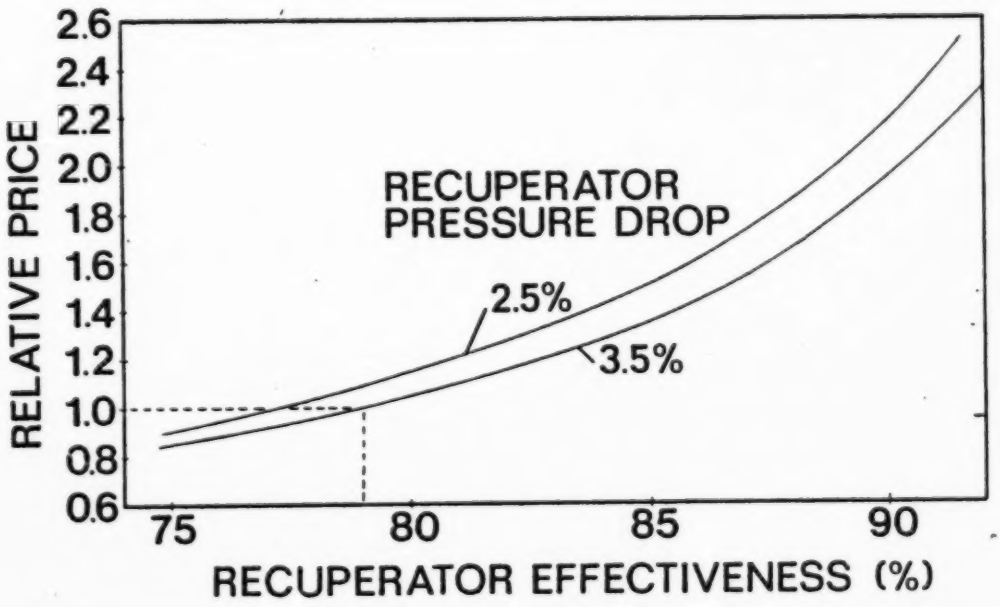

Figure 9. Price Relation for Recuperators as a Function of Effectiveness and Pressure Drop.

7. OPERATING EXPERIENCE

The equipment required for heat recovery from turbine exhaust gas is conventional and generally requires no new technology. This is an important aspect because reliability is highly evaluated by the owners such as Gas and Electric companies and Pipe line companies. Systems as described have been in operation for many years and design improvements have been made to eliminate problems associated with high exhaust gas temperatures and thermal stress. Plate type cross flow heat exchangers for example are subject to differential thermal stress which leads to cracks and internal leakage, which can only be detected by periodic pressure tests or by experiencing a reduction in turbine power output. Therefore, the completely symmetrical shell and tube design which provides zero leakage and no restrictions with respect to the turbine startup operations today outnumbers the plate fin cross flow design. Existing plate fin regenerators are being more and more replaced by the shell and tube design as shown in Figure 10. The operating experience with the design is excellent. Among the units in operation for more than twenty years there are recuperators with 70,000 hours of operation and 5,000 cold starts, which still do not show any leakage. To give an impression of the size of the equipment an overhead mounted recuperator for a Frame 3 gas turbine is shown in Figure 11 during erection. Figure 12 shows a side mounted installation at a gas pipe line compressor station.

CONCLUSIONS

Recovering heat from turbine exhaust gas is the economical choice for new installations and for existing simple cycle gas turbine stations. The equipment required is conventional and reliable designs are available. Using recuperators for gas turbine cycles is the simplest and lowest cost heat recovery system available. The capital investment for recuperator installations can be paid back by the fuel savings in less than one year of operation.

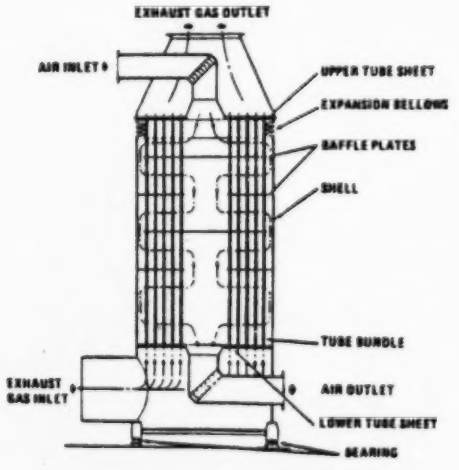

Figure 10. GEA Recuperator

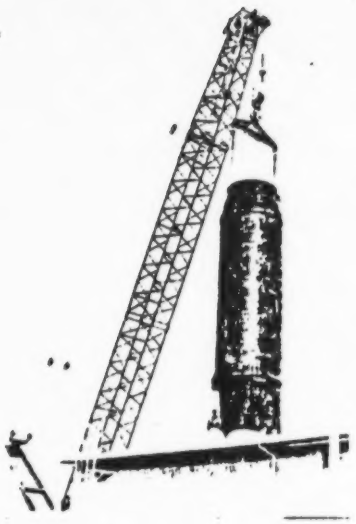

Figure 11.
Overhead Mounted Recuperator
for G.E. Frame 3 - Gas Turbine

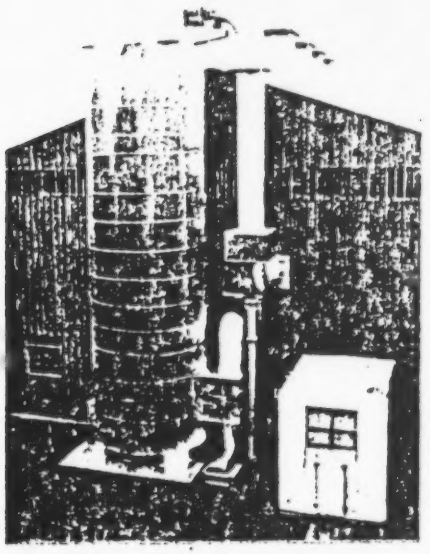

Figure 12.
Sidemounted Recuperator
for G.E. Frame 3 - Gas Turbine

REFERENCES

1. Armstrong, C.H. and Newton, D.H. 1977. Startup and initial operating experience of Braintree's 85 megawatt combined-cycle unit. ASME publication 77-JPGC-GT-1.

2. Meacher, F.S. 1980. Electricity from a gas transmission. MTI report prepared for The Institute of Gas Technology Cogeneration and The Gas Industry Symposium.

3. Axford, M. and Stinger, D. 1980. Combined-cycle operation for pipe line compressor stations. Turbomachinery International, Vol. 21, pp. 17-22.

PB82-228628

PREDICTING THE PERFORMANCE AND COST OF ORC WASTE HEAT RECOVERY SYSTEMS

J. L. Krazinski, H. M. Bushby, and E. H. Buyco[†]
Argonne National Laboratory
Argonne, Illinois 60439

ABSTRACT

Organic Rankine Cycle (ORC) systems have been designed and tested for the recovery of waste heat from low temperature sources. These systems use organic working fluids, rather than steam, in the cycle. A computer code was developed to predict the power outputs and costs of these systems. Six organic fluids and steam are considered in this paper. The thermophysical properties of the seven fluids are compared and their impact upon the system design is discussed. System costs are presented for exhaust gas heat sources with maximum temperatures of 500-1000F. The power outputs in these cases range from approximately 500 kW to 2500 kW. Certain organic fluids are restricted to the lower heat source temperatures because of thermal stability limitations. For the heat source temperatures at which the various fluids were used, however, similar system costs and power output levels were obtained for the six organic fluids.

1. INTRODUCTION

Because of continually rising energy costs, various techniques for conserving energy are being examined more seriously. One particular approach being investigated is the utilization of waste heat. Waste heat streams can be used to generate electricity and/or to produce steam for process or heating requirements. A recent study has identified industrial process streams (liquid, condensate) and gaseous exhaust streams as offering a potential for heat recovery [1]. Typically, these are low temperature streams with maximum temperatures of 1000F or less.

Due to the relatively low temperatures of such sources, systems that operate on the Rankine cycle have been proposed for these applications. However it is difficult to design an efficient and cost-effective system using steam as the working fluid. Consequently, organic chemicals have been selected as working fluids in these cases [2]. The thermodynamic properties of organic fluids allow Organic Rankine Cycle (ORC) systems to achieve high efficiencies and yet remain less expensive than comparable steam systems.

It is the purpose of this paper to examine the performance and predict the cost of waste heat recovery systems. A computer program was developed

---

[†]Purdue University — Calumet, Hammond, Indiana 46323

for conducting the necessary analysis. Results are presented here for six organic fluids and for steam. The organic fluids studied were: Freon R11, Freon R113, methanol, toluene, Fluorinol 85 (85 mole percent organic), and a 2-methyl pyridine/water mixture (20 percent 2-methyl pyridine by volume). These six fluids display a wide variation in their thermodynamic properties and operating characteristics. They have been identified as potential working fluids or have actually been used in heat recovery systems [1-5].

It is assumed here that the heat recovery systems will be used to generate electricity. Power outputs of approximately 500-2500 kW will be examined. These values are typical of the operating ranges of current or proposed units. The available heat sources being considered are exhaust gas streams with maximum temperatures of 500-1000F.

The present study will focus on a comparison of the working fluids from the standpoint of performance and cost. Additional factors, such as fluid toxicity and safety, will not be discussed here, although these factors could be important in the final selection of a working fluid for a specific application.

2. COMPARISON OF FLUID THERMOPHYSICAL PROPERTIES

Thermodynamic properties were acquired for the seven working fluids [6-11]. Table I contains a summary of the key fluid properties which affect system performance. Several of these properties will be examined and compared in this section. Their impact on the design of a heat recovery system will also be discussed.

The maximum fluid stability temperature indicates the highest temperature at which a fluid can be safely operated without significant thermal decomposition. It is difficult to assign a specific stability temperature for each fluid, as this temperature is a function of the cyclic processes undergone by the fluid, the materials of construction to which it is exposed, and the level of contaminants in the system. Frequently, stability temperatures are measured under static conditions at a fixed temperature, rather than the dynamic conditions encountered in an actual system. Therefore a range of maximum stability temperatures was given in Table I.

The maximum fluid temperatures in a heat recovery system will occur in the vaporizer. Thus the stability temperatures limit the range of heat source temperatures over which a particular organic fluid can be used. Of the organic fluids, the Freons and methanol have the lowest stability temperatures, while toluene and 2-methyl pyridine/water have the highest values. When selecting a working fluid for a specific heat source, the vaporizer design must take these temperature limitations into account.

The I-factor describes the nature of the saturated vapor line in the fluid T-s diagram [8]. For ideal gases under conditions far below the critical point, the I factor is given by

$$I(T) = \frac{h_{fg}}{C_p T} \qquad (1)$$

where h_{fg} is the latent heat (enthalpy) of vaporization, C_p is the vapor specific heat at constant pressure, and T is the absolute temperature. Fluids with higher I-factors, such as steam and methanol, are referred to as

Table I Comparison of Fluid Physical and Thermodynamic Properties

Substance	Water	Methanol	2 Methyl Pyridine/H_2O	Fluorinol 85	Toluene	Freon R11	Freon R113
Molecular Weight kg/kmol	18	32	33	88	92	137	187
Boiling Point at 1 ATM (NBPT)							
F	212	148	200	168	231	75	118
(C)	(100)	(64)	(93)	(75)	(110)	(24)	(48)
NBPT Saturated Vapor Specific Volume							
ft^3/lb_m	27.0	12.8	14.0	5.0	5.4	2.7	2.2
(m^3/kg)	(1.69)	(0.80)	(0.87)	(0.31)	(0.34)	(0.17)	(0.14)
Maximum Stability Temperature							
F	—	350-450	700-750	550-625	750-800	300-350	350-450
(C)		(175-230)	(370-400)	(290-330)	(400-425)	(150-175)	(175-230)
NBPT I-Factor	2.81	2.16	1.43	1.26	0.66	1.04	0.69
Liquid Film Coefficient (200F)							
BTU/hr-ft^2-F	1640	585	475	425	375	315	290
(W/m^2-C)	(9300)	(3320)	(2700)	(2410)	(2130)	(1790)	(1650)
Isentropic Turbine Enthalpy Drop							
BTU/lb_m	150-500	70-130	80-230	30-80	50-100	10-20	10-20
(kJ/kg)	(348-1160)	(162-302)	(186-534)	(70-186)	(116-232)	(23-46)	(23-46)

wetting fluids because the turbine exhaust generally contains a certain percentage of moisture. These fluids will usually have to be superheated in the vaporizer to avoid excessive moisture in the turbine.

Toluene and Freon R113 have I-factors which are less than 1. Because the saturated vapor slopes in the T-s plane are positive for these fluids, the turbine expansion will be dry, even without superheating the fluid in the vaporizer. Systems using these fluids may include a regenerator (recuperator) to transfer heat from the superheated turbine exhaust to the (liquid) fluid ahead of the vaporizer, thus improving the system efficiency.

Freon R11 would be classified as an isentropic fluid, since its I-factor ≈ 1.0. Freon R11 contains less superheat in the turbine exhaust than toluene. Fluorinol 85 and 2-methyl pyridine/water have I-factors in the 1.0-2.0 range. These fluids will be either wet or dry at the turbine exit, depending upon the turbine inlet temperature and pressure.

Fluids with lower I-factors, therefore, generally have more energy available for regeneration. In this study, a regenerator was included for systems using Freon R11, Freon R113, and toluene. Methanol and steam systems did not have regenerators. With 2-methyl pyridine/water and Fluorinol 85, a regenerator was only included for dry turbine expansions.

Although systems without a regenerator do have a cost advantage, eliminating the regenerator could increase the potential for corrosion problems in the vaporizer. Corrosion problems result primarily from sulfuric acid condensation on the vaporizer tubes. Because the lowest tube wall temperatures occur in the economizer, this is the area of greatest concern. The minimum recommended metal temperatures to prevent corrosion range from 140-260F, depending on the sulfur content of the exhaust gas [12]. By raising the temperature of the working fluid which enters the vaporizer, a regenerator can be beneficial in reducing or eliminating corrosion problems.

The fluid heat transfer coefficients affect the sizes of the heat transfer equipment. The film coefficients of organic fluids are typically less than those of water. As an example of the relative magnitudes of the fluid heat transfer properties, Table I shows the liquid film coefficients for flow (5 ft/s) in a 1-in. pipe. Water has the highest film coefficient and the Freons have the lowest values. For organic vapors at the same temperature, the relative ranking of the film coefficients could change, depending on the fluid pressure. In the regenerator, for example, the operating pressure of the vapor would be approximately equal to the condensing pressure. For the same condensing temperature, this pressure would be different for each fluid.

The final item presented in Table I is the range of isentropic turbine enthalpy drops for the conditions of this study. Fluids with higher molecular weights generally have lower enthalpy drops. Freon R11, Freon R113, toluene, and Fluorinol 85 have enthalpy drops of about 100 BTU/lb_m or less. Methanol has somewhat higher enthalpy drops. The 2-methyl pyridine/water mixture contains only 20 percent 2-methyl pyridine (by volume) and its enthalpy drops vary from 80-230 BTU/lb_m. Water has the highest enthalpy drops of all the fluids in Table I. The turbine isentropic enthalpy drop has an impact on the turbine design and, consequently, on the overall system cost. The turbine modeling will be discussed in more detail in Section 3.

3. SYSTEM PERFORMANCE AND COST DATA

A computer code was developed to perform the thermodynamic analysis of the Rankine cycle. The major hardware components that were modeled in the analysis are shown in Fig. 1. This design shows a regenerator, although one

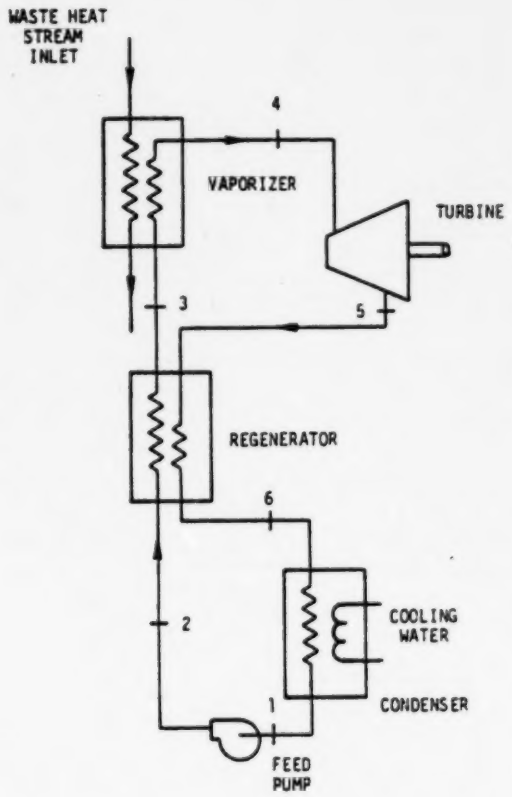

Fig. 1 Waste Heat Recovery System

would not be included for wetting fluids. For each set of turbine inlet conditions, the code determined the pump work, turbine work, heat input, and the cycle efficiency. The unknown fluid enthalpies and temperatures were also calculated throughout the cycle.

For a given waste heat stream, the thermodynamic analysis was conducted over a range of cycle operating temperatures and pressures. The maximum cycle temperature and pressure are limited by the pinch point temperature difference in the vaporizer. The pinch point is the location of the minimum temperature difference between the heat source and the working fluid. A negative temperature difference at the pinch point implies a temperature crossover in the vaporizer. If the pinch point temperature difference was positive for a particular cycle, the corresponding component and system costs were then calculated in the code.

Heat transfer coefficients were calculated for the various heat exchangers, assuming shell- and tube-construction. For the condenser and regenerator, heat transfer coefficients were calculated for each working fluid and included in the input data. The vaporizer heat transfer coefficients depend on the nature of the heat source. For exhaust gas streams, the heat transfer is controlled by the resistance on the gas- (shell-) side. The overall heat

transfer coefficient is relatively insensitive to the film coefficient on the tube side, regardless of the working fluid. Typically, these vaporizer heat transfer coefficients range from 5-6 BTU/hr-ft^2-F [13]. A value of 5.5 BTU/hr-ft^2-F was selected here. It was assumed that finned tubes were used in the vaporizer.

The costs of equipment to a heat recovery system integrator (i.e., manufacturer) were obtained from various vendors. The costs covered the range of equipment sizes encountered in this study. From the data, cost curves were developed for the vaporizer, regenerator, condenser, pump, turbine, gear reducer, and electrical generator. All of these components, except for the vapor generator, were assumed to be enclosed in a building. The building cost, as well as the costs of the cooling tower system and the working fluid, were also included in the overall system cost.

The turbine costs were calculated as a function of the turbine isentropic enthalpy drops. Organic fluids can achieve maximum efficiencies (70-80 percent) with single-stage turbomachinery for isentropic enthalpy drops of approximately 100 BTU/lb$_m$ or less [1]. For steam systems operating at reasonable efficiency levels, however, the turbine enthalpy drops will generally exceed 200 BTU/lb$_m$. These larger enthalpy drops require the use of multistage turbines to maintain reasonable wheel diameters and tip speeds. It was assumed here that single-stage turbines were used for isentropic enthalpy drops of 100 BTU/lb$_m$ or less. Multistage steam turbines were used for enthalpy drops over 200 BTU/lb$_m$. Cost data was obtained for a single-stage turbine, a multistage steam turbine, and a 3-stage turbine. The costs for the 3-stage turbine were used when the isentropic enthalpy drops varied from 100-200 BTU/lb$_m$.

Based on the above criteria, systems with Freon R11, Freon R113, toluene, and Fluorinol 85 used single-stage turbines. Methanol and 2-methyl pyridine/water systems included either single-stage or 3-stage turbines, depending on the cycle conditions. (Several of the high efficiency 2-methyl pyridine/water systems were in the multistage turbine regime.) With water, costs for either the 3-stage turbine or the multistage steam turbine were used.

It was assumed here that a system integrator would purchase the necessary components and assemble the heat recovery system. In addition to the above equipment costs, the integrator manufacturing costs and the system installation costs were also included in the total cost. The manufacturing costs included profit, administration costs, and assembly costs. The installation costs included both direct cost factors (foundation, piping, electrical, etc.) and indirect cost factors (start-up, performance testing, etc.). The indirect costs were taken as constant for all size ranges, while the direct costs were scaled to increase with the system power output.

In this study it was assumed that similar types of equipment could be used for all fluids. For example, carbon steel construction would be used in the vaporizer, regardless of the working fluid. Thus any differences in system performance would be due to fluid property variations, rather than to detailed design variations of the heat recovery units.

4. RESULTS

A number of assumptions were necessary to perform the present analysis. The major assumptions are listed in Table II. A maximum turbine inlet pressure of 500 psia was specified. In calculating the pump cost, an overall

Table II Major Assumptions

1.	Maximum Turbine Inlet Pressure, psia	500
2.	Overall System Pressure Drop, psia	100
3.	Turbine Moisture Limit, percent	10
4.	Turbine Size Limits Based on Isentropic Enthalpy Drops, BTU/lb_m	
	Single-Stage	$\Delta h \leq 100$
	3-Stage	$100 < \Delta h \leq 200$
	Multistage (Steam)	$\Delta h > 200$
5.	Condensing Temperature, F	150
6.	Cooling Water Temperature Range, F	85-110
7.	Exhaust Gas Exit Temperature, F	300
8.	Exhaust Gas Specific Heat, BTU/lb_m-F	0.25
9.	Turbine Efficiency: Single-Stage and 3-Stage	0.75
10.	Multistage Steam Turbine Efficiency (500-2500 kW)	0.65-0.70
11.	Regenerator Effectiveness	0.80
12.	Pump Efficiency	0.75
13.	Gearbox Efficiency	0.97
14.	Electrical Generator Efficiency	0.95
15.	Neglect any Temperature Rise in the Pump	

pressure drop of 100 psia was assumed, based on previous system designs [4,5]. A moisture limit of 10 percent at the turbine exit was imposed to prevent excessive blade erosion [1]. The exhaust gas exit temperature of 300F was selected to minimize potential corrosion problems in the economizer.

Based on these assumptions, system costs were calculated over a range of heat source temperatures. Figures 2-4 show the predicted minimum system costs for 500-1000F exhaust gas streams. The available flow rates of these streams vary widely, depending upon the nature of the heat source. The thermal heat inputs can typically range from 10-100 million BTU/hr [14]. The heat-sources in Figs. 2-4 were taken to have a mass flow rate of 2.5×10^5 lb_m/hr. For an exhaust gas exit temperature of 300F, therefore, the available heat inputs varied from 12.5 million BTU/hr (500F stream) to 43.7 million BTU/hr (1000F stream).

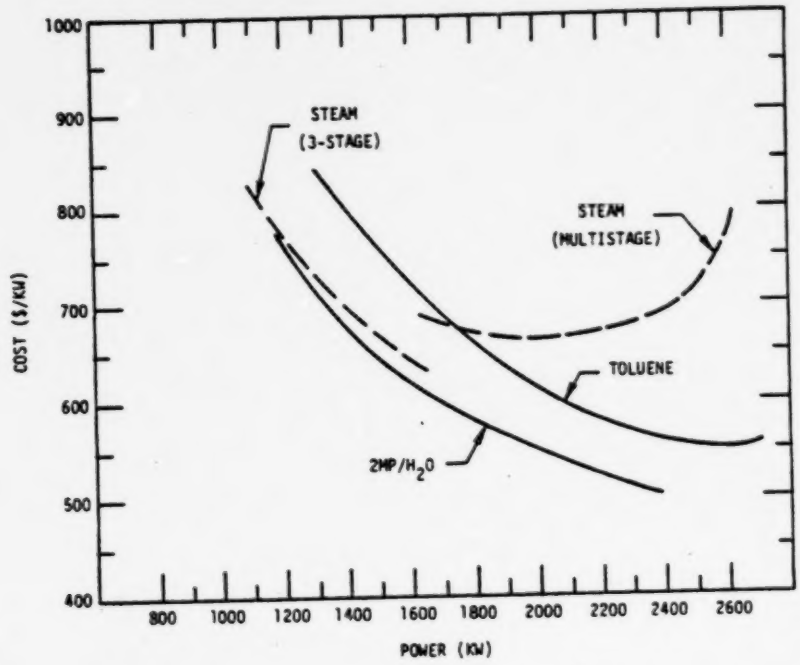

Fig. 2 Predicted System Costs for a 2.5×10^5 lb_m/hr Heat Source at 1000F

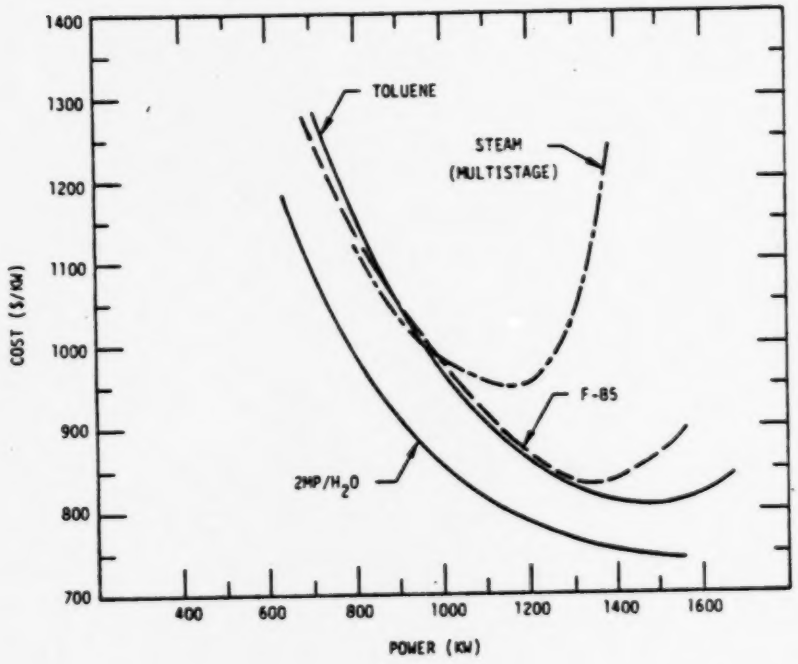

Fig. 3 Predicted System Costs for a 2.5×10^5 lb_m/hr Heat Source at 750F

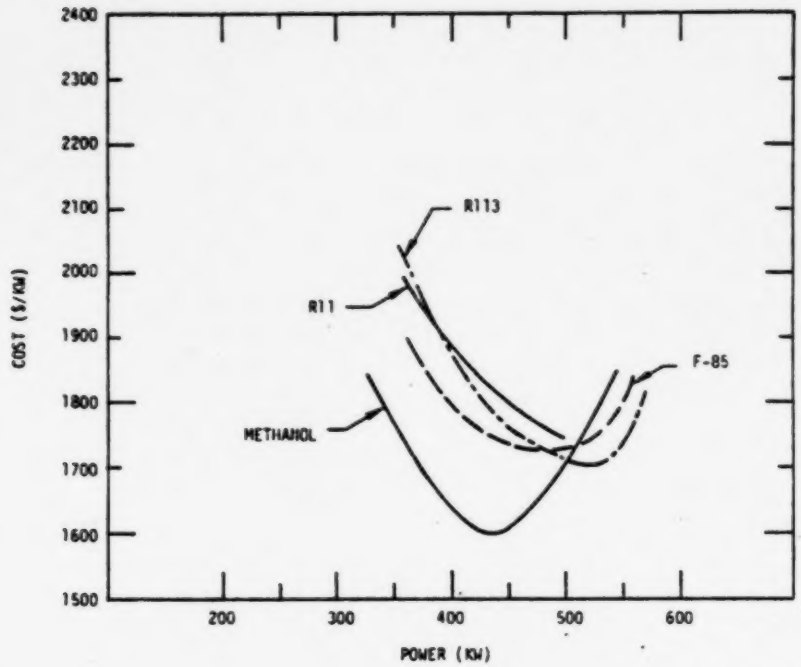

Fig. 4 Predicted System Costs for a 2.5 x 10^5 lb_m/hr Heat Source at 500F

The predicted minimum system costs for a 1000F heat source are shown in Fig. 2. Most organic fluids were not included in Fig. 2 because of temperature stability limitations, as discussed earlier. The higher power outputs imply systems with greater overall efficiencies. For steam systems with higher power outputs, multistage turbines were used. These systems are more expensive than comparable organic systems, as was also shown in earlier studies [1,5]. Single-stage turbines were included in all toluene systems. For 2-methyl pyridine/water, a 3-stage turbine was used at a power output of 2400 kW. Systems with higher power outputs would be in the multistage turbine regime, resulting in significantly higher costs.

Figure 3 shows the system costs for a 750F heat source. The power outputs are less and the predicted costs ($/kW) are higher than those in Fig. 2. The three organic fluids in Fig. 3 have similar system costs over the 600-1600 kW range. Systems with these organic fluids have lower costs and higher power outputs than steam systems.

The most expensive component in the heat recovery system is the vaporizer. Predicted vaporizer costs have typically ranged from 20-30 percent of the total system cost. The system costs in Fig. 3 start to increase at higher power outputs, primarily because of rising vaporizer costs. These higher efficiency systems operate at greater pressures and temperatures. Consequently, the pinch point temperature difference in the vaporizer starts to decrease, resulting in lower log mean temperature differences. The smaller log mean temperature differences, in turn, lead to larger vaporizer areas and higher predicted costs. Because of the nature of the steam saturation curve, the steam systems in Fig. 3 operate at lower pressures than the organic

fluids, due to pinch point temperature limitations in the vaporizer. Thus the steam systems are less efficient, i.e., produce less power, than systems using organic fluids.

The predicted system costs for a 500F heat source temperature are given in Fig. 4. The systems in Fig. 4 have much higher costs ($/kW) than those for the 750F and 1000F heat sources. The power outputs corresponding to the minimum system costs are less than 600 kW. The remaining fluids were not included in Fig. 4 for purposes of clarity. However the minimum predicted costs for toluene, 2-methyl pyridine/water, and steam (3-stage turbine) were also about $1700/kW with power outputs of 400-500 kW.

The heat source mass flow rate in Figs. 2-4 was fixed at 2.5×10^5 lb_m/hr. To determine the effect of the flow rate on the results, system costs were calculated for a 750F heat source with a flow rate of 1.25×10^5 lb_m/hr. The predicted costs for three fluids are shown in Fig. 5. Because of the lower heat input, the power outputs are less than those in Fig. 3. However the minimum predicted costs for both Fluorinol 85 and toluene are approximately the same for the 1.25×10^5 lb_m/hr flow rate.

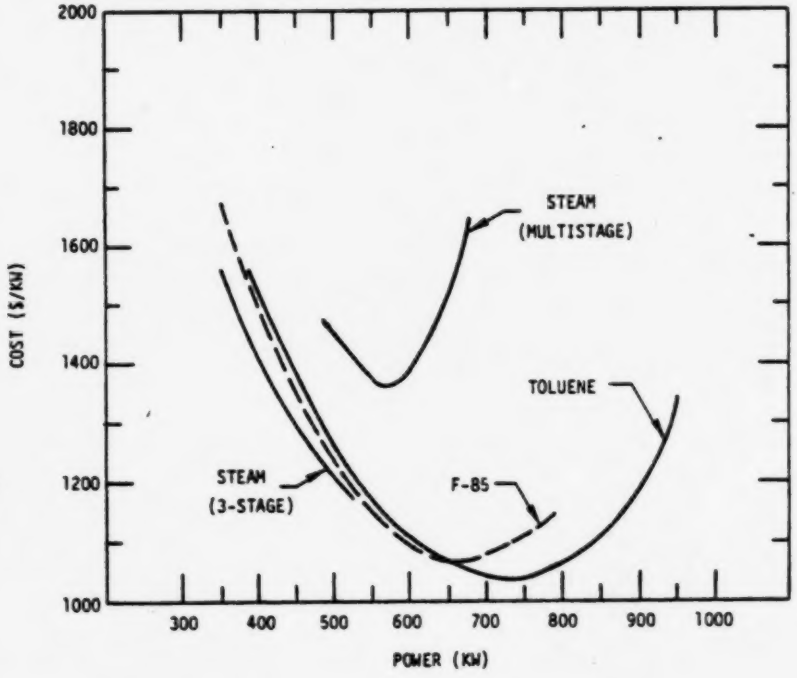

Fig. 5 Predicted System Costs for a 1.25×10^5 lb_m/hr Heat Source at 750F

From the results in Figs. 2-5, two observations can be made. First of all, the system costs showed economies of scale over the 500-2500 kW range. Economies of scale were exhibited in both the equipment costs and the installation costs. With toluene, for example, the minimum predicted system cost for a 750F heat source occurred at a power output of 1500 kW (Fig. 3). The vaporizer cost for this system was $265/kW, while the total installation cost was $275/kW. For the 1000F heat source, however, the minimum system cost for toluene occurred at a power output of 2600 kW (Fig. 2). Here the vaporizer

cost was $168/kW and the total installation cost was approximately $172/kW. The costs of the other system components also showed economies of scale from 500-2500 kW.

Secondly, the predicted power outputs and system costs were similar for the six organic fluids. Because of thermal stability considerations, certain organic fluids would not be used at the higher heat source temperatures. For the heat source temperatures at which a particular organic fluid was used here, however, its predicted system costs were comparable to those of the remaining organic fluids.

5. CONCLUSIONS

The predicted costs and performance levels of waste heat recovery systems were presented in this paper. In obtaining these results, differences in the fluid heat transfer characteristics, turbomachinery requirements, and thermodynamic properties were included. The organic fluids considered here have similar system costs and performance levels for exhaust gas streams between 500F and 1000F. System costs show economies of scale over the 500-2500 kW range, with the minimum costs ($/kW) decreasing at the higher power outputs.

The selection of a potential working fluid depends upon the heat source temperature. Other heat source characteristics, which are site-specific, could also be important. These include the fluid toxicity requirements of a particular site and the exhaust gas sulfur content, the latter of which affects the minimum tube wall temperatures required to prevent corrosion in the vaporizer. Such factors, in addition to the cost and performance data given in this study, need to be considered when evaluating fluids for a specific waste heat recovery application.

ACKNOWLEDGMENTS

This work was undertaken as part of the Rankine Cycle Power System Working Fluid Study, supported by the Office of Industrial Programs, U.S. Department of Energy, under the direction of Mr. John Eustis. Drs. T. J. Marciniak (Program Manager) and J. C. Bratis of Argonne National Laboratory also participated in the study. Their assistance is appreciated.

REFERENCES

1. Drexel University, United Technologies Research Center, and Mathematica, Inc., "Industrial Application Study," Vol. III, DOE Contract No. COO/2862-3 (1978).

2. Curran, H. M., "The Use of Organic Working Fluids in Rankine Engines," Proceedings of the 15th IECEC, p. 985 (1980).

3. Sternlicht, B., "Capturing Energy from Industrial Waste Heat," Mechanical Engineering, p. 30 (1978).

4. Soini, H. E., Patel, P. S., Morgan, D. T., and Batra, S. K., "Combined Diesel-Organic Rankine Cycle Powerplant," Proceedings of the 12th IECEC, p. 1100 (1977).

5. Niggemann, R. E., Greenlee, W. J., and Lacey, P. D., "Fluid Selection and Optimization of an Organic Rankine Cycle Waste Heat Power Conversion System," ASME Paper 78-WA/Ener-6, 8 pp. (1978).

6. ASHRAE Thermodynamic Properties of Refrigerants, American Society of Heating, Refrigerating and Air-Conditioning Engineers, Inc., New York (1969).

7. Pravin, A., Halocarbon Products Corporation, Hackensack, New Jersey, Personal Communication (Feb. 3, 1981).

8. Miller, D. R., Null, H. R., and Thompson, Q. E., "Optimum Working Fluids for Automotive Rankine Engines," APTD-1563, APTD-1564, APTD-1565, and APTD-1566, Vols. I-IV (1973).

9. Keenan, J. H. and Keyes, F. G., Thermodynamic Properties of Steam, John Wiley and Sons, New York (1936).

10. Smith, J. M., "Thermodynamic Properties of Methyl Alcohol," Chemical Engineering Progress, Vol. 44, No. 7, p. 521 (1948).

11. Miller, D. R., Monsanto Industrial Chemicals Co., St. Louis, Missouri, Personal Communication (July 8, 1980).

12. Babcock and Wilcox Co., Steam, Its Generation and Use (38th ed.), Babcock and Wilcox Co., New York (1972).

13. Boyen, J. L., Thermal Energy Recovery (2nd ed.), John Wiley and Sons, New York (1980).

14. Resource Planning Associates, Inc., "Industrial Markets for Organic Rankine Cycle Bottoming Systems," RA-78-1402(3) (1978).

PB82-228636

ENERGY UTILIZATION IN THE PRODUCTION OF ANHYDROUS ETHYL ALCOHOL FOR GASOHOL

Norman B. Smith, P.E.
Stanley Consultants, Inc.
Muscatine, Iowa, U.S.A.

ABSTRACT

Today's literature, both general and technical, is filled with references to the manufacture/use of fuel alcohol. Gasohol, a fuel alcohol product, is by definition a mixture of 90 percent unleaded gasoline and 10 percent anhydrous ethyl alcohol. The ethyl alcohol has traditionally been produced by fermentation methods with corn as a substrate.

Based on substantial federal and state subsidies, a powerful lobby movement, and sustained by the continuing rise in gasoline prices, a fuel alcohol industry has been launched in the USA.

A conventional plant for producing fuel grade ethyl alcohol from corn consists of a series of energy intensive unit processes. Within each of these processes are chemical engineering unit operations which involve the utilization and transfer of energy in one form or another. It is the judicious selection of these "building blocks" or unit operations and equipment that enables the efficient production of fuel alcohol. A special understanding of waste heat recovery techniques is required to integrate an energy efficient design.

1. INTRODUCTION

One of the most controversial topics of the current energy debate is the manufacture of ethyl alcohol from agriculture materials to be used for fuel alcohol. Gasohol, a mixture of 90 percent unleaded gasoline and 10 percent alcohol, is presently being promoted as an extender of our vital oil supply. Other fuel alcohol products consisting of essentially all ethyl alcohol are also being suggested to replace diesel fuel or unleaded gasoline on a gallon-for-gallon basis.

Sides are polarized and debates started around questions, such as:

- Should needed food products be converted into energy fuels?
- Does the alcohol process produce positive net energy?
- Are government subsidies necessary to maintain the industry?
- Will the alcohol/gasoline mix result in additional automobile maintenance?

- Are the basic economics of the industry sound?

- Is there a major technological breakthrough on the horizon?

It is not the intent of this paper to solve, or even address, the many sociological and political issues raised in developing an industry to produce ethyl alcohol for fuel use. However, it is important to keep in mind the variety of factors that influence such an industry even if they have little to do with the technological questions.

2. POSITIVE OR NEGATIVE ENERGY BALANCE

A basic issue that needs to be addressed briefly has been developed on the premise that the production of ethyl alcohol by conventional fermentation/distillation methods requires more energy than is contained in the final alcohol product. Without a fine definition of system boundary, comparison of energy types, end use of all products, and process, this becomes an endless argument.

The fact remains that differences of opinion on the energy balance derive mainly from variations in interpretation of the question. The answer is strongly dependent on basic assumptions.

In general, the energy balance from farm crop to product end use is a near break-even situation. However, there is no question that ethyl alcohol from corn to be used for fuel alcohol can be manufactured as a petroleum substitute supplied for the most part by non-petroleum energy source, coal. If for no other reason, this makes fuel alcohol a viable near term petroleum substitute.

3. PERSPECTIVE OF INDUSTRY

Considering the many positive aspects of developing a fuel alcohol industry based on agriculture crop such as corn, it cannot be assumed that a gasohol product will solve the U.S. energy problem. It is at best a partial solution.

For instance, the U.S. Government has proposed a production goal of 11-12 billion gallons per year of ethyl alcohol by 1990. A production rate of 1-2 billion gallons per year is more realistic based on the present rate of growth.

However, the near term goals (1982) will likely exceed 200 million gallons of ethyl alcohol per year. We cannot minimize this start as it represents over 1 million tons of coal that will be required to provide process steam for the industry.

Iowa, the leader in fuel alcohol use, will utilize almost 20 million gallons of ethyl alcohol in 1981 while burning 200 million gallons of gasohol.

An industry that is as energy intensive as the production of ethyl alcohol for fuel alcohol warrants scrutiny during design and operation. It is critical that the industry be developed taking the advantage of the latest techniques for overall energy conservation. Waste heat utilization is essential to the economic viability of the process.

4. PROCESS DESCRIPTION

In order to better understand the energy requirements/utilization of ethyl alcohol production, it is necessary to briefly describe the process technology as shown on Figure 1:

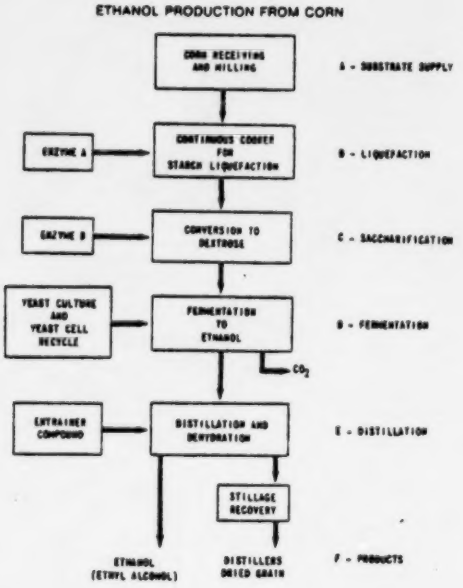

Figure 1. Simplified Process Schematic

4.1 Substrate Supply (A)

Figure 1 illustrates a simplified process schematic for the production of ethyl alcohol (anhydrous) for fuel alcohol. The substrate supply is ground corn. Other materials such as milo or grain sorghum are acceptable.

4.2 Liquefaction (B)

Liquefaction involves cooking of the ground corn mash slurry. Direct injection of steam followed by enzyme digestion results in a starch molecular modification from insoluble to soluble form. Protein and fiber portion of the corn kernel remains essentially unchanged.

4.3 Saccharification (C)

An enzyme (glucoamylase) is required in the saccharification step of the process. Saccharification results in the conversion of the soluble starch and carbohydrate to simple sugar, predominately dextrose.

4.4 Fermentation (D)

The fermentation of the sugar solution results in the products of ethyl alcohol and carbon dioxide. Yeast provide the catalytic reaction to convert sugar to alcohol. By-products of the fermentation can be organic compounds, and the corn residue of protein/fiber.

4.5 Distillation (E)

Recovery of the ethyl alcohol is normally by distillation separation techniques. Since ethyl alcohol forms an azeotrope at approximately 95 percent alcohol and 5 percent water, it is necessary to employ special dehydration techniques to produce an anhydrous product.

4.6 Products and By-products (F)

By-product recovery consists of preconcentration and drying of the stillage material from the distillation separation process. The by-product is a protein enriched feed supplement usually sold in a dry form. An efficient plant will require 0.4 bushels (22.4 lbs.) of corn substrate per gallon of alcohol produced. Approximately 7-8 lbs. of dried feed by-product will also be produced along with the gallon of alcohol product.

5. POTENTIAL ENERGY CONSERVATION

It can be seen from Figure 2, Steam Requirements, for the ethyl alcohol process that approximately 80-118 lbs. of steam is required to produce one gallon of anhydrous fuel grade ethyl alcohol.

The overall energy/material balances were developed for a plant producing 20 million gallons per year anhydrous fuel grade ethyl alcohol.

The wide variation between the steam use is the difference between a "good" design to one termed "excellent" and taking maximum advantage of energy use. Techniques must be used to minimize waste heat discharge in both designs.

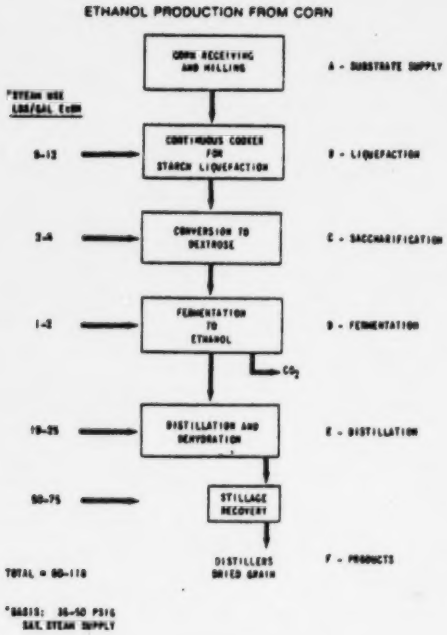

Figure 2. Steam Requirements

6. PROCESS ENERGY ANALYSIS

To better understand the design problem involved to obtain maximum energy efficiencies it is necessary to again refer to Figures 1 and 2.

As in other industrial processes, much of the heat and power used in the ethyl alcohol process is rejected as waste heat to air and water. In such instances the waste is not only costly but can produce environmental problems. In fact, the fermentation process (D) generates a low level heat load to be dissipated.

In general, the waste heat streams available in the plant are of the low temperature type (80-300°F). One exception is the steam generating boiler which may have a flue gas discharge above 300°F.

6.1 Conservation Techniques

Methods for utilizing the waste heat from an alcohol plant can be classified in the following categories:

- Direct utilization, e.g. drying or preheating process flows.
- Preheating with the use of heat exchanger equipment. Can be gaseous or liquid.
- Waste heat boiler or exchanger used to produce process steam.

- Co-generation, in which process steam (low pressure) is produced simultaneously with electricity. This is especially attractive due to the combination of steady state conditions and large low pressure steam requirements.

- Cascading of energy is especially useful with unit operations such as distillation/evaporation. These operations are necessary in an alcohol plant.

6.2 Applied Techniques

Specific waste heat recovery techniques utilized in each manufacturing area follow (Refer to Figure 2):

- A - Substrate supply. Other than electrical power, no energy is used in this process step.

- B - Liquefaction. It is necessary to elevate the corn slurry temperature through a cooking cycle prior to enzyme action. Sparge steam provides both heat input and dilution water for the process. Cooling water required to cool the mash is usually cascaded to preheat the feed and/or act as a supply of water for initial ground corn dilution.

- C - Saccharification. It is necessary to maintain a constant elevated (130-140°F) temperature during this step. A small quantity of sparge steam is used for this purpose to replace heat losses.

- D - Fermentation. Steam use in this area is relatively minor. Sterilization of equipment or heating of cleaning solutions make up the major use. The fermentation reaction is exothermic in nature. However, it is critical that the fermentor temperature be maintained between 85-90°F for yeast viability. In some cases refrigeration is required to supplement a normal cooling water source. The extreme low level of waste heat discharge makes utilization of this form of energy very difficult. Hydroponic gardens are presently being used to take advantage of these streams (A.D.M., Decatur, Illinois).

- E - Distillation. It is in the area of distillation that the concept of waste heat utilization can best be practiced. This unit operation is one of the most energy intensive steps in the plant. Efforts are being focused on techniques, such as:

  - vapor cascading
  - vapor recompression (thermal/mechanical)
  - preheaters for feed
  - reboiler flashing
  - heat pump

Approximately one-fourth of the steam required for the alcohol plant is used in the distillation unit operation. Therefore, it is important to emphasize some of the techniques available to minimize waste heat from the distillation area.

For the most part, the recovery of waste heat is most efficiently accomplished by heat exchange with other process streams that may be related to the same column, another nearby column, or a separate process that could economically use additional heat. The design of heat exchangers which are totally integrated into the system is important. Feed preheaters to the beer still utilizing the alcohol free stillage leaving the system is an example of waste heat recovery utilizing a liquid/liquid heat exchanger.

Vapor cascading is a technique commonly used to conserve energy and transfer heat from one stream to another. In this case, heat exchangers utilizing vapor/liquid heat transfer are used. Since distillation systems are made up of a series of vaporization/condensation stages, vapor cascading external to the tower is also a viable technique to prevent waste heat loss.

In conventional distillation, heat is added to the column at the reboiler (usually from steam or a vapor from an adjacent column) and rejected at the overhead condenser. The overall energy requirements of the column can be reduced significantly by using a heat pump, vapor compression, or reboiler flashing.

Figures 3, 4, and 5 illustrate the energy conservation techniques of heat pumps, vapor recompression and reboiler flashing, respectively. In each case, the applications of such techniques for an alcohol distillation process are very specific and should be considered at the time of the original design.

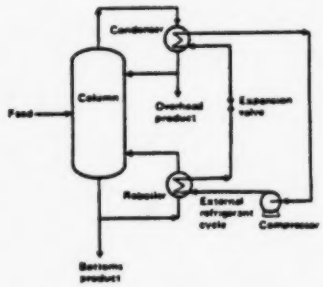

Figure 3. Heat Pumping in Distillation
With an External Refrigerant

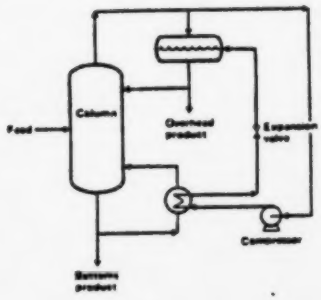

Figure 4. Vapor Recompression

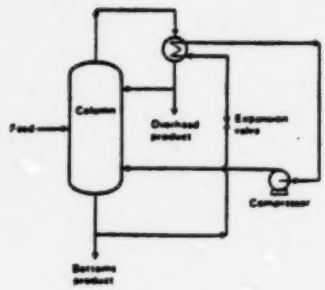

Figure 5. Reboiler Flashing

- F - Product recovery. The feed recovery area utilizes the most steam of any of the production areas in the alcohol plant. Two unit operations, namely, concentration and drying of stillage account for as much as 40 percent of the total plant steam useage. It is sometimes suggested that the stillage be used without concentration or drying. Only in very special cases is this possible.

Evaporation of the stillage is one of the most energy intensive unit operations required in the industry. The engineering evaluation of evaporator equipment has many constraints and can be very complicated. In the past the major criteria for the specification of the evaporator system have been reliability of operation, minimization of capital costs, and the reduction of utility costs. Because the unit operation of evaporation is fundamental, often the final selection of the evaporator has been based on the lowest cost design by competitive bid. It is essential today to consider the overall operation/capital cost to better reflect the cost of energy. Design efforts are being focused on techniques to conserve energy and minimize waste heat, such as:

- Feed preheat using sensible heat in concentrated product
- Multieffect units
- Utilization of waste heat in vacuum ejector system
- Mechanical/thermal recompression methods

Due to the importance of energy conservation in the concentration of the feed product it is worthwhile to elaborate more on the techniques available.

The concentrated product will contain a certain quantity of sensible heat available to preheat the evaporator feed. Heat exchangers of the liquid/liquid variety are normally used for this application. However, occasionally it will be necessary to use an intermediate heat transfer media to minimize fouling of transfer surfaces.

Adding effects to utilize a multieffect arrangement of equipment is expensive so must be evaluated on an operational (energy) basis. Technical considerations to consider when evaluating multieffect evaporators is the overall driving force (ΔT) available and limitations imposed by the product boiling point increase with concentration. However, the adding of effects can greatly reduce overall steam consumption due to the re-use of the vapor latent heat. In general, adding of a second effect will reduce steam use by one half. A third effect will reduce steam by one third of the original single effect. Of course, there are limits to this theory.

Mechanical/thermal recompression offers the highest energy savings potential. Energy recovery is usually above 90 percent theoretical. Previous mechanical limitations of compression ratios and high investment costs are being offset by higher operating costs of more conventional equipment. In operation, mechanical/thermal recompressors are used to compress the overhead vapors to a higher pressure and temperature with a compressor or steam. It is feasible to drive a mechanical compressor by steam turbine or by electric motor making the scheme even more versatile. A mechanical recompression evaporator using electric compression only requires steam for initial start-up. In such a case, steam energy is replaced by electrical energy. However, for most comparisons between conventional multieffect evaporators and mechanical recompression the recompression system is found to be the most efficient and economical.

Energy use in the the drying section of the alcohol plant varies more than any other section. Steam is usually used as a heat source unless a inexpensive source of natural gas is available.

Styles and designs of driers vary considerable. It is important to select a drier with the maximum efficiency along with a gas/gas waste heat recovery system. There are limits to the use of the drier gaseous waste heat due to high moisture, low heat content, and contamination. However, work is progressing in this field to better utilize the drier off gas.

In many cases the hot flue gases from a conventional boiler have been used to assist in drying the feed product directly. Problems with ash contamination and duct arrangements have limited this application, however.

Flash driers are known to provide excellent overall drier efficiencies which integrate reuse of waste heat. This type of drier is always considered for feed drying.

Product cooling is essential, therefore, gas/solid preheaters insure a cool product and utilize the product sensible heat.

7. CONCLUSIONS

It has been emphasized that the manufacture of anhydrous ethyl alcohol to be used as a fuel alcohol is a controversial, but emerging industry. The industry requires large quantities of energy in the form of process steam to produce an acceptable product. Coal can be used to produce process steam.

Considering the type of unit processes required to manufacture fuel ethyl alcohol, there is much potential for energy conservation techniques or some form of waste heat recovery system.

A prudent design will focus on the operation areas of distillation and product recovery (evaporation/drying) to maximize the waste heat recovery. Furthermore, it is essential to evaluate process equipment on a life-cycle type of evaluation considering initial capital costs and energy efficiencies. Energy savings of up to 30-40 percent are possible utilizing energy conservation techniques.

SESSION X-B

THERMAL DISCHARGE VII

Preceding page blank

PB82-228644

DYNAMIC BEHAVIOR OF A THERMAL PLUME

Joseph C. Cataldo
and Stephen Quense

The Cooper Union
for the Advancement of Science and Art
New York, New York

ABSTRACT.

The thermal front phenomenon was observed during field surveys at the Ginna Power Plant. Thermal fronts are rapid temperature oscillations in the near field of a thermal plume and are generally observed in calm receiving water. Temperature oscillations were observed with amplitudes of over 3°C measured from the mean with periods ranging from approximately 100 to 600 seconds. A physical scaled model of the Ginna discharge was used to study the thermal fronts and plume characteristics. The model is 31 feet long and 16 feet wide and geometric scale ratio of 1 to 50 and 1 to 100 were used to model the plume. Temperature versus time for several positions inside the model thermal plume exhibit a clear oscillatory pattern with amplitudes varying from 1 to 5°C. A maximum overall temperature difference of 10°C was recorded at one position, while discharge and ambient temperature traces revealed no significant temperature fluctuations. Predominant periods ranged from 14 to 80 seconds (approximately 100-600 seconds in the prototype). The power of the dominant oscillations tended to increase with depth at the same position inside the plume as did the magnitude of the temperature variations. The mechanism responsible for the thermal fronts is believed to be due to a Kelvin-Helmholtz instability. This instability is induced by vortex formation at a shear layer formed by the movement of the heated surface plume across the cooler ambient lake water.

1. INTRODUCTION

This paper focuses on one natural phenomenon associated with heated water discharges, the observation of significant periodic fluctuations of water temperature referred to by some investigators as "thermal fronts". Thermal fronts are rapid temperature oscillations superimposed on a normally quiescent thermal plume. They are generally observed in the near field of a thermal plume for calm receiving water conditions and extend over the depth of the discharge. The front phenomenon is believed to have important biological implications because of the rapid, large (about 7°C) variation in temperature. The extent of the plume is determined in part by the degree of mixing between the plume and the receiving body of water. Turbulent vertical mixing across the thermocline is observed in the current work to be greatly affected by a Kelvin-Helmholtz instability in the thermocline. This instability is also a potential source of large error in field plume measurements as a result of the large temperature variations with time. Observations of the Ginna Nuclear Power Plant discharge (Lake Ontario, New York) have indicated that rapid temperature oscillations (thermal fronts) can

Preceding page blank

affect both the mixing and accurate modelling of the thermal plume [1]. Although the existence of thermal fronts has been documented, unanswered questions remain as to their nature and origin. The mechanism that produces the thermal fronts has not been established, nor has the connection been explained between the fronts seen in the field and similar wave-like phenomena observed in the laboratory.

Green, Keating, MacKenzie, Roffler, Scarpace, and Sunby [2] and Scarpace and Green [3] in 1972 and 1973 presented field data in the form of aerial infrared surface temperature pictures of the Point Beach Nuclear Power Plant cooling water discharge entering Lake Michigan. During relatively calm weather, the Point Beach thermal plume was shown to often consist of a series of concentric warm and cool fluid regions at the free surface, in alternating bands about 200 meters apart transverse to the plume axis. The authors termed this phenomenon "thermal fronts" and characterized them as rapid internal temperature variations that have been noticed within the Point Beach thermal plume, but which are not unique to this plume. The period of the Point Beach thermal fronts ranged from 5 to 8 minutes. Boat measurements at the same site showed changes of $3^{\circ}C$ in 1 or 2 seconds at 400 feet from the outfall, with an approximate period of 10-30 seconds.

Frigo, Zivi, King, and Levinson [4] conducted field studies of the thermal front phenomenon at the Point Beach, J. H. Campbell and Waukegan Power plants located on Lake Michigan. Their observations made from a small boat revealed systematic oscillations of temperature and current when measured near the end of the power plants surface discharge canals. A thermistor boom was used at the Point Beach site to sense water temperatures simultaneously at 0.5 meter intervals from the water surface to a depth of 3 meters. The water velocity was also measured and recorded at the same time. The temperature records showed a dominant oscillation period of about 140 seconds with a secondary major oscillation period of about 1200 seconds. Their records also show an apparent correlation between velocity and temperature oscillations. These oscillations penetrated the full depth of the plume and for the Point Beach discharge showed a $3\text{-}5^{\circ}C$ change in about 60 seconds, followed by an approximate 80 second recovery.

Kuhlman and Prahl [5] undertook laboratory and field studies of thermal fronts in 1974 that led them to conclude that such fronts were due to a Kelvin-Helmholtz type instability in the plume-ambient interface for densimetric Froude numbers less than 0.50. In the laboratory, bouyant, rectangular surface thermal plumes entering at right angles to a constant temperature uniform crossflow were modelled. For all initial densimetric Froude numbers less than 0.50, definite vortices were observed within a few channel widths from the outfall. These vortices concentrated and formed alternating bands of warm and cold fluid at the free surface which moved nearly with the mean plume flow.

In the Spring and Fall of 1978 Cataldo and Goodman [1] and [6] conducted aerial and insitu surveys of the Ginna Nuclear Power Plant thermal plume on Lake Ontario. During these surveys, two boats simultaneously measured temperature and velocity profiles at a number of fixed locations in the Ginna thermal plume, while an Aztex C aircraft equipped with a Calspan Bendix LN-3 thermal mapper collected surface water infrared data.

In August of 1979 Vahid Alavian [7] completed a Ph.D. thesis involving an analytical and experimental investigation of thermal fronts. In the laboratory, Alavian developed a model of a shoreline, surface, heated water discharge into a large ambient water body. Using thermal imaginary and

fast-responding temperature and velocity probes, he investigated thermal fronts for the cases of a stagnant ambient and an ambient with a uniform cross-flow. From this model study the investigator concluded that thermal fronts were found in the far field region of the discharge mixing zone where the horizontal motion induced by temperature differences between the discharge and the ambient and by the ambient water velocity dominate the discharge behavior. The mean behavior of the heated discharges with thermal fronts was found to be similar to heated discharges without thermal fronts.

2. EXPERIMENT

A laboratory model study has been essayed to quantify the Ginna thermal fronts and, by doing so, to gain a better understanding of the thermal front phenomenon. To facilitate this laboratory study, a physical, hydraulic, scale model was developed and constructed in which the geometric, kinematic, dynamic, and thermal features of a surface, shoreline, heated water discharge into a large, quiescent, receiving water body could be produced.

The Ginna Nuclear Power Plant is situated on the southern shoreline of Lake Ontario in the northwest corner of Wayne County, New York. At full power, 490 MWe (net), the plant removes water from Lake Ontario at a rate of 400,000 GPM (891.2 cfs) and heats it to a temperature approximately 11°C above ambient lake temperature before returning it to the lake as a shoreline surface discharge. The circulating water is withdrawn through a submerged octagonal intake structure located 3,100 feet off shore in 34 feet of water. The heated water is returned to the lake by a trapezoidal open channel surface discharge. The channel is 20 feet wide at the base with side sloped of 1:1 at the lake entry. The 400,000 GPM flow is normally maintained at all power levels and its discharge velocity depends on lake elevation. The lake is shallow at the discharge, generally less than 6 feet deep, and gradually slopes downward away from the shoreline to approximately a 34 foot depth at 3,100 feet measured perpendicular to the shore.

The heated water discharge at the point of exit to the lake is perpendicular to the shoreline. The shoreline is approximately straight running in an easterly direction. To the west is a large promontory, Smokey Point, which extends out into the lake approximately 1,300 feet north of the discharge and is 1,600 feet to the west at its maximum northerly point. The shoreline at the plant site (2,000 feet to the east and to Smokey Point in the west) is at least 10 feet above the lake, rising rapidly to a relatively flatland surface. The effect of Smokey Point and the height of the shoreline relative to the lake elevation tends to shelter the Ginna plume. The winds appear to be lower by at least 10 miles per hour 6 feet above the water surface compared to the top of the Ginna weather tower 60 feet above the shoreline. Hence, the near field jet is almost always perpendicular to the shoreline (at least 1,400 feet from the discharge structure measured along the center line of the plume.

The hydrodynamic phenomenon under consideration involves flow of different temperature and, hence, different density. Therefore, a requirement to achieve dynamic similarity between the model and prototype is that the densimetric Froude number of the model be equal to the densimetric Froude number of the prototype. To minimize the effect of neglected viscous forces, the model must be turbulent as in the prototype. This is achieved by selecting model geometric scale ratios such that the resutling Reynolds number of the model flow remains within the turbulent range. Geometric scale ratios of L_r = 1:50 and L_r = 1:100 were chosen for the Ginna thermal front model.

For the experiments using the 1 to 50 scale ratio, the depth of the water in the tank was kept at 4 inches throughout the tank with a depth of 1.87 inches in the discharge. For the 1 to 100 scale ratio, the tank bottom was contoured to match the prototype bathymetry with experiments run at 0.66 inches and 0.94 inches of water in the discharge. The principal elements of the model include a large main tank which simulates the ambient receiving water body, a discharge structure from which heated water is introduced into the main tank, a series of hot water heaters, a bank of rotameters to control and measure water flows, and an electronic data acquisition system to sense and record water temperatures and velocities in both the main tank and discharge structure.

The 31 foot long by 16 foot wide main tank contained the water and equipment which comprised the model, ambient, receiving water body. Into this tank (whose water depth could be varied from 4 to 10 inches) was discharged a continuous flow of heated water which formed the model thermal plume. This heated water was introduced into the main tank by means of a trapezoidal flume geometrically scaled to the dimensions and shape of the Ginna surface discharge structure at its point of entrance into Lake Ontario. To maintain a constant water level in the main tank, water was withdrawn at the far end of the tank uniformly across its 16 foot width by means of a diffuser pipe and adjustable flow pump. The main tank was also equipped with four long diffusers through which make-up ambient water could be uniformly added with negligible disturbance to the thermal plume.

The main components of the electronic data acquisition system developed for the model studies are an array of Y.S.I. Series 427 thermistors used to sense water temperatures, a Disa 55M constant temperature anemometer system used to sense water velocities, and a microprocessor unit programmed to sample and record on magnetic tape the output signals on all the temperature and velocity probes every 1/4 of a second. The temperature and velocity probes are suspended into the main tank from adjustable depth and position holders which are mounted to a movable beam system.

Data from the model studies in the form of digital output recorded on magnetic tape was reduced and analyzed through the use of the facilities at the Cooper Union Computer Center. For each temperature versus time trace average, standard deviation, maximum and minimum values for temperature were determined. A spectral analysis of the temperature versus time traces was then performed to quantify the predominant period of the temperature oscillations (thermal fronts). The power spectra were used to measure and compare the relative magnitude and strength of temperature oscillations and corresponding periods at various positions inside and outside the model thermal plume.

3. RESULTS

In the Fall of 1977, Spring and Fall of 1978, aerial and in situ surveys were conducted of the Ginna Nuclear Power Plant thermal discharge on Lake Ontario. Quiescent receiving water conditions are believed to be necessary for the thermal fronts to exist. On June 6, 7, October 17, 18 and 20, 1978 two boats measured temperatures and velocity at a number of fixed locations in the Ginna thermal plume. It was difficult to detect a clear oscillatory pattern on June 6 and October 17. The weather on June 6 and October 17 was windy and the lake water was choppy with the plume bending to the east. By contrast, the lake was very calm on June 7 and October 18, 20 and a clear oscillatory pattern was observed. On June 7 at a distance of 100 feet from the discharge, a predominant period of 140 seconds was determined (running a Fourier power spectral analysis of the temperature traces) at the surface,

2 1/2, 4 1/2 and 6 1/2 feet below the surface. These temperature fluctuations varied from 1 to 4°C with a maximum difference of over 7°C at a fixed position. The temperature variation decayed with distance from the discharge along the centerline of the plume. The oscillations did not decay with depth in the plume; in fact for a number of runs, the amplitude of the oscillation at the 6 1/2 foot depth was larger than at the surface. At a fixed location, the predominant temperature oscillations had similar periods with depth and, based on the temperature versus time data, the temperature variations had the same basic pattern with maximum and minimum temperatures occurring at the same times for all four traces (surface, 2 1/2, 4 1/2 and 6 1/2 feet below the surface), Figure 1.

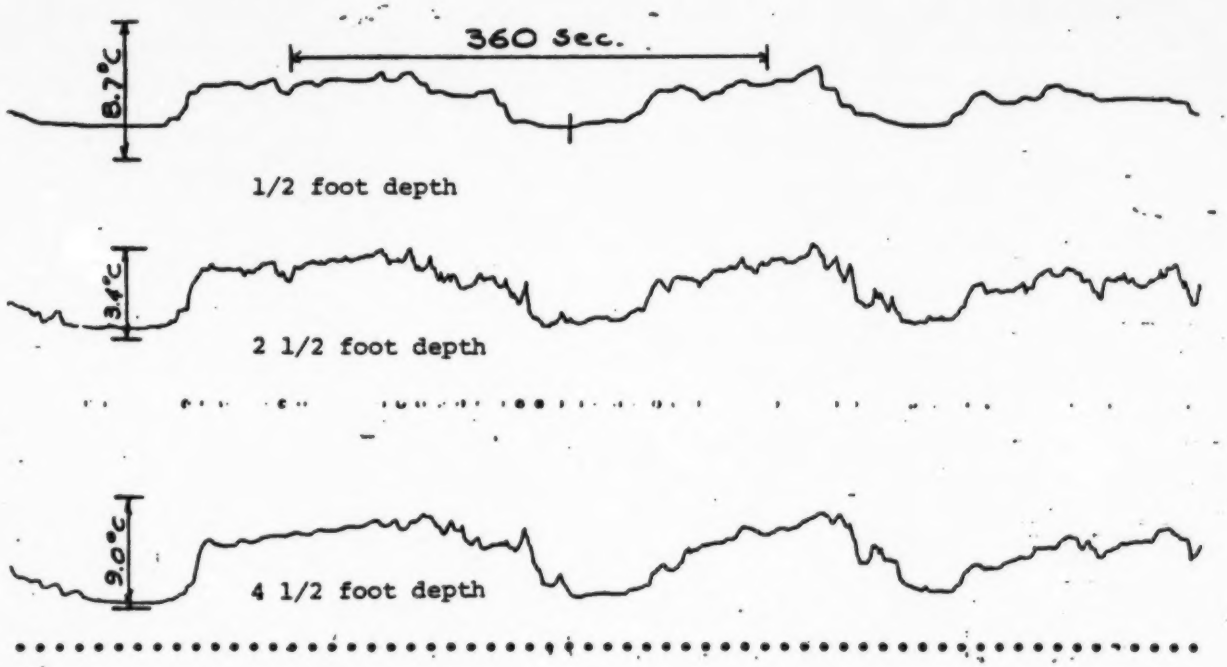

Figure 1: Trace of temperature versus time, Ginna, October 20, 1978, measured at 1/2, 2 1/2 and 4 1/2 feet below the surface of the Lake and 386 feet from the discharge.

A distinct oscillatory pattern was also observed from the velocity measurements 2 1/2 feet below the surface. However, it was impossible to determine the predominant period for the velocity oscillations. The maximum variation in the plume velocity on June 7 was 1.1 ft/sec measured 100 feet from the discharge and decayed to 0.3 ft/sec measured 990 feet from the discharge. Little velocity variation could be measured at distances greater than 1200 feet from the discharge. The average velocities in the plume measured at 100, 350, and 550 feet from the discharge were all about 1.25 ft/sec. (Discharge velocity on June 7 was approximately 3.7 fps.)

From the thermal front surveys at the Ginna site, the following observations are summarized:

1. The temperature fluctuations had the same variation with depth (peaks and troughs all occuring at the same time. The magnitudes of these

oscillations were independent of depth and decayed rapidly across the thermocline

2. Quiescent receiving water conditions appear to be necessary for the thermal fronts to exist.

3. The meteorological, discharge and lake hydraulic conditions were constant (particularly on June 7 and October 18 and 20, when the temperature variations were the largest).

4. The higher the discharge velocity, the larger the magnitude of the temperature fluctuations.

5. The fronts are a near field jet phenomenon and the magnitude of the temperature variations decayed as the survey vessels moved away from the discharge into the far field.

6. For the lower discharge velocities (June 7, 3.7 fps) the periods of the temperature oscillation varied between 140 and 210 seconds. For the higher discharge velocities (6.35 fps, October 18 and 20) the periods of the temperature oscillations were 200 to 700 seconds.

7. Velocity oscillations were measured at 2 1/2 feet from the water surface throughout the near field portion of the plume on June 7, October 18 and October 20. The character of these velocity oscillations was similar to those for temperature, with a period of approximately 120 seconds.

As in the prototype, several positions inside the model thermal plume exhibit a clear oscillatory pattern with amplitude varying from 1 to 5°C. A maximum overall temperature difference of 10°C was recorded at one position, while discharge and ambient temperature traces revealed no significant temperature fluctuations.

Temperature traces from the model were found to have a similar basic pattern for all depths at the same position with respect to the discharge. While the magnitudes of the temperature oscillations tended to increase with depth (maximum temperature differences of 4.6, 4.8, and 6.5°C were recorded at the 1/2, 1 1/2, and 2 1/2 inch depths, respectively 1:50 scale), the frequency of occurrence and location of peaks and troughs in the temperature traces were similar and fairly regular with depth at the same positions. These characteristics were also exemplified in the Ginna field data of which Figure 1 is an example.

Values of maximum recorded temperature differences (measured from the peak to the trough of the temperature oscillation) for a number of centerline positions and depths from the model study runs (1:50) have been compiled and presented in Table 1 (1:50 scale). This table illustrates a characteristic of the front phenomenon which is typical to the June 7 field data. In all cases, the temperature variations decayed with distance from the discharge along the centerline of the plume. Table 1 also shows that the temperature differences tended to increase with depth within the thermal plume. This trend in both the model and field data gives substance to the theories which describe thermal fronts as a near field phenomenon.

Values of maximum recorded temperature differences for a number of centerline positions and depths from the model study runs for the 1:100 scale and a discharge water depth of 0.66 inches at 4 gpm (5.8 feet - October 18 prototype run) have been compiled and presented in Table 2. This table illustrates a characteristic of the front phenomenon which is typical to the October 18 field data, as can be seen from Figure 2. The maximum temperature differences peak 400 to 600 feet from the discharge or 4 to 6 feet from

Washington, D.C. 20235

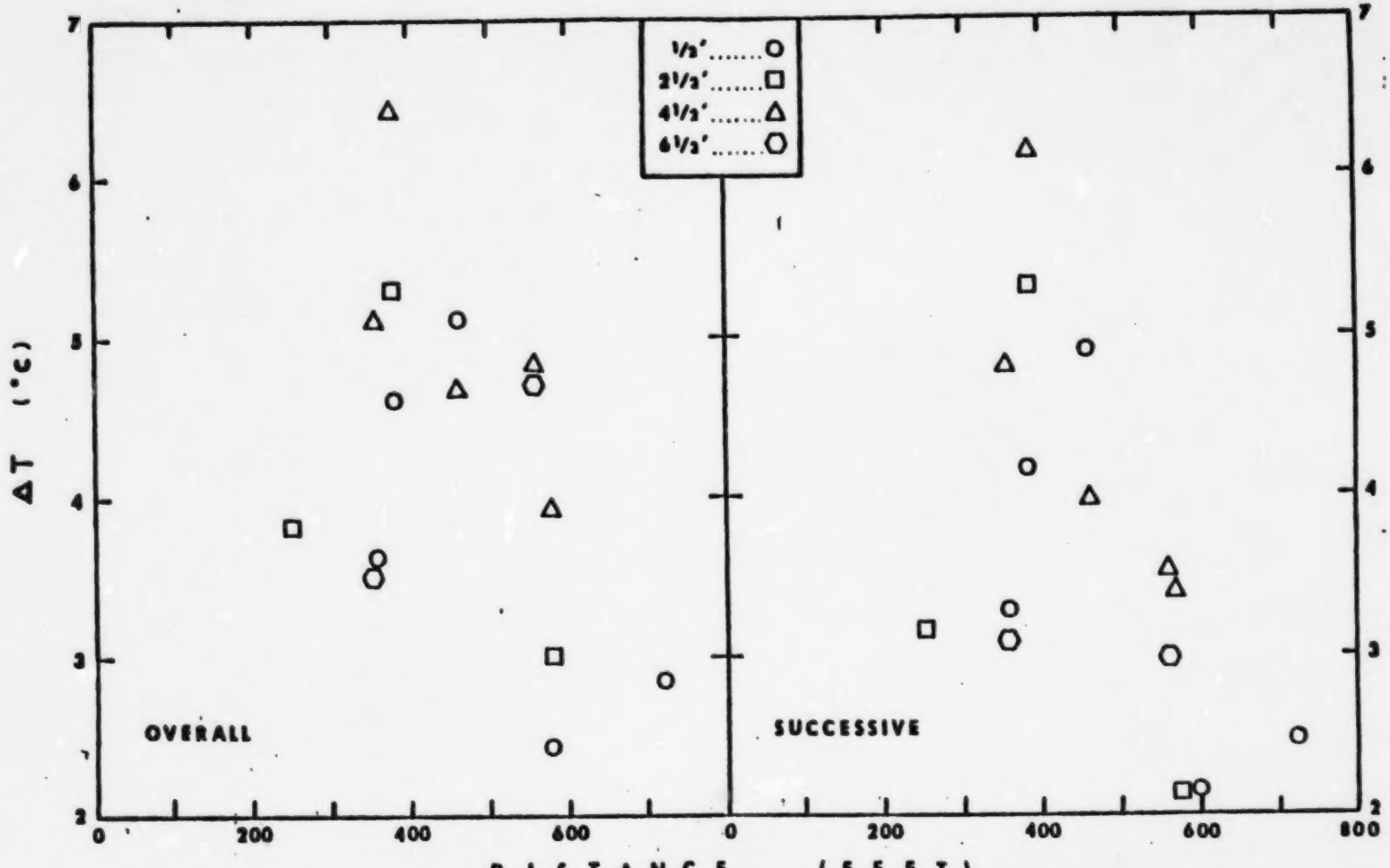

Figure 2: Maximum overall Temperature (°C) difference and maximum successive Temperature (°C) difference versus distance, measured from the Ginna discharge, October 20, 1978.

the model and the temperature differences tend to increase with depth.

TABLE 1

MAXIMUM TEMPERATURE DIFFERENCES (°C)

FROM THE THERMAL FRONT MODEL STUDY (1 to 50 Scale)

Distance from the Discharge (inches)

Depth (inches)	1	12	60	120	180	240
1/2	0.4	4.6	4.4	2.2	1.6	1.5
1	0.5	5.0	3.8	2.4	2.1	1.4
1 1/2	0.4	4.8	4.5	2.3	2.3	1.4
2	10.0	5.7	3.5	2.4	2.7	1.4
2 1/2	3.1	6.4	4.7	2.5	2.6	1.6
3	2.8	5.5	4.0	2.6	2.9	1.1
3 1/2	1.3	6.5	-	-	-	-

TABLE 2

MAXIMUM TEMPERATURE DIFFERENCE (°C)

FROM THE THERMAL FRONT MODEL STUDY (1 to 100 Scale)

Distance from the Discharge (feet)

Depth (inches)	1/2	1	2	3	4	5	6	7	8	9	10	12	14
3/8	0.5	2.3	3.4	3.0	4.6	3.2	1.6	1.5	1.5	1.5	1.5	1.5	1
5/8	0.7	2.5	-	4.0	-	4.5	-	1.8	-	1.8	-	1.7	-
7/8	1.4	2.7	3.4	5.0	4.6	4.0	3.0	2.1	1.8	2.1	2.1	1.7	1.5
1 1/8	1.4	2.9	3.6	5.2	5.7	4.0	3.0	3.3	3.0	3.0	2.4	2.2	2.1
1 3/8	-	-	4.0	-	4.4	-	3.0	-	2.1	-	1.8	-	2.5

Spectral analysis of the model temperature-time traces was performed to determine the predominant periods in the temperature oscillations. The results of the spectral analysis were predominant periods ranging from 10 to 90 seconds (1:50) and 8 to 60 (1:100), equivalent to prototype periods of 71 to 636 seconds and 60 to 600 seconds respectively. These values are in good agreement with predominant periods of 140 to 700 seconds which were determined from spectral analysis of Ginna field data. Also, as observed in the field, periods tended to increase with increased distance from the discharge. Model and prototype periods also increased with increased distance from the discharge. Values of predominant periods for a number of centerline positions and depths from the model study runs (1:50) have been compiled and presented in Table 3.

TABLE 3

PREDOMINANT PERIODS OF TEMPERATURE OSCILLATIONS IN SECONDS FROM THE THERMAL FRONT MODEL STUDY (1 to 50 Scale)

Depth (inches)	Distance from the Discharge 12	60	120	180
1/2	10.6(75)	27.7(196)	42.4(300)	80.1(566)
1	-	22.6(160)	45.1(319)	90.2(638)
1 1/2	25.7(182)	14.4(102)	42.4(300)	80.1(566)
2	-	18.5(131)	90.2(638)	90.2(638)
2 1/2	13.6(96)	21.8(154)	80.0(566)	80.1(566)
3	-	36.1(255)	45.1(319)	90.2(638)

NOTE: The numbers in parentheses are the model periods scaled to prototype time using the time modelling ratio of 7.07.

4. CONCLUSION

From the observations of this model study and previous laboratory field surveys, the thermal fronts appear to result from a Kelvin-Helmholtz instability in the plume thermocline. The Kelvin-Helmholtz instability results from a shear-induced instability in a gravitationally stable stratified fluid. The source of the Kelvin-Helmholtz instability lies in the energy stored in the kinetic energy of relative motion of the different layers of the stratified fluid. The tendency towards mixing and instability will be greater for a larger prevailing shear (as measured by the difference in the velocity across the thermocline for the thermal front phenomenon). A counter-acting force damping this tendency is derived from inertia. As long as inertia maintains a sufficient pressure gradient to prevent mixing, instability will not occur.

It has been shown by Drazin [8] that a sufficient condition for stability is:

$$\left(\frac{dU}{dz}\right)^2 < -4\,\frac{g}{\rho_a}\,\frac{d\rho}{dz} \qquad (1)$$

where: U = velocity of the plume
ρ_a = ambient water density
ρ = density
z = vertical distance measured from the water surface
and g = gravitational constant.

The Richardson number, which measures the dimensionless ratio of bouyancy force to inertia, is defined as:

$$J = -\frac{g}{\rho_a}\frac{\frac{d\rho}{dz}}{\left(\frac{dU}{dz}\right)^2} \qquad (2)$$

Combined with the definition of the Richardson number (equation (2)), the inequality expressed by equation (1) suggests, therefore, that a necessary and sufficient condition for stability is that the Richardson number be everywhere greater than 1/4 in the flow:

$$J > 1/4 \quad \text{for stability.} \qquad (3)$$

The arguments leading to equation (3) do not, of course, justify an inference that its violation must necessarily lead to instability. Although stored energy is available for initiating instability, no mechanism may exist for transforming the energy into the hydrodynamic mode for such instability. An alternate approach to the development of a hydrodynamic stability criterion which would provide the necessary condition for a Kelvin-Helmholtz instability may be evolved from the Taylor-Goldstein equation [9,10]. The Taylor-Goldstein equation is for small disturbances in an inviscid, incompressible, stratified, parallel shear flow, when the Boussinesq approximation is made, with velocity and density variation. These assumptions may be applied to the model thermal plume. Together with suitable boundary conditions, the Taylor-Goldstein equation defines an eigenvalue problem which Hazel [11] expressed in terms of the parameters J a typical Richardson number and the dimensionless wave number, α, defined as:

$$\alpha = \frac{2\pi h}{\lambda} \qquad (4)$$

where h = thermocline thickness
and λ = wavelength of the disturbance

Upon applying hyperbolic tangent profiles for both density and velocity, Hazel obtained a parabolic neutral curve and stability boundary defined by:

$$J = \alpha\ (1-\alpha) \qquad (5)$$

Equation (5) is valid for boundaries of flow at infinity. When the boundaries are not at infinity, as in the case of the model discharge and, in general, most surface discharges, the shape of the neutral curve and stability boundary are shown in Figure 3. The stability curves shown in Figure 3 may be used in general since the shape of the neutral curve only depends slightly on the density and velocity profiles assumed. The numbers against the curves of Figure 3 are the ratios of the depth of the plume to the thermocline thickness. The area below these neutral stability curves or stability boundaries defines the unstable flow region and the area above the curves is considered the stable region.

To determine if the model thermal fronts are unstable as predicted by equation (3) and Figure 3, velocity and density (or temperature) profiles as well as wavelength determinations are needed. The temperature profiles were measured [12] to determine the density gradients ($d\rho/dz$) across the model plume thermocline at 1, 12, 60, 120, 180, and 240 inch distances from the

Hemisphere Publishing Corporation
1025 Vermont Ave., N.W.
Washington, D.C. 20005

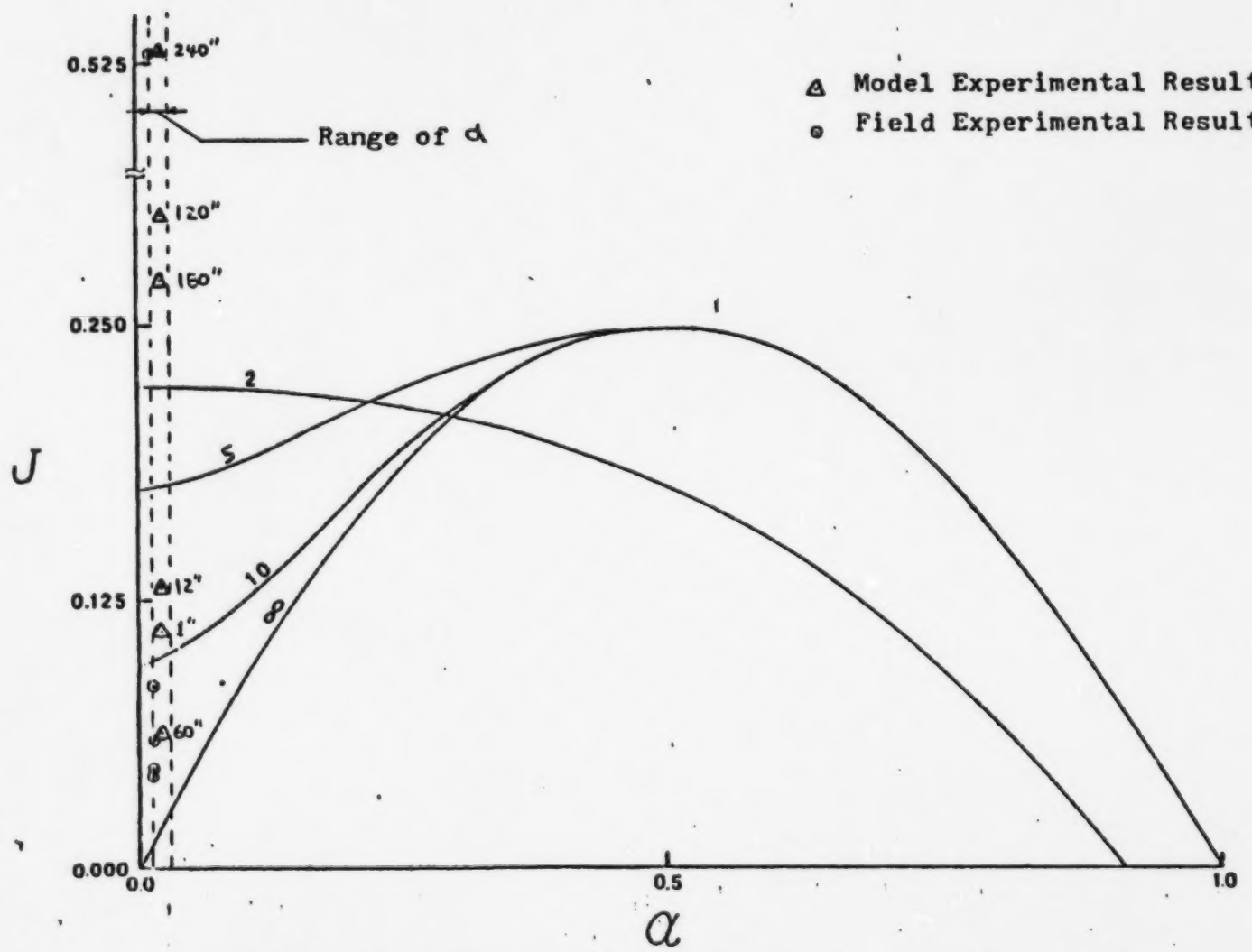

Figure 3: Richardson number (J) versus the dimensionless wave number (α) showing the effect of the stability of a density interface to a Shear (Hazel 1972). The numbers against the curves are the ratios of the depth of the plume to the thickness of the thermocline.

X-B-943

discharge along the plume centerline. Values of fractional excess temperatures (θ/θ_o) from these profiles were converted to four sets of actual temperatures using the four discharge and ambient temperatures recorded. Four sets of density gradients across the plume thermocline were then determined from this temperature data as shown in Figure 3. Similarly, the velocity profiles were used to determine the velocity gradients (dU/dz) or shear across the model plume thermocline at distances from the discharge along the plume centerline of 1, 12, 60, 120, 180, and 240, inches, respectively. The values of the velocity gradients for the model study are also shown in Table 4.

In the field, wavelengths of the thermal fronts were determined from infrared overflight data. These values of wavelength varied from 300 to 440 feet which is equivalent to model values of 72 to 106 inches. In the laboratory, the wavelengths of the model thermal fronts were determined through the use of dye-tracing techniques. Dye patterns were observed and values of λ ranging from 50 to 97 inches were determined. The model thermocline thickness (h) was found to be 1/2 inch at all positions. Using this value of the thermocline thickness and a range of wavelengths from 50 to 106 inches, a range of dimensionless wave numbers from 0.015 to 0.031 was calculated. This range of α values has been indicated on Figure 3. It is clear from this figure that the discrepancies in wavelength values will not seriously affect the validity of the stability analysis for this particular phenomenon. The band or range of dimensionless wave numbers considered is very narrow and will not affect where experiment data points fall with respect to the stability boundary.

The values of the Richardson number, J, have been calculated using equation (2) and are presented in Table 4 for positions 1, 12, 60, 120, 180, and 240 inches from the discharge along the centerline of the plume. The average values of J in Figure 3 are simply the arithmetic mean of the Richardson numbers at each particular position. Note that at the 1, 12, and 60 inch positions all the model study Richardson numbers are less than 1/4. In contrast, the average Richardson numbers at the 120, 180, and 240 inch positions are greater than 1/4.

Six experimental points, corresponding to the average Richardson numbers calculated from model study data at the six different distances from the discharge, have been plotted on Hazel's stability diagram of Figure 3. The ratio of the depth of the plume to the thermocline thickness (numbers against the stability curves of Figure 3) is approximately 5 for the model study. Therefore, the curve marked 5 will be the approximate stability boundary and neutral stability curve for the thermal front model study. The points corresponding to the 1, 12, and 60 inch distances from the discharge on Figure 3 clearly fall below this curve indicating that for distances from the discharge less than 60 inches there is an unstable flow pattern present. The front phenomenon at these three positions is correspondingly very pronounced. At the 120 and 180 inch poisitions, the model thermal fronts showed considerable decay from the three positions closer to the discharge. The 120 and 180 inch experimental points on Figure 3 lie above the stability curve (5) indicating that the flow is stable at these positions. Finally, at the 240 inch position, the thermal fronts no longer exist, and the experimental point on Figure 3 lies well above the stability boundary. From these computations it appears that the model thermal fronts are due to Kelvin-Helmholtz instability in the plume thermocline. The model data satisfies the conditions of equation (3) and those of Hazel's stability diagram (Figure 3). In a similar stability analysis of field data, Cataldo and Goodman [1] also found prototype data to meet the stability conditions of equation (3) and Figure 3.

The thermal fronts observed in both the field and labdratory appear to be due to a Kelvin-Helmholtz-type shear instability caused by a layer of warmer water moving over a cooler receiving water. At the critical Richardson number, vortices can be formed at the thermocline separating the heated plume from the receiving water. Temperature and velocity fluctuations occur in the vortex. A sequence of line vortices of cold and warm fluid roll up in the vortex. Patches of unstable waves spread both laterally and longitudinally in a horizontal plane due to local gradients leading to vertical mixing. The temperature fluctuations (temperature drops) are due to cooler fluid from the crossflow pulled up into the vortex. This cooler water is carried along with the plume in transverse fronts (running throughout the depth of the plume).

TABLE 4

VALUES OF THE RICHARDSON NUMBER (J)

FROM THE THERMAL FRONT MODEL STUDY

Distance From The Discharge (inches)	$\frac{dU}{dz}$ (feet/sec-inches	$\frac{-1}{\rho_a}\frac{d\rho}{dz}$ (1/inches) $\times 10^{-3}$	J
1	0.84	2.56	0.12
1	0.84	1.90	0.087
12	0.50	1.07	0.14
12	0.50	0.808	0.10
60	0.40	0.344	0.069
60	0.40	0.244	0.049
120	0.14	0.194	0.32
120	0.14	0.138	0.23
180	0.12	0.144	0.32
180	0.12	0.0860	0.19
240	0.084	0.140	0.64
240	0.084	0.0980	0.45

REFERENCES

1. J. C. Cataldo and A. S. Goodman, Studies of Thermal Electric Power Plant Heated Discharges, NYS ERDA, Aug. 1978.

2. T. Green, T. Keating, T. MacKenzie, S. Roffler, F. Scarpace and C. Sunby, The Point Beach Thermal Plume, Proc. 15th Conf. Great Lake Res., 1972, p. 588-596.

3. F. Scarpace and T. Green, Dynamic Surface Temperature Structure of Thermal Plumes, Water Resources Res. No. 1, 9; 1973, 138-153.

4. A. A. Frigo, S. M. Zivi, R. F. King, and E. D. Levinson, Field Observations of the Dynamics of Heated Discharge Jets, Proc. 17th Conf. Great Lakes Res., 1974, p. 412-424.

5. J. Kuhlman and J. Prahl, Laboratory Modelling of Surface Thermal Plumes, School of Engineering, Case Western Reserve University, Report FTAS/TS-74-102 (Aug. 1974).

6. J. C. Cataldo and A. S. Goodman, Studies of Thermal Electric Power Plant Heated Discharges, NYS ERDA, Aug. 1978.

7. V. Alavian, Investigation of Thermal Fronts in Heated Water Discharges. Ph.D. Thesis, University of Wisconsin, Madison, Wisconsin, 1979.

8. P. G. Drazin, The Stability of A Shear Layer in an Unbounded Heterogeneous Inviscid Fluid. J. Fluid Mech. 4; 214-224, 1958.

9. G. I. Taylor, Effect of Variation in Density on the Stability of Superposed Streams on Fluid. Proc. Royal Soc. A132, 499-523, 1931.

I0. S. Goldstein, On the Stability of Superimposed Streams of Fluids of Different Densities, Proc. Royal Sec. A 132, 132, 524-548, 1931

11. P. Hazel, Numerical Studies of the Stability of Inviscid Stratified Shear Flows, J. Fluid Mech. 51; 39-61, 1972.

12. G. Keevill, A Physical Model Study of the Thermal Front Phenomenon, M. S. thesis, The Cooper Union for the Advancement of Science and Art, New York, New York, 1980.

PB82-228651

A THREE-DIMENSIONAL FINITE DIFFERENCE MODEL FOR THE PREDICTION OF THERMAL DISCHARGES

R. V. ELLIOTT
Hydraulic Studies & Development
Ontario Hydro
700 University Avenue
TORONTO, Ontario, Canada
M5G 1X6

G. D. RAITHBY
Department of Mechanical Engineering
University of Waterloo
WATERLOO, Ontario, Canada
N2L 3G1

ABSTRACT

An existing three-dimensional finite difference model has been modified in order to accurately account for the interaction of a thermal discharge with the bottom and shoreline of the receiving basin. Predictions are made for a jet entering a quiescent lake, and for convection of a plume along a lakeshore under winter (sinking plume) conditions. Good agreement between predictions and field measurements were achieved.

1. INTRODUCTION

The prediction of thermal discharges entering receiving basins has already received considerable attention. The state-of-the-art was evaluated in 1975 in review articles by Dunn et al [1] and Jirka et al [2]. The accuracy of the phenomenological, integral, and finite difference models described were all shown to be less than adequate. The reasons for this are rooted in the complexity of the problem. The importance of the buoyancy-driven motion, and the site-dependent interaction of the discharge jet with the bottom and shoreline, are particularly difficult to treat accurately.

Recently-developed finite difference models by McGuirk and Rodi [3,4] and by Raithby et al [5,6] are economic to run (less than 20 min. CPU time) and yet are able to account for the complex three-dimensional motion. The McGuirk-Rodi model is applicable only to deep receiving basins and contains several approximations which limit its range of validity. The other model treats bottom interaction crudely (accurately for a uniform bottom) but contains fewer approximations. Both models assume parabolic flow, which permits the solution to be marched forward in the flow direction; the validity of this approximation is questionable however, when the discharge is deflected sharply by a moving ambient fluid.

The present paper describes predictions by a modified version of the model of Raithby et al [5,6] which permit the effect of the bottom and shoreline to be treated more accurately. The predictions of the modified model are first compared to measurements [1] made at the Point Beach Power Station under summer, quiescent lake conditions. The highly irregular bottom at this site is shown to have a pronounced effect on the behaviour of the discharge jet. Good agreement with the reported measurements of gross jet parameters was found.

The model is then applied under winter conditions to the convection of a plume along a shoreline under strong, fairly steady wind conditions where the ambient temperature is such that the density maximum of water is expected to play an important role. The sensitivity of the predicted temperatures to the existence of complex flow, which is driven by the density reversal, was evaluated. Good qualitative agreement was found between predictions and measurements.

2. DESCRIPTION OF THE MODEL

The model for a uniform bottom or very deep receiving basin has been presented previously [6]. By ignoring diffusion in the principal flow direction (y-direction in Fig. 1) and by making a suitable approximation of the pressure gradient in this direction, the solution can be marched forward plane-by-plane. At each y-station at which this solution is obtained, the finite difference analogs of the three momentum equations, the continuity equation, the energy equation and any necessary equations to calculate the turbulence, are solved. Iteration is continued at each plane until a converged solution is obtained; the RUMPIN procedure [7] is used to promote the convergence rate of the equation set.

The original model used Cartesian coordinates with uniform grid spacing in each coordinate direction for each y-station but the spacings were allowed to change from station to station. This permitted the grid to expand or contract as required to follow the active portion of the jet. A typical node layout on the surface is shown in Fig. 1(a), and a similar layout was used in the z-direction. The present model replaced the z-coordinate by σ, where

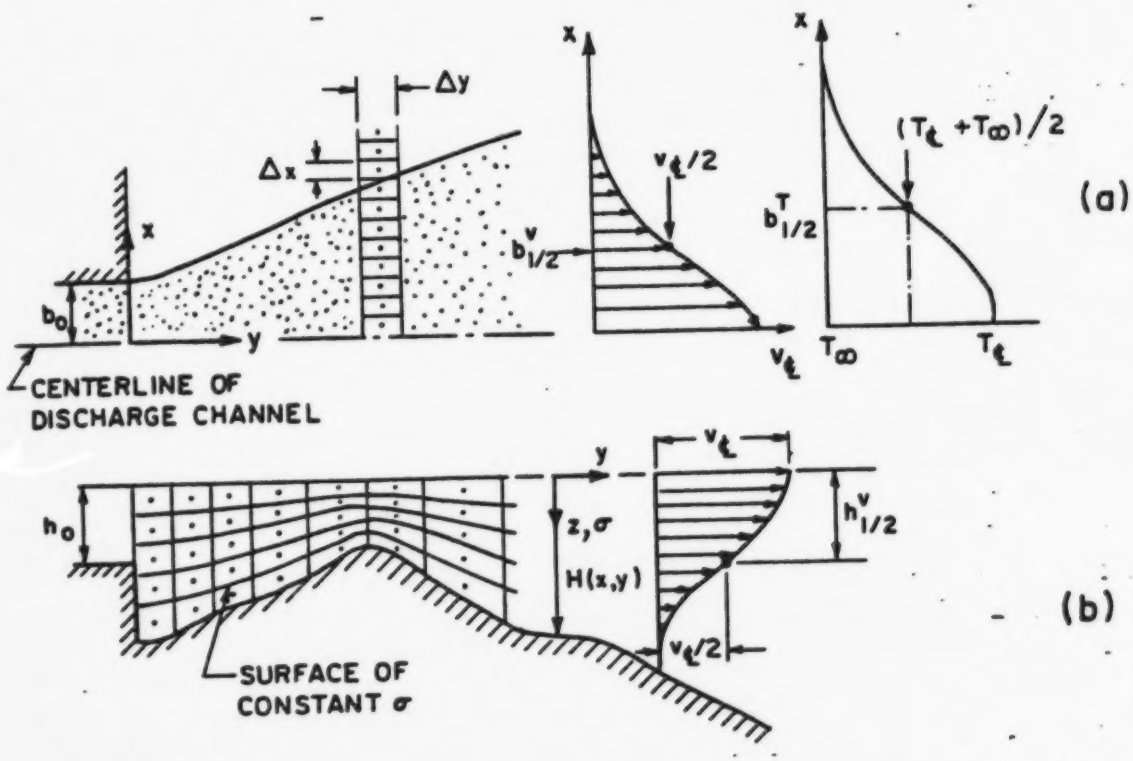

Fig. 1(a) Plan view of water surface and outlet channel showing grid layout, velocity and temperature profiles

(b) Bottom contour along plane x = 0, showing the grid layout and velocity profile.

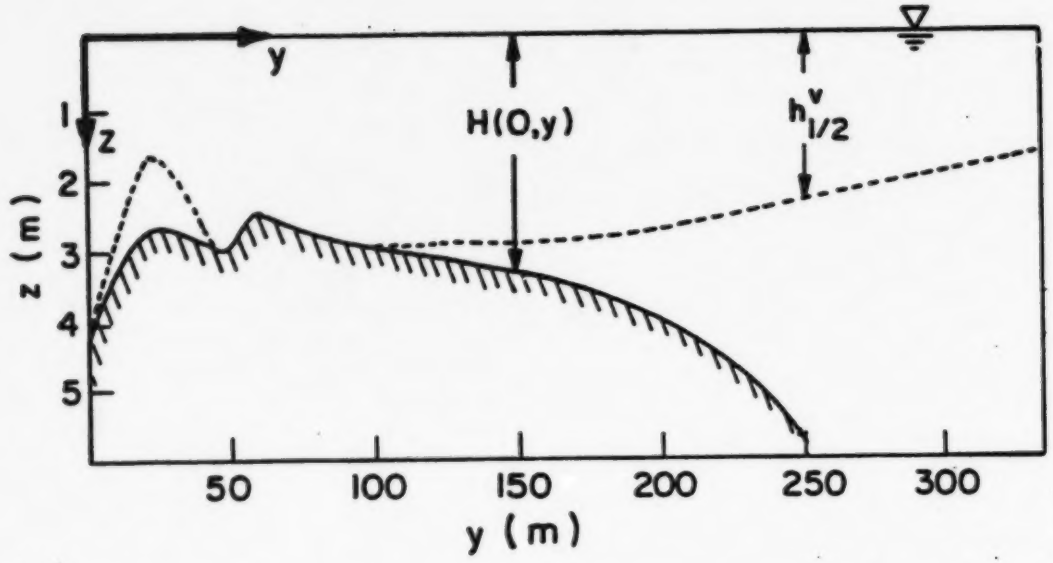

Fig. 2 Bottom contour and velocity half-depth along a line extending from the centre of, and parallel to the sides of, the discharge channel at the Point Beach Power Plant

depth use. With the exception of a region near the outfall, the measured data are seen in Fig. 3(a) to fall between these curves.

The model was then re-run in the present study for the σ-coordinate system, with $\sigma = 1$ along the bottom contour as shown in Fig. 2 and with bottom variations in the x-direction ignored. This yielded predictions depicted by the solid curves in Figs. 3 and 4. The dimensionless centreline predictions in Fig. 3(a) are seen to agree well with the data except very near the outfall where the measured dimensionless temperature did not approach the expected value of unity. Since the outlet velocity profile was not known, runs were made, one with a uniform outlet velocity, and the other with a velocity which varied with the 1/7th-power on distance from the nearest channel wall. Fig. 3(b) shows that the measured dimensionless centreline velocities lie between the curves for these two cases.

The predicted thermal and velocity half-widths shown in Fig. 4 were found to be approximately the same for both inlet velocity profiles. The predicted thermal half-widths are seen from Fig. 4(a) to lie below both sets of measurements (which are in substantial disagreement with one another). A possible explanation is that there is a weak backflow driven by a buoyancy-induced pressure gradient near the edge of the jet that plays a major role in determining the thermal width. Since such a flow would be very sensitive to ambient conditions; this could account for the discrepancy in the measurements. A flow of this type is entirely excluded from the present model by the parabolic approximation which would explain why the thermal half-width predictions are lower than the observations. Since velocities which would arise from this backflow are small, the velocity profiles should not be strongly affected. The good agreement between the measured and observed velocity half-widths shown in Fig. 4(b) supports this hypothesis.

The irregular bottom terrain and the strong buoyancy forces were found to have significant effects on the velocity profile. One indication of this is

$\sigma = z/H(x,y)$, so that surfaces of constant σ lie at a constant fraction of the water depth as shown in Fig. 1(b). The expressions for the finite difference control volumes become somewhat more complicated, however the non-orthogonality is sufficiently small in most real problems (the bottom slope rarely exceeds 10%) so that the solution procedure itself is not adversely affected. Such a coordinate system was originally proposed by Phillips [8], and was first used for lake circulation predictions by Freeman et al [9]; Paul and Lick [10] have applied a similar method to a thermal discharge problem. A typical calculation used 15 control volumes in both the σ- and x-directions and solutions were obtained at up to 30 y-stations. Coarse grids were used to initially establish the plume trajectory and mesh refinement was continued until essentially no further change occurred in the parameters (e.g. velocity and temperature half-widths and half-depths) which characterize the gross jet behaviour.

The boundary conditions along the bottom for velocity require special attention. The velocity at each grid point adjacent to the bottom was obtained and the component of this velocity parallel to the bottom was taken. It was assumed that the velocity decayed from this value to the bottom according to the "universal velocity profile", so that the shear at the bottom could be found and resolved into its x- and y-components. These components were used as boundary conditions on the x- and y-velocities. To determine the z-component of the velocity near the bottom, zero mass flow through the bottom was assumed.

The momentum equations contain eddy diffusivities for momentum and energy transfer which must be specified. For jet calculations, where turbulence is generated by the interaction between the jet and the ambient fluid, a two-equation model is used [6]. This requires the solution of additional equations for the kinetic energy, k, and the dissipation of turbulent kinetic energy, ε. For convection and diffusion of a thermal plume along a shoreline, the turbulence is generated by the large-scale motion of the lake. Since only a small portion of the mean motion near the shore can be calculated by the model, the eddy diffusivities must be specified; the values that were used are described in the relevant section.

3. SURFACE DISCHARGE INTO A QUIESCENT LAKE

Extensive measurements at the Point Beach Power Plant have been reported by Dunn et al [1]. The bathymetry near the power station is quite complex, as indicated by the bottom contour plot along the y-direction shown in Fig. 2. The y-coordinate originates at the centre of the outfall channel where it enters the lake and extends into the lake in a direction parallel to the sides of the outfall channel. Measurements of the centreline temperature and velocity decay of the jet are shown in Fig. 3 for two dates when quiescent conditions prevailed. The measured thermal half-widths of the velocity and temperature profiles near the surface are shown in Fig. 4. The definitions of these quantities can be obtained from Fig. 1(a). It should be noted that the data reported were actually obtained by a curve-fitting procedure and do not represent actual instantaneous or average values. The thermal and velocity half-widths are reported as the best-fit straight lines through the data near the outfall. This accounts for the straight lines shown in Figs. 4(a) and 4(b).

The results obtained from the uniform bottom model were reported earlier [6] and are reproduced as the broken line in Fig. 3(a). When a 3 m constant depth was used, the dimensionless temperature decay along the centreline was predicted to fall to about 0.8 at 100 m from the outfall and thereafter decrease very slowly. When the depth was increased to 4.2 m, the dimensionless temperature dropped more rapidly to level out at lower temperatures than for the 3 m

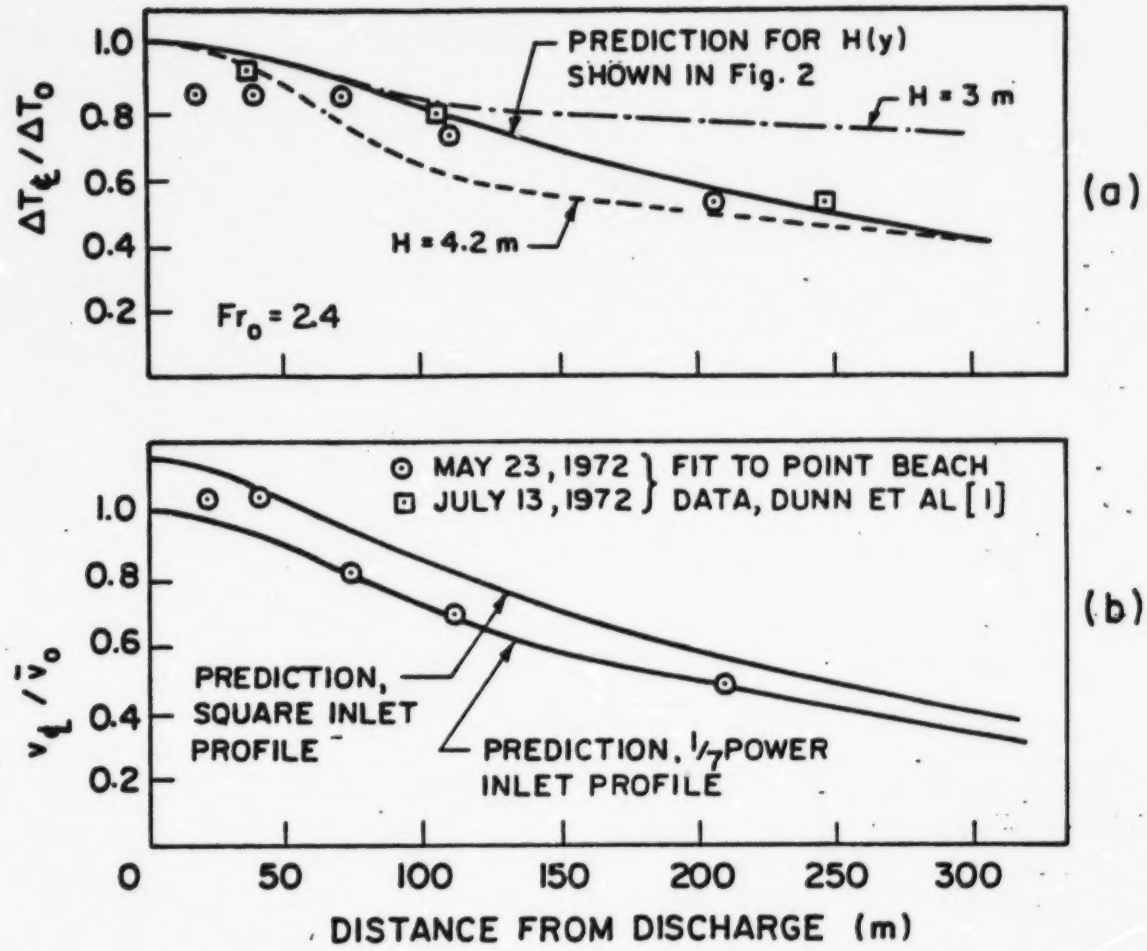

Fig. 3(a) Comparison of measured [1] and predicted temperature decay along the jet centreline
(b) Comparison of velocity decays

the irregular behaviour of the predicted velocity half-depth shown in Fig. 2; for example the change in the bottom terrain at 50 m causes the velocity profile to become much more uniform so that the half-depth approximately follows the bottom up to 100 m from shore.

In summary, with the possible exception of the thermal width of the jet, the present model gives predictions which are in good agreement with observations under conditions where bottom interaction and buoyancy effects are both important.

4. CONVECTION OF A WINTER PLUME ALONG A SHORELINE

4.1 Statement of the Problem

To assess whether winter thermal plumes, which are deflected by longshore currents to impinge on the shoreline, are likely to act to form a barrier for the offshore movement of pollutants, a thermal simulation was performed to study

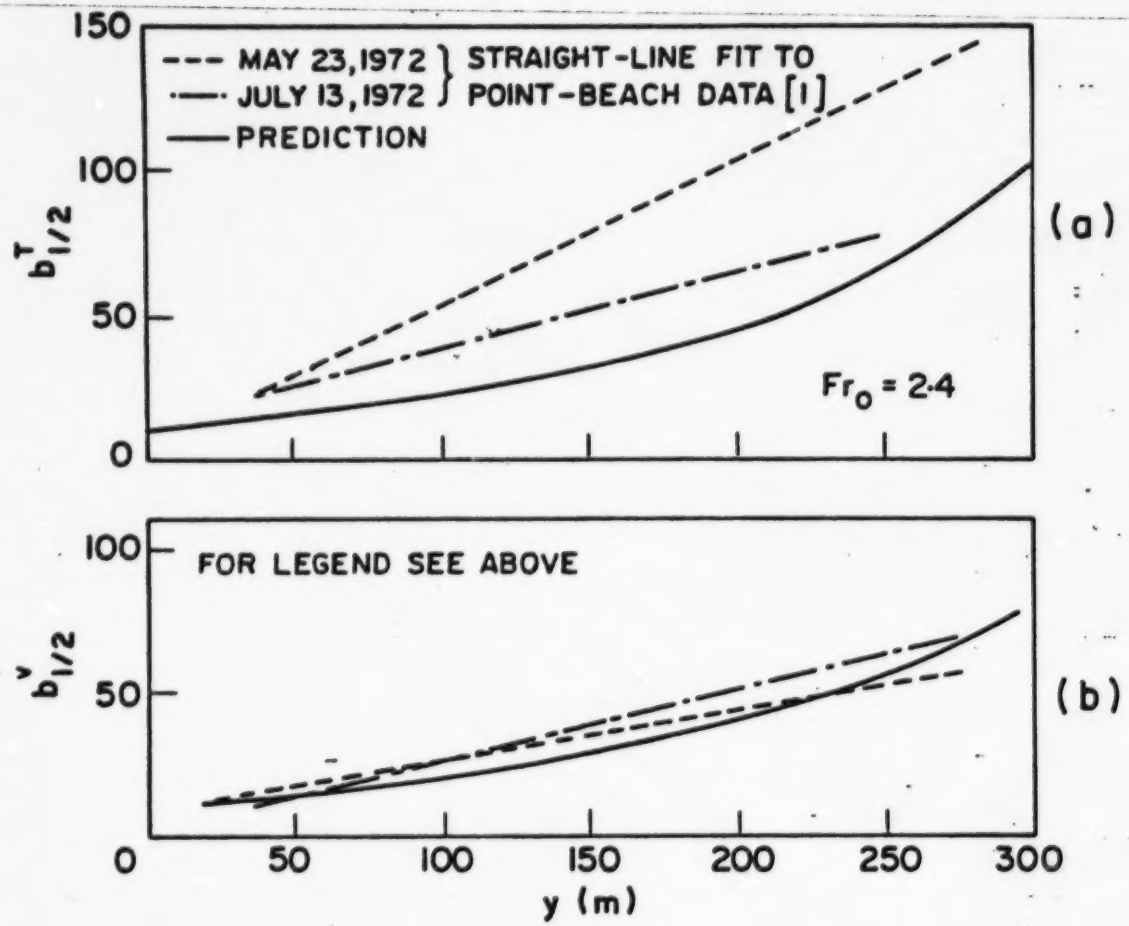

Fig. 4(a) Comparison of measured and predicted thermal half-widths near the surface
(b) Comparison of velocity half-widths

the strength and stability of the temperature-generated density gradients. This was accomplished by mathematically modelling the thermal plumes in the far field after they had been deflected by the currents to follow the shoreline.

4.2 Field Observations

During the winter of 1979-1980, a concerted effort was made by Environment Canada - The National Water Research Institute, The Ontario Ministry of the Environment, and Ontario Hydro to study the behaviour of thermal plumes in Lake Ontario due to the surface discharge of cooling water from the Pickering Nuclear Generating Station. The results of this study are presented in internal reports by the contributing agencies [11,12,13] and have been summarized in a joint report [14]. One result was the observation of persistent, moderate-to-strong (10-45 cm/s) shore-parallel currents with frequency of occurrence of approximately 50%. The average duration of easterly episodes was about 6 days with an average speed of 18 cm/s, compared to 2.5 days with an average speed of 13 cm/s for the westerly episodes. The shoreline runs in an approximate east-west direction near the Pickering station.

Thermal plumes measured during these shore-parallel current episodes were typically less than 800 m wide and tended to follow the shoreline up to distances of 10 km from the source. Measurements of the sub-surface temperature structure in the plumes showed that the temperatures were approximately uniform in the vertical direction at all locations.

The thermal plume which was measured on March 4, 1979, when steady winds maintained a current to the east of about 17 cm/s, was selected for comparison with mathematical model results.

4.3 Specifications of the Grid and Model Parameters

The upstream temperature profile required as input to the model, was specified at a sufficient distance downstream from the outfall so that the plume was travelling parallel to the shore. The starting location and grid layout on the surface are shown in Fig. 5(a). This grid covered a region 166 m wide, with a grid spacing of 89 m, by more than 10 km long, with a longshore grid spacing

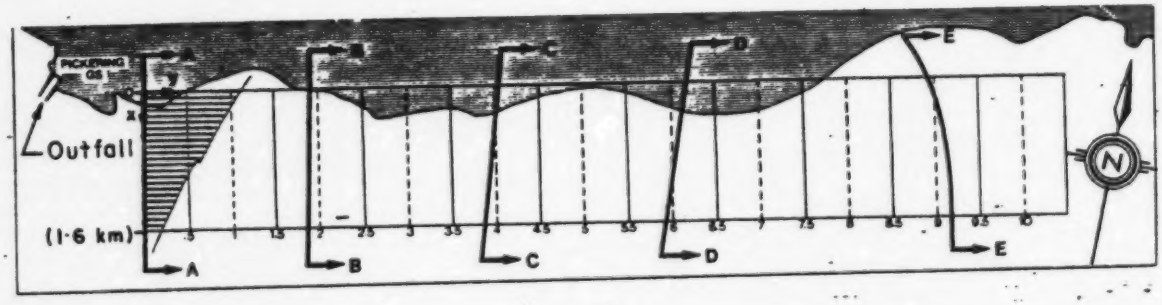

(a)

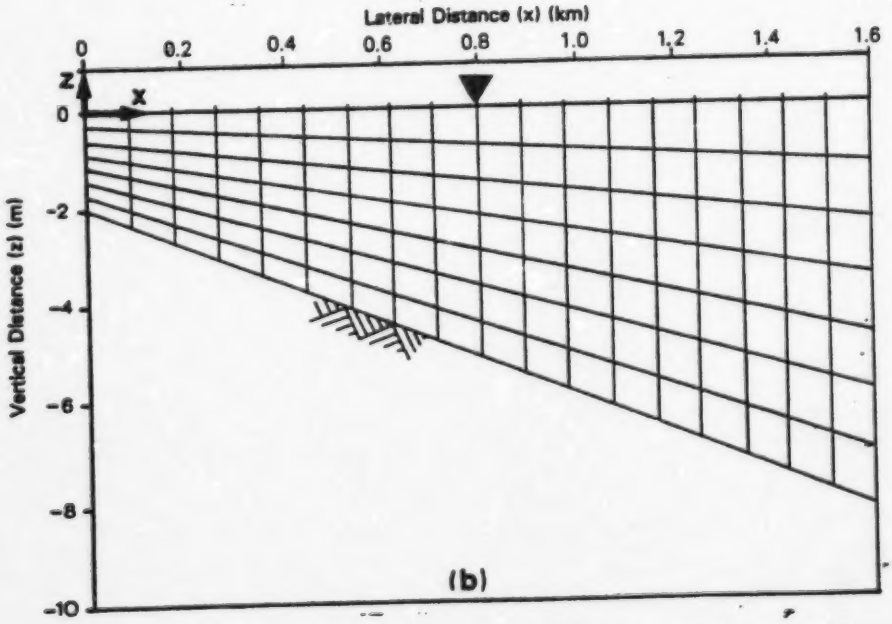

(b)

Fig. 5(a) Drawing of the horizontal (x-y) computation grid showing the orientation relative to the shoreline

(b) Drawing of the vertical (x-z) computation grid distorted 100:1 in the vertical direction

of 1000 m. A cross-section of the grid in a vertical plane appears in Fig. 5(b). The bottom was approximated as a plane with an offshore slope of 0.004, which approximately fitted the measured bathymetry. With this approximation, together with the failure of the grid to follow the shoreline (Fig. 5(a)) only qualitatively correct predictions of the model can be expected. It should be noted that the main flow is in the y-direction for this case and that the σ-coordinate has been denoted by z.

The x- and z-components, of the momentum eddy diffusivity used in the simulation were taken to be $K_x = 0.1$ (from [15]) and $K_z = 0.005\ h(x)(u^2 + v^2)^{1/2}$ [m^2/s] (in which h(x) is the local depth and u and v are, respectively, the calculated x- and y-components of the current velocity).

During the survey, an average wind speed of 6 m/s from a westerly direction, at an angle of 25° toward the shore was measured. A surface drag coefficient of 1.2×10^{-3} was calculated using the methods of Donelan [16]. This produced wind-stress components of $\tau_x = -0.0277$ and $\tau_y = 0.0486$ (N/m^2) respectively. These values were used in the model to calculate current velocity components.

4.4 Tests of Grid Resolution

To ensure that the selected computation grid was fine enough to resolve the gradients involved, a test case was run for a uniform-over-depth step function starting temperature profile to about 600 m from shore in the offshore direction in a constant current. Effects that would cause three-dimensional motion, such as surface heat transfer, wind stress, and temperature-generated density differences, were suppressed in the calculation. The predicted temperature profiles at various distances form the starting plane were compared with results from a depth averaged two-dimensional finite difference model in which very fine grid spacings could be used to ensure grid-independence of the results. The temperature profiles predicted by the two models were in good agreement, thereby validating the horizontal grid spacing chosen for the present simulation. Details can be found in [17].

4.5 Generation of Current Fields

To define starting current velocities for the thermal plume simulation, the model was run for a uniform starting temperature field and zero surface heat transfer. The computation was allowed to proceed to a distance sufficiently far downstream from the starting plane that the current velocity components did not change, i.e. until the flow had become fully established. Typical vertical profiles of the longitudinal velocity components are shown in Fig. 6. Average current velocities measured during the survey by in-situ current meters are also shown on the diagram. It can be seen that these measured velocities are in excellent agreement with predicted values at comparable distances from the bottom.

The surface wind stress generated by the on-shore wind component resulted in the prediction of the current velocities, normal to the main flow, shown in Fig. 7. The flow is, as expected, inward along the surface and outward along the bottom; the magnitudes of the lateral velocity components are less than 2% of the longitudinal components. Although the maximum vertical and lateral components appear to be about the same length in the figure, the vertical components are smaller by a factor of 100 because of the velocity scale distortion that was used in the diagram.

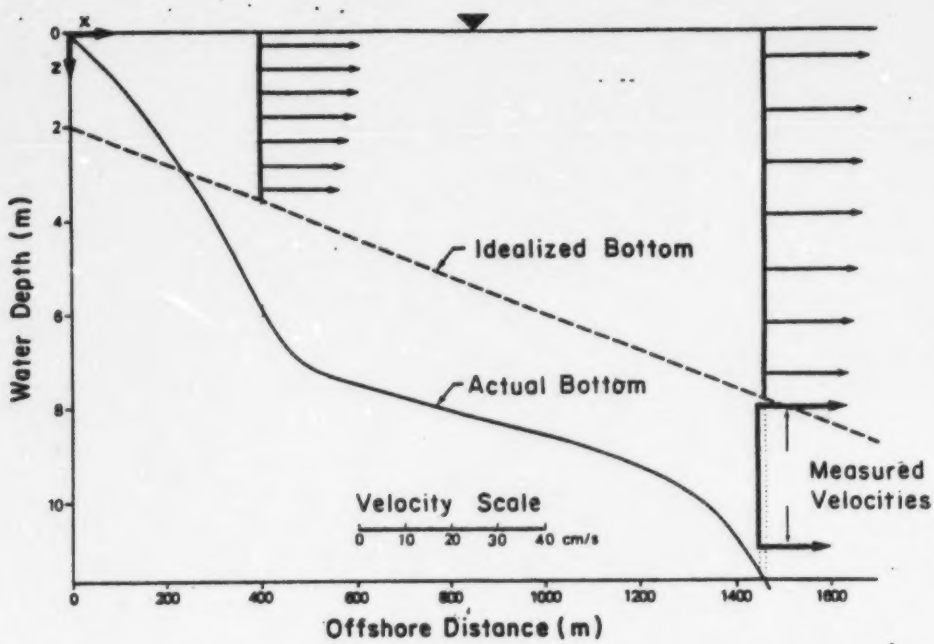

Fig. 6 Typical vertical profiles of calculated longitudinal (y) current velocity components on the starting plane compared with measured values

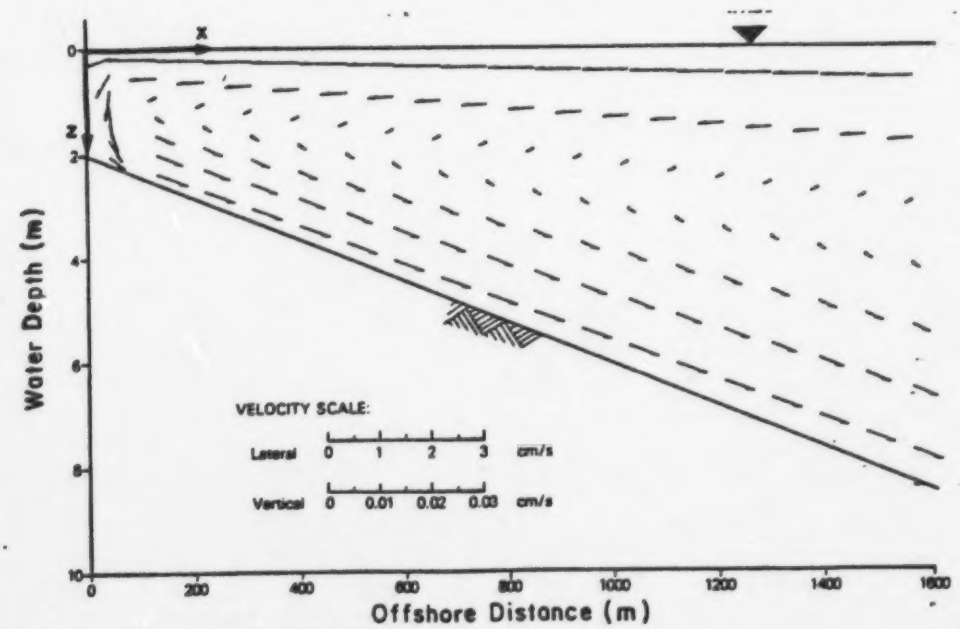

Fig. 7 Predicted current velocity vectors normal to the main flow at the starting plane (cross-section A-A)

4.6 Thermal Boundary Conditions

The meteorological data that was measured just prior to and during the March 4, 1977, thermal plume survey was used to define the following relationship for the rate of surface heat transfer, Q_s, as a function of the water surface temperature T_s: $Q_s = -29(T_s + 1.7)$.

Temperature measurements at Section A-A in Fig. 5 were fitted to grid points on the starting plane for the thermal plume simulation. A comparison between the measured and fitted vertical isotherms is shown in Fig. 8. The ambient temperature of about 1°C lies below the temperature at which water has its maximum density. The vertical uniformity of the plume temperatures can be seen in this figure.

4.7 Simulation of the Temperature Field

A simulation run was made, for the inlet velocity and temperature field presented above, in which surface heat transfer, wind stress, and temperature-driven density variations were included. The predictions at the surface of the thermal plume are compared with the measurements in Fig. 9. The narrow longshore character evident in the observed plume is reproduced in the predictions. The 4°C isotherm (water with maximum density) occurs in the predictions at an offshore distance of approximately 670 m over the length of the plume.

It might be expected that the more dense, warm water would tend to sink to form a diving plume, however, both the measured and predicted results show a uniform temperature structure in the vertical direction. Such behaviour can be explained [17] by noting that the density differences near 4°C are not sufficiently large to cause a noticeable temperature distortion in the presence of the strong longshore currents.

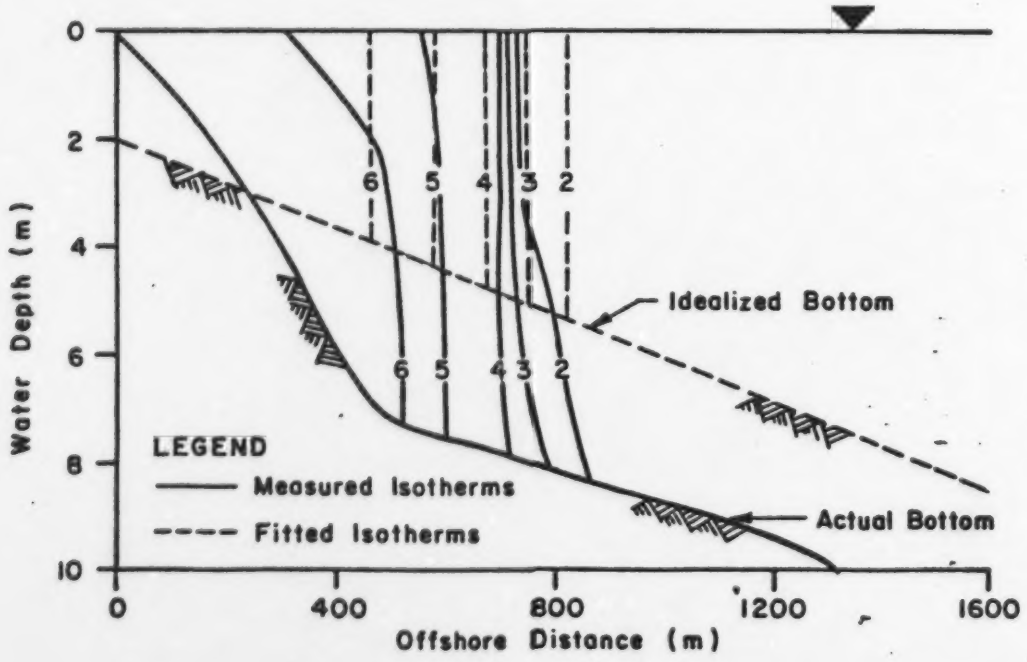

Fig. 8 Comparison of measured and fitted isotherms on the starting plane (cross-section A-A)

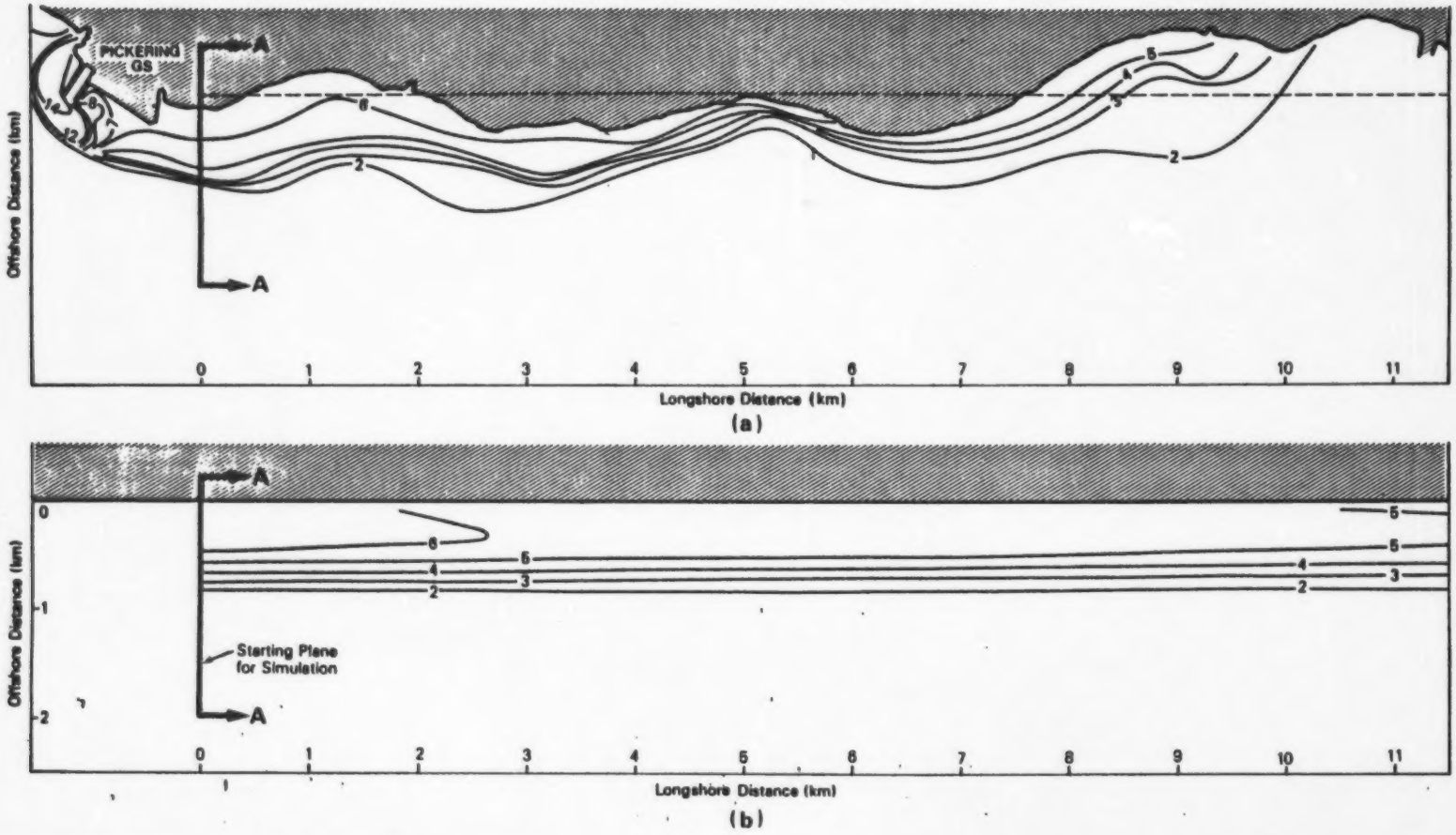

Fig. 9 Comparison of measured surface thermal plume with the results from the simulation run in which temperature-generated density differences were included

The small density differences do have an observable influence on the current velocity components, however. A pronounced gyre in the current pattern due to the sinking action of water near its density maximum is shown in Fig. 10 at a station 5.5 km from the inlet. The largest vertical velocity components occur at approximately 670 m from the shore which is the position of the 4°C isotherm.

Although the relative magnitude of the vertical velocity components are extremely small, the resulting current gyre has a small but noticeable effect on the vertical temperature field when compared with results from a run in which density-induced motion was suppressed. Vertical isotherms at the 10.5 km plane for both cases are compared in Fig. 11. The figure illustrates that the density-induced currents do promote mixing to a small extent, but that this effect is not large enough to alter the essentially uniform vertical temperature distribution.

The simulated vertical temperature fields with and without density variation which are compared in Fig. 11 suggest that density variations tend to promote, rather than inhibit the lateral (offshore) diffusion of the heated water and any other dissolved material that might be carried along with it.

CONCLUSIONS

A three-dimensional finite difference model was applied to two thermal discharge problems and the results have been compared with field observations.

In the first application, which involved a jet of warm water being discharged into a quiescent lake, good agreement was achieved between the predictions and field data. The results showed that the depth and irregular bathymetry of the bottom had a strong effect on the temperature decay of the

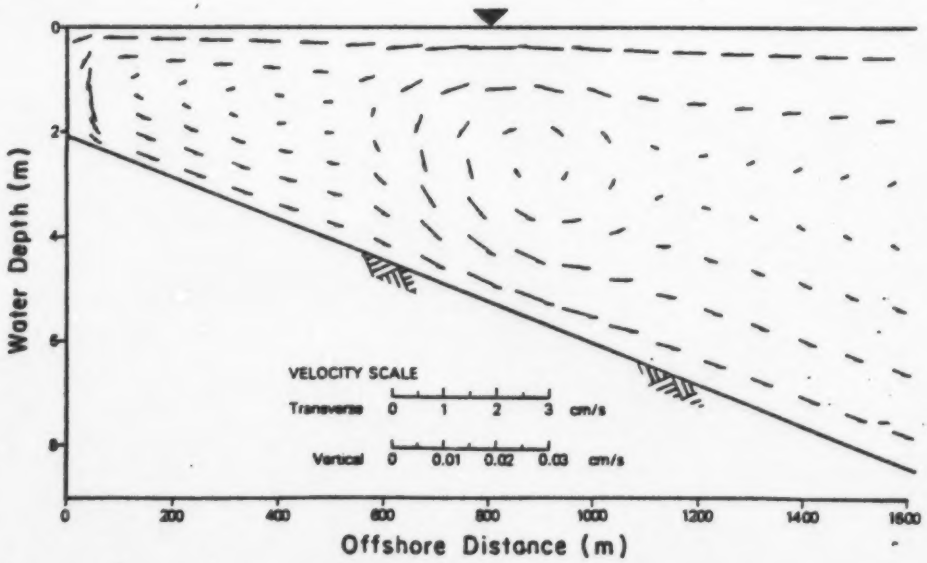

Fig. 10 Predicted current velocity vectors normal to the main flow at the 5.5 km computation plane from the simulation run in which temperature-generated density differences were included

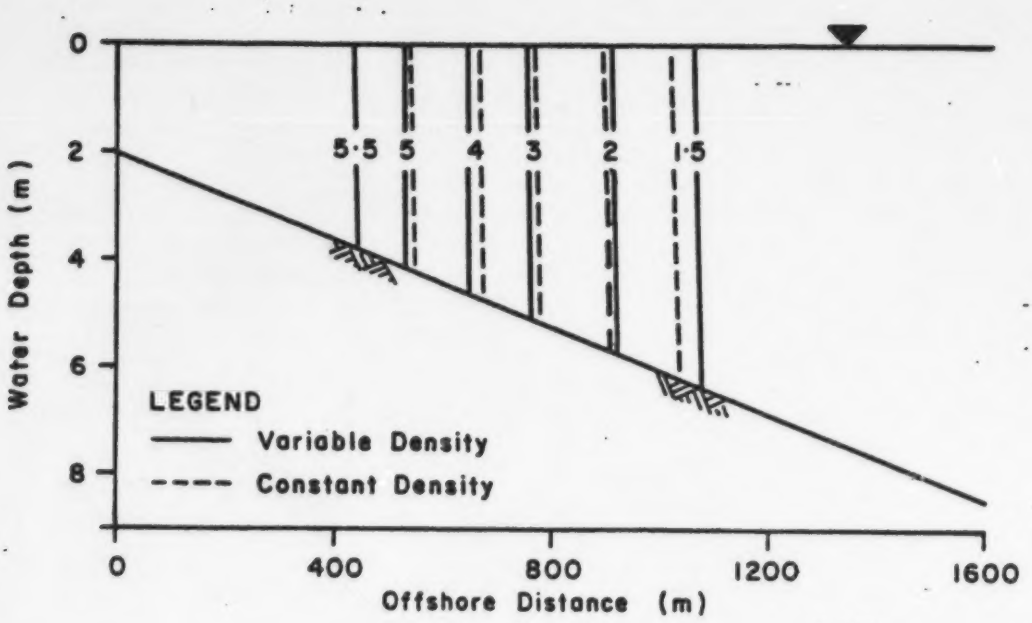

Fig. 11 Comparison of calculated vertical isotherms from simulation runs with and without temperature-generated density differences

discharged water. Thermal half-widths appeared to be under-predicted by the model, which would suggest that backflow along the jet boundary may be partially responsible for spreading of the jet near the discharge.

The second application involved a jet of warm water being discharged under winter (sinking plume) conditions into a moderate-to-strong longshore current to be deflected to follow the lake shoreline. Good qualitative agreement between predictions and observations was found. The main features were the small lateral spreading rate of the plume, and the uniformity of the water temperature from surface to bottom at any location. The sinking of water along the maximum density isotherm was shown to play only a minor role in mixing in the presence of the longshore currents. Under such conditions, the three-dimensional model could be replaced by a depth-averaged two-dimensional model to predict spreading and cooling of the plume.

REFERENCES

1. Dunn, W.E., Policastro, A.J., and Paddock, R.A., Surface Thermal Plumes: Evaluation of Mathematical Models for the Near and Complete Field, Argonne National Laboratory Report No. ANL/WR-75-3, 1975.

2. Jirka, G.H., Abraham, G., and Harlemann, D.R.F., An Assessemnt of Techniques for Hydrothermal Prediction, Ralph M. Parson Laboratory for Water Resources and Hydrodynamics, Report No. 203, Massachusetts Institute of Technology, 1975.

3. McGuirk, J., and Rodi, W., Calculation of Three-Dimensional Heated Surface Jets, Proceedings of the 1976 ICHMT Seminar on Turbulent Buoyant Convection, Dubrovnik, Yugoslavia, pp. 275-288, 1976.

4. McGuirk, J., and Rodi, W., Mathematical Modelling of Three-Dimensional Heated Surface Jets, J. Fluid Mechanics, Vol. 95, Part 4, pp. 609-633, 1979.

5. Raithby, G.D., Prediction of Dispersion by Surface Discharge, Report of the Basin Investigation and Modelling Section, Canada Centre for Inland Waters, Burlington, Ontario, 1976.

6. Raithby, G.S., and Schneider, G.E., The Prediction of Surface Discharge Jets by a Three-Dimensional Finite Difference Model, J. Heat Transfer, Vol. 102, No. 1, pp. 138-145, 1980.

7. Raithby, G.D., and Schneider, G.E., Numerical Solution of Problems in Incompressible Fluid Flow: Treatment of the Velocity-Pressure Coupling, Numerical Heat Transfer, Vol. 2, pp. 417-440, 1979.

8. Phillips, N.A., A coordinate System Having Some Special Advantages for Numerical Forecasting, J. of Meteorology, Vol. 14, pp. 184-185, 1957.

9. Freeman, N.G., Hale, A.M., and Danard, M.B., A Modified Sigma Equations' Approach to the Numerical Modelling of Great Lakes Hydrodynamics, J. Geophysical Research, Vol. 77, No. 6, pp. 1050-1060, 1972.

10. Paul, J.F., and Lick, W.J., A Numerical Model for a Three-Dimensional Variable-Density Jet, Case Institute of Technology Report FTAS/TR 73-9. 1974.

11. Metcalfe, R.P., Lake Ontario Pickering Nuclear Generating Station Winter Thermal Plume Study 1979-1980, Thermal Plume Mapping; Design and Development Division, Ontario Hydro, Toronto, Ontario, Report No. 80294, 1980.

12. Farooqui, R., Lake Ontario, Pickering Nuclear Generating Station, Winter Thermal Plume Study, 1979-1980, Lake Bottom Temperatures; Design and Development Division, Ontario Hydro, Toronto, Ontario, Report No. 80295, 1980.

13. Bull, J.A., Kerman, M., and Lilly, O., Coastal Current Climatological Summary, Pickering Generating Station, December 6, 1979, to March 31, 1980; Environment Canada -National Water Research Institute, Burlington, Ontario, 1980.

14. Winter Thermal Plume Study, 1979-1980 at Pickering Generating Station; Ontario Ministry of the Environment, Environment Canada-National Water Research Institute and Ontario Hydro, Toronto, Ontario, March 1981.

15. Csanady, G.T., Turbulent Diffusion in the Environment, D. Reidel Publishing Company, Dordnecht, Holland, pp. 106-107, 1973.

16. Donelan, M.A., Are Aquatic Micrometeorologists Delivering the Goods or is the Over-Water Drag Coefficient Far From Constant?, Proceedings of Symposium on Modelling of Transport Mechanisms in Ocean and Lakes, Manuscript Report Series 43, Canada Centre for Inland Waters, pp. 325-335, 1975.

17. Elliott, R.V., Pickering Nuclear Generating Station, Winter Thermal Plume Study (1979-1980), Mathematical Simulation of a Selected Longshore Plume; Design and Development Division, Ontario Hydro, Toronto, Ontario, Report No. 80488, 1981.

PB82-228669

PREDICTION OF LOW-FLOW PLUME CONFIGURATIONS FOR 316(a) STUDIES OF OPERATING POWER PLANTS

Paily P. Paily, Ph.D.
School of Civil Engineering
Georgia Institute of Technology
Atlanta, Georgia 30332, U.S.A.

ABSTRACT

316(a) demonstration studies for thermal power plants require that plume configurations corresponding to a specified low river flow be determined. Since field data are normally not available at the low flow, the size of the mixing zone corresponding to the worst-case flow is predicted. Two approaches for the prediction of low -flow plume configurations are illustrated in this paper using case studies.

1. INTRODUCTION

Federal Water Pollution Control Act of 1972 (Public Law 92-500) requires steam electric power plants to be operated in compliance with certain effluent limitations designed to achieve water quality standards. These effluent limitations were promulgated and issued by the Environmental Protection Agency (EPA) at 40 CFR Part 423 in March 1974, under "Proposed Effluent Limitations Guidelines and Standards for Steam Electric Power Plants." For discharge of thermal effluents, the guidelines allow "no discharge of heat except for cold side blowdown for all large base loaded units as reflected by the application of closed cycle evaporative cooling tower systems." However, Section 316(a) of the act allows, for thermal discharges, an exemption from this limitation if a successful demonstration can be made to show that the thermal effluent limitation is "more stringent than necessary to assure the protection and propagation of a balanced, indigenous population of shellfish, fish and wildlife in and on the body of water to which the discharge is to be made." When a 316(a) demonstration is satisfactorily made, the regional EPA administrator can impose a different effluent limitation matching the requirements of the particular thermal discharge.

The Effluent Guidelines and Standards classify power plants that were in operation prior to 1970 as old units, and hence exempt from the "no discharge of heat" limitation. However, in order to demonstrate compliance with applicable state water quality standards, it may be necessary for these plants to submit a 316(a) demonstration. The simplest kind of demonstration possible is the Low Potential Impact Type III, which is permissible when a site is determined to be one of low potential impact for all biotic categories. For this demonstration, field studies are normally conducted for a period of one year, and based on the data collected, a master ecosystem rationale is completed, which will include, besides relevant engineering and hydrological

data, thermal plume configurations for defining a thermal mixing zone at low river flows.

The mixing zone is the region of the stream enclosed by a specified temperature-rise isotherm (usually 5° F) within the thermal plume, and is often characterized by the center-line distance, maximum width, and surface area of this isotherm. The area of noncompliance with the allowable thermal standards, represented by the mixing zone, will be the largest at low river flows. This limiting, or "worst-case", size of mixing zone usually occurs at conditions of maximum design cooling water flow rate, maximum condenser temperature rise, high ambient river temperature, and low river flow. The extreme size of mixing zone may not be directly determined from field measurements, since the river flows may not approach the required low flow during the field survey period. It may thus become necessary to predict plume configurations at low flows.

2. LOW-FLOW PLUME PREDICTION

In order to determine the thermal plume patterns at low river flows, two approaches are possible. The first, and often the simple approach is to develop empirical relationships between plume characteristics and plant operating conditions based on measured data, and then to extrapolate values at low flows. From theoretical considerations, Paily (1980) has shown that the following functional relationships exist between the plume variables:

$$\frac{\Delta T_c}{\Delta T_o} = f_1\left(\frac{Q_R}{Q_o}, \frac{x}{b_o}\right) \qquad (1)$$

$$\frac{A\, Q_R \sqrt{g' h_o}}{Q_o^2} = f_2\left(\frac{\Delta T}{\Delta T_o}\right) \qquad (2)$$

$$\frac{W}{b_o} = f_3\left(\frac{A}{x_o^2}\right) \qquad (3)$$

in which ΔT_o = initial temperature rise; ΔT_c = centerline temperature rise at downstream location, x; ΔT = temperature rise of any isotherm; Q_R = river flow; Q_o = effluent discharge; b_o = width of discharge outlet; h_o = depth of discharge at outlet; W = maximum width of an isotherm; x_o = maximum downstream distance of an isotherm; A = surface area within an isotherm; and $g' = (\Delta\rho / \rho_o)\, g$ = apparent acceleration of gravity, considering the density difference, $\Delta\rho_o$, between effluent and the river flow.

The empirical method based on statistical analysis, as discussed above, for determining thermal plume configurations at low flow may not be applicable if the amount of water diverted through the station condensers at low river flow is a large percentage (above 75%) of the total river flow. In such a case, the discharge from the station will immediately spread across the entire river section, and the temperature within the mixing zone will soon stabilize at the fully mixed value. When considering the downstream extent of the mixing zone, the distance between the discharge outlet and the point of complete mixing can be neglected as being very small in proportion, and

it is reasonable to assume that complete mixing has occurred at the discharge outlet itself. The initial fully mixed excess-temperature within the river due to the plant discharge for this situation will be ΔT_m, given by

$$\Delta T_m = \frac{Q_o}{Q_R} \Delta T_o \qquad (4)$$

The second approach involves the prediction of downstream distribution of temperature, and hence the size of the mixing zone, within a fully mixed river. This can be achieved by the numerical solution of a simplified one-dimensional convection-diffusion equation as presented by Paily and Kennedy (1974). The method involves the evaluation of the heat content of a parcel of water considering the combined actions of advective transport and atmospheric cooling. The simplified heat conservation equation for this case, neglecting tributary inflows and downstream heat sources, is represented by

$$\frac{dT}{d_x} = \frac{B(x)}{Q_R} \frac{\phi^*(T)}{\rho\, c} \qquad (5)$$

where T = water temperature; B(x) = river width, which changes from section to section; and $\phi^*(T)$ = rate of surface heat exchange between water and atmosphere. The quantities ρ and c are the density and specific heat of water, respectively (ρc = 1.0 cal per cm^3 per °C or 62.4 BTU per ft^3 per °F). The surface heat exchange term, $\phi^*(T)$ in the above equation is a complex function of meteorological conditions and water temperature, and represents the net heat transfer to the atmosphere due to solar radiation, atmospheric long-wave radiation, back radiation, evaporation, conduction and precipitation. Methods to determine the magnitude of $\phi^*(T)$ have been given by Paily et al. (1974).

The solution of the heat transport relation, Eq.(5), requires the prior knowledge of an initial condition, which is the water temperature at the starting point (x = 0). In order to determine the excess temperature within the river fue to the plant discharge, this initial temperature can be taken as the equilibrium temperature of water, T_E, corresponding to the specified meteorological conditions. The equilibrium temperature is determined from a trial and error solution of the complex relation for the surface heat exchange rate, $\phi^*(T)$, such that when the water temperature equals the equilibrium temperature, there is no surface heat transfer from water to the atmosphere. The centerline distance of mixing zone is then given by the value of x at which $T - T_E$ is equal to 5°F. The surface area of the plume will be the same as the surface area of the river reach of length x, and maximum plume width will be equal to the maximum river width within that reach.

The numberical method for predicting plume configurations can be made simple, if certain assumptions are possible with respect to the river environment. These will include:

(1) Width of the river is uniform at a fixed value downstream from the location of discharge;

(2) Presence of rapids and pools in the river does not affect the temperature distributions;

(3) There are no inflows or outflows from the river to modify the river flow rate;

(4) Meteorological conditions do not vary along the length of the river; and

(5) Temperature distribution is influenced only by advection, and the surface heat exchange between water and atmosphere.

3. CASE STUDIES

The above discussed predictive approaches for determining low flow plume configurations were applied in 316(a) demonstration studies of two operating power plants in New York State. The first plant, located on the Susquehanna River, has a maximum design flow rate of 4.25 m^3/sec (150 cfs) and a condenser temperature rise of 10°C (18°F). The discharge occurs through a 1m (3.3 ft) wide rectangular outlet canal into the river. A river flow of 17 m^3/sec (600 cfs) with an exceedence probability of 95% at the plant site was designated as the low flow for plume analysis. Hence the applicable flow ratio for low flow plume configurations was 4.0.

As part of the data collection program for 316(a) demonstration studies, six thermal plume surveys were conducted in the river over a one-year period. The background data corresponding to these surveys are provided in Table 1. In order to determine the size of the mixing zone at the desired flow ratio of 4, measured data from the first five plume surveys (December data were excluded due to observed ice conditions in the river) were analyzed to develop empirical relationships. For the downstream location of the edge of mixing zone, the functional relationship in Eq.(1) was represented in the following manner:

for a constant value of Q_R/Q_o:

$$\frac{\Delta T}{\Delta T_o} = a\, e^{-b(x/b_o)} \qquad (6)$$

for a constant value of x/b_o:

$$\frac{\Delta T}{\Delta T_o} = a_1\, e^{-b_1(Q_R/Q_o)} \qquad (7)$$

The relationship between temperature-rise ratio and downstream distance, Eq.(6), can be readily derived from theoretical considerations (e.g., Paily and Kennedy, 1975). For Eq.(7), a similar exponential relationship was assumed based on observed trends in measured data. The required relation between temperature-rise ratio and downstream distance for the low flow situation (Q_R/Q_o = 4.0) was developed from Eqs.(6) and (7) using the following steps:

(1) Measured temperature-rise ratio was plotted as a function of downstream distance for each plume, as shown in Figure 1;
(2) Values of $\Delta T/\Delta T_o$ corresponding to different values of Q_R/Q_o at the same value of x were determined from the plot;
(3) The values of $\Delta T/\Delta T_o$ at each x were fitted to Eq.(7) to determine a_1 and b_1 for that location. Once a_1 and b_1 were known, $\Delta T/\Delta T_o$ at that location for $Q_R/Q_o = 4.0$ was determined;
(4) All values of $\Delta T/\Delta T_o$, corresponding to $Q_R/Q_o = 4$, for different downstream locations were fitted to Eq.(6) to obtain, for $Q_R/Q_o = 4$,

$$\frac{\Delta T}{\Delta T_o} = 1.1183 \exp(-0.0068\, x/b_o) \qquad (8)$$

(5) Solving Eq.(8), maximum downstream distance of an isotherm was given by

$$\frac{x}{b_o} = 164.4 - 1470.6 \ln (\Delta T/\Delta T_o) \qquad (9)$$

Based on Eq.(9), the downstream extent of the mixing zone, defined by ΔT=5°F (for ΔT_o = 18°F) was obtained as 2018m (6720 ft).

For the plume surface area model, a power-law relationship between area and temperature rise is often assumed (Asbury and Frigo, 1971; Elliott and Harkness, 1972) . Hence the functional relationship in Eq.(2) was represented by:

$$A \frac{Q_R}{Q_o 2}\sqrt{g'ho} = C_1 \left(\frac{\Delta T}{\Delta T_o}\right)^{C_2} \qquad (10)$$

The constants C_1 and C_2 were determined using the measured plume data, and the resulting plume area relationship was given by:

$$A \frac{Q_R}{Q_o 2} \sqrt{g'ho} = 3370 \left(\frac{\Delta T}{\Delta T_o}\right)^{-1.309} \qquad (11)$$

For a discharge canal flow depth of 0.5m (1.64 ft), Eq.(11) estimated the surface area of mixing zone to be 16.41 hectares (40.55 acres).

The measured plume data did not provide sufficient information to determine the functional relationship for plume width, given by Eq.(5). Hence, an estimate of the cross-stream extent of the mixing zone was made, considering the maximum river flow within the plume. Using Eq.(4), this flow was estimated, for ΔT_m=5°F, as 15.3 m^3/sec (540 cfs), which was 90% of the total river flow. Hence the maximum width was estimated as about 90% of the maximum river width within the mixing zone.

The second power plant for which the 316(a) studies were conducted was located on the Chemung River. The low flow plume configurations for this plant were required for the following conditions: a plant discharge rate of 3.3 m^3/sec (116 cfs), a condenser temperature rise of 10.3°C (18.54°F), and a river flow, with 95% exceedence probability at the plant site, of 4 m^3/sec (140 cfs). Since the quantity of water diverted through the plant is 83% of the total river flow, the size of the mixing zone was determined assuming the thermal discharge to be fully mixed into the river flow within the entire river cross section at the location of the discharge outlet. The initial

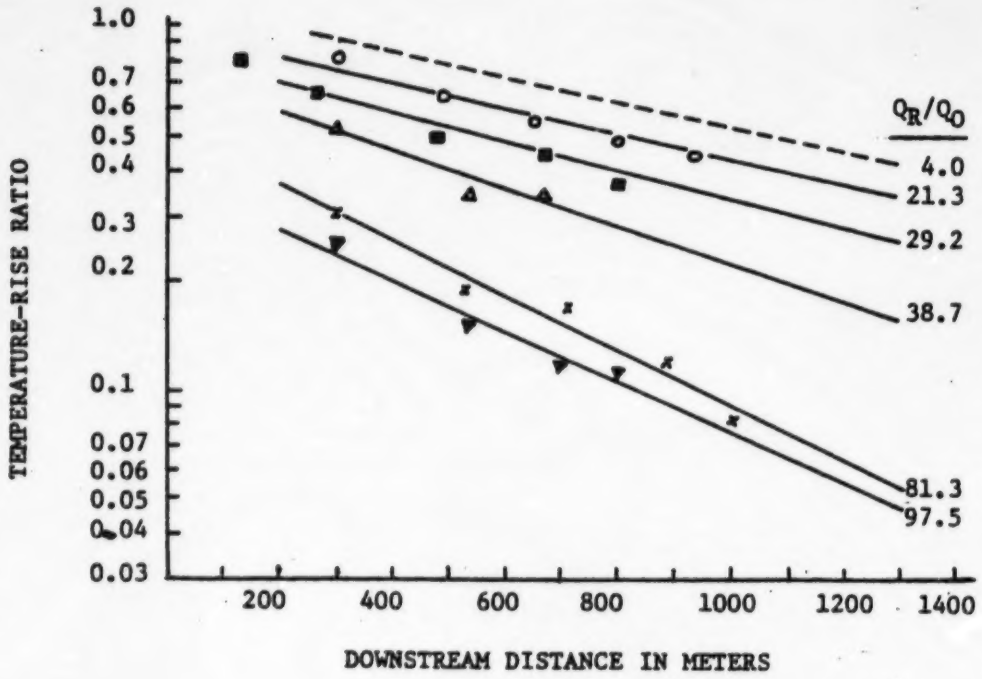

Figure 1: Measured downstream distributions of temperature-rise ratio at various values of flow ratio.

TABLE 3

Predicted mixing zone configuration for August and September, for fully mixed stream flow conditions.

Downstream Distance m (ft)		Temperature Excess August °C (°F)		September °C (°F)	
0	(0)	8.50	(15.30)	8.50	(15.30)
365	(1200)	7.62	(13.72)	7.74	(13.94)
731	(2400)	6.85	(12.33)	7.08	(12.74)
1097	(3600)	6.17	(11.11)	6.46	(11.63)
1463	(4800)	5.57	(10.03)	5.91	(10.64)
1829	(6000)	5.03	(9.06)	5.42	(9.75)
2195	(7200)	4.56	(8.20)	4.97	(8.95)
2560	(8400)	4.13	(7.43)	4.57	(8.22)
2926	(9600)	3.74	(6.74)	4.20	(7.56)
3170	(10,400)	3.51	(6.32)	3.97	(7.15)
3536	(11,600)	3.19	(5.74)	3.66	(6.58)
3901	(12,800)	2.90	(5.22)	3.37	(6.06)
4054	(13,300)	2.78	(5.00)	3.26	(5.86)
4267	(14,000)	-		3.11	(5.59)
4633	(15,200)	-		2.87	(5.16)
4773	(15,600)	-		2.78	(5.00)

TABLE 1

Hydraulic and thermal parameters corresponding to thermal plume surveys.

Date	River Flow Q_R (cfs)	Plant Discharge Q_o (cfs)	Average Plant Load (percent)	Average Heat Rejection Rate (10^8 BTU/hr)	Initial Excess Temperature ΔT_o(C)	Ambient River Temperature, T_R (^oC)	Flow Ratio Q_R/Q_o
16 March	8539	105	87	4.8	15.7	2.9	81.3
04 May	14627	150	93	5.6	14.6	9.6	97.5
29 June	5810	150	95	6.7	12.7	22.7	38.7
03 August	3199	150	89	6.2	10.0	18.5-20.6	21.3
21 August	4376	150	92	6.3	10.2	18.1-19.3	29.2
07 December	6195	105	91	5.3	17.5	0.7	59.0

TABLE 2

Monthly average meteorological conditions at Binghampton, New York based on National Weather Service data for the period 1931 - 1960.

Quantity	August	September
Air Temperature (F)	66.5	59.5
Wind Velocity (mph)	8.5	8.8
Relative humidity (%)	75.2	77.8
Cloud cover (tenths)	6.5	6.4
Atmospheric pressure (in Hg)	28.40	28.31
Solar radiation (langley/min)	415.47	323.66

fully mixed temperature rise in the river, at the discharge point, was determined to be 8.53°C (15.36°F) using Eq.(4).

Since the maximum size of the mixing zone normally corresponds to the warmest periods in a year, monthly mean meteorological conditions for the months of August and September, listed in Table 2, were used to determine the equilibrium temperature, T_E. Using the computed values of T_E (20.7°C or 69.2°F for August; 16.3°C or 61.3°F for September), and Eq.(5), values of fully mixed temperature rise along the stream upto the edge of the mixing zone were computed. The results, listed in Table 3, indicated that the largest downstream extent of the mixing zone, corresponding to September conditions, was 4773m (15660 ft). Within this length, the maximum and average widths of the river were 130m (425 ft) and 91.4m (300ft), respectively. Hence, the total surface area of the mixing zone, based on the average river width was 43.63 hectares (107.9 acres), and the maximum width of the mixing zone was 130m (425 ft).

4. CONCLUSIONS

Low-flow plume configurations required for 316(a) demonstration studies can be predicted using empirical models developed from field data, or from numerical solutions of heat transport equations. For old, operating power plants, the results will help to establish the maximum size of mixing zone under extreme plant operating conditions.

REFERENCES

1. Asbury, J. G., and Frigo, A. A. 1971. A Phenomenological Relationship for the Surface Areas of Thermal Plumes in Lakes. Argonne National Lab. Report No. ANL/ES-5.

2. Elliott, R. V., and Harkness, D. G. 1972. A Phenomenological Model for the Prediction of Thermal Plumes in Large Lakes. Proceed. 5th Conf. of Great Lakes Research.

3. Paily, P. P. 1980. Evaluation of Compliance Criteria for River Plumes. Proceed. ASCE Hydraulics Division Conference, Chicago.

4. Paily, P. P., and Kennedy, J. F. 1975. Determining Ambient Water Temperatures. Discussion of Paper No. 11171 by Markovsky and Binkerd, ASCE Jour. of Hydraulics Division.

5. Paily, P. P., and Kennedy, J. F. 1974. A Computational Model for Predicting the Thermal Regimes of Rivers. Iowa Institute of Hydraulic Research, Report No. 169.

6. Paily, P. P., Macagno, E. O., and Kennedy, J. F. 1974. Winter-regime Surface Heat Loss From Heated Streams. Iowa Institute of Hydraulic Research, Report No. 155.